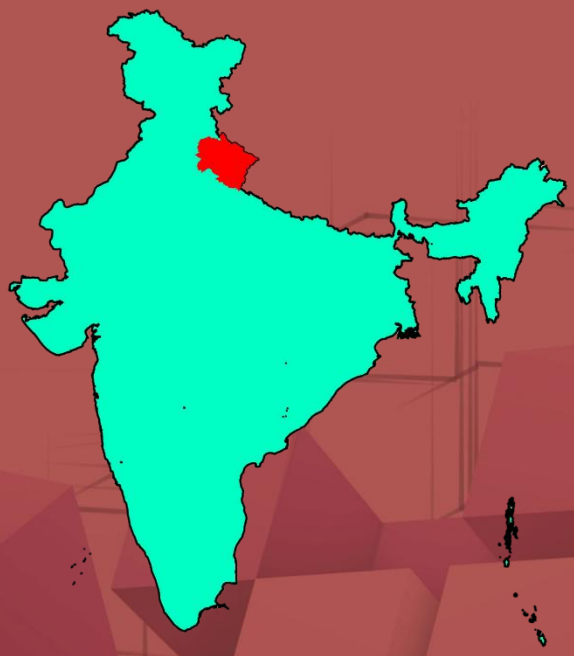

Final Geological Report (GR) on "Reconnaissance Survey (G4 Stage) for Graphite and Vanadium in Matena-Sirar Area (60 sq. km.), Almora District, Uttarakhand"

Geovale Services Pvt. Ltd.

Earth System Science for sustainable Development

June, 2026

3rd Floor, Anaya Chambers
GN 38/5, Salt Lake, Sec –V,
Kolkata - 700091

GEOVALE SERVICES
Planetary Science And Technology for Sustainable Development

Project Title: Reconnaissance Survey (G4 Stage) for Graphite and Vanadium in Matena-Sirar Area (60 sq. km.), Almora District, Uttarakhand.

Project Code: 23/491/2024-NMET-282.

Project Timeline: 21st August 2024 to 30th June 2026.

Project Location: Matena-Sirar, Almora District, Uttarakhand.

National Mineral Exploration and Development Trust Secretariat (NMEDT)
Ministry of Mines
9th Floor, Jeevan Prakash LIC Building
Kasturba Gandhi Marg,
New Delhi-110001

Phone: 011 2307 1006
E-mail Id: nmet-mines@gov.in

Project executed as NPEA:
Geovale Services Pvt. Ltd.

3rd Floor, Anaya Chambers,
GN 38/5, Salt Lake, Sec -V,
Kolkata - 700091

Website: http://geovale.com/

Project Coordinators

Mr. Biplob Chatterjee (Author)

CEO and Director (Consulting)

Dr. Joy Gopal Ghosh (Author)

Principal, Geology and Exploration

Dr. Taraknath Pal (Author)

Principal, Geology and Exploration

Dr. Tapan Pal

Principal, Geology and Exploration

Project Leader

Dr. Tanwita Deb (Author)

Senior Project Manager (Exploration)

Project Managers

Sarita Mahato (Author)

Project Manager (Exploration)

Spandita Kundu (Author)

Project Geologist (Exploration)

Prasen Saha (Author)

Project Geologist (Exploration)

Technical Area Experts

Nupur Adhikary (Author)

Senior Project Manager (Geology and Geospatial Services)

Chiranjib Banerjee (Author)

Senior Project Manager (Geotechnical)

Sujoy Payra (Author)

Senior Project Manager (Geospatial Services)

Team Members

Dr. Suparna Goswami

Senior Project Manager (Exploration)

Arnab Mallick

Project Manager (Exploration)

Shivani Gupta

Project Geologist (Exploration)

Dakshi Sarkar

Project Geologist (Exploration)

Upasana Mondal

Project Geologist (Exploration)

Tanuja Priyadarshani Deo

Project Geologist (Exploration)

Prabir Bhattacharya

Project Manager (Geospatial Services)

Rabiya Parween

Project Scientist (Geospatial Services)

Table of Contents

1 सारांश: 2

2 Introduction: 22

2.1 Administrative Details of the Project: 22

2.2 Investigating Agency: 24

2.3 Objectives of Investigation: 24

2.4 Basis for Taking Up Investigation: 24

2.5 Nature and quantum and timeline of work (NQT): 25

2.6 Personnel Involved: 28

2.7 Mode of Operation of Different Working Components and Associated Agency: 31

2.8 Acknowledgements: 32

2.9 Summary of work strategy and report writing: 33

3 Property Description: 37

3.1 Location and Accessibility: 37

3.2 Topography: 39

3.3 Climate: 40

3.4 Flora and Fauna: 41

3.5 Forest Cover: 42

3.6 Archaeological site: 43

3.7 Satellite Remote Sensing data acquisition and processing: 45

3.8 Environmental, Social and Governance (ESG) framework and Mineability Considerations of the block: 56

4 Previous Work: 63

4.1 Regional Geology: 63

4.2 Structure: 66

4.3 Previous work on exploration 66

5 Geoscientific Activities: Methodological Record of the Almora Graphite Exploration Programme: 76
5.1 Preamble: 76
5.2 Geospatial Analysis (Remote Sensing) 76
5.3 Orientation Survey: 77
5.4 Geological-Structural Mapping: 79
5.5 Surface Sampling - Grab and Chip 82
5.6 Stream Sediment Sampling 84
5.7 Pitting and Trenching 86
5.8 Petrology of Surface and Subsurface Samples 90
5.9 Raman Spectroscopy 91
5.10 X-Ray Diffraction (XRD) 93
5.11 Isodynamic Separation of Heavy Minerals from Stream Sediment Samples 94
5.12 Geophysics - Self Potential (SP) 95
5.13 Geophysics - Vertical Electrical Sounding (VES) 98
5.14 Tumbler Test (Graphite Crystallinity Field Assessment) 101
5.15 Geochemical Assay - XRF (Major Oxide Analysis) 103
5.16 Geochemical Assay - Proximate Analysis (Fixed Carbon) 104
5.17 Geochemical Assay - ICP-MS (Trace Element and REE Analysis) 105
5.18 Geochemical Assay - Total Sulphur 106
5.19 Scout Drilling 107
6 Geology, Structure, Metamorphism, Mineral Systems Analysis: 112
6.1 Geological Mapping: 112
6.2 Description of rock types: 117
6.3 Structure: 138
6.4 Metamorphism: 144
6.5 Graphite and Poly-metals Fertility of the Lesser Himalaya in Mineral System Analysis (MSA) Framework: 151

6.6 Geochemical Analysis for surface sampling: 153
7 Exploration Data Analysis: Characterisation of Graphite Blocks: 183
7.1 Digoli-Gajjola Graphite Block, Almora 184
7.2 Sirar-Bataldeon Graphite Block, Almora 194
7.3 Kalimath Graphite Block, Almora 212
7.4 Phalsima-Pithauni Graphite Block, Almora: 228
7.5 Batgal-Channi Graphite Block 248
8 Exploration by Scout Drilling: 262
8.1 Objectives and Rationale for Scout Drilling 262
8.2 Drilling and Sampling Methodologies 262
8.3 Core Handling and Sampling Protocol 263
8.4 Overview of the Drilling Program 264
8.5 Details of Borehole: 265
9 Exploration Target Potential: Almora Graphite Blocks 314
9.1 Preamble and Reporting Framework 314
9.2 Digoli-Gajjola Graphite Block 317
9.3 Sirar-Bataldeon Graphite Block - Exploration Target Potential 326
9.4 Kalimath Graphite Block 333
9.5 Phalsima-Pithauni Graphite Block-Exploration Target potential 340
9.6 Batgal-Channi Graphite Block - Exploration Target Potential 347
10 Conclusion and Recommendation: 355
10.1 Conclusions 355
10.2 Graphite-Vanadium Exploration Target Potential 358
10.3 Exploration Target Potential 360
10.4 Recommendations for G3 Stage 361
11 Expenditure: 365
12 References: 367

13 Locality Index: 371

14 Annexures: 373

List of Figures:

Figure 1.1: Recommended five G3 graphite blocks within the Almora G4 Block.....20
Figure 2.1: Almora Block Exploration Workflow.....34
Figure 3.1: Location map of Almora Block (G4 Stage) on SOI Toposheet 53O/10.....37
Figure 3.2: Accessibility map of the Almora block.....39
Figure 3.3: Topography map shows the aerial map with drainage pattern.....40
Figure 3.4: Snow Buckwheet plant in Sirar area 42
Figure 3.5: Chir-pine forest at Sirar area.....42
Figure 3.6: Chir-pine forest at Bataldeon area.....42
Figure 3.7: Forest area of the Almora block shown on 50 k geological map. 43
Figure 3.8: Topography map shows the presence of Lakhudiya Archaeological site, Almora Block. 44
Figure 3.9: Culture board from Archeological site given details about Lakhudiyar rock shelter, Almora.....44
Figure 3.10: Rock shelter in Lakhudiyar cave, the Archeological site, Almora. 44
Figure 3.11: Lineament map of the Almora block shows various orientation of lineaments..45
Figure 3.12: Elevation map of the Almora blocks show western part is more elevated than the eastern part. 46
Figure 3.13: Contour map of the Almora block shows higher elevation in the western part than the eastern part. 47
Figure 3.14: Slope Map of the Almora block. 48
Figure 3.15: Hillshade Map of the Almora block.....49
Figure 3.16: Drainage map of the Almora block. 50
Figure 3.17: Red scheme map of the Almora block.....51
Figure 3.18: LULC Map of the Almora Block.....53
Figure 3.19: Clay alteration map of the Almora block. 54
Figure 3.20: Ferrous alteration map of the Almora block. 55
Figure 3.21: Iron oxide map of the Almora block. 56
Figure 4.1: Geological and structural map of the Almora area and surrounding (modified after Pant et. al. 2012).....65
Figure 4.2: NGCM map of the Almora block area.....74
Figure 5.1: Field observation points of the Almora Block. 80
Figure 5.2: Streching lineation within foliated granite rock (Balta area). 80

Figure 5.3: Foliation within quartzite rock (Saura area).....80
Figure 5.4: Litho assemblages as evidenced in the field exposure of Almora Block 82
Figure 5.5: Foliation of the graphite schist.....82
Figure 5.6: Stream sediment location of Almora block.....85
Figure 5.7: Collection of stream sediments.....86
Figure 5.8: Processing the stream sediments.....86
Figure 5.9: Pitting and Trenching location in the Almora block area.....87
Figure 5.10: Marking the pit area for AL/Pit 01, near Pithauni area.....88
Figure 5.11: Excavation of the Pit (AL/Pit 01), near Pithauni area. 88
Figure 5.12: Excavation of pit after marking. 88
Figure 5.13: Labelling and restoration of the ground.....88
Figure 5.14: Excavation of trench (AL/Trench 01) in Pithauni area. 89
Figure 5.15: Labelling and restoration of the ground after trenching, in Pithauni area.....89
Figure 5.16: Self potential (SP) lines of Almora Block 96
Figure 5.17: SP data collection from Aquameter, Bataldeon area. 97
Figure 5.18: SP data collection from Aquameter, Bataldeon area. 97
Figure 5.19: Resistivity survey of Almora block with VES station 98
Figure 5.20: VES data collection in Sirar area. 100
Figure 5.21: VES data collection in Phalsima area 100
Figure 5.22: VES data collection in Pithouni area. 100
Figure 5.23: VES data collection in Pithauni area. 100
Figure 5.24: Collected VES data from Aquameter, Bataldeon area 100
Figure 5.25: Collected VES data from Aquameter, Sirar area. 100
Figure 5.26: Tumbler test for the borehole 04 samples showing majority of graphite flake floating on the water. 102
Figure 5.27: Tumbler test carried on the to verify graphite flake size. 102
Figure 5.28: Borehole 10 drilling site at Sirar area. 109
Figure 5.29: Core box of borehole 03 109
Figure 6.1: Geological Map (scale 1:50000) by GSI. 113
Figure 6.2: Large Scale Geological Map (1:12500) of Almora area (after Santosh and Yadav 2021, Image from GSI Report).....114
Figure 6.3: Map and cross section (1:12500) of Almora area (after Santosh and Yadav 2021, image from GSI Report). 114

Figure 6.4: Large Scale Geological Map (1:12,500) of the Almora block prepared by the Geovale Services Private Limited. *117*
Figure 6.5: Outcrop Section of Graphite Band in the Sirar area, Almora. *119*
Figure 6.6: Outcrop section showing Graphite Schist, Near Dibdiya, Almora. *119*
Figure 6.7: Graphite Flakes in Quartzite layer, near Sirar, Almora. *119*
Figure 6.8: Exposed Graphite Schist in the Hill top near Deora Village, Almora. *119*
Figure 6.9: Road Cut Section of Graphite Schist, near Falsima, Almora. *119*
Figure 6.10: Road Cut Section of Graphite Schist associated with deformed Quartz Vein. . *119*
Figure 6.11: Graphite Schist in outcrop near Falsima, Almora. *120*
Figure 6.12: Graphite Schist with Redox Sensitive Elements *120*
Figure 6.13: Photomicrograph of graphite schist sample showing small grains of graphite distributed in quartz muscovite schist where graphite occurs as pre to syntectonic (Sample Id. 109218), near Digoli, Almora. *121*
Figure 6.14: Photomicrograph of graphite schist sample showing graphite bearing quartz muscovite schist (Sample Id. 109238), near Dinapani, Almora. *121*
Figure 6.15 Photomicrograph of graphite schist sample showing cross-cut quartz vein around the fracture filling zone (Sample Id 109245), near Jakheta, Almora. *122*
Figure 6.16 Photomicrograph of graphite schist sample showing folded graphite flakes, (Sample Id 109202). *122*
Figure 6.17: Photomicrograph of graphite schist sample showing quartz vein with very fine-grained quartz in the vug-filling zone, recrystallized quartz (Sample Id 109245), near Jakheta, Almora. *122*
Figure 6.18 Photomicrograph of graphite schist sample showing crenulation cleavage within graphite schist (Sample Id 109202). *122*
Figure 6.19: Photomicrograph of graphite schist sample showing graphite concentrated in shear along with recrystallized quartz grain (Sample Id 109253), near Mat. *123*
Figure 6.20 Photomicrograph of graphite schist sample showing graphite Flakes observed under reflective light, (Sample Id 109245), near Jhaketa. *123*
Figure 6.21 Photomicrograph of graphite schist sample showing mica-fish in muscovite mica with embedded grains of graphite along the deformation, (Sample Id 109200), near Bintola. *123*
Figure 6.22 Photomicrograph of graphite schist sample showing graphite flakes in recrystallized quartz, Sample Id 109200, near Bintola. *123*

Figure 6.23: The graphite flake, near Kalimath-Mat band (Sample Id 109245), near Jhaketa area. 124
Figure 6.24: Measured graphite flakes, near Kalimath-Mat band (Sample Id 109245).....124
Figure 6.25: Graphite fleke under PPL, Bintola-Digoli area, (Sample Id 109200). 125
Figure 6.26: Measured graphite flakes, Bintola-Digoli graphite (Sample Id 109200).....125
Figure 6.27: Mica Schist associate with Garnet Biotite, near Bataldeon area.....127
Figure 6.28: Mica Schist associated with folded Quartz Vein 127
Figure 6.29: Weathering surface of garnet Mica Schist.....127
Figure 6.30: Garnet Mica Schist showing Boudinage Quartz, near Barakote Area.....127
Figure 6.31: Garnet mica schist showing stretching quartz veins. 128
Figure 6.32: Garnet mica schist, near Kalimath area.....128
Figure 6.33: Biotite with garnet and very rarely developed graphite (Sample Id: 109220) observed. 129
Figure 6.34: Garnetiferous Muscovite Schist (Sample Id: 109154), near Digoli. 129
Figure 6.35: Hand specimen of Quartz Sericite Schist with Tourmaline, near Khas Tilari. 130
Figure 6.36: Quartzite with later forming quartz veins.....130
Figure 6.37: Field outcrop of quartzite near Khas Tilari area. 130
Figure 6.38: Lineation in quartzite near Khas Tilari area.....130
Figure 6.39: Quartzite outcrop near Baman Tilari area.....131
Figure 6.40: Quartzite with prominent F1 foliation, near Channi area. 131
Figure 6.41: Photomicrogry of quartz associated with muscovite (Sample Id 109154, near Khas Tilari).....132
Figure 6.42: Photomicrography of quartz associated with tourmaline (Sample Id 109154, near Khas Tilari).....132
Figure 6.43: Tuffaceous Rock near Balta, Almora, shows banding.....133
Figure 6.44: Tuffaceous Rock shows the presence of lapilli (marked by an arrow) near Jakheta, Almora.....133
Figure 6.45: Tuffaceous bands near Balta, Almora 133
Figure 6.46: Tuffaceous Rock with bands, near Balta, Almora 133
Figure 6.47: Photomicrograph of tuffaceous rock shows fine grained tuffaceous rock (Sample Id 110020).....134
Figure 6.48: Photomicrograph of tuffaceous rock shows fine grained tuffaceous rock contains chlorite (Sample Id 110021). 134

Figure 6.49: Granite intrusive shows foliation, the presence of porphyroclasts of feldspars 135
Figure 6.50: Outcrop of Granite intrusive shows foliation, the presence of porphyroclasts of feldspars.....135
Figure 6.51: Deformed granite intrusive show the presence of zoned feldpar porphyroclast (Sample Id: 109255) 137
Figure 6.52: Deformed granite intrusive show the presence of feldpar porphyroclast wrap by the muscovite and quatz ribbon (Sample Id: 109255). 137
Figure 6.53: Photomicrograph of Granite gneiss shows the presence of elliptical feldspar and quartz (Sample Id: 109242). 138
Figure 6.54: Photomicrograph of Granite gneiss shows the presence of elliptical feldspar and quartz (Sample Id: 109242). 138
Figure 6.55: Field photo shows almost horizontal bed of mica-schist due to thrusting. 139
Figure 6.56: Field photograpgh shows the folding of quartzite in mica schist.....139
Figure 6.57: Quartzite shows the prominent F1 foliation. 140
Figure 6.58: Mylonitized granite intrusive with strong foliation. 141
Figure 6.59: Porphyroclasts (augen-shaped, marked by an arrow) of feldspar in mylonitic granite 141
Figure 6.60: The geological map of the Almora block shows the presence of the 6 thrusts in the block.....144
Figure 6.61: Snowball garnet in the mica-schist.....145
Figure 6.62: Folded muscovite in mica schist.....145
Figure 6.63: The presence of randomely oriented graphite in muscovite.....146
Figure 6.64: The presence of randomely oriented graphite in muscovite.....146
Figure 6.65: Graphite clots in carboneceous phyllite.....146
Figure 6.66: Graphite shows alignment parallel to foliation.....146
Figure 6.67: Foliated granite-gneiss shows the presence of elliptical quartz and muscovite alignment parallel to foliation 147
Figure 6.68: Foliated granite-gneiss shows the presence of elliptical feldspar.....147
Figure 6.69: Ribbon quartz in deformed granite intrusive, near Sirar area.....148
Figure 6.70: Ribbon quartz and muscovite alignments in deformed granite intrusive, near Sirar area. 148
Figure 6.71: Felspar porphyroclased in deformed granite intrusive, near Bintola.....148
Figure 6.72: Quartz prophyroclased in mylonitized granite intrusive, near Digoli. 148

Figure 6.73: Quartzite shows recrystallization of quartz and parallel alignments of muscovite, near Khas Tilari. *149*
Figure 6.74: Recristallized quartz in quarzite, near Khas Tilari. *149*
Figure 6.75: Photomicrograph shows Patchy quartzo-feldspathic masses are associated with sillimanite confirming development of partial melting due to muscovite breakdown reaction. under XPL. *152*
Figure 6.76: Photomicrograph shows sillimanite formation phase after break down of muscovite, under XPL. *152*
Figure 6.77: Photomicrograph shows sillimanite formation after break down of muscovite, under XPL. *152*
Figure 6.78: Histogram of V concentration (ppm) with frequency curve. *164*
Figure 6.79: Histogram of Ni concentration (ppm) with frequency curve. *164*
Figure 6.80: Histogram of Cr concentration (ppm) with frequency curve *164*
Figure 6.81: Histogram of Co concentration (ppm) with frequency curve *164*
Figure 6.82: Histogram of W concentration (ppm) with frequency curve. *164*
Figure 6.83: Histogram of Mo concentration (ppm) with frequency curve. *164*
Figure 6.84: Histogram of Cu concentration (ppm) with frequency curve. *165*
Figure 6.85: Histogram of Zn concentration (ppm) with frequency curve *165*
Figure 6.86: Histogram of Pb concentration (ppm) with frequency curve. *165*
Figure 6.87: Histogram of Sb concentration (ppm) with frequency curve. *165*
Figure 6.88: Histogram of La concentration (ppm) with frequency curve *166*
Figure 6.89: Histogram of Ce concentration (ppm) with frequency curve *166*
Figure 6.90: Histogram of Pr concentration (ppm) with frequency curve. *166*
Figure 6.91: Histogram of Nd concentration (ppm) with frequency curve. *166*
Figure 6.92: Histogram of Tm concentration (ppm) with frequency curve *166*
Figure 6.93: Histogram of Yb concentration (ppm) with frequency curve *166*
Figure 6.94: Histogram of Y concentration (ppm) with frequency curve *167*
Figure 6.95: Histogram of Sulphur concentration (%) with frequency curve *167*
Figure 6.96:Fixed Carbon value in percentange all over the Almora G4 Block *168*
Figure 6.97: Graphical representation of FC values for graphite schist as bedrock samples. *169*
Figure 6.98: XRD spectrum of graphite schist (Sample Id 109999) *172*
Figure 6.99: XRD spectrum of graphite schist (Sample Id: 109938) *174*
Figure 6.100: XRD spectrum of graphite schist (Sample Id: 110004) *175*

Figure 6.101: XRD spectrum of graphite schist (Sample Id: 110001) *176*
Figure 6.102: XRD spectrum of graphite schist (Sample Id: 109923) *177*
Figure 6.103: XRD spectrum of graphite schist (Sample Id: 114229) *177*
Figure 6.104: XRD spectrum of graphite schist (Sample Id: 114232) *178*
Figure 6.105: XRD spectrum of graphite schist (Sample Id: 114233) *179*
Figure 6.106: XRD spectrum of graphite schist (Sample Id: 114235) *179*
Figure 6.107: XRD spectrum of graphite schist (Sample Id: 114239) *180*
Figure 7.1: Geological map showing spatial distribution of five (05) graphite blocks, Almora. *183*
Figure 7.2: Accessibity map of the Digoli-Gajjola Graphite Block. *184*
Figure 7.3: Elevation map of the Digoli-Gajjola Graphite Block *185*
Figure 7.4: LULC map Digoli-Gajjola Graphite Block *185*
Figure 7.5: Drainage map of the Digoli-Gajjola Graphite Block *185*
Figure 7.6: Forest map of the Digoli-Gajjola Graphite Block *185*
Figure 7.7: Details of VES survey at the Digoli-Gajjola Graphite Block. *187*
Figure 7.8: VES 12 Profile showing low resistive zone *188*
Figure 7.9: SP and Elevation Profile of line 01 ..... *189*
Figure 7.10: SP and Elevation Profile of line 02 ..... *189*
Figure 7.11: Geochemical analyses of the (FC, VM, Ash) content of the Digoli-Gajjola block. *191*
Figure 7.12: Geochemical analyses of the Digoli-Gajjola Graphite Block. *192*
Figure 7.13: Geochemical analyses (V, Mo, Cu) of the Digoli-Gajjola Graphite Block *193*
Figure 7.14: Accessibility map of Sirar-Bataldeon Graphite Block *195*
Figure 7.15: Elevation map of the Sirar-Bataldeon Graphite Block, Almora *196*
Figure 7.16: LULC map of the Sirar-Bataldeon Graphite Block, Almora *196*
Figure 7.17: Drainage map of the Sirar-Bataldeon Graphite Block, Almora *196*
Figure 7.18: Forest map of the Sirar-Bataldeon Graphite Block, Almora *196*
Figure 7.19: Road section of the Sirar-Bataldeon graphite block in Sirar area, (Borehole 03) *198*
Figure 7.20: Resistivity VES survey conducted Sirar-Bataldeon Graphite Block *200*
Figure 7.21: Geological section along VES line 04 (VES12, VES13 with Borehole 03), near Sirar area *200*
Figure 7.22: VES profile of VES15, VES16, VES18, VES19 in Sirar area *201*
Figure 7.23: SP survey conducted Sirar-Bataldeon Block. *202*

Figure 7.24: SP and Elevation Profile of Line 03 202
Figure 7.25: SP and Elevation Profile of Line 09 202
Figure 7.26: Geochemical analyses (FC, VM, Ash) of surface graphite bands, Sirar-Bataldeon Block. 208
Figure 7.27: Geochemical analyses (S and SiO2) of surface graphite bands, Sirar-Bataldeon Block. 209
Figure 7.28: Geochemical analyses (V, Cu, and Mo) of surface graphite bands, Sirar-Bataldeon Block. 210
Figure 7.29: Accessibility map of the Kalimath Graphite Block.....212
Figure 7.30: Contour map and elevation map of the Kalimath Graphite Block, Almora. ...213
Figure 7.31: LULC map of the Kalimath Graphite Block, Almora. 213
Figure 7.32: Drainage map of the Kalimath Graphite Block, Almora.....213
Figure 7.33: Forest map of Kalimath Graphite Block, Almora. 213
Figure 7.34: Road section of Kalimath Graphite Block.....216
Figure 7.35: Road section of Kalimath Graphite Block eastern part.....217
Figure 7.36: Road section of eastern part of Kalimath graphite block.....218
Figure 7.37: Details of Graphite Schist rock in Kalimath Graphite Block.....219
Figure 7.38: VES lines and stations map of the Kalimath Graphite Block 220
Figure 7.39: Cross section on the basis of VES Survey of Line 30 221
Figure 7.40: SP Line of Kalimath Graphite Block, Almora 222
Figure 7.41: SP and Elevation Profile of the Kalimath Graphite Block, Almora 223
Figure 7.42: Modal analyses for the surface Graphite Schist thin section, near Mat area (Sample Id 109245).....224
Figure 7.43: Modal analyses counting for the surface Graphite Schist thin section, near Mat area (Sample Id 109245). 224
Figure 7.44: Proximate analyses of the Kalimath Graphite Block 225
Figure 7.45: Geochemical analyses for S and SiO2 from Graphite schist, Kalimath Graphite Block. 225
Figure 7.46: Geochemical analyses for V, Cu, and Mo from Graphite schist, Kalimath Graphite Block. 226
Figure 7.47: Modal Analysis to identify graphite flake size and graphite grain of Sample Id 113514 (BH-05), count by Image J software. 227
Figure 7.48: Accessibility map of Phalsima -Pithauni Graphite Block. 228
Figure 7.49: Elevation map of the Phalsima-Pithauni Graphite Block, Almora. 229

Figure 7.50: LULC map of the Phalsima-Pithauni Graphite Block, Almora.....229
Figure 7.51: Drainage map of the Phalsima-Pithauni Graphite Block, Almora. 229
Figure 7.52: Forest map of the Phalsima-Pithauni Graphite Block, Almora. 229
Figure 7.53: Road section of the Phalsima area. 232
Figure 7.54: Details of Graphite Schist in road section of the Phalshima area. 233
Figure 7.55: Road section and river section of Pithauni area with details of Graphite Schist, near BH06. 234
Figure 7.56:VES profile of the Phalsima-Pithauni block. 236
Figure 7.57: VES Profiles with low resistivity zone identified, Phalsima north band, Almora. 237
Figure 7.58: VES Profiles of VES117 and VES119 with low resistivity zone identified, Phalsima central band, Almora. 238
Figure 7.59: VES Profiles of VES140, VES141, VES142, VES143 with low resistivity zone identified, Phalsima southern band, Almora. 239
Figure 7.60: SP map of the Phalsima-Pithauni Graphite Block, Almora. 240
Figure 7.61: SP and Elevation Profile of Line 04 240
Figure 7.62: SP and Elevation Profile of Line 13 240
Figure 7.63: VES Profiles with low resistivity zone identified at VES Line 26 in Pithauni area, Almora.....241
Figure 7.64: Profile of VES 31 and VES 101 show a low resistivity layer.....242
Figure 7.65: SP and Elevation Profile of Line 05 242
Figure 7.66: SP and Elevation Profile of Line 13 242
Figure 7.67: Geochemical analysis (FC, VM, Ash content) of Phalsima- Pithauni Graphite Block, Almora 245
Figure 7.68: Geochemical analyses show S and SiO2 content of the Graphite, Phasima-Pithauni Graphite Block. 246
Figure 7.69: Geochemical analyses show Vanadium, Copper and Molybdenum content of the Graphite, Phasima-Pithauni Graphite Block. 246
Figure 7.70: Accessibility map of the Batgal-Channi Graphite Block. 248
Figure 7.71: Contour map and elevation map of the Batgal-Channi Graphite Block, Almora. 249
Figure 7.72: LULC map of the Batgal-Channi Graphite Block, Almora. 249
Figure 7.73: Drainage map of the Batgal-Channi Graphite Block, Almora. 249
Figure 7.74: Forest map of Batgal-Channi Graphite Block, Almora.....249

Figure 7.75: Field photographs of graphite schist exposure at Batgal area showing a ~12 m thick graphite schist band interbedded with mica schist. (A) General view of the graphite schist exposure with interbedded mica schist; (B–C) Close-up views showing foliation, schistosity, and graphite-rich bands within the graphite schist; (D) Hand specimen displaying soft, flaky graphite mineralization with characteristic dark grey colour and graphite soiling on hand contact.....252
Figure 7.76: VES Lines and Stations of the Batgal-Channi Graphite Block, Almora.....253
Figure 7.77: Cross Section of Line 23 on the basis of VES Survey, near Batgal area, Almora. 254
Figure 7.78: SP map of the Batgal-Channi Graphite Block, Almora.....255
Figure 7.79: SP and Elevation Profile of Line 12, near Batgal area, Almora.....256
Figure 7.80: SP and Elevation Profile of Line 21, near Batgal area, Almora.....256
Figure 7.81: SP and Elevation Profile of Line 23, north of Batgal area, Almora. 256
Figure 7.82: SP and Elevation Profile of Line 24, north of Batgal area, Almora. 256
Figure 7.83: Surface Geochemical analyses (FC, VM, and Ash content) of the Batgal-Channi Graphite Graphite Block.....258
Figure 7.84: Surface Geochemical analyses (SiO2 and S) of the Batgal-Channi Graphite Block. 259
Figure 7.85: Surface Geochemical analyses (V, Cu, Mo) of the Batgal-Channi Graphite Block. 260
Figure 8.1: 12 Borehole Locations in the Almora G4 Block.....264
Figure 8.2: River cut section showing Graphite Schist Band.....265
Figure 8.3: Banding in Graphite Schist on the surface near to BH-01.....265
Figure 8.4: Litholog of BH01, near Digoli village.....266
Figure 8.5: Photomicrograph of graphite schist sample showing carbonate altered to clay (Sample Id: 114201 at 25.2 m depth).....267
Figure 8.6: Photomicrograph of graphite schist sample showing epidote porphyroblast in graphite bearing schist (Sample Id: 114201 at 25.2 m depth) 267
Figure 8.7: Photomicrograph of graphite schist sample showing jumbo flake of graphite (Sample Id: 114201 at 25.2 m depth).....268
Figure 8.8: Photomicrograph of graphite schist sample showing pyrite in graphite bearing mica schist (Sample Id: 114201 at 25.2 m depth).....268
Figure 8.9: Photomicrograph of graphite schist sample showing foliation in graphite bearing mica schist.....268

Figure 8.10: Photomicrograph of graphite schist sample showing needle like sillimanite in graphite bearing mica schist.....268
Figure 8.11: Photomicrograph of graphite schist sample showing coarse graphite flake ...269
Figure 8.12: Photomicrograph of graphite schist sample showing graphite flake 269
Figure 8.13: Photomicrograph of graphite schist sample showing pyrite associated with graphite 269
Figure 8.14: Photomicrograph of graphite schist sample showing carbonate veins 269
Figure 8.15: Photomicrograph of graphite schist sample showing microcrystals of graphite and associated pyrite. 270
Figure 8.16: Reflected light photomicrograph (20×; scale bar 50 µm) showing disseminated to weakly aligned flaky graphite (black opaque) within a quartz–mica matrix, forming patchy to thin laminae. 270
Figure 8.17: Reflected light photomicrograph (20×; scale bar 50 µm) illustrating banded/laminated graphite with a prominent opaque graphite domain and minor fractures/cleavages in the surrounding silicate matrix, indicating structurally controlled concentration of graphite.....270
Figure 8.18: Reflected light photomicrograph (20×; scale bar 50 µm) showing disseminated to thinly laminated flaky graphite (dark grey to black) aligned along foliation within a quartz–mica matrix. Bright, highly reflective grains represent associated sulphide minerals (likely pyrite), indicating a graphite–sulphide association 271
Figure 8.19: Reflected light photomicrograph (4×; scale bar 200 µm) showing pyrite and chalcopyrite associated with quartz-sericite-graphite schist. 272
Figure 8.20: Reflected light photomicrograph (20×; scale bar 50 µm) showing covellite in chalcopyrite in quartz-sericite-graphite schist. 272
Figure 8.21: Road Cut Section showing Graphite Band near BH-02. 273
Figure 8.22: Thick Graphite Band in Road Cut section near BH-02.....273
Figure 8.23: Drilling team in BH-02.....273
Figure 8.24: Pillaring in BH-02 geavale representative team with Mr. Kandpal GSI, Dehradoon 273
Figure 8.25: Litholog of BH02, near Bataldeon village.....274
Figure 8.26: Graphite Schist layer showing intense Quartz veintaion at 21.5 m depth of borehole 02 275
Figure 8.27: Graphite Schist intruded by folded Quartz vein at 36.40 m depth of borehole 02 275

Figure 8.28: Reflected light photomicrograph (20×; scale bar 50 µm) showing chalcopyrite in graphite bearing muscovite schist. 278
Figure 8.29: Reflected light photomicrograph (10×; scale bar 100 µm) showing quartz rich muscovite schist. 278
Figure 8.30: Exposed wall section near BH-03....279
Figure 8.31: Drilling team in BH-03....279
Figure 8.32: Litholog of BH 03, at Sirar area....280
Figure 8.33: Graphite schist showing schistose layering....281
Figure 8.34: Drillcore sample showing graphite horizons traversed by sulphide bearing quartz vein....281
Figure 8.35: Reflected light photomicrograph (10×; scale bar 100 µm) showing pyrite and chalcopyrite in muscovite schist. 282
Figure 8.36: Reflected light photomicrograph (20×; scale bar 50 µm) showing Chlorite muscovite schist 282
Figure 8.37: Reflected light photomicrograph (4×; scale bar 200 µm) showing foliated granite with mica....283
Figure 8.38: Reflected light photomicrograph (4×; scale bar 200 µm) showing foliated granite with pyrite. 283
Figure 8.39: Reflected light photomicrograph (4×; scale bar 200 µm) showing foliated granite with pyrite 283
Figure 8.40: Reflected light photomicrograph (4×; scale bar 200 µm) showing granite gneiss with contact of graphite bearing mica schist. 284
Figure 8.41: Reflected light photomicrograph (4×; scale bar 200 µm) showing granite gneiss with pyrite and chalcopyrite. 284
Figure 8.42: Reflected light photomicrograph (4×; scale bar 200 µm) showing granite gneiss. 284
Figure 8.43: Reflected light photomicrograph (20×; scale bar 50 µm) showing fine grained quartzite 285
Figure 8.44: Reflected light photomicrograph (20×; scale bar 50 µm) showing Chalcopyrite in fine grained quartzite....285
Figure 8.45: Road Cut Section shows massive Graphite Schist Band 286
Figure 8.46: Drilling team at BH-04....286
Figure 8.47: Pillaring at BH-04....286
Figure 8.48: Litholog of BH 04, at Barakote area 287

Figure 8.49: Road Cut Section near BH-05 shows Graphite Flakes that easily soils on hand, at Kalimath area 289
Figure 8.50: Drilling team at BH-05 289
Figure 8.51: Pillaring at BH-05 289
Figure 8.52: Litholog of BH-05, at Mat area 291
Figure 8.53: Drill core from Borehole-5 at 53.5 m depth, showing graphite-bearing schist with visible foliation and mineralized bands 292
Figure 8.54: Graphite Schist smoothly soils on hand at 26 m depth. 292
Figure 8.55: Graphite Schist band traversed by quartz vein at 74.5 m depth 292
Figure 8.56: Core Box (CB 20) containing graphite schist from 36 m to 40 m depth 292
Figure 8.57: Reflected light photomicrograph (4×; scale bar 200 µm) showing chorite muscovite schist 293
Figure 8.58: Reflected light photomicrograph (4×; scale bar 200 µm) showing pyrite in muscovite schist. 293
Figure 8.59: River section of borehole 06, at Pithauni area 294
Figure 8.60: Road section of borehole 06, at Sironiya area 294
Figure 8.61: Drilling team at BH-06 295
Figure 8.62: Pillaring of BH-06 295
Figure 8.63: Litholog of BH-06, at Pithauni area 296
Figure 8.64: Drill core from Borehole-6 at 32.8 m depth, showing graphitic sericite schist with low sulphide mineralization. 297
Figure 8.65: Drill core from Borehole-6 at 78 m depth, showing graphite-bearing schist with irregular quartz veinlets and foliation-controlled mineralization 297
Figure 8.66: Drilling Team at BH-07 298
Figure 8.67: Litholog of BH-07, at Deora village. 299
Figure 8.68: Drilling team at BH-08 300
Figure 8.69: Pillaring at BH-08 300
Figure 8.70: Litholog of BH-08, at Udalgaon village 301
Figure 8.71: Drilling team at BH-09 302
Figure 8.72: Pillaring at BH-09 302
Figure 8.73: Litholog of Borehole 09, at Batgal village 303
Figure 8.74: Exposed section shows Graphite-Schist banding near BH-10 304
Figure 8.75: Photographs of core box 05 of borehole 10 from 17 m to 22 m 304
Figure 8.76: Drilling team at BH-10 304

Figure 8.77: Pillaring at BH-10 ..... *304*
Figure 8.78: Litholog of BH-10, at Sirar village *305*
Figure 8.79: Drill Core Samples of Graphite Band *306*
Figure 8.80: Folding of Graphite Band near BH-11 ..... *307*
Figure 8.81: Litholog of BH-11, at Digoli village. *308*
Figure 8.82: Drillcore sample of graphite schist associated with cherty layer at 43 m depth *309*
Figure 8.83: Graphite Band traversed by Isoclinal Quartz vein *309*
Figure 8.84: Graphitic Quartzite *309*
Figure 8.85: Sulphidation Channel between Graphite Band *309*
Figure 8.86: Litholog of BH-12, at Sironiya area. *310*
Figure 9.1: Graphite Schist as observed in road cutting section near Sirar Village. *314*
Figure 9.2: Graphitic Quartzite as observed in road cutting section near Digoli Village. *314*
Figure 9.3: Graphitic Sericite Schist as observed in drill core sample of BH-06 (depth 21.1 m), near Pithauni Village. *315*
Figure 9.4: Intercalated Graphite Schist contact with mica schist as observed in road cutting section near Bataldeon Village. *315*
Figure 9.5: Medium to Coarse flake sized, Dark Grey Graphite Schist as observed in BH-03 (depth 43.55 m), near Sirar Village *315*
Figure 9.6: Light to Drak Grey Graphite Schist as observed in BH-02 (depth 19.8 m), near Bataldeon Village *315*
Figure 9.7: Chart shows the exploration target formula for graphite. *317*
Figure 9.8: Location and Accessibility map for Digoli-Gajjola Block *318*
Figure 9.9: Location and Accessibility map for Sirar-Bataldeon Block *326*
Figure 9.10: Location and accessibility and Borehole point map, Kalimath Graphite Block *334*
Figure 9.11: Location and Accessibility map for Phalsima-Pithauni Block *340*
Figure 9.12: Location and Accessibility map for Batgal-Channi Block *348*
Figure 10.1: Recommended five G3 graphite blocks within the Almora G4 Block *363*
Figure 14.1: Raman spectrometry of 109938_1_powder *480*
Figure 14.2: Raman spectrometry of 109938_2_powder *480*
Figure 14.3: Raman spectrometry of 109938_3_powder *480*
Figure 14.4: Raman spectrometry of 110004_1_powder *480*
Figure 14.5: Raman spectrometry of 110004_2_powder *481*

Figure 14.6: Raman spectrometry of 110004_3_powder *480*
Figure 14.7: Raman spectrometry of 11423_1 ..... *481*
Figure 14.8: Raman spectrometry of 11423_2 ..... *481*
Figure 14.9: Raman spectrometry of 11423_3 ..... *481*
Figure 14.10: Raman spectrometry of 11423_4 ..... *481*
Figure 14.11: Raman spectrometry of 14228_1 ..... *481*
Figure 14.12: Raman spectrometry of 14228_2 ..... *481*
Figure 14.13: Raman spectrometry of 14228_3 ..... *482*
Figure 14.14: Raman spectrometry of 14228_4 ..... *482*
Figure 14.15: Raman spectrometry of 14241_1 ..... *482*
Figure 14.16: Raman spectrometry of 14241_2 ..... *482*
Figure 14.17: Raman spectrometry of 14241_3 ..... *482*
Figure 14.18: Raman spectrometry of 14241_4 ..... *482*
Figure 14.19: Raman spectrometry of 114227_1 ..... *482*
Figure 14.20: Raman spectrometry of 114227_2 ..... *482*
Figure 14.21: Raman spectrometry of 114227_3 ..... *482*
Figure 14.22: Raman spectrometry of 114227_4 ..... *483*
Figure 14.23: Raman spectrometry of 114229_1 ..... *483*
Figure 14.24: Raman spectrometry of 114229_2 ..... *483*
Figure 14.25: Raman spectrometry of 114229_3 ..... *483*
Figure 14.26: Raman spectrometry of 114229_4 ..... *483*
Figure 14.27: Raman spectrometry of 114232_1 ..... *483*
Figure 14.28: Raman spectrometry of 114232_2 ..... *483*
Figure 14.29: Raman spectrometry of 114232_3_pyrite *483*
Figure 14.30: Raman spectrometry of 114232_4 ..... *483*
Figure 14.31: Raman spectrometry of 114234_1_carbon *484*
Figure 14.32: Raman spectrometry of 114234_2 ..... *484*
Figure 14.33: Raman spectrometry of 114234_3 ..... *484*
Figure 14.34: Raman spectrometry of 114237_1 ..... *484*
Figure 14.35: Raman spectrometry of 114237_2 ..... *484*
Figure 14.36: Raman spectrometry of 114237_3 ..... *484*
Figure 14.37: Concrete pillaring at Borehole-01 ..... *692*
Figure 14.38: Concrete pillaring at Borehole-02 ..... *692*
Figure 14.39: Concrete pillaring of Borehole-03 ..... *692*

Figure 14.40: Concrete pillaring at Borehole-04.....693
Figure 14.41: Concrete pillaring at Borehole-05.....693
Figure 14.42: Concrete pillaring at Borehole-06.....693
Figure 14.43: Concrete pillaring of Borehole-07.....693
Figure 14.44: Concrete pillaring at Borehole-08.....693
Figure 14.45: Concrete pillaring of Borehole-09.....693
Figure 14.46: Concrete pillaring of Borehole-10.....693
Figure 14.47: Concrete pillaring at Borehole-11.....693
Figure 14.48: Concrete pillaring at Borehole-12.....693

List of Tables:

Table 1.1: अल्मोडा ग्रेफाइट और वैनेडियम कार्यक्रम: ब्लॉक द्वारा अन्वेषण लक्ष्य सारांश। सी = रूढ़िवादी परिदृश्य (सिद्ध डेटा से सीमित एक्सट्रपलेशन)। यह तालिका एक अन्वेषण लक्ष्य का गठन करती है, न कि खनिज संसाधन का।---------- 8

Table 1.2: Almora graphite and vanadium programme: exploration target summary by block. C = Conservative scenario).This table constitutes an Minaral Exploration Target, not a Mineral Resource. ----------16

Table 2.1:Administrative Details of the Almora exploration block----------22

Table 2.2: Details of the investigating agency of the Almora exploration program.----------24

Table 2.3: Details of the approved vs. achieved quantum of targets of the Almora exploration program. ----------25

Table 2.4: List of personnel involved in the Almora exploration program. ----------29

Table 4.1: Stratigraphy of the Himalaya (after Valdiya, 1980)----------64

Table 4.2: Principal legacy work relevant Almora G4 exploration programme by Geovale Services Pvt. Ltd.----------69

Table 4.3: Comparative summary of selected NGCM indicators for the Almora (Matena-Sirar area) and surrounding 53O/10 catchments. (NGDR Portal).----------74

Table 5.1: Anomalous Element Concentration in Orientation Samples ----------79

Table 6.1: Graphite Flake size distriburion of Kalimath-Mat area (Sample Id 109245)---- 124

Table 6.2: Graphite Flake size distriburion of Bintola-Digoli area (Sample Id 109200) --- 125

Table 6.3: Structural Interpretation of stretching and intersection lineation present in granite intrusive. ---------- 142

Table 6.4: Summary table shows various rock and their metamorphic characteristic and estimated temperature of metamorphism.---------- 150

Table 6.5: Details of Raman sample location ---------- 171

Table 7.1: Summary of site characteristics of the Digoli-Gajjola Graphite block ---------- 186

Table 7.2: Geophysical characterics of the Digoli-Gajjola Graphite Block. ---------- 189

Table 7.3: Summary of areal extension and geophysical response for Sirar-Bataldeon Graphite Block---------- 203

Table 7.4: Details of the Kalimath Graphite block---------- 213

Table 7.5: Details of the extension of Kalimath Graphite Block.---------- 215

Table 7.6: Details of the Phalsima -Pithauni Graphite Block ---------- 229

Table 7.7: Details of areal extension of the Phalsima -Pithauni Graphite Block ---------- 230

Table 7.8: Details of Raman spectrum of graphite sample (id: 109938) in Phalsima area. 244

Table 7.9: Summary of site characteristics of the Batgal-Channi Graphite Block. ---------- 250

Table 7.10: Details of the extension of Batgal-Channi Graphite Block ---------- 251

Table 7.11: Integrated interpretation of SP and VES geophysical characterisation of the Batgal-Channi Graphite Block, Almora ---------- 257

Table 8.1: Detailed informations of 12 boreholes in the Almora G4 block ---------- 264

Table 8.2: Analytical results of Fixed Carbon (FC %) and associated base metal concentrations (Cu, Zn, Ni and Co in ppm) for selected drill core samples across specified depth intervals ---------- 276

Table 8.3: Analytical results of Vanadium (V), Chromium (Cr), Molybdenum (Mo) and Uranium (U) concentrations (in ppm) for selected drill core samples across different depth intervals, highlighting variation across the mineralized and transitional zones. ---------- 276

Table 8.4: Analytical results of trace elements including Cd, Se, Sn, Sb, Cs, W and Bi (in ppm) for selected samples as bedrock samples. ---------- 285

Table 8.5: Selected trace element assay results (V, Se, Mo, Cd, Sb, Ba, Bi, W and U; ppm) for representative samples. ---------- 288

Table 8.6: Selected trace element assay results (Zn, Se, Mo, Cd, Sb, Ba and U; ppm) for representative samples ---------- 294

Table 8.7: Assay results of selected trace elements (V, Se, Mo, Cd, Sb, Ba, Bi and U; ppm) for representative bedrock samples. ---------- 300

Table 8.8: Details of true thicknness for all boreholes. ---------- 311

Table 9.1: Band geometry and prospectivity summary, Digoli-Gajjola Block. ---------- 318

Table 9.2: Scout borehole summary, Digoli-Gajjola Block. ---------- 319

*Table 9.3: True thickness derivation, Digoli-Gajjola Block. *Dip from horizontal. --------- 320*

Table 9.4: BH-01 fixed-carbon and vanadium profile by depth. ---------- 321

Table 9.5: BH-04 grade data, Barakote sector. ---------- 321

Table 9.6: Band-by-band exploration target calculations. ---------- 322

Table 9.7: Block-level exploration target summary, Digoli-Gajjola Block. Rock Mass in Mt. ---------- 323

Table 9.8: Borehole-wise vanadium summary, Digoli-Gajjola Block. BH-04 (highest mean V). Clarke = 114 ppm; 5×Clarke = 570 ppm. ---------- 323

Table 9.9: Indicative vanadium exploration target, Digoli-Gajjola Block. V mean = 406.6 ppm (weighted across 52 BH intervals). Conversion: $V \times 1.785 = V_2O_5$. ---------- 324

Table 9.10: Confidence assessment for Digoli-Gajjola Graphite Block. ---------- 324

Table 9.11: Band geometry and prospectivity summary, Sirar-Bataldeon Block. ---------- *327*

Table 9.12: Scout borehole summary, Sirar-Bataldeon Block. ---------- *327*

Table 9.13: True thickness derivation, Sirar-Bataldeon Block. ---------- *328*

Table 9.14: BH-03 fixed-carbon profile by depth, Sirar Band ---------- *329*

Table 9.15: Grade data summary, Sirar-Bataldeon Block. ---------- *329*

Table 9.16: Band-by-band exploration targets of Sirar-Bataldeon Block. ---------- *331*

Table 9.17: Block-level exploration target summary. ---------- *331*

Table 9.18: Indicative vanadium potential, Sirar-Bataldeon Block.. Conversion: V × 1.785 = V_2O_5. ---------- *332*

Table 9.19: Confidence assessment of Sirar-Bataldeon Graphite Block ---------- *332*

Table 9.20: Table summarizes band geometry of each segment of Kalimath graphite band. ---------- *334*

Table 9.21: Graphite Zone of BH05 ---------- *335*

Table 9.22: It presents all FC and V data for eastern and western part of the Kalimath Graphite Block. ---------- *336*

Table 9.23: Exploration target calculation, Kalimath Eastern Part. t = 48 m true thickness; ρ = 2.70 t/m³, graphite bearing zones 75 m. ---------- *337*

Table 9.24: Exploration target calculation, Kalimath Western Part. ---------- *337*

Table 9.25: Kalimath Graphite Block: Block-level exploration target summary. ---------- *338*

Table 9.26: Indicative vanadium exploration target, Kalimath Graphite Block. Conversion: V × 1.785 = V_2O_5. ---------- *338*

Table 9.27: Confidence assessment of Kalimath Graphite Block. ---------- *339*

Table 9.28: Details of Band geometry of the Phalsima-Pithauni Block. ---------- *341*

Table 9.29: Scout borehole summary of Phalsima-Pithauni Block. Both boreholes confirm graphite is open to depth. ---------- *341*

Table 9.30: BH-06 lithological interval breakdown. For detail see Annexure XXIX. ---------- *342*

Table 9.31: BH-12 lithological interval breakdown. For detail see Annexure XXIX ---------- *343*

*Table 9.32: True thickness derivation from BH-06 and BH-12. *Dip convention: measured from horizontal depth.* ---------- *343*

Table 9.33: Surface and subsurface grade data for Phalsima-Pithauni Graphite Block. ---------- *344*

Table 9.34: Exploration target, Pithauni Band. ---------- *345*

Table 9.35: Exploration target estimates, Phalsima North, Central bands, South Band, D-C: depth (m) for Conservative. ---------- *345*

Table 9.36: Block-level exploration target summary, Phalsima-Pithauni Graphite Block. Rock mass in Mt. ---------- *345*

Table 9.37: Indicative vanadium potential, Phalsima-Pithauni block. V concentration: combined BH-06 + BH-12 mean = 223.08 ppm. Conversion factor: 1 tonne V = 1.785 tonnes V_2O_5. ---------- *346*

Table 9.38: Confidence assessment of Phalsima-Pithauni Graphite Block. ---------- *346*

Table 9.39: Band geometry summary, Batgal-Channi Graphite Block. ---------- *348*

Table 9.40: BH-09 litholog summary, Batgal-Channi Block ---------- *349*

Table 9.41: True thickness derivation, BH-09, Batgal-Channi Block. ---------- *350*

Table 9.42: Grade data, Batgal-Channi Block. Clarke value for V = 114 ppm; 5× threshold = 570 ppm. ---------- *351*

Table 9.43: Band 3 exploration target, Batgal-Channi Block. t = 4.82 m true thickness; ρ = 2.70 t/m³. ---------- *352*

Table 9.44: Band 2 and Bands 3-12 exploration target components, Batgal-Channi Block. Bands 1, 2, 4-12 are surface mapping only; thickness (2.5 m) is estimated, not measured. *352*

Table 9.45: Batgal-Channi Block: block-level exploration target summary ---------- *352*

Table 9.46: Indicative vanadium potential, Batgal-Channi Block. V conversion: 1 t V = 1.785 t V_2O_5. Mean V = 787.19 ppm. ---------- *352*

Table 9.47: Confidence assessment of Batgal-Channi Block. ---------- *353*

Table 10.1: Summary of graphite target potential, vanadium association and exploration priority across the identified blocks. ---------- *359*

Table 10.2: Ranking of identified graphite-bearing blocks for G3 exploration based on spatial extent and maximum fixed carbon (FC) values recorded from surface sampling and borehole intersections ---------- *362*

List of Annexures:

Annexure I_Geochemical Data (ICPMS analysis) of Orientation Survey in Almora G4 Block ---------- 373

Annexure II_ Field Observation Points in Almora G4 Block---------- 374

Annexure III_Details of Structural Data in Almora G4 Block ---------- 405

Annexure IV_Details of Graphite Crystallinity for Bedrock---------- 435

Annexure V_Details of Bedrock Petrography ---------- 447

Annexure VI_Pitting and Trenching Details---------- 450

Annexure VII_XRF Data for Surface Samples with 2 Additional Elements Sn, W: (All data in %) ---------- 453

Annexure VIII_XRF Data of Surface Check Samples (All data in %)---------- 462

Annexure IX_XRF Data for 2 Additional Elements- Sn and W of Surafce Check Samples- 463

Annexure X_Proximate Analysis of Graphite for Surface Samples (All Values in %) ------ 464

Annexure XI_ICPMS Data of Surface Samples (All data in ppm) ---------- 466

Annexure XII_ICPMS Data of Surface Check Samples (All data in ppm)---------- 475

Annexure XIII_Total Sulphur Data of Surface Samples (All data in %) ---------- 477

Annexure XIV_Details of Heavy Minerals Seperation ---------- 478

Annexure XV_Raman Spectroscopic Data of Bedrock and Borehole Samples---------- 480

Annexure XVI_XRD Data of Surface and Borehole Samples ---------- 485

Annexure XVII_Self Potential (SP) Raw Data---------- 486

Annexure XVIII_Self Potential (SP) Plots ---------- 522

Annexure XIX_Resistivity (VES) Raw Data---------- 535

Annexure XX_Resistivity (2D) Models ---------- 622

Annexure XXI_Details of Petrographical Description of Borehole Samples---------- 641

Annexure XXII_XRF Data of Borehole Samples with Additional 2 Elements Sn, W (All data in %) ---------- 643

Annexure XXIII_XRF Data of Borehole Check Samples (All data in %) ---------- 645

Annexure XXIV_XRF Data of Borehole Check Samples with 2 Additional Elements (Sn, W) ---------- 645

Annexure XXV_ICPMS Data of Borehole Samples (All data in ppm)---------- 646

Annexure XXVI_ICPMS Data of Borehole Check Samples (All data in ppm) ---------- 671

Annexure XXVII_Proximate Analysis of Graphite for Borehole Samples (All data in %)-- 675

Annexure XXVIII_Details of Borehole Litholog ---------- 677

Annexure XXIX_Details of Drill Core Preservation---------- 689

Annexure XXX_Construction of Concrete Pillar (12"x12"x30") ---------- 692

List of Plates:

Plate-I Large Scale Geological Map (1:12,500) of the Almora G4 Block

Plate-II Recommended Graphite Blocks within the Almora G4 Block

Chapter 1

सारांश

Executive Summary

1 सारांश:

उत्तराखंड के अल्मोडा जिले के मटेना-सिरार क्षेत्र में ग्रेफाइट और वैनेडियम के लिए टोही सर्वेक्षण, G4 स्टेज, जियोवेल सर्विसेज प्राइवेट लिमिटेड द्वारा किया गया था। लिमिटेड, राष्ट्रीय खनिज अन्वेषण और विकास ट्रस्ट, खान मंत्रालय द्वारा वित्त पोषित एक एनपीईए परियोजना के रूप में। यह परियोजना 60 वर्ग किमी को कवर करती है। सर्वे ऑफ इंडिया टोपोशीट 53O/10 में, मटेना, फलसीमा, सिरार, देवरा, बल्टा, कालीमठ और आसपास के गांवों के आसपास। मुख्य उद्देश्य आंतरिक लघु हिमालय के अल्मोडा क्रिस्टलीय में ग्रेफाइटिक क्षितिज की उपस्थिति, सीमा, मोटाई, गुणवत्ता और निरंतरता का मूल्यांकन करना और ग्रेफाइट शिस्ट क्षितिज के भीतर वैनेडियम और अन्य महत्वपूर्ण/पाथफाइंडर तत्वों के लिए संबंधित क्षमता का आकलन करना था।

जाँच इसलिए शुरू की गई क्योंकि अल्मोडा क्षेत्र में ग्रेफाइट की घटनाएँ पहले से ज्ञात थीं, लेकिन पुरानी जानकारी खंडित थी और आधुनिक लक्ष्य मूल्यांकन के लिए अपर्याप्त थी। जीएसआई और पहले के जांचकर्ताओं के विरासती कार्यों ने कालीमठ, सिरार, बटाल्डेऑन, बटगल और आसपास के क्षेत्रों के पास ग्रेफाइट शिस्ट की उपस्थिति स्थापित की थी। पिछले डेटा ने परिवर्तनशील ग्रेफाइट गुणवत्ता का भी संकेत दिया था: थोक ग्रेफाइट शिस्ट में आम तौर पर निम्न से मध्यम स्थिर कार्बन दिखाया गया था, जबकि स्थानीय रूप से कार्बोनेसियस नोड्यूल्स बहुत अधिक कार्बन मान उत्पन्न करते थे। हाल ही में जीएसआई और प्रकाशित कार्य ने अन्वेषण अवधारणा को केवल ग्रेफाइट मॉडल से व्यापक ग्रेफाइट-वैनेडियम-पॉलीमेटेलिक कार्बोनेसियस मेटासेडिमेंटरी सिस्टम में स्थानांतरित कर दिया, जिसमें वैनेडियम, बेरियम, मोलिब्डेनम, टंगस्टन, यूरेनियम और रूपांतरित ब्लैक शेल/ग्रेफाइट शिस्ट क्षितिज के साथ अन्य तत्वों के संभावित सहयोग पर प्रकाश डाला गया।

अल्मोडा ब्लॉक एक ऊबड़-खाबड़ हिमालयी इलाके में स्थित है जो क्षेत्रीय रूप से सुलभ है लेकिन अन्वेषण के लिए स्थानीय रूप से चुनौतीपूर्ण स्थानों पर है। क्षेत्रीय पहुंच अल्मोडा शहर, NH-309A, NH-309B और जुड़ी हुई ग्रामीण सड़कों के माध्यम से उपलब्ध है; हालाँकि, कुछ क्षेत्र खड़ी ढलानों, विच्छेदित जल निकासी, वन क्षेत्रों, निवास स्थान, खेती योग्य छतों और अंतिम मील तक पहुंच बाधाओं द्वारा नियंत्रित होता है। अल्मोडा ब्लॉक के कुछ क्षेत्रों में पर्यावरण और सामाजिक रूप से संवेदनशील तत्व भी शामिल हैं, जिनमें आरक्षित/नागरिक वन क्षेत्र, घने जल निकासी नेटवर्क, झरने, ग्राम भूमि उपयोग और लखुडियार पुरातात्विक स्थल शामिल हैं। ये कारक न केवल भविष्य के फील्ड लॉजिस्टिक्स के लिए बल्कि खनन योग्यता स्क्रीनिंग के लिए भी महत्वपूर्ण हैं, क्योंकि अकेले ग्रेफाइट की उपस्थिति सभी क्षेत्रों को भविष्य की खोज या विकास के लिए समान रूप से उपयुक्त नहीं बनाती है।

इस अल्मोडा G4 ब्लॉक के प्रमुख लिथोलॉजिकल एसोसिएशन में मीका शिस्ट, क्वार्टजाइट, ग्रेफाइट शिस्ट, टफेसियस रॉक्स, ग्रेनाइट गनीस और युवा घुसपैठ वाले फोलेटेड ग्रेनाइट शामिल हैं। अभ्रक शिस्ट प्रमुख लिथोलॉजी बनाता है, जबकि ग्रेफाइट शिस्ट मेटासेडिमेंटरी इकाइयों के भीतर अलग लेकिन संरचनात्मक रूप से दोहराए गए बैंड के रूप में होता है। युवा ग्रेनाइटिक घुसपैठ आमतौर पर जली हुई होती है और स्थानीय रूप से फोलिएशन/थ्रस्ट विमानों के साथ स्थापित होती है, जो महत्वपूर्ण है क्योंकि थर्मल और विरूपण-सहायता वाले पुनर्क्रिस्टलीकरण ने अनुकूल क्षेत्रों में ग्रेफाइट ऑर्डर को बढ़ाया हो सकता है।

अन्वेषण कार्यक्रम ने स्थापित किया कि ग्रेफाइट खनिजकरण प्रमुख रूप से स्तरित, फैब्रिक-नियंत्रित और संरचनात्मक रूप से संशोधित है। ग्रेफाइट जंबो में मध्यम और महीन परतदार अनाज के रूप में होता है जो पत्ते के समानांतर संरेखित होता है और क्वार्ट्ज-मस्कोवाइट-समृद्ध शिस्ट के भीतर ग्रेफाइट-समृद्ध लैमिना में केंद्रित होता है। पेट्रोग्राफिक अवलोकन मुड़े हुए ग्रेफाइट के गुच्छे, कतरनी लेंस में ग्रेफाइट, अभ्रक मछली से जुड़े ग्रेफाइट और विरूपण कपड़ों के साथ पुनर्वितरित क्वार्ट्ज और ग्रेफाइट का संकेत देते हैं। यह पुष्टि करता है कि ग्रेफाइट को कार्बोनेसियस तलछटी प्रोटोलिथ से विरासत में मिला था और बाद में क्षेत्रीय रूपांतर, कतरनी, तह, जोर पुनरावृत्ति और स्थानीय ग्रेनाइट-संबंधित थर्मल प्रभावों द्वारा संशोधित किया गया था।

G4 का कार्य बहु-विषयक था और संरचनात्मक रूप से जटिल ग्रेफाइट इलाके के लिए उचित रूप से डिज़ाइन किया गया था। इसमें 60 वर्ग कि.मी. शामिल था। मल्टीस्पेक्ट्रल और डीईएम व्याख्या, बड़े पैमाने पर भूवैज्ञानिक मानचित्रण (1:12,500), व्यवस्थित सतह नमूनाकरण, पिटिंग और ट्रेंचिंग, पेट्रोग्राफी, और मॉडल विश्लेषण रमन और एक्सआरडी, और अन्य खनिज कार्य, एक्सआरएफ, आईसीपीएमएस, अनुमानित विश्लेषण, कुल सल्फर विश्लेषण, एसपी और वीईएस भूभौतिकी और स्काउट ड्रिलिंग। प्राप्त फ़ील्ड मात्रा में 450.68 घन मीटर शामिल है। एम। पिटिंग और ट्रेंचिंग, एसपी की 32.6 लाइन-किमी, वीईएस की 31.4 लाइन-किमी और कोर ड्रिलिंग की 801.2 मीटर, सतह और बोरहोल भू-रासायनिक विश्लेषण द्वारा समर्थित। अन्वेषण वर्कफ़्लो तार्किक रूप से विरासत की समीक्षा और रिमोट सेंसिंग से मैपिंग, नमूनाकरण, भूभौतिकीय परीक्षण, उत्खनन और स्काउट ड्रिलिंग तक चला गया।

रिमोट सेंसिंग और डीईएम व्याख्या ने लाइनियेमेंट, ढलान वर्ग, जल निकासी, पहुंच गलियारे, वन आवरण, भूमि उपयोग और इलाके की बाधाओं की पहचान करने में मदद की। भूवैज्ञानिक मानचित्रण ने ग्रेफाइट बैंड का पता लगाने, मेजबान लिथोलॉजी की पहचान करने, संरचनात्मक दृष्टिकोण रिकॉर्ड करने और लक्ष्य गलियारों को परिभाषित करके सबसे महत्वपूर्ण प्राथमिक ढांचा प्रदान किया। मिट्टी से ढके या खराब मौसम वाले क्षेत्रों में गड्ढा खोदने और खाई खोदने से एक्सपोज़र में सुधार हुआ। एसपी और वीईएस

प्रवाहकीय ग्रेफाइटिक क्षितिज का पता लगाने में उपयोगी थे, खासकर जहां सतह का जोखिम खराब था। हालाँकि, रिपोर्ट इस बात पर जोर देती है कि भूभौतिकीय चालकता आर्थिक ग्रेफाइट ग्रेड के लिए प्रत्यक्ष प्रॉक्सी नहीं है, क्योंकि ग्रेफाइट निरंतरता, सल्फाइड, मिट्टी, नमी और संरचनात्मक विघटन सभी चालकता को प्रभावित कर सकते हैं। इसलिए सबसे अधिक आत्मविश्वास वाले लक्ष्य वे हैं जहां मैपिंग, जियोकेमिस्ट्री, एसपी/वीईएस प्रतिक्रिया और ड्रिलिंग परिणाम मेल खाते हैं।

ग्रेफाइट खनिजीकरण मुख्यतः अभ्रक-युक्त ग्रेफाइट शिस्ट, ग्रेफाइटिक क्वार्टजाइट तथा ग्रेफाइट सेरीसाइट शिस्ट में सेमीमीटर से मीटर स्तर तक की पतली अंतःस्तरित पट्टियों के रूप में विकसित है, जो इसके प्रमुख होस्ट रॉक हैं। ग्रेफाइट मुख्य रूप से फोलिएशन तल के साथ संकेंद्रित है, किंतु यह मध्यम से मोटे दानेदार फ्लेक्स, शिराओं तथा सूक्ष्म शिरिकाओं के रूप में भी फैला हुआ पाया जाता है, जिससे कई स्थानों पर पूरा होस्ट रॉक गहरे धूसर से काले रंग का ग्रेफाइट-समृद्ध पिंड जैसा प्रतीत होता है। इस खनिजीकरण की उत्पत्ति कार्बनयुक्त अवसादी पदार्थों से मानी जाती है, जो विरूपण एवं क्षेत्रीय कायांतरण से प्रभावित हुए तथा बाद में युवा ग्रेनाइट के lit-par-lit अंत:क्षेपण से संबंधित संपर्क कायांतरण के कारण ग्रेफाइट की क्रिस्टलीयता में वृद्धि हुई।

इस कार्यक्रम का एक प्रमुख परिणाम 60 वर्ग किमी में वितरित 30 ग्रेफाइट बैंड की पहचान है। G4 अन्वेषण क्षेत्र. ग्रेफाइट प्रणाली को पांच प्रमुख ग्रेफाइट-असर डोमेन में वर्गीकृत किया गया है: कालीमथ, सिरार-बटाल्डेओन, डिगोली-गज्जोला, फाल्सिमा-पिथौनी और बटगल-चन्नी। ये भूवैज्ञानिक निरंतरता, ग्रेड, उपसतह पुष्टि, पहुंच, ईएसजी संवेदनशीलता या भविष्य की अन्वेषण प्राथमिकता में समकक्ष नहीं हैं। कुल मिलाकर, पांच डोमेन लगभग 36.46 किमी संचयी मैप करने योग्य ग्रेफाइट-बैंड स्ट्राइक लंबाई और 5.14 वर्ग किमी के क्रम पर एक मैप किए गए ग्रेफाइट पदचिह्न के लिए जिम्मेदार हैं, हालांकि ये आंकड़े एकल निरंतर अयस्क के बजाय संरचनात्मक रूप से दोहराए गए और खंडित बैंड निशान का प्रतिनिधित्व करते हैं। जी4 चरण में, ये डेटा एक अन्वेषण लक्ष्य को परिभाषित करते हैं, न कि किसी खनिज संसाधन या रिजर्व को।

कालीमठ ग्रेफाइट ब्लॉक महत्वपूर्ण ग्रेफाइट-वैनेडियम लक्ष्यों में से एक है। यह लगभग 4.93 वर्ग किमी में फैला है। और इसमें पूर्वी और पश्चिमी ग्रेफाइट-बैंड खंड शामिल हैं। पूर्वी खंड में लगभग 2.32 किमी मैप करने योग्य स्ट्राइक लंबाई और गहराई पर 35-55 मीटर मोटे प्रवाहकीय क्षेत्रों के भूभौतिकीय संकेत हैं, जबकि पश्चिमी खंड में लगभग 3.53 किमी स्ट्राइक लंबाई है। BH05 ने मुख्य रूप से 22.9-45.67 मीटर और 46.62-75 मीटर के दो ग्रेफाइट-असर अंतरालों को प्रतिच्छेद किया, जो लगभग 48.65 मीटर वास्तविक मोटाई का प्रतिनिधित्व करता है। कालीमठ ने मजबूत वैनेडियम संवर्धन भी दर्ज किया

है, जिसमें BH05 नमूने ने अल्मोडा जी4 ब्लॉक में एफसी को 5.74% वैनेडियम मान 3,739 ppm तक रिपोर्ट किया है।

सिरार-बटाल्डेऑन ग्रेफाइट ब्लॉक एक अन्य उच्च प्राथमिकता वाला डोमेन है। इसमें कई मैप करने योग्य ग्रेफाइट बैंड शामिल हैं, जिनमें से बैटलडियन ईस्ट बैंड 2 सबसे पार्श्व व्यापक में से एक है, जिसकी स्ट्राइक लंबाई लगभग 3.40 किमी, औसत चौड़ाई लगभग 0.132 किमी और लगभग 0.449 वर्ग किमी है। मानचित्रित क्षेत्र. सिरार के पास BH03 लगभग 12.5 मीटर से 75 मीटर तक ग्रेफाइट को काटता है, जिसमें 31.45-42 मीटर के आसपास अच्छी गुणवत्ता वाला ग्रेफाइट भी शामिल है। बीएच03 ने अल्मोडा जी4 ब्लॉक में उच्चतम एफसी मूल्य 8.4% और वैनेडियम 2758 ppm तक दर्ज किया है। इस ब्लॉक में मजबूत वॉल्यूमेट्रिक क्षमता है, लेकिन जल निकासी, वन, स्थानीय आवरण और सल्फाइड/गुणवत्ता के मुद्दों पर सावधानीपूर्वक मूल्यांकन की आवश्यकता है।

डिगोली-गज्जोला ग्रेफाइट ब्लॉक एक महत्वपूर्ण अनुवर्ती लक्ष्य है क्योंकि इसमें कई थ्रस्ट-बाउंड ग्रेफाइट बैंड शामिल हैं और BH01, BH04, BH07 और BH11 में उपसतह पुष्टि है। BH01 लगभग 16 मीटर से 91.7 मीटर तक ग्रेफाइट खनिजकरण को रिकॉर्ड करता है, जिसमें 5.28-7.56% स्थिर कार्बन ले जाने वाला 35-37 मीटर से 2 मीटर का अंतराल भी शामिल है। ब्लॉक में एक मजबूत वैनेडियम (बीएच01 पर 1594 ppm तक) -पॉलीमेटेलिक हस्ताक्षर भी है, जिसमें सिस्टम के कुछ हिस्सों में वैनेडियम संवर्धन और संबंधित मोलिब्डेनम, बेरियम, तांबा, जस्ता, यूरेनियम और चांदी शामिल है।

फाल्सिमा-पिथौनी ग्रेफाइट ब्लॉक अपनी उथली-डुबकी ज्यामिति और अपेक्षाकृत अनुकूल पहुंच के कारण महत्वपूर्ण है। चार मैप किए गए ग्रेफाइट बैंड की संयुक्त स्ट्राइक लंबाई लगभग 6.96 किमी और मैप किया गया क्षेत्र लगभग 0.872 वर्ग किमी है, जिसमें उत्तर-पूर्व की ओर लगभग 3°-15° का हल्का उतार-चढ़ाव होता है। वीईएस डेटा लगभग 20-60 मीटर मोटाई के प्रवाहकीय क्षेत्रों की पहचान करता है और पिथौनी उपसतह मूल्यांकन 26 मीटर मोटे ग्रेफाइट क्षेत्र को रिकॉर्ड करता है, जिसके बाद लगभग 10 मीटर ओवरबर्डन के नीचे लगभग 40 मीटर इंटरकलेटेड ग्रेफाइट-अभ्रक शिस्ट होता है। हालाँकि, उपलब्ध सतह स्थिर-कार्बन मान आम तौर पर 2.14-5.67% के आसपास होते हैं और ग्रेफाइट शिस्ट स्थानीय रूप से उच्च राख के साथ अत्यधिक सिलिसियस होता है। इसलिए इस ब्लॉक में अच्छी ज्यामितीय और उथली-गहराई क्षमता है। BH06 और BH12 उस ब्लॉक में आयोजित किए जाते हैं जहां एफसी उपज 6.92% तक और वैनेडियम 1380 ppm तक होती है।

बटगल-चन्नी ग्रेफाइट ब्लॉक संरचनात्मक रूप से दिलचस्प है लेकिन वॉल्यूमेट्रिक क्षमता के लिए इसे निचले स्थान पर रखा गया है। इसमें लगभग 12 संकीर्ण और असंतुलित ग्रेफाइट बैंड हैं, जिनकी संचयी स्ट्राइक लंबाई लगभग 3.53 किमी और लगभग 0.242 वर्ग किमी है। मानचित्रित क्षेत्र. बैंड खड़ी हैं,

आमतौर पर 50°-70° और BH09 दो अंतरालों में केवल 6.07 मीटर कुल वास्तविक ग्रेफाइट मोटाई की पुष्टि करता है। यद्यपि सतह पर स्थिर कार्बन स्थानीय रूप से लगभग 7.05% तक पहुँच जाता है और वैनेडियम मान स्थानीय रूप से लगभग 3,536 ppm तक असमान होते हैं, लेकिन अधिक धीरे-धीरे डुबाने वाले ब्लॉकों की तुलना में तेज गिरावट, संकीर्ण लेंस और संरचनात्मक विखंडन उच्च स्ट्रिप अनुपात और कम थोक-निरंतरता क्षमता का संकेत देते हैं। BH09 उस ब्लॉक में मौजूद है जहां FC 2.99% तक और वैनेडियम 1502 ppm तक पहुंचता है।

ग्रेड और उत्पाद की गुणवत्ता के संदर्भ में, अल्मोडा ग्रेफाइट प्रणाली को बड़ी मात्रा में, संरचनात्मक रूप से दोहराया गया, मध्यम से उच्च ग्रेड फ्लेक-ग्रेफाइट शिस्ट प्रणाली के रूप में वर्णित किया गया है। सतह के नमूनों में स्थिर-कार्बन 7.05% एफसी तक पहुंच गया, जबकि उपसतह मान 8.40% एफसी तक पहुंच गया। परत के आकार का डेटा कालीमठ, पिथौनी और सिरार क्षेत्रों में ग्रेफाइट के मोटे और महीन अंश के साथ-साथ जंबो अंश की उपस्थिति को दर्शाता है।

वैनेडियम एसोसिएशन G4 कार्यक्रम का एक प्रमुख सकारात्मक परिणाम है। वैनेडियम कई ग्रेफाइटिक क्षितिजों में विसंगतिपूर्ण है, विशेष रूप से कालीमथ, सिरार-बटाल्डियन, डिगोली-गज्जोला और बटगल-चन्नी में। रिपोर्ट किए गए मूल्यों में कालीमठ में बीएच05 में 3,739 ppm वी तक, सिरार-बटाल्डेऑन में 2,414 ppm तक सतह वैनेडियम, 710-1,022 ppm के आसपास BH02 मान, डिगोली-गज्जोला एक्सआरएफ-व्युत्पन्न डेटासेट में 2,296 ppm तक और चयनित बटगल-चन्नी बैंड में 3,536 ppm तक शामिल हैं। यह इस व्याख्या का समर्थन करता है कि ग्रेफाइट शिस्ट कम कार्बनयुक्त मेटासेडिमेंटरी क्षितिज का प्रतिनिधित्व करते हैं जो रेडॉक्स-संवेदनशील तत्वों को केंद्रित करने में सक्षम हैं।

इस G4 कार्यक्रम ने पिछले प्रदर्शनों से अल्मोडा ग्रेफाइट घटनाओं को एक सुसंगत ब्लॉक-वार ग्रेफाइट-वैनेडियम अन्वेषण मॉडल में सफलतापूर्वक उन्नत किया है। सबसे अच्छा ग्रेफाइट विकास वहां होता है जहां अनुकूल कार्बोनेसियस प्रोटोलिथ को संरचनात्मक रूप से गाढ़ा किया जाता है, थ्रस्ट-संबंधित गलियारों, फोल्ड क्लोजर और कम से मध्यम-डिप पैनलों के साथ दोहराया या संरक्षित किया जाता है। पहचाने गए सबसे संभावित क्षेत्रों में सिरार-बटाल्डेऑन, डिगोली-गज्जोला, कालीमठ पूर्व, फाल्सिमा-पिथौनी और बटगल-चन्नी ग्रेफाइट ब्लॉक हैं।

यूएनएफसी ढांचे के तहत, जी4-चरण (टोही) जांच औपचारिक खनिज संसाधन अनुमान उत्पन्न नहीं करती है। हालाँकि, अल्मोडा ग्रेफाइट इन्वेस्टिगेशन जैसा G4 कार्यक्रम अन्वेषण लक्ष्यों का एक सेट तैयार कर सकता है: "संभावित" टन भार और खनिजकरण के ग्रेड का मात्रात्मक, "भौगोलिक रूप से बाधित अनुमान"। एक मानक अभ्यास के रूप में इन्हें श्रेणियों के रूप में प्रस्तुत किया जाता है और बताई गई

भूवैज्ञानिक धारणाओं के अधीन किया जाता है। अध्याय 9 में अल्मोडा ग्रेफाइट और वैनेडियम कार्यक्रम के लिए विकसित अन्वेषण लक्ष्यों का सारांश नीचे दिया गया है।

60 वर्ग किमी के जी4 अन्वेषण क्षेत्र के भीतर, 30 ग्रेफाइट-असर बैंड को चित्रित किया गया है और इन्हें पांच संरचनात्मक रूप से नियंत्रित अन्वेषण ब्लॉकों में वितरित किया गया है, जिनकी पुष्टि संचयी स्ट्राइक लंबाई लगभग 36.46 किमी और संयुक्त मैप्ड ग्रेफाइट-शिस्ट क्षेत्र लगभग 5.14 वर्ग किमी है। अलग-अलग बैंड की औसत मैप की गई चौड़ाई लगभग 4.1 मीटर (संकीर्ण लेंसोइडल बॉडी) से लेकर लगभग 783.6 मीटर (बटगल ब्लॉक) तक भिन्न होती है, स्थानीय मानचित्र-ट्रेस की चौड़ाई संभावित रूप से उच्च-राहत इलाके में अधिक होती है। ग्रेफाइट-असर संरचनाओं की गिरावट दृढ़ता से सेक्टर पर निर्भर है: दक्षिणी फाल्सिमा सेक्टर में हल्का (क्षैतिज से 3°-15°), मध्य सिरार, डिगोली, कालीमठ और बाराकोट गलियारों में मध्यम (15°-26°), और उत्तरी बटगल-चन्नी ब्लॉकों में तीव्र से बहुत तीव्र (अनुमानित 40°-75°) तक। स्थानीय भिन्नताओं के साथ प्रहार की दिशा आम तौर पर NW-SE होती है; दक्षिणी और मध्य ब्लॉकों में ढलान की दिशा मुख्य रूप से उत्तर से उत्तर-पूर्व की ओर है। 12 स्काउट बोरहोल, कुल 801.2 मीटर डायमंड कोर, 800 मीटर की कुल स्वीकृत मात्रा तक पूरा कर लिया गया है। बोरहोल पांच ब्लॉकों के भीतर दस ग्रेफाइट बैंड में वितरित किए गए हैं। प्रतिच्छेदित खनिज स्तंभ - जिसमें ग्रेफाइट शिस्ट, ग्रेफाइट-सेरीसाइट शिस्ट और ग्रेफाइटिक क्वार्टजाइट शामिल हैं - बारह बोरहोल में लगभग 501.56 मीटर है, जो ड्रिल किए गए कोर का लगभग 62% प्रतिनिधित्व करता है। अलग-अलग ग्रेफाइट-असर वाले कॉलम 7.07 मीटर वास्तविक मोटाई (BH-09, बटगल-चन्नी) से लेकर 68 मीटर (BH-01, डिगोली) तक होते हैं, कई बोरहोल इस बात की पुष्टि करते हैं कि ग्रेफाइट खनिजकरण छेद के आधार पर गहराई तक खुला है। निरंतर ग्रेफाइट शिस्ट में सबसे लंबा ग्रेफाइट-असर स्तंभ 58.73 मीटर वास्तविक मोटाई (BH-03, सिरार बैंड) है, जहां ग्रेफाइट 75 मीटर बोरहोल बेस तक बना रहता है। सतही आधार चट्टान का नमूना (57 नमूने) पांच ब्लॉकों में 0.82% से 7.05% के निश्चित कार्बन (FC%) मान दिखाता है; इनमें से छह नमूने स्क्रीनिंग के लिए उपयोग किए जाने वाले अनंतिम 2% आंतरिक कट-ऑफ से नीचे आ गए। लगभग 54 ड्रिल-कोर नमूनों के उप-सतह निकटतम विश्लेषण से 0.49% से 8.40% के एफसी% मान प्राप्त हुए, बीएच-03 (सिरार बैंड, सिरार-बटाल्डेऑन ब्लॉक) में 5.72% (n= 11 नमूने) में दर्ज उच्चतम उप-सतह औसत के साथ, एक ही बोरहोल में 38-39 मीटर की गहराई पर 8.40% का उच्चतम एकल मूल्य, और चरम मान BH-01 (डिगोली-गज्जोला) में 36.5-37 मीटर पर 7.56%। ये परिणाम इस ब्लॉक के ग्रेफाइट-शिस्ट क्षितिज में आर्थिक रूप से महत्वपूर्ण ग्रेफाइट एकाग्रता क्षमता की पुष्टि करते हैं, हालांकि डेटासेट कार्यक्रम क्षेत्र के सापेक्ष स्थानिक कवरेज में सीमित रहता है और संसाधन वर्गीकरण से पहले व्यवस्थित कंपोजिंग की आवश्यकता होती है। सभी पांच ब्लॉकों में लगातार और अत्यधिक

विषम वैनेडियम संवर्धन की पहचान की गई है। उप-सतह आईसीपी-एमएस विश्लेषण ने 1,594.6 ppm (BH-01, डिगोली-गज्जोला), 1,502 ppm (BH-09, बटगल-चन्नी), 2,758 ppm (BH-03, सिरार-बटाल्डेओन), और 3,486 ppm (BH-05, कालीमठ) के अधिकतम वैनेडियम मान लौटाए, जो 158 ppm के क्लार्क मूल्य से काफी अधिक है। सभी ब्लॉकों में. लगभग 594 ppm की प्रोग्राम-स्तरीय भारित माध्य उप-सतह वैनेडियम सांद्रता लगातार वैनैडीफेरस ग्रेफाइट प्रणाली की पुष्टि करती है। वैनेडियम को इस परियोजना के लिए सह-प्राथमिक अन्वेषण उद्देश्य के रूप में मान्यता दी गई है, जो जी3 चरण में समर्पित धातुकर्म परीक्षण कार्य की गारंटी देता है। सूत्र $T = L \times t \times D \times \rho$ ($\rho = 2.70$ t/m^3) का उपयोग करते हुए, प्रति ब्लॉक लागू तीन एक्सट्रपलेशन परिदृश्यों के साथ, अल्मोडा G4 ब्लॉक के लिए प्रोग्राम-स्तरीय अन्वेषण लक्ष्य को नीचे Table 1.1 में संक्षेपित किया गया है।

Table 1.1: अल्मोडा ग्रेफाइट और वैनेडियम कार्यक्रम: ब्लॉक द्वारा अन्वेषण लक्ष्य सारांश। सी = रूढ़िवादी परिदृश्य (सिद्ध डेटा से सीमित एक्सट्रपलेशन)। यह तालिका एक अन्वेषण लक्ष्य का गठन करती है, न कि खनिज संसाधन का।

Graphite Block	Graphite Schist Bands	Strike (km)	Exposed Graphite Schist Area (sq.km)	BH control	C: Graphite Schist Rock (Mt)	FC %	V in ppm (Subsurface)	Open to depth
Kalimath	2	5.85	1.08	1 (BH-05)	18.10	Surface: Max- 6.54, Min- 3.46, n-4 Subsurface: Max- 5.74, Min- 1.51, n-5	Max: 3739.38, Min: 67.1, n=19, avg: 1538.791	YES (BH-05)
Sirar–Bataldeon	6	8.82	0.98	4 (BH-02,03,08,10)	20.40	Surface: Max- 7, Min- 2.19, n-9 Subsurface: Max-	Max: 2758.56, Min: 29.64, n=44, avg:721.98	YES (BH-03, BH-10)

						8.4, Min-0.81, n-22		
Digoli–Gajjola	6	11.309	1.97	4 (BH-01,04,07,11)	42.30	Surface: Max-6.98, Min-0.82, n-18 Subsurface: Max-7.56, Min-0.49, n-20	Max: 1594.6, Min:51.9, n=53, avg:406.66	YES (BH-01)
Phalsima–Pithauni	4	6.957	0.85	2 (BH-06, BH-12)	42.40	Surface: Max-5.67, Min-2.14, n-5 Subsurface: Max-6.92, Min- 1, n-6	Max: 1380.52, Min: 17.22, n=30, avg:226.85	YES (both BH)
Batgal–Channi	12	3.529	0.26	1 (BH-09)	0.431	Surface: Max-7.05, Min-2.46, n-11 Subsurface: 2.99	Max:1502.34, Min:35.75, n=6, avg:414.25	Not confirmed
PROGRAMME TOTAL	**30**	**36.465**	**5.14**	12 boreholes 801.2 m	**123.6**			6 of 12 BH open

बिना किसी साइट-विशिष्ट माप के थोक घनत्व 2.70 t/m³ माना गया है; यह बड़े पैमाने पर अनुमान में अनुमानित ±2% व्यवस्थित त्रुटि का परिचय देता है। इस चरण में कोई डाउनहोल विचलन सर्वेक्षण या औपचारिक भूभौतिकीय लॉगिंग नहीं की गई, जिससे गहराई पर संरचनात्मक विश्वास सीमित हो गया। अन्वेषण लक्ष्य पार्श्व और ऊर्ध्वाधर निरंतरता मान्यताओं पर भी निर्भर हैं जिनका परीक्षण संसाधन-पैटर्न ड्रिलिंग द्वारा नहीं किया गया है। अन्वेषण लक्ष्य क्षमता के पैमाने और ऊपर वर्णित आत्मविश्वास सीमाओं

दोनों को ध्यान में रखते हुए, अध्ययन उच्चतम प्राथमिकता वाले गलियारों पर केंद्रित जी3-चरण प्रारंभिक अन्वेषण कार्यक्रम के लिए चयनात्मक उन्नति की सिफारिश करता है। सिरार-बटाल्डियन ब्लॉक (सिरार बैंड और बटालडियन ईस्ट बैंड 2) और डिगोली-गज्जोला ब्लॉक (बैंड-1/ई.डिगोली और अनड्रिल्ड बैंड-3) को पहली प्राथमिकता वाले लक्ष्य के रूप में स्थान दिया गया है, कालीमठ (BH-05 पूर्वी भाग) और फाल्सिमा-पिथौनी (उत्तरी फाल्सिमा बैंड, वर्तमान में अनड्रिल) को दूसरी प्राथमिकता के रूप में, बटगल-चन्नी को तीसरी प्राथमिकता के रूप में रखा गया है।

सभी G3-स्टेज ड्रिलिंग को संरचनात्मक रूप से निर्देशित किया जाना चाहिए (डीजीपीएस-नियंत्रित बैंड ट्रेसिंग, नजदीकी दूरी वाले एसपी और वीईएस या ईआरटी प्रोफाइलिंग, और सेक्शन-नियंत्रित कॉलर प्लेसमेंट को शामिल करते हुए)। प्रत्येक बोरहोल को निम्नलिखित द्वारा समर्थित किया जाना चाहिए: व्यवस्थित 0.5-1.0 मीटर चैनल-मिश्रित कोर नमूना; निकटतम विश्लेषण; LECO दहन द्वारा कुल ग्रेफाइटिक कार्बन जहां निकटतम डेटा अस्पष्ट है; एक्सआरएफ द्वारा प्रमुख ऑक्साइड भू-रसायन; बहु-तत्व आईसीपी-एमएस (वैनेडियम, मोलिब्डेनम और पूर्ण आरईई सूट सहित); ग्रेफाइट क्रिस्टलीयता, संरचनात्मक क्रम और चरण संयोजन निर्धारित करने के लिए मिश्रित कोर पर रमन स्पेक्ट्रोस्कोपी और एक्सआरडी; छवि विश्लेषण सॉफ्टवेयर द्वारा ग्रेफाइट फ्लेक-आकार मोडल विश्लेषण; साइट-विशिष्ट थोक घनत्व माप (जल-विसर्जन विधि); और मिश्रित ग्रेफाइट-शिस्ट सामग्री (फ्लोटेशन प्रतिक्रिया, ध्यान केंद्रित शुद्धता, और वैनेडियम डिपोर्टमेंट) पर प्रारंभिक चरण लाभकारी परीक्षण। पर्यावरण, सामाजिक और शासन (ईएसजी) स्क्रीनिंग - विशेष रूप से आरक्षित वन ओवरलैप, जल-स्रोत निकटता, और निवास संवेदनशीलता - को अंतिम G3 ड्रिल स्थान चयन से पहले पूरा किया जाना चाहिए, विशेष रूप से कालीमठ (आरक्षित वन) और डिगोली-गज्जोला (फर्कनौला और मटेना आरएफ) ब्लॉक में।

संक्षेप में, अल्मोडा ब्लॉक एक भूवैज्ञानिक रूप से संभावित ग्रेफाइट-वैनेडियम प्रणाली है जिसमें पर्याप्त सतह पदचिह्न, सार्थक उपसतह चौराहे, मजबूत संरचनात्मक नियंत्रण और महत्वपूर्ण वैनेडियम संवर्धन है। वर्तमान G4 डेटा आगे की खोज और G3 लक्ष्य परीक्षण को उचित ठहराने के लिए पर्याप्त है। परियोजना का भविष्य का मूल्य सर्वोत्तम निम्न-से-मध्यम-डिप पैनलों में निरंतरता साबित करने, ग्रेड वितरण में आत्मविश्वास में सुधार, लाभकारी के माध्यम से ग्रेफाइट पुनर्प्राप्ति स्थापित करने, वैनेडियम खनिज निवास का निर्धारण करने और ढलान, वन, जल निकासी, निवास और विरासत बाधाओं के साथ भविष्य के सभी कार्यों को एकीकृत करने पर निर्भर करेगा।

Executive Summary:

The Reconnaissance Survey, G4 Stage, for Graphite and Vanadium in the Matena–Sirar area, Almora District, Uttarakhand was undertaken by Geovale Services Pvt. Ltd. as an NPEA project funded by the National Mineral Exploration and Development Trust, Ministry of Mines. The project covers 60 sq. km. in Survey of India Toposheet 53O/10, around Matena, Phalsima, Sirar, Deora, Balta, Kalimath and adjoining villages. The principal objective was to evaluate the presence, extent, thickness, quality and continuity of graphitic horizons in the Almora Crystalline of the Inner Lesser Himalaya and to assess the associated potential for vanadium and other critical/pathfinder elements within graphite schist horizons.

The investigation was taken up because graphite occurrences in the Almora region have been known previously, but the older information was fragmented and insufficient for modern target appraisal. Legacy work by GSI and earlier investigators had established the presence of graphite schist near Kalimath, Sirar, Bataldeon, Batgal and adjoining areas. Previous data also indicated variable graphite quality: bulk graphite schist generally showed low to moderate fixed carbon, whereas carbonaceous nodules locally yielded much higher carbon values. More recent GSI and published work shifted the exploration concept from a graphite-only model to a broader graphite–vanadium–polymetallic carbonaceous metasedimentary system, highlighting the potential association of vanadium, barium, molybdenum, tungsten, uranium and other elements with metamorphosed black shale/graphite schist horizons.

The Almora block lies within a rugged Himalayan terrain that is regionally accessible but at places locally challenging for exploration. Regional access is available through Almora town, NH-309A, NH-309B and connected village roads; however, some of the area is controlled by steep slopes, dissected drainage, forest patches, habitation, cultivated terraces and last-mile access constraints. A few areas in the Almora block also includes environmentally and socially sensitive elements, including reserve/civil forest areas, dense drainage networks, springs, village land use and the Lakhudiyar archaeological site. These factors are important not only for future field logistics but also for mineability screening, because the presence of graphite alone does not make all sectors equally suitable for future exploration or development.

The dominant lithological association of this Almora G4 Block includes mica schist, quartzite, graphite schist, tuffaceous rocks, granite gneiss and younger intrusive foliated granite. Mica schist forms the dominant lithology, while graphite schist occurs as discrete but structurally repeated bands within the metasedimentary units. The younger granitic intrusions are commonly lit-par-lit and locally emplaced along foliation/thrust planes, which is significant

because thermal and deformation-assisted recrystallization may have enhanced graphite ordering in favourable sectors.

The exploration programme established that the graphite mineralisation is dominantly stratabound, fabric-controlled and structurally modified. Graphite occurs jumbo to as medium and fine flaky grains aligned parallel to foliation and concentrated in graphite-rich laminae mainly within quartz–muscovite-rich schists. Petrographic observations indicate folded graphite flakes, graphite in shear lenses, graphite associated with mica fish and recrystallized quartz and graphite redistributed along deformation fabrics. This confirms that graphite was inherited from carbonaceous sedimentary protoliths and later modified by regional metamorphism, shearing, folding, thrust repetition and local granite-related thermal effects.

The G4 work was multi-disciplinary and appropriately designed for a structurally complex graphite terrain. It included 60 sq. km. of multispectral and DEM interpretation, large-scale geological mapping (1:12,500), systematic surface sampling, pitting and trenching, petrography, and modal analyses,Raman and XRD, and other mineralogical work, XRF, ICPMS, proximate analysis, total sulphur analysis, SP and VES geophysics and scout drilling. The achieved field quantum included 450.68 cu. m. of pitting and trenching, 32.6 line-km of SP, 31.4 line-km of VES and 801.2 m of core drilling, supported by surface and borehole geochemical analyses. The exploration workflow moved logically from legacy review and remote sensing to mapping, sampling, geophysical testing, excavation and scout drilling.

Remote sensing and DEM interpretation helped identify lineaments, slope classes, drainage, access corridors, forest cover, land use and terrain constraints. Geological mapping provided the most important primary framework by tracing graphite schist bands, identifying host lithologies, recording structural attitudes and defining target corridors. Pitting and trenching improved exposure in soil-covered or weathered areas. SP and VES were useful in tracing conductive graphitic horizons, particularly where surface exposure was poor. However, the report emphasizes that geophysical conductivity is not a direct proxy for economic graphite grade, because graphite continuity, sulphides, clay, moisture and structural dismemberment may all affect conductivity. The highest confidence targets are therefore those where mapping, geochemistry, SP/VES response and drilling results coincide.

Graphite mineralization is developed as thin, cm- to metre-scale intercalated bands within mica-rich graphite schist, graphitic quartzite, and graphite sericite schist, which serve as the principal host rocks. The graphite is chiefly localized along foliation planes, though it also occurs as medium- to coarse-grained disseminated flakes, veins, and veinlets, commonly giving the host rocks a dark grey to black, graphite-rich appearance. The mineralization is

considered to have formed from carbonaceous sedimentary precursors that were deformed and regionally metamorphosed, with enhanced crystallinity produced by later contact metamorphism related to lit-par-lit injection of younger granite.

A major outcome of this programme is the recognition of 30 graphite schist bands distributed over the 60 sq. km. G4 exploration area. The graphite system has been classified into five principal graphite-bearing domains: Kalimath, Sirar–Bataldeon, Digoli–Gajjola, Phalsima–Pithauni and Batgal–Channi. These are not equivalent in geological continuity, grade, subsurface confirmation, accessibility, ESG sensitivity or future exploration priority. Together, the five domains account for approximately 36.46 km of cumulative mappable graphite-band strike length and a mapped graphite footprint on the order of 5.14 sq. km., although these figures represent structurally repeated and segmented band traces rather than a single continuous orebody. At G4 stage, these data define an mineral exploration target, not a mineral resource or reserve.

The Kalimath Graphite Block is one of the important graphite–vanadium targets. It covers about 4.93 sq. km. and comprises eastern and western graphite-band segments. The eastern segment has about 2.32 km mappable strike length and geophysical indications of 35–55 m thick conductive zones at depth, while the western segment has about 3.53 km strike length. BH05 intersected mainly two graphite-bearing intervals from 22.9–45.67 m and 46.62–75 m, representing about 48.65 m true thickness. Kalimath also records strong vanadium enrichment, with BH05 samples reporting FC upto 5.74% vanadium values upto 3,739 ppm in Almora G4 Block.

The Sirar–Bataldeon Graphite Block is another high-priority domain. It includes several mappable graphite bands, of which Bataldeon East Band 2 is one of the most laterally extensive, with about 3.40 km strike length, about 0.132 km average width and about 0.449 sq. km. mapped area. BH03 near Sirar intersects graphite bearing rocks from about 12.5 m to 75 m, including a good quality graphite around 31.45–42 m. BH03 records highest FC value 8.4% in Almora G4 Block and vanadium upto 2758 ppm. This block has strong volumetric potential, but drainage, forest, local cover and sulphide/quality issues need careful evaluation.

The Digoli–Gajjola Graphite Block is a significant follow-up target because it contains multiple thrust-bounded graphite bands and has subsurface confirmation in the BH01, BH04, BH07 and BH11. BH01 records graphite bearing mineralisation from about 16 m to 91.7 m, including a 2 m interval from 35–37 m carrying 5.28–7.56% fixed carbon. The block also has a strong vanadium (upto 1594 ppm at BH01) -polymetallic signature, with vanadium

enrichment and associated molybdenum, barium, copper, zinc, uranium and silver in parts of the system.

The Phalsima–Pithauni Graphite Block is significant because of its shallow-dipping geometry and relatively favourable access. The four mapped graphite bands have a combined strike length of about 6.96 km and mapped area of about 0.872 sq. km., with gentle dips of about 3°–15° toward the north-east. VES data identify conductive zones of about 20–60 m thickness and the Pithauni subsurface assessment record a 26 m thick graphite zone followed by about 40 m of intercalated graphite–mica schist below about 10 m overburden. However, available surface fixed-carbon values are generally around 2.14–5.67% and the graphite schist locally with highly siliceous with high ash. This block therefore has good geometric and shallow-depth potential. BH06 and BH12 are conducted in the block where FC yield upto 6.92% and vanadium upto 1380 ppm.

The Batgal–Channi Graphite Block is structurally interesting but is ranked lower for volumetric potential. It contains about 12 narrow and discontinuous graphite bands, with about 3.53 km cumulative strike length and about 0.242 sq. km. mapped area. The bands are steep, commonly 50°–70° and BH09 confirms only about 6.07 m total true graphite thickness in two intervals. Although surface fixed carbon locally reaches about 7.05% and vanadium values are locally anomalous up to about 3,536 ppm, the steep dips, narrow lenses and structural fragmentation imply higher strip ratio and lower bulk-continuity potential than the more gently dipping blocks. BH09 present in the block where FC reaches upto 2.99% and vanadium upto 1502 ppm.

In terms of grade and product quality, the Almora graphite system is best described as a large-volume, structurally repeated, moderate to high grade flake-graphite schist system. Fixed-carbon in surface samples reaching upto 7.05% FC, with subsurface values reaching upto 8.40% FC. Flake-size data shows the presence of jumbo fraction along with coarse, medium, and fine fraction of graphite in Kalimath, Pithauni and Sirar areas.

The vanadium association is a major positive result of the G4 programme. Vanadium is anomalous in several graphitic horizons, particularly in Kalimath, Sirar–Bataldeon, Digoli–Gajjola and Batgal–Channi. Reported values include up to 3,739 ppm V in BH05 at Kalimath, surface vanadium up to 2,414 ppm in Sirar–Bataldeon, BH02 values around 710–1,022 ppm, up to 2,296 ppm in Digoli–Gajjola XRF-derived datasets and up to 3,536 ppm in selected Batgal–Channi bands. This supports the interpretation that the graphite schists represent reduced carbonaceous metasedimentary horizons capable of concentrating redox-sensitive elements.

This G4 programme has successfully upgraded the Almora graphite occurrences from previous showings into a coherent block-wise graphite–vanadium exploration model. The best graphite development occurs where favourable carbonaceous protoliths are structurally thickened, repeated or preserved along thrust-related corridors, fold closures and low- to moderate-dip panels. The most prospective sectors identified are Sirar–Bataldeon, Digoli–Gajjola, Kalimath East, Phalsima-Pithauni and Batgal-Channi graphite blocks.

Under the UNFC framework, a G4-stage (Reconnaissance) investigation does not produce a formal Mineral Resource estimate. However, a G4 program like Almora Graphite Investigation can produce a set of Mineral Exploration Targets.: As a standard practice these are presented as ranges and subject to the stated geological assumptions. The **exploration targets** developed for the Almora graphite and vanadium programme in Chapter 9 are summarised below.

Within the G4 exploration area of 60 sq. km., 30 graphite-bearing bands have been delineated and these are distributed across five structurally controlled exploration blocks, with a confirmed cumulative strike length of approximately 36.46 km and a combined mapped graphite-schist area of approximately 5.14 sq. km. The average mapped width of the individual bands varies from roughly 4.1 m (narrow lensoidal bodies) to roughly 783.6 m (Batgal block) with local map-trace width potentially greater in high-relief terrain. Dip of the graphite-bearing formations is strongly sector-dependent: gentle (3°–15° from horizontal) in the southern Phalsima sector, moderate (15°–26°) in the central Sirar, Digoli, Kalimath and Barakote corridors, and steep to very steep (estimated 40°–75°) in the northern Batgal–Channi blocks. Strike direction is generally NW–SE with local variations; dip direction is predominantly northward to north-eastward across the southern and central blocks. 12 scout boreholes, totalling 801.2 m of diamond core, have been completed to the total sanctioned quantum of 800 m. Boreholes are distributed across ten graphite bearing bands within the five blocks. ***The mineralised column intersected - comprising graphite schist, graphite–sericite schist, and graphitic quartzite - totals approximately 501.56 m across the twelve boreholes, representing approximately 62% of the drilled core***. Individual graphite-bearing columns range from 7.07 m true thickness (BH-09, Batgal–Channi) to 68 m (BH-01, Digoli), with several boreholes confirming that graphite mineralisation is open to depth at the hole base. The longest graphite-bearing column in continuous graphite schist is 58.73 m true thickness (BH-03, Sirar Band), where graphite persists to the 75 m borehole base. ***Surface bedrock sampling (57 samples) shows fixed carbon (FC%) values of 0.82% to 7.05% across the five blocks***; only six of these

samples fell below the provisional 2% internal cut-off used for screening. ***Sub-surface proximate analysis of approximately 54 drill-core samples yielded FC% values of 0.49% to 8.40%,*** with the highest sub-surface mean recorded in BH-03 (Sirar Band, Sirar-Bataldeon block) at 5.72% (n = 11 samples), the highest single value of 8.40% at 38–39 m depth in the same borehole, and other peak value in BH-01 of 7.56% (Digoli–Gajjola) at 36.5–37 m. These results confirm economically significant graphite concentration potential in the graphite-schist horizons of this block, though the dataset remains limited in spatial coverage relative to the programme area and requires systematic compositing before resource classification. Consistent and strongly anomalous vanadium enrichment has been identified across all five blocks. Sub-surface ICP-MS analyses returned peak vanadium values of 1,594.6 ppm (BH-01, Digoli–Gajjola), 1,502 ppm (BH-09, Batgal–Channi), 2,758 ppm (BH-03, Sirar–Bataldeon), and 3,486 ppm (BH-05, Kalimath), significantly exceeding the Clarke value of 158 ppm in all blocks. The programme-level weighted mean sub-surface vanadium concentration of approximately 594 ppm confirms a consistently vanadiferous graphite system. Vanadium is recognised as a co-primary exploration objective for this project, warranting dedicated metallurgical testwork in the G3 stage. Using the formula $T = L \times t \times D \times \rho$; $\rho = 2.70$ t/m³), the programme-level exploration target for the Almora G4 block is summarised in Table 1.2 below.

Table 1.2: Almora graphite and vanadium programme: exploration target summary by block. C = Conservative scenario).This table constitutes an Minaral Exploration Target, not a Mineral Resource.

Graphite Block	Graphite Schist Bands	Strike (km)	Exposed Graphite Schist Area (sq.km)	BH control	C: Graphite Schist Rock (Mt)	FC %	V in ppm (Subsurface)	Open to depth
Kalimath	2	5.85	1.08	1 (BH-05)	18.10	Surface: Max-6.54, Min-3.46, n-4 Subsurface: Max-5.74,	Max: 3739.38, Min: 67.1, n=19, avg: 1538.791	YES (BH-05)

						Min- 1.51, n-5		
Sirar– Bataldeon	6	8.82	0.98	4 (BH-02,03,08,10)	20.4	Surface: Max- 7, Min- 2.19, n-9 Subsurface: Max- 8.4, Min- 0.81, n-22	Max: 2758.56, Min: 29.64, n=44, avg:721.98	YES (BH-03, BH-10)
Digoli– Gajjola	6	11.309	1.97	4 (BH-01,04,07,11)	42.3	Surface: Max- 6.98, Min- 0.82, n-18 Subsurface: Max- 7.56, Min- 0.49, n-20	Max: 1594.6, Min:51.9, n=53, avg:406.66	YES (BH-01)
Phalsima– Pithauni	4	6.957	0.85	2 (BH-06, BH-12)	42.4	Surface: Max- 5.67, Min- 2.14, n-5 Subsurface: Max- 6.92, Min- 1, n-6	Max: 1380.52, Min: 17.22, n=30, avg:226.85	YES (both BH)
Batgal– Channi	12	3.529	0.26	1 (BH-09)	0.431	Surface: Max- 7.05, Min- 2.46, n-11 Subsurface: 2.99	Max:1502.34, Min:35.75, n=6, avg:414.25	Not confirmed

PROGRAM ME TOTAL	**30**	**36.465**	**5.14**	12 boreholes 801.2 m	**123.6**			6 of 12 BH open

Bulk density has been assumed at 2.70 t/m³ with no site-specific measurements; this introduces an estimated ±2% in mass estimates. No downhole deviation surveys or formal geophysical logging were conducted in this phase, limiting structural confidence at depth. The exploration targets are also contingent on lateral and vertical continuity assumptions that have not been tested by resource-pattern drilling. **Considering both the scale of the exploration target potential and the confidence limitations, the study recommends selective advancement to a G3-stage preliminary exploration programme focused on the highest-priority corridors. The Sirar–Bataldeon block (Sirar Band and Bataldeon East Band 2) and the Digoli–Gajjola block (Band-1/E.Digoli and the undrilled Band-3) are ranked as the first-priority targets, with Kalimath (BH-05 eastern part) and Phalsima–Pithauni (north Phalsima band, currently undrilled) as second priority, with Batgal-Channi as the third priority**.

All G3-stage drilling should be structurally guided (incorporating DGPS-controlled band tracing, closer-spaced SP and VES or ERT profiling, and section-controlled collar placement). Each borehole should be supported by: systematic 0.5–1.0 m channel-composited core sampling; proximate analysis; total graphitic carbon by LECO combustion where proximate data are ambiguous; major oxide geochemistry by XRF; multi-element ICP-MS (including vanadium, molybdenum, and full REE suite); Raman spectroscopy and XRD on composited core to determine graphite crystallinity, structural order, and phase assemblage; graphite flake-size modal analysis by image analysis software; site-specific bulk density measurements (water-immersion method); and early-stage beneficiation testing on composited graphite-schist material (flotation response, concentrate purity, and vanadium deportment). Environmental, social, and governance (ESG) screening - specifically reserved forest overlap, water-source proximity, and habitation sensitivity - must be completed before final G3 drill location selection, particularly in the Kalimath (Reserve Forest) and Digoli–Gajjola (Pharhkanaula and Matena RF) blocks.

In summary, the Almora block is a geologically prospective graphite–vanadium system with a substantial surface footprint, meaningful subsurface intersections, strong structural controls and significant vanadium enrichment. The present G4 data are sufficient to justify further exploration and G3 target testing. The future value of the project will depend on proving

continuity in the best low- to moderate-dip panels, improving confidence in grade distribution, establishing graphite recoverability through beneficiation, determining vanadium mineral residence and integrating all future work with slope, forest, drainage, habitation and heritage constraints.

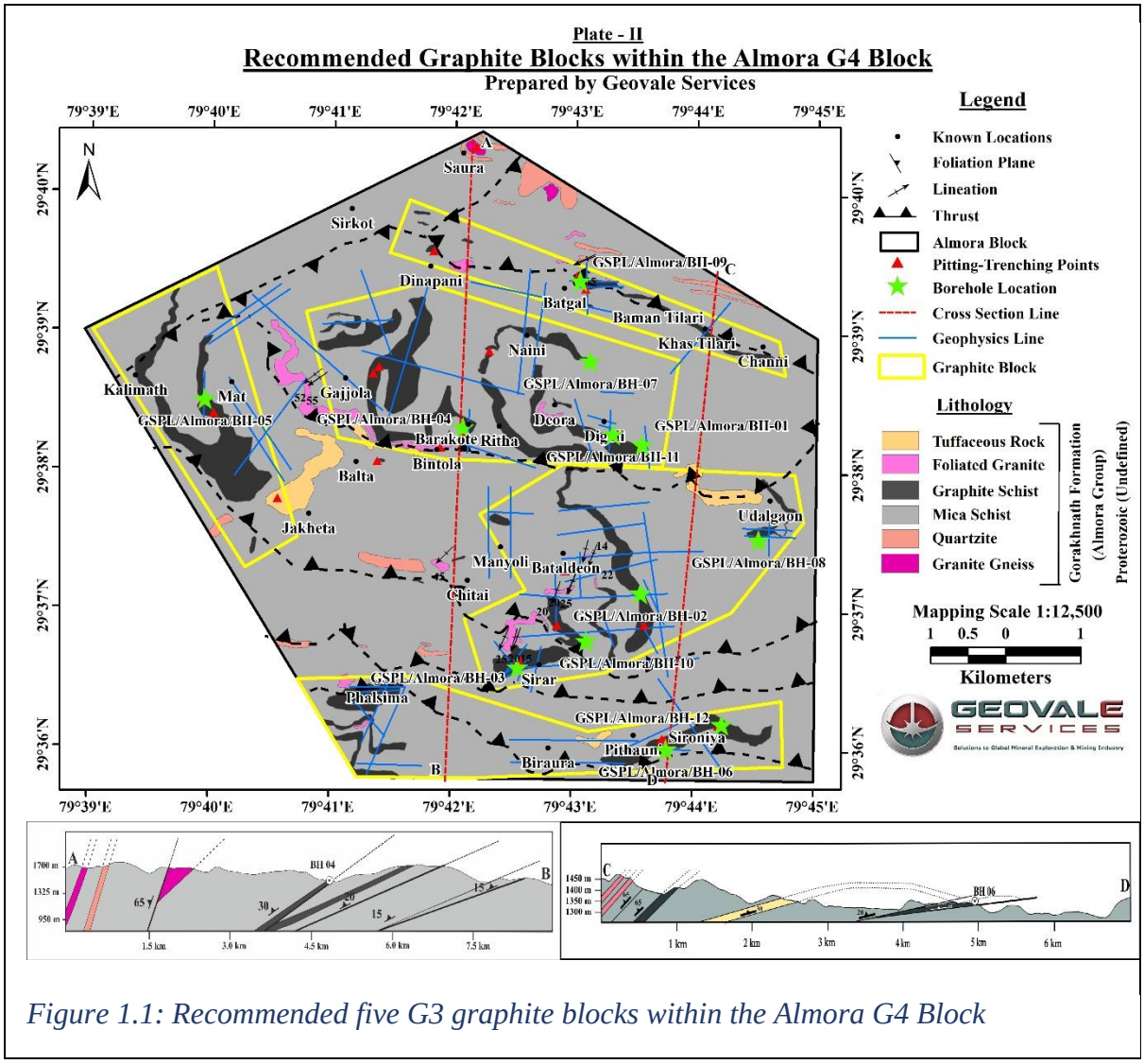

Figure 1.1: Recommended five G3 graphite blocks within the Almora G4 Block

Chapter 2

Introduction

2 Introduction:

The National Mineral Exploration and Development Trust (NMEDT) of Ministry of Mines, India awards different exploration projects to different Notified Private Exploration Agencies (NPEAs) after thorough review of proposals received from them. Accordingly, M/s. Geovale Services (one of the NPEAs) was given a G4 stage exploration project titled "Reconnaissance Survey (G4 Stage) for Graphite and Vanadium in the Matena-Sirar Area (60 sq. km.), Almora District, Uttarakhand."

The project area is near the Almora Town in Uttarakhand and is part of Survey of India toposheet number 53O/10 and covers an area of 60 sq. km.

This report documents the G4 stage exploration work and findings for graphite and vanadium using data from remote sensing, detailed geological mapping, geochemical sampling, geophysical investigations, petrographic and mineralogical analyses, and drilling. The exploration was conducted on a Mineral Systems Analysis framework. The objective of this project has been to understand the thickness and distribution of graphite bands in the area and to know the extent of graphitization. If found suitable then few G3 stage exploration projects would be generated. In addition to the extent of ordering of graphite bands, their usefulness for extraction of vanadium and other polymetals would also be explored.

2.1 Administrative Details of the Project:

The following table (Table 2.1) summarizes key details of the project, including geographical coverage, administrative jurisdictions, target commodities and project timeline:

Table 2.1:Administrative Details of the Almora exploration block

Features		Details
1	**Project Name:**	**Reconnaissance Survey (G4 Stage) for Graphite and Vanadium in Matena-Sirar Area (60 sq. km.), Almora District, Uttarakhand.**
2	**Project Code:**	**23/491/2024-NMET-282**
3	**Block ID**	**GSPL/NMET/UK/2024/282**

Features		Details		
4	Exploration Agency	Geovale Services Private Limited		
5	Commodity	Graphite and Vanadium		
6	Mineral Belt	Almora Crystalline of the Inner Lesser Himalaya		
7	Nearby villages	Matena, Falshima, Sirar, Deora, Balta and Kalimath		
8	Tehsil	Almora		
9	District	Almora		
10	State	Uttarakhand		
11	Project area	60 sq. km.		
12	Survey of India Toposheet No.	53O/10		
13	Date of commencement of the project	1st September, 2024		
10	Boundary coordinates of the project area	Boundary Coordinates	Latitude	Longitude
		A	29.67419714	79.70360564
		B	29.64965410	79.75000285
		C	29.59650200	79.75000000
		D	29.59650189	79.68720717
		E	29.65003641	79.64906903

2.2 Investigating Agency:

The key information about the investigating agency is provided in the table (Table 2.2) below:

Table 2.2: Details of the investigating agency of the Almora exploration program.

Name:	Geovale Services Private Limited.
Postal address:	3rd Floor, Anaya Chambers, Block GN, Plot 38/5, Sector V, Salt Lake, Kolkata- 700091, West Bengal, India.
Telephone Number (Office):	033 4601 2887
Mobile No.:	+91 9007706145
Telephone Number:	+91 9874320018
E-Mail address:	biplob.chatterjee@geovale.com
Date of accreditation granted by QCI-NABET:	23rd March, 2022; 23rd March, 2025
Date of expiry of accreditation:	22 March, 2030
Category of the NPEA	Category A

2.3 Objectives of Investigation:

i. To explore the extent and ordering of graphitization within the block area (60 sq. km.).
ii. To identify target areas for possible G3 stage of exploration for graphite and polymetals.

2.4 Basis for Taking Up Investigation:

Inner Lesser Himalayan rocks of the Almora Crystalline include medium to high amphibolite grade meta-pelllites, quartzites, graphite schists that are closely associated with ~1.8 Ga and ~500 (?) Ma granites. The younger granite (?500 Ma) occurs as lit-par-lit injections to the metapelites.

Thick carbonaceous schists (or graphite schists) occur as multiple discrete bands in the area. At places these bands are quite thick (5-10m) and have substantial sulphide minerals in them (Rawat and Sharma, 2011; Vishnu and Yadav, 2021).

GSI's recent Specialized Thematic Mapping (STM) and exploration studies in the area brought out some exciting information on these metamorphosed black shales (Santosh and Yadav, 2021; Bauri and Raut, 2021):

i. Some of the metamorphosed black shale horizons may be categorized as High Carbon (>7%) High Sulphur (>4%) (HCHS) category.
ii. Some spot sample analyses by GSI have yielded V concentration >0.4% and Ba concentration >4% in addition to very high concentration of a host of critical metals like Mo, U, REE etc.
iii. An exploration work for tungsten in the area by the GSI (Santosh and Yadav, 2021) using detailed stream sampling and a few channel samplings in a part of the present block also reported tungsten and tin from stream-sediment and bedrock samples.

The block is considered prospective for graphite and graphite associated polymetals especially vanadium. As the graphite schist occur in close association with medium to high-amphibolite grade metasediments some reaching upto sillimanite grade of metamorphism along with evidences of in situ partial melting, there is high chance of getting highly ordered graphite in the area.

2.5 Nature and quantum and timeline of work (NQT):

The project followed a structured work plan to systematically evaluate the graphite potential of the area. The following table (Table 2.3) presents a comparison between the approved scope of work and actual achievements during project execution.

Table 2.3: Details of the approved vs. achieved quantum of targets of the Almora exploration program.

Sl. No.	Nature of work	Approved Quantum	Achieved Quantum	Remarks
1	Multispectral and DEM data analysis	60 sq. km.	60 sq. km.	Achieved

Sl. No.	Nature of work	Approved Quantum	Achieved Quantum	Remarks
2	Large Scale Geological Mapping (LSM) (1:12,500 scale) and Sampling	60 sq. km.	60 sq. km.	Achieved
3	Pitting (up to 2m depth)	400 cu. m for graphite and V (200 cu.m trench, 200 cu.m pitting)	450.68 cu. m. Pitting and Trenching; (234.46 cu.m for pitting, 216.22 cu. m. for trenching)	Achieved
4	Geochemical Analysis (Phase I)			
	a. Separation of heavy minerals from stream sediment samples of -2mm size through gravity and magnetic separation	25 samples	25 samples	Achieved
	b. XRF (major oxides)	200 samples	200 samples	Achieved
	c. External Check samples for XRF	20 samples	22 samples	Achieved
	d. XRF 10 % samples for 2 additional elements)- Sn and W	20 samples	20 samples	Achieved
	e. Check samples XRF 10 % samples for 2 additional elements)	2 samples	2 samples	Achieved
	f. ICPMS (To analyse V and REEs)	100 samples	100 samples	Achieved
	g. Check samples ICPMS	10 samples	10 samples	Achieved

Sl. No.	Nature of work	Approved Quantum	Achieved Quantum	Remarks
	(To analyse V and REEs)			
	h. Proximate analysis of Graphite (FC)	50 samples	57 samples	Achieved
	i. Total Sulphur	25 samples	25 samples	Achieved
5	Petrological Studies			
	a. Thin section preparation	20 samples	21 samples	Achieved
	b. Microscopic study	20 samples	21 samples	Achieved
	c. Raman Spectrometry (graphite crystallinity)	10 samples	10 samples	Achieved
	d. XRD	10 samples	10 samples	Achieved
6	Geophysical Survey			
	a. Self-Potential and shallow electrical resistivity (VES)	30 line-km	32.6 line-km (SP) 31.4 line-km (VES)	Achieved
7	Drilling In-House			
	a. Core Drilling	800 m	801.2 m	Achieved
	b. Transportation of drill rig and truck associated per drill (2 rigs)- Two way	6000 m	4455 m	Achieved
	c. Construction of concrete pillar (12”12”30”)	12 nos.	12 nos.	Achieved
	d. Drill Core Preservation	300 m	301.6 m	Achieved
8	Geochemical Investigation (BH Samples)			

Sl. No.	Nature of work	Approved Quantum	Achieved Quantum	Remarks
	a. XRF (Major oxide)	50 samples	51 samples	Achieved
	b. External Check samples for XRF	5 samples	5 samples	Achieved
	c. XRF 10 % samples for 2 additional elements (Sn, W)	5 samples	5 samples	Achieved
	d. Check samples XRF 10 % samples for 12 additional elements)	1 sample	1 sample	Achieved
	e. ICPMS 34 elements	150 samples	150 samples	Achieved
	f. Check samples of ICPMS 34 elements	15 samples	15 samples	Achieved
	g. Proximate analysis of Graphite	50 samples	54 samples	Achieved
9	Petrological Studies (BH samples)			
	a. Thin section preparation	25 samples	25 samples	Achieved
	b. Microscopic studies	25 samples	25 samples	Achieved
10	Geological Report	1	1	Achieved

2.6 Personnel Involved:

The successful execution of the project was made possible through the efforts of a dedicated team of geoscientists, field personnel and technical experts. The table (Table 2.4) below lists the team members and their respective roles.

Table 2.4: List of personnel involved in the Almora exploration program.

Sl. No.	Team Members	Designation/ Role	Project Responsibilities
1	**Biplob Chatterjee**	Director and CEO, PC (NABET)	Overall project supervision, strategic oversight, verification of project protocols, review of outcomes and report.
2	**Dr. Joy Gopal Ghosh**	Principal Consultant (Exploration), PC (NABET)	Conceptualization of exploration models, Mineral System Analyses (MSA) study, determination of project protocols, technical design and guidance, peer review of findings and report.
3	**Dr. Taraknath Pal**	Principal Consultant (Exploration), PC (NABET)	Project management and project administration.
4	**Dr. Tapan Pal**	Principal Consultant (Exploration)	Geological, petrological supervision and review of report.
5	**Dr. Tanwita Deb**	Senior Project Manager (Exploration), TM (NABET)	Overall coordination of field operations, lithological and structural mapping, interpretation of geochemical data, petrographical and modal analyses of graphite, all data integration and analyses.
6	**Sarita Mahato**	Project Manager (Exploration), TM (NABET)	Project Manager; field logistics coordination, field assistance, sampling supervision, pitting and trenching managements.

Sl. No.	Team Members	Designation/ Role	Project Responsibilities
7	**Spandita Kundu**	Project Geologist (Exploration), TM (NABET)	Field assistance, sample processing, laboratory coordination, geophysical data acquisition, data documentation, core logging and litho-log preparation.
8	**Dr. Suparna Goswami**	Senior Project Manager (Exploration), TM (NABET)	Project administration.
9	**Nupur Adhikary**	Senior Project Manager (Geology and Geospatial Services, TAE (NABET)	Supervision on geospatial data management and project administration.
10	**Chiranjib Banerjee**	Senior Project Manager (Geotechnical), TAE (NABET)	Drilling and project management plan supervision.
11	**Arnab Mallick**	Project Manager, (Exploration), TM (NABET)	Geological mapping and sampling.
12	**Krishna Prasad**	Senior Consultant (Geophysics), TAE (NABET)	Geophysical survey design, data quality assessment and supervising.
13	**Dakshi Sarkar**	Project Geologist (Exploration), TM (NABET)	Geological mapping and sampling.
14	**Shivani Gupta**	Project Geologist (Exploration), TM (NABET)	Geological mapping and sampling.

Sl. No.	Team Members	Designation/ Role	Project Responsibilities
15	**Tanuja Priyadarshini Deo**	Project Geologist (Exploration), TM (NABET)	Geophysical data acquisition, data documentation and compilation.
16	**Upasana Mondal**	Project Geologist (Exploration), TM (NABET)	Geophysical data acquisition, data documentation and compilation.
17	**Prasen Saha**	Project Geologist (Exploration), TM (NABET)	Core logging, litho-log preparation.
18	**Sujay Payra**	Senior Project Manager (Geospatial Services), TAE (NABET)	Overall coordination of geospatial activities and remote sensing interpretation.
19	**Prabir Bhattacharya**	Project Manager (Geospatial Services)	Satellite data processing, map generation, DEM analysis and GIS integration.
20	**Rabiya Parween**	Project Scientist (Geospatial Services), TM (NABET)	GIS database preparation and figure generation.

2.7 Mode of Operation of Different Working Components and Associated Agency:

The "Reconnaissance Survey (G4 Stage) for Graphite and Vanadium in the Matena-Sirar Area (60 sq. km.), Almora District, Uttarakhand " was conducted through a multi-disciplinary approach that integrated geological, geophysical, mineralogical and geochemical methodologies. All field-based activities-including large scale geological mapping, systematic

sampling, sample processing, geophysical surveys and drilling were carried out in-house by Geovale Services Private Limited.

For geochemical analyses, the project partnered with the Inspectorate Griffith India Pvt. Ltd. (IGI), Bureau Veritas, at its Gandhidham Laboratory in Gujarat, to ensure high analytical precision. Additionally, check sample analyses were conducted at Shiva Analytical, Bengaluru, Karnataka, to validate data accuracy and reproducibility.

Advanced mineralogical and characterization studies, including X-ray Diffraction (XRD), Raman Spectroscopy and Isodynamic Separation analysis, were carried out at the Geological Survey of India (GSI), Kolkata and Nagpur.

This integrated and collaborative approach ensured the highest standards of analytical accuracy, data reliability and interpretational robustness in evaluating the Graphite and Vanadium deposits of the Almora.

2.8 Acknowledgements:

This project was funded by the National Mineral Exploration and Development Trust (NMEDT), Ministry of Mines, Government of India, under Project Sanction File No: 23/491/2024-NMET-282, dated 21st August, 2024. The project's technical design and periodic review were undertaken by the Technical and Cost Committee (TCC) and the Executive Committee (EC) of NMEDT, whose valuable insights and guidance are gratefully acknowledged.

We express our sincere gratitude to EC, PSC, TCC and HOD of NMEDT for awarding us this project. Technical and Financial review by the GSI SU Uttarakhand is sincerely acknowledged. Administrative support extended by the State DGM, Government of Uttarakhand is highly acknowledged. We are indebted to Shri Binod Kumar, Dy. Director General (Retd.), GSI, the NMEDT nominated Peer Reviewer, for his critical review and recommendations.

Lastly, we express our sincere gratitude to the local administration, forest officials and the villagers in and around the Matena-Sirar area of Uttarakhand for their cooperation, logistical assistance and steadfast support during the fieldwork, which was instrumental in the successful completion of the project.

2.9 Summary of work strategy and report writing:

Almora Block Exploration Workflow: The systematic execution of the project workflow is illustrated in the figure (Figure 2.1) below, highlighting the sequential stages from planning and field investigation to data analysis and reporting.

i. Review of legacy data.
ii. Large Scale Mapping (LSM, 1:12,500 scale)
iii. Detailed geochemical characterization (by XRF, ICPMS and FCC analyses) of graphite schist / black-shale units, along with validation of vanadium enrichment within the carbonaceous horizons.
iv. Subsurface studies including shallow geophysical methods (SP and Resistivity)
v. Trenching and pitting to delineate drilling targets.

The project work provides the following outputs:

i. An updated geological map.
ii. Channel and stream/bedrock geochemical datasets
iii. Graphite crystallinity analyses (by XRD and Raman Spectrometry)
iv. Self Potential (SP) and Vertical Electrical Sounding (VES) anomaly maps
v. A prioritized list of targets for subsequent core drilling and exploration. The targets are also tested through scout drilling.

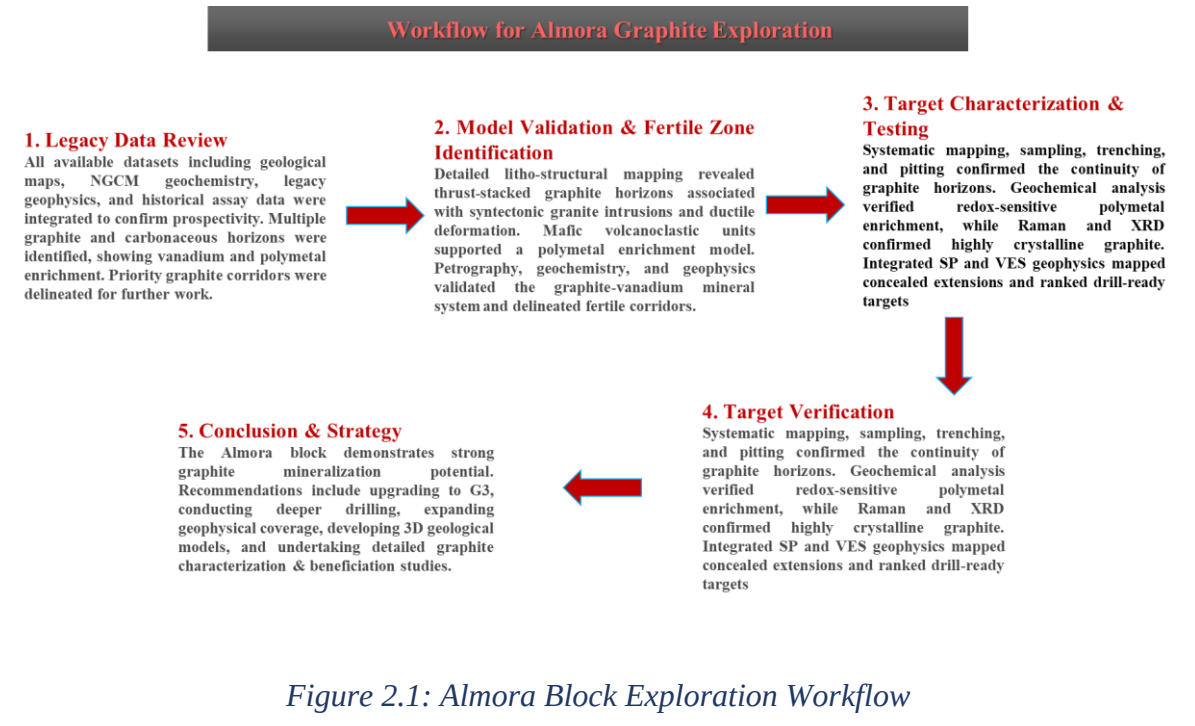

Figure 2.1: Almora Block Exploration Workflow

Detailed Report Structure:

A comprehensive overview describing the project rationale, geological and tectonic setting, exploration strategy, nature and extent of work carried out, geological and geochemical outcomes, identification of graphite-vanadium bearing zones, geophysical data analyses, metallogenic interpretation, target prioritisation, drilling findings and recommended forward exploration strategy leading to upgrading.

- Chapter 1. Executive Summary.
- Chapter 2. Introduction: Project background, objectives, methodology overview (including the exploration workflow) and administrative details.
- Chapter 3. Property Description: Location and accessibility, description of the project location, accessibility, climate, physiography and archaeological site present in the block.
- Chapter 4. Previous Work: Regional geological setting of the project area, summary of known mineral occurrences and previous explorations in and around the project area and analysis of NGCM geochemical data. This chapter establishes the exploration rationale and explains why the project area was selected.
- Chapter 5. Geoscientific Activities: Methodological record of the Almora Graphite Exploration Programme: Process description, SOPs, QC protocol adopted, data

collected, annexures listing, point to analytical description: a) Remote Sensing, b) Geological - structural mapping, c) Surface Sampling - grab, stream sediment, channel sample, pitting and trenching, d) Geophysics - SP, VES, e) Petrology, f) Raman spectrometry, g) XRD, h) Chemical Assay (XRF, ICPMS, PA, i) Isodynamic heavies seperation) Drilling.

- Chapter 6. Geology, structure, metamorphism, mineral systems analysis.
- Chapter 7. Exploration data analysis: characterisation of graphite occurrence block wise: Discuss about five graphite blocks and its characteristics
- Chapter 8. Exploration by Scout Drilling: Discuss about drilling process and 12 boreholes in Almora G4 block and its geochemical result.
- Chapter 9. Exploration Target Potential: Almora Graphite Blocks
- Chapter 10. Conclusion and Reccomendation.
- Chapter 11. Expenditure.
- Chapter 12. References.
- Chapter 13. Locality Index.
- Chapter 14. Annexures.

Chapter 3

Property Description

3 Property Description:

3.1 Location and Accessibility:

The project area (hereafter named as the Almora block) is situated within the Almora District, Uttarakhand state, is part of the Survey of India toposheet 53O/10. The bounding coordinates are: Latitude 29.59650189 to 29.67419714°N and Longitude 79.64906903°E to 79.75000285°E (Figure 3.1). The block is a part of the Almora Crystallines of the Inner Lesser Kumaon Himalaya and is characterized by undulating to steep.

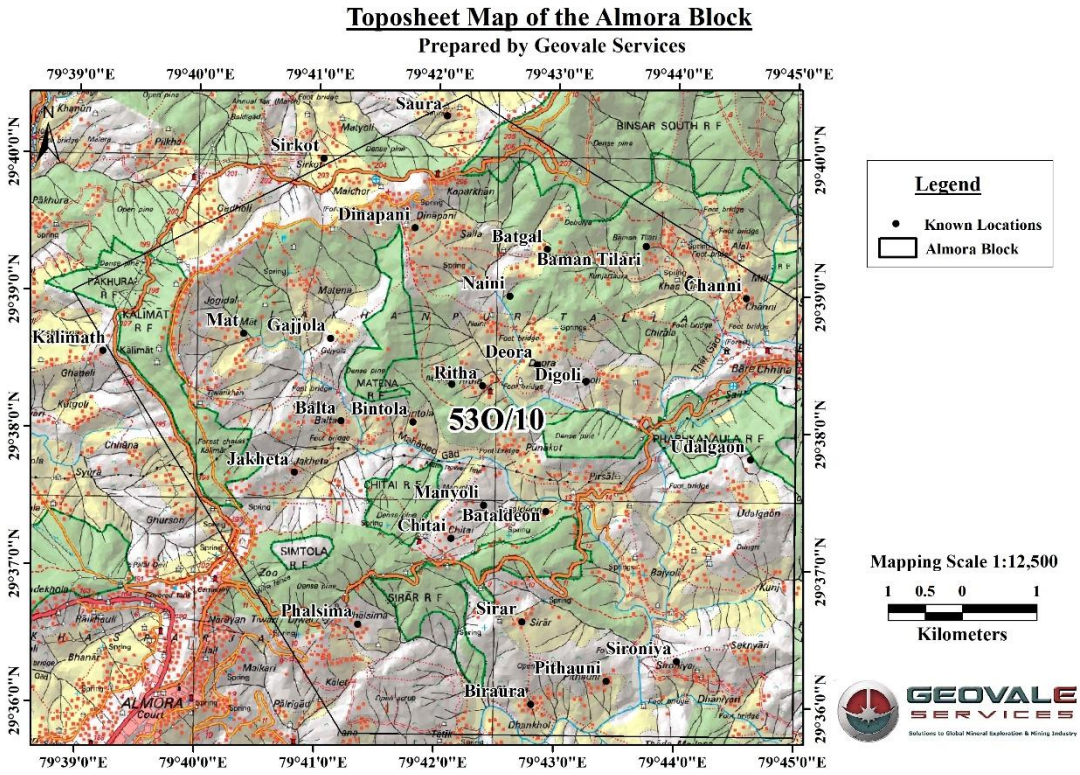

Figure 3.1: Location map of Almora Block (G4 Stage) on SOI Toposheet 53O/10

Accessibility to the block is feasible through multiple modes of transport.

By Road: The block area is approximately 30-40 km from Almora town and can be reached via well-connected with major cities such as Haldwani, Kathgodam and Ranikhet, using the NH-109 and state highways. From Almora, the site is accessible via the Almora-Dwarahat or Almora-Ranikhet roads, with several village tracks leading toward the various part of the block, particularly near northern part (Kalimath). In the block, NH 309A, is present in the western part of the block connecting Kalimath, Sirkot areas while NH 309B is situated

in the center part of the block connecting Phalsima, Sirar, Udalgaon areas. Manyconneting road from these two NH joins the other area of the block.

By Rail: The nearest major railway station is Kathgodam, located approximately 100-110 km from the block. Kathgodam serves as the principal railhead for the Kumaon region and maintains direct rail links with major cities including Delhi and Lucknow, thereby facilitating transportation of manpower and material. From Kathgodam, the journey to Almora and onward to the block can be completed by road in 3-4 hours via Car or Bus.

By Air: The closest airport is Pantnagar Airport, about 125-130 km from the site, which mainly offers flights to and from Delhi. Alternatively, Dehradun's Jolly Grant Airport, approximately 300 km away, serves as a more prominent air travel with wider connectivity. From both airports, the remaining distance is covered by road.

In addition, On Helipad, situated in the block near Tatik area, in the Almora block (Figure 3.2). Helicopter connectivity operates between Haldwani and Almora, significantly reducing travel time across mountainous terrain. Similarly, helicopter services between Pithoragarh and Almora facilitate inter-district coordination within the Kumaon region. These aerial services provide an important alternative mode of transport when road connectivity is temporarily disrupted due to landslides or extreme weather conditions.

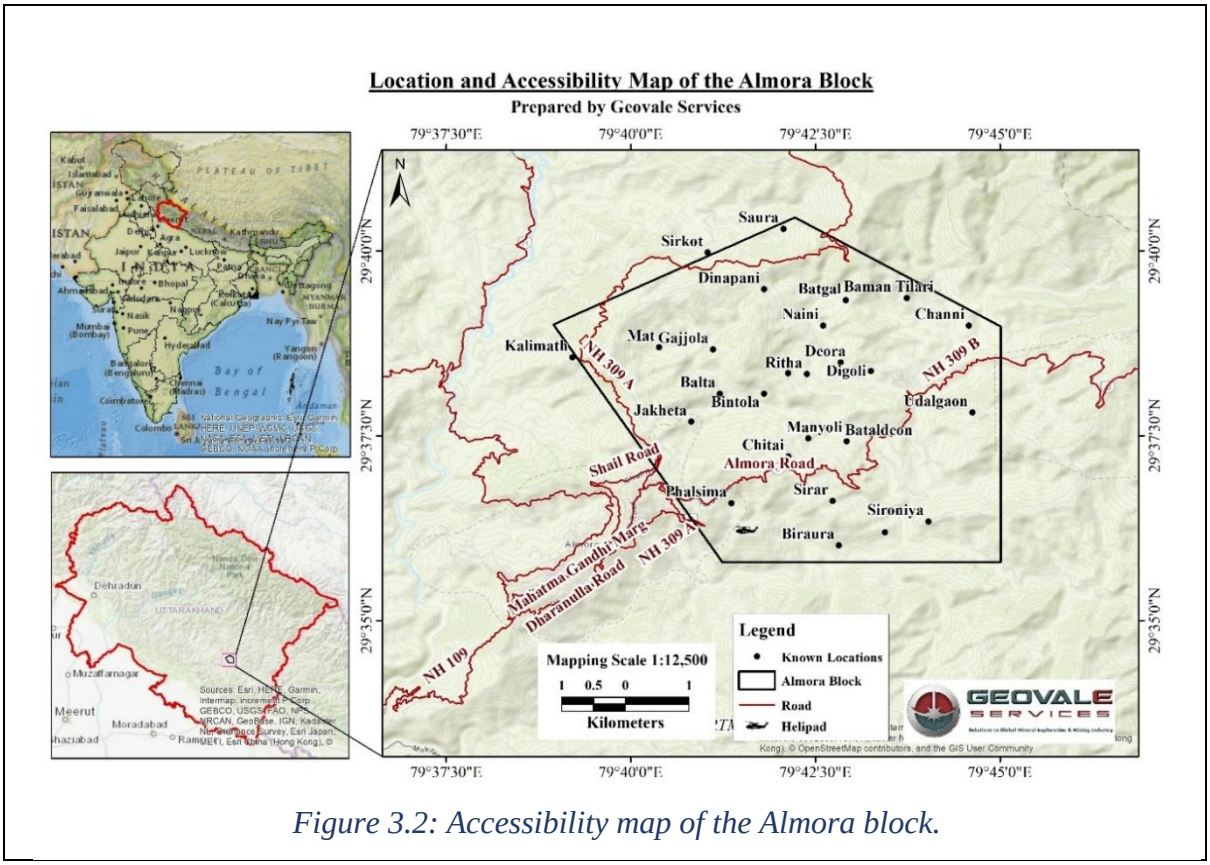

Figure 3.2: Accessibility map of the Almora block.

3.2 Topography:

The Almora area is characterized by rugged and undulating mountainous terrain (Figure 3.3) typical of the Himalayan belt, with prominent ridge systems, steep hill slopes and narrow intervening valleys. The overall topographic expression reflects intense tectonic activity and prolonged denudational processes that have produced the present geomorphology of the region (*Valdiya, 1980*).

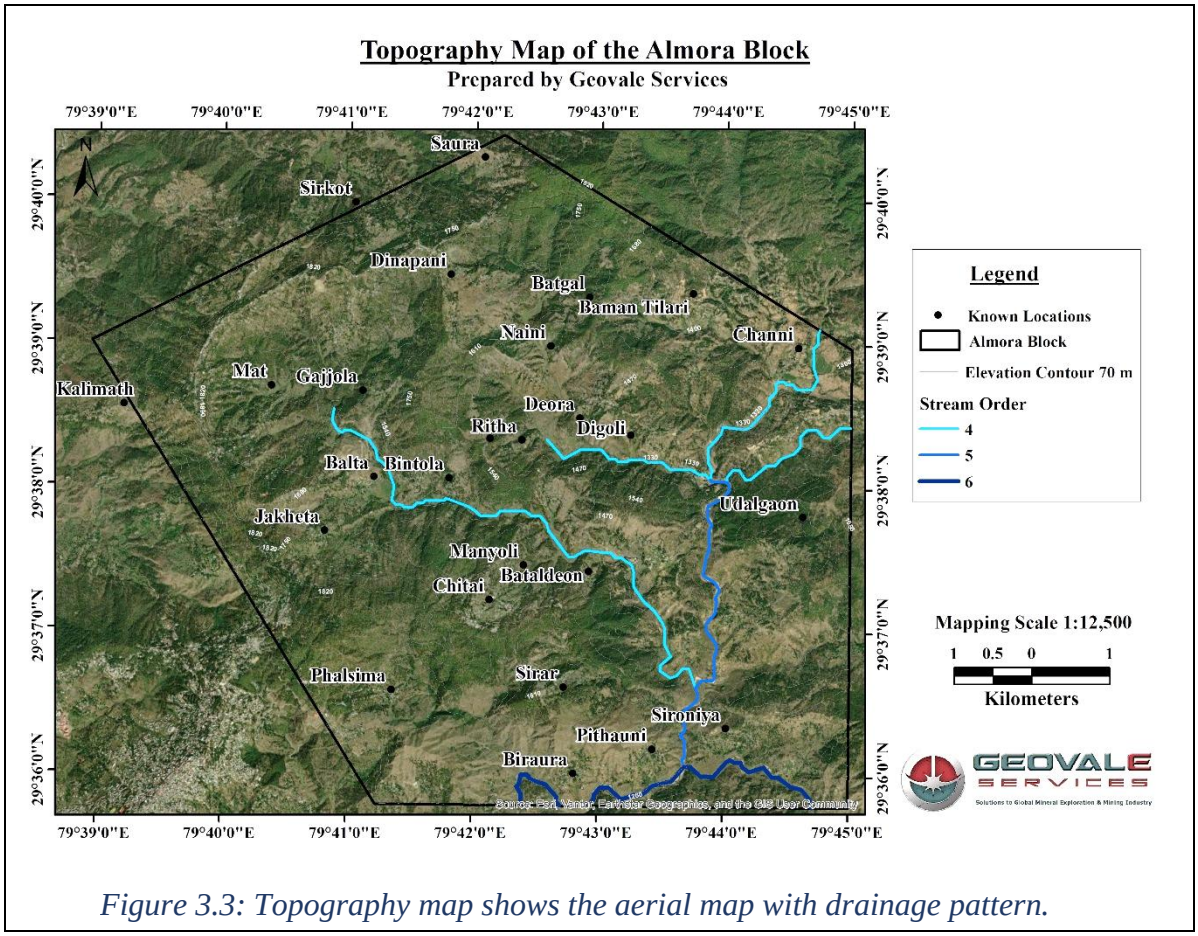

Figure 3.3: Topography map shows the aerial map with drainage pattern.

Elevation within the block varies considerably, generally ranging between 1,200 m and 1,800 m above mean sea level, though local variations may occur depending on ridge crest and valley positions. The relief is moderate to highwith slopes are predominantly moderate to steep (15°-35° or more at places), particularly along ridge flanks and escarpments, whereas gentler slopes are observed near habitation zones, river sides and terraced hill sections.

The topography exhibits a predominantly NW-SE to WNW-ESE ridge alignment consistent with the regional structure of the Almora Crystalline Zone of the Kumaon Himalaya (*Valdiya, 1980*).

3.3 Climate:

Almora, located in the Kumaon Himalaya of Uttarakhand at an elevation of around 1,638 meters above sea level, exhibits a pleasant mountain climate.

Temperature and Seasonal Variability: Summers (March to June), temperature ranges 15°C to 30°C and dry conditions. The monsoon season (July to September) brings temperatures

down and ranges 15°C to 25°C. Winter (November to February) is cold, with temperatures ranging from 1°C to 15°C, sometimes dropping below freezing.

Humidity and Wind Condition: Almora remains dry in winter, with humidity between 30%-40% while monsoon month experienced high humidity levels (80%-90%). Winds are generally mild to moderate, though winter months can have cold, dry breezes that increase wind chill in higher elevations.

Rainfall and Hydrological Impact: Annual rainfall ranges from 1100 mm to 1300 mm, concentrated during the monsoon season.

3.4 Flora and Fauna:

Almora district, exhibits a distinct altitudinal and habitat gradient that produces a varities of vegetation and associated fauna across relatively short distances. Lower slopes and warmer area are commonly occupied by subtropical chir-pine (*Pinus roxburghii*) (Figure 3.5, Figure 3.6), mid-elevations support broad-leaved temperate forests dominated by banj oak (*Quercus leucotrichophora*), *Quercus floribunda*, *Rhododendron arboreum*, *Acer* spp., *Eriogonum niveum (*Figure 3.4*)* and *Alnus nepalensis* and higher ridges carry sub-alpine shrubs and meadows. This zonation is strongly influenced by various parameters including soil depth and local land use (terraced agriculture, orchards and village woodlots) etc. (*Champion and Seth, 1968; Singh and Singh, 1992*).

The botanical wealth of Almora includes a large suite of medicinal and ethnobotanically important species that local communities have used for generations; regional surveys document on the order of 150-200 traditionally used species spanning many families (e.g., *Berberis aristata*, *Myrica esculenta*, *Centella asiatica*, *Acorus calamus*, *Urtica dioica*), which supply remedies, food, fodder, fuelwood and small-scale income (*Kumari et. al., 2011*). Beyond direct economic uses, intact broad-leaved forests-especially oak stands-perform critical ecosystem services in the Almora landscape: stabilizing slopes, enhance soil development, reducing soil erosion, retain moisture and sustain perennial springs and small streams that are the main source of village water supplies and agricultural land. (*Singh and Singh, 1992*).

Almora area has higher vertebrate diversity, including Himalayan mammals such as Himalayan black bear (*Ursus thibetanus*), goral (*Naemorhedus goral*), barking deer (*Muntiacus* spp.), leopard (*Panthera pardus*) and a range of smaller carnivores (martens,

civets), primates and rodents. Avifauna is rich and varied: pheasants (e.g., Kalij, Koklass) and montane passerines, woodpeckers, nuthatches and raptors are well represented where mature trees and structural heterogeneity persist. Reptiles and amphibians are moderately presented, typically associated with moist microhabitats, streams and terraced agricultural margins (*Rodgers and Panwar, 1988*).

Figure 3.4: Snow Buckwheet plant in Sirar area

Figure 3.5: Chir-pine forest at Sirar area

Figure 3.6: Chir-pine forest at Bataldeon area.

3.5 Forest Cover:

The Almora block is characterized by significant forest cover (approx. 19.26 sq. km. area) is governed by altitude, slope gradient, aspect and climatic conditions, resulting in a heterogeneous pattern of moderately dense to open forest patches scattered with revenue land and agricultural terrace.

As per the latest assessment by the Forest Survey of India, Uttarakhand is one of the most forest-rich states in India (Figure 3.7). The forest cover in and around the Almora Block are classified as Reserved Forest (RF), Open Forest area, Civil Soyam Forest (CSF), and Van

Panchayat lands. The block area is characterized by moderately dense forest (canopy density 40-70%) along mid-slope zones and open forest (canopy density 10-40%).

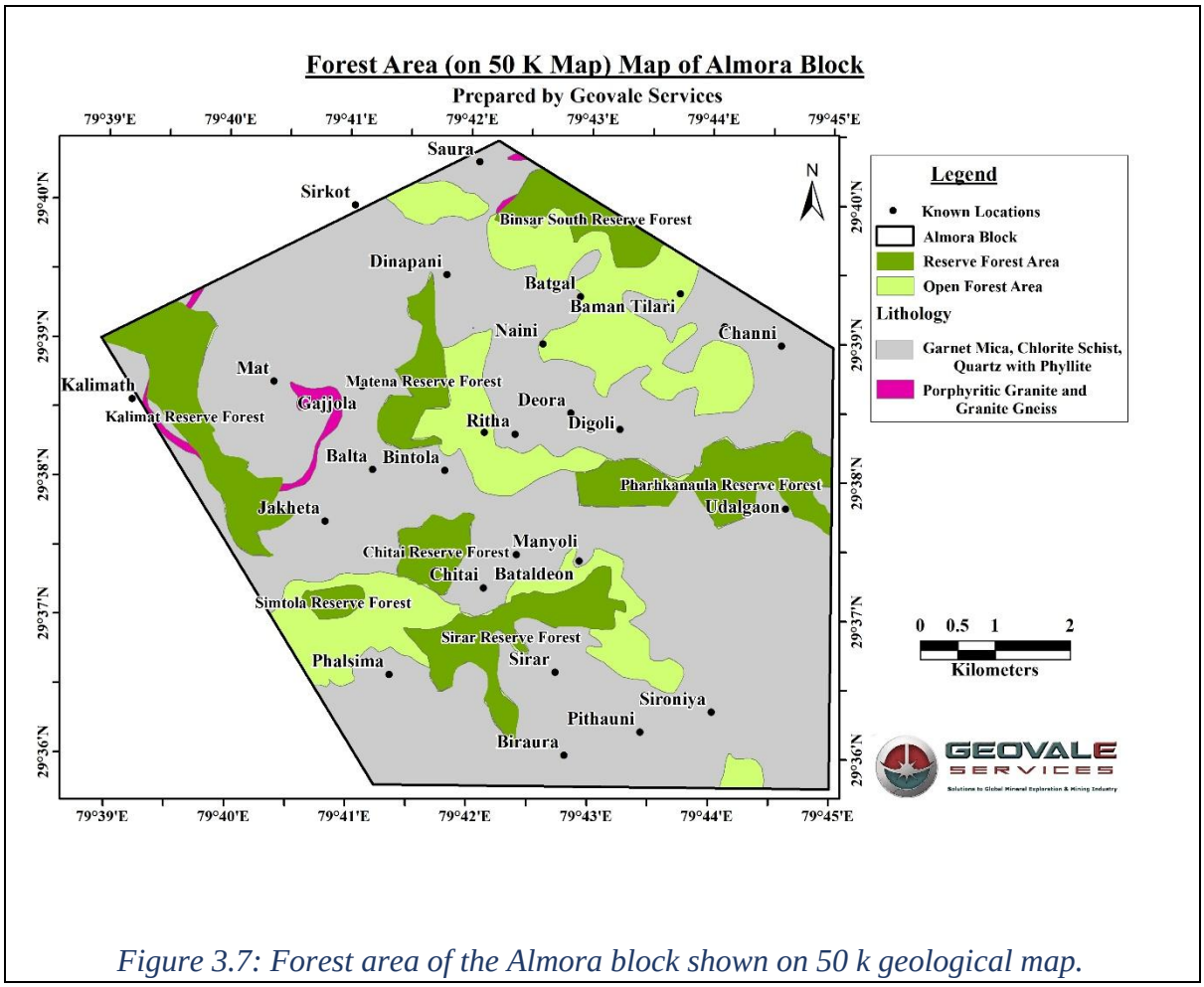

Figure 3.7: Forest area of the Almora block shown on 50 k geological map.

3.6 Archaeological site:

A Painted Rock Shelter of the early man stone age time is situated in the Lakhudiyar area (29.62° N and 79.67° E), in the northern part of the Almora block (Figure 3.8). The rock shelter is, used as a natural rock shelter by the stone aged human to prevent themselves from natural disaster. In this cave, human figure, trees, animal, hunting scene, geometric lines were made by them with red, black, white colour are also observed.

Geologically, the cave is developed within quartzite and schist formations of the Lesser Himalaya, forming natural rock shelters that have preserved the paintings over time. The surrounding area is characterized by hilly terrain with moderate to steep slopes. Due to its archaeological importance, the site is protected under the Archaeological Survey of India and should be treated as a restricted zone for any exploration activities (Figure 3.9, Figure 3.10).

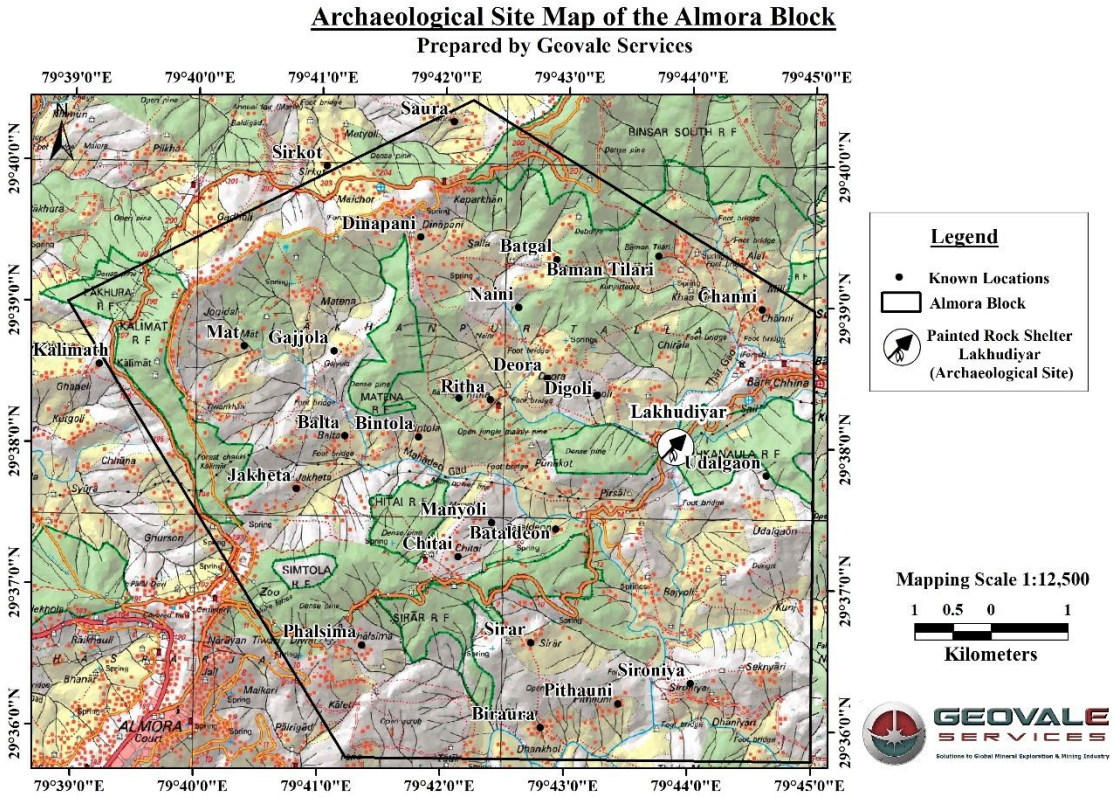

Figure 3.8: Topography map shows the presence of Lakhudiya Archaeological site, Almora Block.

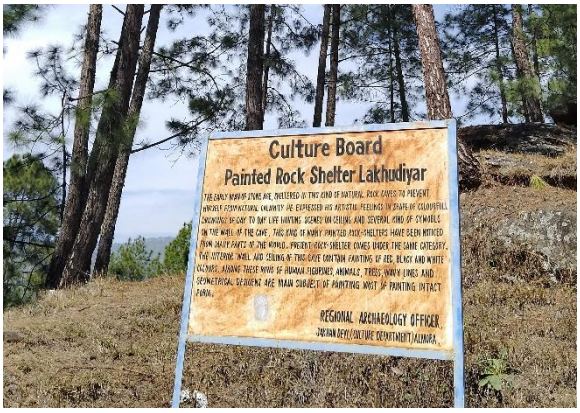

Figure 3.9: Culture board from Archeological site given details about Lakhudiyar rock shelter, Almora.

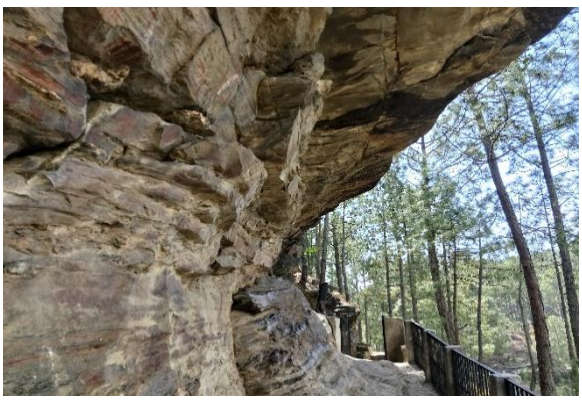

Figure 3.10: Rock shelter in Lakhudiyar cave, the Archeological site, Almora.

3.7 Satellite Remote Sensing data acquisition and processing:

3.7.1 Lineament map:

The lineaments drawn on Shuttle Radar Topography Mission (SRTM) imageries of the Almora block are of different orientations. The most prominent being the NE–SW trending lineaments in the north-western part of the block, near Jhaketa and Mat areas. Besides, two prominent NW–SE trending lineament zones are present in the block-one located in the southern part, along Sironiya-Sirar area and another in the north-eastern part of the block, along Udalgaon-Digoli area. A few N–S and E–W trending lineaments are also present in the Almora block (Figure 3.11).

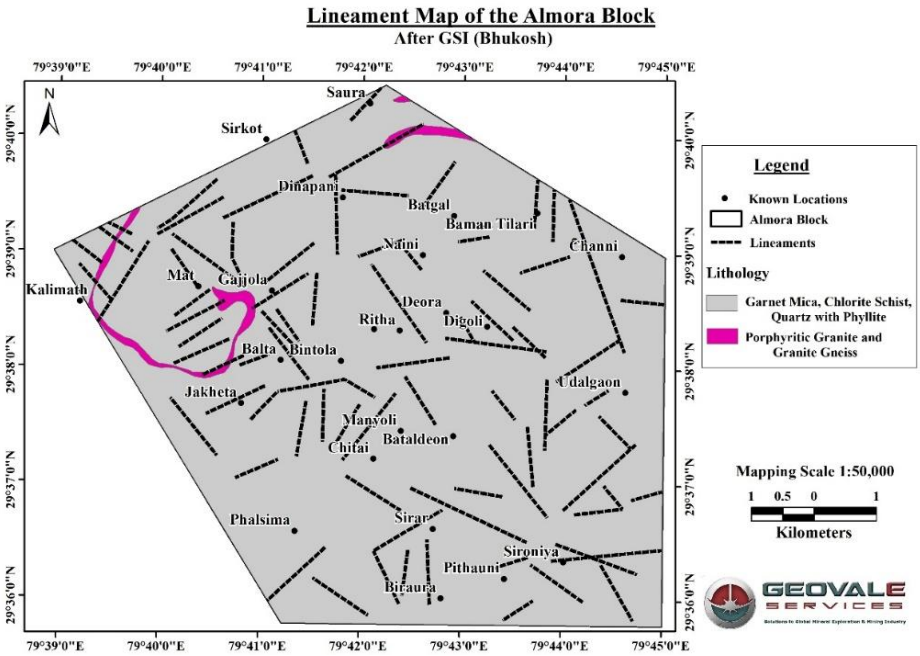

Figure 3.11: Lineament map of the Almora block shows various orientation of lineaments.

3.7.2 Elevation map

The elevation map of the Almora block has been prepared using SRTM-DEM data (Figure 3.12). The area is characterized by an elevation range from ~700 m to 2400 m, indicating a faily high-relief, undulatory topography with rugged and dissected terrain comprising mountainous to hilly landscapes.

Based on elevation, the area can be broadly divided into two parts:

(i) Elevated zone (1500–2400 m), mainly occupying the north-western part of the block; (elevation between 1700 m and 1900 m, form a curved pattern extending from Phalsima

through Sirkot towards Saura). Another N-S trending linear belt of similar elevation (1700–1900 m) is observed to the west of the Mat area.

(ii) Moderately elevated zone (700–1500 m), present in the south-eastern part of the Almora block (around Udalgaon, Sironiya and Pithauni areas), with elevations ranging between 700 m and 1100 m occurring along the river bank areas.

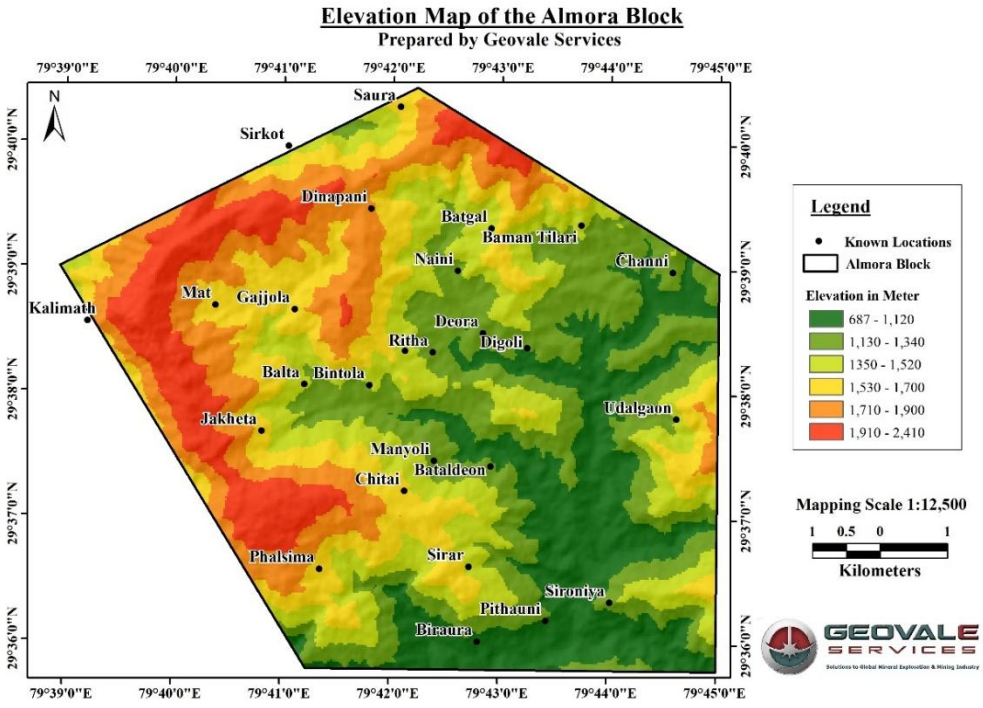

Figure 3.12: Elevation map of the Almora blocks show western part is more elevated than the eastern part.

3.7.3 Contour Map:

For use of ground mapping, a contour map of the Almora block and surrounding area was prepared from SRTM-DEM data by generating 30 m interval contour lines representing elevation variations across the terrain (Figure 3.13).

Closely spaced contour lines, indicating steep slopes, are generally observed in the western part along Phalsima and Kalimath; and northern parts along Sirkot, Saura and Baman Tilari area. Additionally, two major steep slopes which are exhibit almost NW–SE linear trends (detected by joining closely spaced contour lines) are present in the central (near Bintola area) and southern parts (near Pithauni-Phalsima areas) of the block.

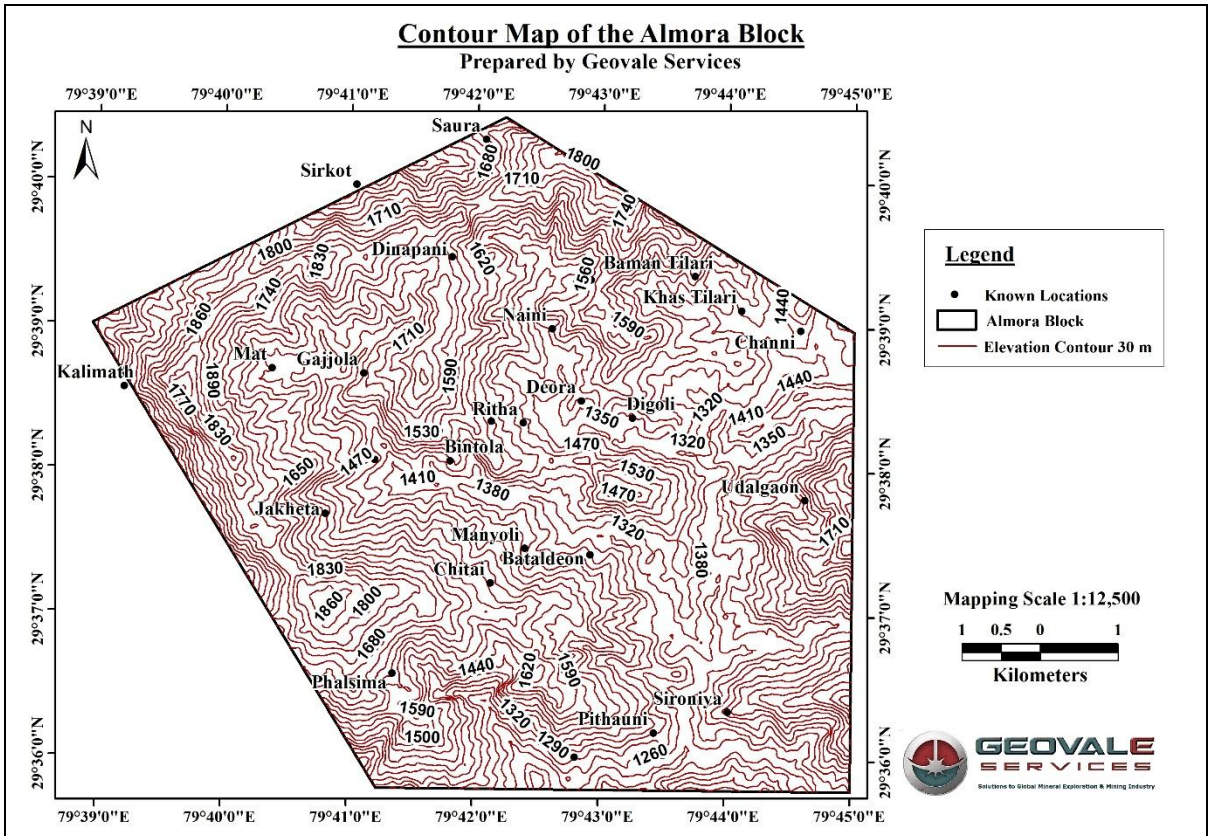

Figure 3.13: Contour map of the Almora block shows higher elevation in the western part than the eastern part.

3.7.4 Slope Map:

The slope map has been prepared using SRTM-DEM data (Figure 3.14).

The map categorizes the terrain's steepness into five distinct classes:

a) 0 – 10° (Light Green): These represent the gentlest slopes, generally found in the central part of the block, in valley floors and along a N-S trending river bank area present in the eastern side of the block and along a E-W trending river bank in the southern part of the block.

b) 11 – 20° (Dark Green): Areas with slightly more inclination but still considered relatively mild terrain. Generally, found in the central part of the block, around the gentle slope.

c) 21 – 30° (Yellow): These are moderate slopes that often serve as transitional zones between flatlands and steeper ridges.

d) 31 – 40° (Light Red): These represent steep slopes, indicating more rugged and challenging terrain.

e) 41 – 54° (Deep Red/Brown): These are the steepest areas within the study site, likely representing sharp ridges, escarpments, or cliff-like features. Predominantly observed in the

western part of the Almora block, along Phalsima, Kalimath and Chhana area; and northern parts along Sirkot, Saura and Baman Tilari area.

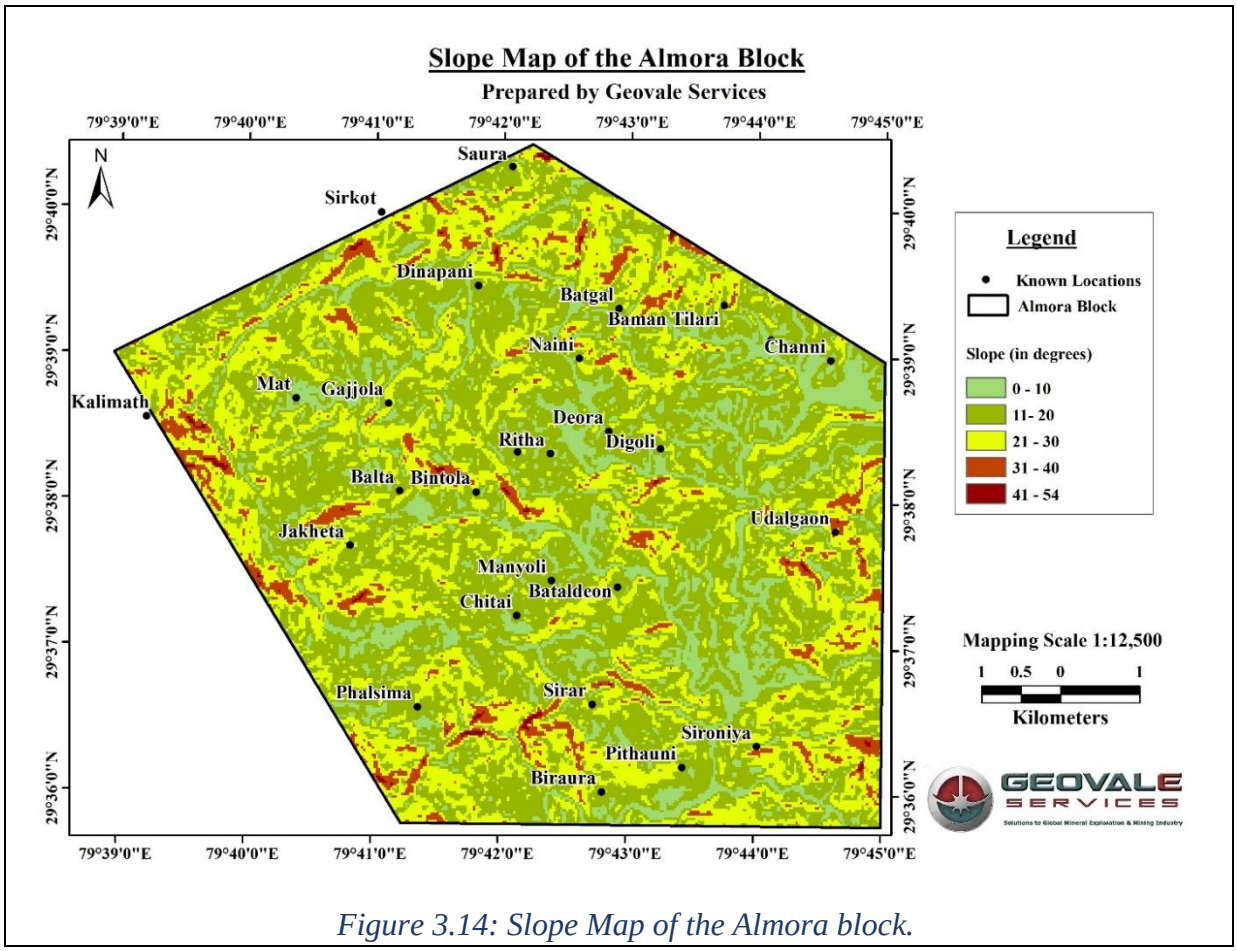

Figure 3.14: Slope Map of the Almora block.

3.7.5 Hillshade Map:

Hillshade, a shading technique, adds depth and dimension to maps by creating a 3D-like representation of the terrain (Figure 3.15). On the hillshade map, the steeper parts of the terrain are visually represented by areas of intense contrast, where deep shadows immediately follow bright highlights. This visual pattern indicates the presence of the sharp ridges and narrow, deep valleys.

Based on the Almora block hill-shade map, the following things are observed:

a) In the north-eastern part of the block, between the Gadholi and Saura area, the NE-SW trending dense network of high-relief ridges (i.e. deep shadows immediately follow bright highlights) are present, indicating very rugged and steep slopes.

b) The south-eastern region: Near Saknyari villages, the hillshading becomes particularly dark and complex, suggesting a highly dissected landscape with steep gradients. From Sironiya

to Sirar, a prominent NW-SE trending dark linear hillshade is present, indication of NW-SE trending sharp ridges.

c) In the western flank of the Almora block, the terrain surrounding Gadholi, Chhana and Phalsima villages exhibits light-and-dark shifts, marking the steep descent from ridges into the valley systems.

d) In the central part of the block, another WNW-ESE trending sharp hill shade is present implying sharp ridges. Incidentally, this WNW-ESE trend corresponds with our interpreted major thurst planes.

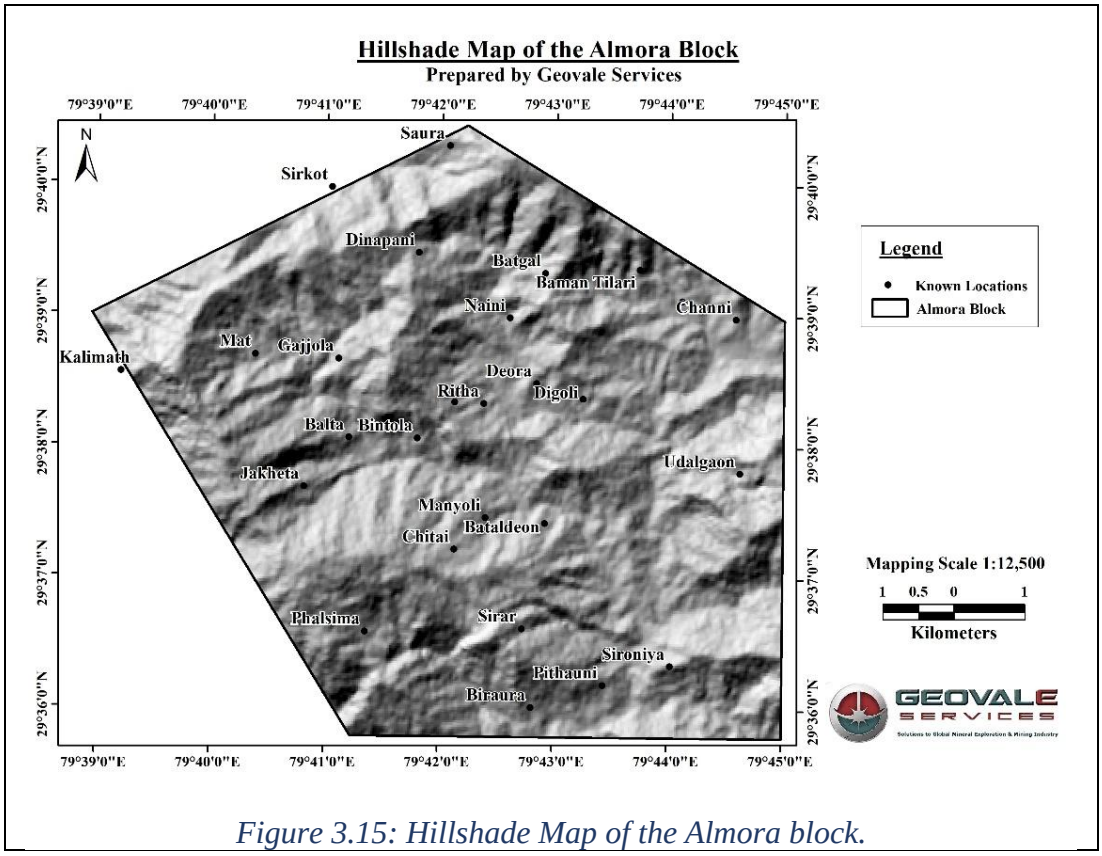

Figure 3.15: Hillshade Map of the Almora block.

3.7.6 Drainage Map:

The drainage map represents the stream order of a watershed, delimited by a block boundary. The drainage map for this region, also derived from SRTM-DEM data, illustrates a complex hydrological network classified by stream order.

The drainage map (Figure 3.16) of the Almora block and the surrounding displays a dendritic drainage pattern. The map categorizes streams based on Strahler's stream order classification ranging from order 1 to order 6.

a) Watershed Characteristics: The first-order and second-order streams are widely distributed throughout the block area, indicating dense drainage, especially in the northern and western parts near Gajjola and Chhana villages. In the western part of the block, near Gadholi and Chhana villages, the drainage is dominated by numerous 1st and 2nd-order streams that flow down from the high ridges identified in the hillshade map. The central area around Deora and Bataldeon is highly dissected by 3rd and 4th-order streams.

b) Major Tributaries: A prominent 5th-order stream runs longitudinally, through the eastern portion of the block, flowing south from the area between Udalgaon and Sironiya villages to join the main 6th-order channel near Biraura and Saknyari villages.

c) Main Stream: The most significant feature is a 6th-order stream (the highest order on the map) that flows along the southern boundary of the Almora block, where Swal Nadi moving generally towards west and Suwal Nadi moving towards eastern part of the map.

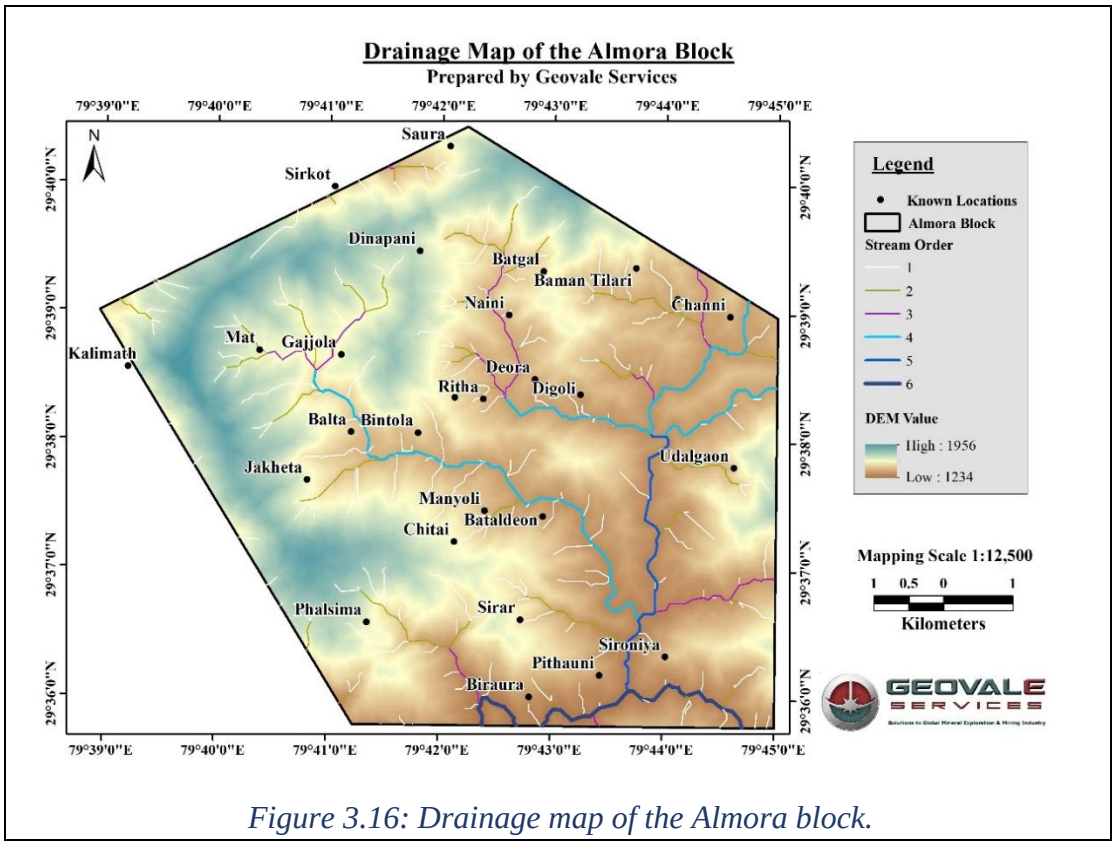

Figure 3.16: Drainage map of the Almora block.

3.7.7 RED Scheme Mapping:

The RED (Residual, Erosional, Depositional) scheme landform map (Figure 3.17) represents a detailed geological analysis of a project area in Almora, Uttarakhand.

i. Highly dissected structural hill and valley: Dominated in the Almora block. Mineral-rich zones are interspersed within the erosional lands, appearing most prominently in the north-western and southern part of the block.

ii. Depositional Landforms: These zones in the block including piedmont alluvial plains and younger alluvial plains, are areas where sediment accumulation occurs due to fluvial processes, mainly present in the eastern side of the block. Such regions could potentially support agriculture due to the nutrient-rich sediment and they often mark lower-lying, relatively stable lands. These depositional zones indicate past or current river activity that contributes to soil fertility.

iii. Rivers: The rivers and streams dissecting the area are essential for drainage and groundwater recharge. They likely influence soil moisture and could contribute to fluvial deposits in the alluvial plains. The river network also plays a role in the erosional dynamics of the surrounding landscape.

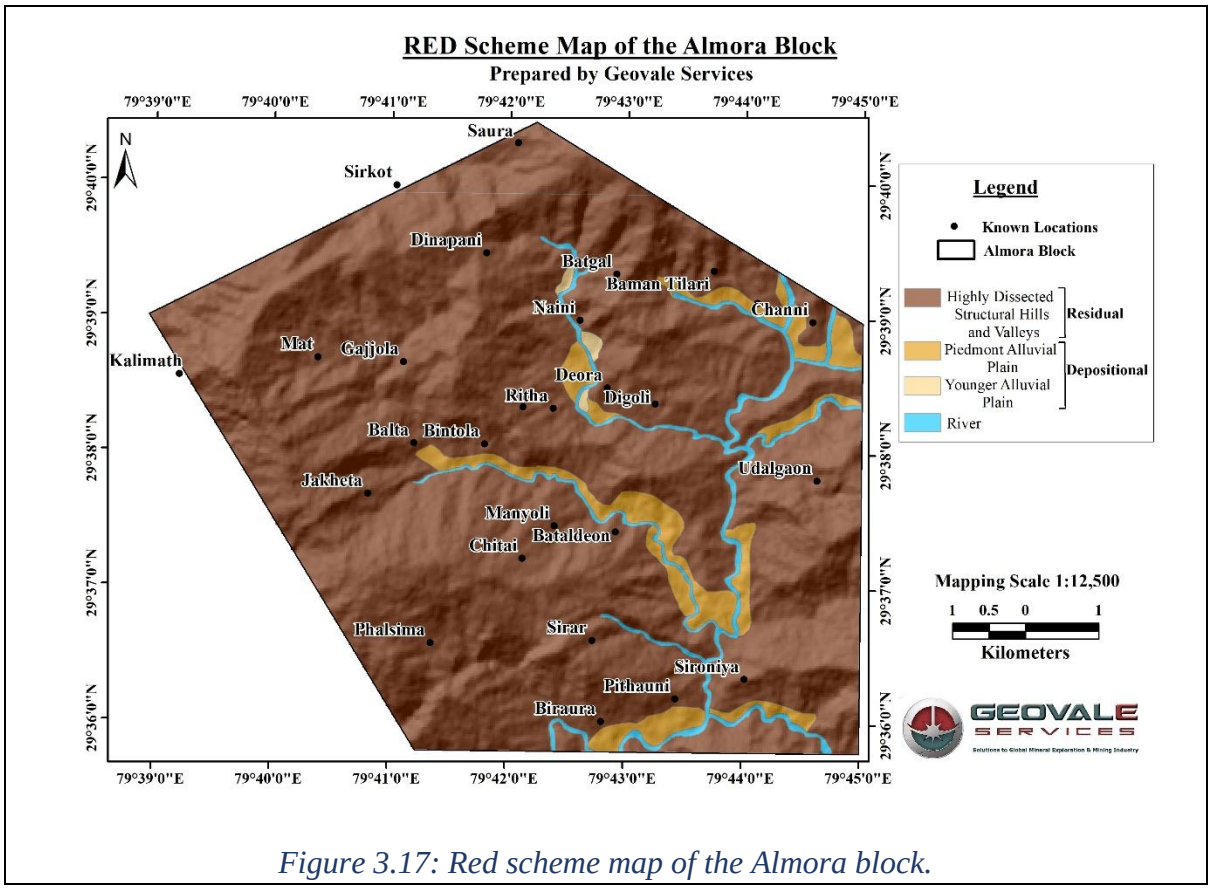

Figure 3.17: Red scheme map of the Almora block.

3.7.8 Land Use and Land Cover (LULC):

The LULC map shows the Land Use Land Cover (LULC) classification prepared using Sentinel 2A multispectral imageries for block area, delineated by boundary points A-B-C-D-E (Figure 3.18). The map classifies the area into five major categories: Water Bodies, Vegetation, Cropland, Built-up areas and Rangeland.

a) **Vegetation:** The dominant category across the block is Vegetation (green) with 267.94 sq. km., indicating that most of the area is covered with forests or dense natural vegetation. Significant patches of Rangeland (gray) are also observed throughout the region, particularly in the northern and central parts, suggesting areas with sparse vegetation, grasslands, or degraded land.

b) **Cropland and Agricultural Activity:** The Cropland areas (yellow) occuping 34.87 sq. km. are prominently concentrated around the central, north-easternand southern parts of the block near villages such as Deora, Bataldeon, Sirar, Saknyari and parts near Phalsima and Baman Tilari. These areas suggest the presence of active agricultural fields, likely serving as key agricultural zones for the local population. The spatial distribution of cropland near settlement areas indicates the strong dependence of the community on agriculture for livelihood.

c) **Built-up Areas and Human Settlements:** Spans 40.41 sq. km., the Built-up areas (red) are mainly clustered near village locations such as Saura, Gadholi, Chhana, Phalsima, Baman Tilari, Deora and Sirar. These areas represent settlements, roads, or other infrastructural developments. The distribution of built-up zones shows that settlements are scattered throughout the region, generally surrounded by cropland and vegetation, reflecting a typical rural settlement pattern.

d) **Water Bodies and Hydrological Features:** Small patches of Water Bodies (blue) covering 0.0018 sq. km. are present in limited areas, mostly along stream courses or valleys. These water bodies are minimal in extent but play an essential role in supporting local agriculture and daily needs. The limited extent of water bodies also suggests a relatively dry region with dependency on seasonal streams or groundwater resources.

e) **Rangeland:** The rangeland (Grey) area covers 196.86 sq. km., indicating open land or areas used for grazing. This class is widespread, particularly in the northern, central,

southern and southwestern portions of the block, representing less developed or cultivated areas.

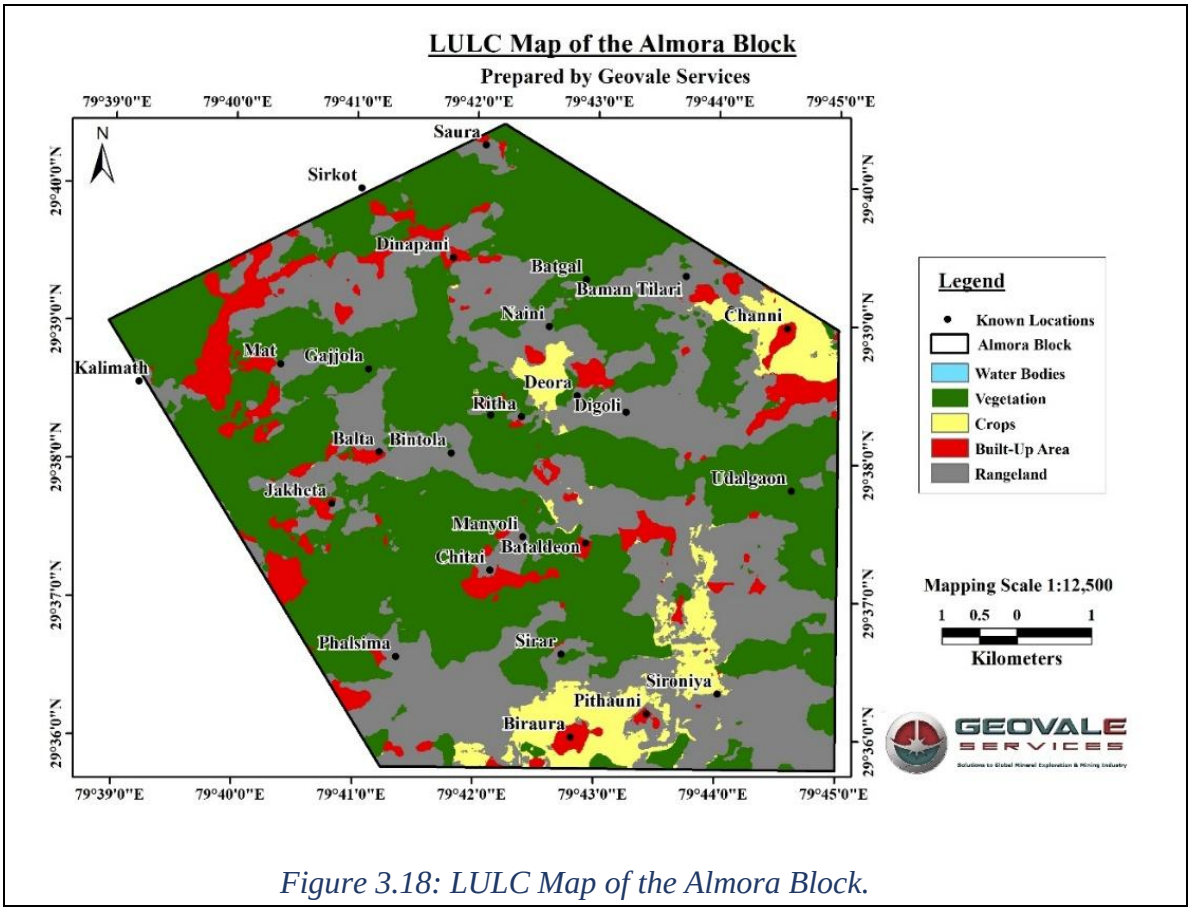

Figure 3.18: LULC Map of the Almora Block.

3.7.9 Alteration Mapping:

The alteration maps provided different mineralogical and lithological attributes in the Almora project area using satellite remote sensing data. By analysing band ratios and multispectral datasets, key mineral signatures- such as clays, ferrous minerals and iron oxides- are identified, which are indicative of hydrothermal alteration processes. These maps provide insights into the spatial distribution of altered zones and the types of mineral deposits in the area.

i. Clay alteration mapping:

The clay map highlights areas with significant clay mineral presence, typically associated with weathering and hydrothermal alteration. Using the band ratio for clay detection (such as ASTER bands 6/7 for kaolinite), the regions marked in yellow reveal areas likely to contain kaolinite and other phyllosilicate minerals. Clay minerals often indicate alteration zones related to low-temperature hydrothermal processes, which could signify the upper parts of mineralized sytems or sedimentary deposits (Figure 3.19).

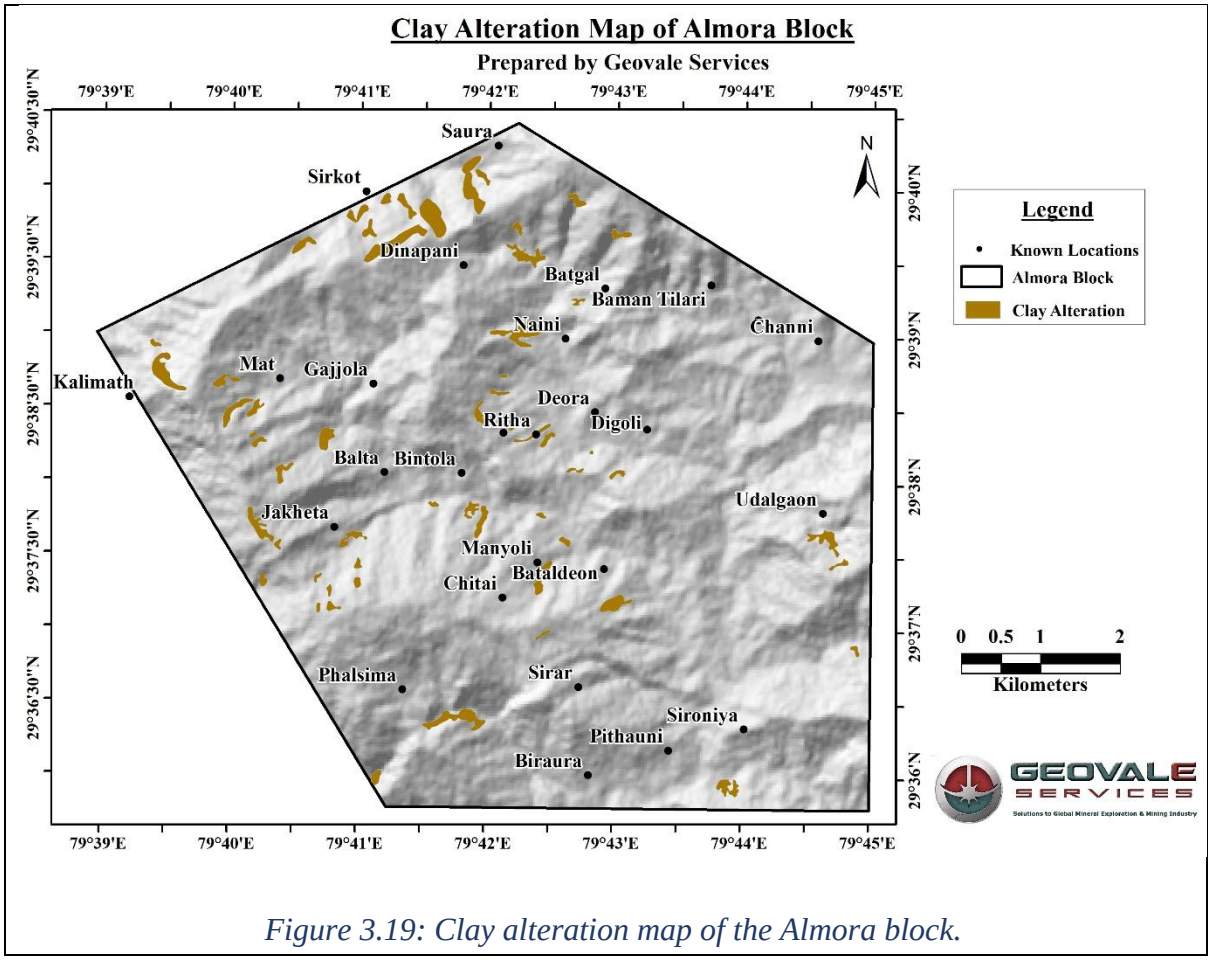

Figure 3.19: Clay alteration map of the Almora block.

ii. Ferrous alteration mapping:

The map illustrates regions with high ferrous mineral content, marked in red with hatching (Figure 3.20). Ferrous minerals, often detected through the use of bands sensitive to iron absorption and reflectance (such as ASTER's SWIR bands 4/5), point to areas with primary or secondary iron mineralization. The presence of ferrous minerals in these areas could be related to iron-bearing rock units or iron-enriched alteration zones, which are often valuable for exploring mineral deposits.

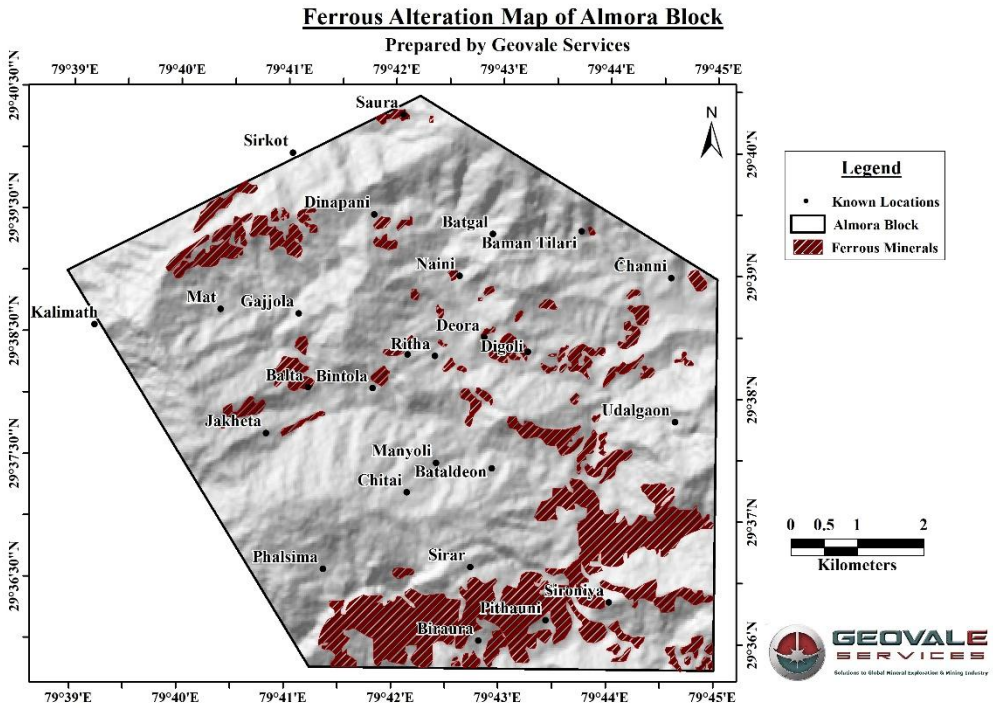

Figure 3.20: Ferrous alteration map of the Almora block.

iii. Iron Oxides alteration mapping:

The iron oxides map identifies zones with an abundance of hematite, limonite, or other oxidized iron minerals, marked in solid red. Iron oxides are typically detected using specific band ratios that highlight their distinct spectral signature, such as Landsat 8 band ratios 4/2. These oxides form in oxidizing conditions and can be indicative of supergene alteration zones or gossan formations, which serve as valuable exploration guides for underlying sulphide mineralization (Figure 3.21).

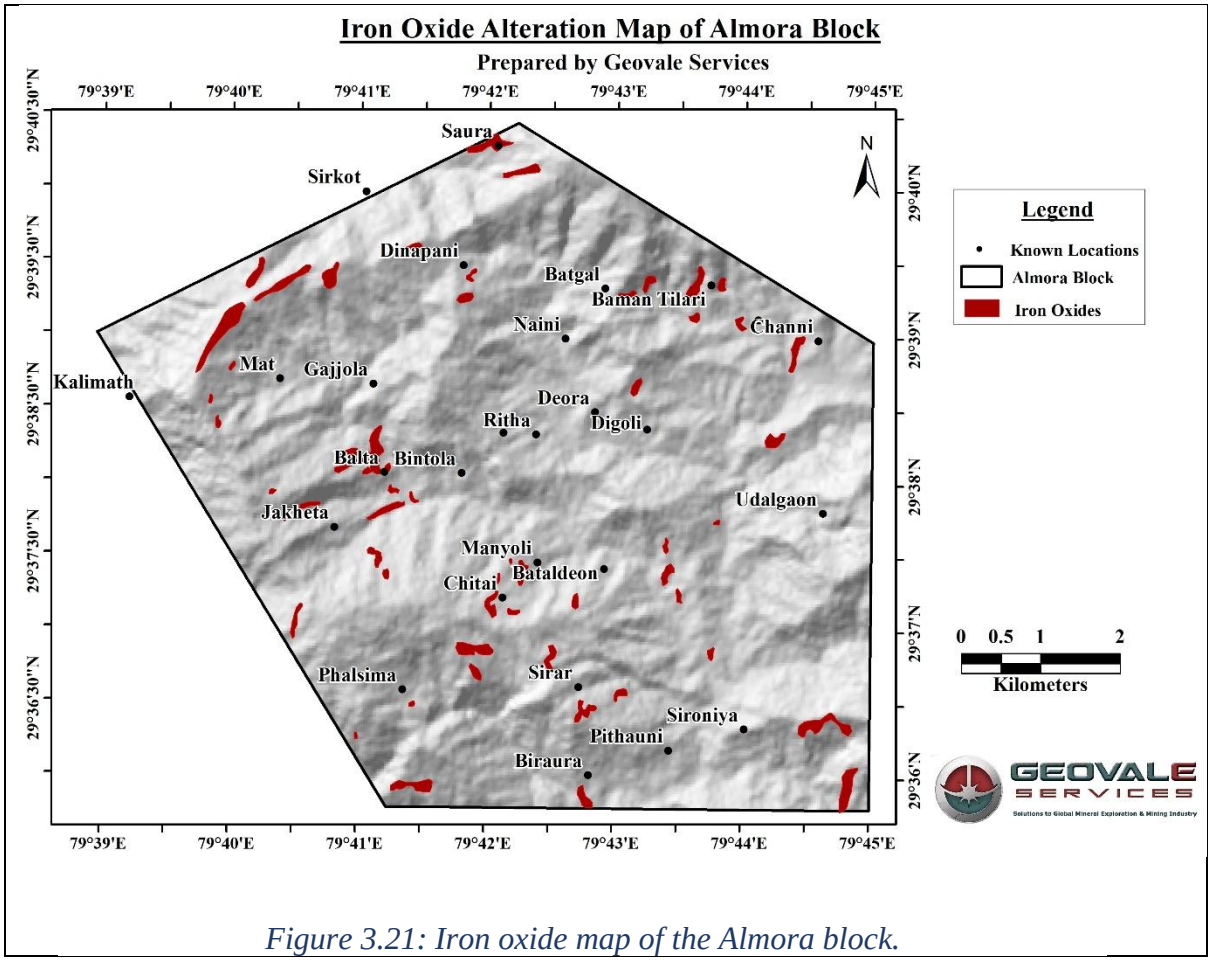

Figure 3.21: Iron oxide map of the Almora block.

3.8 Environmental, Social and Governance (ESG) framework and Mineability Considerations of the block:

The mineability of the Almora block cannot be evaluated based on the presence of graphite, its thickness, structure, and degree of continuity. Given the current Himalayan context, mineability is as much dependent upon environmental sensitivity, socio-economic conditions, legal status of land, geological stability, hydrological sensitivity, and operational feasibility of implementing planned surface mining activities without excessive disruption. It is already clear from the current report that the block occurs in a mountainous hill zone with extensive forest cover, abundant drainage network, varying soil cover, proximity to habitation, and an area of archaeological importance, whereas the completion of the exploration campaign also proves that controlled entry, trenching, geophysical surveys, and scout drilling could be feasibly undertaken in certain areas within the zone. Thus, the Almora block may be considered as a selectively mineable terrain subject to constraints.

3.8.1 Soil, Regolith and Overburden Conditions

The Almora block is characterized by typical Himalayan hill soils derived from metamorphic parent rocks, with shallow to moderate thickness, variable texture, moderate organic content under forest cover and strong spatial variation controlled by slope, lithology and drainage position. The mid-hill and settled sectors generally preserve comparatively thicker soil and colluvium cover, whereas ridge sections and steeper slopes tend to have thinner, erosion-prone soil mantles and better rock exposure. Such variability directly affects mineability because it governs stripping behaviour, pad preparation, trench stability, sediment generation and the volume of topsoil that would need to be preserved and reinstated during future works. In practical terms, areas with shallow stony soil on steep slopes are less favourable for large-scale disturbance, while gentler interfluves and colluvium-bearing slopes may offer comparatively better working ground, though with higher requirements for erosion and sediment control.

From an ESG perspective, soil in Almora is not merely an overburden unit but also a rehabilitation resource. Because the field SOP for excavation already requires replacement of topsoil after trenching and controlled site restoration, future mineability assessment should explicitly consider topsoil salvage, separate storage, slope-wise reuse and avoidance of unnecessary stripping in steep sectors. Thus, soil conditions in the block support only carefully managed and spatially selective ground disturbance, rather than indiscriminate surface development.

3.8.2 Surface Water, Springs and Drainage Sensitivity

Hydrological sensitivity is a major mineability control in the Almora block. The drainage interpretation (Figure 3.16) prepared from SRTM-DEM shows a dense dendritic system with widespread first- and second-order streams in the northern and western sectors, more dissected third- and fourth-order drainage in the central block, a prominent fifth-order stream in the east and a sixth-order master channel along the southern boundary. This means that even localized disturbance may transmit sediment, runoff and turbidity downstream if not tightly controlled. In a hill environment such as Almora, these drainage characteristics directly affect safe excavation periods, drainage diversion feasibility, erosion risk and the design of water-management systems for future mining.

Spring protection and riparian zones have been recognized as significant features in the Almora report's ecological portion and need to be safeguarded through buffer zone creation and minimal disturbance designs. Such considerations become highly pertinent when it comes to mineability since the factors that contribute towards ensuring water security such as spring

discharge and catchment health have direct links with the stability of the slopes and community well-being. Thus, hydrologically sensitive areas need to be designated as mitigation or no-go zones and mineability may be considered relatively better only if it does not disturb springs and drainage areas.

.

3.8.3 Slope Stability, Erosion and Geo-Hazard Sensitivity

Topography and slope (Figure 3.14) are among the strongest limiting factors on mineability in Almora. The terrain includes moderate to very steep hill slopes and the slope interpretation already identifies sectors with gradients reaching about 35.1° to 67.6°, especially in the north-western and south-eastern parts of the block, where erosion and landslide susceptibility are comparatively high. The hillshade and topographic interpretation further indicate sharp ridges, deeply incised valleys and strongly dissected hill terrain, all of which reduce the suitability of broad-scale excavation, waste placement and road widening. Such conditions do not rule out mineral development altogether, but they greatly increase the technical threshold for safe extraction.

The flora-fauna and forest sections reinforce this constraint by explicitly linking habitat degradation, unplanned infrastructure and slope disturbance with increased landslide susceptibility and spring failure. In terms of mineability, this means that the physically accessible portions of the block are not automatically the most developable ones; rather, the most favourable areas will be those where slope angle, exposure, access geometry and drainage can be managed together without materially increasing instability. Accordingly, future mine planning in Almora would need to be based on a stability-screened corridor approach, avoiding very steep slopes, ridge-edge cuttings and highly dissected sectors unless supported by detailed geotechnical justification.

3.8.4 Forest Cover, Biodiversity and Ecological Constraints

The Almora exploration block lies within a moderately to significantly forested Himalayan landscape that includes Reserved Forest, Civil Soyam Forest and Van Panchayat land (Figure 3.7). The report specifically notes that forest distribution is controlled by altitude, slope, aspect and climate and that the presence of forest can directly affect accessibility and operational planning. From a mineability standpoint, this is critical because forested sectors are not only ecologically sensitive but also legally and operationally restrictive. Any requirement for clearing for drilling pads, approach tracks, camps, or future mine infrastructure would be subject to statutory permissions and disturbance-minimization measures.

Ecologically, the report emphasizes that intact broad-leaved and mixed forest stands contribute to biodiversity conservation, water security and slope stability and therefore cannot be treated as neutral land. Exploration and future mining in such zones would require ecological baseline studies, buffer maintenance around springs and riparian strips, minimization of fragmentation and restoration using locally suitable species. This significantly affects mineability: areas with dense ecologically important forest cover may still be mineralized, but they carry a higher environmental cost, longer approval timelines and greater mitigation burden. Hence, ESG-based mineability ranking in Almora should classify forested target zones into permissible with mitigation, high-sensitivity and practical no-go categories depending on forest type, slope and ecological function.

3.8.5 Land Use, Habitation and Livelihood Sensitivity

The Almora block is not an empty mountain area; it is a living landscape, which is linked to village settlements like Matena, Falshima, Sirar, Deora, Balta, and Kalimath. Moreover, the descriptions of topography and soil reveal that gentler gradients and deeper soil layers near the settlement zones are also more accessible to human use.

The report's ecological discussion explicitly states that local livelihoods are closely tied to forest resources, water and ecological condition. The trenching SOP also requires prior communication with local communities, landowner consent and prompt rehabilitation. These are not only exploration-stage good practices; they are early indicators that future mineability in Almora will depend heavily on social licence, local acceptance and visible disturbance control. Therefore, areas close to settlements, terraces, community-use land, springs, or NTFP-use zones should be treated as socially sensitive mineability domains, where even geologically favourable ground may face reduced development potential unless community engagement is strong and the disturbance footprint remains low.

3.8.6 Archaeological and Heritage Sensitivity

A major governance-related mineability constraint in the Almora block is the presence of the Lakhudiyar archaeological site (Figure 3.8), a painted rock shelter of prehistoric significance located in the northern part of the block. The report identifies this site on the topography map and records it as a culturally important rock shelter developed within quartzite-schist terrain. Such a feature cannot be treated as a descriptive curiosity; it must be considered a heritage exclusion or high-buffer zone in all future mineability evaluation.

From a mineability perspective, this means that any target zone spatially associated with the Lakhudiyar area, or requiring access, blasting, excavation, vibration-generating activity, or visual disturbance near it, should be screened out or subjected to the highest level of heritage

protection review. Accordingly, the archaeological site represents a clear no-go or restricted-governance zone within the broader mineability framework of the block.

3.8.7 Statutory and Governance Constraints

Mineability issues are highly relevant in Almora, considering that the block contains various forest-land classifications along with other special types of surface uses. The Almora SOP specifically mentions that any earth disturbance is not supposed to be done in forest land without clearance, along with mentioning the importance of landowner consent, community involvement, and quick rehabilitation of the land as important operational aspects. This clearly indicates that mineability in the future will be contingent upon geological and non-geological issues such as the process of obtaining approvals, etc.

This governance setting implies that the Almora block should be assessed through a permit-linked mineability model. In such a model, technically favourable target areas may still be ranked lower if they fall in forest-restricted sectors, near sensitive ecological corridors, or within socially and culturally constrained areas. Conversely, zones on accessible non-forest or lower-sensitivity land may become relatively more mineable even at moderate grade, because their approval path and disturbance footprint may be more manageable.

3.8.8 Access, Infrastructure and Operational Supportability

Despite all these limitations, it can be clearly seen that the G4 exercise successfully shows that the Almora block has practical operational supportability in some selected areas. The work done involved 60 sq. km of geological mapping and sampling, 450 cu. m of pitting and trenching, 30-line km of SP survey and also VES survey and 800 m of core drilling. It is worth mentioning here that the accomplished worktables involve drilling camp establishment, construction of approach road in difficult hilly/rough terrain and also core handling logistics.

However, operational supportability should not be confused with universal mineability across the entire block. The existing field success indicates that phased, selective, logistics-supported work is possible, especially where access tracks, drill pads and work sites can be created with controlled disturbance.. For Almora, the realistic inference is that infrastructure and access are sufficient for continued exploration and selective future development studies, but larger-scale mineability would remain strongly dependent on terrain, land status and ESG screening.

3.8.9 Rehabilitation and Disturbance Reversibility

An important positive ESG factor for Almora is that the project SOP framework already incorporates rehabilitation-oriented operational practice. Trenching procedures require backfilling, replacement of topsoil, gentle compaction and post-work communication with the

local community, while ecological management guidance emphasizes restoration with locally appropriate native species and ongoing monitoring where disturbance occurs. This suggests that at least for exploration-scale activities, the block is capable of being worked under a low-footprint and reversible-disturbance model.

For future mineability assessment, this is significant because the reversibility of disturbance is a major determinant of ESG feasibility. In relatively limited-access Himalayan terrain, mineability improves where disturbance can be confined, rehabilitated and monitored and weakens where long linear cuttings, permanent slope modification, forest fragmentation, or hydrological disruption would be required. Almora therefore appears more suitable for targeted and corridor-based development concepts than for broad, high-footprint surface disturbance.

.

Chapter 4

Previous Work

4 Previous Work:

4.1 Regional Geology:

The Almora Block is in the Kumaon Himalya of Uttarakhand state. The Himalaya Mountain Range (HMR) may be subdivided longitudinally five divisions. These divisions are thought to be separated by major fault/thurst zones (Table 4.1). From north to south these are:

i. **The Tethyan Himalayan Sequence (THS) or Trans-Himalaya**. This includes Phanerozoic sedimentary rocks such as limestone, shale, sandstone and fossiliferous formations

ii. **Greater Himalayan Complex (GHC)**: This lies south of the THS and is occupied by Proterozoic to Ordovician, comprises of high-grade metamorphic rocks such as gneiss, schist, migmatite and granite

iii. **Inner Lesser Himalaya**: It comprises of major areas occupied by low greenschist facies rocks of meta-arenites, meta-argillites and carbonates. It includes many interlayered sequence of metamorphosed mafic and felsic volcanic rocks. Within the generally low greenschist facies rocks exists a few crystalline inliers comprising high amphibolite to granulite facies metasediements and metavolcanic rocks. These high-grade crystallines are variably interpreted as nappes of GHC thrusted over the low-grade metasediments and metavolcanics. Alternatively, they may also represent paraautochthonous sheets equivalent to the low-grade rocks emplaced due to thrusting.

iv. **Outer Lesser Himalayan sequence**: South of the Inner Lesser Himalaya lies low-grade to very low-grade metasediments ranging in age from Neoproterozoic to Paleozoic. The predominant rock types include slate, phyllite, quartzite, limestone, dolomite and low- to medium-grade metamorphic rocks

v. **Sub-Himalaya or the Siwalik Group**: This group include Neogene to Quaternary fluvial sedimentary rock including sandstone, shale, clay and conglomerate of the Himalayan foreland basin.

Table 4.1: Stratigraphy of the Himalaya (after Valdiya, 1980)

North
Tethyan Himalayan Belt: limestone, shale, sandstone and fossiliferous formations
South Tibetan detachment (STD)
Higher Himalayan Belt: as gneiss, schist, migmatite and granite
Main Central Thrust (MCT)
Inner Lesser Himalaya: Greenschist facies Interlayered sequence of metasediments and metavolcanis with many mappable inliers of upper amphibolite facies to granulite facies metasediments, granite gneiss and granite intrusives.
Outer Lesser Himalaya: slate, phyllite, quartzite, limestone, dolomite and low greenschist facies metasediments
Main Boundary Thrust (MBT)
Sub -Himalayan Belt: Neogene sedimentary rocks such as sandstone, shale, clay and conglomerate
Himalayan Frontal Thrust (HFT)
Quaternary sediments: Gangetic Alluvium sediments (Quaternary age)
South

4.1.1 Regional geology of the Almora Block:

The Almora Block is within the Almora Crystalline inlier within the Inner Lesser Himalayan sequence. The Almora Crystallines is also referred to as the Almora Group. The Crystalline is supposed to be bounded by E-W trending thrust planes, the northern bounding thrust plane is termed as the North Almora Thrust (NAT) in the north and the South Almora Thrust (SAT) in the south (Figure 4.1).

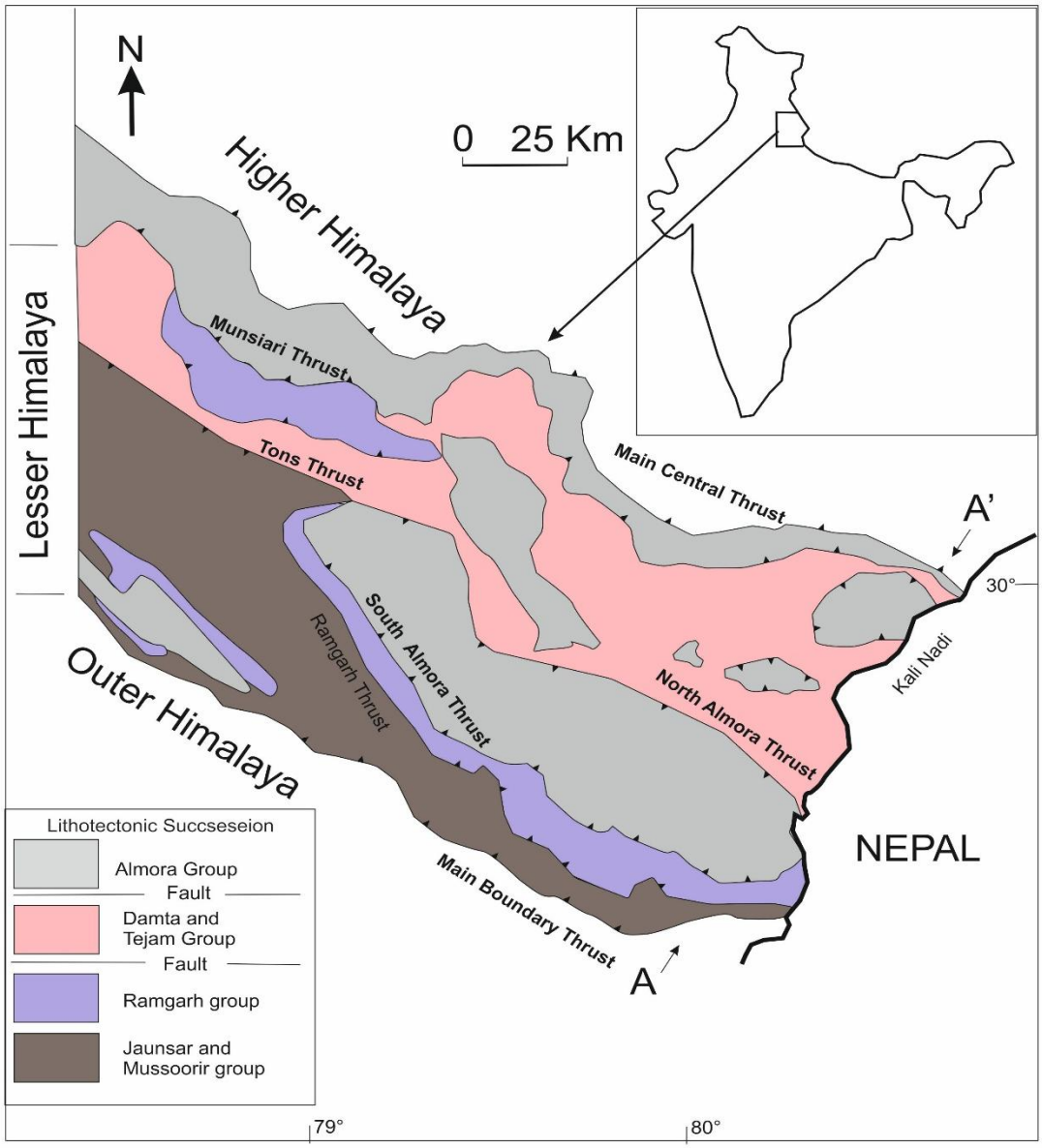

Figure 4.1: Geological and structural map of the Almora area and surrounding (modified after Pant et. al. 2012).

4.1.2 The Geology of the Block:

The Almora Group or the Almora Crystalline of KLH is extended over an area approximately 6,000 sq. km. and consists mainly of quartzite with phyllites, graphite schist, interbedded mica schist and garnet-mica schist associated with granite and gneiss.

Valdiya (1980) noted that Kumaun klippes mainly consist high-grade metasediments and granodioritic rocks around 1800 million years old. Peak metamorphism in the Crystalline was caused partial melting also Cambrian–Ordovician granitoids intruded at several places (Kumar

et. al. 1985). The Palaeoproterozoic granitic gneisses formed under peak regional metamorphism (Joshi and Tiwari, 2009). However, it is found that the highest-grade sillimanite-K-feldspar zone occupy the core areas of anticlines, which means the earlier idea of inverted metamorphism does not apply here. Recently, Santosh and Yadav (2021) proposed that Almora Nappe show mineral assemblages and textures typical of Amphibolite facies, indicating high-temperature regional metamorphism. Garnetiferous mica-schists, quartzites and graphite schists contain minerals like garnet, sillimanite, kyanite and staurolite, reflecting progressive metamorphic conditions.

4.2 Structure:

4.2.1 Almora Block and surrounding Structure:

Santosh and Yadav, 2021 opined that the block area experienced three phases of deformation. Diastrophic structures, including foliations of different generations, folds and their interference patterns, stretching and pucker lineations, folded lineations and faults, all developed within the metamorphic rocks of the Almora Block area.

4.3 Previous work on exploration

Previous work in and around Almora nearly two centuries and ranges from early descriptions of graphite nodules to few systematic explorations aided by electrical surveys and drilling.

- Merbert (1829) reported graphite in the form of nodules weathered out from a band of mica schist on the ridge between Almora and Kalimat. Medlicott (1865) and Drumond obtained samples of graphite in the Almora area.
- Heim and Gansser (1939) noted the occurrence of graphite schist northeast of Almora (at Pirsal and near Bari Chhina), Nautiyal (1949) reported the occurrence of graphite (poor quality) in the schist of Kalimat and Sirar and good quality at Phalsima in Almora.
- Raina (1949) investigated the occurrence of graphite at Deveri, Lakakot and Barechia of Almora district and was of the view that these were of no economic importance. Tiwari (1962-63) (1963-64) noted the occurrence of graphite schist at Channi-Khastiwari (near Bari chhina) Deolikhan-Diodiya and Channa. Bhattacharyya (1965) examined the occurrence of Kalimat, Sirar and Pirsal and mapped these areas in detail.

- Investigation for graphite was taken up by Raina (1949), Tewari (1963-64). Tewari (op. cit.) reported fixed carbon content as much as 31.5% in some part of the Almora Block.
- Bhattacherjee (1964) reported graphite bands from a very wide area with fixed carbon content varying between 2.38% and 8.36%. Further exploration for graphite was pursued using electrical surveys (Srivastava et. al. 1976) to delineate prospective graphite horizons.
- Recently, GSI carried out comprehensive research for origin and prospectivity of carbonaceous horizons in the Almora Crystallines (Bauri and Raut, FS 2020-2021). Another important recent work in the area has been by Santosh and Yadav (FS 2020-2021). These works brought out several interesting things that warrants a relook on the prospectivity of the graphite horizons of the whole Almora Crystallline belt).
    - Graphite horizons are very extensive and ran as continuous layers alternated by late quartzite, mica schist, even though intricately folded and dismembered by later deformation.
    - At many locations, late granites (part of ~500Ma old Almora Granite) injected lit-par-lit into the graphite bearing metasediments. This intrusion resulted in significant crystallinity of the graphite along with other high-grade minerals like sillimanite etc. This brings out possibility of identifying horizons of flake graphite in the area that are very demanding economically.
- GSI's publication (Misc. Pub. V. 30, Part 13, 2002) records the following:
    - Graphite schist samples from the area have analysed 5.86% Carbon and 94.12% ash.
    - Samples of carbonaceous nodules have analysed carbon from 30.36% to 37. 1 1 %.
    - The possible reserves estimated for the Kalimati and the Sirar areas (both areas falling within the present project area) are of the order of 10.7 million tonnes upto a depth of 30m

Thus, even though early explorations have not indicated substantial Resource for graphite, those works indicated good possibility of getting such substantial Resource. This is more important as much of the area where graphite schists are present display high grade metapelites. Thus, it is possible that the graphite in the Almora Block might represent high-ordered graphite. However, the graphite in the area is not classified in terms of its crystallinity, which is very crucial in determining economic prospect of any graphite deposit.

4.3.1 Chronological development of previous work:

The collective work of multiple authors establishes a coherent understanding of the Almora graphite system. Verma and Rawat (2020) provide regional stratigraphic context, while Santosh and Yadav (2021) identifying graphite horizons as hosts to significant vanadium and barium enrichment within a structurally controlled setting. Bauri and Raut (2021), followed by Shankar and Misra (2023), further demonstrate that black shale and graphite schist units contain appreciable vanadium and represent shale-hosted mineralization formed under anoxic conditions. Kumar and Manna (2023) confirming the regional continuity of the graphite–vanadium system. Earlier, Mehrotra (1955) highlighted the economic relevance of even low-grade graphite, while Rawat and Sharma (2011) established its origin as metamorphosed biogenic carbon later modified by deformation. Supporting tectonometamorphic studies by Joshi and Tiwari (2009), Célérier et. al. (2009) and Mandal et. al. (2015) collectively show that the geometry, continuity and enrichment of graphite-bearing horizons are strongly controlled by polyphase deformation within a long-lived tectonic framework.

The table (Table 4.2) summarizes the principal strands of previous work that materially shaped geological understanding of the Almora graphite belt and its regional extensions. The later sections expand the technical significance of these investigations.

Table 4.2: Principal legacy work relevant Almora G4 exploration programme by Geovale Services Pvt. Ltd.

Period	Study	Spatial focus	Nature of work	Key relevance to present exploration
1829-1964	Bhattacharji (1964), including Herbert, Medlicott, Lawder, Nautiyal, Raina, Tewari and Mehdi	Almora-Kalimat-Barichhina sector	Reconnaissance observations, district-scale mapping and early sampling	Established the presence of graphite and carbonaceous nodules; recognized strong local variation in quality; documented continuity of graphite schist horizons beyond isolated ridge-top showings; and introduced the idea of an organic precursor to some carbonaceous material.
1939	Heim and Gansser	Central Himalaya / Almora-Barichhina	Regional structural synthesis	Defined the Persal-Barichhina asymmetrical syncline and described the repetition of graphite schist on its limbs, providing the first structural explanation for the Almora graphite belt.

Period	Study	Spatial focus	Nature of work	Key relevance to present exploration
1965	Bhattacharji, GSI	Sirar, Persal-Punakot, Kalimat	Detailed geological mapping, pitting, sampling.	Mapped the classical graphite belt on 1:63,360 scale; dug 71 pits; demonstrated synclinal and isoclinal controls on graphite schist geometry; reported fixed carbon mostly in the 2.28%-8.36% range in bulk schist, but much higher in nodules; and published previous geological tonnage estimates for Sirar and Kalimat.
1975-1978	Srivastava et. al.; Chauhan et. al.	Kalimat-Sirar-Pirsal and Sirar-Phalsima	Self-potential, resistivity and limited drilling	It showed that graphitic horizons could be traced as conductive bodies, but also demonstrated that anomaly intensity depended strongly on graphite texture and continuity, not simply graphite presence. Helped to identify depth continuation and the limitations of geophysical anomalies as direct proxies for economic graphite.

Period	Study	Spatial focus	Nature of work	Key relevance to present exploration
1979	Bajapai	Parts of Pauri, Almora and Nainital districts	Photogeological interpretation with limited field check	Clarified nappe-scale architecture, broad lithostratigraphic divisions and fracture patterns across the Kumaon Lesser Himalaya, strengthening the regional framework for later exploration.
1983-1988	Kumar and Krishnamurthy; Srivastava and Kumar	Bageshwar-Didihat-Champawat regional belt; Jakheta-Petshal block	Regional integrated W-Sn-Au survey and detailed scheelite/tungsten investigation	Demonstrated that the broader Almora Group terrane is metallogenically fertile beyond graphite. Tungsten investigations in Jakheta-Petshal traced scheelite-bearing zones by mapping, trenching and drilling, while also highlighting the disconnect between surface tenor and subsurface continuity in folded Himalayan terrain.

Period	Study	Spatial focus	Nature of work	Key relevance to present exploration
1988-2006	Ramaiah and Mehta; Chittora and Kacker; Mehta et. al.	Binsar-Mukteshwar, Devidhura-Naya Sangrauli-Chhira and Jeolikote-Betalghat sectors	Regional petrological work and specialized thematic mapping	Refined granitoid petrogenesis, standardization of regional stratigraphy, South Almora Thrust relationships and polyphase deformation (F1-F4), including shear-related sulphide mineralization in adjacent Almora Group rocks.
2011	Rawat and Sharma, Sharma et. al.	Multiple graphite occurrences within Almora crystallines	Mineralogical and genetic study (SEM-EDX, XRD, Raman)	Established that Almora graphite is mostly ordered graphite derived from metamorphism of organic-rich precursors, with formation temperatures of approximately 485-568 °C and a close association with V- and P-bearing mineral assemblages.
2013-2020	Das et. al.; Singh and Bishakha; Verma and Rawat	Ramgarh Group footwall, Siwalik belt and Agalgarhdhar area	G-4 mineral investigation and specialized thematic mapping	Improved the regional geological framework around the Almora block, including thrust geometry, stratigraphic relationships and additional evidence for multi-commodity mineral potential in adjacent belts.

Period	Study	Spatial focus	Nature of work	Key relevance to present exploration
2020-2023	Santosh and Yadav; Bauri and Raut; Shankar and Misra; Kumar and Manna	Almora, Nishni-Malta and Chaura-Sirmoli-Lohaghat sectors	Graphite-vanadium-associated metal investigations	Reframed the Almora graphite belt as part of a broader carbonaceous metasedimentary mineral system. Demonstrated elevated vanadium, barium and locally Y-Mo values in graphite schist and black shale/graphite schist, highlighted fold closures and structurally thickened carbonaceous packages as priority targets and linked follow-up work to legacy NGCM W anomalies (140-887 ppm) east of Almora.

The NGCM data (Figure 4.2, Table 4.3) therefore provide a catchment-scale test of various elements of the present block lies within the Jakheta-Bataldeon-Phalsima sector.

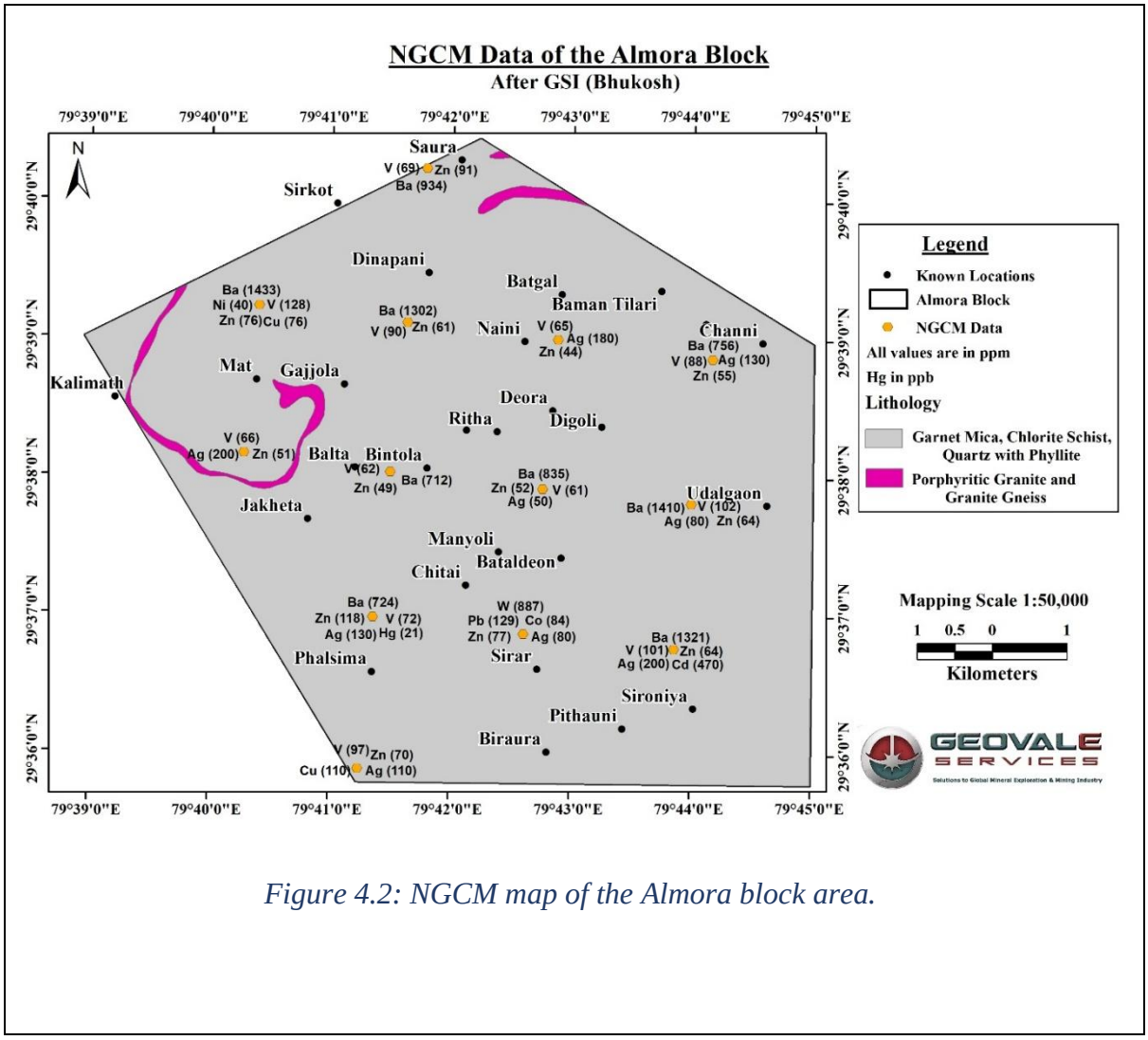

Figure 4.2: NGCM map of the Almora block area.

Table 4.3: Comparative summary of selected NGCM indicators for the Almora (Matena-Sirar area) and surrounding 53O/10 catchments. (NGDR Portal).

Indicator	Within-block median (n of samples= 13), in ppm	Toposheet 53O/10 median (no of samples = 156)
Vanadium (V)	72	66
Tungsten (W)	3.00	4.03
Tin (Sn)	3.48	5.15
Chromium (Cr)	112	80
Cobalt (Co)	15	14

Chapter 5

Geoscientific Activities

5 Geoscientific Activities: Methodological Record of the Almora Graphite Exploration Programme:

5.1 Preamble:

The current chapter presents the methodology behind the exploration report of Almora. This includes the integration of remote sensing, field geology, sampling, excavation, lab characterization, geophysical surveying, and drilling techniques applied for the investigation of graphite- and vanadium-bearing carbonaceous formations in the Matena-Sirar block. The current chapter will act as the documentation of the geoscientific activities that are being evaluated further in other chapters.

The Almora block required a multi-disciplinary exploration design because the target mineralization occurs within a structurally complex metamorphic terrane of the Almora Group, where carbonaceous and graphitic horizons are folded, sheared, repeated and variably exposed. No single dataset is sufficient in isolation; geological observations must be checked against geochemical signatures, graphite quality assessed through petrographic and spectroscopic methods, geophysical anomalies matched with mapped graphite schist and trench exposures and drilling justified by the convergence of multiple lines of evidence.

The approved exploration plan included 60 sq. km. of multispectral and DEM-based analysis, 60 sq. km. of geological mapping, 450.68 cu. m of combined pitting and trenching, 32.6 line-km of self-potential survey, 31.4 line-km of VES survey, petrological and mineralogical studies, a multi-stream laboratory assay programme and 800 m of core drilling.

5.2 Geospatial Analysis (Remote Sensing)

Remote sensing formed the first geoscientific screening layer of the programme. Before detailed field traverses were undertaken, satellite imagery and digital elevation data were compiled and interpreted over the full Matena–Sirar block so that terrain, geomorphology, drainage behaviour, structural grain and land-use constraints could be understood in a spatially consistent manner. It was used as a decision-support tool for planning traverses, recognizing structurally favourable zones, organizing stream-sediment catchments and identifying terrain sectors requiring direct ground validation. The entire approved quantum of multispectral and DEM-based analysis, covering 60 sq. km., was completed under the programme.

5.2.1 Process, Derivatives and Their Exploration Significance

The remote sensing process combined multiple bands of imagery (Landsat, Sentinel-2A, ASTER) and digital elevation models (SRTM-DEM) using a Geographic Information System (GIS). This involved a series of steps such as downloading and filtering the images, creating the DEM, extracting lineaments, creating terrain derivatives, preparing the LULC and drainage products, and integrating them into GIS. Past geological thematic derivatives generated, their figure references (Section 3.7) and exploration significance are as follows:

Lineament map, Elevation map, Contour map, slope map, Hillshade map, Drainage map, LULC map, RED landform map, Spectral alteration maps- clay, ferrous, iron oxide.

5.2.2 SOP and QA/QC Protocol

The SOP required: (i) acquisition of cloud-free imagery (preferably <10% cloud cover) using Landsat, Sentinel and ASTER datasets together with DEM products; (ii) lineament extraction and azimuth validation against regional structural grain; (iii) generation of DEM derivatives - slope, aspect, hillshade, drainage, contour and elevation profiles; (iv) preparation of LULC and drainage morphometry products; and (v) integration of all outputs into the project GIS with preserved metadata. Specific risks addressed in the SOP included persistent cloud cover (mitigated through multi-date and dry-season imagery), vegetation masking (addressed through field validation), DEM artefacts in steep terrain (checked by comparing multiple elevation sources and field GPS) and spectral anomalies (explicitly not to be interpreted as geological fact without ground evidence).

QC procedures entailed field mapping of GIS-interpretation ground truthing; DEM spot height validation based on GPS control points (tolerance ±5 m); and archiving of all raw imagery and associated derivatives with their metadata documentation. The remote-sensing-derived results were treated as hypotheses, which were verified or rejected through field mapping.

5.3 Orientation Survey:

Prior to the commencement of systematic exploration under the G4 stage, an orientation survey was undertaken within the Almora Graphite-Vanadium exploration block in the vicinity of Almora to assess the occurrence of graphite-bearing lithological units and to evaluate the appropriate sampling strategy for geochemical investigation. Reconnaissance visits were conducted to selected locations exhibiting graphite schist exposures, particularly around Digoli and Bataldeon areas.

The exposures of graphite schist with polymetallic characteristics at Digoli were extensively studied. The graphite was present as flake graphite within schist-like rocks. It was found that flake graphite has shown a tendency to behave in a buoyant manner using the tumbler test. This is because graphite particles suspended in water rose to the surface in the tumbler test, and hence there was the existence of graphitic carbon. Disseminated pyrite in addition to fine quartz veins were seen in the graphite schist.

At Bataldeon, a well-exposed roadside cross section of graphite schist was studied to understand the lithological continuity and structural disposition of the graphite-bearing horizon. In the same locality, an exposure of deformed granite was also examined to assess the possibility of associated mineralization. However, no visible mineralization or sulphide occurrence was observed in the granite during field inspection.

Geochemical analysis of the four representative rock samples (Annexure I) collected during the orientation survey from the graphite schist exposures near Digoli and Bataldeon indicates enrichment of several trace elements associated with graphite-bearing metasedimentary rocks.

Vanadium values range from 110 ppm to 362 ppm, with the highest values recorded in samples 106311 (360 ppm) and 106313 (362 ppm). These values are considered anomalous compared to average crustal abundance (~120 ppm) and suggest a possible association of vanadium with graphite-bearing schist horizons. Such enrichment is commonly observed where vanadium substitutes within organic-rich sedimentary precursors that later metamorphose into graphite schist. Arsenic shows elevated concentrations in samples 106311 (213 ppm) and 106312 (111 ppm), which indicates polymetallic sulphide association within the graphite schist. This observation correlates with the presence of pyrite observed megascopically in the field. A particularly strong anomaly is recorded for Zn in sample 106312 (3041 ppm), which is significantly higher than normal background levels and may indicate localized sulphide mineralization within the graphite-bearing horizon. The occurrence of sulphur-rich graphite schist in this sample further supports this interpretation. Tungsten values are also moderately elevated, reaching 198 ppm in sample 106311, suggesting possible trace enrichment within hydrothermal or metamorphic fluid pathways associated with quartz veining observed in the graphite schist (Table 5.1)

Table 5.1: Anomalous Element Concentration in Orientation Samples

Sample Id	Lithology	V (ppm)	As (ppm)	W (ppm)	Zn (ppm)	Cu (ppm)	Remarks
106310	Graphite schist	219	17	53	52	109	Moderate V enrichment
106311	Sulphide-rich mafic rock	360	213	198	85	16	Strong V, As and W anomaly
106312	Graphite schist with sulphur	110	111	70	**3041**	**307**	Very strong Zn and Cu anomaly
106313	Graphite schist	**362**	10	107	33	10	Strong V enrichment

The results obtained from the orientation survey and subsequent geochemical analysis indicate that the graphite schist horizons exposed around Digoli and Bataldeon show notable enrichment of vanadium (Table 5.1) along with localized polymetallic sulphide signatures (Zn-Cu-As). The presence of flaky graphite, visible pyrite dissemination and quartz veining within the graphite schist further supports the geochemical indications of mineralization.

Based on the above results, the graphite-bearing metasedimentary formation of the region may be viewed as a geologically favourable setting for the formation of graphite-vanadium ore deposits through the metamorphism of organic sedimentation followed by sulfidation. As such, geological mapping, sampling, and analysis of rocks, and geochemical surveying in the fourth geophysical stage is seen as necessary to outline the limits of graphite-bearing formations and ore occurrences in the study area.

5.4 Geological-Structural Mapping:

Geological-structural mapping (Figure 5.1, Figure 5.2, Figure 5.3) constituted the principal ground-validation component of the programme and formed the bridge between remote-sensing-based screening and all subsequent sampling, geophysical, trenching and drilling decisions. In the Almora block, graphite and vanadium are hosted within a multiply deformed metamorphic package where carbonaceous horizons are folded, repeated, locally sheared and variably weathered. Mapping had therefore to establish lithological continuity,

structural attitude, relative position of graphitic horizons and the tectonic framework controlling their surface expression and Subsurface geometry.

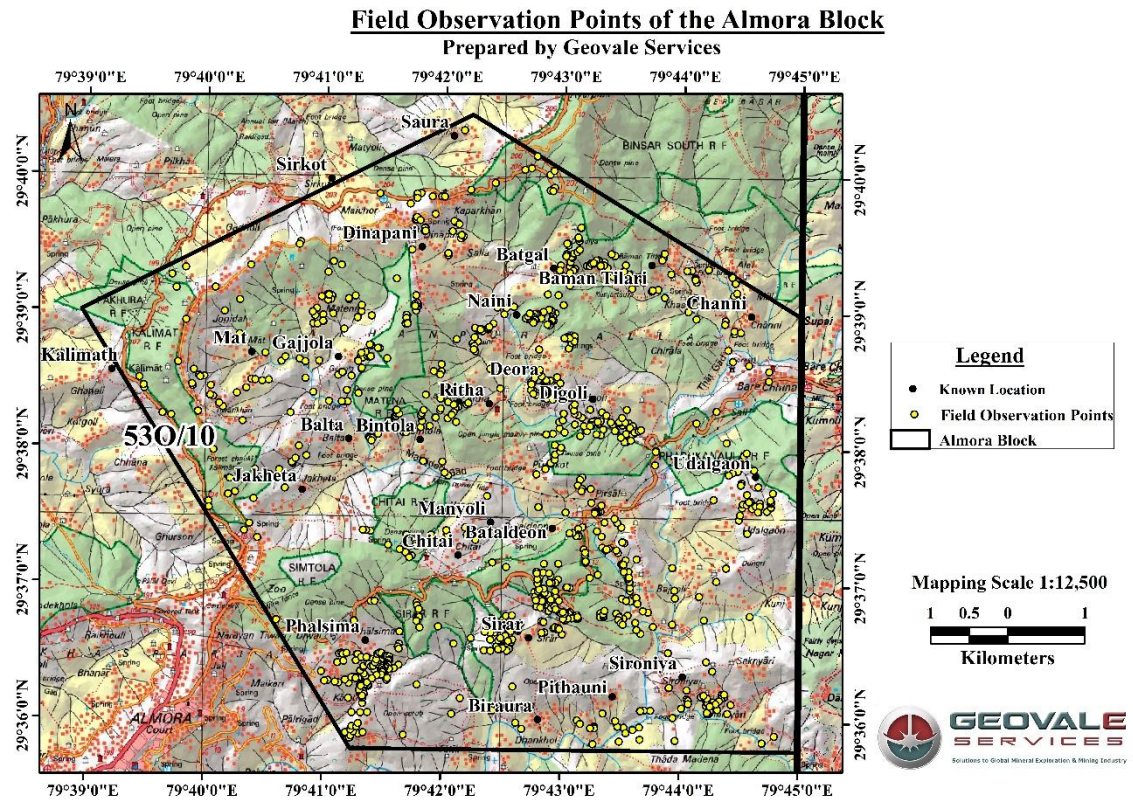

Figure 5.1: Field observation points of the Almora Block.

Figure 5.2: Streching lineation within foliated granite rock (Balta area).

Figure 5.3: Foliation within quartzite rock (Saura area).

5.4.1 Process and Derivative Mapping Inputs

The mapping program covered the entire approved block area of 60 square kilometers at a working scale of 1:12,500. Geologists planned traverses both along and across the main lithological belts. At each observation point, they recorded the GPS location, host lithology, rock description, visible mineralization, structural features, and took photographs. The inputs for mapping came in two levels. The first level included legacy and remote-sensing layers: (a) the GSI 1:50,000 lithological map, which served as a regional guide. This map mainly featured garnet mica-schist and chlorite-schist terrain with porphyritic granite bodies; and (b) the more detailed GSI 1:12,500 scale map. This map identified one granite-gneiss band, three foliated tourmaline granite bands, eight sheared quartzite bands, 18 folded shallow-dipping graphite-schist bands, 27 folded quartzite bands, and 22 injected gneiss bodies. This served as the immediate template for field verification. Remote-sensing derivatives such as lineament, slope, hillshade, drainage, and land use/land cover offered context for terrain and access during traverse planning.

The second tier comprised the field-derived data compilations: the observation-point file (Annexure II) contains more than 800 georeferenced point records; the structural compilation files (Annexure III) contain more than 500 planar measurements with strike, dip amount and dip direction and 16 lineation measurements with plunge amount and plunge direction (Table 6.3). These formed the working backbone of the geological and structural map.

5.4.2 SOP and QA/QC Protocol

The SOP required: systematic traverses across and along strike; recording of GPS coordinates, rock type and structural measurements at every station; specific notation of graphite occurrences and host lithology; scale photography; end-of-day digital database transfer; and continuous updating of lithological boundaries on the working map. Each field day was to begin with a traverse plan and end with digital compilation, so that the map evolved in near real time - critical in Himalayan terrain where access, exposure quality and structural repetition can bias interpretation.

QC relied on repeat observation and interpretation. A senior geologist was to independently revisit and relog about 10% of observation points, both random stations and areas where interpretation was doubtful. Map review sessions at the end of each week would resolve discrepancies in lithological descriptions, interpretations of contacts and structures. In cases where weathering prevented a proper identification of lithology, additional chip sampling and testing would be needed, while doubtful interpretations would be sent to the petrographic lab

for verification. The process of entering data into the database at the end of each day provided an independent quality check by requiring that the interpretations made in the field notebook, GPS coordinates, photos, and new GIS layers be compared with one another.

5.4.3 Data Collected and Generated

The programme completed 60 sq. km. of geological mapping at 1:12,500 scale. The structural compilation preserves over 700 planar measurements of strike, dip amount and dip direction and 16 linear measurements of plunge and plunge direction. Dominant structural trend is WNW–ESE to NW–SE foliation, with strong dip variation by sector - very gentle dips in the south, moderate dips around Barakot/Bintola/Digoli/Udalgaon and steep to near-vertical attitudes in the north (Channi, Khas Tilari, Baman Tilari). Stretching lineations cluster in the 230°–270° plunge direction sector with a secondary group around 300°–330°, supporting interpretation of thrust-related flat and ramp geometries within a compressional deformational framework.

Mapped units include graphite schist, mica-schist and garnet-mica-schist, quartzite, foliated granite, granite gneiss and tuffaceous rocks. Geological products generated include working and final 1:12,500 lithological map, structural overlays, graphite-band traces, domain-wise observation compilations, cross-section control points, photo-linked outcrop records (Figure 5.4, Figure 5.5) and the attribute database used for all downstream targeting.

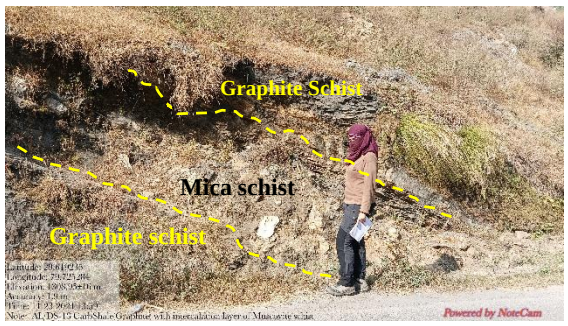

Figure 5.4: Litho assemblages as evidenced in the field exposure of Almora Block

Figure 5.5: Foliation of the graphite schist

5.5 Surface Sampling - Grab and Chip

Surface grab and chip sampling became the first direct geochemical link between the geologic map and the analytical work, translating the field identification of graphite mineralization into geologically situated physical samples for chemical analysis in the lab.

Sampling was confined to graphite schist and associated host rocks in natural exposures, road cuts, ridges and other exposed outcrops in the whole 60 sq.km block, which included locations such as Sirar, Bataldeon, Digoli, Bajyoli, Debdiya, Ritha, Balta, Udalgaon, Deora and Phalsima.

5.5.1 Process and Derivative Outputs

Unweathered surface was exposed using a hammer and chisel, avoiding rind weathering and recording sample locations while noting the geological data at hand such as rock type, pencil style, sulphide relationships and field setting. Samples were taken in individual exposures, although chip sampling was employed when a more representative sample needed to be made from a restricted area. Field samples were assigned a set of geographical and geological information including sample identification, GPS coordinates, description and digital photos before being shipped with sample forms.

Surface samples were routed into a staged analytical programme comprising: XRF major oxide analysis (200 samples + 20 external checks + 20 Sn/W extension checks with 2 further checks); ICPMS multi-element analysis including vanadium and REE characterization (100 samples + 10 checks); proximate/fixed-carbon determination for graphite-bearing material (50 samples); and total sulphur analysis (25 samples). The derivative outputs comprise a georeferenced bedrock sample inventory in GIS, field sample registers and photo logs and an assay database that can be interrogated lithology-wise, horizon-wise and locality-wise.

5.5.2 SOP and QA/QC Protocol

The SOP included: specimen collection with the geological hammer and chisel; recording in the sample register with a unique serial number for each sample, coordinates, and description (no repeat of serial numbers); packaging in labeled bags; cleaning of all equipment using a wire brush after each sample; photographing of each lot before shipping; and completion of sample submission forms with project code, tests to be conducted, and other relevant information.

QC was built around four concerns: representativeness, contamination control, sample identity integrity and sample-to-lithology reconciliation. Core measures included: (i) field duplicate collected from the same site for repeatability check; (ii) senior geologist review of sample descriptions against mapped lithology; and (iii) complete documentation uploaded to the project cloud repository. Key risks - high-grading or selective sampling bias, cross-contamination, mislabelling, moisture damage - were mitigated through representative selection under geological supervision, tool cleaning, independent field ID verification, dry

labelled bag storage and photo retention. External check assays for XRF and ICPMS subsets extended QC through the geochemical pipeline.

5.6 Stream Sediment Sampling

Stream sediment sampling provided the reconnaissance-scale geochemical component for testing whether the drainage network draining the graphite-bearing package carries a detectable geochemical and mineralogical signal. In the Almora block, where steep terrain, forest cover and transported cover locally limit direct bedrock observation, stream sediment acts as an integrated catchment response and therefore functions as an efficient first-pass screening medium.

5.6.1 Process and Derivative Outputs

Site selection was guided by the GIS drainage derivatives (stream order, catchment geometry, access), targeting first-order and second-order catchment outlets. The field team walked upstream from each planned site to confirm suitability and identify contamination sources. Multiple scoops of fine stream sediment were collected from active stream-bed trap sites using a cleaned stainless-steel scoop, composited in the field (~10–15 kg), excess water drained naturally and each sample recorded with sample Id and GPS coordinates. The programme generated 25 primary stream-sediment locations (**Error! Reference source not found.**), with paired preparation entries per location reflecting internal splitting or fraction control.

The main outputs from the derivative work were:

- Stream sediment locations layer;

- Catchment-based sample data base;

- Laboratory ready sample data set that had been separated by gravity and magnetic separation of heavy minerals (25 samples – 2mm excluded);

- Catchment-level screening layer for anomaly identification (similar to geological mapping, structure interpretation and bedrock sampling).

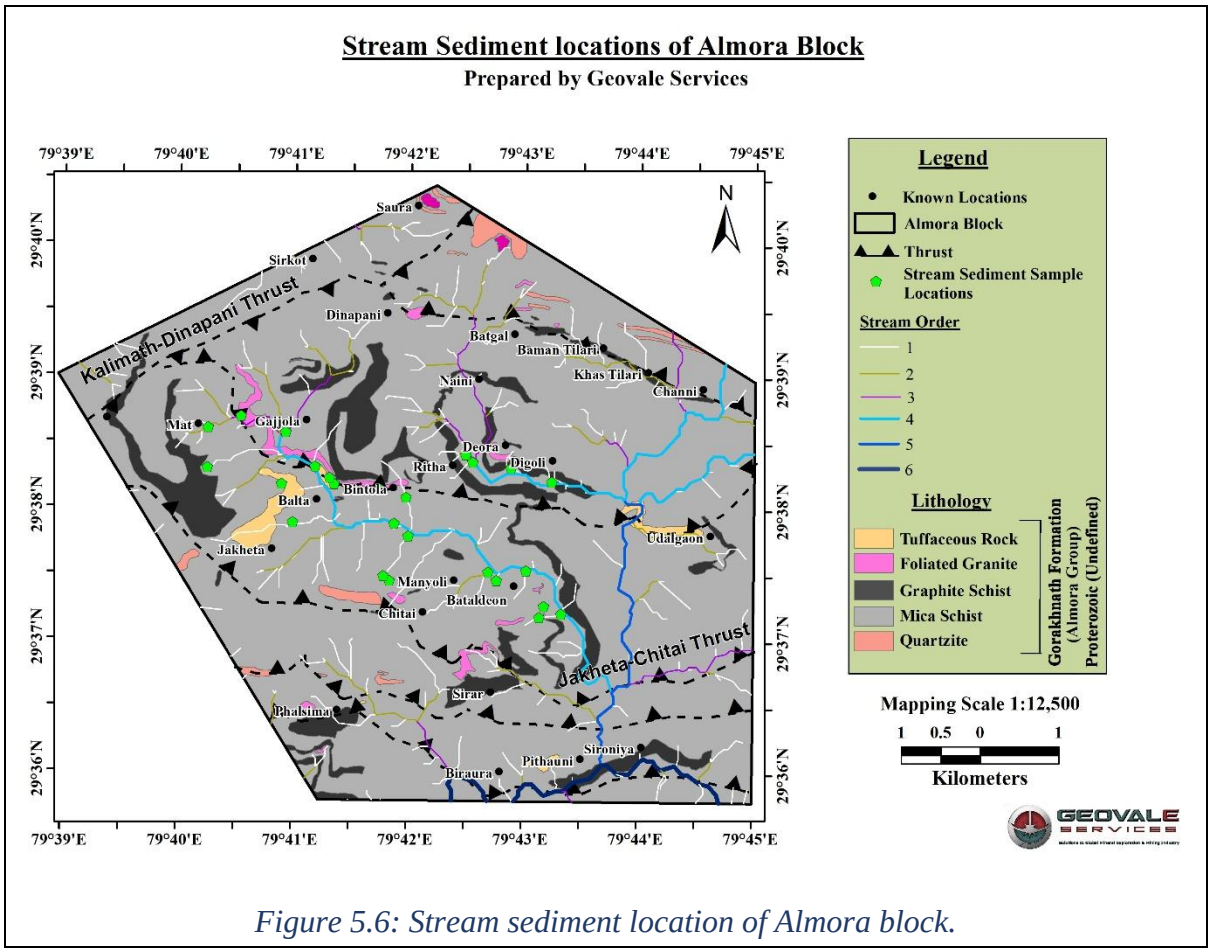

Figure 5.6: Stream sediment location of Almora block.

5.6.2 SOP and QA/QC Protocol

The SOP required: sample sites selected from GIS-based drainage analysis targeting first- and second-order catchments; upstream walk before collection to identify contamination; active stream-bed trap site selected for sampling; use of a cleaned stainless-steel scoop; organic matter removed before collection; approximately 10–15 kg of composite sediment collected; bag not overfilled to permit homogenisation; excess water drained naturally (not squeezed); sample homogenised within the bag, labelled, recorded with GPS and accompanied by a Sample Submission Form before dispatch (Figure 5.7**Error! Reference source not found.**, Figure 5.8**Error! Reference source not found.**).

QC focused on representativeness, contamination awareness, homogenisation and equipment cleanliness. The SOP required: field duplicates at selected locations for repeatability assessment; explicit recording and flagging of any contamination source observed during upstream walk; mandatory homogenisation before any split; scoop scrubbed in flowing water between every site. Dry-season sampling was preferred; clay-silt fine fractions were prioritised; sites downstream of anthropogenic disturbance were to be avoided.

Figure 5.7: Collection of stream sediments

Figure 5.8: Processing the stream sediments.

5.7 Pitting and Trenching

Pitting and trenching (Figure 5.9) constituted the principal shallow subsurface exposure techniques to verify geological interpretation beneath soil-covered slopes, expose graphite-bearing horizons and obtain fresh channel samples from controlled excavation faces. The approved-versus-achieved work statement records a combined excavation of 450.68 cu. m, comprising 234.43 cu. m from pitting and 216.22 cu. m from trenching against total sactioned excavationed target 400 cu. m (Annexure VI).

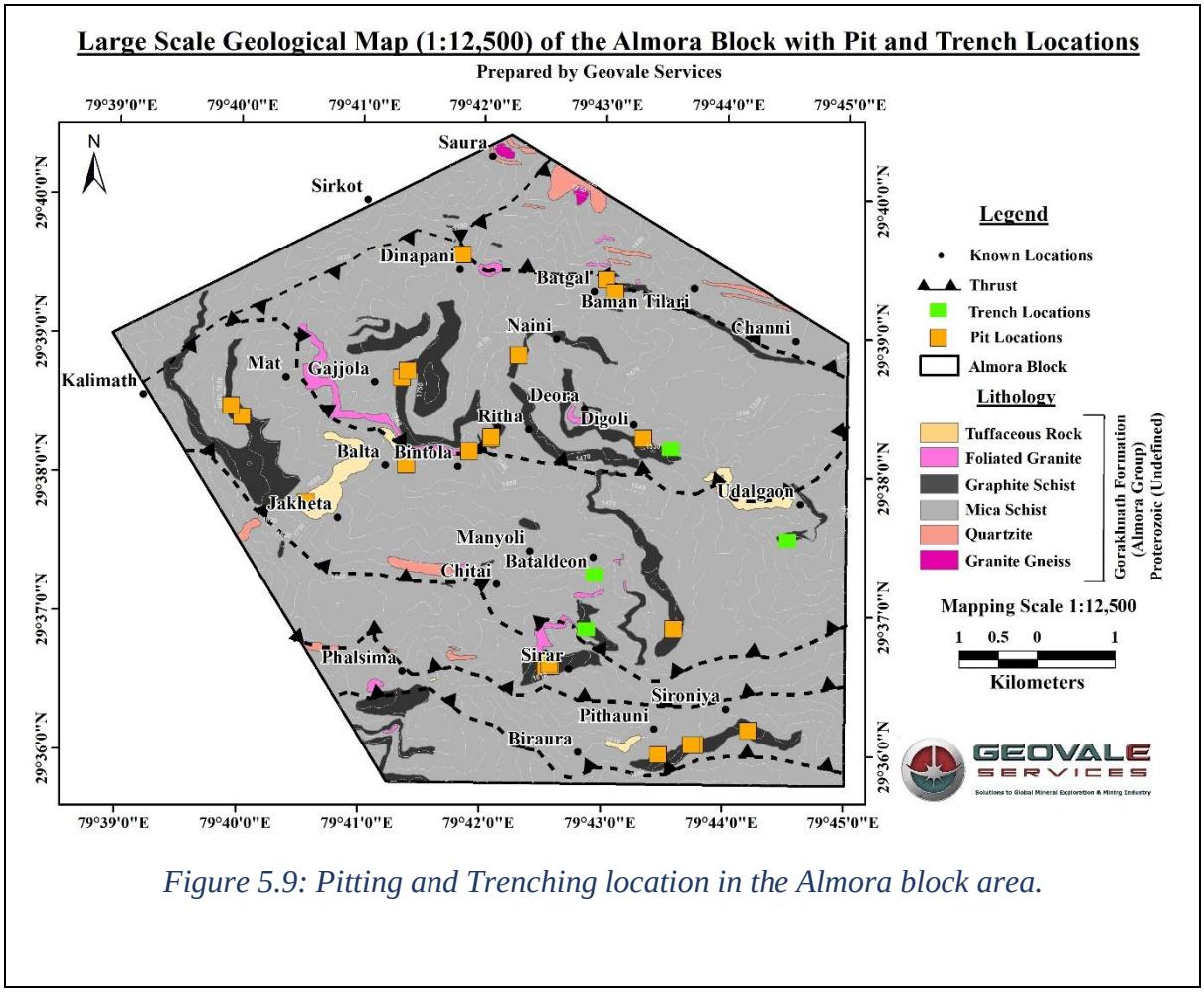

Figure 5.9: Pitting and Trenching location in the Almora block area.

5.7.1 Pitting - Process, SOP and QA/QC

Pitting was undertaken to examine shallow vertical continuity, expose fresh bedrock below soil cover and test the immediate subsurface expression of graphite schist, sulphidic horizons, lithological contacts and weathered mineralised ground. Site selection was based on the integrated interpretation of geological mapping, surface graphite and sulphide indications, lithological contacts, structural features and terrain accessibility (excluding reserve forest areas). Pits were excavated by JCB at approximately 2 m × 2 m plan dimensions to depths of ~2–3 m and walls manually cleaned for geological logging. Representative channel samples were collected from cleaned faces at 0.5–1.0 m intervals, labelled with pit number, interval, lithology and structural information (Figure 5.10, Figure 5.11, Figure 5.12, Figure 5.13).

Figure 5.10: Marking the pit area for AL/Pit 01, near Pithauni area.

Figure 5.11: Excavation of the Pit (AL/Pit 01), near Pithauni area.

Figure 5.12: Excavation of pit after marking.

Figure 5.13: Labelling and restoration of the ground.

SOP indicated that the extent of the excavation had to be marked before starting, permission had to be granted before excavation and at least one face had to remain clean for mapping and sampling purposes. Large samples were homogenized through coning and quartering process. Quality Control had to focus on the quality of exposure, accuracy in terms of location, sampling and excavation safety. According to SOP, it was necessary to: correlate geology obtained from excavation with the geological map; measure true width of mineralization based on the measured dip; clean walls prior to logging; reconcile pit descriptions with field notebooks, photos and dispatch reports. Excavation safety meant that any wall over ~1.5 meters high should have been battered or shored.

The excavation register records 24 pits completed, contributing ~234.43 cu. m of excavation. Pit dimensions ranged from ~2.05–2.40 m length, ~1.90–2.30 m width and ~1.0–2.4 m depth; per-pit volumes from ~4.305 cu. m to ~12.144 cu. m. Pits were distributed across Sirar, Naini, Debdiya, Bintola, Gajjola, Pithuani, Mat, Dinapani, Bataldeon, Sironiya, Jakheta, Saura,

Udalgaon and Deora. Fixed carbon values broadly in the 2–7% range (highest reported: 7.05%); associated vanadium, molybdenum and zinc anomalies recognized in graphite-bearing northern block exposures.

5.7.2 Trenching - Process, SOP and QA/QC

Trenching was adopted where the principal requirement was lateral continuity along prospective graphite-bearing zones and exposure across mapped lithological or geophysical targets. Trenches were mechanically excavated by JCB, typically 1.5–3 m wide, 2–3 m deep and 5-7 m long, aligned perpendicular to the strike of mineralised structures. After excavation, walls were manually dressed and cleaned. Channel sampling along cleaned faces was at 0.5–1.0 m intervals (7–10 samples per trench), with grooves cut perpendicular to strike, every interval labelled against trench number, sample interval, lithology and structural data (Figure 5.14, Figure 5.15).

Orientation, face quality, and post-excavation rehabilitation were stressed in the SOP. Lot sizes greater than 5 kg were to be reduced through coning and quartering. Once the trenches were photographed, logged, and verified, they were to be filled with the material removed, topsoil reinstated, and the area secured for both people and animals. Quality control was more specific with regard to geometry compared to other operations. The geological observations made in one trench had to be compared with those found in another trench and on the surface maps to ensure consistency and accuracy; true width correction using the dip angle was required; a constant channel depth and width had to be used during sampling; and excavations were not to be performed during unfavorable weather because of wall instability.

Figure 5.14: Excavation of trench (AL/Trench 01) in Pithauni area.

Figure 5.15: Labelling and restoration of the ground after trenching, in Pithauni area.

The trenching register records 6 trenches completed for a cumulative excavated volume of ~216.22 cu. m. Trenches were located at Pithuani, Naini, Digoli, Bataldeon, Sirar and

Udalgaon. Recorded trench lengths: ~5.2–7.3 m; widths: ~2.1–3.0 m; depths: ~2.1–2.9 m; volumes: ~29.568–45.24 cu. m per trench.

5.8 Petrology of Surface and Subsurface Samples

Petrological investigation formed the microscopic bridge between field observations, laboratory mineralogical studies and the evolving geological model. It was used to verify the true mineral assemblages of graphite-bearing and host rocks, establish the textural character of graphite in surface and drill-core samples and recognise metamorphic and deformational processes controlling graphitization, sulphide association and lithological repetition.

5.8.1 Process and Derivative Outputs

The representative samples were obtained from all major lithological formations and graphite deposits that had been located by mapping during the field work - surface samples from fresh outcrops, pits and trenches; underground samples from core samples of graphite bearing horizons, Graphite Schist, mica-schist and other lithologically important rocks. The thin section samples were made to be examined under PPL, XPL, and reflected light.

Surface petrology revealed that graphite schist is dominated by graphite, quartz and muscovite, with minor biotite and feldspar, with graphite as fine- to medium-grained flakes aligned parallel to foliation. Key microscopic observations include: small graphite grains in quartz-muscovite schist (pre- to syn-tectonic); folded graphite flakes; crenulation cleavage; graphite concentrated in shear lenses with muscovite inside recrystallized quartz; graphite flakes in reflected light; and graphite associated with mica-fish and quartz-vein-related microstructures. Photomicrograph documentation of surface samples covers graphite schist, garnet-mica schist, mica schists, quartz-sericite and quartz-mica schist and tuffaceous rocks. Tuffaceous rock petrography confirmed a very fine-grained fragmental texture comprising quartz, feldspar, chlorite and minor opaques in a fine groundmass, confirming volcaniclastic input into the metasedimentary sequence. Garnet-mica schist petrography confirmed boudinage, folded quartz veins and shearing. Borehole petrology validated lithological continuity at depth and enabled comparison of drill-core graphite textures with surface occurrences.

The programme completed 21 thin sections and 21 microscopic studies for surface material (Annexure V); 25 thin sections and 25 microscopic studies from subsurface (borehole) samples (Annexure XXI). Key interpretive derivatives include a microscopic lithology-validation dataset; a photomicrograph library (PPL, XPL, reflected light); qualitative to semi-quantitative

modal observations for major minerals (graphite, quartz, muscovite, biotite, garnet, feldspar, chlorite, tourmaline, opaques); and a metamorphic interpretation supporting progressive graphitization under directed stress and medium- to high-grade metamorphic overprint locally enhanced near intrusive granite bodies.

5.8.2 SOP and QA/QC Protocol

The SOP required representative sample selection from all mapped lithological units and every graphite mineralisation style, entry in the register with sample Id, GPS/locality reference, rock type and analytical purpose, followed by polished thin section preparation and systematic examination in PPL, XPL and reflected light. Mineral identification and modal percentage were to be recorded systematically, followed by a written petrographic description, applied identically to both surface and borehole samples.

The QC process was carried out based on representativeness, section quality, mineral identification accuracy, and interpretation consistency. For instance, in the SOP, the procedure included a requirement for independent examination of sections by another petrographer, modal analysis using a grid pattern sufficiently close not to cause selection bias, preparation of new sections where previous ones were below standard, comparison of uncertain fine-grained minerals to XRD and whole rock chemistry, and marking of thin sections to maintain directionality during preparation. In case of integration-based QC, it involved correlation of petrological descriptions of each rock unit type to maps, structures, and geochemistry.

5.9 Raman Spectroscopy

Raman spectroscopy was used to assess the structural order of carbonaceous material and to distinguish well-ordered flaky crystalline graphite from poorly ordered or amorphous carbon, functioning as an interpretive bridge between field recognition of graphite schist and laboratory confirmation of graphite maturity. It was recognised in the project as one of the methods to confirm enhanced graphite crystallinity, particularly in horizons affected by metamorphic recrystallization and local thermal influence of granite injections. Work was carried out at the Geological Survey of India, Kolkata. The approved work programme provided for 10 Raman analyses (Annexure XV).

Laser Raman Spectroscopy is a method of vibrational spectroscopy that involves the inelastic scattering of a monochromatic light, which originates in most cases from a laser source, and is applied in analyzing molecular movements and identification of chemical compositions of solid, fluid and gaseous samples. The principle behind this technology entails

illumination of the sample with a monochromatic light of laser at UV, Vis or NIR range. The photons of this light are absorbed and then reemitted by the sample. Frequency of a few photons from the sample shifts up or down relative to the original photon frequency. This shift is referred to as the Raman effect and gives information about the vibrational and rotational frequencies.

5.9.1 Process and Derivative Outputs

Analyzing setup:

• Laboratory: Laser Raman spectroscopy, NCEGR, CHQ

• LASER: 514 nm edge Ar+ laser (gratings: 2400 lines/mm)

• Spot beam Diameter: ~ 1.2 µm

• Focus Energy: 12 – 15 mW

• Spectrum Accumulations time: 20 s.

The room temperature was maintained at 22 ± 1ºC. The peak positions of Raman spectra were determined by the Wire program (Version 3.4). The spectral resolution for each Raman vibrational mode is on the order of ± 1-2 cm-1. (Dennison et. al., 1996; Neubick et. al., 2020; Zhang et. al. 2022)

The adopted process required representative graphite-bearing material from mineralised zones to be subjected to Raman spectral acquisition over the range 1,100–3,200 cm^{-1} to capture the diagnostic D band, G band and 2D band. Low laser power was mandated to avoid thermal damage; either 532 nm or 785 nm laser was permitted depending on fluorescence behaviour. Required outputs per sample: band positions and intensities, full width at half maximum (FWHM) of the G band and derived ratios I_D/I_G and I_2D/I_G. Multi-spot analysis per sample (minimum 3 spots) was required to characterize intra-sample graphite-order heterogeneity.

Derivative outputs include: (i) the graphite-order dataset (I_D/I_G as primary indicator of structural order and defect density; I_2D/I_G as supporting indicator) classifying carbonaceous material into highly ordered, moderately ordered, defective, or highly disordered graphite; (ii) the intra-sample heterogeneity profile distinguishing uniform graphite populations from mixed recrystallization histories; and (iii) a cross-disciplinary graphite-quality layer when Raman results are correlated with XRD d002 spacing and fixed-carbon (FC) results - the SOP specifically requires this correlation. The currently available Raman dataset is reconnaissance-

level (3 surface bedrock samples) and should be treated as confirmatory rather than exhaustive; 8 subsurface sample for Raman were identified in chapter 6.6.5.

5.9.2 SOP and QA/QC Protocol

The SOP required: representative sample selection covering the full range of graphite habits and grades; spectral acquisition at 532 nm or 785 nm at low power; recording of D-band, G-band and 2D-band positions and intensities, G-band FWHM and calculated I_D/I_G and I_2D/I_G; a minimum of 3 spots per sample including both large and small grains and visually bright and dull graphite domains (anti-bias rule - analysts were explicitly instructed not to target only coarse flakes). Samples for Raman trace back to the same controlled field-sampling chain used for surface grab or bedrock sampling.

The quality control process accounted for the following four types of uncertainty: (i) instrument calibration – the use of a reference standard (HOPG) that will be analyzed at the beginning of each analytical run; (ii) repeatability – analysis of 5% of samples twice with the same instrument but by another analyst; (iii) thermal effects – using low laser power and defocused beam when necessary and monitoring for any changes in Raman bands due to burning; and (iv) fluorescence – using 785 nm laser, extending exposure time, and applying baseline correction in case of organic fluorescence.

5.10 X-Ray Diffraction (XRD)

XRD formed part of the advanced mineralogical characterisation programme to identify crystalline mineral phases in graphite-bearing rocks and associated host lithologies, distinguishing graphite-rich schist from quartz-rich, mica-rich, chloritic, clay-bearing, or sulphidic variants. Work was carried out at the Geological Survey of India, Kolkata and Nagpur. The approved work programme provided for 10 XRD analyses (Annexure XVI).

5.10.1 Process and Derivative Outputs

Representative graphite-bearing and host-rock samples were dried, powdered and mounted for X-ray powder diffraction analysis. Diffractograms were generated over the prescribed 2-theta scan range (4.0954–79.5784° 2θ, step size 0.0170°, count time 50.8 seconds per step, Cu Kα radiation) and matched against reference mineral databases. The programme generated graphite-specific structural information including d002 spacing and a crystallinity indicator, in addition to the standard phase list and semi-quantitative mineral abundances.

Principal phases recorded: quartz, graphite and muscovite; with clinochlore, albite, pyrite and rectorite in selected samples. Samples 109923, 109999 and 110001 are most quartz-rich

(graphite schist with graphite in minor to moderate proportions). Sample 109938 is richer in muscovite with minor albite and pyrite. Sample 110004 is markedly different, containing abundant rectorite and only trace graphite. The key explorational derivative is the d002 spacing: values close to 3.354 Å are indicative of well-ordered crystalline graphite; substantially higher values reflect poorly ordered carbonaceous material.

5.10.2 SOP and QA/QC Protocol

SOP required random mounts of powders obtained through back-loading in order to avoid preferred orientation (more so with respect to platy graphite and mica). The analysis requirements included qualitative phase determination, semi-quantitative phase determination, d002 spacing of graphite, and an index for graphite crystallinity. XRD data were to be interpreted using a multidisciplinary approach, where the list of minerals was correlated with modal analysis from petrography and geochemical analysis using XRF/XRD techniques.

QC was based on internal consistency and instrument verification: (i) XRD mineralogy checked against XRF chemistry (e.g., quartz-rich interpretations must correspond to elevated SiO_2; muscovite-rich samples must be compatible with Al_2O_3 and K_2O); (ii) periodic analysis of certified mineralogical reference standards to confirm diffractometer calibration and phase identification stability. Analytical risks and mitigations: preferred orientation bias addressed through back-loading preparation (any orientation correction applied must be documented); peak overlap between quartz, mica, chlorite and clay phases must be checked against multiple peaks per phase and reconciled with petrography, Raman and geochemistry before final use.

5.11 Isodynamic Separation of Heavy Minerals from Stream Sediment Samples

Isodynamic separation was the mineral-separation stage applied to the heavy-mineral concentrate stream from the stream-sediment programme, carried out at the Geological Survey of India, Kolkata. The main project report records that 25 stream sediment samples were advanced for heavy-mineral separation through gravity and magnetic techniques. The isodynamic stage sat between field sediment collection and downstream mineralogical interpretation, serving as a mineralogical screening tool to refine the stream-sediment programme (Annexure XIV).

5.11.1 Process and Derivative Outputs

The working procedure began with the heavy-mineral concentrate obtained from the sediment sample. Material was first dried to constant mass, size-fractionated through sieves (usable grain-size range 63–500 µm, with 63–250 µm identified as the usual target fraction for

graphite/vanadium-bearing minerals) and cleaned to remove adhering fines and coatings. The Frantz Isodynamic Separator then passed the dry feed through a stepped sequence of magnetic field strengths - sequential stages at 0.3 A, 0.5 A, 0.7 A, 1.0 A, 1.5 A and 1.7 A, followed by 5° magnetic and 5° non-magnetic end fractions - with each stage producing a labelled split for subsequent examination. Annexure XIV records fraction weights for all 25 sample entries at each amperage step, together with total sample weight. That allows each drainage to be described by its fraction-wise magnetic susceptibility distribution, identifying whether it is dominated by strongly magnetic minerals, carries a significant weakly magnetic fraction, or retains a meaningful non-magnetic fraction warranting examination for graphite and associated minerals.

5.11.2 SOP and QA/QC Protocol

Primary equipment specified: Frantz Isodynamic Separator, analytical balance, binocular microscope, ultrasonic bath, drying oven, vibrating sieve shaker, fume hood and non-magnetic laboratory tools. Standard setup: forward tilt at −5°, side tilt 10°–15°, vibration adjusted to steady single-file grain flow, warm-up before the run. Separation proceeds from low to high field strength generating strongly magnetic, moderately magnetic, weakly magnetic, very weakly magnetic and residual non-magnetic fractions.

QC was instrument-based: (i) instrument blank every 10 samples or at start of each operator session; (ii) mass-balance check for every sample (summed fraction masses within ±2% of initial feed weight - direct check on recovery); (iii) blind duplicates on 1 in 10 samples; (iv) one certified reference material per batch of 20 samples; (v) amperage calibration before each analytical session; (vi) cross-contamination checks between samples; (vii) operator competency checks for new or periodically reviewed personnel; (viii) trough-angle verification at the start of every session. Contamination controls: instrument cleaned between samples with brushing and acetone wipe-down; only one sample actively processed at a time on the bench. Dry sieving and separation are dust-generating operations requiring controlled handling, ventilation and PPE.

5.12 Geophysics - Self Potential (SP)

Self-Potential survey was the first passive geophysical method applied, used primarily to detect graphite-bearing horizons because graphite schist generates distinct negative SP responses when contrasted with enclosing resistive lithologies. A total of 32.6 line-km of SP profiling (Annexure XVII, Figure 5.16) was completed across the block (approved quantum: 30 line-km). Profiles were laid perpendicular to the interpreted strike of graphite-bearing units;

station readings at generally 50 m intervals using non-polarising copper sulphate electrodes. The method was used for rapid screening and integrated with mapped graphite schist, trench and pit exposures and VES-derived conductive layers - not as a stand-alone ore-detection tool.

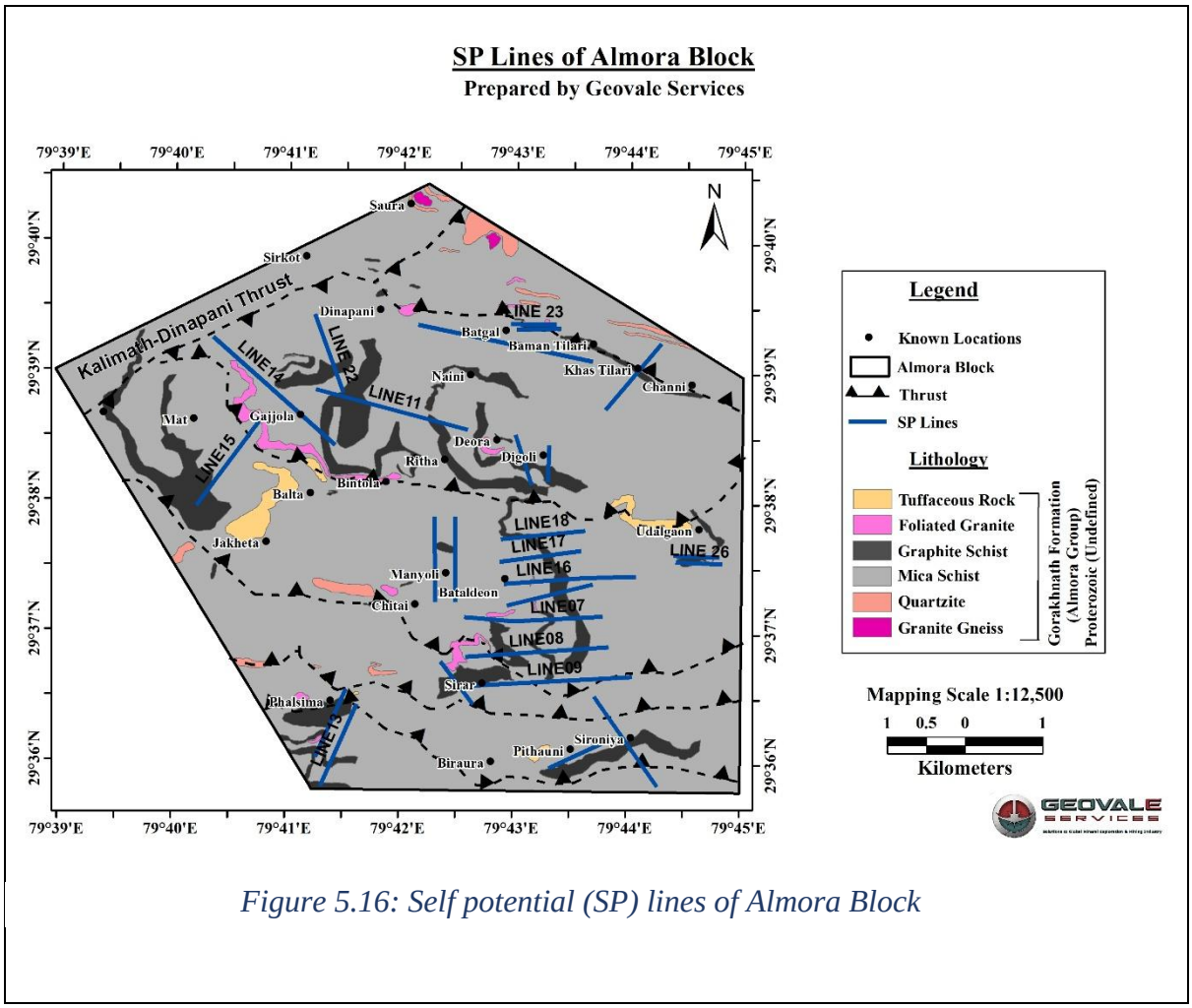

Figure 5.16: Self potential (SP) lines of Almora Block

5.12.1 Process and Derivative Outputs

The SP survey has been carried out by using Anvic Aquameter CRM 500. One electrode was kept as the fixed reference; the second moved sequentially along the line. At each station, the natural potential difference relative to the base point was recorded in millivolts together with station number, coordinates, elevation and observation time. The raw field datasheet preserves base-station entries, station-wise measurements and revised columns tracking subsequent correction. Two representative responses from the block: a sharp negative anomaly in the Pithauni area (narrow but intense conductor) and a broader negative anomaly in the Bataldeon area (SP values down to ~−400 mV, suggesting a thicker graphitic horizon) (Figure 5.17, Figure 5.18).

Derivative outputs include: (i) line-wise SP profiles (corrected potential vs. station distance), with representative SP-elevation plots prepared for Pithauni and Bataldeon areas and processed line models referred to as Annexure XVIII line models; (ii) spatial GIS line-coverage layer relating survey lines to mapped lithology and structure; (iii) corrected SP anomaly map with 30 m contour interval, overlaying SP observation points, mapped graphite schist and tentative VES locations; and (iv) an integrated graphite-conductor model combining SP polarity with lithological and resistivity information - the report notes that coincidence of resistivity conductors with SP anomalies strengthens the interpretation of graphite mineralisation over clay-rich or water-saturated ground.

Figure 5.17: SP data collection from Aquameter, Bataldeon area.

Figure 5.18: SP data collection from Aquameter, Bataldeon area.

5.12.2 SOP and QA/QC Protocol

The SOP entailed: the necessity of performing profile planning in GIS prior to field work; profile interval between 50 and 100 meters; consistent spacing of stations at 50 meters; extending the lines beyond the target zones interpreted for obtaining local background data; locating the base electrode in geologically neutral zone; use of non-polarized Cu-$CuSO_4$ electrodes, tested to match each other within ±2 mV using saturated copper sulphate solution. At the stations: ensuring good contact with the ground by watering if necessary; giving time for stabilization; making multiple measurements; visiting the base at every 60 minutes for drift correction.

QC focused on repeatability, drift control and geological consistency: (i) repeated base-station occupation at regular intervals for drift correction (ii) daily electrode conditioning and cup matching; (iii) geological cross-validation - SP anomalies accepted only when compared with mapped graphite schist, trench/pit observations and VES-derived conductive zones; multi-

dataset consistency used as a QC filter to reduce false positives. The survey was to avoid metallic fences, pipelines and powerlines within ~50 m where possible and to suspend work during rain or lightning.

5.13 Geophysics - Vertical Electrical Sounding (VES)

VES was the principal active geophysical method used to investigate vertical variations in subsurface resistivity and to identify conductive graphite-bearing horizons beneath areas of poor or discontinuous exposure. The method was used to trace concealed graphitic bands, estimate their depth disposition and support drill-location selection. Schlumberger array soundings were conducted using an Anvic Aquameter CRM 500 resistivity meter. In total, 154 vertical soundings amounting to 31.4 line-km (Annexure XIX, Figure 5.19) of coverage were completed (approved quantum: refer to Chapter 6). Sounding sites were preferentially selected along contours to reduce the effect of topographic breaks.

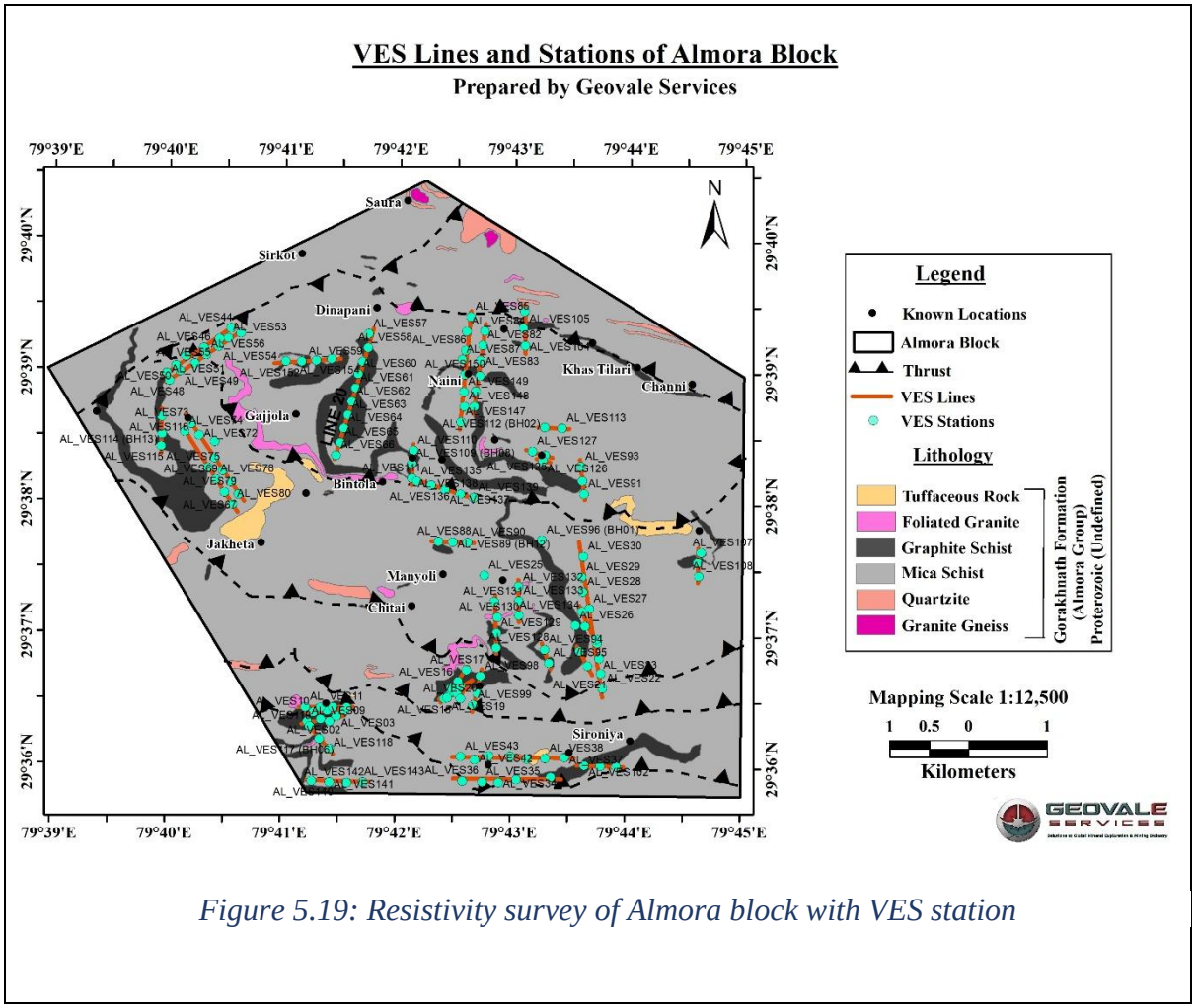

Figure 5.19: Resistivity survey of Almora block with VES station

5.13.1 Process and Derivative Outputs

At each sounding location, current was injected through two outer electrodes and the resulting potential difference measured through two inner electrodes; resistance was calculated for each expansion step and converted to apparent resistivity using the Schlumberger geometric factor. The raw sheets preserve sounding number, date, area name, coordinates, elevation, orientation, AB/2 spacing, MN/2 spacing, resistance, geometric factor K and derived apparent resistivity (Figure 5.20, Figure 5.21, Figure 5.22, Figure 5.23, Figure 5.24, Figure 5.25). Representative examples illustrating the block variability: AL_VES01 (Phalshima, 04/03/2025) shows apparent resistivity decreasing from ~614 at small spacing to ~47 at AB/2 = 100, suggesting progressively more conductive response at depth; AL_VES29 (Bajyoli) shows a generally rising curve; AL_VES32 (Pithauni) declines from ~2,124 at shallow spacing to ~100 at larger spacings. Soundings were distributed across Phalshima, Sirar, Bajyoli, Pithauni, Biraura/Bhirora and Matena.

Derivative outputs include: (i) field sounding curves (apparent resistivity vs. AB/2 spacing); (ii) 1D resistivity inversion models (depth vs. resistivity layer interpretation), with representative models illustrated for VES28, VES29 and VES30; (iii) spatial VES layout layer in GIS; and (iv) integrated interpretation products in which selected VES models are compared with SP anomalies and mapped graphite schist (Annexure XX).

Figure 5.20: VES data collection in Sirar area.

Figure 5.21: VES data collection in Phalsima area

Figure 5.22: VES data collection in Pithouni area.

Figure 5.23: VES data collection in Pithauni area.

Figure 5.24: Collected VES data from Aquameter, Bataldeon area

Figure 5.25: Collected VES data from Aquameter, Sirar area.

5.13.2 SOP and QA/QC Protocol

SOP requirements included: Schlumberger geometry usage (ratio of current-electrode spacing to potential-electrode spacing ≥5 during each stage of expansion); GPS location for

each sounding point; array direction orthogonal to geological formation trend whenever possible; insertion of electrodes to ≥80% depth; application of water at points of contact when necessary; pre-reading inspection of all cables and crocodile clips; testing of instrument at maximum current setting initially; ≥3 readings per electrode arrangement with the average being recorded; real-time plotting of apparent resistivity using log-log paper or digital method to pinpoint any erroneous data.

The QC protocol involved four linked controls: (i) repeatability - minimum 3 readings per configuration, mean value for apparent resistivity; full sounding repeated at 5% of locations on a different day; (ii) instrument and field-condition control - battery condition, cable integrity and contact resistance checked systematically; (iii) independent re-processing - 10% of soundings independently processed by a second geophysicist for model comparison; the SOP explicitly recognises inversion non-uniqueness and requires geological constraints and equivalence analysis where ambiguity is present; and (iv) geological cross-validation - lateral heterogeneity near sharp contacts or faults to be flagged and checked against mapping. Sounding sites preferentially along contours in highly undulating terrain to improve data quality and current distribution.

5.14 Tumbler Test (Graphite Crystallinity Field Assessment)

The tumbler test was used as a rapid field-scale method for distinguishing crystalline flaky graphite from carbonaceous material and for recording the mechanical behaviour of graphite-bearing samples under gentle water-assisted agitation. It was applied at outcrop, trench, pit and drill-core stages wherever graphite-bearing rock was visibly present, occupying an important place between geological observation and laboratory confirmation - providing an immediate field proxy for flake preservation, graphite habit and likely beneficiation relevance. In the field we collected 70 high responses, 207 moderate responses and 113 poor responses, predominantly from graphite schist with a smaller subset from graphite-schist-bearing hosts and related garnet-mica schist associations (Annexure IV).

5.14.1 Process and Derivative Outputs

A graphite-bearing specimen was carefully exposed (not crushed). A small representative fragment (~10–30 g) was placed in a standard hard-plastic cup, submerged in clean water, soaked for ~5–10 minutes to soften the clay/mica matrix, then gently rotated in circular motion to simulate low-energy stress. The slurry was decanted and replaced with clean water through repeated wash cycles, during which the geologist observed whether graphite remained as flexible recognisable flakes, degraded into fines, floated preferentially, or behaved as dull

carbonaceous matter. Powdered material floating in water indicated flaky graphite; sinking material was more consistent with graphite schist or amorphous carbonaceous matter. The Almora block's graphite textural variability (fine- to medium-flaky at Sirar, Balta, Bajyoli, Ritha and Udalgaon; coarser at Debdiya and Khas Tilari; more nodular/thread-like at Kalimat) made rapid field discrimination between preserved flakes and lower-crystallinity carbonaceous matter essential for directing follow-up work (Figure 5.26, Figure 5.27).

Derivative outputs include: (i) a field quality classification (High/Good, Moderate, or Poor) per sample, forming a repeatable record comparable across graphite bands, pits, trenches and drill intersections; (ii) a point-based graphite crystallinity/flake-quality dataset - Annexure IV stores location-wise coordinates, host lithology, surface mineralization and field crystallinity class - which can be symbolised as a thematic GIS layer; (iii) a prioritisation matrix for follow-up analytical work (Raman, XRD, proximate analysis, beneficiation studies, trenching, drilling support); and (iv) a photographic evidence package (before-and-after photographs) providing a visual audit trail of sample behaviour.

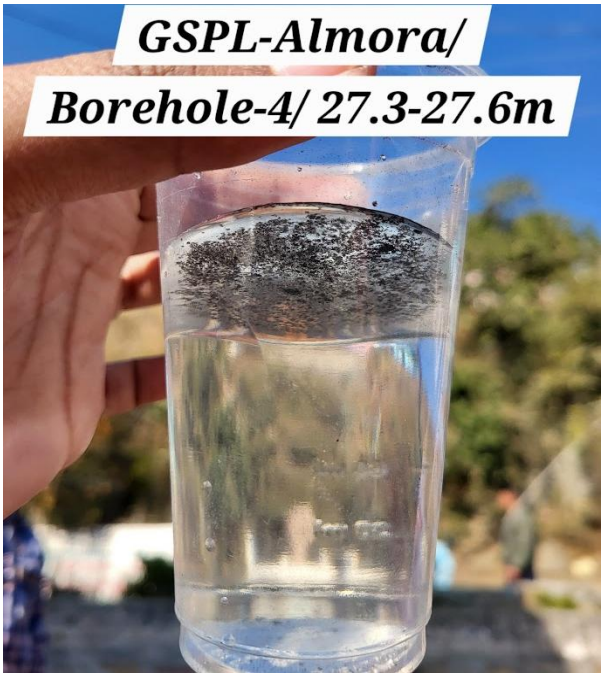

Figure 5.26: Tumbler test for the borehole 04 samples showing majority of graphite flake floating on the water.

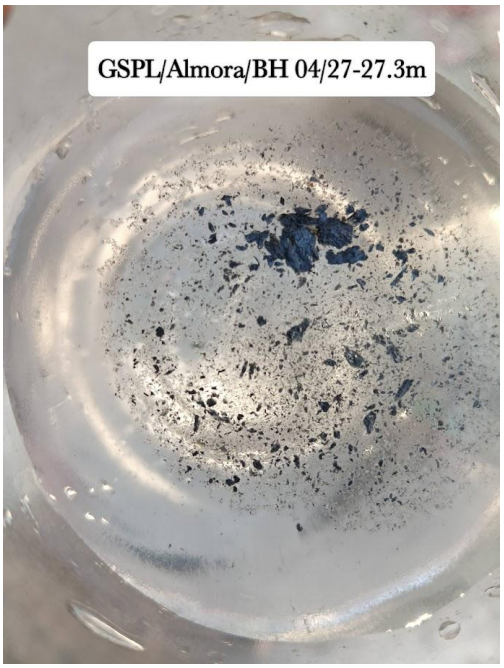

Figure 5.27: Tumbler test carried on the to verify graphite flake size.

5.14.2 SOP and QA/QC Protocol

SOP expected the following: gentle pounding to produce fresh surface without crushing the core; 10-30 g in a standard plastic cup, with clean water added; soaking; carefully controlled circular motions to agitate the contents, then wash; determination of behaviour class; record of sample identification/number, location, lithology, field behaviour class, date and operator; before and after photographs with scale. SOP was not just the handling procedure, but also a way of documenting the process.

Quality Control aimed to limit operator biases: (i) replicate testing for ~10% of samples by another geologist; (ii) field campaign calibration when starting the sampling campaign – calibration for each geologist on cup size, volume of water, degree of agitation, and class cut-off criteria (essential because any procedural changes would dramatically alter outcomes); (iii) daily review of anomalous results or questionable samples before interpretation was firmly established in sampling routine; (iv) field photos as an extra tool for quality control. Risk mitigation strategies included: standardized handling, favoring of fresher material, use of clean water, cross-geologist checking, and explicit statement that tumbler test was a qualitative field indicator only.

5.15 Geochemical Assay - XRF (Major Oxide Analysis)

XRF was the principal whole-rock major oxide assay stream for lithological characterization, discrimination of graphitic and non-graphitic host rocks, recognition of iron-rich or sulphide-bearing variants and preliminary appraisal of vanadium-associated carbonaceous horizons. The executed work comprised: Phase I surface programme - 200 major oxide samples (Annexure VII) + 20 external check samples (Annexure VIII) + 20 Sn/W extension XRF samples with 2 associated checks (Annexure IX); borehole programme - 50 samples for major oxides (Annexure XXII) with external checks (Annexure XXIII) and limited additional-element verification. Analyses were executed through Inspectorate Griffith Commodities Division, Bureau Veritas, Gandhidham, with check analyses at Shiva Analytical, Bengaluru.

5.15.1 Process and Derivative Outputs

Representative surface, trench and drill-core samples were submitted with unique sample Ids linked to coordinates, lithology and sampling medium. The analytical method was wavelength-dispersive XRF on fused glass beads (lithium-borate fusion) for major oxide determinations; the reporting suite comprises SiO_2, Al_2O_3, Fe_2O_3 (total), MgO, CaO, Na_2O,

K_2O, TiO_2, P_2O_5, MnO, Cr_2O_3 and LOI, with V_2O_5, SnO_2 and WO_3 for selected early pathfinder screening. The main dataset includes fields for sample number, sample Id, coordinates, lithology, sample type and full oxide suite.

5.15.2 SOP and QA/QC Protocol

The SOP required fused glass bead preparation (lithium-borate fusion) for major oxide determinations; pressed pellets accepted only for trace-element work. Every sample moved through a disciplined submission chain maintaining sample identity, analytical request and geological context from field to laboratory. The laboratory side preserved method references, units and quantification limits; the external-check sheet preserved paired results between primary and check laboratories.

Three QC layers were applied: (i) internal chemical consistency - major oxide totals must fall between 99.5–100.5%; all outliers investigated (especially important given that LOI is strongly influenced by graphite combustion in this project); matrix effects minimised through fused-bead preparation; (ii) external checks - 20 external XRF checks for the 200-sample Phase I programme; 5 external checks for the 50-sample borehole programme; the Annexure VII preserves a paired comparison sheet with two analytical rows per selected sample Id; and (iii) geological reconciliation - high-SiO_2 quartzites must correspond to quartz-rich mapped lithologies; graphite schists must show chemistry compatible with carbonaceous and locally sulphidic horizons; iron-rich materials must show corresponding Fe enrichment in both field description and assay. This filters out chemically improbable results before targeting decisions.

5.16 Geochemical Assay - Proximate Analysis (Fixed Carbon)

50 samples for the surface (Annexure X) and 50 borehole samples (Annexure XXVII), for FC, moisture (IM), volatile matter (VM) and ash were analyses.

5.16.1 Process and Derivative Outputs

Representative graphitic samples were submitted to a current NABL-accredited laboratory. The SOP specified two permissible analytical routes: (i) LECO combustion - total carbon measured under high-temperature oxygen combustion, corrected for total inorganic carbon to obtain fixed carbon (preferred route); and (ii) proximate analysis - moisture determined at 105°C, volatile matter at 950°C under nitrogen, ash at 750°C in air, with fixed carbon calculated as 100 minus the sum of moisture, volatile matter and ash (accepted alternative). A homogenised pulp aliquot of ~0.5–1.0 g per determination was required.

5.16.2 SOP and QA/QC Protocol

The SOP stipulated that there must be compulsory reporting of FC, ash, volatile matter, and moisture for each sample, submission to NABL-accredited laboratories, and applying the same logic for grade for both surface and subsurface materials. With regards to documentation/report writing, the proximate data set needs to be kept in two versions: one in the raw data from the laboratory and another version after eliminating all formulaic and/or erroneous entries.

QC was based on: (i) accuracy - blind insertion of certified reference materials at ~1 in 20 samples, spanning low-, medium- and high-FC ranges, with acceptable performance within ±2 standard deviations of certified value; (ii) precision - laboratory pulp duplicates at ~1 in 20 samples, relative difference below 10% required; (iii) internal consistency check - FC and associated proximate components must reconcile (low FC → high ash; higher FC must not be contradicted by implausible proximate balances); and (iv) database management - the working analytical file should be archived in both raw and cleaned forms as separate documents for auditability.

5.17 Geochemical Assay - ICP-MS (Trace Element and REE Analysis)

ICPMS was adopted as the principal trace-element and rare-earth-element assay stream for evaluating vanadium enrichment, associated base and critical metals and the broader elemental character of graphitic, carbonaceous and barren host lithologies. Two executed ICPMS streams were completed: 100 Phase I surface samples (Annexure XI) with + 10 check samples (Annexure XII) and 150 borehole samples (Annexure XXV) with + 15 check samples (Annexure XXVI). Analyses were executed through Inspectorate Griffith Commodities Division, Bureau Veritas, Gandhidham, with check analyses at Shiva Analytical, Bengaluru.

5.17.1 Process and Derivative Outputs

The analytical route specified is 4-acid digestion (HF-HNO_3-$HClO_4$-HCl) for near-total dissolution, with an explicit caution that resistant phases (chromite, zircon, cassiterite, some Ti oxides) may not dissolve completely; lithium-borate fusion followed by ICP-MS is required where those minerals are material to interpretation. The minimum reporting suite includes V, Cr, Ni, Cu, Zn, Rb, Sr, Y, Zr, Nb, Mo, Sn, Ba, full REE group (La to Lu), Hf, Ta, W, Pb, Th, U and sulphur, with vanadium at low detection limit (key by-product indicator in the Almora black-shale/graphite-schist system). The Annexure XI and Annexure XXV contain 250 rows

with assay columns extending from Li, Be through V, Cr, Co, Ni, Cu, Zn, Rb, Sr, Y, Zr, Nb, Mo, Sn, Sb, Ba, La-Ce-Nd and other REEs, to Hf, Ta, W, Tl, Pb, Bi, Th, U.

5.17.2 SOP and QA/QC Protocol

This SOP mandates that the digestion procedure, detection limits, analytical precision, and units of reporting be stated for each batch. This methodology involves a selective sampling process as opposed to a blanket analysis. The ICP-MS is presented as the analytical stream that identifies vanadium enrichment and metallogenic signatures and REE patterns in graphite-hosted and non-graphite-hosted environments.

QC comprised: (i) accuracy - certified reference materials at ~1 in 20 samples; (ii) contamination - blanks at ~1 in 30; (iii) precision - pulp duplicates at ~1 in 20; (iv) umpire analysis - 5% of samples at a second laboratory; and (v) control-chart monitoring of vanadium, REEs and other critical pathfinder elements. A project-specific QC concern: possible BaO spectral interference on Eu in High-Ba samples (samples with Ba >1,000 ppm are to be flagged for Eu data review - directly relevant given extreme Ba values in the Almora dataset). Additional QC should include lithology-against-assay reconciliation, duplicate comparison of High-V populations and consistency checks between sulphur-bearing samples, field sulphide observations and geophysical responses.

5.18 Geochemical Assay - Total Sulphur

Total sulphur (TS) analysis was adopted to quantify sulphur content in graphite-bearing, carbonaceous and locally sulphidic rock samples, distinguishing relatively clean graphitic material from units containing pyrite and related sulphides. The executed work comprised 25 samples (approved: 25; achieved: 25). Samples were drawn chiefly from bedrock exposures, with additional selected samples from pits and trenches, weighted toward graphite schist, graphite schist, sulphur-bearing graphitic material, metallic carbonaceous layers and a small number of associated host lithologies (Annexure XIII).

5.18.1 Process and Derivative Outputs

Samples were selected on geological grounds from graphite-bearing and carbonaceous units, especially where field descriptions indicated sulphidic character. Material was dried, crushed, pulverised and homogenised before dispatch to an accredited laboratory for total sulphur determination. The SOP required maintaining a chain-of-custody from field to laboratory, with the sample number, medium description and submission identity preserved

throughout. TS values were integrated with lithological descriptions, XRF major-oxide data, ICP-MS trace-element data and fixed-carbon results.

Derivative outputs: (i) sample-wise sulphur dataset (TS%); (ii) sulphur histogram and frequency curves for identifying anomalous sulphur populations (Chapter 6 plot); (iii) geological discrimination layer - elevated TS values matched with graphite schist, graphite schist, field pyrite pits, metallic layers and associated descriptions to identify intervals where graphite mineralisation is accompanied by iron sulphides; and (iv) integrated targeting product - TS used as a discriminant variable explaining why certain graphitic units show stronger Fe-S signatures, why some geophysical responses may reflect conductive sulphidic graphite and why vanadium-bearing carbonaceous horizons can be geochemically more fertile than visually similar but less sulphidic units.

5.18.2 SOP and QA/QC Protocol

The SOP required: geological selection of samples indicating sulphidic character; maintenance of unique sample number and submission identity throughout the chain; dry, representative, homogenised pulp dispatched to an accredited laboratory; total sulphur reported together with method information, units, batch identity and QC records. TS analysis was explicitly not to be interpreted in isolation: it was to remain comparable with fixed carbon, XRF major oxides and ICP-MS trace-element results.

QC involved: (i) accuracy, by laboratory standards or certified reference material within the assay batch; (ii) precision, by duplicate analyses or pulp duplicates, or by laboratory repeats for certain samples; (iii) geological validation – the presence of exceptionally high sulphur values was anticipated where there were carbonaceous or graphitic rocks with sulphide signature characteristics; exceptionally high TS content in visibly barren rock formations needed to be confirmed to ensure no sample mislabelling or contamination occurred, or problems with the analysis itself; and (iv) reconciliations between datasets – TS data compared with XRF sulphide content and ICP-MS elements with redox properties, and proximate analysis data.

5.19 Scout Drilling

Scout drilling represented the first direct Subsurface validation stage of the programme, undertaken only after lithological, structural, geochemical, pitting-trenching and geophysical evidence had been integrated into a ranked target set. The programme was conceived to test the integrated geological-geophysical model, confirm the depth persistence of graphite-bearing

horizons, recover continuous core for logging and laboratory characterization and examine whether the surface graphite-schist bands continue coherently below cover. The method adopted was diamond core drilling for 800 m using standard wireline practice (HQ and NQ core; HQ preferred, NQ where required by ground conditions or depth; water circulation for cooling and cuttings removal; sludge collected as a supplementary geological record where formation disintegration reduced core recovery). Holes were kept vertical; no downhole geophysical logging or formal deviation survey was carried out in this phase.

A total of 300 m of NQT-sanctioned drill core has been preserved at the GSI Core Library, Lucknow, in accordance with the prescribed protocol for safe custody and future reference. The preserved core (Annexure XXIX) represents an important geological archive for detailed re-examination, validation of observations and supporting future exploration studies. In addition, pillaring construction work (Annexure XXX) has been initiated for the G4 stage exploration programme to facilitate systematic drilling operations, ensure stable access and support efficient execution of the proposed field activities.

5.19.1 Process, Hole Inventory and Derivative Outputs

Twelve scout boreholes were planned (Figure 8.1). The tabulated collar table presently documents BH01 to BH12. Holes are distributed across Digoli, Bataldeon, Sirar, Barakote, Mat, Pithauni, Deora, Udalgaon and Batgal, ranging from 28.5 m to 106 m depth. The documented 12 holes total 801.2 m; this should be reconciled against the broader project summary recording 800 m of core drilling as the achieved work quantum (Figure 5.28, Figure 5.29). Collar selection was guided by mapped graphite bands, favourable surface fixed-carbon values, anomalous multi-element geochemistry and supportive VES responses. Holes are spatially spread 3–4 km apart across central, southern and northern sectors to test multiple target corridors.

Key hole-wise results: BH01 - significant graphite-bearing intervals below shallow weathered cap, from ~16 m to 91.7 m. BH02 - graphite intervals from ~14–15 m to 40 m. BH03 - graphite from 12.5 m to end of hole (75 m), with strong high-grade interval at ~31.45–42 m. BH05 - graphite-rich intervals persistent below ~25.4 m. BH06 - two notable high-grade zones at ~41–45.3 m and ~84.8–88.9 m. BH11 - principal graphite interval from ~23.6 m, including a localized sulphidic high-grade band at ~58.35–59.7 m. Graphite in core occurs as laminated/banded graphite schist, graphite-sericite schist, graphitic quartzite, or quartz-muscovite-graphite schist, commonly with pyrite and locally chalcopyrite. Overall core

recovery was generally good at ~90%; local reductions linked to sludge zones, brecciated intervals and strongly fractured ground.

The drilling programme generated: collar register with BH01–BH12 data; run-wise core recovery and RQD records; box-wise geological logs; core photographs; interval-wise channel sample registers; sludge records; petrographic/mineralogical follow-up on selected core intervals; and analytical datasets from XRF, ICPMS, proximate analysis, and XRD submissions. Interpretive derivatives include borehole lithological logs, mineralized interval summaries, depth-wise graphite-zone interpretations, core-photo plates, drillhole-to-surface correlation tables and the first defensible three-dimensional control on thickness, continuity, lithological association, sulphide relationship and depth behaviour of the Almora graphite system.

Figure 5.28: Borehole 10 drilling site at Sirar area.

Figure 5.29: Core box of borehole 03

5.19.2 SOP and QA/QC Protocol

The SOP required: approved drill plan documenting collar position, orientation, planned depth, geological rationale and relationship to the interpreted target; surveyed collar coordinates and RL after rig setup; triple-tube barrels in broken/weathered ground (double-tube in competent rock). On retrieval: orientation marking, run-measured recovery vs. drilled interval, core recovery and RQD calculated per run (target >90% in mineralised zones); steel tags at run boundaries and core-loss intervals; complete logging within 24 hours; photography before cutting; logging by rock type, mineral assemblage, mineralisation and geotechnical condition.

Sampling SOP required: longitudinal core cutting with retention of three-quarters in the box for future reference; quarter-core dispatch for laboratory analysis; sample intervals at ~1 m through mineralised zones or to geological contact boundaries; each sample linked to Hole ID, from-to depth, sample length and lithology. QC comprised four linked controls: (i) recovery monitoring per run with sludge documentation where recovery falls below threshold; (ii) logging and sampling reproducibility - daily reconciliation of measured core length against driller's depth; re-logging of 10% of core by a senior geologist; pre-printed sample tags with metal identifiers; blind quarter-core duplicates at 1 in 20; (iii) umpire assays at an independent accredited laboratory on 10% of analysed samples (principal assays through Bureau Veritas, check work at Shiva Analytics); and (iv) accurate collar control and depth discipline - given that no formal deviation logging was sanctioned, quality of collar survey, RL capture, run-wise depth reconciliation, core photography and box control was especially important. The drillhole database in the final report should include: collar register, run-wise recovery and RQD sheets, box photo catalogue, logged lithological intervals, analytical sample register, assay tables and hole sections or fence diagrams.

Chapter 6

Geology, Structure, Metamorphism, Mineral Systems Analysis

6 Geology, Structure, Metamorphism, Mineral Systems Analysis:

6.1 Geological Mapping:

Geological mapping of the Almora block was carried out to develop a clear understanding of the lithological variation, structural framework, and the surface expression of graphite horizons. The block is situated within a highly deformed metamorphic terrain, where various lithologies are modified by folding, shearing, and local intrusive bodies. In such a geological setting, detailed mapping is essential for interpreting the distribution and continuity of graphite-bearing horizons and their relationship with the surrounding host rocks.

The following sections describe the geological interpretation is based on published Geological Survey of India maps at regional and large scales, following the Geovale's mapped lithological units, their field characteristics, and the tectonism of the graphite-bearing horizons, providing the geological basis for interpretation of mineralization within the Almora block.

6.1.1 Geological Map by GSI:

The geological map of the Almora area at 1:50,000 scale was prepared by GSI (Figure 6.1). Based on this map, two litho-units are identified within the Almora block namely garnet mica-schist-chlorite-schist-quartz with phyllite and porphyritic granite-granite-gneiss. Garnet mica-schist and chlorite-schist (quartz with phyllite) is the dominant rock types, occupying approximately 90% area of the Almora block. In the north-eastern part of the block, within the garnet mica and chlorite schist terrain, thin band of porphyritic granite associated with granite-gneiss body is observed, exhibiting a folded nature. In the northern part, adjacent to the block boundary, two parallel WNW–ESE trending linear bodies of porphyritic granite - granite-gneiss are present, a portion of one such body extending into the northern part of the block. In the south-eastern part, along the block margin, graphite schist along with quartzite and schist bodies are present.

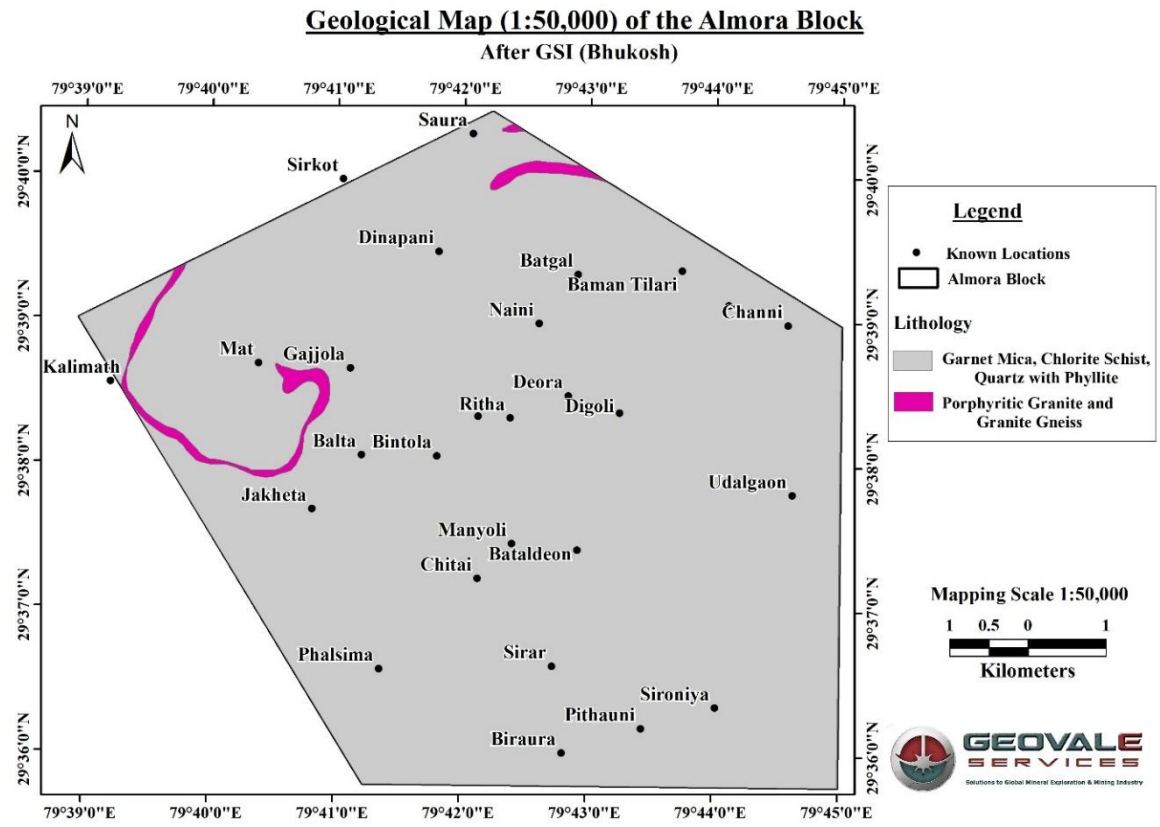

Figure 6.1: Geological Map (scale 1:50000) by GSI.

6.1.2 Large Scale Geological Map by GSI:

The area had been mapped in 1:12,500 scale recently by GSI (Santosh and Yadav, 2021) (Figure 6.2, Figure 6.3). Based on their map, the dominant rock type of the block is garnet mica-schist. In the northern part of the block, the WNW- ESE trending one granite-gneiss band, three foliated tourmaline granite bands and eight sheared quartzite bands are present. In the central part of the block, 18 the folded shallow dipping graphite-schist, 27 folded quartzite bands are marked. All over the block 22 injected gneiss rock bodies are present.

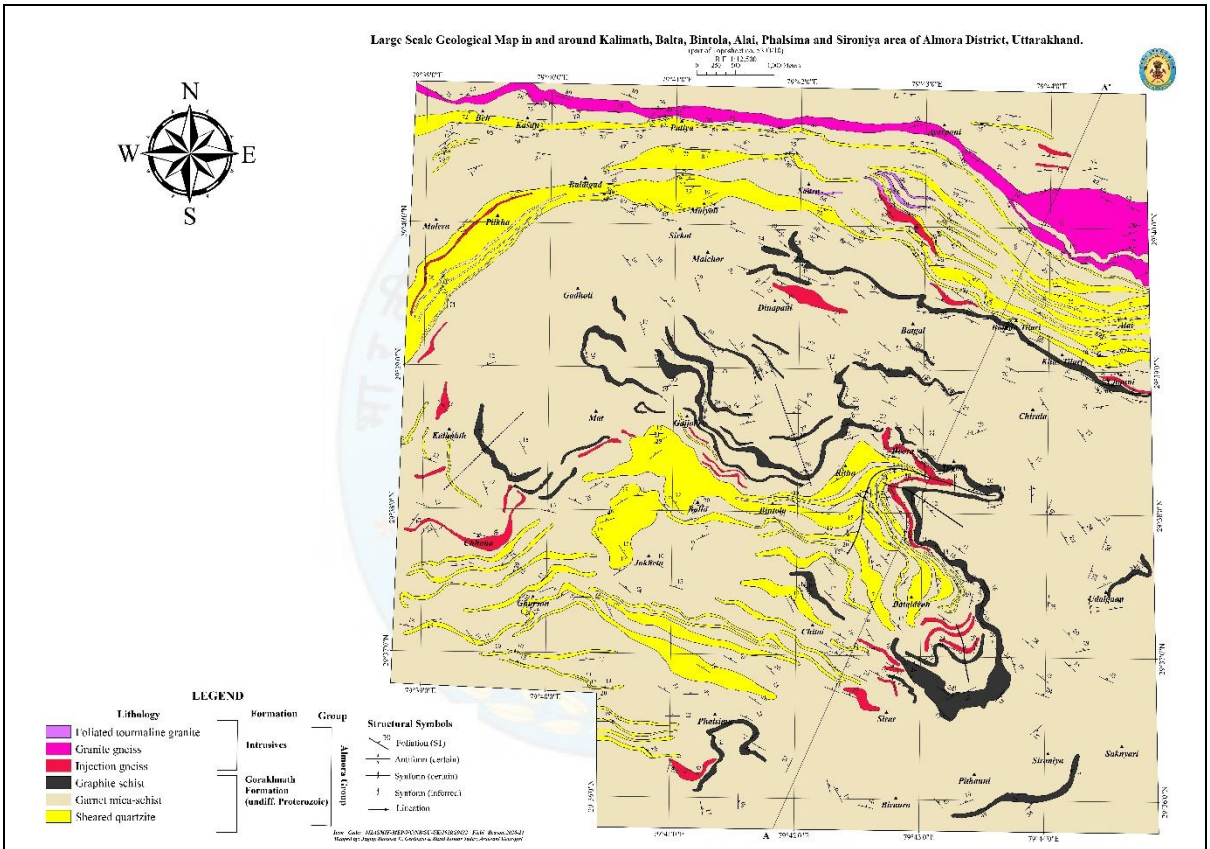

Figure 6.2: Large Scale Geological Map (1:12500) of Almora area (after Santosh and Yadav 2021, Image from GSI Report)

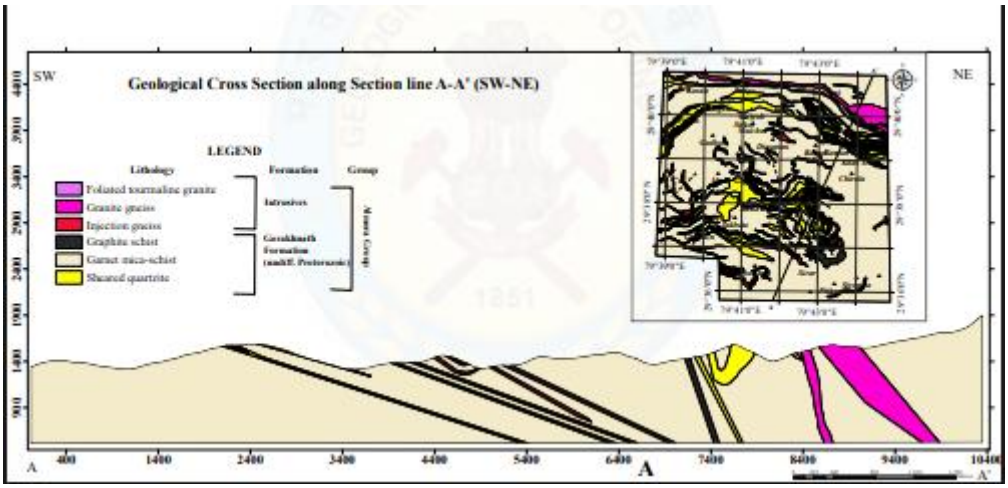

Figure 6.3: Map and cross section (1:12500) of Almora area (after Santosh and Yadav 2021, image from GSI Report).

6.1.3 Large Scale Mapping (LSM) by Geovale Services:

Large Scale Geological Mapping (LSM) on 1:12,500 scale was prepared over a 60 sq. km² Almora block area by Geovale Services Private Limited (Figure 6.4). The mapping was carried out using Survey of India topographic sheets (53O/10) as base map, along with SRTM DEM-derived contour data and high-resolution satellite imagery. The systematic ground verification was carried out through detailed field traverses and involved systematic documentation of lithology, structural measurements (fault, foliation and lineation), mineral assemblages, and occurrence of quartz veins and sulphide mineralization. Traverses were designed to cover the western, northern and southern parts of the Matena-Sirar sector, extending across the areas around Deora, Digoli, Petshal and Bintola and continuing along the settlements of Phalsima, Pithouni, Barechhina, Kalimath and Saura villages.

The mica-schist is the dominant rock covered almost 65% of the block area. The mica-schist (±garnet) rocks occur widely around Dinapani, Mat, Matena, Chitai, Sironiya, Batgal, Maichor, Pithauni, Jogidal and Udalgaon areas. In the northern and north-eastern part, around Saura, Kaparkhan, Baman Tilari and Khas Tilari areas, the schist contains higher amount of sillimanite, whereas in the souther-eastern sector around Udalgaon, the rocks are represented by kyanite bearing garnetiferous mica-schist (±kyanite).

The discrete ~E-W trending quartzite (quartz-sericite schist ± tourmaline) bands are reported from the northern part around Baman Tilari, Khas Tilari, Channi, Saura areas and south-western part of the block around Kaparkhan, Manyoli, around Phalsima villages.

In this Almora block, Geovale Services Private Limited had identified two types of granite rocks, i) older (1.8 Ga) granite-gneiss (having solid-state deformation) and ii) and younger (?500 Ma) intrusive granite that mostly occur as lit-per-lit within the meta-sedimentary package.The older granite-gneiss are well-exposed in the northern part of the block, around Saura areas whereas younger (?500 Ma) intrusive granites are generally intruded along the thrust planes and mostly occur as lit-per-lit granite within the meta-sedimentary package.

Another finding by Geovale Services is the mafic tuffaceous rock exposed near Birora, Badyura, Jhakheta, Balta, Udalgaon and Thana Matena villages. The rock is characterized by a fine- to medium-grained grey-coloured rock composed of volcanic ash, with occasional lapilli-sized fragments and clasts of feldspar and quartz. The matrix is often compact, showing layering, cross bedding or bedding due to deposition from pyroclastic flows or air-fall material.

The distribution of the graphite schist rocks is modified by the Geovale Services. A total 29 graphite bands are traced in the Almora block.

In the western sector of the block, graphite occurs as thin graphite schist bands ranging from ~10-60 cm in thickness, hosted within quartzite (quartz-sericite schist) rock. In contrast, the eastern sector of the block hosts thicker graphite-bearing bands ranging from ~ 2 m to 50 m in thickness, generally occurring along the contact with mica-schist. Overall, the graphite commonly occurs in flaky crystalline form (understand by simple field-based tumbler test,to differentiate graphite flakes from carbonaceous material; i.e. powdered samples that float in water indicate the presence of flaky graphite, whereas sinking material generally implying graphite schist or amorphous carbonaceous matter), especially in areas proximal to deformed granite bodies where thermal influence and metamorphic recrystallization appear to have enhanced graphite crystallinity. Structurally, the graphite schist bands exhibit significant variation in orientation across the block. In the central and southern parts of the block, the graphite horizons generally show low-angle dips ranging from about 5° to 15° and dip toward the north-east, while in the north-eastern sector the bands display moderate to steep dips ranging from approximately 60° to 86° and dip towards north-east. Based on the presence of graphite associated with the thrust planes, the graphite bands are grouped into five (05) distinct blocks. i) Digoli-Gajjola Graphite Block present between Batgal-Channi and Bintola-Udalgaon thrusts, ii) Sirar-Bataldeon Graphite Block associated with the Phalsima–Sironiya, Bintola–Udalgaon and Jakheta-Chitai thrusts, iii) Kalimath Graphite Block is aligned with the Kalimath-Dinapani thrust, iv) Phalsima-Pithauni Graphite Block lies between the Biraura–Pithauni and Phalsima–Sironiya thrusts, and v) Batgal -Channi Graphite Block occurs along the Batgal–Channi thrust.

Quartz veins and veinlets are widely developed throughout the Almora block area, especially around Chitai and Deora villages and occur along fractures, shear zones and foliation planes within the mica-schist rocks. These crystalline quartz veins are generally coarse-grained, milky white to translucent and at places associated with graphite-bearing horizons and contains sulphide mineralization.

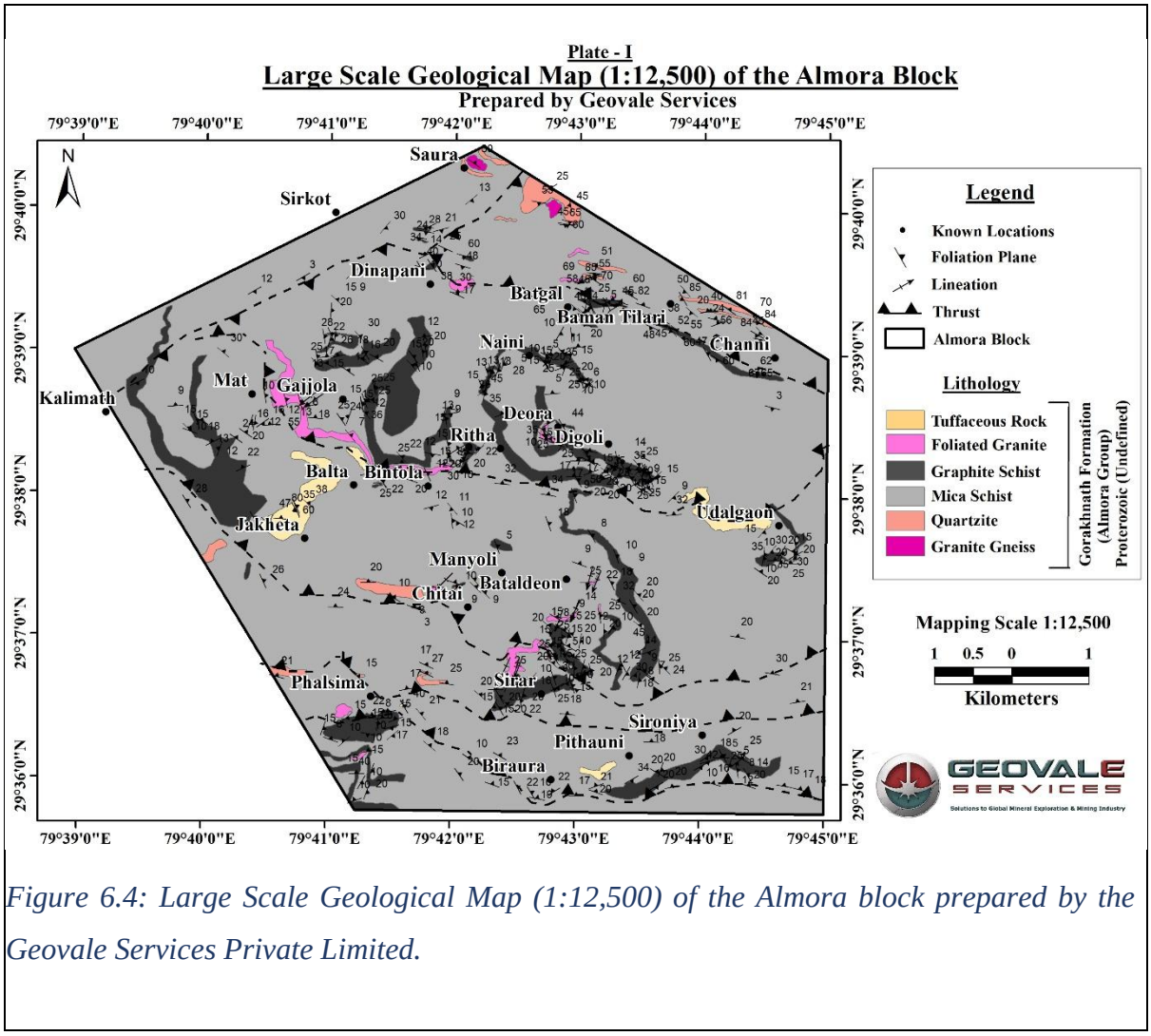

Figure 6.4: Large Scale Geological Map (1:12,500) of the Almora block prepared by the Geovale Services Private Limited.

6.2 Description of rock types:

The lithological units identified within the Almora block were studied through detailed field observations supported by petrographic analysis, with the objective of understanding their composition, texture, deformation, metamorphism, and relationship with graphite mineralization.

The following sub-sections present detailed descriptions of the individual rock types, including their field characteristics, mineralogical composition, textural features, and their significance in relation to graphite–vanadium mineralization within the Almora block. A total of 21 samples for different rock types has been studied under microscope (Annexure V).

6.2.1 Graphite schist:

Field Observation: In the Almora block, the graphite schist is typically dark grey to black in colour, showing steel grey to silvery luster on fresh surfaces due to the presence of abundant graphite flakes, whereas weathered surfaces appear grey to dull grey occasionally

with brownish staining. The rock is generally fine- to medium-grained (although locally medium- to coarse flaky graphite is observed) feels smooth and greasy, and soil hands. The rock exhibits moderate to well-developed foliation, and splits easily into thin platy or flaky sheets along schistosity planes (Figure 6.5, Figure 6.6, Figure 6.7, Figure 6.8). The foliation surfaces often show a shiny metallic to sub-metallic lustre, imparted by aligned graphite flakes and micaceous minerals. Mineralogically, the rock is composed predominantly of graphite, quartz and muscovite, which together define the schistose fabric. Graphite occurs mainly as fine to medium flaky crystals oriented parallel to the foliation planes, forming continuous graphite-rich laminae. Quartz is present as fine to medium recrystallized grains or thin discontinuous lenses, while muscovite occurs as silvery micaceous flakes aligned parallel to the foliation. Minor amounts of biotite, feldspar are also present as accessory minerals.

In the study area, graphite schist occurs extensively around Sirar, Bataldeon, Digoli, Phalsima, Pithauni, Mat, Kalimath, Bajyoli, Debdiya, Ritha, Balta and Udalgaon, where it forms distinct strata-bound bands within the mica-schist. In several locations, particularly around Digoli (Figure 6.12), Bataldeon (Figure 6.10), Bajyoli, Phalsima (Figure 6.9, Figure 6.11) and Sirar, southern part of the Almora block, the graphite schist bands show visible occurrences of sulphide minerals, mainly pyrite and chalcopyrite, present as disseminations, specks, or small veinlets. Occasional traces of bornite are also observed in association with quartz veins cutting the graphite schist. Around Sirar, Balta, Bajyoli, Ritha and Udalgaon, central part of the block, graphite typically occurs as fine- to medium-grained flakes aligned parallel to foliation, forming continuous graphite-rich layers and imparting a prominent luster to the rock surface. In contrast, in the Kalimat area, graphite occurs as intercalated layers within garnet-mica schist, forming alternating mica-rich and graphite-rich bands. In these zones, graphite flakes tend to be relatively coarser and irregular and the rock locally contains threads and nodular concentrations of carbonaceous material, indicating comparatively moderate to lower crystallinity based on tumbler test at field. In the Debdiya and Khas Tilari areas, northern part of the Almora block, graphite schist commonly contains medium to coarse graphite flakes aligned parallel to foliation, forming relatively thicker graphite-bearing bands with well-developed schistosity and prominent shining luster on broken surfaces. Contacts between graphite schist and mica schist are generally gradational to sharp. In several locations, the graphite schist bands are observed to be structurally controlled and parallel to the regional foliation.

Figure 6.5: Outcrop Section of Graphite Band in the Sirar area, Almora.

Figure 6.6: Outcrop section showing Graphite Schist, Near Dibdiya, Almora.

Figure 6.7: Graphite Flakes in Quartzite layer, near Sirar, Almora.

Figure 6.8: Exposed Graphite Schist in the Hill top near Deora Village, Almora.

Figure 6.9: Road Cut Section of Graphite Schist, near Falsima, Almora.

Figure 6.10: Road Cut Section of Graphite Schist associated with deformed Quartz Vein.

Figure 6.11: Graphite Schist in outcrop near Falsima, Almora.

Figure 6.12: Graphite Schist with Redox Sensitive Elements.

Petrological Study of Graphite Schist: A total 11 thin sections (109193, 109202, 109208, 109218, 109238, 109244, 109245, 109252, 1059253, 110027, 109200) of graphite schist were studied (Annexure V). Overall, it is a fine- to medium grained, strongly foliated rock composed of quartz, feldspar, muscovite and graphite with minor opaque minerals (Figure 6.13). The rock is characterized by a well-developed schistose texture, defined primarily by the preferred alignment of fine sericite-muscovite flakes and graphite along the foliation planes. The matrix is dominated by recrystallized quartz grains, which are mostly fine to medium-grained and subhedral to anhedral in shape. In several areas, quartz grains exhibit polygonal grain boundaries and sutured contacts. Local development of quartz ribbons and elongated quartz aggregates is also observed, reflecting strain-induced grain elongation within high-strain domains. Muscovite and fine sericite flakes occur abundantly, typically forming parallel aggregates that define the principal schistosity of the rock (Figure 6.14). These micaceous minerals display bending, kinking and slight rotation (Figure 6.15, Figure 6.16, Figure 6.17, Figure 6.18). In several parts of the thin section, the sericite flakes show multiple orientations, suggesting the development of secondary foliation or crenulation cleavage associated with successive deformation phases. The graphite grains are typically elongated and aligned parallel to the schistosity, and in many cases form continuous streaks that wrap around quartz and mica grains, imparting a distinctly layered appearance to the rock. In certain zones, graphite concentration increases along shear planes and micro-shear bands, suggesting its mechanical mobilization and redistribution during deformation. Feldspar occurs as subhedral to anhedral grains, commonly showing partial alteration to sericite, indicating secondary alteration under metamorphic conditions. In some instances, feldspar grains show fractures and minor recrystallization, reflecting deformation. Certain quartz veins are parallel or subparallel to the

foliation, whereas others crosscut the foliation at high angles, indicating multiple phases of fracturing and fluid infiltration during progressive deformation. These veins are composed of fine-grained quartz aggregates that differ texturally from the coarser recrystallized quartz present in the host matrix. Some veins show irregular margins and vug-filling textures, while others appear structurally controlled along micro-fractures or shear planes. A few veins exhibit cross-cut or stepped geometries, suggesting emplacement along fractures influenced by localized stress regimes. Localized zones of intense deformation are evident within the thin section, characterized by grain size reduction, development of quartz ribbons, and concentration of graphite along narrow shear bands (Figure 6.16, Figure 6.17, Figure 6.19, Figure 6.20, Figure 6.21, Figure 6.22).

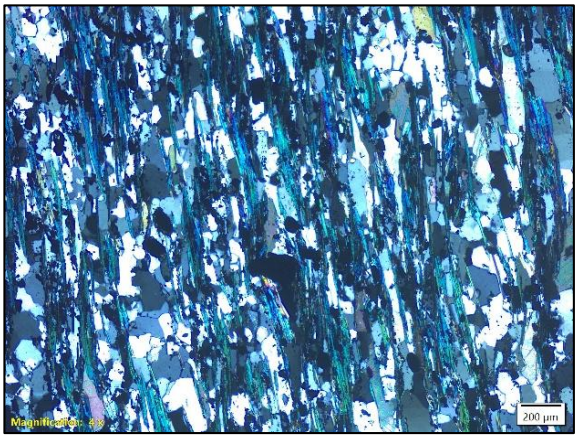

Figure 6.13: Photomicrograph of graphite schist sample showing small grains of graphite distributed in quartz muscovite schist where graphite occurs as pre to syntectonic (Sample Id. 109218), near Digoli, Almora.

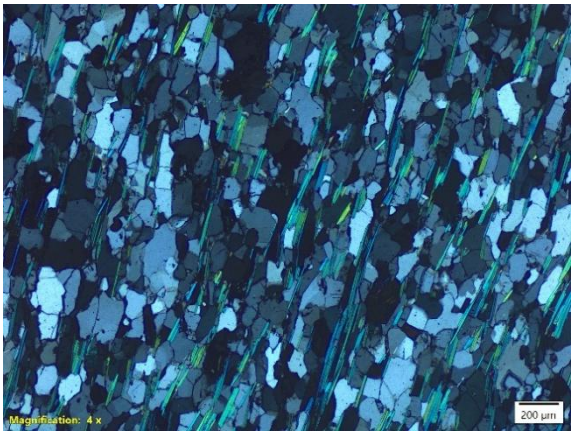

Figure 6.14: Photomicrograph of graphite schist sample showing graphite bearing quartz muscovite schist (Sample Id. 109238), near Dinapani, Almora.

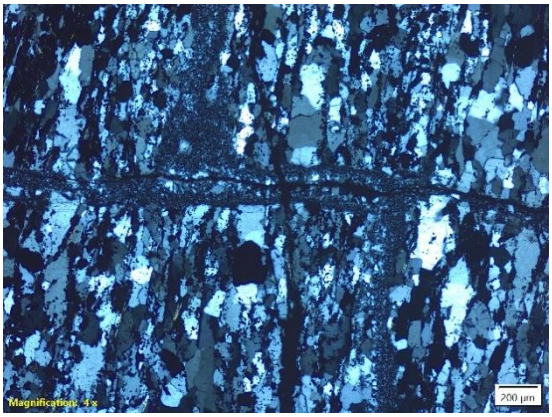

Figure 6.15 Photomicrograph of graphite schist sample showing cross-cut quartz vein around the fracture filling zone (Sample Id 109245), near Jakheta, Almora.

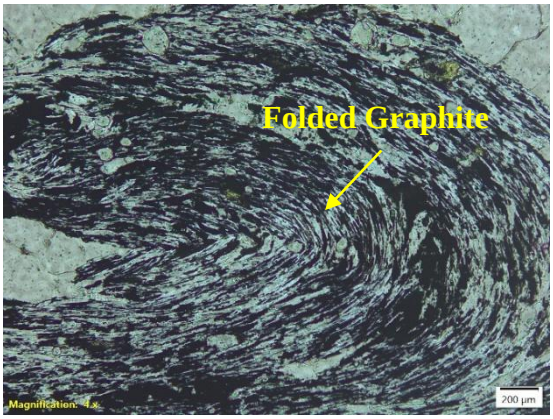

Figure 6.16 Photomicrograph of graphite schist sample showing folded graphite flakes, (Sample Id 109202).

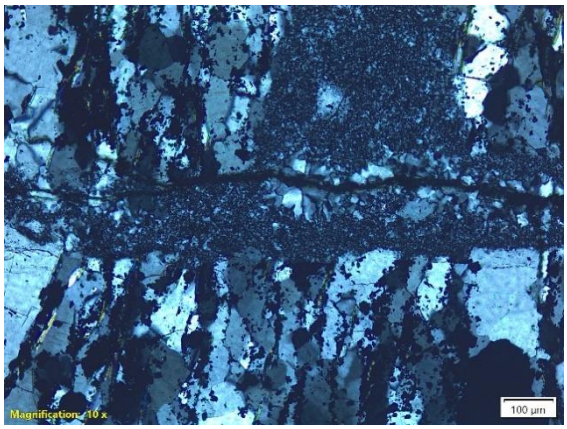

Figure 6.17: Photomicrograph of graphite schist sample showing quartz vein with very fine-grained quartz in the vug-filling zone, recrystallized quartz (Sample Id 109245), near Jakheta, Almora.

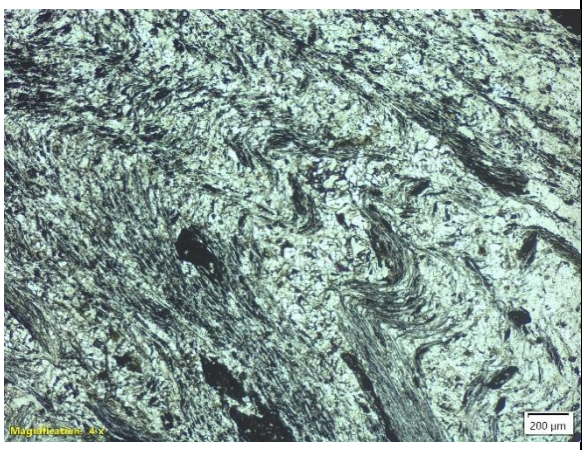

Figure 6.18 Photomicrograph of graphite schist sample showing crenulation cleavage within graphite schist (Sample Id 109202).

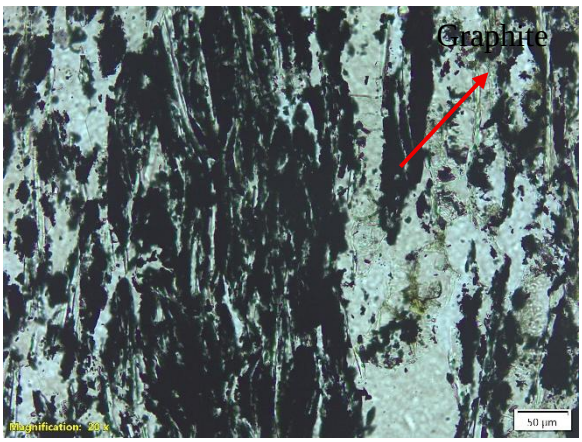

Figure 6.19: Photomicrograph of graphite schist sample showing graphite concentrated in shear along with recrystallized quartz grain (Sample Id 109253), near Mat.

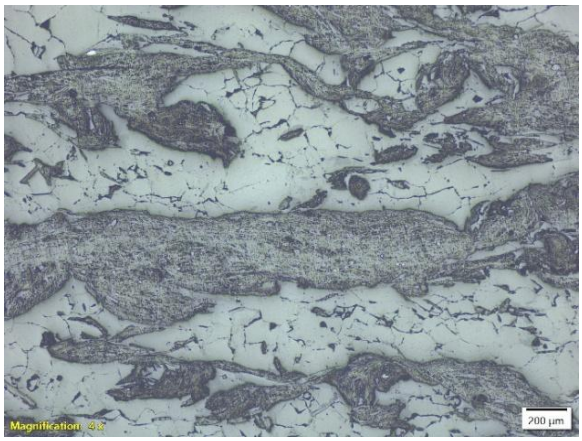

Figure 6.20 Photomicrograph of graphite schist sample showing graphite Flakes observed under reflective light, (Sample Id 109245), near Jhaketa.

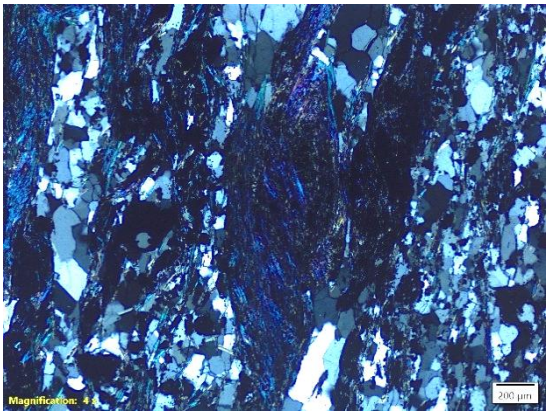

Figure 6.21 Photomicrograph of graphite schist sample showing mica-fish in muscovite mica with embedded grains of graphite along the deformation, (Sample Id 109200), near Bintola.

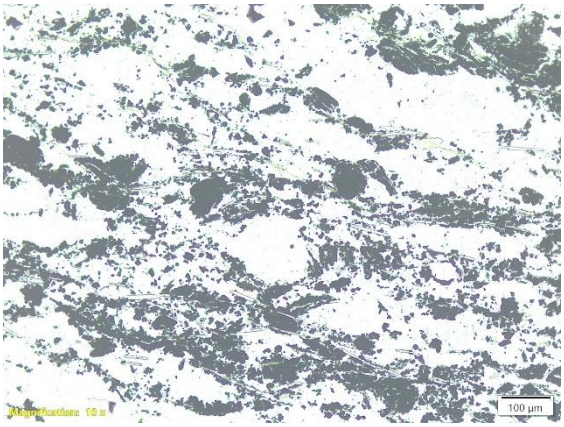

Figure 6.22 Photomicrograph of graphite schist sample showing graphite flakes in recrystallized quartz, Sample Id 109200, near Bintola.

Modal analyses of Surface Graphite flake distribution:

Kalimath- Mat Graphite Band, present along Chitai-Kalimath Thrust: Elongated graphite mostly parallel to the alignments of the quartz are present (Figure 6.23,Figure 6.24).

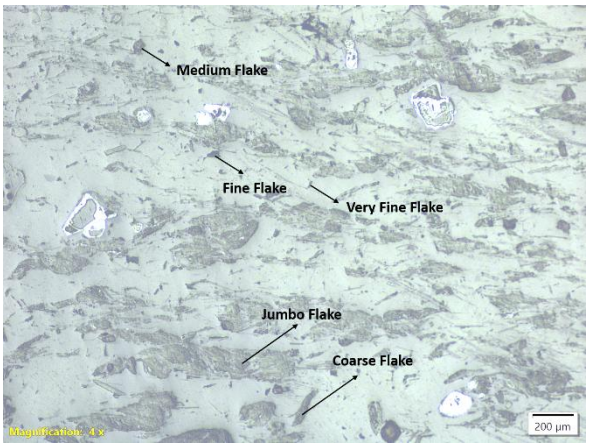

Figure 6.23: The graphite flake, near Kalimath-Mat band (Sample Id 109245), near Jhaketa area.

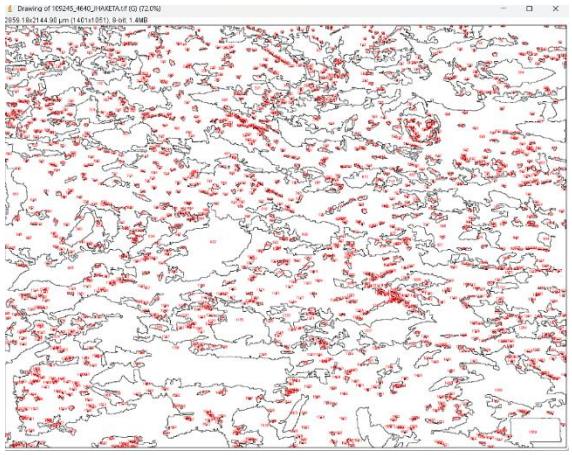

Figure 6.24: Measured graphite flakes, near Kalimath-Mat band (Sample Id 109245).

Table 6.1: Graphite Flake size distriburion of Kalimath-Mat area (Sample Id 109245)

Category	Flake Size Range	Number (No.)	Area Percentage of total area (µm2)
Jumbo	Greater than 300 µm	11	95.96%
Coarse	180–300 µm	25	1.23%
Medium	150–180 µm	9	0.25%
Fine	75–150 µm	63	1.03%
Very Fine	Less than 75 µm	1,532	1.53%
Total		**1,640**	**100.00%**

Particle Size Distribution of Kalimath-Mat Graphite (Table 6.1**):**

- **Jumbo to Coarse Fraction:** 95.96% area is occupied by the Jumbo graphite flake, with 1.23% area with coarse flakes.
- **Predominantly Very Fine-Grained:** 0.25% area is occupied by the medium graphite flakes, 1.03% area with fine and 1.53% area is occupied by the very fine flakes of graphite.

Graphite flake size distribution (Figure 6.25**,** Figure 6.26**,** Table 6.2**) of Bintola-Digoli Graphite Zone (Sample Id 109200):**

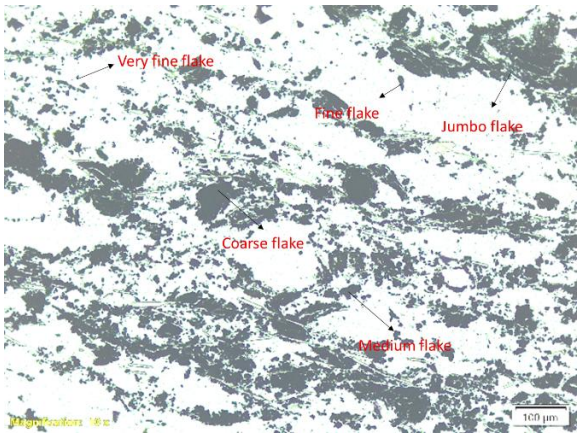

Figure 6.25: Graphite fleke under PPL, Bintola-Digoli area, (Sample Id 109200).

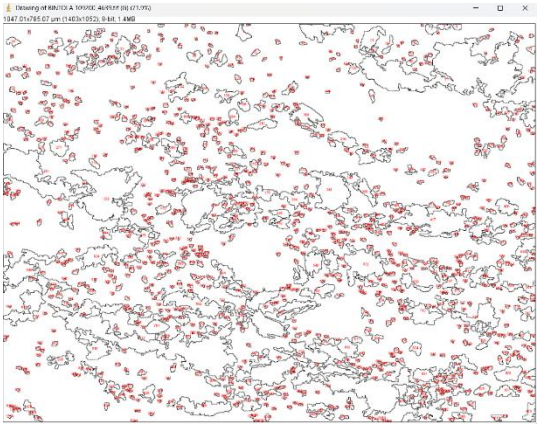

Figure 6.26: Measured graphite flakes, Bintola-Digoli graphite (Sample Id 109200).

- **Jumbo (> 300 µm):** 86.15% area is occupied by the jumbo flakes of graphite.
- **Coarse (180 - 300 µm):** 2.94%area is occupied by the coarse graphite flakes.
- **Medium (150 - 180 µm):** 0.98% area is occupied by the medium graphite flakes.
- **Fine (75 - 150 µm):** 4.10%area is occupied by the fine graphite flakes.
- **Very Fine (< 75 µm):** 5.83%area is occupied by the very fine flakes.

Table 6.2: Graphite Flake size distriburion of Bintola-Digoli area (Sample Id 109200)

Category	Size Range (µm)	Number of Particles	Area Percentage of total area (µm2)
Jumbo	> 300 µm	2	86.15%
Coarse	180 - 300 µm	2	2.94%
Medium	150 - 180 µm	0	0.98%
Fine	75 - 150 µm	14	4.10%
Very Fine	< 75 µm	666	5.83%
Total		**684**	**100%**

6.2.2 Mica Schist:

Field Observation: The mica-schist rock typically displays a grey to dark grey, brownish grey, or greenish grey colour, depending on the relative abundance of biotite, muscovite, and

chlorite. Unweathered surfaces show a silvery to sub-metallic sheen, produced by the alignment of mica minerals, whereas weathered surfaces often appear dull grey to brownish. The rock is generally medium-grained, with individual mineral flakes visible to the naked eye. On unwesthered surfaces, the rock exhibits a distinctly schistose texture, and it tends to split easily along foliation planes, producing thin slabs with smooth, glistening surfaces. On hand, the rock commonly gives a slightly rough to flaky feel, particularly where mica plates are abundant.

A common variety found in the Almora block is garnetiferous biotite-muscovite schist, which appears dark grey to brownish grey with a pronounced glittery lustre in surface due to abundant aligned mica flakes (Figure 6.27, Figure 6.28). The rock is typically medium- to coarse-grained and strongly foliated, allowing it to break readily along the schistosity planes. The rock shows the presence of randomely oriented reddish-brown to wine-coloured garnet grains, usually ranging from a few millimetres to occasionally centimetre scale. These garnet crystals are generally dodecahedron and slightly protrude from the foliated surface, giving the rock a rough, uneven texture despite its overall planar cleavage. Quartz commonly occurs as interlocking grains or thin segregated bands, and in some exposures the foliation surfaces display a pearly lustre under sunlight due to abundant muscovite flakes.

Another lithology is kyanite bearing mica schist, mainly present in the Udalgaon area, which can be recognized by its bluish-grey to silvery grey colour and strongly developed foliation. The rock generally a medium- to coarse-grained, and exhibits silky to shiny lustre on foliation surfaces due to aligned muscovite and biotite. A distinctive field feature is the presence of elongated bladed kyanite crystals, typically pale blue to deep blue, occurring either aligned parallel to foliation or slightly oblique to it. These blades may occur as isolated crystals or clustered aggregates within the foliated matrix. Because of the hardness of kyanite, the rock surface often appears uneven and rough where the crystals project from the schistose matrix. Quartz occurs as fine- to medium-grained interlocking grains or thin lenses parallel to foliation, contributing to the banded appearance of the rock in certain exposures.

Hornblende-chlorite-biotite schist is also locally present at Udalgaon area, and can be distinguished by its dark green to greenish-brown colour and comparatively coarser mineral assemblage. Unweathered exposures show a slightly greasy to moderately shiny lustre, resulting from aligned chlorite and biotite flakes. The rock typically displays well-developed schistosity, with mineral alignment producing clear foliation planes along which the rock tends

to split. Hornblende commonly occurs as elongated prismatic crystals, generally aligned with the foliation or distributed irregularly within the matrix. Chlorite imparts a greenish tint and soft, slightly greasy lustre to the rock surfaces, whereas biotite contributes to the dark brownish tones and glittery lustre. Quartz occurs as fine- to medium-grained interstitial grains or thin segregated bands, occasionally forming quartz-rich layers that contrast with the darker mafic mineral assemblage (Figure 6.29, Figure 6.31).

Across the region, these mica schist varieties commonly show well-developed foliation (Figure 6.30, Figure 6.32), mineral alignment and locally visible banding, giving exposures a distinct layered appearance. In several outcrops, the foliation surfaces display minor crenulations, quartz streaks and ribbon-like quartz bands, reflecting intense deformation and recrystallization. The overall appearance in the field is therefore characterized by shiny micaceous surfaces, strong planar fabric and easily recognizable mineral alignment, making mica schist one of the most visually distinctive rock types within the Almora crystalline terrain.

Figure 6.27: Mica Schist associate with Garnet Biotite, near Bataldeon area

Figure 6.28: Mica Schist associated with folded Quartz Vein

Figure 6.29: Weathering surface of garnet Mica Schist.

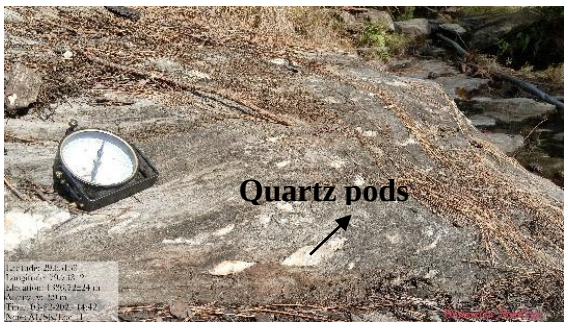

Figure 6.30: Garnet Mica Schist showing Boudinage Quartz, near Barakote Area

Figure 6.31: Garnet mica schist showing stretching quartz veins.

Figure 6.32: Garnet mica schist, near Kalimath area.

Petrological Study of Mica Schist: Total 6 samples (109212, 109220, 109233, 109251, 109254, 109256) of mica schist were studied. The thin section is a medium- to coarse-grained, foliated consist mainly of quartz, plagioclase/orthoclase (minor amount), muscovite ± biotite, garnet, kyanite, hornblende, chlorite and subordinate opaque (magnetite ± ilmenite). The dominant matrix comprises finely to medium-grained recrystallized quartz (≈40-50 vol.%) that commonly displays undulose extinction, sub grains and polygonal sutured grain boundaries, diagnostic of dynamic recrystallization under ductile strain. Quartz occurs both as equant recrystallized grains and as elongate quartz ribbons aligned parallel to the fabric in high-strain domains. Micas (muscovite ± biotite, ~20-25 vol.%) form pervasive lath-like and tabular grains that define the foliation. Micas are commonly bent, kinked and locally crenulated, recording progressive, polyphase deformation; biotite is strongly pleochroic and commonly shows chloritization along margins and cleavage planes. Kyanite occurs as elongate bladed porphyroblasts or aggregates (pale blue/colourless in thin section) oriented either parallel or oblique to foliation; many kyanite blades show partial replacement by fine-grained biotite/sericite. Garnet porphyroblasts (± garnet cores, 5-10 vol.%) are visible, subhedral to euhedral, commonly 0.5-5 mm in size, and display inclusion trails (snowball/rolled-inclusions) of quartz and mica aligned sub-parallel to regional fabric, suggesting syn-kinematic growth during deformation. Garnet rims show minor alteration to chlorite/sericite in places (Figure 6.33, Figure 6.34). Hornblende occurs as prismatic to elongate crystals that commonly cross-cut foliation or are wrapped by mica, locally forming a more equigranular/hornfelsic texture in discrete patches-suggestive of locally elevated thermal conditions or intrusion-related thermal overprint. Accessory opaque (magnetite ± ilmenite) occurs as scattered anhedral grains and

aggregates; some magnetite grains display martitization rims and are associated with fine sulphide blebs in places. Feldspar is subordinate and commonly sericitized; where present it is fractured and partially recrystallized. The evidence for prograde/peak amphibolite-facies metamorphism is preserved in garnet + kyanite + hornblende assemblages, while dynamic recrystallization of quartz and mica deformation fabrics show to syn-tectonic recrystallization. Subsequent retrogression under more hydrous, lower-grade conditions is indicated by partial kyanite to biotite/sericite reaction, chloritization of biotite rims and local development of fine sericite. Localized brittle-ductile interplay is recorded by micro-shear bands, grain-size reduction zones and quartz veining that post-date the main foliation. Mica schist also contains disseminated graphite flakes at places.

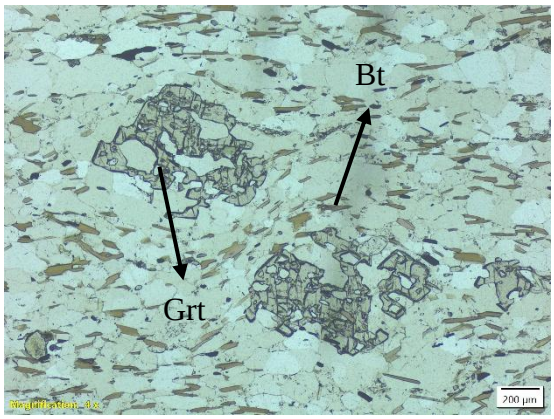

Figure 6.33: Biotite with garnet and very rarely developed graphite (Sample Id: 109220) observed.

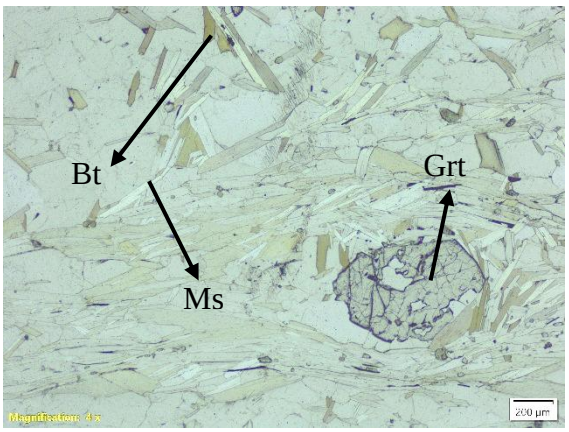

Figure 6.34: Garnetiferous Muscovite Schist (Sample Id: 109154), near Digoli.

6.2.3 Quartzite:

Field Observation: In field, the quartz sericite schist is reported from the Phalsima, Chitai, Khas Tilari area.

The rock is light grey to silvery-white (pale buff to brownish tone where iron oxides are present), fine- to medium-grained (Figure 6.35, Figure 6.36), foliated (foliation surfaces show a silky luster produced by aligned sericite plates) (Figure 6.37, Figure 6.38) and in hand specimen feels smooth, soft and slightly soapy/slippery owing to the pervasive fine-sericite matrix. The schist splits readily into thin, flexible sheets parallel to schistosity and fresh cleavage surfaces exhibit a clean, shiny luster. Quartz occurs as fine to medium, elongate interlocking grains, commonly forming lenticular or streaky quartz-rich bands that stand out

against the sericite-rich matrix; these quartz lenses are discontinuous and vary from a few centimetres to metre scale in outcrop. Accessory phases visible in the field include chlorite (greenish tint in some exposures), tourmaline (small black prismatic needles), minor feldspar and scattered iron-oxide stains. Fracturing is common: small, closely spaced joint sets and narrow quartz veinlets cut the foliation at varying angles and in some exposures the veins show vuggy, fine-grained quartz infill. At mapped localities such as Kaparkhan, Saura, Dinapani, Manyoli and Balta the unit forms distinct, laterally persistent sericite-rich bands that are useful field markers and commonly host narrow quartz streaks or tourmaline-bearing stringers (Figure 6.39, Figure 6.40). Al, places, quartzite served as the host rock for graphite.

Figure 6.35: Hand specimen of Quartz Sericite Schist with Tourmaline, near Khas Tilari.

Figure 6.36: Quartzite with later forming quartz veins.

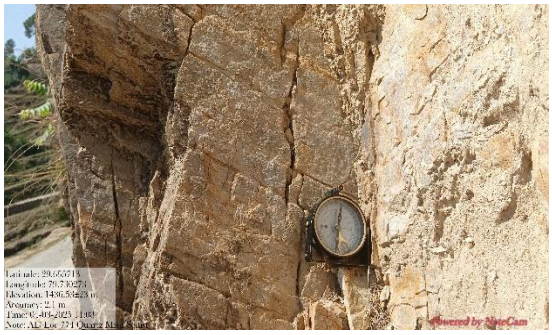

Figure 6.37: Field outcrop of quartzite near Khas Tilari area.

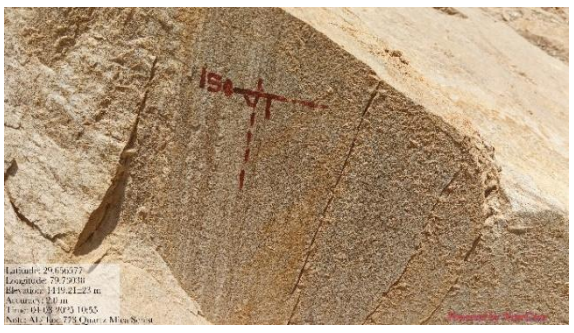

Figure 6.38: Lineation in quartzite near Khas Tilari area.

Figure 6.39: Quartzite outcrop near Baman Tilari area.

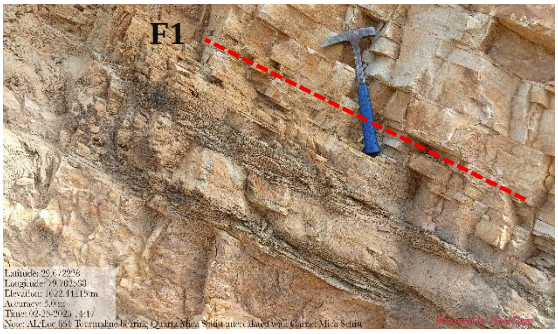

Figure 6.40: Quartzite with prominent F1 foliation, near Channi area.

Petrological Study of Quartzite: One thin section (Sample Id: 109154) is studied. Under thin section, the quartz-sericite schist is predominantly composed of quartz and fine-grained sericite, with minor biotite occurring as accessory phases. Quartz forms the major framework of the rock and occurs as fine- to medium-grained, recrystallized anhedral grains showing undulose extinction, sub-grain development and sutured grain boundaries, indicating dynamic recrystallization during deformation. In several domains, quartz grains display polygonal aggregates and local grain-size reduction, suggesting progressive recrystallization under metamorphic conditions. The quartz crystals are commonly arranged in elongated ribbons and discontinuous bands, which are parallel to the main foliation and contribute to the overall schistose fabric of the rock. The micaceous component is dominated by sericite, which occurs as very fine, platy flakes forming a dense micaceous matrix that defines the principal schistosity (Figure 6.41). These sericite plates are typically aligned parallel to the foliation and locally show slight bending and crenulation, reflecting deformation associated with the development of the schistosity. Biotite occurs in minor proportions as small pleochroic flakes, generally aligned with the foliation but locally appearing as relict grains within the sericite-rich matrix. In several areas, muscovite has developed at the expense of earlier biotite, forming fine lath-like crystals that partially replace biotite along cleavage planes and grain margins, indicating a later stage of mineral growth or retrograde alteration during the metamorphic evolution. The texture of the rock is lepidoblastic to grano-lepidoblastic, characterized by the intergrowth of recrystallized quartz with fine sericite aggregates. The preferred orientation of sericite flakes together with the elongation of quartz grains defines a well-developed schistose fabric, reflecting deformation and recrystallization under low- to medium-grade metamorphic conditions. At places tourmaline also present and shows parallel orientation (Figure 6.42).

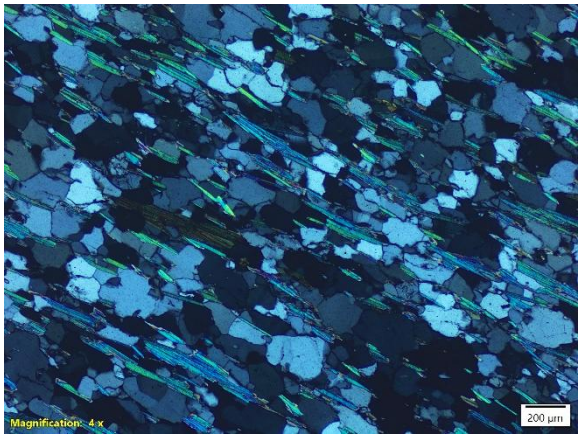

Figure 6.41: Photomicrogry of quartz associated with muscovite (Sample Id 109154, near Khas Tilari).

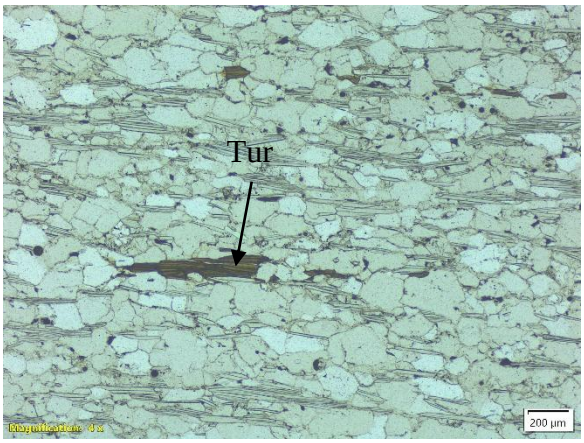

Figure 6.42: Photomicrography of quartz associated with tourmaline (Sample Id 109154, near Khas Tilari).

6.2.4 Tuffaceous rock:

Field Observation: It appears light grey to greenish-grey in colour, locally showing a slightly mottled or patchy appearance on fresh surfaces. The rock is generally fine- to medium-grained and displays bading texture and sometimes with lapilli (Figure 6.43, Figure 6.44, Figure 6.45 and Figure 6.46), with small broken mineral and lithic fragments embedded within a comparatively finer groundmass. Unweathered exposures commonly show angular to sub-angular fragments of quartz and feldspar, occasionally visible as small white to translucent grains scattered within the matrix. The rock surface tends to be dull to slightly earthy in lustre and when broken it commonly exhibits irregular to subconchoidal fracture surfaces. The rock is generally massive to weakly foliated, although in some exposures a subtle planar fabric can be observed where elongated mineral fragments or lithic particles show a slight preferred orientation, suggesting mild deformation after deposition. In weathered sufaces, the rock may display greenish patches or streaks, attributed to the presence of alteration minerals such as chlorite and epidote, which impart a faint green tint to the matrix. The rock is moderately hard and compact, but locally shows slightly porous or vesicular features, particularly where volcanic fragments or cavities were originally present. At several outcrops (in Balta area), dark needle-like or elongated dark green to black mineral grains are scattered throughout the rock, likely representing altered mafic minerals or chlorite aggregates. These elongated grains occasionally show a weak alignment, giving the rock a faintly streaked appearance in certain sections. The overall texture reflects a volcanoclastic origin, where fragmented volcanic

materials were deposited and subsequently subjected to mild metamorphic overprinting. Within the mapped area, these tuffaceousrocks commonly occur interbedded with schistose lithologies, forming discontinuous bands and lenses that can be traced along strike for short distances, indicating localized episodes of volcanic input within the regional sedimentary-metamorphic sequence.

Figure 6.43: Tuffaceous Rock near Balta, Almora, shows banding.

Figure 6.44: Tuffaceous Rock shows the presence of lapilli (marked by an arrow) near Jakheta, Almora.

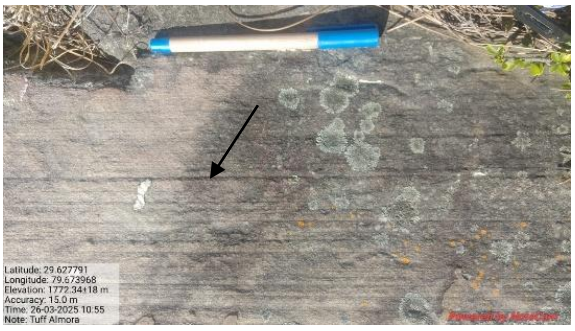

Figure 6.45: Tuffaceous bands near Balta, Almora

Figure 6.46: Tuffaceous Rock with bands, near Balta, Almora

Petrological Study: A total two samples (110020, 110021) were studied. It is characterized by a fine- to medium grained volcaniclastic texture, composed mainly of quartz, feldspar, chlorite and minor opaque minerals embedded within a very fine, partly vitrified groundmass (Figure 6.47). The rock shows a distinctly fragmental fabric, where discrete mineral fragments and crystal clasts are set within a fine matrix, reflecting its pyroclastic origin. Quartz occurs predominantly as broken crystal fragments, ranging from angular to sub-angular forms. Many quartz grains exhibit polygonal outlines, embayed margins and wedge-shaped fragments, suggesting magmatic crystallization followed by mechanical fragmentation during volcanic activity. Some quartz grains also display slight undulose extinction, indicating mild post-

depositional deformation. Feldspar occurs mainly as altered phenocryst fragments, commonly showing partial to complete sericitization. In several areas, feldspar crystals are preserved only as pseudomorphic outlines replaced by fine sericite aggregates, indicating alteration during low-grade metamorphism or hydrothermal processes. These quartz and feldspar crystal fragments locally act as porphyritic clasts, floating within the very fine-grained matrix. The groundmass is composed of very fine fragmented quartz grains, altered orthoclase feldspar and chloritic material, giving the rock a microcrystalline to cryptocrystalline appearance. Chlorite occurs as patches, sometimes forming diffuse clusters within the matrix (Figure 6.48). These chloritic masses may be interpreted to represent altered volcanic glass or devitrified glassy components, suggesting that part of the original volcanic ash or glass fragments underwent secondary alteration. Minor opaque minerals occur as fine disseminated grains within the groundmass. The thin section shows a vitroclastic to crystal-lithic tuffaceous texture, where crystal fragments of quartz and feldspar are embedded within a fine altered matrix composed of devitrified volcanic material. The observed mineralogical assemblage and alteration features indicate volcaniclastic deposition followed by low-grade metamorphism and hydrothermal alteration, which resulted in recrystallization of the matrix and transformation of primary feldspar into sericite and chloritic aggregates.

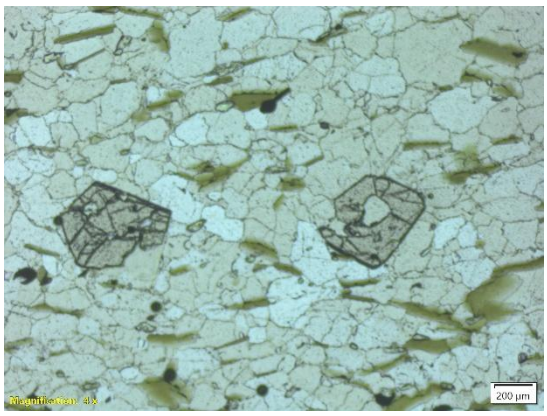

Figure 6.47: Photomicrograph of tuffaceous rock shows fine grained tuffaceous rock (Sample Id 110020)

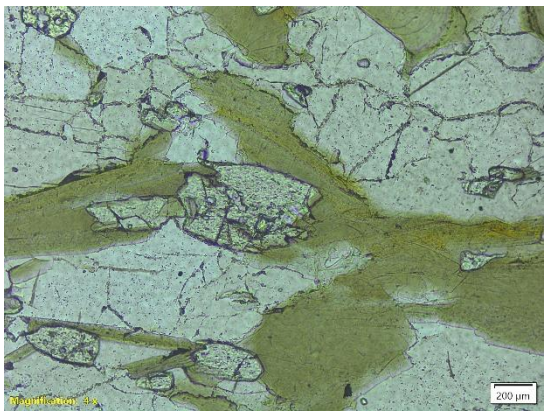

Figure 6.48: Photomicrograph of tuffaceous rock shows fine grained tuffaceous rock contains chlorite (Sample Id 110021).

6.2.5 Granite Intrusive:

Field Observation: It shows a light grey to whitish grey colour on fresh surfaces, while weathered exposures often appear pale brown to slightly yellowish due to surface alteration of feldspar and mica minerals. The rock is generally medium- to coarse-grained, foliated with quartz and feldspar porphyroclasts in the quartzo-feldspathic matrix, with individual mineral grains of quartz and feldspar clearly visible to the naked eye. The quartz occurs as translucent grey grains and feldspar as whitish to pinkish crystals, while biotite appears as dark brown to black flaky minerals scattered throughout the rock. The overall lustre is dull to slightly vitreous, although foliation surfaces locally show a faint luster due to aligned mica minerals. The rock exhibits weak to moderate foliation, which becomes more evident in zones affected by stronger deformation. This foliation is defined by the preferred orientation of biotite and muscovite flakes, along with the elongation and stretching of quartz grains. In several exposures, feldspar crystals appear augen-shaped, indicating ductile deformation under compressive stress (Figure 6.49). Quartz grains commonly occur as elongated streaks or ribbon-like aggregates, giving the rock a slightly streaked appearance parallel to the foliation. In zones of stronger deformation, it may show sheared textures and feldspar crystals may appear fractured or partially recrystallized along grain margins (Figure 6.50). Biotite and muscovite tend to concentrate along foliation planes, giving some surfaces micaceous luster when exposed to sunlight. The rock preserves both primary granitic fabric and deformation-related planar structures, representing a transitional stage between undeformed granite and well-developed gneiss within the metamorphic sequence of the region.

Figure 6.49: Granite intrusive shows foliation, the presence of porphyroclasts of feldspars

Figure 6.50: Outcrop of Granite intrusive shows foliation, the presence of porphyroclasts of feldspars.

Petrological Study: A total three samples (Sample Id: 109255, 110029, 110028) were studied. It represents a medium- to fine-grained foliated granitoid, composed predominantly of quartz (~40 vol.%), feldspar (~45 vol.%) and mica minerals including muscovite and biotite (~10 vol.%), with minor accessory phases such as epidote, garnet, apatite and opaque minerals (~5 vol.%). The rock exhibits a strongly developed planar fabric defined by the preferred alignment of quartz ribbons and mica flakes, indicating deformation under ductile conditions. Quartz occurs both as recrystallized granular aggregates and elongated ribbon-like grains. The ribbon quartz commonly shows undulose extinction and dynamic recrystallization, reflecting deformation under high strain conditions. In several domains, quartz ribbons together with aligned biotite wrap around larger feldspar grains, indicating strain partitioning within the rock matrix. Feldspar is represented by both orthoclase and albite, occurring largely as porphyroclasts within a finer recrystallized matrix. Many of the larger feldspar grains display mortar texture, where smaller recrystallized feldspar phenocrysts grains develop along the margins of larger porphyroclasts. Some feldspar crystals show sigmoidal shapes and associated pressure-shadow zones, indicating rotational deformation of the porphyroclasts within the shear fabric (Figure 6.51). Zoned feldspar grains are also observed, where the core portions commonly exhibit sericitic alteration with visible albitic lamellae, whereas the outer rims remain comparatively unaltered and lack lamellar structures. In addition to zoned grains, unzoned albite and orthoclase crystals are also present within the matrix. Mica minerals occur mainly as biotite and muscovite flakes aligned parallel to the deformation fabric, forming the principal foliation within the rock. In several areas, mica fish structures are observed, which are characteristic indicators of ductile shear deformation. The foliation defined by the alignment of quartz ribbons and mica minerals is mylonitic in nature (Figure 6.52). Garnet occurs locally as porphyroblastic crystals within the foliated matrix, often showing post-tectonic growth relationships, as indicated by their relatively undeformed margins and cross-cutting relationships with the surrounding foliation. Epidote is present as fine to medium grains occurring both parallel to and cross-cutting biotite flakes, suggesting syn- to post-deformation crystallization. Zoned epidote crystals are also observed in certain areas. Apatite occurs as small accessory grains, commonly included within feldspar crystals. The thin section records a strongly deformed granitoid protolith that has undergone dynamic recrystallization, feldspar porphyroclast rotation and development of mylonitic foliation within a ductile shear regime.

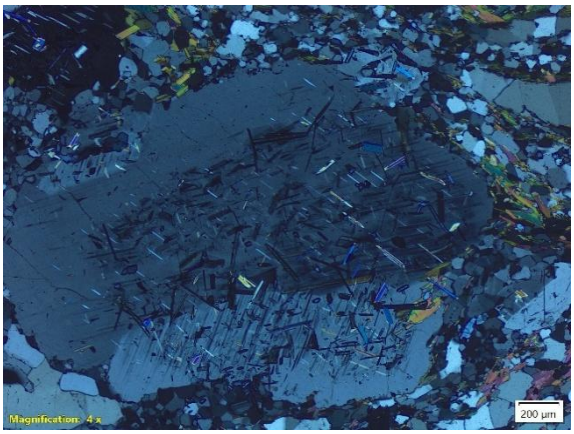

Figure 6.51: Deformed granite intrusive show the presence of zoned feldpar porphyroclast (Sample Id: 109255)

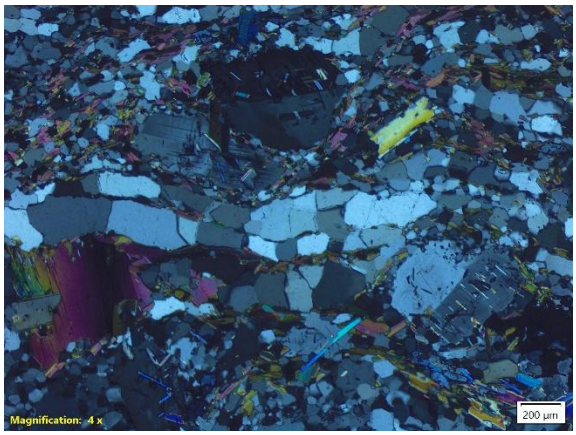

Figure 6.52: Deformed granite intrusive show the presence of feldpar porphyroclast wrap by the muscovite and quatz ribbon (Sample Id: 109255).

6.2.6 Granite gneiss:

Field Observation: The granite gneiss rock of Almora is reported from the northern part of the block, near Saura and Sirkot area. The rock is medium grained, foliated, having the distinct felsic and mafic bands. In hand specimen, the rock is composed of quartz, feldspar and mafic like biotite, muscovite. The foliation is marked by parallel alignments of mafic. Beside quartz shows elliptical to ribbon shape, parallel to foliation, feldspar also elliptical and parallel to foliation.

Petrological Study: Total 2 thin section were studied (109242, 109250). In thin section, the rock exhibits a well-developed gneissose texture with bands of felsic (quartz and feldspar) and mafic (biotite ± muscovite). Quartz appears colourless with low relief and shows undulose extinction under crossed polars, often forming elongated ribbon-like grains parallel to foliation. Feldspars, including alkali and plagioclase feldspar, are colourless, showing characteristic twinning (simple and polysynthetic) and are commonly altered to sericite. These feldspar grains are often elliptical or lens-shaped and aligned with the foliation. Biotite and muscovite arranged parallel to foliation (Figure 6.53, Figure 6.54).

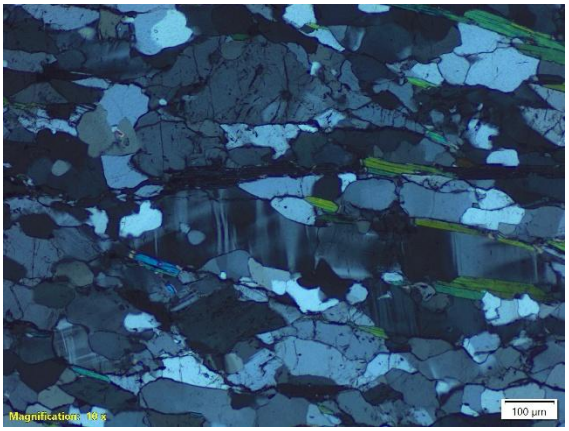

Figure 6.53: Photomicrograph of Granite gneiss shows the presence of elliptical feldspar and quartz (Sample Id: 109242).

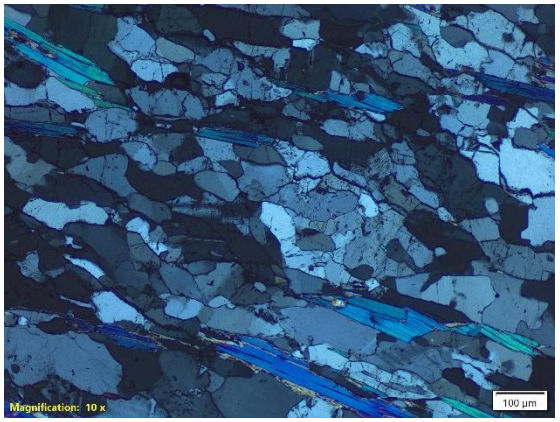

Figure 6.54: Photomicrograph of Granite gneiss shows the presence of elliptical feldspar and quartz (Sample Id: 109242).

6.3 Structure:

6.3.1 Field observation on structures in different lithologies:

The field study indicates that the presence of a strong WNW–ESE trending foliation almost all rock types in the Almora block.

The mica schist of the Almora block exhibits a strongly developed schistosity defined by the preferred orientation of muscovite and biotite minerals. At places, the foliation also folded developing 2nd ordered schistosity. The foliation shows variable orientations, dominantly WNW–ESE trending with a few NW-SE to NE–SW trending. Dip values are highly variable, ranging from very gentle angles all over the block due to thrusting and about 3°-15° in the southern part of the block specially around Biraura, Pithauni, Sironiya, Phalsima, Sirar areas to about ~20° near Barakot, Bintola, Digoli, Udalgaon area for thrust flat geometry (Figure 6.55, Figure 6.56) to steep and near-vertical attitudes up to 88° in the northern part of the block, near Channi, Khas Tilari, Baman Tilari area due to folding to ramp/ imbricate thrust for continuous compression. In the norther-western part, near Sirkot, Saura area, the foliation is generally NE-SW trending with low dip toward south-east. The dip directions of the foliation in mica-schist are predominantly toward NE with ESE and SE, with occasional reversals toward the SW, reflecting local structural complexity.

Figure 6.55: Field photo shows almost horizontal bed of mica-schist due to thrusting.

Figure 6.56: Field photograpgh shows the folding of quartzite in mica schist.

Graphite schists show a well-developed and penetrative foliation (F1) characterized by the alignment of graphite and muscovite. The dominant orientation of the foliation is WNW–ESE to NW–SE, with minor NE–SW variations. Dip angles are generally gentle to moderate, ranging from 5° to 45°, with local steepening in structurally disturbed zones. The dip value is similar to mica-schist, i.e. ranging from very gentle angles of about 3°-15° in the southern part of the block specially around Biraura, Pithauni, Sironiya, Phalsima, Sirar areas to about ~20° near Barakot, Bintola, Digoli, Udalgaon area to steep and near-vertical attitudes up to 88° in the northern part of the block, near Channi, Khas Tilari, Baman Tilari area. The dip directions are mainly toward NE and SSW.

Quartzite (±quartz mica schist) rocks (Figure 6.57) show strong alignment with the regional NW–SE structural trend (varies between 100° and 155°). However, they exhibit a wide range of dip values from gentle (7°–20°) to very steep and vertical (up to 90°). Variation of the dip is similar as seen in the mica schist and graphite schist. Dip directions vary significantly, including SW, NE and locally towards N.

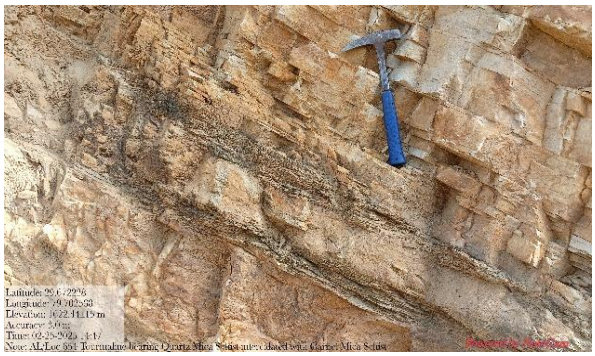

Figure 6.57: Quartzite shows the prominent F1 foliation.

The younger granitic intrusive shows a well-developed strong mylonitic foliation. The foliation is defined by the parallel alignment of recrystallized quartz, feldspar and mafic minerals. Quartz occurs as elongated elliptical to ribbon-shaped grains, while feldspar porphyroclasts exhibit augen (eye-shaped) (Figure 6.59), σ-type and fish-like forms as a result of intense ductile shearing. These porphyroclasts are commonly elongated with their long axes inclined to the foliation and their strain shadows or tails are consistently curved in the sense of shear. The asymmetric shape and systematic orientation of feldspar porphyroclasts provide reliable kinematic indicators, confirming sinistral (left-lateral) shear movement. The orientation of the mylonitic foliation vary from NW–SE to NE–SW, while generally moderate (25°–40°) dip, with local steep dips reaching up to about 85°.

The granite intrusive also exhibits two distinct types of lineations: dominantly the stretching lineation and a few intersection lineation (Figure 6.58). Stretching lineation is the most widely developed linear structure in the study area and is associated with ductile deformation within mylonitic and sheared rocks. It is represented by the elongation and alignment of minerals and mineral aggregates, mainly quartz ribbons and feldspar porphyroclasts, within the foliation plane. The stretching lineations show a wide range of plunge values, from very low angles (~5°–25°) to moderately high angles (~45°–70°). Azimuthal orientations are relatively consistent, with dominant trends between 230°–270° and a secondary set around 300°–330°. In contrast, intersection lineations are comparatively rare and are characterized by low plunge angles (15°–20°), with orientations towards Southwest (220°) and Northeast (50°), suggesting relatively gentle structural features.

Figure 6.58: Mylonitized granite intrusive with strong foliation.

Figure 6.59: Porphyroclasts (augen-shaped, marked by an arrow) of feldspar in mylonitic

Tuffaceous rocks also show foliation trends similar to surrounding rocks, ranging from NW–SE to NE–SW. Dip values are generally moderate (11°–38°), with occasional higher values up to about 55°. Dip directions are mainly toward NE with rarely SE.

6.3.2 Structural Interpretation:

The structural data from the Almora Block indicates a dominantly thrust-related compressional tectonic regime affecting all lithological units, including mica schist, graphite schist, quartzite, tuffaceous rocks and granitic intrusives. The pervasive development of regional foliation with a general WNW–ESE to NW–SE trend reflects strong crustal shortening and consistent tectonic transport during orogenesis.

The wide variation in foliation dip, ranging from gently inclined attitudes (3°–15°) in the southern sector to steep and near-vertical orientations (up to ~88°) in the northern part, indicates progressive deformation associated with thrust stacking and crustal thickening. The coexistence of gentle and steep dipsmay be due to the presence of thrust-related flat and ramp geometries, where shallowly dipping foliations represent flat detachment levels and steep foliations represent ramp zones and imbricate thrust slices and thrust related folding.

Quartzite and schistose units preserve the structural grain, confirming region-wide thrust deformation, while local variations in dip and dip direction reflect folding and rotation associated with thrust propagation and imbrication. The consistent regional alignment of foliation indicates a unified tectonic transport direction, typical of compressional thrust belts.

In the younger granitic intrusives, the development of mylonitic foliation and ductile fabrics further supports thrust-related deformation at deeper structural levels. The presence of stretching lineations with variable plunge (5°–70°) and consistent azimuthal orientation (230°–270°) indicates tectonic transport within a ductile thrust shear system, where low-plunge

lineations correspond to thrust flat zones and high-plunge lineations represent ramp-related shear zones.

Intersection lineations (Table 6.3) represent earlier structural overprinting during initial shortening and are consistent with early stages of thrust-related folding prior to intense shear localization.

Table 6.3: Structural Interpretation of stretching and intersection lineation present in granite intrusive.

S No	Location No	Lineation Type	Plunge (°)	Azimuth	Structural Interpretation
1	GSPL-Almora-24/11/728	Intersection	15	220	Fold-related structure
2	GSPL-Almora-24/11/728	Stretching	20	240	Transitional deformation
3	GSPL-Almora-24/11/728	Stretching	22	330	Transitional deformation
4	GSPL-Almora-24/11/731	Stretching	25	260	Transitional / weak thrust influence
5	GSPL-Almora-24/11/734	Intersection	20	50	Fold-related structure
6	GSPL-Almora-24/11/735	Stretching	20	230	Transitional deformation
7	GSPL-Almora-24/11/735	Stretching	25	310	Transitional deformation

S No	Location No	Lineation Type	Plunge (°)	Azimuth	Structural Interpretation
8	GSPL-Almora-24/11/738	Stretching	45	90	Transitional to weak thrust zone
9	GSPL-Almora-24/11/744	Stretching	22	35	Transitional deformation
10	GSPL-Almora-24/11/746	Stretching	14	270	Transitional / approaching thrust zone
11	GSPL-Almora-24/11/749	Stretching	7	145	Thrust-related (flat zone)
12	GSPL-Almora-24/11/749	Stretching	65	325	Thrust-related (ramp zone)
13	GSPL-Almora-24/11/750	Stretching	52	325	Thrust-related shear zone
14	GSPL-Almora-24/11/751	Stretching	55	255	Thrust-related flat
15	GSPL-Almora-24/11/756	Stretching	65	260	Thrust-related ramp zone
16	GSPL-Almora-24/11/756	Stretching	69	265	Thrust-related high-strain zone

Based on integrated field observations, remote sensing analysis and structural data, six thrusts have been identified within the Almora Block. Out of these, five thrusts exhibit WNW–ESE trend and are arranged from south to north of the block, with their dip increasing northward from approximately 15° to 65° (ramp structure). One thrust shows a NE–SE trend

situated western part of the block. The identified thrusts (Figure 6.60) are (WNW–ESE trending, from south to north): (1) Biraura–Pithauni Thrust, (2) Phalsima–Sironiya Thrust, (3) Jakheta–Chitan Thrust, (4) Bintola–Udalgaon Thrust, (5) Batgal–Channi Thrust and NE-SE trending (6) Kalimath–Dinapani Thrust.

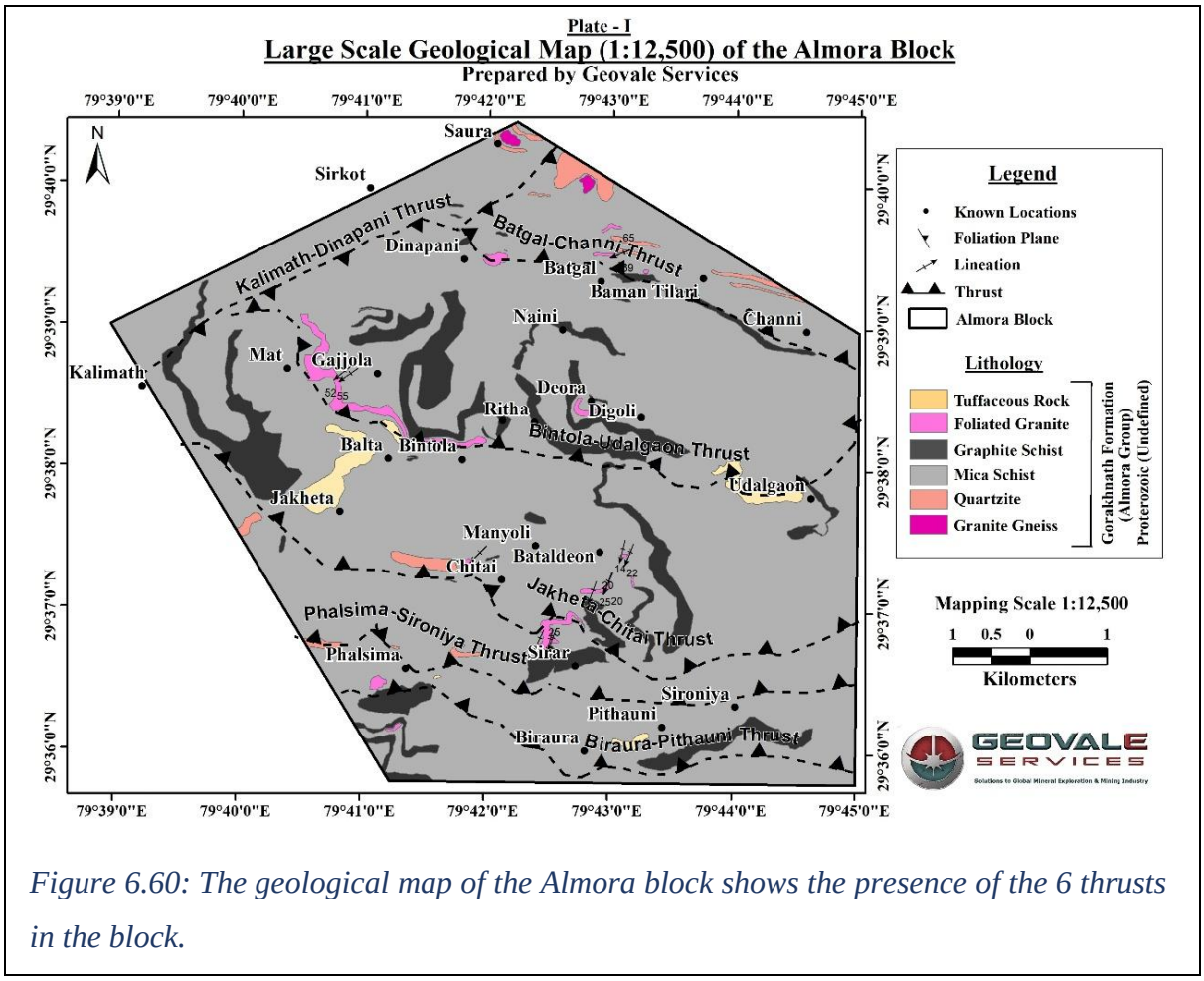

Figure 6.60: The geological map of the Almora block shows the presence of the 6 thrusts in the block.

6.4 Metamorphism:

6.4.1 Mica-schist:

The mica-schist exposed in the Sironiya area, in the south-eastern part of the block, is medium- to coarse-grained and exhibits a well-developed schistosity defined by the preferred alignment of muscovite and biotite, giving rise to a typical lepidoblastic texture. A characteristic feature of this rock is the presence of snowball garnet porphyroblasts (Figure 6.61), which contain spiral inclusion trails and are wrapped by the surrounding muscovite–biotite matrix, indicating their syn-tectonic growth. In several samples, muscovite flakes are observed to be folded and kinked, (Figure 6.62) reflecting deformation after initial mineral growth. In the Udalgaon area, the mica-schist shows comparatively higher garnet content along with the presence of hornblende, suggesting mineralogical variation within the block. In contrast, the central and

northeastern parts of the area display mica-schist with relatively lower garnet abundance, indicating spatial variation in mineral distribution and textural development.

The mica-schists of the area represent regionally metamorphosed pelitic rocks formed under medium-grade metamorphic conditions. The mineral assemblage of muscovite, biotite and garnet indicates metamorphism within the greenschist to lower amphibolite facies. The development of snowball garnets in the Sironiya area suggests syn-tectonic growth during progressive metamorphism, where garnet formed contemporaneously with deformation. The inclusion trails and their spiral pattern reflect continuous deformation and recrystallization during metamorphism. The presence of hornblende in the Udalgaon area indicates relatively higher temperature and pressure conditions, marking a transition toward amphibolite facies. In contrast, the reduced garnet content in the central and northeastern parts suggests comparatively lower metamorphic grade. The metamorphic variation across the Almora block indicates a progressive increase in grade from the central and northeastern regions toward the southeastern and Udalgaon areas, likely controlled by differences in burial depth, temperature conditions and tectonic activity during regional metamorphism.

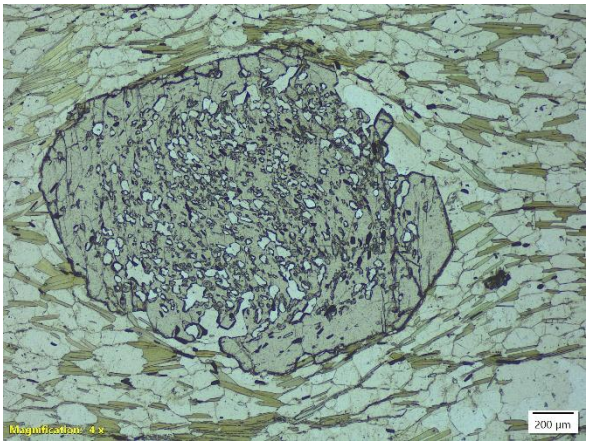

Figure 6.61: Snowball garnet in the mica-schist

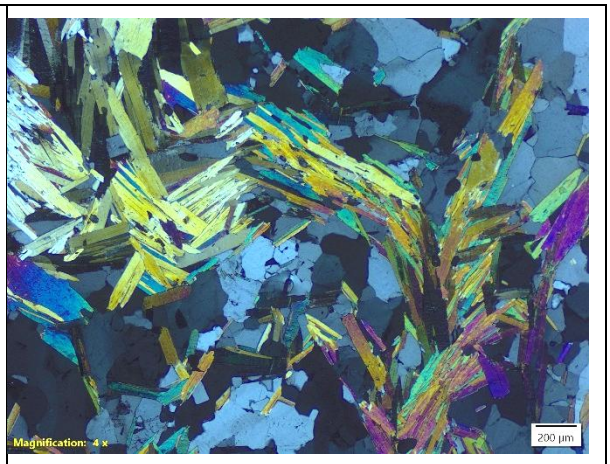

Figure 6.62: Folded muscovite in mica schist.

6.4.2 Graphite schist:

In graphite schist, the rock is typically medium- to coarse-grained with a well-developed schistosity defined by aligned mica minerals such as muscovite and biotite, along with abundant flaky graphite (Figure 6.63, Figure 6.64, Figure 6.65, Figure 6.66). The graphite may occur as disseminated flakes or concentrated along foliation planes. The mineral assemblage commonly includes quartz, muscovite, biotite and graphite and in higher-grade conditions. With increasing temperature and pressure, the original organic matter undergoes progressive

transformation into crystalline graphite, reflecting a higher degree of carbon ordering. The well-developed schistosity, defined by aligned muscovite and biotite, indicates metamorphism under directed pressure, where deformation and recrystallization occurred simultaneously. The presence of mineral assemblages such as quartz, muscovite, biotite and graphite suggests amphibolite facies condition.

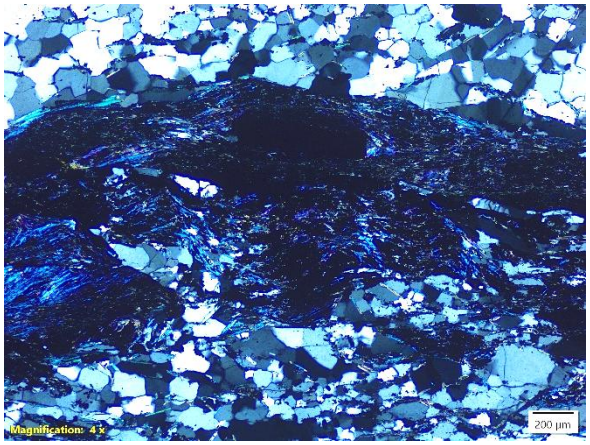

Figure 6.63: The presence of randomely oriented graphite in muscovite.

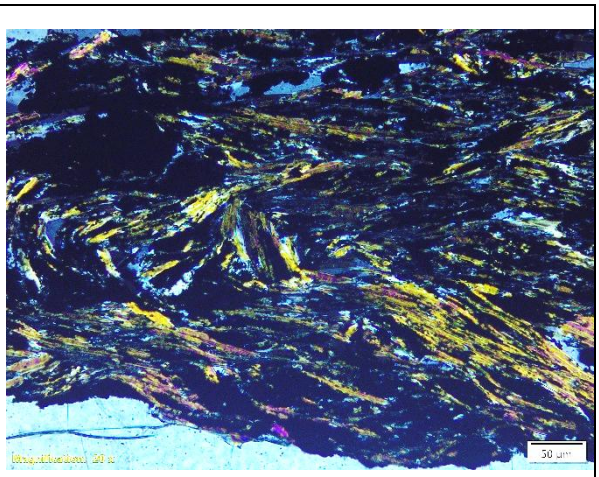

Figure 6.64: The presence of randomely oriented graphite in muscovite.

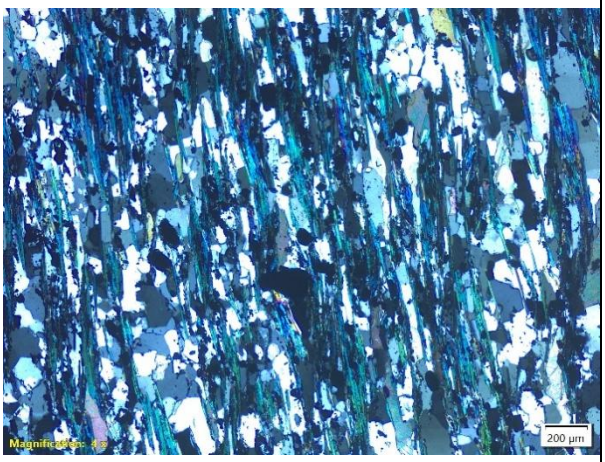

Figure 6.65: Graphite clots in carboneceous phyllite.

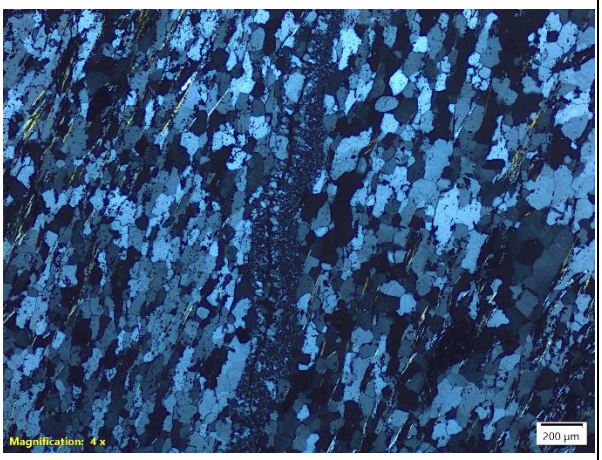

Figure 6.66: Graphite shows alignment parallel to foliation.

6.4.3 Granite-gneiss:

The granite-gneiss present in the northern part of the block shows the presence of quartz, muscovite and biotite and feldspar which have been reoriented and recrystallized. Quartz displays elongated, ribbon-like forms with sutured boundaries, reflecting dynamic

recrystallization and ductile deformation (Figure 6.67, Figure 6.68). The strong alignment of mica flakes forms a distinct foliation. Feldspars show elliptical grain, grain-size reduction. These features collectively indicate that the rock has undergone regional metamorphism, likely within a tectonically active zone, where both heat and stress contributed to the transformation of the original igneous rock into a foliated metamorphic rock such as gneiss.

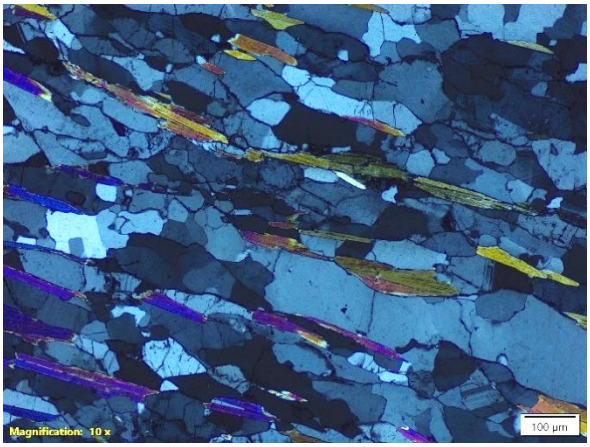

Figure 6.67: Foliated granite-gneiss shows the presence of elliptical quartz and muscovite alignment parallel to foliation

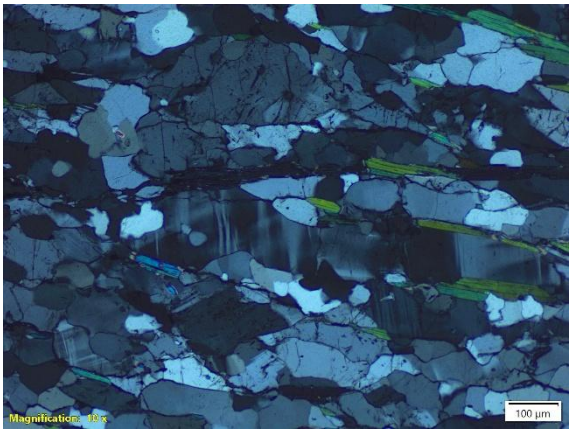

Figure 6.68: Foliated granite-gneiss shows the presence of elliptical feldspar.

6.4.4 Younger granite intrusive:

The younger granite intrusive are generally present along the thrusts, near Sirar, Bintola and Digoli, cenral part of the block, shows strongly foliated granite rock composed mainly of quartz, feldspar, biotite and muscovite. Quartz occurs as well-developed ribbon grains (Figure 6.69, Figure 6.70) with strong elongation and preferred orientation. Biotite and muscovite are aligned parallel to the foliation, defining a continuous planar fabric. Feldspar occurs as porphyroclasts and are wrapped by quartz ribbons and biotite muccovite, indicating strong deformation. The ribbon quartz reflects dynamic recrystallization and crystal plastic flow under elevated temperature and directed stress. The strong preferred alignment of biotite and muscovite indicates the development of foliation due to rotation and recrystallization of platy minerals perpendicular to maximum compressive stress. The wrapping of feldspar porphyroclasts (Figure 6.71, Figure 6.72) by quartz and mafic material suggests progressive deformation and high strain. Based on the observed microstructures, the estimated temperature of metamorphism is approximately 450–650°C. This interpretation is supported by the presence of ribbon quartz, which indicates dynamic recrystallization and ductile flow of quartz

at elevated temperatures. The strong preferred alignment of biotite and muscovite further suggests deformation under conditions where platy minerals can rotate and recrystallize, typically within the upper greenschist to lower amphibolite facies. Feldspar occurs as porphyroclasts that are not completely recrystallized, indicating that temperatures were not high enough for feldspar plasticity, which commonly develops at higher amphibolite facies conditions.

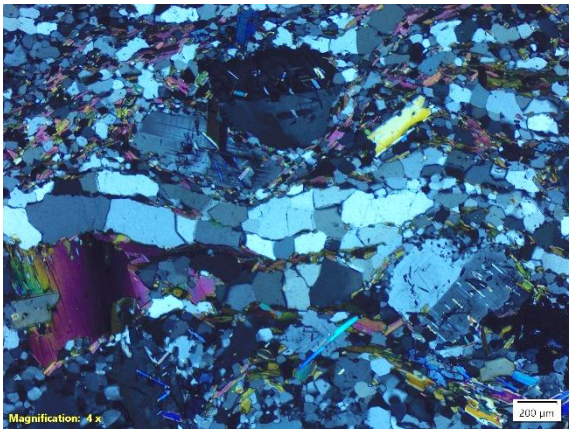

Figure 6.69: Ribbon quartz in deformed granite intrusive, near Sirar area.

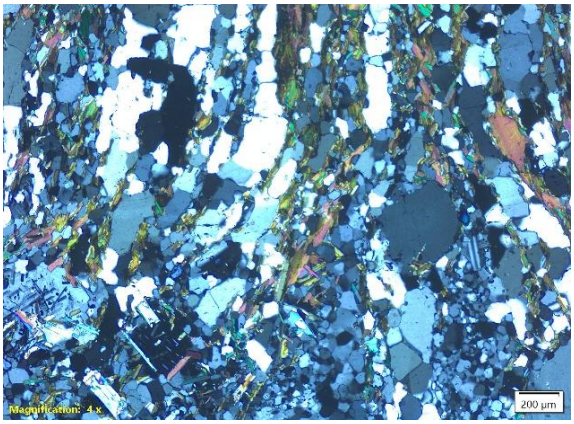

Figure 6.70: Ribbon quartz and muscovite alignments in deformed granite intrusive, near Sirar area.

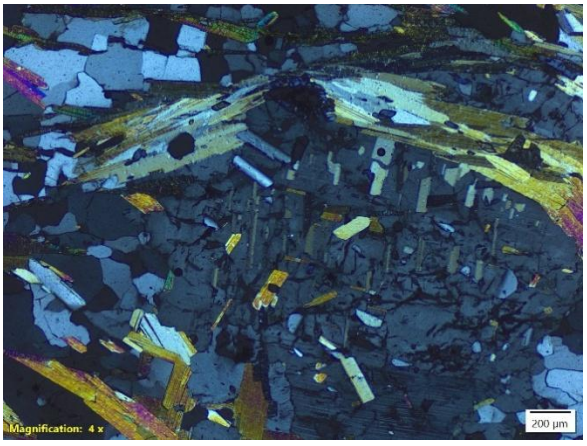

Figure 6.71: Felspar porphyroclased in deformed granite intrusive, near Bintola.

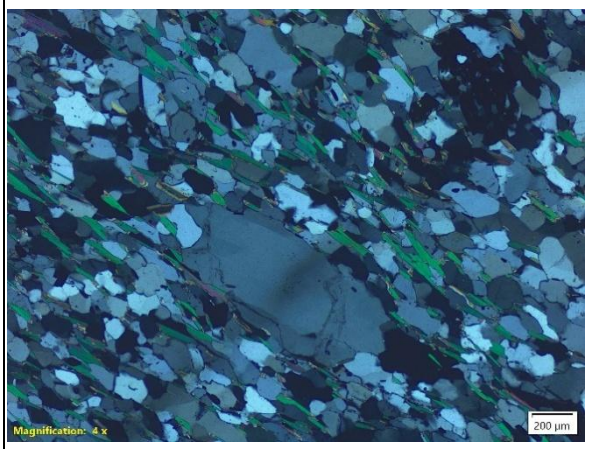

Figure 6.72: Quartz prophyroclased in mylonitized granite intrusive, near Digoli.

6.4.5 Quartzite:

Quartzite from Mat, Khas Tilari area, northern part of the block shows well-developed recrystallization textures, including undulose extinction and subgrain formation, indicating

progressive recovery and dynamic recrystallization. The quartz forms an interlocking mosaic texture typical of recrystallized metamorphic rocks. Minor mica and tourmaline grains show a distinct preferred orientation (Figure 6.73, Figure 6.74), defining a weak foliation and indicating the influence of directed stress during deformation.

The quartzite microstructures indicate that the rock has undergone recrystallization under medium-grade metamorphic conditions with both static and dynamic recrystallization processes active. The presence of 120° triple junctions suggests grain boundary energy minimization, typical of annealing at elevated temperatures, while undulose extinction and sub-grains reflect ongoing deformation. The preferred orientation of mica and tourmaline indicates mild ductile deformation under differential stress. Based on these features, the estimated temperature of metamorphism is approximately 450–650°C, corresponding to upper greenschist to lower amphibolite facies conditions. At this range, quartz is highly ductile, allowing recrystallization, while accessory minerals align to form a weak foliation under directed pressure.

For detail understanding metamorphism and associated temperature are discussed below the table (Table 6.4).

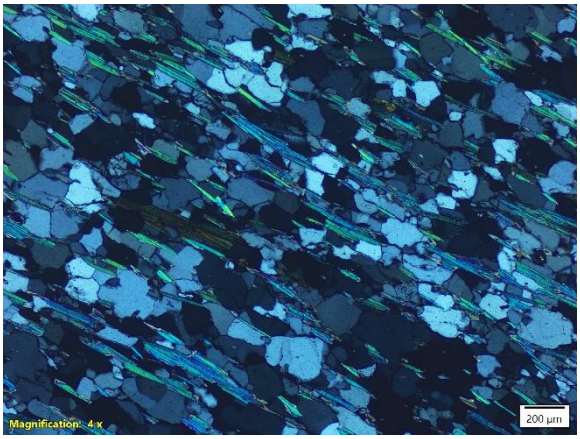

Figure 6.73: Quartzite shows recrystallization of quartz and parallel alignments of muscovite, near Khas Tilari.

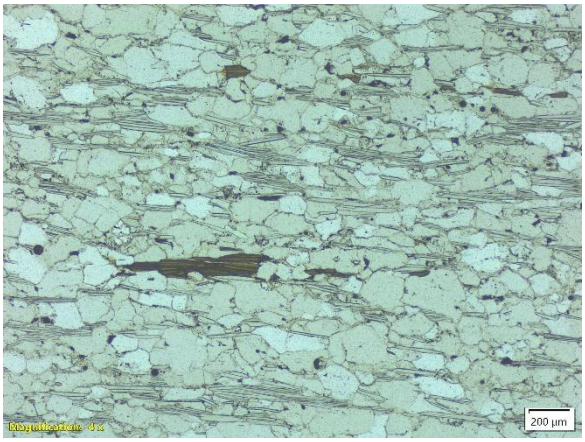

Figure 6.74: Recristallized quartz in quarzite, near Khas Tilari.

Table 6.4: Summary table shows various rock and their metamorphic characteristic and estimated temperature of metamorphism.

Rock Type	Area	Metamorphic Features (Key Observations)	Metamorphic Facies
Mica Schist	Sironiya (SE), Udalgaon, south eastern part of the block	Well-developed schistosity; lepidoblastic texture; aligned muscovite and biotite; snowball garnet with spiral inclusion trails (syn-tectonic growth); folded/kinked micas; hornblende in Udalgaon indicates higher grade variation	**Greenschist to Lower Amphibolite facies**
Graphite Schist	All over the block along the thrusts	Strong foliation defined by muscovite, biotite and graphite; graphite flakes along foliation planes; progressive graphitization of organic matter; recrystallization under directed stress.	**Greenschist facies (upper transition locally)**
Granite Gneiss	Northern part of block	Quartz,feldspar, and mica reoriented; ribbon quartz with sutured boundaries; strong foliation; feldspar grain-size reduction and deformation; ductile flow textures	**Upper Greenschist to Amphibolite facies**
Younger Granite Intrusive (Foliated granite)	Sirar, Bintola, Digoli	Ribbon quartz; strong mica alignment; feldspar porphyroclasts wrapped by quartz and mafic minerals; dynamic recrystallization; high-strain shear zone fabric	**Upper Greenschist to Lower Amphibolite facies (shear zone metamorphism)**
Quartzite	Mat, Khas Tilari (Northern	Recrystallized quartz mosaic; undulose extinction; sub-grain formation; 120° triple junctions; weak	**Greenschist to Lower Amphibolite facies**

Rock Type	Area	Metamorphic Features (Key Observations)	Metamorphic Facies
	part of the block)	foliation due to mica and tourmaline alignment	

6.5 Graphite and Poly-metals Fertility of the Lesser Himalaya in Mineral System Analysis (MSA) Framework:

Geovale Services Private Limited adopts the Mineral System Analysis (MSA) technique as its primary approach for mineral exploration in the Almora block. MSA is based on the concept that mineral deposits occur only when several critical geological processes occur together in space and time. A combined role of fertile host rocks, metal-bearing fluids, tectonic framework and trapping mechanisms are necessary to form a potential mineralization.

6.5.1 Fertile Host Rocks

The host rocks for graphite and vanadium mineralization are the Graphite Schist that occur intercalated with other high grade pelitic and psamitic schists. The Graphite Schist rocks are rich in organic carbon and their thickness varies from less than a meter to more than ten meters. The intercalated pelitic schists show evidence of insitu partial melting leading to development of patchy granitic rocks within it with indistinct outlines (Figure 6.75). Under thin sections, patchy quartzo-feldspathic masses are intimately associated with sillimanite confirming development of partial melting due to muscovite breakdown reaction (Figure 6.76). Thus, the host carbonaceous layers have also suffered a high-grade metamorphism to the tune of temperature exceeding 700°C. Under such high temperature, the carbonaceous matter is expected to have converted into highly ordered graphite. However, post graphitization thrusting might have affected sizes of graphite and their ordering. The deposition of thick carbonaceous layers is likely to have occurred in shallow sea environment due to massive dumping of algal matters. Such massive dumping of algal matters might have been triggered by onset of unusual toxicity in the ocean and/or sudden changes in the changes of ocean water. The one possible cause for such toxicity for temperature changes of ocean water is concomitant oceanic hydrothermal activity. Such hydrothermal activity might as well contribute a number of rare metals (for example, V, Co, Cr, Zn, Cu, Au, W, Sn, PGE etc.). Thus, it is possible that carbonaceous layer would also be hosting leached concentration of above base metals. Of course, some redox sensitive trace metals (V, Cr) might also be contributed by input from continental sources that gets trapped in the reducing environment of the carbonaceous matters.

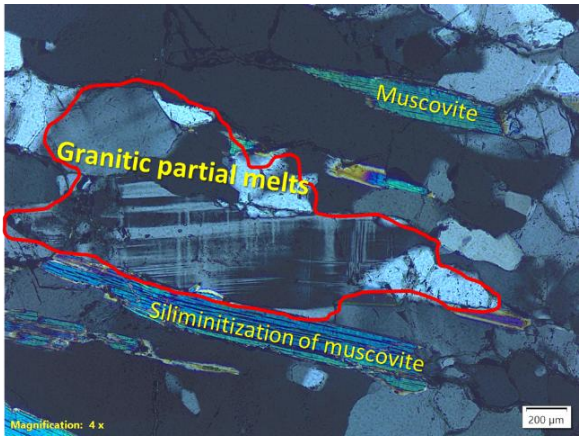

Figure 6.75: Photomicrograph shows Patchy quartzo-feldspathic masses are associated with sillimanite confirming development of partial melting due to muscovite breakdown reaction. under XPL.

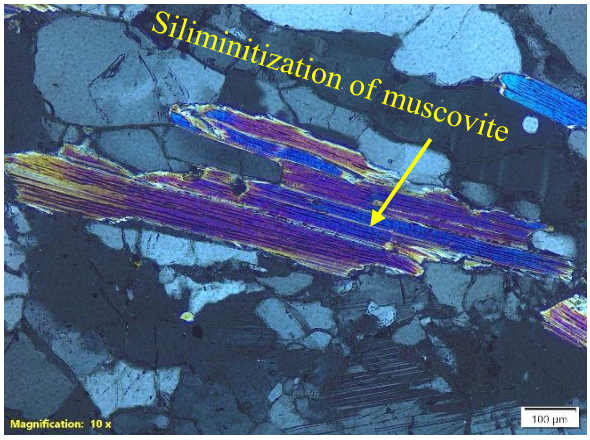

Figure 6.76: Photomicrograph shows sillimanite formation phase after break down of muscovite, under XPL.

6.5.2 Fluids to scavenge metals from fertile host rocks

Carbonaceous layers are stratiform and syn-depositional in nature so there is no role of fluids concentrating carbonaceous matters other than what for metamorphism to have taken place. Critical trace metals that might have been deposited alongside the carbonaceous matters would require some sub-sea hydrothermal activity. Post -depositional fluid activity associated with subsequent deformation might rearrange concentration of critical metals along some weaker planes.

6.5.3 Tectonic Controls and Structural Architecture

Graphitisation in present area are related to increase in geothermal gradient due to the burial deep inside the crust related to some tectonic activity. Subsequent upthrust would be required for the graphite to get exposed at the present level. Deeper part that might have been exposed are expected to have higher order of graphitization. Thus, it is important to find out the zones of graphite layers that might have upthrusted deeper level of the crust.

6.5.4 Structural and Lithological Traps:

Preservation of upthrusted deeper level of the crust is a primary requirement for the high-order graphite to have been exposed at the surface. Again, critical trace metals are liable to subsequent mobilization during deformation and accompanied fluid activity. Suitable structural traps like axial traces of folds, fault or thrust planes are likely loci for trapping of remobilized trace metals.

6.6 Geochemical Analysis for surface sampling:

6.6.1 XRF data analyses and interpretation:

The analysed samples comprise a diverse assemblage of metamorphic, igneous and hydrothermal rock types, each characterised by distinct geochemical signatures obtained through XRF analysis. Among these, mica schist and its variants-including garnet mica schist, quartz mica schist, muscovite schist and biotite–muscovite schist-form the most abundant lithological group. These rocks show a wide range in SiO_2 content (approximately 41.8% to 88.8%) and consistently high Al_2O_3 values (10%–27%), with K_2O typically between 1.5% and 4%, reaching up to 8.91% in muscovite-rich samples. Fe_2O_3 content is variable but generally falls between 1% and 8%, with occasional higher values. These characteristics indicate aluminous metamorphic rocks derived from pelitic or psammitic sedimentary protoliths, with higher silica values reflecting quartz-rich precursors. The presence of garnet and muscovite suggests formation under medium- to high-grade regional metamorphic conditions.

Graphite schist represents another important lithology, characterised by significant carbonaceous content and commonly occurring as interlayered units within mica schists. These rocks exhibit highly variable SiO_2 values (27.8% to 92.2%) and elevated loss on ignition (LOI) values ranging from 3% to 20%, reflecting the presence of graphite and volatiles. Fe_2O_3 content can be particularly high, reaching up to 47% in mineralised samples. The geochemical and field characteristics suggest derivation from organic-rich sedimentary rocks such as shales or mudstones. The presence of features such as pyrite pits and sulphur further indicates the occurrence of iron sulphides, particularly pyrite, within these graphitic horizons.

Granitic rocks in the study area include younger granite, foliated granite and sheared granite, often displaying augen textures indicative of deformation. These rocks are characterised by relatively high SiO_2 content (60%–77%), moderate Al_2O_3 (10%–16%) and elevated alkali contents, with Na_2O ranging from 1.9% to 3.5% and K_2O from 1.3% to 4.8%. These geochemical signatures are typical of felsic igneous rocks. The presence of foliation and augen structures indicates that these granites have undergone deformation and metamorphism, resulting in orthogneissic textures. The designation of "younger granite" suggests emplacement during a later intrusive phase relative to the surrounding lithological units.

Quartzite occurs both as bedrock and as detrital components within stream sediments. It is characterised by very high SiO_2 content, typically ranging from 74% to 92%, with Al_2O_3 varying between 3.6% and 14.7% depending on impurity levels and generally low LOI values (<1.5%). These features indicate formation through the metamorphism of quartz-rich

sandstones. Samples with higher Al_2O_3 content suggest the presence of micaceous material, indicating a gradation toward micaceous quartzite or quartz schist.

Quartz veins are widely observed as hydrothermal features cutting across mica schists and granitic rocks. These veins are typically composed almost entirely of silica, with SiO_2 values ranging from 91% to over 99%. However, one anomalous sample shows significantly lower SiO_2 (19.49%) along with elevated CaO, P_2O_5 and LOI values, suggesting a composition dominated by carbonate or phosphate minerals rather than pure quartz. Overall, these veins are interpreted as products of hydrothermal fluid activity, with local variations in fluid chemistry reflected in their composition.

Volcanic or tuffaceous rocks are also present in both bedrock and stream sediment samples. These rocks display SiO_2 values between 71.3% and 82.0%, Al_2O_3 between 7.7% and 9.9% and Fe_2O_3 between 2.5% and 4.6%. Such compositions are consistent with felsic volcanic or volcaniclastic materials, indicating that the geological history of the area includes episodes of explosive volcanic activity.

The geochemical composition of mica schist and its variants indicate an aluminous nature, with consistently high Al_2O_3 and variable but often elevated SiO_2 content. This suggests derivation from pelitic to psammitic sedimentary protoliths, such as clay-rich shales and sandy sediments. Elevated K_2O values, particularly in muscovite-rich samples, reflect the abundance of K-bearing minerals like muscovite and biotite. Variations in Fe_2O_3 are attributed to differing proportions of ferromagnesian minerals and accessory phases such as garnet. High silica samples (>80% SiO_2) indicate quartz-rich precursors, while the presence of garnet and mica points to medium- to high-grade regional metamorphism.

The geochemical signature of graphite schist is marked by highly variable SiO_2 and significantly elevated loss on ignition (LOI), which reflects the presence of carbonaceous material (graphite) and volatiles. High Fe_2O_3 values in certain samples suggest the presence of iron-bearing minerals, particularly sulphides such as pyrite. These characteristics indicate that the protoliths were organic-rich sedimentary rocks, such as black shales or mudstones, deposited in reducing environments. The enrichment of sulphur and iron further supports the interpretation of syngenetic or diagenetic sulphide mineralisation within these rocks.

Granitic rocks exhibit high SiO_2 and moderate Al_2O_3, along with elevated alkali contents (Na_2O and K_2O), confirming their felsic igneous origin. The relatively high total alkalis indicate a composition dominated by feldspar minerals (both plagioclase and K-feldspar). Geochemical variations between samples likely reflect fractional crystallisation and minor alteration processes. The presence of foliation and deformation-related textures, combined with their

chemistry, suggests that these granites have undergone metamorphism and deformation, forming orthogneissic equivalents. The identification of "younger granite" further implies a later intrusive phase distinct from earlier metamorphic events.

Quartzite samples are characterised by very high SiO_2 content and low concentrations of other oxides, reflecting their origin from quartz-rich sandstones. The chemical purity of many samples indicates extensive recrystallization and removal of impurities during metamorphism. However, samples with higher Al_2O_3 suggest the presence of clay or mica impurities, indicating incomplete purification or transitional compositions toward micaceous quartzite. The low LOI values further confirm the absence of volatile-rich minerals and the dominance of stable quartz. Quartz veins show extremely high SiO_2 values, consistent with precipitation from silica-rich hydrothermal fluids. Their chemical simplicity reflects limited incorporation of other elements during formation. However, anomalous samples with elevated CaO, P_2O_5 and LOI indicate the presence of carbonate and phosphate minerals, suggesting variation in hydrothermal fluid composition and possible multi-stage mineralisation. These geochemical features point to hydrothermal processes associated with fluid circulation through fractures and structural zones. Volcanic or tuffaceous rocks display moderately high SiO_2 along with lower Al_2O_3 and Fe_2O_3, consistent with felsic volcanic compositions. These geochemical characteristics suggest derivation from explosive volcanic activity, producing ash and pyroclastic material that later lithified. The relatively uniform composition implies limited post-depositional alteration, although minor variations may reflect differences in source magma composition or degree of weathering and reworking.

From a geochemical perspective, elevated loss on ignition (LOI) values are a key indicator of graphite content, as they reflect the presence of carbonaceous material that burns off during analysis. The wide variation in SiO_2 suggests heterogeneous protolith composition, ranging from clay-rich to siliceous sediments. High Fe_2O_3 values, especially where associated with sulphur indications, point to the presence of iron sulphides such as pyrite. This association is significant because it indicates that graphite-bearing rocks were formed in reducing environments, where organic matter was preserved and sulphide minerals could precipitate. Such conditions are typical of anoxic sedimentary basins, often marine in origin.

From a genetic and geological standpoint, graphite mineralisation indicates that the original sediments were rich in organic matter, such as black shales or carbonaceous mudstones. During regional metamorphism, this organic carbon was progressively transformed into crystalline graphite. The degree of graphitisation generally increases with metamorphic grade, meaning that well-crystallised graphite can be an indicator of medium- to high-grade metamorphic

conditions. Thus, graphite schists can serve as markers of metamorphic intensity and thermal history.

In terms of structural and exploration significance, graphite is often concentrated along foliation planes, shear zones and fold hinges due to its platy nature and mobility during deformation. This makes structurally controlled zones particularly favourable targets for graphite enrichment. Additionally, the presence of associated sulphides (e.g., pyrite) may indicate hydrothermal fluid activity, which can further upgrade graphite concentration or introduce other economically valuable minerals.

From an economic perspective, graphite mineralisation is important due to its wide range of industrial applications, including use in batteries (especially lithium-ion batteries), refractories, lubricants and conductive materials. High-grade, flake graphite-typically formed under higher metamorphic conditions-is especially valuable. Therefore, zones showing high LOI, consistent carbon content and favourable structural controls are considered potential targets for resource evaluation.

Finally, graphite-rich horizons can also act as pathfinders in mineral exploration, particularly for sulphide deposits, as both graphite and sulphides form under similar reducing conditions. Their coexistence may therefore signal favourable conditions for base metal or gold mineralisation in certain geological settings.

6.6.2 Surface ICPMS data analyses and interpretation:

Graphite schist samples show very high concentrations of several trace elements. Vanadium reaches up to 3536 ppm (sample 110030), while Barium shows an extreme peak of 24,699 ppm (sample 109946). Copper and Zinc are also elevated, reaching 436.18 ppm (sample 110013) and 1690.39 ppm (sample 109218) respectively.

Mica schist samples also show significant trace element variation. Vanadium reaches up to 1150 ppm (sample 109205).

Foliated Granite and Granite Gniess samples show enrichment in incompatible and radioactive elements. Tin reaches up to 33.19 ppm (sample 110061) and Tungsten reaches up to 1047 ppm (sample 110063). Lithium reaches 99.57 ppm (sample 110054), Rubidium 366.57 ppm (sample 110054), Thorium 31.54 ppm (sample 110061), Uranium 4.22 ppm (sample 110054).

In case of Tuffaceous rocks, Tungsten yielded up to 127.41 ppm (sample 110020), and Tin 8.53 ppm (sample 110044).

The high vanadium, zinc, copper and extremely elevated barium in graphite schist indicate strong metal enrichment under reducing, carbon-rich conditions. These rocks act as geochemical traps where organic matter and sulphide phases concentrate redox-sensitive and ore-related elements.

Graphite schist show similar enrichment patterns, suggesting interaction with hydrothermal fluids. High zinc and barium values indicate localized sulphide mineralisation and sulfate-bearing fluid influence, while elevated vanadium reflects reducing depositional environments.

Granite intrusive is enriched in lithium, rubidium, uranium, thorium and hafnium, indicating strong magmatic differentiation. These elements are typically concentrated during late-stage crystallisation, suggesting evolved felsic magmatism with potential for rare metal mineralisation.

Mica schists show moderate to high enrichment in barium, lithium and cerium, reflecting their role as both source and host rocks. Element distribution is controlled by metamorphic reworking and fluid-assisted redistribution, with REEs likely hosted in accessory minerals such as monazite.

Volcanic and tuffaceous rocks show enrichment in tungsten, zirconium, gallium and REEs, indicating a felsic volcanic source with significant accessory mineral control. Hydrothermal overprinting may have further enhanced trace element concentrations.

6.6.3 Statistical analysis of surface geochemical data and Interpretation of anomalous zones

The high-V anomalies likely reflect sampling of graphite-bearing black shales or altered mafic units. In Almora block, graphitic schists often host vanadium (e.g. in trace titanomagnetite or vanadiferous clays). Histogram of Vanadium (V) concentration (ppm) showing a strong positive skew and a heavy high-end tail. The Vanadium histogram is sharply right-skewed: most samples have low V values (clustered near tens of ppm), but a few samples reach extremely high concentrations (up to ~3500 ppm). The median V (~129 ppm) is much lower than the mean (~466 ppm), indicating a few anomalously V-rich samples. This suggests that only a few sampled zones contain the strongly vanadium-enriched lithologies, while most samples have background levels. Black shale horizons worldwide are known to concentrate “critical” metals (V, Ni, Co, W) during diagenesis and metamorphism. Thus, the few very High-V samples likely come from zones of Graphite Schist (“graphite schist”) identified in the pits. Vanadium’s distribution suggests it may serve as an exploration pathfinder for the graphite

horizon. Nickel and Co (both compatible with mafic minerals and sulphides) also have occasional high values, consistent with sulfide-bearing graphite schist (e.g. pentlandite-pyrrhotite zones). In general, elevated Ni–Co–V in the geochemical data support the interpretation that several pits sampled graphite schist rich in minor sulphides (pyrite/pyrrothite or magnetite), in agreement with field notes.

These transition-metal anomalies help delineate the graphite schist ore horizon. Samples with outlying V and Ni-Co point to pockets of richer graphite+ magnetite/sulfide. Lower and broadly distributed values of base metals (e.g. Cu, Zn, Pb) likely reflect host-rock background compositions (schist), whereas the spikes in V (and, to lesser extent, Ni, W, Mo) indicate a special lithology. In summary, the positively skewed V histograms highlight anomalous graphite-schist horizons, consistent with the reconnaissance focus on vanadium-graphite targets.

Geologically, Sb is not a primary graphite indicator but can trace minor hydrothermal or metamorphic sulfides. The histogram suggests Sb anomalies are rare, implying most rocks are leached of Sb except where subtle veinlets or sulfide patches occur. W and Mo, being siderophile/chalcophile, tend to concentrate in magnetite and scheelite. A few samples containing W-bearing veins or disseminations would explain the extreme W. Interpretively, the heavy right-tails of Sb, W and Mo indicate rare high-grade spots. These could determine shear zones or quartz veins intersecting the graphite layer. For example, a graphite schist cut by brittle quartz-sulfide veins might yield a high-Sb anomaly. On the other hand, the low baseline of these elements in most samples suggests a relatively “fresh” metasediment.

REEs in the Almora crystalline rocks likely reflect the source sediments of the metasediments. High-grade metamorphism tends to remobilize light REEs somewhat, but graphitic black shales can retain REE enrichments. The measured Ce (and La, Nd) anomalies likely correspond to portions of the sequence with higher detrital input or palaeo-sediment layers. Histogram of Cerium (Ce) concentration (ppm) with a near-normal distribution (moderate skew). The Ce histogram is moderately skewed to the right: most samples cluster around 30–60 ppm, with a few samples reaching >100 ppm. A similar pattern holds for other LREEs (La, Pr, Nd) – the histograms show gentle right tails but no extreme outliers like the V case. HREEs (e.g. Tm, Yb, HREE like-Y) have low absolute values (~0.5–5 ppm) and more pronounced skew, but these are geochemically expected.

Since the reconnaissance goal includes vanadium (often enriched in black shales), REE anomalies can co-occur with graphite horizons. However, in these samples the REE distributions are relatively moderate, suggesting the bulk of the samples are schist (with LREEs at crustal levels) and that only a subset has elevated REEs. The REE histograms show that most samples have LREE content typical of pelitic schists (tens of ppm Ce), with the slightly heavy-tailed shape hinting at minor enrichment in certain samples that may coincide with the V-rich zones.

Histogram of Sulfur (%) showing extreme skew toward low values. The sulfur distribution is highly positively skewed: almost all samples have very low S (<0.5%), while a few have significantly higher S (max ~5.3%). The median S (~0.04%) is far below the mean (~0.31%) because of these few high values. In other words, most samples are essentially sulphur-poor (barren schist), but a minority are sulphide-rich.

This pattern is geologically meaningful. Graphite schist in Almora is well-known to contain "substantial sulphide minerals" in places. Sulfur in the ICPMS data likely reflects pyrite/pyrrhotite content. Samples from the continuous graphite horizon show elevated S; others do not. Thus, the sulfur histogram directly maps the graphite-proxy: the anomalous S values coincide with the graphite-schist ore horizon. In exploration, detecting those rare high-S outliers is significant. It corroborates the visual logging of sulphides in pits and the SP/resistivity anomalies (graphite plus pyrrhotite). The S histogram confirms that graphite-ore zones are discrete. The strong skewness (many zeros with few spikes) indicates graphite facies rocks are limited in extent. Sulfur serves as an excellent pathfinder for graphite here: any sample falling on the S tail is almost certainly from graphite schist. This assists in delineating the mineralized horizon. The combination of sulphur peaks with high V and moderate Ni/Co in the same samples would flag the best graphite-vanadium targets.

The geochemical histograms reveal that most trace metals cluster at low baseline levels, whereas elements tied to graphite/mineralization (V, S, W, Ni, Co) have heavy right-tails. This supports the geological picture of a continuous graphite schist horizon (amphibolite-facies graphite schist) hosting vanadium and minor sulfides. Transition metals and REEs have relatively typical background distributions, with only a few pronounced anomalies. Sulfur and vanadium stand out as the clearest pathfinder signatures: their histograms highlight the anomalous samples. These geochemical signatures align with the rock descriptions in the Almora block and help target the graphite-vanadium mineralized layer for exploration.

Vanadium (V)

The vanadium (V) concentration histogram is highly right-skewed: most samples are at low ppm and a few have very large values. The KDE (Kernel Density Estimation, red curve) clearly shows one main peak near the low end and a long tail to high concentrations. Indeed, the mean (466 ppm) is much larger than the median (129 ppm), indicating extreme outliers (maximum ~3536 ppm). The mode (at the 6.7 ppm detection limit) highlights that many values cluster at the minimum. In *Vanadium (V) concentration histogram (n=100): Mean = 466 ppm, Median = 129 ppm, Mode = 6.7 ppm (*Figure 6.78*)*

Nickel (Ni)

Nickel shows a similar positive skew: a large cluster of low-concentration samples and a few very high values (max ~127 ppm). The KDE (red curve) smooths the histogram bins, capturing the main peak near the lower concentrations without the abrupt jumps of the bars. The mean (24.24 ppm) exceeds the median (11.09 ppm), reflecting a long right tail. The mode is at 0.5 ppm (detection limit), indicating many samples at the minimum measurable Ni. In *Nickel (Ni) concentration histogram (n=100): Mean = 24.2 ppm, Median = 11.1 ppm, Mode = 0.5 ppm (*Figure 6.79*).*

Chromium (Cr)

Chromium concentrations are moderately skewed right. The histogram peak is around 150–200 ppm, with a tail to higher values (max ~485 ppm). The KDE overlay (red line) again smooths the distribution shape. Here the mean (213.7 ppm) is only slightly above the median (189.8 ppm), so the skew is mild compared to other elements. The mode (204.2 ppm) is close to the peak of the histogram, indicating the most frequent value range. *In Chromium (Cr) concentration histogram (n=100): Mean = 213.7 ppm, Median = 189.8 ppm, Mode = 204.2 ppm (*Figure 6.80*).*

Cobalt (Co)

Cobalt shows a pronounced right-skewed distribution. The vast majority of samples are at very low values and a few samples (max ~98.98 ppm) produce a long tail. This yields a mean (6.73 ppm) well above the median (4.22 ppm). The KDE curve emphasizes this shape, smoothly tracing the main peak at low ppm and the extended tail. The mode (0.5 ppm) again reflects a cluster at the detection limit. *In Cobalt (Co) concentration histogram (n=100): Mean = 6.73 ppm, Median = 4.22 ppm, Mode = 0.5 ppm (*Figure 6.81*).*

Tungsten (W)

Tungsten concentrations are extremely skewed: nearly all samples are at 0.5–1 ppm (mode at 0.5 ppm) and only a very few are higher (maximum ~127.41 ppm). The mean (4.11 ppm) far exceeds the median (2.46 ppm). The KDE overlay highlights the single large peak at the low end and the sparse data in the tail. *In Tungsten (W) concentration histogram (n=100): Mean = 4.11 ppm, Median = 2.46 ppm, Mode = 0.5 ppm (*Figure 6.82*).*

Molybdenum (Mo)

Molybdenum distribution is also highly skewed right. A few samples have very high Mo (max ~142.75 ppm) while most are low. The KDE (red) smooths between bins, showing the main peak at low ppm and a long right tail. Mean (18.80 ppm) is much greater than median (3.62 ppm), reflecting the heavy tail; mode at 0.5 ppm (detection limit) again indicates many low-end values. *In Molybdenum (Mo) concentration histogram (n=100): Mean = 18.8 ppm, Median = 3.62 ppm, Mode = 0.5 ppm (*Figure 6.83*).*

Copper (Cu)

Copper concentrations show a strong right skew. Most samples are at very low Cu (many at 0.5 ppm, the detection limit), with a few very high values (max ~436.18 ppm). The KDE curve follows the same overall pattern as the histogram but without its jagged bins. This yields a mean (40.99 ppm) far above the median (3.33 ppm). The mode is 0.5 ppm (detection limit), indicating that the most common value is the lowest measurable Cu. *In Copper (Cu) concentration histogram (n=100): Mean = 41.0 ppm, Median = 3.33 ppm, Mode = 0.5 ppm (*Figure 6.84*).*

Zinc (Zn)

Zinc exhibits one of the strongest skewness. The histogram peak is at the low end (~2–86 ppm), but a few samples reach very high Zn (max ~1690 ppm), creating a long tail. The KDE overlay clearly shows one large peak at the low concentrations and a stretched tail toward higher values. The mean (80.95 ppm) far exceeds the median (46.16 ppm), confirming heavy right skew. The mode (16.63 ppm) is near the lower end where most data cluster. *In Zinc (Zn) concentration histogram (n=100): Mean = 80.95 ppm, Median = 46.16 ppm, Mode = 16.6 ppm (*Figure 6.85*).*

Lead (Pb)

Lead concentration data are strongly right-skewed. Many samples are at the detection limit (0.5 ppm) or low tens of ppm, but a few outliers reach ~296.46 ppm. The KDE (red line) follows the main peak at low ppm and smooths the long tail. The mean (26.68 ppm) is much higher than the median (14.11 ppm). The mode is 0.5 ppm, again highlighting the frequent occurrence

of the minimum value. *In Lead (Pb) concentration histogram (n=100): Mean = 26.7 ppm, Median = 14.1 ppm, Mode = 0.5 ppm (*Figure 6.86*).*

Antimony (Sb)

Antimony shows a somewhat different pattern: while 23 samples are at 0.5 ppm, many others cluster around ~15–25 ppm (the histogram's main peak). This bimodal-like appearance (one cluster at the limit, one around 20 ppm) yields a median (16.97 ppm) slightly above the mean (13.62 ppm). The KDE overlay reveals the strong low-end peak and the broader feature near ~20 ppm. The mode (0.5 ppm) reflects the detection-limit cluster, but the histogram shows the most samples are in the 15–25 ppm range. *In Antimony (Sb) concentration histogram (n=100): Mean = 13.6 ppm, Median = 17.0 ppm, Mode = 0.5 ppm (*Figure 6.87*).*

Lanthanum (La)

Lanthanum (a rare-earth element) is moderately skewed. The histogram has a single main peak around 15–30 ppm with a tail to higher values (max ~78.02 ppm). The KDE smooth curve captures this main peak smoothly. The mean (25.69 ppm) slightly exceeds the median (22.87 ppm), indicating modest right skew. The mode (0.5 ppm, detection limit) is technically the highest bar, but most data are between ~15–25 ppm. *In Lanthanum (La) concentration histogram (n=100): Mean = 25.7 ppm, Median = 22.9 ppm, Mode = 0.5 ppm (*Figure 6.88*).*

Cerium (Ce)

Cerium is similarly skewed. Most Ce concentrations lie in the 30–50 ppm range, but a few samples go up to ~132.46 ppm. The KDE overlay again shows one main smooth peak and the high-end tail. The mean (44.58 ppm) is slightly above the median (40.80 ppm). The mode (0.5 ppm, detection limit) indicates many low-level occurrences, but the distribution is concentrated around ~40–45 ppm. *In Cerium (Ce) concentration histogram (n=100): Mean = 44.6 ppm, Median = 40.8 ppm, Mode = 0.5 ppm (*Figure 6.89*).*

Praseodymium (Pr)

Praseodymium (Pr) shows a moderately skewed distribution. The main bulk of data is around 3–7 ppm, with a maximum of ~17.86 ppm. The KDE curve highlights a single peak in the lower range. The mean (5.86 ppm) is above the median (5.06 ppm). The mode (0.5 ppm) reflects that several samples are at the detection limit, but most data cluster around 5–6 ppm. *In Praseodymium (Pr) concentration histogram (n=100): Mean = 5.86 ppm, Median = 5.06 ppm, Mode = 0.5 ppm (*Figure 6.90*).*

Neodymium (Nd)

Neodymium (Nd) is right-skewed. Its concentrations cluster around 10–30 ppm with some extending up to ~77.88 ppm. The KDE (red) captures one primary peak and a right-hand tail. Mean (21.53 ppm) is higher than the median (18.63 ppm), indicating skewness. The mode (0.5 ppm) again shows many low-limit values, but the bulk of data is around 15–20 ppm. *In Neodymium (Nd) concentration histogram (n=100): Mean = 21.53 ppm, Median = 18.63 ppm, Mode = 0.5 ppm (*Figure 6.91*).*

Thulium (Tm)

Thulium concentrations are heavily clustered at the low end. Most samples (85 of 100) are at 0.5 ppm, with only a few higher (max ~2.52 ppm). This yields a distribution almost degenerate at 0.5 ppm. The KDE overlay shows a sharp peak at the minimum and tiny values beyond. The mean (0.585 ppm) is slightly above the median (0.5 ppm). Mode is 0.5 ppm, reflecting the overwhelming low-end cluster. *In Thulium (Tm) concentration histogram (n=100): Mean = 0.585 ppm, Median = 0.5 ppm, Mode = 0.5 ppm (*Figure 6.92*).*

Ytterbium (Yb)

Ytterbium is also heavily skewed low. Most samples are around 0.5–3 ppm, with a maximum ~17.85 ppm. The KDE highlights a strong low-end peak and a long tail (on the log scale). The mean (2.33 ppm) is above the median (1.54 ppm). The mode (0.5 ppm) indicates many values at the detection limit. *In Ytterbium (Yb) concentration histogram (n=100): Mean = 2.33 ppm, Median = 1.54 ppm, Mode = 0.5 ppm (*Figure 6.93*).*

Yttrium (Y)

Yttrium concentrations are right-skewed. Most values lie between 5–25 ppm, but a few go up to ~178.54 ppm, creating a long tail. The KDE shows one large low-concentration peak and a stretched tail. The mean (23.30 ppm) significantly exceeds the median (16.23 ppm). The mode (0.5 ppm) indicates the many samples at the detection limit, but most data cluster around ~10–20 ppm. *In Yttrium (Y) concentration histogram (n=100): Mean = 23.30 ppm, Median = 16.23 ppm, Mode = 0.5 ppm (*Figure 6.94*).*

Sulfur (S)

Sulfur is unusual: most samples are very low (mode = 0.01 ppm) with a few higher readings (max ~5.33 %). The distribution is extremely skewed; the KDE shows a sharp peak at near-zero and a long tail. Because only 28 samples had measurable S (the rest are missing), the caption notes n=28. The mean (0.309 %) is much higher than the median (0.04 %). *In Sulphur (S) concentration histogram (n=28): Mean = 0.31 %, Median = 0.04 %, Mode = 0.01 % (*Figure 6.95*).*

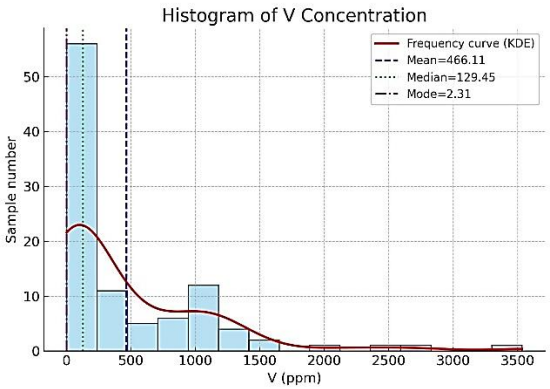

Figure 6.78: Histogram of V concentration (ppm) with frequency curve.

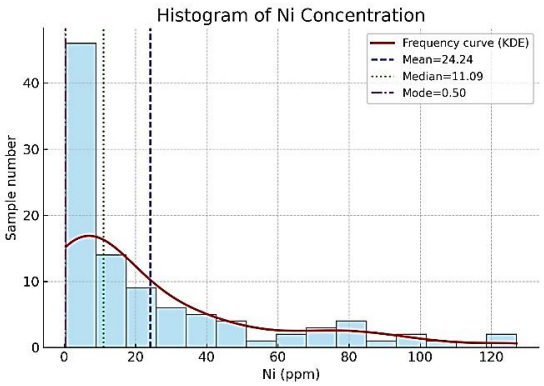

Figure 6.79: Histogram of Ni concentration (ppm) with frequency curve.

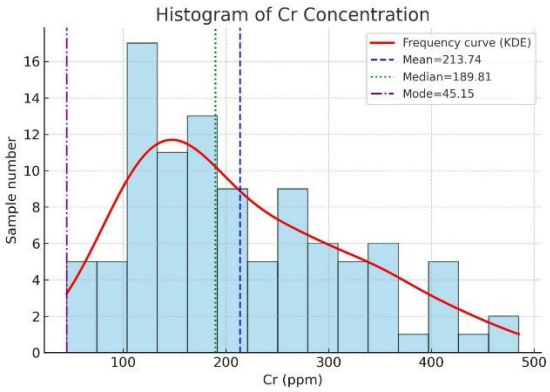

Figure 6.80: Histogram of Cr concentration (ppm) with frequency curve.

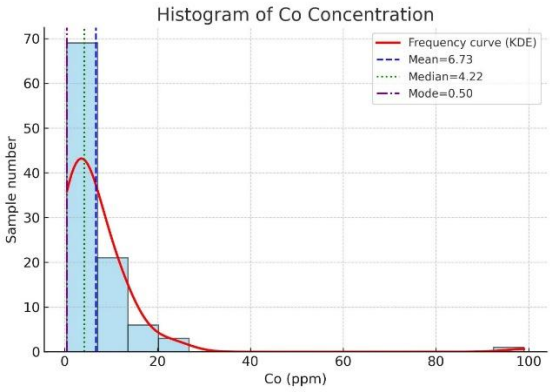

Figure 6.81: Histogram of Co concentration (ppm) with frequency curve

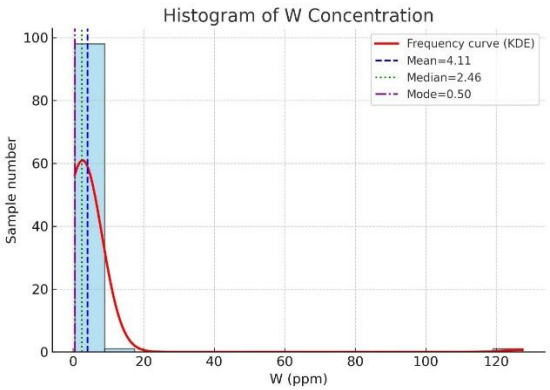

Figure 6.82: Histogram of W concentration (ppm) with frequency curve.

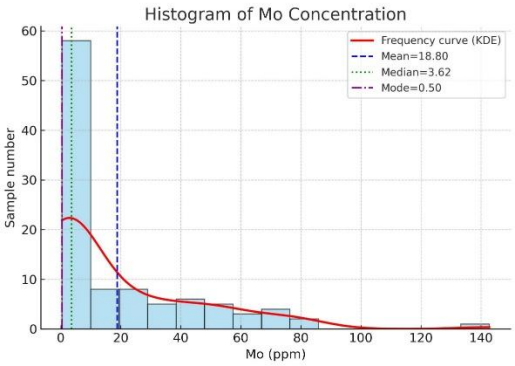

Figure 6.83: Histogram of Mo concentration (ppm) with frequency curve.

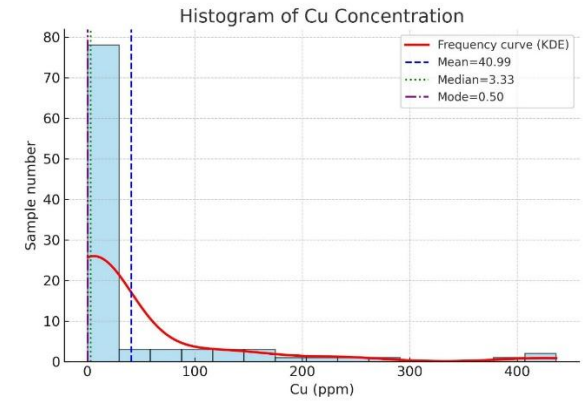

Figure 6.84: Histogram of Cu concentration (ppm) with frequency curve.

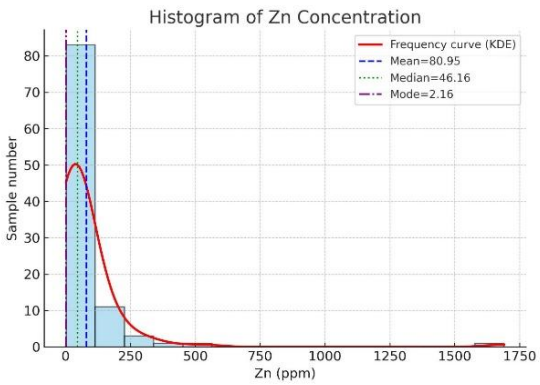

Figure 6.85: Histogram of Zn concentration (ppm) with frequency curve.

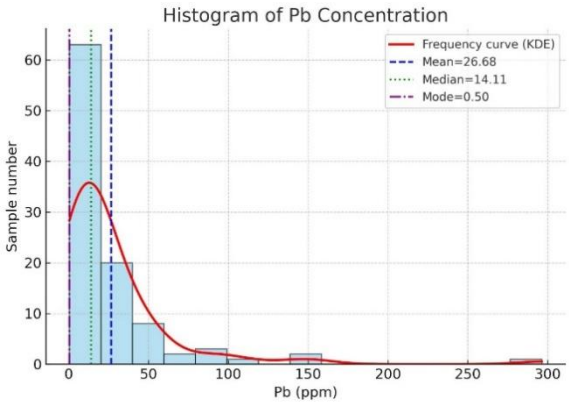

Figure 6.86: Histogram of Pb concentration (ppm) with frequency curve.

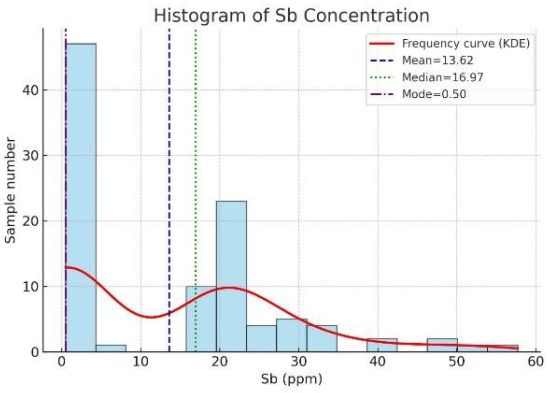

Figure 6.87: Histogram of Sb concentration (ppm) with frequency curve.

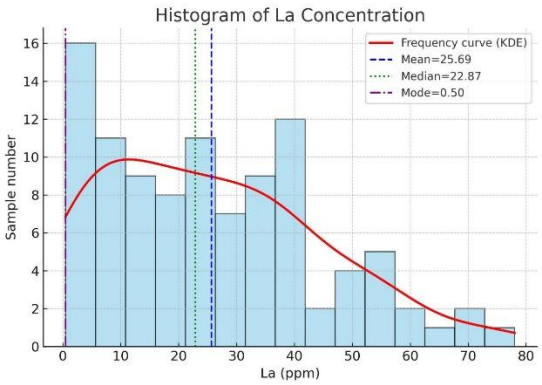

Figure 6.88: Histogram of La concentration (ppm) with frequency curve

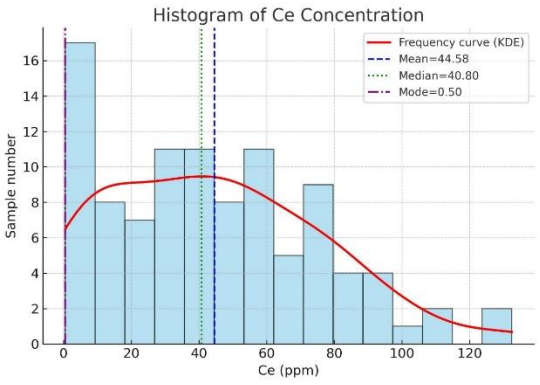

Figure 6.89: Histogram of Ce concentration (ppm) with frequency curve

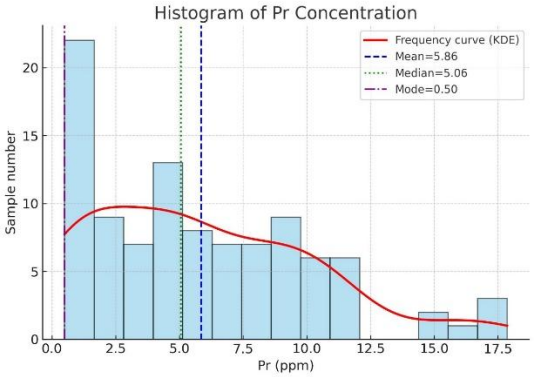

Figure 6.90: Histogram of Pr concentration (ppm) with frequency curve.

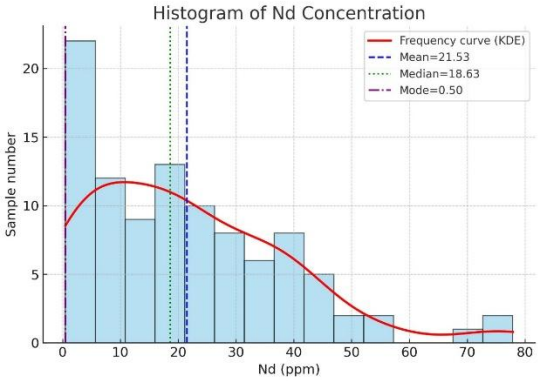

Figure 6.91: Histogram of Nd concentration (ppm) with frequency curve.

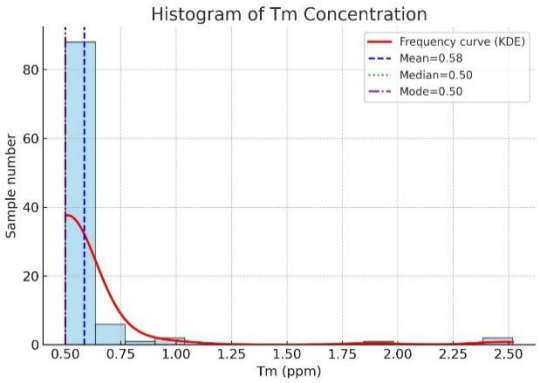

Figure 6.92: Histogram of Tm concentration (ppm) with frequency curve.

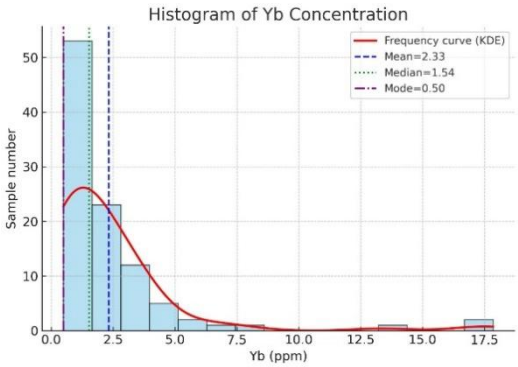

Figure 6.93: Histogram of Yb concentration (ppm) with frequency curve.

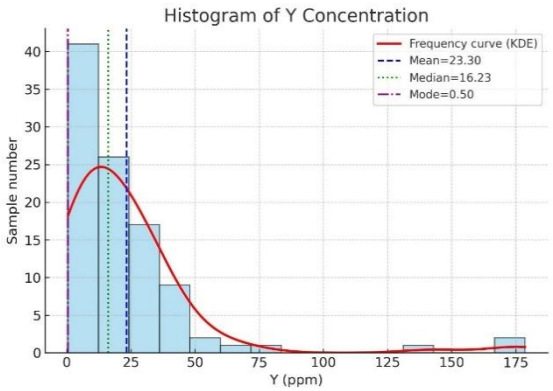

Figure 6.94: Histogram of Y concentration (ppm) with frequency curve.

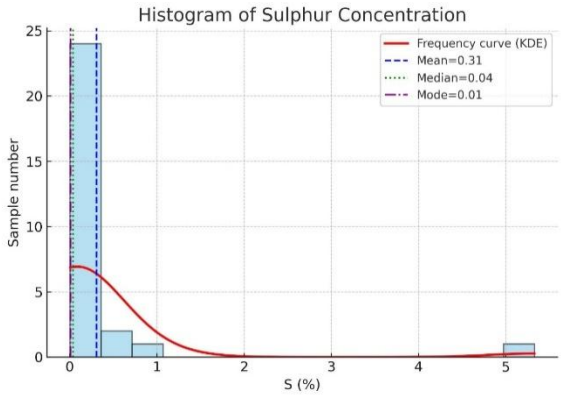

Figure 6.95: Histogram of Sulphur concentration (%) with frequency curve.

6.6.4 Proximate Analysis:

A total of 57 surface samples were analyzed for proximate analysis to evaluate the graphite potential of the study area based on Fixed Carbon (FC) content. The analyzed samples show FC values ranging from 0.82% to **7.05%**, with an average FC content of 3.84%.

Out of the total analyzed 57 samples, 51 samples (89.47%) recorded more than 2% FC, which is considered the indicative cut-off value for graphite mineralization in the area. Further, 23 samples (40.35%) yielded more than 4% FC, indicating comparatively good graphite concentration and favorable graphite mineralization potential.

The proximate analysis results suggest widespread occurrence of graphitic material within the investigated zones, with several samples exhibiting moderate to good fixed carbon values suitable for further detailed exploration and evaluation (Figure 6.96, Figure 6.97).

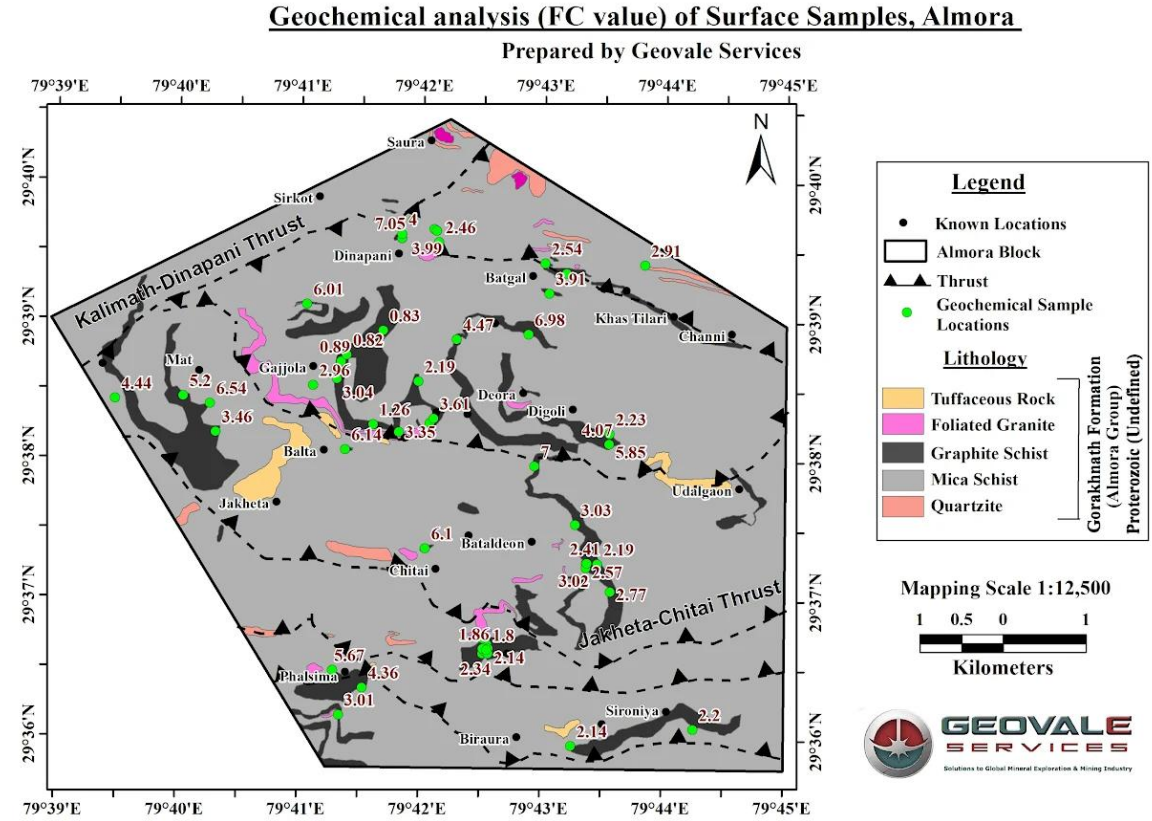

Figure 6.96:Fixed Carbon value in percentange all over the Almora G4 Block

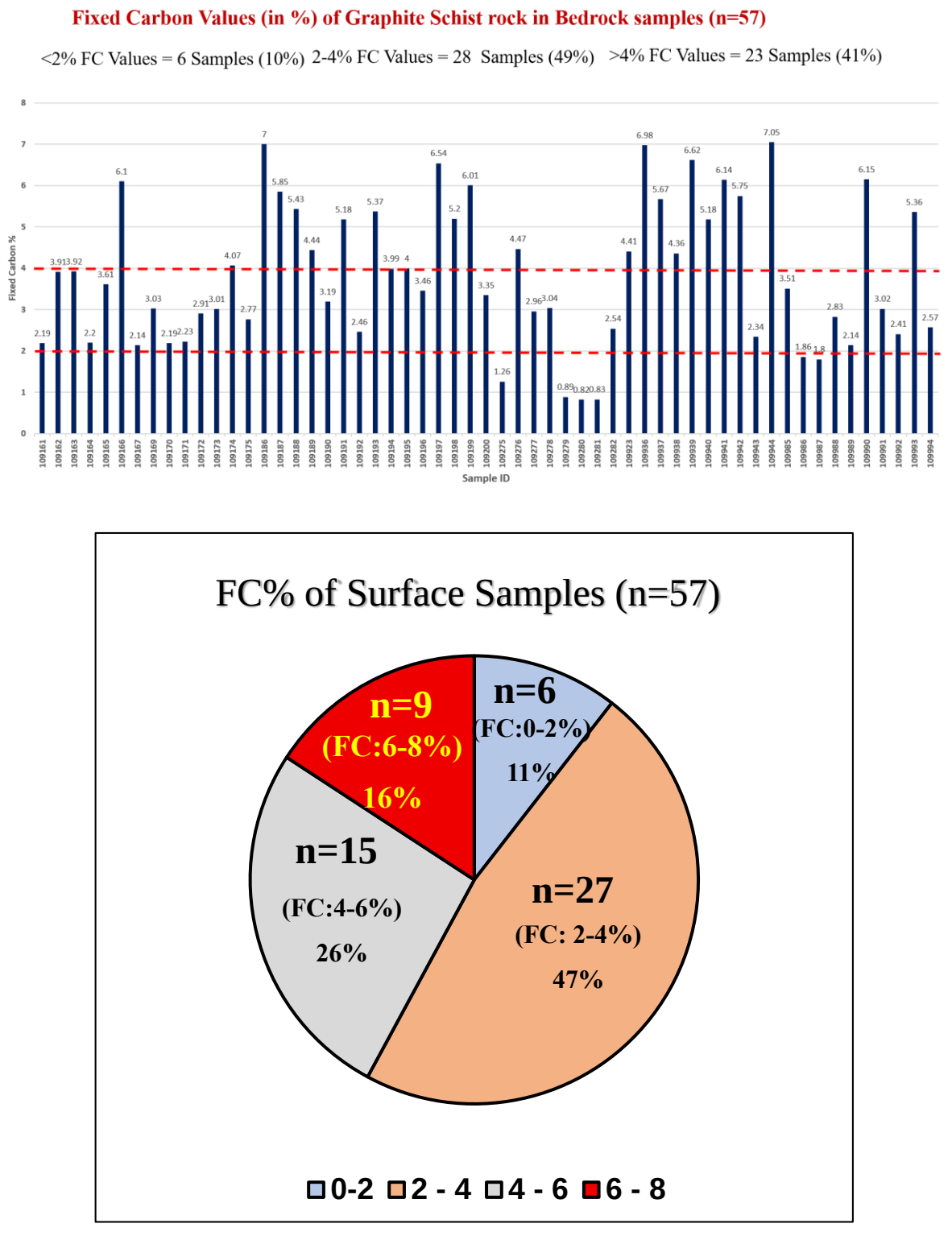

Figure 6.97: Graphical representation of FC values for graphite schist as bedrock samples.

6.6.5 RamanAnalysis:

Raman spectroscopy has been carried out for 10 samples (02- BR, 08- Drill core) in Almora G4 block. (Table 6.5)

a) 109938: (Surface sample, collected from Falshima area**)** It characterized by a sharp G band at 1579–1580 cm^{-1}, accompanied by a distinct D band at 1354–1361 cm^{-1}, a clear shoulder / D′ band at 1619–1623 cm^{-1} and a strong second-order 2D band at 2717–2729 cm^{-1}. In addition, smaller low-wave number peaks around 261, 413, 463 and 701 cm^{-1} indicate the presence of associated gangue/mineral phases within the graphite-bearing matrix. It is more characteristic of vein-type or structurally recrystallized crystalline graphite.

b) 110004: (Surface sample, collected from Digoli area**)** It dominated by a sharp G band at 1565–1577 cm^{-1}, associated with smaller D bands at 1355–1363 cm^{-1} and strong second-order 2D bands at 2697–2718 cm^{-1}. Compared with sample 109938, the D′ shoulder near 1620 cm^{-1} is weak to absent, indicating relatively lower lattice disorder in most analysed spots. Minor low-wavenumber peaks around 202, 263, 462 and 702 cm^{-1} suggest limited gangue contribution. Overall, this spectral assemblage indicates comparatively more ordered and texturally more uniform crystalline graphite and is more indicative of massive graphite to massive flaky graphite.

c) 114231: (Borehole 03 at 15.2 m depth) The sharp Raman peak at 1577–1580 cm^{-1}, accompanied by shoulder peaks at 1618–1621 cm^{-1}, smaller peaks at 1353–1354 cm^{-1} and second-order peaks at 2721–2727 cm^{-1}, is characteristic of vein-type graphite. In contrast, a sharp peak at ~1570 cm^{-1}, along with smaller peaks at ~1354 cm^{-1} and second-order peaks around 2705 cm^{-1}, is indicative of massive graphite.

d) 114228: (Borehole 05 at 23.5 m depth) The Raman peak at 1578–1579 cm^{-1}, accompanied by shoulder peaks at 1619–1621 cm^{-1}, smaller peaks at 1353–1354 cm^{-1} and second-order peaks at 2712 2725 cm^{-1}, is characteristic of vein-type graphite.

e) 114241: (Borehole 01 at 91.3 m depth) The Raman peak at 1576–1578 cm^{-1}, with weak shoulder features, accompanied by smaller peaks at 1353–1362 cm^{-1} and second-order peaks at 2721–2725 cm^{-1}, is characteristic of vein-type graphite. A Raman peak at ~1577 cm^{-1}, along with smaller peaks at ~1359 cm^{-1} and second-order peaks at ~2719 cm^{-1}, is indicative of massive graphite. A Raman peak at ~1577 cm^{-1}, associated with smaller peaks at ~1345 cm^{-1} and ~2726 cm^{-1}, represents poorly crystalline graphite.

f) 114237: (Borehole 01 at 18.4 m depth) The Raman peak at ~1578 cm^{-1}, with shoulder features, accompanied by smaller peaks at ~1352 cm^{-1} and second-order peaks at ~2714 cm^{-1}, is characteristic of vein-type graphite. Raman peaks at 1573–1576 cm^{-1}, along with smaller

peaks at 1355–1359 cm^{-1} and second-order peaks at 2698–2721 cm^{-1}, are indicative of massive graphite.

g) 114232: (Borehole 03 at 27.9 m depth) The Raman peak at ~1580 cm^{-1}, with shoulder peaks at 1619–1621 cm^{-1}, accompanied by smaller peaks at 1354–1357 cm^{-1} and second-order peaks at 2715–2725 cm^{-1}, is characteristic of vein-type graphite. Raman peaks at ~348 cm^{-1} and ~383 cm^{-1} are indicative of pyrite.

h) 114229: (Borehole 05 at 32.3 m depth) The Raman peak at 1579–1580 cm^{-1}, with shoulder peaks at 1620–1623 cm^{-1}, accompanied by smaller peaks at 1351–1355 cm^{-1} and second-order peaks at 2717 2726 cm^{-1}, is characteristic of vein-type graphite. A Raman peak at ~1579 cm^{-1}, along with smaller peaks at ~1356 cm^{-1} and second-order peaks at ~2714 cm^{-1}, is indicative of massive graphite.

i) 114227: (Borehole 10 at 24.8 m depth) Raman peaks at 1576–1578 cm^{-1}, accompanied by smaller peaks at ~1343 cm^{-1} and second-order peaks at 2718–2721 cm^{-1}, are indicative of poorly crystalline graphite. A Raman peak at ~1577 cm^{-1}, with smaller peaks at ~1339 cm^{-1} and ~2722 cm^{-1}, also represents poorly crystalline graphite. Raman peaks at ~1351 cm^{-1} and ~1593 cm^{-1} indicate the presence of amorphous carbon.

j) 114234: (Borehole 02 at 36 m depth) The Raman peak at ~1579 cm^{-1}, with a shoulder feature, accompanied by smaller peaks at ~1355 cm^{-1} and second-order peaks at ~2726 cm^{-1}, is characteristic of vein-type graphite. A Raman peak at ~1591 cm^{-1}, along with smaller peaks at ~1352 cm^{-1}, is indicative of amorphous carbon. A Raman peak at ~1577 cm^{-1}, associated with a smaller peak at ~610 cm^{-1}, also represents amorphous carbon.

Single LRS peaks at 1580–1581 cm^{-1} are indicative of the flaky/massive nature of graphite (Neubeck et. al. 2020). Raman peaks at 1580–1581 cm^{-1}, accompanied by shoulder peaks at 1618–1624 cm^{-1} and smaller peaks at 1348–1355 cm^{-1}, are characteristic of vein-type graphite. The representative samples contain small disseminated specks of graphite (both massive and vein types) within amorphous carbon.

Table 6.5: Details of Raman sample location

S. no	Sample Id	Latitude	Longitude	Remarks
1	110004	29.636403	79.723705	Digoli Village
2	109938	29.605957	79.692265	Falshima Village
3	114231	29.609816	79.709241	BH-03, 15.2 m
4	114228	29.64173	79.66583	BH-05, 23.5 m
5	114241	29.63673	79.72611	BH-01, 91.3 m
6	114227	29.6131	79.71863	BH-10, 24.8 m
7	114229	29.64173	79.66583	BH-05, 32.3 m

S. no	Sample Id	Latitude	Longitude	Remarks
8	114232	29.609816	79.709241	BH-03, 27.9 m
9	114234	29.61886	79.72608	BH-02, 36 m
10	114237	29.63673	79.72611	BH-01, 18.4 m

6.6.6 XRD data analyses and interpretation:

XRD has been carried out for 10 samples (05- BR, 05- Drill core) in Almora G4 block.

a) Sample 1099999: The X-ray diffraction (XRD) analysis (Figure 6.98) of surface sample 109999 at Bataldeon area, indicates that Muscovite is the dominant mineral phase in the sample, as evidenced by its strong and well-defined reflections at 9.82 Å, 4.94 Å and a particularly intense peak at 3.30 Å. Quartz is identified as a significant secondary phase, with characteristic diffraction peaks observed at 4.23 Å, 3.34 Å, 2.12 Å, 1.81 Å and 1.37 Å. Graphite 2H is also present and is notably responsible for an overlapping reflection with Quartz at approximately 3.34 Å, indicating the coexistence of both phases contributing to the same diffraction position. Additionally, Rectorite is confirmed through diagnostic reflections at 11.84 Å and 2.97 Å, along with a weak contribution at 1.31 Å. The diffraction pattern exhibits sharp, high-intensity peaks with a maximum count rate of approximately 110,000 counts, suggesting that the sample is highly crystalline. Overall, the mineral assemblage reflects a complex, phyllosilicate-rich system dominated by Muscovite with subordinate Quartz, Graphite 2H and Rectorite, indicative of specific geological formation conditions or subsequent alteration processes.

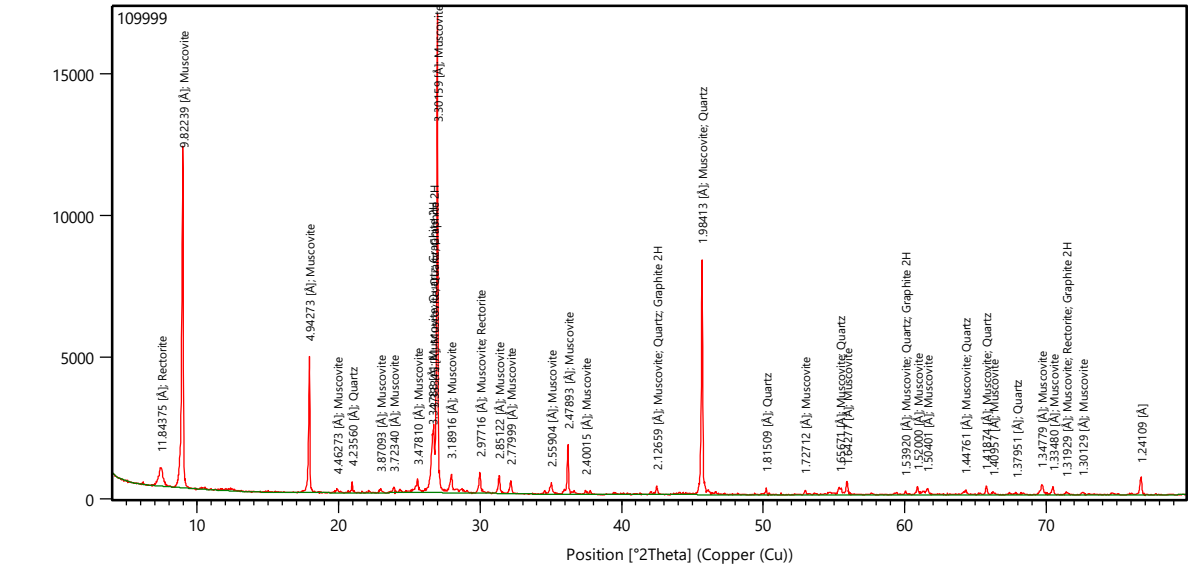

Figure 6.98: XRD spectrum of graphite schist (Sample Id 109999)

The presence of Rectorite is significant as it is a mixed-layer clay mineral (chlorite–smectite type) that typically forms under specific diagenetic to low-grade metamorphic conditions, indicating chemical alteration processes and variable environmental conditions during rock evolution. Its occurrence suggests a transitional mineralogical environment and provides insight into the degree of alteration and fluid interaction experienced by the host rock. The diffraction pattern exhibits sharp, high-intensity peaks with a maximum count rate of approximately 110,000 counts, suggesting that the sample is highly crystalline. Rectorite is a mixed-layer clay mineral with useful physical and chemical properties such as high surface area, ion-exchange capacity and layered structure, which make it valuable in several applications. It is widely used in ceramics and refractory materials to improve plasticity and thermal stability. In environmental applications, rectorite is used as an adsorbent for removing heavy metals and organic pollutants from wastewater due to its strong ion-exchange behavior. It is also applied in drilling mud formulations in the petroleum industry, where it helps control viscosity and fluid loss. Additionally, rectorite is used as a filler and reinforcing material in polymer nanocomposites, improving mechanical strength, thermal resistance and barrier properties. In some cases, it also serves as a catalyst support material in chemical processes.

b) Sample 109938: The X-ray diffraction (XRD) analysis (Figure 6.99) of the surface sample 109938 at Phalsima area, reveals a highly crystalline material characterized by sharp and intense diffraction peaks. Muscovite is identified as the dominant mineral phase, with characteristic reflections observed at 9.90 Å, 4.96 Å, 2.56 Å and 1.50 Å and a particularly strong peak at 3.33 Å, which represents the most intense reflection in the pattern. Quartz is present as a secondary phase, with diagnostic peaks at 4.25 Å, 2.45 Å, 2.28 Å and 1.82 Å. Notably, the strongest Quartz reflection at 3.33 Å overlaps with the primary Muscovite peak, indicating that both minerals contribute to this diffraction position. The diffraction pattern exhibits a high maximum intensity of approximately 109,938 counts and the sharpness of the peaks confirms that the sample is well-crystallised. The coexistence of Muscovite and Quartz suggests a phyllosilicate-rich composition, typical of metamorphic rocks such as mica-schist. Overall, the analysis indicates that the sample is predominantly composed of Muscovite with a significant contribution from Quartz, reflecting a relatively simple and well-defined mineralogical assemblage.

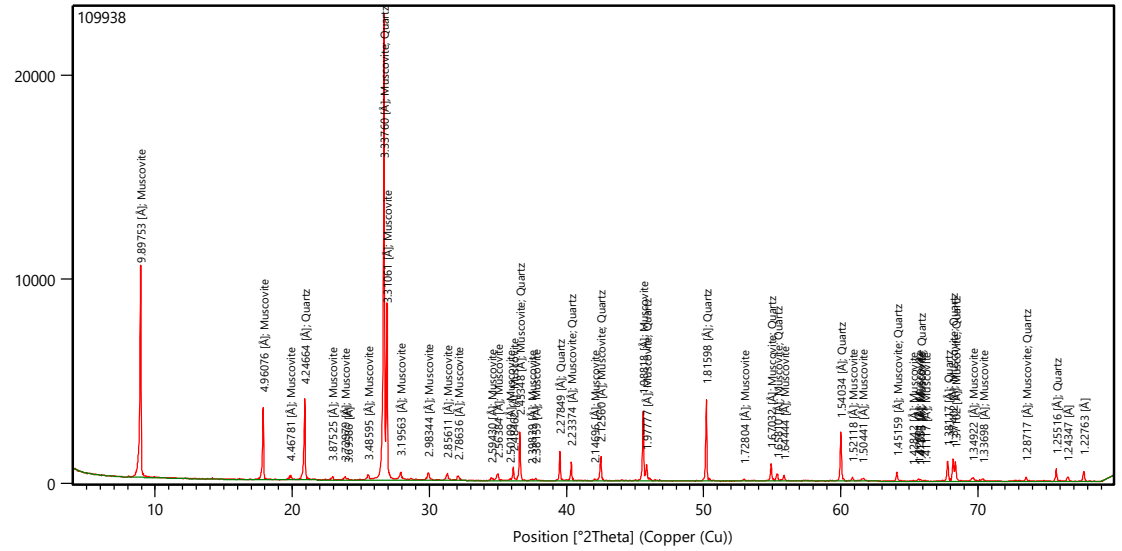

Figure 6.99: XRD spectrum of graphite schist (Sample Id: 109938)

c) Sample 110004: The X-ray diffraction (XRD) analysis (Figure 6.100) of surface sample 110004 at Digoli area, indicates that the sample is a well-crystallised multi-phase material, as evidenced by the presence of sharp and high-intensity reflections in the diffraction pattern. Muscovite is identified as the dominant mineral phase, with characteristic peaks at 9.90 Å, 4.96 Å and 4.47 Å and a particularly strong reflection at 3.31 Å, which represents the most intense peak in the pattern. Quartz is present as a secondary phase, with diagnostic reflections observed at 4.25 Å, 2.45 Å and 1.82 Å. Notably, the primary Quartz reflection at approximately 3.34 Å overlaps with the Muscovite peak in the same region, indicating the contribution of both mineral phases to this diffraction position. The diffraction pattern exhibits a high maximum intensity of approximately 110,004 counts, confirming a high degree of crystallinity. The sharpness and narrowness of the peaks suggest relatively large crystallite sizes and minimal lattice strain within the sample. The coexistence of Muscovite and Quartz is characteristic of silicate-rich metamorphic or igneous materials, indicating a well-defined mineralogical composition dominated by these two phases, with no significant presence of additional mineral.

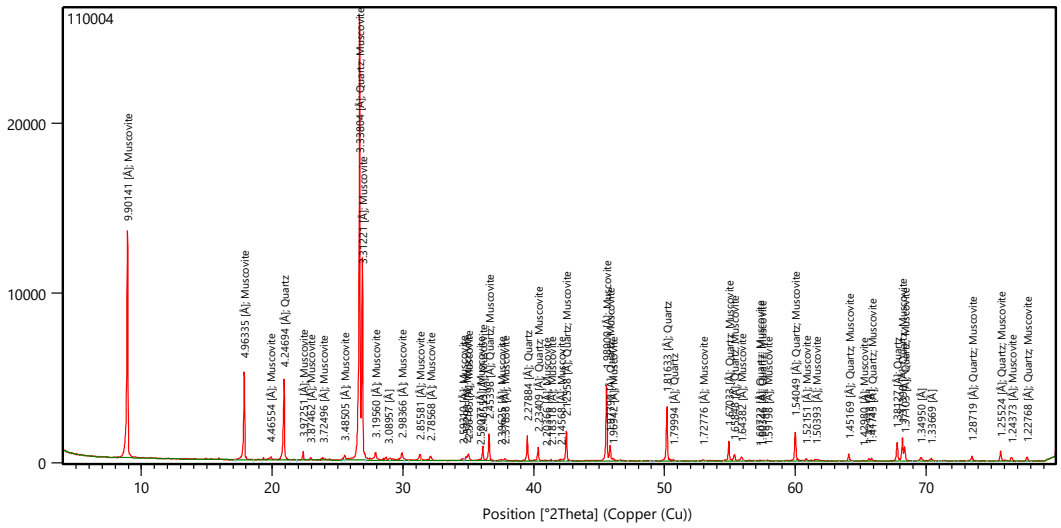

Figure 6.100: XRD spectrum of graphite schist (Sample Id: 110004)

d) Sample 110001: The X-ray diffraction (XRD) analysis (Figure 6.101) of surface sample 110001 at Gajjola area, reveals that the sample is a highly crystalline multi-phase material, as indicated by the presence of sharp and well-defined diffraction peaks. Muscovite is identified as the dominant mineral phase, exhibiting strong reflections at 9.87 Å, 4.95 Å and 1.99 Å, with its most intense peak occurring at 3.34 Å. This reflection overlaps with contributions from other mineral phases present in the sample. Clinochlore is clearly recognized by its characteristic low-angle reflections at 14.06 Å and 7.13 Å, along with a prominent peak at 3.54 Å, confirming its presence as a significant constituent. Quartz is identified as a secondary phase, with diagnostic reflections at 4.23 Å and 1.81 Å and its primary peak at 3.34 Å contributing to the major overlapping reflection in the pattern. Additionally, Graphite 2H is detected through its reflections at 3.34 Å and 1.81 Å, further contributing to peak overlap and indicating the coexistence of multiple phases. The diffraction pattern exhibits a high maximum intensity of approximately 110,001 counts, confirming a high degree of crystallinity, while the sharpness of the peaks suggests well-ordered crystal structures with minimal lattice strain. The mineral assemblage of Muscovite, Clinochlore and Quartz is characteristic of chlorite–muscovite schists or similar metamorphic rocks and the presence of Graphite 2H suggests carbon-rich formation conditions. The analysis confirms that the sample is a complex multi-phase system dominated by Muscovite, with significant contributions from Clinochlore and Quartz and a minor but notable presence of Graphite 2H.

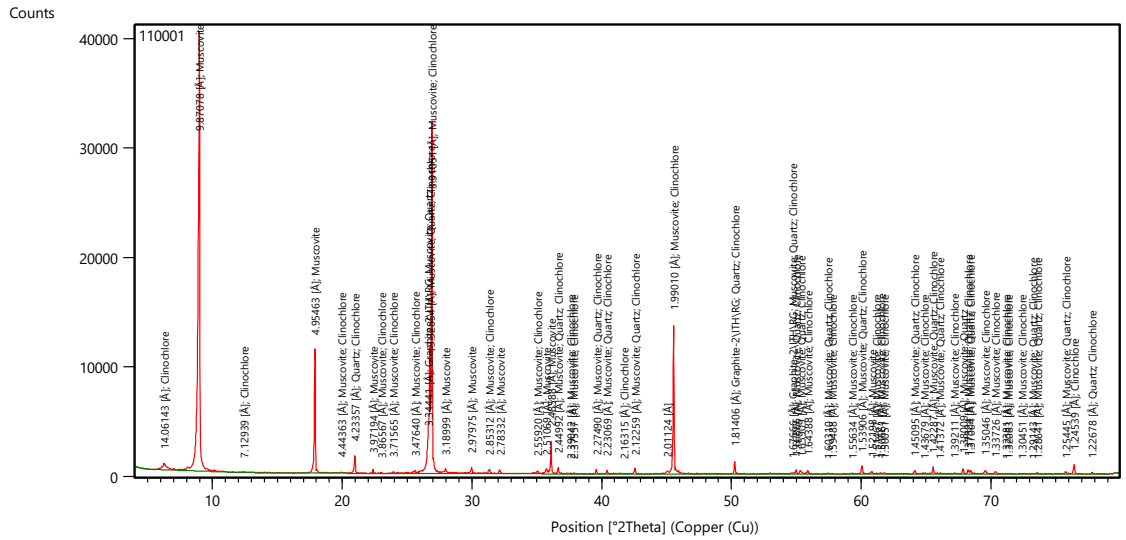

Figure 6.101: XRD spectrum of graphite schist (Sample Id: 110001)

e) Sample 109923: The X-ray diffraction (XRD) analysis (Figure 6.102) of surface sample 109923 at Sirar area, indicates that the sample is a well-crystallised material, as evidenced by the presence of sharp and high-intensity reflections in the diffraction pattern. Muscovite is identified as the dominant mineral phase, with characteristic peaks at 9.91 Å, 4.96 Å and 4.48 Å and a particularly strong reflection at 3.34 Å, which represents the most intense peak in the pattern. Quartz is present as a secondary phase, with diagnostic reflections observed at 4.26 Å, 1.82 Å and 1.54 Å. Notably, the primary Quartz reflection at 3.34 Å overlaps with the dominant Muscovite peak, indicating that both mineral phases contribute to the highest intensity observed in the diffraction pattern. The maximum intensity reaches approximately 109,923 counts, confirming a high degree of crystallinity, while the sharp and narrow peaks suggest relatively large crystallite sizes and a stable crystal structure. The coexistence of Muscovite and Quartz is characteristic of silicate-rich metamorphic or igneous rocks, such as mica-schists, indicating a well-defined mineralogical composition dominated by these two phases with no significant presence of additional minerals.

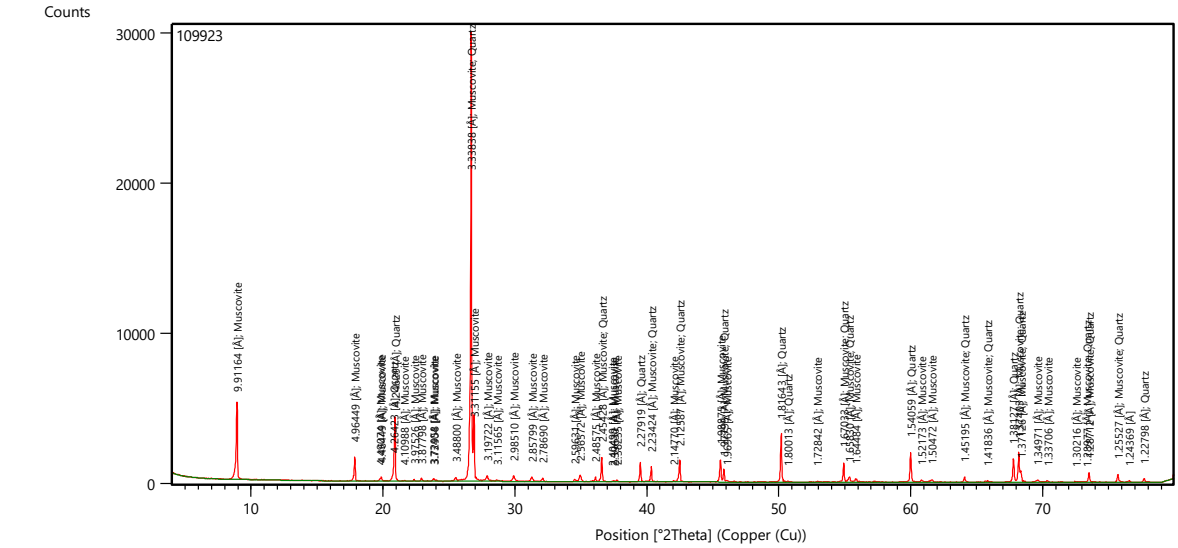

Figure 6.102: XRD spectrum of graphite schist (Sample Id: 109923)

f) Sample 114229 (Figure 6.103) was taken from borehole 05 at 32.3 m depth, in Mat area reveals a sample heavily dominated by Quartz, which accounts for approximately 90.00% of the mineralogical composition. The diffractogram shows a high-intensity primary peak for Quartz reaching nearly 20,000 counts at a position of roughly 26.6° 2θ. In addition to Quartz, the sample contains a minor amount of Muscovite (~08.00%) and a small fraction of Pyrite (~02.00%).

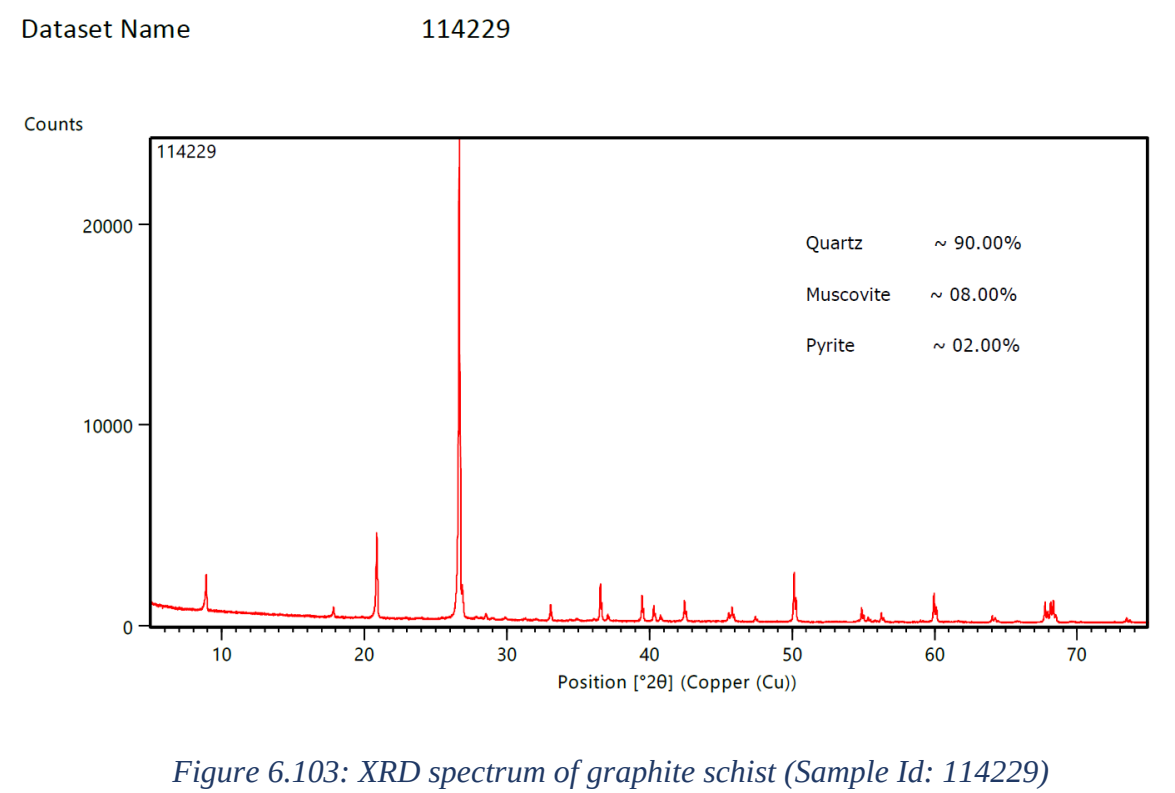

Figure 6.103: XRD spectrum of graphite schist (Sample Id: 114229)

g) Sample 114232 (Figure 6.104), was taken from borehole 03 at 27.9 m depth, in Sirar area indicates a significant presence of Quartz at ~75.00%, although this represents a decrease in silica content compared to the previous sample. There is a notable increase in Muscovite, which constitutes 20.00% of the sample, accompanied by a small increase in Pyrite to ~05.00%. The primary Quartz peak in the graph remains prominent, with an intensity exceeding 15,000 counts.

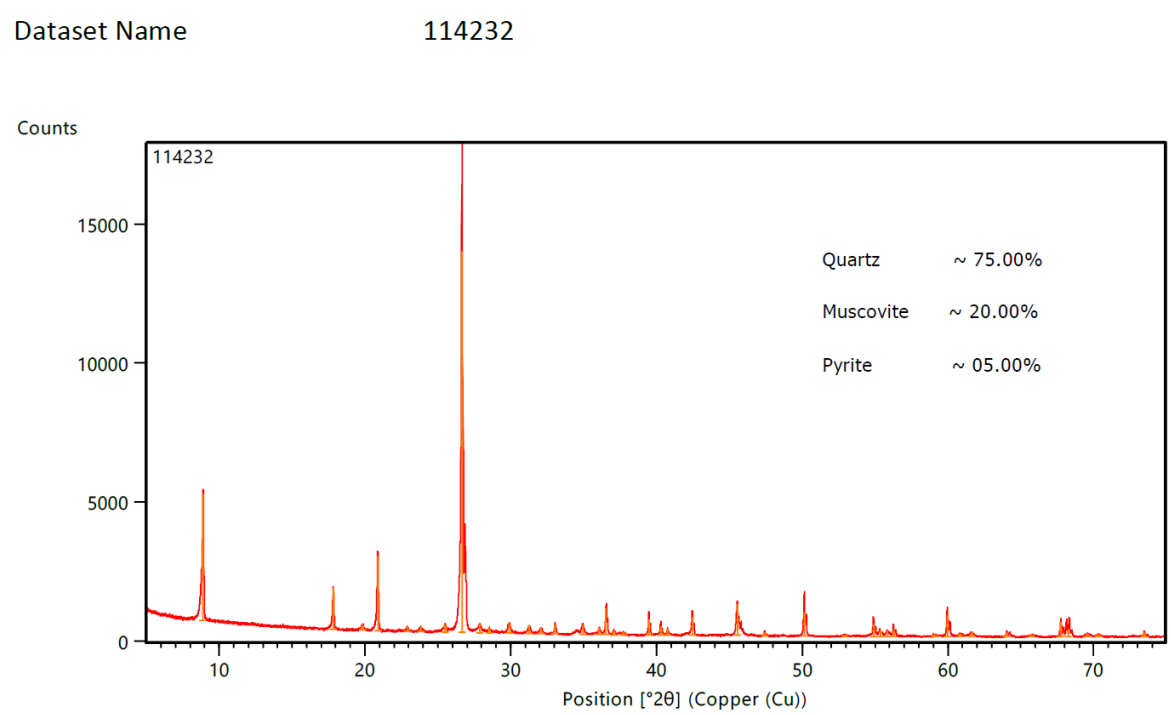

Figure 6.104: XRD spectrum of graphite schist (Sample Id: 114232)

h) Sample 114233 (Figure 6.105), was taken from borehole 03 at 73 m depth, in Sirar area represents the most siliceous sample in the group, with Quartz comprising approximately 95.00% of the total mineral content. The corresponding XRD graph displays an exceptionally high-intensity peak for Quartz. Trace amounts of Muscovite (~04.00%) are present and this is the only sample in the set where Fluorite was detected, although in a very small quantity of ~01.00%.

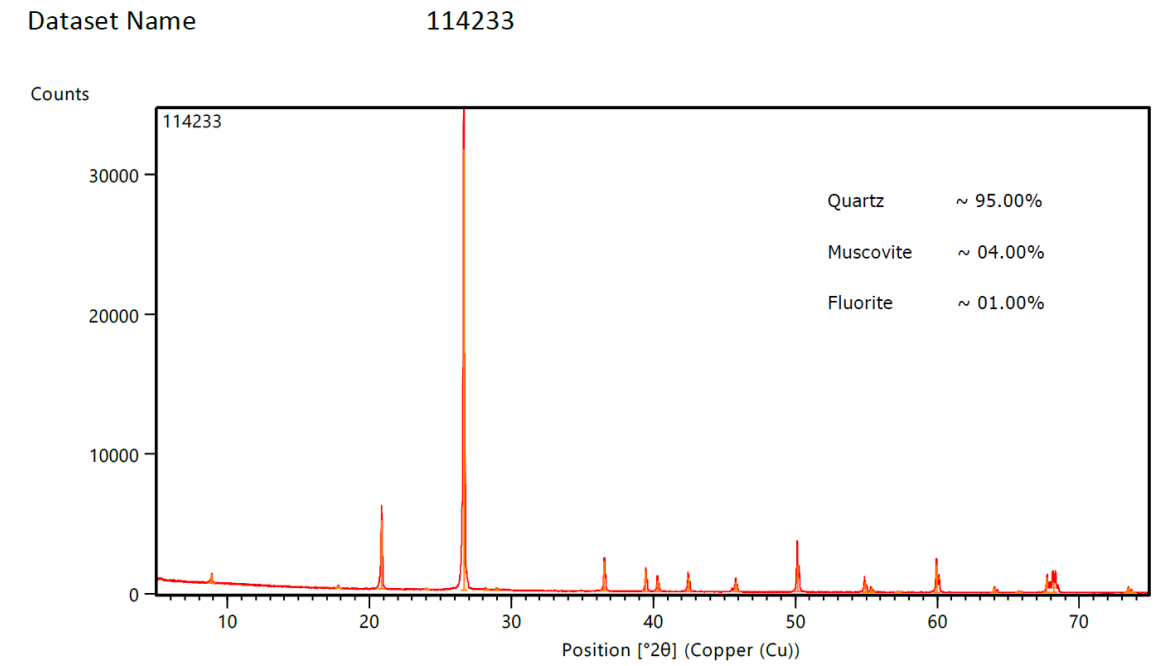

Figure 6.105: XRD spectrum of graphite schist (Sample Id: 114233)

i) Sample 114235 (Figure 6.106), was taken from borehole 02 at 24.3 m depth, in Sirar area the mineralogical profile shows 65.00% Quartz and a substantial 33.00% Muscovite. The diffractogram clearly illustrates the increased presence of Muscovite with a distinct peak at approximately 8.8° 2θ, while the primary Quartz peak remains the most intense at over 15,000 counts. This sample is unique in the series for containing a small trace of Sphalerite (~02.00%).

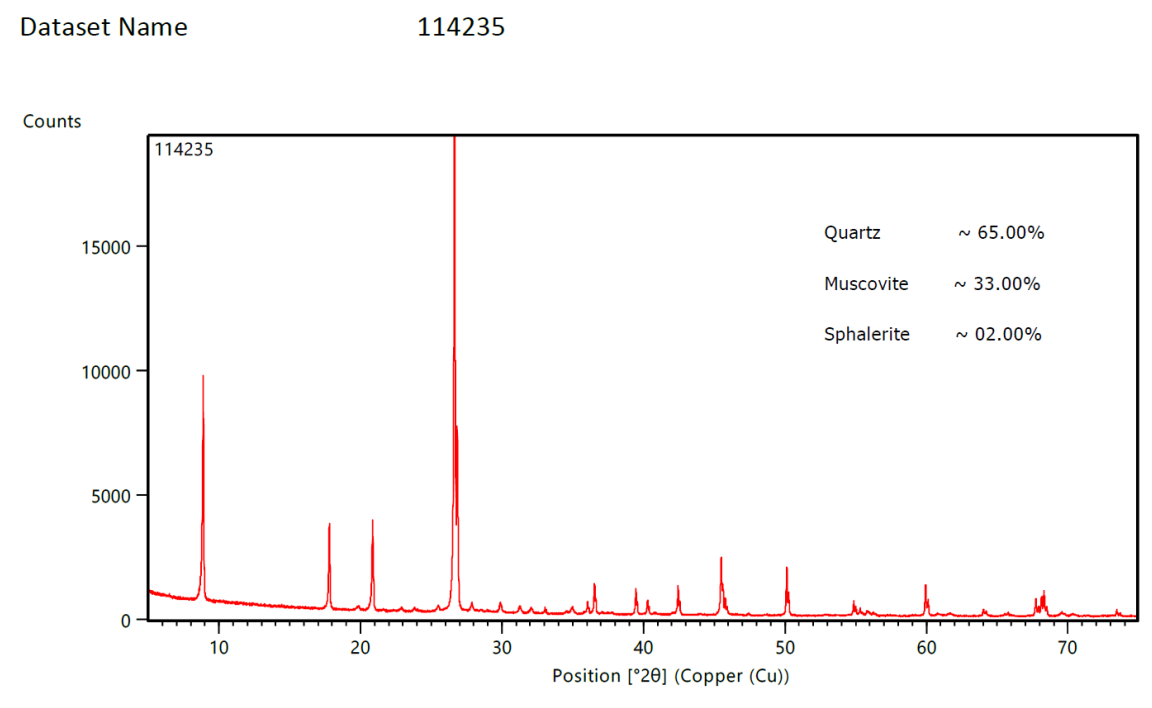

Figure 6.106: XRD spectrum of graphite schist (Sample Id: 114235)

j) Sample 114239 (Figure 6.107), was taken from borehole 01 at 64.6 m depth, in Sirar area is the most mineralogically diverse sample, featuring the lowest Quartz concentration at 45.00%. It contains a nearly equal amount of Muscovite at 40.00%, which is reflected in the graph where the Muscovite peak at ~8.8° 2θ is comparable in height to the Quartz peak. This sample is further distinguished by a significant Albite content of ~13.00% and a minor amount of Calcite (~02.00%), with the overall peak intensities being lower than the other samples, peaking at approximately 8,000 counts.

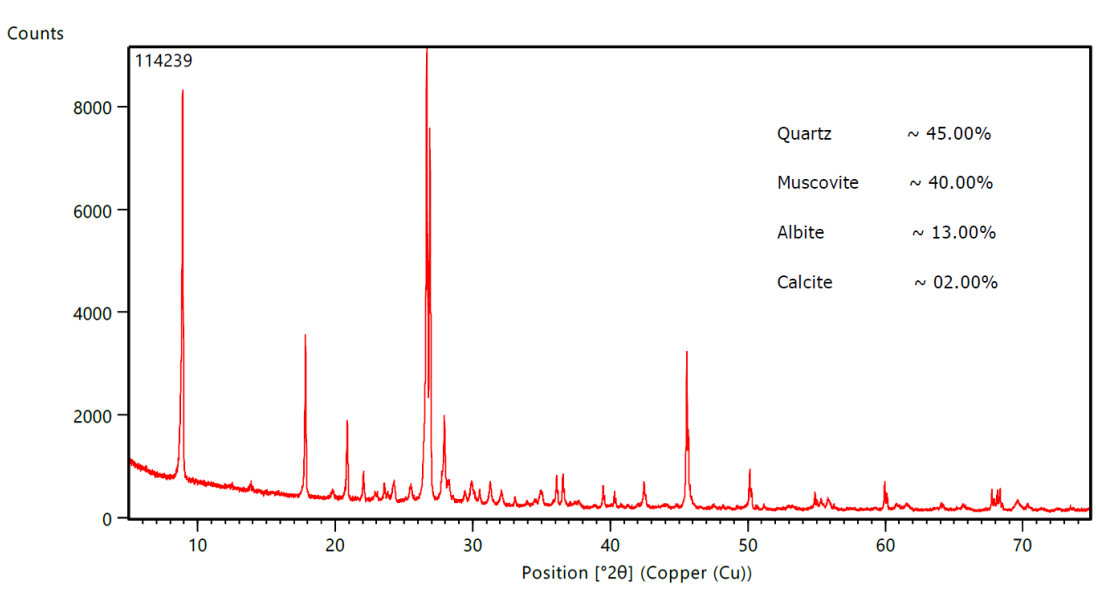

Figure 6.107: XRD spectrum of graphite schist (Sample Id: 114239)

Significance of XRD:

The XRD interpretations from the above analyses collectively indicate that the samples are dominated by muscovite with consistent occurrences of quartz and, in some cases, accessory minerals such as clinochlore, graphite and rectorite. This mineral assemblage is characteristic of silicate-rich metamorphic environments, particularly mica-schists and related lithologies, which are commonly associated with regional metamorphism and hydrothermal alteration processes. The dominance of muscovite suggests potassium-rich conditions and potential alteration of feldspathic precursor rocks, while quartz indicates silica saturation and stability under a wide range of geological conditions. The presence of clinochlore points to low- to medium-grade metamorphism, whereas rectorite signifies transitional clay mineral formation

and fluid–rock interaction during diagenesis or alteration. Graphite, when present, is particularly significant as it reflects carbon-rich conditions and may indicate organic matter transformation under metamorphic environments. From an economic and ore-deposit perspective, such mineral assemblages are important indicators of hydrothermal systems and metamorphic fluid activity, which are often associated with the formation of economically valuable deposits such as gold, base metals and industrial minerals. Additionally, muscovite- and quartz-rich rocks themselves may have industrial applications, including use in ceramics, fillers and refractory materials. Overall, the mineralogical composition provides valuable insight into the geological history, physicochemical conditions of formation and potential economic significance of the studied material.

Rectorite, though often present as minor or accessory phases in XRD analyses, carry significant geological and economic importance. Rectorite is a mixed-layer clay mineral typically formed under conditions of diagenesis to low-grade metamorphism and is indicative of active fluid–rock interaction and chemical alteration processes. Its presence suggests transitional environmental conditions, often associated with hydrothermal systems or weathering of aluminosilicate minerals. From an industrial perspective, rectorite is valued for its swelling behavior, ion-exchange capacity and adsorption properties, making it useful in ceramics, drilling fluids, environmental remediation and as a component in nanocomposite materials.

Graphite, on the other hand, is a highly significant mineral both geologically and economically. Its occurrence indicates carbon-rich conditions, often derived from the metamorphism of organic matter or precipitation from carbon-bearing fluids. In ore deposit studies, graphite can act as a pathfinder mineral, suggesting reducing environments that are favorable for the deposition of certain metals, including gold. Industrially, graphite is extremely valuable due to its excellent electrical conductivity, thermal stability and lubricating properties. It is widely used in electrodes, batteries (especially lithium-ion batteries), refractories, lubricants and advanced materials. Therefore, the presence of rectorite and graphite not only provides insight into the formation conditions of the sample but also enhances its potential economic and industrial significance.

Chapter 7

Exploration Data Analysis

7 Exploration Data Analysis: Characterisation of Graphite Blocks:

The distribution of graphite mineralization in the area is mainly tectonically controlled, with graphite bands occurring either along these thrust planes or in the intervening zones between two thrusts. Based on their spatial association with thrust structures, clustering of band in the specific area, the graphite blocks have been classified into five (05) distinct blocks. i) Digoli-Gajjola Graphite Block present between Batgal-Channi and Bintola-Udalgaon thrusts, ii) Sirar-Bataldeon Graphite Block associated with the Phalsima–Sironiya, Bintola–Udalgaon and Jakheta-Chitai thrusts, iii) Kalimath Graphite Block is aligned with the Kalimath-Dinapani thrust, iv) Phalsima-Pithauni Graphite Block lies between the Biraura–Pithauni and Phalsima–Sironiya thrusts and v) Batgal-Channi Graphite Block occurs along the Batgal–Channi thrust (Figure 7.1).

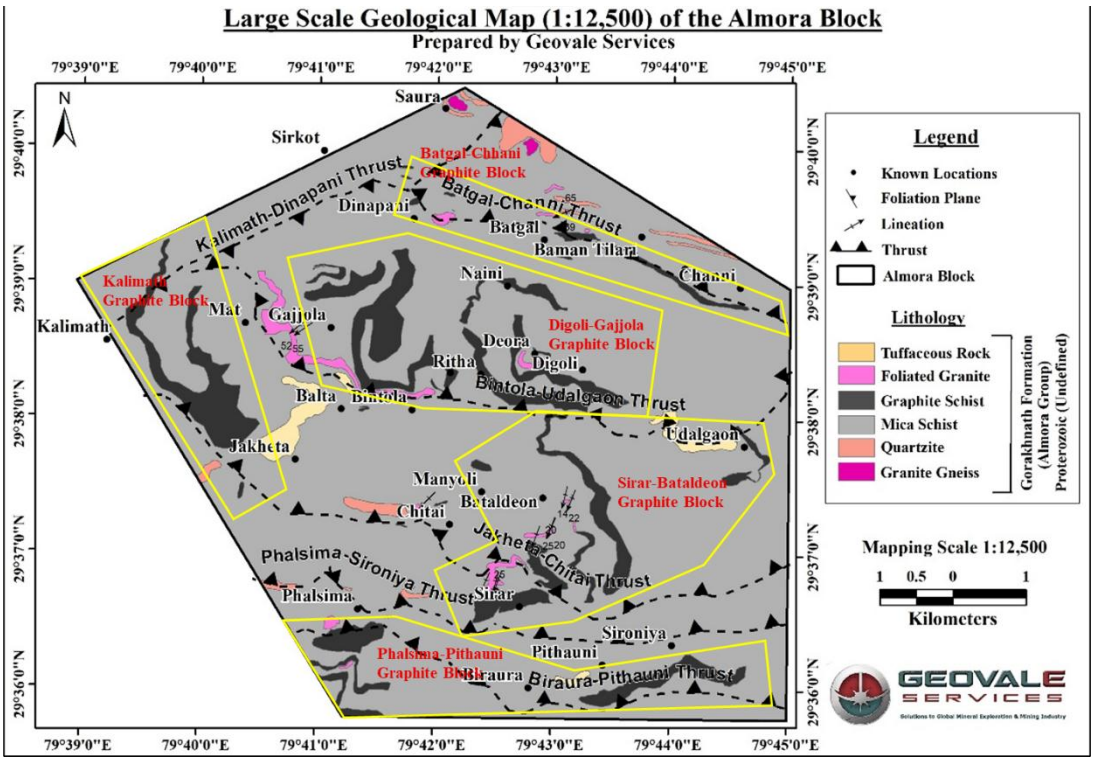

Figure 7.1: Geological map showing spatial distribution of five (05) graphite blocks, Almora.

7.1 Digoli-Gajjola Graphite Block, Almora

7.1.1 Site Characteristics

The Digoli–Gajjola graphite block (Table 7.1) is situated in the northern part of the Almora G4 block and bounded by the Bintola–Udalgaon and Batgal–Channi thrust systems. The Bintola block has eight discontinuous bands distributed across western Digoli, central transition zones and the eastern Bintola–Naini sector. The area is accessible via NH-309B, although last-mile connectivity remains limited and may require infrastructure development for exploration activities. (Figure 7.2)

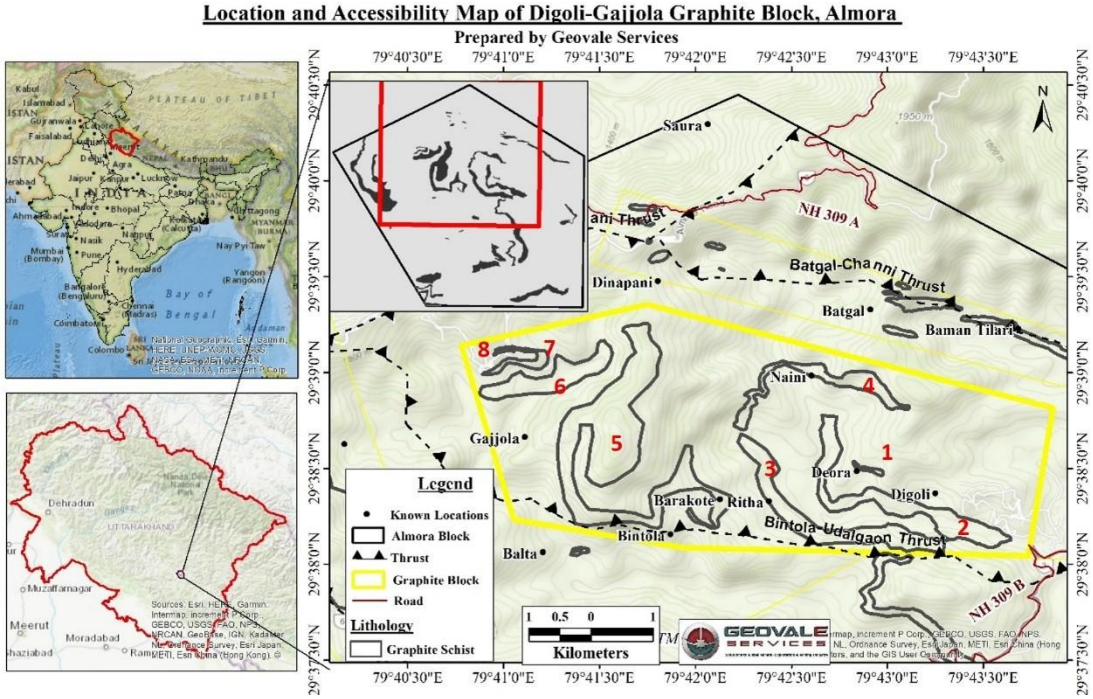

Figure 7.2: Accessibity map of the Digoli-Gajjola Graphite Block.

The terrain ranges from approximately 1000 m to 1700 m RL and is characterized by moderate to steep slopes, typical of a dissected Lesser Himalayan hill-slope environment.

Water availability is relatively favourable due to the presence of the perennial Mahadeo Gad river, which can support both field operations and potential processing needs. The region is characterized by forest cover in parts, particularly in Pharhkanaula to the south and Matena to the west, along with scattered pine vegetation, which may impose regulatory constraints on exploration. The drainage system ranges from 1st to 4th order streams, reflecting moderate dissection of the terrain. Topographically, the area transitions from piedmont zones to younger alluvial plains, interspersed with hilly slopes, resulting in elevations ranging between 1000 and

1700 meters. Slopes vary from moderate to steep, influencing both accessibility and the stability of exploration sites, while habitation remains low, reducing immediate socio-environmental conflicts but necessitating logistical planning for workforce accommodation. (Figure 7.3, Figure 7.4, Figure 7.5, Figure 7.6)

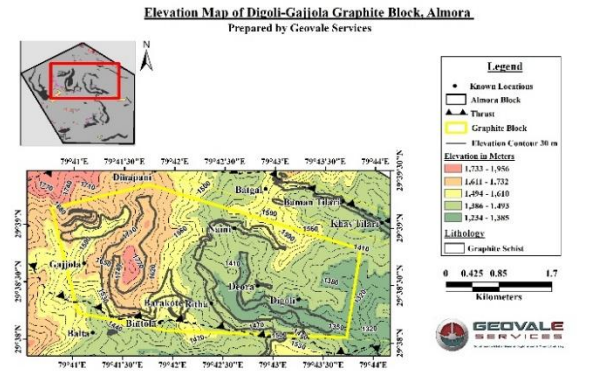

Figure 7.3: Elevation map of the Digoli-Gajjola Graphite Block

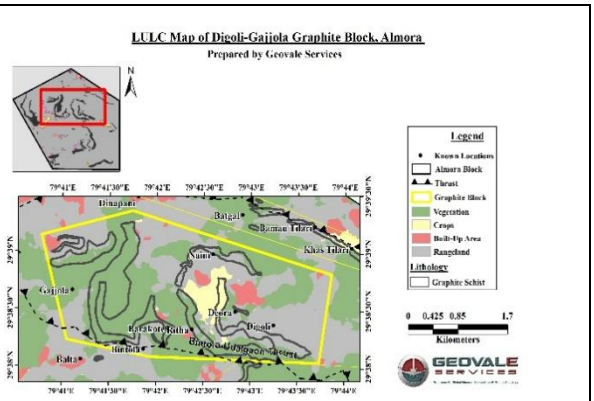

Figure 7.4: LULC map Digoli-Gajjola Graphite Block

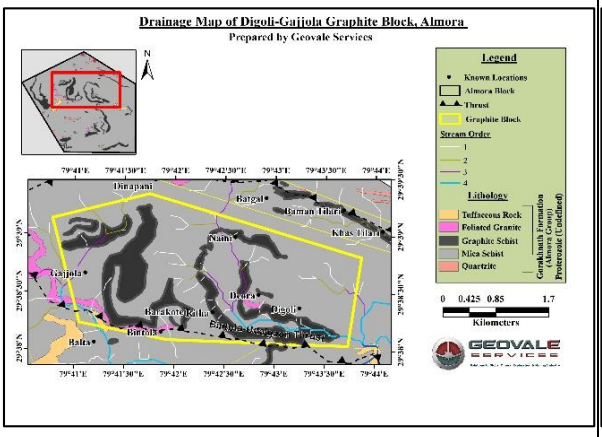

Figure 7.5: Drainage map of the Digoli-Gajjola Graphite Block

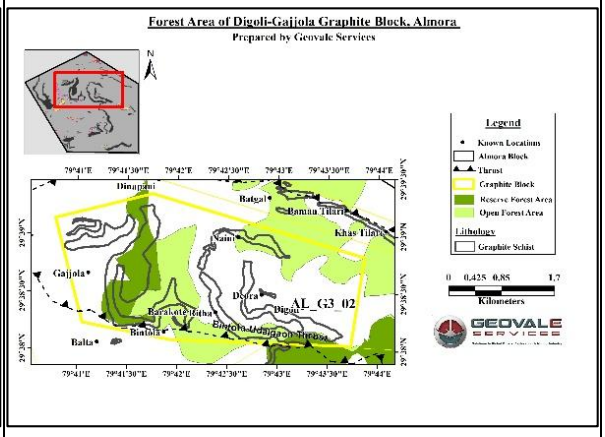

Figure 7.6: Forest map of the Digoli-Gajjola Graphite Block

Table 7.1: Summary of site characteristics of the Digoli-Gajjola Graphite block

Parameter	Block-specific interpretation
Regional access	Approached from NH-309B
Water availability	Mahadeo Gad river / perennial water sources.
Forest / vegetation	Mixed vegetation and rangeland; southern Pharhkanaula RF and western Matena RF; scattered pine forest.
Drainage	1st- to 4th-order drainage network
Topography	Piedmont to younger alluvial lower surfaces bordered by moderate-to-steep hill slopes and ridges.
Habitation	Low overall, but rural land-use interaction remains relevant for future drilling and trenching.
Elevation	Approximately 1,000-1,700 m RL.

7.1.2 Geological and Resource Characterization (Graphite and Vanadium)

The Digoli–Gajjola graphite block lies between the Bintola–Udalgaon and Batgal–Channi thrusts and graphite schist is associated with quartzite, graphite schist and mica-schist assemblages, with localized influence from deformed granitic intrusions that may enhance graphitization. Structurally, the graphite horizons are strongly governed by thrusting, folding and wrapping, resulting in significant variability in orientation. Foliation in graphite schist and other associated rock type indicates a wide range of strikes (005°–170°) and predominantly low to moderate dips (8°–30°). This variability reflects a folded and thrust-flat ramp geometry.

Thickness and continuity:

The Digoli-Gajjola graphite block is characterised by eight distinct graphite bands that display significant variation in strike continuity and geometric disposition. Among these, Graphite Band-1 (1.86 km long and 0.0903 km width), Band-2 (~0.28 km long and 0.0321 km wider), where Band-3 (~2.21 km long and ~0.158 km wider) represents the longest and most laterally persistent unit. Band-4 (~2.027 km long and ~0.2931 wider), Band-5 (0.578 km long and ~0.0603 km wider), Band-6 (~1.17 km long and ~0.1769 km wider), Band-7 further reflects

structural complexity, as it is divided into two limbs with separate strike lengths, suggesting deformation of the same graphitic horizon rather than independent bodies where 0.060 km and 0.025 km across two limbs, Band-8 (~0.17 km long and ~0.0117 km wider).

Band-1 and Band-6 are indicating that graphite mineralization is not uniformly distributed but concentrated along the structurally favourable zones. In contrast, shorter bands such as Band-2 and Band-8 are reflected more localized or lensoidal occurrences, likely controlled by folding and segmentation within the thrust regime, where Band-8 is extremely thin and lensoidal.

7.1.3 Geophysical analyses of Digoli-Gajjola graphite bands:

VES and SP was carried out in the Graphite Bands 2 to 8 (Table 7.2).

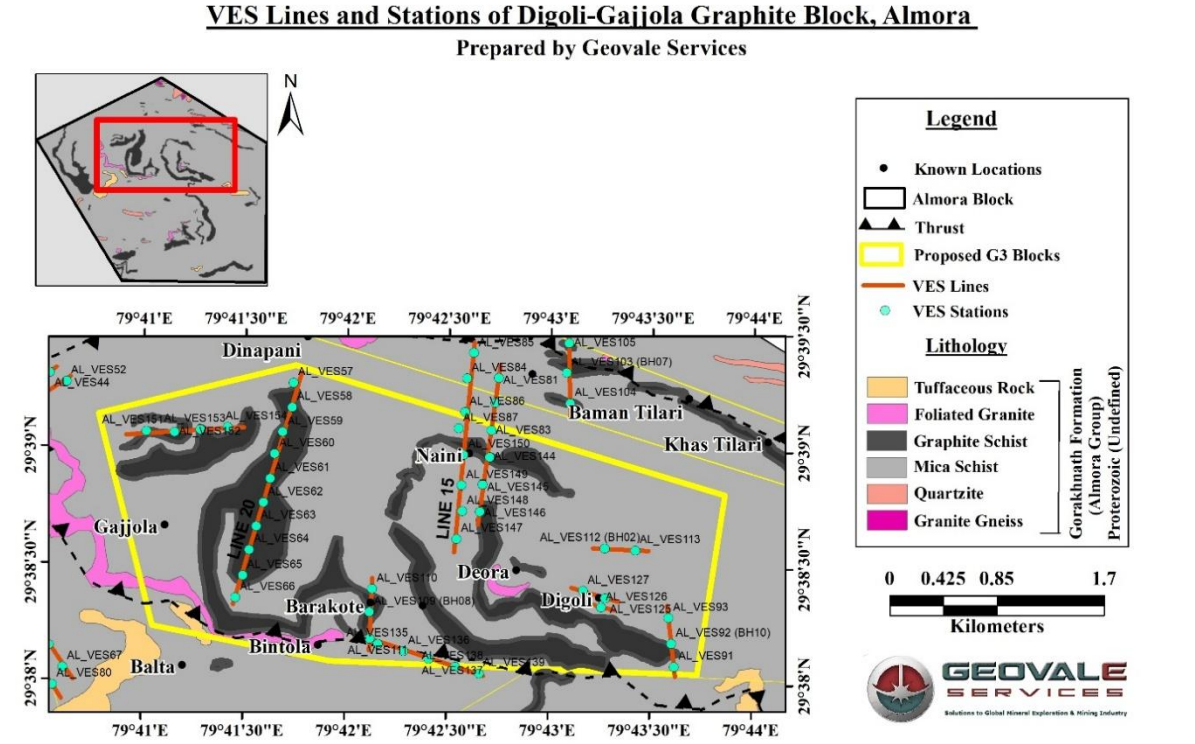

Figure 7.7: Details of VES survey at the Digoli-Gajjola Graphite Block.

Vertical Electrical Sounding (VES):

A total of three VES profile lines (Line 11, Line 12 and Line 24) were carried out in the area to investigate subsurface resistivity distribution and delineate possible mineralized zones (Figure 7.7).

Line 11: Only VES-12 was conducted along this profile line. The interpreted data indicates a comparatively conductive subsurface zone, showing resistivity values ranging from 230–270 ohm·m at depth about 30 m from surface (Figure 7.8).

Line 12: Two VES stations (VES-125 and VES-127) were completed along this line. Both stations exhibit high resistivity values exceeding 700–1200 ohm·m, suggesting the presence of compact, resistive lithologies such as fresh bedrock or mica schist lithologies.

Line 24: Three VES stations (VES-91, VES-92 and VES-93) were conducted along Line 24. All stations show high resistivity values ranging between 400–1300 ohm·m, indicating dominantly resistive subsurface conditions.

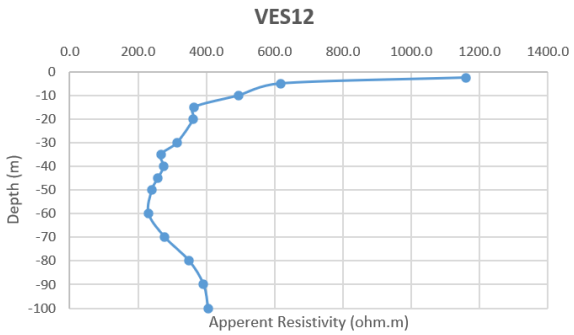

Figure 7.8: VES 12 Profile showing low resistive zone

Self Potential (SP):

Two SP Profiles (Line 01, 02) were carried out in the area.

Line 01: The SP profile exhibits partialy positive potential values and partial negative value reaching up to −303 mV is observed at specific locations along the profile. Such localized negative SP responses generally indicate the presence of conductive subsurface zones, which may be related to graphite mineralization and/or sulphide concentration (Figure 7.9).

Line 02: The SP profile predominantly exhibits positive potential values along most parts of the survey line. However, a localized negative anomaly reaching up to −503 mV is recorded at specific locations along the profile (Figure 7.10).

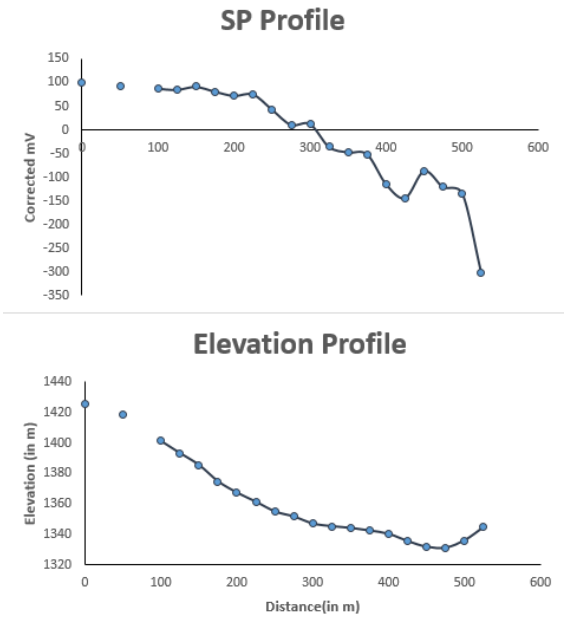

Figure 7.9: SP and Elevation Profile of line 01

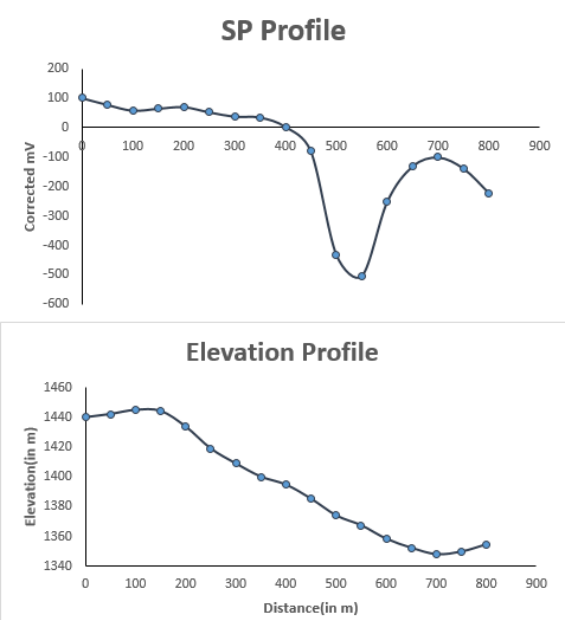

Figure 7.10: SP and Elevation Profile of line 02

Table 7.2: Geophysical characterics of the Digoli-Gajjola Graphite Block.

Bands	Geophysical characterics
Band-1	No SP or VES profile recorded.
Band-2	SP lows to ~-303 to -503 mV; VES-12 conductive at ~230-270 ohm.m; adjacent stations locally high-resistivity.
Band-3	Line-22 VES stations largely high resistivity (700-3000 ohm.m, locally higher), suggesting limited conductive continuity.
Band-4	VES-84 ~10 m conductive zone (~200 ohm.m); VES-81/82 define 35-40 m zones around 190-250 ohm.m.
Band-5	VES-62 and VES-65 define ~20 m conductive layers around 264-300 ohm.m; VES-66 falls to ~20 ohm.m below ~40 m.
Band-6	No VES, but SP Line-22 shows strong ~-590 mV anomaly.
Band-7	Band-7 VES largely high-resistivity.
Band-8	Band-8 has no SP / VES control.

7.1.4 Qualitative Features and Analytical Results

Tumbler test carried out in the field Bands-1 shows moderate to poor characteristics, while Bands 3, 7 and 8 are consistently moderate. Band-6 exhibits relatively better quality, ranging

from moderate to high, whereas Bands 2 and 5 show generally high tumbler values but with localized reduction due to intercalation and weathering effects. Surface modal analyses show the presence of

- **Jumbo (> 300 µm):** 86.15% area is occupied by the jumbo flakes of graphite.
- **Coarse (180 - 300 µm):** 2.94% area is occupied by the coarse graphite flakes.
- **Medium (150 - 180 µm):** 0.98% area is occupied by the medium graphite flakes.
- **Fine (75 - 150 µm):** 4.10% area is occupied by the fine graphite flakes.
- **Very Fine (< 75 µm):** 5.83% area is occupied by the very fine flakes.

Geochemical analyses of the surface graphite sample from different band shows,

Band-1:

Geochemical parameters are largely unavailable; however, sulphur values are low (≈0.008–0.026 ppm) and silica content is high (≈67–84% SiO_2), indicating a highly siliceous, impurity-rich host with limited direct assessment of graphite grade.

Band-2:

Shows moderate FC values (~4.07–5.84%) and VM (~3.38–3.9%), indicating relatively better graphite concentration compared to other bands. Sulphur is generally low but locally elevated (up to ~1.61 ppm). Ash content is very high (~90.59–98.41%) and silica/alumina impurities are significant. Vanadium is highly variable (511–1220 ppm), suggesting geochemical enrichment and lithological variability.

Band-3:

Displays comparatively low FC 2.19%, VM 3.13%.

Band-4:

Displays comparatively higher FC (up to ~6.98%) with moderate VM (~2.44–2.49%) and no detectable sulphur. Ash remains high (~90–93%), indicating graphite within a siliceous matrix. Represents one of the better-grade bands in terms of carbon content.

Band-5:

Highly variable geochemical character, with FC ranging from very low (~0.82%) to moderate (~5.75%) and VM between ~1.46–4.97%. Sulphur is low but present in minor amounts. Ash is consistently high (~89–97%) and silica content is also high, indicating strong dilution. This band reflects significant heterogeneity along strike.

Band-6:

Limited data available; sulphur shows minor presence (~0.021–0.48 ppm) and silica values are high (~83–92%), suggesting impurity-rich composition. FC and VM data are absent.

Band-7: No data.

Band-8:

Shows relatively higher FC (~6.01%) and VM (~6.16%), indicating moderate graphite presence but with higher volatile content. Ash is still high (~87.6%), implying impurity-rich graphite.

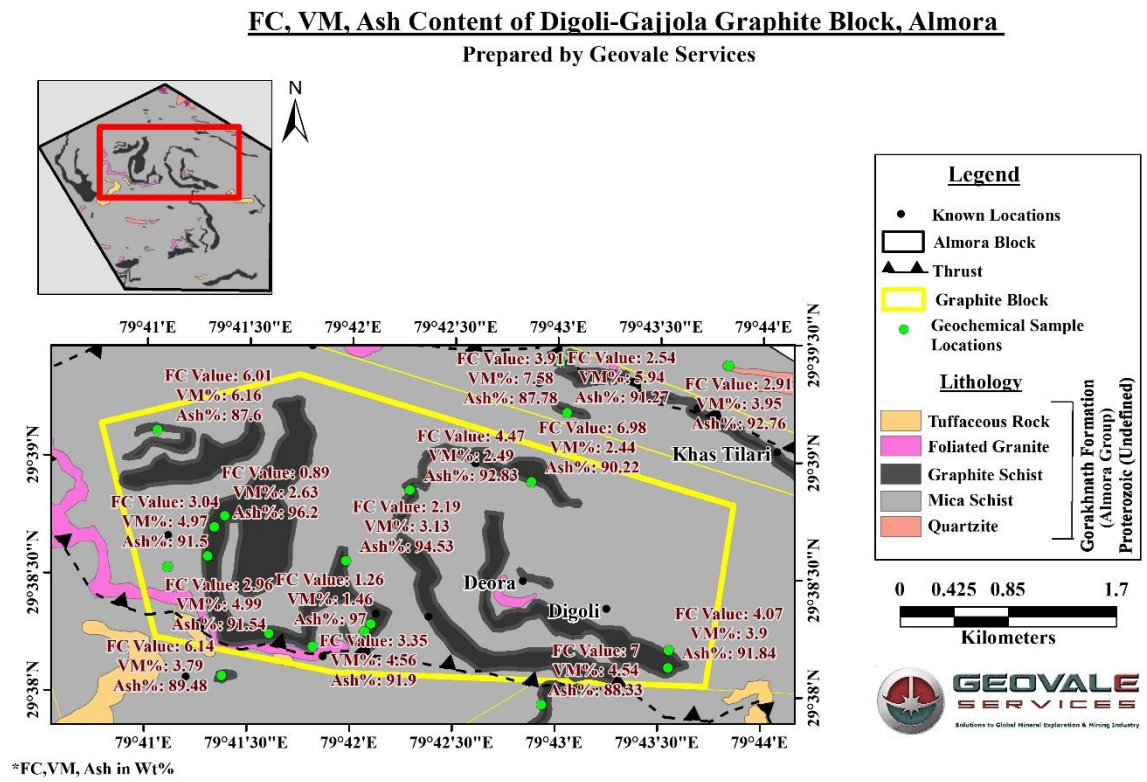

Figure 7.11: Geochemical analyses of the (FC, VM, Ash) content of the Digoli-Gajjola block.

Surface XRF results.

XRF analysis of graphitic and carbonaceous samples confirms the strongly gangue-rich nature of the block. Silica (SiO_2) is consistently dominant, ranging from ~58.60 to 96.21 wt% (median ~76.78 wt%), while Al_2O_3 varies between ~0.91 and 19.64 wt% (median ~8.37 wt%) and Fe_2O_3 from ~0.49 to 8.40 wt% (median ~1.43 wt%), indicating a siliceous to micaceous host assemblage. SO_3 is generally low but locally elevated up to ~4.03 wt%, supporting the presence of sulphidic and oxidized graphitic zones observed in the field. Vanadium, derived

from V_2O_5, shows a wide range (~61.6–2,296 ppm; median ~392 ppm), with distinct high-value clusters (>1,400 ppm) associated with graphitic zones and pyrite-bearing occurrences. This confirms that vanadium enrichment is significant but spatially variable, controlled by lithology and structural repetition within the graphitic package. (Figure 7.12)

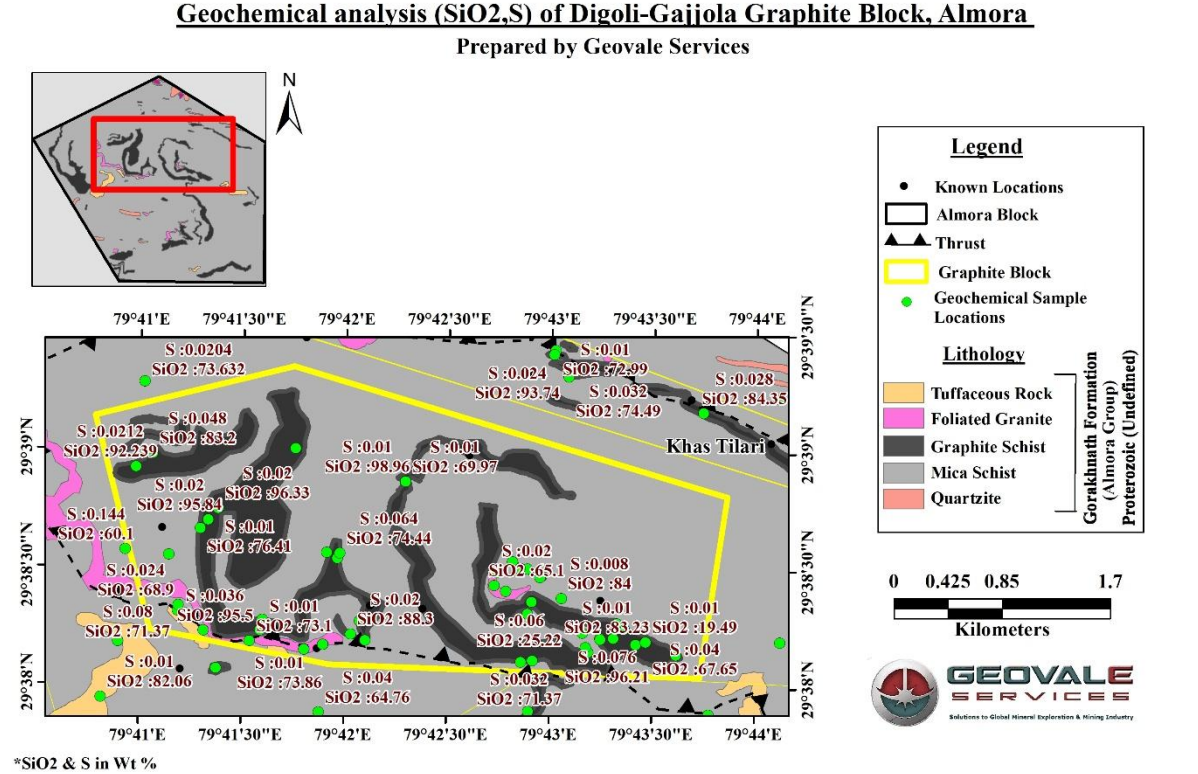

Figure 7.12: Geochemical analyses of the Digoli-Gajjola Graphite Block.

Surface ICP-MS results and associated commodities.

The ICP-MS dataset, though limited, highlights a clear polymetallic association within the graphitic system. A graphite schist sample records ~1,220 ppm V along with 32.97 ppm Mo, 1,690 ppm Zn, 101 ppm Cu, 140 ppm Ba, 15.15 ppm Pb, 14.35 ppm U and minor sulphur, whereas a graphite-schist sample shows ~511 ppm V, higher Mo (~52.9 ppm), very high Ba (~4,899 ppm) and elevated Cu, Zn, Pb and U. These results indicate that mineralization is not restricted to vanadium-bearing graphite but includes a broader suite of associated elements, with variations depending on host lithology. (Figure 7.13)

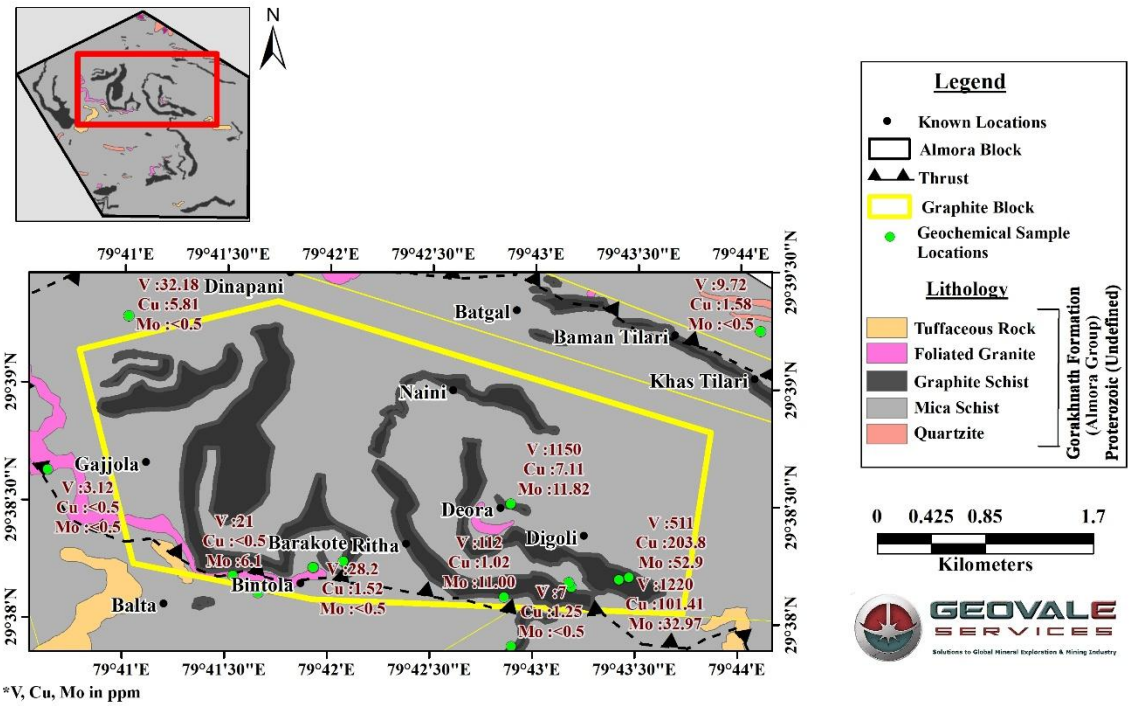

Figure 7.13: Geochemical analyses (V, Mo, Cu) of the Digoli-Gajjola Graphite Block

Raman and XRD:

One sample (Sample Id 110004) was analysed for Raman and XRD. Raman analysis confirms the graphite is massive and flakey in nature. XRD analysis shows sample containing Rectorite along with Graphite.

Tumbler test from drill core samples implies the Subsurface graphite flake size characteristics, based on tumbler test observations, indicate moderate to high variability across the Digoli-Gajjola bands with clear depth-wise fluctuations. In Band-2, boreholes BH-01 and BH-11 show overall moderate to high graphite characteristics, with distinct high zones at depths such as 35–37.5 m, 48–58 m, 72–72.5 m and 80.4–83.4 m in BH-01 and 23.6–30.5 m and 58.35–59.7 m in BH-11; however, intervals intercalated with mica schist show reduced graphite quality. Band-4 (BH-07) is consistently moderate, indicating relatively uniform but not enriched graphite zones. Band-5 (BH-04) shows moderate to high characteristics, with stronger zones between 30–42.4 m and moderate intervals between 5–30 m, along with localized enrichment. Other bands lack Subsurface data.

Geochemically, the Borehole 01 intersects a well-developed graphitic zone up to ~72 m depth beneath ~17.8 m overburden. Fixed carbon (FC) values range from ~2.06% to 7.56%, with higher concentrations between 35–37 m, while volatile matter (VM) varies from ~2.65% to 8.50%, indicating internal variability in graphite content. A very high vanadium value (~1594 ppm at 36–36.5 m) marks strong localized enrichment at depth. Barium (Ba) values are consistently elevated (up to ~1594 ppm in upper intervals) and copper (Cu) shows a significant peak (~524 ppm at 36.5–37 m). Molybdenum (Mo) is also enriched, reaching up to ~163 ppm in upper sections and showing variability with depth. Silver (Ag) occurs throughout the borehole (0.79–15.69 ppm from 35–90 m).

Drill-core analytical character. Subsurface analytical control is strongest in BH01 and moderate in BH07. In BH01, proximate data show FC from 0.91% to 7.56% (mean ~3.10%) with ash from 83.25% to 95.79%; the best FC interval occurs at 36.5-37.0 m. Borehole XRF at 36.5-37.0 m and 81.0-82.0 m gives V of about 1,405.6 ppm and 408.8 ppm respectively, with sulphur from about 412 ppm to 9,939 ppm. ICP-MS across BH01 records V from about 105.7 ppm to 1,594.6 ppm, Mo up to about 163.4 ppm, Ba up to about 7,067 ppm, Cu up to about 524 ppm, Zn up to about 950 ppm and U up to about 43.45 ppm. The strongest geochemical enrichment broadly coincides with the graphitic intervals identified in the Annexure XXV (35-37.5 m; 48-58 m; 72-72.5 m; 80.4-83.4 m). In BH07, XRF and ICP-MS still demonstrate graphitic-sulphidic fertility: XRF sulphur reaches about 3,043 ppm and 3,003 ppm, while ICP-MS records V up to about 309 ppm, Ba up to about 4,685 ppm and Mo up to about 23.2 ppm.

7.1.5 Raman and XRD Data:

The project report confirms that a Raman sample (Annexure XV) and an XRD sample at 29.636403/79.723705 (sample 110004) (Figure 14.6, Figure 14.5, Figure 14.4) come from this block. The Raman evidence can be used to confirm that the block was sampled for crystallinity testing, not to assign a quantitative Raman rank. XRD evidence is somewhat stronger: the project report states that sample 110004 is rectorite-rich and contains only trace graphite. This is an important cautionary result, because it shows that some surface graphitic exposures in the block are clay- / mica-rich and graphitically diluted even where field appearance suggests graphite-bearing schist.

7.2 Sirar-Bataldeon Graphite Block, Almora

7.2.1 Site Characteristics

The Sirar-Bataldeon Graphite Block situated in the central part of the Almora G4 block. The Sirar-Bataldeon Graphite Block is composed of eight mappable bands distributed between the

Ugalgaon–Bataldeon-Sirar eastern sector, the Bataldeon south sector and Sirar area. The block is regionally accessible from NH-309B, which forms the principal approach route to the belt; however, internal approach to individual bands is governed by slope, reserve-forest cover and drainage dissection. (Figure 7.14)

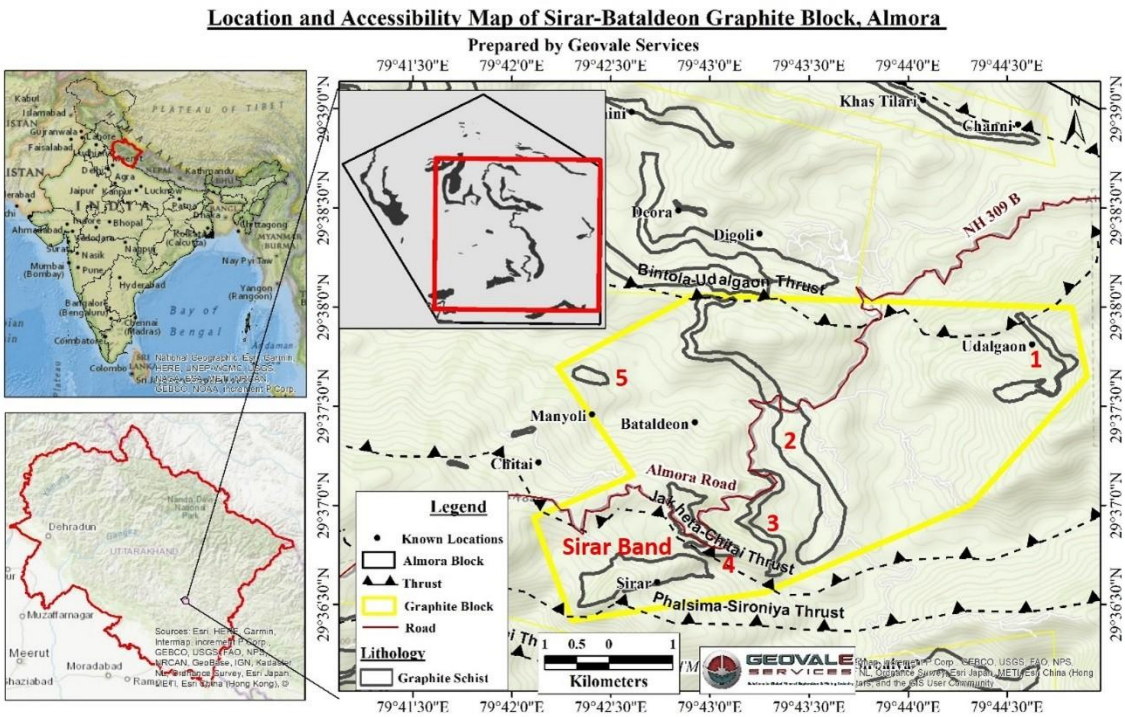

Figure 7.14: Accessibility map of Sirar-Bataldeon Graphite Block.

The Sirar-Bataldeon Graphite Block occupies a piedmont younger alluvial plain to lower hill-slope transitional setting, with elevations ranging from ~1380 m to 1710 m and moderate to steep slopes, where surface continuity is irregular due to partial burial under alluvio-colluvial cover; and near in the Sirar area, the terrain is more structurally dissected and hilly (1300–1700 m), dominated by ridges and valleys that provide relatively better exposure but lead to segmentation of graphite bodies (Figure 7.15). Structurally, the Bataldeon–Udalgaon band shows thrust-controlled graphite mineralization with NW–SE trending lineaments defining major structural trends, indicating stronger structural localization and possible shear/thrust dominance. LULC map indicates that the Bataldeon–Udalgaon band is dominated by dense vegetation with minor cropland and rangeland and lies largely within Sirar and Pharhkanaula Reserve Forests, making it environmentally sensitive (Figure 7.16). Drainage in the Bataldeon–Udalgaon-Sirar block is dendritic, controlled by Mahadeo Gad and That Gad rivers forming a

1st to 5th order network that ensures water availability but creates access barriers due to incised channels (Figure 7.17). Habitation in the Bataldeon–Udalgaon-Sirar band is moderate, indicating some settlement interaction. The open forest area is 0.924 sq. km and reserved forest area is 2.087 sq. km. (Figure 7.18).

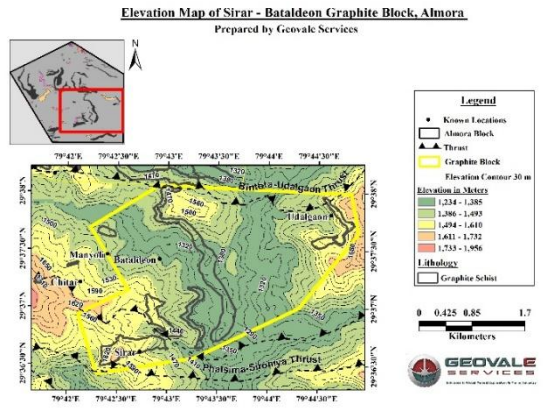

Figure 7.15: Elevation map of the Sirar-Bataldeon Graphite Block, Almora

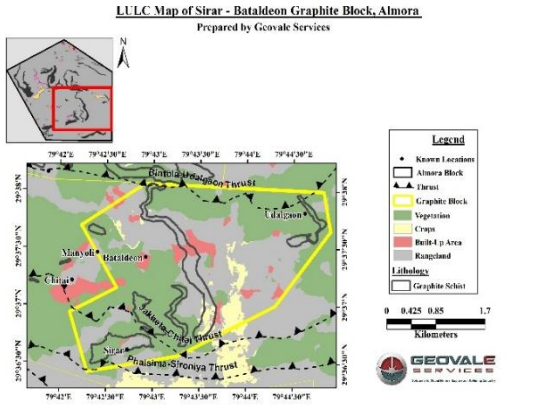

Figure 7.16: LULC map of the Sirar-Bataldeon Graphite Block, Almora

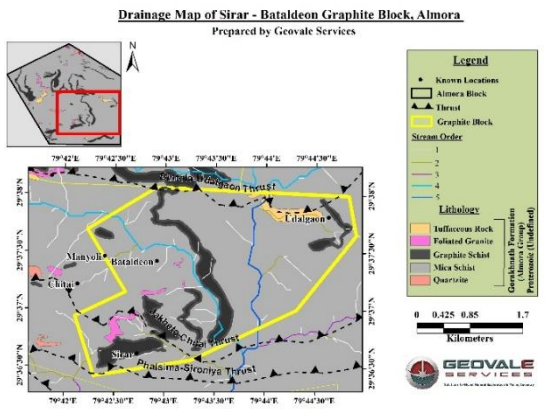

Figure 7.17: Drainage map of the Sirar-Bataldeon Graphite Block, Almora

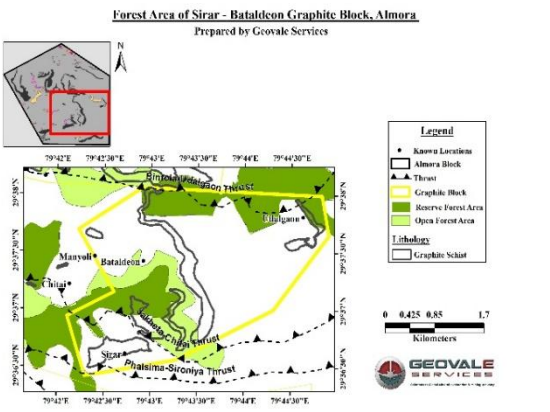

Figure 7.18: Forest map of the Sirar-Bataldeon Graphite Block, Almora

7.2.2 Geological and Resource Characterization

The graphite mineralization in the Sirar-Bataldeon Graphite Block is structurally controlled and foliation in graphite schist and associated rock is generally NW–SE trending with gently to moderately dipping (10°–35°) graphite schist bands with local folding and shearing and ramp-flat thrust structure.

7.2.3 Thickness and continuity

The graphite mineralization is distributed across multiple bands with variable geometry and continuity. Band 1 (near Udalgaon) has a strike length of ~1.52 km with a highly variable and narrow width (0.010–0.159 km, avg. 0.065 km), covering ~0.099 sq. km, indicating limited but discontinuous potential. Bataldeon East Band 2 is the most extensive, with ~3.40 km strike length, ~0.132 km average width and 0.449 sq. km area, representing the most significant and laterally continuous graphite zone. Bataldeon South Band 3 (~1.51 km strike, 0.063 km width, 0.095 sq. km) and Band 4 (~0.84 km strike, 0.173 km width, 0.145 sq. km) show moderate but more localized development. Bataldeon Band 5, despite a strike length of ~0.3 km, has a relatively narrow width (~0.097 km) and small mapped area (~0.029 sq. km), suggesting discontinuous or poorly exposed mineralization. Bands 6–7 are not robustly constrained due to insufficient data. In comparison, the Sirar Band has a strike length of ~1.03 km, an average width of ~0.459 km (with local variation from narrow to moderately wide zones) and a mapped area of ~0.473 sq. km, indicating a comparatively well-developed but structurally segmented graphite zone with moderate lateral continuity.

7.2.4 Road Section:

(Figure 7.19)

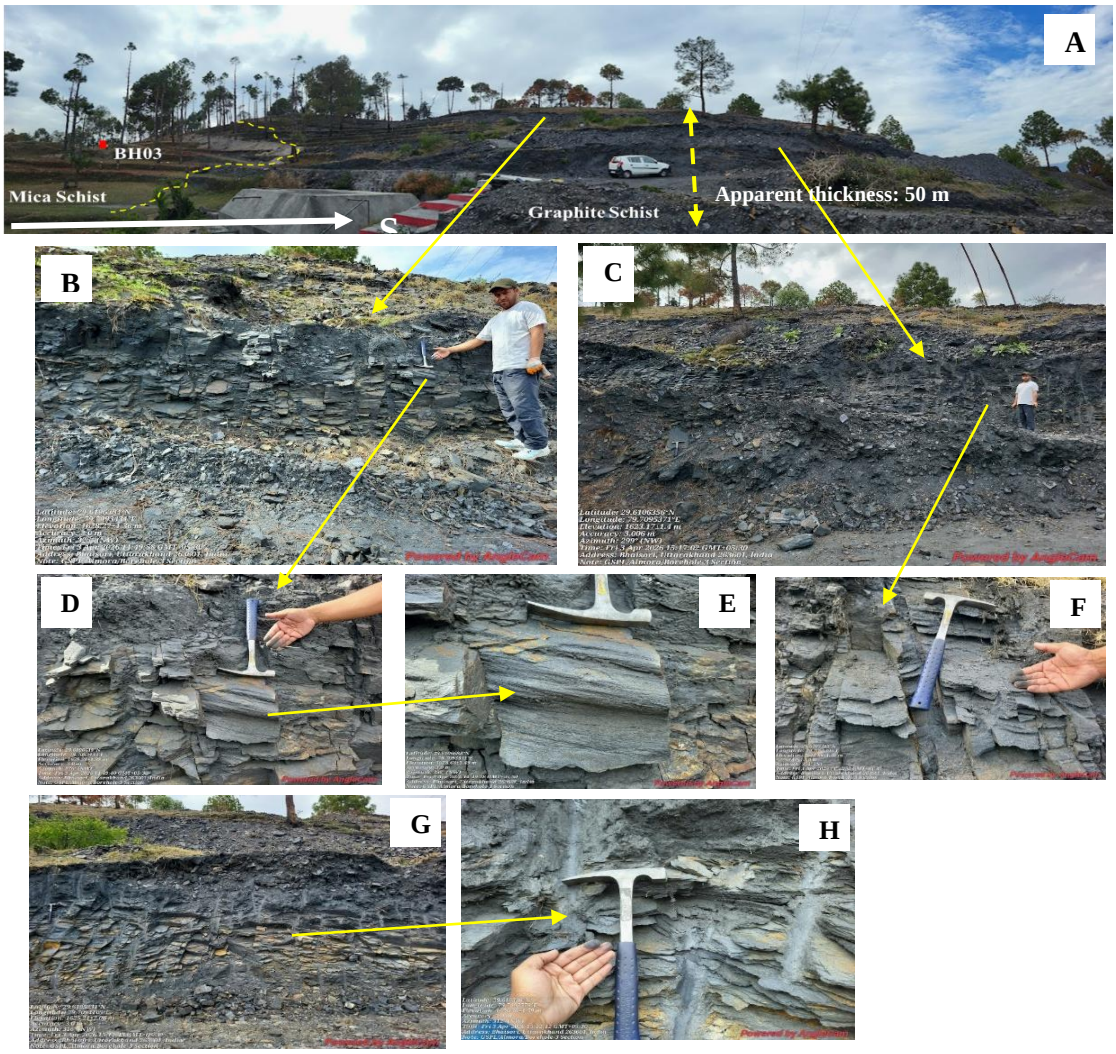

Figure 7.19: Road section of the Sirar-Bataldeon graphite block in Sirar area, (Borehole 03)

7.2.5 Geophysical Data Analyses:

VES study near Sirar area: A total of five VES profile lines (Line 04, 05, 06, 07 and 25) were conducted across the graphite-bearing zone to delineate subsurface lithological variation and identify conductive horizons related to graphite mineralization (Figure 7.20).

Line 04: Two VES stations (VES-12 and VES-13) were carried out along this profile. VES-13 exhibits high apparent resistivity values ranging from 400 to 1400 Ω·m. In contrast, VES-12 reveals a conductive subsurface layer approximately 35 m thick with apparent resistivity around 230 Ω·m, indicating a probable graphite-bearing horizon at a depth of 30-35 m from

surface. The execution of Borehole-03 in proximity to this location supports the geophysical interpretation and indicates exploration targeting based on resistivity response (Figure 7.21).

Line 05: Three VES stations (VES-14, VES-15 and VES-19) were conducted. VES-14 shows high resistivity (>900 Ω·m), indicating resistive country rock with negligible conductive mineralization. VES-15 and VES-19 delineate a 20–30 m thick conductive layer at a depth of ~70 m, with resistivity values between 153–190 Ω·m, suggesting continuity of graphite mineralization or associated conductive lithological units along this segment (Figure 7.22).

Line 06: Two VES stations (VES-16 and VES-18) were completed. Both stations clearly indicate a well-developed conductive layer having thickness 20–30 m and apparent resistivity approximately 49 Ω·m (depth ~70 m from surface). Such very low resistivity values strongly suggest graphite-rich conductive horizons, possibly representing the most promising segment of the investigated graphite band (Figure 7.22).

Line 07: Only one VES station (VES-20) was conducted along this line. The station records very high resistivity values (>1500 Ω·m).

Line 25: Three VES stations (VES-97, VES-98 and VES-99) were conducted. All stations display very high apparent resistivity values, exceeding 500 Ω·m and locally reaching up to 37,000 Ω·m, indicating extremely resistive formations such as compact granitoids, quartz veins, or barren host rocks.

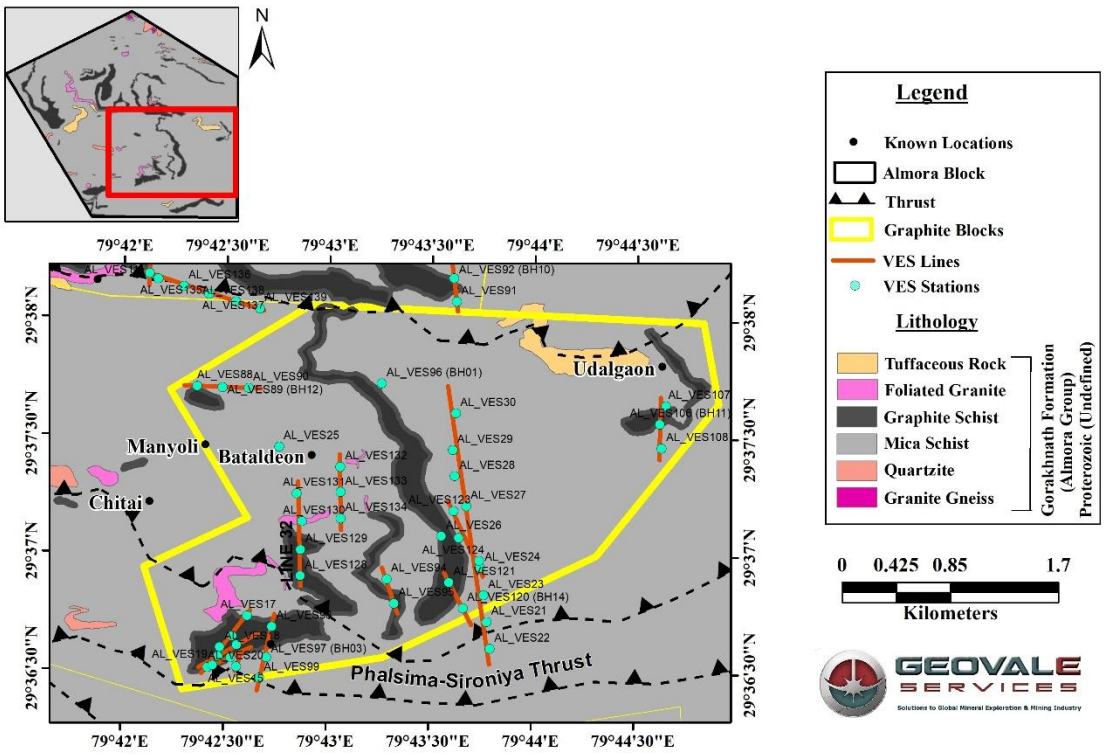

Figure 7.20: Resistivity VES survey conducted Sirar-Bataldeon Graphite Block

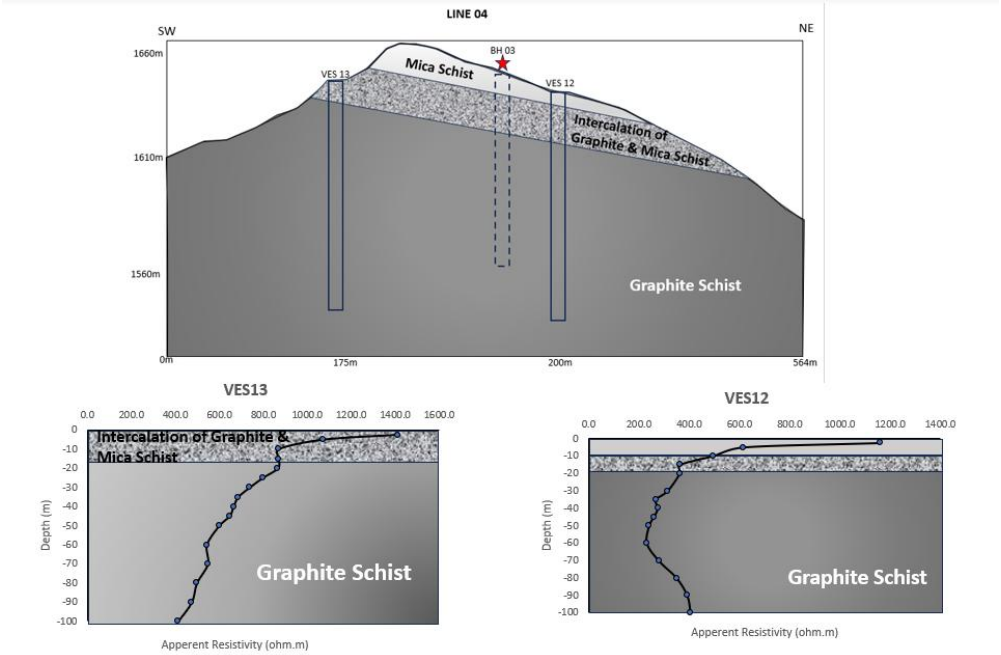

Figure 7.21: Geological section along VES line 04 (VES12, VES13 with Borehole 03), near Sirar area

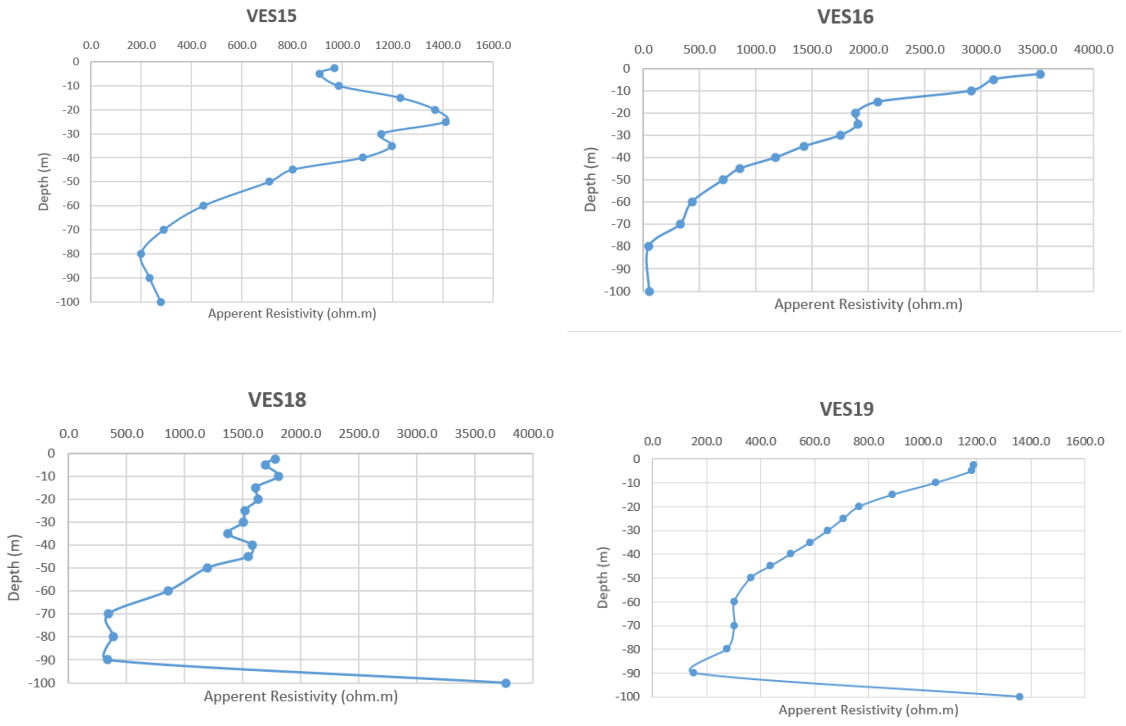

Figure 7.22: VES profile of VES15, VES16, VES18, VES19 in Sirar area

One Self Potential (SP) profile, Line 03 and Line 09 has been conducted, near Sirar area. (Figure 7.23**)**

Line 03: The SP measurements predominantly show positive values, reaching a maximum of approximately +422 mV. A localized negative anomaly of about –17 mV is observed along the profile (Figure 7.24).

Line 09: The SP measurements predominantly show positive values, reaching a maximum of approximately +450 mV. A localized negative anomaly of about –100 mV is observed along the profile (Figure 7.25).

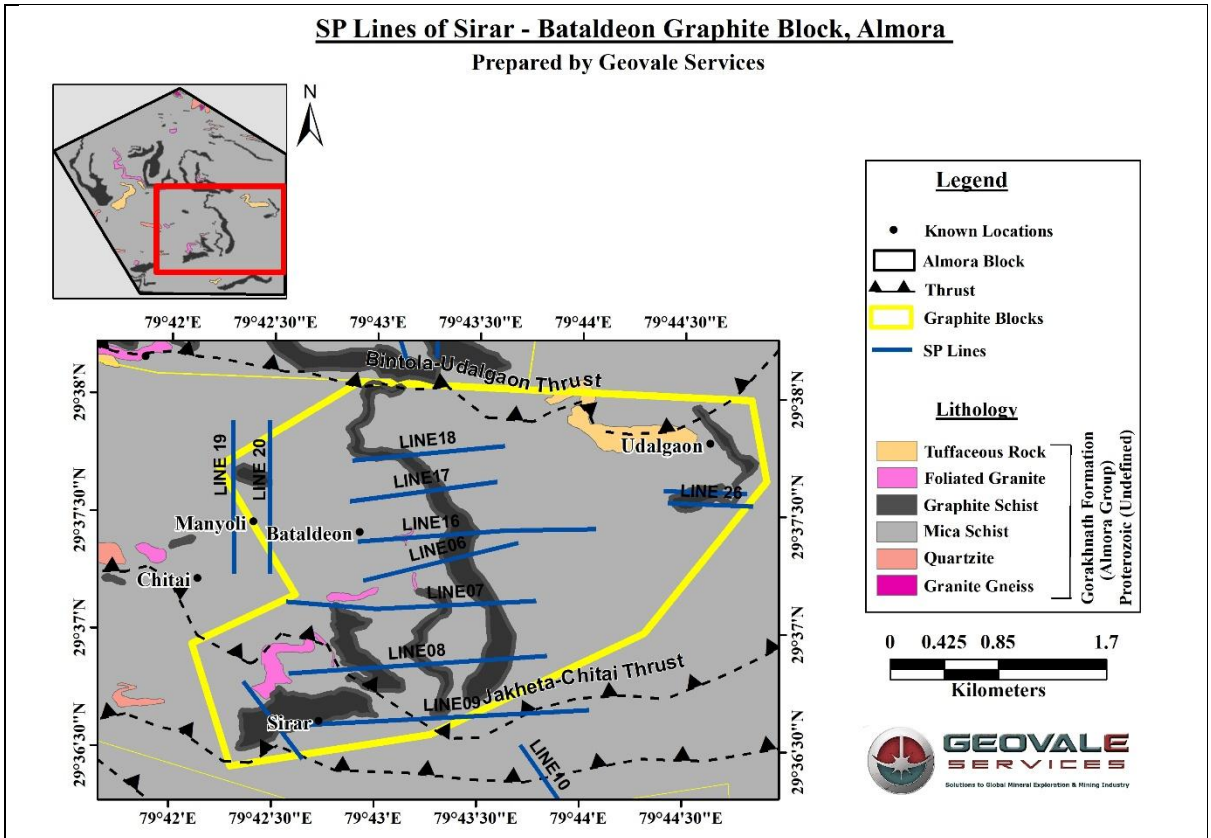

Figure 7.23: SP survey conducted Sirar-Bataldeon Block.

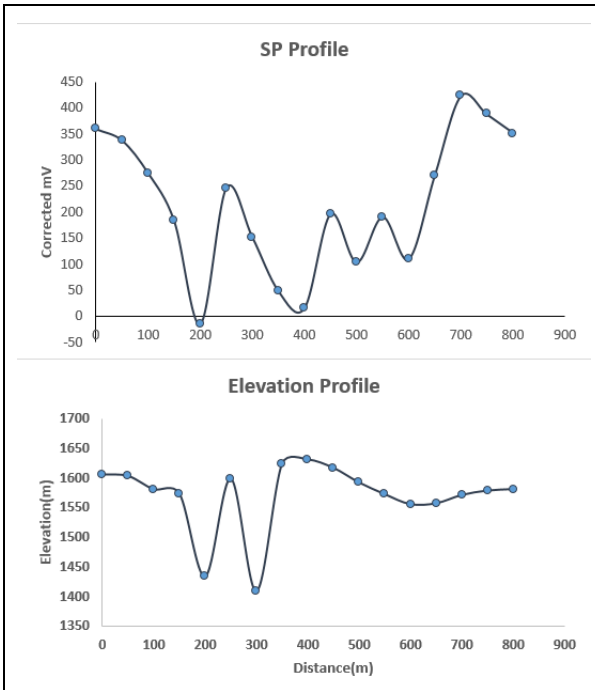

Figure 7.24: SP and Elevation Profile of Line 03

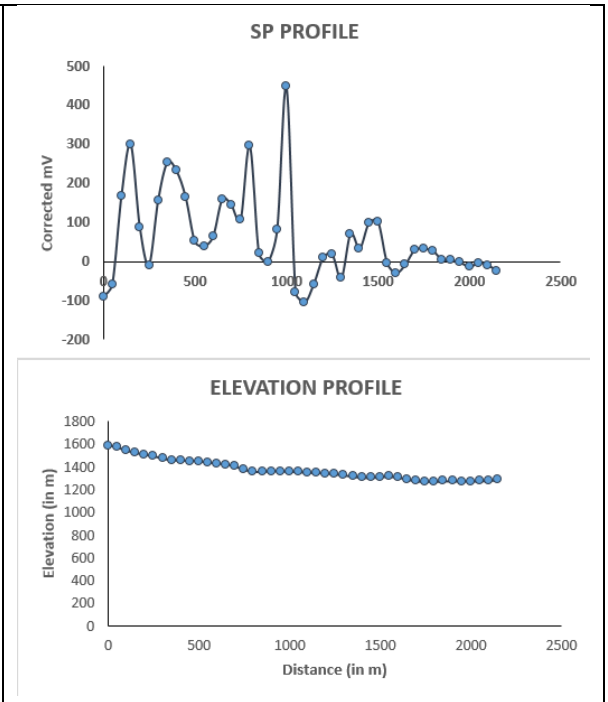

Figure 7.25: SP and Elevation Profile of Line 09

Geophysical data near Baladeon-Udalgaon area (Table 7.3**).**

Bataldeon Band 1 (Near Ugalgaon): Moderate graphite potential with localized conductive zone (~20 m, 86 Ω·m) supported by strong negative SP anomalies (–319 to –481 mV).

Bataldeon East Band 2: High graphite potential with thick conductive horizons (up to 50 m, very low resistivity ~6 Ω·m) and strong, consistent negative SP anomalies (up to –451 mV).

Bataldeon South Band 3: Low graphite potential dominated by high resistivity (~1800 Ω·m) indicating mostly barren or weakly mineralized zones.

Bataldeon South Band 4: Moderate graphite potential with localized thick conductive zone (~90 m, 150–220 Ω·m) but largely discontinuous due to surrounding resistive formations.

Bataldeon Band 5: Very low graphite potential with consistently high resistivity (900–1300 Ω·m) indicating barren formations.

Table 7.3: Summary of areal extension and geophysical response for Sirar-Bataldeon Graphite Block

Bands / sector	Strike length (km)	Average width (km)	Mapped area (sq. km.)	Geophysical data	Remark
Band 1 (near Ugalgaon)	1.520	0.065	0.099	Line 25 VES 106–108; VES 108 conductive layer ~20 m at ~86 ohm·m; SP Lines 25–26 with valley lows –319 to –481 mV	Discontinuous but conductive western/central target; fine flake response and lower surface quality than eastern sectors.

Bands / sector	Strike length (km)	Average width (km)	Mapped area (sq. km.)	Geophysical data	Remark
Bataldeon East Band 2	3.400	0.132	0.449	VES 26 conductive ~10 m at ~262 ohm·m and VES 121 strong ~50 m conductor at ~6 ohm·m; multiple SP lows to ~–451 mV	Most laterally persistent and geophysically strongest sector; priority target for follow-up.
Bataldeon South Band 3	1.51	0.063	0.095	Profile 34 (VES 94–95) mostly resistive to ~1800 ohm·m; conductive response weaker and likely localized	Moderate continuity but limited subsurface conductive support in current dataset.

Bands / sector	Strike length (km)	Average width (km)	Mapped area (sq. km.)	Geophysical data	Remark
Bataldeon South Band 4	0.840	0.173	0.145	Profiles 32–33; VES 129 conductive zone ~90 m thick with ~150–220 ohm·m; adjacent stations resistive	Compact but comparatively thick target; supported by BH-10 collar and log evidence.
Bataldeon Band 5	~0.3	0.097	0.029	Profile 27 (VES 88–90) predominantly resistive (900–1300 ohm·m)	Long but thin and currently lower confidence.

Bands / sector	Strike length (km)	Average width (km)	Mapped area (sq. km.)	Geophysical data	Remark
Sirar Band	1.026695	0.459	0.472652	Profile 06 and parts of Profile 04–05 host thick (20–35 m), low-resistivity conductive horizons (≈49–230 Ω·m) suggestive of graphite mineralization, whereas Lines 07 and 25 are dominated by high-resistivity (>500–37,000 Ω·m) barren formation	Moderate graphite potential

.

7.2.6 Qualitative Features and Analytical Results

Tumbler test carried out in the field near Bataldeon area shows moderate to high variability, reflecting differences in graphite quality and recovery potential. Bataldeon Band 1 (near Ugalgaon) exhibits moderate flake size, indicating average liberation with limited development of jumbo flakes. In contrast, Bataldeon East Band 2 shows high flake size, suggesting strong potential for coarse to jumbo graphite recovery. Bataldeon South Bands 3 and 4 display moderate to high flake size, indicating generally favorable graphite quality with localized enrichment of coarser flakes. Bataldeon Band 5 again reflects moderate flake size, implying

average quality and recovery potential. Bataldeon Band 6 stands out with high flake size, indicating strong potential for coarse graphite concentration, while Bataldeon Band 7 shows moderate to high flake size, reflecting moderately good graphite quality with some degree of variability across the band. Near Sirar area, Field observations indicate dark grey to black graphite with metallic lustre, strong streak and occurrence within quartz veinlets along with redox-sensitive elements; tumbler test suggests overall high flake size with local moderate variation due to intercalation, while modal analysis indicates dominance of fine to medium flakes with subordinate coarse fractions, reflecting generally good but locally variable flake size distribution.

Geochemical analyses have been carried out from various surface graphite ands of Udalgaon-Sirar block, indicates Bataldeon Geochemical data for Band 1 (Near Ugalgaon) band indicate sulphur content remains low (0.015–0.116 ppm) and silica values are relatively high (≈47–68% SiO_2), indicating a dominance of siliceous impurities. Bataldeon East Band 2 band shows relatively better data coverage, with FC values ranging from ~2.19% to 7% and VM between ~1.57% and 4.54%. Despite this, ash content remains very high (~88–95%) and silica impurities are significant, indicating dilution of graphite concentration. Low sulphur values (0.08–0.18 ppm) are favourable. Bataldeon South Band 4: has sulphur (~0.044 ppm) and silica (~65%) reported. The low sulphur is favourable; however, the relatively high silica content indicates significant impurity presence. Bataldeon Band 6 band shows FC ~6.1% and VM ~5.49%, indicating moderate carbon content. However, ash content is high (~87.9%), suggesting significant gangue material. The overall geochemical signature indicates moderate grade graphite but with high impurities, which may impact recovery and beneficiation efficiency. The Sirar band shows FC values ranging from ~3.5% to 5.43% and VM from ~3.02% to 4.48%, indicating low to moderate graphite grade. Sulphur values (0.02–0.24 ppm) and the presence of moderate pyrite suggest some sulphide association. Ash content is high (~90–93%) and silica impurities (≈75–85% SiO_2) are significant, indicating dilution by gangue minerals (Figure 7.26).

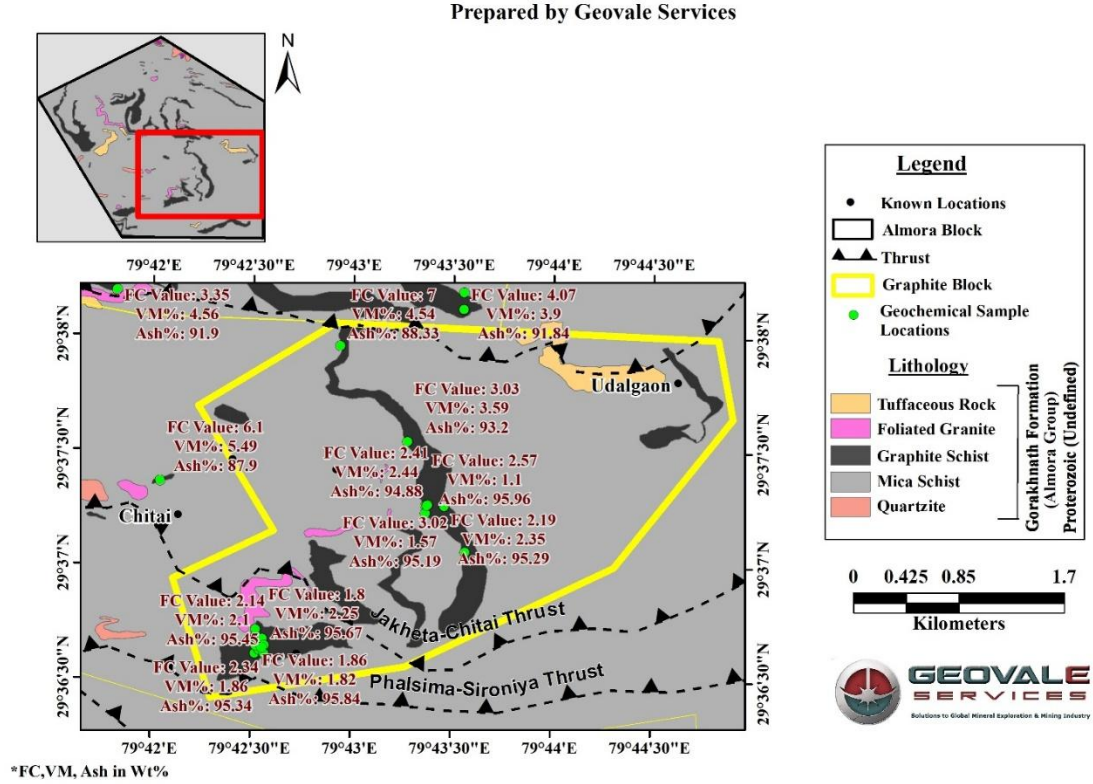

Figure 7.26: Geochemical analyses (FC, VM, Ash) of surface graphite bands, Sirar-Bataldeon Block.

Whole-rock XRF data (Figure 7.27) of the surface graphite sample (annexture) indicate that the graphite-bearing horizons are silicate-rich and strongly diluted, with SiO_2 ranging from ~47.7% to 89.8% (avg. ~74%), Al_2O_3 from ~4–19% and Fe_2O_3 from ~0.6–7.2%, confirming a quartz–mica dominated graphite-schist/graphite schist system rather than high-purity graphite; although LOI locally reaches ~20% in graphitic zones (notably eastern Bataldeon), overall mineralogy remains polymineralic. Importantly, vanadium (as V_2O_5) reaches up to ~0.20 wt% in XRF and shows consistent association with graphitic lithologies.

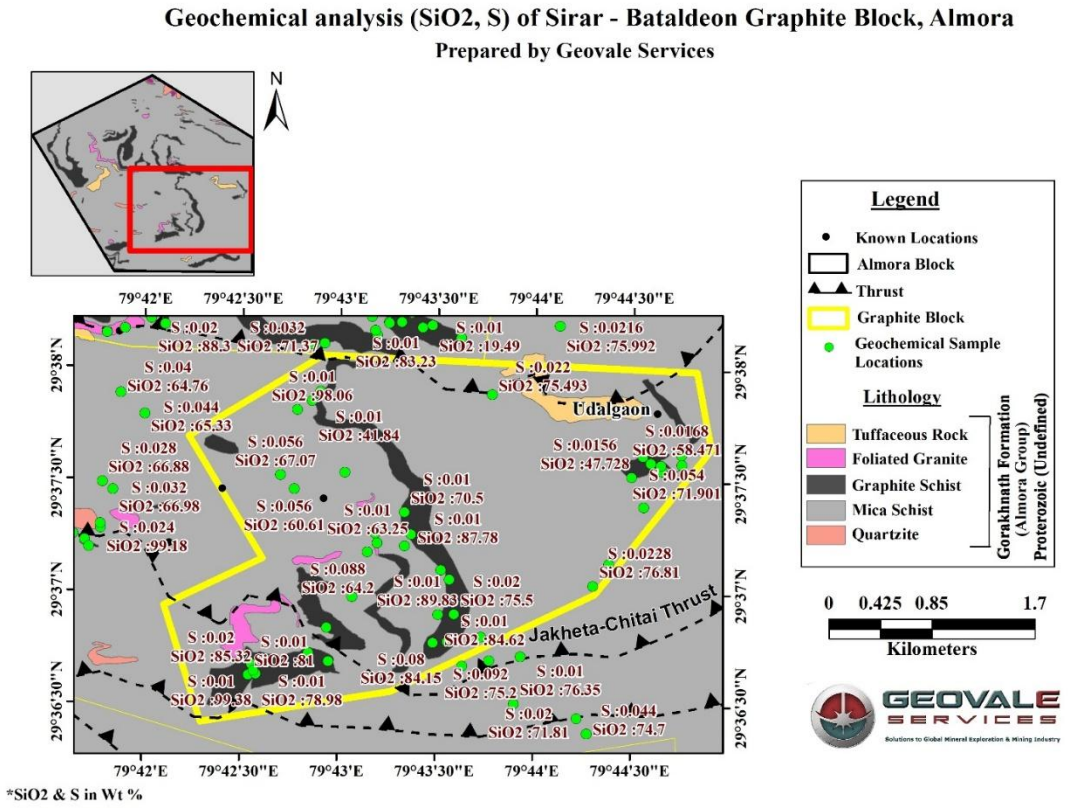

Figure 7.27: Geochemical analyses (S and SiO2) of surface graphite bands, Sirar-Bataldeon Block.

ICPMS data further strengthen this interpretation, with vanadium ranging from 85 to 2,060 ppm, accompanied by elevated Ba (up to ~13,668 ppm), Mo (up to ~73 ppm) and U (up to ~37 ppm), highlighting a distinct redox-controlled graphite–vanadium–barium–molybdenum association. High-value anomalies such as sample 109990 (2,060 ppm V) and the eastern Bataldeon cluster (729–1,128 ppm V) confirm that the block is not merely graphite-bearing but geochemically fertile and exploration should integrate graphite targeting with trace-element enrichment criteria. (Figure 7.28)

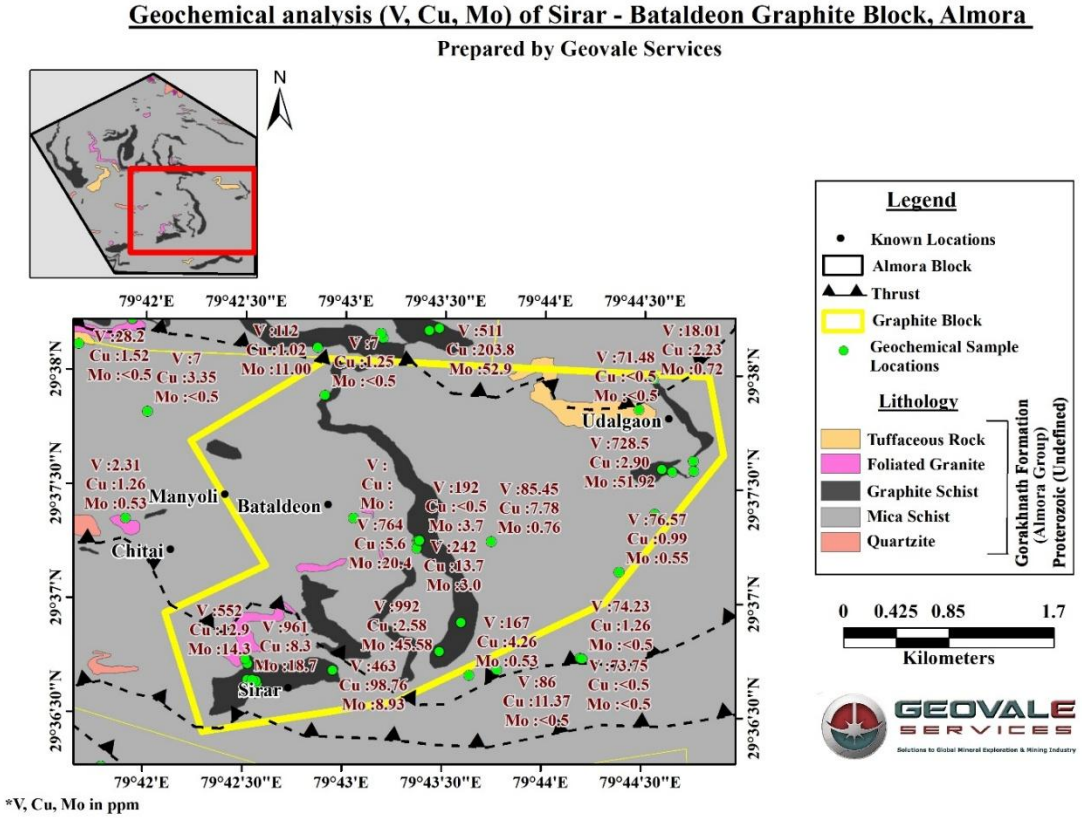

Figure 7.28: Geochemical analyses (V, Cu, and Mo) of surface graphite bands, Sirar-Bataldeon Block.

7.2.7 Borehole Information in the Sirar-Bataldeon Graphite Block:

In the Sirar graphite band, Borehole-3 was drilled with a total depth of 75 m out of which 58 m (true thickness) of Graphite Schist thickness was established based on lithologging data. All proximate analysis (except one sample) have shown >6% Fixed Carbon value with the highest value of 8.4% out of the 111 analyzed graphite sample within the Almora G4 Project Area.

7.2.8 Tumbler Test in the Sirar-Bataldeon Graphite Block:

Modal analysis of Subsurface samples near Bataldeon East Band 2 indicates very fine graphite flakes (<75 µm), accounting for ~98.53% of the total population, with only minor contributions from the 75–150 µm (≈1.13%) and 150–180 µm (≈0.34%) fractions. Notably, no course (>180 µm) or jumbo flakes are recorded.

Subsurface modal analysis (BH-03), near Sirar area shows that 300 µm flake size graphite occupy about 98.71% of the area. 300 – 180 µm flake size occupies about 0.87% of the area. Flake size between 180 – 150 µm occupies about 0.21% of the area. Flak size between 150 –

75 µm occupies about 0.18% of the total area. Flake size <75 µm occupies about 0.03% of the area.

Geochemical analyses from subsurface data from BH-02, near Bataldeon East Band 2 indicates a moderately thick graphite horizon (~27 m) beneath ~13 m overburden, with FC values ranging from ~2.13% to 5.73% and VM between ~2.92% and 4.43%, reflecting low to moderate grade graphite. However, sulphur values are significantly high (≈4185–16675 ppm), suggesting strong sulphide association, while vanadium content (≈710–1022 ppm) indicates notable trace element enrichment linked to graphitic zones.

7.2.9 Raman and XRD Data:

Based on Raman analysis (Annexure XV) Graphite within the Sirar Band is mainly massive type Graphite with minor vein controlled (Sample Id- 114231, 114232). Based on XRD Analysis Quartz and Muscovite are nearly in equal proportion (Sample Id 114239).

7.3 Kalimath Graphite Block, Almora

7.3.1 Site Characteristics

The Kalimath Graphite Block (Table 7.4) lies in the north-western part of the Almora G4 block, near Kalimath, Mat and Saura villages. This block consists of the one curved graphite bands divided into two parts, namely western and eastern part (Figure 7.29). The area is easily accessible by road from Almora via NH 309A, along with connected village roads.

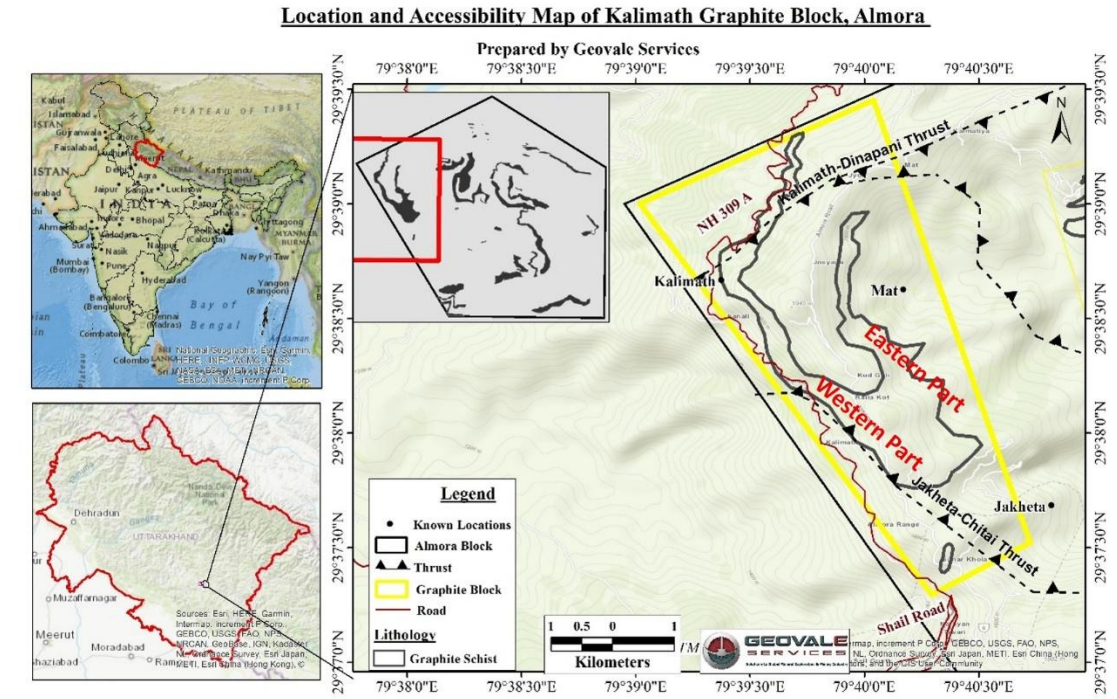

Figure 7.29: Accessibility map of the Kalimath Graphite Block

Topographically, the Kalimath area is characterized by rugged and high-relief terrain, with elevations ranging between 1910 m and 2400 m (Figure 7.30). The area represents a residual environment characterized by highly dissected, structurally controlled hilly terrain with steep hill slopes, narrow ridges and deeply incised valleys (Figure 7.31). The higher elevations are mainly confined to ridge tops, while the slopes descend sharply towards adjoining valleys. Drainage is dendritic type and is mainly by first and second-order seasonal channels (Figure 7.32), springs and short feeder gullies draining away from the ridges are present near Kalimath and Mat areas. Water availability in this area is limited and largely seasonal in nature. Land use and land cover (Figure 7.33) in the Kalimath-Mat area shows vegetation is dominant with a few rangeland and human build-up. Despite the challenging terrain, the region exhibits relatively higher habitation levels compared to other part. This is partly due to its proximity to

tourist spot near Kasar area. The presence of local communities can provide labour and basic support services. A part of this G3 block falls within the Kalimath Reserve Forest, indicating the presence of dense forest cover and associated ecological sensitivity.

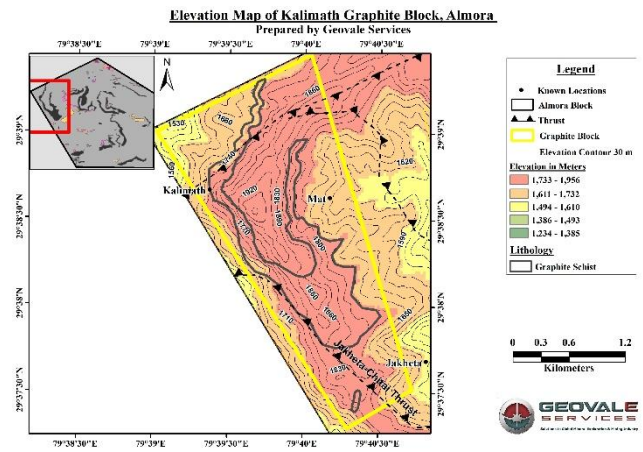

Figure 7.30: Contour map and elevation map of the Kalimath Graphite Block, Almora.

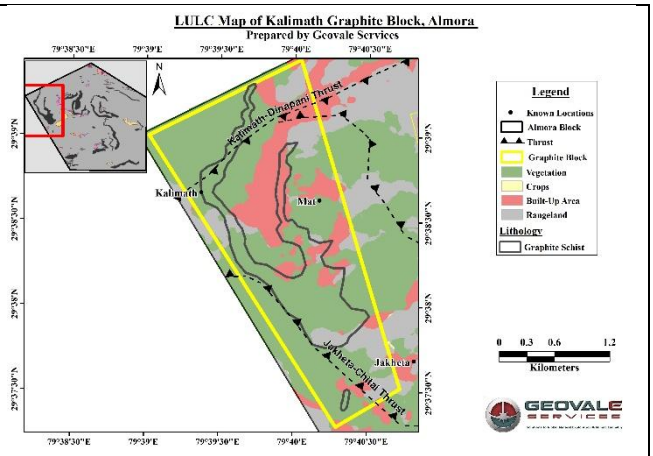

Figure 7.31: LULC map of the Kalimath Graphite Block, Almora.

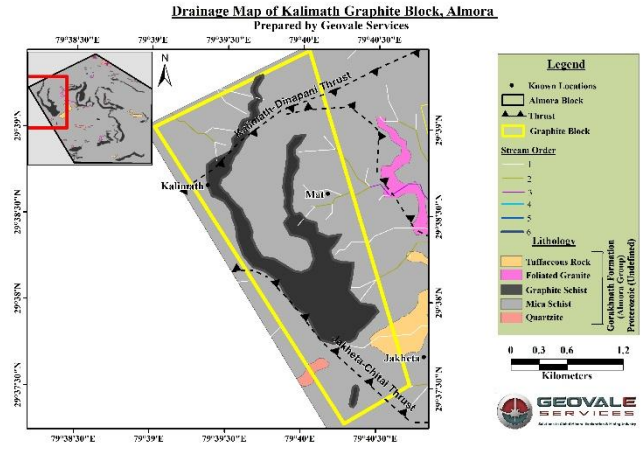

Figure 7.32: Drainage map of the Kalimath Graphite Block, Almora.

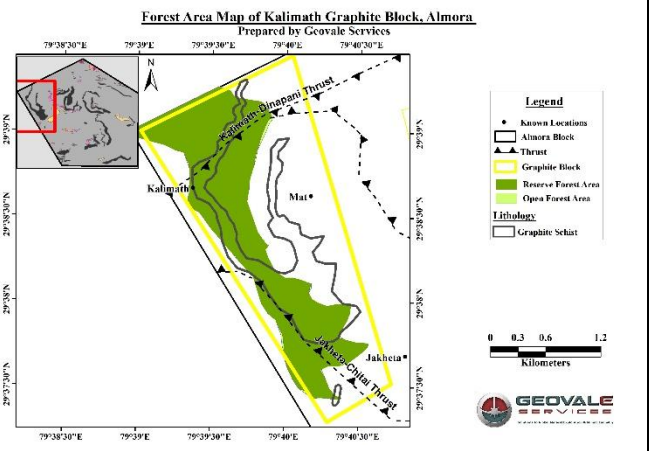

Figure 7.33: Forest map of Kalimath Graphite Block, Almora.

Table 7.4: Details of the Kalimath Graphite block

Parameter	Details of the Kalimath G3 Block
Area	4.93 sq. km
Toposheet No.	53 O/10
Access	Approached through NH-309A from Almora Town.
Elevation	~1,910–2,400 m RL; high-elevation block sector.

Parameter	Details of the Kalimath G3 Block
Topography	Hilly, undulated to steep
Drainage	1st- and 2nd-order streams; short, slope-controlled drainage
Forest / vegetation	Rangeland and vegetation; within Kalimath Reserve Forest.
Water availability	Limited, seasonal; dependent on tanker supply.
Habitation	Moderate to high due to nearby Kasar tourist influence.
Hillshade / Structure	Thrust-controlled; graphite aligned with structural geometry.
RED Scheme	Residual, highly dissected hilly and valley terrain.
LULC	Vegetation-dominated with limited built-up area.

7.3.2 Geological and Resource Characterization

The graphite band of the Kalimath Graphite Block is surrounded by the with mica-schist. Towards the south eastern part of the block, tuffaceous rock and quartzite rock exposures are reported.

The block cover about 4.93 sq. km. with mappable graphite are is 1.08 sq. km. The detail of eastern and western bands is given below:

Thickness and Continuity (Table 7.5**)**

Eastern Part

The eastern part of the Kalimath G3 graphite band has 2.32 km mappable strike length and average 0.179 km width which imply greater variability in thickness. While surface exposures from the road cross section shows the graphite is ~5–10 meters near surface, geophysical data suggests significantly thicker zones (up to 35–55 meters) at depth, indicating potential for larger accumulation.

Western Part

The western part exhibits a strike length of approximately 3.53 km and a relatively narrow width of 0.14 km. The graphite band here is thin, ranging from 5–7 meters in in road cut section.

Table 7.5: Details of the extension of Kalimath Graphite Block.

Bands / Segment	Approx. Strike Length (km)	Average / Mapped Width (km)	Approx. Mapped Area (sq. km.)	Interpretation from Road Section
Western Part	3.53	0.14	0.494	Mappable graphite band (5–7 m) exposed at surface along the road cut section.
Eastern Part	2.32	0.179	0.415	Band with variable thickness; surface exposure (5–10 m) with strong geophysical indication of thicker zones (up to 35–55 m) at depth, suggesting significant subsurface graphite accumulation and high exploration potential.

7.3.3 Road section

Kalimat graphite block (western Limb): (Figure 7.34**)**

Figure 7.34: Road section of Kalimath Graphite Block

Kalimath Graphite Block: Eastern part (Figure 7.35, Figure 7.36, Figure 7.37).

Figure 7.35: Road section of Kalimath Graphite Block eastern part

Figure 7.36: Road section of eastern part of Kalimath graphite block

Figure 7.37: Details of Graphite Schist rock in Kalimath Graphite Block

7.3.4 Geophysical Data Analyses

Resistivity (VES Survey)

In the western part of the Kalimath graphite band, a total of five Vertical Electrical Sounding (VES) lines (Figure 7.38), namely Line 13, Line 14, Line 17, Line 18 and Line 30, were conducted to investigate the subsurface resistivity distribution and delineate conductive horizons associated with graphite mineralization.

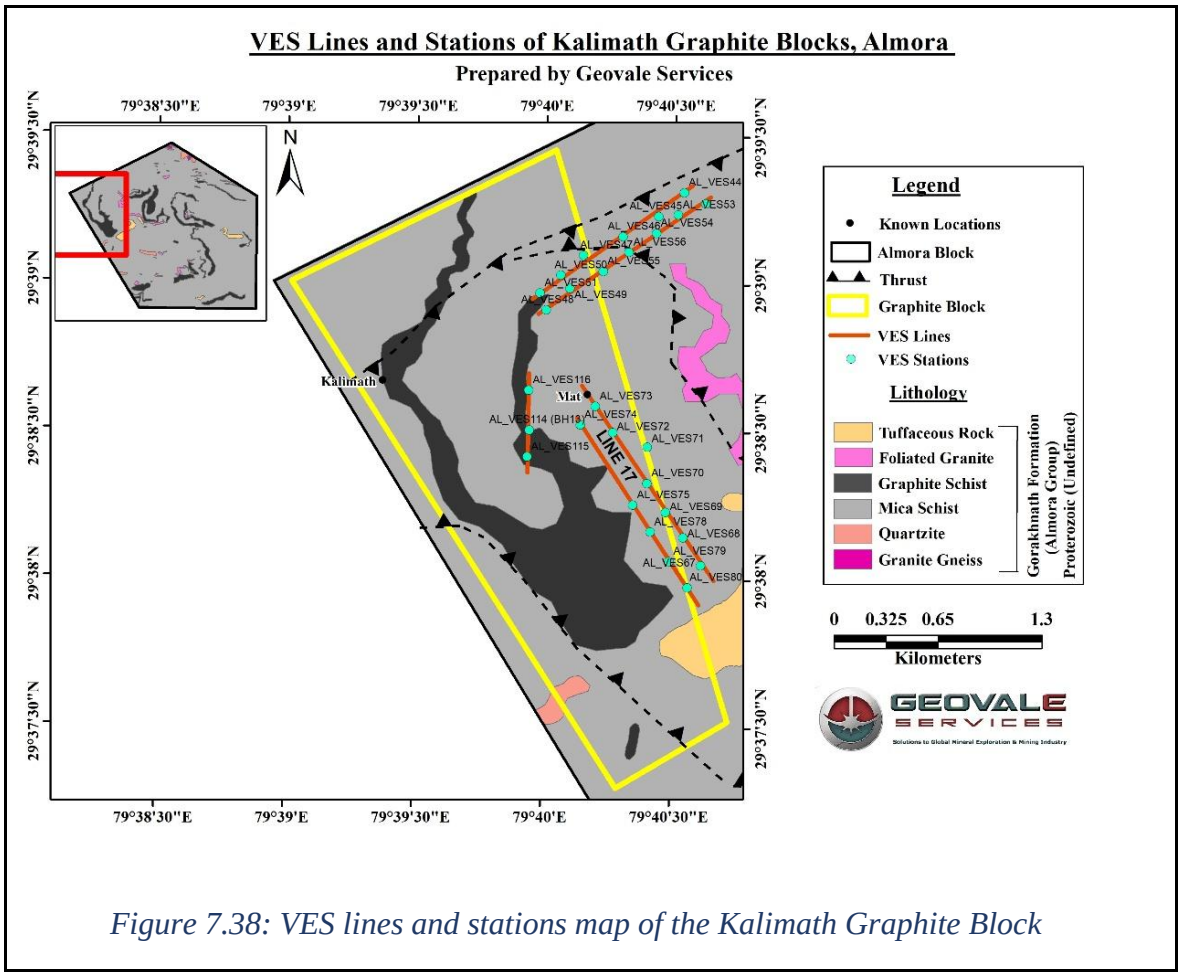

Figure 7.38: VES lines and stations map of the Kalimath Graphite Block

Line 30: A total of three VES stations were carried out along this line. Interpretation reveals a distinct conductive zone at VES 114 (~15m depth) and VES 115 (~25 m depth), exhibiting an estimated thickness of approximately 40 m, which is indicative of a potential graphite-bearing horizon. Notably, Borehole-05 was drilled in close proximity to VES 114, providing subsurface verification support for the geophysical interpretation. In contrast, VES 116 shows relatively high resistivity values, suggesting transition into resistive lithology or absence of conductive mineralization (Figure 7.39).

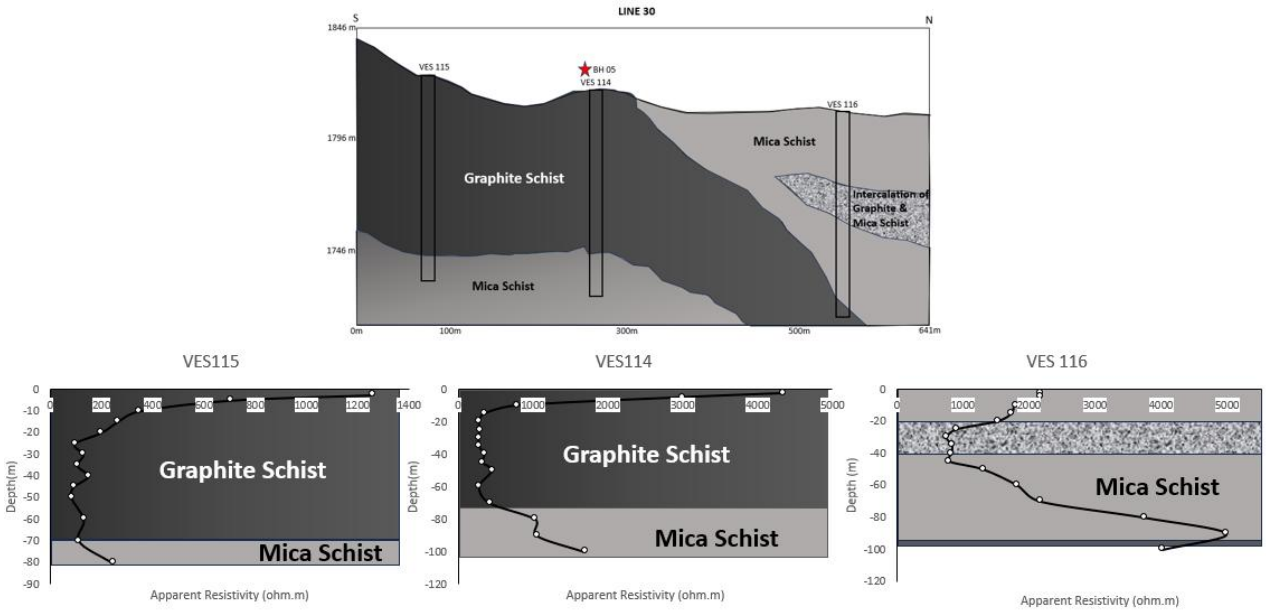

Figure 7.39: Cross section on the basis of VES Survey of Line 30

Line 13: Interpretation of VES data indicates the presence of a prominent conductive zone at VES 44 (~17m depth) and VES 45 (~ 33m depth), characterized by a resistivity value of approximately 15.7 ohm·m and an estimated thickness of nearly 40 m. This low-resistivity horizon is interpreted to represent a graphite-bearing conductive layer. In contrast, VES stations 46, 47, 50 and 51 exhibit comparatively higher resistivity values, suggesting either reduced graphite concentration, transition into less conductive host rock.VES Profiles have been attached in Annexure XX.

Line 14: A total of seven Vertical Electrical Soundings (VES 48,49,52,53,54,55,56) were conducted along Line 14 to evaluate subsurface resistivity variations within the eastern graphite band. The interpretation reveals a relatively low-resistivity zone at VES 49 (~5 m depth) and 54 (~30 m depth), characterized by an average thickness of approximately 10 m and 70 m respectively and resistivity values around 139 -175 ohm·m. This moderately conductive horizon may indicate the presence of graphite-bearing or altered lithological zones. In contrast, VES stations 48, 52, 53 and 56 exhibit comparatively higher resistivity values, suggesting resistive country rocks, reduced graphite content, or absence of significant conductive mineralization.VES Profiles have been attached in Annexure XX.

Line 17: Total five VES (VES 74, 75, 78, 79, 80) have been done here with resistivity high. No significant conductive zone identified.VES Profiles have been attached in Annexure XXII.

Line 18: Total seven VES (VES 67, 68, 69, 70, 71, 72, 73) have been done with high resistivity. No significant conductive zone identified.VES Profiles have been attached in Annexure XX.

Self-Potential (SP) Survey

In the western part of the Kalimath Graphite Block, one Self Potential (SP) profile (Line 15) was conducted to delineate conductive subsurface zones associated with graphite mineralization (Figure 7.40). The SP measurements show a pronounced negative anomaly, with values reaching up to –82 mV (Figure 7.41).

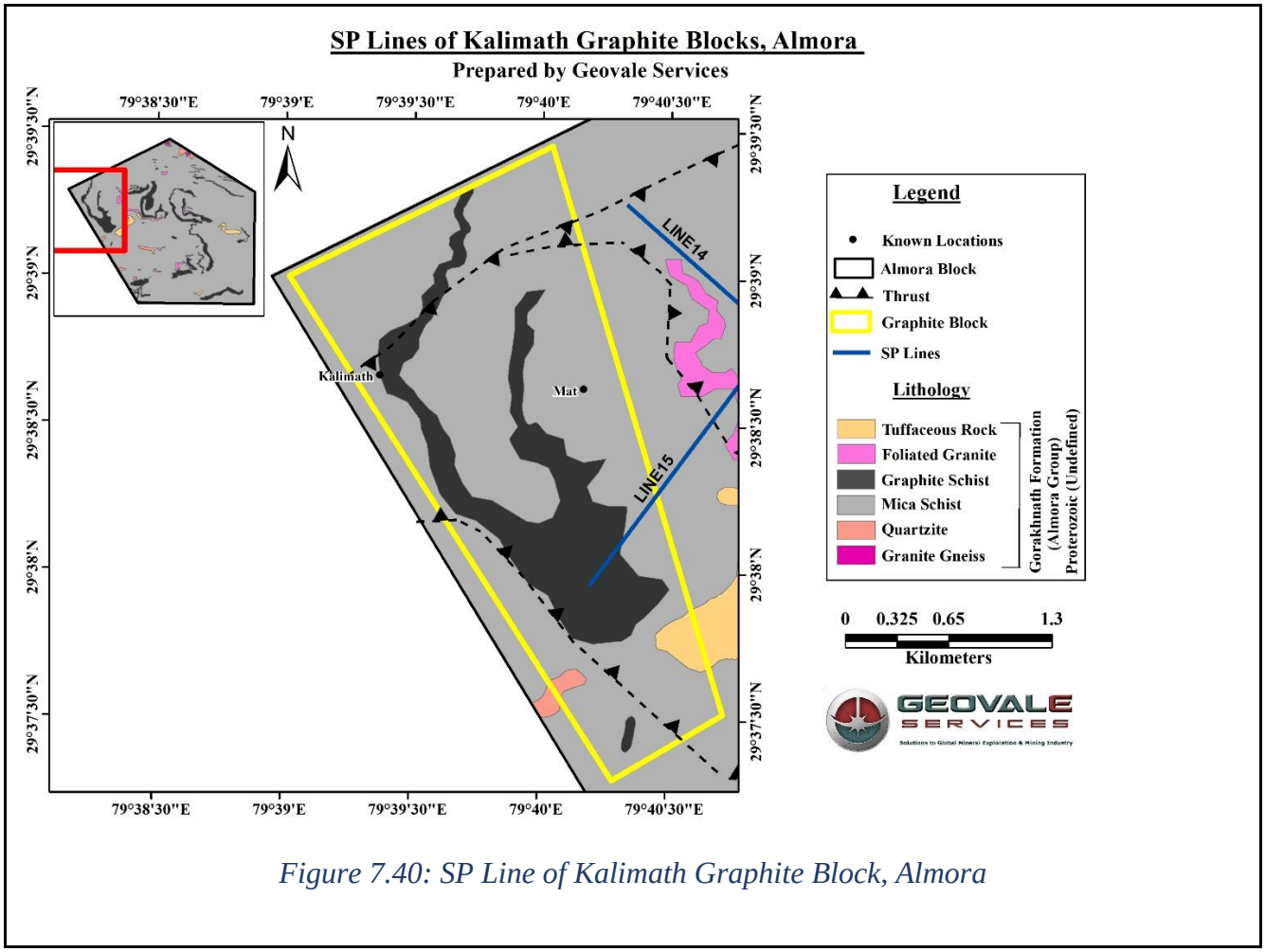

Figure 7.40: SP Line of Kalimath Graphite Block, Almora

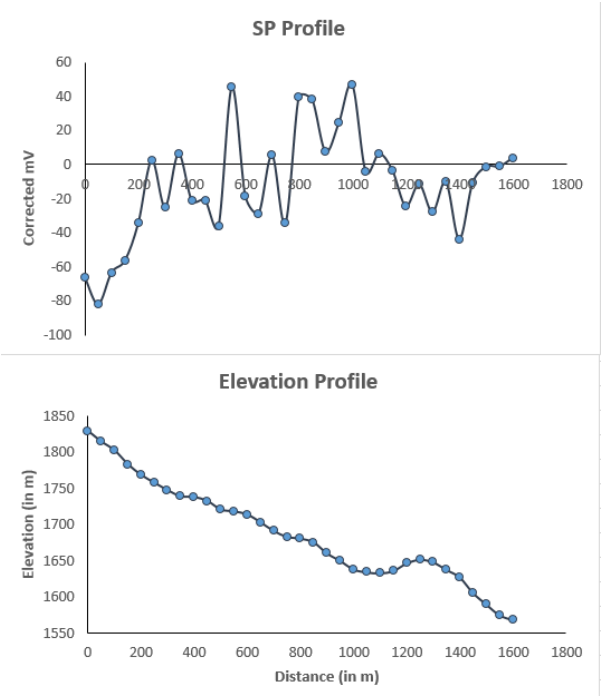

Figure 7.41: SP and Elevation Profile of the Kalimath Graphite Block, Almora

7.3.5 Qualitative Features and Analytical Results

Western Part:

The Tumbler Test carried out in the field in the western part of Kalimath-Mat indicates generally moderate flake size, primarily due to intercalation with mica schist in the host rock, which restricts the development and preservation of larger graphite flakes. However, locally some zones exhibit high flake size, suggesting limited pockets of better crystalline development.

Eastern Part:

The Tumbler Test carried out in the field, from the eastern part of the block, indicate moderate to high flake size, with certain zones showing relatively better flake development. In some locations, graphite occurs in nodular form and is mixed with water, suggesting secondary alteration or weathering effects that may influence flake integrity and recovery.

- **Modal analysis**
- **Surface modal analyses shows the presence of the**
- **Jumbo to Coarse Fraction:** 95.96% area is occupied by the Jumbo graphite flake, with 1.23% area with coarse flakes.
- **Predominantly Very Fine-Grained:** 0.25% area is occupied by the medium graphite flakes, 1.03% area with fine and 1.53% area is occupied by the very fine flakes of graphite.

(Figure 7.42, Figure 7.43).

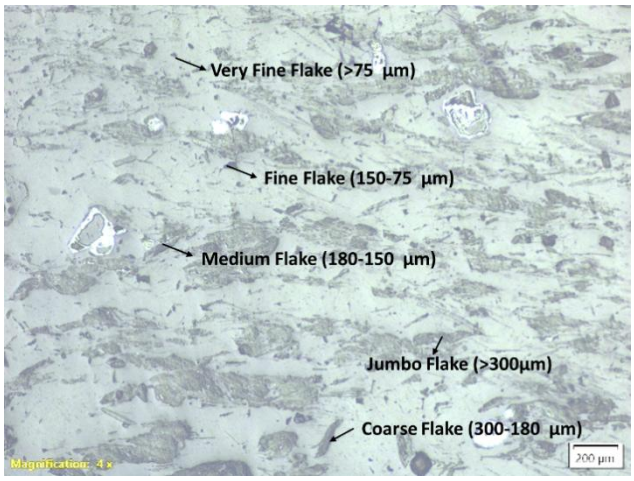

Figure 7.42: Modal analyses for the surface Graphite Schist thin section, near Mat area (Sample Id 109245).

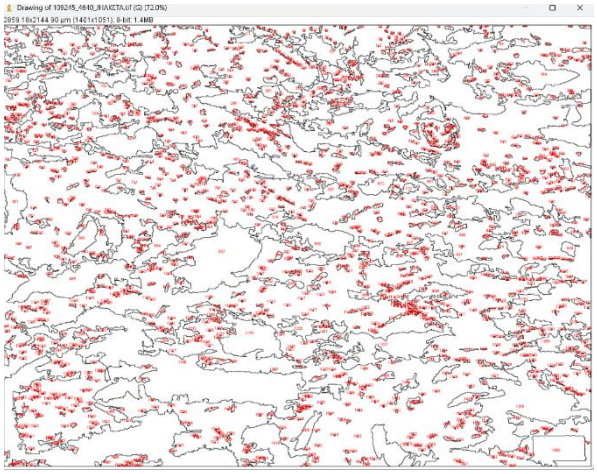

Figure 7.43: Modal analyses counting for the surface Graphite Schist thin section, near Mat area (Sample Id 109245).

Geochemically, the analysed sample from the western part shows a fixed carbon (FC) value (Figure 7.44) of 4.44% and volatile matter (VM) of 4.51%, indicating low to moderate graphite grade. No sulphur analysis is available for this portion. Redox indicators observed in the field include the presence of pyrites and sulphate enrichment, suggesting reducing conditions favourable for graphite formation. The ash content is 90.81%, indicating a high proportion of gangue material. The impurity level is also significantly high, with 67.21% silica (SiO_2), reflecting strong siliceous association and low graphite purity (Figure 7.45).

The fixed carbon (FC) values (Figure 7.44) from surface graphite samples range from 6.54% in the central, 5.20% in the northern, to 3.46% in the southern zone of the eastern part. The volatile matter (VM) also shows variation, with values of 6.41% (central), 3.91% (northern) and 4.32% (southern), suggesting heterogeneity in organic maturity and composition. Sulphur (S) content from ranges between 0.0184 and 0.320 ppm, indicating minor sulphide presence. Redox conditions are supported by the presence of pyrites and pyrite pits, confirming reducing depositional environments. The ash content is consistently high, varying from 90.59% (northern), 86.65% (central), to 92.01% (southern), indicating dominance of non-carbonaceous material. Impurity levels are also very high, with silica (SiO_2) ranging from 73.26% to 83.765%, associated with graphite schist intercalated with cherty quartz, which adversely affects graphite quality (Figure 7.45).

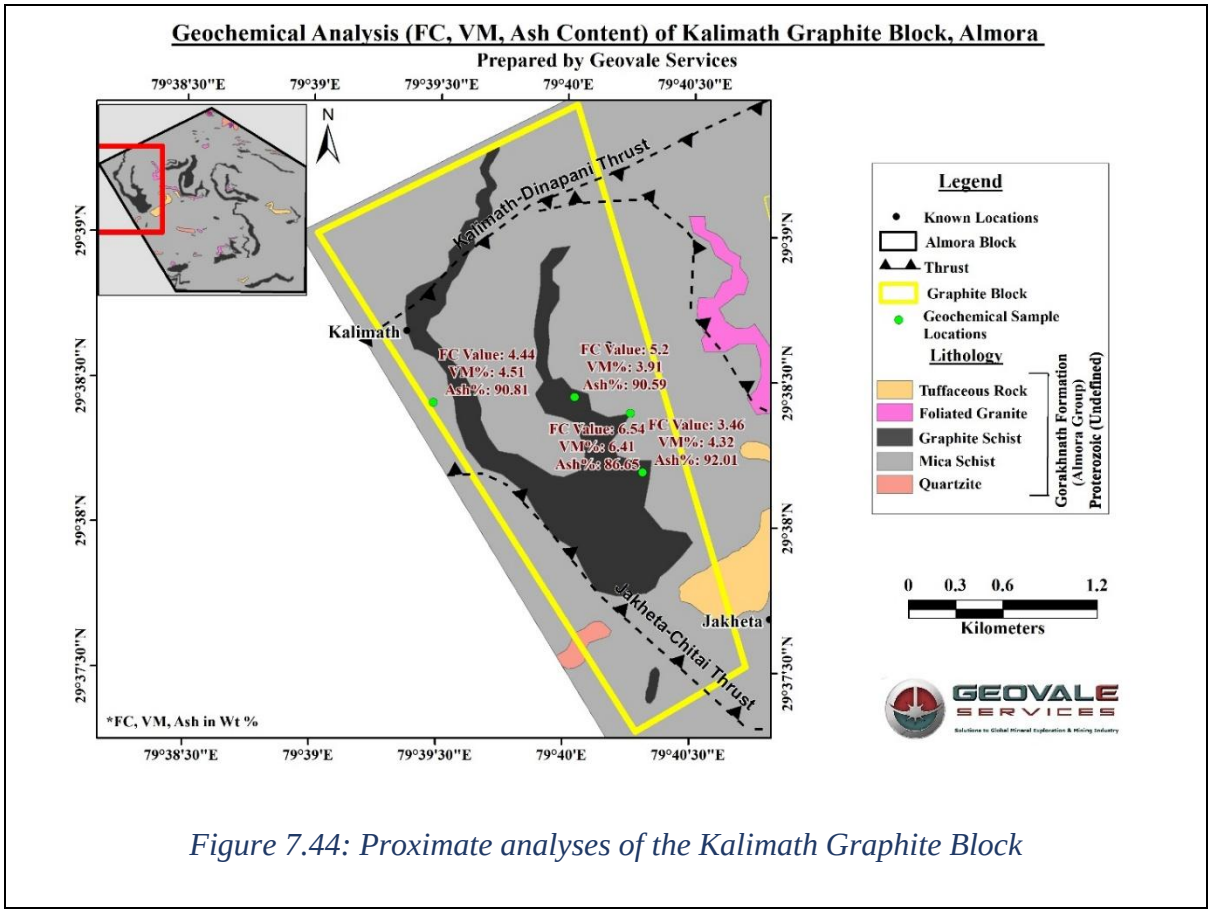

Figure 7.44: Proximate analyses of the Kalimath Graphite Block

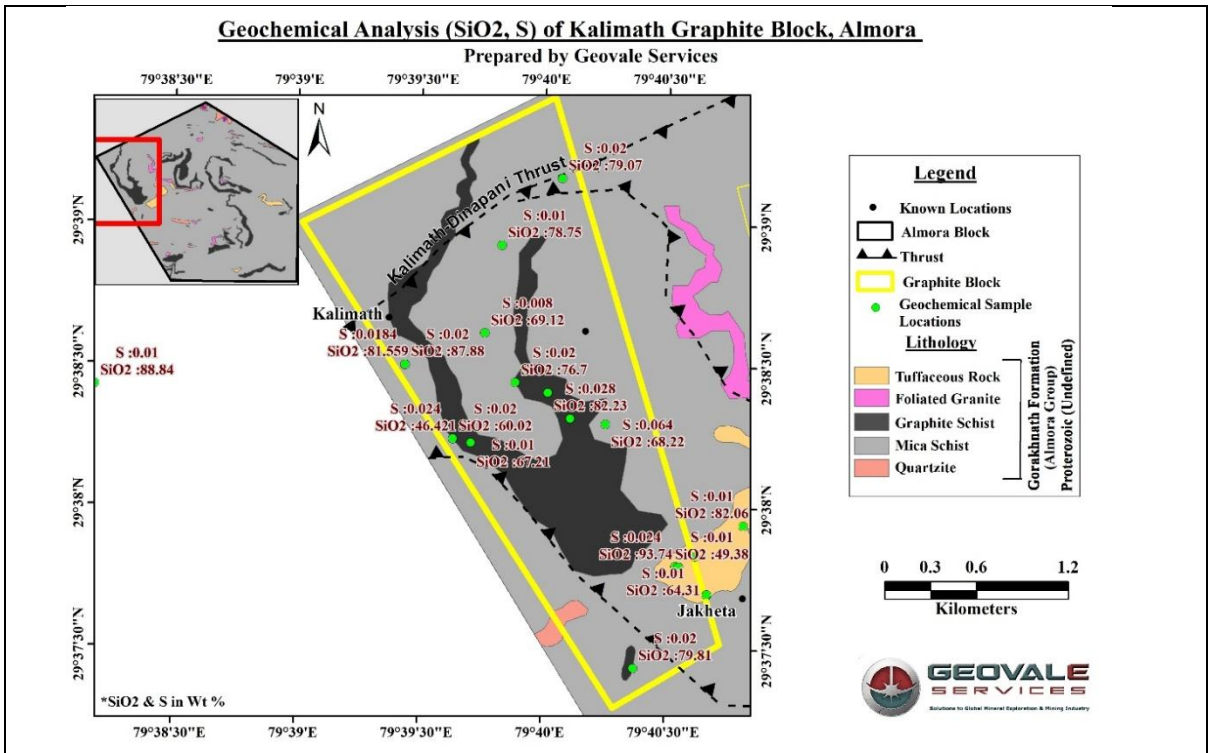

Figure 7.45: Geochemical analyses for S and SiO2 from Graphite schist, Kalimath Graphite Block.

Surface Vanadium and other elemental values: Out of 3 graphite schist samples from the east part of the Kalimath Graphite Block, 2 samples show anomalous Vanadium (1153 ppm and 2765 ppm), Mo upto 47 ppm in ICPMS analyses (Figure 7.46).

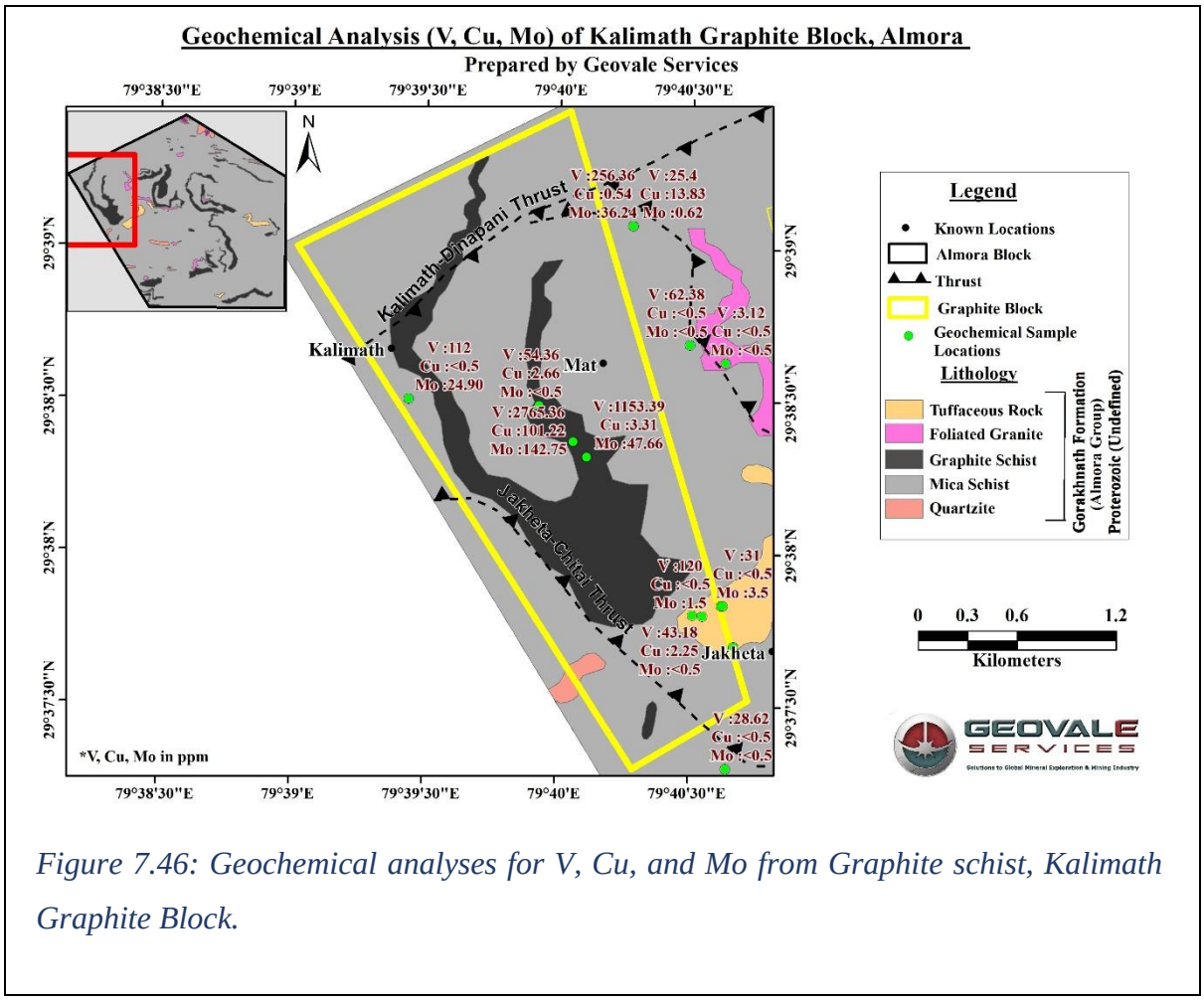

Figure 7.46: Geochemical analyses for V, Cu, and Mo from Graphite schist, Kalimath Graphite Block.

7.3.6 Subsurface Characterization:

One core-drilling (BH05) (29.641725, 79.665825) has been carried out in the eastern part of the Kalimath Graphite Block (65.5 m) indicates a graphite-bearing zone with a total true thickness of 48.65 m, Borehole information there are two graphite bands with occurring at the depth from 22.9 to 45.67 m. width the borehole thickness of 22.77 m and true thickenss of 21.66 m Other band starts from depth 46.62 m to 75 m with borehole thickness of 28.38 m and true thickness of 26.99 m.

In the eastern band, subsurface flake size analysis indicates a moderate to high flake size overall, as inferred from the tumbler test from drill core samples, suggesting good mechanical preservation of graphite flakes.

Modal analysis of thin sections of drill core samples reveals that the graphite comprises jumbo flakes, 300 µm flake size occupy about 99.47% of the area. 300 – 180 µm flake size occupies

about 0.15% of the area. Flake size between 180 – 150 µm occupies about 0.06% of the area. Flak size between 150 – 75 µm occupies about 0.13% of the total area. Flake size <75 µm occupies about 0.19% of the area.

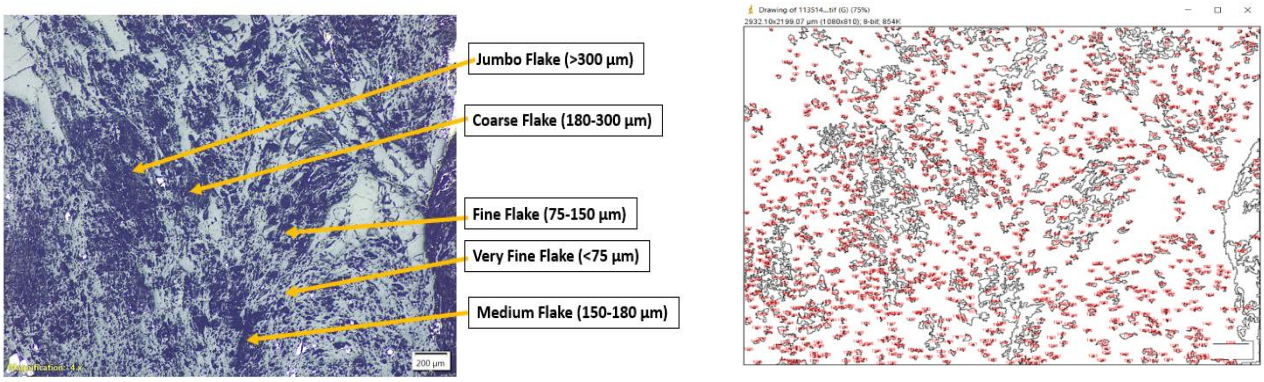

Figure 7.47: Modal Analysis to identify graphite flake size and graphite grain of Sample Id 113514 (BH-05), count by Image J software.

Subsurface Vanadium value from ICPMS: In the BH05, the graphite samples show anomalous Vanadium values (1170, 2089, 2443, 3486, 909, 3739 and 1502 ppm) (Annexure XXV). In borehole Zinc has 2368, 1478, 1724 ppm, Se 7-28 ppm, Mo upto 119 ppm, Ag upto 17 ppm and Cu upto 239 ppm, Bi upto 0.89 ppm.

Subsurface geochemical analysis: XRF data reveals variable sulphur content ranging from 1761.98 ppm (6–7 m) to significantly elevated values of 57664.8 ppm (72–73 m), suggesting localized sulphide enrichment at depth.

Geologically, the zone is characterized as highly to moderately weathered, with prominent pyrite pits and visible pyrite mineralization, consistent with the elevated sulphur values. The impurity content (silica, alumina, etc.) is relatively high, estimated at ~40–60%, suggesting significant gangue material within the graphite-bearing horizons.

7.3.7 Raman and XRD Data:

Based on two Raman Samples (Annexure XV) from Borehole-5 (Sample Id 114228 and 114229) the graphite is characterised as vein type Graphite. One XRD Sample (Sample Id 114229) reveals a sample heavily dominated by Quartz, which accounts for approximately 90.00% of the mineralogical composition. The diffractogram shows a high-intensity primary peak for Quartz reaching nearly 20,000 counts at a position of roughly 26.6° 2θ. In addition to Quartz, the sample contains a minor amount of Muscovite (~08.00%) and a small fraction of Pyrite (~02.00%).

7.4 Phalsima-Pithauni Graphite Block, Almora:

7.4.1 Site Characteristics

The Phalsima–Pithauni Graphite Block lies in the southern part of the Almora G4 block, in the vicinity of Phalsima, Pithauni, Sironiya and Biraura villages. The block encompasses four mappable graphite bands: three within the Phalsima area (north, central and south) and one near Pithauni (Figure 7.48). Road access is available from Almora via NH 309A and 309B, supplemented by connected village roads.

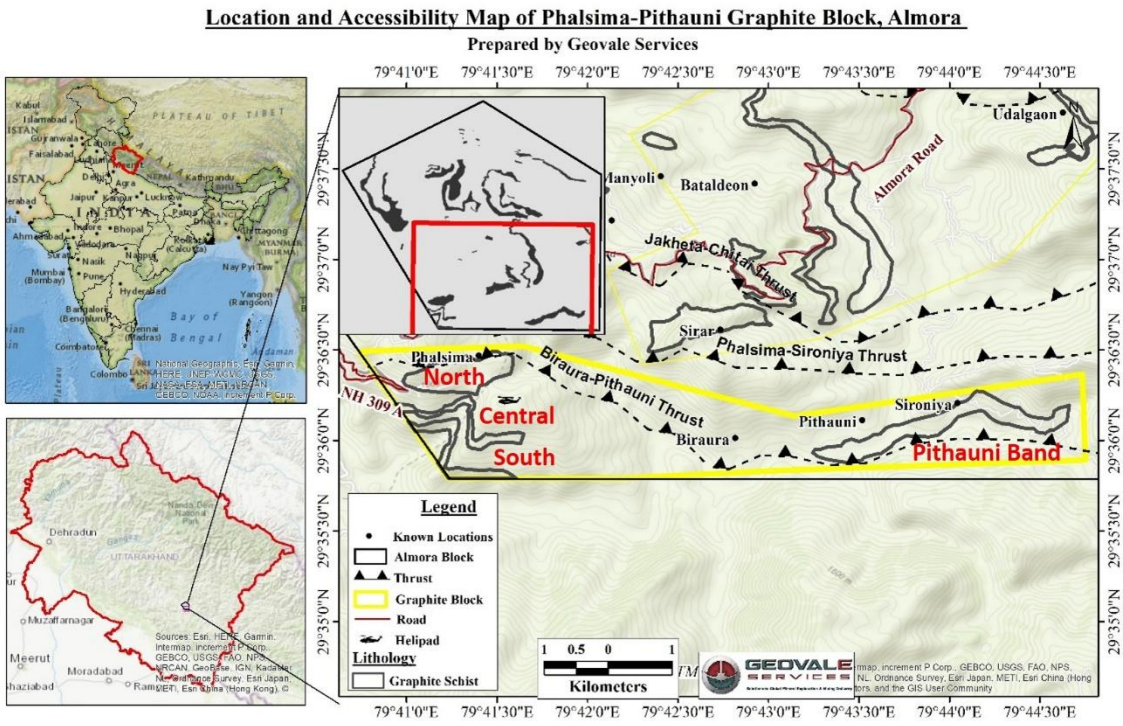

Figure 7.48: Accessibility map of Phalsima -Pithauni Graphite Block.

Topographically, near the Phalsima area slopes down toward the south-west (~1300 m) from north-east (~1600 m). Overall, the graphite-bearing area situated at moderate elevations between roughly 1100 and 1600 m, with uneven and occasionally steep slopes (Figure 7.49). LULC map shows the most of the area occupied by the rangeland, crops and little bit of vegetation (Figure 7.50). Drainage is dendritic type and is mainly by first-order seasonal channels, springs and short feeder gullies draining away from the ridges are present near Phalsima area whereas near Pithauni area 5 and 6 th ordered drainage is present (Figure 7.51). The Pithauni area has lower elevation (680-1200 m) with presence of the mainly 5 and 6 ordered streams (Figure 7.52). Habitation mainly found around Phalsima and Pithauni villages.

Forest area is open forest (0.1194 sq. km.), Reserved Forest (0.1219 sq. km.) and a few Van Panchayat lands.

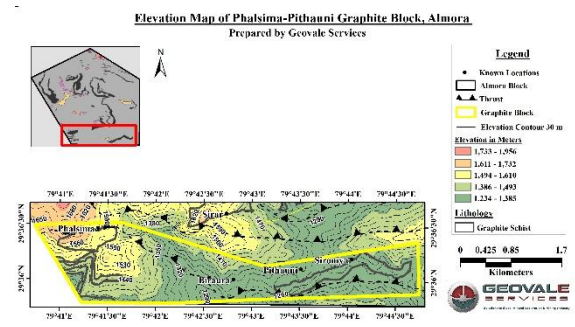

Figure 7.49: Elevation map of the Phalsima-Pithauni Graphite Block, Almora.

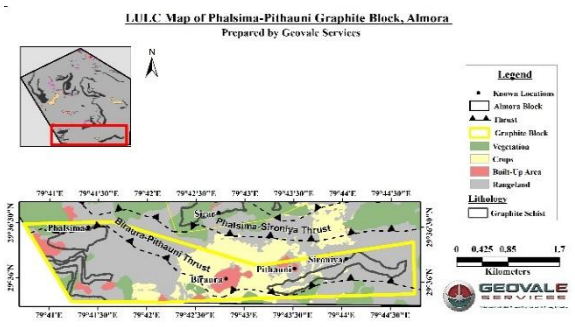

Figure 7.50: LULC map of the Phalsima-Pithauni Graphite Block, Almora.

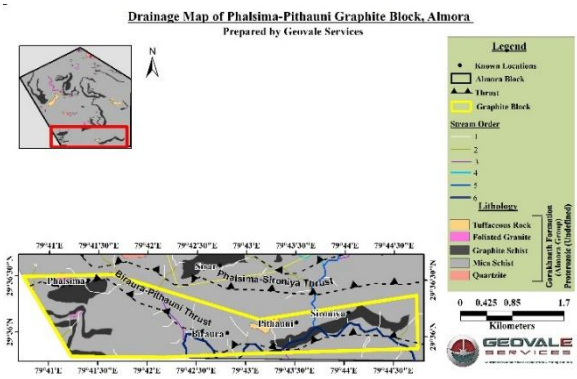

Figure 7.51: Drainage map of the Phalsima-Pithauni Graphite Block, Almora.

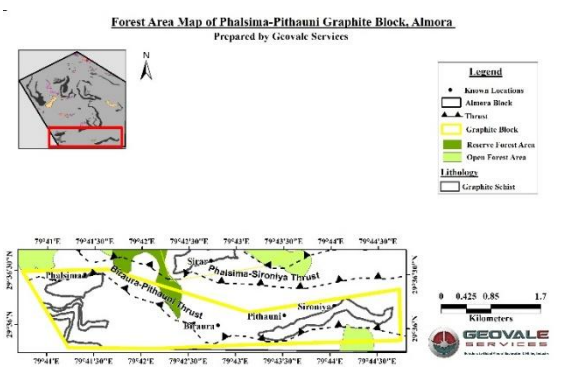

Figure 7.52: Forest map of the Phalsima-Pithauni Graphite Block, Almora.

Below the Table contains details of the Phalsima-Pithauni Graphite Block (Table 7.6).

Table 7.6: Details of the Phalsima -Pithauni Graphite Block

Parameters	Phalsima-Pithauni Graphite Block
Area	9.19 sq. km.
Toposheet No.	53O/10
Accessibility	Road-accessible from Almora through NH 309A and 309B.

Parameters	Phalsima-Pithauni Graphite Block
Topography and elevation	Undulatory to moderately steep hill terrain (680-1600 m).
Slope character	Moderate.
LULC	Vegetation and rangeland dominant; local cropland and settlement patches occur around Phalsima and Pithauni areas.
Forest and land status	Open forest and Van Panchayat land.
Habitation	Moderate habitation sensitivity in and around Phalsima and Pithauni villages.
Drainage and water	First-order streams and springs; dendritic drainage, near Phalsima and 5 to 6 ordered drainages near Pithauni.

7.4.2 Geological and Resource Characterization

The Phalsima-Pithauni Graphite bands are surrounded by the mica-schist. Near Phalsima are 3 mappable graphite band are present: north (linear), central (folded) and south (folded) band whereas one band (almost linear, E-W trending) is present near Phithauni area. The foliation in the graphite-bearing bands dips very gently, about 3 degrees to 15 degrees, toward the north-east.

The Phalsima-Pithauni Graphite Block covers about 5.59 sq. km (area of the total mappable 4 graphite bands are 0.511 sq. km), the detail of each band extension is given below (Table 7.7).

Table 7.7: Details of areal extension of the Phalsima -Pithauni Graphite Block

Bands	Approx. strike length (km)	Average or mapped width	Approx. mapped area (sq. km.)	Interpretation
North Band Phalsima	0.997	Variable width, ranges between 0.122 and 0.388 km, avg. 0.2597	0.259	Elliptical band with largest volumetric component.

Bands	Approx. strike length (km)	Average or mapped width	Approx. mapped area (sq. km.)	Interpretation
Central Band Phalsima	1.736	Very narrow width of the band, about 0.0581 km	0.101	Folded band with excellent strike persistence with variable width.
Southern Band Phalsima	1.611	Variable width, rnges between 0.036 and 0.136 km, avg. 0.069 km	0.112	Folded band with variable width.
Pithauni Band	2.613	Variable width, ranges between 0.2242-0.099 km, avg. 0.153 km	0.0397	Almost E-W trending linear band

7.4.3 Road section of the Phalsima -Pithauni Graphite Block:

Road section of Phalsima and Pthauni area are showing below (Figure 7.53, Figure 7.54, Figure 7.55).

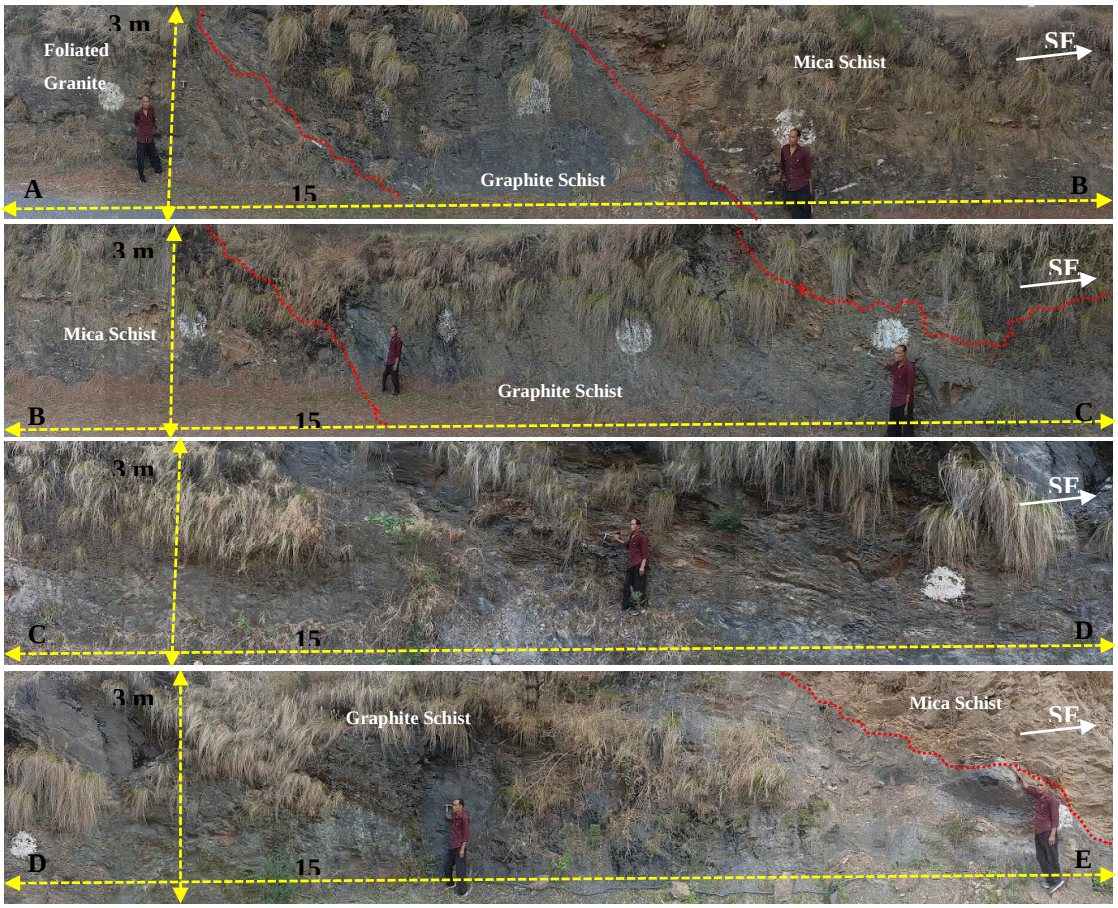

Figure 7.53: Road section of the Phalsima area.

Figure 7.54: Details of Graphite Schist in road section of the Phalshima area.

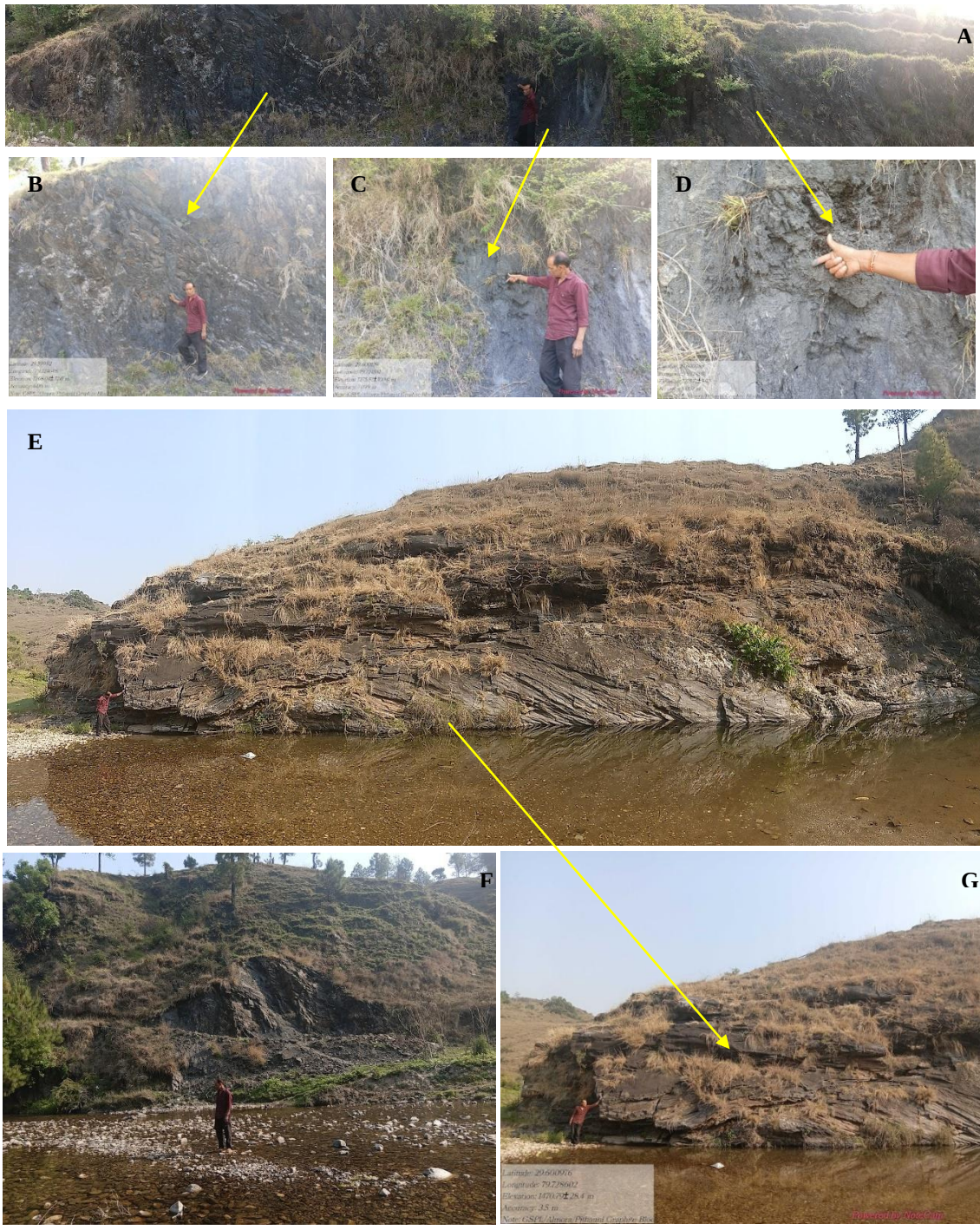

Figure 7.55: Road section and river section of Pithauni area with details of Graphite Schist, near BH06.

7.4.4 Geophysical Data Analyses (VES) Of the Phalsima-Pithauni Graphite Block:

North Band

A total of three VES profiles (Line 02, 03 and 37) were conducted along the north graphite band to delineate subsurface conductive horizons associated with graphite mineralization (Figure 7.56, Figure 7.57).

Line 2: Three VES stations (VES 02, 03 and 09) were carried out along Line 2. Interpretation of the sounding data indicates the presence of a prominent conductive zone at VES 02 and VES 03, having a probable thickness of approximately 55–60 m with apparent resistivity values ranging between 38–56 ohm·m (at depth ~20-35m) These low resistivity signatures are indicative of graphite-bearing formations or conductive lithological units. In contrast, VES 09 exhibits comparatively higher resistivity values, suggesting either thinning of the conductive horizon or transition into resistive country rock.

Line 3: Four VES stations (VES 06, 07, 08 and 11) were conducted along Line 3. The interpretation shows that VES 08 contains a conductive layer with an estimated thickness of about 40 m (depth ~60 m from surface) and an apparent resistivity of approximately 68 ohm·m, indicating a probable graphite mineralized zone. VES 06 displays consistently low apparent resistivity values (< 200 ohm·m) extending up to a depth of nearly 100 m, suggesting the presence of a thick conductive formation or persistent graphite-rich lithology at depth. However, VES 07 and VES 11 show relatively higher resistivity responses, implying dominance of resistive host rocks or limited conductive mineralization along this location.

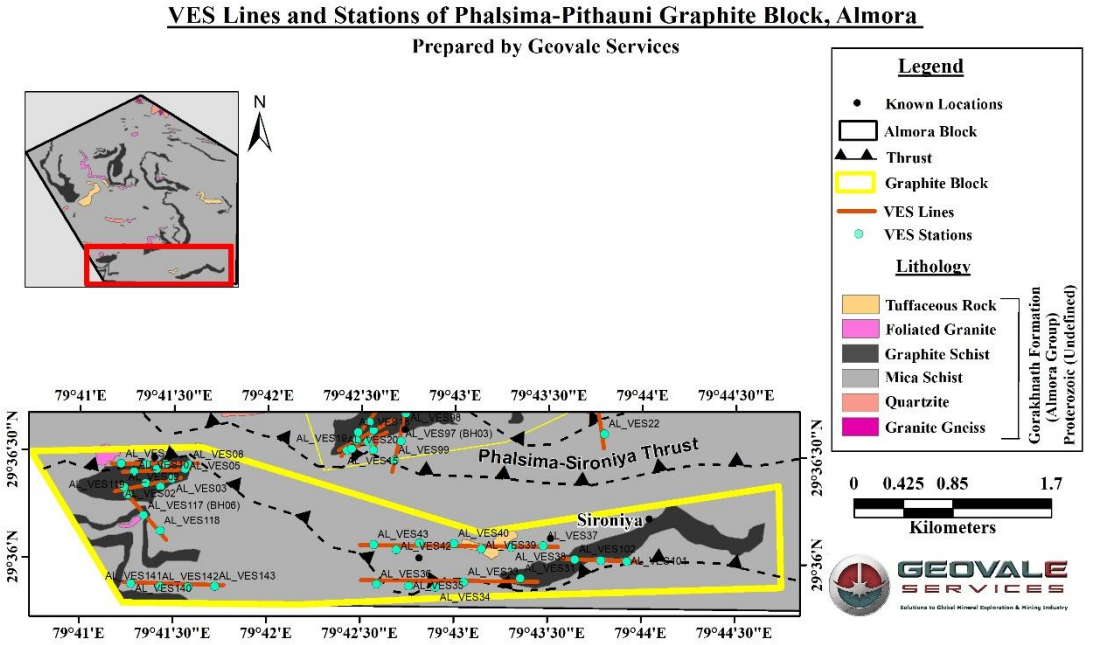

Figure 7.56:VES profile of the Phalsima-Pithauni block.

Line 37: Three VES stations were completed along Line 37. VES 05 and VES 10 predominantly show high resistivity characteristics, indicating resistive lithologies and absence of significant conductive horizons. In contrast, VES 04 reveals two distinct conductive zones (one at depth of 100 m and another one at 130 m depth): A shallow conductive layer approximately 20 m thick with apparent resistivity around 64 ohm·m and A deeper and more significant conductive horizon about 60 m thick, exhibiting very low apparent resistivity (~15 ohm·m). These conductive responses strongly suggest the presence of graphite mineralization and represent a promising exploration target.

A significant conductive zone is identified with thickness ranging from ~20 m to ~60 m, occurring at depths between approximately 20 m and 130 m across different VES stations. These zones are characterized by low apparent resistivity values (≈15–68 ohm·m), indicating potential graphite-bearing formations or other conductive lithologies.

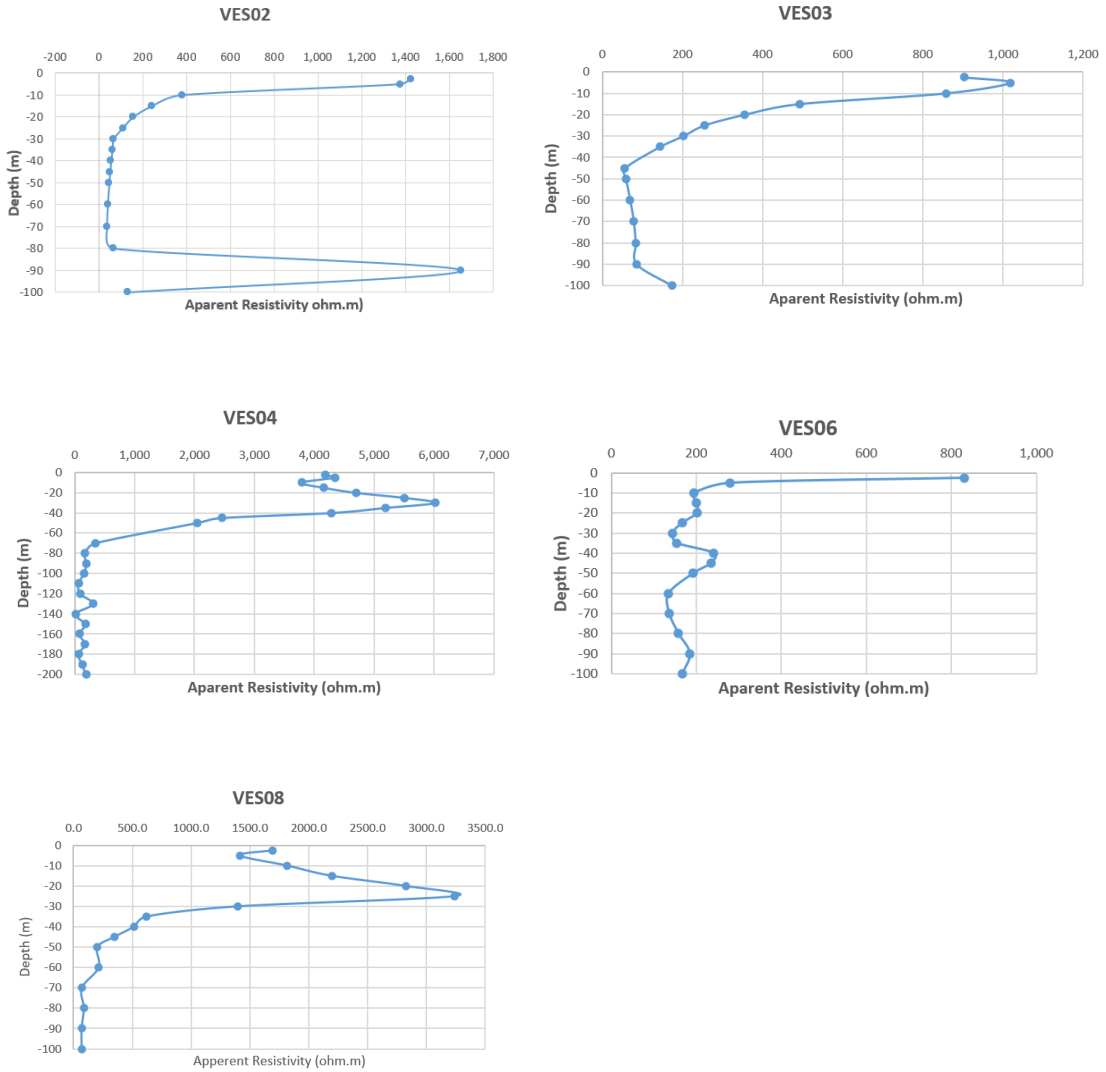

Figure 7.57: VES Profiles with low resistivity zone identified, Phalsima north band, Almora.

Central Band

Only one VES profile (Line 29) was conducted along the graphite band comprising three VES stations (VES 117, 118 and 119).

Interpretation of the resistivity data of VES 117 (Figure 7.58) reveals a well-defined conductive zone with an estimated thickness of approximately 50 m (depth ~10 m) and apparent resistivity values reaching up to 30 ohm·m, suggesting the presence of a graphite-bearing or conductive lithological horizon. At VES 119, a comparatively deeper conductive layer at a depth of 40-45m with thickness of 5 m, is identified, exhibiting apparent resistivity values around 21 ohm·m, which may represent a localized graphite-rich or altered zone. In contrast, VES 118

shows relatively higher resistivity values compared to adjacent stations, indicating resistive country rock.

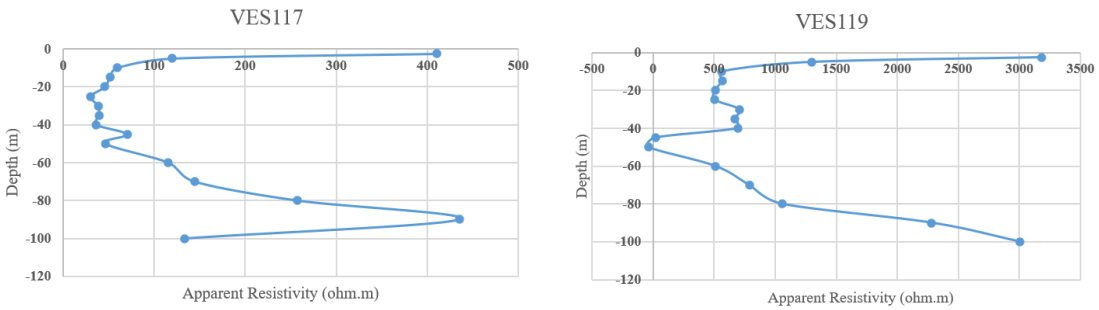

Figure 7.58: VES Profiles of VES117 and VES119 with low resistivity zone identified, Phalsima central band, Almora.

Southern Band

A single VES profile (Line 19) was conducted outside the graphite band within the Mica Schist host rock to establish a comparative resistivity framework and correlate apparent resistivity responses with those observed over the graphite mineralized zone.

A total of four VES stations (VES 140, 141, 142 and 143) were executed along this profile (Figure 7.59). Interpretation of the sounding data indicates consistently high resistivity values at all stations. These results are characteristic of resistive schistose lithologies and confirm the absence of significant conductive horizons in this sector.

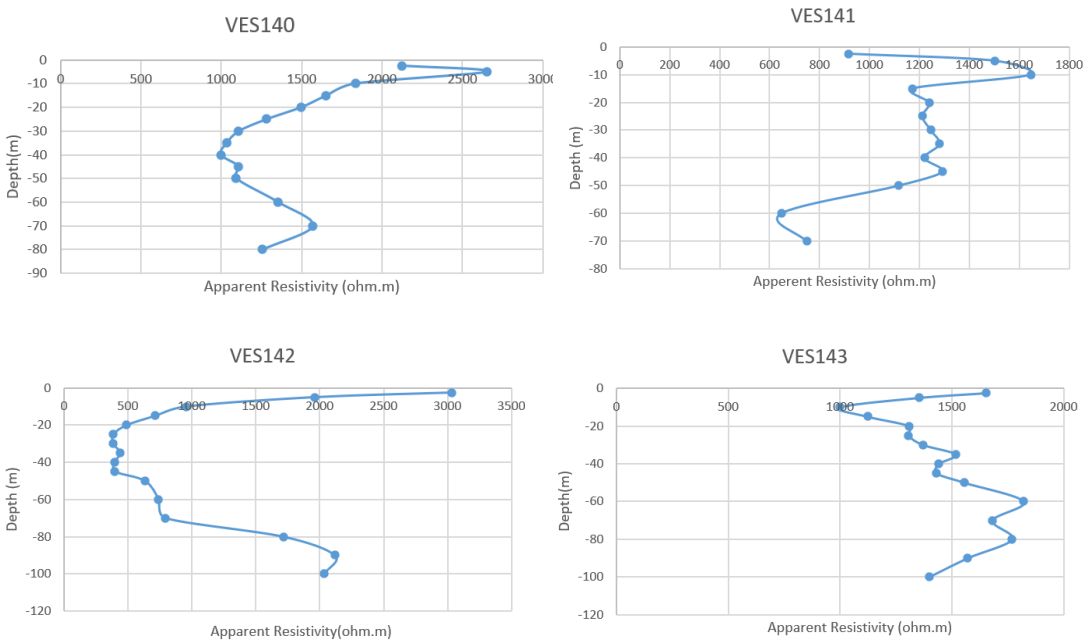

Figure 7.59: VES Profiles of VES140, VES141, VES142, VES143 with low resistivity zone identified, Phalsima southern band, Almora.

Self-Potential near Phalsima Area:

Two Self Potential (SP) profiles were conducted across the three graphite bands to delineate conductive zones associated with graphite mineralization (Figure 7.60).

Line 04: The SP data along Line 04 exhibit strong negative anomalies, with values reaching up to –259 mV. Such intense negative SP responses indicate the presence of highly conductive subsurface horizons, most likely corresponding to graphite-rich bands or associated sulphide mineralization zones (Figure 7.61).

Line 13: SP measurements along Line 13 show negative potential values up to –128 mV, indicating the presence of conductive subsurface material. Although comparatively weaker than Line 04, the anomaly still reflects probable graphite-bearing horizons or zones of enhanced electrical conductivity (Figure 7.62).

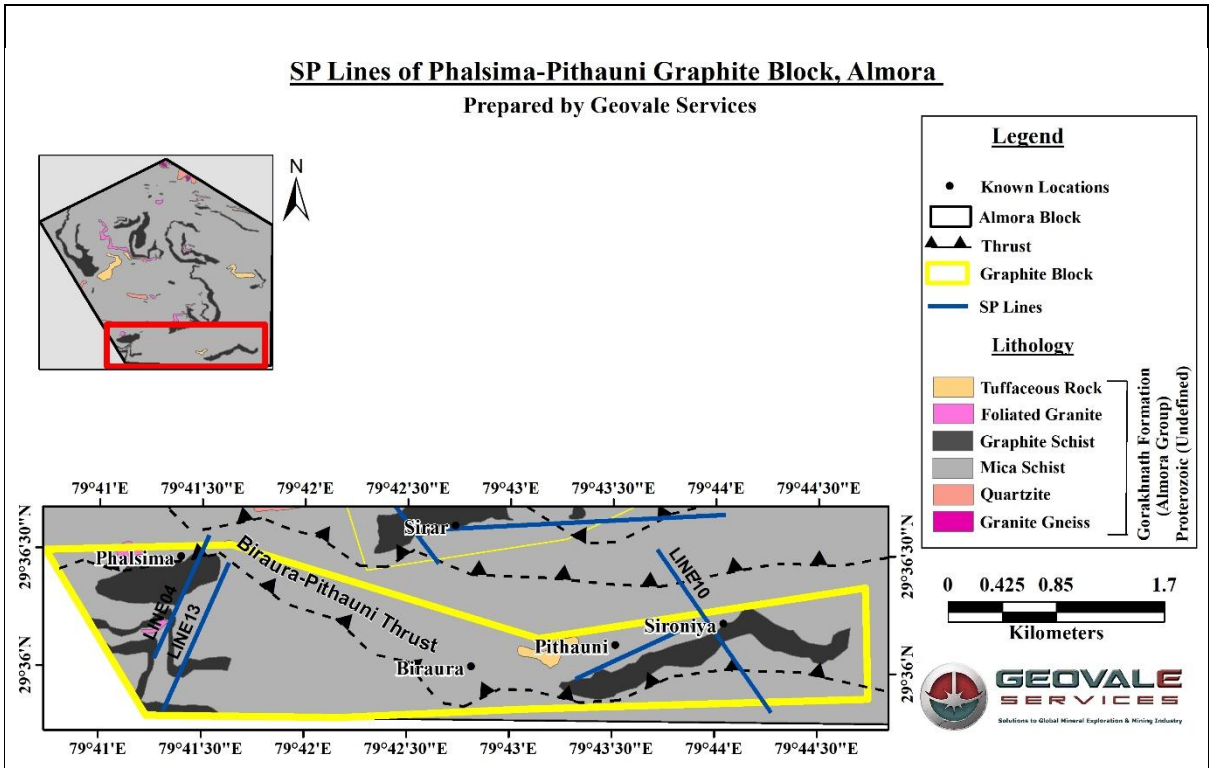

Figure 7.60: SP map of the Phalsima-Pithauni Graphite Block, Almora.

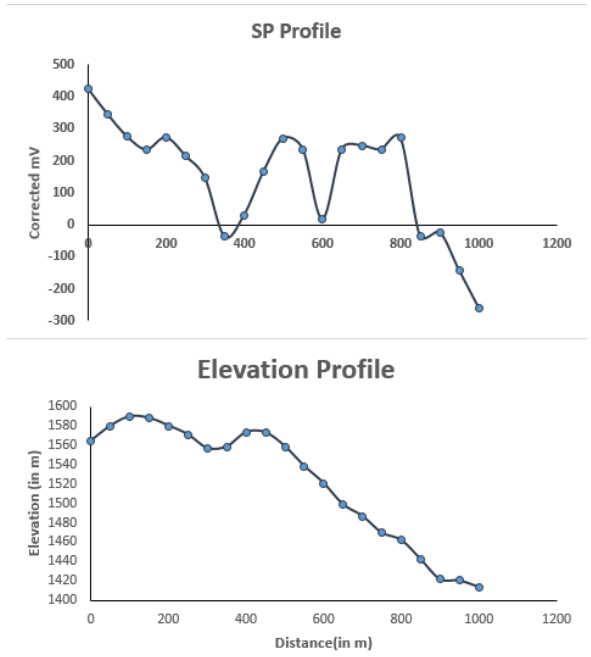

Figure 7.61: SP and Elevation Profile of Line 04

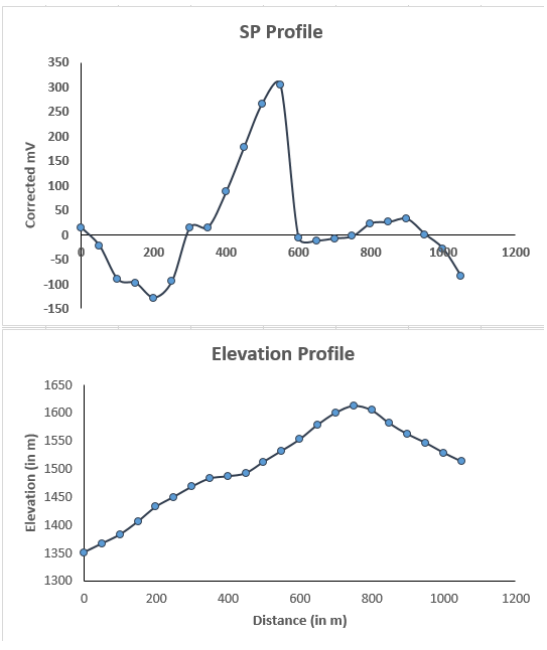

Figure 7.62: SP and Elevation Profile of Line 13

Geophysical survey at Pithauni area:

A total of three Resistivity (VES) profile lines (Line 09, Line 10 and Line 26) were conducted to evaluate subsurface resistivity variations and assess the continuity of graphite mineralization of Pithauni area.

Line 09: Five VES stations (VES 31, 33, 34, 35 and 36) were carried out. Interpretation indicates that VES 33 to VES 36 exhibit higher resistivity values, suggesting dominance of resistive country rocks with limited conductive mineralization. In contrast, VES 31 (~20m depth), located in the vicinity of the graphite band, shows comparatively lower apparent resistivity (~200 ohm·m) (Figure 7.64), which may indicate weak conductive characteristics associated with graphite-bearing horizons.

Line 10: This profile consists of seven VES stations (VES 37, 38, 39, 40, 41, 42 and 43). All stations display consistently high resistivity signatures, which are interpreted to represent mica schist lithology.

Line 26: A total of three VES stations were conducted along Line 26 (Figure 7.63). VES 100 and VES 101 (Figure 7.64) show predominantly high resistivity responses, indicating resistive host rocks. However, VES 102 reveals a distinct low-resistivity zone (< 50 ohm·m) extending up to a depth of approximately 100 m, suggesting the presence of a substantial conductive horizon likely associated with graphite mineralization.

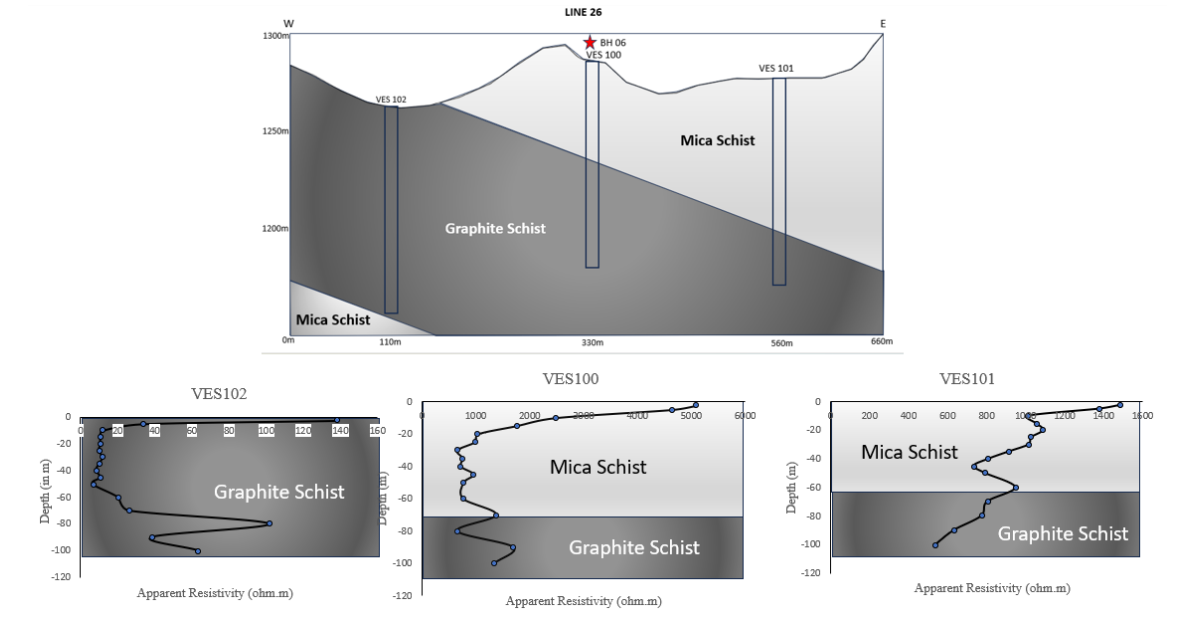

Figure 7.63: VES Profiles with low resistivity zone identified at VES Line 26 in Pithauni area, Almora.

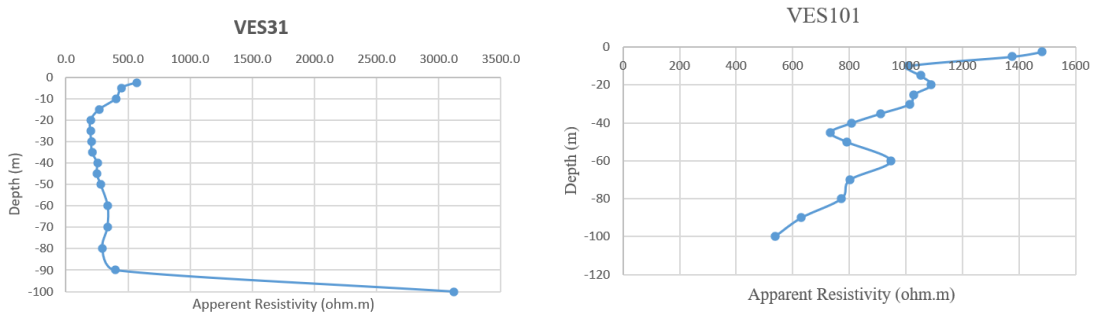

Figure 7.64: Profile of VES 31 and VES 101 show a low resistivity layer

Two Self Potential (SP) profile lines were executed across the Pithauni area.

Line 05: SP measurements along Profile reveal very strong negative potential anomalies, reaching values up to –853 mV in the vicinity of the graphite zone. The anomaly spatially coincides with graphite mineralization that has been physically identified during field mapping. (Figure 7.65)

Line 10: Another SP profile was conducted across the graphite band. The SP data show a pronounced negative anomaly of about –691 mV at the point where the profile intersects the graphite band (Figure 7.66).

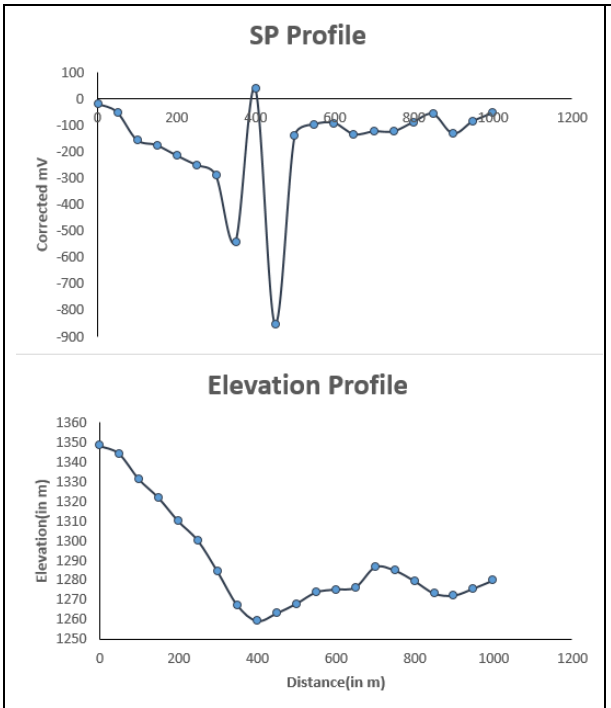

Figure 7.65: SP and Elevation Profile of Line 05

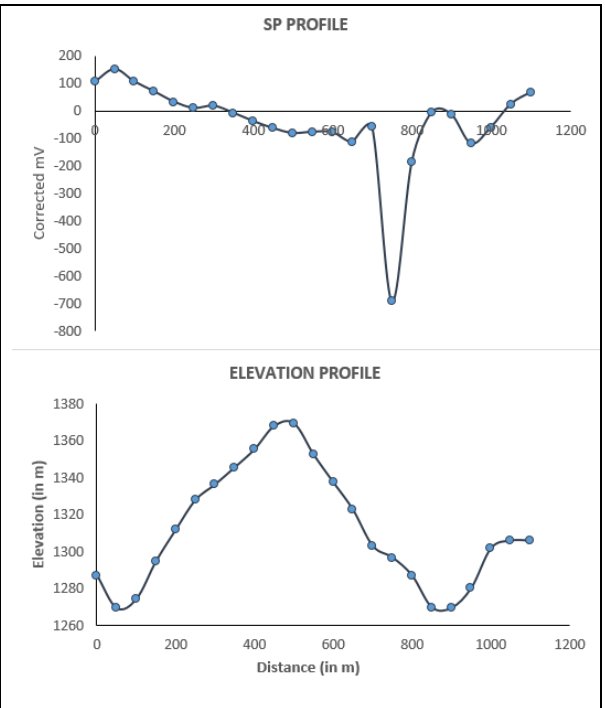

Figure 7.66: SP and Elevation Profile of Line 13

7.4.5 Qualitative Features and Analytical Results

Tumbler Test:

The Tumbler Test carried out in the field indicates that the North Band has overall high flake size with some locally moderate variations, suggesting strong durability and good resistance to mechanical degradation, with minor localized instability. The Tumbler Test carried out in the field southern band indicates consistently moderate flake size, reflecting uniform but comparatively lower resistance to degradation than the North Band. The Tumbler Test carried out in the field for central band indicates moderate to high values, reflecting the presence of almost good quality graphite.

Geochemically, one sample analysed from northern band which shows the fixed carbon (FC) value of 4.36% and very low volatile matter (VM) at 0.54%, indicating relatively better graphite quality. However, the ash content is very high (94.58%), reflecting significant non-carbonaceous material. The presence of pyrite and pyrite pits suggests sulphide mineralization under reducing conditions. One Raman analyses is carried out for bedrock graphite-schist specimen collected from North B29.605957 N, 79.692265 E (sample 109938) (Table 7.8). Three spot spectra from this sample show a highly stable first-order graphitic G band at 1578.9 to 1580.2 cm^-1 and a clear second-order 2D band at 2717.1 to 2728.9 cm^-1. A weak disorder band D is resolved at 1354.2 to 1360.9 cm^-1 in two of the three spots, whereas the third analysed spot shows no clearly resolved D band and therefore represents the most ordered graphite micro-domain in the sample. The defect-bearing spots also show a minor D' shoulder near 1620 to 1623 cm^-1. Approximate intensity ratios derived from the displayed spectral pick tables give I_D/I_G values of about 0.05 and 0.12 for the two spots in which D is resolved, while I_2D/I_G varies approximately from 0.60 to 0.76. These values are consistent with well-ordered crystalline graphite with low defect density and only limited spot-scale heterogeneity. The Raman result is therefore fully compatible with the field inference of crystalline flaky to locally coarse graphite in Phalsima. At the same time, Raman is a micro-domain method: it confirms structurally ordered graphite where the laser is focused, but it does not override the low bulk fixed-carbon and high-ash proximate results, which still show that the ordered graphite domains occur within a gangue-rich mica-quartz schist.

Table 7.8: Details of Raman spectrum of graphite sample (id: 109938) in Phalsima area.

Sample	Spot	G band (cm^-1)	D band (cm^-1)	2D band (cm^-1)	Approx. I_D/I_G	Approx. I_2D/I_G	Interpretation
109938	1	1580.17	1354.20	2728.89	0.05	0.64	Ordered graphite; weak disorder band and clear 2D response
109938	2	1579.70	1360.85	2723.53	0.12	0.60	Ordered graphite with slightly stronger local defect response
109938	3	1578.86	Not clearly resolved	2717.05	Not resolved / very low	0.76	Most ordered analysed micro-domain; D band effectively absent

Geochemical analysis one sample analyses central part of the Phalsima which reveals a lower FC value (3.01%) and higher VM (3.41%), suggesting reduced graphite purity and higher volatile content. For northern band FC value is upto 5.67%. Ash content is also high (93.25%). The occurrence of pyrite pits indicates similar sulphide association and redox conditions. Geochemically, FC and VM data are unavailable, but sulphur content is very low (0.028 ppm), suggesting minimal sulphide presence despite observed pyrite pits. A high silica content (66.54% SiO_2) indicates that the band is highly siliceous and less suitable for high-grade graphite extraction. Geochemically, one sample was analysed for southern band for FC value, the fixed carbon content of the Pithauni–Sironiya graphite deposit is inferred to be low (2.41%), primarily due to the extremely high proportion of silicate gangue minerals present in the ore. Although direct FC analytical values are not extensively available, the geochemical dataset indicates very high silica content ranging from ~59% to >95% SiO_2, which implies that the carbon fraction is correspondingly low because of the presence of cherty layer in graphite. The ash content of the deposit is extremely high, consistent with the silica-rich composition observed in the dataset. With SiO_2 values commonly between ~70% and 90% and reaching up to >95% in one analyzed sample. Fron XRF analyses, it is reported that the silica is the dominant impurity in the Pithauni graphite band, with recorded values ranging from ~59.38% to as high as ~95.2% SiO_2. This confirms a strong association with quartz-rich host rocks, particularly quartz-mica schist. In addition to silica, alumina-bearing minerals (derived from

mica) are also present, further contributing to the impurity load. The volatile matter content in the Pithauni–Sironiya graphite is inferred to be low to moderate, which is typical of metamorphic graphite deposits. VM value (1.52%) indicates the geological setting and degree of metamorphism relatively low volatile components (Figure 7.67, Figure 7.68). The northern band of the Phalsima shows the presence of 83 ppm V and in the Pithauni band V is up to 430 ppm and Mo up to 59 ppm (Figure 7.69).

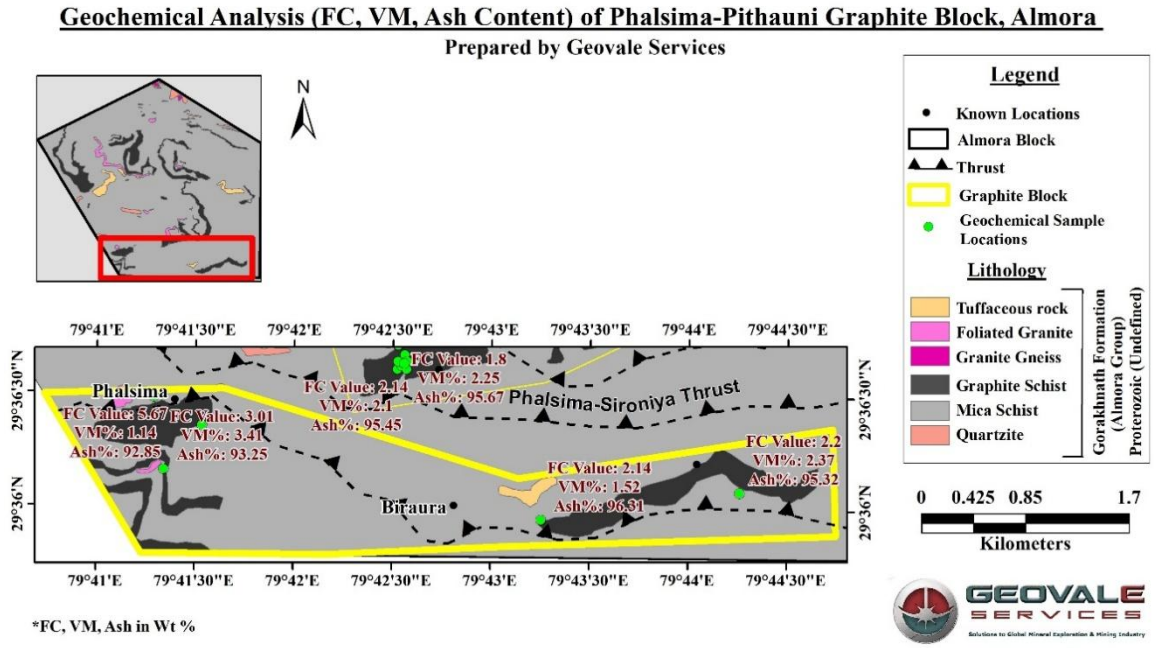

Figure 7.67: Geochemical analysis (FC, VM, Ash content) of Phalsima- Pithauni Graphite Block, Almora

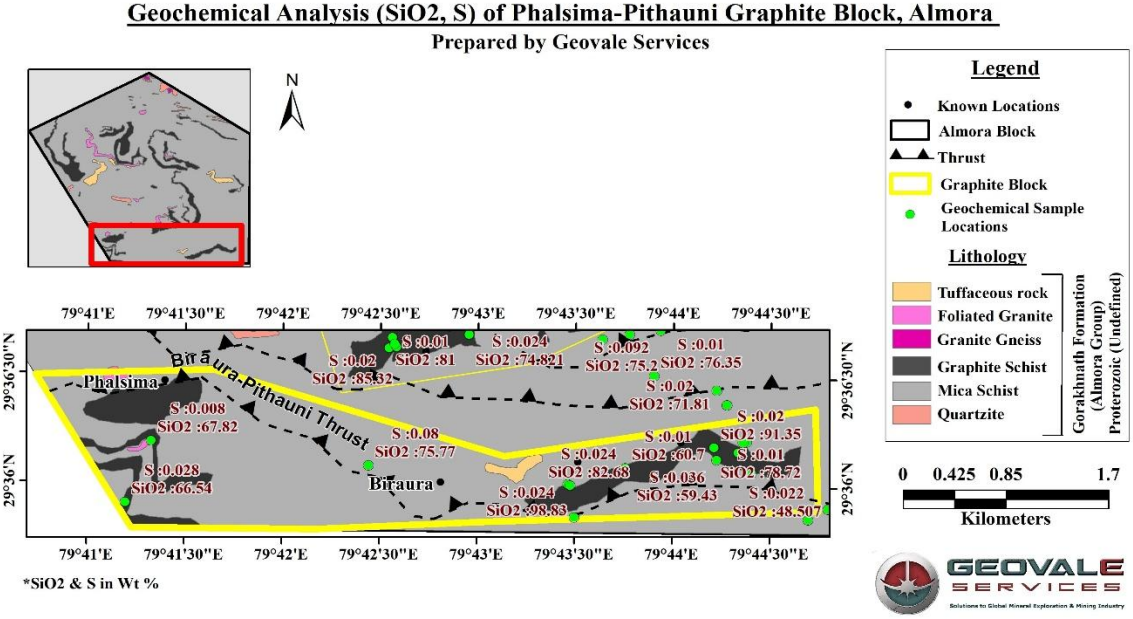

Figure 7.68: Geochemical analyses show S and SiO2 content of the Graphite, Phasima-Pithauni Graphite Block.

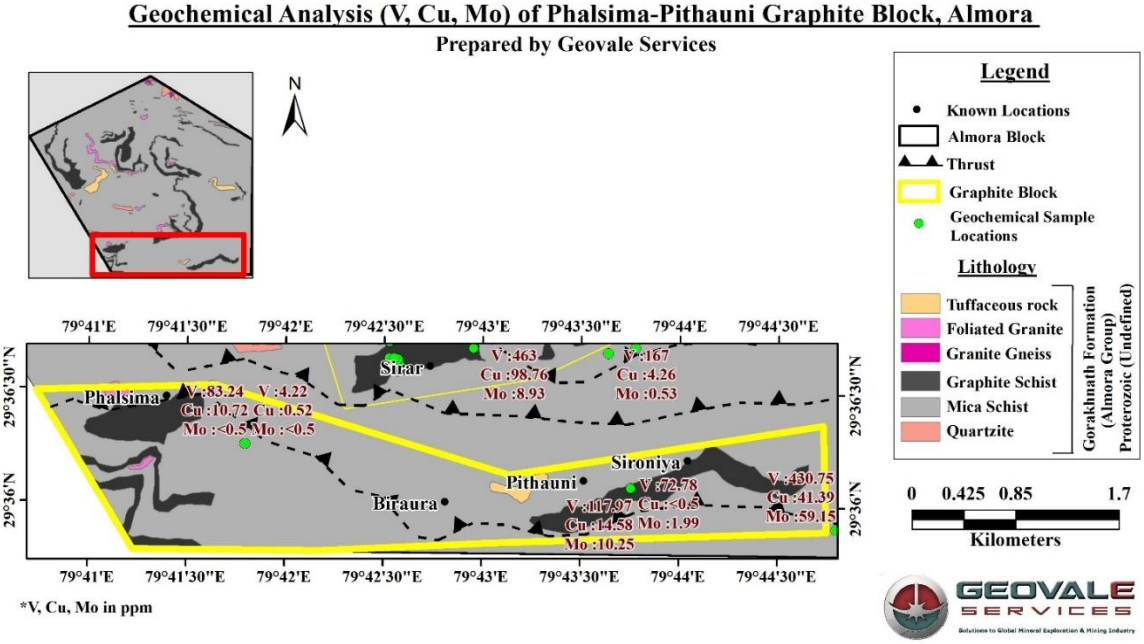

Figure 7.69: Geochemical analyses show Vanadium, Copper and Molybdenum content of the Graphite, Phasima-Pithauni Graphite Block.

7.4.6 Subsurface Characterization:

Drilling details:

Two Boreholes are drilled (BH-06, Depth 106 m and BH-12, Depth 64 m) within this Graphite Block. Total Graphite Ture thickness establised from BH-06 is 69 m and BH-12 is 42 m. FC% from these boreholes are upto 6.92%.

Tumbler Test (Subsurface Graphite):

The tumbler test result is classified as moderate, indicating a fair level of resistance of graphite flakes to mechanical degradation.

The modal analysis of the drill core sample thin section reveals the presence of jumbo (zambo) graphite flakes, >300 µm flake size occupy about 90.97% of the area. 300 –180 µm flake size occupies about 3.95% of the area. Flake size between 180 –150 µm occupies about 1.58% of the area. Flak size between 150 – 75 µm occupies about 3.14% of the total area. Flake size <75 µm occupies about 0.37% of the area.

The Subsurface geochemical assessment of the Pithauni Graphite Band indicates the presence of a 26 m thick high-grade graphite zone, followed by 40 m of intercalated graphite associated with mica schist. The thickness of overburden is recorded as 10 m. However, trace element analysis shows a significant presence of vanadium, with a value of 582.7 ppm recorded at a depth of 102–103 m. Molybdenum (Mo) values vary across depths, ranging from 14.56 ppm to 38.61 ppm, indicating moderate enrichment within the graphite-bearing horizons.

7.4.7 XRD Data:

One sample (109938) was analysed from the Phalsima Village shows rich in muscovite, albite, pyrite along with Graphite.

7.5 Batgal-Channi Graphite Block

7.5.1 Site Characteristics

The Batgal-Channi Graphite Block is situated on the northern part of the Almora G4 block. The block is regionally connected through NH-309B and local roads (Figure 7.70).

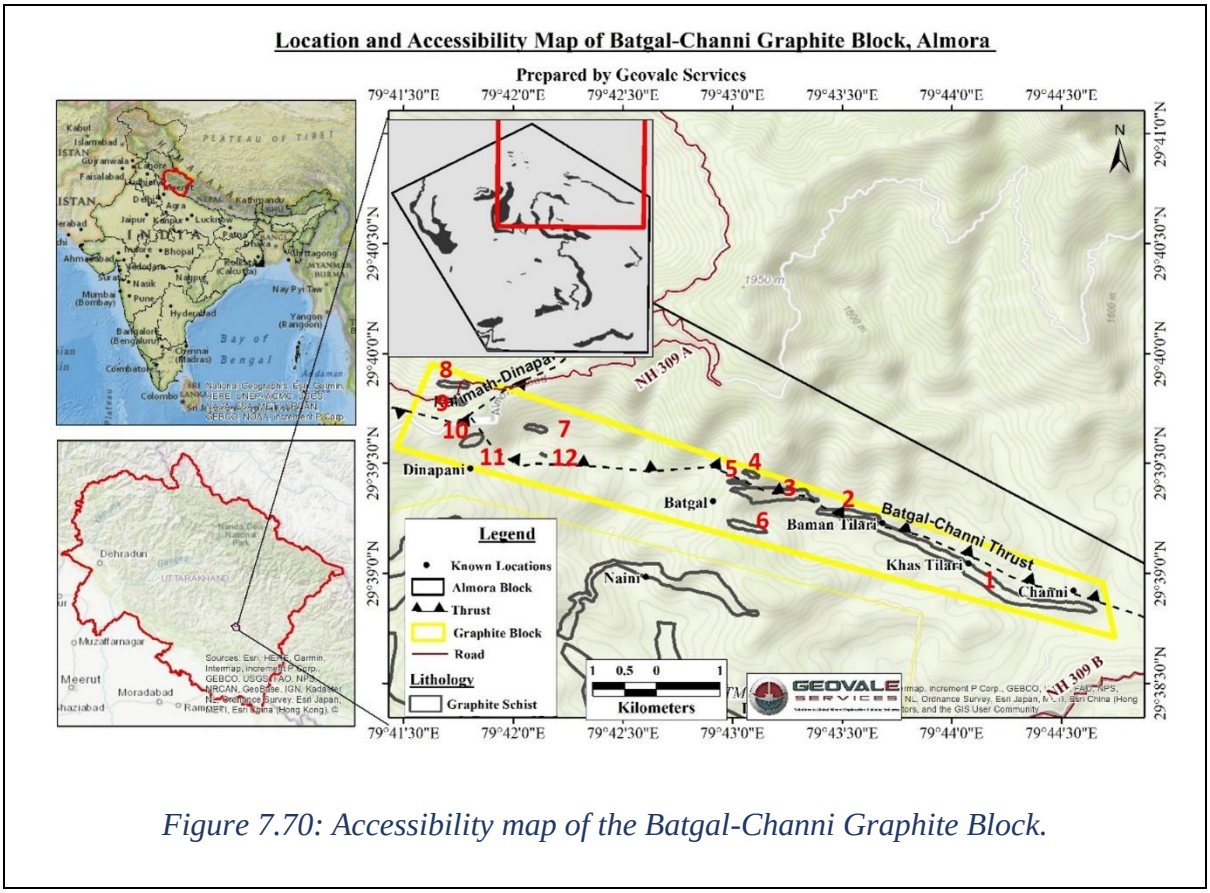

Figure 7.70: Accessibility map of the Batgal-Channi Graphite Block.

The area is characterized by hilly, steep terrain and elevations ranging from 1,400 m to 1,800 m RL, reflecting a high-relief, dissected hill–valley setting with graphite exposures occurring discontinuously along ridge flanks and slope breaks (Figure 7.71). Remote sensing and terrain analysis indicate a residual to highly dissected structurally controlled landscape with limited hillshade resolution of thrust features, supporting interpretation of the graphite band as a narrow, tectonically controlled zone within a rugged Himalayan slope environment rather than a broad, laterally extensive deposit. Land Use Land Cover data (Figure 7.72) shows that the area is predominantly covered by vegetation with minimal cropland, built-up land and rangeland, indicating that the graphite mineralization lies within vegetated hill slopes rather than agricultural or urban zones. Reserved Forest Cover area is nil (Figure 7.74). Settlement density is low, which reduces direct anthropogenic interference, though nearby rural presence requires consideration of land-use interaction and slope stability during exploration; The

drainage system (Figure 7.73) is dendritic with dominated by first-order streams typical of steep terrain, promoting localized exposure of graphite but also indicating susceptibility to seasonal runoff, erosion and slope instability, necessitating proper drainage and sediment management.

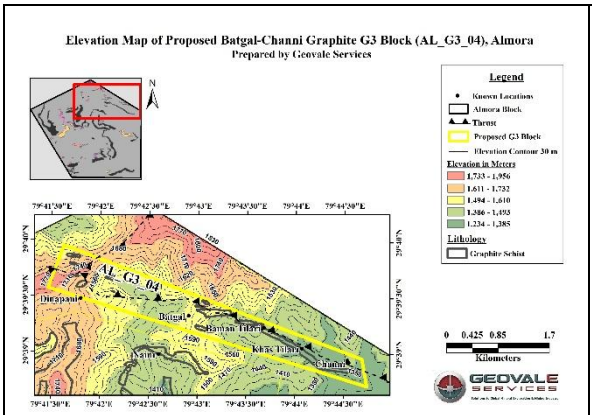

Figure 7.71: Contour map and elevation map of the Batgal-Channi Graphite Block, Almora.

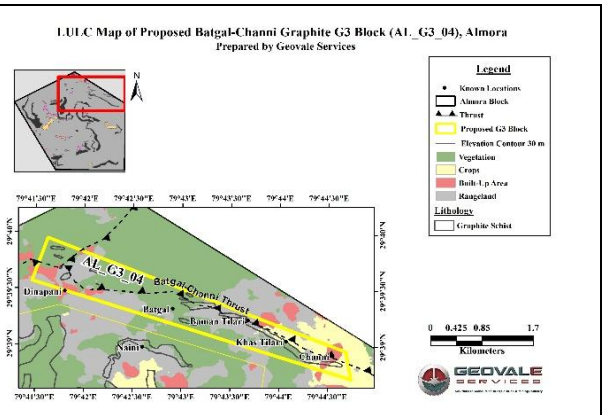

Figure 7.72: LULC map of the Batgal-Channi Graphite Block, Almora.

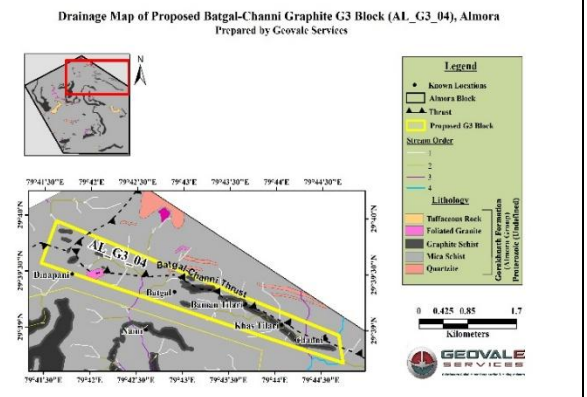

Figure 7.73: Drainage map of the Batgal-Channi Graphite Block, Almora.

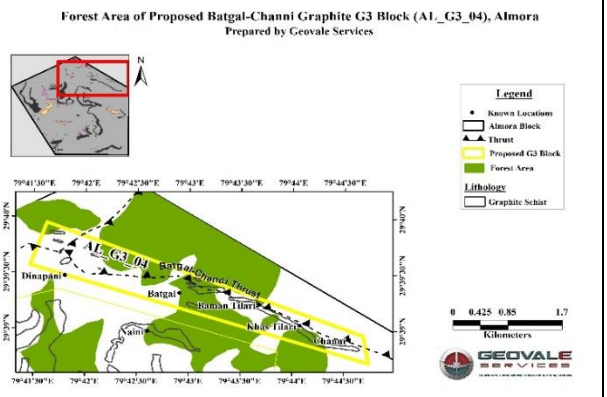

Figure 7.74: Forest map of Batgal-Channi Graphite Block, Almora.

Below the table contains details of the Batgal-Channi Graphite Block (Table 7.9).

Table 7.9: Summary of site characteristics of the Batgal-Channi Graphite Block.

Parameter	Batgal-Channi Graphite Block
Area	3.09 sq. km
Toposheet No.	53O/10
Accissibility	Approached from NH-309B vial Almora Town.
Topography	Hilly to steep, structurally rugged terrain on dissected ridge and hill-slope sectors.
Elevation	Approximately 1,400-1,800 m RL.
Drainage	Predominantly first-order stream development.
LULC	Vegetation dominant; cropland low; built-up low; rangeland very low.
Habitation	Low overall within the mapped graphite corridor.

7.5.2 Geological and Resource Characterization

The Batgal-Channi Graphite Block is a structurally controlled graphite zone developed along a steep thrust-related shear (Ramp), where mineralization is mainly confined to graphite schist with associations of mica schist, quartzite and related metamorphic rocks. The foliation in graphite is mainly marked by moderate to steep dips, typically between 50° and 70°, indicating strong deformation. The graphite occurs in multiple narrow and discontinuous bands (total 12 bands) rather than as a single continuous body, showing limited lateral spread despite having moderate overall strike length. Intense shearing combined with high-grade metamorphism has improved graphitization in localized zones, but at the same time has led to fragmentation and reduced continuity of the graphite bands across the corridor.

Thickness of the Band:

The Batgal graphite corridor is segmented into multiple bands (Band 1 to Band 12) showing significant variability in strike continuity, width and areal extent, collectively reflecting a discontinuous but structurally controlled mineralized system. The strike length ranges from as high as 1.765 km in Band 1 to as low as 0.015 km in Band 7, indicating that only a few segments exhibit notable lateral persistence while several others are short and fragmented. The average width also varies considerably, from a of about 0.07 km in Band 3 to as little as 0.0041 km in Band 7, suggesting irregular thickening and pinching typical of structurally controlled graphite bands. In terms of mappable area, Band 1 dominates with approximately 0.12587 sq. km, followed by moderate contributions from Bands 3 (0.050435 sq. km) and 2 (0.020221 sq. km),

whereas most other bands represent very small and localized occurrences with areas less than 0.015 sq. km. Several bands such as 7, 10 and 12 show extremely limited areal extent, indicating isolated or weakly developed graphite lenses.

Table (Table 7.10**) below shows detail of the Batgal-Channi Graphite Block.**

Table 7.10: Details of the extension of Batgal-Channi Graphite Block

Bands	Strike Length (Km)	Avg. Width (Km)	Total Mappable Area (Sq. Km.)	Prospectivity Rank
Band 1	1.765	0.0713	0.12587	High
Band 2	0.453	0.0447	0.020221	High
Band 3	0.064	0.07836	0.050435	High
Band 4	0.118	0.0307	0.003621	Low
Band 5	0.156	0.0238	0.00372	Low
Band 6	0.298	0.0454	0.013517	Moderate
Band 7	0.015	0.0041	0.00006	Very Low
Band 8	0.224	0.0371	0.008283	Moderate
Band 9	0.155	0.0246	0.003803	Low
Band 10	0.068	0.0110	0.000745	Very Low
Band 11	0.173	0.0687	0.011912	Moderate
Band 12	0.041	0.0049	0.000202	Very Low

7.5.3 Road section of the Batgal-Channi Graphite Block:

Road section of Batgal and Debdiya area are showing below (Figure 7.75).

Figure 7.75: Field photographs of graphite schist exposure at Batgal area showing a ~12 m thick graphite schist band interbedded with mica schist. (A) General view of the graphite schist exposure with interbedded mica schist; (B–C) Close-up views showing foliation, schistosity, and graphite-rich bands within the graphite schist; (D) Hand specimen displaying soft, flaky graphite mineralization with characteristic dark grey colour and graphite soiling on hand contact.

7.5.4 Geophysical Data Analyses (VES) of the Batgal-Channi Graphite Block:

Resistivity (VES) survey:

One VES profile (Line 23) (with three VES points, VES 103,104,105) has been carried out in this block (Figure 7.76, Figure 7.77).

Interpretation of these data indicates the presence of multiple subsurface layers, including a relatively shallow conductive layer of approximately 15 m thickness with resistivity up to ~250 ohm·m, a more prominent conductive zone of about 70 m thickness with resistivity ranging from ~35 to 250 ohm·m and a distinctly resistive horizon exceeding 1,000 ohm·m. This variation reflects alternating conductive and resistive units within the subsurface.

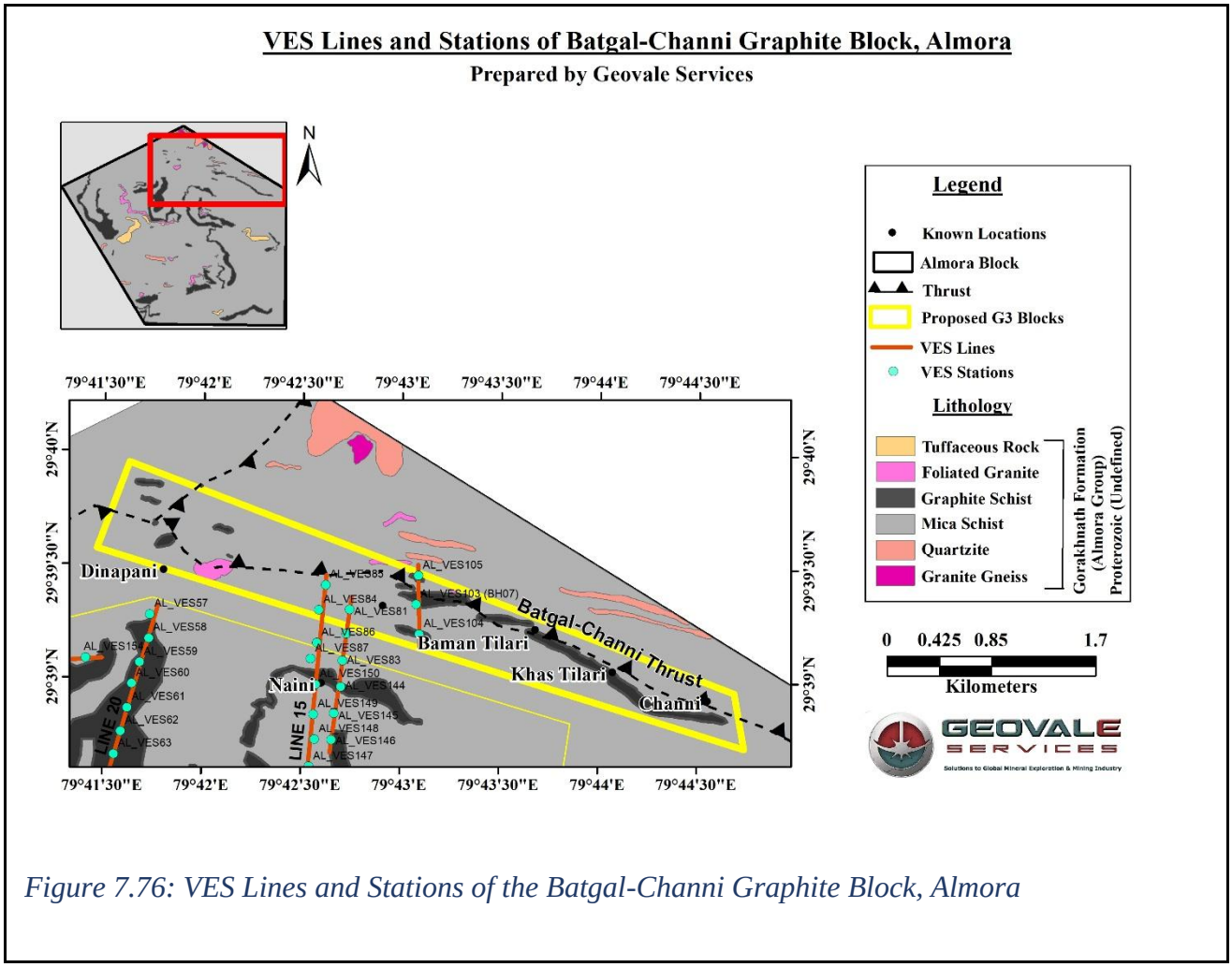

Figure 7.76: VES Lines and Stations of the Batgal-Channi Graphite Block, Almora

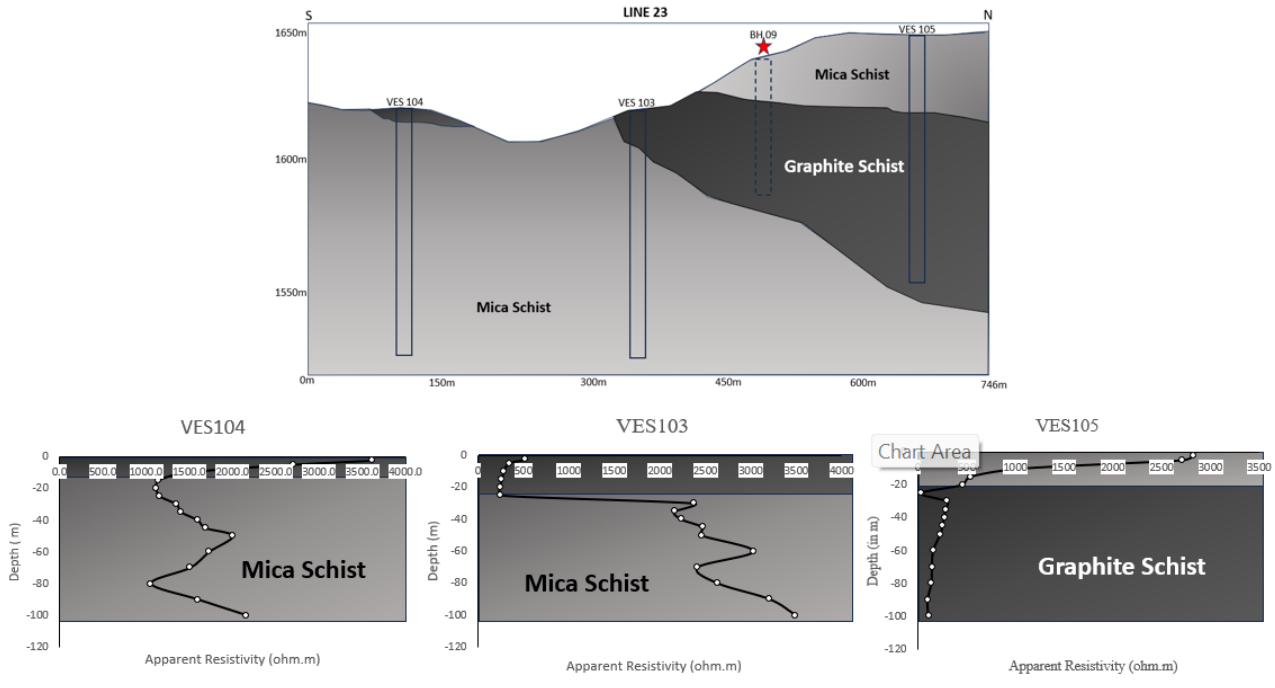

Figure 7.77: Cross Section of Line 23 on the basis of VES Survey, near Batgal area, Almora.

Self Potential Survey (SP):

Four SP (Profile Line 12, 21, 23 and 24) has been carried out in this block (Figure 7.78).

Self-Potential (SP) data are available only for a few bands, with Band 1 showing a local anomaly of approximately –87 mV, Band 2 recording stronger responses up to about –170 mV and Band 6 indicating values around –123 mV. These responses confirm the presence of conductive zones associated with graphite and/or graphite–sulphide mineralization; however, their moderate intensity and restricted distribution suggest localized conductors rather than a continuous, high-intensity conductive horizon along the entire strike (Figure 7.79, Figure 7.80, Figure 7.81, Figure 7.82).

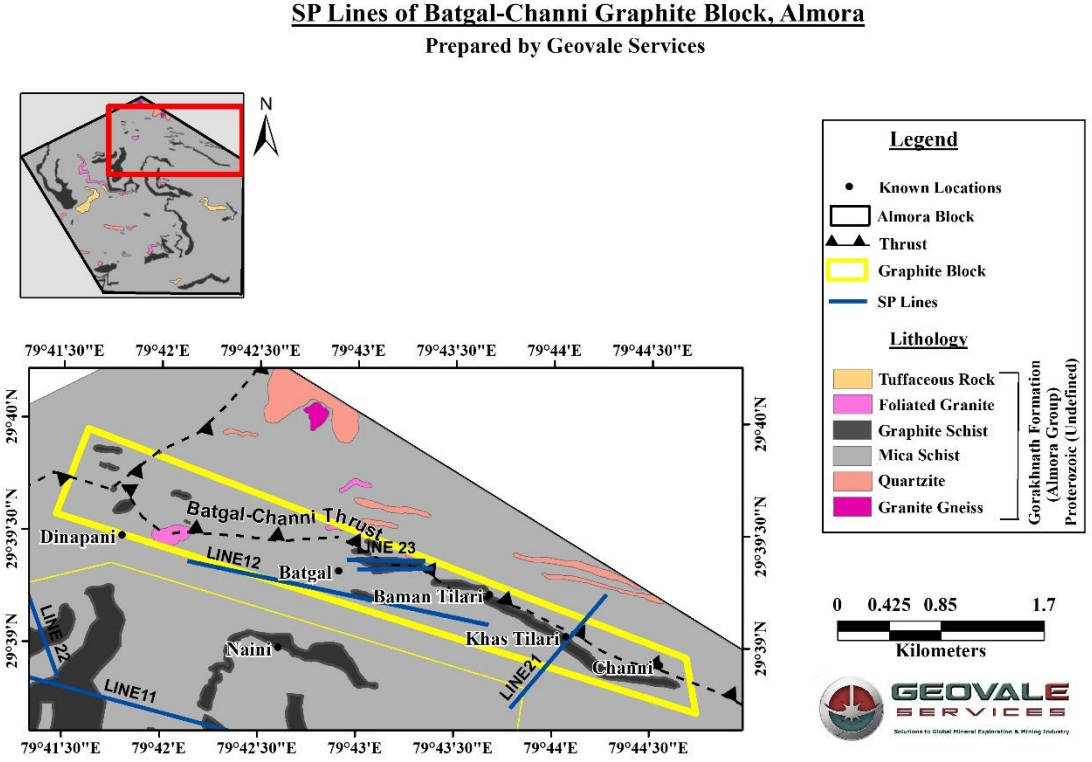

Figure 7.78: SP map of the Batgal-Channi Graphite Block, Almora

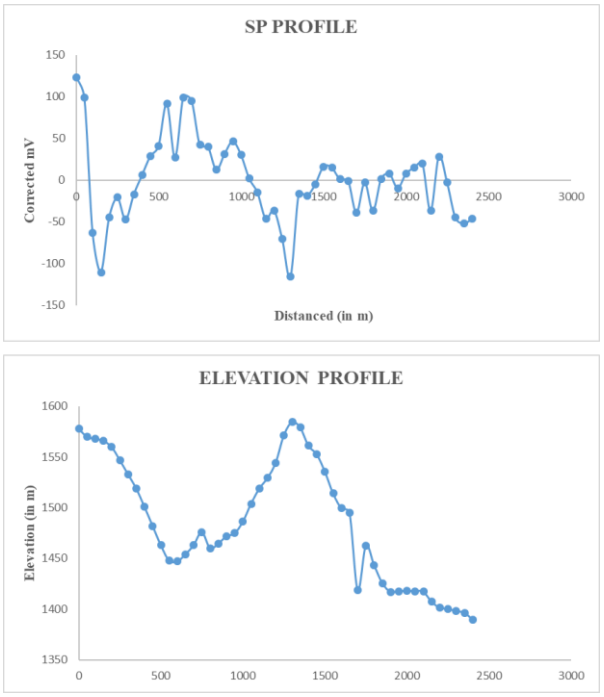

Figure 7.79: SP and Elevation Profile of Line 12, near Batgal area, Almora.

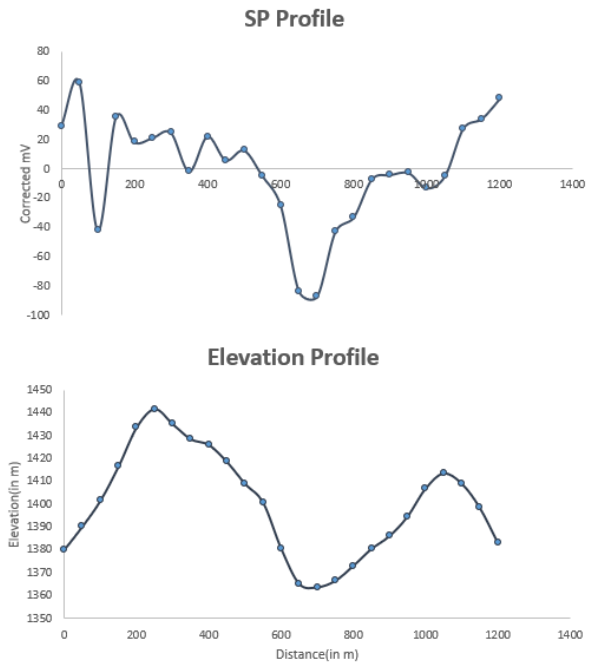

Figure 7.80: SP and Elevation Profile of Line 21, near Batgal area, Almora.

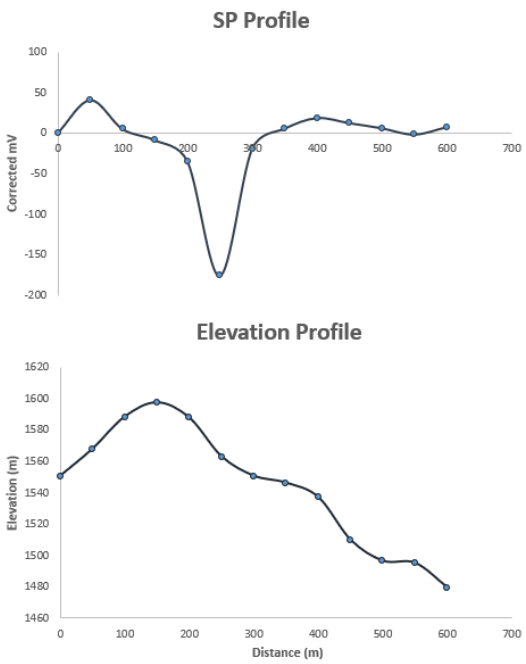

Figure 7.81: SP and Elevation Profile of Line 23, north of Batgal area, Almora.

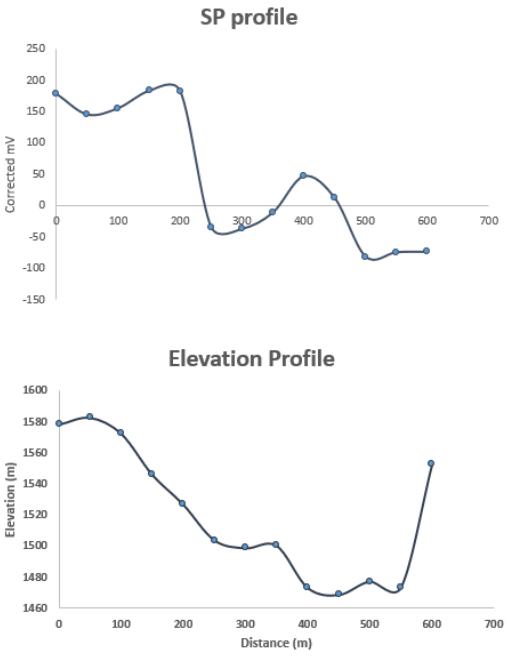

Figure 7.82: SP and Elevation Profile of Line 24, north of Batgal area, Almora.

Geophysical summary of the Batgal-Channi are discussed as below (Table 7.11**).**

Table 7.11: Integrated interpretation of SP and VES geophysical characterisation of the Batgal-Channi Graphite Block, Almora

Bands / data source	Observed response	Interpretation from SP data
SP line, Bands 1	Mostly positive profile with local low about -87 mV	Weak-to-moderate localized conductive response.
SP lines, Bands 2	Local low about -170 mV	More distinct conductor, but still limited spatially.
SP line, Bands 6	Local low about -123 mV	Moderate localized conductive corridor.
VES 102 / 103 interpretation	Conductive layer about 15 m thick, resistivity up to about 250 ohm.m	Thin to moderate graphite-bearing conductor.
VES 105 interpretation	Conductive zone about 70 m thick, resistivity about 35-250 ohm.m	Most promising subsurface graphite lens in the Batgal area by geophysics control.
VES 104 interpretation	High resistivity >1,000 ohm.m	Likely non-graphitic host rock or barren structural sector.

7.5.5 Qualitative Features and Analytical Results

Field observations show typical graphitic characteristics such as dark streak, metallic lustre and locally coarse flakes, though these are not uniform across the corridor. Tumbler test carried on the field indicate predominantly moderate quality with some poor zones and limited high-grade pockets, reflecting a structurally controlled, heterogeneous graphite system with better zones around Batgal and Dinapani. In the Batgal graphite bands, tumbler test carried on the field showed considerable variability, ranging from poor to high grades. Bands such as 6 and 9 exhibit high ratings, indicating the presence of relatively coarse and durable graphite flakes, while Bands 3, 5, 7, 8, 10 and 11 show moderate to high characteristics, suggesting moderate flake size with some localized degradation. Bands 1 and 12 are classified as moderate, whereas Bands 2 and 4 show moderate to poor and poor responses respectively, indicating finer or more fragile graphite. This variation reflects the strong influence of structural deformation and metamorphic conditions on graphite quality within the corridor.

The surface geochemical data for the Batgal graphite bands indicate overall low to moderate fixed carbon (FC) values, generally ranging from about 2.5% to 7.05%. Band 7, 11 and 12 also show higher FC values (above ~5%), indicating comparatively better graphite concentration, whereas Bands 5 and 6 show lower FC and higher VM, suggesting comparatively poorer quality. Volatile matter (VM) values vary between approximately 2.18% and 7.58%, indicating variable thermal maturity and possible influence of host rock composition and metamorphic conditions. Geochemical analyses of surface graphite samples show the Ash content is notably high across most bands, typically ranging between ~87% and 92%, reflecting significant gangue presence and indicating that the graphite is highly intergrown with silicate minerals. (Figure 7.83)

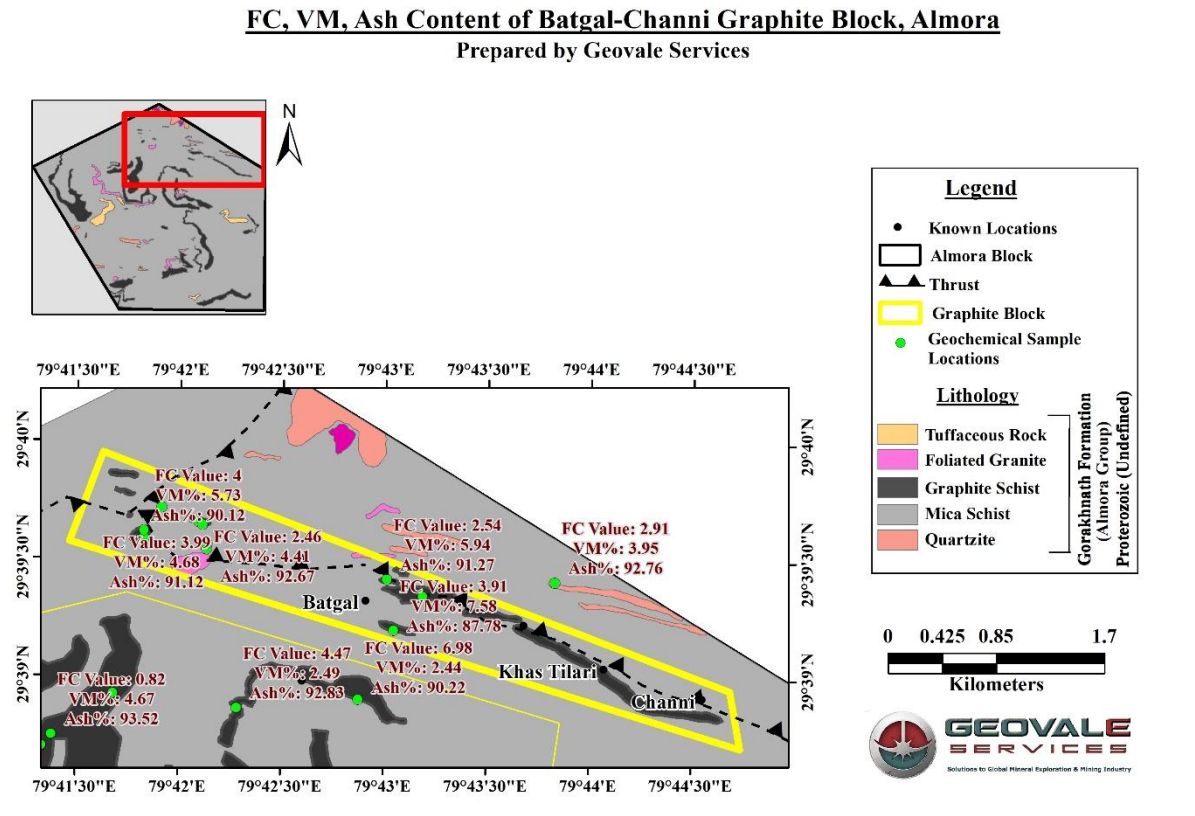

Figure 7.83: Surface Geochemical analyses (FC, VM, and Ash content) of the Batgal-Channi Graphite Graphite Block.

Sulphur (S) content is consistently low (typically ~0.02–0.05 ppm where available), which is favorable from a beneficiation perspective as it implies minimal sulphide contamination. This is further supported by high impurity levels (silica, alumina, etc.), which range from ~68% to

as high as ~94%, confirming that the graphite occurs within impure, schistose host rocks and would require substantial beneficiation. (Figure 7.84)

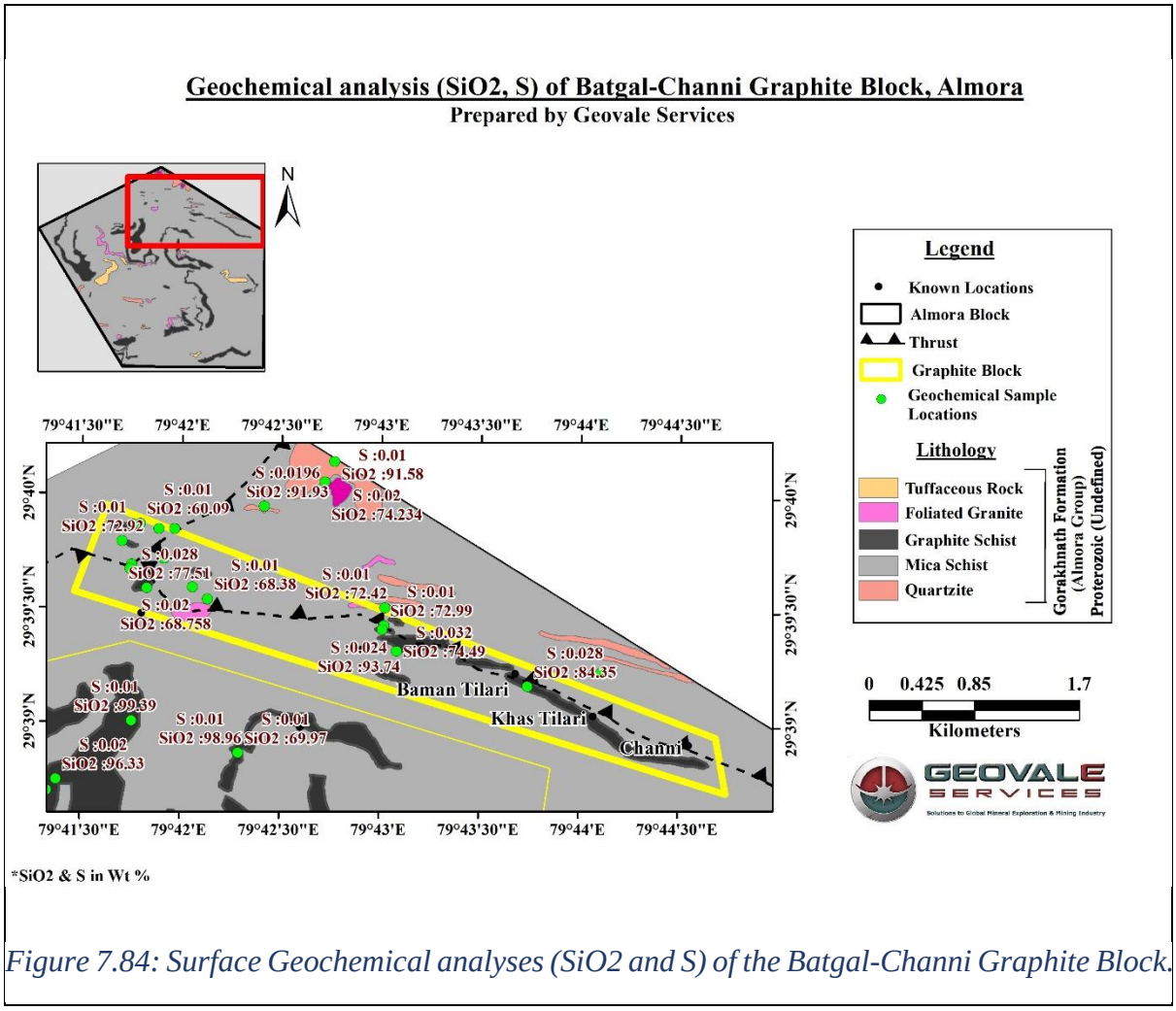

Figure 7.84: Surface Geochemical analyses (SiO2 and S) of the Batgal-Channi Graphite Block.

ICPMS: However, ICPMS analyses show (reported Band 10 and Band 11) anomalous enrichment (up to ~3536 ppm) of Vanadium (V) values, upto 74 ppm Mo, 260ppm Cu suggesting possible trace element association with the graphitic horizons. (Figure 7.85)

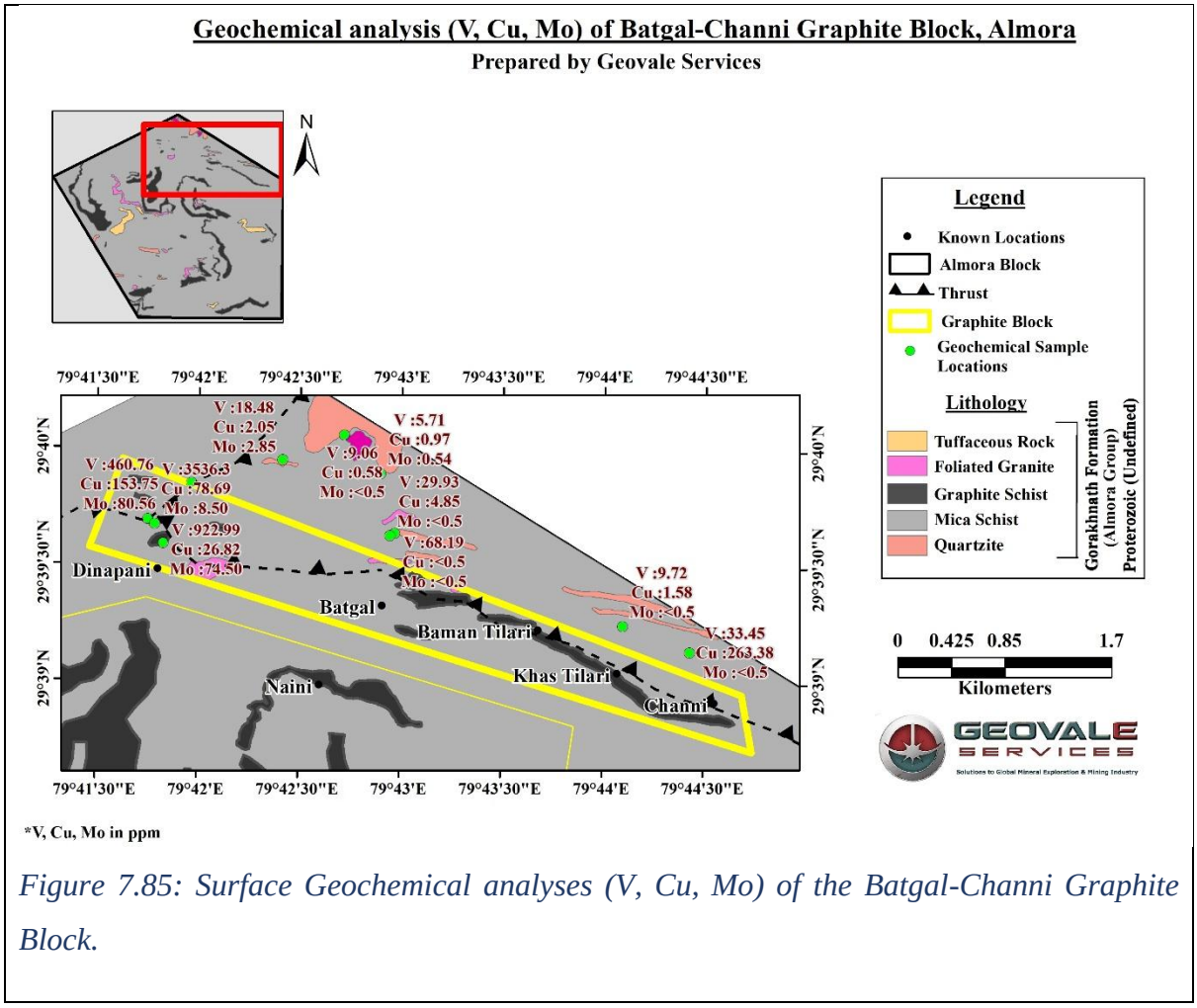

Figure 7.85: Surface Geochemical analyses (V, Cu, Mo) of the Batgal-Channi Graphite Block.

7.5.6 Subsurface Characterization:

One core-drilling (BH09) has been carried out in the eastern part of the Batgal-Channi Graphite Block (65.5 m) indicates a graphite-bearing zone with a total true thickness of 6.07 m (from depth to depth in the vertical borehole where the graphite band dip 50º toward east), Bore hole information there are two graphite bands with occurring at the depth from 0.5 to 8 m. width the borehole thickness of 7.5 m and true thickenss of 4.82 m Other band starts from depth 16 m to 19.5 m with borehole thickness of 3.5 m and true thickness of 2.25 m.

Chemical analysis reveals FC value upto 2.99% and Vanadium upto 1502 ppm.

Chapter 8

Exploration by Scout Drilling

8 Exploration by Scout Drilling:

8.1 Objectives and Rationale for Scout Drilling

Scout drillhole locations were selected through systematic integration of geological mapping, geochemical assays, laboratory studies and geophysical surveys, designed to test the depth continuity and Graphite quality - including associated Vanadium mineralisation - of ranked target zones.

Geological mapping and cross-section analyses across the Almora G4 Block defined graphite-bearing formations (Graphite Schist), their structural attitudes and tectonic controls. Predicted subsurface continuity and band geometry from these cross-sections provided the primary geometric framework for target selection. Vertical Electrical Sounding (VES) surveys delineating low-resistivity zones in conjugation with low SP values are indicative of conductive graphite bodies at depth. Where VES conductive zones and SP anomalies coincided with mapped geological units, these intersections were ranked as primary drilling targets.

Petrological modal analysis of surface specimens determined graphite flake size as an indicator of economic significance; Raman spectroscopy confirmed crystallinity and graphite ordering; geochemical analyses quantified FC, vanadium and pathfinder-element association. Drillhole collars were positioned where favourable geology, strong geophysical anomalies and positive graphite quality indicators converged.

Due to terrain constraints, forest cover and restricted accessibility in parts of the Almora G4 Block, the extent of drilling was limited at specific locations. Within these operational constraints, the scout programme was planned with two objectives:

- To establish the depth continuity of graphite mineralization within the structurally and foliation-controlled Graphite Schist and to characterise its 3D disposition.
- To evaluate flake size and crystallinity alongwith depth-wise variation of graphitic carbon (FC) and associated vanadium across different bands as intersected by multiple boreholes.

Accordingly, a few conceptual target zones were identified and tested through scout boreholes.

8.2 Drilling and Sampling Methodologies

Diamond core drilling was adopted as the primary subsurface exploration method. The technique employs a rotary drilling system fitted with a diamond-impregnated bit, capable of penetrating mica-schist and graphite schist sequences and yielding continuous cylindrical core samples for systematic lithological, structural and mineralogical examination.

Sludge samples were systematically collected where poorly consolidated formation reduced core recovery (used triple tube barrel for maximum best possible recovery); these provided supplementary geological and geochemical continuity across intervals of structural weakening or intense weathering.

All holes were drilled using standard wireline diamond core technique. HQ core (63.5 mm diameter) was used in upper sections, reducing to NQ (47.6 mm) at depth where ground conditions required. Water circulation was maintained throughout for bit cooling and cuttings removal.

8.3 Core Handling and Sampling Protocol

Cores were recovered in 0.5-3 m runs, stored in depth-marked core boxes in a box-shaped pattern. Core recovery was monitored routinely and was generally good at approximately 90%; local reductions correlate with brecciated and strongly fractured zones, supplemented by sludge samples.

Cores were quarter-cut longitudinally:

- Half-core preserved as reference in the core boxes.
- One quarter retained for petrographic and mineralogical thin-section study.
- One quarter used for geochemical sampling at nominal 1–1.5 m intervals, with shorter intervals over visually mineralised zones.

Selective intervals were submitted for XRF (Annexure XXII, Annexure XXIII, Annexure XXIV), ICP-MS (Annexure XXV, Annexure XXVI), Proximate (Annexure XXVII), Raman (Annexure XV) and XRD (Annexure XVI) to characterise graphite quality and base-metal associations.

No downhole geophysical logging or borehole deviation surveys were conducted in this scout phase. All boreholes were designed as vertical holes; collar positions and orientations are adequate for G4-level geological interpretation.

8.4 Overview of the Drilling Program

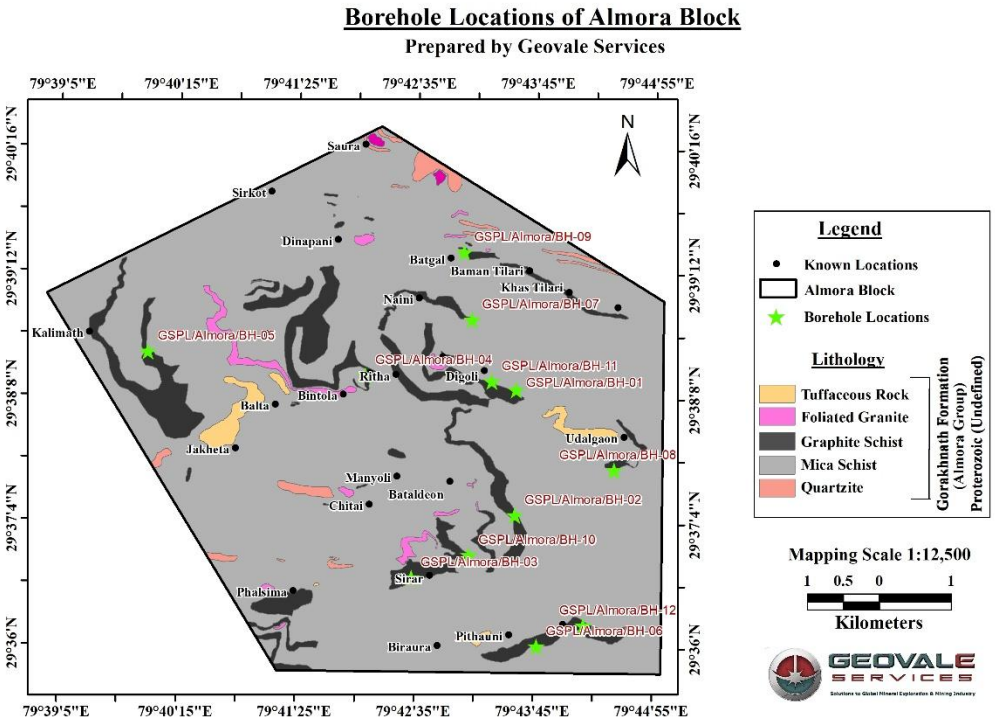

Figure 8.1: 12 Borehole Locations in the Almora G4 Block.

The boreholes are spatially distributed across the central, southern and northern sectors of the block approximately 3-4 km apart from each other (Figure 8.1).

Detailed information on the boreholes is given in the following table (Table 8.1, Table 8.8).

Table 8.1: Detailed informations of 12 boreholes in the Almora G4 block

S No	Borehole ID	Latitude	Longitude	Village	Collar Height (m)	Inclination	Depth
1	GSPL_Almora_BH01	29.636734	79.726113	Digoli	1363	Vertical	91.7 m
2	GSPL_Almora_BH02	29.618863	79.726083	Bataldeon	1322	Vertical	60 m
3	GSPL_Almora_BH03	29.609816	79.709241	Sirar	1622	Vertical	75 m
4	GSPL_Almora_BH04	29.638587	79.701410	Barakote	1531	Vertical	64 m
5	GSPL_Almora_BH05	29.641725	79.665825	Mat	1890.15	Vertical	75 m
6	GSPL_Almora_BH06	29.600162	79.729779	Pithauni	1275.07	Vertical	106 m
7	GSPL_Almora_BH07	29.64667	79.718822	Deora	1540.16	Vertical	50 m
8	GSPL_Almora_BH08	29.625384	79.742246	Udalgaon	1533.25	Vertical	50 m
9	GSPL_Almora_BH09	29.656291	79.717376	Batgal	1554	Vertical	45 m
10	GSPL_Almora_BH10	29.613099	79.718628	Sirar	1469.72	Vertical	28.5 m
11	GSPL_Almora_BH11	29.637927	79.722081	Digoli	1329	Vertical	92 m
12	GSPL_Almora_BH12	29.603202	79.737426	Sironiya	1359	Vertical	64 m
Total							**801.2 m**

8.5 Details of Borehole:

8.5.1 GSPL_Almora_BH01

Surface Selection Criteria- The borehole 1 location was selected at Digoli Village within a prominent NW–SE trending graphite bearing band, extending over a strike length of about 2 km with an average thickness of 200 m and an overall dip towards the NE. Surface selection was primarily guided by the presence of this well-defined and continuous graphite-bearing zone (Figure 8.2, Figure 8.3).

Grab samples of graphite schist collected near the borehole 01 site showed promising proximate analysis results, with fixed carbon (FC) values of 5.85%, 4.07% and 2.23%, all exceeding the 2% cut-off grade for graphite in India, indicating economically significant mineralization.

In addition, surface sampling and chemical analysis revealed a wide range of anomalous values, including Mo up to 52.9 ppm, Ba up to 4899.2 ppm, U up to 22.1 ppm, V up to 1220 ppm, Zn up to 1690.39 ppm, Se up to 29.31 ppm, Cd up to 44.91 ppm and Sb up to 26.47 ppm.

These geochemical anomalies, along with favorable geological characteristics, supported the selection of this site for drilling to test the continuity, thickness and quality of graphite mineralisation at depth.

Figure 8.2: River cut section showing Graphite Schist Band

Figure 8.3: Banding in Graphite Schist on the surface near to BH-01

Geophysical Signature- VES profiling also shows lowering the resistivity between 20 m to 45 m (value drop from 800 ohm-m to 568 ohm-m to 778 ohm-m), indicating a conducting layer (probably Graphite bearing horizon).

BH-01 – Lithologging and Mineralization:

The graphite mineralization starts at ~16 m depth and continues to ~91.7 m as laminated to banded graphite schist (Figure 8.4).

The borehole shows a transition from near-surface weathered mica schist (0–15 m) to graphite-bearing metamorphic horizons below ~16 m. Graphite occurs within quartz–muscovite–graphite schist as laminated to banded units, alternating between low-, moderate- and high-graphite bands. Notable enriched zones appear at ~35–37.5 m, 48–58 m, 72–72.5 m and 80.4–83.4 m, characterized by darker colour, strong foliation, shearing and medium-luster flaky graphite with pyrite stringers along foliation.

Overall, the core represents a stratabound metamorphosed sedimentary sequence where graphite mineralization is structurally controlled along foliation and shear-parallel laminae, forming multiple graphite-rich horizons of moderate to good quality.

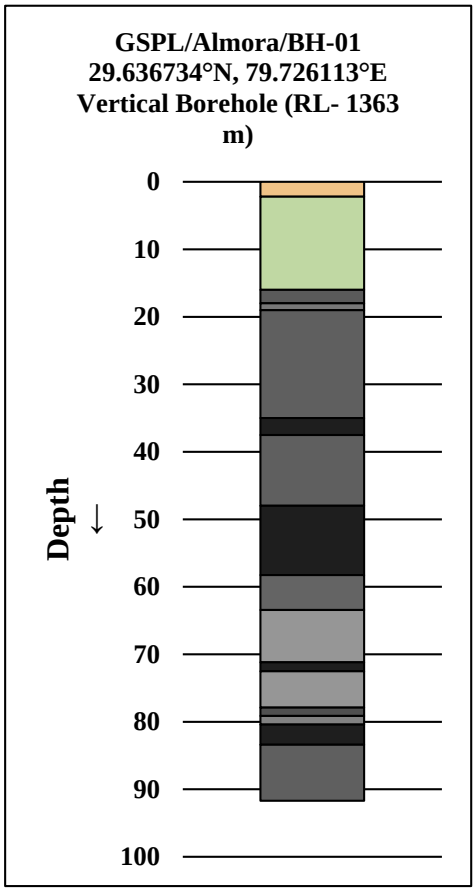

Colour Code	From (m)	To (m)	Lithology
	0	2.2	Weathered mica schist with topsoil
	2.2	16	Sericite–Mica Schist
	16	18	Weathered graphite schist
	18	19	Graphite schist with quartz vein
	19	35	Medium Grade Graphite schist
	35	37.5	High Grade Graphite schist
	37.5	48	Medium Grade Graphite schist
	48	58.25	High Grade Graphite schist
	58.25	63.43	Medium Grade Graphite schist (partly weathered)
	63.43	71.18	Low Grade Graphite schist
	71.18	72.5	High Grade Graphite schist
	72.5	77.9	Low Grade Graphite schist
	77.9	79.13	Weathered high-grade graphite
	79.13	80.4	Low to Medium Grade Graphite schist
	80.4	83.4	High Grade Graphite schist
	83.4	91.7	Medium Grade Graphite schist

Figure 8.4: Litholog of BH01, near Digoli village

Chemical Analysis-

Proximate Analysis for Graphite schist shows a good continuous zone of 2 m (35 m- 37 m) of FC% between 5.28 to 7.56.

Petrography Details-

Sample Id- 114201 (AL-BH-01) Depth- 25.2 m

Alternate bands of quartz with secondary carbonates and bands rich in muscovite, chlorite, graphite and pyrite. Graphite occurs as concordant bands within the schist, with very fine graphite flakes/sringers are aligned parallel to the schistosity. Three distinct graphite-bearing bands have been identified, of which the middle band contains the highest concentration of graphite, comprising approximately 15–20% of the band. Apatite and epidote are noted within the graphite-rich bands. Pyrite is abundantly present and is closely associated with the graphite-rich horizons (Figure 8.5, Figure 8.6, Figure 8.7, Figure 8.8, Figure 8.9, Figure 8.10).

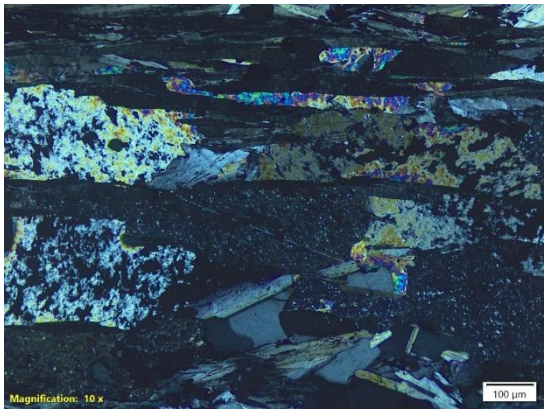

Figure 8.5: Photomicrograph of graphite schist sample showing carbonate altered to clay (Sample Id: 114201 at 25.2 m depth)

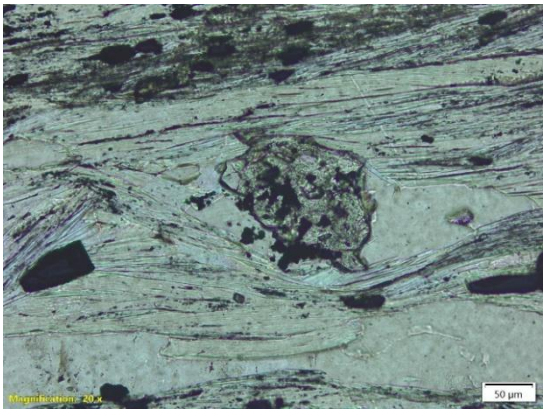

Figure 8.6: Photomicrograph of graphite schist sample showing epidote porphyroblast in graphite bearing schist (Sample Id: 114201 at 25.2 m depth)

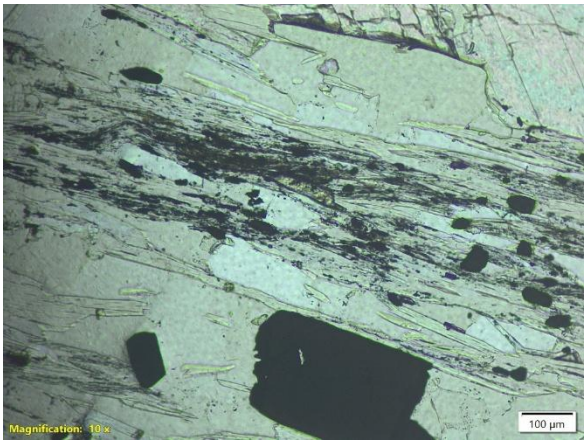

Figure 8.7: Photomicrograph of graphite schist sample showing jumbo flake of graphite (Sample Id: 114201 at 25.2 m depth)

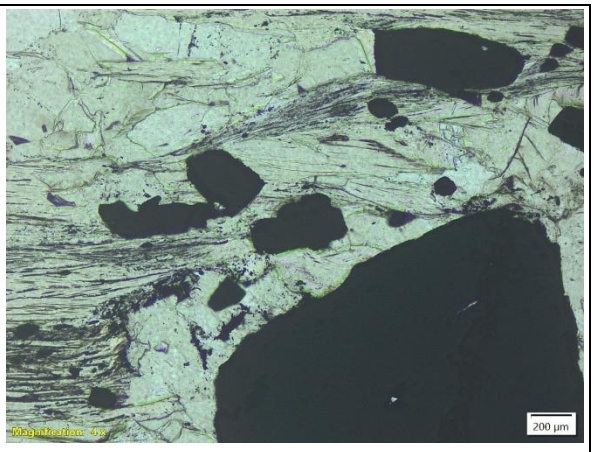

Figure 8.8: Photomicrograph of graphite schist sample showing pyrite in graphite bearing mica schist (Sample Id: 114201 at 25.2 m depth)

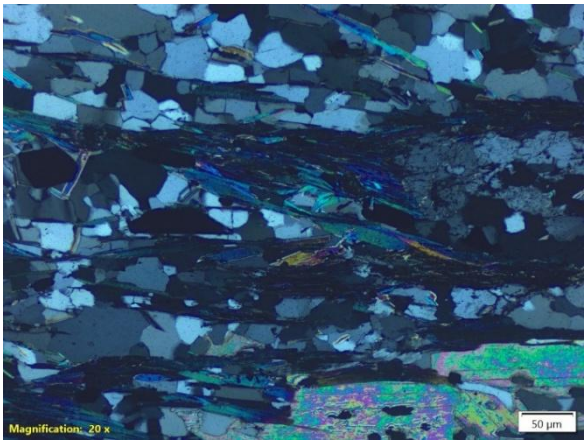

Figure 8.9: Photomicrograph of graphite schist sample showing foliation in graphite bearing mica schist.

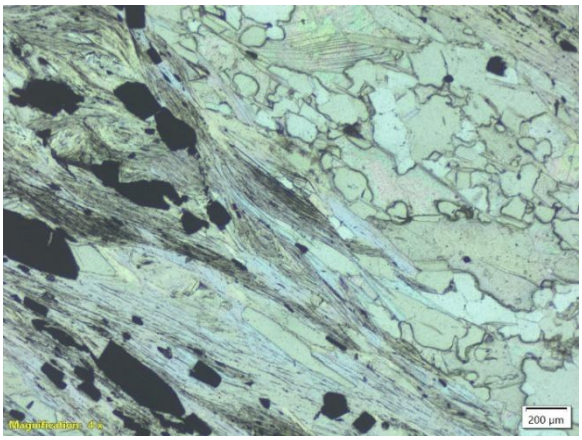

Figure 8.10: Photomicrograph of graphite schist sample showing needle like sillimanite in graphite bearing mica schist.

Sample Id- 110071 (ALBH-01) Depth- 36.75 m

Quartz-sericite-graphite schist with quartz- carbonate veins. Coarse grained flakey graphite notes which are not parallel to the foliation (post deformation graphite formation). Smaller graphite flakes are syn deformational. Pyrite present. (Figure 8.11, Figure 8.12, Figure 8.13, Figure 8.14)

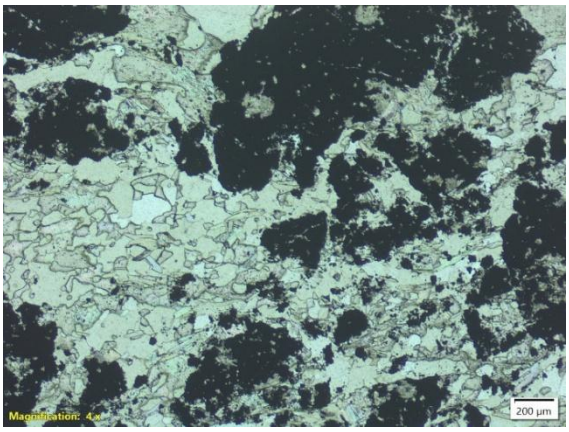

Figure 8.11: Photomicrograph of graphite schist sample showing coarse graphite flake

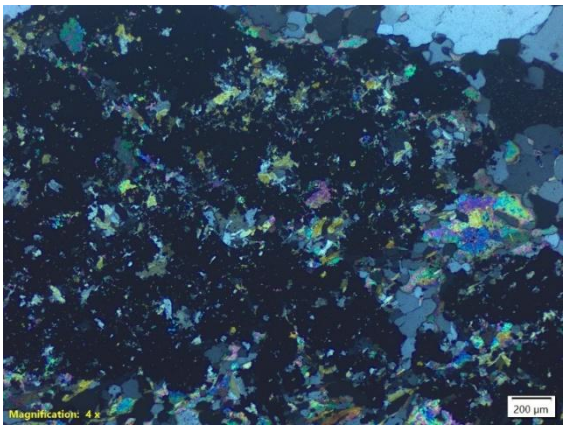

Figure 8.12: Photomicrograph of graphite schist sample showing graphite flake

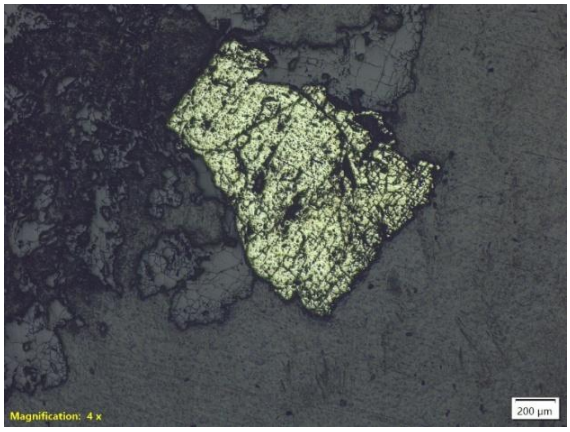

Figure 8.13: Photomicrograph of graphite schist sample showing pyrite associated with graphite

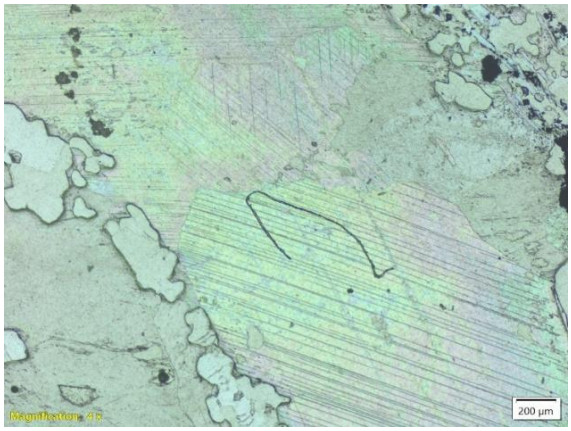

Figure 8.14: Photomicrograph of graphite schist sample showing carbonate veins

Sample Id- 114202 (ALBH-01) Depth- 40.5 m

Quartz–muscovite/sericite–graphite schist with a few quartz veins. The veins comprise polycrystalline quartz with secondary carbonates. Fine specks of graphite with irregular grain boundaries are disseminated throughout the thin section. Pyrite is profusely developed and minor chalcopyrite is also observed. (Figure 8.15)

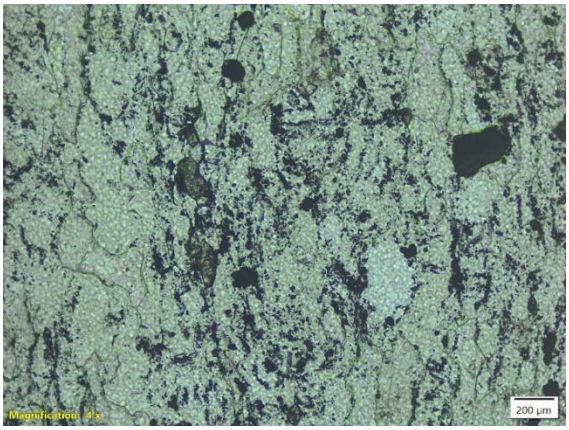

Figure 8.15: Photomicrograph of graphite schist sample showing microcrystals of graphite and associated pyrite.

Sample Id- 114203 (ALBH-01) Depth- 58.3 m

Graphite bearing quartz-mica schist. Dessiminated pyrite of various size. Medium sized grains of graphite with irregular grain boundary scattered in the rock (Figure 8.16, Figure 8.17, Figure 8.18).

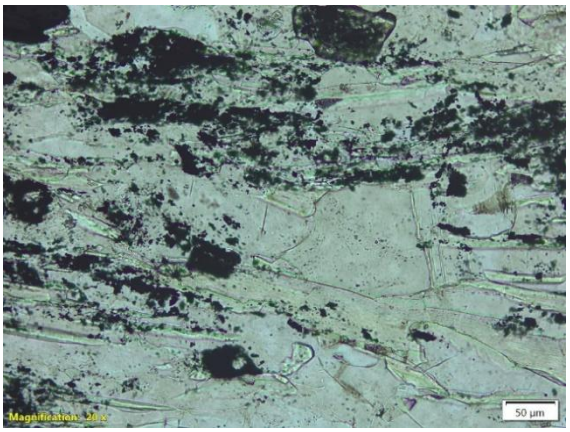

Figure 8.16: Reflected light photomicrograph (20×; scale bar 50 µm) showing disseminated to weakly aligned flaky graphite (black opaque) within a quartz–mica matrix, forming patchy to thin laminae.

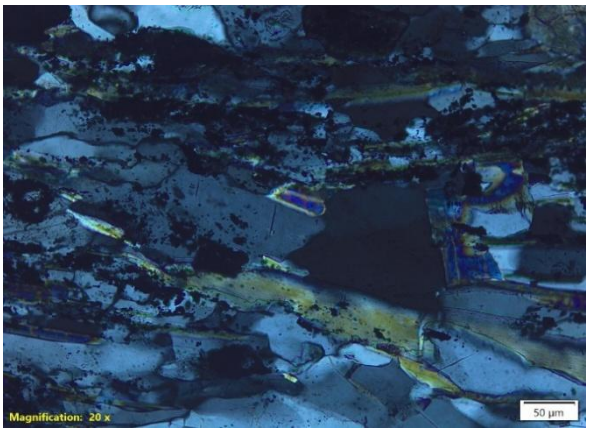

Figure 8.17: Reflected light photomicrograph (20×; scale bar 50 µm) illustrating banded/laminated graphite with a prominent opaque graphite domain and minor fractures/cleavages in the surrounding silicate matrix, indicating structurally controlled concentration of graphite.

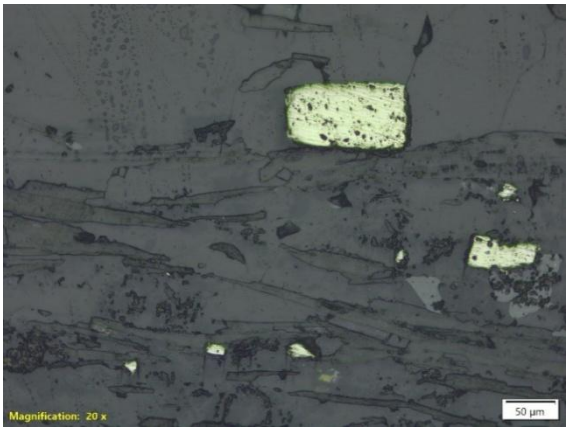

Figure 8.18: Reflected light photomicrograph (20×; scale bar 50 µm) showing disseminated to thinly laminated flaky graphite (dark grey to black) aligned along foliation within a quartz–mica matrix. Bright, highly reflective grains represent associated sulphide minerals (likely pyrite), indicating a graphite–sulphide association

Sample Id- 110076 (ALBH-01) Depth- 81.4 m

Quartz-sericite-graphite schist. Dessiminated pyrite of various size. Amorphos graphite scattered in the slide.

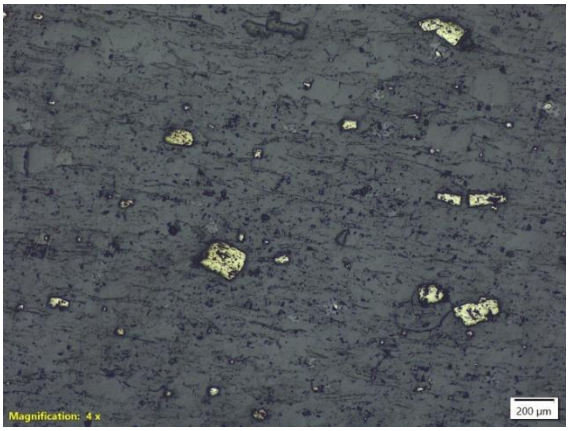

Figure 8.19: Reflected light photomicrograph (4×; scale bar 200 µm) showing pyrite and chalcopyrite associated with quartz-sericite-graphite schist.

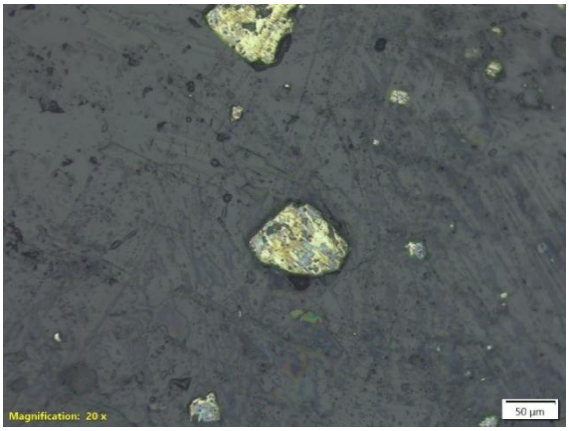

Figure 8.20: Reflected light photomicrograph (20×; scale bar 50 µm) showing covellite in chalcopyrite in quartz-sericite-graphite schist.

8.5.2 GSPL_Almora_BH02

Surface Selection Criteria- The Borehole is located near Bataldeon Village in a Graphite Schist band extending NNW-SSE, having a strike length ~3.1 km and thickness ~80 m. The band dips towards NNE (Figure 8.21, Figure 8.22).

Grab Sample near Borehole-2 Proximate Analysis of Fixed Carbon shows promising Values; i.e, FC% = 6.15 (Sample Id-109990), 5.36 (Sample Id-109993), 3.02 (Sample Id-109991), 2.57 (Sample Id-109994), 2.41 (Sample Id-109992), 2.19 (Sample Id-109170), 2.77 (Sample Id-109177).

Northern Part of this band also shows 7% (Sample Id-109186), 3.03% (Sample Id-109169) good FC%.

Surface Sampling chemical analysis data Shows a wide range of anomalous values.

V (ppm)= 2060 (Sample Id-109990), 764 (Sample Id-109992), 727 (Sample Id-109994), 580 (Sample Id-110005), 1040 (Sample Id-110009)

Mo (ppm)= 53.1 (Sample Id-109990), 10.3 (Sample Id-109991), 20.4 (Sample Id-109992), 22.6 (Sample Id-109994), 3.7 (Sample Id-109997), 10.28 (Sample Id-110005), 9.14 (Sample Id-110006), 6.97 (Sample Id-110007), 8.38 (Sample Id-110008), 27.60 (Sample Id-110009)

Geophysical Signature- VES profiling also shows drop of resistivity (from 559 ohm-m to 482 ohm-m) in between 15 m to 60 m, indicating a conducting layer (probably Graphite bearing horizon).

Figure 8.21: Road Cut Section showing Graphite Band near BH-02.

Figure 8.22: Thick Graphite Band in Road Cut section near BH-02

Figure 8.23: Drilling team in BH-02

Figure 8.24: Pillaring in BH-02 geavale representative team with Mr. Kandpal GSI, Dehradoon

Core Logging- Graphite mineralisation begins at ~14–15 m depth and persists upto ~40m (Figure 8.25). The dominant lithology below this depth is graphite schist, with high-grade graphite zones occurring repeatedly, especially between ~15–35 m. These high-grade intervals indicate strong and continuous graphite enrichment (Figure 8.23, Figure 8.24).

Moderate-grade graphite schist occurs as thinner interbands, separating high-grade zones and suggesting banded/stratabound mineralization. The alternation of high- and moderate-grade graphite schist reflects structural and lithological control, likely along foliation planes. (Figure 8.26, Figure 8.27)

Overall, BH02 confirms a thick, persistent graphite-bearing horizon with multiple high-grade bands, indicating good continuity and favourable potential for further graphite resource delineation.

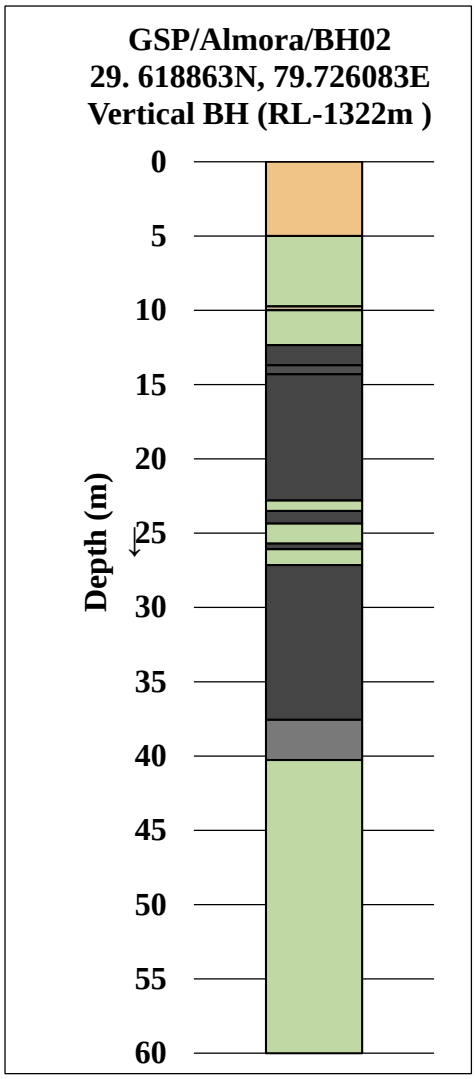

Colour Code	From (m)	To (m)	Lithology
	0	5	Weathered mica schist with topsoil
	5	9.74	Sericite Mica Schist
	9.74	10	Quartz Graphite Schist
	10	12.35	Sericite Mica Schist
	12.35	13.7	High Grade Graphite Schist (sulphide-rich)
	13.7	14.3	Moderate to High Grade Graphite Schist
	14.3	22.8	High Grade Graphite Schist (sulphide-rich)
	22.8	23.5	Sericite Mica Schist
	23.5	24.36	High Grade Graphite Schist (sulphide-rich)
	24.36	25.7	Sericite Mica Schist
	25.7	26.08	High Grade Graphite Schist (sulphide-rich)
	26.08	27.15	Sericite Mica Schist
	27.15	37.56	High Grade Graphite Schist (sulphide-rich)
	37.56	40.27	Moderate Grade Graphite Schist
	40.27	60	Sericite Mica Schist

Figure 8.25: Litholog of BH02, near Bataldeon village

Figure 8.26: Graphite Schist layer showing intense Quartz veintaion at 21.5 m depth of borehole 02

Figure 8.27: Graphite Schist intruded by folded Quartz vein at 36.40 m depth of borehole 02

Chemical Analysis- The dataset is characterized by a hyper-enriched, highly carbonaceous upper zone extending approximately from 13 meters to 20 meters, which abruptly and decisively transitions into a geochemically depleted, carbon-poor lower zone approximately from 22 meters downward. To systematically dissect these anomalies, the data has been organized into distinct thematic tables.

Proximate Analysis and Base Metals: Fixed Carbon (FC%) concentrations alongside the primary base metals—Copper (Cu), Zinc (Zn) and Nickel (Ni)—demonstrating the absolute covariance between organic carbon preservation and base metal sequestration (Table 8.2).

Table 8.2: Analytical results of Fixed Carbon (FC %) and associated base metal concentrations (Cu, Zn, Ni and Co in ppm) for selected drill core samples across specified depth intervals

Sample Id	Depth Interval (m)	FC (%)	Cu (ppm)	Zn (ppm)	Ni (ppm)	Co (ppm)
110080	13 - 14	4.85	323.89	555.81	205.81	10.26
110093	17 - 18	2.92	380.21	511.48	217.18	13.88
110081	19 - 20	5.64	246.35	382.90	149.67	9.78
110082	22 - 23	0.96	27.51	124.90	29.65	12.04
110083	27 - 28	2.13	120.83	260.19	75.39	9.62
110086	29.3 - 30.3	0.81	31.78	82.12	33.70	15.98
110084	34 - 35	0.89	16.86	31.38	7.52	2.79

The upper 7 meters of the sampled section (13 to 20 m) exhibit an intense accumulation of base metals, with Zinc peaking at 555.81 ppm, Copper at 409.49 ppm and Nickel at 225.26 ppm. These values exceed average continental crustal abundances by orders of magnitude. The stark drop-off below 22 meters, where Copper falls to 27.51 ppm and Nickel to 29.65 ppm, indicates a profound shift in the depositional environment, terminating the metal-scavenging process. Notably, Cobalt (Co) remains relatively low and stable across the entire sequence (ranging loosely between 2.79 ppm and 17.37 ppm).

Redox Sensitive Elements: The concentration of highly redox-sensitive transition metals and paleoproductivity indicators reveal the chemical state of the ancient water column (Table 8.3).

Table 8.3: Analytical results of Vanadium (V), Chromium (Cr), Molybdenum (Mo) and Uranium (U) concentrations (in ppm) for selected drill core samples across different depth intervals, highlighting variation across the mineralized and transitional zones.

Sample Id	Depth Interval (m)	V (ppm)	Cr (ppm)	Mo (ppm)	U (ppm)
110080	13 - 14	1022.08	123.21	87.76	29.11
110092	15 - 16	819.12	172.12	77.97	30.00
110093	17 - 18	789.05	190.31	75.08	28.84
110094	19 - 20	710.55	165.90	59.14	28.55
Transition	----------	-------	------	-----	-----

Sample Id	Depth Interval (m)	V (ppm)	Cr (ppm)	Mo (ppm)	U (ppm)
110082	22 - 23	98.47	211.15	3.13	2.72
110083	27 - 28	424.79	423.79	38.33	19.83
110086	29.3 - 30.3	81.32	527.87	1.51	2.11
110084	34 - 35	29.64	136.30	1.16	1.91
110085	42 - 43	68.54	725.07	0.23	2.53
110087	48 - 49	81.64	566.10	2.52	2.56

Vanadium dominates the redox trace element suite, surpassing an astonishing 1000 ppm in the uppermost interval. Molybdenum and Uranium show identical stratigraphic covariance, tightly bound to the vanadium and carbon peaks. Conversely, Chromium (Cr) behaves inversely to Vanadium, demonstrating lower concentrations in the heavily organic zones and reaching maximums (up to 725.07 ppm at 42-43 m) in the lower, carbon-poor silty intervals. Thorium remains exceptionally stable (averaging around 10 to 12 ppm) throughout most of the core, confirming its role as an immobile, detrital background indicator against which the wildly fluctuating, authigenic Uranium can be measured. Barium (Ba) operates as a clear proxy for bioproductivity, exhibiting massive peaks (up to 2272.13 ppm) precisely where the organic carbon is preserved.

Vanadium and Molybdenum Geochemistry: The exceptional enrichment of Vanadium (V) and Molybdenum (Mo) provides the clearest evidence of profound euxinia (a water column completely devoid of oxygen and saturated with free hydrogen sulfide). The concurrent extreme spikes of Mo (up to 87.76 ppm) and V (up to 1022.08 ppm) at the 13–14 m interval mandate the presence of a highly sulfidic, toxic bottom-water environment.

Petrographic Description-

Sample Id- 114207 (ALBH-02) Depth- 27.8 m

In thin section, pyrite and chalcopyrite occurring in schist appear as opaque sulphide minerals. In transmitted light (PPL and XPL), both remain black due to their opacity. In reflected light, pyrite shows a pale brass-yellow colour with high reflectance and commonly cubic form, whereas chalcopyrite appears deeper brassy yellow with slightly lower reflectance and may show anisotropy. These sulphides commonly occur as disseminated grains or along foliation planes within the schist (Figure 8.28, Figure 8.29).

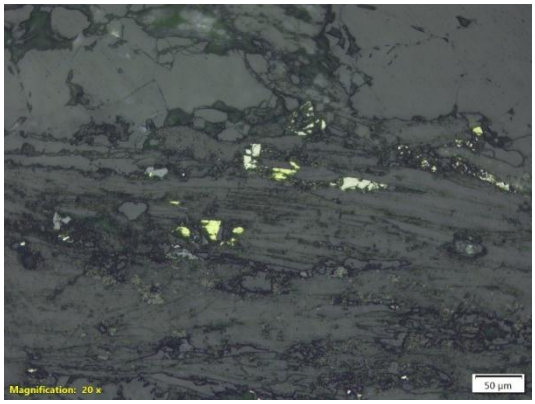

Figure 8.28: Reflected light photomicrograph (20×; scale bar 50 µm) showing chalcopyrite in graphite bearing muscovite schist.

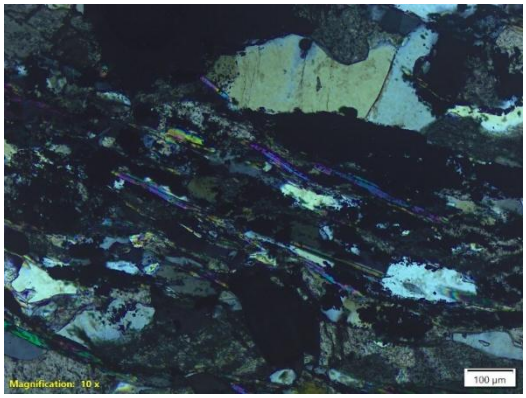

Figure 8.29: Reflected light photomicrograph (10×; scale bar 100 µm) showing quartz rich muscovite schist.

8.5.3 GSPL_Almora_BH03

Surface Selection Criteria- This borehole is located in Sirar Village in a band that extends along East- west and extends ~1 km in length and ~210 m in width (Figure 8.30). Generally, dips Northerly.

Surface Sample Geochemistry shows a wide range of Geochemical Anomaly as follows-

Grab Sample near Borehole-3 Proximate Analysis of Fixed Carbon shows promising Values; i.e, FC% = 6.62 (Sample Id- 109939), 5.43 (Sample Id- 109168), 4.41 (Sample Id- 109923), 3.51 (Sample Id- 109985), 2.83 (Sample Id- 109988), 2,34 (Sample Id- 109943), 2.14 (Sample Id- 109989), 1.86 (Sample Id- 109986), 1.8 (Sample Id- 109987).

Geophysical Signature- VES-12 profiling also shows drop of resistivity (from 495 ohm-m to 278 ohm-m) in between 10 m to 70 m, indicating a conducting layer (probably Graphite bearing horizon).

VES-20 profiling also shows drop of resistivity (from 4121 ohm-m to 1560 ohm-m) in between 25 m to 60 m, indicating a conducting layer (probably Graphite bearing horizon).

Figure 8.30: Exposed wall section near BH-03

Figure 8.31: Drilling team in BH-03

Core Logging-

BH-03 (0–75 m) penetrates an initial overburden of loose, dark-brown soil with minor sericite up to 12.5 m depth, marking a non-graphitic weathered zone (Figure 8.32). This is followed by the onset of graphite mineralization from 12.5 m, initially as moderate-grade graphite associated with redox-sensitive elements and thin quartz veining. Between 17.5 m and 23.5 m, the borehole intersects a dominantly graphitic sludge zone, indicating intense weathering or structural weakening. From 23.5 m to 31.45 m (Figure 8.33), graphite occurs as coherent schist with increasing sulphide content (mainly pyrite) and thin quartz veins, representing an improvement in graphite quality. A thick, continuous high-grade graphite schist zone is encountered from 31.45 m to 42 m, locally marked by very high sulphidation, including an interval of extreme sulphide concentration around 39–39.5 m, suggesting strong structural and redox control on mineralization. Below 42 m, the lithology transitions into graphite–sericite schist (42–47 m) (Figure 8.34) and then into relatively uniform graphite schist up to 55.8 m. This is succeeded by a graphitic quartzite horizon between 55.8 m and 64.8 m, characterized by reduced graphite content and increased silica. The borehole terminates in graphite schist from 64.8 m to 75 m, indicating the persistence of a graphite-bearing horizon at depth and confirming vertical continuity of mineralization in BH03 (Figure 8.31).

Colour Code	From (m)	To (m)	Lithology
	0	12.5	Weathered mica schist with topsoil
	12.5	23.5	Moderate Grade Graphite Schist
	23.5	42	High Grade Graphite Schist
	42	55.8	Graphitic Sericite Schist
	55.8	64.8	Graphitic Quartzite
	64.8	75	High Grade Graphite Schist

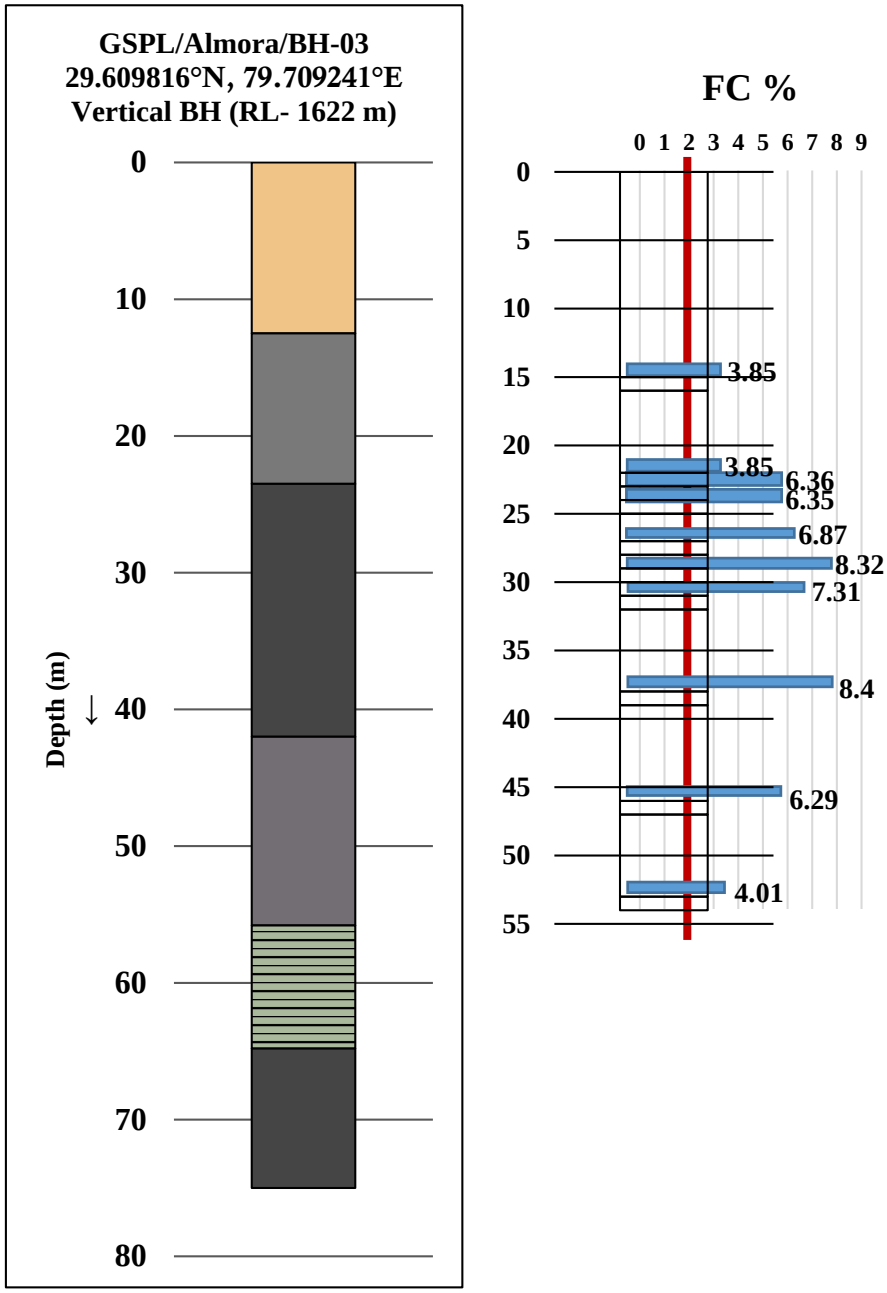

Figure 8.32: Litholog of BH 03, at Sirar area.

Figure 8.33: Graphite schist showing schistose layering

Figure 8.34: Drillcore sample showing graphite horizons traversed by sulphide bearing quartz vein

Chemical Analysis-

Al2O3 shows a decreasing trend while SiO2 shows an increasing tendency with depth. Vanadium is the significant in BH-03, with concentrations exceeding the anomaly threshold (570 ppm) in the majority of sampled intervals. Out of 16 samples that were analyzed, V shows anomaly (5 times Clarke) in 13 samples with a range between 712 ppm to 2758 ppm. Highest value recorded in between 53-54 m. Cu shows anomaly in 10 samples with highest recorded in 608.12 ppm at 65-66 m interval. Mo is highly anomalous with an avg of 133 ppm. Ranges from 2.3 ppm to 211.25 ppm. The highest Mo (191.9–211.2 ppm) at 38–39 m, 59–60 m and 65–66 m coincides with elevated Ni, Se and V. FC ranges from 1.31 to 8.4% with an avg of 5.72% (as per analyzed 11 samples).

Petrographic Description-

Sample Id- 114204 (ALBH-03) Depth- 39.2 m

In thin section, the rock shows a well-developed schistose texture with strong foliation defined by the parallel alignment of platy minerals of chlorite and muscovite with traces of graphite.

Chlorite appears pale to green in plane-polarized light with weak pleochroism and shows low first-order interference colour under crossed polars. Muscovite is colourless in PPL, exhibits perfect cleavage and displays bright second-order interference colours in XPL. Quartz is commonly present as colourless, anhedral grains with low first-order gray interference colours. Pyrite and Chalcopyrite are also associated with this rock. The rock is graphite bearing chlorite muscovite schist (Figure 8.35, Figure 8.36).

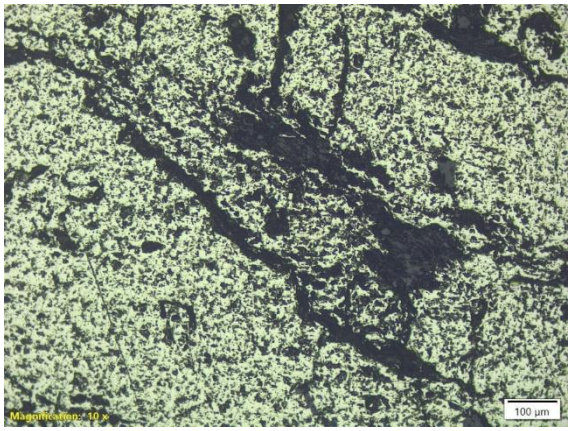

Figure 8.35: Reflected light photomicrograph (10×; scale bar 100 µm) showing pyrite and chalcopyrite in muscovite schist.

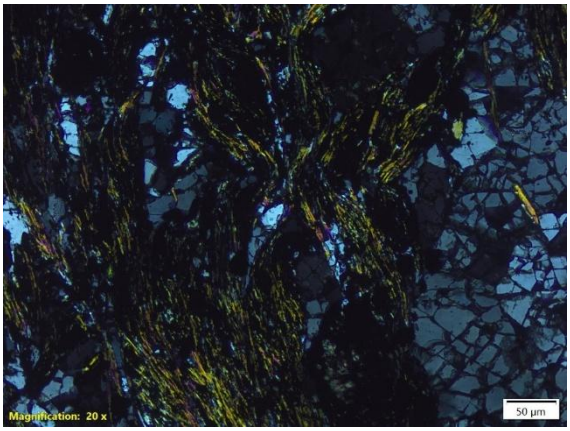

Figure 8.36: Reflected light photomicrograph (20×; scale bar 50 µm) showing Chlorite muscovite schist

Sample Id- 114205 (ALBH-03) Depth- 43.5 m

In this sample, rock is composed of quartz, muscovite, feldspar, graphite and minor of pyrite. Pyrite appears pale brass-yellow in reflected light with high reflectance and cubic crystal form although in section part of it shows. In transmitted light it is opaque, appearing black in both PPL and XPL with no interference colours (Figure 8.37, Figure 8.38, Figure 8.39).

Figure 8.37: Reflected light photomicrograph (4×; scale bar 200 µm) showing foliated granite with mica

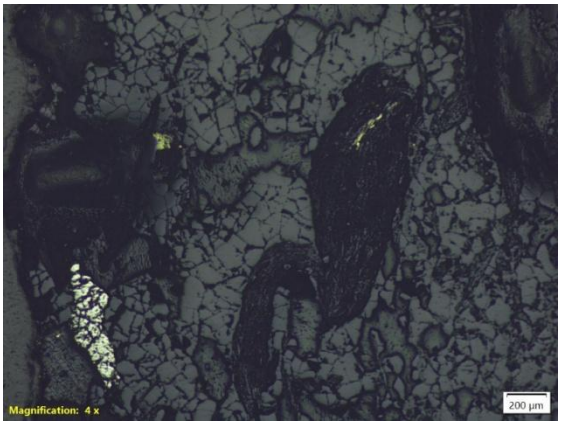

Figure 8.38: Reflected light photomicrograph (4×; scale bar 200 µm) showing foliated granite with pyrite.

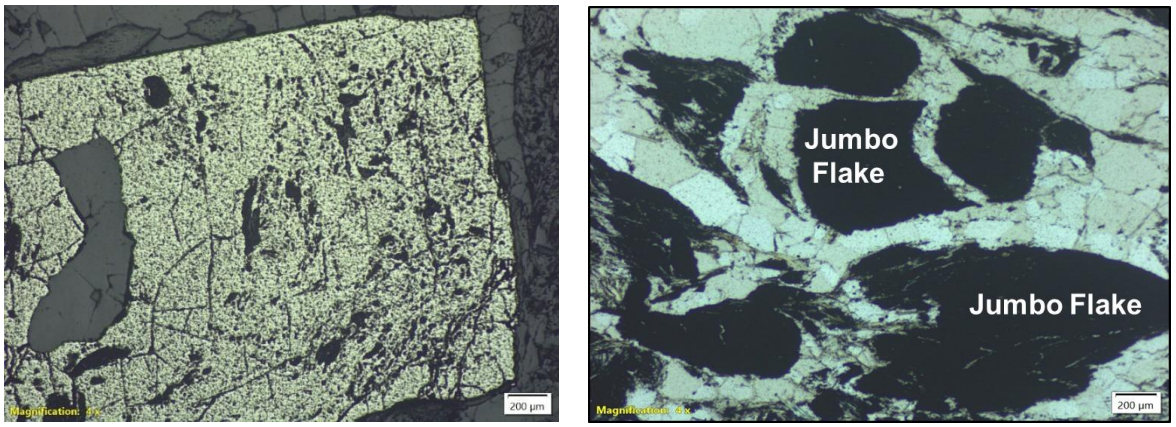

Figure 8.39: Reflected light photomicrograph (4×; scale bar 200 µm) showing foliated granite with pyrite

Sample Id- 113501 (ALBH-03) Depth- 53.36 m

Under the petrographic microscope, graphite appears completely opaque in plane- polarized light (PPL), showing black colour with sharp grain boundaries. It commonly occurs in flaky and often aligned parallel to the foliation in schists. In crossed polars (XPL), graphite remains black due to its opacity and does not show interference colour. The chalcopyrite occurs in disseminated form (Figure 8.40, Figure 8.41, Figure 8.42).

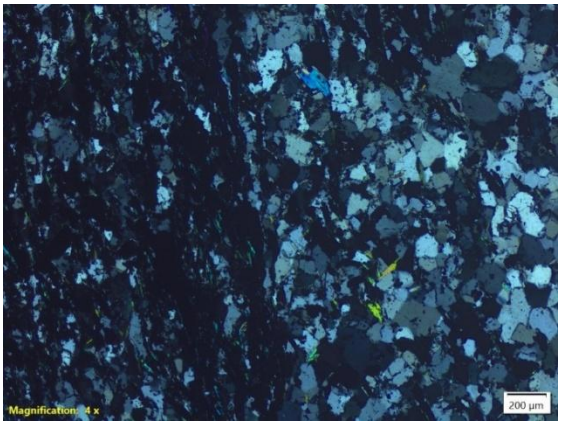

Figure 8.40: Reflected light photomicrograph (4×; scale bar 200 µm) showing granite gneiss with contact of graphite bearing mica schist.

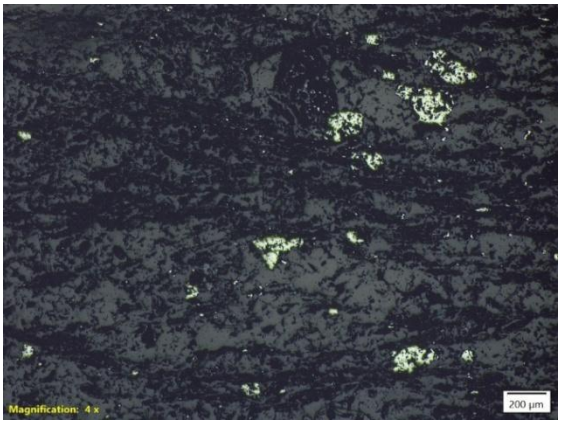

Figure 8.41: Reflected light photomicrograph (4×; scale bar 200 µm) showing granite gneiss with pyrite and chalcopyrite.

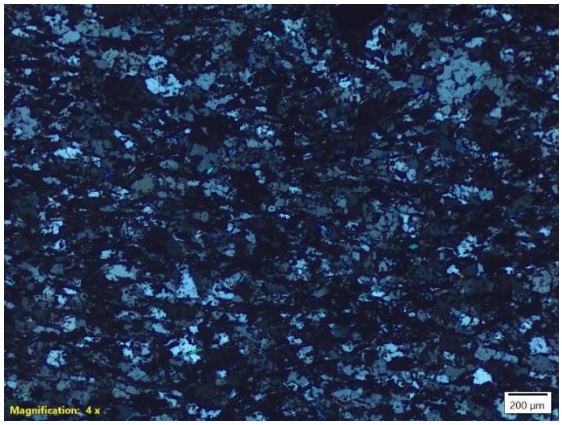

Figure 8.42: Reflected light photomicrograph (4×; scale bar 200 µm) showing granite gneiss.

Sample Id- 114206 (ALBH-03) Depth- 66.7 m

Graphite flakes occurring within recrystallized quartz appear as opaque, black, platy to flaky grains in thin section. In plane-polarized light (PPL) and crossed polars (XPL), graphite remains completely black due to its opacity, while the surrounding quartz is colourless in PPL and shows low first-order gray interference colours in XPL. The quartz typically exhibits a granoblastic texture with interlocking, equigranular crystals formed by recrystallization during metamorphism. Graphite flakes may occur as inclusions within quartz grains or along grain boundaries, sometimes showing alignment parallel to foliation (Figure 8.43, Figure 8.44).

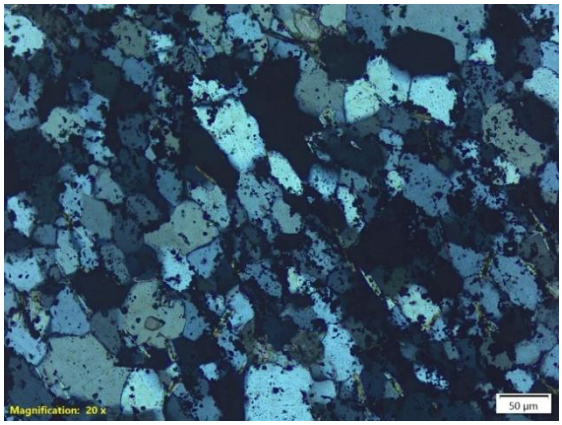

Figure 8.43: Reflected light photomicrograph (20×; scale bar 50 µm) showing fine grained quartzite

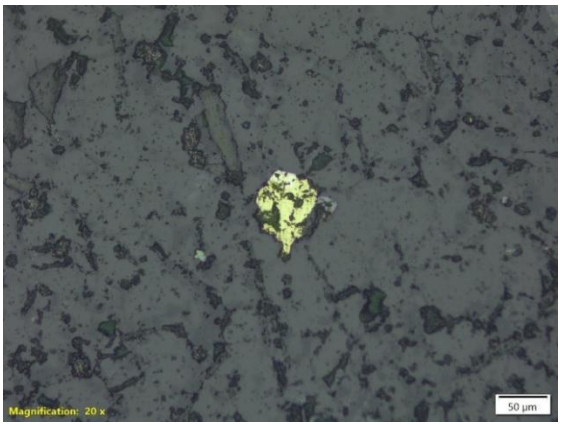

Figure 8.44: Reflected light photomicrograph (20×; scale bar 50 µm) showing Chalcopyrite in fine grained quartzite.

8.5.4 GSPL_Almora_BH04

Surface Selection Criteria- This Borehole is located in Barakote village in a Graphite Schist band which has a Strike length of ~4 km and width of ~180 m. (Figure 8.45)

Surface Geochemistry shows a wide range of Anomalies as follows (Table 8.4)-

Table 8.4: Analytical results of trace elements including Cd, Se, Sn, Sb, Cs, W and Bi (in ppm) for selected samples as bedrock samples.

Sample Id	Cd	Se	Sn	Sb	Cs	W	Bi
110055	3.1						
110061	1.08	2.59	33.18	1.09	25.31	8.17	
110063	1.38	1.98	10.65		18.77	10.47	0.79

Grab Sample near Borehole-4 Proximate Analysis of Fixed Carbon shows promising Values; i.e, FC%= 5.18 (Sample Id- 109940), 3.61 (Sample Id- 109165), 3.35 (Sample Id- 109200), 5.75 (Sample Id- 109942).

Geophysical Signature- VES profiling also shows drop of resistivity (from 309 ohm-m to 140 ohm-m) in between 15 m to 70 m, indicating a conducting layer (probably graphite bearing horizon).

Figure 8.45: Road Cut Section shows massive Graphite Schist Band

Figure 8.46: Drilling team at BH-04

Figure 8.47: Pillaring at BH-04

Core Logging-

This borehole is conducted near Barakote area (Figure 8.46, Figure 8.47).

This borehole begins with 4 m of weathered mica schist with topsoil, underlain by loose mica schist and highly weathered garnet–mica schist. From ~5.5 m, intercalations of graphite schist and mica schist appear, transitioning into very highly to moderately weathered graphite schist with thin quartz veins and occasional thick quartz bands. Between ~13.6–21 m, graphite schist becomes more prominent, showing moderate to dark grey streaks, thin quartz layers and pyrite

within quartz bands, though core recovery is locally poor with chip and sludge samples. A well-developed graphite zone occurs from ~21–40.6 m, comprising dominantly flaky graphite schist with minor amorphous graphite, interlayered quartz, muscovite and sulphides (mainly pyrite). This is followed by graphitic quartzite and intercalated graphite–sericite–quartz–mica schist up to ~46.6 m, then sericite schist with quartz veins. From ~48.7–52 m, graphite–quartz schist with pyrite stringers is present. The lower section (52–64 m) is dominated by biotite mica schist intercalated with thin graphite layers and quartz veins, including a distinct graphite band at 63.20–63.60 m, indicating continued but reduced graphite mineralization at depth (Figure 8.48).

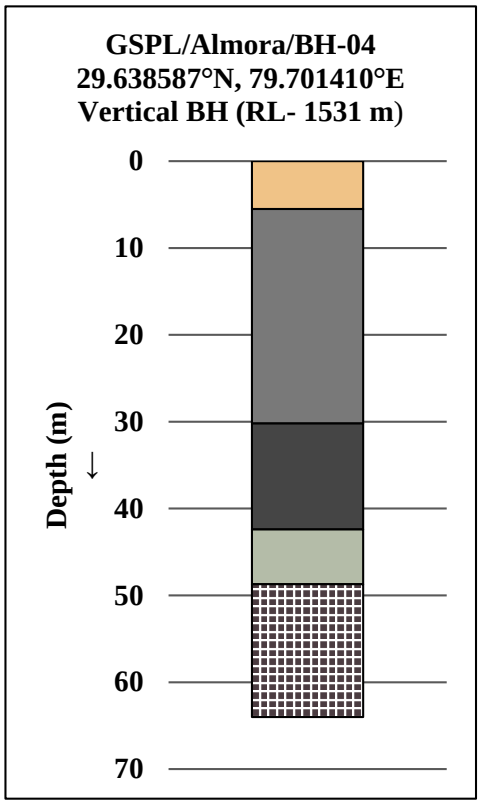

Colour Code	From (m)	To (m)	Lithology
	0	5.5	Weathered mica schist with topsoil
	5.5	30.2	Moderate Grade Graphite Schist
	30.2	42.4	High Grade Graphite Schist
	42.4	48.7	Graphite Quartzite intercalated with Sericite Schist
	48.7	64	Biotite Mica Schist intercalated with thin Graphite Band

Figure 8.48: Litholog of BH 04, at Barakote area

Geochemical Analysis:

Vanadium exhibits the enrichment pattern, with concentrations ranging from 95 ppm at 54.5 m to 1,460 ppm at 15 m, against a Clarke value of 114 ppm and a threshold of 570 ppm. Four of seven samples exceed the anomaly threshold. The highest concentrations are confined to the 10–19 m interval. The mean/Clarke ratio of 6.41 classifies V as the most strongly anomalous major element. Molybdenum is strongly anomalous throughout the borehole, with a mean of 43.52 ppm against a Clarke value of 1 ppm (43.5times enrichment). Individual values range

from 1.23 ppm at 54.5 m to 107.5 ppm at 15 m. Vanadium and Molybdenum are strongly positively correlated. (r = 0.88). Copper displays a highly variable distribution, ranging from 22.6 ppm at 54.5 m to 335 ppm at 18 m (threshold = 280 ppm), with a mean of 128 ppm - 2.3 times the Clarke value. Two samples at 18 m and 19 m exceeds the 5 times Clarke threshold. Silver ranges from 0.61 to 1.36 ppm (Clarke = 0.075 ppm; threshold = 0.375 ppm), with three samples exceeding the threshold (15-16, 18-19 and 19-20 m). Fixed Carbon (FC%), the geochemically relevant indicator of graphite grade, ranges from 1.05% to 6.29% across the sampled interval (as per 3 analyzed samples), with the highest value recorded at 15 m (6.29%) and the lowest at 31 m (1.05%). All three samples exhibit very high ash contents (89.89–96.11%). The Volatile Matter at 18-19 m (6.19%) is notably elevated compared to other samples.

8.5.5 GSPL_Almora_BH05

Surface Selection Criteria- This Borehole is located near Mat Village in a Graphite Schist band having a strike length of ~5.5 km and width ~200 m. This Band Extends along NS. (Figure 8.49)

Surface Geochemistry shows a wide range of Anomalies as follows (

Table 8.5)-

Table 8.5: Selected trace element assay results (V, Se, Mo, Cd, Sb, Ba, Bi, W and U; ppm) for representative samples.

Sample Id	V	Se	Mo	Cd	Sb	Ba	Bi	W	U
109244	1153	0.69	47.66	1.62	57.72		0.53		
109245	2765		142.75	2.06	25.70	4062.61	0.73	6.64	17.38
109962		1.26		1.27	1.07				

Grab Sample near Borehole-05 Proximate Analysis of Fixed Carbon shows promising Values; i.e, FC%= 6.54 (Sample Id- 109197), 5.2 (Sample Id- 109198), 3.46 (Sample Id- 109196)

Geophysical Signature- VES profiling also shows drop of resistivity (from 783 ohm-m to 278 ohm-m) in between 10 m to 60 m, indicating a conducting layer (probably Graphite bearing horizon).

Figure 8.49: Road Cut Section near BH-05 shows Graphite Flakes that easily soils on hand, at Kalimath area

Figure 8.50: Drilling team at BH-05

Figure 8.51: Pillaring at BH-05

Core Logging- (Figure 8.50, Figure 8.51)

This borehole (0–75 m) (Figure 8.52) intersects a shallow weathered zone comprising loose topsoil and sludge overlying weathered mica schist up to 4 m depth. This is followed by mica schist with minor thin graphite (5.15–5.30 m) and occasional quartz veins, transitioning through an intercalated sludge horizon into a progressively graphite-bearing sequence from 8.7 m downward. Between ~8.7 m and 25.4 m, graphite occurs intercalated with mica and sericite

schists, commonly traversed by mm–cm scale quartz veins and accompanied by vugs, limonitic alteration and increasing redox-sensitive elements; sulphur content is visually low near the top but becomes more prominent with depth. From 25.4 m onward (Figure 8.54), the borehole is dominated by graphite schist, locally interbedded with sericite schist and thin quartzose layers, showing clear evidence of ductile shearing, folding and fracture development. High-grade graphite zones are observed particularly between ~29.7–33.8 m and continue intermittently to the bottom of the hole, with coarse graphite flakes occasionally noted within silica-rich bands. Sulphide mineralization, likely pyrite, is moderate to high below ~22.9 m and is typically associated with quartz veins and fold hinge zones, suggesting structurally controlled enrichment. Several sludge/soft intervals occur throughout the borehole, but overall the deeper section (below ~36.5 m) (Figure 8.53,Figure 8.56) maintains a persistent high-grade graphite schist with alternate quartzose layers (locally 2–5 cm thick), pervasive shearing fabrics and continued sulphide association, indicating a laterally continuous and structurally deformed graphite-bearing horizon (Figure 8.55).

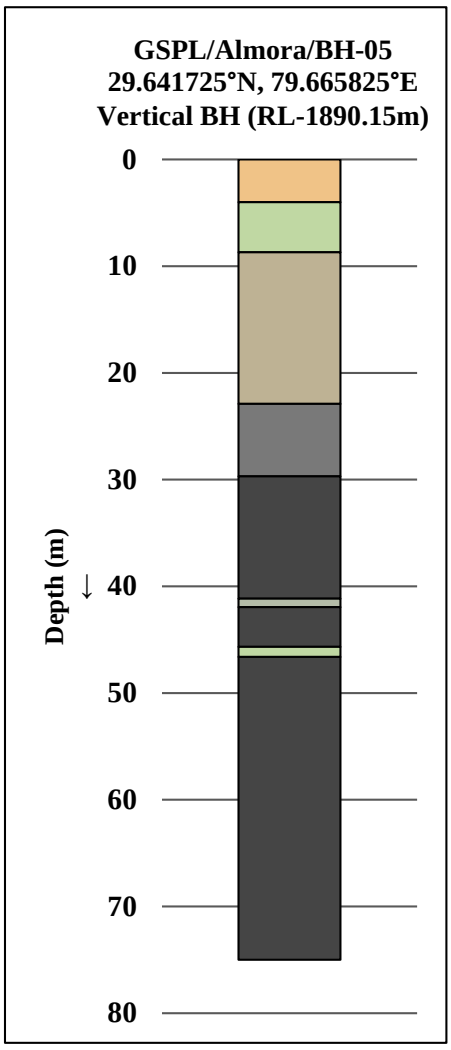

Colour Code	From (m)	To (m)	Lithology
	0	4	Weathered mica schist with topsoil
	4	8.7	Sericite Mica Schist
	8.7	22.9	Quartz Graphitic Schist
	22.9	29.7	Moderate Grade Graphite Schist
	29.7	41.15	High Grade Graphite Schist
	41.15	41.95	Sericitic Graphite Schist
	41.95	45.67	High Grade Graphite Schist
	45.67	46.62	Sericite Mica Schist
	46.62	75	High Grade Graphite Schist

Figure 8.52: Litholog of BH-05, at Mat area

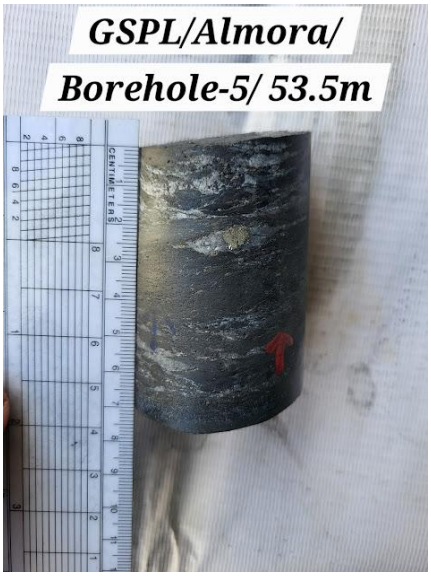

Figure 8.53: Drill core from Borehole-5 at 53.5 m depth, showing graphite-bearing schist with visible foliation and mineralized bands

Figure 8.54: Graphite Schist smoothly soils on hand at 26 m depth.

Figure 8.55: Graphite Schist band traversed by quartz vein at 74.5 m depth

Figure 8.56: Core Box (CB 20) containing graphite schist from 36 m to 40 m depth

Geochemical Analysis:

Vanadium displays one of the most spectacular anomalies in the dataset, with concentrations ranging from 67 ppm to 3,739 ppm (mean: 1,539 ppm). A total of 13 out of 19 samples exceed

the 5× Clarke threshold. The maximum value (3,739 ppm) occurs at 48–49 m and concentrations remain consistently elevated from 15 m depth downward. Copper ranges from 16.9 to 663.1 ppm with a mean of 213.5 ppm. Three samples exceed the anomaly threshold: 23–24 m (663 ppm), 44–45 m (340 ppm) and 72–73 m (296 ppm). The extreme Cu at 23–24 m is notable (663.13 ppm). Molybdenum exhibits extreme enrichment throughout the graphite-schist section, ranging from 1.2 to 119.7 ppm (mean: 58.2 ppm). Fourteen samples exceed the threshold, with peak values in the 32–56 m interval (63–120 ppm). Vanadium and Mo show positive correlation. The fixed carbon (FC%) values of 1.51–5.74%. The highest FC% at 48–49 m (5.74%) coincides with the V-Zn-Mo-U peak.

Petrographic Description-

Sample Id- 114208 (ALBH-05) Depth- 47.8 m

Intense chlorite–muscovite schist in thin section shows a strongly foliated, lepidoblastic texture with well-aligned platy minerals. Chlorite appears pale to green in plane-polarized light (PPL) with weak pleochroism and low first-order interference colour in crossed polars (XPL). Muscovite is colourless in PPL, displays perfect basal cleavage and shows bright second-order interference colour in XPL. Quartz is present as interlocking, anhedral grains with low first-order gray interference colour. The strong alignment of chlorite and muscovite reflects high foliation development during low- to medium-grade regional metamorphism (Figure 8.57, Figure 8.58).

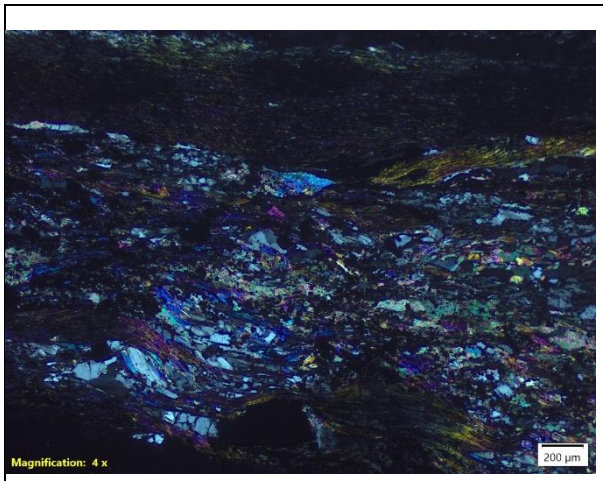

Figure 8.57: Reflected light photomicrograph (4×; scale bar 200 µm) showing chorite muscovite schist

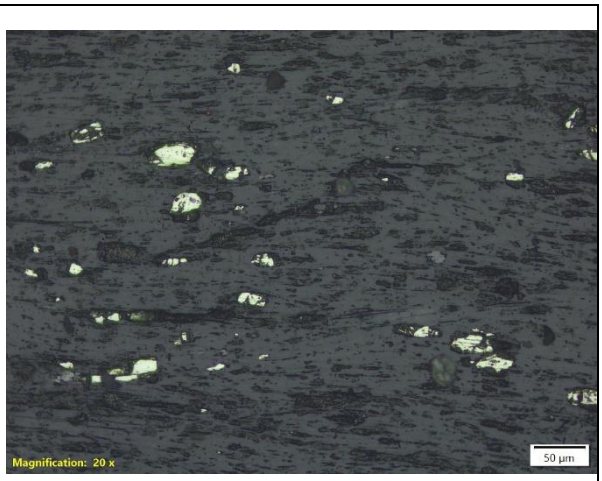

Figure 8.58: Reflected light photomicrograph (4×; scale bar 200 µm) showing pyrite in muscovite schist.

8.5.6 GSPL_Almora_BH06

Surface Selection Criteria- This Borehole is located at Pithauni village in Mica Schist near north of Graphite Schist band having strike length of ~2.4 km and width of ~200 m. The band generally dips southwards (Figure 8.59, Figure 8.60).

Surface Geochemistry shows a wide range of Geochemical Anomalies as follows (Table 8.6)-

Table 8.6: Selected trace element assay results (Zn, Se, Mo, Cd, Sb, Ba and U; ppm) for representative samples

Sample Id	Zn	Se	Mo	Cd	Sb	Ba	U
110058		2.77	10.25	4.48	19.72	4719.19	7.24
110060	520	4.08		3.07	19.03	6112.07	

Grab Sample near Borehole-06 Proximate Analysis of Fixed Carbon shows promising Values; i.e, FC%= 2.14 (Sample Id- 109167), 2.2 (Sample Id- 109164).

Geophysical Signature- VES profiling also shows drop of resistivity (from 1043 ohm-m to 763 ohm-m) in between 20 m to 60 m, indicating a conducting layer (probably Graphite bearing horizon).

Figure 8.59: River section of borehole 06, at Pithauni area

Figure 8.60: Road section of borehole 06, at Sironiya area

Figure 8.61: Drilling team at BH-06

Figure 8.62: Pillaring of BH-06

Core Logging- (Figure 8.61, Figure 8.62)

(0–106 m) begins (Figure 8.63) with weathered mica schist with topsoil followed by shallow, oxidized graphite–sericite schist and intermittent weathered zones up to ~21.5 m depth. Between 21.5 m and 41 m (Figure 8.64), the sequence is dominated by sericite schist with minor graphite pockets and increasing quartzose banding, indicating a transitional graphitic horizon within a micaceous host. A significant high-grade graphite schist zone with strong sulphidation is encountered between 41–45.3 m, representing the first major enriched graphite interval. Below this, the lithology transitions into dominantly graphitic sericitic quartzite and graphitic quartzite (48.8–84.8 m), characterized by fine alternations of quartzose and graphitic bands with moderate sulphide dissemination. A distinct high-grade graphite schist band reappears at 84.8–88.9 m, followed by continued graphitic quartzite and finely intercalated graphite–sericite layers down to the final depth of 106 m (Figure 8.65).

Overall, BH06 represents a quartzose-dominant graphitic sequence with two significant high-grade graphite schist horizons (41–45 m and 84.8–88.9 m), separated by thick graphitic quartzite and sericitic intercalations, indicating vertically discontinuous but structurally controlled graphite enrichment.

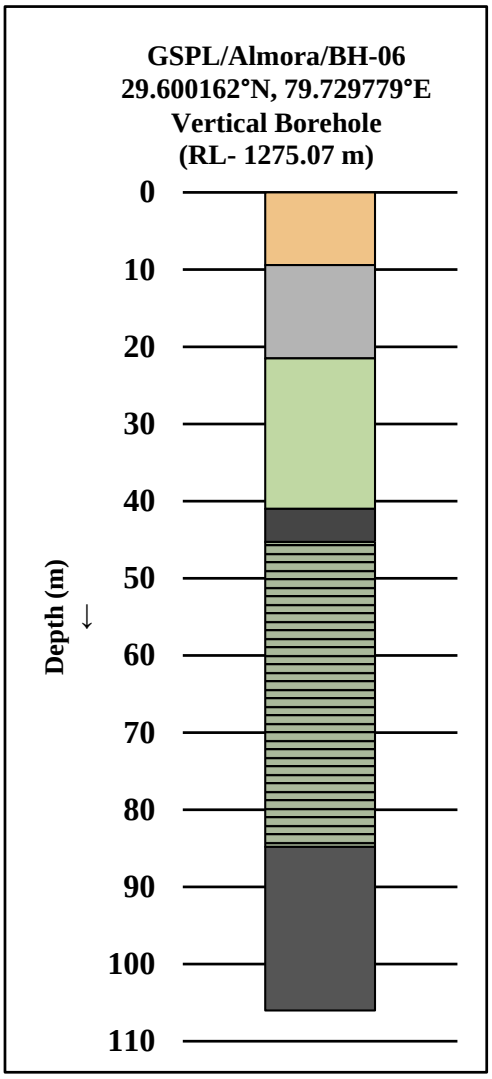

Colour Code	From (m)	To (m)	Lithology
	0	9.4	Weathered mica schist with topsoil
	9.4	21.5	Graphite–Sericite Schist
	21.5	41	Sericite Mica Schist
	41	45.3	High Grade Graphite Schist
	45.3	84.8	Graphitic Quartzite
	84.8	106	High-Grade Graphite Schist to Graphitic Quartzite

Figure 8.63: Litholog of BH-06, at Pithauni area

Figure 8.64: Drill core from Borehole-6 at 32.8 m depth, showing graphitic sericite schist with low sulphide mineralization.

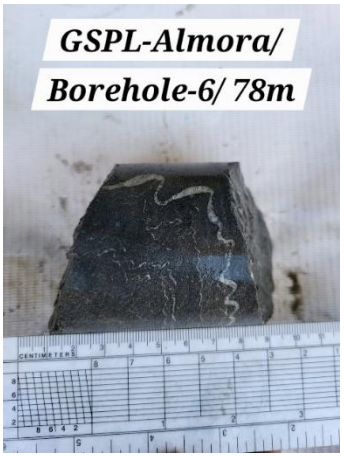

Figure 8.65: Drill core from Borehole-6 at 78 m depth, showing graphite-bearing schist with irregular quartz veinlets and foliation-controlled mineralization

Chemical Analysis-

Vanadium shows a generally moderate enrichment (mean 1.28 times Clarke) with a single strong anomaly at 102–103 m (582.7 ppm). The spike at depth coincides with the Mo-U-Bi-Cd deep anomaly cluster, reinforcing the interpretation of a strongly reducing euxinic zone in the lower borehole. V also correlates strongly with Ni (r = 0.92), Cd (r = 0.99) and Bi (r = 0.92).

Molybdenum (Mo) shows a strongly bimodal depth distribution. In the upper portion (14–67 m), Mo values are near or slightly above background (0.43–2.17 ppm). A moderate spike at 41–42 m (20.3 ppm) is followed by low values before a pronounced, sustained deep anomaly at 81–82 m (14.56 ppm) and 97–106 m (31–38 ppm). This deep anomaly zone is interpreted as a redox-controlled precipitation front, where Mo was transported by oxidizing hydrothermal fluids and precipitated upon encountering the reduced, carbonaceous/sulphidic graphite schist environment. The strong positive correlations of Mo with Ni (r = 0.94), U (r = 0.97) and Bi (r = 0.93) are strongly consistent with a euxinic/organic trap mechanism.

8.5.7 GSPL_Almora_BH07

Figure 8.66: Drilling Team at BH-07

Core Logging- (0-50 m) (Figure 8.66, Figure 8.67) is dominated by sericite–mica schist with intermittent graphite-bearing horizons. The borehole begins with a mixed topsoil–graphitic sludge zone (0–6 m), followed by thick mica schist with quartz veining and local shear indicators up to ~24.7 m, indicating a structurally influenced metamorphic sequence. Graphite mineralization occurs as discontinuous intercalations between 9.55–10.3 m and more consistently between 24.68 m and 35.73 m, comprising graphite–mica schist, moderate-grade graphite schist and graphitic quartzite. These zones are generally moderate in grade and structurally controlled, with occasional quartz veins (locally up to 2 cm thick). Below ~36.9 m, the lithology transitions back into predominantly mica schist with minor graphitic intercalations and the borehole terminates in non-graphitic mica schist at 50 m depth.

Overall, BH07 indicates discontinuous, structurally intercalated moderate-grade graphite horizons within a dominant sericite–mica schist host.

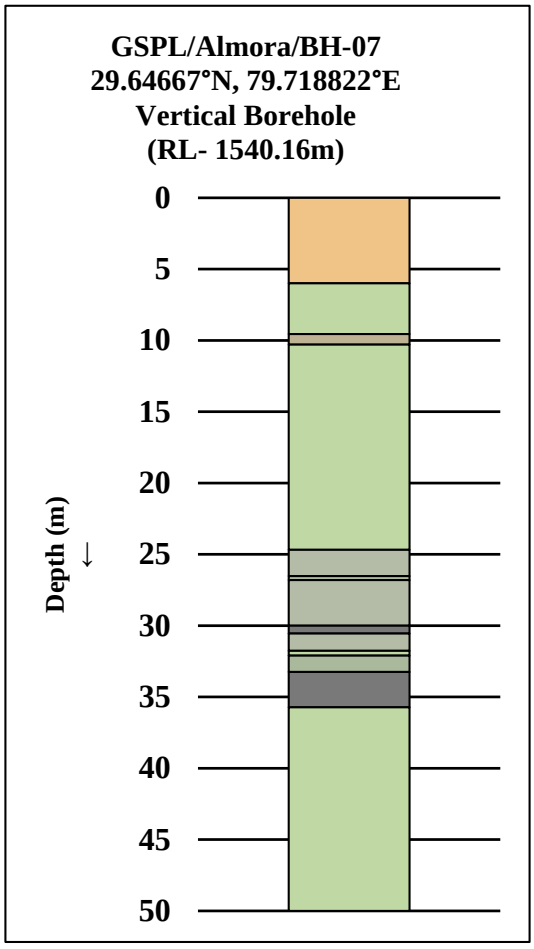

Colour Code	From (m)	To (m)	Lithology
	0	6	Weathered mica schist with topsoil
	6	9.55	Sericite Mica Schist
	9.55	10.3	Quartz Graphitic Schist
	10.3	24.7	Sericite Mica Schist
	24.68	26.5	Graphitic Sericite Schist
	26.52	26.8	Graphitic Quartzite
	26.81	30	Graphitic Sericite Schist
	30	30.6	Medium Grade Graphite Schist
	30.55	31.8	Graphitic Sericite Schist
	31.77	32.1	Sericite Mica Schist
	32.1	33.3	Graphitic Quartzite
	33.25	35.7	Medium Grade Graphite Schist
	35.73	50	Sericite Mica Schist

Figure 8.67: Litholog of BH-07, at Deora village.

Chemical Analysis-

Vanadium (V) shows near-Clarke overall (mean 113 ppm, EF 0.99 times) but with a spike at 35-36 m (309 ppm; 2.7× Clarke). V is strongly enriched in organic-rich sediments and graphite schists owing to organic matter affinity and ilmenite/biotite substitution. The extreme V at 35–36 m, co-varying with Mo (r=0.94) and U (r=0.97), constitutes the core redox-sensitive element signature. This co-enrichment is the most powerful geochemical indicator of the graphite-rich, originally euxinic horizon.

Molybdenum (Mo) shows anomalous values in two samples i.e. 13.2 ppm (9-10 m) and 23.2 ppm (35-36 m). Mo shows strong correlation with V (r=0.94) and U (r=0.98). Uranium (U) shows anomalous value in one sample (11.6 ppm at 35-35 m). 113522 (35–36 m depth) represents the most geochemically anomalous single horizon in the borehole. Five elements simultaneously exceed their respective anomaly thresholds at this depth: Ba (4685 ppm; 4× threshold), Mo (23.2 ppm; 4.6× threshold), U (11.6 ppm; 1.5× threshold), Ag (1.24 ppm; 3.3× threshold) and Cd (1.10 ppm; 1.6× threshold). In addition, V reaches 309 ppm (2.7× Clarke),

LOI peaks at 4.55% and Cu reaches 77.1 ppm. This multi-element convergence at a single depth is interpreted as the axis of a structurally controlled, graphite-rich shear zone with significant hydrothermal overprinting.

The 9–10 m interval (peak Sb 38.4 ppm, anomalous Mo 13.2 ppm and Ag 0.42 ppm) constitutes the secondary anomalous zone.

8.5.8 GSPL_Almora_BH08

Surface Selection Criteria- This Borehole is located in Batgal Village in a graphite Schist band extending NS with a bend in EW, having a strike length ~620 m and width ~85 m. The band dips northerly (Table 8.7).

Table 8.7: Assay results of selected trace elements (V, Se, Mo, Cd, Sb, Ba, Bi and U; ppm) for representative bedrock samples.

Sample Id	V	Se	Mo	Cd	Sb	Ba	Bi	U
109227	969	5.52	73.35	1.79	29.01	2516.01	0.54	8.46
109228	1128.34	0.95	45.59	1.78	27.71			37.34
109229	943.15	9.63	64.90	1.72	31.72	7574.09		11.93
109230	728.5	8.14	51.92	1.68	28.17	13668.18		13.96

Figure 8.68: Drilling team at BH-08

Figure 8.69: Pillaring at BH-08

Core Logging- (0–50 m) (Figure 8.68, Figure 8.69) begins with a thick weathered mica schist with topsoil and highly weathered mixed zone up to 16 m depth. From 16–28.14 m, the borehole is dominated by sericite–mica schist with minor graphite stringers and quartz veins, indicating weak and discontinuous mineralization. Between 28.14–37.3 m, graphite occurs as fine flaky laminae aligned with foliation within graphite–sericite schist, representing low- to

moderate-grade mineralization. A moderate-grade graphite schist band is intersected at 37.3–39 m, followed by a non-graphitic mica schist interval from 39–43 m. The principal mineralized horizon occurs at 43–45 m as high-grade, sulphide-rich graphite schist. Below this, intercalated graphite–sericite schist and moderate-grade graphite schist persist up to 48.4 m, before transitioning back to mica schist at the borehole termination depth of 50 m (Figure 8.70). BH08 indicates localized, structurally controlled high-grade graphite enrichment at 43–45 m within a dominantly mica schist host.

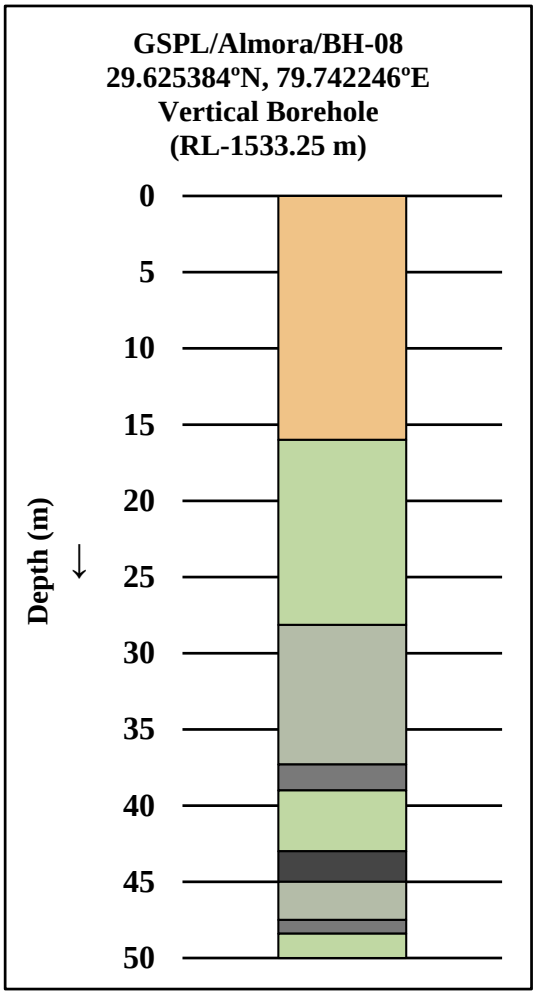

Colour Code	From (m)	To (m)	Lithology
	0	16	Weathered mica schist with topsoil
	16	28.14	Sericite Mica Schist
	28.14	37.3	Graphitic Sericite Schist
	37.3	39	Medium Grade Graphite Schist
	39	43	Sericite Mica Schist
	43	45	High Grade Graphite Schist
	45	47.5	Graphitic Sericite Schist
	47.5	48.4	Medium Grade Graphite Schist
	48.4	50	Sericite Mica Schist

Figure 8.70: Litholog of BH-08, at Udalgaon village

Geochemical Analysis:

Out of 9 samples analyzed, Vanadium shows no anomaly with an overall mean of 141 ppm. Vanadium ranges from 68 – 365 ppm with highest value in the 48 -49 m interval. Se is anomalous throughout the Borehole. Ag shows 9.37 ppm within the interval of 21.5 to 22.5 m. Mo is anomalous in three samples out of 9 samples (mean 18.25 ppm) analyzed.

Highest value recorded in 48 - 49 m interval. (26.82 ppm) FC analysis was done for a sample that shows 3.02% fixed carbon.

8.5.9 GSPL_Almora_BH09

Surface Selection Criteria- This borehole is located at Batgal village in a graphite schist band (extending EW and dips southerly) having a strike length of ~650 m and width ~70 m.

Grab Sample near Borehole-09 Proximate Analysis of Fixed Carbon shows promising Values; i.e, FC%= 3.92 (Sample Id- 109163), 2.54 (Sample Id- 109282).

Figure 8.71: Drilling team at BH-09

Figure 8.72: Pillaring at BH-09

BH-09 is conducted near Batgal area (Figure 8.71, Figure 8.72)

Core Logging-

The borehole (Figure 8.73) intersects a thin weathered mica schist with topsoil cover overlying a succession of highly weathered to fresh mica schist and graphite schist, with local intercalation and mixed zones. The upper part is dominated by sludgy/decomposed schist, while the lower part shows comparatively fresh mica schist with occasional weathered intervals.

Geochemical Analysis:

Out of 6 samples analyzed, Vanadium (mean 368 ppm) is anomalous in a single sample (1502.34 ppm) within the depth interval of 3-4 m. Mo shows (out of 6 samples) mean value of 9.71 ppm with highest recorded in between 3-4 m (44.41 ppm). 3 samples exceed the threshold of 5 times Clarke. 1 Sample analyzed for FC that shows 2.99% fixed carbon.

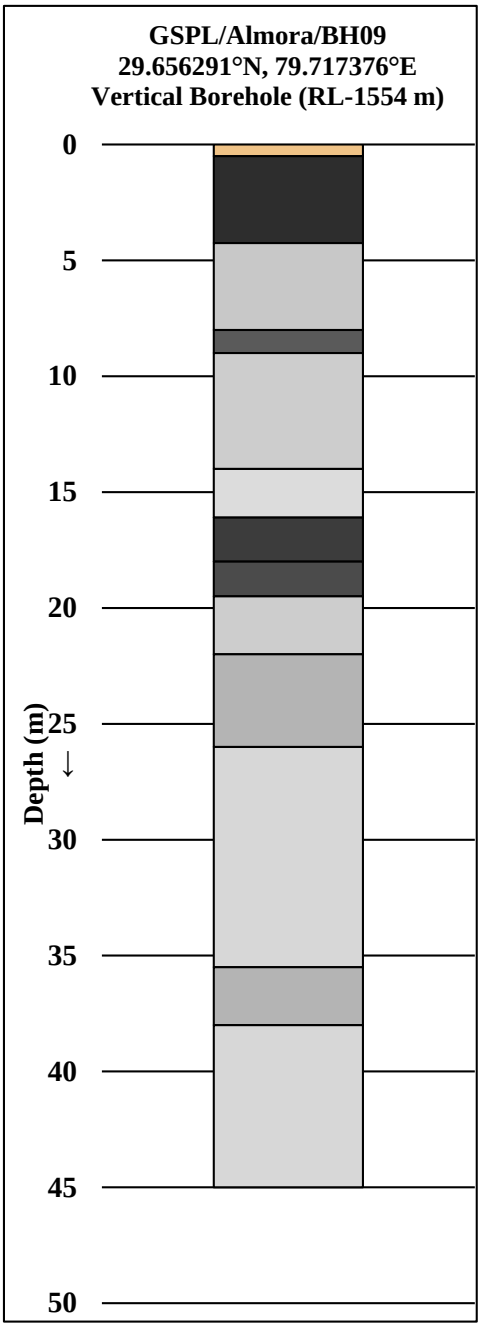

Colour Code	From (m)	To (m)	Lithology
	0	0.5	Weathered mica schist with topsoil
	0.5	4.25	Highly weathered graphitic schist, sludgy
	4.25	8	Highly weathered mica schist, sludgy
	8	9	Intercalated mica schist and graphitic schist
	9	14	Highly weathered mica schist, sludgy
	14	16.1	Loose / highly weathered mica schist
	16.1	18	Loose / highly weathered graphitic schist
	18	19.5	Loose mixed mica schist with dominant graphitic schist
	19.5	22	Highly weathered mica schist, sludgy
	22	26	Mica schist
	26	35.5	Loose/ weathered mica schist
	35.5	38	Mica schist
	38	45	Loose/ weathered mica schist

Figure 8.73: Litholog of Borehole 09, at Batgal village

8.5.10 GSPL_Almora_BH10

Surface Selection Criteria- Extension of Sirar Graphite band on which BH-03 was drilled. Here the outcrops in the road section shows prominent graphite exposures (Figure 8.74).

Geophysical Signature- VES profiling shows preodic rise and drop (overall drop) of resistivity (from 3343 ohm-m to 1855 ohm-m) in between 10 m to 80 m, indicating a conducting layer (probably Graphite bearing horizon).

Figure 8.74: Exposed section shows Graphite-Schist banding near BH-10

Figure 8.75: Photographs of core box 05 of borehole 10 from 17 m to 22 m

Figure 8.76: Drilling team at BH-10

Figure 8.77: Pillaring at BH-10

Core Logging-

The BH-10 is conducted in Sirar area **(**Figure 8.75**,** Figure 8.76**,** Figure 8.77**).**

The borehole (Figure 8.79) reveals a surficial weathered mica schist with topsoil horizon admixed with sericite, underlain by a thick zone of high-grade graphite schist enriched in

redox-sensitive elements. This transitions downward into comparatively low redox graphite schist with occasional greenish coloration, followed by zones of highly weathered and decomposed greenish and graphite schist. The lower section comprises loose to weathered high-grade graphite schist (Figure 8.78).

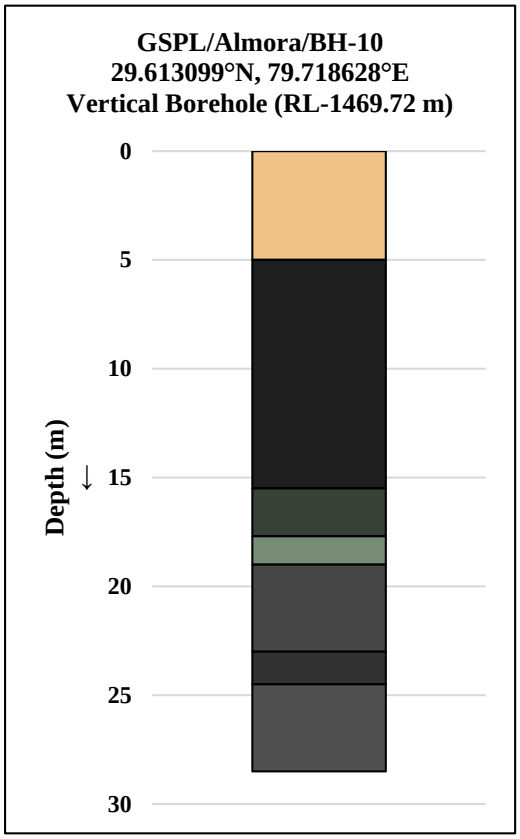

Colour Code	From (m)	To (m)	Lithology
	0	5	Top Soil mixed with Sericite.
	5	15.5	High-grade graphitic schist (enriched in redox-sensitive elements)
	15.5	17.7	Graphitic schist (low redox-sensitive elements), locally greenish
	17.7	19	Highly weathered greenish schist (sludgy)
	19	23	Highly weathered graphitic schist (sludgy)
	23	24.5	Loose / friable high-grade graphitic schist
	24.5	28.5	Weathered high-grade graphitic schist

Figure 8.78: Litholog of BH-10, at Sirar village

Figure 8.79: Drill Core Samples of Graphite Band

Chemical Analysis-

Out of 8 samples analyzed, Vanadium shows (mean 596.76 ppm) a range of 123-1216 ppm with highest value of 1216 ppm (16-17 m). Vanadium exceeds threshold value of 5 times Clarke in 5 samples within the depth interval of 9 – 23 m. Within the 8 analyzed samples Cu (mean 134 ppm) exceeds threshold value in 2 samples in between 21 – 23 m. Highest value is 385 ppm (22-23 m). All 8 samples show anomalous (9.53 ppm – 58.36 ppm) Mo (mean 39.94 ppm) throughout the borehole with highest 58.36 ppm. (15-16 m). FC values range from 2.15% to 3.1% (as per 3 analyzed samples)

8.5.11 GSPL_Almora_BH11

Surface Selection Criteria-

Extension of Sirar Graphite band on which BH-01 was drilled. Here the outcrops in the road section shows prominent graphite exposures (Figure 8.80).

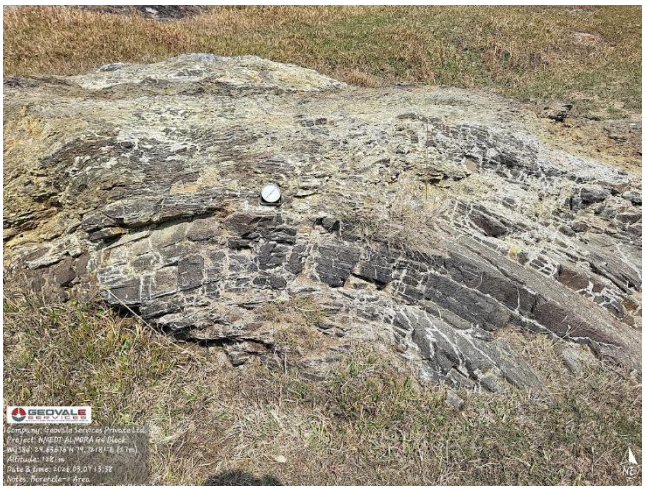

Figure 8.80: Folding of Graphite Band near BH-11

Core Logging- The borehole (Figure 8.81) commences with a weathered mica schist with topsoil horizon containing graphitic sludge (0–5 m), underlain by a thick weathered graphite–sericite zone (5–17 m) and a sericite-dominant interval (17–23.6 m), indicating intense surface weathering and leaching. This is followed by a high-grade graphite schist zone (23.6–30.5 m) representing the primary mineralized horizon, which transitions downward into an intercalated sequence of graphite and mica schist (30.5–41.1 m) and a moderate-grade graphite zone (41.1–43.3 m), reflecting lithological and structural control. The interval from 43.3 to 75.8 m is dominated by mica schist hosting disseminated and banded graphite, commonly associated with quartz veins and includes a localized high-grade sulphidic graphite band at 58.35–59.7 m; overall, the mineralization in this zone is discontinuous and stratabound, occurring as thin bands and lenses. Below 75.8 m, the sequence comprises relatively barren mica schist up to 90 m, with the borehole terminating in foliated granite (90–92 m) (Figure 8.82, Figure 8.83, Figure 8.84, Figure 8.85).

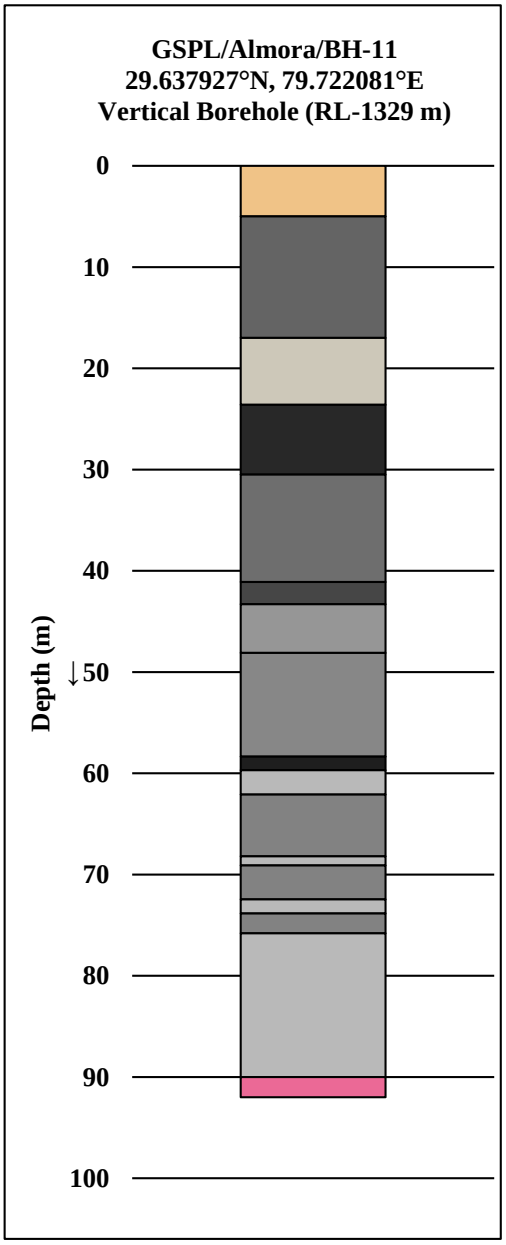

Colour Code	From (m)	To (m)	Lithology
	0	5	Weathered mica schist with topsoil
	5	17	Graphite–sericite (sludgy/weathered)
	17	23.6	Sericite (minor graphite)
	23.6	30.5	High-grade graphite schist
	30.5	41.1	Intercalated graphite & mica schist
	41.1	43.3	Moderate-grade graphite schist
	43.3	48.1	Mica schist with disseminated graphite (altered, quartz veins)
	48.1	58.4	Mica schist with graphite bands (with quartz)
	58.4	59.7	High-grade graphite band (sulphidic)
	59.7	62.1	Mica schist
	62.1	68.2	Mica schist with thin graphite bands (repetitive)
	68.2	69.1	Mica schist
	69.1	72.5	Mica schist with thin graphite bands
	72.5	73.9	Mica schist
	73.9	75.8	Mica schist with thin graphite bands
	75.8	90	Mica schist
	90	92	Foliated granite

Figure 8.81: Litholog of BH-11, at Digoli village.

Figure 8.82: Drillcore sample of graphite schist associated with cherty layer at 43 m depth

Figure 8.83: Graphite Band traversed by Isoclinal Quartz vein

Figure 8.84: Graphitic Quartzite

Figure 8.85: Sulphidation Channel between Graphite Band

Chemical Analysis-

Out of 17 samples analyzed, Vanadium shows a range of 53 to 573 ppm with a mean of 200.45 ppm. One sample exceeds the 5x Clarke threshold (573.01 ppm at 2-3 m interval). Within the 17 samples analyzed (mean 11.45 ppm), Mo is anomalous in 8 samples with highest value 29.72 ppm at 29-30 m interval. One proximate analysis was performed on sample 113559 (31–32 m): IM = 0.47%, VM = 2.46%, Ash = 96.06%, FC = 1.01%.

8.5.12 GSPL_Almora_BH-12

Surface Selection Criteria-

Extension of Sirar Graphite band on which BH-06 was drilled. Here the outcrops in the road section shows prominent graphite exposures.

Geophysical Signature- VES profiling shows overall low resistivity following a continuous declining from 50 m depth (apparent resistivity 636 ohm-m) upto investigation depth of 100 m (apparent resistivity 0 ohm-m).

Core Logging-

First 16 m is top soil followed by a thin Sericite zone (16-17.5 m) and from then continues upto 64 m High Grade Graphite Schist mixed with occasional Graphite Sludge (Figure 8.86).

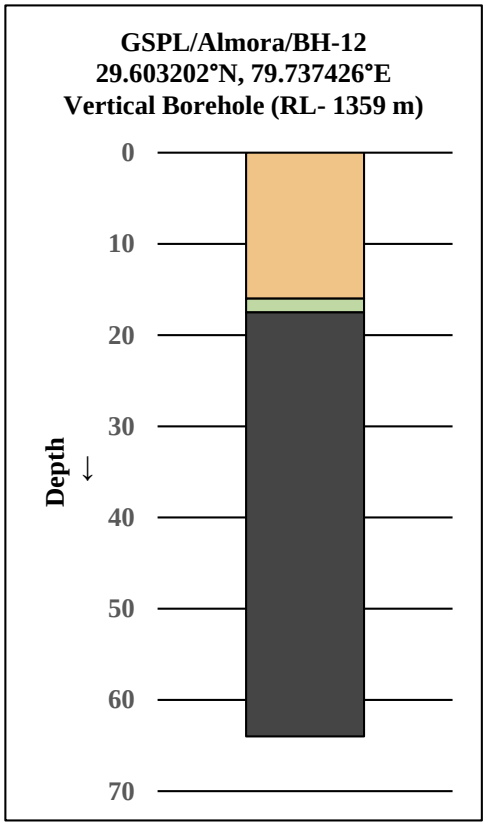

Colour code	From (m)	To (m)	Lithology
	0	16	Weathered mica schist with topsoil
	16	17.5	Sericite Mica Schist
	17.5	64	Graphite Schist

Figure 8.86: Litholog of BH-12, at Sironiya area.

Chemical Analysis-

Out of 11 samples analyzed, Vanadium (mean 326 ppm) shows anomalous values in two samples (662 ppm at 45-46 m and 1380 ppm at 54.5-56 m).

Out of those analyzed 11 samples Cu shows anomalous values within 26.5 to 31 m (evident from 2 samples) with a mean of 711 ppm.

Molybdenum (mean 23.82 ppm) exceeds threshold values in 8 samples with anomalous range of in between 5.48 ppm to 79.35 ppm.

Out of 4 Proximate analyses, 3 samples exceed 2% cutoff (4.06%, 2.34%, 6.92%).

Summerized true thickness of the graphite bands obtains for all boreholes (Table 8.8) are given below.

Table 8.8: Details of true thicknness for all boreholes.

Borehole No	Band Name	From (m)	To (m)	Thickness of Graphite in Vertical Borehole	Dip Amount of Graphite Band	True thickness of graphite band
BH-01	Digoli-Gajjola Graphite Block	16	91.7	75.7	26	68
BH-02	Sirar-Bataldeon Graphite Band	12.35	22.8	10.45	22	9.69
		23.5	24.36	0.86	22	0.79
		27.15	40.27	13.12	22	12.16
BH-03	Sirar-Bataldeon Graphite Band	12.5	75	62.5	20	58.73
BH-04	Digoli-Gajjola Graphite Block	5.5	48.7	43.2	20	40.59
BH-05	Kalimath Graphite Band	22.9	45.67	22.77	18	21.66
		46.62	75	28.38	18	26.99
BH-06	Phalsima-Pithauni Graphite Block	9.4	21.5	12.1	25	10.96
		41	106	65	25	58.91
BH-07	Digoli-Gajjola Graphite Block	24.68	31.8	7.12	20	6.69
		32.1	35.7	3.6	20	3.38

Borehole No	Band Name	From (m)	To (m)	Thickness of Graphite in Vertical Borehole	Dip Amount of Graphite Band	True thickness of graphite band
BH-08	Sirar-Bataldeon Graphite Band	28.14	39	10.86	20	10.21
		43	48.4	5.4	20	5.07
BH-09	Batgal-Channi Graphite Block	0.5	8	7.5	50	4.82
		16	19.5	3.5	50	2.25
BH-10	Sirar-Bataldeon Graphite Band	5	28.5	23.5	25	21.3
BH-11	Digoli-Gajjola Graphite Block	5	17	12	15	11.59
		23.6	59.7	36.1	15	34.87
		62.1	68.2	6.1	15	5.89
		69.1	72.5	3.4	15	3.28
		73.9	75.8	1.9	15	1.83
BH-12	Phalsima-Pithauni Graphite Block	17.5	64	46.5	24	42.48

Chapter 9

Exploration Target Potential: Reconnaissance-Scale Resource Assessment

9 Exploration Target Potential: Almora Graphite Blocks

9.1 Preamble and Reporting Framework

This chapter presents the exploration target potential of each of the five graphite-bearing blocks identified and characterised in Chapters 7 and 8 of the Almora G4 reconnaissance report. The blocks are: i) Digoli-Gajjola, ii) Sirar-Bataldeon, iii) Kalimath, iv) Phalsima-Pithauni and v) Batgal-Channi.

Graphite mineralization occurs as thin intercalated bands (with thickness varying cm to m scale) within graphite schist (mica bearing), graphitic quartzite, graphite sericite schist; all these forms as the host rocks for graphite (Figure 9.1, Figure 9.2, Figure 9.3). The graphite is mostly concentrated along the foliation plane but also found to occur as disseminated flake/vein/veinlets within the host rocks. In many of the cases, the intercalation as well as dissemination are so intensed that the entire host rocks look like a graphite body as a whole (Figure 9.4). Graphite is present mostly as medium to coarse grained flakes, imparting a characteristic dark-grey to black colour to the rock (Figure 9.5 and Figure 9.6). The graphite mineralization is interpreted to have originated from carbonaceous sedimentary material that underwent deformation and regional metamorphism, followed by increase in crystallinity due to contact metamorphism during lit- per-lit injection of younger granite. The overall colour of the host rock varies from light grey to dark grey depending on its graphite contents (FC), as evidenced through proximate analyses.

Figure 9.1: Graphite Schist as observed in road cutting section near Sirar Village.

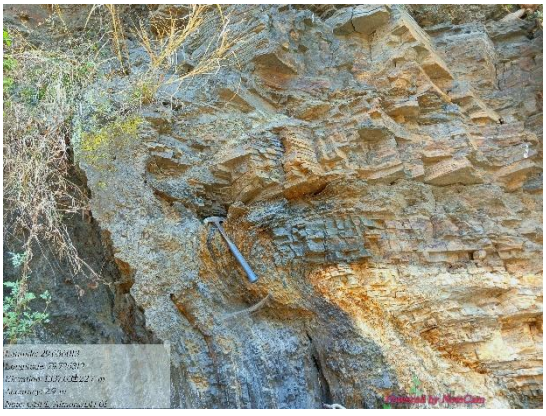

Figure 9.2: Graphitic Quartzite as observed in road cutting section near Digoli Village.

Figure 9.3: Graphitic Sericite Schist as observed in drill core sample of BH-06 (depth 21.1 m), near Pithauni Village.

Figure 9.4: Intercalated Graphite Schist contact with mica schist as observed in road cutting section near Bataldeon

Figure 9.5: Medium to Coarse flake sized, Dark Grey Graphite Schist as observed in BH-03 (depth 43.55 m), near Sirar Village

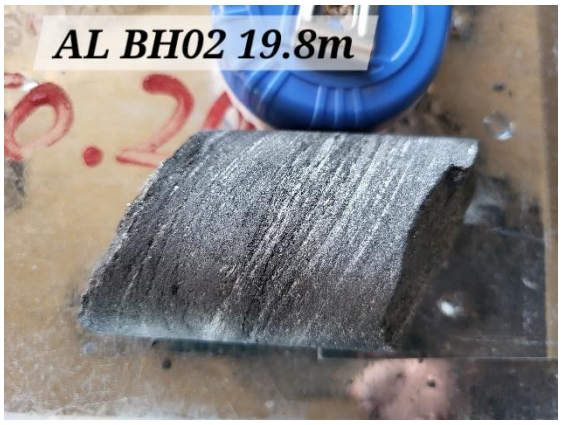

Figure 9.6: Light to Drak Grey Graphite Schist as observed in BH-02 (depth 19.8 m), near Bataldeon Village.

We described the graphite zones and its width on the basis of lithological indexing, mostly on the basis of colour intensity in the shades of grey, tumbler test and flake size. Accordingly, we classified the graphitic rocks as low grade (light grey colour, low in tumbler test, more micaceous quantity than graphite), moderate grade (grey, moderate in tumbler test, medium micaceous quantity than graphite) and high grade (dark grey, very high in tumbler test, less micaceous quantity than graphite). Confirming these grade connotations by chemical

analysis could not be achieved due to limited sanctioned quantity of proximate analysis (50 sanctioned quantities were distributed across 12 boreholes each for multiple depths, against our drilled cumulative graphite bearing host rocks of ~ 500 m). We could not make continuous composite sample analysis for any of the 12 boreholes. The chemical analysis, though limited in numbers, but majority of the analysis samples show FC > 2%, the highest FC value recored as 8.40%. Possibilities of higher FC values in this block cannot be nullified.

Reconnaissance resource assessment in identifying mineralized zones in corroboration with chemical assay could not be done. Lithologically, we marked the thickness of the graphitic rock mass in each of the boreholes, and accordingly, we assessed the volume of the rock mass.

The current project constitutes a G4 (Reconnaissance) stage Geological Report. At this stage, mineralisation is established through systematic mapping, surface and sub-surface geochemistry, geophysics, scout drilling, and identifying the graphite-vanadium mineral potential zones. In this G4 (Reconnaissance) stage, the quantitative outputs of this chapter are therefore presented strictly as Exploration Target Potential.

The exploration target formula is applied throughout by below equation:

$$\text{Tonnage (tonnes)} = \text{Length (m)} \times \text{True Thickness (m)} \times \text{Depth (m)} \times \text{Density } (\rho\text{- t/m}^3)$$

True thickness formula for all vertical boreholes: t = Borehole Thickness × cos (dip angle), where dip is the measured dip from horizontal of the graphite band. Bulk density ρ graphite schist±mica schist= 2.70 t/m³ throughout. Conservative measuments of the exploration target potential of the graphite schist associated with host rocks are given below (Figure 9.7).

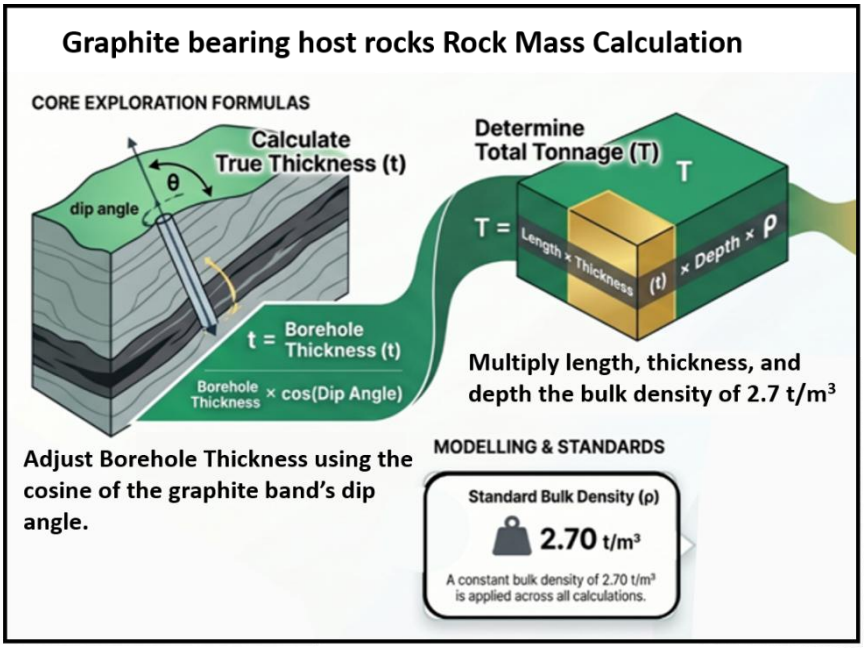

Figure 9.7: Chart shows the exploration target formula for graphite.

9.2 Digoli-Gajjola Graphite Block

9.2.1 Block Location and Geological Setting

The Digoli-Gajjola Graphite Block (Figure 9.8) lies in the north-central part of the Almora G4 area, bounded by the Bintola-Udalgaon and Batgal-Channi thrust systems (Chapter 7.1). Eight discontinuous graphite bands are present in this block.

Access is via NH-309B; last-mile connectivity is limited and will require road improvement for full-scale exploration. Water supply is reliable from the perennial Mahadeo Gad river (Figure 7.5). Partial forest cover (Pharhkanaula RF to the south; Matena RF to the west) imposes selective environmental constraints but is not a block-wide limitation (Figure 7.6).

In this block, the graphite system is vanadiferous: sub-surface ICP-MS data from BH-01 and BH-04 consistently record V concentrations well above 5× Clarke (570 ppm) within graphitic intervals - peaking at 1,594.6 ppm (BH-01, 36-36.5 m) and 1,459.7 ppm (BH-04, 15-16 m) - making vanadium a co-primary exploration objective alongside graphite.

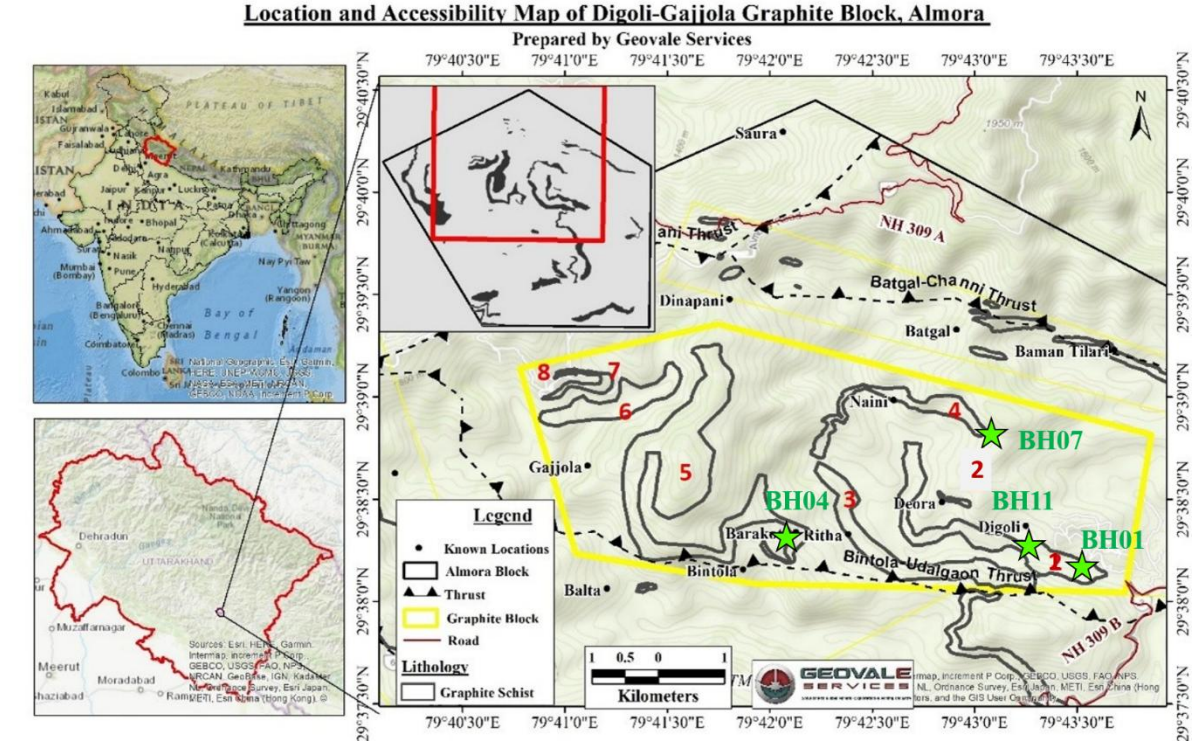

Figure 9.8: Location and Accessibility map for Digoli-Gajjola Block

9.2.2 Band Geometry

Eight graphite bands have been mapped across the block, spanning a total strike length of 8.82 km and combined area of 1.410 sq. km (Table 10.4.1). Band-3 (2.21 km; largest mapped areaand Band-4/Barakote (2.03 km; partially drilled by BH-07) are the two dominant units by strike and area. Band-1/Digoli (1.86 km) is the best-drilled segment, while Band-6 (1.17 km) is a significant undrilled target (Table 9.1). Bands-2, 7, and 8 are minor lensoidal or isolated occurrences.

Table 9.1: Band geometry and prospectivity summary, Digoli-Gajjola Block.

Band	Strike (km)	Avg Width (km)	Area (sq.km)	BH Control	Key Characteristics
Band-1	1.86	0.0903	0.168	BH-01 + BH-11	Two boreholes; thick graphite (avg TT 62.8 m); V peaks >1,300 ppm.
Band-2	0.28	0.0321	0.009	None	Very small, narrow lens; no drilling

Band	Strike (km)	Avg Width (km)	Area (sq.km)	BH Control	Key Characteristics
Band-3	2.21	0.1579	0.349	None	Undrilled band in block; no subsurface data; major exploration upside.
Band-4	2.03	0.2931	0.595	BH-07	Drilled
Band-5	0.58	0.0603	0.035	BH-04	Drilled
Band-6	1.17	0.1769	0.207	None	Significant strike; undrilled; moderate potential based on surface geochemistry.
Band-7	1.02	0.0441	0.045	None	Structurally deformed, no drilling.
Band-8	0.17	0.0117	0.002	None	Isolated thin lens; minimal.
TOTAL	**9.32**	**0.8664**	**1.410**	-	-

9.2.3 Scout Drilling Overview

Four vertical diamond-core boreholes (BH-01, BH-04, BH-07, BH-11) have been completed across three band clusters (Table 9.2). BH-01 and BH-11 are in the Band-1/Digoli corridor (~460 m apart), BH-04 is on Band-5, and BH-07 is at Deora (Band-4).

Table 9.2: Scout borehole summary, Digoli-Gajjola Block.

BH	Coordinates	RL (m)	Depth (m)	Band	Open to depth	True thickness of graphite (m)	Dip (°)
BH-01	29.636734°N, 79.726113°E	1,363	**91.7**	Band-1 (Digoli)	Yes (graphite at hole base)	**68**	26
BH-04	29.638587°N, 79.701410°E	1,531	**64.0**	Band-4 (Barakote)	No - graphite ends at 48.7 m	**40.59**	20
BH-07	29.646670°N, 79.718822°E	1,540	**50.0**	Band-5 (Deora)	Not confirmed, borehole ends at sericite mica schist	**10.07**	20

BH-11	29.637927°N, 79.722081°E	1,329	**92.0**	Band-1 (Digoli)	No - terminates in foliated granite	**57.47**	15

9.2.4 True Thickness Derivation

True thicknesses are derived using TT = BH graphite thickness ×cos (dip). Dip convention: measured from horizontal, consistent with project methodology. Table 9.3 presents the full derivation.

*Table 9.3: True thickness derivation, Digoli-Gajjola Block. *Dip from horizontal.*

BH / Zone	Band	Interval (m)	BH graphite Thickness (m)	Dip (°)*	Factor	True TT of graphite (m)
BH-01	Band-1	16-91.7	75.70	26	cos (26°) =0.899	**68.04**
BH-04	Band-5	5.5-48.7	43.20	20	cos (20°) =0.940	**40.59**
BH-07 (Int.1)	Band-4	24.68-31.8	7.12	20	cos (20°) =0.940	**6.69**
BH-07 (Int.2)	Band-4	32.1-35.7	3.60	20	cos (20°) =0.940	**3.38**
BH-07 TOTAL	Band-4	-	**10.72**	-	-	**10.07**
BH-11 (5 ivs)	Band-1	5-75.8	59.50	15	cos (15°) =0.966	**57.47**
Band-1 Average TT	-	-	-	-	-	**62.8**

9.2.5 Grade Data - Fixed Carbon and Vanadium

9.2.5.1 BH-01 (FC and Vanadium Profile)

Table 9.4 presents the full BH-01 FC and ICP-MS vanadium profile. The critical observation is the spatial co-occurrence of peak FC (5.28-7.56%) and peak V (1,028-1,594 ppm) in the 35-37 m interval, confirming that the highest-quality graphite in this borehole is simultaneously the most vanadium-enriched.

Table 9.4: BH-01 fixed-carbon and vanadium profile by depth.

Sample Id	Depth (m)	FC (%)	Lithology	V (ppm)
110068	35.0-35.5	**6.44**	High grade graphite schist	1,383.4
110069	35.5-36.0	**5.28**	High grade graphite schist	1,405.8
110070	36.0-36.5	**5.80**	High grade graphite schist	1,594.6
110071	36.5-37.0	**7.56**	High grade graphite schist - FC peak	1,028.7
110072	49.0-50.0	1.11	High Grade Graphite Schist	260.3
110073	53.0-54.0	1.34	Medium Grade Graphite schist (partly weathered)	641.6
110074	57.0-58.0	0.91	Low Grade Graphite schist	391.7
110077	58.25-59.25	0.49	Low Grade Graphite schist	333.5
110088	62.0-63.0	2.18	Low Grade Graphite schist	748.8
110075	72.0-72.5	2.50	Low Grade Graphite schist	794.5
110078	73.0-74.0	2.06	Low Grade Graphite schist	218.2
110089	78.0-79.0	4.32	Weathered high-grade graphite	784.4
110090	79.0-80.0	2.87	Graphite schist (low-moderate)	759.9
110076	81.0-82.0	1.08	High Grade Graphite Schist	381.3
110079	84.0-85.0	2.09	High Grade Graphite Schist	187.1
110091	89.0-90.0	0.96	Medium Grade Graphite schist	250.7
BH-01 MEAN	**-**	**2.94%**	**n=16; range 0.49-7.56%; best FC zone at 35-37 m (5.28-7.56%)**	**609.6**

9.2.5.2 BH-04 Data (Barakote Sector)

Table 9.5 presents BH-04 FC and vanadium data. The Barakote sector is the most strongly vanadiferous in the block: BH-04 mean V is 730.5 ppm (6.4× Clarke), with four of seven samples exceeding the 5× Clarke anomaly threshold. However, the high-grade graphite zone (30.2-42.4 m).

Table 9.5: BH-04 grade data, Barakote sector.

Sample Id	Depth (m)	FC (%)	V (ppm)	Lithology
113503	10-11	No FC sample	1,052.4	Medium Grade Graphite Schist

Sample Id	Depth (m)	FC (%)	V (ppm)	Lithology
113504	15-16	6.29	1,459.7	Medium grade graphite schist - V peak
113505	18-19	3.40	1,041.1	Medium Grade Graphite Schist
113506	19-20	No FC sample	784.2	Medium Grade Graphite Schist
113507	23-24	No FC sample	135.3	Medium Grade Graphite Schist
113508	31-32	1.05	546.1	High grade graphite schist
113509	54.5-55.5	No FC sample	95.0	Biotite mica schist (non-graphitic zone)
BH-04 MEAN	**-**	**3.58% (n=3)**	**730.5 ppm**	**6.4× Clarke (114 ppm); 4 of 7 samples exceed 5×Clarke threshold**

BH-07 (Band-4/Deora) has no FC data; the exploration target for this band uses an estimated 3.35% surface FC. BH-11 (Band-1/Digoli) has a single FC sample (1.01% at 31-32 m) from the intercalated graphite-mica schist zone, which is not representative of the full 57.47 m true thickness.

9.2.6 Exploration Target Calculation

$T = L \times t \times D \times \rho$, with $\rho = 2.70$ t/m³, where T=Tonnage of rock mass hosting graphite bands. Band-4 Conservative scenario caps depth at 48.7 m (graphite termination in BH-04) (Table 9.6, Table 9.7).

Table 9.6: Band-by-band exploration target calculations.

Band	True t (m)	Open to D	FC%	Eff. Strike/ Area	D (m)	Rock Mass in million ton (Mt)
Band-1 (BH-01, BH-11)	62.8	Yes (BH-01)	2.94	1,209	92 (actual)	**18.8**
Band-5 (BH-04)	40.59	No	3.58	346	48.7	**1.8**
Band-4 (BH-07)	10.07	N/C	3.35*	1216	35.7	**1.2**
Band-3 (undrilled)	Var.	N/A	3.5-4.0	0.349 sq.km	15	**14.1**
Band-6 (undrilled)	Var.	N/A	3.5-4.0	0.207 sq.km	10	**5.6**
Bands 2+7+8 (undrilled)	Var.	N/A	3.0-3.8	0.056 sq.km	5	**0.8**

Table 9.7: Block-level exploration target summary, Digoli-Gajjola Block. Rock Mass in Mt.

B1 Rock	B4 Rock	B5 Rock	B3 Rock	B6 Rock	Mn Rock	TOT Rock Mass in million ton (Mt)
18.8	1.8	1.2	14.1	5.6	0.8	**42.3**

9.2.7 Vanadium Co-product Potential

The Digoli-Gajjola block is explicitly identified in the project as a vanadiferous graphite system. Two boreholes (BH-01, BH-04) consistently deliver V >5× Clarke in graphitic intervals, making this the most reliably anomalous vanadium sector in the Almora programme on a per-graphite-zone basis. Table 9.8 summarises the vanadium characterisation across all four boreholes.

Table 9.8: Borehole-wise vanadium summary, Digoli-Gajjola Block. BH-04 (highest mean V). Clarke = 114 ppm; 5×Clarke = 570 ppm.

BH	Mean V (ppm)	n	Range (ppm)	>5×Clarke	Key observation
BH-01	609.6	19	105.7-1,594.6	9/19 (47%)	1,594.6 ppm at 36-36.5 m (high FC zone)
BH-04	730.5	7	95.0-1,459.7	4/7 (57%)	1,459.7 ppm at 15-16 m; 6.4× Clarke (highest BH-mean V)
BH-07	113.2	9	51.9-309.2	0/9 (0%)	All below 5×Clarke; weakest V in block
BH-11	201.6	17	53.7-573.0	1/17 (6%)	573 ppm at 2-3 m only; mostly below threshold
Mean	**406.6**	52	-	14/52 (27%)	Predominantly elevated above Clarke (3.6×) across drilled block

The co-location of peak FC and peak V in BH-01 at 35-37 m (FC 5.28-7.56%; V 1,028-1,594 ppm) is the most significant finding: the highest-quality graphite in the block is simultaneously the most vanadium-enriched. Both organic carbon and redox-sensitive metals (V, Mo, U) are co-enriched. In BH-04, V peaks of 1,052-1,459 ppm at 10-19 m depth are in the moderate-grade graphite zone (FC 3.40-6.29%); the high-grade zone (30.2-42.4 m) with no FC data may carry even higher V (Table 9.9).

Table 9.9: Indicative vanadium exploration target, Digoli-Gajjola Block. V mean = 406.6 ppm (weighted across 52 BH intervals). Conversion: V × 1.785 = V_2O_5.

Total Rock Mass (Mt)	V mean (ppm)	V Potential (t)	V_2O_5 Equiv. (t)
46.3	406.6	**18,819**	**33,593**

The block vanadium potential of 18,819 V (33,593tonnes V_2O_5) is comparable to the Sirar-Bataldeon block.

9.2.8 Confidence Assessment:

Below the table (Table 9.10) show the details of confidence assessment for Digoli-Gajjola Graphite Block.

Table 9.10: Confidence assessment for Digoli-Gajjola Graphite Block.

Parameter	Value / Status	Confidence	Remarks
Band-1 TT (BH-01+11)	BH-01: 68.04 m (16-91.7m); BH-11: 57.47 m (multiple intervals)	Moderate	TT is robust for BH-01. BH-11 has complex multi-interval structure; dip 15° applied uniformly but may vary.
Band-1 FC (BH-01)	Mean 2.94% (n=16); high-grade zone at 35-37 m (5.28-7.56%)	Moderate	BH-01 with 16 samples is the best-constrained FC dataset in the block. However, the 35-37 m high-FC cluster is localised and the lower borehole shows low FC (0.49-2.5%).
BH-11 FC (Band-1)	1.01% (n=1 sample only; 31-32 m)	Very Low	Single sample from intercalated graphite/mica schist zone. Completely unrepresentative of the 57.47 m true thickness. Must not be used for grade estimation.
Band-5 depth (BH-04)	No FC data available	Very Low	No grade characterisation possible for Band-5 at depth. Exploration target for this band is grade-unsupported.

Parameter	Value / Status	Confidence	Remarks
BH-07 FC (Band-4)	Graphite terminates at 48.7 m; not open to depth	Low	Graphite confirmed absent below 48.7 m at BH-04. VES evidence for deeper material is uncertain for this specific location.
Band-4 FC (BH-07)	Mean 3.58% (n=3); only moderate and low-grade zones sampled	Low	Critical gap: the high-grade zone (30.2-42.4 m) has NO FC sample. 3 samples from 43.2 m of graphite is grossly inadequate.
Bands 3 and 6 (undrilled)	No subsurface data; surface geochemistry only	Very Low	These contribute 40-60% of block rock mass in Moderate-Optimistic scenarios but are entirely speculative. Surface V up to 1,220 ppm (Band-2) and 2,296 ppm (XRF V_2O_5 range) suggests potential.
Vanadium characterisation	BH-01 mean 609.6 ppm; BH-04 mean 730.5 ppm; both >5×Clarke in graphitic zones	Moderate	Two boreholes consistently show anomalous V (>570 ppm) in graphitic intervals. BH-07 and BH-11 are weaker. V appears highest in moderate-grade FC zones (Barakote area).

9.3 Sirar-Bataldeon Graphite Block - Exploration Target Potential

9.3.1 Block Location and Geological Setting

The Sirar-Bataldeon Graphite Block occupies the central part of the Almora G4 area. It comprises six mappable graphite bands (Chapter 7.2). Graphite mineralisation is structurally controlled along thrust-bounded corridors; foliation in graphite schist trends generally NW-SE with gentle to moderate dips (10°-35°) and locally steeper attitudes. Significant access via NH-309B; last-mile connectivity varies by band. Four boreholes have been drilled (BH-02, BH-03, BH-08, BH-10), spanning four of the six mappable bands. The Sirar Band, drilled by BH-03, carries the highest sub-surface fixed-carbon grades in the entire Almora project (mean 5.72%; maximum 8.40%). The Pharhkanaula and Matena Reserve Forests impose constraints in parts of the block (Figure 9.9).

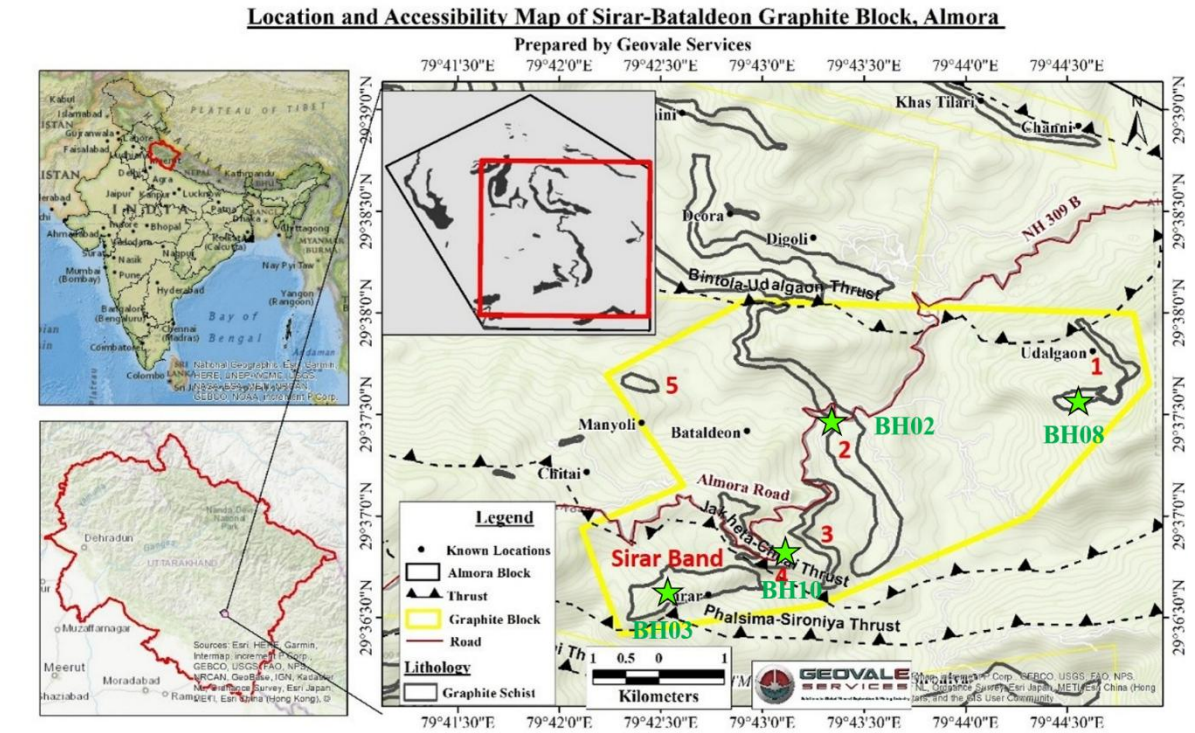

Figure 9.9: Location and Accessibility map for Sirar-Bataldeon Block

9.3.2 Band Geometry

Six graphite bands with a combined strike length of 8.80 km and a mapped area of 1.290 sq. km. have been identified. Table 9.11 summarises geometry and key characteristics.

Table 9.11: Band geometry and prospectivity summary, Sirar-Bataldeon Block.

Band	Strike (km.)	Avg Width (km.)	Area (sq.km.)	BH Control	Key Characteristics
Band 1	1.52	0.065	0.099	BH-08 (50 m)	Very narrow, discontinuous; surface V up to 1,128 ppm.
Band 2	3.40	0.132	0.449	BH-02 (60 m)	Longest band; VES 6 Ω·m deep conductor; NOT open to depth at BH-02.
Band 3	1.51	0.063	0.095	None	High resistivity (~1,800 Ω·m); limited graphite potential.
Band 4	0.84	0.173	0.145	BH-10 (28.5 m)	Near-surface graphite; V mean 596.8 ppm; open to depth.
Band 5	0.30	0.097	0.029	None	Short, narrow; VES profile 27 predominantly resistive.
Sirar Band	1.03	0.459	0.473	BH-03 (75 m)	Best drilled; highest FC in Almora programme; open to depth.
Total	**8.60**	**0.989**	**1.290**	-	-

9.3.3 Scout Drilling Overview

Four vertical diamond-core boreholes are distributed across the block. Table 9.12 gives collar details and open-to-depth status.

Table 9.12: Scout borehole summary, Sirar-Bataldeon Block.

BH	Collar	RL (m)	Depth (m)	Band	Open to depth
BH-02	29.618863°N, 79.726083°E	1,322	**60**	Band 2 (Bataldeon East)	No - graphite terminates at ~40.27 m
BH-03	29.609816°N, 79.709241°E	1,622	**75**	Sirar Band	Yes- graphite at hole base; best borehole
BH-08	29.625384°N, 79.742246°E	1,533	**50**	Band 1 (Udalgaon)	Not confirmed; graphite in 28.14-48.4 m interval
BH-10	29.613099°N, 79.718628°E	1,470	**28.5**	Band 4 (Bataldeon South)	Essentially yes; graphite at 5-28.5 m (base of hole)

BH-03 (Sirar Band) is the most significant subsurface result in the Almora programme. Graphite mineralisation begins at 12.5 m depth and continues to the borehole base at 75 m, confirmed open to depth. The mineralised column includes Moderate Grade Graphite Schist (12.5-23.5 m), High Grade Graphite Schist (23.5-42 m), Graphitic Sericite Schist (42-55.8 m), Graphitic Quartzite (55.8-64.8 m), and a further High Grade Graphite Schist zone (64.8-75 m). Total graphite column: 62.5 m vertical (true thickness 58.73 m).

BH-02 (Band 2) intersects multiple high-grade graphite-schist intervals between 12.35 and 40.27 m, separated by thin sericite mica schist. The graphite terminates at 40.27 m with barren sericite mica schist to the hole base at 60 m. Graphite is confirmed not open to depth at this location, a critical distinction for depth extrapolation in the exploration target potential.

BH-08 (Band 1, Udalgaon) intersects graphitic sericite schist and moderate- to high-grade graphite schist across two intervals: 28.14-39 m and 43-48.4 m. BH-10 (Band 4, Bataldeon South) intersects near-surface graphite schist from 5 m to the hole base at 28.5 m, essentially open to depth at this shallow termination.

9.3.4 True Thickness Derivation

The formula TT = BH × cos(dip) is applied consistently, where dip is measured from horizontal. Table 9.13 presents the derivation for all four boreholes.

Table 9.13: True thickness derivation, Sirar-Bataldeon Block.

BH	Band	Interval (m)	BH Thickness (m)	Dip (°) *	True Thickness (m)
BH-02	Band 2	12.35-22.80	10.45	22	**9.69**
BH-02	Band 2	23.50-24.36	0.86	22	**0.79**
BH-02	Band 2	27.15-40.27	13.12	22	**12.16**
BH-02 TOTAL	Band 2	-	**24.43**	-	**22.64**
BH-03	Sirar Band	12.50-75.00	62.50	20	**58.73**
BH-08	Band 1	28.14-39.00	10.86	20	**10.21**
BH-08	Band 1	43.00-48.40	5.40	20	**5.07**
BH-08 TOTAL	Band 1	-	**16.26**	-	**15.28**
BH-10	Band 4	5.00-28.50	23.50	25	**21.30**

9.3.5 Grade Data - Fixed Carbon and Vanadium

Table 9.14 details the BH-03 fixed-carbon profile. Two of 11 samples reach 8.40% FC (38-39 m) and 8.32% FC (29-30 m); six of eleven samples exceed 6% FC, giving a mean of 5.72% - the highest sub-surface FC mean in the Almora programme.

Table 9.14: BH-03 fixed-carbon profile by depth, Sirar Band

Sample Id	Depth (m)	FC (%)	Lithology
113616	15-16	**3.85**	Medium Grade Graphite Schist
110095	22-23	**3.85**	Medium Grade Graphite Schist
113615	23-24	**6.36**	High Grade Graphite Schist
113614	24-25	**6.35**	High Grade Graphite Schist
110097	27-28	**6.87**	High Grade Graphite Schist
113613	29-30	**8.32**	High Grade Graphite Schist - peak
113612	31-32	**7.31**	High Grade Graphite Schist
110096	38-39	**8.40**	High Grade Graphite Schist - peak
110098	46-47	**6.29**	Graphitic sericite schist
113501	53-54	**4.01**	Graphitic quartzite
110100	59-60	**1.31**	Graphitic quartzite / transition
BH-03 MEAN	-	**5.72%**	**n=11; range 1.31-8.40%; highest sub-surface FC mean in Almora programme**

Table 9.15 consolidates all grade data (fixed carbon and vanadium) across all four boreholes and available surface samples.

Table 9.15: Grade data summary, Sirar-Bataldeon Block.

Sample Type	Sample Id / Band	FC (%)	V (ppm)	Note
Surface	109186 (Band 2)	7.00	-	Surface grab; Band 2 area; highest surface FC
Surface	109990 (Band 2)	6.15	2,060	Surface grab; V anomalous
Surface	109939 (Sirar)	6.62	-	Surface grab; Sirar band
Surface	Band 2 range	·2.19-7.00	-	Multiple surface samples; Band 2 corridor

Sample Type	Sample Id / Band	FC (%)	V (ppm)	Note
Surface	Sirar range	·3.50-5.43	-	Multiple surface samples; Sirar Band
Surface	110019 (Sirar)	-	2,414	Peak surface V in block, channel sampling
Surface (BH-08 area)	109227-109230	-	942 (mean)	V range 728-1,128 ppm; Band 1/Udalgaon
BH-02 sub-surface	110081 (19-20 m)	5.64	882.95	High-grade graphite zone
BH-02 sub-surface	110080 (13-14 m)	4.85	1,022.1	High-grade graphite zone; peak V in BH-02
BH-02 sub-surface	7 samples total (mean)	2.60	-	Range 0.81-5.64%; diluted by low-grade intervals
BH-03 sub-surface	11 samples (mean)	**5.72**	**1,852 (mean, n=2 from 2 graphite zone at 38-39 m and 53-54 m)**	Range 1.31-8.40%; best FC in Almora programme
BH-08 sub-surface	113528 (37.5-38.5 m)	3.02	-	Single sample
BH-10 sub-surface	3 samples (mean)	2.56	597 (mean, n=8)	Range 2.15-3.10% FC; V 123-1,216 ppm; 5 of 8 samples >5×Clarke

9.3.6 Exploration Target Calculation

$T = L \times t \times D \times \rho$, with $\rho = 2.70$ t/m³ throughout. Table 9.16 presents band-by-band calculations; Table 9.17 gives block totals.

Table 9.16: Band-by-band exploration targets of Sirar-Bataldeon Block.

Band	True t (m)	Open to D		Eff. Strike or Area (m)	D (m)	Rock (Mt)
Sirar (BH-03)	58.73	Yes		721(67% of the full strike 1030 m)	75 (as open to depth)	**8.6**
Band 2 (BH-02)	22.64	NO	2.60	2,380 (70 % of the full strike)	40*	**5.8**
Band 1 (BH-08)	15.28	N/C	3.02	912 (60% of the full strike length)	50	**1.9**
Band 4 (BH-10)	21.30	Yes	2.56	504	28.5 (as open to depth)	**0.8**
Bands 3+5 (undrilled) Band 3	Var.	N/A	3.5-4.0	Area 0.124 sq.km	10	**3.3**

Table 9.17: Block-level exploration target summary.

Scenario	Bd2 Rock	Sirar Rock	Bd1 Rock	Bd4 Rock	Undr. Rock	TOTAL Rock (Mt)
Conservative	5.8	8.6	1.9	0.8	3.3	**20.4**

9.3.7 Vanadium Co-Product Potential

Vanadium enrichment is consistently strong across all four boreholes, with sub-surface values ranging from 597 ppm (BH-10 weighted mean, 8 samples) to 1,361 ppm (BH-03 graphite-zone mean, 18 samples). Surface ICP-MS records 2,414 ppm (Sirar Band vicinity), 2,060 ppm (Band 2 vicinity), and 942 ppm mean in the Band 1/Udalgaon area. The sub-surface V mean across all borehole intervals is 721 ppm, which is 5.5× Clarke value - a consistently anomalous signature block-wide. Table 9.18 presents the vanadium potential.

Table 9.18: Indicative vanadium potential, Sirar-Bataldeon Block.. Conversion: V × 1.785 = V_2O_5.

Rock (Mt)	V mean (ppm)*	V Potential (t)	V_2O_5 Equiv. (t)
20.4	721	**14,708**	**26,254**

The block vanadium potential of ~14,700 tonnes V (~26,250 tonnes V_2O_5).

9.3.8 Confidence Assessment

Below the table (Table 9.19) show the details of confidence assessment for Sirar-Bataldeon Graphite Block.

Table 9.19: Confidence assessment of Sirar-Bataldeon Graphite Block

Parameter	Value / Status	Confidence	Remarks
Band mapping (6 bands) 5 bands	Four bands drilled; two undrilled	Moderate (Bands 1,2,4, Sirar) Low (Bands 3,5)	Bands 3 and 5 are poorly constrained; VES on Band 3 corridor shows high resistivity.
BH-03 true thickness (Sirar)	TT = 58.73 m from 12.5-75 m; dip 20°; open to depth	Moderate-High	Best sub-surface evidence in the block. Single hole limits along-strike characterisation.
BH-02 depth/open status (Band 2)	Graphite terminates at 40.27 m; not open to depth at BH-02	Low for depth extrapolation	VES 121 (6 Ω·m) supports deeper conductor. Must resolve discrepancy with second hole.
BH-02 FC grade (Band 2)	Mean 2.60% (n=7); range 0.81-5.64%	Low	High variance; low-grade intervals dilute mean. Surface grab at Band 2 returns 6.15-7.00%.
BH-03 FC grade (Sirar)	Mean 5.72% (n=11); range 1.31-8.40%	Moderate	11 composited samples; wide variance but dominated by high-FC core (FC >6% in 6 of 11). Supports averaging.

Parameter	Value / Status	Confidence	Remarks
BH-10 depth (Band 4)	28.5 m only; open to depth; graphite essentially at hole base	Low-Moderate	Short hole limits down-dip confidence. V strong (>5×Clarke in 5 of 8 samples).
Bulk density	2.70 t/m³ assumed throughout	Moderate	No site-specific measurements; standard reconnaissance value.

9.4 Kalimath Graphite Block

9.4.1 Block Location and Geological Setting

The Kalimath Graphite Block lies in the north-western part of the Almora block, situated in and around Kalimath, Mat, and Saura areas. The block consists of a single curved graphite band classified into a western and an eastern part. The graphite band is hosted within mica-schist of the Almora Group. Tectonically, the Kalimath graphite block is present along the Jakheta-Chitai thrust system.

9.4.2 Exploration Prospects and Constraints

The Kalimath Graphite Block shows promising exploration potential due to the presence of continuous graphite bands and structurally controlled terrain with well-exposed rock formations. Good road connectivity through National Highway 309A and nearby settlements around Almora and Kasar provide logistical support, labour availability, and easier access for exploration activities. Although the area has rugged topography and moderate to steep slopes, the deeply incised valleys provide excellent geological exposures useful for detailed investigation. However, the western part of the block is largely covered by dense forest within the Kalimath Reserve Forest, which may require careful environmental management during exploration activities, whereas the eastern part is completely free from forest cover, providing comparatively easier access and operational flexibility. The seasonal water availability will require careful environmental planning and systematic resource management during exploration activities (Figure 9.10).

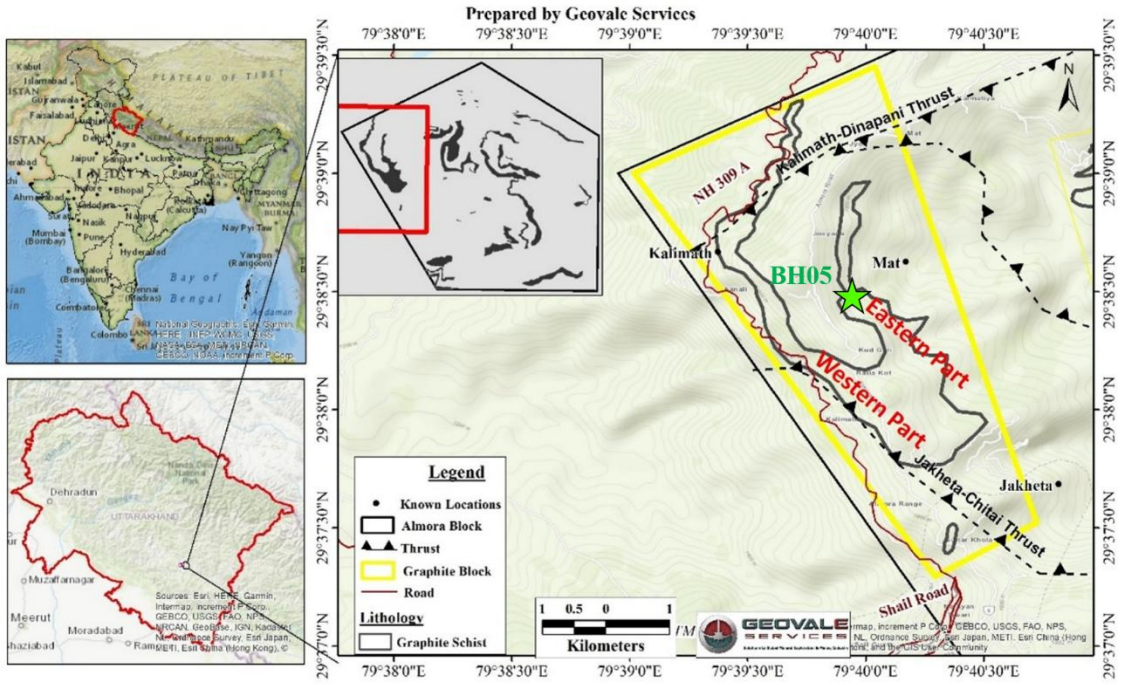

Figure 9.10: Location and accessibility and Borehole point map, Kalimath Graphite

The total Kalimath graphite block area is 4.93 sq. km. The combined mapped graphite area is 0.909 sq. km across the two segments.

9.4.3 Band Geometry and Mapping Data

Table 9.20: Table summarizes band geometry of each segment of Kalimath graphite band.

Segment	Approx. Strike Length (km)	Avg. Mapped Width (km)	Mapped Area (sq. km)
Western Part	3.530	0.140	0.494
Eastern Part	2.320	0.179	0.415
Total	**5.850**	**0.319**	**0.909**

The eastern part, though shorter in strike, is the priority segment. Following the stronger geophysical responses (VES conductive zones of ~35-55 m thickness at depth, SP anomaly to −82 mV), eastern part is drilled (BH-05), and the borehole confirms graphite is open to depth at the 75 m.

The western part has longer strike but is constrained only by surface sampling, road-section observations, confirming the presence of conductive graphitic material but without drill verification (Table 9.20).

9.4.4 Scout Drilling - BH-05 in Eastern part

One vertical diamond core borehole (BH-05) was completed in the eastern part of the Kalimath block (Location: 29.641725°N, 79.665825°E; RL 1890.15 m; Vertical; Total depth 75 m) to test sub-surface continuity of the graphite schist (Figure. photographs A-L, see Chapter 7). The borehole intersected a non-graphitic overburden interval of 22.9 m before entering continuous graphite-bearing schist.

The graphite mineralisation in BH-05 occurs in two principal structural bands (see the Chapter 8 drilling data).

The BH-05 graphite interval breakdown is given in Table 9.21.

Table 9.21: Graphite Zone of BH05

BH05	From (m)	To (m)	Total intersected graphite bearing zone (m)	Grade of graphite
1	22.9	29.7	6.8	Medium Grade Graphite Schist
2	29.7	41.15	11.45	High Grade Graphite Schist
3	41.95	45.67	3.72	High Grade Graphite Schist
5	41.15	41.95	0.80	Low Grade Sericitic graphite schist
4	46.62	75	28.38	High Grade Graphite Schist
Total			**51.15**	

Medium grade graphite: 6.8 m.

High grade graphite: 43.55 m

Total intersected graphite bearing zone in BH05= 51.15 m.

The borehole terminated at 75 m, and open to depth

9.4.5 Grade Data - Surface and Sub-surface

Grade of graphite for the Kalimath block is available from surface sampling (FC% and V ppm) (Table 9.22) and from proximate analysis of BH-05 core samples. Surface FC% values

range from 3.46% to 6.54% with a mean of 4.91%. Sub-surface FC% values from BH-05 (five core samples across the mineralised interval) range from 1.51% to 5.74%, with a mean of 3.11%. The sub-surface mean of 3.11% is the more conservative and defensible grade parameter for resource-target calculations.

Vanadium is the principal critical-metal co-product. Surface ICPMS yields two highly anomalous values - 2,765 ppm (sample 109245) and 1,153 ppm (sample 109244) - from the eastern part, together with a cluster of moderate values (43-120 ppm). The mean of all surface values is 477ppm. Sub-surface ICPMS data from BH-05 core yields high V values of 1,170 ppm, 2,089 ppm, 2,443 ppm, 3,486 ppm, 909 ppm, and 1,502 ppm, across the graphite-mineralised interval (Annexure XI).

Table 9.22: It presents all FC and V data for eastern and western part of the Kalimath Graphite Block.

Sample Type	Sample Id	V (ppm)	FC (%)	Depth / Locality
Surface	109197	-	6.54	Eastern part
Surface	109196	-	3.46	Eastern part
Surface	109198	-	5.20	Eastern part
Surface	109189	-	4.44	Western part
Surface	109216	112	-	Western part
Surface	109962	54	-	Eastern part
Surface	109245	2,765	-	Eastern part
Surface	109244	1,153	-	Eastern part
Surface	110043	43	-	Along the curvature
Surface	109995	120	-	Along the curvature
Surface	109996	31	-	Along the curvature
Surface	110045	4	-	Along the curvature
Surface	110034	18	-	Along the curveture
Subsurface / BH-05	113512	-	1.84	28-29 m
Subsurface / BH-05	113513	-	3.09	32-33 m
Subsurface / BH-05	113515	-	3.35	44-45 m
Subsurface / BH-05	113605	-	5.74	48-49 m
Subsurface / BH-05	113516	-	1.51	61-62 m

9.4.6 Exploration Target Calculation

The following calculations apply the volumetric formula: $T = L \times t \times D \times \rho$, with in-situ bulk density $\rho = 2.70$ t/m³ for graphite-bearing mica-schist (a standard reconnaissance value for pelitic-graphitic schist, within the range 2.65-2.75 t/m³). Calculations are presented separately for the eastern and western parts, then combined at block scale.

9.4.6.1 Eastern Part - BH-05

BH-05 is conducted in the eastern part of this block. A 70% strike continuity factor is applied for the Conservative (reflecting the high likelihood of locally discontinuous grade, structural repetition, and undrilled sectors across the 2.32 km strike). Down-dip depth extent is varied from the proven 51 m (Table 9.23).

Table 9.23: Exploration target calculation, Kalimath Eastern Part. t = 48 m true thickness; ρ = 2.70 t/m³, graphite bearing zones 75 m.

Eff. Strike (m)	True t (m)	Depth D (m)	Density (t/m³)	Rock Mass (Mt)
1,624 (70% continuity)	48	75 (proven BH-05 depth)	2.70	**15.8**

9.4.6.2 Western Part - Geophysics-Controlled, No Drilling

The western part has no drill verification. True thickness is estimated from field investigation i.e.: (i) road-section exposures showing ~5-7 m of graphite schist; Grade data are from surface FC% is 4.44%, and this is applied uniformly across all scenarios as no sub-surface grade data exist for the western part. A 70% continuity factor is applied for Conservative and Moderate; the Optimistic scenario uses the full 3,530 m strike. it is anchored to the proven BH-05 depth (75 m) with a conservative 67% depth extension, applies a 70% strike continuity factor to account for expected geological variation across an undrilled strike of 3.53 km, and uses true thickness directly derived from the borehole. (Table 9.24).

Table 9.24: Exploration target calculation, Kalimath Western Part.

Eff. Strike (m)	True t (m)	Depth D (m)	Density (t/m³)	Rock Mass (Mt)
2,471 (70% continuity of full strike 3530)	7 +	50	2.70	**2.3**

9.4.6.3 Block-Scale Exploration Target

Table 9.25 combines eastern and western part of Kalimath graphite block results to produce the block-level exploration target range.

Table 9.25: Kalimath Graphite Block: Block-level exploration target summary.

Eastern (Mt)	Western (Mt)	Total Rock (Mt)
15.8	2.3	**18.1**

.

9.4.7 Vanadium Co-Product Potential

Vanadium is a key critical-mineral co-product of the Kalimath graphite system, consistently enriched in the graphite schist horizons. Sub-surface ICPMS data from BH-05 core samples (Annexure XXV) record V values of mostly 67.1-3,739.38 ppm, with a mean of 1,538 ppm. This is approximately 9 times the crustal Clarke value (~158 ppm), confirming strong vanadium enrichment associated with graphite.

The indicative vanadium potential is computed by applying the sub-surface mean V concentration (1,538 ppm) to the conservative and moderate rock mass estimates. V_2O_5 equivalent is derived using the conversion factor: 1 tonne V = 1.785 tonnes V_2O_5.

Table 9.26 summarises the vanadium potential.

Table 9.26: Indicative vanadium exploration target, Kalimath Graphite Block. Conversion: V × 1.785 = V_2O_5.

Rock Mass (Mt)	Mean V (ppm, sub-surface)	V Potential (kt)	V_2O_5 Equivalent (kt)
13	1,538	**19.99**	**35.68**

The vanadium potential of ~19-32 kt V (equivalent to 35.68-58.46 kt V_2O_5) across the Kalimath Block.

9.4.8 Confidence Assessment

Table 9.27 summarises the key geological, geometric, and analytical parameters underpinning the Kalimath exploration target, together with an assessment of confidence.

Table 9.27: Confidence assessment of Kalimath Graphite Block.

Parameter	Value / Status	Confidence	Remarks
Band mapping and strike	Eastern: 2.32 km; Western: 3.53 km (from 1:12,500 mapping)	Moderate	Single curved band may be structurally repeated or offset by faults not yet resolved.
True thickness	Eastern: ~48 m (from BH-05; dip 70° assumed); Western: 7-25 m (range)	Eastern: Moderate Western: Low	Dip angle uncertainty (±10°) introduces ~15% in true thickness. Western part has no drill control.
Down-dip extent	Eastern: 75 m proven (BH-05, open to depth); Western: undrilled	Eastern: Low Western: Very low	Graphite is open to depth at BH-05 but continuity and grade persistence beyond 75 m are unverified. Western part has no drill control.
Strike continuity	70% assumed (Conservative/Moderate); 100% (Optimistic)	Low	Single borehole: insufficient to establish along-strike grade and thickness variation. Structural repetition possible.
Sub-surface FC% grade	Mean 3.11% (n=5 BH-05 samples); range 1.51-5.74%	Low-Moderate	Only 5 samples analysed from 75 m hole. High variance (CV ~56%). Composited channel sampling over mineralised intervals required.
Bulk density	2.70 t/m³ (standard; no site-specific measurement)	Moderate	No specific gravity determinations available. ±0.05 t/m³ introduces ~2% mass uncertainty.
Vanadium grade	Mean 1,538 ppm	Low	High inter-sample variability (909-3,739.38 ppm). Spatial continuity of V not established. No metallurgical data.

9.5 Phalsima-Pithauni Graphite Block-Exploration Target potential

9.5.1 Block Location and Geological Setting

The Phalsima-Pithauni Graphite Block lies in the southern part of the Almora block, encompassing the villages of Phalsima, Pithauni, Sironiya, and Biraura. The block includes four mappable graphite bands: three within the Phalsima area (north, central, and south) and one near the Pithauni graphite band. All four bands are enclosed within mica-schist of the Almora Group and are structurally associated with the WNW-ESE trending Biraura-Pithauni thrust.

9.5.2 Exploration Prospects and Constraints

The Phalsima-Pithauni Graphite Block shows good mining potential due to the presence of four mappable graphite bands, indicating continuity of mineralisation. Good road connectivity via NH 309A, NH 309B, and village roads facilitates transportation and mine access. The area has moderate to low elevation and partly exposed slopes, which are favourable for geological investigation and mine planning. The block is with limited forest cover, reducing major forest clearance constraints. However, careful environmental and slope management will be required in areas affected by steep terrain and seasonal drainage channels (Figure 9.11).

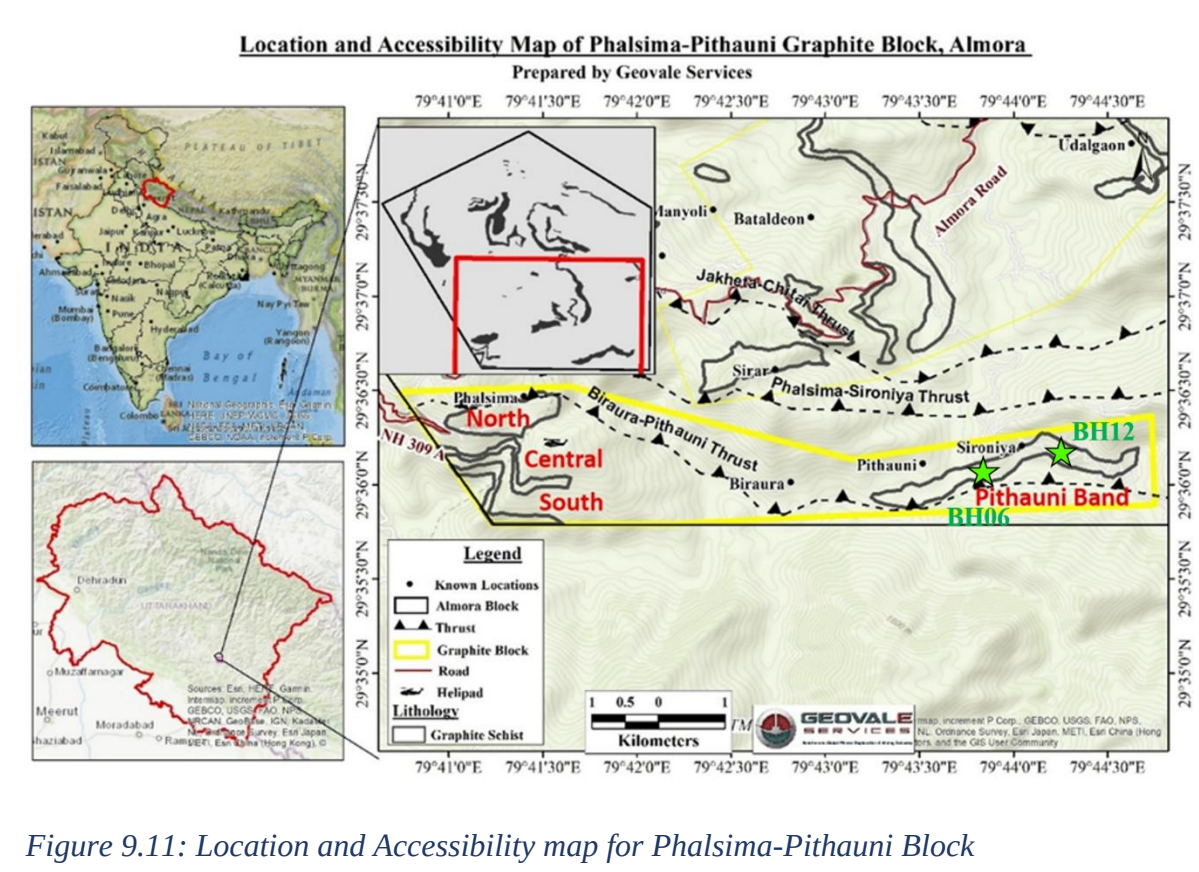

Figure 9.11: Location and Accessibility map for Phalsima-Pithauni Block

9.5.3 Geological and Resource Characterization

The total Phalsima-Pithauni graphite block covers total is 9.19 sq. km. The four graphite bands together occupy a mapped area of approximately 0.872 sq. km.

9.5.4 Band Geometry and Mapping Data

Table 9.28 shows summarise the four-band geometry of the Phalsima-Pithauni Block.

Table 9.28: Details of Band geometry of the Phalsima-Pithauni Block.

Band	Strike (km)	Ava. Width (km)	Area (sq. km.)
Phalsima North Band	0.997	0.2597	0.259
Phalsima Central Band	1.736	0.0581	0.101
Phalsima South Band	1.611	0.069	0.112
Pithauni Band	2.613	0.153	0.40
TOTAL	6.957	0.5398	0.872

Among the four bands, the Phalsima North Band is the highest-priority surface target: it carries the largest mapped area (0.259 sq. km), the strongest SP anomaly (−259 mV on Line 04), VES conductive zones of 20-60 m thickness at 15-68 Ω·m (Lines 02, 03), and the highest surface FC% (5.67%). Raman spectroscopy on sample 109938 from the north band confirms very well-ordered crystalline graphite (I_D/I_G = 0.05-0.12; 2D band clearly resolved at 2,717-2,729 cm^{-1}), establishing graphite quality at the surface. The Pithauni Band is the best-controlled segment, with two drilled boreholes (BH06 and BH12) and the strongest SP anomaly in the block (−853 mV, Line 05).

9.5.5 Scout Drilling - BH-06 and BH-12

Two vertical diamond core boreholes have been completed within this block (Table 9.29), both within the Pithauni Band.

Table 9.29: Scout borehole summary of Phalsima-Pithauni Block. Both boreholes confirm graphite is open to depth.

BH	Location	RL (m)	Depth (m)	Open to depth	Band
BH-06	29.600162°N, 79.729779°E	1,275.07	**106**	Yes	Pithauni Band
BH-12	29.603202°N, 79.737426°E	1,359.00	**64**	Yes	Pithauni Band

9.5.6 BH-06 Lithological Profile

BH-06 (Pithouni, 106 m) intersects a complex graphitic sequence. Overburden (weathered mica schist with topsoil) extends to 9.4 m, followed by a Graphite-Sericite Schist zone (9.4-21.5 m), a non-graphitic Sericite Mica Schist gap (21.5-41 m), and then graphitic lower section (41-106 m) comprising High Grade Graphite Schist (41-45.3 m), Graphitic Quartzite (45.3-84.8 m), and High-Grade Graphite Schist to Graphitic Quartzite (84.8-106 m). Graphite is confirmed open to depth at 106 m (Table 9.30).

Table 9.30: BH-06 lithological interval breakdown. For detail see Annexure XXIX.

From (m)	To (m)	Thickness (m)	Lithology	Note
0	9.4	**9.4**	Weathered mica schist with topsoil	Overburden
9.4	21.5	**12.1**	Graphite-Sericite Schist	Lower graphite-sericite zone; BH thickness 12.1m, true 10.96m
21.5	41.0	**19.5**	Sericite Mica Schist	Non-graphitic intercalation
41.0	45.3	**4.3**	High Grade Graphite Schist	High-grade; strong geochemical signature
45.3	84.8	**39.5**	Graphitic Quartzite	Intermediate; lower FC; graphitic but siliceous
84.8	106.0	**21.2**	High-Grade Graphite Schist to Graphitic Quartzite	High-grade base zone; V peaks to 582.7 ppm at 102-103 m; open to depth

9.5.7 BH-12 Lithological Profile

BH-12 (Pithauni, 64 m) presents a simpler, highly favourable profile: thin weathered mica schist with topsoil (0-16 m) and sericite mica schist transition (16-17.5 m), followed by continuous Graphite Schist from 17.5 m to the base of the hole at 64 m. Graphite is confirmed open to depth. With only 17.5 m of non-graphitic overburden and continuous graphite schist spanning 46.5 m (true thickness 42.48 m), BH-12 represents the most direct and accessible graphite intersection in the Phalsima-Pithauni block (Table 9.31).

Table 9.31: BH-12 lithological interval breakdown. For detail see Annexure XXIX

From (m)	To (m)	Thickness (m)	Lithology	Note
0	16.0	**16.0**	Weathered mica schist with topsoil	Overburden
16.0	17.5	**1.5**	Sericite Mica Schist	Thin transition interval
17.5	64.0	**46.5**	Graphite Schist	Continuous graphite schist; true thickness 42.48 m; open to depth at 64 m

9.5.8 True Thickness Derivation

For True thicknesses, following formula applied is:

True thickness (TT) of graphite associated with host rocks= Borehole thickness (BH) × cos(dip)

This is consistent with a convention in which the reported dip angle (α) is measured from the horizontal (i.e., α = 25° from horizontal = 65° from vertical).

*Table 9.32: True thickness derivation from BH-06 and BH-12. *Dip convention: measured from horizontal depth.*

BH	Zone	Interval (m)	BH Thickness (m)	Dip (°)	Factor Applied	True Thickness (m)
BH-06	Upper graphite zone	9.4-21.5	12.10	25	cos (25°) = 0.906	10.96
BH-06	Lower graphite zone	41-106	65.00	25	cos (25°) = 0.906	58.91
BH-06	TOTAL	9.4-21.5 + 41-106	77.10	-	-	69.87 (~70)
BH-12	Graphite zone	17.5-64	46.50	24	cos (24°) = 0.914	42.48 (~42)

BH-06 total true graphite thickness: ~70 m (combining upper zone 10.96 m + lower zone 58.91 m; these are separated by ~19.5 m of barren mica schist). BH-12 true graphite thickness: ~42

m (continuous). The average across both boreholes is 56 m, which is used as the representative true thickness for Pithauni band exploration target calculations (Table 9.32).

9.5.9 Grade Data - Fixed Carbon and Vanadium

Table 9.33 presents all available grade data for the block from surface and subsurface analyses. The sample 113629 (BH-12, 54.5-56 m) is particularly significant: it carries the highest FC in the block at 6.92% combined with the highest V at 1,380.5 ppm, and is given below.

Table 9.33: Surface and subsurface grade data for Phalsima-Pithauni Graphite Block.

Sample Type	Sample Id / Depth	FC (%)	V (ppm)	Note
Surface	109164 (Phalsima)	2.20	-	Surface grab; Phalsima north/central area
Surface	Central band sample	3.01	-	Surface grab; central Phalsima band
Surface	South band sample	214	-	Surface grab; south Phalsima / Pithauni
Surface	North band sample	4.36	-	Surface grab; north Phalsima band
Surface	Phalsima	5.67		Surface grab sample
BH-06 subsurface	113541 (75-76 m)	1.00	187.5	Graphitic quartzite zone
BH-06 subsurface	113543 (87-88 m)	1.20	355.1	High-grade base zone
BH-12 subsurface	113622 (26.5-27.8 m)	4.06	396.4	Upper graphite schist; high V
BH-12 subsurface	113623 (29.5-31 m)	2.34	250.8	Mid graphite zone
BH-12 subsurface	113624 (31-33 m)	1.83	143.1	Mid graphite zone
BH-12 subsurface	113629 (54.5-56 m)	**6.92**	**1380.5**	Best FC + highest V in block

The contrast between BH-06 and BH-12 FC averages is diagnostically important: BH-06 intersects a mixed graphite-schist-graphitic quartzite assemblage in which the quartzite dilutes the carbon content; BH-12 shows substantially purer graphite schist throughout.

Exploration targets for the Pithauni band should be understood as representing this mixed assemblage, with pockets of higher-grade graphite.

9.5.10 Exploration Target Calculation

Calculations use the formula $T = L \times t \times D \times \rho$, where L = effective strike length (m), t = average true thickness (m), D = down-dip extent (m), and $\rho = 2.70$ t/m³ (in-situ bulk density of graphite-bearing schist).

9.5.10.1 Pithauni Band (BH-06 and BH-12)

Two boreholes have been drilled in the Pithauni band. Down-dip depth from Conservative (proven BH-06 depth, 90 m effective) and average true thickness of BH-06 and BH-12. (Table 9.34).

Table 9.34: Exploration target, Pithauni Band.

Eff. Strike (m)	True t (m)	Depth D (m)	ρ (t/m³)	Rock (Mt)
1,568 (60% of 2,613m full strike)	56	90 (proven BH depth)	2.70	**21.3**

9.5.10.2 Phalsima Bands (Surface and Geophysics Only)

The three Phalsima bands (north, central, south) are undrilled. Exploration targets are estimated using field road cut section, mapped plan area and a vertically interpreted depth parameter (from VES conductive zone thickness and SP anomaly extent). (Table 9.35)

Table 9.35: Exploration target estimates, Phalsima North, Central bands, South Band, D-C: depth (m) for Conservative.

Band	Area (sq.m)	D-C (m)	Rock-C (Mt)
North Band	259000	20	14.0
Central Band	101000	15	4.1
South Band	112000	10	3.0

9.5.10.3 Block-Scale Exploration Target

Table 9.36 combines all four bands to produce the block-level range.

Table 9.36: Block-level exploration target summary, Phalsima-Pithauni Graphite Block. Rock mass in Mt.

Pithauni (Mt)	N-Band (Mt)	C-Band (Mt)	S- Band (Mt)	Total Rock (Mt)
21.3	14.0	4.1	3	**42.4**

9.5.11 Vanadium Co-Product Potential

Vanadium data are available from sub-surface ICPMS analyses across BH-06 and BH-12. Combined, 31 analytical intervals across both holes (19 from BH-06, 12 from BH-12) yield a block-average V of 223.08 ppm. Depth-wise, V increases significantly in the lower sections of both boreholes: BH-06 peaks at 582.7 ppm (102-103 m, Zone 3) and 355.1 ppm (87-88 m); BH-12 peaks at 1,380.5 ppm (54.5-56 m, a strongly anomalous value) and 662.0 ppm (45-46 m). The BH-12 peak value (1,380.5 ppm) at 54.5-56 m is coincident with the highest FC value in the block (6.92%), confirming a strong positive association between vanadium enrichment and graphite quality (Table 9.37).

Table 9.37: Indicative vanadium potential, Phalsima-Pithauni block. V concentration: combined BH-06 + BH-12 mean = 223.08 ppm. Conversion factor: 1 tonne V = 1.785 tonnes V_2O_5.

Rock (Mt)	Mean V (ppm, combined BH)	V Potential (tonnes)	V_2O_5 Equivalent (tonnes)
42.4	223.08	**9,458**	**16,883**

9.5.12 Confidence Assessment

Below the table (Table 9.38) show the details of confidence assessment for Phalsima-Pithauni Graphite Block.

Table 9.38: Confidence assessment of Phalsima-Pithauni Graphite Block.

Parameter	Value / Status	Confidence	Remarks
Band mapping	Four bands mapped at 1:12,500; moderate quality	Moderate	Phalsima North and Pithauni well-mapped; Central and South narrow and hard to constrain.
True thickness	BH-06: 69.87 m (two zones); BH-12: 42.48 m. Formula: TT = BH × cos(dip)	Moderate (Pithauni) Low (Phalsima)	Dip uncertainty ±5° adds ±~8% to TT. Phalsima bands have no drilling.
Down-dip extent	BH-06: 106 m proven; BH-12: 64 m proven. Both open to depth.	Low-Moderate	Depth extension beyond proven values is speculative. Phalsima bands entirely undrilled.

Parameter	Value / Status	Confidence	Remarks
Strike continuity	60-70% continuity applied. Two BHs in Pithauni.	Low	BHs are ~850 m apart within a 2.6 km band. Grade interpolation between holes is unconstrained.
Sub-surface FC grade	Mean 2.89% (n=6). BH-06 mean 1.1%; BH-12 mean 3.79%.	Low	High variance; BH-06 data dominated by graphitic quartzite (low FC). Only 4 samples each. No systematic compositing.
Graphite quality	Raman (sample 109938, north band): I_D/I_G ≈ 0.05-0.12; very well-ordered crystalline graphite.	Moderate (north band only)	Raman data are surface-only and from one sample. Core petrography (BH-06) is pending.
Bulk density	2.70 t/m³ assumed; no site measurements	Moderate	Standard reconnaissance value; ±0.05 t/m³ = ~2% .

The current estimate should be understood as rock-mass inclusive of the graphitic quartzite, and the economic cut-off decision remains to be made on the basis of metallurgical testing (Table 9.38).

9.6 Batgal-Channi Graphite Block - Exploration Target Potential

9.6.1 Block Location and Geological Setting

The Batgal-Channi Graphite Block lies in the northern part of the Almora G4 exploration area, in the vicinity of Batgal, Channi, and Dinapani villages, accessible via NH-309B (Chapter 7.5). The block area is 3.09 sq. km (Toposheet 53O/10). The graphite mineralization is structurally controlled, developed along steep thrust-related ramp geometry with foliations dipping at 50°-70°, and occurs as 12 narrow, discontinuous bands rather than a single continuous body. No Reserve Forest coverage is recorded within the block boundary. Terrain is hilly to steep (1,400-1,800 m RL), and drainage is predominantly first-order. Habitation is low (Figure 9.12).

The Batgal corridor represents the most tectonically complex and fragmented graphite block in the Almora programme. Intense shearing combined with high-grade metamorphism has locally improved graphitization but has also segmented the bands, reduced lateral continuity, and created a structurally controlled, heterogeneous system. This character is reflected directly

in the exploration target, which is considerably smaller and more uncertain than the Kalimath block.

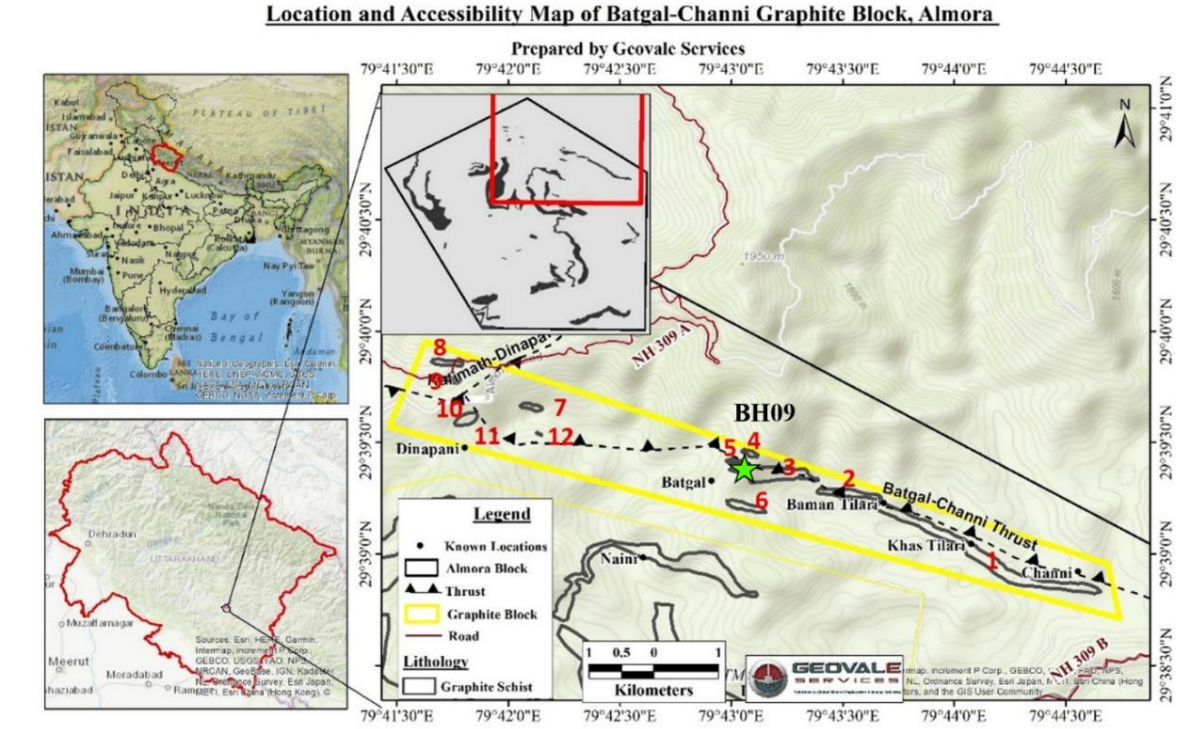

Figure 9.12: Location and Accessibility map for Batgal-Channi Block

9.6.2 Band Geometry and Mapping Data

The Batgal block comprises 12 mapped graphite bands with highly variable strike length and width, reflecting the fragmented structural character of the corridor. Band 1 is by far the most areally significant (0.126 sq. km, 1.765 km strike), constituting over 52% of the total mapped graphite area. Bands 10 and 11, though small in area, carry the strongest surface vanadium anomalies. Table 9.39 provides the full band geometry.

Table 9.39: Band geometry summary, Batgal-Channi Graphite Block.

Band	Strike (km)	Avg. Width (km)	Mapped Area (sq. m.)
Band 1	1.765	0.0713	125.87
Band 2	0.453	0.0447	20.22
Band 3	0.6444	0.07836	50.44
Band 4	0.118	0.0307	3.62
Band 5	0.156	0.0238	3.72

Band	Strike (km)	Avg. Width (km)	Mapped Area (sq. m.)
Band 6	0.298	0.0454	13.52
Band 7	0.015	0.0041	0.06
Band 8	0.224	0.0371	8.28
Band 9	0.155	0.0246	3.80
Band 10	0.068	0.0110	0.75
Band 11	0.173	0.0687	11.91
Band 12	0.041	0.0049	0.20
TOTAL	**3.529**	**1.1498**	**242.39**

Total mapped graphite area: 0.242 sq. km across all 12 bands (Block 7.4 total: 3.09 sq. km). Band 3, the only drilled bands, account for 0.07836 sq. kmof the total graphite area. The geophysical footprint (SP anomalies from Lines 12, 21, 23, 24; VES from Line 23) provides limited additional spatial control, with SP lows reaching −170 mV (Band 2) and VES identifying a conductive zone approximately 70 m thick at 35-250 Ω·m (VES-105). A second shallower conductor (~15 m thick, ~250 Ω·m) is identified at VES-102 and VES-103, consistent with Band 1 at shallow depth.

9.6.3 Scout Drilling - BH-09

One vertical diamond core borehole (BH-09) was completed in the eastern part of Band 3 of the Batgal-Channi Block. Collar: 29.656291°N, 79.717376°E; RL 1554 m; vertical; total depth 45 m. Two graphite bands are intersected, as summarised in Table 9.40.

Table 9.40: BH-09 litholog summary, Batgal-Channi Block

From (m)	To (m)	Lithology	Mineralisation Note
0.0	0.5	Weathered mica schist with topsoil	Non-mineralised
0.5	4.25	Highly weathered graphitic schist, sludgy	Band 1 (graphitic)
4.25	8.0	Highly weathered mica schist, sludgy	Minor graphitic flake present (internal dilution within Band 1 zone)
8.0	9.0	Intercalated mica schist and graphitic schist	Transition; minor graphite
9.0	16.1	Highly weathered mica schist, sludgy	Non-mineralised

From (m)	To (m)	Lithology	Mineralisation Note
16.1	19.5	Loose/weathered graphitic schist + mixed dominant graphitic schist	Band 2 (graphitic)
19.5	45.0	Mica schist (weathered)	Non-mineralised; graphite not open to depth

A critical observation is that graphite mineralization does not continue below 19.5 m in BH-09: the borehole enters mica schist at 19.5 m and remains non-graphitic to hole termination at 45 m.

9.6.4 True Thickness Calculation

True thicknesses for BH-09 are derived from the borehole horizontal intersections using the formula: True Thickness = Borehole Thickness × cos (dip angle). The dip of the graphite band is recorded as 50°.Table 9.41 presents the derivation.

Table 9.41: True thickness derivation, BH-09, Batgal-Channi Block.

Band	Interval (m)	BH Thickness (m)	Dip Angle	True Thickness (m)	Notes
Graphite Zone in BH-09 (Zone-1)	0.5-8.0	7.50	50°	4.82	Vertical borehole; formula: T = Bh × cos(dip)
Graphite Zone in BH-09 (Zone-2)	16.0-19.5	3.50	50°	2.25	Vertical borehole; same formula
Combined	-	11.00	50°	**7.07**	Write-up states 6.07 m - arithmetic discrepancy; 7.07 m adopted (from spreadsheet data)

The adopted total true thickness for BH-09 is 7.07 m.

9.6.5 Grade Data

Grade data for the Batgal block is highly limited. Sub-surface data from BH-09 comprises only one FC% determination and six vanadium analyses. Table 9.42 presents all available grade data.

Table 9.42: Grade data, Batgal-Channi Block. Clarke value for V = 114 ppm; 5× threshold = 570 ppm.

Type	Sample Id	Borehole/Source	Depth (m)	FC (%)	V (ppm)
Sub-surface	113571	GSPL/AL/BH-09	3-4	2.99	1,502
Sub-surface	113572	GSPL/AL/BH-09	8-9	-	36
Sub-surface	113573	GSPL/AL/BH-09	16-17	-	494
Sub-surface	113574	GSPL/AL/BH-09	26-27	-	186
Sub-surface	113575	GSPL/AL/BH-09	39-40	-	175
Sub-surface	113576	GSPL/AL/BH-09	44-45	-	91
Surface	Multiple	Bands 1-12	-	2.5-7.05	Up to 3,536

Sub-surface FC data: a single proximate analysis on sample 113571 (3-4 m, Band 1 graphitic zone) yields FC = 2.99%. This is the only quantitative sub-surface graphite grade measurement for the entire block. Surface FC values range from ~2.5% to 7.05%, with Bands 7, 11, and 12 exceeding ~5%, while Bands 5 and 6 are lower; average surface FC is approximately 3.5-4.0%. The single-sample sub-surface dataset, grade confidence is Very Low (as assessed in Table 9.47), and the FC value used in Conservative and Moderate calculations (2.99%) is treated as tentative only.

Vanadium signature: Band 1 at 3-4 m carries 1,502 ppm V (13.2× Clarke) - a strongly anomalous value. Band 2 at 16-17 m carries 494 ppm V (4.3× Clarke, below the 5× threshold). Intervals in mica schist between and below the graphite bands record near-background to low V (36-186 ppm), confirming that the vanadium enrichment is confined to the graphitic horizons. Of additional note, surface ICPMS from Bands 10 and 11 records V up to 3,536 ppm - the highest V value in the entire Almora Block.

9.6.6 Exploration Target Calculation

9.6.6.1 Band 3 - BH-09

Band 3 is the dominant target in the Batgal block: strike (0.644 km), area (0.050 sq. km.), highest V in BH-09, and directly drilled. A conservative 60% strike continuity factor is applied for Conservative (reflecting the narrow, fragmented band character with only one borehole). Down-dip depth is limited to 20 m for Conservative (anchored to BH-09 graphite base at 19.5 m). (Table 9.43).

Table 9.43: Band 3 exploration target, Batgal-Channi Block. t = 4.82 m true thickness; ρ = 2.70 t/m³.

Eff. Strike (m)	True t (m)	Depth D (m)	ρ (t/m³)	Rock (Mt)
386 (60% continuity)	7.07	20 (BH-09 proven zone)	2.70	**0.15**

9.6.6.2 Band 2 and Bands 1 and 4-12

Band 2 (strike 453 m, true thickness 2.5 m) is treated at lower confidence than Band 3, using 60-65% continuity and identical depth assumptions. Bands 1,2, 4-12 collectively have strike lengths of 14-298 m each and no drill control; their true thickness is estimated conceptually at 2.5 m (thinner than the drilled bands). Table 9.44 presents these calculations.

Table 9.44: Band 2 and Bands 3-12 exploration target components, Batgal-Channi Block. Bands 1, 2, 4-12 are surface mapping only; thickness (2.5 m) is estimated, not measured.

Eff. Strike (m)	True t (m)	Depth (m)	ρ (t/m³)	Rock (Mt)
272 (60%)	2.5 (est.)	20	2.70	0.037
1807 (3013 of 60%)	2.5 (est.)	20	2.70	0.244

9.6.6.3 Block-Level Exploration Target

Table 9.45: Batgal-Channi Block: block-level exploration target summary

Band 3 (Mt)	Band 2 (Mt)	Bands 3-12 (Mt)
0.15	0.037	0.244

9.6.7 Vanadium Co-Product Potential

The vanadium enrichment in BH-09 (Band 1: 1,502 ppm, Band 2: 494 ppm) confirms a geochemically significant reducing depositional environment, consistent with organic-rich black-shale precursors. The mean V across (surface and Subsurface) the mineralised bands is 787.19 ppm. (Table 9.46).

Table 9.46: Indicative vanadium potential, Batgal-Channi Block. V conversion: 1 t V = 1.785 t V_2O_5. Mean V = 787.19 ppm.

Rock Mass (Mt)	Mean V (ppm)	V Potential (t)	V_2O_5 Equivalent (t)

0.431	787.19	**339.27**	**605.61**

At 339.27 tonnes V (605.61 tonnes V_2O_5) across Conservative, vanadium does not constitute an economically significant standalone co-product at this scale.

9.6.8 Confidence Assessment

Below the table (Table 9.47) show the details of confidence assessment for Batgal-Channi Graphite Block.

Table 9.47: Confidence assessment of Batgal-Channi Block.

Parameter	Value / Status	Confidence	Remarks
Band mapping (Bands 1-12)	12 bands mapped at 1:12,500	**Moderate**	Complex multi-band geometry; structural repetition possible; Bands 3-12 poorly constrained in thickness.
True thickness (BH-09 bands)	Band 1: 4.82 m; Band 2: 2.25 m; Total: 7.07 m	**Moderate**	6.07 m of graphite zone
Down-dip extent	20 m proven (BH-09); graphite NOT open to depth	**Low**	Only 19.5 m of graphite in BH-09 before terminating in mica schist; depth extension to 50-100 m supported by geophysics only.
Strike continuity	Single BH; 60-65% assumed	**Very Low**	Single borehole. Narrow, fragmented bands characteristic of thrust-related systems.
Grade (FC%)	2.99% sub-surface (n=1); 2.5-7.05% surface	**Very Low**	Only 01 FC sample from BH-09. Extremely limited grade confidence. Composite channel sampling essential.
Bulk density	2.70 t/m³ assumed	**Moderate**	No site-specific SG measurements. Standard value for graphitic schist.
Vanadium	Band 1: 1,502 ppm; Band 2: 494 ppm	**Low**	Two data points only. No metallurgical data. V tonnage is small (<6,000 t V_2O_5 even optimistically).

Chapter 10

Conclusion and Recommendation

10 Conclusion and Recommendation:

10.1 Conclusions

The G4 reconnaissance survey in the Matena-Sirar area has established the Almora block as a prospective, graphite-vanadium terrain within the Almora Crystalline of the Inner Lesser Himalaya. The present work has moved the project beyond previous graphite occurrences and confirmed a structurally repeated system of graphite schist bands distributed across multiple thrust-bounded corridors. The principal outcome is therefore a block-wise graphite-vanadium exploration model, not a single continuous deposit model.

10.1.1 Location, Terrain and Surface Constraints

The block covers about 60 sq. km. in SOI Toposheet 53O/10 around Matena, Phalsima/Falshima, Sirar, Deora, Balta, Kalimath, Bataldeon, Digoli and adjoining villages. It is regionally accessible from Almora through NH-309A, NH-309B and village roads and this access was adequate for mapping, sampling, geophysics, pitting, trenching and scout drilling. At target scale, however, operations are controlled by steep slopes, dissected valleys, forest patches, cultivated terraces, settlements..

Topography limitations are key filters for future work. Kalimath occupies higher and steeper terrain, while Sirar-Bataldeon and Phalsima-Pithauni include ridge, lower-slope and piedmont/alluvio-colluvial settings. Forest land, dense drainage, springs, habitation, cultivated terraces and the Lakhudiyar archaeological site require early screening. Hence, the presence of graphite cannot be equated with uniform mineability; G3 targets have selected after slope, drainage, forest, settlement, water and heritage constraints are considered.

10.1.2 Legacy Work and Geological Setting

Graphite has been known in the Almora region for nearly two centuries. Legacy GSI and regional work recognised graphite schist around Kalimath, Sirar, Bataldeon/Pirsal, Bari Chhina and nearby areas and showed variable graphite quality: low to moderate fixed carbon in bulk graphite schist, with locally higher fixed carbons. Earlier electrical geophysical surveys also established that graphite occurs in mappable bands and that folding, repetition and thrust-related architecture strongly influence band repetition and apparent thickening.

Recent work upgraded the concept from a graphite-only occurrence to a graphite-vanadium-polymetallic carbonaceous metasedimentary system. The present G4 programme has filled a major legacy gap by integrating geological mapping, structural interpretation, geochemistry, graphite quality, SP-VES geophysics, petrography and modal analyses, Raman and XRD data, proximate analysis, ICPMS and scout drilling in one framework.

The block belongs to the Almora Crystalline or Almora Group and comprises mica schist, (±garnet), quartzite (quartz-sericite schist), graphite schist, mafic tuffaceous rocks, older granite-gneiss and younger intrusive granite. Mica schist is the dominant lithology, while graphite schist occurs as discrete but repeated bands within the metasedimentary rocks. Lit-par-lit younger granite along foliation/thrust planes may have locally enhanced graphite recrystallization and ordering.

Geological mapping (1:12,500) traced 30 graphite - beraingbands. Graphite occurs mainly as jumbo size (>300 µm contains maximum area %)- to medium--fine flaky grains aligned parallel to foliation and concentrated in graphite-rich laminae, confirming a stratabound, fabric-controlled origin inherited from carbonaceous protoliths and modified by metamorphism, deformation and local intrusion-related effects.

10.1.3 Structure, Graphitisation Controls and Exploration Method

Structure is the principal control on graphite disposition. The dominant WNW-ESE to NW-SE structural grain, variable foliation dips, thrust-related flat-ramp architecture, folding and structural repetition control the thickness, continuity and present exposure pattern of graphite bands. Five graphite blocks have been classified in this project: these are Kalimath, Sirar-Bataldeon, Digoli-Gajjola, Phalsima-Pithauni and Batgal-Channi.

Graphitisation reflects original carbonaceous sedimentation followed by regional metamorphism, strain localisation and local thermal/fluid modification. Graphite flakes aligned with foliation, folded graphite laminae, graphite in shear lenses, mica fish and recrystallised quartz support pre- to syn-tectonic graphite growth and redistribution. The same deformation that created structural thickening also introduced boudinage, segmentation and local discontinuity. The best targets are therefore expected where carbonaceous protoliths coincide with thrust repetition, fold closures, low- to moderate-dip panels, surface continuity, geophysical conductors and reasonable access.

The G4 workflow was appropriately multidisciplinary: 60 sq. km. of remote sensing/DEM work, 60 sq. km. geological mapping, pitting/trenching, surface and stream sampling, SP and VES geophysics, petrography/mineralogy, multi-element geochemistry and 801.2 m of scout core drilling. SP and VES were useful for detecting conductive horizons, however, graphite, sulphides, clay, moisture and structural breaks were taken into account as these are produced anomalies. Target confidence is highest where mapping, geochemistry, geophysics and drilling coincide.

10.1.4 Block-wise Exploration Outcomes

Kalimath is one of the strongest targets. The block covers about 4.93 sq. km. and has eastern and western graphite segments. The eastern segment has about 2.32 km mappable strike length and geophysical indications of thicker conductive zones at depth. BH05 intersected two graphite-bearing intervals with a combined true thickness of about 48.65 m below about 22 m overburden. Surface FC values are about 3.46-6.54% and BH05 records FC upto 5.74% and vanadium up to 3,739 ppm, with associated Zn, Se, Mo, Ag, Cu and S enrichment. The main constraints are steep terrain, forest sensitivity at places.

Sirar-Bataldeon is another high-priority domain. It contains several mappable bands, with Bataldeon East Band 2 showing about 3.40 km strike length, about 0.25 km average width and about 0.449 sq. km mapped area. BH02 confirms about 27 m graphite below about 13 m overburden, with FC of about 2.13-5.73% and V of about 710-1,022 ppm. BH03 records graphite bearing zones from about 12.5 m to 75 m, including a stronger interval around 31.45-42 m. Forest, drainage, cover and sulphide/quality issues require careful management. BH-03 records FC upto 8.4% and Vanadium 2758 ppm with associated Zn, Se, Mo, Ag, Cu and S enrichment.

Digoli-Gajjola contains multiple thrust-bounded graphite bands and strong subsurface confirmation around BH01-BH11. BH01 intersected graphite hosted rocks from about 16 m to 91.7 m, including a 2 m interval from 35-37 m with FC of about 5.28-7.56%. The block also carries a vanadium (1,594 ppm) -polymetallic signature with V, Mo, Ba, Cu, Zn, U and Ag enrichment. Its main risk is structural segmentation and discontinuity.

Phalsima-Pithauni is attractive for shallow-dip geometry and access. Four mapped bands give about 6.96 km cumulative strike length, with gentle dips of about 3-15 degrees NE. VES indicates conductive zones of about 20-60 m and Pithauni records a 26 m graphite bearing zone followed by about 40 m intercalated graphite-mica schist below about 10 m overburden. The key limitation is quality: surface FC is commonly about 2.41-5.67% and the graphite schist is siliceous at places. BH-12 records FC upto 6.92% and Vanadium upto 1380 ppm.

Batgal-Channi is a valid but lower-priority target. It contains about 12 narrow and discontinuous graphite bearing bands with steep dips, commonly about 50-70 degrees. BH09 confirms only about 6.07 m total true graphite bearing rock thickness in two intervals. Surface FC locally reaches about 7.05% and selected bands contain V up to about 3,536 ppm, but steep geometry and discontinuity imply higher strip ratio and lower bulk-continuity potential.

Taken together, the five blocks show a clear priority pattern. Sirar-Bataldeon, Digoli-Gajjola, Kalimath offer the best combination of thickness, continuity, geophysical support and

vanadium enrichment. Phalsima-Pithauni has favourable shallow geometry. Batgal-Channi is geologically valid, but its steep and discontinuous geometry makes it a selective target.

10.1.5 Grade, Quality and Economic Significance

Most of the surface and subsurface FC values in the range of about 0.49%-8.40%. This is consistent with graphite disseminated through quartz-mica-rich schist rather than massive high-carbon graphite. Most graphite has jumbo fraction (have high % of area) with very fine to medium flake with, coarse fractions are also occurring in Kalimath, Pithauni and Sirar. Economic potential will therefore depend on beneficiation performance, graphite recovery, flake preservation and impurity rejection.

The vanadium association is one of the strongest positive outcomes of the G4 project. Vanadium is anomalous in several graphite/carbonaceous horizons, especially Kalimath, Sirar-Bataldeon, Digoli-Gajjola and Batgal-Channi. The best reported results include up to 3,739 ppm V in Kalimath BH05, Sirar-Bataldeon surface values up to about 2,758 ppm in Sirar BH03 and BH02 values of about 710-1,022 ppm, Digoli-Gajjola values up to about 2,296 ppm in XRF-derived datasets and Batgal-Channi values up to about 3,536 ppm. This supports a reduced carbonaceous metasedimentary system capable of concentrating redox-sensitive metals. Vanadium should be retained as a key associated exploration target until its mineral residence and recoverability are resolved.

10.2 Graphite-Vanadium Exploration Target Potential

In volumetric terms, the key exploration opportunity is shallow to moderate-depth graphite schist where low- to moderate-dip panels can be followed down dip with limited stripping. The main geological risk is structural dismemberment, particularly in steep ramp zones. The main quality risk is dilution by quartz-mica gangue, expressed as high ash and high SiO2. The main upside is the repeated association of graphite with vanadium and other redox-sensitive elements.

The strongest shallow-volume opportunities occur where mapped area, strike length, subsurface thickness and low- to moderate-dip geometry coincide. Gently dipping sectors such as Phalsima-Pithauni and parts of Sirar-Bataldeon offer better shallow depth and potential low-strip conditions. Steeper ramp zones, particularly Batgal-Channi, may host locally enriched graphite and vanadium but have higher strip ratio and continuity risk. Kalimath and Sirar-Bataldeon are the leading volumetric targets because they combine surface continuity, geophysical support and robust drill confirmation (Table 10.1).

Table 10.1: Summary of graphite target potential, vanadium association and exploration priority across the identified blocks.

Graphite Block	Graphite target potential	Vanadium significance	G3 implication
1. Kalimath	About 5.85 km combined strike. Kalimath East has about 2.32 km strike and BH05 gives about 48.65 m true graphite bearing rock thickness below about 22 m overburden. FC about 3.46-6.54%. BH-05, FC: 5.74%	Strongest drilled BH-05 V result: up to 3,739 ppm; associated Zn, Se, Mo, Ag and Cu.	High-priority G3 block. Requires drilling, full graphite quality work, beneficiation and V deportment studies; terrain/forest and silica-ash risks remain.
2. Sirar-Bataldeon	Largest constrained strike/area: about 8.82 km cumulative strike and about 1.29 sq. km mapped area. BH02 gives about 27 m graphite bearing rocks; BH03 intersects graphite from about 12.5-75 m. FC about 2.13-7%. BH-03, FC-8.4 %	V in BH02 about 710-1,022 ppm; surface values locally up to about 2,060 ppm. BH-03 (V- 2758 ppm)	Very high G3 priority. Need to test Bataldeon East Band 2 and Sirar; address forest, drainage, cover and sulphide/quality issues at places.
3. Digoli-Gajjola	About 11.309 km cumulative strike. BH01 records graphite from about 16-91.7 m and a 2 m interval with FC about 5.28-7.56%.	V-polymetallic signature with V, Mo, Ba, Cu, Zn, U and Ag; V locally up to about 2,296 ppm in XRF datasets.	High-priority follow-up around BH01-BH11 and persistent bands; structural segmentation must be resolved.
4. Phalsima-Pithauni	About 6.96 km cumulative strike and about 0.872 sq. km	V lower than Kalimath and Digoli, but	Good shallow/low-strip potential, but high silica/ash at places and

Graphite Block	Graphite target potential	Vanadium significance	G3 implication
	mapped area. Gentle 3-15 degree dips and Pithauni subsurface graphite zone of about 26 m plus 40 m intercalated graphite-mica schist. BH-12: FC- 6.92%	anomalous; reported up to about 430 ppm at surface and 582.7 ppm at depth. BH-12: V- 1380 ppm	lower FC make beneficiation testing decisive.
5. Batgal-Channi	About 3.53 km cumulative strike and about 0.242 sq. km mapped area. Narrow, steep and discontinuous bands; BH09 gives about 6.07 m true graphite thickness.	Selected bands show V up to about 3,536 ppm.	Conditional G3 target only. Focus on compact lenses after confirmatory mapping, trenching and geophysics.

The target value lies in cumulative tonnage potential, structural repetition and associated vanadium enrichment. Accordingly, the conversion of exploration target potential into a defendable G3 model will depend on proving continuity in the best panels, quantifying recoverable graphite through beneficiation and determining whether vanadium is recoverable or remains only an exploration/pathfinder attribute.

10.3 Exploration Target Potential

- The Almora graphite–vanadium G4 investigation has delineated a sizeable vanadiferous graphite Exploration Target across five structurally controlled blocks, comprising 30 graphite-bearing bands over a cumulative strike length of about 36.46 km and an exposed graphite-schist area of approximately 5.14 sq. km.
- Graphite mineralization occurs as thin cm- to metre-scale intercalated bands within mica-bearing graphite schist, graphitic quartzite, and graphite sericite schist. It is mainly concentrated along foliation planes, with medium- to coarse-grained flakes also disseminated as veins and veinlets, locally making the entire host rock appear graphitic and dark grey to black. The mineralization is interpreted to have originated from

carbonaceous sediments that underwent deformation, regional metamorphism, and increased crystallinity during contact metamorphism associated with lit-par-lit injection of younger granite.

- Drilling results from 12 scout boreholes totalling 801.2 m confirmed approximately 501.56 m of graphitic lithologies, including graphite schist, graphite–sericite schist, and graphitic quartzite.
- Analytical results indicate encouraging graphite and vanadium potential, with drill-core FC values reaching up to 8.40% and vanadium values reaching up to 3,486 ppm, confirming the potential for a regionally significant vanadiferous graphite system.
- The programme has generated a project-level Exploration Target potential of 123.6 Mt rock mass under the Conservative scenario..

10.4 Recommendations for G3 Stage

G3 programmes are recommended for all the 5 blocks; 1) Sirar-Bataldeon, 2) Digoli-Gajjola, 3) Kalimath, 4) Phalsima-Pathouni and 5) Batgal-Channi (Figure 10.1). Phase I should refine targets through close-spaced geological and structural mapping, DGPS band tracing, trenching/channel sampling where permissible, additional SP/VES or preferably ERT profiles and reconciliation of all pending Raman, XRD, proximate, ICPMS, sulphur and borehole datasets. The integrated 3D interpretation should be completed before committing to larger drilling.

The G3 ranking should remain dynamic. If beneficiation tests show strong graphite recovery and impurity rejection, Phalsima-Pithauni may improve in priority because of its gentle dip and shallow strip potential. Conversely, any block with poor recovery, high deleterious sulphur or poorly recoverable vanadium should be downgraded even if thickness is locally attractive.

Phase II should comprise systematic core drilling on cross-sections perpendicular to the main graphite-band strike. Kalimath East and Sirar-Bataldeon should be explored first by drilling fences, followed by selected Digoli-Gajjola and Phalsima-Pithauni targets. Batgal-Channi should be tested only where compact, higher-grade structural lenses are confirmed. All core should be logged for lithology, structure, graphite habit, sulphides, recovery and RQD and analysed for FC, total graphitic carbon, ash, volatile matter, sulphur, major oxides, ICPMS multi-elements, mineralogy, graphite flake size and vanadium deportment.

Beneficiation testing must be taken up during the G3 stage.

According to the highest fixed carbon (FC) values obtained from surface and borehole samples and mineability, the graphite-bearing blocks have been prioritized and ranked as follows (Table 10.2).

Table 10.2: Ranking of identified graphite-bearing blocks for G3 exploration based on spatial extent and maximum fixed carbon (FC) values recorded from surface sampling and borehole intersections

Rank	Block Name	Block Area (Sq. Km.)	Highest Surface FC (%)	Highest Sub-surface FC (%)
1	Sirar-Bataldeon Block	9.19	7	8.4 (BH03, at 38-39 m depth)
2	Digoli-Gajjola Block	8.94	5.85	7.56 (BH01, at 36.5-37 m depth)
3	Kalimath Block	4.93	6.54	5.74 (BH05, at 48-49 m depth)
4	Phalsima-Pithauni Block	5.59	5.67	6.92 (BH12, at 54.5-56 m depth)
5	Batgal-Channi Block	3.1	7.05	2.99 (BH09, at 3-4 m depth)

The Almora G4 work confirms a structurally controlled, graphite-bearing, carbonaceous metasedimentary system with locally significant vanadium and polymetallic enrichment. At G4 stage the data justify selective G3 follow-up. The project should advance through structurally guided, ESG-screened and beneficiation-aware exploration.

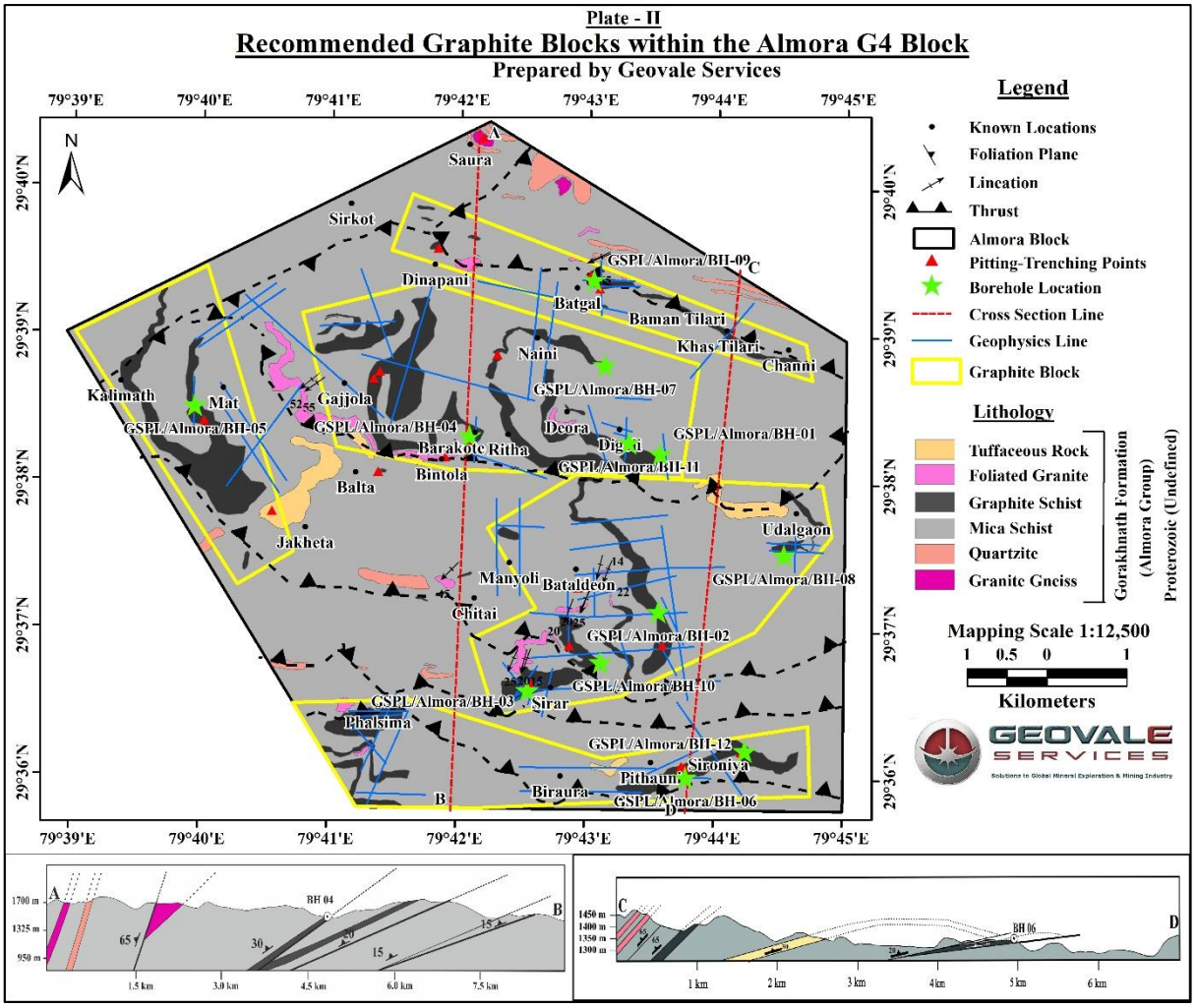

Figure 10.1: Recommended five G3 graphite blocks within the Almora G4 Block

Chapter 11

Expenditure

11 Expenditure:

Project Initiation Date	Sanctioned Amount	Total Expenditure till June 30, 2026
1st September, 2024	Rs. 2.80 Crores (including GST)	Rs. 2.80 Crores (including GST)

Chapter 12

References

12 References:

1. Bajapai, I.P., 1979. Geology of part of Kumaon Himalaya covering parts of Pauri, Almora and Nainital districts, Uttar Pradesh. Geological Survey of India. Unpublished Report.
2. Bauri, D. and Rout, D., 2021. Petro-geochemical characterization of Graphite Schists of the Almora Group, Uttarakhand. Geological Survey of India. Unpublished Report.
3. Bhattacharji, T.K., 1964. An interim note on the graphite schist occurrences of Sirar, Persal and Kalimat areas, Almora District, U.P. Geological Survey of India. Unpublished Report.
4. Bhattacharyya, A. and Bhattacharji, A., 1965. Mapping and laboratory studies of the Kalimat-Sirar-Pirsal belt. Geological Survey of India. Unpublished Report.
5. Bhattacharyya, A., 1965. Report on graphite occurrences in the Almora district, Uttar Pradesh. Unpublished Report. Geological Survey of India. Unpublished Report.
6. Célérier, J., Harrison, T.M., Webb, A.A.G. and Yin, A., 2009. The Kumaun and Garhwal Lesser Himalaya, India: Part 1. Structure and stratigraphy. Geological Society of America Bulletin, 121(9–10), pp.1262–1280.
7. Champion, H.G. and Seth, S.K., 1968. A revised survey of the forest types of India. New Delhi: Government of India Press.
8. Chauhan, D.P.S., Pathak, R.C. and Srivastava, V.M., 1978. Report on the continuation of geophysical investigations for graphite in the Sirar and Phalsima areas of Almora District, U.P. (Field season 1977–78). Geological Survey of India. Unpublished Report.
9. Chittora, V.K. and Kacker, A.K., 1988. Report on the standardisation and correlation of Garhwal Group in parts of Pithoragarh district, Uttar Pradesh (Field seasons 1986–87 and 1987–88). Geological Survey of India. Unpublished Report.
10. Das, A., Modak, A., Nag, R. and Mishra, A.K., 2015. Final report on search for iron and sulphide mineralization in undifferentiated Ramgarh Group in parts of Toposheets 53O/6, 7 and 11, Nainital District, Uttarakhand (G-4 stage). Geological Survey of India. Unpublished Report.
11. Dennison, Holtz and Swain.1996) Raman Spectroscopy of Carbon Materials. Journal of Spectroscopy, Vol. 11/8, pp 38-45
12. Heim, A. and Gansser, A., 1939. Central Himalaya: Geological observations of the Swiss expedition 1936. Delhi: Hindustan Publishing Corporation.
13. Joshi, M. and Tiwari, A.N., 2009. Structural events and metamorphic consequences in Almora Nappe during Himalayan collision tectonics. Journal of Asian Earth Sciences, 34(3), pp.326–335.
14. Kumar, S. and Krishnamurthy, K.V., 1985. Report on regional integrated survey for tungsten, tin and gold occurrences (Field season 1983–84). Geological Survey of India. Unpublished Report.

15. Kumar, S. and Manna, S., 2023. Reconnaissance survey for vanadium and allied metals mineralization. Geological Survey of India. Unpublished Report.

16. Kumari, P., Joshi, G.C. and Tewari, L.M., 2011. Indigenous uses of medicinal plants in Almora district. African Journal of Plant Science, 5(7), pp.453–461.

17. Lawder, A.W., 1869. Mineralogical statistics of Kumaon Division. Records of the Geological Survey of India, 3(4), p.87.

18. Mandal, S., Robinson, D.M., Khanal, S. and Das, O., 2015. Redefining the tectonostratigraphic and structural architecture of the Almora klippe and the Ramgarh–Munsiari thrust sheet in NW India. In: Tectonics of the Himalaya. Geological Society of London, pp.247–269.

19. Medlicott, H. B. 1865. Notes on the geology of Kumaun Himalaya. Records of the Geological Survey of India. Unpublished Report.

20. Mehrotra, M.N., 1955. Graphite: Occurrence and production. Transactions of the Indian Ceramic Society, 14(1), pp.20–25.

21. Mehta, J.S., Tripathi, S. C., Durai, P. R., 2006. Thematic Mapping of Kumaon Himalaya (2001–02). Geological Survey of India. Unpublished Report.

22. Mehta, J.S., Tripathi, S. C., Pippal, P. S., 2002. Final Report on the Specialised Thematic Mapping of Devidhura-Naya Sangrauli-Chhira Area, Almora and Champawat Districts, Uttaranchal (F.S. 1997-98 and 1998-99). Geological Survey of India. Unpublished Report.

23. Merbert, J. 1829. Geological observations in the Almora region of Kumaun Himalaya. Geological Survey of India. Unpublished Report.

24. Nautiyal, S. P. 1949. A note on the stability of certain hill sides in and around Nainital. Geological Survey of India. Unpublished Report.

25. Neubeck, A., Broman, C., Magnus Ivarsson, M., Holm, N. G., Martin Whitehouse, Sara Nilsson, Wolf Geppert and Fernando Gervilla (2020) Isotopic Signatures of Carbon in the 'Los Pobres' Graphite Mine, Ronda, Spain. Journal of Petrology, Vol. 61-4, pp 1-13.

26. Pant, N.C. and Singh, R.K., 2005. Prospecting and sampling reports in Almora block. Geological Survey of India. Unpublished Report.

27. Raina, V.K., 1949. Investigation of graphite occurrences in Almora district. Geological Survey of India. Unpublished Report.

28. Ramaiah, A. and Mehta, J.S., 1991. Granite study report (1990–91). Geological Survey of India. Unpublished Report.

29. Rawat, R. and Sharma, R., 2011. Characterization of graphite in Almora crystallines. Journal of Asian Earth Sciences, 42(1–2), pp.51–64.

30. Rodgers, W.A. and Panwar, H.S., 1988. Planning a wildlife protected area network in India. Wildlife Institute of India.

31. Santosh, J.V. and Yadav, S.K., 2021. Reconnaissance survey for tungsten, tin and associated mineralization around Almora District, Uttarakhand (G-4 stage). Geological Survey of India. Unpublished Report.

32. Shankar, B. and Misra, R., 2023. Reconnaissance survey for vanadium in Almora District. Geological Survey of India. Unpublished Report.

33. Sharma, R., Rawat, R. and Law, R.D., 2011. Carbon isotopic evidence for Himalayan graphite. Current Science, 100(8), pp.1216–1220.

34. Singh, J.S. and Singh, S.P., 1992. Forests of Himalaya. Delhi: International Book Distributors.

35. Singh, N. and Bishakha, 2014. Thematic mapping report (2013–14). Geological Survey of India. Unpublished Report.

36. Srivastava, I.P. and Kumar, A., 1988. Exploration of scheelite mineralization. Geological Survey of India. Unpublished Report.

37. Srivastava, V.N. et. al. 1976. Geophysical investigation for graphite (1975–76). Geological Survey of India. Unpublished Report.

38. Tewari, R.C., 1963–64. Chemical analyses of Almora samples. Geological Survey of India. Unpublished Report.

39. Tiwari, R.N., 1963–64. Field mapping of Almora region. Geological Survey of India. Unpublished Report.

40. Valdiya, K.S., 1980. Geology of Kumaun Lesser Himalaya. Dehradun: Wadia Institute of Himalayan Geology.

41. Verma, S. and Rawat, S., 2020. Reconnaissance survey for limestone in [specific region]. Geological Survey of India. Unpublished Report.

42. Zhang, He., Qian, G., Yunafeng Cal., Gibson, C. and Pring, A. 2022. Crystal chemistry of the arsenian pyrites: A Raman spectroscopic study. Journal of American Mineralogist, Vol. 107, pp 274-281

Chapter 13

Locality Index

13 Locality Index:

Toposheet No: 53O/10			
S No	**Location**	**Latitude**	**Longitude**
1	Balta	29.63436	79.68675
2	Baman Tilari	29.65593	79.72896
3	Barakote	29.63896	79.70214
4	Bataldeon	29.62362	79.7154
5	Batgal	29.65545	79.71519
6	Bintola	29.63433	79.69675
7	Biraura	29.6002	79.71361
8	Channi	29.64974	79.74299
9	Chitai	29.62024	79.70224
10	Debdiya	29.65817	79.71638
11	Deora	29.64141	79.71402
12	Digoli	29.63949	79.72084
13	Dinapani	29.65793	79.69675
14	Gajjola	29.64437	79.68519
15	Jakheta	29.62807	79.68031
16	Kalimath	29.64259	79.65349
17	Khas Tilari	29.65201	79.73515
18	Manyoli	29.62429	79.70674
19	Mat	29.64486	79.67305
20	Naini	29.64971	79.71008
21	Phalsima	29.6097	79.68937
22	Pithauni	29.60309	79.72404
23	Ritha	29.6388	79.70639
24	Saura	29.67155	79.70109
25	Sirar	29.61019	79.71223
26	Sirkot	29.6662	79.68399
27	Sironiya	29.60557	79.73382
28	Udalgaon	29.63015	79.74379

Chapter 14

Annexures

14 Annexures:

Annexure I_Geochemical Data (ICPMS analysis) of Orientation Survey in Almora G4 Block

Sample Id.	Lat	Long	Lithology	Ag	Al	As	Ba	Bi	Ca	Cd	Co	Cr	Cu	Fe	Ga	K	Mg
106310	29.64706	79.7589	Graphite	1	8.59	17	883	5	0.54	5	14	276	109	0.72	30	3.46	0.51
106311	29.64706	79.7589	Sulphide rich mafic	2	1.83	213	319	5	0.44	5	41	110	16	12.49	6	1.06	0.29
106312	29.64706	79.7589	Graphite with sulfur	1	3.27	111	326	5	0.18	5	120	93	307	31.62	5	1.5	0.24
106313	29.61924	79.72155	Graphite	1	8.53	10	957	5	0.2	5	17	328	10	0.51	28	4.42	0.69

Sample Id.	Lat	Long	Lithology	Mn	Mo	Na	Ni	P	Pb	S	Sb	Sn	Sr	Te	Ti	Tl	V
106310	29.64706	79.7589	Graphite	0.01	8	0.24	33	0.83	46	0.19	5	4	1005	5	0.23	29	219
106311	29.64706	79.7589	Sulphide rich mafic	0.01	21	0.14	89	0.01	33	13.53	9	3	32	5	0.09	5	360
106312	29.64706	79.7589	Graphite with sulfur	0.06	83	0.24	252	0.38	55	0.26	26	3	41	24	0.1	5	110
106313	29.61924	79.72155	Graphite	0.01	20	0.25	15	0.02	39	0.11	11	6	87	5	0.35	30	362

Annexure II_ Field Observation Points in Almora G4 Block

S No	Location	Latitude	Longitude	Lithology
1	GSPL-Almora-1/11/24	29.614028	79.715725	Graphite Schist and Mica Schist
2	GSPL-Almora-2/11/24	29.614	79.7157	Graphite Schist
3	GSPL-Almora-3/11/24	29.614	79.7157	Graphite Schist
4	GSPL-Almora-4/11/24	29.6135	79.7163	Mica schist
5	GSPL-Almora-5/11/24	29.6135	79.7163	Mica schist
6	GSPL-Almora-6/11/24	29.6132	79.7174	Graphite Schist
7	GSPL-Almora-7/11/24	29.6132	79.7174	Graphite Schist
8	GSPL-Almora-8/11/24	29.6132	79.7174	Graphite Schist
9	GSPL-Almora-9/11/24	29.6151	79.7161	Mica schist
10	GSPL-Almora-10/11/24	29.6151	79.7161	Graphite Schist and Mica Schist
11	GSPL-Almora-24/11/28	29.6176	79.7207	Graphite Schist
12	GSPL-Almora-24/11/29	29.6275	79.7062	Graphite Schist
13	GSPL-Almora-24/11/30	29.618	79.7218	Graphite Schist
14	GSPL-Almora-24/11/31	29.618	79.7218	Mica schist
15	GSPL-Almora-24/11/32	29.6257	79.7221	Graphite Schist
16	GSPL-Almora-24/11/33	29.6257	79.7218	Graphite Schist
17	GSPL-Almora-24/11/34	29.6257	79.7215	Graphite Schist
18	GSPL-Almora-24/11/35	29.6257	79.7213	Graphite Schist
19	GSPL-Almora-24/11/36	29.6268	79.7208	Graphite Schist and Mica Schist
20	GSPL-Almora-24/11/37	29.6285	79.7207	Garnet Mica Schist
21	GSPL-Almora-24/11/38	29.6285	79.7207	Garnet Mica Schist
22	GSPL-Almora-24/11/39	29.6299	79.7195	Garnet Mica Schist
23	GSPL-Almora-24/11/40	29.6296	79.7192	Garnet Mica Schist
24	GSPL-Almora-24/11/41	29.6289	79.7189	Graphite Schist
25	GSPL-Almora-24/11/42	29.6285	79.7195	Graphite Schist
26	GSPL-Almora-24/11/43	29.6282	79.7194	Graphite Schist
27	GSPL-Almora-24/11/44	29.6255	79.7213	Graphite Schist
28	GSPL-Almora-24/11/45	29.615097	79.726584	Graphite Schist
29	GSPL-Almora-24/11/46	29.616036	79.726352	Graphite Schist
30	GSPL-Almora-24/11/47	29.616417	79.726329	Graphite Schist
31	GSPL-Almora-24/11/48	29.617139	79.726244	Graphite Schist and Mica Schist
32	GSPL-Almora-24/11/49	29.61752	79.726046	Graphite Schist
33	GSPL-Almora-24/11/50	29.6184	79.7261	Graphite Schist

S No	Location	Latitude	Longitude	Lithology
34	GSPL-Almora-24/11/51	29.6184	79.7254	Graphite Schist and Mica Schist
35	GSPL-Almora-24/11/52	29.6192	79.7252	Graphite Schist
36	GSPL-Almora-24/11/53	29.6193	79.7251	Graphite Schist and Mica Schist
37	GSPL-Almora-24/11/54	29.6198	79.7257	Graphite Schist and Mica Schist
38	GSPL-Almora-24/11/55	29.6207	79.7246	Graphite Schist and Mica Schist
39	GSPL-Almora-24/11/56	29.621	79.7244	Graphite Schist and Mica Schist
40	GSPL-Almora-24/11/57	29.6219	79.7255	Garnet Mica Schist
41	GSPL-Almora-24/11/58	29.622	79.7252	Garnet Mica Schist
42	GSPL-Almora-24/11/59	29.623795	79.725035	Graphite Schist and Mica Schist
43	GSPL-Almora-24/11/60	29.624369	79.72445	Graphite Schist and Mica Schist
44	GSPL-Almora-24/11/61	29.624851	79.724094	Graphite Schist
45	GSPL-Almora-24/11/62	29.622664	79.722291	Graphite Schist
46	GSPL-Almora-24/11/63	29.62131	79.72241	Graphite Schist and Mica Schist
47	GSPL-Almora-24/11/64	29.621003	79.72287	Graphite Schist and Mica Schist
48	GSPL-Almora-24/11/65	29.623313	79.721633	Garnet Mica Schist
49	GSPL-Almora-24/11/66	29.624405	79.72268	Graphite Schist and Mica Schist
50	GSPL-Almora-24/11/67	29.626484	79.722232	Graphite Schist
51	GSPL-Almora-24/11/68	29.603155	79.736417	Graphite Schist and Mica Schist
52	GSPL-Almora-24/11/69	29.602918	79.737055	Graphite Schist
53	GSPL-Almora-24/11/70	29.602542	79.737229	Mica schist
54	GSPL-Almora-24/11/71	29.602086	79.73715	Graphite Schist
55	GSPL-Almora-24/11/72	29.602516	79.738126	Graphite Schist and Mica Schist
56	GSPL-Almora-24/11/73	29.602376	79.737397	Mica schist
57	GSPL-Almora-24/11/74	29.602971	79.737294	Graphite Schist and Mica Schist
58	GSPL-Almora-24/11/75	29.603312	79.736802	Mica schist
59	GSPL-Almora-24/11/76	29.614818	79.726658	Graphite Schist and Mica Schist
60	GSPL-Almora-24/11/77	29.614825	79.726541	Graphite Schist
61	GSPL-Almora-24/11/78	29.6385	79.718	Graphite Schist and Mica Schist
62	GSPL-Almora-24/11/79	29.638863	79.685909	Garnet Mica Schist
63	GSPL-Almora-24/11/80	29.637042	79.698817	Granite
64	GSPL-Almora-24/11/81	29.636968	79.70056	Graphite Schist and Mica Schist
65	GSPL-Almora-24/11/82	29.638236	79.701726	Graphite Schist and Mica Schist
66	GSPL-Almora-24/11/83	29.636525	79.701742	Graphite Schist
67	GSPL-Almora-24/11/84	29.634596	79.689543	Graphite Schist and Mica Schist
68	GSPL-Almora-24/11/85	29.637549	79.665578	Graphite Schist

S No	Location	Latitude	Longitude	Lithology
69	GSPL-Almora-24/11/86	29.637556	79.665581	Graphite Schist
70	GSPL-Almora-24/11/87	29.642686	79.699634	Graphite Schist
71	GSPL-Almora-24/11/88	29.643574	79.699637	Graphite Schist and Mica Schist
72	GSPL-Almora-24/11/89	29.647829	79.70488	Graphite Schist and Mica Schist
73	GSPL-Almora-24/11/90	29.640386	79.701566	Mica schist
74	GSPL-Almora-24/11/91	29.646665	79.701705	Mica schist
75	GSPL-Almora-24/11/92	29.664127	79.698129	Mica schist
76	GSPL-Almora-24/11/93	29.664499	79.696561	Mica schist
77	GSPL-Almora-24/11/94	29.664439	79.695985	Graphite Schist and Mica Schist
78	GSPL-Almora-24/11/95	29.663216	79.695062	Graphite Schist and Mica Schist
79	GSPL-Almora-24/11/96	29.640691	79.664802	Graphite Schist and Mica Schist
80	GSPL-Almora-24/11/97	29.642669	79.664938	Graphite Schist and Mica Schist
81	GSPL-Almora-24/11/98	29.641966	79.66566	Mica schist
82	GSPL-Almora-24/11/99	29.643591	79.662716	Mica schist
83	AL-DS-01	29.648776	79.66381	Mica schist
84	AL-DS-02	29.652766	79.667847	Mica schist
85	AL-DS-03	29.655513	79.672813	Mica schist
86	GSPL-Almora-24/11/100	29.658453	79.679743	Mica schist
87	GSPL-Almora-24/11/101	29.658926	79.686369	Mica schist
88	GSPL-Almora-24/11/102	29.601803	79.738437	Graphite Schist and Mica Schist
89	GSPL-Almora-24/11/103	29.601595	79.738726	Mica schist
90	GSPL-Almora-24/11/104	29.601297	79.737719	Phylitic Graphite Schist
91	GSPL-Almora-24/11/105	29.601078	79.737447	Seritic micaceous phylite
92	GSPL-Almora-24/11/106	29.601204	79.737283	Graphite Schist and Mica Schist
93	GSPL-Almora-24/11/107	29.602851	79.734428	Graphite Schist and Mica Schist
94	GSPL-Almora-24/11/108	29.602653	79.734618	Graphite Schist
95	GSPL-Almora-24/11/109	29.602265	79.734624	Graphite Schist and Mica Schist
96	GSPL-Almora-24/11/110	29.601714	79.733682	Mica Schist
97	AL-DS-04	29.600565	79.7325	Graphite Schist and Mica Schist
98	AL-DS-05	29.601416	79.729362	Graphite Schist
99	AL-DS-06	29.601435	79.728485	Graphite Schist
100	AL-DS-07	29.599358	79.727826	Mica Schist
101	AL-DS-08	29.599049	79.726917	Mica Schist
102	AL-DS-09	29.598651	79.725917	Graphite Schist and Mica Schist
103	AL-DS-10	29.599318	79.725664	Graphite Schist and Mica Schist

S No	Location	Latitude	Longitude	Lithology
104	AL-DS-11	29.599427	79.724799	Graphite Schist and Mica Schist
105	AL-DS-12	29.5994205	79.721516	Graphite Schist and Mica Schist
106	AL-DS-13	29.599204	79.72152	Graphite Schist and Mica Schist
107	AL-DS-14	29.601031	79.722689	Mica Schist
108	GSPL-Almora-24/11/111	29.600117	79.724477	Graphite Schist and Mica Schist
109	GSPL-Almora-24/11/112	29.601356	79.72792	Graphite Schist
110	GSPL-Almora-24/11/113	29.601351	79.727983	Graphite Schist and Mica Schist
111	GSPL-Almora-24/11/114	29.617683	79.726185	Graphite Schist and Mica Schist
112	GSPL-Almora-24/11/115	29.61521	79.727248	Graphite Schist
113	GSPL-Almora-24/11/116	29.614488	79.727413	Mica Schist
114	GSPL-Almora-24/11/117	29.601113	79.740133	Graphite Schist and Garnet Mica Schist
115	GSPL-Almora-24/11/118	29.603154	79.739701	Garnet Mica Schist
116	GSPL-Almora-24/11/119	29.603463	79.739393	Graphite Schist and Mica Schist
117	GSPL-Almora-24/11/120	29.603017	79.739298	Mica Schist
118	AL-DS-15	29.603485	79.739698	Graphite Schist
119	AL-DS-16	29.602665	79.738968	Graphite Schist
120	AL-DS-17	29.602275	79.738492	Graphite Schist and Mica Schist
121	AL-DS-18	29.604203	79.731898	Garnet Mica Schist
122	AL-DS-19	29.608492	79.731753	Garnet Mica Schist
123	AL-DS-20	29.619225	79.725267	Graphite Schist and Mica Schist
124	AL-DS-21	29.620363	79.719983	Garnet Mica Schist and Sheared Granite
125	AL-DS-23	29.598406	79.686671	Graphite Schist and Garnet Mica Schist
126	AL-DS-24	29.60085	79.687551	Graphite Schist and Mica Schist
127	AL-DS-25	29.59767	79.687036	Mica Schist
128	AL-DS-25	29.597826	79.687325	Graphite Schist and Mica Schist
129	AL-DS-26	29.598494	79.687721	Graphite Schist and Mica Schist
130	AL-DS-27	29.600858	79.688774	Mica Schist
131	AL-DS-28	29.602	79.689028	Mica Schist
132	AL-DS-29	29.602637	79.689009	Graphite Schist and Mica Schist
133	AL-DS-30	29.603238	79.688715	Graphite Schist and Lit per lit granite
134	AL-DS-31	29.634305	79.72573	Garnet Mica Schist
135	AL-DS-32	29.63562	79.724124	Graphite Schist and Garnet Mica Schist
136	AL-DS-33	29.636586	79.724532	Graphite Schist
137	AL-DS-34	29.636703	79.724847	Graphite Schist
138	AL-DS-35	29.636815	79.721908	Graphite Schist

S No	Location	Latitude	Longitude	Lithology
139	AL-DS-36	29.636863	79.721228	Graphite Schist
140	AL-DS-37	29.636758	79.72088	Garnet Mica Schist
141	AL-DS-38	29.636687	79.720728	Granite
142	AL-DS-39	29.637197	79.719378	Jhama like (?)
143	AL-DS-40	29.63751	79.7188	Graphite Schist and Mica Schist
144	AL-DS-41	29.637677	79.718332	Graphite Schist
145	AL-DS-42	29.63806	79.718228	Graphite Schist
146	AL-DS-43	29.63881	79.71832	Graphite Schist and Mica Schist
147	AL-DS-44	29.65288	79.729088	Graphite Schist
148	AL-DS-45	29.65296	79.729871	Graphite Schist and Mica Schist
149	AL-DS-46	29.652733	79.728953	Graphite Schist and Mica Schist
150	AL-DS-47	29.653843	79.727833	Graphite Schist and Mica Schist
151	AL-DS-48	29.65445	79.727528	Graphite Schist and Garnet Mica Schist
152	AL-DS-49	29.654463	79.726945	Graphite Schist and Mica Schist
153	AL-DS-50	29.653825	79.726868	Garnet Mica Schist
154	AL-DS-51	29.654027	79.726073	Garnet Mica Schist
155	AL-DS-52	29.654798	79.725748	Graphite Schist and Mica Schist
156	AL-DS-53	29.654229	79.726293	Graphite Schist and Mica Schist
157	AL-DS-54	29.655116	79.725071	Mica Schist
158	AL-DS-55	29.655922	79.725288	Mica Schist
159	AL-DS-56	29.65704	79.723787	Mica Schist
160	AL-DS-57	29.656272	79.722283	Graphite Schist and Mica Schist
161	AL-DS-58	29.655783	79.721742	Graphite Schist
162	AL-DS-59	29.656087	79.721658	Graphite Schist and Mica Schist
163	AL-DS-60	29.65649	79.721443	Granite and Mica Schist
164	AL-DS-61	29.656471	79.721132	Granite and Mica Schist
165	AL-DS-62	29.656081	79.720913	Graphite Schist
166	AL-DS-63	29.653041	79.726208	Mica Schist
167	AL-DS-64	29.655578	79.72272	Graphite Schist
168	AL-DS-65	29.654498	79.723483	Graphite Schist and Mica Schist
169	AL-DS-66	29.645598	79.739748	Garnet Mica Schist
170	AL-DS-67	29.64778	79.741482	Graphite Schist and Mica Schist
171	AL-DS-68	29.647632	79.740627	Graphite Schist
172	AL-DS-69	29.647947	79.740588	Graphite Schist and Mica Schist
173	AL-DS-70	29.653902	79.735225	Quartz mica schist

S No	Location	Latitude	Longitude	Lithology
174	AL-DS-71	29.654408	79.73505	Quartz mica schist and Mica Schist
175	AL-DS-72	29.655323	79.734567	Quartz mica schist and Mica Schist
176	AL-DS-73	29.655429	79.736916	Quartz mica schist and Mica Schist
177	AL-DS-74	29.65529	79.734321	Quartz mica schist and Mica Schist
178	AL-DS-75/141	29.656833	79.730544	Quartz mica schist and Mica Schist
179	AL-DS-76/142	29.653358	79.717475	Graphite Schist And Garnet Mica Schist
180	AL-DS-77/143	29.655015	79.717665	Mica Schist
181	GSPL-Almora-24/11/220	29.65545	79.718048	Graphite Schist and Mica Schist
182	GSPL-Almora-24/11/221	29.655775	79.71983	Graphite Schist and Mica Schist
183	GSPL-Almora-24/11/222	29.655855	79.721817	Graphite Schist
184	GSPL-Almora-24/11/223	29.65199	79.73078	Graphite Schist and Mica Schist
185	GSPL-Almora-24/11/224	29.65026	79.734123	Graphite Schist and Mica Schist
186	GSPL-Almora-24/11/225	29.649376	79.735253	Graphite Schist and Mica Schist
187	GSPL-Almora-24/11/226	29.622725	79.700718	Graphite Schist and Mica Schist
188	GSPL-Almora-24/11/227	29.623607	79.70317	Quartz Mica Schist
189	GSPL-Almora-24/11/228	29.622757	79.70342	Garnet Mica Schist
190	GSPL-Almora-24/11/229	29.622108	79.704612	Mica Schist and quartz sericite schist
191	GSPL-Almora-24/11/230	29.623055	79.7045	Mica Schist
192	GSPL-Almora-24/11/231	29.623258	79.700542	Quartz sericite schist
193	GSPL-Almora-24/11/233	29.620119	79.695742	Graphite Schist and Mica Schist
194	GSPL-Almora-24/11/234	29.620326	79.695103	Graphite Schist and Mica Schist
195	GSPL-Almora-24/11/235	29.620448	79.695019	Pegmatite
196	GSPL-Almora-24/11/236	29.630212	79.71307	Mica Schist
197	GSPL-Almora-24/11/237	29.630883	79.714322	Graphite Schist and Mica Schist
198	GSPL-Almora-24/11/238	29.631603	79.715032	Pegmatite
199	GSPL-Almora-24/11/239	29.632012	79.715605	Quartz vein and Graphite Schist
200	GSPL-Almora-24/11/240	29.632645	79.715648	Graphite Schist and Mica Schist
201	GSPL-Almora-24/11/241	29.633052	79.716362	Graphite Schist and Mica Schist
202	GSPL-Almora-24/11/242	29.633515	79.716495	Pegmatite and Graphite Schist
203	GSPL-Almora-24/11/243	29.633824	79.715608	Graphite Schist and Quartz Mica Schist
204	GSPL-Almora-24/11/244	29.635199	79.715345	Graphite Schist and Mica Schist
205	GSPL-Almora-24/11/245	29.635852	79.716246	Graphite Schist
206	GSPL-Almora-24/11/246	29.636653	79.716196	Pegmatite and Garnet Mica Schist
207	GSPL-Almora-24/11/247	29.63684	79.716685	Graphite Schist and Mica Schist
208	GSPL-Almora-24/11/248	29.63768	79.716796	Graphite Schist and Mica Schist

S No	Location	Latitude	Longitude	Lithology
209	GSPL-Almora-24/11/249	29.636366	79.718373	Graphite Schist and Mica Schist
210	GSPL-Almora-24/11/250	29.635816	79.719848	Graphite Schist and Mica Schist
211	GSPL-Almora-24/11/251	29.635563	79.720086	Graphite Schist and Mica Schist
212	GSPL-Almora-24/11/252	29.635076	79.722031	Graphite Schist and Mica Schist
213	GSPL-Almora-24/11/253	29.636284	79.725738	Graphite Schist
214	GSPL-Almora-24/11/254	29.636164	79.726026	Graphite Schist and Mica Schist
215	GSPL-Almora-24/11/255	29.636588	79.725912	Graphite Schist and Mica Schist
216	GSPL-Almora-24/11/256	29.636255	79.726492	Mica Schist
217	GSPL-Almora-24/11/257	29.635649	79.726191	Graphite Schist and Mica Schist
218	GSPL-Almora-24/11/258	29.635157	79.725868	Graphite Schist and Mica Schist
219	GSPL-Almora-24/11/259	29.635255	79.725878	Graphite Schist and Mica Schist
220	GSPL-Almora-24/11/260	29.635355	79.725887	Graphite Schist
221	GSPL-Almora-24/11/261	29.635593	79.727267	Graphite Schist and Mica Schist
222	GSPL-Almora-24/11/262	29.635672	79.726995	Graphite Schist and sericite Mica Schist
223	GSPL-Almora-24/11/263	29.635082	79.71441	Graphite Schist and Mica Schist
224	GSPL-Almora-24/11/264	29.635105	79.714393	Graphite Schist and Mica Schist
225	GSPL-Almora-24/11/265	29.639632	79.717638	Mica Schist
226	GSPL-Almora-24/11/266	29.640069	79.71615	Mica Schist
227	GSPL-Almora-24/11/267	29.641098	79.715909	Graphite Schist and Mica Schist
228	GSPL-Almora-11/11/24	29.642124	79.715824	Garnet Mica schist
229	GSPL-Almora-12/11/24	29.641709	79.714861	Graphite Schist and Mica Schist
230	GSPL-Almora-13/11/24	29.641405	79.716276	Graphite Schist and Mica Schist
231	GSPL-Almora-14/11/24	29.641528	79.714378	Graphite Schist and Mica Schist
232	GSPL-Almora-15/11/24	29.641752	79.714284	Graphite Schist and Mica Schist
233	GSPL-Almora-16/11/24	29.642209	79.713659	Graphite Schist and Mica Schist
234	GSPL-Almora-17/11/24	29.642718	79.713309	Mica Schist
235	GSPL-Almora-18/11/24	29.643014	79.713387	Mica Schist
236	GSPL-Almora-19/11/24	29.618382	79.725446	Quartz Graphite Schist and Mica Schist
237	GSPL-Almora-21/11/24	29.616348	79.717888	Graphite Schist
238	GSPL-Almora-22/11/24	29.600893	79.689726	Granite and Graphite Schist
239	GSPL-Almora-23/11/24	29.602683	79.689068	Graphite Schist and Mica Schist
240	GSPL-Almora-24/11/24	29.5992	79.72097	Graphite Schist and Mica Schist
241	GSPL-Almora-25/11/24	29.597265	79.721335	River bed
242	GSPL-Almora-26/11/24	29.603156	79.688851	Granite
243	GSPL-Almora-27/11/24	29.611253	79.70936	Graphite Schist

S No	Location	Latitude	Longitude	Lithology
244	GSPL-Almora-24/11/268	29.611713	79.708745	Graphite Schist and Mica Schist
245	GSPL-Almora-24/11/269	29.61103	79.710713	Graphite Schist
246	GSPL-Almora-24/11/270	29.612148	79.714207	Graphite Schist
247	GSPL-Almora-24/11/271	29.611528	79.715905	Graphite Schist
248	GSPL-Almora-24/11/272	29.611315	79.71608	Graphite Schist and Mica Schist
249	GSPL-Almora-24/11/273	29.613433	79.728892	Mica Schist
250	GSPL-Almora-24/11/274	29.611678	79.729612	Garnet Mica Schist
251	GSPL-Almora-24/11/275	29.610833	79.72788	Garnet Mica Schist
252	GSPL-Almora-24/11/276	29.611263	79.727305	Garnet Mica Schist
253	GSPL-Almora-24/11/277	29.612147	79.727135	Garnet Mica Schist
254	GSPL-Almora-24/11/278	29.613047	79.726045	Graphite Schist and Mica Schist
255	GSPL-Almora-24/11/279	29.612963	79.724822	Graphite Schist
256	GSPL-Almora-24/11/280	29.613277	79.724468	Graphite Schist and Mica Schist
257	GSPL-Almora-24/11/281	29.615068	79.725232	Graphite Schist and Mica Schist
258	GSPL-Almora-24/11/282	29.637335	79.660615	Graphite Schist and Mica Schist
259	GSPL-Almora-24/11/283	29.640338	79.65802	Mica Schist
260	GSPL-Almora-24/11/284	29.641695	79.657337	Mica Schist
261	GSPL-Almora-24/11/285	29.626595	79.66721	Mica Schist and Quartzite
262	GSPL-Almora-24/11/286	29.638197	79.725623	Garnet Mica schist
263	GSPL-Almora-24/11/287	29.637882	79.722155	Graphite Schist
264	GSPL-Almora-24/11/288	29.637492	79.722783	Graphite Schist and Mica Schist
265	GSPL-Almora-24/11/289	29.636403	79.723705	Graphite Schist
266	GSPL-Almora-24/11/290	29.63656	79.725463	Graphite Schist and Mica Schist
267	GSPL-Almora-24/11/291	29.640513	79.719095	Garnet Mica Schist
268	GSPL-Almora-24/11/292	29.638213	79.720517	Mica Schist
269	GSPL-Almora-24/11/293	29.636173	79.719654	Garnet Mica Schist
270	GSPL-Almora-24/11/294	29.63674	79.72085	Lit per lit granite
271	GSPL-Almora-24/11/296	29.641847	79.745487	Garnet Mica Schist
272	GSPL-Almora-24/11/297	29.638098	79.738217	Garnet Mica Schist
273	GSPL-Almora-24/11/298	29.63663056	79.73541667	Garnet Mica Schist
274	GSPL-Almora-24/11/299	29.63322222	79.72980556	Garnet Mica Schist
275	GSPL-Almora-24/11/300	29.63147222	79.72966667	Mica Schist and Lit per lit granite
276	GSPL-Almora-24/11/301	29.626942	79.742592	Graphite Schist and Mica Schist
277	GSPL-Almora-24/11/302	29.625837	79.744223	Rock (?)
278	GSPL-Almora-24/11/303	29.626358	79.745898	Graphite Schist and Mica Schist

S No	Location	Latitude	Longitude	Lithology
279	GSPL-Almora-24/11/304	29.627081	79.745878	Graphite Schist and Mica Schist
280	GSPL-Almora-24/11/305	29.628157	79.746225	Mica Schist
281	GSPL-Almora-24/11/306	29.626294	79.744137	Graphite Schist and Mica Schist
282	GSPL-Almora-24/11/307	29.627084	79.743134	Mica Schist
283	GSPL-Almora-24/11/308	29.626436	79.743254	Graphite Schist
284	GSPL-Almora-24/11/309	29.625402	79.741634	Graphite Schist and Mica Schist
285	GSPL-Almora-24/11/310	29.623181	79.74268	Mica Schist
286	GSPL-Almora-24/11/311	29.627295	79.737915	Garnet Mica Schist
287	GSPL-Almora-24/11/312	29.618908	79.739762	Mica Schist
288	GSPL-Almora-24/11/313	29.61728	79.73842	Garnet Mica Schist
289	GSPL-Almora-24/11/314	29.624828	79.741488	Garnet Mica Schist
290	GSPL-Almora-24/11/315	29.615423	79.73602	Garnet Mica Schist
291	GSPL-Almora-24/11/316	29.597559	79.744998	Garnet Mica Schist
292	GSPL-Almora-24/11/317	29.598399	79.7467047	Garnet Mica Schist
293	GSPL-Almora-24/11/318	29.661522	79.69587	Graphite Schist and Mica Schist
294	GSPL-Almora-24/11/319	29.661362	79.696147	Graphite Schist and Mica Schist
295	GSPL-Almora-24/11/320	29.661193	79.695755	Quartzite and Garnet Mica Schist
296	GSPL-Almora-24/11/321	29.661252	79.695917	Graphite Schist and Garnet Mica Schist
297	GSPL-Almora-24/11/322	29.661952	79.698568	Garnet Mica Schist
298	GSPL-Almora-24/11/323	29.664138	79.699485	Mica Schist
299	GSPL-Almora-24/11/324	29.664125	79.699451	Mica Schist
300	GSPL-Almora-24/11/325	29.664963	79.703502	Garnet Mica Schist
301	GSPL-Almora-24/11/326	29.66583	79.706938	Quartzite and Garnet Mica Schist
302	GSPL-Almora-24/11/327	29.667667	79.711977	Quartzite and Mica Schist
303	GSPL-Almora-24/11/328	29.664972	79.714648	Garnet Mica Schist
304	GSPL-Almora-24/11/329	29.656915	79.700418	Garnet Mica Schist
305	GSPL-Almora-24/11/330	29.659027	79.702238	Graphite Schist and Garnet Mica Schist
306	GSPL-Almora-24/11/331	29.659013	79.70213	Graphite Schist and Garnet Mica Schist
307	GSPL-Almora-24/11/332	29.6593	79.702525	Garnet Mica Schist
308	GSPL-Almora-24/11/333	29.659407	79.702255	Garnet Mica Schist
309	GSPL-Almora-24/11/334	29.659875	79.700982	Garnet Mica Schist
310	GSPL-Almora-24/11/335	29.66094	79.701612	Graphite Schist and Garnet Mica Schist
311	GSPL-Almora-24/11/336	29.66095	79.701357	Graphite Schist and Garnet Mica Schist
312	GSPL-Almora-24/11/337	29.661103	79.701203	Graphite Schist and Garnet Mica Schist
313	GSPL-Almora-24/11/338	29.660738	79.70191	Graphite Schist and Garnet Mica Schist

S No	Location	Latitude	Longitude	Lithology
314	GSPL-Almora-24/11/339	29.660305	79.697163	Graphite Schist and Garnet Mica Schist
315	GSPL-Almora-24/11/340	29.636452	79.671847	Garnet Mica Schist
316	GSPL-Almora-24/11/341	29.641532	79.673018	Garnet Mica Schist
317	GSPL-Almora-24/11/342	29.64149	79.673573	Garnet Mica Schist
318	GSPL-Almora-24/11/343	29.641343	79.674538	Garnet Mica Schist
319	GSPL-Almora-24/11/344	29.641477	79.675442	Garnet Mica Schist
320	GSPL-Almora-24/11/345	29.640468	79.672313	Garnet Mica Schist
321	GSPL-Almora-24/11/346	29.639835	79.671003	Garnet Mica Schist
322	GSPL-Almora-24/11/347	29.638145	79.66907	Garnet Mica Schist
323	GSPL-Almora-24/11/348	29.63859	79.668533	Graphite Schist
324	GSPL-Almora-24/11/349	29.63943	79.66769	Graphite Schist
325	GSPL-Almora-24/11/350	29.640733	79.667333	Graphite Schist
326	GSPL-Almora-24/11/351	29.639557	79.66727	Garnet Mica Schist
327	GSPL-Almora-24/11/352	29.654743	79.683657	Garnet Mica Schist
328	GSPL-Almora-24/11/353	29.651853	79.684228	Graphite Schist and Garnet Mica Schist
329	GSPL-Almora-24/11/354	29.65142	79.684037	Garnet Mica Schist
330	GSPL-Almora-24/11/355	29.651322	79.683635	Garnet Mica Schist
331	GSPL-Almora-24/11/356	29.649655	79.684368	Graphite Schist
332	GSPL-Almora-24/11/357	29.649503	79.682975	Garnet Mica Schist
333	GSPL-Almora-24/11/358	29.648703	79.683013	Graphite Schist
334	GSPL-Almora-24/11/359	29.649423	79.681858	Garnet Mica Schist
335	GSPL-Almora-24/11/360	29.65197	79.683552	Garnet Mica Schist
336	GSPL-Almora-24/11/361	29.652043	79.683758	Graphite Schist and Garnet Mica Schist
337	GSPL-Almora-24/11/362	29.642723	79.698558	Garnet Mica Schist
338	GSPL-Almora-24/11/363	29.642317	79.699435	Graphite Schist
339	GSPL-Almora-24/11/365	29.637907	79.699488	Graphite Schist
340	GSPL-Almora-24/11/366	29.638152	79.699563	Graphite Schist and Garnet Mica Schist
341	GSPL-Almora-24/11/367	29.635853	79.696792	Gneiss
342	GSPL-Almora-24/11/368	29.636595	79.696992	Graphite Schist and Garnet Mica Schist
343	GSPL-Almora-24/11/369	29.637203	79.696825	Graphite Schist and Garnet Mica Schist
344	GSPL-Almora-24/11/370	29.637293	79.69681	Graphite Schist and Garnet Mica Schist
345	GSPL-Almora-24/11/371	29.637548	79.696937	Graphite Schist and Garnet Mica Schist
346	GSPL-Almora-24/11/372	29.637937	79.697197	Graphite Schist and Garnet Mica Schist
347	GSPL-Almora-24/11/373	29.635767	79.69432	Quartzite
348	GSPL-Almora-24/11/374	29.629405	79.67013	Garnet Mica Schist

S No	Location	Latitude	Longitude	Lithology
349	GSPL-Almora-24/11/375	29.628275	79.67787	Mafic rock? And Graphite Schist
350	GSPL-Almora-24/11/376	29.629923	79.675737	Gray Phyllite
351	GSPL-Almora-24/11/377	29.661558	79.695972	Graphite Schist
352	GSPL-Almora-24/11/378	29.660257	79.697092	Graphite Schist
353	GSPL-Almora-24/11/379	29.639818	79.697478	Graphite schist
354	GSPL-Almora-24/11/380	29.659865	79.697045	QBSS
355	GSPL-Almora-24/11/381	29.659895	79.697201	QBSS
356	GSPL-Almora-24/11/382	29.639353	79.699532	QSS and QBSS
357	GSPL-Almora-24/11/383	29.657185	79.700407	QSS and Granite
358	GSPL-Almora-24/11/384	29.623908	79.672935	Graphite Schist
359	GSPL-Almora-24/11/385	29.61213	79.676832	QSS
360	GSPL-Almora-24/11/386	29.614506	79.690073	QSS
361	GSPL-Almora-24/11/387	29.656075	79.684382	Garnet bearing Q B Sch
362	GSPL-Almora-24/11/388	29.651945	79.683767	Graphite Schist
363	GSPL-Almora-24/11/389	29.651745	79.682758	Graphite Schist
364	GSPL-Almora-24/11/390	29.650308	79.682083	QBSS
365	GSPL-Almora-24/11/391	29.649847	79.68151	Graphite Schistand Q Mica S
366	GSPL-Almora-24/11/392	29.648443	79.681597	Graphite Schist
367	GSPL-Almora-24/11/393	29.648398	79.6822	Graphite Schist
368	GSPL-Almora-24/11/394	29.648748	79.682948	Graphite Schist
369	GSPL-Almora-24/11/395	29.655641	79.685517	QBSS
370	GSPL-Almora-24/11/396	29.664115	79.699845	Graphite Schist
371	GSPL-Almora-24/11/397	29.640728	79.657935	Ph. (NG)
372	GSPL-Almora-24/11/398	29.637112	79.661835	Graphite Schist
373	GSPL-Almora-24/11/399	29.625867	79.66725	QSS
374	GSPL-Almora-24/11/400	29.619465	79.720092	Graphite Schistand Deformed Granite
375	GSPL-Almora-24/11/401	29.621203	79.723318	Graphite Schist
376	GSPL-Almora-24/11/402	29.619262	79.725398	Graphite Schist
377	GSPL-Almora-24/11/403	29.612637	79.725457	Graphite Schist
378	GSPL-Almora-24/11/404	29.60425	79.731945	QBS
379	GSPL-Almora-24/11/405	29.603959	79.734416	Graphite Schist
380	GSPL-Almora-24/11/406	29.602012	79.737677	Graphite Schist
381	GSPL-Almora-24/11/407	29.602225	79.740608	Mica Schist
382	GSPL-Almora-24/11/408	29.614778	79.726418	Graphite Schist
383	GSPL-Almora-24/11/409	29.61483	79.725837	Graphite Schist

S No	Location	Latitude	Longitude	Lithology
384	GSPL-Almora-24/11/410	29.612834	79.724886	Graphite Schist
385	GSPL-Almora-24/11/411	29.612472	79.724767	Graphite Schist
386	GSPL-Almora-24/11/412	29.612108	79.725122	Graphite Schistand Q Mica S
387	GSPL-Almora-24/11/413	29.61191	79.725382	Quartzite
388	GSPL-Almora-24/11/422	29.64918	79.739358	Quartz Biotite Sericite Schist
389	GSPL-Almora-24/11/423	29.654017	79.740818	Quartz Biotite Sericite Schist
390	GSPL-Almora-24/11/424	29.654555	79.74037	Quartzite
391	GSPL-Almora-24/11/426	29.652869	79.729068	Graphite Schist
392	GSPL-Almora-24/11/427	29.655912	79.722012	Graphite Schist
393	GSPL-Almora-24/11/428	29.65565	79.722018	Graphite Schist
394	GSPL-Almora-24/11/429	29.655783	79.720208	Graphite Schist
395	GSPL-Almora-24/11/430	29.656122	79.720452	Graphite Schist
396	GSPL-Almora-24/11/431	29.611993	79.732298	Garnet Biotite Sericite Schist
397	GSPL-Almora-24/11/432	29.61518	79.73265	Garnet Biotite Sericite Schist
398	GSPL-Almora-24/11/433	29.61616	79.732557	Garnet Biotite Sericite Schist
399	GSPL-Almora-24/11/434	29.618923	79.732243	Garnet Biotite Sericite Schist
400	GSPL-Almora-24/11/435	29.651405	79.686548	Graphite Schist
401	GSPL-Almora-24/11/436	29.651537	79.686562	Graphite Schist and Garnet Biotite Sericite Schist
402	GSPL-Almora-24/11/437	29.651867	79.687485	Garnet Biotite Sericite Schist
403	GSPL-Almora-24/11/438	29.649957	79.688332	Graphite Schist
404	GSPL-Almora-24/11/439	29.650715	79.688363	Graphite Schist
405	GSPL-Almora-24/11/440	29.64927	79.68784	Graphite Schist
406	GSPL-Almora-24/11/441	29.649212	79.687808	Graphite Schist
407	GSPL-Almora-24/11/442	29.647808	79.685932	Quartz Biotite Sericite Schist
408	GSPL-Almora-24/11/442	29.630522	79.677053	Quartzite
409	GSPL-Almora-24/11/443	29.631282	79.678918	Quartzite
410	GSPL-Almora-24/11/443	29.631443	79.678797	Quartzite
411	GSPL-Almora-24/11/444	29.631907	79.679313	Quartzite
412	GSPL-Almora-24/11/445	29.634533	79.68963	Garnet Mica Schist
413	GSPL-Almora-24/11/446	29.634443	79.689695	Graphite Schist and Garnet Mica Schist
414	GSPL-Almora-24/11/459	29.619907	79.695393	Quartz Biotite rich Sericite Schist
415	GSPL-Almora-24/11/460	29.62054	79.694825	Biotite rich Sericite Schist
416	GSPL-Almora-24/11/461	29.620875	79.69405	Quartz Biotite rich Sericite Schist
417	GSPL-Almora-24/11/462	29.62141	79.69242	Sericite Schist and Quartzite
418	GSPL-Almora-24/11/463	29.623095	79.689917	Quartzite

S No	Location	Latitude	Longitude	Lithology
419	GSPL-Almora-24/11/464	29.623193	79.689317	Sericite Schist and Quartzite
420	GSPL-Almora-24/11/465	29.623212	79.688862	Quartzite
421	GSPL-Almora-24/11/466	29.622647	79.694987	Quartzite
422	GSPL-Almora-24/11/467	29.62215	79.696173	Quartz Sericite Schist
423	GSPL-Almora-24/11/468	29.621622	79.696343	Silica rich Quartz vein
424	GSPL-Almora-24/11/469	29.621313	79.696377	Quartzite
425	GSPL-Almora-24/11/470	29.598178	79.694753	Quartz Biotite Sericite Schist
426	GSPL-Almora-24/11/471	29.60079	79.701505	Quartz Biotite Sericite Schist
427	GSPL-Almora-24/11/472	29.601425	79.707417	Quartz Biotite Sericite Schist
428	GSPL-Almora-24/11/473	29.597598	79.725015	Garnetiferous Quartz Biotite Sericite Schist
429	GSPL-Almora-24/11/482	29.607435	79.737102	Garnet Quartz Biotite Sericite Schist
430	GSPL-Almora-24/11/483	29.606313	79.737987	Garnet Quartz Biotite Sericite Schist
431	GSPL-Almora-24/11/484	29.638907	79.686535	Garnet Quartz Biotite Sericite Schist
432	GSPL-Almora-24/11/485	29.6403	79.686393	Garnet Quartz Biotite Sericite Schist
433	GSPL-Almora-24/11/487	29.639933	79.68803	Quartz vein
434	GSPL-Almora-24/11/488	29.634518	79.690125	Graphite Schist and Garnet Biotite Sericite Schist
435	GSPL-Almora-24/11/489	29.634983	79.690702	Graphite schist
436	GSPL-Almora-24/11/490	29.63498	79.69083	Garnet Mica Schist
437	GSPL-Almora-24/11/491	29.636412	79.692355	Incipient Gneiss/ Deformed Granite
438	GSPL-Almora-24/11/492	29.636567	79.692262	Graphite Schist and Garnet Biotite Sericite Schist
439	GSPL-Almora-24/11/493	29.6371	79.69311	Graphite Schist
440	GSPL-Almora-24/11/494	29.637171	79.693191	Graphite Schist
441	GSPL-Almora-24/11/495	29.637185	79.693352	Graphite Schist
442	GSPL-Almora-24/11/496	29.63748	79.693458	Graphite Schist
443	GSPL-Almora-24/11/497	29.637833	79.693298	Graphite Schist
444	GSPL-Almora-24/11/498	29.637472	79.693755	Chert like alternate mafic felsic layer
445	GSPL-Almora-24/11/499	29.637923	79.693398	Garnet Sericite schist interlayer with Graphite schist
446	GSPL-Almora-24/11/500	29.647758	79.704782	Garnet mica schist and Graphite Schist
447	GSPL-Almora-24/11/501	29.64773	79.70513	Garnet mica schist and Graphite Schist
448	GSPL-Almora-24/11/502	29.647915	79.704658	Garnet mica schist and Graphite Schist
449	GSPL-Almora-24/11/503	29.648072	79.70427	Graphite schist and Mica schist
450	GSPL-Almora-24/11/504	29.64767	79.705282	Graphite Schist and Garnet mica schist
451	GSPL-Almora-24/11/505	29.64789	79.706078	Graphite Schist and Garnet mica schist
452	GSPL-Almora-24/11/505	29.648075	79.706116	Garnet sericite schist intercalted layer of graphite schist
453	GSPL-Almora-24/11/506	29.646397	79.704653	Graphite Schist

S No	Location	Latitude	Longitude	Lithology
454	GSPL-Almora-24/11/507	29.646918	79.704223	Graphite Schist and mica schist
455	GSPL-Almora-24/11/508	29.646153	79.703937	Graphite Schist
456	GSPL-Almora-24/11/509	29.645857	79.704157	Graphite Schist
457	GSPL-Almora-24/11/510	29.645213	79.704315	Graphite Schist
458	GSPL-Almora-24/11/511	29.645432	79.704127	Graphite Schist
459	GSPL-Almora-24/11/512	29.643067	79.7064443	Graphite Schist and mica schist
460	GSPL-Almora-24/11/513	29.640672	79.707891	Garnet Biotite Sericite schist
461	GSPL-Almora-24/11/514	29.64437	79.688287	Garnet Sericite Biotite Schist
462	GSPL-Almora-24/11/515	29.644272	79.68856	Garnet sericite schist intercalted layer of graphite schist and Graphite Schist
463	GSPL-Almora-24/11/516	29.643948	79.687927	Garnet Sericite Schist and Graphite Schist
464	GSPL-Almora-24/11/517	29.643858	79.687945	Garnet Sericite Schist and Graphite Schist
465	GSPL-Almora-24/11/517	29.642453	79.685793	Graphite Schist
466	GSPL-Almora-24/11/518	29.64215	79.685167	Graphite Schist
467	GSPL-Almora-24/11/518	29.642495	79.685752	Mafic rock? And No Graphite Schist
468	GSPL-Almora-24/11/519	29.642052	79.687023	Garnet Sericite Biotite Schist
469	GSPL-Almora-24/11/520	29.642922	79.688403	Graphite Schist
470	GSPL-Almora-24/11/520	29.643033	79.688442	Garnet Sericite Schist
471	GSPL-Almora-24/11/520	29.644435	79.689243	Graphite Schist
472	GSPL-Almora-24/11/520	29.644415	79.689553	Garnet Sericite Schist and Graphite Schist
473	GSPL-Almora-24/11/520	29.649462	79.68978	Graphite Schist
474	GSPL-Almora-24/11/520	29.644472	79.689693	Garnet Sericite Schist
475	GSPL-Almora-24/11/520	29.645005	79.688953	Graphite Schist
476	GSPL-Almora-24/11/520	29.64578	79.68976	Garnet Sericite Schist with intercalated layer of Graphite Schist
477	GSPL-Almora-24/11/520	29.645893	79.689533	Garnet Sericite Schist with intercalated layer of Graphite Schist
478	GSPL-Almora-24/11/520	29.645487	79.690945	Garnet Sericite Schist with intercalated layer of Graphite Schist
479	GSPL-Almora-24/11/520	29.64549	79.690682	Garnet Sericite Schist with intercalated layer of Graphite Schist
480	GSPL-Almora-24/11/521	29.644242	79.692001	Garnet Sericite Biotite Schist
481	GSPL-Almora-24/11/521	29.648743	79.694727	Graphite Schist layer in Garnet Sericite Schist
482	GSPL-Almora-24/11/521	29.648537	79.694528	Graphite Schist
483	GSPL-Almora-24/11/521	29.649533	79.694738	Graphite Schist
484	GSPL-Almora-24/11/521	29.6495	79.694665	Graphite Schist
485	GSPL-Almora-24/11/521	29.649567	79.69464	Graphite Schist
486	GSPL-Almora-24/11/521	29.649213	79.694632	Graphite Schist
487	GSPL-Almora-24/11/522	29.648587	79.694808	Graphite Schist
488	GSPL-Almora-24/11/523	29.648512	79.694647	Graphite Schist

S No	Location	Latitude	Longitude	Lithology
489	GSPL-Almora-24/11/523	29.64847	79.694568	Quartz Vein
490	GSPL-Almora-24/11/523	29.654028	79.69322	Quartz Vein
491	GSPL-Almora-24/11/523	29.648518	79.694808	Graphite Schist layer in Garnet Sericite Schist
492	GSPL-Almora-24/11/524	29.650097	79.69597	Graphite Schist layer in Garnet Sericite Schist
493	GSPL-Almora-24/11/525	29.65083	79.696287	Graphite Schist layer in Garnet Sericite Schist
494	GSPL-Almora-24/11/526	29.65069	79.696263	Quartz Vein
495	GSPL-Almora-24/11/527	29.650927	79.696192	Quartz Vein
496	GSPL-Almora-24/11/528	29.651062	79.696108	Quartz Vein
497	GSPL-Almora-24/11/529	29.650927	79.695811	Quartz Vein
498	GSPL-Almora-24/11/530	29.650668	79.695838	Quartz Vein
499	GSPL-Almora-24/11/531	29.652248	79.714392	Garnet Sericite Biotite Schist
500	GSPL-Almora-24/11/532	29.657213	79.71701	Graphite Schist layer in Garnet Sericite Schist
501	GSPL-Almora-24/11/533	29.657153	79.71699	Graphite Schist in Garnet Sericite Schist
502	GSPL-Almora-24/11/534	29.656963	79.7169	Graphite Schist
503	GSPL-Almora-24/11/535	29.656933	79.716947	Graphite Schist
504	GSPL-Almora-24/11/535	29.658505	79.717097	Deformed Granite
505	GSPL-Almora-24/11/536	29.65827	79.717243	Quartz Vein
506	GSPL-Almora-24/11/537	29.655817	79.71618	Graphite Schist layer in Garnet Sericite Schist
507	GSPL-Almora-24/11/538	29.655215	79.716053	Garnet Sericite Biotite Schist
508	GSPL-Almora-24/11/539	29.639915	79.714992	Garnet Sericite Biotite Schist and Graphite Schist
509	GSPL-Almora-24/11/540	29.640475	79.712515	Garnet Sericite Biotite Schist
510	GSPL-Almora-24/11/541	29.640515	79.712177	Deformed Granite
511	GSPL-Almora-24/11/542	29.640102	79.71312	Deformed Granite
512	GSPL-Almora-24/11/543	29.639898	79.712945	Garnet Sericite Biotite Schist
513	GSPL-Almora-24/11/544	29.640072	79.712517	Deformed Granite
514	GSPL-Almora-24/11/544	29.641398	79.712388	Deformed Granite
515	GSPL-Almora-24/11/544	29.641495	79.71221	Deformed Granite
516	GSPL-Almora-24/11/544	29.641247	79.712238	Garnet Sericite Biotite Schist
517	GSPL-Almora-24/11/545	29.642015	79.712698	Garnet Sericite Biotite Schist and Graphite Schist
518	GSPL-Almora-24/11/545	29.640052	79.713783	Deformed Granite
519	GSPL-Almora-24/11/546	29.640067	79.713878	Deformed Granite
520	GSPL-Almora-24/11/546	29.639592	79.713973	Deformed Granite intercalated with Garnet Sericite schist
521	GSPL-Almora-24/11/546	29.63947	79.714392	Garnet Sericite Biotite Schist
522	GSPL-Almora-24/11/546	29.639364	79.715226	Quartz vein and ???
523	GSPL-Almora-24/11/547	29.652175	79.715897	Garnet Sericite Biotite Schist

S No	Location	Latitude	Longitude	Lithology
524	GSPL-Almora-24/11/548	29.65096	79.716637	Graphite Schist in garnet mica schist
525	GSPL-Almora-24/11/548	29.649962	79.715508	Graphite schist as thin layer in garnet sericite schist
526	GSPL-Almora-24/11/549	29.64954	79.71517667	Graphite schist as thin layer in garnet sericite schist
527	GSPL-Almora-24/11/550	29.649048	79.715242	Graphite schist as thin layer in garnet sericite schist
528	GSPL-Almora-24/11/550	29.65005833	79.71498833	Garnet Sericite Biotite schist
529	GSPL-Almora-24/11/551	29.65028167	79.71488667	Garnet Sericite Biotite schist
530	GSPL-Almora-24/11/552	29.65038333	79.71459333	Garnet Sericite Biotite schist
531	GSPL-Almora-24/11/553	29.65008519	79.71384176	Garnet Sericite Biotite schist
532	GSPL-Almora-24/11/554	29.649825	79.71304833	Garnet Sericite Biotite schist
533	GSPL-Almora-24/11/555	29.64979333	79.71287333	Garnet Sericite Biotite schist
534	GSPL-Almora-24/11/556	29.649065	79.715015	Garnet Sericite Biotite schist
535	GSPL-Almora-24/11/557	29.648643	79.714672	Graphite schist layer in garnet mica schist
536	GSPL-Almora-24/11/557	29.648528	79.714775	Intercalated layer between Graphite Schist and Garnet Sericite Schist
537	GSPL-Almora-24/11/557	29.64983333	79.712595	Graphite Schist layer in Sericite schist
538	GSPL-Almora-24/11/558	29.648441	79.714639	Graphite Schist layer in Garnet Sericite Biotite schist
539	GSPL-Almora-24/11/559	29.648448	79.714648	Contact between Graphite Schist and Garnet Sericite schist
540	GSPL-Almora-24/11/560	29.648567	79.714385	Graphite Schist
541	GSPL-Almora-24/11/561	29.649493	79.71242	Graphite schist layer in garnet mica schist
542	GSPL-Almora-24/11/562	29.649318	79.712317	Graphite Schist layer in Sericite schist
543	GSPL-Almora-24/11/562	29.649147	79.71215	Graphite schist layer in garnet mica schist
544	GSPL-Almora-24/11/563	29.648945	79.712197	Contact between Graphite Schist and Garnet Sericite schist
545	GSPL-Almora-24/11/564	29.649304	79.713531	Quartz Biotite Schist
546	GSPL-Almora-24/11/565	29.649105	79.712742	Contact between Sericite Schist and Graphite Schist
547	GSPL-Almora-24/11/566	29.64911	79.712632	Graphite Schist
548	GSPL-Almora-24/11/567	29.648913	79.712372	Graphite Schist
549	GSPL-Almora-24/11/568	29.648765	79.712425	Contact between Graphite Schist and Quartz Sericite schist
550	GSPL-Almora-24/11/569	29.64922	79.71160333	Graphite in Garnet Sericite schist
551	GSPL-Almora-24/11/570	29.649295	79.71134667	Graphite in Garnet Sericite schist
552	GSPL-Almora-24/11/571	29.649535	79.711663	Graphite schist intercalted with Garnet Sericite Schist
553	GSPL-Almora-24/11/572	29.649895	79.711915	Garnet Sericite Biotite Schist
554	GSPL-Almora-24/11/573	29.603425	79.689068	Graphite Schist
555	GSPL-Almora-24/11/574	29.603413	79.689103	Graphite Schist , Garnet sericite schist
556	GSPL-Almora-24/11/575	29.603487	79.689095	Garnet Sericite Biotite Schist
557	GSPL-Almora-24/11/576	29.60316	79.689132	Garnet Sericite schist, Graphite Schist
558	GSPL-Almora-24/11/577	29.603127	79.689243	Garnet Sericite Schist

S No	Location	Latitude	Longitude	Lithology
559	GSPL-Almora-24/11/578	29.604112	79.689862	Garnet Sericite Biotite Schist
560	GSPL-Almora-24/11/579	29.604248	79.689817	Graphite Schist , Sericite schist
561	GSPL-Almora-24/11/579	29.60434	79.689438	Graphite Schist, Sericite schist
562	GSPL-Almora-24/11/580	29.604438	79.6871	Graphite Schist and Biotite sericite schist
563	GSPL-Almora-24/11/581	29.604438	79.6871	Graphite Schist
564	GSPL-Almora-24/11/582	29.605023	79.690128	Garnet Sericite Biotite Schist
565	GSPL-Almora-24/11/582	29.605433	79.69115	Graphite Schist, Sericite schist
566	GSPL-Almora-24/11/583	29.606073	79.690685	Graphite Schist
567	GSPL-Almora-24/11/584	29.605232	79.688167	Sericite Biotite Schist
568	GSPL-Almora-24/11/585	29.605193	79.687838	Graphite Schist
569	GSPL-Almora-24/11/586	29.605138	79.687482	Graphite Schist
570	GSPL-Almora-24/11/587	29.60485	79.686568	Graphite Schist
571	GSPL-Almora-24/11/588	29.604487	79.685662	Graphite Schist
572	GSPL-Almora-24/11/589	29.614385	79.696493	Garnet quartz bioite sericte schist
573	GSPL-Almora-24/11/590	29.614018	79.696572	Garnet quartz bioite sericte schist
574	GSPL-Almora-24/11/591	29.613592	79.696808	Garnet quartz bioite sericte schist
575	GSPL-Almora-24/11/592	29.612783	79.696757	Garnet quartz bioite sericte schist
576	GSPL-Almora-24/11/593	29.612608	79.696855	Quarzite (?)/ Quartz biotite schist
577	GSPL-Almora-24/11/594	29.612175	79.696495	Quartzite
578	GSPL-Almora-24/11/595	29.612125	79.696488	Garnet sericite biotite schist
579	GSPL-Almora-24/11/596	29.61133	79.696935	Quartzite
580	GSPL-Almora-24/11/596	29.611475	79.699525	Quartzite
581	GSPL-Almora-24/11/596	29.610803	79.694142	Garnet biotite sericite schist
582	GSPL-Almora-24/11/596	29.609303	79.694095	Garnet sericite biotite schist
583	GSPL-Almora-24/11/596	29.60896	79.693927	mafic hard rock(?) Graphite Schist
584	GSPL-Almora-24/11/596	29.60869	79.694055	Mafic hard rock(?) .
585	GSPL-Almora-24/11/597	29.606738	79.694043	Graphite Schist
586	GSPL-Almora-24/11/598	29.606315	79.6934	Graphite Schist
587	GSPL-Almora-24/11/599	29.605957	79.692265	Graphite Schist
588	GSPL-Almora-24/11/599	29.60509	79.6893162	Graphite Schist
589	GSPL-Almora-24/11/600	29.61213	79.687738	Quartzite
590	GSPL-Almora-24/11/601	29.612065	79.687735	Quartzite and Garnet Biotite Sricite schist
591	GSPL-Almora-24/11/602	29.609743	79.708707	Garnet mica schist
592	GSPL-Almora-24/11/602	29.609868	79.708725	Garnet mica schist and Graphite Schist
593	GSPL-Almora-24/11/602	29.610001	79.70867	Garnet mica schist and Graphite Schist

S No	Location	Latitude	Longitude	Lithology
594	GSPL-Almora-24/11/603	29.610683	79.709524	Graphite Schist
595	GSPL-Almora-24/11/604	29.610173	79.708728	Garnet mica schist and Graphite Schist
596	GSPL-Almora-24/11/604	29.610405	79.708942	Graphite Schist
597	GSPL-Almora-24/11/605	29.610972	79.709708	Garnet mica schist
598	GSPL-Almora-24/11/605	29.60911	79.707712	Graphite Schist
599	GSPL-Almora-24/11/605	29.608737	79.708102	Quartz vein
600	GSPL-Almora-24/11/605	29.608757	79.70831	Chert like rock (?)
601	GSPL-Almora-24/11/606	29.609405	79.7096	Graphite Schist and Quartz sericite schist
602	GSPL-Almora-24/11/607	29.619907	79.727227	Garnet quartz mica schist
603	GSPL-Almora-24/11/608	29.60803	79.685722	Deformed Granite
604	GSPL-Almora-24/11/609	29.608127	79.686045	Deformed Granite
605	GSPL-Almora-24/11/610	29.607968	79.686228	Deformed Granite
606	GSPL-Almora-24/11/611	29.608112	79.68676	Garnet quartz biotite sericite schist
607	GSPL-Almora-24/11/612	29.608	79.688202	Graphite Schist and Garnet Mica Schist
608	GSPL-Almora-24/11/613	29.607985	79.688335	Graphite Schist and Mica schist
609	GSPL-Almora-24/11/613	29.60758	79.689678	Graphite Schist
610	GSPL-Almora-24/11/614	29.60757	79.689773	Quartz Sericite Schist
611	GSPL-Almora-24/11/615	29.607308	79.689893	Graphite Schist
612	GSPL-Almora-24/11/616	29.607485	79.689827	Graphite Schist
613	GSPL-Almora-24/11/617	29.607375	79.69038	Graphite Schist
614	GSPL-Almora-24/11/618	29.608032	79.691043	Graphite Schist
615	GSPL-Almora-24/11/618	29.607812	79.692015	Graphite Schist
616	GSPL-Almora-24/11/619	29.607428	79.691927	Chert like rock
617	GSPL-Almora-24/11/620	29.655755	79.717402	Sericite schist
618	GSPL-Almora-24/11/621	29.65622	79.717519	Graphite Schist
619	GSPL-Almora-24/11/622	29.656775	79.717792	Graphite Schist
620	GSPL-Almora-24/11/623	29.656878	79.717717	Quartz vein
621	GSPL-Almora-24/11/624	29.656878	79.717668	Graphite Schist
622	GSPL-Almora-24/11/625	29.657285	79.718003	Graphite Schist and Mica schist
623	GSPL-Almora-24/11/625	29.657473	79.718492	Graphite Schist and Mica schist
624	GSPL-Almora-24/11/625	29.657762	79.718822	Garnet white sericite schist
625	GSPL-Almora-24/11/626	29.658797	79.71876	White Sericite muscovite schist
626	GSPL-Almora-24/11/626	29.659132	79.718657	Quartzite
627	GSPL-Almora-24/11/627	29.659265	79.718615	Garnet white sericite schist
628	GSPL-Almora-24/11/628	29.660385	79.718972	Quartzite

S No	Location	Latitude	Longitude	Lithology
629	GSPL-Almora-24/11/629	29.660475	79.718992	Sericite schist
630	GSPL-Almora-24/11/630	29.648632	79.706828	Garnet quartz biotite sericite schist
631	GSPL-Almora-24/11/631	29.648632	79.706828	Quartz biotite sericite schist
632	GSPL-Almora-24/11/632	29.649783	79.70835	Quartz biotite muscovite schist
633	GSPL-Almora-24/11/633	29.650575	79.707382	Graphite Schist and Chert
634	GSPL-Almora-24/11/634	29.650572	79.70866	Graphite Schist, Sericite biotite schist
635	GSPL-Almora-24/11/635	29.65663	79.708622	Sericite biotite schist
636	GSPL-Almora-24/11/636	29.650537	79.708642	Sericite biotite schist
637	GSPL-Almora-24/11/637	29.6507	79.709688	Graphite Schist, Sericite biotite schist
638	GSPL-Almora-24/11/638	29.650677	79.709685	Sericite biotite schist
639	GSPL-Almora-24/11/639	29.64819	79.706258	Graphite Schist, Sericite schist
640	GSPL-Almora-24/11/640	29.644865	79.688377	Mica Schist
641	GSPL-Almora-24/11/641	29.622493	79.69845	Granite
642	GSPL-Almora-24/11/642	29.629963	79.70071	Quartz biotite sericite schist
643	GSPL-Almora-24/11/643	29.630303	79.700202	Garnet Quartz Sericite biotite schist
644	GSPL-Almora-24/11/643	29.631647	79.699875	Granite, Garnet Mica Schist
645	GSPL-Almora-24/11/644	29.631702	79.697182	Garnet Quartz Sericite biotite schist
646	GSPL-Almora-24/11/645	29.625592	79.717213	Garnet Quartz Sericite biotite schist
647	GSPL-Almora-24/11/646	29.626205	79.713403	Garnet Biotite Sericite Schist
648	GSPL-Almora-24/11/647	29.6455	79.713262	Garnet Mica Schist
649	GSPL-Almora-24/11/648	29.666888	79.714573	Older Granite
650	GSPL-Almora-24/11/649	29.628282	79.677865	Tuffaceous Rock
651	GSPL-Almora-24/11/650	29.62111	79.723005	Graphite Schist
652	GSPL-Almora-24/11/650	29.636001	79.698062	Foliated Granite
653	GSPL-Almora-24/11/651	29.637048	79.698823	Foliated Granite
654	GSPL-Almora-24/11/651	29.637043	79.698888	Foliated Granite and Garnet Mica Schist
655	GSPL-Almora-24/11/652	29.63521	79.694403	Garnet Mica Schist
656	GSPL-Almora-24/11/652	29.6389	79.685705	Garnet Mica Schist
657	GSPL-Almora-24/11/653	29.632257	79.6808293	Tuffaceous Rock
658	GSPL-Almora-24/11/653	29.6329	79.66781	Garnet Mica Schist and Graphite Schist
659	GSPL-Almora-24/11/654	29.669152	79.712775	Quartz Mica Schist/ Granite?
660	GSPL-Almora-24/11/654	29.66737	79.715138	Quartz Mica Schist
661	GSPL-Almora-24/11/655	29.665313	79.715235	Quartz Mica Schist and Garnet Mica Schist
662	GSPL-Almora-24/11/656	29.664913	79.715007	Garnet Mica Schist
663	GSPL-Almora-24/11/657	29.667482	79.711065	Garnet Mica Schist

S No	Location	Latitude	Longitude	Lithology
664	GSPL-Almora-24/11/658	29.672238	79.702542	Tourmaline foliated Granite
665	GSPL-Almora-24/11/659	29.611752	79.708471	Garnet Mica Schist
666	GSPL-Almora-24/11/660	29.611732	79.707845	Garnet Mica Schist and Foliated Granite
667	GSPL-Almora-24/11/661	29.610088	79.704115	Graphite Schist
668	GSPL-Almora-24/11/662	29.60939	79.701721	Foliated Granite
669	GSPL-Almora-24/11/663	29.604867	79.6924	Mica Schist
670	GSPL-Almora-24/11/664	29.604335	79.696618	Garnet Mica Schist
671	GSPL-Almora-24/11/665	29.638943	79.68391	Foliated Granite
672	GSPL-Almora-24/11/666	29.64003	79.68169	Foliated Granite
673	GSPL-Almora-24/11/667	29.651268	79.671318	Graphite Schist with chert
674	GSPL-Almora-24/11/668	29.649858	79.669197	Graphite Schist
675	GSPL-Almora-24/11/669	29.647085	79.671312	Quartz Biotite Sericite Schist
676	GSPL-Almora-24/11/670	29.64478	79.674937	Quartz Biotite Sericite Schist
677	GSPL-Almora-24/11/671	29.643795	79.677203	Quartz Vein
678	GSPL-Almora-24/11/672	29.644325	79.677742	Mica Schist and older Granite
679	GSPL-Almora-24/11/674	29.612305	79.708582	Foliated Granite
680	AL/SK/LOC 01	29.612855	79.709002	Mica Schist and Foliated Granite
681	AL/SK/LOC 03	29.615808	79.71296	Quartz vein
682	AL/SK/LOC 04	29.615252	79.7131	Foliated Granite
683	AL/SK/LOC 05	29.61403	79.713277	Mica Schist and Foliated Granite
684	AL/SK/LOC 06	29.613502	79.715013	Graphite Schist
685	AL/UM/LOC 01	29.612358	79.717265	Graphite Schist with Chert
686	AL/UM/LOC 02	29.612597	79.718973	Graphite Schist (stone)
687	AL/UM/LOC 03	29.612545	79.73674	Garnet Mica schist
688	AL/UM/LOC 04	29.613033	79.743132	Garnet Mica schist
689	AL/UM/LOC 05	29.629343	79.741825	Garnet Mica Schist
690	AL/UM/LOC 06	29.630777	79.741287	Tuffaceous Rock
691	AL/UM/LOC 07	29.630592	79.740548	Tuffaceous Rock
692	AL/UM/LOC 08	29.630315	79.740007	Tuffaceous Rock
693	AL/UM/LOC 09	29.629096	79.7417173	Graphite Schist
694	AL/UM/LOC 12	29.62795	79.742588	Graphite Schist
695	GSPL-Almora-24/11/675	29.628901	79.744165	Garnet Mica Schist
696	GSPL-Almora-24/11/676	29.630965	79.743557	Garnet Mica Schist
697	GSPL-Almora-24/11/677	29.631873	79.742421	Graphite Schist
698	GSPL-Almora-24/11/678	29.632314	79.741917	Graphite Schist

S No	Location	Latitude	Longitude	Lithology
699	GSPL-Almora-24/11/679	29.632683	79.742106	Graphite Schist
700	GSPL-Almora-24/11/680	29.633041	79.742488	Tuffaceous Rock
701	GSPL-Almora-24/11/681	29.634248	79.739658	Garnet Mica Schist
702	GSPL-Almora-24/11/682	29.602622	79.687053	Mica Schist and Foliated Granite
703	GSPL-Almora-24/11/683	29.599788	79.710494	Tuffaceous Rock
704	GSPL-Almora-24/11/684	29.600148	79.719098	Mica Schist
705	GSPL-Almora-24/11/689	29.661188	79.696457	Graphite schist
706	GSPL-Almora-24/11/690	29.659962	79.695658	Mica Schist
707	GSPL-Almora-24/11/691	29.657587	79.695343	Mica Schist
708	GSPL-Almora-24/11/692	29.65198	79.695972	Graphite Schist and Mica Schist
709	GSPL-Almora-24/11/693	29.660112	79.695693	Mica Schist
710	GSPL-Almora-24/11/694	29.658122	79.679573	Mica Schist
711	GSPL-Almora-24/11/695	29.623036	79.672212	Graphite Schist and Mica Schist
712	GSPL-Almora-24/11/696	29.622173	79.674075	Mica Schist
713	GSPL-Almora-24/11/697	29.652695	79.662402	Mica Schist
714	GSPL-Almora-24/11/698	29.654308	79.661783	Graphite Schist
715	GSPL-Almora-24/11/699	29.655202	79.663692	Mica Schist
716	GSPL-Almora-24/11/702	29.664427	79.690788	Tuffaceous Rock and Mica Schist
717	GSPL-Almora-24/11/703	29.663898	79.695998	Mica Schist
718	GSPL-Almora-24/11/704	29.627735	79.670887	Graphite
719	GSPL-Almora-24/11/705	29.626936	79.673489	Tuffaceous Rock
720	GSPL-Almora-24/11/706	29.627451	79.669907	Graphite Schist
721	GSPL-Almora-24/11/707	29.630536	79.673662	Mica Schist
722	GSPL-Almora-24/11/709	29.637493	79.678542	Tuffaceous Rock
723	GSPL-Almora-24/11/710	29.63343	79.679777	Tuffaceous Rock
724	GSPL-Almora-24/11/712	29.629995	79.675263	Tuffaceous Rock
725	GSPL-Almora-24/11/713	29.635833	79.684229	Tuffaceous Rock
726	GSPL-Almora-24/11/714	29.635929	79.688601	Tuffaceous Rock
727	GSPL-Almora-24/11/715	29.635196	79.694786	Tuffaceous Rock
728	GSPL-Almora-24/11/716	29.63415	79.689922	Tuffaceous Rock
729	GSPL-Almora-24/11/717	29.614515	79.690601	Quartz Mica Schist
730	GSPL-Almora-24/11/718	29.61292	79.709848	Foliated Granite
731	GSPL-Almora-24/11/719	29.612531	79.7069923	Foliated Granite
732	GSPL-Almora-24/11/720	29.61714	79.713557	Graphite Schist
733	GSPL-Almora-24/11/721	29.617693	79.713685	Graphite Schist

S No	Location	Latitude	Longitude	Lithology
734	GSPL-Almora-24/11/722	29.618188	79.714163	Foliated Granite
735	GSPL-Almora-24/11/723	29.619298	79.71628	Foliated Granite
736	GSPL-Almora-24/11/724	29.61524	79.714308	Graphite Schist
737	GSPL-Almora-24/11/725	29.614265	79.714693	Graphite Schist
738	GSPL-Almora-24/11/726	29.622703	79.698427	Tourmaline Quartz Mica Schist (Granite?)
739	GSPL-Almora-24/11/727	29.619363	79.707022	Quartz Mica Schist
740	GSPL-Almora-24/11/728	29.618825	79.708947	Mica Schist
741	GSPL-Almora-24/11/729	29.623803	79.719575	Deformed Granite, Mica Schist
742	GSPL-Almora-24/11/730	29.623588	79.719015	Garnet Mica Schist
743	GSPL-Almora-24/11/731	29.622895	79.718993	Garnet Mica Schist
744	GSPL-Almora-24/11/732	29.622708	79.719097	Deformed Granite
745	GSPL-Almora-24/11/733	29.62271	79.718732	Garnet Mica Schist
746	GSPL-Almora-24/11/734	29.623083	79.718232	Deformed Granite
747	GSPL-Almora-24/11/735	29.62306	79.717793	Graphite Schist
748	GSPL-Almora-24/11/736	29.641732	79.680595	Foliated Granite
749	GSPL-Almora-24/11/737	29.644092	79.679728	Foliated Granite
750	GSPL-Almora-24/11/738	29.643767	79.680543	Foliated Granite
751	GSPL-Almora-24/11/739	29.64388	79.682488	Foliated Granite
752	GSPL-Almora-24/11/740	29.65852	79.717105	Foliated Granite
753	GSPL-Almora-24/11/741	29.658492	79.717056	Foliated Granite
754	GSPL-Almora-24/11/742	29.643012	79.7455171	Mica Schist
755	GSPL-Almora-24/11/743	29.643737	79.742687	Mica Schist
756	GSPL-Almora-24/11/744	29.644207	79.740413	Mica Schist
757	GSPL-Almora-24/11/745	29.648758	79.73927	Mica Schist
758	GSPL-Almora-24/11/746	29.65176	79.74098	Quartz Mica Schist
759	GSPL-Almora-24/11/747	29.652278	79.740488	Quartz Mica Schist
760	GSPL-Almora-24/11/748	29.652595	79.740903	Mica Schist
761	GSPL-Almora-24/11/749	29.653793	79.740683	Mica Schist
762	GSPL-Almora-24/11/750	29.65466	79.740185	Quartz Mica Schist
763	GSPL-Almora-24/11/751	29.654525	79.740255	Quartz Mica Schist
764	GSPL-Almora-24/11/754	29.655327	79.73457	Mica Schist
765	GSPL-Almora-24/11/755	29.654358	79.720442	Garnet Mica Schist
766	GSPL-Almora-24/11/756	29.654358	79.735007	Quartz Mica Schist
767	GSPL-Almora-24/11/756	29.654192	79.735068	Quartz Mica Schist
768	GSPL-Almora-24/11/757	29.65529	79.733895	Mica Schist and Quartz Mica Schist

S No	Location	Latitude	Longitude	Lithology
769	GSPL-Almora-24/11/758	29.65737	79.730713	Quartz Mica Schist
770	GSPL-Almora-24/11/759	29.656543	79.730378	Quartz Mica Schist
771	GSPL-Almora-24/11/760	29.656943	79.71694	Graphite Schist
772	GSPL-Almora-24/11/761	29.654503	79.71666	Mica Schist
773	GSPL-Almora-24/11/762	29.655177	79.717956	Mica Schist
774	GSPL-Almora-24/11/763	29.65485	79.731663	Quartz Mica Schist
775	GSPL-Almora-24/11/764	29.616398	79.71743	Mica Schist
776	GSPL-Almora-24/11/765	29.601255	79.707233	Mica Schist
777	GSPL-Almora-24/11/765	29.597762	79.732815	Greisen
778	GSPL-Almora-24/11/766	29.597853	79.727897	Quartz Mica Schist
779	GSPL-Almora-24/11/767	29.59865	79.725922	Greisen
780	GSPL-Almora-24/11/768	29.599713	79.71954	Mica Schist
781	GSPL-Almora-24/11/769	29.599043	79.711345	Greisen
782	GSPL-Almora-24/11/770	29.604202	79.710018	Greisen
783	GSPL-Almora-24/11/770	29.60272	79.702688	Mica Schist
784	GSPL-Almora-24/11/771	29.645672	79.717423	Graphite Schist
785	GSPL-Almora-24/11/772	29.646352	79.717793	Mica Schist
786	GSPL-Almora-24/11/773	29.647043	79.717923	Graphite schist intercalted with Garnet Mica Schist
787	GSPL-Almora-24/11/774	29.616235	79.713638	Mica Schist
788	GSPL-Almora-24/11/775	29.616207	79.71395	Graphite Schist
789	GSPL-Almora-24/11/776	29.615888	79.714085	Graphite Schist
790	GSPL-Almora-24/11/777	29.614394	79.715511	Graphite Schist
791	GSPL-Almora-24/11/778	29.613879	79.71533	Mica Schist
792	GSPL-Almora-24/11/779	29.61348	79.716378	Graphite Schist
793	GSPL-Almora-24/11/780	29.613879	79.715933	Graphite Schist
794	GSPL-Almora-24/11/781	29.613375	79.717952	Graphite Schist
795	GSPL-Almora-24/11/782	29.615095	79.716078	Graphite Schist
796	GSPL-Almora-24/11/783	29.61514	79.71596	Contact between graphite schist and mica schist
797	GSPL-Almora-24/11/784	29.61514	79.71596	Graphite Schist
798	GSPL-Almora-24/11/785	29.61514	79.71596	Mica Schist
799	GSPL-Almora-24/11/786	29.616422	79.717515	Mica Schist
800	GSPL-Almora-24/11/787	29.621083	79.719805	Mica Schist
801	GSPL-Almora-24/11/788	29.620684	79.720014	Granite
802	GSPL-Almora-24/11/789	29.61963	79.720098	Granite
803	GSPL-Almora-24/11/790	29.613282	79.7222118	Mica Schist

S No	Location	Latitude	Longitude	Lithology
804	GSPL-Almora-24/11/791	29.612797	79.722225	Mica Schist and Graphite Schist
805	GSPL-Almora-24/11/792	29.612832	79.722692	Graphite Schist
806	GSPL-Almora-24/11/793	29.612965	79.722685	Graphite Schist
807	GSPL-Almora-24/11/794	29.61317	79.722645	Graphite Schist
808	GSPL-Almora-24/11/795	29.613603	79.722807	Graphite Schist
809	GSPL-Almora-24/11/796	29.635113	79.725871	Graphite Schist
810	GSPL-Almora-24/11/797	29.636009	79.726091	Graphite Schist
811	GSPL-Almora-24/11/798	29.636308	79.725034	Graphite Schist
812	GSPL-Almora-24/11/799	29.636573	79.724528	Graphite Schist
813	GSPL-Almora-24/11/800	29.636672	79.724761	Graphite Schist
814	GSPL-Almora-24/11/801	29.636718	79.724582	Graphite Schist
815	GSPL-Almora-24/11/802	29.636643	79.725435	Graphite Schist
816	GSPL-Almora-24/11/803	29.635453	79.726761	Graphite Schist with sulphosalts
817	GSPL-Almora-24/11/804	29.637221	79.724982	Mica schist
818	GSPL-Almora-24/11/805	29.609628	79.709755	Graphite Schist
819	GSPL-Almora-24/11/806	29.609823	79.707996	Graphite Schist
820	GSPL-Almora-24/11/807	29.61014	79.708268	Graphite Schist
821	GSPL-Almora-24/11/808	29.609964	79.709922	Graphite Schist
822	GSPL-Almora-24/11/809	29.611554	79.710628	Graphite Schist
823	GSPL-Almora-24/11/810	29.609492	79.70967	Graphite Schist mica schist contact
824	GSPL-Almora-24/11/811	29.60978	79.709337	Mica schist
825	GSPL-Almora-24/11/812	29.609209	79.7093	Mica schist
826	GSPL-Almora-24/11/813	29.608787	79.709502	Mica schist
827	GSPL-Almora-24/11/814	29.608566	79.709176	Mica schist
828	GSPL-Almora-24/11/815	29.608918	79.708546	Mica schist and Graphite Schist cntct
829	GSPL-Almora-24/11/816	29.635113	79.725871	Graphite Schist
830	GSPL-Almora-24/11/817	29.636009	79.726091	Graphite Schist
831	GSPL-Almora-24/11/818	29.636308	79.725034	Graphite Schist
832	GSPL-Almora-24/11/819	29.636573	79.724528	Graphite Schist
833	GSPL-Almora-24/11/820	29.636672	79.724761	Graphite Schist
834	GSPL-Almora-24/11/821	29.636718	79.724582	Graphite Schist
835	GSPL-Almora-24/11/822	29.636643	79.725435	Graphite Schist
836	GSPL-Almora-24/11/823	29.63537	79.716952	Graphite Schist
837	GSPL-Almora-24/11/824	29.634953	79.719146	Graphite Schist
838	GSPL-Almora-24/11/825	29.635332	79.726696	Graphite Schist

S No	Location	Latitude	Longitude	Lithology
839	GSPL-Almora-24/11/826	29.635033	79.72611	Graphite Schist
840	GSPL-Almora-24/11/827	29.635255	79.725565	Graphite Schist
841	GSPL-Almora-24/11/828	29.63562	79.724004	Graphite Schist
842	GSPL-Almora-24/11/829	29.635793	79.722363	Graphite Schist
843	GSPL-Almora-24/11/830	29.636475	79.721721	Graphite Schist
844	GSPL-Almora-24/11/831	29.6368	79.721998	Graphite Schist
845	GSPL-Almora-24/11/832	29.636667	79.723413	Graphite Schist
846	GSPL-Almora-24/11/833	29.635189	79.72644	Graphite Schistwith qtz interlayered
847	GSPL-Almora-24/11/834	29.635453	79.726761	Graphite Schistwith sulphosalts
848	GSPL-Almora-24/11/835	29.635662	79.727316	Graphite Schist and Mica Schist Contact
849	GSPL-Almora-24/11/836	29.635635	79.727345	Graphite Schist and Mica Schist Contact
850	GSPL-Almora-24/11/837	29.636708	79.721578	Graphite Schist and Mica Schist Contact
851	GSPL-Almora-24/11/838	29.635753	79.727649	Mica schist
852	GSPL-Almora-24/11/839	29.637221	79.724982	Mica schist
853	GSPL-Almora-24/11/840	29.635196	79.721414	Mica schist
854	GSPL-Almora-24/11/841	29.634259	79.725351	Mica schist
855	GSPL-Almora-24/11/842	29.634462	79.726256	Mica schist
856	GSPL-Almora-24/11/843	29.633102	79.729754	Mica schist
857	GSPL-Almora-24/11/844	29.634821	79.724855	Mica schist
858	GSPL-Almora-24/11/845	29.636313	79.720737	Mica schist
859	GSPL-Almora-24/11/846	29.636179	79.720501	Mica schist
860	GSPL-Almora-24/11/847	29.609628	79.709755	Graphite Schist
861	GSPL-Almora-24/11/848	29.609823	79.707996	Graphite Schist
862	GSPL-Almora-24/11/849	29.61014	79.708268	Graphite Schist
863	GSPL-Almora-24/11/850	29.609964	79.709922	Graphite Schist
864	GSPL-Almora-24/11/851	29.611554	79.710628	Graphite Schist
865	GSPL-Almora-24/11/852	29.611129	79.707781	Graphite Schist
866	GSPL-Almora-24/11/853	29.610798	79.707465	Graphite Schist
867	GSPL-Almora-24/11/854	29.610734	79.706844	Graphite Schist
868	GSPL-Almora-24/11/855	29.610867	79.706073	Graphite Schist
869	GSPL-Almora-24/11/856	29.609921	79.706866	Graphite Schist
870	GSPL-Almora-24/11/857	29.608589	79.705973	Graphite Schist
871	GSPL-Almora-24/11/858	29.608553	79.706873	Graphite Schist
872	GSPL-Almora-24/11/859	29.608746	79.707957	Graphite Schist
873	GSPL-Almora-24/11/860	29.611923	79.708377	Graphite Schist and mica schist contact

S No	Location	Latitude	Longitude	Lithology
874	GSPL-Almora-24/11/861	29.60978	79.709337	Mica schist
875	GSPL-Almora-24/11/862	29.611258	79.707869	Mica schist
876	GSPL-Almora-24/11/863	29.613582	79.72817	Mica schist
877	GSPL-Almora-24/11/864	29.614083	79.715783	Graphite Schist
878	GSPL-Almora-24/11/865	29.613465	79.716434	Graphite Schist
879	GSPL-Almora-24/11/866	29.613205	79.71781	Graphite Schist
880	GSPL-Almora-24/11/867	29.613022	79.71896	Graphite Schist
881	GSPL-Almora-24/11/868	29.61257	79.718941	Graphite Schist
882	GSPL-Almora-24/11/869	29.612631	79.718221	Graphite Schist
883	GSPL-Almora-24/11/870	29.612593	79.71766	Graphite Schist
884	GSPL-Almora-24/11/871	29.612535	79.716992	Graphite Schist
885	GSPL-Almora-24/11/872	29.613215	79.717346	Graphite Schist
886	GSPL-Almora-24/11/873	29.613168	79.717202	Graphite Schist
887	GSPL-Almora-24/11/874	29.613233	79.716774	Graphite Schist
888	GSPL-Almora-24/11/875	29.613722	79.715968	Graphite Schist
889	GSPL-Almora-24/11/876	29.614763	79.716418	Graphite Schist
890	GSPL-Almora-24/11/877	29.612588	79.7191	Graphite Schist and mica schist contact
891	GSPL-Almora-24/11/878	29.612792	79.719028	Graphite Schist and mica schist contact
892	GSPL-Almora-24/11/879	29.613371	79.716995	Gossan in Graphite Schist
893	GSPL-Almora-24/11/880	29.615943	79.715889	Mica schist
894	GSPL-Almora-24/11/881	29.61546	79.71492	Graphite Schist
895	GSPL-Almora-24/11/882	29.619274	79.714266	Deformed Granite
896	GSPL-Almora-24/11/883	29.614671	79.7152	Graphite Schist
897	GSPL-Almora-24/11/884	29.615728	79.714415	Graphite Schist
898	GSPL-Almora-24/11/885	29.616229	79.714269	Graphite Schist
899	GSPL-Almora-24/11/886	29.615886	79.713467	Graphite Schist
900	GSPL-Almora-24/11/887	29.616118	79.713633	Graphite Schist
901	GSPL-Almora-24/11/888	29.616861	79.713375	Graphite Schist
902	GSPL-Almora-24/11/889	29.618293	79.713246	Graphite Schist
903	GSPL-Almora-24/11/890	29.617354	79.716266	Graphite Schist
904	GSPL-Almora-24/11/891	29.616953	79.715895	Graphite Schist
905	GSPL-Almora-24/11/892	29.616933	79.715377	Graphite Schist
906	GSPL-Almora-24/11/893	29.616938	79.715079	Graphite Schist
907	GSPL-Almora-24/11/894	29.614901	79.715299	Graphite Schist
908	GSPL-Almora-24/11/895	29.617782	79.715194	Graphite Schist and mica schist contact

S No	Location	Latitude	Longitude	Lithology
909	GSPL-Almora-24/11/896	29.617387	79.71336	Graphite Schist near contact
910	GSPL-Almora-24/11/897	29.618113	79.715016	Mica schist
911	GSPL-Almora-24/11/898	29.61808	79.713275	Mica schist Graphite Schist contact
912	GSPL-Almora-24/11/899	29.655878	79.72223	Graphite Schist
913	GSPL-Almora-24/11/900	29.655812	79.721772	Graphite Schist
914	GSPL-Almora-24/11/901	29.656051	79.72051	Graphite Schist
915	GSPL-Almora-24/11/902	29.65543	79.71817	Graphite Schist
916	GSPL-Almora-24/11/903	29.65614	79.720754	Mica schist Graphite Schist contact
917	GSPL-Almora-24/11/904	29.655204	79.717945	Mica schist Graphite Schist contact
918	GSPL-Almora-24/11/905	29.654899	79.717472	Mica schist
919	GSPL-Almora-24/11/906	29.657247	79.723274	Mica schist
920	GSPL-Almora-24/11/907	29.641873	79.666418	Graphite Schist
921	GSPL-Almora-24/11/908	29.641778	79.665853	Mica schist Graphite Schist contact
922	GSPL-Almora-24/11/909	29.64092	79.664718	Mica schist with thin interlayered Graphite Schist
923	GSPL-Almora-24/11/910	29.626328	79.741919	Graphite Schist
924	GSPL-Almora-24/11/911	29.626782	79.742043	Graphite Schist
925	GSPL-Almora-24/11/912	29.626693	79.74255	Graphite Schist
926	GSPL-Almora-24/11/913	29.626236	79.743317	Graphite Schist
927	GSPL-Almora-24/11/914	29.62655	79.743823	Graphite Schist
928	GSPL-Almora-24/11/915	29.626931	79.744393	Graphite Schist
929	GSPL-Almora-24/11/916	29.626544	79.7444	Graphite Schist
930	GSPL-Almora-24/11/917	29.627044	79.74289	Mica schist Graphite Schist contact
931	GSPL-Almora-24/11/918	29.625931	79.745411	Mica schist
932	GSPL-Almora-24/11/919	29.625849	79.744152	Mica schist
933	GSPL-Almora-24/11/920	29.615089	79.713816	Graphite Schist
934	GSPL-Almora-24/11/921	29.615039	79.713807	Graphite Schist
935	GSPL-Almora-24/11/922	29.614405	79.714143	Graphite Schist
936	GSPL-Almora-24/11/923	29.611238	79.710741	Graphite Schist
937	GSPL-Almora-24/11/924	29.612237	79.714001	Graphite Schist
938	GSPL-Almora-24/11/925	29.61214	79.714284	Graphite Schist
939	GSPL-Almora-24/11/926	29.611369	79.71569	Graphite Schist
940	GSPL-Almora-24/11/927	29.611488	79.715875	Graphite Schist
941	GSPL-Almora-24/11/928	29.610662	79.716868	Graphite Schist
942	GSPL-Almora-24/11/929	29.610871	79.714415	Graphite Schist
943	GSPL-Almora-24/11/930	29.610811	79.714016	Graphite Schist

S No	Location	Latitude	Longitude	Lithology
944	GSPL-Almora-24/11/931	29.611905	79.71105	Graphite Schist
945	GSPL-Almora-24/11/932	29.614675	79.714146	Mica schist Graphite Schist contact
946	GSPL-Almora-24/11/933	29.611437	79.716332	Contact Graphite Schist mica schist
947	GSPL-Almora-24/11/934	29.614936	79.713959	Mica schist
948	GSPL-Almora-24/11/935	29.614694	79.714056	Mica schist
949	GSPL-Almora-24/11/936	29.613902	79.713833	Mica schist
950	GSPL-Almora-24/11/937	29.614786	79.713196	Mica schist
951	GSPL-Almora-24/11/938	29.611294	79.716479	Mica schist
952	GSPL-Almora-24/11/939	29.626426	79.745967	Graphite Schist
953	GSPL-Almora-24/11/940	29.626915	79.745969	Graphite Schist
954	GSPL-Almora-24/11/941	29.627077	79.746028	Graphite Schist and Mica schist contact
955	GSPL-Almora-24/11/942	29.627267	79.745891	Graphite Schist and Mica schist contact
956	GSPL-Almora-24/11/943	29.625434	79.74165	Graphite Schist and Mica schist contact
957	GSPL-Almora-24/11/944	29.638366	79.702035	Graphite Schist
958	GSPL-Almora-24/11/945	29.638254	79.70165	Graphite Schist
959	GSPL-Almora-24/11/946	29.637729	79.70138	Graphite Schist
960	GSPL-Almora-24/11/947	29.638687	79.701506	Graphite Schist and Mica schist contact
961	GSPL-Almora-24/11/948	29.637391	79.701102	Mica schist
962	GSPL-Almora-24/11/949	29.638942	79.700597	Mica schist
963	GSPL-Almora-24/11/950	29.638697	79.703156	Mica schist
964	GSPL-Almora-24/11/951	29.63886	79.703432	Mica schist
965	GSPL-Almora-24/11/952	29.638615	79.701392	Bh Naini 01
966	GSPL-Almora-24/11/953	29.647933	79.705077	Bh_Naini02
967	GSPL-Almora-24/11/954	29.646948	79.716942	Graphite Schist
968	GSPL-Almora-24/11/955	29.64702	79.7172	Graphite Schist
969	GSPL-Almora-24/11/956	29.646992	79.717442	Graphite Schist
970	GSPL-Almora-24/11/957	29.646958	79.71782	Graphite Schist
971	GSPL-Almora-24/11/958	29.64699	79.718118	Graphite Schist
972	GSPL-Almora-24/11/959	29.647007	79.718213	Graphite Schist
973	GSPL-Almora-24/11/960	29.646863	79.71718	Graphite Schist contact
974	GSPL-Almora-24/11/961	29.64681	79.718173	Graphite Schist and Mica schist contact
975	GSPL-Almora-24/11/962	29.647072	79.717192	Graphite Schist and Mica schist contact
976	GSPL-Almora-24/11/963	29.647147	79.718225	Graphite Schist and Mica schist contact
977	GSPL-Almora-24/11/964	29.64787	79.705022	Graphite Schist and Mica schist contact
978	GSPL-Almora-24/11/965	29.646546	79.71818	Mica schist

S No	Location	Latitude	Longitude	Lithology
979	GSPL-Almora-24/11/966	29.646922	79.717503	Mica schist
980	GSPL-Almora-24/11/967	29.6469	79.716795	Mica schist
981	GSPL-Almora-24/11/968	29.607866	79.692004	Graphite Schist
982	GSPL-Almora-24/11/969	29.607224	79.688081	Graphite Schist
983	GSPL-Almora-24/11/970	29.597734	79.687256	Graphite Schist
984	GSPL-Almora-24/11/971	29.598015	79.687439	Graphite Schist
985	GSPL-Almora-24/11/972	29.598261	79.688448	Graphite Schist
986	GSPL-Almora-24/11/973	29.598922	79.687568	Graphite Schist
987	GSPL-Almora-24/11/974	29.598522	79.687788	Graphite Schist
988	GSPL-Almora-24/11/975	29.602889	79.689014	Graphite Schist
989	GSPL-Almora-24/11/976	29.604571	79.685174	Graphite Schist
990	GSPL-Almora-24/11/977	29.605147	79.688383	Graphite Schist
991	GSPL-Almora-24/11/978	29.605166	79.688735	Graphite Schist
992	GSPL-Almora-24/11/979	29.605271	79.689098	Graphite Schist
993	GSPL-Almora-24/11/980	29.605181	79.68893	Graphite Schist
994	GSPL-Almora-24/11/981	29.60518	79.689357	Graphite Schist
995	GSPL-Almora-24/11/982	29.60512	79.68944	Graphite Schist
996	GSPL-Almora-24/11/983	29.605179	79.689513	Graphite Schist
997	GSPL-Almora-24/11/984	29.605225	79.689437	Graphite Schist
998	GSPL-Almora-24/11/985	29.605303	79.689446	Graphite Schist
999	GSPL-Almora-24/11/986	29.605606	79.689203	Graphite Schist
1000	GSPL-Almora-24/11/987	29.605958	79.688697	Graphite Schist
1001	GSPL-Almora-24/11/988	29.606411	79.689135	Graphite Schist
1002	GSPL-Almora-24/11/989	29.606521	79.689171	Graphite Schist
1003	GSPL-Almora-24/11/990	29.607612	79.688837	Graphite Schist
1004	GSPL-Almora-24/11/991	29.606934	79.68971	Graphite Schist
1005	GSPL-Almora-24/11/992	29.606782	79.689887	Graphite Schist
1006	GSPL-Almora-24/11/993	29.606501	79.690195	Graphite Schist
1007	GSPL-Almora-24/11/994	29.606553	79.690489	Graphite Schist
1008	GSPL-Almora-24/11/995	29.606966	79.690786	Graphite Schist
1009	GSPL-Almora-24/11/996	29.607338	79.690943	Graphite Schist
1010	GSPL-Almora-24/11/997	29.608012	79.691087	Graphite Schist
1011	GSPL-Almora-24/11/998	29.60817	79.691346	Graphite Schist
1012	GSPL-Almora-24/11/999	29.60816	79.691638	Graphite Schist
1013	GSPL-Almora-24/11/1000	29.607815	79.692221	Graphite Schist

S No	Location	Latitude	Longitude	Lithology
1014	GSPL-Almora-24/11/1001	29.607789	79.692447	Graphite Schist
1015	GSPL-Almora-24/11/1002	29.607722	79.69275	Graphite Schist
1016	GSPL-Almora-24/11/1003	29.607348	79.692799	Graphite Schist
1017	GSPL-Almora-24/11/1004	29.607247	79.69262	Graphite Schist
1018	GSPL-Almora-24/11/1005	29.606935	79.692404	Graphite Schist
1019	GSPL-Almora-24/11/1006	29.606753	79.692391	Graphite Schist
1020	GSPL-Almora-24/11/1007	29.60672	79.692587	Graphite Schist
1021	GSPL-Almora-24/11/1008	29.606475	79.692387	Graphite Schist
1022	GSPL-Almora-24/11/1009	29.606612	79.691918	Graphite Schist
1023	GSPL-Almora-24/11/1010	29.60656	79.691868	Graphite Schist
1024	GSPL-Almora-24/11/1011	29.606204	79.692732	Graphite Schist
1025	GSPL-Almora-24/11/1012	29.606397	79.692117	Graphite Schist
1026	GSPL-Almora-24/11/1013	29.606326	79.691749	Graphite Schist
1027	GSPL-Almora-24/11/1014	29.606093	79.691946	Graphite Schist
1028	GSPL-Almora-24/11/1015	29.605876	79.691968	Graphite Schist
1029	GSPL-Almora-24/11/1016	29.605806	79.691794	Graphite Schist
1030	GSPL-Almora-24/11/1017	29.605493	79.69167	Graphite Schist
1031	GSPL-Almora-24/11/1018	29.604555	79.689669	Graphite Schist
1032	GSPL-Almora-24/11/1019	29.604292	79.688735	Graphite Schist
1033	GSPL-Almora-24/11/1020	29.604779	79.684154	Graphite Schist
1034	GSPL-Almora-24/11/1021	29.606973	79.685477	Graphite Schist
1035	GSPL-Almora-24/11/1022	29.607131	79.68633	Graphite Schist
1036	GSPL-Almora-24/11/1023	29.605848	79.683221	Graphite Schist
1037	GSPL-Almora-24/11/1024	29.598913	79.687563	Graphite Schist and Mica schist contact
1038	GSPL-Almora-24/11/1025	29.60504	79.688061	Graphite Schist and Mica schist contact
1039	GSPL-Almora-24/11/1026	29.60544	79.691012	Graphite Schist and Mica schist contact
1040	GSPL-Almora-24/11/1027	29.604229	79.688695	Graphite Schist and Mica schist contact
1041	GSPL-Almora-24/11/1028	29.60362	79.688557	Granite
1042	GSPL-Almora-24/11/1029	29.59843	79.689128	Mica schist
1043	GSPL-Almora-24/11/1030	29.59877	79.68741	Mica schist
1044	GSPL-Almora-24/11/1031	29.599182	79.687575	Mica schist
1045	GSPL-Almora-24/11/1032	29.599122	79.688234	Mica schist
1046	GSPL-Almora-24/11/1033	29.599537	79.688443	Mica schist
1047	GSPL-Almora-24/11/1034	29.607616	79.689563	Mica schist
1048	GSPL-Almora-24/11/1035	29.605092	79.692467	Mica schist

S No	Location	Latitude	Longitude	Lithology
1049	GSPL-Almora-24/11/1036	29.605025	79.69036	Mica schist
1050	GSPL-Almora-24/11/1037	29.604096	79.688807	Mica schist
1051	GSPL-Almora-24/11/1038	29.604691	79.683681	Mica schist

Annexure III_Details of Structural Data in Almora G4 Block

S No	Location	Latitude	Longitude	Lithology	Foliation		
					Strike	Dip Amount	Dip Direction
1	AL1	29.61403	79.71573	Graphite Schist and Mica Schist	175	23	85
2	AL2	29.614	79.7157	Graphite Schist	170	25	80
3	AL3	29.614	79.7157	Graphite Schist	140	45	50
4	AL4	29.6135	79.7163	Mica Schist	000	15	90
5	AL5	29.6132	79.7174	Graphite Schist	100	25	10
6	AL6	29.6132	79.7174	Graphite Schist	105	27	15
7	AL7	29.6132	79.7174	Graphite Schist	120	17	30
8	AL8	29.6151	79.7161	Mica Schist	100	45	10
9	AL9	29.6151	79.7161	Graphite Schist and Mica Schist	150	32	60
10	AL10	29.6176	79.7207	Graphite Schist	180	20	90
11	AL11	29.6275	79.7062	Graphite Schist	160	5	70
12	AL12	29.618	79.7218	Graphite Schist	035	12	125
13	AL13	29.618	79.7218	Mica Schist	030	10	120
14	AL14	29.6257	79.7221	Graphite Schist	110	26	20
15	AL15	29.6257	79.7218	Graphite Schist	150	12	60
16	AL16	29.6257	79.7215	Graphite Schist	130	18	40
17	AL17	29.6257	79.7213	Graphite Schist	140	27	50
18	AL18	29.6268	79.7208	Graphite Schist and Mica Schist	140	28	50
19	AL19	29.6285	79.7207	Mica Schist	090	10	0
20	AL20	29.6285	79.7207	Mica Schist	135	5	45
21	AL21	29.6299	79.7195	Mica Schist	140	10	50
22	AL22	29.6296	79.7192	Mica Schist	150	15	60
23	AL23	29.6289	79.7189	Graphite Schist	150	8	60
24	AL24	29.6255	79.7213	Graphite Schist	150	35	60

S No	Location	Latitude	Longitude	Lithology	Foliation		
					Strike	Dip Amount	Dip Direction
25	AL25	29.6151	79.72658	Graphite Schist	050	45	160
26	AL26	29.61604	79.72635	Graphite Schist	040	20	150
27	AL27	29.61642	79.72633	Graphite Schist	010	45	100
28	AL28	29.61752	79.72605	Graphite Schist	010	20	100
29	AL29	29.6184	79.7261	Graphite Schist	100	18	10
30	AL30	29.6184	79.7254	Graphite Schist and Mica Schist	130	20	40
31	AL31	29.6192	79.7252	Graphite Schist	140	22	50
32	AL32	29.6198	79.7257	Graphite Schist and Mica Schist	140	35	50
33	AL33	29.6207	79.7246	Graphite Schist and Mica Schist	150	20	60
34	AL34	29.621	79.7244	Graphite Schist and Mica Schist	140	32	50
35	AL35	29.6219	79.7255	Mica Schist	150	22	60
36	AL36	29.622	79.7252	Mica Schist	140	20	50
37	AL37	29.6238	79.72504	Graphite Schist and Mica Schist	140	28	50
38	AL38	29.62437	79.72445	Graphite Schist and Mica Schist	160	10	70
39	AL39	29.62485	79.72409	Graphite Schist	140	9	50
40	AL40	29.62266	79.72229	Graphite Schist	150	12	60
41	AL41	29.62131	79.72241	Graphite Schist and Mica Schist	110	32	20
42	AL42	29.621	79.72287	Graphite Schist and Mica Schist	180	11	90
43	AL43	29.62331	79.72163	Mica Schist	155	18	65
44	AL44	29.62441	79.72268	Graphite Schist and Mica Schist	155	18	65
45	AL45	29.62648	79.72223	Graphite Schist	160	10	70
46	AL46	29.60316	79.73642	Graphite Schist and Mica Schist	090	18	0
47	AL47	29.60292	79.73706	Graphite Schist	040	36	130
48	AL48	29.60254	79.73723	Mica Schist	000	20	90
49	AL49	29.60209	79.73715	Graphite Schist	060	45	150
50	AL50	29.60252	79.73813	Graphite Schist and Mica Schist	000	20	90

S No	Location	Latitude	Longitude	Lithology	Foliation		
					Strike	Dip Amount	Dip Direction
51	AL51	29.60238	79.7374	Mica Schist	040	40	130
52	AL52	29.60297	79.73729	Graphite Schist and Mica Schist	020	50	110
53	AL53	29.60331	79.7368	Mica Schist	150	5	60
54	AL54	29.61482	79.72666	Graphite Schist and Mica Schist	150	18	60
55	AL55	29.61483	79.72654	Graphite Schist	020	20	110
56	AL56	29.6385	79.718	Graphite Schist and Mica Schist	145	18	55
57	AL57	29.63886	79.68591	Mica Schist	150	15	60
58	AL58	29.63704	79.69882	Granite	070	50	340
59	AL59	29.64269	79.69963	Graphite Schist	080	15	170
60	AL60	29.64357	79.69964	Graphite Schist and Mica Schist	100	9	10
61	AL61	29.66413	79.69813	Mica Schist	075	21	165
62	AL62	29.6645	79.69656	Mica Schist	065	23	155
63	AL63	29.66444	79.69599	Graphite Schist and Mica Schist	095	34	185
64	AL64	29.66322	79.69506	Graphite Schist and Mica Schist	100	24	190
65	AL65	29.64069	79.6648	Graphite Schist and Mica Schist	110	10	20
66	AL66	29.64267	79.66494	Graphite Schist and Mica Schist	170	28	80
67	AL67	29.64359	79.66272	Mica Schist	086	9	356
68	AL68	29.64878	79.66381	Mica Schist	170	19	80
69	AL69	29.65277	79.66785	Mica Schist	150	17	60
70	AL70	29.65551	79.67281	Mica Schist	180	9	90
71	AL71	29.65845	79.67974	Mica Schist	060	3	150
72	AL72	29.65893	79.68637	Mica Schist	050	9	140
73	AL73	29.6016	79.73873	Mica Schist	170	12	80
74	AL74	29.6013	79.73772	Graphite Schist	160	15	70
75	AL75	29.60108	79.73745	Seritic micaceous phylite	060	30	150
76	AL76	29.60285	79.73443	Graphite Schist and Mica Schist	055	10	145

S No	Location	Latitude	Longitude	Lithology	Foliation		
					Strike	Dip Amount	Dip Direction
77	AL77	29.60227	79.73462	Graphite Schist and Mica Schist	074	30	164
78	AL78	29.60171	79.73368	Mica Schist	060	42	150
79	AL79	29.60057	79.7325	Graphite Schist and Mica Schist	060	50	150
80	AL80	29.60142	79.72936	Graphite Schist	055	47	145
81	AL81	29.60144	79.72849	Graphite Schist	020	20	110
82	AL82	29.59936	79.72783	Mica Schist	060	50	150
83	AL83	29.59865	79.72592	Graphite Schist and Mica Schist	058	48	148
84	AL84	29.59943	79.7248	Graphite Schist and Mica Schist	065	48	155
85	AL85	29.5992	79.72152	Graphite Schist and Mica Schist	060	58	150
86	AL86	29.60012	79.72448	Graphite Schist and Mica Schist	060	34	150
87	AL87	29.60136	79.72792	Graphite Schist	120	20	30
88	AL88	29.61768	79.72619	Graphite Schist and Mica Schist	120	25	30
89	AL89	29.60111	79.74013	Graphite Schist and Mica Schist	150	14	60
90	AL90	29.60346	79.73939	Graphite Schist and Mica Schist	125	25	35
91	AL91	29.60302	79.7393	Mica Schist	120	8	30
92	AL92	29.60349	79.7397	Graphite Schist	150	88	60
93	AL93	29.60228	79.73849	Graphite Schist and Mica Schist	055	5	145
94	AL94	29.60849	79.73175	Mica Schist	050	5	320
95	AL95	29.61923	79.72527	Graphite Schist and Mica Schist	180	17	90
96	AL96	29.61923	79.72527	Graphite Schist and Mica Schist	160	26	70
97	AL98	29.59841	79.68667	Graphite Schist and Mica Schist	080	40	350
98	AL99	29.60085	79.68755	Graphite Schist and Mica Schist	090	15	0
99	AL100	29.59783	79.68733	Graphite Schist and Mica Schist	120	20	30
100	AL101	29.59849	79.68772	Graphite Schist and Mica Schist	015	18	105
101	AL102	29.60086	79.68877	Mica Schist	085	30	175
102	AL103	29.60264	79.68901	Graphite Schist and Mica Schist	040	30	130

S No	Location	Latitude	Longitude	Lithology	Foliation		
					Strike	Dip Amount	Dip Direction
103	AL104	29.60324	79.68872	Graphite Schist and Lit per lit Granite	040	30	130
104	AL105	29.63431	79.72573	Mica Schist	120	15	30
105	AL106	29.63562	79.72412	Graphite Schist and Mica Schist	150	12	60
106	AL107	29.63659	79.72453	Graphite Schist	105	10	15
107	AL108	29.6367	79.72485	Graphite Schist	080	60	350
108	AL109	29.63682	79.72191	Graphite Schist	050	30	140
109	AL110	29.63686	79.72123	Graphite Schist	110	20	200
110	AL111	29.63676	79.72088	Mica Schist	150	9	60
111	AL112	29.63669	79.72073	Granite	075	50	335
112	AL113	29.63751	79.7188	Graphite Schist and Mica Schist	110	28	20
113	AL114	29.63768	79.71833	Graphite Schist	120	84	30
114	AL115	29.63806	79.71823	Graphite Schist	140	45	50
115	AL116	29.63881	79.71832	Graphite Schist and Mica Schist	100	39	10
116	AL117	29.65288	79.72909	Graphite Schist	140	50	230
117	AL118	29.65296	79.72987	Graphite Schist and Mica Schist	140	60	230
118	AL119	29.65273	79.72895	Graphite Schist and Mica Schist	140	52	230
119	AL120	29.65384	79.72783	Graphite Schist and Mica Schist	120	58	210
120	AL121	29.65445	79.72753	Graphite Schist and Mica Schist	140	50	230
121	AL122	29.65446	79.72695	Graphite Schist and Mica Schist	100	55	190
122	AL123	29.65383	79.72687	Mica Schist	045	46	155
123	AL124	29.65403	79.72607	Mica Schist	105	48	195
124	AL125	29.6548	79.72575	Graphite Schist and Mica Schist	100	90	190
125	AL126	29.65423	79.72629	Graphite Schist and Mica Schist	090	60	180
126	AL127	29.65512	79.72507	Mica Schist	020	35	290
127	AL128	29.65592	79.72529	Mica Schist	110	88	20
128	AL129	29.65704	79.72379	Mica Schist	120	82	30

S No	Location	Latitude	Longitude	Lithology	Foliation		
					Strike	Dip Amount	Dip Direction
129	AL130	29.65627	79.72228	Graphite Schist and Mica Schist	110	88	20
130	AL131	29.65578	79.72174	Graphite Schist	060	43	330
131	AL132	29.65609	79.72166	Graphite Schist and Mica Schist	090	50	180
132	AL133	29.65649	79.72144	Granite and Mica Schist	110	32	10
133	AL134	29.65647	79.72113	Granite and Mica Schist	095	57	5
134	AL135	29.65304	79.72621	Mica Schist	115	45	205
135	AL136	29.6545	79.72348	Graphite Schist and Mica Schist	105	43	195
136	AL137	29.6456	79.73975	Mica Schist	065	25	155
137	AL138	29.64778	79.74148	Graphite Schist and Mica Schist	085	67	175
138	AL139	29.64763	79.74063	Graphite Schist	105	65	195
139	AL140	29.64795	79.74059	Graphite Schist and Mica Schist	100	62	190
140	AL141	29.6539	79.73523	Quartzite	070	50	340
141	AL142	29.65441	79.73505	Quartzite and Mica Schist	105	56	15
142	AL143	29.65532	79.73457	Quartzite and Mica Schist	115	56	25
143	AL144	29.65543	79.73692	Quartzite and Mica Schist	125	81	35
144	AL145	29.65529	79.73432	Quartzite and Mica Schist	090	24	0
145	AL146	29.65683	79.73054	Quartzite and Mica Schist	120	68	30
146	AL147	29.65336	79.71748	Graphite Schist and Mica Schist	120	20	210
147	AL148	29.65502	79.71767	Mica Schist	015	18	105
148	AL149	29.65545	79.71805	Graphite Schist and Mica Schist	165	45	255
149	AL150	29.65578	79.71983	Graphite Schist and Mica Schist	015	5	285
150	AL151	29.65586	79.72182	Graphite Schist	030	48	300
151	AL152	29.65199	79.73078	Graphite Schist and Mica Schist	130	55	220
152	AL153	29.65026	79.73412	Graphite Schist and Mica Schist	150	47	240
153	AL154	29.64938	79.73525	Graphite Schist and Mica Schist	120	60	210
154	AL155	29.62273	79.70072	Graphite Schist and Mica Schist	060	26	330

S No	Location	Latitude	Longitude	Lithology	Foliation		
					Strike	Dip Amount	Dip Direction
155	AL156	29.62361	79.70317	Quartzite	140	14	50
156	AL157	29.62276	79.70342	Mica Schist	135	9	45
157	AL158	29.62211	79.70461	Mica Schist and Quartzite	135	9	45
158	AL159	29.62306	79.7045	Mica Schist	030	10	300
159	AL160	29.62326	79.70054	Quartzite	110	7	20
160	AL162	29.62012	79.69574	Graphite Schist and Mica Schist	110	3	20
161	AL163	29.62033	79.6951	Graphite Schist and Mica Schist	110	3	20
162	AL164	29.62045	79.69502	Mica Schist	150	21	60
163	AL165	29.63021	79.71307	Mica Schist	160	18	70
164	AL166	29.63088	79.71432	Graphite Schist and Mica Schist	160	18	70
165	AL167	29.6316	79.71503	Mica Schist	160	10	70
166	AL168	29.63201	79.71561	Quartz vein and Graphite Schist	150	27	60
167	AL169	29.63265	79.71565	Graphite Schist and Mica Schist	150	10	60
168	AL170	29.63305	79.71636	Graphite Schist and Mica Schist	160	9	70
169	AL171	29.63352	79.7165	Mica Schist and Graphite Schist	160	9	70
170	AL172	29.63382	79.71561	Graphite Schist and Quartzite	155	7	65
171	AL173	29.6352	79.71535	Graphite Schist and Mica Schist	010	12	100
172	AL174	29.63585	79.71625	Graphite Schist	090	7	0
173	AL175	29.63665	79.7162	Quartzite and Mica Schist	090	17	0
174	AL176	29.63684	79.71669	Graphite Schist and Mica Schist	090	17	0
175	AL177	29.63768	79.7168	Graphite Schist and Mica Schist	090	17	0
176	AL178	29.63637	79.71837	Graphite Schist and Mica Schist	070	20	340
177	AL179	29.63582	79.71985	Graphite Schist and Mica Schist	070	20	340
178	AL180	29.63556	79.72009	Graphite Schist and Mica Schist	070	20	340
179	AL181	29.63508	79.72203	Graphite Schist and Mica Schist	140	20	50
180	AL182	29.63628	79.72574	Graphite Schist	010	59	100

S No	Location	Latitude	Longitude	Lithology	Foliation		
					Strike	Dip Amount	Dip Direction
181	AL183	29.63616	79.72603	Graphite Schist and Mica Schist	130	54	40
182	AL184	29.63659	79.72591	Graphite Schist and Mica Schist	160	50	70
183	AL185	29.63626	79.72649	Mica Schist	160	50	70
184	AL186	29.63565	79.72619	Graphite Schist and Mica Schist	010	59	100
185	AL187	29.63516	79.72587	Graphite Schist and Mica Schist	050	50	140
186	AL188	29.63526	79.72588	Graphite Schist and Mica Schist	050	20	140
187	AL189	29.63536	79.72589	Graphite Schist	150	9	60
188	AL190	29.63559	79.72727	Graphite Schist and Mica Schist	050	10	140
189	AL191	29.64171	79.71486	Graphite Schist and Mica Schist	150	44	60
190	AL193	29.60089	79.68973	Granite and Graphite Schist	020	40	110
191	AL194	29.60268	79.68907	Graphite Schist and Mica Schist	022	55	112
192	AL195	29.5992	79.72097	Graphite Schist and Mica Schist	080	60	170
193	AL196	29.61125	79.70936	Graphite Schist	065	18	155
194	AL197	29.61171	79.70875	Graphite Schist and Mica Schist	115	15	25
195	AL198	29.61171	79.70875	Graphite Schist and Mica Schist	065	18	155
196	AL199	29.61103	79.71071	Graphite Schist	055	34	145
197	AL200	29.61132	79.71608	Graphite Schist and Mica Schist	175	16	85
198	AL201	29.61343	79.72889	Mica Schist	135	24	45
199	AL202	29.61168	79.72961	Mica Schist	135	20	45
200	AL203	29.61126	79.72731	Mica Schist	135	12	45
201	AL204	29.61215	79.72714	Mica Schist	125	7	35
202	AL205	29.61305	79.72605	Graphite Schist and Mica Schist	125	9	35
203	AL206	29.61296	79.72482	Graphite Schist	010	32	100
204	AL207	29.61507	79.72523	Graphite Schist and Mica Schist	055	14	145
205	AL208	29.63734	79.66062	Graphite Schist and Mica Schist	165	12	75
206	AL209	29.64034	79.65802	Mica Schist	055	16	145

S No	Location	Latitude	Longitude	Lithology	Foliation		
					Strike	Dip Amount	Dip Direction
207	AL210	29.6266	79.66721	Mica Schist and Quartzite	020	12	110
208	AL211	29.6382	79.72562	Mica Schist	120	14	30
209	AL212	29.63786	79.72216	Graphite Schist	170	14	80
210	AL213	29.63788	79.72216	Graphite Schist	020	15	110
211	AL214	29.63749	79.72278	Graphite Schist and Mica Schist	160	16	70
212	AL215	29.6364	79.72371	Graphite Schist	030	20	120
213	AL216	29.63656	79.72546	Graphite Schist and Mica Schist	147	18	57
214	AL217	29.63674	79.72085	Foliated Granite	075	50	345
215	AL219	29.63663	79.73542	Mica Schist	045	10	315
216	AL220	29.63322	79.72981	Mica Schist	045	9	135
217	AL221	29.63147	79.72967	Mica Schist and Folited Granite	085	8	355
218	AL222	29.62694	79.74259	Graphite Schist and Mica Schist	050	17	140
219	AL223	29.62708	79.74588	Graphite Schist and Mica Schist	160	15	250
220	AL224	29.62816	79.74623	Mica Schist	165	12	75
221	AL225	29.62629	79.74414	Graphite Schist and Mica Schist	180	8	270
222	AL226	29.6254	79.74163	Graphite Schist and Mica Schist	070	20	340
223	AL227	29.6273	79.73792	Mica Schist	020	8	110
224	AL228	29.61891	79.73976	Mica Schist	060	6	330
225	AL229	29.61728	79.73842	Mica Schist	100	20	10
226	AL230	29.62483	79.74149	Mica Schist	150	20	35
227	AL231	29.66152	79.69587	Graphite Schist and Mica Schist	165	22	255
228	AL232	29.66195	79.69857	Mica Schist	115	25	205
229	AL233	29.66496	79.7035	Mica Schist	165	35	255
230	AL234	29.66497	79.71465	Mica Schist	100	45	190
231	AL235	29.65692	79.70042	Mica Schist	115	17	25
232	AL236	29.65903	79.70224	Graphite Schist and Mica Schist	145	27	235

S No	Location	Latitude	Longitude	Lithology	Foliation		
					Strike	Dip Amount	Dip Direction
233	AL237	29.6593	79.70253	Mica Schist	165	12	255
234	AL238	29.65988	79.70098	Mica Schist	107	48	197
235	AL239	29.66094	79.70161	Graphite Schist and Mica Schist	107	58	197
236	AL240	29.6611	79.7012	Graphite Schist and Mica Schist	105	60	195
237	AL241	29.66031	79.69716	Graphite Schist and Mica Schist	080	22	350
238	AL242	29.63645	79.67185	Mica Schist	065	22	335
239	AL243	29.64153	79.67302	Mica Schist	020	12	110
240	AL244	29.64149	79.67357	Mica Schist	010	16	100
241	AL245	29.64134	79.67454	Mica Schist	055	12	145
242	AL246	29.64148	79.67544	Mica Schist	085	16	355
243	AL247	29.64047	79.67231	Mica Schist	125	20	35
244	AL248	29.63984	79.671	Mica Schist	125	24	35
245	AL249	29.63859	79.66853	Graphite Schist	020	12	290
246	AL250	29.63943	79.66769	Graphite Schist	063	13	333
247	AL251	29.65474	79.68366	Mica Schist	005	20	95
248	AL252	29.65185	79.68423	Graphite Schist and Mica Schist	005	22	95
249	AL253	29.65142	79.68404	Mica Schist	015	16	105
250	AL254	29.65132	79.68364	Mica Schist	015	12	105
251	AL255	29.64966	79.68437	Graphite Schist	075	26	345
252	AL256	29.6495	79.68298	Mica Schist	085	13	355
253	AL257	29.6487	79.68301	Graphite Schist	113	15	23
254	AL258	29.64942	79.68186	Mica Schist	170	25	80
255	AL259	29.65204	79.68376	Graphite Schist and Mica Schist	155	28	65
256	AL260	29.64272	79.69856	Mica Schist	010	13	280
257	AL261	29.64232	79.69944	Graphite Schist	170	8	80
258	AL262	29.64229	79.69917	Graphite Schist and Mica Schist	170	9	80

S No	Location	Latitude	Longitude	Lithology	Foliation		
					Strike	Dip Amount	Dip Direction
259	AL263	29.63791	79.69949	Graphite Schist	010	8	100
260	AL264	29.63815	79.69956	Graphite Schist and Mica Schist	165	12	75
261	AL265	29.63585	79.69679	Foliated Granite	155	12	65
262	AL266	29.6366	79.69699	Graphite Schist and Mica Schist	070	42	160
263	AL267	29.63755	79.69694	Graphite Schist and Mica Schist	170	25	80
264	AL268	29.63794	79.6972	Graphite Schist and Mica Schist	100	12	190
265	AL269	29.63577	79.69432	Quartzite	125	15	35
266	AL270	29.62992	79.67574	Graphite Schist	028	45	118
267	AL271	29.66156	79.69597	Graphite Schist	063	14	333
268	AL272	29.66026	79.69709	Graphite Schist	145	38	55
269	AL273	29.65987	79.69705	Mica Schist	080	14	170
270	AL274	29.6599	79.6972	Mica Schist	080	14	170
271	AL275	29.63935	79.69953	Quartzite and Mica Schist	165	15	75
272	AL276	29.65719	79.70041	Quartzite and Granite Gneiss	080	30	0
273	AL277	29.62391	79.67294	Graphite Schist	010	2	280
274	AL278	29.61213	79.67683	Quartzite	105	21	15
275	AL279	29.61451	79.69007	Quartzite	010	3	280
276	AL280	29.65608	79.68438	Mica Schist	133	15	43
277	AL281	29.65195	79.68377	Graphite Schist	150	35	60
278	AL282	29.65175	79.68276	Graphite Schist	170	22	80
279	AL283	29.64844	79.6816	Graphite Schist	130	17	220
280	AL284	29.6484	79.6822	Graphite Schist	130	17	220
281	AL285	29.64073	79.65794	Mica Schist	015	18	105
282	AL286	29.63711	79.66184	Graphite Schist	060	15	150
283	AL287	29.61947	79.72009	Graphite Schist	170	25	80
284	AL288	29.6212	79.72332	Graphite Schist	140	22	50

S No	Location	Latitude	Longitude	Lithology	Foliation		
					Strike	Dip Amount	Dip Direction
285	AL289	29.61926	79.7254	Graphite Schist	140	27	50
286	AL290	29.60396	79.73442	Graphite Schist	150	50	60
287	AL291	29.60201	79.73768	Graphite Schist	020	25	110
288	AL292	29.60223	79.74061	Mica Schist	030	24	120
289	AL293	29.61478	79.72642	Graphite Schist	150	15	60
290	AL294	29.61483	79.72584	Graphite Schist	040	15	310
291	AL295	29.61283	79.72489	Graphite Schist	030	38	120
292	AL296	29.61247	79.72477	Graphite Schist	050	18	140
293	AL297	29.61191	79.72538	Quartzite	010	8	100
294	AL307	29.64918	79.73936	Mica Schist	130	50	220
295	AL308	29.65456	79.74037	Quartzite	180	52	270
296	AL310	29.65287	79.72907	Graphite Schist	145	50	235
297	AL311	29.65591	79.72201	Graphite Schist	100	45	10
298	AL312	29.65565	79.72202	Graphite Schist	010	40	280
299	AL313	29.65578	79.72021	Graphite Schist	150	25	240
300	AL314	29.65612	79.72045	Graphite Schist	165	42	75
301	AL315	29.61199	79.7323	Mica Schist	150	9	60
302	AL316	29.61518	79.73265	Mica Schist	170	15	80
303	AL317	29.61616	79.73256	Mica Schist	160	20	70
304	AL318	29.61892	79.73224	Mica Schist	005	20	95
305	AL319	29.65187	79.68749	Mica Schist	140	30	50
306	AL320	29.64996	79.68833	Graphite Schist	150	18	60
307	AL321	29.64927	79.68784	Graphite Schist	125	16	35
308	AL322	29.64921	79.68781	Graphite Schist	125	16	35
309	AL323	29.64781	79.68593	Mica Schist	125	12	35
310	AL324	29.63052	79.67705	Quartzite	095	47	5

S No	Location	Latitude	Longitude	Lithology	Foliation		
					Strike	Dip Amount	Dip Direction
311	AL325	29.63128	79.67892	Quartzite	160	60	250
312	AL326	29.63144	79.6788	Quartzite	150	80	240
313	AL327	29.63191	79.67931	Quartzite	155	35	65
314	AL335	29.61991	79.69539	Mica Schist	160	9	70
315	AL336	29.62088	79.69405	Mica Schist	160	13	70
316	AL337	29.62141	79.69242	Quartzite	120	10	30
317	AL338	29.62321	79.68886	Quartzite	090	20	0
318	AL339	29.62265	79.69499	Quartzite	090	23	180
319	AL340	29.62131	79.69638	Quartzite	005	15	95
320	AL341	29.59818	79.69475	Mica Schist	040	15	135
321	AL342	29.60079	79.70151	Mica Schist	145	20	55
322	AL343	29.60143	79.70742	Mica Schist	160	15	70
323	AL346	29.60744	79.7371	Mica Schist	110	15	20
324	AL347	29.60631	79.73799	Mica Schist	060	20	330
325	AL348	29.63891	79.68654	Mica Schist	195	18	105
326	AL349	29.6403	79.68639	Mica Schist	140	7	50
327	AL351	29.63498	79.6907	Graphite schist	140	25	50
328	AL352	29.63498	79.69083	Mica Schist	150	22	60
329	AL353	29.63717	79.69319	Graphite Schist	090	25	0
330	AL354	29.63748	79.69346	Graphite Schist	015	27	105
331	AL355	29.63783	79.6933	Graphite Schist	140	22	50
332	AL356	29.64776	79.70478	Mica schist and Graphite Schist	115	10	115
333	AL357	29.64792	79.70466	Mica schist and Graphite Schist	160	17	70
334	AL358	29.64767	79.70528	Mica schist and Graphite Schist	020	13	110
335	AL359	29.64789	79.70608	Mica schist and Graphite Schist	020	13	110
336	AL360	29.6464	79.70465	Graphite Schist	010	20	100

S No	Location	Latitude	Longitude	Lithology	Foliation		
					Strike	Dip Amount	Dip Direction
337	AL361	29.64615	79.70394	Graphite Schist	160	15	70
338	AL362	29.64586	79.70416	Graphite Schist	015	20	105
339	AL363	29.64521	79.70432	Graphite Schist	010	26	100
340	AL364	29.64543	79.70413	Graphite Schist	050	45	140
341	AL365	29.64307	79.70644	Graphite Schist and Mica schist	070	35	340
342	AL366	29.64067	79.70789	Mica schist	160	12	70
343	AL367	29.64437	79.68829	Mica schist	160	15	70
344	AL368	29.64427	79.68856	Mica schist intercalted layer of graphite schist and Graphite Schist	095	36	5
345	AL369	29.64395	79.68793	Mica Schist and Graphite Schist	170	15	80
346	AL370	29.64386	79.68795	Mica Schist and Graphite Schist	170	15	80
347	AL371	29.64245	79.68579	Graphite Schist	020	25	290
348	AL372	29.64215	79.68517	Graphite Schist	145	24	55
349	AL373	29.64292	79.6884	Graphite Schist	140	12	50
350	AL374	29.64444	79.68924	Graphite Schist	120	25	30
351	AL375	29.64946	79.68978	Graphite Schist	120	20	30
352	AL376	29.64578	79.68976	Mica Schist and Graphite Schist	170	25	80
353	AL377	29.64589	79.68953	Mica Schist and Graphite Schist	170	25	80
354	AL378	29.64874	79.69473	Mica Schist and Graphite Schist	140	10	50
355	AL379	29.64854	79.69453	Graphite Schist	140	10	50
356	AL380	29.64953	79.69474	Graphite Schist	145	15	55
357	AL381	29.6495	79.69467	Graphite Schist	145	17	55
358	AL382	29.64957	79.69464	Graphite Schist	150	18	60
359	AL383	29.64921	79.69463	Graphite Schist	150	18	60
360	AL384	29.64852	79.69481	Mica Schist and Graphite Schist	160	10	250
361	AL385	29.6501	79.69597	Mica Schist and Graphite Schist	170	20	80

S No	Location	Latitude	Longitude	Lithology	Foliation		
					Strike	Dip Amount	Dip Direction
362	AL386	29.65083	79.69629	Mica Schist and Graphite Schist	170	20	80
363	AL387	29.65225	79.71439	Mica Schist	030	10	120
364	AL388	29.65721	79.71701	Mica Schist and Graphite Schist	105	60	195
365	AL389	29.65715	79.71699	Mica Schist and Graphite Schist	115	58	205
366	AL390	29.65696	79.7169	Graphite Schist	100	70	190
367	AL391	29.65693	79.71695	Graphite Schist	105	72	195
368	AL392	29.65522	79.71605	Mica Schist	130	35	220
369	AL394	29.63992	79.71499	Mica Schist and Graphite Schist	145	22	55
370	AL395	29.64048	79.71252	Mica Schist	160	25	70
371	AL396	29.64052	79.71218	Foliated Granite	130	10	40
372	AL397	29.6401	79.71312	Foliated Granite	120	35	30
373	AL398	29.64007	79.71252	Foliated Granite	110	40	20
374	AL399	29.64125	79.71224	Mica Schist	120	35	30
375	AL400	29.64202	79.7127	Mica Schist and Graphite Schist	060	35	330
376	AL401	29.64005	79.71378	Foliated Granite	145	40	55
377	AL402	29.64007	79.71388	Foliated Granite	135	25	45
378	AL403	29.63959	79.71397	Foliated Granite intercalated with Mica Schist	110	25	20
379	AL404	29.63947	79.71439	Mica Schist	030	15	300
380	AL405	29.65218	79.7159	Mica Schist	175	15	85
381	AL406	29.65096	79.71664	Graphite Schist in Mica Schist	085	15	355
382	AL407	29.64996	79.71551	Graphite schist as thin layer in Mica Schist	020	37	290
383	AL409	29.65006	79.71499	Mica Schist	130	10	40
384	AL410	29.65038	79.71459	Mica Schist	140	11	50
385	AL411	29.64983	79.71305	Mica Schist	020	20	110
386	AL412	29.64907	79.71502	Mica Schist	070	25	340
387	AL413	29.64864	79.71467	Graphite schist layer in Mica Schist	100	20	10

S No	Location	Latitude	Longitude	Lithology	Foliation		
					Strike	Dip Amount	Dip Direction
388	AL414	29.64983	79.7126	Graphite Schist layer in Sericite schist	155	15	65
389	AL415	29.64845	79.71465	Contact between Graphite Schist and Mica Schist	020	25	290
390	AL416	29.64857	79.71439	Graphite Schist	070	35	340
391	AL417	29.64949	79.71242	Graphite schist layer in Mica Schist	120	5	210
392	AL418	29.64932	79.71232	Graphite Schist layer in Sericite schist	140	5	50
393	AL419	29.64915	79.71215	Graphite schist layer in Mica Schist	140	10	50
394	AL420	29.64895	79.7122	Contact between Graphite Schist and Mica Schist	140	11	50
395	AL421	29.64911	79.71263	Graphite Schist	020	15	290
396	AL422	29.64891	79.71237	Graphite Schist	165	20	55
397	AL423	29.60343	79.68907	Graphite Schist	240	18	330
398	AL424	29.60349	79.6891	Mica Schist	260	15	350
399	AL425	29.60411	79.68986	Mica Schist	160	15	70
400	AL426	29.60425	79.68982	Graphite Schist and Sericite schist	170	50	80
401	AL427	29.60434	79.68944	Graphite Schist and Sericite schist	080	15	170
402	AL428	29.60444	79.6871	Graphite Schist and Mica Schist	160	15	70
403	AL429	29.60444	79.6871	Graphite Schist	010	30	100
404	AL430	29.60543	79.69115	Graphite Schist and Sericite schist	170	35	80
405	AL431	29.60607	79.69069	Graphite Schist	230	20	320
406	AL432	29.60514	79.68748	Graphite Schist	175	15	85
407	AL433	29.60485	79.68657	Graphite Schist	215	25	125
408	AL434	29.60449	79.68566	Graphite Schist	230	10	320
409	AL435	29.61439	79.69649	Mica Schist	070	20	160
410	AL436	29.61402	79.69657	Mica Schist	060	15	150
411	AL437	29.61359	79.69681	Mica Schist	115	17	25

S No	Location	Latitude	Longitude	Lithology	Foliation		
					Strike	Dip Amount	Dip Direction
412	AL438	29.61278	79.69676	Mica Schist	055	20	195
413	AL439	29.61261	79.69686	Quarzite(?)/ Quartz biotite schist	115	27	25
414	AL440	29.61218	79.6965	Quartzite	070	10	160
415	AL441	29.61133	79.69694	Quartzite	025	27	115
416	AL442	29.61148	79.69953	Quartzite	110	25	10
417	AL443	29.6108	79.69414	Garnet Mica Schist	080	17	350
418	AL444	29.60869	79.69406	Mafic hard rock(?) .	150	40	60
419	AL445	29.60632	79.6934	Graphite Schist	075	35	165
420	AL446	29.60596	79.69227	Graphite Schist	075	17	165
421	AL447	29.60509	79.68932	Graphite Schist	050	88	140
422	AL448	29.61213	79.68774	Quartzite	065	35	335
423	AL449	29.61207	79.68774	Quartzite and Garnet Biotite Sricite schist	130	15	40
424	AL450	29.60974	79.70871	Mica Schist	015	25	115
425	AL451	29.60987	79.70873	Mica Schist andGraphite Schist	015	25	115
426	AL452	29.61	79.70867	Mica Schist andGraphite Schist	015	25	115
427	AL453	29.61068	79.70952	Graphite Schist	050	40	140
428	AL454	29.60911	79.70771	Graphite Schist	140	20	50
429	AL455	29.60876	79.70831	Chert like rock (?)	170	20	80
430	AL456	29.60941	79.7096	Graphite Schist and Quartzite	170	22	80
431	AL457	29.60813	79.68605	Foliated Granite	140	18	50
432	AL458	29.60811	79.68676	Mica Schist	125	20	35
433	AL459	29.608	79.6882	Graphite Schist and Mica Schist	165	10	75
434	AL460	29.60799	79.68834	Graphite Schist and Mica schist	165	6	75
435	AL461	29.60758	79.68968	Graphite Schist	190	25	280
436	AL462	29.60749	79.68983	Graphite Schist	105	17	15
437	AL463	29.60781	79.69202	Graphite Schist	240	20	330

S No	Location	Latitude	Longitude	Lithology	Foliation		
					Strike	Dip Amount	Dip Direction
438	AL464	29.65622	79.71752	Graphite Schist	120	50	30
439	AL465	29.65678	79.71779	Graphite Schist	130	50	40
440	AL466	29.65688	79.71767	Graphite Schist	050	55	320
441	AL467	29.65747	79.71849	Graphite Schist and Mica schist	160	45	250
442	AL468	29.6588	79.71876	Quartzite	125	70	35
443	AL469	29.65913	79.71866	Quartzite	070	55	340
444	AL470	29.65927	79.71862	Mica Schist	095	45	185
445	AL471	29.66039	79.71897	Quartzite	110	51	20
446	AL472	29.64863	79.70683	Mica schist	020	28	110
447	AL473	29.65058	79.70738	Graphite Schist and Chert	070	15	160
448	AL474	29.65057	79.70866	Graphite Schist and Mica Schist	090	5	180
449	AL475	29.62249	79.69845	Granite	115	20	25
450	AL476	29.62996	79.70071	Mica schist	120	12	210
451	AL477	29.6303	79.7002	Mica Schist	175	10	85
452	AL478	29.63165	79.69988	Granite and Mica Schist	140	11	230
453	AL479	29.6317	79.69718	Mica Schist	075	12	165
454	AL480	29.62559	79.71721	Mica Schist	110	9	20
455	AL481	29.6455	79.71326	Mica Schist	065	5	355
456	AL482	29.63705	79.69882	Foliated Granite	100	30	10
457	AL483	29.63704	79.69889	Foliated Granite and Mica Schist	100	52	10
458	AL484	29.63521	79.6944	Mica Schist	110	20	20
459	AL485	29.6389	79.68571	Mica Schist	130	15	60
460	AL486	29.63226	79.68083	Tuffaceous Rock	130	38	40
461	AL487	29.6329	79.66781	Mica Schist and Graphite Schist	020	10	110
462	AL488	29.66915	79.71278	Quartzite	060	25	150
463	AL489	29.66737	79.71514	Quartzite	170	45	260

S No	Location	Latitude	Longitude	Lithology	Foliation		
					Strike	Dip Amount	Dip Direction
464	AL490	29.66531	79.71524	Quartzite and Mica Schist	100	60	190
465	AL491	29.66491	79.71501	Mica Schist	090	65	180
466	AL492	29.66748	79.71107	Mica Schist	100	55	190
467	AL493	29.67224	79.70254	Tourmaline foliated Granite	120	30	35
468	AL494	29.61009	79.70412	Graphite Schist	130	20	40
469	AL495	29.60487	79.6924	Mica Schist	035	30	305
470	AL496	29.63966	79.6829	Foliated Granite	170	12	90
471	AL497	29.64003	79.68169	Foliated Granite	170	14	85
472	AL498	29.64124	79.6813	Foliated Granite	045	20	115
473	AL499	29.64233	79.68151	Mica Scist	275	18	5
474	AL500	29.65127	79.67132	Graphite Schist with chert	356	22	86
475	AL501	29.64986	79.6692	Graphite Schist	130	30	40
476	AL502	29.64478	79.67494	Mica Schist	340	10	80
477	AL503	29.64433	79.67774	Mica Schist and older Granite	345	12	75
478	AL504	29.64112	79.68091	Mica Scist	175	8	265
479	AL505	29.61231	79.70858	Foliated Granite	060	20	150
480	AL506	29.61525	79.7131	Foliated Granite	340	30	70
481	AL507	29.61236	79.71727	Graphite Schist with Chert	330	50	60
482	AL508	29.6126	79.71897	Graphite Schist (stone)	090	14	180
483	AL509	29.61255	79.73674	Mica Schist	210	12	120
484	AL510	29.61303	79.74313	Mica Scist	280	30	10
485	AL511	29.62934	79.74183	Mica Schist	040	15	130
486	AL512	29.63078	79.74129	Tuffaceous Rock	030	11	120
487	AL513	29.63059	79.74055	Tuffaceous Rock	155	20	65
488	AL514	29.63268	79.74211	Graphite Schist	170	11	80
489	AL515	29.59979	79.71049	Tuffaceous Rock	335	18	70

S No	Location	Latitude	Longitude	Lithology	Foliation		
					Strike	Dip Amount	Dip Direction
490	AL516	29.62154	79.67723	Mica Scist	215	25	300
491	AL517	29.61218	79.72349	Mica Scist	050	25	140
492	AL518	29.61258	79.72377	Mica Scist	040	30	120
493	AL519	29.65996	79.69566	Mica Schist	150	10	60
494	AL520	29.65198	79.69597	Graphite Schist and Mica Schist	080	12	350
495	AL521	29.66011	79.69569	Mica Schist	105	40	15
496	AL522	29.62217	79.67408	Mica Schist	070	10	340
497	AL523	29.6552	79.66369	Mica Schist	140	10	50
498	AL525	29.66443	79.69079	Tuffaceous Rock and Mica Schist	040	30	130
499	AL526	29.6639	79.696	Mica Schist	100	28	190
500	AL527	29.62694	79.67349	Tuffaceous Rock	210	55	120
501	AL528	29.62745	79.66991	Graphite Schist	070	15	340
502	AL529	29.63054	79.67366	Mica Schist	150	10	60
503	AL531	29.63	79.67526	Tuffaceous Rock	140	20	50
504	AL532	29.63583	79.68423	Tuffaceous Rock	310	29	40
505	AL533	29.63593	79.6886	Tuffaceous Rock	260	20	350
506	AL534	29.61292	79.70985	Foliated Granite	330	20	60
507	AL535	29.61253	79.70699	Foliated Granite	070	5	160
508	AL536	29.61769	79.71369	Graphite Schist	110	16	20
509	AL537	29.61819	79.71416	Foliated Granite	050	8	320
510	AL538	29.6193	79.71628	Foliated Granite	050	9	140
511	AL539	29.61524	79.71431	Graphite Schist	050	18	320
512	AL540	29.61427	79.71469	Graphite Schist	045	16	135
513	AL541	29.6227	79.69843	Tourmaline Quartzite (Granite?)	090	18	0
514	AL542	29.6238	79.71958	Foliated Granite and Mica Schist	005	25	95
515	AL543	29.62359	79.71902	Mica Schist	160	10	70

S No	Location	Latitude	Longitude	Lithology	Foliation		
					Strike	Dip Amount	Dip Direction
516	AL544	29.6229	79.71899	Mica Schist	075	11	345
517	AL545	29.62271	79.7191	Foliated Granite	035	17	125
518	AL546	29.62308	79.71823	Foliated Granite	090	25	180
519	AL547	29.64173	79.6806	Foliated Granite	145	25	55
520	AL548	29.64409	79.67973	Foliated Granite	165	13	75
521	AL549	29.64377	79.68054	Foliated Granite	075	6	345
522	AL550	29.65852	79.71711	Foliated Granite	080	72	350
523	AL551	29.65849	79.71706	Foliated Granite	085	85	355
524	AL552	29.64374	79.74269	Mica Schist	105	3	195
525	AL553	29.64421	79.74041	Mica Schist	105	15	195
526	AL554	29.64876	79.73927	Mica Schist	115	48	205
527	AL555	29.65176	79.74098	Quartzite	100	86	190
528	AL556	29.65228	79.74049	Quartzite	120	84	210
529	AL557	29.6526	79.7409	Mica Schist	140	45	230
530	AL558	29.65379	79.74068	Mica Schist	130	84	220
531	AL559	29.65466	79.74019	Quartzite	120	70	210
532	AL560	29.65453	79.74026	Quartzite	015	32	285
533	AL562	29.65533	79.73457	Mica Schist	160	45	70
534	AL563	29.65436	79.72044	Quartzite	035	10	125
535	AL564	29.65436	79.73501	Quartzite	085	30	355
536	AL565	29.65419	79.73507	Quartzite	060	50	330
537	AL566	29.65529	79.7339	Mica Schist and Quartzite	080	40	350
538	AL567	29.65737	79.73071	Quartzite	140	50	230
539	AL568	29.65654	79.73038	Quartzite	150	85	240
540	AL569	29.65694	79.71694	Graphite Schist	110	70	200
541	AL570	29.6545	79.71666	Mica Schist	080	25	170

S No	Location	Latitude	Longitude	Lithology	Foliation		
					Strike	Dip Amount	Dip Direction
542	AL571	29.65518	79.71796	Mica Schist	130	40	40
543	AL572	29.65485	79.73166	Quartzite	130	20	220
544	AL573	29.6164	79.71743	Mica Schist	164	30	74
545	AL574	29.60126	79.70723	Mica Schist	015	20	105
546	AL575	29.59776	79.73282	Tuffaceous Rock	170	15	80
547	AL576	29.59785	79.7279	Quartzite	020	20	110
548	AL577	29.59865	79.72592	Tuffaceous Rock	120	15	30
549	AL578	29.59971	79.71954	Mica Schist	070	20	340
550	AL579	29.59904	79.71135	Greisen	020	7	110
551	AL580	29.6042	79.71002	Greisen	060	5	150
552	AL581	29.60272	79.70269	Mica Schist	125	10	35
553	AL582	29.64635	79.71779	Mica Schist	045	6	315
554	AL583	29.64704	79.71792	Graphite schist intercalted with Mica Schist	130	25	40
555	AL584	29.61624	79.71364	Mica Schist	030	15	120
556	AL585	29.61589	79.71409	Graphite Schist	115	28	25
557	AL586	29.61388	79.71593	Graphite Schist	070	4	340
558	AL587	29.61338	79.71795	Graphite Schist	150	18	105
559	AL588	29.6151	79.71608	Graphite Schist	010	20	100
560	AL589	29.61514	79.71596	Graphite Schist	010	20	100
561	AL590	29.61514	79.71596	Mica Schist	100	23	10
562	AL591	29.61642	79.71752	Mica Schist	010	22	100
563	AL592	29.61283	79.72269	Graphite Schist	030	2	300
564	AL593	29.61297	79.72269	Graphite Schist	045	15	315
565	AL594	29.61317	79.72265	Graphite Schist	020	12	110
566	AL595	29.6136	79.72281	Graphite Schist	155	12	245
567	AL596	29.63511	79.72587	Graphite Schist	005	20	95

S No	Location	Latitude	Longitude	Lithology	Foliation		
					Strike	Dip Amount	Dip Direction
568	AL597	29.63601	79.72609	Graphite Schist	020	26	110
569	AL598	29.63631	79.72503	Graphite Schist	040	10	130
570	AL599	29.63657	79.72453	Graphite Schist	135	12	45
571	AL600	29.63667	79.72476	Graphite Schist	100	60	10
572	AL601	29.63672	79.72458	Graphite Schist	090	60	0
573	AL602	29.63664	79.72544	Graphite Schist	130	25	40
574	AL603	29.63545	79.72676	Graphite Schist with sulphosalts	160	10	70
575	AL604	29.63722	79.72498	Mica schist	140	25	50
576	AL605	29.60963	79.70976	Graphite Schist	000	35	90
577	AL606	29.60982	79.708	Graphite Schist	000	12	90
578	AL607	29.61014	79.70827	Graphite Schist	020	20	110
579	AL608	29.60996	79.70992	Graphite Schist	015	20	105
580	AL609	29.61155	79.71063	Graphite Schist	005	20	95
581	AL611	29.60978	79.70934	Mica schist	025	20	115
582	AL616	29.63511	79.72587	Graphite Schist	185	20	95
583	AL617	29.63601	79.72609	Graphite Schist	200	26	110
584	AL618	29.63631	79.72503	Graphite Schist	040	10	130
585	AL619	29.63657	79.72453	Graphite Schist	135	12	45
586	AL620	29.63667	79.72476	Graphite Schist	100	60	10
587	AL621	29.63672	79.72458	Graphite Schist	090	60	0
588	AL622	29.63664	79.72544	Graphite Schist	130	25	40
589	AL623	29.63537	79.71695	Graphite Schist	150	17	60
590	AL624	29.63495	79.71915	Graphite Schist	170	14	80
591	AL625	29.63533	79.7267	Graphite Schist	050	10	140
592	AL626	29.63503	79.72611	Graphite Schist	040	25	130
593	AL627	29.63526	79.72557	Graphite Schist	000	10	90

S No	Location	Latitude	Longitude	Lithology	Foliation		
					Strike	Dip Amount	Dip Direction
594	AL628	29.63562	79.724	Graphite Schist	110	22	20
595	AL629	29.63579	79.72236	Graphite Schist	030	20	120
596	AL630	29.63648	79.72172	Graphite Schist	020	20	110
597	AL631	29.6368	79.722	Graphite Schist	120	25	30
598	AL632	29.63667	79.72341	Graphite Schist	130	35	40
599	AL633	29.63519	79.72644	Graphite Schist with qtz interlayered	020	30	100
600	AL634	29.63545	79.72676	Graphite Schist with sulphosalts	160	10	70
601	AL635	29.63566	79.72732	Graphite Schist and Mica Schist Contact	165	22	75
602	AL636	29.63564	79.72735	Graphite Schist and Mica Schist Contact	160	20	70
603	AL637	29.63671	79.72158	Graphite Schist and Mica Schist Contact	120	25	200
604	AL638	29.63575	79.72765	Mica schist	000	15	90
605	AL639	29.63722	79.72498	Mica schist	140	25	50
606	AL640	29.6352	79.72141	Mica schist	180	17	90
607	AL641	29.63426	79.72535	Mica schist	140	25	50
608	AL642	29.63446	79.72626	Mica schist	125	15	35
609	AL643	29.6331	79.72975	Mica schist	180	25	90
610	AL644	29.63482	79.72486	Mica schist	060	10	150
611	AL645	29.63631	79.72074	Mica schist	130	15	40
612	AL646	29.63618	79.7205	Mica schist	030	35	120
613	AL647	29.60963	79.70976	Graphite Schist	000	35	90
614	AL648	29.60982	79.708	Graphite Schist	000	12	90
615	AL649	29.61014	79.70827	Graphite Schist	200	20	120
616	AL650	29.60996	79.70992	Graphite Schist	015	20	105
617	AL651	29.61155	79.71063	Graphite Schist	005	20	95
618	AL652	29.61113	79.70778	Graphite Schist	020	18	110
619	AL653	29.6108	79.70747	Graphite Schist	030	20	120

S No	Location	Latitude	Longitude	Lithology	Foliation		
					Strike	Dip Amount	Dip Direction
620	AL654	29.61073	79.70684	Graphite Schist	135	10	45
621	AL655	29.61087	79.70607	Graphite Schist	090	35	0
622	AL656	29.60992	79.70687	Graphite Schist	150	15	60
623	AL657	29.60859	79.70597	Graphite Schist	030	15	120
624	AL658	29.60855	79.70687	Graphite Schist	150	20	60
625	AL659	29.60875	79.70796	Graphite Schist	170	20	80
626	AL660	29.61192	79.70838	Graphite Schist and mica schist contact	170	15	80
627	AL661	29.60978	79.70934	Mica schist	025	20	115
628	AL662	29.61126	79.70787	Mica schist	040	18	130
629	AL663	29.61358	79.72817	Mica schist	175	25	85
630	AL664	29.61408	79.71578	Graphite Schist	020	25	110
631	AL665	29.61347	79.71643	Graphite Schist	040	35	130
632	AL666	29.61321	79.71781	Graphite Schist	040	20	130
633	AL667	29.61302	79.71896	Graphite Schist	170	20	80
634	AL668	29.61257	79.71894	Graphite Schist	070	17	150
635	AL669	29.61263	79.71822	Graphite Schist	080	25	170
636	AL670	29.61259	79.71766	Graphite Schist	095	5	5
637	AL671	29.61254	79.71699	Graphite Schist	100	20	10
638	AL672	29.61322	79.71735	Graphite Schist	020	15	100
639	AL673	29.61317	79.7172	Graphite Schist	170	25	80
640	AL674	29.61323	79.71677	Graphite Schist	000	10	90
641	AL675	29.61372	79.71597	Graphite Schist	060	10	150
642	AL676	29.61476	79.71642	Graphite Schist	110	22	20
643	AL677	29.61259	79.7191	Graphite Schist and mica schist contact	040	10	130
644	AL678	29.61279	79.71903	Graphite Schist and mica schist contact	000	10	90
645	AL679	29.61337	79.717	Gossan in Graphite Schist	020	35	110

S No	Location	Latitude	Longitude	Lithology	Foliation		
					Strike	Dip Amount	Dip Direction
646	AL680	29.61594	79.71589	Mica schist	120	25	30
647	AL681	29.61546	79.71492	Graphite Schist	000	15	90
648	AL682	29.61927	79.71427	Foliated Granite	120	20	30
649	AL683	29.61467	79.7152	Graphite Schist	050	35	140
650	AL684	29.61573	79.71442	Graphite Schist	120	10	210
651	AL685	29.61623	79.71427	Graphite Schist	015	10	105
652	AL686	29.61589	79.71347	Graphite Schist	130	27	40
653	AL687	29.61612	79.71363	Graphite Schist	105	15	15
654	AL688	29.61686	79.71338	Graphite Schist	135	25	45
655	AL689	29.61829	79.71325	Graphite Schist	130	15	40
656	AL690	29.61735	79.71627	Graphite Schist	140	10	50
657	AL691	29.61695	79.7159	Graphite Schist	015	20	105
658	AL692	29.61693	79.71538	Graphite Schist	005	15	95
659	AL693	29.61694	79.71508	Graphite Schist	000	15	90
660	AL694	29.6149	79.7153	Graphite Schist	140	5	50
661	AL695	29.61778	79.71519	Graphite Schist and mica schist contact	125	15	35
662	AL696	29.61739	79.71336	Graphite Schist near contact	140	25	50
663	AL697	29.61811	79.71502	Mica schist	140	25	50
664	AL698	29.61808	79.71328	Mica schist Graphite Schist contact	150	15	60
665	AL699	29.65588	79.72223	Graphite Schist	100	80	10
666	AL700	29.65581	79.72177	Graphite Schist	070	35	340
667	AL701	29.65605	79.72051	Graphite Schist	120	30	30
668	AL702	29.65543	79.71817	Graphite Schist	130	24	240
669	AL703	29.65614	79.72075	Mica schist Graphite Schist contact	120	25	30
670	AL704	29.6552	79.71795	Mica schist Graphite Schist contact	110	50	20
671	AL705	29.6549	79.71747	Mica schist	130	35	40

S No	Location	Latitude	Longitude	Lithology	Foliation		
					Strike	Dip Amount	Dip Direction
672	AL706	29.65725	79.72327	Mica schist	110	60	200
673	AL707	29.64187	79.66642	Graphite Schist	120	18	30
674	AL708	29.64178	79.66585	Mica schist Graphite Schist contact	160	15	70
675	AL709	29.64092	79.66472	Mica schist with thin interlayered Graphite Schist	130	15	45
676	AL710	29.62633	79.74192	Graphite Schist	010	10	100
677	AL711	29.62678	79.74204	Graphite Schist	180	35	90
678	AL712	29.62669	79.74255	Graphite Schist	040	35	130
679	AL713	29.62624	79.74332	Graphite Schist	090	35	0
680	AL714	29.62655	79.74382	Graphite Schist	140	40	50
681	AL715	29.62693	79.74439	Graphite Schist	030	10	120
682	AL716	29.62654	79.7444	Graphite Schist	115	15	20
683	AL717	29.62704	79.74289	Mica schist Graphite Schist contact	040	30	130
684	AL718	29.62593	79.74541	Mica schist	090	25	0
685	AL719	29.62585	79.74415	Mica schist	020	20	110
686	AL720	29.61509	79.71382	Graphite Schist	090	20	0
687	AL721	29.61504	79.71381	Graphite Schist	120	15	30
688	AL722	29.61441	79.71414	Graphite Schist	140	18	50
689	AL723	29.61124	79.71074	Graphite Schist	040	35	130
690	AL724	29.61224	79.714	Graphite Schist	160	15	70
691	AL725	29.61214	79.71428	Graphite Schist	150	10	60
692	AL726	29.61137	79.71569	Graphite Schist	060	25	150
693	AL727	29.61149	79.71588	Graphite Schist	000	10	90
694	AL728	29.61066	79.71687	Graphite Schist	100	15	190
695	AL729	29.61087	79.71442	Graphite Schist	060	16	150
696	AL730	29.61081	79.71402	Graphite Schist	160	10	70

S No	Location	Latitude	Longitude	Lithology	Foliation		
					Strike	Dip Amount	Dip Direction
697	AL731	29.61191	79.71105	Graphite Schist	040	10	130
698	AL732	29.61468	79.71415	Mica schist Graphite Schist contact	130	20	40
699	AL733	29.61144	79.71633	Contact Graphite Schist mica schist	000	10	90
700	AL734	29.61494	79.71396	Mica schist	140	30	50
701	AL735	29.61469	79.71406	Mica schist	150	25	60
702	AL736	29.6139	79.71383	Mica schist	130	15	40
703	AL737	29.61479	79.7132	Mica schist	090	15	0
704	AL738	29.61129	79.71648	Mica schist	160	10	70
705	AL739	29.62643	79.74597	Graphite Schist	090	30	0
706	AL740	29.62692	79.74597	Graphite Schist	050	20	330
707	AL741	29.62708	79.74603	Graphite Schist and Mica schist contact	010	20	280
708	AL742	29.62727	79.74589	Graphite Schist and Mica schist contact	120	15	30
709	AL743	29.62543	79.74165	Graphite Schist and Mica schist contact	090	20	0
710	AL744	29.63837	79.70204	Graphite Schist	080	20	350
711	AL745	29.63825	79.70165	Graphite Schist	030	20	300
712	AL746	29.63773	79.70138	Graphite Schist	020	20	290
713	AL747	29.63869	79.70151	Graphite Schist and Mica schist contact	080	20	350
714	AL748	29.63739	79.7011	Mica schist	060	10	330
715	AL749	29.63894	79.7006	Mica schist	060	15	330
716	AL750	29.6387	79.70316	Mica schist	050	20	320
717	AL751	29.63886	79.70343	Mica schist	040	22	310
718	AL753	29.64793	79.70508	Graphite Schist	170	18	80
719	AL754	29.64695	79.71694	Graphite Schist	100	22	10
720	AL759	29.64701	79.71821	Graphite Schist	090	15	0
721	AL762	29.64707	79.71719	Graphite Schist and Mica schist contact	340	10	70
722	AL765	29.64655	79.71818	Mica schist	110	10	20

S No	Location	Latitude	Longitude	Lithology	Foliation		
					Strike	Dip Amount	Dip Direction
723	AL766	29.64692	79.7175	Mica schist	000	25	90
724	AL767	29.6469	79.7168	Mica schist	100	20	10
725	AL770	29.59773	79.68726	Graphite Schist	070	10	340
726	AL771	29.59802	79.68744	Graphite Schist	090	20	0
727	AL780	29.60518	79.68893	Graphite Schist	100	10	190
728	AL781	29.60518	79.68936	Graphite Schist	040	35	130
729	AL782	29.60512	79.68944	Graphite Schist	020	47	110
730	AL783	29.60518	79.68951	Graphite Schist	060	55	150
731	AL784	29.60523	79.68944	Graphite Schist	050	43	140
732	AL785	29.6053	79.68945	Graphite Schist	035	65	135
733	AL786	29.60561	79.6892	Graphite Schist	035	35	125
734	AL789	29.60652	79.68917	Graphite Schist	025	35	110
735	AL791	29.60693	79.68971	Graphite Schist	070	15	160
736	AL792	29.60678	79.68989	Graphite Schist	000	20	90
737	AL793	29.6065	79.6902	Graphite Schist	020	15	110
738	AL794	29.60655	79.69049	Graphite Schist	010	8	100
739	AL796	29.60734	79.69094	Graphite Schist	085	8	355
740	AL797	29.60801	79.69109	Graphite Schist	090	10	0
741	AL798	29.60817	79.69135	Graphite Schist	120	10	30
742	AL799	29.60816	79.69164	Graphite Schist	080	30	350
743	AL804	29.60725	79.69262	Graphite Schist	030	15	340
744	AL810	29.60656	79.69187	Graphite Schist	070	20	160
745	AL812	29.6064	79.69212	Graphite Schist	075	25	165
746	AL815	29.60588	79.69197	Graphite Schist	090	35	180
747	AL816	29.60581	79.69179	Graphite Schist	080	40	170
748	AL817	29.60549	79.69167	Graphite Schist	085	30	175

S No	Location	Latitude	Longitude	Lithology	Foliation		
					Strike	Dip Amount	Dip Direction
749	AL818	29.60456	79.68967	Graphite Schist	070	30	160
750	AL819	29.60429	79.68874	Graphite Schist	040	15	130
751	AL820	29.60478	79.68415	Graphite Schist	110	8	20
752	AL821	29.60697	79.68548	Graphite Schist	020	15	110
753	AL822	29.60713	79.68633	Graphite Schist	050	15	140
754	AL823	29.60585	79.68322	Graphite Schist	020	15	110
755	AL824	29.59891	79.68756	Graphite Schist and Mica schist contact	005	15	275
756	AL825	29.60504	79.68806	Graphite Schist and Mica schist contact	125	10	215
757	AL826	29.60544	79.69101	Graphite Schist and Mica schist contact	050	25	140
758	AL827	29.60423	79.6887	Graphite Schist and Mica schist contact	110	10	20
759	AL828	29.60362	79.68856	Granite	120	10	30
760	AL829	29.59843	79.68913	Mica schist	020	20	110
761	AL830	29.59877	79.68741	Mica schist	020	20	110
762	AL831	29.59918	79.68758	Mica schist	010	5	100
763	AL832	29.59912	79.68823	Mica schist	000	15	90
764	AL833	29.59954	79.68844	Mica schist	030	10	120
765	AL834	29.60762	79.68956	Mica schist	085	22	355
766	AL835	29.60509	79.69247	Mica schist	050	15	140
767	AL836	29.60503	79.69036	Mica schist	120	20	30
768	AL837	29.6041	79.68881	Mica schist	100	20	10
769	AL838	29.60469	79.68368	Mica schist	060	25	150

Annexure IV_Details of Graphite Crystallinity for Bedrock

SL No.	Location No.	Latitude	Longitude	Host Lithology	Surface Mineralization	Graphite Crystallinity
1	AL1	29.61403	79.71573	Graphite Schist	Graphite	Moderate
2	AL2	29.614	79.7157	Graphite Schist	Graphite	Moderate
3	AL3	29.614	79.7157	Graphite Schist	Graphite	Moderate
4	AL4	29.6132	79.7174	Graphite Schist	Graphite	Moderate
5	AL5	29.6132	79.7174	Graphite Schist	Graphite	Moderate
6	AL6	29.6132	79.7174	Graphite Schist	Graphite	Moderate
7	AL7	29.6151	79.7161	Graphite Schist	Graphite	Moderate
8	AL8	29.6176	79.7207	Graphite Schist	Graphite	Moderate
9	AL9	29.6275	79.7062	Graphite Schist	Graphite	Moderate
10	AL10	29.618	79.7218	Graphite Schist	Graphite	Moderate
11	AL11	29.6257	79.7221	Graphite Schist	Graphite	High
12	AL12	29.6257	79.7218	Graphite Schist	Graphite	High
13	AL13	29.6257	79.7215	Graphite Schist	Graphite	High
14	AL14	29.6257	79.7213	Graphite Schist	Graphite	High
15	AL15	29.6268	79.7208	Graphite Schist	Graphite	Poor
16	AL16	29.6289	79.7189	Graphite Schist	Graphite	High
17	AL17	29.6285	79.7195	Graphite Schist	Graphite	High
18	AL18	29.6282	79.7194	Graphite Schist	Graphite	High
19	AL19	29.6255	79.7213	Graphite Schist	Graphite	High
20	AL20	29.6151	79.72658	Graphite Schist	Graphite	High
21	AL21	29.61604	79.72635	Graphite Schist	Graphite	Moderate
22	AL22	29.61642	79.72633	Graphite Schist	Graphite	Poor
23	AL23	29.61714	79.72624	Graphite Schist	Graphite	Poor
24	AL24	29.61752	79.72605	Graphite Schist	Graphite	High
25	AL25	29.6184	79.7261	Graphite Schist	Graphite	Poor
26	AL26	29.6184	79.7254	Graphite Schist	Graphite	Poor
27	AL27	29.6192	79.7252	Graphite Schist	Graphite	High
28	AL28	29.6193	79.7251	Graphite Schist	Graphite	Poor
29	AL29	29.6198	79.7257	Graphite Schist	Graphite	Moderate
30	AL30	29.6207	79.7246	Graphite Schist	Graphite	Moderate
31	AL31	29.621	79.7244	Graphite Schist	Graphite	High
32	AL32	29.6238	79.72504	Graphite Schist	Graphite	Moderate
33	AL33	29.62437	79.72445	Graphite Schist	Graphite	Poor

SL No.	Location No.	Latitude	Longitude	Host Lithology	Surface Mineralization	Graphite Crystallinity
34	AL34	29.62485	79.72409	Graphite Schist	Graphite	Moderate
35	AL35	29.62266	79.72229	Graphite Schist	Graphite	High
36	AL36	29.62131	79.72241	Graphite Schist	Graphite	High
37	AL37	29.621	79.72287	Graphite Schist	Graphite	Moderate
38	AL38	29.62331	79.72163	Mica Schist	Graphite	Moderate
39	AL39	29.62441	79.72268	Graphite Schist	Graphite	High
40	AL40	29.62648	79.72223	Graphite Schist	Graphite	High
41	AL41	29.60316	79.73642	Graphite Schist	Graphite	Moderate
42	AL42	29.60292	79.73706	Graphite Schist	Graphite	Poor
43	AL43	29.60254	79.73723	Mica Schist	Graphite	Poor
44	AL44	29.60209	79.73715	Graphite Schist	Graphite	Poor
45	AL45	29.60252	79.73813	Graphite Schist	Graphite	Poor
46	AL46	29.60238	79.7374	Mica Schist	Graphite	Poor
47	AL47	29.60297	79.73729	Graphite Schist	Graphite	Poor
48	AL48	29.60331	79.7368	Mica Schist	Graphite	Poor
49	AL49	29.61482	79.72666	Graphite Schist	Graphite	Poor
50	AL50	29.61483	79.72654	Graphite Schist	Graphite	Poor
51	AL51	29.6385	79.718	Graphite Schist	Graphite	Moderate
52	AL52	29.63697	79.70056	Graphite Schist	Graphite	High
53	AL53	29.63824	79.70173	Graphite Schist	Graphite	High
54	AL54	29.63653	79.70174	Graphite Schist	Graphite	Moderate
55	AL55	29.6346	79.68954	Graphite Schist	Graphite	Poor
56	AL56	29.63755	79.66558	Graphite Schist	Graphite	Poor
57	AL57	29.63756	79.66558	Graphite Schist	Graphite	Moderate
58	AL58	29.64269	79.69963	Graphite Schist	Graphite	Moderate
59	AL59	29.64357	79.69964	Graphite Schist	Graphite	Moderate
60	AL60	29.64783	79.70488	Graphite Schist	Graphite	Moderate
61	AL61	29.66444	79.69599	Graphite Schist	Graphite	Moderate
62	AL62	29.66322	79.69506	Graphite Schist	Graphite	Poor
63	AL63	29.64069	79.6648	Graphite Schist	Graphite	Poor
64	AL64	29.64267	79.66494	Graphite Schist	Graphite	Poor
65	AL65	29.64197	79.66566	Mica Schist	Graphite	Poor
66	AL66	29.6018	79.73844	Graphite Schist	Graphite	Poor
67	AL67	29.6013	79.73772	Graphite Schist	Graphite	High
68	AL68	29.60108	79.73745	Mica Schist	Graphite	Poor

SL No.	Location No.	Latitude	Longitude	Host Lithology	Surface Mineralization	Graphite Crystallinity
69	AL69	29.6012	79.73728	Graphite Schist	Graphite	Moderate
70	AL70	29.60285	79.73443	Graphite Schist	Graphite	Poor
71	AL71	29.60265	79.73462	Graphite Schist	Graphite	Moderate
72	AL72	29.60227	79.73462	Graphite Schist	Graphite	Moderate
73	AL73	29.60057	79.7325	Graphite Schist	Graphite	Moderate
74	AL74	29.60142	79.72936	Graphite Schist	Graphite	Moderate
75	AL75	29.60144	79.72849	Graphite Schist	Graphite	Poor
76	AL76	29.59865	79.72592	Graphite Schist	Graphite	Poor
77	AL77	29.59932	79.72566	Graphite Schist	Graphite	Poor
78	AL78	29.59943	79.7248	Graphite Schist	Graphite	Poor
79	AL79	29.59942	79.72152	Graphite Schist	Graphite	Moderate
80	AL80	29.5992	79.72152	Graphite Schist	Graphite	Moderate
81	AL81	29.60012	79.72448	Graphite Schist	Graphite	Poor
82	AL82	29.60136	79.72792	Graphite Schist	Graphite	Moderate
83	AL83	29.60135	79.72798	Graphite Schist	Graphite	High
84	AL84	29.61768	79.72619	Graphite Schist	Graphite	Poor
85	AL85	29.61521	79.72725	Graphite Schist	Graphite	Moderate
86	AL86	29.60111	79.74013	Graphite Schist	Graphite	Poor
87	AL87	29.60346	79.73939	Graphite Schist	Graphite	Poor
88	AL88	29.60349	79.7397	Graphite Schist	Graphite	Poor
89	AL89	29.60267	79.73897	Graphite Schist	Graphite	Poor
90	AL90	29.61923	79.72527	Graphite Schist	Graphite	Moderate
91	AL91	29.59841	79.68667	Graphite Schist	Graphite	Moderate
92	AL92	29.60085	79.68755	Graphite Schist	Graphite	Moderate
93	AL93	29.59783	79.68733	Graphite Schist	Graphite	Poor
94	AL94	29.59849	79.68772	Graphite Schist	Graphite	Moderate
95	AL95	29.60264	79.68901	Graphite Schist	Graphite	Poor
96	AL96	29.60324	79.68872	Graphite Schist	Graphite	Poor
97	AL97	29.63562	79.72412	Graphite Schist	Graphite	Moderate
98	AL98	29.63659	79.72453	Graphite Schist	Graphite	Moderate
99	AL99	29.6367	79.72485	Graphite Schist	Graphite	Poor
100	AL100	29.63682	79.72191	Graphite Schist	Graphite	Poor
101	AL101	29.63686	79.72123	Graphite Schist	Graphite	Poor
102	AL102	29.63768	79.71833	Graphite Schist	Graphite	Moderate
103	AL103	29.63806	79.71823	Graphite Schist	Graphite	Poor

SL No.	Location No.	Latitude	Longitude	Host Lithology	Surface Mineralization	Graphite Crystallinity
104	AL104	29.63806	79.71823	Graphite Schist	Graphite	Moderate
105	AL105	29.63881	79.71832	Graphite Schist	Graphite	Moderate
106	AL106	29.65288	79.72909	Graphite Schist	Graphite	Poor
107	AL107	29.65296	79.72987	Graphite Schist	Graphite	Moderate
108	AL108	29.65273	79.72895	Graphite Schist	Graphite	Moderate
109	AL109	29.65384	79.72783	Graphite Schist	Graphite	Moderate
110	AL110	29.65445	79.72753	Graphite Schist	Graphite	Poor
111	AL111	29.65446	79.72695	Graphite Schist	Graphite	Moderate
112	AL112	29.6548	79.72575	Graphite Schist	Graphite	Poor
113	AL113	29.65423	79.72629	Graphite Schist	Graphite	Poor
114	AL114	29.65627	79.72228	Graphite Schist	Graphite	Poor
115	AL115	29.65578	79.72174	Graphite Schist	Graphite	Moderate
116	AL116	29.65609	79.72166	Graphite Schist	Graphite	Poor
117	AL117	29.65608	79.72091	Graphite Schist	Graphite	Moderate
118	AL118	29.65558	79.72272	Graphite Schist	Graphite	Poor
119	AL119	29.6545	79.72348	Graphite Schist	Graphite	Poor
120	AL120	29.64778	79.74148	Graphite Schist	Graphite	Moderate
121	AL121	29.64763	79.74063	Graphite Schist	Graphite	Moderate
122	AL122	29.64795	79.74059	Graphite Schist	Graphite	Moderate
123	AL123	29.65683	79.73054	Mica Schist	Graphite	Moderate
124	AL124	29.65336	79.71748	Graphite Schist	Graphite	High
125	AL125	29.65545	79.71805	Graphite Schist	Graphite	Poor
126	AL126	29.65578	79.71983	Graphite Schist	Graphite	High
127	AL127	29.65586	79.72182	Graphite Schist	Graphite	Moderate
128	AL128	29.65199	79.73078	Graphite Schist	Graphite	Moderate
129	AL129	29.65026	79.73412	Graphite Schist	Graphite	Moderate
130	AL130	29.64938	79.73525	Graphite Schist	Graphite	Moderate
131	AL131	29.62273	79.70072	Graphite Schist	Graphite	High
132	AL132	29.6222	79699617	Mica Schist	Graphite	Moderate
133	AL133	29.62012	79.69574	Graphite Schist	Graphite	Poor
134	AL134	29.62033	79.6951	Graphite Schist	Graphite	Poor
135	AL135	29.63088	79.71432	Graphite Schist	Graphite	Moderate
136	AL136	29.63201	79.71561	Graphite Schist	Graphite	Moderate
137	AL137	29.63265	79.71565	Graphite Schist	Graphite	Poor
138	AL138	29.63305	79.71636	Graphite Schist	Graphite	Moderate

SL No.	Location No.	Latitude	Longitude	Host Lithology	Surface Mineralization	Graphite Crystallinity
139	AL139	29.63352	79.7165	Graphite Schist	Graphite	Moderate
140	AL140	29.63382	79.71561	Graphite Schist	Graphite	Poor
141	AL141	29.6352	79.71535	Graphite Schist	Graphite	Poor
142	AL142	29.63585	79.71625	Graphite Schist	graphite	Moderate
143	AL143	29.63684	79.71669	Graphite Schist	graphite	Moderate
144	AL144	29.63768	79.7168	Graphite Schist	graphite	Moderate
145	AL145	29.63637	79.71837	Graphite Schist	graphite	Moderate
146	AL146	29.63582	79.71985	Graphite Schist	graphite	Moderate
147	AL147	29.63556	79.72009	Graphite Schist	graphite	Moderate
148	AL148	29.63508	79.72203	Graphite Schist	graphite	Moderate
149	AL149	29.63628	79.72574	Graphite Schist	Graphite	Moderate
150	AL150	29.63616	79.72603	Graphite Schist	Graphite	Moderate
151	AL151	29.63659	79.72591	Graphite Schist	Graphite	Moderate
152	AL152	29.63565	79.72619	Graphite Schist	Graphite	Moderate
153	AL153	29.63516	79.72587	Graphite Schist	Graphite	Moderate
154	AL154	29.63526	79.72588	Graphite Schist	Graphite	Moderate
155	AL155	29.63536	79.72589	Graphite Schist	Graphite	Moderate
156	AL156	29.63559	79.72727	Graphite Schist	Graphite	Moderate
157	AL157	29.63567	79.727	Graphite Schist	Graphite	Moderate
158	AL158	29.63508	79.71441	Graphite Schist	Graphite	Moderate
159	AL159	29.63511	79.71439	Graphite Schist	Graphite	Moderate
160	AL160	29.6411	79.71591	Graphite Schist	Graphite	Poor
161	AL161	29.64171	79.71486	Graphite Schist	Graphite	Moderate
162	AL162	29.64141	79.71628	Graphite Schist	Graphite	Moderate
163	AL163	29.64153	79.71438	Graphite Schist	Graphite	Moderate
164	AL164	29.64175	79.71428	Graphite Schist	Graphite	Poor
165	AL165	29.64221	79.71366	Graphite Schist	Graphite	Moderate
166	AL166	29.61838	79.72545	Graphite Schist	Graphite	Moderate
167	AL167	29.64696	79.75891	Graphite Schist	Graphite	High
168	AL168	29.61635	79.71789	Graphite Schist	Graphite	High
169	AL169	29.60089	79.68973	Graphite Schist	Graphite	Moderate
170	AL170	29.60268	79.68907	Graphite Schist	Graphite	Moderate
171	AL171	29.5992	79.72097	Graphite Schist	Graphite	Moderate
172	AL172	29.61125	79.70936	Graphite Schist	Graphite	High
173	AL173	29.61171	79.70875	Graphite Schist	Graphite	Moderate

SL No.	Location No.	Latitude	Longitude	Host Lithology	Surface Mineralization	Graphite Crystallinity
174	AL174	29.61103	79.71071	Graphite Schist	Graphite	High
175	AL175	29.61215	79.71421	Graphite Schist	Graphite	Moderate
176	AL176	29.61153	79.71591	Graphite Schist	Graphite	Moderate
177	AL177	29.61132	79.71608	Graphite Schist	Graphite	Moderate
178	AL178	29.61305	79.72605	Graphite Schist	Graphite	Poor
179	AL179	29.61296	79.72482	Graphite Schist	Graphite	Moderate
180	AL180	29.61328	79.72447	Graphite Schist	Graphite	Moderate
181	AL181	29.61507	79.72523	Graphite Schist	Graphite	Moderate
182	AL182	29.63734	79.66062	Graphite Schist	Graphite	Moderate
183	AL183	29.64034	79.65802	Mica Schist	Graphite	Poor
184	AL184	29.63788	79.72216	Graphite Schist	Graphite	High
185	AL185	29.63749	79.72278	Graphite Schist	Graphite	High
186	AL186	29.6364	79.72371	Graphite Schist	Graphite	High
187	AL187	29.63656	79.72546	Graphite Schist	Graphite	High
188	AL188	29.62694	79.74259	Graphite Schist	Graphite	Poor
189	AL189	29.62636	79.7459	Graphite Schist	Graphite	Poor
190	AL190	29.62708	79.74588	Graphite Schist	Graphite	Poor
191	AL191	29.62629	79.74414	Graphite Schist	Graphite	Moderate
192	AL192	29.62644	79.74325	Graphite Schist	Graphite	Moderate
193	AL193	29.6254	79.74163	Graphite Schist	Graphite	Moderate
194	AL194	29.66152	79.69587	Graphite Schist	Graphite	Poor
195	AL195	29.66136	79.69615	Graphite Schist	Graphite	Poor
196	AL196	29.66125	79.69592	Graphite Schist	Graphite	Poor
197	AL197	29.66195	79.69857	Mica Schist	Graphite	High
198	AL198	29.66414	79.69949	Mica Schist	Graphite	Moderate
199	AL199	29.66413	79.69945	Mica Schist	Graphite	Moderate
200	AL200	29.65903	79.70224	Graphite Schist	Graphite	Moderate
201	AL201	29.65901	79.70213	Graphite Schist	Graphite	Moderate
202	AL202	29.65941	79.70226	Mica Schist	Graphite	Moderate
203	AL203	29.66094	79.70161	Graphite Schist	Graphite	High
204	AL204	29.66095	79.70136	Graphite Schist	Graphite	High
205	AL205	29.6611	79.7012	Graphite Schist	Graphite	Moderate
206	AL206	29.66074	79.70191	Graphite Schist	Graphite	Moderate
207	AL207	29.66031	79.69716	Graphite Schist	Graphite	High
208	AL208	29.63645	79.67185	Mica Schist	Graphite	High

SL No.	Location No.	Latitude	Longitude	Host Lithology	Surface Mineralization	Graphite Crystallinity
209	AL209	29.63984	79.671	Mica Schist	Graphite	High
210	AL210	29.63859	79.66853	Graphite Schist	Graphite	Moderate
211	AL211	29.63943	79.66769	Graphite Schist	Graphite	Moderate
212	AL212	29.64073	79.66733	Graphite Schist	Graphite	Moderate
213	AL213	29.65185	79.68423	Graphite Schist	Graphite	Moderate
214	AL214	29.64966	79.68437	Graphite Schist	Graphite	Moderate
215	AL215	29.6487	79.68301	Graphite Schist	Graphite	Poor
216	AL216	29.65204	79.68376	Graphite Schist	Graphite	Moderate
217	AL217	29.64232	79.69944	Graphite Schist	Graphite	High
218	AL218	29.64229	799.6992	Graphite Schist	Graphite	Moderate
219	AL219	29.63791	79.69949	Graphite Schist	Graphite	Moderate
220	AL220	29.63815	79.69956	Graphite Schist	Graphite	Moderate
221	AL221	29.6366	79.69699	Graphite Schist	Graphite	High
222	AL222	29.6372	79.69683	Graphite Schist	Graphite	Poor
223	AL223	29.63729	79.69681	Graphite Schist	Graphite	Poor
224	AL224	29.63755	79.69694	Graphite Schist	Graphite	Poor
225	AL225	29.63794	79.6972	Graphite Schist	Graphite	Poor
226	AL226	29.62828	79.67787	Graphite Schist	Graphite	Poor
227	AL227	29.66156	79.69597	Graphite Schist	Graphite	Moderate
228	AL228	29.66026	79.69709	Graphite Schist	Graphite	Moderate
229	AL229	29.63982	79.69748	Graphite Schist	Graphite	Moderate
230	AL230	29.62391	79.67294	Graphite Schist	Graphite	Moderate
231	AL231	29.65195	79.68377	Graphite Schist	Graphite	Moderate
232	AL232	29.65175	79.68276	Graphite Schist	Graphite	Moderate
233	AL233	29.64985	79.68151	Graphite Schist	Graphite	Moderate
234	AL234	29.64844	79.6816	Graphite Schist	Graphite	Moderate
235	AL235	29.6484	79.6822	Graphite Schist	Graphite	Moderate
236	AL236	29.64875	79.68295	Graphite Schist	Graphite	Moderate
237	AL237	29.66412	79.69985	Graphite Schist	Graphite	Moderate
238	AL238	29.63711	79.66184	Graphite Schist	Graphite	High
239	AL239	29.61947	79.72009	Graphite Schist	Graphite	Poor
240	AL240	29.6212	79.72332	Graphite Schist	Graphite	High
241	AL241	29.61926	79.7254	Graphite Schist	Graphite	Moderate
242	AL242	29.61264	79.72546	Graphite Schist	Graphite	Moderate
243	AL243	29.60396	79.73442	Graphite Schist	Graphite	High

SL No.	Location No.	Latitude	Longitude	Host Lithology	Surface Mineralization	Graphite Crystallinity
244	AL244	29.60201	79.73768	Graphite Schist	Graphite	High
245	AL245	29.61478	79.72642	Graphite Schist	Graphite	Moderate
246	AL246	29.61483	79.72584	Graphite Schist	Graphite	Moderate
247	AL247	29.61283	79.72489	Graphite Schist	Graphite	Moderate
248	AL248	29.61247	79.72477	Graphite Schist	Graphite	Moderate
249	AL249	29.61211	79.72512	Graphite Schist	Graphite	Moderate
250	AL250	29.65287	79.72907	Graphite Schist	Graphite	Moderate
251	AL251	29.65591	79.72201	Graphite Schist	Graphite	High
252	AL252	29.65565	79.72202	Graphite Schist	Graphite	High
253	AL253	29.65578	79.72021	Graphite Schist	Graphite	Moderate
254	AL254	29.65612	79.72045	Graphite Schist	Graphite	High
255	AL255	29.65141	79.68655	Graphite Schist	Graphite	Moderate
256	AL256	29.65154	79.68656	Graphite Schist	Graphite	Moderate
257	AL257	29.64996	79.68833	Graphite Schist	Graphite	Poor
258	AL258	29.65072	79.68836	Graphite Schist	Graphite	High
259	AL259	29.64927	79.68784	Graphite Schist	Graphite	High
260	AL260	29.64921	79.68781	Graphite Schist	Graphite	High
261	AL261	29.63453	79.68963	Mica Schist	Graphite	High
262	AL262	29.63444	79.6897	Graphite Schist	Graphite	Moderate
263	AL263	29.61991	79.69539	Mica Schist	Graphite	High
264	AL264	29.60328	79.74435	Graphite Schist	Graphite	Poor
265	AL265	29.62694	79.74346	Graphite Schist	Graphite	Moderate
266	AL266	29.6569	79.71657	Graphite Schist	Graphite	High
267	AL267	29.63452	79.69013	Graphite Schist	Graphite	Moderate
268	AL268	29.63498	79.6907	Graphite Schist	Graphite	Moderate
269	AL269	29.63657	79.69226	Graphite Schist	Graphite	Poor
270	AL270	29.6371	79.69311	Graphite Schist	Graphite	Poor
271	AL271	29.63717	79.69319	Graphite Schist	Graphite	Moderate
272	AL272	29.63719	79.69335	Graphite Schist	Graphite	Poor
273	AL273	29.63748	79.69346	Graphite Schist	Graphite	High
274	AL274	29.63783	79.6933	Graphite Schist	Graphite	High
275	AL275	29.63792	79.6934	Graphite Schist	Graphite	Moderate
276	AL276	29.64776	79.70478	Graphite Schist	Graphite	High
277	AL277	29.64773	79.70513	Graphite Schist	Graphite	High
278	AL278	29.64792	79.70466	Graphite Schist	Graphite	Moderate

SL No.	Location No.	Latitude	Longitude	Host Lithology	Surface Mineralization	Graphite Crystallinity
279	AL279	29.64807	79.70427	Graphite Schist	Graphite	Moderate
280	AL280	29.64767	79.70528	Graphite Schist	Graphite	Moderate
281	AL281	29.64789	79.70608	Graphite Schist	Graphite	Moderate
282	AL282	29.64808	79.70612	Graphite Schist	Graphite	Moderate
283	AL283	29.6464	79.70465	Graphite Schist	Graphite	Poor
284	AL284	29.64692	79.70422	Graphite Schist	Graphite	Poor
285	AL285	29.64615	79.70394	Graphite Schist	Graphite	Poor
286	AL286	29.64586	79.70416	Graphite Schist	Graphite	Moderate
287	AL287	29.64521	79.70432	Graphite Schist	Graphite	Moderate
288	AL288	29.64543	79.70413	Graphite Schist	Graphite	Moderate
289	AL289	29.64307	79.70644	Graphite Schist	Graphite	Moderate
290	AL290	29.64427	79.68856	Graphite Schist	Graphite	Moderate
291	AL291	29.64395	79.68793	Graphite Schist	Graphite	Poor
292	AL292	29.64386	79.68795	Graphite Schist	Graphite	Poor
293	AL293	29.64245	79.68579	Graphite Schist	Graphite	Moderate
294	AL294	29.64215	79.68517	Graphite Schist	Graphite	Moderate
295	AL295	29.64292	79.6884	Graphite Schist	Graphite	High
296	AL296	29.64444	79.68924	Graphite Schist	Graphite	Poor
297	AL297	29.64442	79.68955	Graphite Schist	Graphite	Poor
298	AL298	29.64946	79.68978	Graphite Schist	Graphite	Poor
299	AL299	29.64501	79.68895	Graphite Schist	Graphite	High
300	AL300	29.64578	79.68976	Graphite Schist	Graphite	High
301	AL301	29.64549	79.69095	Graphite Schist	Graphite	High
302	AL302	29.64549	79.69068	Graphite Schist	Graphite	High
303	AL303	29.64874	79.69473	Graphite Schist	Graphite	High
304	AL304	29.64854	79.69453	Graphite Schist	Graphite	High
305	AL305	29.64953	79.69474	Graphite Schist	Graphite	Moderate
306	AL306	29.6495	79.69467	Graphite Schist	Graphite	Moderate
307	AL307	29.64957	79.69464	Graphite Schist	Graphite	Moderate
308	AL308	29.64921	79.69463	Graphite Schist	Graphite	Moderate
309	AL309	29.64859	79.69481	Graphite Schist	Graphite	Moderate
310	AL310	29.64851	79.69465	Graphite Schist	Graphite	Moderate
311	AL311	29.64852	79.69481	Graphite Schist	Graphite	Moderate
312	AL312	29.6501	79.69597	Graphite Schist	Graphite	Moderate
313	AL313	29.65083	79.69629	Graphite Schist	Graphite	Moderate

SL No.	Location No.	Latitude	Longitude	Host Lithology	Surface Mineralization	Graphite Crystallinity
314	AL314	29.65225	79.71439	Mica Schist	Graphite	Moderate
315	AL315	29.65721	79.71701	Graphite Schist	Graphite	Poor
316	AL316	29.65715	79.71699	Graphite Schist	Graphite	Moderate
317	AL317	29.65696	79.7169	Graphite Schist	Graphite	High
318	AL318	29.65693	79.71695	Graphite Schist	Graphite	High
319	AL319	29.65582	79.71618	Graphite Schist	Graphite	Moderate
320	AL320	29.68912	79.71701	Graphite Schist	Graphite	Moderate
321	AL321	29.63992	79.71499	Graphite Schist	Graphite	Moderate
322	AL322	29.64202	79.7127	Graphite Schist	Graphite	Moderate
323	AL323	29.65096	79.71664	Graphite Schist	Graphite	Moderate
324	AL324	29.64996	79.71551	Graphite Schist	Graphite	Moderate
325	AL325	29.64954	79.71518	Graphite Schist	Graphite	Moderate
326	AL326	26.64929	79.71529	Graphite Schist	Graphite	Moderate
327	AL327	29.64905	79.71524	Graphite Schist	Graphite	Moderate
328	AL328	29.64864	79.71467	Graphite Schist	Graphite	Moderate
329	AL329	29.64853	79.71478	Graphite Schist	Graphite	Moderate
330	AL330	29.64983	79.7126	Graphite Schist	Graphite	Moderate
331	AL331	29.64844	79.71464	Graphite Schist	Graphite	Moderate
332	AL332	29.64845	79.71465	Graphite Schist	Graphite	Moderate
333	AL333	29.64857	79.71439	Graphite Schist	Graphite	Moderate
334	AL334	29.64949	79.71242	Graphite Schist	Graphite	Moderate
335	AL335	29.64932	79.71232	Graphite Schist	Graphite	Moderate
336	AL336	29.64915	79.71215	Graphite Schist	Graphite	Moderate
337	AL337	29.64895	79.7122	Graphite Schist	Graphite	Moderate
338	AL338	29.64911	79.71274	Graphite Schist	Graphite	Moderate
339	AL339	29.64911	79.71263	Graphite Schist	Graphite	Moderate
340	AL340	29.64891	79.71237	Graphite Schist	Graphite	Moderate
341	AL341	29.64877	79.71243	Graphite Schist	Graphite	Moderate
342	AL342	29.64922	79.7116	Mica Schist	Graphite	Moderate
343	AL343	29.6493	79.71135	Mica Schist	Graphite	Moderate
344	AL344	29.64954	79.71166	Graphite Schist	Graphite	Moderate
345	AL345	29.60343	79.68907	Graphite Schist	Graphite	Poor
346	AL346	29.60341	79.6891	Graphite Schist	Graphite	Poor
347	AL347	29.60316	79.68913	Graphite Schist	Graphite	Moderate
348	AL348	29.60425	79.68982	Graphite Schist	Graphite	Poor

SL No.	Location No.	Latitude	Longitude	Host Lithology	Surface Mineralization	Graphite Crystallinity
349	AL349	29.60434	79.68944	Graphite Schist	Graphite	Poor
350	AL350	29.60444	79.6871	Graphite Schist	Graphite	High
351	AL351	29.60444	79.6871	Graphite Schist	Graphite	Poor
352	AL352	29.60543	79.69115	Graphite Schist	Graphite	Poor
353	AL353	29.60607	79.69069	Graphite Schist	Graphite	Moderate
354	AL354	29.60519	79.68784	Graphite Schist	Graphite	Poor
355	AL355	29.60514	79.68748	Graphite Schist	Graphite	Poor
356	AL356	29.60485	79.68657	Graphite Schist	Graphite	Poor
357	AL357	29.60449	79.68566	Graphite Schist	Graphite	Poor
358	AL358	29.6108	79.69414	Mica Schist	Graphite	Poor
359	AL359	29.6093	79.6941	Mica Schist	Graphite	Poor
360	AL360	29.60896	79.69393	Graphite Schist	Graphite	Moderate
361	AL361	29.60674	79.69404	Graphite Schist	Graphite	Moderate
362	AL362	29.60632	79.6934	Graphite Schist	Graphite	Moderate
363	AL363	29.60596	79.69227	Graphite Schist	Graphite	High
364	AL364	29.60509	79.68932	Graphite Schist	Graphite	Moderate
365	AL365	29.60987	79.70873	Graphite Schist	Graphite	Moderate
366	AL366	29.61	79.70867	Graphite Schist	Graphite	Moderate
367	AL367	29.61068	79.70952	Graphite Schist	Graphite	Moderate
368	AL368	29.61017	79.70873	Graphite Schist	Graphite	High
369	AL369	29.61041	79.70894	Graphite Schist	Graphite	High
370	AL370	29.60911	79.70771	Graphite Schist	Graphite	Poor
371	AL371	29.60941	79.7096	Graphite Schist	Graphite	Moderate
372	AL372	29.608	79.6882	Graphite Schist	Graphite	Poor
373	AL373	29.60799	79.68834	Graphite Schist	Graphite	High
374	AL374	29.60758	79.68968	Graphite Schist	Graphite	Poor
375	AL375	29.60731	79.68989	Graphite Schist	Graphite	Poor
376	AL376	29.60749	79.68983	Graphite Schist	Graphite	Moderate
377	AL377	29.60738	79.69038	Graphite Schist	Graphite	Poor
378	AL378	29.60803	79.69104	Graphite Schist	Graphite	Poor
379	AL379	29.60781	79.69202	Graphite Schist	Graphite	Poor
380	AL380	29.65576	79.7174	Mica Schist	Graphite	Moderate
381	AL381	29.65622	79.71752	Graphite Schist	Graphite	Poor
382	AL382	29.65678	79.71779	Graphite Schist	Graphite	Moderate
383	AL383	29.65688	79.71767	Graphite Schist	Graphite	Moderate

SL No.	Location No.	Latitude	Longitude	Host Lithology	Surface Mineralization	Graphite Crystallinity
384	AL384	29.65729	79.718	Graphite Schist	Graphite	Poor
385	AL385	29.65747	79.71849	Graphite Schist	Graphite	Poor
386	AL386	29.65058	79.70738	Graphite Schist	Graphite	Poor
387	AL387	29.65057	79.70866	Graphite Schist	Graphite	Poor
388	AL388	29.6507	79.70969	Graphite Schist	Graphite	Poor
389	AL389	29.64819	79.70626	Graphite Schist	Graphite	Poor
390	AL390	29.64487	79.68838	Mica Schist	Graphite	Moderate

Annexure V_Details of Bedrock Petrography

S No	Field ID	Sample tag	Latitude	Longitude	Host Lithology	Petrographic Description
1	AL/DS- 54	109154	29.653902	79.735225	Quartzite	Mainly composed of quartz, sericite. Minor mineral- biotite. Where muscovite has grown later than biotite at some places. Quartz grain are recrystallized.
2	GSPL-Almora-24/11/336	109193	29.66094	79.701357	Graphite Schist	The sample is medium to fine grained equidimensional biotite schist; biotite (50% by volume),quartz (40% by volume),opaque (5% by volume).Few garnet porphyroblast present showing pre tectonic relationships.
3	GSPL-Almora-24/11/234	109202	29.635816	79.719848	Graphite Schist	The sample is medium to coarse grained graphite bearing quartz muscovite schist. Quartz (45% by volume), muscovite (30% by volume), feldspar (20% by volume), graphite (5% by volume). Muscovite schists are well developed and deformed in a folded pattern due to different sets of deformation. Graphite grains are generally embedded along the deformation and associated with muscovite grains. Presence of mica fish indicates about shear sense direction in ductile shear zone.
4	GSPL-Almora-24/11/271	109208	29.612148	79.714207	Graphite Schist	The sample is fine grained, equidimensional garnet bearing phyllitic rock where 2sets of foliation present. Quartz (55% by volume),Feldspar(20% by volume),muscovite(20% by volume) and opaque(5% by volume).Garnet present as porphyroblast but garnet converted into quartz and feldspar which shows retrogradation process ,garnet become unstable under decreasing temperature and pressure conditions, leading to breakdown and replacement by lower-grade minerals.
5	GSPL-Almora-24/11/275	109212	29.611678	79.729612	Mica Schist	The sample is a garnet bearing quartz-biotite-chlorite-muscovite schist with mineral proportions are quartz (30% by volume), biotite (25% by volume), chlorite (10% by volume), muscovite (25% by volume), garnet (5% by volume), opaque minerals (5% by volume). Garnet occur as porphyroblast and shows syntectonism that means garnet develops during tectonic evolution and schistosity wrapped around it. Development of biotite shows retrogradation process. Chlorite and muscovite also develop after garnet. Few magnetite present parallel to foliation. Magnetite generally occur as inclusion within garnet which means magnetite is prior to garnet.
6	GSPL-Almora-24/11/290	109218	29.636403	79.723705	Graphite Schist	The sample is medium to coarse grained quartz muscovite schist with quartz (40% by volume), muscovite (50%by volume), Opaque minerals (10% by volume) where schistosity is well developed. Small grains of graphite distributed in quartz muscovite schist where graphite occur as pre to syntectonic. Graphites are generally aligned along the foliation plane. Presence of mica fish depicts about internal deformation, bending and folding of mica grains. Apart from that few Chalcopyrite and pyrite grains are present.
7	GSPL-Almora-24/11/295	109220	29.63674	79.72085	Mica schist	The sample is medium to coarse grained garnetiferrous quartz muscovite schist with garnet (5% by volume), quartz (50% by volume), muscovite (40% by volume), opaque (5% by volume). Garnet is pre tectonic in nature and occur as porphyroblast. From the reflected microscopy analysis , the opaque minerals are deduced to be pyrite and chalcopyrite.
8	GSPL-Almora-24/11/313	109233	29.618908	79.739762	Mica schist	The sample is coarse to medium grained garnetiferous muscovite biotite schist. Garnet occur as porphyroblast. Few garnet show pre tectonic relationship which implies tectonic deformation takes place after formation of garnet. Snowball garnet shows syntectonism.
9	GSPL-Almora-24/11/321	109238	29.661252	79.695755	Graphite Schist	The sample is medium to fine grained graphite bearing quartz muscovite schist with few quartz crystals are elongated and some are equidimensional in nature. Quartz (40% by volume), muscovite (50% by volume), graphite (5% by volume), opaque (5% by volume). Muscovite showing high order interference colour with

S No	Field ID	Sample tag	Latitude	Longitude	Host Lithology	Petrographic Description
						moderate R.I Presence of quartz ribbon indicates dynamic recrystallization, commonly in ductile shear conditions with well-developed schistosity.
10	GSPL-Almora-24/11/328	109242	29.664972	79.711977	Granite Gniess	Medium- to coarse-grained rock showing well-developed gneissose texture with alternating felsic (quartz, feldspar) and mafic (biotite ± muscovite) bands. Quartz is colourless, low relief, displaying undulose extinction and occurring as elongated ribbon-like grains aligned with foliation. Feldspars (alkali and plagioclase) are colourless, showing simple and polysynthetic twinning, commonly sericitized and occur as elliptical to lens-shaped grains aligned with foliation. Biotite and muscovite are present as flaky minerals arranged parallel to foliation.
11	GSPL-Almora-24/11/349	109244	29.63859	79.668533	Graphite Schist	The sample is medium to fine grained graphite bearing quartz muscovite schist, quartz (55% by volume), muscovite (35% by volume), Graphite (10% by volume). Graphite concentrated in shear lenses along with muscovite grains. Quartz crystals are elongated like ribbon depicts about dynamic recrystallization, commonly in ductile shear conditions. Recrystallized quartz grains are present in few places.
12	GSPL-Almora-24/11/350	109245	29.63943	79.66769	Graphite Schist	The sample is medium to fine grained phyllites, quartz (50% by volume), feldspar (30% by volume), muscovite (15% by volume), opaque minerals (5% by volume). Feldspar mainly altered to sericite showing orientation due to deformation bounded by dark black grains of graphite and altered quartz rich bands with deformation signatures. Quartz vein with very fine grained quartz in the vug-filling zone , the veins is oriented in a different direction as compared to the recrystalized quartz grains (deformation)
13	GSPL-Almora-24/11/369	109250	29.635853	79.696792	Granite Gniess	The sample shows coarse to medium grained granite which is mainly a foliated(deformed) with quartz(35% by volume),feldspar(45% by volume),muscovite(10% by volume),garnet(5% by volume),opaque(5% by volume).Foliation is not very consistent. Graphic growth present within feldspar. Few veins of granite are intruded within the garnet biotite schistose rock. Garnets are present shows post tectonic relationships.
14	AL/P1/L 02	109251	29.646968	79.758927	Mica Schist	The sample is coarse to medium grained quartz muscovite schist, quartz (45% by volume), muscovite (30% by volume), kyanite (5% by volume), feldspar (15% by volume), opaque (5% by volume) muscovite grains oriented along 2 sets of deformation. Muscovite has moderate RI with higher order interference color. Muscovite schist with presence of bladed kyanite depicts about intense pressure and moderate to high temperatures under which the rock deformed.
15	GSPL-Almora-24/11/377	109252	29.628275	79.67787	Graphite Schist	The sample is coarse to medium grained phyllites with quartz(45% by volume), feldspar(30% by volume),muscovite(20% by volume),opaque(5% by volume).Schistosity is poorly developed. Bimodal distribution of grains, muscovite(larger) and quartz and feldspar(smaller in size).Under reflected microscopic analysis, opaque minerals are magnetite and pyrite.
16	GSPL-Almora-24/11/390	109253	29.654975	79.683767	Graphite Schist	The sample is coarse to medium grained graphite bearing muscovite schist. Quartz (55% by volume), muscovite (30% by volume), sillimanite (5% by volume),opaque(10% by volume).alternate coarse and fine grained band present. Muscovite develops along with graphite because presence of carbon-rich protolith under high temperature and pressure conditions. In some places muscovite is converted to sillimanite due to muscovite breakdown reaction. Under reflected light opaque minerals can be deduced to sphalerite. Sphalerite develops after than graphite.
17	GSPL-Almora-24/11/406	109254	29.60425	79.731945	Mica schist	The sample is coarse to medium grained ganetiferous quartz muscovite biotite schist. Quartz(35% by volume),muscovite(25% by volume),biotite(25% by volume),garnet(10% by volume),opaque(5% by volume). Garnet shows pre tectonic relation with biotite and muscovite. Biotite mainly forms after

S No	Field ID	Sample tag	Latitude	Longitude	Host Lithology	Petrographic Description
						muscovite during 2nd stage of deformation. Muscovite biotite schist are folded due to later deformational event.
18	GSPL-Almora-24/11/402	109255	29.619463	79.720092	Foliated Granite	The sample is medium to fine grained granitoid (foliated). This rock contains major minerals: Quartz (40% by volume), feldspar (45% by volume), mica- muscovite and biotite (10% by volume), minor minerals (epidote, garnet, apatite, opaque - 5% by volume). Large feldspar grain often shows morter texture where small feldspar grain develops around the rim of large grains. At some places, ribbon quartz along with biotite wraps around the large grain of feldspar. Feldspar represents by both orthoclase and albite. Feldspar mostly occurs as porphyries of zone grains where core part having sericitic alteration and rim without alteration. The core part shows mainly albitic laminae and rim part does not show any laminae. Besides, unzoned grains of albite and orthoclase are also found. Here, rotation of porphyroclast of feldspar grain produces sigmoidal grain and pressure-shadow zone. Here, quartz ribbon and biotite given a foliation without any gneissic banding. Therefore, this foliation could be a mylonite foliation. Also, mica fish structure indicates the ductile shear zone. Growth of epidote is generally found parallel and cross cut the biotite, which indicate syn to post deformation stage for epidote. Zoned epidote is also present. Apatite is also found in feldspar. Garnet as porphyroblast has also developed at shuttle places and biotite is forming after garnet.
19	GSPL-Almora-24/11/389	109256	29.656075	79.684382	Mica Schist	Garnet–mica schist shows a well-developed foliated under the microscope, with biotite, muscovite minerals aligned in parallel layers. The rock is mainly composed of biotite and muscovite, which appear as platy, flaky minerals giving a schistose structure. Quartz occurs as canhedral grains, often showing undulose extinction. Garnet appears as subhedral to euhedral porphyroblasts, commonly containing inclusions of quartz or mica. The overall texture reflects mineral alignment due to metamorphism under directed pressure.
20	Al/SK/04	110021	29.617	79.701	Tuffaceous Rock	Very fine-grained, fragmental felsic tuff composed of broken crystal fragments within a compact ash matrix. Quartz occurs as angular to sub-angular grains showing pyramidal, embayed and wedge-shaped forms. Feldspar is present as fine grains with partial pseudomorphic alteration. The groundmass is very fine and dominated by glassy material. Chlorite occurs as a secondary phase. Opaque minerals (magnetite) are present as disseminated grains. Overall colour is dark brown.
21		110027	29.62267	79.717522	Graphite Schist	Graphite mica schist is a foliated metamorphic rock that shows a well-developed schistose texture under thin section. It is mainly composed of fine to medium-grained platy minerals such as muscovite and biotite, along with abundant graphite, which appears as opaque black flakes. The strong foliation is defined by the parallel alignment of mica minerals, giving the rock a layered appearance. Quartz is commonly present as anhedral grains interspersed between the mica layers, often showing undulose extinction under crossed polars due to deformation.

Annexure VI_Pitting and Trenching Details

S No	SL No	Type	Latitude	Longitude	Pitting Description	Area	Rock Type	Length (in m)	Width (in m)	Depth (in m)	Volume (cubic m)
1	AL/Pit 01	Pit	29.600032	79.724657	0.35 m of surface soil, rest of part is Graphite Schist (high graphite crystallinity) and quartz vein.	Pithauni	Graphite Schist	2.06	2.03	2.17	9.074506
2	AL/Pit 02	Pit	29.659791	79.697149	0.5 m of soil, 1 m of Graphite Schist (High graphite crystallinity), 0.5 m of Mica Schist	Dinapani	Graphite Schist	2.05	2.01	2.1	8.65305
3	AL/Pit 03	Pit	29.610453	79.70908	Pyrite pits presnet in Graphite Schist, High graphite crystallinity, quartz vein	Sirar	Graphite Schist	2.35	2.27	2.1	11.20245
4	AL/Pit 04	Pit	29.610535	79.70972	Surface soil (0.4 m) and rest of Graphite Schist	Sirar	Graphite Schist	2.4	2.1	2.1	10.584
5	AL/Pit 05	Pit	29.610768	79.709548	Rock of Graphite Schist (Graphite high crystallinity, Pyrites pits) and quartz vein	Sirar	Graphite Schist	2.2	2.1	1.8	8.316
6	AL/Pit 06	Pit	29.647805	79.704923	1.5 m ofd Graphite Schist (High crystallinity of graphite) and 0.6 m of Mica Schist	Naini	Graphite Schist	2.2	1.9	2.1	8.778
7	AL/Pit 07	Pit	29.637687	79.701228	Surface part (0.2 m) of weathered Graphite Schist and Mica Schist, then 0.7m of Graphite Schist (High crystalline graphite), then rest of part is intercalted layer of Graphite Schist and Mica Schist.	Naini	Graphite Schist	2.3	2	1.9	8.74
8	AL/Pit 08	Pit	29.637896	79.701271	Surface part (0.3 m) weathered Graphite Schist, then rest of part is Graphite Schist (High graphite crystallinity with pyrite pits) and quartz vein.	Naini	Graphite Schist	2.4	2.2	1.9	10.032
9	AL/Pit 09	Pit	29.656921	79.716897	0.2 m of soil zone (highly weathered zone). Graphite Schist, quartz vein (pyrite pits and weathered pyrite), Quartz Sericite Schist and Chert like layer rock.	Debdiya	Graphite Schist	2.4	2.2	2.1	11.088
10	AL/Pit 10	Pit	29.655345	79.718097	Graphite Schist, Quartz vein (Pyrite pits and weathered pyrites)	Debdiya	Graphite Schist	2.4	2.1	1.9	9.576
11	AL/Pit 11	Pit	29.634467	79.68964	High crystalline graphite in Graphite Schist layer with highly altered (weathered) sericite schist with quartz vein.	Bintola	Graphite Schist	2.4	2.2	2.2	11.616
12	AL/Pit 12	Pit	29.644975	79.688927	0.5 m of altered sericite schist, 0.5-1.3 m of Graphite Schist (High crystalline graphite), 1.3-2.1 m of sericite schist. Highly altered sericite schist (red, yellow, blue alteration indicates presence of redox sensitive elements) with moderately weathered Graphite Schist	Gajjola	Graphite Schist with Mica Schist	2.4	2.2	2.1	11.088

S No	SL No	Type	Latitude	Longitude	Pitting Description	Area	Rock Type	Length (in m)	Width (in m)	Depth (in m)	Volume (cubic m)
13	AL/Pit 13	Pit	29.6458	79.689707	0.1 m of soil zone of pitting. Very thin threads of graphite in sericite schist throughout pitting. Very thin layer of graphite (1-4 cm thick) at 2m depth. Alteration of sericite schist with sulpher pits indicates presence of redox sensitive elements.	Gajjola	Quartz Sericite schist with quartz vein (No Graphite Schist)	2.3	2.2	2.2	11.132
14	AL/Pit 14	Pit	29.60304	79.736917	0.2 m of soil zone (highly weathered zone). In Graphite Schist, pyrite pits and weathered pyrite got with low cryastalline of graphite. Graphite Schist with intercalated layer of sericite schist.	Sironiya	Graphite Schist with quartz vein	2.1	1.9	1.8	7.182
15	AL/Pit 15	Pit	29.615107	79.726605	0.2 m of soil zone (highly weathered zone). Next 0.4 m of weathered mica schist, then 1 m of Graphite Schist layer (moderate graphite crystallinity) with quartz vein. Next, 0.4 m of yellow altered mica schist.	Bataldeon	Graphite Schist with intercalated layer of Mica Schist	2.3	2.1	2.2	10.626
16	AL/Pit 16	Pit	29.629902	79.675958	0.2 m of soil zone (highly weathered zone). Rest of part is granite with black elongated mineral contact with granite with felsic and mafic layer.	Jakheta	Granite	2.15	1.9	2.1	8.5785
17	AL/Pit 17	Pit	29.636193	79.69831	0-1 m of soil zone (highly weathered zone). Next rest of the part is deformed granite with intercalated layer of quartz biotite sericite schist.	Bintola	Deformed Granite	2.3	2.1	2.4	11.592
18	AL/Pit 18	Pit	29.640091	79.667015	Weathered Graphite Schist bed with presence of sulpher. Quartz vein from Graphite Schist also contained sulpher.	Mat	Graphite Schist	2.2	2.1	2.15	9.933
19	AL/Pit 19	Pit	29.641397	79.665528	0.3 m of soil zone of graphite schist. Then 1 m of graphite schist (consists of moderate crystallinity graphite with quartz vein). Next 1 m of graphite schist (contain graphite flakes with quartz vein and some white flaky minerals)	Mat	Graphite Schist	2.2	2.15	2.3	10.879
20	AL/Pit 20	Pit	29.672352	79.702942	0.5 m of soil zone. Then after hard rocks are found with intruded quartz vein .	Saura	Tourmaline rich Foliated Granites	2.1	2.25	2.05	9.68625
21	AL/Pit 21	Pit	29.601433	79.729225	Weathered Graphite Schist bed with presence of sulpher. Quartz vein was found from Graphite Schist.	Pithuani	Graphite Schist with Quartz vein	2.1	2.3	2.15	10.3845
22	AL/Pit 22	Pit	29.601277	79.729614	From the soil after 1m of depth found Black soil then Hard rock are found.	Udal	Mica Schist	2.1	2.05	1	4.305
23	AL/ Pit 23	Pit	29.601276	79.729128	From the surface Mica Schist are found at depth of 1m.after that black hard rock are found.	Pithuani	Mica Schist	2.1	2.2	2	9.24
24	AL/ Pit 24	Pit	29.63792	79.722147	Graphite found in Graphite Schist from surface (0 m) to 2 m depth. Next 0.4 m depth, altered mica schist was found. Folded elongated quartz vein was found in Graphite Schist.	Deora	Graphite Schist	2.3	2.2	2.4	12.144

S No	SL No	Type	Latitude	Longitude	Pitting Description	Area	Rock Type	Length (in m)	Width (in m)	Depth (in m)	Volume (cubic m)
25	AL/ Trench 01	Trench	29.601307	79.729308	From the surface found Graphite Schist with quartz vein. In some zone, sulphur was found. At 1.2 m depth, there is found hard Graphite Schist which sounded like metals.	Pithauni	Graphite Schist	7.2	2.1	2.1	31.752
26	AL/ Trench 02	Trench	29.63749	79.701315	From the surface HCHS zone found (Graphite Schist). The found thin layer of graphite after that Mica Schist found. And Quartz vein found.	Naini	Mica Schist intercalation with Graphite Schist	6.1	2.2	2.25	30.195
27	AL/ Trench 03	Trench	29.636647	79.72594	From the surface found mica schist zone, at the 2.3 m depth get sharp contact with graphite schist, where graphite is high crystalline and flaky	Digoli	Mica Schist	5.2	3	2.9	45.24
28	AL/ Trench 04	Trench	29.621512	79.715658	From the surface found soil mixed with mica schist zone, not get any traces of graphitic layer.	Bataldeon	Mica Schist	6.4	2.2	2.1	29.568
29	AL/ Trench 05	Trench	29.614975	79.714587	From the surface found soil mixed with graphitic layer, contain moderate to high grade of graphite crystalline.	Sirar	Graphite Schist	7.1	2.2	2.4	37.488
30	AL/ Trench 06	Trench	29.625869	79.74209	From the surface found graphitic layer, contain high grade of graphite crystalline and flakes.	Udalgaon	Graphite Schist	7.3	2.3	2.5	41.975
Total											**450.65**

Annexure VII_XRF Data for Surface Samples with 2 Additional Elements Sn, W: (All data in %)

S No	Sample ID	Latitude	Longitude	Lithology	Type	Al_2O_3	BaO	CaO	Cr_2O_3	Fe_2O_3	K_2O	MgO	MnO	Na_2O	P_2O_5	TiO_2	SiO_2	LOI	SO_3	V_2O_5	SnO_2	WO_3
1	109151	29.643591	79.662716	Mica Schist	Bedrock	13.8	0.01	1.53	0.01	5.49	2.49	2.45	0.09	2.41	0.2	0.84	69.12	1.36	0.02	-	-	-
2	109152	29.600117	79.724477	Graphite Schist	Bedrock	7.43	0.27	0.2	0.03	1.74	1.11	0.42	<0.01	0.29	0.17	0.31	80.96	6.71	0.03	-	-	-
3	109153	29.620363	79.719983	Mica Schist	Bedrock	15.88	0.03	2.83	<0.01	4.31	3.4	1.41	0.07	2.8	0.16	0.57	67.52	0.81	0.02	-	-	-
4	109154	29.653902	79.735225	Mica Schist	Bedrock	6.06	<0.01	0.15	<0.01	0.88	1.71	0.15	<0.01	0.81	0.07	0.31	88.88	0.75	0.02	-	-	-
5	109155	29.620448	79.695019	Mica Schist	Bedrock	0.91	<0.01	0.12	0.01	0.26	0.1	<0.01	<0.01	<0.01	0.07	<0.01	98.15	0.23	0.02	-	-	-
6	109156	29.635672	79.726995	Graphite Schist	Bedrock	14.3	0.04	0.13	0.01	1.03	4.07	1.11	<0.01	0.26	0.08	0.85	75.35	2.44	0.07	-	-	-
7	109157	29.641098	79.715909	Graphite Schist	Bedrock	12.03	0.02	1.17	<0.01	4.11	1.95	1.39	<0.01	2.69	0.18	0.73	74.62	0.83	0.02	-	-	-
8	109158	29.618382	79.725446	Mica Schist	Bedrock	11.5	0.03	0.13	0.01	6.46	3.13	0.75	<0.01	0.23	0.22	1.05	73.76	2.53	0.03	-	-	-
9	109159	29.639632	79.717638	Mica Schist	Bedrock	7.4	<0.01	0.41	0.01	2.4	0.49	0.69	<0.01	2.62	0.11	0.43	84	1.23	0.02	-	-	-
10	109160	29.603156	79.688851	Foliated Granite	Bedrock	16.2	0.05	1.72	<0.01	4	2.98	1.16	0.08	2.67	0.14	0.53	67.82	2.48	0.02	-	-	-
11	109177	29.620152	79.722328	Mica Schist	Stream sediment (<-125 micron)	9.06	0.08	1.48	<0.05	3.81	1.76	0.84	0.06	1.93	0.1	1.17	75.76	3.6	0.15	<0.05	<0.05	<0.05
12	109181	29.638534	79.686488	Tuffaceous Rock	Stream sediment (<-125 micron)	9.95	0.13	1.11	<0.05	4.61	1.74	0.93	0.06	1.92	0.11	1.18	71.37	6.35	0.2	<0.05	<0.05	<0.05
13	109183	29.6385	79.714892	Mica Schist	Stream sediment (<-125 micron)	12.52	0.16	1.52	<0.05	5.76	2.3	1.44	0.16	2.11	0.25	0.94	62.54	9.84	0.23	<0.05	<0.05	<0.05
14	109185	29.636802	79.720817	Mica Schist	Stream sediment (<-125 micron)	13.1	0.14	1.55	<0.05	5.2	2.1	1.45	0.09	2.34	0.23	0.97	64.94	7.46	0.22	<0.05	<0.05	<0.05
15	109201	29.631603	79.715032	Quartz Vain	Bedrock	2.698	<0.01	0.323	0.027	0.78228	0.13	0.153	<0.01	0.423	0.098	<0.01	94.83	0.43	0.047	<0.01	<0.01	0.011
16	109202	29.635816	79.719848	Mica Schist	Bedrock	13.5299	0.023	0.171	0.015	0.44096	3.812	1.056	<0.01	0.408	0.102	0.873	76.642	2.71	0.048	<0.01	0.011	<0.01
17	109203	29.635672	79.726995	Graphite Schist	Bedrock	13.7883	0.013	0.135	0.011	1.65784	3.95	1.094	<0.01	0.262	0.091	0.79	75.398	2.56	0.06	<0.01	<0.01	<0.01
18	109204	29.635105	79.714393	Mica Schist	Bedrock	7.83275	0.466	0.142	0.032	4.9237	2.001	0.522	<0.01	0.087	0.148	0.417	77.358	5.71	0.043	0.093	<0.01	<0.01
19	109205	29.641709	79.714861	Mica Schist	Bedrock	15.1297	0.114	1.312	<0.01	5.92752	3.971	2.485	0.015	1.385	0.182	0.975	67.76	0.31	0.065	<0.01	0.013	<0.01

S No	Sample ID	Latitude	Longitude	Lithology	Type	Al_2O_3	BaO	CaO	Cr_2O_3	Fe_2O_3	K_2O	MgO	MnO	Na_2O	P_2O_5	TiO_2	SiO_2	LOI	SO_3	V_2O_5	SnO_2	WO_3
20	109206	29.623	79.723	Graphite Schist	Bedrock	7.7197	<0.01	0.151	<0.01	47	2.092	0.366	0.056	0.175	0.849	0.322	27.865	13.4	0.037	<0.01	<0.01	<0.01
21	109207	29.616348	79.717888	Mica Schist	Bedrock	13.7551	0.197	0.808	<0.01	4.0545	2.258	2.229	0.125	2.52	0.105	0.628	68.911	4.06	0.054	0.023	<0.01	<0.01
22	109208	29.612148	79.714207	Graphite Schist	Bedrock	4.5752	<0.01	2.493	0.016	0.93704	0.902	0.329	<0.01	0.063	0.099	0.108	85.593	4.5	0.116	<0.01	<0.01	<0.01
23	109209	29.612148	79.714207	Graphite Schist	Bedrock	10.5042	0.03	0.172	0.012	0.61162	2.068	0.866	<0.01	0.652	0.097	0.324	82.214	2.31	0.065	<0.01	<0.01	<0.01
24	109210	29.611528	79.715905	Graphite Schist	Bedrock	11.6784	0.045	0.195	0.033	2.53658	3.02	0.728	<0.01	0.493	0.123	0.582	74.821	5.57	0.06	0.059	<0.01	<0.01
25	109211	29.613433	79.728892	Mica Schist	Bedrock	11.5995	<0.01	1.18	<0.01	5.4007	2.001	1.648	0.082	2.332	0.211	1.04	72.65	1.41	0.053	<0.01	<0.01	<0.01
26	109212	29.611678	79.729612	Mica Schist	Bedrock	11.2186	0.01	0.989	0.01	5.49928	2.4	1.761	0.085	1.502	0.207	0.775	74.005	1.08	0.047	<0.01	0.014	<0.01
27	109213	29.611263	79.727305	Mica Schist	Bedrock	18.0643	0.031	0.578	0.012	8.12172	3.812	3.76	0.085	1.536	0.194	1.018	58.342	4.1	0.05	0.013	0.01	<0.01
28	109214	29.612963	79.724822	Graphite Schist	Bedrock	4.8469	<0.01	0.132	0.05	1.42358	1.183	0.259	<0.01	0.052	0.106	0.188	87.167	4.18	0.045	0.135	0.011	<0.01
29	109215	29.637335	79.660615	Mica Schist	Bedrock	24.9014	1.015	0.563	0.01	7.1868	7.656	5.217	0.035	0.995	0.179	1.145	46.421	4.2	0.06	0.029	<0.01	<0.01
30	109216	29.641695	79.657337	Mica Schist	Bedrock	6.0192	<0.01	0.146	0.053	2.3426	1.472	0.353	<0.01	0.054	0.138	0.26	81.559	7.13	0.046	0.158	<0.01	<0.01
31	109217	29.637492	79.722783	Graphite Schist	Bedrock	12.9989	0.02	0.131	0.014	1.24762	3.856	0.938	<0.01	0.199	0.09	0.873	76.783	2.57	0.05	0.011	<0.01	<0.01
32	109218	29.636403	79.723705	Graphite Schist	Bedrock	9.8192	0.401	5.582	0.036	8.39732	2.567	1.078	0.039	0.397	0.136	0.285	58.597	8	4.028	0.14	<0.01	<0.01
33	109219	29.636173	79.719654	Quartz vein	Bedrock	1.4706	<0.01	0.16	0.024	0.52788	0.079	0.039	<0.01	0.074	0.073	<0.01	97.382	0.13	0.05	<0.01	0.012	0.012
34	109220	29.63674	79.72085	Mica Schist	Bedrock	10.0102	<0.01	1.402	<0.01	4.70534	1.305	1.244	0.052	2.081	0.198	0.818	77.033	0.62	0.064	<0.01	<0.01	<0.01
35	109221	29.641847	79.745487	Mica Schist	Bedrock	13.3903	<0.01	1.7	0.012	5.81728	1.863	1.906	0.089	3.082	0.189	0.837	69.495	1.39	0.063	<0.01	<0.01	<0.01
36	109222	29.638098	79.738217	Mica Schist	Bedrock	12.3291	<0.01	1.734	<0.01	4.80392	0.71	1.744	0.085	2.56	0.19	0.698	72.764	2.08	0.056	<0.01	<0.01	<0.01
37	109223	29.636631	79.735417	Mica Schist	Bedrock	11.2376	<0.01	1.143	<0.01	4.08418	1.812	1.451	0.058	2.218	0.175	0.662	75.992	0.73	0.054	<0.01	<0.01	<0.01
38	109224	29.631472	79.729667	Mica Schist	Bedrock	11.8769	<0.01	0.906	<0.01	4.0121	1.898	1.378	0.041	1.994	0.155	0.612	75.493	1.33	0.055	<0.01	<0.01	<0.01
39	109225	29.626942	79.742592	Mica Schist	Bedrock	11.0181	0.23	1.128	<0.01	4.89826	1.843	1.533	0.049	2.46	0.212	0.869	74.081	1.25	0.047	<0.01	<0.01	<0.01
40	109226	29.625837	79.744223	Mica Schist	Bedrock	13.1262	0.456	0.886	<0.01	4.70958	2.605	1.721	0.041	2.026	0.184	0.68	70.563	2.53	0.046	<0.01	<0.01	<0.01
41	109227	29.626358	79.745898	Graphite Schist	Bedrock	10.9896	0.635	1.092	0.01	1.73734	1.507	0.594	<0.01	2.312	0.103	0.678	64.808	15.1	0.059	0.047	<0.01	<0.01
42	109228	29.627081	79.745878	Graphite Schist	Bedrock	10.4282	2.697	0.271	0.015	2.8514	2.871	0.935	<0.01	0.195	0.138	0.687	64.604	13.7	0.192	0.165	<0.01	<0.01
43	109229	29.626294	79.744137	Graphite Schist	Bedrock	12.046	2.352	1.137	0.018	3.1376	2.367	1.272	0.014	1.601	0.109	0.855	67.694	7	0.291	0.041	<0.01	<0.01
44	109230	29.626436	79.743254	Graphite Schist	Bedrock	12.0308	2.794	0.755	0.019	7.20906	2.796	1.32	<0.01	0.322	0.179	0.861	58.471	12.7	0.042	0.135	<0.01	<0.01

S No	Sample ID	Latitude	Longitude	Lithology	Type	Al_2O_3	BaO	CaO	Cr_2O_3	Fe_2O_3	K_2O	MgO	MnO	Na_2O	P_2O_5	TiO_2	SiO_2	LOI	SO_3	V_2O_5	SnO_2	WO_3
45	109231	29.625402	79.741634	Graphite Schist	Bedrock	19.1881	0.83	0.763	<0.01	4.66294	2.11	1.731	0.024	1.159	0.166	1.384	47.728	20.1	0.039	0.023	<0.01	<0.01
46	109232	29.623181	79.74268	Mica Schist	Bedrock	12.1657	0.506	0.161	0.012	5.61588	2.878	0.681	<0.01	0.271	0.126	0.713	71.901	4.58	0.135	0.064	<0.01	<0.01
47	109233	29.618908	79.739762	Mica Schist	Bedrock	10.5935	<0.01	1.245	<0.01	4.56966	1.618	1.339	0.051	2.499	0.187	0.842	76.054	0.6	0.047	<0.01	0.01	<0.01
48	109234	29.61728	79.73842	Mica Schist	Bedrock	10.925	<0.01	0.864	<0.01	3.95062	2.1	1.331	0.062	1.934	0.168	0.64	76.81	0.88	0.057	<0.01	<0.01	<0.01
49	109235	29.597559	79.744998	Mica Schist	Bedrock	26.2067	0.138	0.797	0.012	8.9464	7.17	3.934	0.114	1.407	0.196	1.186	45.679	3.96	0.054	0.019	<0.01	<0.01
50	109236	29.598399	79.746705	Mica Schist	Bedrock	27.0323	0.127	0.18	0.011	6.78188	6.15	1.477	0.011	0.946	0.178	1.34	48.507	6.87	0.055	0.056	<0.01	<0.01
51	109237	29.661522	79.69587	Graphite Schist	Bedrock	11.3421	1.945	0.167	0.046	0.79606	2.412	1.931	<0.01	0.156	0.097	0.589	68.936	11	0.063	0.195	<0.01	<0.01
52	109238	29.661193	79.695755	Mica Schist	Bedrock	11.9149	<0.01	1.049	0.012	1.02078	1.533	0.574	<0.01	2.546	0.097	0.889	78.639	1.43	0.071	<0.01	<0.01	<0.01
53	109239	29.661952	79.698568	Mica Schist	Bedrock	12.2332	0.212	0.387	0.022	17.5398	3.328	1.02	<0.01	0.708	0.349	0.723	53.401	10	0.069	0.04	<0.01	<0.01
54	109240	29.664125	79.699451	Mica Schist	Bedrock	16.4398	0.791	0.167	0.015	3.5457	3.706	1.326	<0.01	0.308	0.147	1.143	58.892	13.2	0.045	0.047	<0.01	<0.01
55	109241	29.66583	79.706938	Mica Schist	Bedrock	4.3776	<0.01	0.296	0.015	1.10558	0.497	0.123	<0.01	0.534	0.087	0.085	91.93	0.73	0.049	<0.01	0.011	<0.01
56	109242	29.667667	79.711977	Quartzite	Bedrock	14.7336	<0.01	0.456	<0.01	0.8904	4.882	0.17	<0.01	3.052	0.259	0.032	74.234	0.94	0.05	<0.01	0.01	<0.01
57	109243	29.659875	79.700982	Mica Schist	Bedrock	13.4872	<0.01	2.047	<0.01	5.7399	1.328	1.673	0.07	3.104	0.216	0.763	68.758	2.73	0.05	<0.01	<0.01	<0.01
58	109244	29.63859	79.668533	Graphite Schist	Bedrock	6.78585	0.288	0.138	0.068	0.92114	1.549	0.485	<0.01	0.077	0.093	0.263	83.765	4.89	0.049	0.361	<0.01	<0.01
59	109245	29.63943	79.66769	Graphite Schist	Bedrock	6.19875	0.236	0.154	0.042	2.22176	1.444	0.462	<0.01	0.094	0.141	0.219	81.286	6.91	0.046	0.242	<0.01	<0.01
60	109246	29.654743	79.683657	Quartz vein	Bedrock	13.035	<0.01	1.485	<0.01	3.88914	1.794	1.4	0.021	2.998	0.154	0.403	73.632	1.03	0.051	<0.01	0.011	<0.01
61	109247	29.648703	79.683013	Graphite Schist	Bedrock	3.7221	<0.01	0.14	0.027	0.7632	0.587	0.176	<0.01	0.04	0.109	0.062	92.239	1.93	0.053	0.014	<0.01	<0.01
62	109248	29.642723	79.698558	Mica Schist	Bedrock	11.0561	<0.01	0.784	0.012	5.1198	0.674	1.769	0.022	2.433	0.109	0.519	75.521	1.62	0.056	<0.01	<0.01	<0.01
63	109249	29.642317	79.699435	Graphite Schist	Bedrock	15.353	0.027	0.136	0.021	0.636	3.87	1.017	<0.01	0.277	0.086	0.698	73.783	3.8	0.052	0.026	<0.01	<0.01
64	109250	29.635853	79.696792	Foliated Granite	Bedrock	14.4534	<0.01	0.649	<0.01	1.88574	4.196	0.355	0.023	3.038	0.257	0.211	73.283	1.27	0.047	<0.01	<0.01	<0.01
65	109258	29.636306	79.681662	Mica Schist	Stream sediment (<-125 micron)	8.83	0.09	0.88	<0.05	3	1.44	0.66	<0.05	1.86	0.07	1.24	79.02	2.39	0.15	<0.05	<0.05	<0.05
66	109260	29.642837	79.682194	Mica Schist	Stream sediment (<-125 micron)	14.01	0.3	1.29	<0.05	6.67	2.34	1.87	0.12	2.22	0.2	1.04	60.1	9.31	0.36	<0.05	<0.05	<0.05
67	109266	29.637122	79.688612	Mica Schist	Stream sediment (<-125 micron)	13.21	0.12	1.19	<0.05	4.79	2.27	1.49	<0.05	2.13	0.11	1.12	65.3	7.95	0.12	<0.05	<0.05	<0.05

S No	Sample ID	Latitude	Longitude	Lithology	Type	Al_2O_3	BaO	CaO	Cr_2O_3	Fe_2O_3	K_2O	MgO	MnO	Na_2O	P_2O_5	TiO_2	SiO_2	LOI	SO_3	V_2O_5	SnO_2	WO_3
68	109268	29.621075	79.71979	Mica Schist	Stream sediment (<-125 micron)	18.47	0.09	0.89	<0.05	8.15	3.14	1.91	0.12	2.15	0.15	1.22	54.87	8.37	0.13	<0.05	<0.05	<0.05
69	109270	29.619697	79.719138	Mica Schist	Stream sediment (<-125 micron)	14.28	0.15	1.21	<0.05	5.25	2.62	1.59	0.08	2.48	0.13	1.04	64.2	6.5	0.22	<0.05	<0.05	<0.05
70	109272	29.638278	79.670908	Mica Schist	Stream sediment (<-125 micron)	11.53	0.11	0.94	<0.05	5.24	1.77	1.28	0.07	2.19	0.14	1.43	68.22	6.71	0.16	<0.05	<0.05	<0.05
71	109283	29.647	79.678	Foliated Granite	Bed rock	15.55	<0.05	0.45	<0.05	1.95	4.39	0.32	0.12	2.8	0.21	0.11	72.01	1.83	0.05	<0.05	<0.05	<0.05
72	109284	29.621313	79.696377	Quartz vein	Bed rock	0.11	<0.05	<0.05	<0.05	0.38	<0.05	<0.05	<0.05	<0.05	<0.05	<0.05	99.07	0.24	0.06	<0.05	<0.05	<0.05
73	109285	29.601425	79.707417	Mica Schist	Bed rock	11.23	<0.05	1.08	<0.05	4.06	1.74	1.33	0.07	2.54	0.11	0.58	75.77	1.16	0.2	<0.05	<0.05	<0.05
74	109286	29.597598	79.725015	Mica Schist	Bed rock	16.36	<0.05	3.59	<0.05	7.1	1.07	2.03	0.19	3.11	0.14	0.74	63.41	1.86	0.13	<0.05	<0.05	<0.05
75	109287	29.597598	79.725015	Quartz vein	Bed rock	0.21	<0.05	<0.05	<0.05	0.41	<0.05	<0.05	<0.05	0.08	<0.05	<0.05	98.83	0.17	0.06	<0.05	<0.05	<0.05
76	109288	29.609	79.749	Mica Schist	Bed rock	9.38	<0.05	1.69	<0.05	5.29	2.26	1.5	0.1	3	0.15	0.87	74.53	0.87	<0.05	<0.05	<0.05	<0.05
77	109289	29.615	79.726	Graphite Schist	Bed rock	15.17	0.12	<0.05	0.05	2.42	4.64	1.25	<0.05	0.29	<0.05	0.91	71.01	3.68	0.06	<0.05	<0.05	<0.05
78	109290	29.605	79.749	Mica Schist	Bed rock	10.04	<0.05	0.07	<0.05	0.92	2.64	0.82	<0.05	0.28	<0.05	0.52	81.94	2.34	0.07	<0.05	<0.05	<0.05
79	109291	29.607435	79.737102	Mica Schist	Bed rock	12.43	<0.05	0.94	<0.05	5.58	2.69	1.82	0.07	2.23	0.13	0.76	71.81	1.29	0.05	<0.05	<0.05	<0.05
80	109292	29.606313	79.737987	Mica Schist	Bed rock	10.17	<0.05	1.18	<0.05	5.94	1.58	1.5	0.12	2.17	0.15	1.39	74.7	0.88	0.11	<0.05	<0.05	<0.05
81	109293	29.606313	79.737987	Mica Schist	Bed rock	3.08	<0.05	0.79	<0.05	1.57	0.43	0.29	<0.05	0.76	0.08	0.11	91.94	0.66	0.07	<0.05	<0.05	<0.05
82	109294	29.638907	79.686535	Mica Schist	Bed rock	16.07	<0.05	1.53	<0.05	4.11	2.14	1.39	<0.05	3.24	0.06	0.68	68.9	1.54	0.06	<0.05	<0.05	<0.05
83	109295	29.621	79.677	Mica Schist	Bed rock	5.54	<0.05	0.38	<0.05	1.31	1.69	0.27	<0.05	0.31	<0.05	0.33	88.84	0.93	<0.05	<0.05	<0.05	<0.05
84	109296	29.636412	79.692355	Foliated Granite	Bed rock	14.29	<0.05	0.55	<0.05	2.27	3.92	0.42	0.06	3.09	0.22	0.28	73.1	1.46	<0.05	<0.05	<0.05	<0.05
85	109297	29.637472	79.693755	Graphite Schist	Bed rock	1.67	<0.05	<0.05	<0.05	0.48	0.23	0.08	<0.05	0.06	<0.05	<0.05	96.36	0.88	0.07	<0.05	<0.05	<0.05
86	109298	29.637923	79.693398	Graphite Schist	Bed rock	13.64	0.06	<0.05	<0.05	1.67	4.08	0.97	<0.05	0.25	<0.05	0.69	75.11	3.12	0.05	<0.05	<0.05	<0.05
87	109299	29.642495	79.685752	Mica Schist	Bed rock	12.55	0.3	0.59	<0.05	2.86	2.26	1.38	<0.05	1.91	<0.05	0.51	72.25	4.99	0.06	<0.05	<0.05	<0.05
88	109300	29.64578	79.68976	Graphite Schist	Bed rock	11.21	0.14	0.36	<0.05	1.16	1.98	0.59	<0.05	1.35	<0.05	0.65	79.39	2.81	0.09	<0.05	<0.05	<0.05
89	109851	29.650097	79.69597	Quartz vein	Bed rock	0.12	<0.05	<0.05	<0.05	0.15	<0.05	<0.05	<0.05	<0.05	<0.05	<0.05	99.39	0.22	<0.05	<0.05	<0.05	<0.05

S No	Sample ID	Latitude	Longitude	Lithology	Type	Al_2O_3	BaO	CaO	Cr_2O_3	Fe_2O_3	K_2O	MgO	MnO	Na_2O	P_2O_5	TiO_2	SiO_2	LOI	SO_3	V_2O_5	SnO_2	WO_3
90	109852	29.658505	79.717097	Foliated Granite	Bed rock	14.7	<0.05	0.57	<0.05	2.19	4.88	0.45	<0.05	2.79	0.19	0.27	72.42	1.24	<0.05	<0.05	<0.05	<0.05
91	109853	29.628275	79.67787	Tuffaceous Rock	Bed rock	28.55	0.1	4.62	<0.05	2.2	1.12	0.88	0.07	1.52	0.23	1.31	47.06	11.1	<0.05	<0.05	<0.05	<0.05
92	109854	29.628275	79.67787	Tuffaceous Rock	Bed rock	28.98	0.34	1.19	<0.05	2.09	9.02	1.01	0.06	0.63	0.11	1.38	50.26	4.56	<0.05	<0.05	<0.05	<0.05
93	109855	29.628275	79.67787	Tuffaceous Rock	Bed rock	21.04	0.12	0.76	<0.05	1.94	6.1	0.76	<0.05	0.3	0.08	1	64.31	3.22	<0.05	<0.05	<0.05	<0.05
94	109856	29.629923	79.675737	Tuffaceous Rock	Bed rock	15.4	0.08	1.55	<0.05	5	4.47	1.24	<0.05	0.85	0.07	0.81	67.81	2.16	0.29	<0.05	<0.05	<0.05
95	109857	29.623908	79.672935	Graphite Schist	Bed rock	9.9	0.06	0.13	<0.05	2.04	3.07	0.56	<0.05	1.27	<0.05	1.22	79.81	1.59	0.05	<0.05	<0.05	<0.05
96	109858	29.637112	79.661835	Graphite Schist	Bed rock	13.16	1.16	0.13	0.09	0.38	4.74	1.37	<0.05	0.25	<0.05	0.89	67.21	9.73	<0.05	0.55	<0.05	<0.05
97	109859	29.652869	79.729068	Graphite Schist	Bed rock	2.58	0.09	0.07	<0.05	8.11	0.46	0.17	0.09	0.18	0.3	0.07	84.35	3.26	0.07	<0.05	<0.05	<0.05
98	109860	29.611993	79.732298	Mica Schist	Bed rock	10.59	<0.05	1.1	<0.05	5.01	1.95	1.52	0.06	2.36	0.12	0.75	75.2	0.93	0.23	<0.05	<0.05	<0.05
99	109861	29.630522	79.677053	Tuffaceous Rock	Bed rock	18.22	0.15	0.88	<0.05	2.04	7.46	0.66	0.05	0.94	0.06	0.94	66.43	1.89	<0.05	<0.05	<0.05	<0.05
100	109862	29.656	79.689	Mica Schist	Bed rock	18.37	0.07	0.07	<0.05	3.31	4.76	0.92	0.06	0.74	<0.05	0.73	68.02	2.63	0.06	<0.05	<0.05	<0.05
101	109863	29.619907	79.695393	Mica Schist	Bed rock	15.16	0.08	0.47	<0.05	3.32	4.02	0.96	<0.05	0.97	0.06	0.78	67.84	5.3	0.87	<0.05	<0.05	<0.05
102	109864	29.620875	79.69405	Mica Schist	Bed rock	1.09	<0.05	0.11	<0.05	0.39	0.32	<0.05	<0.05	0.09	<0.05	<0.05	97.62	0.23	0.08	<0.05	<0.05	<0.05
103	109865	29.62141	79.69242	Quartzite	Bed rock	4.02	<0.05	0.23	<0.05	0.65	1.56	0.13	<0.05	0.82	<0.05	0.1	91.64	0.53	<0.05	<0.05	<0.05	<0.05
104	109866	29.621622	79.696343	Mica Schist	Bed rock	<0.05	<0.05	0.13	<0.05	0.21	0.05	<0.05	<0.05	<0.05	<0.05	<0.05	99.18	0.31	0.06	<0.05	<0.05	<0.05
105	109867	29.637171	79.693191	Graphite Schist	Bed rock	1.48	<0.05	0.2	<0.05	0.56	0.42	0.08	<0.05	0.05	0.06	<0.05	95.5	1.31	0.09	<0.05	<0.05	<0.05
106	109868	29.64437	79.688287	Graphite Schist	Bed rock	10.05	0.11	0.94	<0.05	3.94	2.18	1.19	<0.05	1.49	0.1	0.65	76.41	2.7	<0.05	<0.05	<0.05	<0.05
107	109869	29.657213	79.71701	Mica Schist	Bed rock	11.92	0.61	0.49	<0.05	3.07	2.44	1.22	<0.05	1.66	0.05	0.48	72.99	4.78	<0.05	<0.05	<0.05	<0.05
108	109870	29.640515	79.712177	Foliated Granite	Bed rock	15.72	<0.05	3.65	<0.05	5.15	3.04	1.63	0.08	2.94	0.14	0.6	65.1	1.63	0.05	<0.05	<0.05	<0.05
109	109871	29.640102	79.71312	Foliated Granite	Bed rock	14.96	<0.05	2.28	<0.05	3.89	3.57	1.1	0.06	2.72	0.15	0.49	68.97	1.52	<0.05	<0.05	<0.05	<0.05
110	109872	29.641398	79.712388	Foliated Granite	Bed rock	14.14	<0.05	0.93	<0.05	1.62	2.94	0.33	0.05	2.48	0.23	0.21	74.85	1.86	<0.05	<0.05	<0.05	<0.05
111	109873	29.639364	79.715226	Graphite Schist	Bed rock	3.82	<0.05	0.46	<0.05	63.58	0.39	0.82	4.86	0.15	0.42	0.15	25.22	<0.1	0.15	<0.05	<0.05	<0.05
112	109874	29.618382	79.725446	Graphite Schist	Bed rock	5.14	<0.05	0.17	<0.05	1.87	1.44	0.37	<0.05	0.11	0.08	0.36	86.72	3.22	<0.05	0.08	<0.05	<0.05
113	109875	29.631603	79.715032	Mica Schist	Bed rock	0.61	<0.05	0.13	<0.05	0.48	<0.05	<0.05	<0.05	<0.05	<0.05	<0.05	98.27	0.34	0.11	<0.05	<0.05	<0.05
114	109876	29.637335	79.660615	Mica Schist	Bed rock	17.6	0.57	0.72	<0.05	5.08	3.87	3.17	<0.05	1.42	0.13	0.68	60.02	6.34	0.05	0.05	<0.05	<0.05

S No	Sample ID	Latitude	Longitude	Lithology	Type	Al_2O_3	BaO	CaO	Cr_2O_3	Fe_2O_3	K_2O	MgO	MnO	Na_2O	P_2O_5	TiO_2	SiO_2	LOI	SO_3	V_2O_5	SnO_2	WO_3
115	109877	29.641695	79.657337	Mica Schist	Bed rock	5.49	<0.05	1.06	<0.05	1.36	0.94	0.44	<0.05	0.76	<0.05	0.19	87.88	1.5	0.05	<0.05	<0.05	<0.05
116	109878	29.649655	79.684368	Graphite Schist	Bed rock	7.39	0.34	0.17	0.05	1.04	1.16	0.51	<0.05	0.3	<0.05	0.29	83.2	5.03	0.12	0.13	<0.05	<0.05
117	109879	29.636403	79.723705	Graphite Schist	Bed rock	6.13	0.27	0.45	<0.05	3.05	1.3	0.45	<0.05	0.47	0.05	0.18	80.07	5.41	1.89	0.1	<0.05	<0.05
118	109880	29.613047	79.726045	Graphite Schist	Bed rock	7.82	0.06	0.15	0.07	0.76	1.96	0.55	<0.05	0.16	<0.05	0.38	84.15	3.48	0.2	<0.05	<0.05	<0.05
119	109881	29.635199	79.715345	Graphite Schist	Bed rock	13.97	0.64	0.16	<0.05	1.47	3.82	1.32	<0.05	0.39	<0.05	0.52	71.37	5.79	0.08	0.12	<0.05	<0.05
120	109882	29.630883	79.714322	Mica Schist	Bed rock	25.05	0.17	0.22	<0.05	5.7	8.91	1.69	<0.05	0.19	<0.05	1.24	41.84	14.5	<0.05	<0.05	<0.05	<0.05
121	109883	29.615068	79.725232	Graphite Schist	Bed rock	4.96	<0.05	0.14	0.08	2.19	1.48	0.34	<0.05	0.1	<0.05	0.26	84.62	5.4	<0.05	0.2	<0.05	<0.05
122	109884	29.642209	79.713659	Graphite Schist	Bed rock	5.47	0.06	0.19	<0.05	1.91	2.18	0.56	<0.05	0.11	<0.05	0.45	83.1	5.42	0.06	0.09	<0.05	<0.05
123	109885	29.622664	79.722291	Graphite Schist	Bed rock	10.86	1.61	0.15	0.07	2.43	3.09	1.2	<0.05	0.19	<0.05	0.69	70.5	8.74	<0.05	0.18	<0.05	<0.05
124	109886	29.642686	79.699634	Graphite Schist	Bed rock	15.07	0.06	0.14	<0.05	0.49	4.01	1.09	<0.05	0.33	<0.05	0.74	74.44	3.12	0.16	<0.05	<0.05	<0.05
125	109887	29.641752	79.714284	Graphite Schist	Bed rock	6.54	<0.05	0.16	0.07	1.43	1.85	0.45	<0.05	0.14	<0.05	0.4	84.42	4.1	0.05	0.1	<0.05	<0.05
126	109888	29.664439	79.695985	Mica Schist	Bed rock	13.52	0.31	0.62	<0.05	5.02	2.9	1.79	<0.05	1.9	0.08	0.63	68.85	3.9	0.13	<0.05	<0.05	<0.05
127	109889	29.637882	79.722155	Graphite Schist	Bed rock	19.64	0.87	0.14	<0.05	0.58	5.67	1.9	<0.05	0.28	<0.05	0.83	62.95	6.45	0.06	0.29	<0.05	<0.05
128	109890	29.630212	79.71307	Mica Schist	Bed rock	0.08	<0.05	0.13	<0.05	0.88	0.23	0.06	<0.05	<0.05	<0.05	<0.05	98.06	0.3	<0.05	<0.05	<0.05	<0.05
129	109891	29.664125	79.699451	Mica Schist	Bed rock	16.6	0.66	0.29	<0.05	1.78	2.83	1.43	<0.05	1.08	0.08	1.01	58.72	15.1	<0.05	<0.05	<0.05	<0.05
130	109892	29.598406	79.686671	Graphite Schist	Bed rock	17.18	<0.05	0.84	<0.05	4.15	2.86	1.1	<0.05	2.55	<0.05	0.61	66.54	3.72	0.07	<0.05	<0.05	<0.05
131	109893	29.659027	79.702238	Graphite Schist	Bed rock	12.11	0.77	0.41	<0.05	2.58	1.95	0.69	<0.05	1.87	0.05	0.82	68.38	9.9	<0.05	0.11	<0.05	<0.05
132	109894	29.635853	79.696792	Foliated Granite	Bed rock	<0.05	<0.05	0.12	<0.05	0.28	<0.05	<0.05	<0.05	<0.05	<0.05	<0.05	99.41	0.29	<0.05	<0.05	<0.05	<0.05
133	109895	29.611253	79.70936	Graphite Schist	Bed rock	8.39	0.59	0.16	0.05	1.41	2.48	0.7	<0.05	0.85	<0.05	0.55	76.99	7.36	<0.05	0.2	<0.05	<0.05
134	109896	29.611253	79.70936	Quartz vein	Bed rock	<0.05	<0.05	0.12	<0.05	0.31	<0.05	<0.05	<0.05	<0.05	<0.05	<0.05	99.38	0.23	<0.05	<0.05	<0.05	<0.05
135	109897	29.602086	79.73715	Graphite Schist	Bed rock	13.02	0.24	0.15	<0.05	11.88	2.93	1.04	<0.05	0.18	0.14	0.62	59.43	10.1	0.09	0.11	<0.05	<0.05
136	109898	29.636586	79.724532	Graphite Schist	Bed rock	11.96	0.67	0.62	<0.05	2.3	3.19	1.06	<0.05	1.56	<0.05	0.64	67.65	9.87	0.1	0.1	<0.05	<0.05
137	109899	29.636968	79.70056	Graphite Schist	Bed rock	2.88	0.26	0.13	<0.05	3.08	0.94	0.27	<0.05	0.07	<0.05	0.15	88.3	3.63	0.05	0.07	<0.05	<0.05
138	109900	29.621003	79.72287	Graphite Schist	Bed rock	4.65	0.32	0.13	0.05	0.64	1.39	0.42	<0.05	0.09	<0.05	0.15	87.78	3.89	<0.05	0.17	<0.05	<0.05
139	109901	29.663216	79.695062	Graphite Schist	Bed rock	11.83	0.21	0.99	<0.05	3.32	2	1.19	<0.05	1.94	0.06	0.42	72.92	4.86	<0.05	<0.05	<0.05	<0.05

S No	Sample ID	Latitude	Longitude	Lithology	Type	Al_2O_3	BaO	CaO	Cr_2O_3	Fe_2O_3	K_2O	MgO	MnO	Na_2O	P_2O_5	TiO_2	SiO_2	LOI	SO_3	V_2O_5	SnO_2	WO_3
140	109902	29.603485	79.739698	Graphite Schist	Bed rock	12.9	0.73	0.18	<0.05	6.75	3.47	1.08	<0.05	0.22	0.22	0.63	66.03	7.32	0.05	0.28	<0.05	<0.05
141	109903	29.652766	79.667847	Mica Schist	Bed rock	9.06	<0.05	1.09	<0.05	3.88	1.78	1.22	0.05	1.99	0.1	0.66	79.07	0.94	0.05	<0.05	<0.05	<0.05
142	109904	29.614028	79.715725	Graphite Schist	Bed rock	10.92	1.45	0.24	<0.05	7.23	2.79	0.89	<0.05	0.63	0.21	0.58	65.21	9.68	0.11	0.06	<0.05	<0.05
143	109905	29.664127	79.698129	Mica Schist	Bed rock	14.13	0.13	0.79	<0.05	15.74	3.4	8	0.14	1.14	0.18	0.59	48.46	7.13	0.07	<0.05	<0.05	<0.05
144	109906	29.640691	79.664802	Mica Schist	Bed rock	10.18	0.11	1.38	<0.05	4.11	2.18	1.32	0.07	1.9	0.12	0.63	76.7	1.08	0.05	<0.05	<0.05	<0.05
145	109907	29.636525	79.701742	Graphite Schist	Bed rock	8.37	0.6	0.14	0.07	4.81	3.01	0.66	<0.05	0.14	0.08	0.49	73.11	7.8	<0.05	0.41	<0.05	<0.05
146	109908	29.647829	79.70488	Quartz vein	Bed rock	0.1	0.13	0.12	<0.05	0.21	0.09	<0.05	<0.05	<0.05	<0.05	<0.05	98.96	0.26	<0.05	<0.05	<0.05	<0.05
147	109909	29.648776	79.66381	Mica Schist	Bed rock	9.26	<0.05	1.24	<0.05	3.63	1.34	1.23	<0.05	2.5	0.1	0.58	78.75	0.95	<0.05	<0.05	<0.05	<0.05
148	109910	29.603463	79.739393	Mica Schist	Bed rock	11.47	0.61	0.65	<0.05	3.62	2.11	1.65	<0.05	2.32	0.07	0.43	72.42	4.37	0.09	<0.05	<0.05	<0.05
149	109911	29.601113	79.740133	Mica Schist	Bed rock	10.31	0.11	0.58	<0.05	3.77	2.07	1.21	<0.05	0.95	<0.05	0.54	77.29	2.81	0.05	<0.05	<0.05	<0.05
150	109912	29.617683	79.726185	Graphite Schist	Bed rock	0.86	0.1	0.12	<0.05	0.28	0.47	0.07	<0.05	<0.05	<0.05	<0.05	96.93	0.92	<0.05	<0.05	<0.05	<0.05
151	109913	29.636586	79.724532	Graphite Schist	Bed rock	6.01	0.46	0.14	0.07	0.98	2.32	0.69	<0.05	<0.05	0.05	0.34	83.23	5.17	<0.05	0.29	<0.05	<0.05
152	109914	29.620363	79.719983	Mica Schist	Bed rock	16.93	0.05	0.61	0.08	8.39	3.79	1.7	0.18	1.45	0.14	0.84	63.25	2.32	<0.05	<0.05	<0.05	<0.05
153	109915	29.636586	79.724532	Quartz vein	Bed rock	2.03	0.08	16.57	<0.05	1.25	0.5	0.27	<0.05	<0.05	13.19	<0.05	19.49	46.4	<0.05	<0.05	<0.05	<0.05
154	109916	29.637197	79.719378	Mica Schist	Bed rock	1.89	<0.05	0.57	<0.05	70.92	0.43	2.09	3.4	<0.05	0.34	0.11	20.07	<0.1	0.12	<0.05	<0.05	<0.05
155	109917	29.601416	79.729362	Graphite Schist	Bed rock	14.2	2.47	0.11	0.09	1.45	4.88	1.47	<0.05	0.17	0.14	1.1	60.7	12.6	<0.05	0.54	<0.05	<0.05
156	109918	29.636815	79.721908	Graphite Schist	Bed rock	0.91	<0.05	0.33	<0.05	0.81	0.18	0.06	<0.05	0.54	0.07	<0.05	96.21	0.45	0.19	<0.05	<0.05	<0.05
157	109919	29.608492	79.731753	Mica Schist	Bed rock	10.03	<0.05	1.44	<0.05	4.93	1.35	1.44	0.09	2.72	0.13	0.78	76.35	0.45	<0.05	<0.05	<0.05	<0.05
158	109920	29.658453	79.679743	Mica Schist	Bed rock	10.16	<0.05	1.5	<0.05	4.89	1.53	1.74	0.08	2.54	0.14	0.87	74.93	1.31	<0.05	<0.05	<0.05	<0.05
159	109921	29.602665	79.738968	Graphite Schist	Bed rock	1.7	<0.05	<0.05	<0.05	0.49	0.67	0.14	<0.05	<0.05	<0.05	0.1	95.16	1.32	0.05	<0.05	<0.05	<0.05
160	109922	29.664499	79.696561	Mica Schist	Bed rock	15.69	0.39	0.92	<0.05	8.29	3.81	2.91	0.08	2.51	0.22	0.79	60.09	4.05	<0.05	<0.05	<0.05	<0.05
161	109945	29.600032	79.724657	Graphite Schist	Pitting	5.42	0.46	0.18	<0.05	1.35	1.41	0.59	<0.05	0.44	0.08	0.32	82.68	6.79	0.06	0.21	<0.05	<0.05
162	109946	29.659791	79.697149	Graphite Schist	Pitting	6.03	2.34	0.23	0.09	0.51	1.53	0.88	<0.05	0.1	<0.05	0.37	77.51	9.33	0.07	0.63	<0.05	<0.05
163	109947	29.610453	79.70908	Graphite Schist	Pitting	8.5	0.31	<0.05	0.07	0.4	2.84	0.78	<0.05	0.11	<0.05	0.58	81	4.85	<0.05	0.36	<0.05	<0.05
164	109948	29.610535	79.70972	Graphite Schist	Pitting	6.85	0.2	<0.05	<0.05	2.22	1.88	2.39	<0.05	0.06	<0.05	0.43	78.98	6.59	<0.05	0.13	<0.05	<0.05

S No	Sample ID	Latitude	Longitude	Lithology	Type	Al_2O_3	BaO	CaO	Cr_2O_3	Fe_2O_3	K_2O	MgO	MnO	Na_2O	P_2O_5	TiO_2	SiO_2	LOI	SO_3	V_2O_5	SnO_2	WO_3
165	109949	29.610768	79.709548	Graphite Schist	Pitting	5.87	0.22	<0.05	0.09	0.42	1.98	0.56	<0.05	0.08	<0.05	0.38	85.32	4.49	0.05	0.37	<0.05	<0.05
166	109950	29.647805	79.704923	Graphite Schist	Pitting	11.17	4.66	0.16	0.06	1.01	2.92	0.95	<0.05	0.34	<0.05	0.65	69.97	7.54	<0.05	0.29	<0.05	<0.05
167	109951	29.637896	79.701271	Graphite Schist	Pitting	5.68	0.28	0.09	0.09	3.7	1.92	0.87	<0.05	0.16	<0.05	0.46	77.57	8.51	0.05	0.25	<0.05	<0.05
168	109952	29.656921	79.716897	Graphite Schist	Pitting	1.03	0.08	0.12	<0.05	1.05	0.49	0.11	<0.05	0.06	0.19	0.1	93.74	2.71	0.06	<0.05	<0.05	<0.05
169	109953	29.655345	79.718097	Mica Schist	Pitting	7.67	3.35	<0.05	0.07	2.89	2.29	1.24	<0.05	0.22	0.12	0.37	74.49	6.44	0.08	0.33	<0.05	<0.05
170	109954	29.634467	79.68964	Quartz vein	Pitting	<0.05	<0.05	<0.05	<0.05	1.27	0.15	<0.05	<0.05	0.07	<0.05	<0.05	98.73	0.4	<0.05	<0.05	<0.05	<0.05
171	109955	29.644975	79.688927	Graphite Schist	Pitting	8.06	0.17	0.36	<0.05	4.29	2.16	0.41	<0.05	0.91	0.06	0.82	76.51	5.78	0.08	0.07	<0.05	<0.05
172	109956	29.6458	79.689707	Graphite Schist	Pitting	9.82	0.23	0.22	<0.05	1.25	3.16	0.97	<0.05	0.4	<0.05	0.78	79.87	2.93	0.06	<0.05	<0.05	<0.05
173	109957	29.60304	79.736917	Graphite Schist	Pitting	7.05	0.53	0.27	0.06	1.68	1.7	0.68	<0.05	1.29	<0.05	0.53	78.72	7.02	<0.05	0.18	<0.05	<0.05
174	109958	29.615107	79.726605	Graphite Schist	Pitting	4.01	<0.05	<0.05	<0.05	0.62	1.69	0.28	<0.05	0.07	<0.05	0.34	89.83	2.71	<0.05	0.11	<0.05	<0.05
175	109959	29.629902	79.675958	Tuffaceous Rock	Pitting	17.85	0.09	0.74	<0.05	1.53	4.91	0.63	<0.05	0.18	<0.05	0.81	70.47	2.34	0.06	<0.05	<0.05	<0.05
176	109960	29.636193	79.69831	Foliated Granite	Pitting	12.95	<0.05	0.69	<0.05	2.46	4.69	0.4	<0.05	2.78	0.19	0.33	73.86	1.24	<0.05	<0.05	<0.05	<0.05
177	109961	29.640091	79.667015	Graphite Schist	Pitting	8.02	0.7	0.16	0.07	1.02	2.06	0.52	<0.05	1.25	<0.05	0.44	80.16	4.98	0.08	0.28	<0.05	<0.05
178	109962	29.641397	79.665528	Graphite Schist	Pitting	12.02	0.09	0.77	<0.05	2.33	1.43	1.84	<0.05	3.51	<0.05	0.5	73.26	3.99	0.07	<0.05	<0.05	<0.05
179	109963	29.636193	79.69831	Mica Schist	Pitting	17.91	0.05	0.23	<0.05	4.61	4.83	1.26	0.07	0.8	<0.05	0.8	66.14	2.75	0.06	<0.05	<0.05	<0.05
180	109964	29.629902	79.675958	Tuffaceous Rock	Pitting	29.7	0.19	1.05	<0.05	2.35	9.44	0.99	<0.05	0.31	0.1	1.5	49.38	4.58	<0.05	<0.05	<0.05	<0.05
181	109965	29.615107	79.726605	Graphite Schist	Pitting	13.32	0.09	<0.05	<0.05	1.36	4.5	0.84	<0.05	0.23	<0.05	0.85	75.5	2.85	0.05	0.05	<0.05	<0.05
182	109966	29.60304	79.736917	Graphite Schist	Pitting	9.8	0.5	0.63	<0.05	4	2.28	3.49	<0.05	2.02	0.17	0.54	66.66	9.23	0.07	0.18	<0.05	<0.05
183	109967	29.644975	79.688927	Quartz vein	Pitting	1.5	<0.05	<0.05	<0.05	0.76	0.5	0.11	<0.05	<0.05	<0.05	0.07	95.84	0.81	0.05	<0.05	<0.05	<0.05
184	109968	29.644975	79.688927	Graphite Schist	Pitting	10.05	0.26	<0.05	<0.05	5.56	3.16	0.58	<0.05	0.21	<0.05	0.77	74.08	4.92	0.07	0.12	<0.05	<0.05
185	109969	29.6458	79.689707	Quartz vein	Pitting	0.74	<0.05	<0.05	<0.05	0.78	0.58	0.1	<0.05	0.11	<0.05	0.15	96.33	0.7	0.05	<0.05	<0.05	<0.05
186	109970	29.60304	79.736917	Quartz vein	Pitting	2.09	0.17	0.14	<0.05	1.71	0.7	0.15	<0.05	0.65	<0.05	0.16	91.35	2.45	0.05	0.06	<0.05	<0.05
187	109971	29.615107	79.726605	Quartz vein	Pitting	1.16	<0.05	<0.05	<0.05	0.61	0.64	0.11	<0.05	<0.05	<0.05	0.15	96.22	0.71	0.06	<0.05	<0.05	<0.05
188	109972	29.629902	79.675958	Quartz vein	Pitting	2.21	<0.05	0.35	<0.05	1.25	0.82	0.18	<0.05	<0.05	<0.05	<0.05	93.74	0.9	0.06	<0.05	<0.05	<0.05
189	109973	29.636193	79.69831	Quartz vein	Pitting	16.66	<0.05	0.59	<0.05	1	1.35	0.24	0.11	6.08	0.28	<0.05	72.59	0.83	0.07	<0.05	<0.05	<0.05

S No	Sample ID	Latitude	Longitude	Lithology	Type	Al_2O_3	BaO	CaO	Cr_2O_3	Fe_2O_3	K_2O	MgO	MnO	Na_2O	P_2O_5	TiO_2	SiO_2	LOI	SO_3	V_2O_5	SnO_2	WO_3
190	109974	29.640091	79.667015	Quartz vein	Pitting	6.88	0.7	<0.05	0.09	0.84	2.12	0.61	<0.05	0.14	<0.05	0.43	82.23	5.29	0.07	0.39	<0.05	<0.05
191	109975	29.641397	79.665528	Quartz vein	Pitting	<0.05	<0.05	0.15	<0.05	0.65	0.18	0.29	<0.05	0.49	<0.05	<0.05	97.44	0.59	<0.05	<0.05	<0.05	<0.05
192	109976	29.669152	79.712775	Quartzite	Bedrock	3.66	<0.05	0.12	<0.05	0.68	2.29	0.06	<0.05	0.79	<0.05	<0.05	91.58	0.48	<0.05	<0.05	<0.05	<0.05
193	109977	29.632357	79.680293	Tuffaceous Rock	Bedrock	7.72	<0.05	2.52	<0.05	2.53	1.08	1.05	<0.05	1.41	<0.05	0.54	82.06	0.72	<0.05	<0.05	<0.05	<0.05
194	109978	29.624178	79.697392	Mica Schist	Stream sediment (<-125 micron)	14.44	0.1	0.62	<0.05	3.47	3.88	0.77	0.06	2.7	0.06	0.85	66.98	5.62	0.08	<0.05	<0.05	<0.05
195	109979	29.624757	79.696493	Mica Schist	Stream sediment (<-125 micron)	14.51	0.1	0.58	<0.05	3.57	3.8	0.77	0.07	3	0.07	0.85	66.88	5.37	0.07	<0.05	<0.05	<0.05
196	109980	29.629825	79.70005	Mica Schist	Stream sediment (<-125 micron)	14.16	0.09	0.81	<0.05	3.86	3.36	0.77	0.08	2.94	0.09	0.98	65.33	7.14	0.11	<0.05	<0.05	<0.05
197	109981	29.631394	79.698021	Mica Schist	Stream sediment (<-125 micron)	14.72	0.09	0.69	<0.05	4.55	3.38	0.96	0.07	2.93	0.07	1.23	64.76	6.12	0.1	<0.05	<0.05	<0.05
198	109982	29.625578	79.717188	Mica Schist	Stream sediment (<-125 micron)	14.44	0.09	1.1	<0.05	5.14	2.97	1.11	0.08	2.26	0.1	1.08	64.82	6.52	0.14	<0.05	<0.05	<0.05
199	109983	29.624315	79.712884	Mica Schist	Stream sediment (<-125 micron)	15.57	0.08	1.02	<0.05	5.89	3.09	1.17	0.08	2.56	0.13	1.22	60.61	8.23	0.14	<0.05	<0.05	<0.05
200	109984	29.625355	79.711702	Mica Schist	Stream sediment (<-125 micron)	13.25	0.06	1.28	<0.05	5.21	2.61	0.79	0.11	2.11	0.12	1.04	67.07	5.88	0.14	<0.05	<0.05	<0.05

Annexure VIII_XRF Data of Surface Check Samples (All data in %)

S No	Sample ID	Latitude	Longitude	Lithology	Type	Lab	Al_2O_3	BaO	CaO	Cr_2O_3	Fe_2O_3	K_2O	MgO	MnO	Na_2O	P_2O_5	TiO_2	SiO_2	LOI	SO_3	V_2O_5
1	109201	29.631603	79.715032	Quartz Vain	Bedrock	BV	2.698	<0.01	0.323	0.027	0.782	0.130	0.153	<0.01	0.423	0.098	<0.01	94.830	0.430	0.047	<0.01
						Shiva	0.742	<0.05	0.070	0.125	2.067	0.060	0.078	<0.05	0.149	<0.05	<0.05	95.947	0.390	0.241	<0.05
2	109202	29.635816	79.719848	Mica Schist	Bedrock	BV	13.530	0.023	0.171	0.015	0.441	3.812	1.056	<0.01	0.408	0.102	0.873	76.642	2.710	0.048	<0.01
						Shiva	14.065	0.066	<0.05	0.072	1.235	4.338	1.211	<0.05	0.324	0.064	0.768	74.675	2.920	0.134	<0.05
3	109204	29.635105	79.714393	Mica Schist	Bedrock	BV	7.833	0.466	0.142	0.032	4.924	2.001	0.522	<0.01	0.087	0.148	0.417	77.358	5.710	0.043	0.093
						Shiva	5.635	0.410	<0.05	0.135	5.457	1.562	0.439	<0.05	0.078	0.122	0.315	80.720	4.880	0.078	0.087
4	109210	29.611528	79.715905	Graphite Schist	Bedrock	BV	11.678	0.045	0.195	0.033	2.537	3.020	0.728	<0.01	0.493	0.123	0.582	74.821	5.570	0.060	0.059
						Shiva	10.501	0.089	<0.05	0.110	3.397	3.252	0.727	<0.05	0.109	0.072	0.517	75.063	5.770	0.161	0.076
5	109213	29.611263	79.727305	Mica Schist	Bedrock	BV	18.064	0.031	0.578	0.012	8.122	3.812	3.760	0.085	1.536	0.194	1.018	58.342	4.100	0.050	0.013
						Shiva	19.233	0.101	0.374	<0.05	7.762	4.387	3.582	<0.05	1.150	0.134	0.904	57.999	4.250	<0.05	<0.05
6	109216	29.641695	79.657337	Mica Schist	Bedrock	BV	6.019	<0.01	0.146	0.053	2.343	1.472	0.353	<0.01	0.054	0.138	0.260	81.559	7.130	0.046	0.158
						Shiva	13.993	0.138	1.228	<0.05	5.869	3.563	2.373	<0.05	1.284	0.136	0.742	58.568	6.900	5.109	<0.05
7	109218	29.636403	79.723705	Graphite Schist	Bedrock	BV	9.819	0.401	5.582	0.036	8.397	2.567	1.078	0.039	0.397	0.136	0.285	58.597	8.000	4.028	0.140
						Shiva	10.102	0.558	4.857	<0.05	3.838	3.145	1.220	<0.05	0.657	0.098	0.367	61.469	8.380	4.921	0.192
8	109227	29.626358	79.745898	Graphite Schist	Bedrock	BV	10.990	0.635	1.092	0.010	1.737	1.507	0.594	<0.01	2.312	0.103	0.678	64.808	15.130	0.059	0.047
						Shiva	4.296	0.378	0.380	0.155	2.012	0.991	0.364	<0.05	0.498	<0.05	0.291	82.041	7.340	0.925	0.242
9	109228	29.627081	79.745878	Graphite Schist	Bedrock	BV	10.428	2.697	0.271	0.015	2.851	2.871	0.935	<0.01	0.195	0.138	0.687	64.604	13.680	0.192	0.165
						Shiva	8.796	2.730	<0.05	0.103	3.614	2.900	0.772	<0.05	0.160	0.089	0.591	66.114	13.830	<0.05	0.210
10	109229	29.626294	79.744137	Graphite Schist	Bedrock	BV	12.046	2.352	1.137	0.018	3.138	2.367	1.272	0.014	1.601	0.109	0.855	67.694	7.000	0.291	0.041
						Shiva	7.524	3.509	0.738	<0.05	4.670	2.647	1.333	<0.05	0.595	0.061	0.850	63.340	14.270	0.136	0.110
11	109230	29.626436	79.743254	Graphite Schist	Bedrock	BV	12.031	2.794	0.755	0.019	7.209	2.796	1.320	<0.01	0.322	0.179	0.861	58.471	12.700	0.042	0.135
						Shiva	11.274	3.450	0.723	<0.05	5.093	3.200	1.505	<0.05	0.310	0.099	0.822	60.916	12.380	<0.05	0.118
12	109232	29.623181	79.74268	Mica Schist	Bedrock	BV	12.166	0.506	0.161	0.012	5.616	2.878	0.681	<0.01	0.271	0.126	0.713	71.901	4.580	0.135	0.064
						Shiva	14.281	0.488	<0.05	<0.05	8.299	3.950	0.893	<0.05	0.255	0.112	0.771	64.119	6.020	0.569	0.103
13	109233	29.618908	79.739762	Mica Schist	Bedrock	BV	10.593	<0.01	1.245	<0.01	4.570	1.618	1.339	0.051	2.499	0.187	0.842	76.054	0.600	0.047	<0.01
						Shiva	10.588	<0.05	1.348	<0.05	5.000	1.880	1.534	<0.05	2.692	0.159	0.844	74.943	0.840	<0.05	<0.05
14	109236	29.598399	79.746705	Mica Schist	Bedrock	BV	27.032	0.127	0.180	0.011	6.782	6.150	1.477	0.011	0.946	0.178	1.340	48.507	6.870	0.055	0.056
						Shiva	22.856	0.156	0.077	<0.05	7.267	5.976	1.175	<0.05	0.901	0.110	1.077	54.169	5.950	0.123	0.053
15	109237	29.661522	79.69587	Graphite Schist	Bedrock	BV	11.342	1.945	0.167	0.046	0.796	2.412	1.931	<0.01	0.156	0.097	0.589	68.936	11.030	0.063	0.195
						Shiva	9.325	2.239	<0.05	0.054	2.137	2.331	1.013	<0.05	0.089	0.077	0.412	75.455	6.410	<0.05	0.310
16	109239	29.661952	79.698568	Mica Schist	Bedrock	BV	12.233	0.212	0.387	0.022	17.540	3.328	1.020	<0.01	0.708	0.349	0.723	53.401	10.010	0.069	0.040
						Shiva	14.071	0.260	0.813	0.117	9.570	4.173	2.296	<0.05	0.683	0.077	0.707	59.690	7.060	0.311	0.106
17	109240	29.664125	79.699451	Mica Schist	Bedrock	BV	16.440	0.791	0.167	0.015	3.546	3.706	1.326	<0.01	0.308	0.147	1.143	58.892	13.150	0.045	0.047
						Shiva	15.774	0.951	0.072	0.083	3.792	3.906	1.380	<0.05	0.313	0.089	0.992	60.074	12.260	0.165	0.065
18	109241	29.66583	79.706938	Mica Schist	Bedrock	BV	4.378	<0.01	0.296	0.015	1.106	0.497	0.123	<0.01	0.534	0.087	0.085	91.930	0.730	0.049	<0.01
						Shiva	6.780	<0.05	0.128	0.063	1.481	1.792	0.219	<0.05	0.489	<0.05	0.308	87.519	1.100	<0.05	<0.05
19	109242	29.667667	79.711977	Quartzite	Bedrock	BV	14.734	<0.01	0.456	<0.01	0.890	4.882	0.170	<0.01	3.052	0.259	0.032	74.234	0.940	0.050	<0.01
						Shiva	14.876	<0.05	0.451	<0.05	1.641	4.474	0.252	<0.05	3.353	0.356	0.142	73.104	1.230	<0.05	<0.05
20	109244	29.63859	79.668533	Graphite Schist	Bedrock	BV	6.786	0.288	0.138	0.068	0.921	1.549	0.485	<0.01	0.077	0.093	0.263	83.765	4.890	0.049	0.361
						Shiva	4.267	0.286	<0.05	0.093	1.377	1.303	0.441	<0.05	0.078	<0.05	0.216	86.824	4.440	<0.05	0.355
21	109246	29.654743	79.683657	Quartz vein	Bedrock	BV	13.03495	<0.01	1.485	<0.01	3.88914	1.794	1.4	0.021	2.998	0.154	0.403	73.632	1.03	0.051	<0.01
						Shiva	5.031	<0.05	0.515	<0.05	2.176	0.911	0.671	<0.05	0.947	0.073	0.183	88.864	0.520	<0.05	<0.05
22	109212	29.611678	79.729612	Mica Schist	Bedrock	BV	11.21855	0.01	0.989	0.01	5.49928	2.4	1.761	0.085	1.502	0.207	0.775	74.005	1.08	0.047	<0.01
						Shiva	14.133	<0.05	0.977	<0.05	7.543	2.705	3.020	0.106	2.657	0.176	0.746	66.523	1.250	<0.05	<0.05

Annexure IX_XRF Data for 2 Additional Elements- Sn and W of Surafce Check Samples

S No	Sample ID	Latitude	Longitude	Lithology	Type	Lab	SnO2 (in %)	WO3 (in %)	Sn (in ppm)	W (in ppm)
1	109202	29.635816	79.719848	Mica Schist	Bedrock	BV	0.011	<0.01	86.625	<79.3
						Shiva	-	-	<50	<50
2	109205	29.641709	79.714861	Mica Schist	Bedrock	BV	0.013	<0.01	102.375	<79.3
						Shiva	-	-	<50	<50
3	109212	29.611678	79.729612	Mica Schist	Bedrock	BV	0.014	<0.01	110.25	<79.3
						Shiva	-	-	<50	<50
4	109213	29.611263	79.727305	Mica Schist	Bedrock	BV	0.01	<0.01	78.75	<79.3
						Shiva	-	-	<50	<50
5	109214	29.612963	79.724822	Graphite Schist	Bedrock	BV	0.011	<0.01	86.625	<79.3
						Shiva	-	-	<50	<50
6	109219	29.636173	79.719654	Quartz vein	Bedrock	BV	0.012	0.012	94.5	95.16
						Shiva	-	-	<50	<50

Annexure X_Proximate Analysis of Graphite for Surface Samples (All Values in %)

S No	Sample ID	Latitude	Longitude	Sample Type	Fixed Carbon	Moisture Content	Volatile Matter	Ash Content
1	109161	29.64269	79.69963	BR	2.19	0.15	3.13	94.53
2	109162	29.65336	79.71748	BR	3.91	0.73	7.58	87.78
3	109163	29.65578	79.71983	BR	3.92	0.29	3.91	91.88
4	109164	29.6013	79.73772	BR	2.2	0.11	2.37	95.32
5	109165	29.63824	79.70173	BR	3.61	0.02	3.40	92.97
6	109166	29.62273	79.70072	BR	6.1	0.51	5.49	87.90
7	109167	29.5992	79.72097	BR	2.14	0.03	1.52	96.31
8	109169	29.625700	79.721300	BR	3.03	0.18	3.59	93.20
9	109170	29.62100	79.7244	BR	2.19	0.17	2.35	95.29
10	109171	29.63659	79.72591	BR	2.23	0.05	2.01	95.71
11	109172	29.65683	79.73054	BR	2.91	0.38	3.95	92.76
12	109173	29.60268	79.68907	BR	3.01	0.33	3.41	93.25
13	109174	29.63536	79.72589	BR	4.07	0.19	3.90	91.84
14	109175	29.61768	79.72619	BR	2.77	0.22	4.09	92.92
15	109186	29.63265	79.71565	BR	7	0.13	4.54	88.33
16	109187	29.63536	79.72589	BR	5.85	0.18	3.38	90.59
17	109188	29.61125	79.70936	BR	5.43	0.34	4.18	90.05
18	109189	29.64034	79.65802	BR	4.44	0.24	4.51	90.81
19	109190	29.66195	79.69857	BR	3.19	0.38	5.42	91.01
20	109191	29.65903	79.70224	BR	5.18	0.15	3.79	90.88
21	109192	29.65941	79.70226	BR	2.46	0.46	4.41	92.67
22	109193	29.66094	79.70161	BR	5.37	0.16	4.44	90.03
23	109194	29.66074	79.70191	BR	3.99	0.21	4.68	91.12
24	109195	29.66031	79.69716	BR	4	0.15	5.73	90.12
25	109196	29.63645	79.67185	BR	3.46	0.21	4.32	92.01
26	109197	29.63984	79.671	BR	6.54	0.40	6.41	86.65
27	109198	29.64073	79.66733	BR	5.2	0.30	3.91	90.59
28	109199	29.65185	79.68423	BR	6.01	0.23	6.16	87.60
29	109200	29.6366	79.69699	BR	3.35	0.19	4.56	91.90
30	109275	29.63748	79.69346	BR	1.26	0.28	1.46	97.00
31	109276	29.64776	79.70478	BR	4.47	0.21	2.49	92.83
32	109277	29.64215	79.68517	BR	2.96	0.51	4.99	91.54
33	109278	29.64292	79.6884	BR	3.04	0.49	4.97	91.50

S No	Sample ID	Latitude	Longitude	Sample Type	Fixed Carbon	Moisture Content	Volatile Matter	Ash Content
34	109279	29.64501	79.68895	BR	0.89	0.28	2.63	96.20
35	109280	29.64578	79.68976	BR	0.82	0.99	4.67	93.52
36	109281	29.64874	79.69473	BR	0.83	0.14	3.61	95.42
37	109282	29.65696	79.7169	BR	2.54	0.25	5.94	91.27
38	109923	29.61077	79.70955	BR	4.41	0.36	1.27	93.96
39	109936	29.64845	79.71465	BR	6.98	0.36	2.44	90.22
40	109937	29.608	79.6882	BR	5.67	0.34	1.14	92.85
41	109938	29.60596	79.69227	BR	4.36	0.52	0.54	94.58
42	109939	29.61017	79.70873	BR	6.62	0.62	0.92	91.84
43	109940	29.63769	79.70123	PIT	5.18	1.41	4.07	89.34
44	109941	29.63447	79.68964	PIT	6.14	0.59	3.79	89.48
45	109942	29.64498	79.68893	PIT	5.75	0.65	3.31	90.29
46	109943	29.61045	79.70908	PIT	2.34	0.46	1.86	95.34
47	109944	29.65979	79.69715	PIT	**7.05**	0.32	2.18	90.45
48	109985	29.61195	79.7088	BR	3.51	0.46	3.02	93.01
49	109986	29.61077	79.70878	BR	1.86	0.48	1.82	95.84
50	109987	29.61062	79.7093	BR	1.8	0.28	2.25	95.67
51	109988	29.61051	79.70913	BR	2.83	0.22	2.14	94.81
52	109989	29.61018	79.70952	BR	2.14	0.31	2.10	95.45
53	109990	29.62114	79.72303	BR	6.15	0.25	1.86	91.74
54	109991	29.6211	79.72303	BR	3.02	0.22	1.57	95.19
55	109992	29.62107	79.72298	BR	2.41	0.27	2.44	94.88
56	109993	29.62106	79.72286	BR	5.36	0.23	2.14	92.27
57	109994	29.62051	79.72286	BR	2.57	0.37	1.10	95.96

Annexure XI_ICPMS Data of Surface Samples (All data in ppm)

SL No	Sample ID	Latitude	Longitude	Lithology	Li	Be	Sc	V	Cr	Co	Ni	Cu	Zn	Ga	Ge	Se	Rb	Sr	Y	Zr
1	109296	29.636412	79.692355	Incipient Gneiss/ Younger Granite	63.7	3.0	3.5	21	47.0	3.7	8.2	<0.5	61.5	19.1	<0.5	1.1	292.7	68.3	14.7	1.5
2	109985	29.611948	79.708797	Graphite Schist	27.0	2.9	10.5	552	144.3	7.4	44.2	12.9	199.5	18.7	<0.5	4.1	111.8	94.3	17.9	1.6
3	109986	29.610765	79.708783	Graphite Schist	19.2	2.0	6.5	961	149.7	<0.5	7.2	8.3	31.8	12.9	<0.5	3.3	80.9	66.1	21.6	6.9
4	109987	29.610622	79.709302	Graphite Schist	16.7	2.2	10.4	1504	219.3	0.7	15.6	5.1	23.9	13.5	<0.5	3.7	77.8	33.4	27.6	4.5
5	109988	29.61051	79.709127	Graphite Schist	18.8	2.4	11.5	1499	298.5	<0.5	10.4	<0.5	11.8	14.6	<0.5	3.2	83.5	30.2	27.1	2.7
6	109989	29.610179	79.709517	Graphite Schist	16.8	1.3	8.5	789	270.2	0.7	19.7	14.5	47.4	12.1	<0.5	1.0	63.2	48.8	20.5	2.2
7	109990	29.621137	79.723032	Graphite Schist	23.5	2.9	9.7	2060	342.2	<0.5	5.2	<0.5	7.7	18.5	<0.5	3.4	129.8	19.6	3.7	2.0
8	109991	29.621103	79.723027	Graphite Schist	**11.9**	**2.2**	**6.8**	**503**	**130.3**	**5.2**	**11.3**	**<0.5**	**2.3**	**13.8**	**<0.5**	**3.4**	**65.8**	**106.0**	**9.7**	**1.2**
9	109992	29.62107	79.722977	Graphite Schist	19.3	2.8	9.5	764	140.7	4.1	9.2	5.6	7.7	16.6	<0.5	5.3	100.8	106.9	1.5	1.6
10	109993	29.621058	79.722862	Graphite Schist	13.0	2.4	8.2	242	127.9	9.7	24.0	13.7	20.3	15.9	<0.5	3.5	68.8	156.7	16.4	1.8
11	109994	29.620512	79.722855	Graphite Schist	10.3	1.6	4.7	727	164.5	0.5	5.3	<0.5	18.8	8.7	<0.5	3.0	48.2	41.9	10.8	1.1
12	109995	29.629941	79.675877	Volcanic tuffaceous	62.5	5.8	18.7	120	98.2	9.8	17.9	<0.5	57.4	37.0	<0.5	4.0	243.6	100.2	42.4	13.0
13	109996	29.630513	79.677048	Volcanic tuffaceous	28.3	1.6	4.1	31	72.5	2.4	6.4	<0.5	13.9	12.4	<0.5	1.0	103.2	48.2	15.4	1.8
14	109997	29.62111	79.723005	Graphite Schist	8.2	1.8	6.8	192	153.3	7.9	17.4	<0.5	14.8	12.9	<0.5	6.1	47.8	170.9	27.4	1.4
15	109998	29.636586	79.724532	Graphite Schist	23.1	3.0	12.6	511	210.4	12.3	76.7	203.8	336.5	18.8	<0.5	12.7	110.1	151.3	51.5	1.5
16	110005	29.621075	79.723056	Graphite Schist	24.24	2.01	10.22	580	146.01	6.36	16.32	27.25	10.89	15.92	<0.5	7.80	63.98	156.30	18.44	5.45
17	110006	29.621075	79.723056	Graphite Schist	15.28	1.71	7.47	330	119.77	4.42	33.86	69.07	167.02	15.36	<0.5	7.38	51.25	181.07	23.19	2.64
18	110007	29.621075	79.723056	Graphite Schist	12.56	2.16	7.01	283	105.84	6.55	29.33	50.76	82.61	13.21	<0.5	8.45	46.72	153.17	17.36	2.13
19	110008	29.621075	79.723056	Graphite Schist	18.29	3.56	10.74	339	116.54	14.12	69.25	125.15	252.19	17.47	<0.5	9.04	74.93	147.84	59.50	2.05
20	110009	29.621075	79.723056	Graphite Schist	47.83	2.90	13.22	1040	213.25	3.68	19.07	<0.5	19.76	22.04	<0.5	6.51	128.74	61.78	3.11	2.50
21	110010	29.610435	79.70963	Graphite Schist	11.26	2.14	10.42	1150	337.38	4.62	62.08	151.31	160.95	14.44	<0.5	10.11	69.50	30.18	37.60	2.78
22	110011	29.610435	79.70963	Graphite Schist	6.59	<0.5	11.73	1240	368.33	4.58	73.75	231.05	173.11	16.21	<0.5	11.17	75.65	32.93	72.23	3.41
23	110012	29.610435	79.70963	Graphite Schist	**34.45**	**1.59**	**10.84**	**1285**	**353.90**	**4.47**	**75.48**	**399.72**	**148.58**	**14.34**	<0.5	**9.51**	**75.52**	**36.40**	**60.00**	**3.42**
24	110013	29.610435	79.70963	Graphite Schist	30.78	3.69	11.88	1052	357.37	4.95	91.03	436.18	143.17	15.41	<0.5	3.63	68.48	40.35	47.43	2.91
25	110014	29.610435	79.70963	Graphite Schist	21.57	3.43	10.61	1142	404.78	4.53	81.26	433.69	132.14	14.21	<0.5	6.23	70.82	34.48	38.15	2.49
26	110015	29.610692	79.709507	Graphite Schist	16.90	3.37	10.10	1335.16	333.84	8.06	127.07	234.46	271.93	16.87	<0.5	3.95	56.90	138.84	142.24	4.41
27	110016	29.610692	79.709507	Graphite Schist	15.27	3.32	10.14	1140.19	350.72	4.94	79.12	138.59	149.92	14.18	<0.5	6.56	45.64	148.45	178.54	4.11
28	110017	29.610692	79.709507	Graphite Schist	14.27	1.99	9.36	997.04	356.38	3.59	104.24	155.39	122.13	12.17	<0.5	2.77	41.03	39.85	19.44	4.09
29	110018	29.610692	79.709507	Graphite Schist	13.16	1.43	2.31	321.90	239.30	2.14	39.55	72.12	52.92	2.92	<0.5	1.86	10.73	19.24	8.12	1.59
30	110019	29.610692	79.709507	Graphite Schist	12.59	1.68	18.25	2414.28	400.09	1.55	32.79	24.52	18.81	21.23	<0.5	3.88	106.47	63.89	22.55	6.75
31	109201	29.631603	79.715032	Qtz. Vain of Mica Schist	7.20	0.66	<0.5	6.72	204.20	1.66	<0.5	1.25	16.63	1.28	<0.5	1.57	8.13	28.44	0.82	0.71

32	109202	29.635816	79.719848	Mica Schist	36.91	2.56	14.74	129.20	168.73	1.52	1.28	<0.5	9.69	17.37	<0.5	2.25	161.26	28.70	1.30	2.39

Continue.

SL No	Sample ID	Latitude	Longitude	Lithology	Nb	Mo	Cd	In	Sn	Sb	Te	Cs	Ba	La	Ce	Pr	Nd	Sm	Eu	Gd
1	109296	29.636412	79.692355	Incipient Gneiss/ Younger Granite	14.5	6.1	<0.5	<0.5	27.5	<0.5	<0.5	20.7	276.7	21.5	43.0	5.7	20.9	4.8	0.6	3.9
2	109985	29.611948	79.708797	Graphite Schist	9.4	14.3	1.9	<0.5	5.2	<0.5	<0.5	3.6	8642.5	18.0	31.2	4.1	15.1	3.0	1.0	2.8
3	109986	29.610765	79.708783	Graphite Schist	6.7	18.7	0.7	<0.5	4.2	1.7	<0.5	2.5	3025.1	13.6	21.3	3.1	11.5	2.6	0.7	2.8
4	109987	29.610622	79.709302	Graphite Schist	9.8	56.7	<0.5	<0.5	4.0	5.6	<0.5	2.6	2315.6	27.7	41.1	7.5	30.4	6.3	1.2	5.4
5	109988	29.61051	79.709127	Graphite Schist	11.9	28.1	<0.5	<0.5	3.4	2.0	<0.5	2.8	2565.1	34.1	50.6	9.4	38.1	7.9	1.4	6.2
6	109989	29.610179	79.709517	Graphite Schist	7.3	23.1	<0.5	<0.5	1.7	0.9	<0.5	2.6	3622.9	19.6	31.5	5.4	22.1	5.1	1.0	4.3
7	109990	29.621137	79.723032	Graphite Schist	9.4	53.1	<0.5	<0.5	5.8	0.7	<0.5	3.2	5076.8	3.0	3.5	<0.5	1.5	<0.5	<0.5	<0.5
8	109991	29.621103	79.723027	Graphite Schist	**8.1**	**10.3**	**<0.5**	**<0.5**	**2.8**	**<0.5**	**<0.5**	**2.1**	**2190.1**	**16.6**	**33.2**	**4.0**	**14.3**	**2.7**	**0.7**	**2.4**
9	109992	29.62107	79.722977	Graphite Schist	11.3	20.4	<0.5	<0.5	0.6	<0.5	<0.5	2.4	4559.1	3.4	5.1	0.6	1.8	<0.5	<0.5	<0.5
10	109993	29.621058	79.722862	Graphite Schist	8.9	3.0	<0.5	<0.5	<0.5	<0.5	<0.5	2.0	2693.6	22.4	44.2	5.1	17.9	3.5	0.9	3.0
11	109994	29.620512	79.722855	Graphite Schist	4.7	22.6	<0.5	<0.5	<0.5	<0.5	<0.5	1.1	3544.7	14.3	21.8	3.5	13.4	2.7	0.6	2.3
12	109995	29.629941	79.675877	Volcanic tuffaceous	23.0	1.5	<0.5	<0.5	<0.5	<0.5	<0.5	11.0	1538.5	64.4	130.5	15.4	54.5	10.4	2.0	8.3
13	109996	29.630513	79.677048	Volcanic tuffaceous	5.7	3.5	<0.5	<0.5	<0.5	<0.5	<0.5	6.1	511.0	27.1	54.8	6.3	22.2	4.6	0.9	3.6
14	109997	29.62111	79.723005	Graphite Schist	9.2	3.7	<0.5	<0.5	1.6	<0.5	<0.5	2.7	1185.8	30.6	54.7	6.6	23.7	5.0	1.2	4.7
15	109998	29.636586	79.724532	Graphite Schist	9.8	52.9	4.0	<0.5	<0.5	1.0	<0.5	2.9	4899.2	33.5	54.2	8.1	30.8	6.9	1.7	7.4
16	110005	29.621075	79.723056	Graphite Schist	11.47	10.28	2.38	<0.5	2.58	20.98	<0.5	2.41	2343.72	23.99	38.93	4.68	16.59	3.62	0.96	3.00
17	110006	29.621075	79.723056	Graphite Schist	8.40	9.14	3.75	<0.5	1.85	20.69	<0.5	4.02	1282.08	34.18	55.18	6.79	24.70	4.93	1.20	4.04
18	110007	29.621075	79.723056	Graphite Schist	8.41	6.97	2.89	<0.5	1.87	20.02	<0.5	3.26	1544.36	21.20	38.54	5.01	17.98	3.63	0.83	3.00
19	110008	29.621075	79.723056	Graphite Schist	10.34	8.38	3.54	<0.5	2.05	22.32	<0.5	5.91	2470.39	41.44	76.51	10.69	43.66	10.55	2.69	9.47
20	110009	29.621075	79.723056	Graphite Schist	13.46	27.60	2.30	<0.5	3.88	21.91	<0.5	3.30	4662.31	4.78	7.56	0.99	3.36	0.70	0.59	0.55
21	110010	29.610435	79.70963	Graphite Schist	9.62	76.08	1.96	<0.5	3.54	28.60	<0.5	5.74	2041.20	33.44	52.41	8.66	34.10	7.59	1.71	6.08
22	110011	29.610435	79.70963	Graphite Schist	10.28	84.84	1.58	<0.5	4.60	28.30	<0.5	6.37	2175.25	45.53	65.86	11.98	47.16	11.37	2.48	10.62
23	110012	29.610435	79.70963	Graphite Schist	**9.14**	**59.45**	**1.77**	<0.5	**3.91**	**34.72**	<0.5	**6.22**	**2309.89**	**39.34**	**60.47**	**10.67**	**41.63**	**10.69**	**2.48**	**9.71**
24	110013	29.610435	79.70963	Graphite Schist	9.64	30.63	1.67	<0.5	2.97	41.21	<0.5	6.32	1865.35	40.62	66.94	10.35	41.94	9.09	2.32	8.60
25	110014	29.610435	79.70963	Graphite Schist	8.99	35.65	1.85	<0.5	3.27	34.74	<0.5	5.93	2120.17	36.84	57.29	9.59	38.78	8.19	2.07	7.96
26	110015	29.610692	79.709507	Graphite Schist	14.82	32.86	2.38	<0.5	2.09	49.44	<0.5	3.01	1749.22	58.33	95.13	16.87	71.68	19.53	4.65	20.58
27	110016	29.610692	79.709507	Graphite Schist	14.50	22.86	1.69	<0.5	1.42	47.65	<0.5	2.06	1643.34	53.56	82.25	15.74	76.52	23.84	5.96	26.80
28	110017	29.610692	79.709507	Graphite Schist	13.93	40.88	1.75	<0.5	1.56	51.16	<0.5	1.90	1344.14	36.81	54.53	8.79	32.50	6.52	1.32	4.89
29	110018	29.610692	79.709507	Graphite Schist	3.27	24.75	1.08	<0.5	0.86	33.43	<0.5	0.54	357.31	7.85	11.63	1.97	7.56	1.33	<0.5	1.35
30	110019	29.610692	79.709507	Graphite Schist	19.00	74.53	1.41	<0.5	2.98	39.87	0.58	4.00	2966.32	47.61	61.33	11.34	44.66	9.30	2.09	6.40
31	109201	29.631603	79.715032	Qtz. Vain of Mica Schist	<0.5	<0.5	1.49	<0.5	<0.5	17.31	<0.5	0.68	48.30	1.20	0.94	<0.5	1.15	<0.5	<0.5	<0.5
32	109202	29.635816	79.719848	Mica Schist	10.90	<0.5	1.76	<0.5	3.56	22.29	<0.5	2.46	610.10	7.65	10.86	0.75	2.04	0.55	<0.5	<0.5

Continue.

SL No	Sample ID	Latitude	Longitude	Lithology	Tb	Dy	Ho	Er	Tm	Yb	Lu	Hf	Ta	W	Tl	Pb	Bi	Th	U
1	109296	29.636412	79.692355	Incipient Gneiss/ Younger Granite	0.6	3.0	0.5	1.6	<0.5	1.2	<0.5	<0.5	3.8	6.2	<0.5	29.4	1.4	14.6	2.5
2	109985	29.611948	79.708797	Graphite Schist	<0.5	2.8	0.6	2.1	<0.5	1.6	<0.5	<0.5	0.6	2.9	<0.5	38.6	0.5	8.8	9.2
3	109986	29.610765	79.708783	Graphite Schist	<0.5	3.1	0.7	2.3	<0.5	1.9	<0.5	<0.5	<0.5	1.4	<0.5	29.2	<0.5	4.3	9.5
4	109987	29.610622	79.709302	Graphite Schist	0.7	4.2	0.9	2.9	<0.5	2.5	<0.5	<0.5	0.6	3.4	<0.5	24.5	<0.5	9.0	5.9
5	109988	29.61051	79.709127	Graphite Schist	0.8	4.3	0.9	2.8	<0.5	2.4	<0.5	<0.5	0.7	3.5	<0.5	21.8	<0.5	8.6	6.7
6	109989	29.610179	79.709517	Graphite Schist	0.6	3.8	0.7	2.4	<0.5	2.1	<0.5	<0.5	0.6	4.0	<0.5	14.8	<0.5	6.9	5.7
7	109990	29.621137	79.723032	Graphite Schist	<0.5	<0.5	<0.5	<0.5	<0.5	<0.5	<0.5	<0.5	0.6	4.3	<0.5	31.1	0.6	2.7	1.8
8	109991	29.621103	79.723027	Graphite Schist	**<0.5**	**1.9**	**<0.5**	**1.2**	**<0.5**	**1.0**	**<0.5**	**<0.5**	**<0.5**	**1.1**	**<0.5**	**11.8**	**<0.5**	**6.4**	**2.2**
9	109992	29.62107	79.722977	Graphite Schist	<0.5	<0.5	<0.5	<0.5	<0.5	<0.5	<0.5	<0.5	0.8	1.8	<0.5	18.4	<0.5	7.3	3.7
10	109993	29.621058	79.722862	Graphite Schist	<0.5	2.8	0.6	1.8	<0.5	1.4	<0.5	<0.5	0.7	0.8	<0.5	20.3	<0.5	7.0	4.2
11	109994	29.620512	79.722855	Graphite Schist	<0.5	1.9	<0.5	1.3	<0.5	1.1	<0.5	<0.5	<0.5	1.5	<0.5	90.3	1.6	2.9	2.6
12	109995	29.629941	79.675877	Volcanic tuffaceous	1.3	7.9	1.6	5.2	0.7	4.2	0.6	0.6	2.3	4.6	<0.5	43.8	<0.5	26.4	3.7
13	109996	29.630513	79.677048	Volcanic tuffaceous	0.5	2.9	0.6	1.8	<0.5	1.5	<0.5	<0.5	0.5	1.7	<0.5	20.1	<0.5	7.7	1.4
14	109997	29.62111	79.723005	Graphite Schist	0.7	4.3	0.9	2.9	<0.5	2.2	<0.5	<0.5	0.7	<0.5	<0.5	13.7	<0.5	9.5	3.3
15	109998	29.636586	79.724532	Graphite Schist	1.2	8.0	1.7	5.5	0.7	4.2	0.5	<0.5	0.6	2.4	<0.5	28.7	<0.5	8.3	22.1
16	110005	29.621075	79.723056	Graphite Schist	0.52	3.09	0.62	2.08	<0.5	1.87	<0.5	0.94	1.86	1.62	1.74	39.42	<0.5	9.63	4.56
17	110006	29.621075	79.723056	Graphite Schist	0.61	4.18	0.90	3.02	<0.5	2.68	<0.5	<0.5	1.02	1.02	1.09	47.07	<0.5	9.96	13.20
18	110007	29.621075	79.723056	Graphite Schist	0.51	3.00	0.55	2.10	<0.5	2.00	<0.5	<0.5	1.10	0.93	1.00	46.65	<0.5	9.69	13.03
19	110008	29.621075	79.723056	Graphite Schist	1.60	10.60	2.01	6.82	0.87	6.12	0.76	<0.5	1.27	1.48	1.59	62.30	<0.5	11.50	18.10
20	110009	29.621075	79.723056	Graphite Schist	<0.5	0.50	<0.5	<0.5	<0.5	<0.5	<0.5	<0.5	1.44	3.75	4.03	110.50	0.54	5.68	2.22
21	110010	29.610435	79.70963	Graphite Schist	1.10	6.28	1.28	4.41	0.59	4.04	0.57	<0.5	0.73	4.06	4.36	144.02	0.75	9.88	14.95
22	110011	29.610435	79.70963	Graphite Schist	1.86	11.97	2.55	8.51	1.04	7.77	1.10	<0.5	1.19	4.69	5.04	29.27	<0.5	12.06	15.25
23	110012	29.610435	79.70963	Graphite Schist	**1.65**	**10.77**	**2.04**	**6.89**	**0.91**	**6.87**	**1.00**	<0.5	**0.90**	**4.75**	**5.10**	**36.90**	<0.5	**10.42**	**16.36**
24	110013	29.610435	79.70963	Graphite Schist	1.40	8.51	1.69	5.61	0.71	5.85	0.74	<0.5	0.79	3.18	3.42	63.11	<0.5	11.57	18.79
25	110014	29.610435	79.70963	Graphite Schist	1.21	7.11	1.36	4.66	0.55	4.12	0.64	<0.5	0.74	4.32	4.64	24.09	<0.5	10.42	17.11
26	110015	29.610692	79.709507	Graphite Schist	3.64	23.98	4.88	15.59	1.88	13.36	1.81	0.54	0.69	2.55	2.73	52.64	<0.5	10.00	27.97
27	110016	29.610692	79.709507	Graphite Schist	4.51	31.74	6.40	18.94	2.45	17.14	2.35	0.59	0.93	2.78	2.98	57.54	<0.5	11.28	23.86
28	110017	29.610692	79.709507	Graphite Schist	0.67	3.53	0.73	2.21	<0.5	2.41	<0.5	<0.5	0.52	2.08	2.24	44.71	<0.5	9.61	17.14
29	110018	29.610692	79.709507	Graphite Schist	<0.5	1.29	<0.5	0.90	<0.5	0.95	<0.5	<0.5	<0.5	0.94	1.01	6.32	<0.5	2.89	7.26
30	110019	29.610692	79.709507	Graphite Schist	0.85	4.89	0.81	2.58	<0.5	2.69	<0.5	<0.5	0.66	5.81	6.25	153.17	0.77	12.54	15.54
31`	109201	29.631603	79.715032	Qtz. Vain of Mica Schist	<0.5	<0.5	<0.5	<0.5	<0.5	<0.5	<0.5	<0.5	<0.5	0.54	<0.5	<0.5	<0.5	<0.5	<0.5
32	109202	29.635816	79.719848	Mica Schist	<0.5	<0.5	<0.5	<0.5	<0.5	<0.5	<0.5	<0.5	0.72	2.30	1.36	<0.5	2.03	9.55	1.48

Continue.

SL No	Sample ID	Latitude	Longitude	Lithology	Li	Be	Sc	V	Cr	Co	Ni	Cu	Zn	Ga	Ge	Se	Rb	Sr	Y	Zr
33	109204	29.635105	79.714393	Mica Schist	9.32	<0.5	0.95	111.60	289.81	2.67	0.58	1.02	19.54	1.83	<0.5	<0.5	11.75	9.38	2.69	0.78
34	109205	29.641709	79.714861	Mica Schist	40.52	0.68	6.79	1150.20	436.43	1.83	13.89	7.11	43.23	12.13	<0.5	<0.5	82.01	19.76	15.01	3.61
35	109210	29.611528	79.715905	Carb. Phyllite	7.23	1.56	11.06	462.81	423.66	5.89	94.15	98.76	217.09	17.91	<0.5	3.35	143.68	35.90	34.05	2.79
36	109212	29.611678	79.729612	Mica Schist	24.23	1.34	12.96	86.32	183.31	14.22	35.54	11.37	54.34	17.19	<0.5	1.66	106.27	59.65	23.12	2.51
37	109213	29.611263	79.727305	Mica Schist	65.21	1.57	23.35	166.90	225.08	23.60	79.93	4.26	65.31	31.81	<0.5	<0.5	213.95	64.24	37.51	2.42
38	109214	29.612963	79.724822	Carb. Phyllite	9.40	0.70	6.00	992.07	417.00	1.35	<0.5	2.58	11.61	7.93	<0.5	1.76	63.70	24.40	4.07	2.58
39	109216	29.641695	79.657337	Mica Schist	28.98	2.94	14.53	112.11	160.19	12.92	29.29	<0.5	52.12	22.23	<0.5	7.21	161.55	132.22	37.86	2.08
40	109218	29.636403	79.723705	Carb. Phyllite	31.45	1.83	6.09	1219.86	413.20	14.14	126.62	101.41	1690.39	17.72	<0.5	29.31	127.07	151.72	37.77	1.53
41	109219	29.636173	79.719654	Qtz. Vain of Mica Schist	9.18	<0.5	3.30	25.08	174.56	3.77	<0.5	<0.5	18.12	4.85	<0.5	1.04	38.03	32.09	7.50	1.21
42	109227	29.626358	79.745898	Carb. Phyllite	18.78	2.12	3.33	969.45	262.66	1.41	0.96	<0.5	17.77	8.85	<0.5	5.52	50.23	135.68	5.70	4.16
43	109228	29.627081	79.745878	Carb. Phyllite	17.02	2.97	7.60	1128.34	260.25	2.00	<0.5	0.88	19.91	17.66	<0.5	9.05	118.54	139.23	7.50	4.79
44	109229	29.626294	79.744137	Carb. Phyllite	11.18	1.17	5.02	943.15	253.13	1.72	1.02	0.54	6.91	12.48	<0.5	9.63	101.35	219.92	2.17	7.81
45	109230	29.626436	79.743254	Carb. Phyllite	22.54	2.00	7.44	728.50	261.66	3.02	7.62	2.90	23.52	17.03	<0.5	8.14	103.22	216.54	4.95	7.42
46	109232	29.623181	79.74268	Mica Schist	22.59	1.99	11.91	521.39	269.96	1.37	2.01	1.00	22.71	25.14	<0.5	5.42	124.67	42.95	0.74	2.44
47	109233	29.618908	79.739762	Mica Schist	14.46	1.43	8.22	76.57	152.30	10.64	18.63	0.99	51.13	16.86	<0.5	<0.5	90.36	97.40	30.78	3.32
48	109236	29.598399	79.7467047	Mica Schist	27.20	4.04	21.54	430.75	168.67	9.12	12.39	41.39	51.75	40.12	<0.5	1.69	289.62	132.76	21.06	2.23
49	109237	29.661522	79.69587	Carb. Phyllite	25.50	1.77	23.45	460.76	338.28	2.45	8.35	153.75	46.21	16.96	<0.5	9.81	129.11	30.60	22.78	2.34
50	109240	29.664125	79.699451	Mica Schist	30.31	3.83	16.45	466.52	228.13	4.63	14.13	25.03	95.54	25.53	<0.5	6.07	153.26	59.90	23.58	7.18
51	109241	29.66583	79.706938	Quarzite	4.35	<0.5	0.65	18.48	185.49	1.54	<0.5	2.05	6.82	1.87	<0.5	<0.5	10.95	30.36	7.06	1.24
52	109242	29.667667	79.711977	Quarzite	258.27	2.78	4.14	9.06	108.61	1.49	<0.5	0.58	49.70	17.46	<0.5	<0.5	517.27	28.28	13.03	1.68
53	109244	29.63859	79.668533	Carb. Phyllite	5.32	<0.5	3.89	1153.39	350.54	2.03	0.78	3.31	23.42	4.88	<0.5	0.70	32.72	14.49	12.22	2.48
54	109245	29.63943	79.66769	Carb. Phyllite	4.56	3.59	14.06	2765.36	472.79	3.54	28.80	101.22	50.94	16.79	<0.5	<0.5	99.70	27.78	35.70	3.79
55	109246	29.654743	79.683657	Qtz. Vain of Mica Schist	14.36	1.27	2.60	32.18	190.84	4.43	9.49	5.81	23.42	5.40	<0.5	1.72	51.07	36.53	5.44	2.10
56	110020	29.630777	79.741287	Tuffaceous	5.69	2.57	7.91	71.48	223.93	23.41	21.42	<0.5	46.14	14.97	<0.5	3.08	44.63	169.73	25.97	5.57
57	110021	29.617	79.701	Greisen	71.49	2.94	19.60	124.62	177.48	19.97	53.97	6.63	66.72	31.67	<0.5	2.54	183.75	81.14	32.63	2.32
58	110022	29.628	79.694	Greisen	18.70	4.91	15.51	106.75	192.34	22.87	46.99	<0.5	61.99	25.65	<0.5	1.57	24.50	137.60	33.68	4.41
59	110023	29.630	79.686	Quartz Mica Schist	14.88	<0.5	0.65	6.93	288.84	2.79	2.01	6.82	26.09	2.07	<0.5	2.85	5.93	7.59	0.90	0.70

60	110024	29.622	79.691	Quartz Vein	15.14	<0.5	<0.5	3.37	326.43	1.80	0.52	<0.5	3.99	<0.5	<0.5	0.96	2.87	8.58	0.77	<0.5
61	110025	29.65228	79.740522	Slug	3.72	1.24	4.68	33.45	45.15	10.59	0.66	263.38	80.41	25.34	<0.5	3.76	20.91	56.29	33.32	51.20
62	110026			River sample	2.91	<0.5	8.66	41.19	62.67	11.48	2.77	<0.5	38.93	6.64	<0.5	4.64	8.54	5.79	9.00	1.42
63	110027	29.62267	79.717522	Graphite Mica Schist	21.12	1.11	8.11	728.44	263.66	3.14	6.21	2.54	21.30	16.22	<0.5	7.68	102.55	214.65	4.96	6.88
64	110028	29.64478	79.674937	QBSS	24.05	2.09	10.25	62.38	163.71	9.57	14.38	<0.5	56.35	15.16	<0.5	2.89	102.94	147.70	26.45	2.73
65	110029	29.643795	79.677203	Quartz vein	5.35	<0.5	<0.5	3.12	274.84	0.94	0.66	<0.5	2.34	<0.5	<0.5	4.56	1.15	6.55	<0.5	0.77

Continue.

SL No	Sample ID	Latitude	Longitude	Lithology	Nb	Mo	Cd	In	Sn	Sb	Te	Cs	Ba	La	Ce	Pr	Nd	Sm	Eu	Gd
33	109204	29.635105	79.714393	Mica Schist	0.83	11.00	1.24	<0.5	0.77	18.48	<0.5	<0.5	678.54	2.34	4.24	<0.5	1.74	0.68	<0.5	<0.5
34	109205	29.641709	79.714861	Mica Schist	5.22	11.82	1.49	<0.5	1.83	23.85	<0.5	3.58	309.80	24.07	47.15	5.19	17.56	3.62	0.62	3.08
35	109210	29.611528	79.715905	Carb. Phyllite	6.81	8.93	4.52	<0.5	2.53	21.02	<0.5	5.67	780.77	37.42	68.36	9.29	36.83	6.83	1.34	4.94
36	109212	29.611678	79.729612	Mica Schist	9.53	<0.5	1.45	<0.5	3.25	20.78	<0.5	4.04	457.63	26.88	56.20	6.49	23.29	5.41	0.96	4.43
37	109213	29.611263	79.727305	Mica Schist	19.36	0.53	1.01	<0.5	6.35	20.48	<0.5	8.20	865.41	51.83	96.69	11.16	42.05	7.83	1.61	7.51
38	109214	29.612963	79.724822	Carb. Phyllite	2.92	45.58	1.80	<0.5	1.72	20.03	<0.5	1.82	290.88	7.41	11.32	1.25	4.33	0.72	<0.5	0.67
39	109216	29.641695	79.657337	Mica Schist	14.26	24.90	1.47	<0.5	4.15	20.34	<0.5	4.80	952.80	72.64	132.46	14.70	51.46	9.80	2.08	8.04
40	109218	29.636403	79.723705	Carb. Phyllite	6.56	32.97	44.91	<0.5	2.97	26.47	<0.5	4.12	140.12	14.26	29.97	4.95	19.30	4.69	0.88	4.49
41	109219	29.636173	79.719654	Qtz. Vain of Mica Schist	1.88	0.59	1.52	<0.5	1.86	17.15	<0.5	1.35	369.95	12.92	26.99	3.08	10.11	2.58	<0.5	1.88
42	109227	29.626358	79.745898	Carb. Phyllite	7.02	73.35	1.79	<0.5	2.95	29.01	<0.5	3.03	2516.01	16.04	24.04	2.62	8.22	1.64	<0.5	1.31
43	109228	29.627081	79.745878	Carb. Phyllite	9.02	45.59	1.78	<0.5	4.12	27.71	<0.5	1.99	1685.30	26.28	39.59	4.18	12.79	2.70	0.55	1.63
44	109229	29.626294	79.744137	Carb. Phyllite	11.44	64.90	1.72	<0.5	2.72	31.72	<0.5	1.65	7574.09	12.76	17.80	1.29	3.92	0.84	0.80	0.51
45	109230	29.626436	79.743254	Carb. Phyllite	11.47	51.92	1.68	<0.5	2.84	28.17	<0.5	2.06	13668.18	32.17	39.40	3.71	10.54	2.31	1.79	1.50
46	109232	29.623181	79.74268	Mica Schist	8.94	52.77	1.64	<0.5	3.40	18.79	<0.5	4.22	4148.03	24.50	31.12	2.20	4.90	0.84	<0.5	<0.5
47	109233	29.618908	79.739762	Mica Schist	12.03	0.55	1.40	<0.5	3.04	20.37	<0.5	5.80	408.76	49.39	91.29	10.42	37.60	7.52	1.52	6.97
48	109236	29.598399	79.7467047	Mica Schist	18.74	59.15	3.73	<0.5	7.47	21.55	<0.5	5.12	1512.17	31.84	51.67	7.21	25.50	4.58	1.04	4.33
49	109237	29.661522	79.69587	Carb. Phyllite	7.70	80.56	4.65	<0.5	3.30	21.58	<0.5	7.28	4889.20	48.91	75.32	10.49	37.84	7.56	1.58	5.06
50	109240	29.664125	79.699451	Mica Schist	15.56	44.62	2.06	<0.5	4.13	26.85	<0.5	10.60	7369.98	53.05	76.31	8.56	27.57	4.99	1.31	3.84
51	109241	29.66583	79.706938	Quarzite	1.83	2.85	1.61	<0.5	0.83	16.32	<0.5	0.95	186.34	8.98	20.70	2.22	8.08	2.43	<0.5	1.70
52	109242	29.667667	79.711977	Quarzite	16.19	<0.5	1.28	<0.5	50.56	21.15	<0.5	78.93	149.13	9.54	20.18	2.47	9.40	2.77	<0.5	2.14
53	109244	29.63859	79.668533	Carb. Phyllite	4.84	47.66	1.62	<0.5	1.77	57.72	<0.5	0.92	1414.35	8.53	11.58	2.34	10.71	2.79	0.56	2.23
54	109245	29.63943	79.66769	Carb. Phyllite	12.65	142.75	2.06	<0.5	2.85	25.70	<0.5	3.18	4062.61	17.60	27.76	4.67	19.92	5.42	1.62	4.90
55	109246	29.654743	79.683657	Qtz. Vain of Mica Schist	3.33	<0.5	1.32	<0.5	2.90	0.59	<0.5	2.62	152.89	6.80	13.51	1.50	4.64	1.09	<0.5	0.99
56	110020	29.630777	79.741287	Tuffaceous	7.20	<0.5	1.40	<0.5	2.69	17.05	<0.5	2.71	212.92	40.77	79.35	8.66	33.32	6.48	1.27	5.50
57	110021	29.617	79.701	Greisen	18.32	<0.5	1.47	<0.5	4.99	21.79	<0.5	5.31	633.12	57.48	106.65	11.64	42.09	8.26	1.78	7.15
58	110022	29.628	79.694	Greisen	9.99	<0.5	1.38	<0.5	6.58	20.62	<0.5	1.30	82.95	39.35	75.57	8.33	30.18	6.57	1.52	6.36
59	110023	29.630	79.686	Quartz Mica Schist	0.67	<0.5	1.21	<0.5	0.66	16.90	<0.5	<0.5	27.04	1.25	2.51	<0.5	0.94	<0.5	<0.5	<0.5

60	110024	29.622	79.691	Quartz Vein	<0.5	0.61	1.20	<0.5	<0.5	17.17	<0.5	<0.5	21.03	1.90	4.40	<0.5	1.24	<0.5	<0.5	<0.5
61	110025	29.65228	79.740522	Slug	2.40	<0.5	1.22	<0.5	12.98	0.67	<0.5	1.24	90.81	14.65	31.32	3.71	14.34	3.93	1.35	4.89
62	110026			River sample	<0.5	<0.5	1.33	0.78	4.88	0.74	<0.5	<0.5	18.95	8.50	18.73	1.87	7.35	2.74	<0.5	3.33
63	110027	29.62267	79.717522	Graphite Mica Schist	12.55	51.66	1.61	<0.5	3.17	30.06	<0.5	1.80	13242.63	32.02	38.96	3.62	9.89	2.27	1.51	1.4
64	110028	29.64478	79.674937	QBSS	9.34	<0.5	1.15	<0.5	2.01	19.94	<0.5	4.73	523.62	45.58	88.28	9.22	34.07	6.12	1.45	5.35
65	110029	29.643795	79.677203	Quartz vein	<0.5	<0.5	1.26	<0.5	0.75	<0.5	<0.5	<0.5	17.59	<0.5	<0.5	<0.5	<0.5	<0.5	<0.5	<0.5

Continue.

SL No	Sample ID	Latitude	Longitude	Lithology	Tb	Dy	Ho	Er	Tm	Yb	Lu	Hf	Ta	W	Tl	Pb	Bi	Th	U
33	109204	29.635105	79.714393	Mica Schist	<0.5	0.50	<0.5	<0.5	<0.5	<0.5	<0.5	<0.5	<0.5	1.40	<0.5	7.35	<0.5	1.19	1.48
34	109205	29.641709	79.714861	Mica Schist	<0.5	2.23	<0.5	1.55	<0.5	1.61	<0.5	<0.5	0.54	6.69	1.89	16.03	<0.5	21.73	2.18
35	109210	29.611528	79.715905	Carb. Phyllite	0.77	4.10	0.83	2.83	<0.5	2.22	<0.5	<0.5	0.60	6.82	1.12	1.31	0.51	11.22	2.69
36	109212	29.611678	79.729612	Mica Schist	0.62	4.02	0.80	2.54	<0.5	2.54	<0.5	<0.5	0.75	3.34	<0.5	5.18	<0.5	11.56	2.04
37	109213	29.611263	79.727305	Mica Schist	1.21	6.88	1.22	3.72	0.64	3.47	<0.5	<0.5	2.07	6.25	0.99	4.79	<0.5	21.07	3.73
38	109214	29.612963	79.724822	Carb. Phyllite	<0.5	0.60	<0.5	<0.5	<0.5	<0.5	<0.5	<0.5	<0.5	4.47	<0.5	5.15	<0.5	1.95	1.93
39	109216	29.641695	79.657337	Mica Schist	1.32	7.03	1.24	4.05	0.61	3.63	0.52	<0.5	1.12	5.15	1.36	4.58	0.64	18.56	15.52
40	109218	29.636403	79.723705	Carb. Phyllite	0.75	5.01	1.12	3.41	0.62	3.56	0.69	<0.5	<0.5	3.00	2.29	15.15	<0.5	7.25	14.35
41	109219	29.636173	79.719654	Qtz. Vain of Mica Schist	<0.5	1.43	<0.5	0.80	<0.5	0.89	<0.5	<0.5	<0.5	0.85	<0.5	<0.5	<0.5	5.14	1.09
42	109227	29.626358	79.745898	Carb. Phyllite	<0.5	1.20	<0.5	0.54	<0.5	0.75	<0.5	<0.5	<0.5	3.37	1.21	11.65	0.54	5.25	8.46
43	109228	29.627081	79.745878	Carb. Phyllite	<0.5	1.10	<0.5	0.76	<0.5	0.70	<0.5	<0.5	<0.5	4.02	3.23	0.91	<0.5	9.15	37.34
44	109229	29.626294	79.744137	Carb. Phyllite	<0.5	<0.5	<0.5	<0.5	<0.5	<0.5	<0.5	<0.5	<0.5	4.34	3.48	9.97	0.51	11.59	11.93
45	109230	29.626436	79.743254	Carb. Phyllite	<0.5	1.00	<0.5	0.51	<0.5	0.52	<0.5	<0.5	0.62	3.98	3.76	15.55	<0.5	14.77	13.96
46	109232	29.623181	79.74268	Mica Schist	<0.5	<0.5	<0.5	<0.5	<0.5	<0.5	<0.5	<0.5	<0.5	5.25	1.30	9.09	0.71	15.57	6.76
47	109233	29.618908	79.739762	Mica Schist	0.92	5.97	1.11	3.41	<0.5	3.00	<0.5	<0.5	1.09	2.62	<0.5	2.25	<0.5	19.35	2.57
48	109236	29.598399	79.7467047	Mica Schist	0.67	3.92	0.75	2.23	<0.5	2.28	<0.5	<0.5	1.33	6.45	1.40	48.03	2.13	15.26	8.53
49	109237	29.661522	79.69587	Carb. Phyllite	0.56	3.44	0.69	2.15	<0.5	2.14	<0.5	<0.5	<0.5	3.69	2.05	<0.5	<0.5	13.74	13.36
50	109240	29.664125	79.699451	Mica Schist	0.55	3.26	0.65	2.27	<0.5	2.14	<0.5	<0.5	0.65	5.69	3.12	35.64	0.71	21.50	16.36
51	109241	29.66583	79.706938	Quarzite	<0.5	1.52	<0.5	0.74	<0.5	0.71	<0.5	<0.5	<0.5	0.77	<0.5	<0.5	<0.5	3.52	1.29
52	109242	29.667667	79.711977	Quarzite	<0.5	2.42	<0.5	1.29	<0.5	1.31	<0.5	<0.5	4.72	8.39	2.20	3.42	2.11	4.96	1.23
53	109244	29.63859	79.668533	Carb. Phyllite	<0.5	1.80	<0.5	1.06	<0.5	1.08	<0.5	<0.5	<0.5	4.05	<0.5	6.80	0.53	3.03	6.21
54	109245	29.63943	79.66769	Carb. Phyllite	0.82	5.38	1.18	3.54	0.64	3.91	0.61	<0.5	0.82	6.64	1.69	6.81	0.73	11.75	17.38
55	109246	29.654743	79.683657	Qtz. Vain of Mica Schist	<0.5	0.92	<0.5	<0.5	<0.5	0.53	<0.5	<0.5	<0.5	0.82	0.63	12.66	<0.5	2.02	0.52
56	110020	29.630777	79.741287	Tuffaceous	0.86	5.79	1.07	3.00	<0.5	2.31	<0.5	0.57	0.66	127.41	<0.5	38.98	1.23	13.58	2.08
57	110021	29.617	79.701	Greisen	1.21	6.92	1.23	4.21	0.56	3.53	<0.5	<0.5	2.18	5.20	0.69	8.13	<0.5	22.46	4.30

58	110022	29.628	79.694	Greisen	1.03	6.25	1.27	3.80	0.50	3.42	0.57	<0.5	1.50	4.97	<0.5	49.07	4.42	13.78	3.24
59	110023	29.630	79.686	Quartz Mica Schist	<0.5	<0.5	<0.5	<0.5	<0.5	<0.5	<0.5	<0.5	<0.5	1.10	<0.5	11.12	<0.5	0.59	<0.5
60	110024	29.622	79.691	Quartz Vein	<0.5	<0.5	<0.5	<0.5	<0.5	<0.5	<0.5	<0.5	<0.5	0.88	<0.5	5.03	<0.5	<0.5	<0.5
61	110025	29.65228	79.740522	Slug	0.83	6.41	1.08	4.09	0.59	3.63	0.70	1.58	<0.5	0.54	4.29	91.94	<0.5	5.40	9.70
62	110026			River sample	0.51	2.27	<0.5	0.62	<0.5	0.57	<0.5	<0.5	<0.5	<0.5	3.62	39.53	<0.5	<0.5	3.08
63	110027	29.62267	79.717522	Graphite Mica Schist	<0.5	0.98	<0.5	0.59	<0.5	0.61	<0.5	<0.5	0.83	4.22	3.52	17.59	<0.5	14.58	13.56
64	110028	29.64478	79.674937	QBSS	0.90	5.34	0.97	3.29	<0.5	2.89	<0.5	<0.5	0.67	0.91	<0.5	4.47	<0.5	17.79	3.03
65	110029	29.643795	79.677203	Quartz vein	<0.5	<0.5	<0.5	<0.5	<0.5	<0.5	<0.5	<0.5	<0.5	<0.5	<0.5	11.45	<0.5	<0.5	<0.5

Continue.

SL No	Sample ID	Latitude	Longitude	Lithology	Li	Be	Sc	V	Cr	Co	Ni	Cu	Zn	Ga	Ge	Se	Rb	Sr	Y	Zr
66	110030	29.661188	79.696457	Graphite schist with sulphur	26.35	5.30	16.49	3536.30	485.14	3.66	36.32	78.69	166.03	20.64	<0.5	4.33	122.89	74.47	172.65	4.43
67	110031	29.651268	79.671318	Quartz vein	14.90	2.44	14.32	256.36	286.83	1.31	1.49	0.54	61.36	20.60	<0.5	9.61	162.35	28.75	6.63	2.69
68	110032	29.633041	79.742488	Chert	3.37	<0.5	1.23	18.01	165.58	1.64	<0.5	2.23	9.32	1.18	<0.5	5.05	4.24	9.98	1.92	0.93
69	110033	29.612305	79.708582	Mica schist with elongated mineral	70.62	3.45	14.22	71.33	107.83	2.99	0.66	7.16	52.77	25.58	<0.5	5.40	146.69	96.42	24.02	3.33
70	110034	29.628282	79.677865	Tuffaceous	3.02	<0.5	1.61	17.91	107.54	4.15	0.92	<0.5	49.46	6.52	<0.5	4.40	31.76	68.54	13.75	3.17
71	110035	29.621045	79.72905	Poly metallic layer of Graphite Schist	5.16	1.60	7.67	85.45	200.16	9.36	24.82	7.78	15.25	16.15	<0.5	14.29	59.28	181.97	16.10	1.82
72	110036	29.610765	79.70919	Quartz vein in Carb Phyllite	11.74	<0.5	1.13	224.15	264.07	1.29	3.02	26.35	10.63	2.60	<0.5	7.92	9.18	11.93	7.90	1.28
73	110037	29.621603	79.677427	Younger Granite	24.45	1.45	3.62	28.62	165.64	3.41	<0.5	<0.5	21.89	11.14	<0.5	2.20	100.30	76.88	11.76	1.88
74	110038	29.612545	79.73674	Lit per lit	15.81	1.57	5.96	50.95	90.20	8.03	16.27	1.47	37.24	14.34	<0.5	3.13	19.23	176.02	35.12	5.21
75	110039				24.15	2.25	12.09	73.75	133.27	12.35	23.09	<0.5	59.82	16.33	<0.5	3.99	112.61	126.74	36.20	2.69
76	110040	29.651268	79.671318	Chert	5.37	<0.5	4.77	25.40	167.15	1.02	3.22	13.83	7.40	2.27	<0.5	3.16	15.05	28.51	14.93	0.84
77	110041	29.612545	79.73674	Lit per lit	10.77	2.50	10.94	74.23	132.16	11.31	34.62	1.26	53.22	18.66	<0.5	3.15	61.16	165.10	35.48	3.33
78	110042	29.614515	79.690601	Quartz Mica Schist	9.34	<0.5	1.78	17.54	91.64	2.77	6.63	1.53	14.40	8.30	<0.5	3.93	73.05	54.85	11.60	1.25
79	110043	29.629995	79.675263	Tuffaceous	49.28	1.33	5.98	43.18	108.68	10.33	8.80	2.25	62.09	13.46	<0.5	6.96	68.81	197.43	27.99	7.89
80	110044	29.635	79.682	Tuffaceous	72.38	4.88	14.58	87.25	120.11	6.47	10.91	2.56	73.30	24.32	<0.5	3.34	231.76	52.37	30.70	2.83
81	110045	29.630517	79.67716	Tuffaceous	6.16	<0.5	<0.5	4.36	285.35	0.96	6.47	5.75	3.66	<0.5	<0.5	<0.5	4.88	7.35	0.80	0.85
82	109971	29.615107	79.726605	Quartz vein at depth 1-2.2 m (XRF)	15.26	0.96	1.94	182.60	292.56	0.99	2.96	22.32	4.37	2.32	<0.5	3.05	20.16	9.07	2.51	2.72
83	109946	29.659791	79.697149	Graphite in Carb Phyllite	32.16	5.65	14.97	922.99	324.34	4.29	19.29	26.82	40.94	21.05	<0.5	8.59	150.08	47.83	8.19	3.64
84	110046	29.622493	79.69845	Quartz vein	<0.5	<0.5	<0.5	2.31	239.32	1.14	1.58	1.26	2.16	<0.5	<0.5	<0.5	1.63	5.65	<0.5	<0.5
85	110047	29.664913	79.715007	Quartz vein	4.51	<0.5	0.56	5.71	198.95	2.60	1.87	0.97	9.85	0.88	<0.5	1.75	11.19	15.12	2.52	1.13
86	110048	29.604335	79.696618	Quartz vein	2.66	<0.5	<0.5	4.22	211.13	1.18	0.94	0.52	3.64	<0.5	<0.5	1.29	3.21	7.20	<0.5	0.80
87	110049	29.604335	79.696618	Mica Schist	60.91	4.86	12.04	83.24	142.38	12.28	32.95	10.72	65.25	17.39	<0.5	1.80	127.22	78.52	27.60	4.76
88	110050	29.660631	79.716183	Tuffaceous	64.52	6.28	10.81	68.19	109.59	6.62	1.03	<0.5	65.05	20.03	<0.5	3.56	224.50	77.58	7.27	3.25
89	110054	29.660463	79.715814	Younger Granite	99.57	5.47	5.42	29.93	94.00	4.97	7.13	4.85	78.17	23.13	<0.5	2.07	366.57	63.84	11.90	2.53
90	110055	29.63749	79.701315	Quartz vein in Mica Schist	46.37	4.73	5.49	38.92	188.78	9.39	40.47	31.02	112.44	7.82	<0.5	1.73	69.29	73.06	12.09	1.27
91	110056	29.65412	79.735008	Quartz Mica Schist	20.38	<0.5	1.14	9.72	132.67	1.49	5.58	1.58	11.66	5.79	<0.5	1.52	96.47	50.61	11.19	1.61
92	110057	29.630303	79.700202	Quartz Vein	19.59	<0.5	0.52	7.00	198.25	1.68	1.89	3.35	11.76	1.67	<0.5	1.42	19.26	14.73	2.18	0.64

93	110058	29.601307	79.729308	Carb phyllite with sulphur	35.28	3.41	10.15	117.97	135.76	13.31	48.72	14.58	344.24	18.31	<0.5	2.77	116.61	212.77	12.13	1.39
94	110059	29.615107	79.726605	Quartz vein	30.76	2.44	6.62	129.70	258.92	2.29	6.93	11.52	33.90	5.90	<0.5	4.02	51.57	16.50	3.98	2.73
95	110060	29.601307	79.729308	Metallic layer of Carb phyllite	35.44	2.92	5.14	72.78	156.75	13.97	94.20	<0.5	521.00	14.69	<0.5	4.08	110.18	246.75	14.73	3.47
96	109962	29.641397	79.665528	Carb phyllite	84.39	<0.5	5.70	54.36	127.53	13.87	47.95	2.66	22.47	15.78	<0.5	1.26	71.04	93.14	12.66	3.43
97	110061	29.637043	79.698888	Younger Granite	62.28	8.50	20.39	131.10	119.29	4.67	5.59	4.25	49.27	40.26	<0.5	2.59	286.63	148.29	47.41	3.77
98	110062	29.628282	79.677865	Tuffaceous	27.36	4.75	10.97	75.08	125.79	8.17	11.94	1.96	48.99	22.46	<0.5	0.99	166.76	89.35	28.18	12.66
99	110063	29.637048	79.698823	Younger Granite	41.74	4.27	6.58	28.20	95.73	5.64	4.28	1.52	46.18	18.48	<0.5	1.98	225.70	147.99	22.68	1.84
100	110064	29.63521	79.694403	Quartz vein in Mica Schist	25.82	1.87	3.65	21.52	74.30	3.46	4.70	2.57	34.80	9.17	<0.5	2.68	114.24	36.62	16.94	2.67

Continue.

SL No	Sample ID	Latitude	Longitude	Lithology	Nb	Mo	Cd	In	Sn	Sb	Te	Cs	Ba	La	Ce	Pr	Nd	Sm	Eu	Gd
66	110030	29.661188	79.696457	Graphite schist with sulphur	12.28	8.50	2.24	<0.5	5.52	23.05	<0.5	3.06	19806.86	70.03	81.46	17.86	77.88	20.48	6.77	21.51
67	110031	29.651268	79.671318	Quartz vein	6.93	36.24	2.32	<0.5	6.64	0.67	<0.5	3.30	2942.28	3.89	3.89	0.56	1.84	0.57	<0.5	0.60
68	110032	29.633041	79.742488	Chert	0.58	0.72	1.36	<0.5	1.20	<0.5	<0.5	<0.5	195.57	1.97	3.28	<0.5	1.59	<0.5	<0.5	<0.5
69	110033	29.612305	79.708582	Mica schist with elongated mineral	13.54	0.83	1.50	<0.5	10.90	0.65	<0.5	24.44	588.14	40.81	82.68	9.42	31.16	6.90	1.26	5.31
70	110034	29.628282	79.677865	Tuffaceous	6.07	<0.5	1.72	<0.5	4.36	0.55	<0.5	2.78	230.52	22.32	43.15	4.62	14.67	3.08	0.73	2.92
71	110035	29.621045	79.72905	Poly metallic layer of Graphite Schist	8.80	0.76	1.23	<0.5	4.24	0.63	<0.5	2.16	544.89	27.15	50.96	5.72	18.72	4.15	0.91	2.96
71	110036	29.610765	79.70919	Quartz vein in Carb Phyllite	1.16	8.45	1.21	<0.5	1.06	0.68	<0.5	0.54	253.67	6.29	8.92	1.55	5.72	1.79	<0.5	1.19
73	110037	29.621603	79.677427	Younger Granite	6.12	<0.5	1.03	<0.5	5.60	19.62	<0.5	11.38	768.95	23.33	49.89	5.34	18.83	3.85	0.70	3.00
74	110038	29.612545	79.73674	Lit per lit	7.34	<0.5	1.54	<0.5	7.32	0.74	<0.5	1.02	58.23	33.81	61.85	6.76	22.60	5.37	1.15	4.82
75	110039				8.61	<0.5	1.41	<0.5	3.58	0.58	<0.5	5.78	404.35	56.22	111.18	11.67	41.05	7.92	1.46	7.94
76	110040	29.651268	79.671318	Chert	1.15	0.62	1.43	<0.5	2.11	<0.5	<0.5	<0.5	1452.73	13.02	29.46	3.95	10.67	1.97	<0.5	1.97
77	110041	29.612545	79.73674	Lit per lit	8.67	<0.5	1.90	<0.5	7.07	0.61	<0.5	3.43	131.21	38.08	73.87	8.40	28.71	6.21	1.51	5.99
78	110042	29.614515	79.690601	Quartz Mica Schist	4.32	<0.5	1.10	<0.5	2.54	0.59	<0.5	4.29	532.31	20.45	40.52	4.44	14.54	2.98	0.82	2.37
79	110043	29.629995	79.675263	Tuffaceous	6.61	<0.5	1.39	<0.5	4.34	0.61	<0.5	5.91	486.76	36.81	74.82	8.46	26.90	6.32	1.26	5.94
80	110044	29.635	79.682	Tuffaceous	13.00	<0.5	1.62	<0.5	8.53	0.65	<0.5	17.41	1098.84	32.54	65.82	7.42	24.41	5.77	1.18	5.14
81	110045	29.630517	79.67716	Tuffaceous	<0.5	0.73	1.12	<0.5	1.16	0.57	<0.5	0.83	22.07	1.49	3.38	<0.5	0.67	<0.5	<0.5	<0.5
82	109971	29.615107	79.726605	Quartz vein at depth 1-2.2 m (XRF)	0.97	11.15	1.14	<0.5	<0.5	<0.5	<0.5	0.89	112.79	4.49	9.15	1.21	3.74	0.77	<0.5	0.66
83	109946	29.659791	79.697149	Graphite in Carb Phyllite	15.16	74.50	2.98	<0.5	4.16	22.80	<0.5	2.49	24699.70	6.43	8.34	1.33	5.21	1.25	2.87	1.01
84	110046	29.622493	79.69845	Quartz vein	<0.5	0.53	1.45	<0.5	0.54	<0.5	<0.5	<0.5	15.90	<0.5	<0.5	<0.5	<0.5	<0.5	<0.5	<0.5
85	110047	29.664913	79.715007	Quartz vein	0.79	0.54	1.25	<0.5	0.56	<0.5	<0.5	1.35	46.58	2.46	6.63	0.67	2.58	0.62	<0.5	<0.5
86	110048	29.604335	79.696618	Quartz vein	<0.5	<0.5	1.06	<0.5	0.54	<0.5	<0.5	<0.5	22.09	0.60	1.24	<0.5	<0.5	<0.5	<0.5	<0.5
87	110049	29.604335	79.696618	Mica Schist	11.71	<0.5	0.90	<0.5	2.87	0.61	<0.5	5.23	466.08	41.42	75.41	8.49	30.17	7.25	0.98	5.56
88	110050	29.660631	79.716183	Tuffaceous	11.09	<0.5	1.41	<0.5	5.02	<0.5	<0.5	13.77	608.02	53.82	94.11	11.13	35.69	7.08	1.26	5.53
89	110054	29.660463	79.715814	Younger Granite	19.42	<0.5	1.20	<0.5	4.82	0.59	<0.5	21.34	323.73	32.73	77.69	9.60	33.26	7.45	0.70	5.54
90	110055	29.63749	79.701315	Quartz vein in Mica Schist	4.23	0.90	3.10	<0.5	0.98	<0.5	<0.5	4.78	983.73	11.03	25.27	2.79	10.03	1.80	<0.5	2.10
91	110056	29.65412	79.735008	Quartz Mica Schist	3.86	<0.5	1.44	<0.5	1.80	<0.5	<0.5	2.75	389.25	17.99	32.83	4.61	16.55	3.67	0.67	2.93

92	110057	29.630303	79.700202	Quartz Vein	1.19	<0.5	1.21	<0.5	0.77	<0.5	<0.5	1.44	110.56	4.19	9.62	1.13	3.52	0.76	<0.5	0.65
93	110058	29.601307	79.729308	Carb phyllite with sulphur	6.14	10.25	4.48	<0.5	2.81	19.72	<0.5	6.63	4719.20	27.60	56.19	6.04	22.50	4.70	1.58	3.19
94	110059	29.615107	79.726605	Quartz vein	2.59	39.75	1.64	<0.5	1.53	20.50	<0.5	1.46	284.00	8.93	17.75	2.06	7.55	1.40	<0.5	0.91
95	110060	29.601307	79.729308	Metallic layer of Carb phyllite	7.07	1.99	3.07	<0.5	2.28	19.04	<0.5	7.76	6112.07	31.18	52.03	5.96	21.76	4.52	1.48	3.66
96	109962	29.641397	79.665528	Carb phyllite	6.65	<0.5	1.27	<0.5	2.18	1.07	<0.5	4.39	965.60	17.40	38.32	3.95	13.29	2.98	0.55	2.39
97	110061	29.637043	79.698888	Younger Granite	18.78	<0.5	1.08	<0.5	33.19	1.09	<0.5	25.32	1722.31	78.02	70.03	16.89	56.13	12.40	2.04	10.77
98	110062	29.628282	79.677865	Tuffaceous	14.64	<0.5	1.12	<0.5	4.50	<0.5	<0.5	18.33	977.09	55.10	98.14	10.67	37.56	7.81	1.19	5.88
99	110063	29.637048	79.698823	Younger Granite	15.01	<0.5	1.38	<0.5	10.65	<0.5	<0.5	18.77	245.32	22.11	47.27	5.47	18.55	4.53	0.63	3.75
100	110064	29.63521	79.694403	Quartz vein in Mica Schist	5.57	<0.5	1.36	<0.5	1.76	<0.5	<0.5	17.05	436.09	21.19	39.50	4.96	17.97	3.70	0.71	3.94

Continue.

SL No	Sample ID	Latitude	Longitude	Lithology	Tb	Dy	Ho	Er	Tm	Yb	Lu	Hf	Ta	W	Tl	Pb	Bi	Th	U
66	110030	29.661188	79.696457	Graphite schist with sulphur	3.88	27.24	6.02	20.27	2.52	17.85	2.29	<0.5	0.91	8.39	1.15	296.46	1.31	15.46	13.34
67	110031	29.651268	79.671318	Quartz vein	<0.5	0.90	<0.5	0.56	<0.5	0.66	<0.5	<0.5	<0.5	1.58	1.48	18.35	0.67	1.91	11.76
68	110032	29.633041	79.742488	Chert	<0.5	<0.5	<0.5	<0.5	<0.5	<0.5	<0.5	<0.5	<0.5	<0.5	<0.5	10.25	<0.5	<0.5	<0.5
69	110033	29.612305	79.708582	Mica schist with elongated mineral	0.87	4.76	0.90	2.11	<0.5	2.07	<0.5	<0.5	1.01	4.82	0.64	17.68	0.70	15.42	1.88
70	110034	29.628282	79.677865	Tuffaceous	<0.5	2.82	0.51	1.20	<0.5	1.18	<0.5	<0.5	<0.5	0.69	<0.5	10.52	<0.5	9.26	0.95
71	110035	29.621045	79.72905	Poly metallic layer of Graphite Schist	<0.5	2.67	0.57	1.47	<0.5	1.63	<0.5	<0.5	0.62	0.92	1.02	13.49	<0.5	5.49	3.03
71	110036	29.610765	79.70919	Quartz vein in Carb Phyllite	<0.5	1.11	<0.5	0.66	<0.5	0.68	<0.5	<0.5	<0.5	0.95	<0.5	15.73	<0.5	1.17	1.68
73	110037	29.621603	79.677427	Younger Granite	<0.5	2.33	<0.5	1.42	<0.5	1.18	<0.5	<0.5	0.57	3.36	<0.5	93.16	<0.5	9.78	2.53
74	110038	29.612545	79.73674	Lit per lit	0.88	5.34	1.13	2.58	0.50	2.81	0.51	<0.5	0.84	0.53	1.29	26.94	4.80	7.80	1.52
75	110039				1.13	7.70	1.33	3.61	0.63	3.67	0.64	<0.5	0.65	0.96	<0.5	19.84	<0.5	18.33	2.70
76	110040	29.651268	79.671318	Chert	<0.5	2.32	<0.5	1.12	<0.5	1.42	<0.5	<0.5	<0.5	0.80	<0.5	9.03	<0.5	2.14	0.96
77	110041	29.612545	79.73674	Lit per lit	1.00	6.14	1.16	3.10	0.51	3.13	0.59	<0.5	0.55	<0.5	<0.5	8.09	2.76	11.96	2.62
78	110042	29.614515	79.690601	Quartz Mica Schist	<0.5	1.99	<0.5	0.95	<0.5	1.01	<0.5	<0.5	<0.5	1.20	<0.5	11.71	<0.5	5.63	0.97
79	110043	29.629995	79.675263	Tuffaceous	0.83	5.56	0.95	2.52	<0.5	2.29	<0.5	0.62	<0.5	0.51	<0.5	10.18	<0.5	11.52	1.63
80	110044	29.635	79.682	Tuffaceous	0.86	5.59	1.04	2.90	0.51	3.01	0.63	<0.5	0.90	3.88	0.90	12.50	<0.5	17.26	2.80
81	110045	29.630517	79.67716	Tuffaceous	<0.5	<0.5	<0.5	<0.5	<0.5	<0.5	<0.5	<0.5	<0.5	<0.5	<0.5	11.83	<0.5	0.91	<0.5
82	109971	29.615107	79.726605	Quartz vein at depth 1-2.2 m (XRF)	<0.5	<0.5	<0.5	<0.5	<0.5	<0.5	<0.5	<0.5	<0.5	2.71	<0.5	10.25	<0.5	1.69	0.73
83	109946	29.659791	79.697149	Graphite in Carb Phyllite	<0.5	1.34	<0.5	1.04	<0.5	0.97	<0.5	<0.5	1.57	4.13	4.07	5.29	<0.5	11.06	11.94
84	110046	29.622493	79.69845	Quartz vein	<0.5	<0.5	<0.5	<0.5	<0.5	<0.5	<0.5	<0.5	<0.5	<0.5	<0.5	11.23	<0.5	<0.5	<0.5
85	110047	29.664913	79.715007	Quartz vein	<0.5	<0.5	<0.5	<0.5	<0.5	<0.5	<0.5	<0.5	<0.5	0.53	<0.5	7.58	<0.5	0.56	<0.5
86	110048	29.604335	79.696618	Quartz vein	<0.5	<0.5	<0.5	<0.5	<0.5	<0.5	<0.5	<0.5	<0.5	<0.5	<0.5	9.05	<0.5	<0.5	<0.5
87	110049	29.604335	79.696618	Mica Schist	0.79	4.95	0.98	2.82	<0.5	2.28	<0.5	<0.5	1.46	3.52	<0.5	14.48	<0.5	14.79	2.13
88	110050	29.660631	79.716183	Tuffaceous	0.54	2.65	<0.5	0.61	<0.5	<0.5	<0.5	<0.5	0.77	2.30	<0.5	20.54	<0.5	20.00	2.19
89	110054	29.660463	79.715814	Younger Granite	0.61	2.95	<0.5	1.15	<0.5	0.94	<0.5	<0.5	2.68	2.05	<0.5	21.54	0.58	24.15	4.22
90	110055	29.63749	79.701315	Quartz vein in Mica Schist	<0.5	2.01	<0.5	1.16	<0.5	0.96	<0.5	<0.5	<0.5	1.39	<0.5	9.69	<0.5	5.32	6.04

91	110056	29.65412	79.735008	Quartz Mica Schist	<0.5	1.95	<0.5	1.01	<0.5	0.79	<0.5	<0.5	<0.5	1.90	<0.5	1.52	<0.5	8.72	0.77
92	110057	29.630303	79.700202	Quartz Vein	<0.5	<0.5	<0.5	<0.5	<0.5	<0.5	<0.5	<0.5	<0.5	0.74	<0.5	9.58	<0.5	1.48	<0.5
93	110058	29.601307	79.729308	Carb phyllite with sulphur	0.59	2.50	<0.5	1.22	<0.5	1.06	<0.5	<0.5	<0.5	2.00	0.71	16.72	<0.5	11.78	7.24
94	110059	29.615107	79.726605	Quartz vein	<0.5	0.54	<0.5	<0.5	<0.5	<0.5	<0.5	<0.5	<0.5	1.48	<0.5	22.97	<0.5	3.59	1.57
95	110060	29.601307	79.729308	Metallic layer of Carb phyllite	0.51	2.27	<0.5	1.41	<0.5	1.18	<0.5	<0.5	0.71	2.49	2.08	8.44	<0.5	25.09	5.27
96	109962	29.641397	79.665528	Carb phyllite	<0.5	2.39	<0.5	1.48	<0.5	1.06	<0.5	<0.5	1.17	1.58	<0.5	10.25	<0.5	9.07	1.15
97	110061	29.637043	79.698888	Younger Granite	1.54	10.35	1.67	4.97	0.72	3.99	0.62	<0.5	2.20	8.17	<0.5	10.07	<0.5	31.54	3.84
98	110062	29.628282	79.677865	Tuffaceous	0.87	5.27	0.94	2.64	<0.5	2.29	<0.5	<0.5	1.41	4.41	<0.5	18.82	<0.5	20.28	2.99
99	110063	29.637048	79.698823	Younger Granite	0.56	3.64	0.74	2.31	<0.5	2.36	<0.5	<0.5	3.27	10.47	<0.5	20.53	0.79	9.11	2.60
100	110064	29.63521	79.694403	Quartz vein in Mica Schist	0.62	3.15	0.58	1.57	<0.5	1.15	<0.5	<0.5	<0.5	2.57	<0.5	12.16	<0.5	6.51	0.74

Annexure XII_ICPMS Data of Surface Check Samples (All data in ppm)

Sl. No.	Sample ID	Latitude	Longitude	Sample type	Lithology	Lab	Li	Be	B	Sc	V	Cr	Co	Ni	Cu	Zn	Ga	Ge	Se	Rb	Sr	Y
1	109296	29.63641	79.69236	BR	Foliated Granite	BV	63.7	3	-	3.5	21	47	3.7	8.2	<0.5	61.5	19.1	<0.5	1.1	292.7	68.3	14.7
	113591					Shiva	62.87	2.51	<5	1.67	-	-	4.33	-	-	-	16.25	<0.5	<0.5	308.08	-	11.97
2	110014	29.61044	79.70963	BR	Graphite Schist	BV	21.57	3.43	-	10.61	1142	404.78	4.53	81.26	433.69	132.14	14.21	<0.5	6.23	70.82	34.48	38.15
	113592					Shiva	23.27	1.85	<5	9.1	-	-	4.5	-	-	-	12.5	<0.5	5.09	76.35	-	36.41
3	110037	29.6216	79.67743	BR	Foliated Granite	BV	24.45	1.45	-	3.62	28.62	165.64	3.41	<0.5	<0.5	21.89	11.14	<0.5	2.2	100.3	76.88	11.76
	113593					Shiva	71.82	4.23	<5	14.16	-	-	6.38	-	-	-	33.46	<0.5	<0.5	313.87	-	12.26
4	110019	29.61069	79.70951	BR	Graphite Schist	BV	12.59	1.68	-	18.25	2414	400.09	1.55	32.79	24.52	18.81	21.23	<0.5	3.88	106.47	63.89	22.55
	113594					Shiva	21.31	2.19	<5	15.7	-	-	1.53	-	-	-	17.32	<0.5	3.26	106.3	-	21.87
5	110013	29.61044	79.70963	BR	Graphite Schist	BV	30.78	3.69	-	11.88	1052	357.37	4.95	91.03	436.18	143.17	15.41	<0.5	3.63	68.48	40.35	47.43
	113595					Shiva	23.89	1.92	<5	11.65	-	-	4.7	-	-	-	12.89	<0.5	3.71	73.9	-	44.78
6	109995	29.62994	79.67588	BR	Tuffaceous Rock	BV	62.5	5.8	-	18.7	120	98.2	9.8	17.9	<0.5	57.4	37	<0.5	4	243.6	100.2	42.4
	113596					Shiva	56.48	3.06	<5	17.06	-	-	18.53	-	-	-	26.03	<0.5	0.91	239.58	-	29.6
7	109987	29.61062	79.7093	BR	Graphite Schist	BV	16.7	2.2	-	10.4	1504	219.3	0.7	15.6	5.1	23.9	13.5	<0.5	3.7	77.8	33.4	27.6
	113597					Shiva	16.7	1.72	<5	10.9	-	-	1.68	-	-	-	13.45	<0.5	2.44	80.52	-	22.89
8	109998	29.63659	79.72453	BR	Graphite Schist	BV	23.1	3	-	12.6	511	210.4	12.3	76.7	203.8	336.5	18.8	<0.5	12.7	110.1	151.3	51.5
	113598					Shiva	18.08	2.18	<5	12.41	-	-	13.95	-	-	-	16.53	<0.5	24.16	103.2	-	54.9
9	110012	29.61044	79.70963	BR	Graphite Schist	BV	34.45	1.59	-	10.84	1285	353.9	4.47	75.48	399.72	148.58	14.34	<0.5	9.51	75.52	36.4	60
	113599					Shiva	23.28	1.97	<5	11.36	-	-	4	-	-	-	13.65	<0.5	10.2	79.06	-	54.17
10	109993	29.62106	79.72286	BR	Graphite Schist	BV	13	2.4	-	8.2	242	127.9	9.7	24	13.7	20.3	15.9	<0.5	3.5	68.8	156.7	16.4
	113600					Shiva	23.26	1.87	<5	11.43	-	-	4.65	-	-	-	13.72	<0.5	8.84	80.79	-	55.22

Sl. No.	Sample ID	Latitude	Longitude	Sample type	Lithology	Lab	Zr	Nb	Mo	Cd	In	Sn	Sb	Te	Cs	Ba	La	Ce	Pr	Nd	Sm	Eu
1	109296	29.63641	79.69236	BR	Foliated Granite	BV	1.5	14.5	6.1	<0.5	<0.5	27.5	<0.5	<0.5	20.7	276.7	21.5	43	5.7	20.9	4.8	0.6
	113591					Shiva	-	8.75	<0.5	<0.5	<0.5	13.99	<0.5	1.1	19.4	-	26.97	57.49	6.8	25.82	5.51	0.78
2	110014	29.61044	79.70963	BR	Graphite Schist	BV	2.49	8.99	35.65	1.85	<0.5	3.27	34.74	<0.5	5.93	2120.17	36.84	57.29	9.59	38.78	8.19	2.07
	113592					Shiva	-	5.23	20.25	<0.5	<0.5	2.98	12.92	<0.5	5.76	-	35.2	56.62	9.71	40	8.57	3.39
3	110037	29.6216	79.67743	BR	Foliated Granite	BV	1.88	6.12	<0.5	1.03	<0.5	5.6	19.62	<0.5	11.38	768.95	23.33	49.89	5.34	18.83	3.85	0.7
	113593					Shiva	-	20.15	0.68	<0.5	<0.5	54.22	<0.5	0.55	28.28	-	27.22	69.7	8.47	29.94	6	2.08
4	110019	29.61069	79.70951	BR	Graphite Schist	BV	6.75	19	74.53	1.41	<0.5	2.98	39.87	0.58	4	2966.32	47.61	61.33	11.34	44.66	9.3	2.09
	113594					Shiva	-	13.13	40.52	2.36	<0.5	4.1	20.77	<0.5	3.58	-	40.97	56.6	10.6	41.76	7.99	4.11
5	110013	29.61044	79.70963	BR	Graphite Schist	BV	2.91	9.64	30.63	1.67	<0.5	2.97	41.21	<0.5	6.32	1865.35	40.62	66.94	10.35	41.94	9.09	2.32
	113595					Shiva	-	6.53	18.15	<0.5	<0.5	2.5	18.82	<0.5	5.8	-	38.39	66.07	10.46	43.02	9.27	3.28
6	109995	29.62994	79.67588	BR	Tuffaceous Rock	BV	13	23	1.5	<0.5	<0.5	<0.5	<0.5	<0.5	11	1538.5	64.4	130.5	15.4	54.5	10.4	2
	113596					Shiva	-	13.27	0.52	<0.5	<0.5	4.22	<0.5	<0.5	19.48	-	52.5	104.84	13.18	50	9.68	2.75
7	109987	29.61062	79.7093	BR	Graphite Schist	BV	4.5	9.8	56.7	<0.5	<0.5	4	5.6	<0.5	2.6	2315.6	27.7	41.1	7.5	30.4	6.3	1.2
	113597					Shiva	-	6.15	31.35	<0.5	<0.5	1.62	13.83	<0.5	2.55	-	34.57	51.08	9.08	37.39	6.93	3.29
8	109998	29.63659	79.72453	BR	Graphite Schist	BV	1.5	9.8	52.9	4	<0.5	<0.5	1	<0.5	2.9	4899.2	33.5	54.2	8.1	30.8	6.9	1.7
	113598					Shiva	-	5.85	37.8	4.49	<0.5	2.14	6.06	<0.5	2.67	-	34.47	54.42	8.04	33.36	6.94	4.61
9	110012	29.61044	79.70963	BR	Graphite Schist	BV	3.42	9.14	59.45	1.77	<0.5	3.91	34.72	<0.5	6.22	2309.89	39.34	60.47	10.67	41.63	10.69	2.48
	113599					Shiva	-	5.28	33.08	<0.5	<0.5	2.78	11.9	<0.5	5.75	-	36.21	59.77	10.43	43.16	9.91	3.7
10	109993	29.62106	79.72286	BR	Graphite Schist	BV	1.8	8.9	3	<0.5	<0.5	<0.5	<0.5	<0.5	2	2693.6	22.4	44.2	5.1	17.9	3.5	0.9
	113600					Shiva	-	5.37	32.13	<0.5	<0.5	2.94	13.18	<0.5	5.79	-	35.92	58.41	10.29	43.17	9.77	3.63

Sl. No.	Sample ID	Latitude	Longitude	Sample type	Lithology	Lab	Gd	Tb	Dy	Ho	Er	Tm	Yb	Lu	Hf	Ta	W	Re	Tl	Pb	Bi	Th	U
1	109296	29.63641	79.69236	BR	Foliated Granite	BV	3.9	0.6	3	0.5	1.6	<0.5	1.2	<0.5	<0.5	3.8	6.2	-	<0.5	29.4	1.4	14.6	2.5
	113591					Shiva	5.96	0.57	2.81	<0.5	1.1	<0.5	0.82	<0.5	1.34	3.6	6.16	<0.5	1.45	-	1.61	18.33	2.19
2	110014	29.61044	79.70963	BR	Graphite Schist	BV	7.96	1.21	7.11	1.36	4.66	0.55	4.12	0.64	<0.5	0.74	4.32	-	4.64	24.09	<0.5	10.42	17.11
	113592					Shiva	8.83	1.09	6.83	1.3	3.67	0.54	3.79	0.58	<0.5	0.6	2.54	<0.5	1.6	-	<0.5	10.66	16.26
3	110037	29.6216	79.67743	BR	Foliated Granite	BV	3	<0.5	2.33	<0.5	1.42	<0.5	1.18	<0.5	<0.5	0.57	3.36	-	<0.5	93.16	<0.5	9.78	2.53
	113593					Shiva	6.21	0.59	3.69	0.66	1.72	<0.5	1.87	<0.5	0.97	3.49	12.12	<0.5	1.31	-	<0.5	30.49	2.73
4	110019	29.61069	79.70951	BR	Graphite Schist	BV	6.4	0.85	4.89	0.81	2.58	<0.5	2.69	<0.5	<0.5	0.66	5.81	-	6.25	153.17	0.77	12.54	15.54
	113594					Shiva	7.79	0.75	4.01	0.75	2.22	<0.5	2.16	<0.5	<0.5	0.98	5.01	<0.5	1.32	-	0.59	13.79	14.57
5	110013	29.61044	79.70963	BR	Graphite Schist	BV	8.6	1.4	8.51	1.69	5.61	0.71	5.85	0.74	<0.5	0.79	3.18	-	3.42	63.11	<0.5	11.57	18.79
	113595					Shiva	9.69	1.25	8.09	1.62	4.71	0.76	4.87	0.77	<0.5	0.63	2.42	<0.5	1.73	-	<0.5	12.91	18.01
6	109995	29.62994	79.67588	BR	Tuffaceous Rock	BV	8.3	1.3	7.9	1.6	5.2	0.7	4.2	0.6	0.6	2.3	4.6	-	<0.5	43.8	<0.5	26.4	3.7
	113596					Shiva	11.14	1.19	6.71	1.14	3.05	<0.5	2.44	<0.5	<0.5	2.1	3.6	<0.5	1.01	-	<0.5	25.67	1.79
7	109987	29.61062	79.7093	BR	Graphite Schist	BV	5.4	0.7	4.2	0.9	2.9	<0.5	2.5	<0.5	<0.5	0.6	3.4	-	<0.5	24.5	<0.5	9	5.9
	113597					Shiva	7.26	0.69	3.97	0.82	2.26	<0.5	2.17	<0.5	<0.5	<0.5	2.3	<0.5	1.15	-	<0.5	9.13	6.24
8	109998	29.63659	79.72453	BR	Graphite Schist	BV	7.4	1.2	8	1.7	5.5	0.7	4.2	0.5	<0.5	0.6	2.4	-	<0.5	28.7	<0.5	8.3	22.1
	113598					Shiva	8.76	1.26	8.51	1.92	5.09	0.76	4.66	0.64	<0.5	0.67	2.23	<0.5	1.04	-	<0.5	12.45	28.94
9	110012	29.61044	79.70963	BR	Graphite Schist	BV	9.71	1.65	10.77	2.04	6.89	0.91	6.87	1	<0.5	0.9	4.75	-	5.1	36.9	<0.5	10.42	16.36
	113599					Shiva	9.72	1.49	9.55	1.97	5.51	0.86	5.87	1.02	<0.5	0.59	3.39	<0.5	1.4	-	<0.5	11.05	14.97
10	109993	29.62106	79.72286	BR	Graphite Schist	BV	3	<0.5	2.8	0.6	1.8	<0.5	1.4	<0.5	<0.5	0.7	0.8	-	<0.5	20.3	<0.5	7	4.2
	113600					Shiva	10	1.49	9.21	1.81	5.39	0.83	5.81	0.85	<0.5	0.57	3.37	<0.5	1.46	-	<0.5	11.15	14.26

Annexure XIII_Total Sulphur Data of Surface Samples (All data in %)

Sl. No.	Sample number	Latitude	Longitude	Lithology	Total Sulphur (%)
1	109218	29.636403	79.723705	Graphite Schist	5.33
2	109946	29.659791	79.697149	Graphite Schist	0.037
3	110005	29.621075	79.723056	Graphite Schist	0.97
4	110006	29.621075	79.723056	Graphite Schist	0.31
5	110007	29.621075	79.723056	Graphite Schist	0.03
6	110008	29.621075	79.723056	Graphite Schist	0.04
7	110009	29.621075	79.723056	Graphite Schist	0.09
8	110010	29.610435	79.70963	Graphite Schist	0.01
9	110011	29.610435	79.70963	Graphite Schist	0.01
10	110012	29.610435	79.70963	Graphite Schist	0.01
11	110013	29.610435	79.70963	Graphite Schist	0.01
12	110014	29.610435	79.70963	Graphite Schist	0.01
13	110015	29.610692	79.709507	Graphite Schist	0.14
14	110016	29.610692	79.709507	Graphite Schist	0.04
15	110017	29.610692	79.709507	Graphite Schist	0.04
16	110018	29.610692	79.709507	Graphite Schist	0.01
17	110019	29.610692	79.709507	Graphite Schist	0.07
18	110020	29.630777	79.741287	Tuffaceous Rock	<0.01
19	110024	29.584899	79.725847	Quartz Vein	0.019
20	110028	29.64478	79.674937	Mica Schist	0.07
21	110030	29.661188	79.696457	Graphite Schist	<0.01
22	110037	29.621603	79.677427	Foliated Granite	0.028
23	110058	29.601307	79.729308	Graphite Schist	0.66
24	110059	29.615107	79.726605	Quartz vein	0.02
25	110060	29.601307	79.729308	Graphite Schist	0.37

Annexure XIV_Details of Heavy Minerals Seperation

S No	Sample No	Latitude	Longitude	Location	Size Range	Ampere	0.3	0.5	0.7	1.0	1.5	1.7	1.7	1.7	Total weight
						Tilt	20°	20°	20°	20°	20°	20°	5° Magnetic	5° Non Magnetic	
1	109934	29.6433	79.670958	AL/SS 24	from -500 to +125	Wt in gm	4.647	2.513	0.761	0.400	0.327	0.278	0.356	0.388	9.670
						Wt in %	48.056	25.988	7.870	4.137	3.382	2.875	3.681	4.012	100.000
2	109182	29.6385	79.714892	AL/SS 04	from -500 to +125	Wt in gm	6.682	1.233	0.462	0.361	0.311	0.289	0.299	0.350	9.987
						Wt in %	66.907	12.346	4.626	3.615	3.114	2.894	2.994	3.505	100.000
3	109932	29.6392	79.709323	AL/SS 22	from -500 to +125	Wt in gm	7.898	1.288	0.459	0.380	0.307	0.269	0.324	0.402	11.327
						Wt in %	69.727	11.371	4.052	3.355	2.710	2.375	2.860	3.549	100.000
4	109933	29.6448	79.675704	AL/SS 23	from -500 to +125	Wt in gm	5.636	5.110	1.664	0.537	0.337	0.270	0.341	0.353	14.248
						Wt in %	39.556	35.865	11.679	3.769	2.365	1.895	2.393	2.478	100.000
5	109184	29.6368	79.720817	AL/SS 05	from -500 to +125	Wt in gm	3.318	1.395	0.509	0.356	0.314	0.266	0.303	0.351	6.812
						Wt in %	48.708	20.479	7.472	5.226	4.610	3.905	4.448	5.153	100.000
6	109269	29.6197	79.719138	AL/SS 12	from -500 to +125	Wt in gm	2.740	1.809	0.741	0.420	0.325	0.266	0.277	0.288	6.866
						Wt in %	39.907	26.347	10.792	6.117	4.733	3.874	4.034	4.195	100.000
7	109931	29.6401	79.708332	AL/SS 21	from -500 to +125	Wt in gm	2.012	1.139	0.550	0.386	0.332	0.280	0.272	0.320	5.291
						Wt in %	38.027	21.527	10.395	7.295	6.275	5.292	5.141	6.048	100.000
8	109930	29.6254	79.711702	AL/SS 20	from -500 to +125	Wt in gm	1.184	1.382	0.707	0.465	0.377	0.275	0.336	0.272	4.998
						Wt in %	23.689	27.651	14.146	9.304	7.543	5.502	6.723	5.442	100.000
9	109178	29.6347	79.699705	AL/SS 02	from -500 to +125	Wt in gm	4.907	2.455	0.941	0.476	0.336	0.277	0.317	0.347	10.056
						Wt in %	48.797	24.413	9.358	4.733	3.341	2.755	3.152	3.451	100.000
10	109261	29.6357	79.695928	AL/SS 08	from -500 to +125	Wt in gm	12.697	6.851	0.315	1.036	0.530	0.300	0.402	0.495	22.626
						Wt in %	56.117	30.279	1.392	4.579	2.342	1.326	1.777	2.188	100.000
11	109926	29.6298	79.70005	AL/SS 16	from -500 to +125	Wt in gm	1.258	0.523	0.316	0.299	0.286	0.253	0.251	0.288	3.474
						Wt in %	36.212	15.055	9.096	8.607	8.233	7.283	7.225	8.290	100.000
12	109924	29.6242	79.697392	AL/SS 14	from -500 to +125	Wt in gm	0.613	0.437	0.324	0.275	0.250	0.247	0.240	0.328	2.714
						Wt in %	22.587	16.102	11.938	10.133	9.211	9.101	8.843	12.085	100.000
13	109265	29.6371	79.688612	AL/SS 10	from -500 to +125	Wt in gm	5.115	3.914	1.396	0.600	0.396	0.300	0.336	0.364	12.421
						Wt in %	41.180	31.511	11.239	4.831	3.188	2.415	2.705	2.931	100.000
14	109925	29.6248	79.696493	AL/SS 15	from -500 to +125	Wt in gm	0.670	0.452	0.395	0.302	0.288	0.257	0.304	0.278	2.946
						Wt in %	22.743	15.343	13.408	10.251	9.776	8.724	10.319	9.437	100.000
15	109263	29.6363	79.6893	AL/SS 09	from -500 to +125	Wt in gm	1.674	1.782	1.018	0.419	0.280	0.261	0.274	0.312	6.020
						Wt in %	27.807	29.601	16.910	6.960	4.651	4.336	4.551	5.183	100.000
16	109267	29.6211	79.71979	AL/SS 11	from -500 to +125	Wt in gm	5.585	3.344	1.079	0.495	0.338	0.276	0.284	0.271	11.672
						Wt in %	47.850	28.650	9.244	4.241	2.896	2.365	2.433	2.322	100.000
17	109176	29.6202	79.722328	AL/SS 01	from -500 to +125	Wt in gm	5.539	4.653	1.782	0.688	0.461	0.419	0.460	0.350	14.352
						Wt in %	38.594	32.421	12.416	4.794	3.212	2.919	3.205	2.439	100.000
18	109935	29.6314	79.683298	AL/SS 25	from -500 to +125	Wt in gm	1.298	1.695	1.209	0.852	0.540	0.373	0.396	0.310	6.673
						Wt in %	19.452	25.401	18.118	12.768	8.092	5.590	5.934	4.646	100.000

S No	Sample No	Latitude	Longitude	Location	Size Range	Ampere	0.3	0.5	0.7	1.0	1.5	1.7	1.7	1.7	Total weight
						Tilt	20º	20º	20º	20º	20º	20º	5º Magnetic	5º Non Magnetic	
19	109928	29.6256	79.717188	AL/SS 18	from -500 to +125	Wt in gm	1.986	2.202	1.172	0.737	0.421	0.321	0.338	0.299	7.476
						Wt in %	26.565	29.454	15.677	9.858	5.631	4.294	4.521	3.999	100.000
20	109180	29.6385	79.686488	AL/SS 03	from -500 to +125	Wt in gm	1.971	1.193	0.504	0.351	0.315	0.260	0.300	0.288	5.182
						Wt in %	38.036	23.022	9.726	6.773	6.079	5.017	5.789	5.558	100.000
21	109271	29.6383	79.670908	AL/SS 13	from -500 to +125	Wt in gm	0.344	1.554	1.052	0.404	0.310	0.269	0.256	0.343	4.532
						Wt in %	7.590	34.289	23.213	8.914	6.840	5.936	5.649	7.568	100.000
22	109257	29.6363	79.681662	AL/SS 06	from -500 to +125	Wt in gm	2.695	2.653	1.297	0.675	0.440	0.294	0.303	0.325	8.682
						Wt in %	31.041	30.557	14.939	7.775	5.068	3.386	3.490	3.743	100.000
23	109929	29.6243	79.712884	AL/SS 19	from -500 to +125	Wt in gm	1.310	1.183	0.690	0.419	0.343	0.299	0.305	0.289	4.838
						Wt in %	27.077	24.452	14.262	8.661	7.090	6.180	6.304	5.974	100.000
24	109259	29.6428	79.682194	AL/SS 07	from -500 to +125	Wt in gm	9.682	8.641	1.299	0.502	0.344	0.287	0.400	0.501	21.656
						Wt in %	44.708	39.901	5.998	2.318	1.588	1.325	1.847	2.313	100.000
25	109927	29.6314	79.698021	AL/SS 17	from -500 to +125	Wt in gm	1.182	0.594	0.351	0.295	0.300	0.262	0.258	0.291	3.533
						Wt in %	33.456	16.813	9.935	8.350	8.491	7.416	7.303	8.237	100.000

Annexure XV_Raman Spectroscopic Data of Bedrock and Borehole Samples

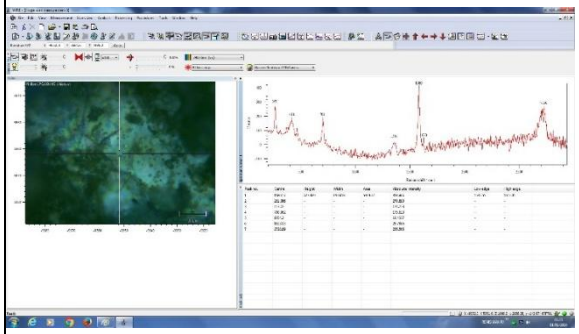

Figure 14.1: Raman spectrometry of 109938_1_powder

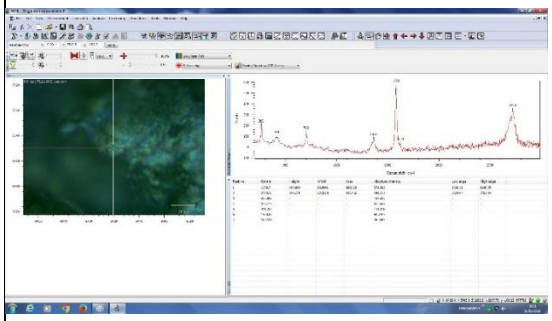

Figure 14.2: Raman spectrometry of 109938_2_powder

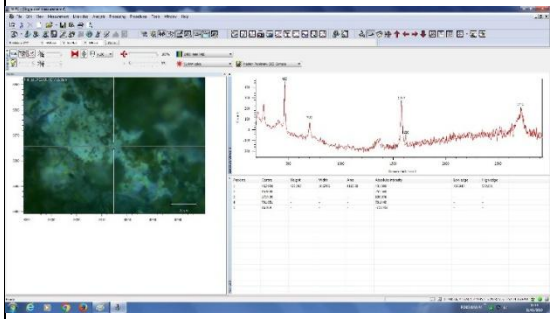

Figure 14.3: Raman spectrometry of 109938_3_powder

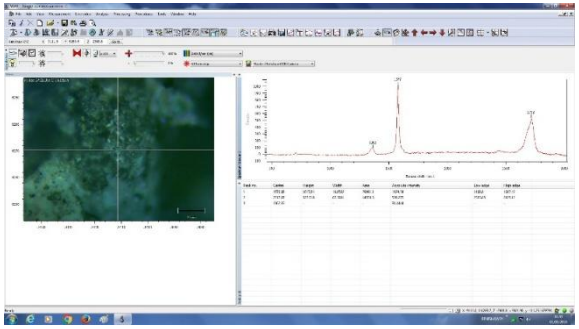

Figure 14.4: Raman spectrometry of 110004_1_powder

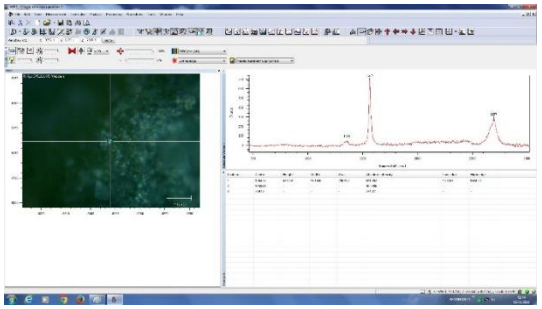

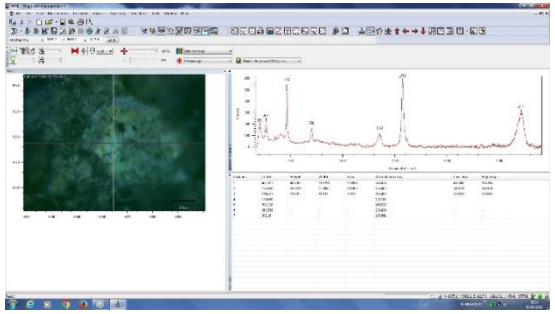

Figure 14.6: Raman spectrometry of 110004_3_powder

	Figure 14.5: Raman spectrometry of 110004_2_powder	
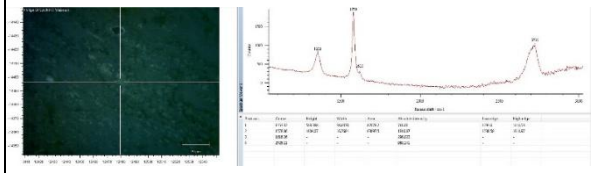 *Figure 14.7: Raman spectrometry of 11423_1*	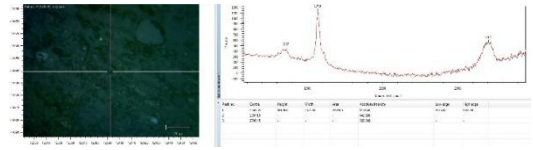 *Figure 14.8: Raman spectrometry of 11423_2*	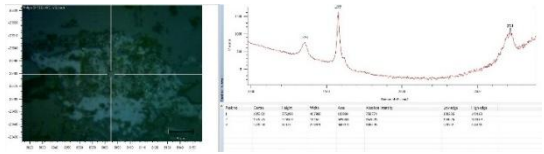 *Figure 14.9: Raman spectrometry of 11423_3*
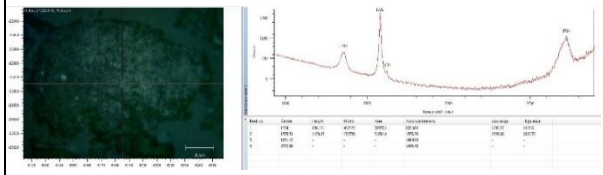 *Figure 14.10: Raman spectrometry of 11423_4*	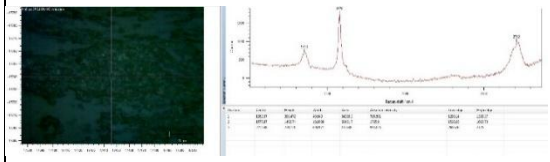 *Figure 14.11: Raman spectrometry of 14228_1*	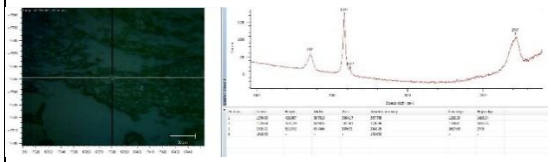 *Figure 14.12: Raman spectrometry of 14228_2*

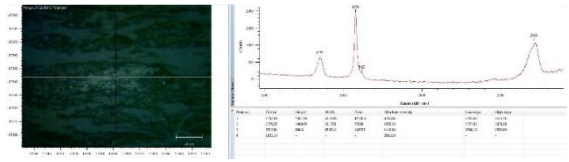

Figure 14.13: Raman spectrometry of 14228_3

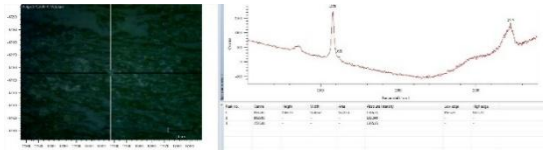

Figure 14.14: Raman spectrometry of 14228_4

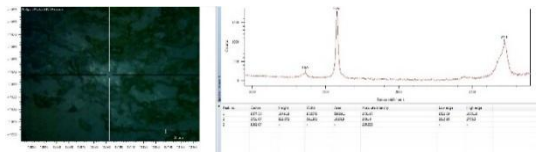

Figure 14.15: Raman spectrometry of 14241_1

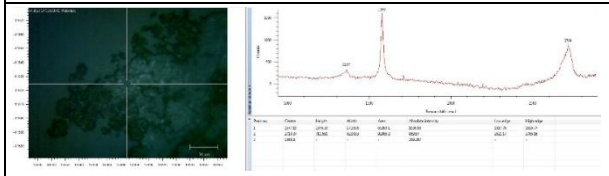

Figure 14.16: Raman spectrometry of 14241_2

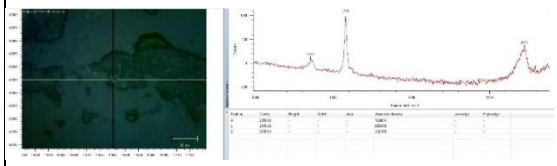

Figure 14.17: Raman spectrometry of 14241_3

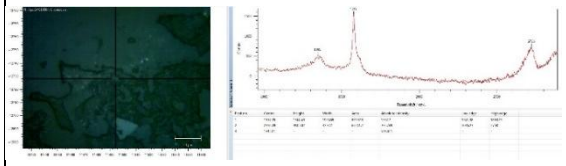

Figure 14.18: Raman spectrometry of 14241_4

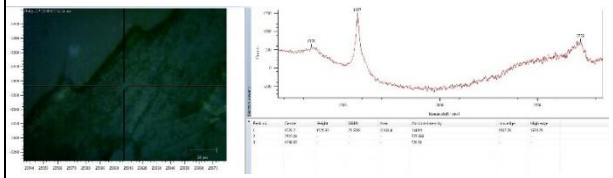

Figure 14.19: Raman spectrometry of 114227_1

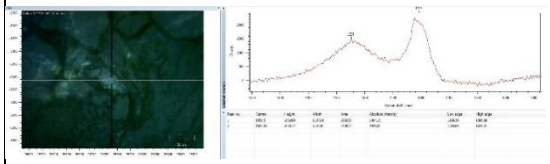

Figure 14.20: Raman spectrometry of 114227_2

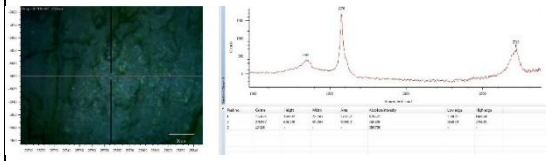

Figure 14.21: Raman spectrometry of 114227_3

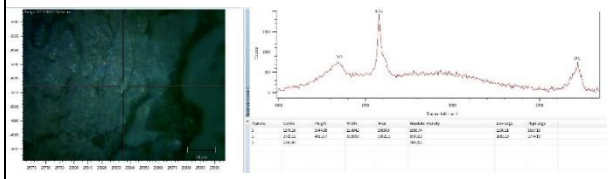

Figure 14.22: Raman spectrometry of 114227_4

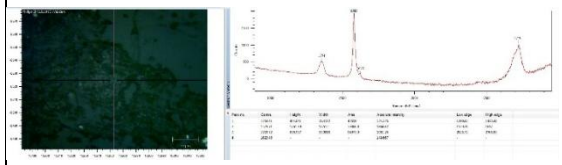

Figure 14.23: Raman spectrometry of 114229_1

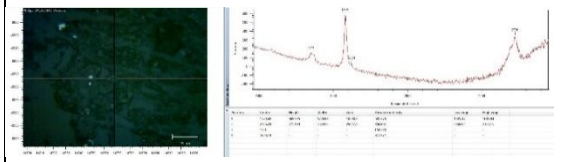

Figure 14.24: Raman spectrometry of 114229_2

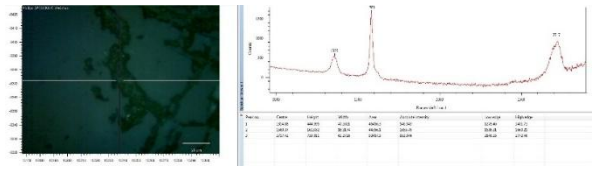

Figure 14.25: Raman spectrometry of 114229_3

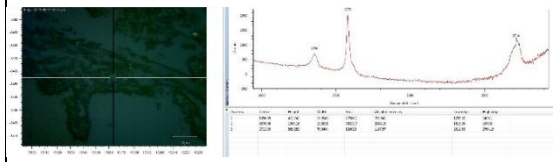

Figure 14.26: Raman spectrometry of 114229_4

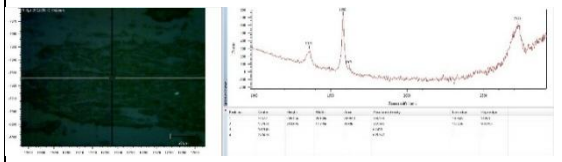

Figure 14.27: Raman spectrometry of 114232_1

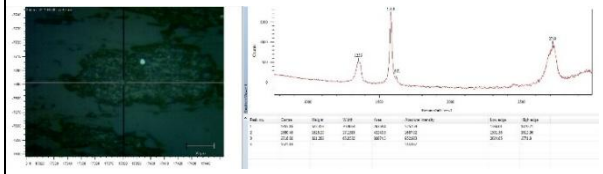

Figure 14.28: Raman spectrometry of 114232_2

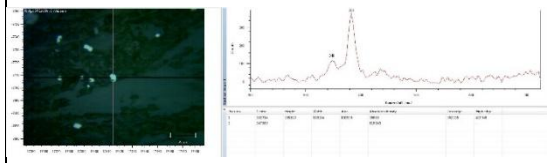

Figure 14.29: Raman spectrometry of 114232_3_pyrite

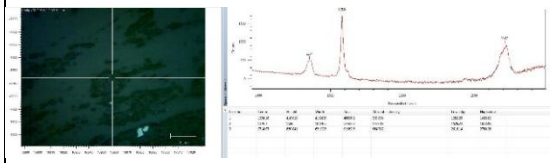

Figure 14.30: Raman spectrometry of 114232_4

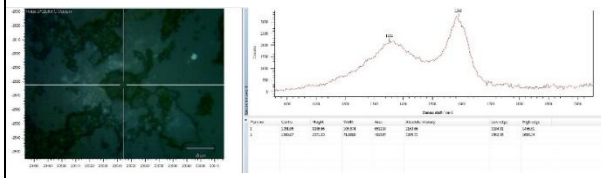

Figure 14.31: Raman spectrometry of 114234_1_carbon

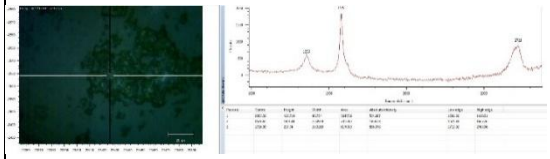

Figure 14.32: Raman spectrometry of 114234_2

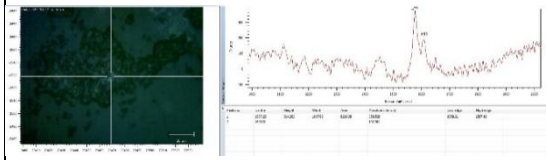

Figure 14.33: Raman spectrometry of 114234_3

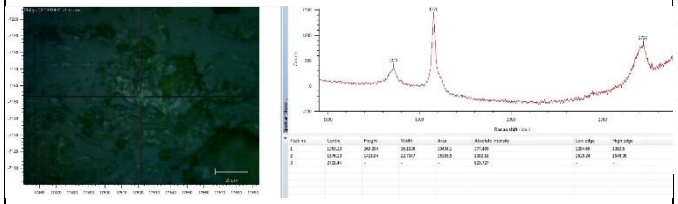

Figure 14.34: Raman spectrometry of 114237_1

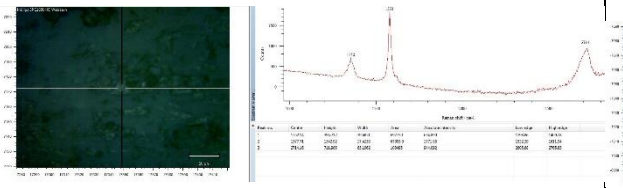

Figure 14.35: Raman spectrometry of 114237_2

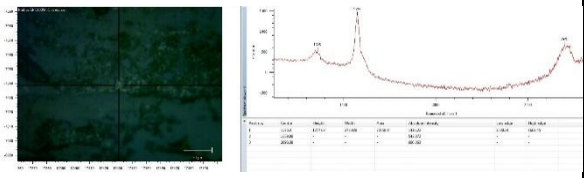

Figure 14.36: Raman spectrometry of 114237_3

Annexure XVI_XRD Data of Surface and Borehole Samples

SL No	Analysis	Sample no.	Latitude	Longitude	Sample type	Lithology	Depth (m)
1	XRD	109923	29.610768	79.709548	BR	Graphite Schist	Surface
2	XRD	109999	29.6211441	79.723035	BR	Graphite Schist	Surface
3	XRD	110001	29.651829	79.684433	BR	Graphite Schist	Surface
4	XRD	109938	29.605957	79.692265	BR	Graphite Schist	Surface
5	XRD	110004	29.636403	79.723705	BR	Graphite Schist	Surface
6	XRD	114239	29.636734	79.726113	BH-01	Graphite Schist	64.6
7	XRD	114232	29.609816	79.709241	BH-03	Graphite Schist	27.9
8	XRD	114233	29.609816	79.709241	BH-03	Graphite Schist	73
9	XRD	114229	29.641725	79.665825	BH-05	Graphite Schist	32.3
10	XRD	114235	29.618863	79.726083	BH-02	Graphite Schist	24.3

Annexure XVII_Self Potential (SP) Raw Data

SP Line-1

			Elevation	mV	Time	Time Difference	Corrected mV	Factor	Remark	Revised 1 (mV)		Revised 2 (mV)	
B1(@300m)			1347.20m	12.7	11.24 AM					Time	mV	Time	mV
Station No.	Latitude	Longitude	Elevation							12.54 PM	8.34 mV	1.56 PM	7.42 mV
0	29.64071	79.722158	1425.35m	103.4	12:40pm	76	99.71822256	0.04844444					
25													
50	29.64027	79.7219	1418.47m	96.575	12:31pm	67	93.32922252	0.04844444					
75													
100	29.63985	79.721772	1401.28m	90.42	12:21pm	57	87.65866692	0.04844444					
125	29.63963	79.721707	1393.33m	87.4	12:16pm	52	84.88088912	0.04844444					
150	29.63946	79.721688	1385.51m	93.4	12:09pm	45	91.2200002	0.04844444					
175	29.63925	79.72159	1374.75m	83.1	12:04pm	40	81.1622224	0.04844444					
200	29.63906	79.721518	1367.27m	73.4	11:49am	25	72.188889	0.04844444					
225	29.63887	79.72143	1361.28m	76.4	11:46am	22	75.33422232	0.04844444					
250	29.63867	79.721382	1354.87m	43.8	11:36am	12	43.21866672	0.04844444					
275	29.63851	79.721408	1351.49m	11.1875	11.31 am	7	10.84838892	0.04844444					
300	29.63822	79.72136	1346.90m	12.7	11:24am	0	12.7	0.04844444					
325	29.638	79.721343	1345.14m	-30.625	12:58pm	4	-35.96435484	0.01483871					
350	29.63779	79.721382	1344.01m	-41.875	01:02pm	8	-47.27370968	0.01483871					
375	29.63756	79.721353	1342.29m	-46	1:11pm	17	-51.53225807	0.01483871					
400	29.63736	79.721448	1340.05m	-109.375	1:14pm	20	-114.9517742	0.01483871					
425	29.63712	79.72144	1335.27m	-138	1:22pm	28	-143.6954839	0.01483871					
450	29.63693	79.721515	1331.53m	-80.9	1:31pm	37	-86.72903227	0.01483871					
475	29.63669	79.721535	1330.995	-115	1.39pm	45	-120.947742	0.01483871					
500	29.6365	79.721495	1335.894	-128	1.50pm	56	-134.1109678	0.01483871					
525	29.6363	79.721533	1344.66m	-297	1:56pm	62	-303.2	0.01483871					

SP Line-2

			Elevation	mV	Time	Time Difference	Corrected mV	Factor	Remark	Revised 1 (mV)		Revised 2 (mV)		Revised 3(mV)		Revised 4(mV)	
B1(@400m)			1394.7253	3.97	11.51am					Time	mV	Time	mV	Time	mV	Time	mV
Station No.	Latitude	Longitude	Elevation							12:06pm	0.66	1:05pm	-4.97	2:02pm	-4.7	3:18pm	-7.62
0	29.64202833	79.716408	1440.0663	101.975	12:55pm	64	101.8888688	0.0013458									
50	29.64157	79.716545	1442.2167	79	12:45pm	54	78.9273268	0.0013458									
100	29.64117	79.716535	1445.0071	59.225	12:33pm	42	59.1684764	0.0013458									
150	29.64077833	79.716652	1444.29	65.75	12:29pm	38	65.6988596	0.0013458									
200	29.64035333	79.716822	1433.8	71.3	12:22pm	31	71.2582802	0.0013458									
250	29.64001667	79.71709	1419.04	53.8	12:18pm	27	53.7636634	0.0013458									
300	29.63967667	79.71743	1408.98	38.8	12:12pm	21	38.7717382	0.0013458									
350	29.63931833	79.717727	1400.12	35.9	12.08pm	17	35.8771214	0.0013458									
400	29.63896167	79.718042	1394.7253	3.97	11.51am	0	3.97	0.0013458									
450	29.63858	79.718135	1385.2781	-78.6	1:38pm	33	-79.4863144	0.0047368									
500	29.63819167	79.718392	1374.05	-430	1:42pm	37	-430.9052616	0.0047368									
550	29.63782167	79.71866	1367.39	-502	1:46pm	41	-502.9242088	0.0047368									
600	29.63738	79.718853	1358.35	-249	1:49pm	44	-249.9384192	0.0047368									
650	29.63695667	79.719033	1352.28	-129	1:54pm	49	-129.9621032	0.0047368									
700	29.63658167	79.719195	1348	-96.3	2:08pm	6	-100.1805263	0.03842105									
750	29.63612333	79.719095	1349.812	-134	2:19pm	17	-138.3031579	0.03842105									
800	29.635737	79.719558	1354.77	-216	2:54pm	52	-221.6478946	0.03842105									

SP Line-3

			Elevation	mV	Time	Time Difference	Corrected mV	Factor	Remark	Revised 1 (mV)		Revised 2 (mV)		Revised 3(mV)		Revised 3(mV)	
B1(@400m)			1631.16	13.9	11:17am					Time	mV	Time	mV				
Station No.	Latitude	Longitude	Elevation							12:21pm	14.4mv	1:18pm	0.38mv	14:19pm	2.92mv	14:54pm	-18.3
0	29.60768	79.711222	1605.93	376	12:38pm	17	358.2985967	0.2459649									
50	29.60795	79.710982	1603.322	353	12:34pm	13	336.2824563	0.2459649									
100	29.60837	79.710762	1580.812	273	12:14pm	57	273.4453125	0.0078125									
150	29.60873	79.7105	1573.392	181	12:04m	47	181.3671875	0.0078125									
200	29.64035	79.716822	1433.801	-17	11:54m	37	-16.7109375	0.0078125									
250	29.60929	79.709853	1598.773	245	11:48pm	31	245.2421875	0.0078125									
300	29.63968	79.71743	1408.98	150	11:38pm	21	150.1640625	0.0078125									
350	29.60994	79.709148	1624.18	46.5	11:24pm	7	46.5546875	0.0078125									
400	29.61023	79.70882	1631.16	13.9	11:17pm	0	13.9	0.0078125									
450	29.61058	79.708533	1617.044	207	1:41pm	23	195.0622961	0.0416393									
500	29.61081	79.708175	1592.381	114.4	1:53pm	35	101.9626245	0.0416393									
550	29.61111	79.707987	1572.628	202	2:00pm	42	189.2711494	0.0416393									
600	29.61143	79.707738	1555.797	121	2:06pm	48	108.0213136	0.0416393									
650	29.61183	79.707497	1557.215	282	2:11pm	53	268.8131171	0.0416393									
700	29.61225	79.707245	1571.228	435	2:17pm	59	421.5632813	0.0416393									
750	29.6126	79.706913	1578.759	395	2:28pm	9	386.6451429	0.43942857									
800	29.61287	79.70653	1581.193	364	2:38pm	19	351.2508572	0.43942857									

SP Line-4

			Elevation	mV	Time	Time Difference	Corrected mV	Factor	Remark	Revised 1 (mV)		Revised 2 (mV)		Revised 3(mV)		Revised 3(mV)	
B1(@400m)				30.1	11:16am					Time	mV	Time	mV				
Station No.	Latitude	Longitude	Elevation							12:18pm	22.1mv	01:33pm	23.1mv	2:34	17.4mv	03:58pm	18.0mv
0	29.60887	79.69173	1564.88 m	434	1.07pm	49	426.3466683	0.0133333									
50	29.60847	79.69144	1580.06 m	354	1:03pm	45	346.4000015	0.0133333									
100	29.60814	79.69136	1589.58 m	284	12:51pm	33	276.5600011	0.0133333									
150	29.60769	79.69126	1587.83 m	242	12:34pm	16	234.7866672	0.0133333									
200	29.60731	79.69108	1579.93 m	280	12:31pm	13	272.8266671	0.0133333									
250	29.60687	79.69095	1570.79 m	222	12:08pm	52	215.2903256	0.1290322									
300	29.60641	79.69091	1556.85 m	148	11:34am	18	145.6774204	0.1290322									
350	29.60603	79.69075	1558.59 m	-35.6	11:29am	13	-37.2774186	0.1290322									
400	29.60564	79.69059	1573.33 m	30.1	11:16am	0	30.1	0.1290322									
450	29.6053	79.69038	1572.96 m	179	2.38pm	4	166.8714284	0.0071429									
500	29.60493	79.69021	1558.64 m	283	2:43pm	9	270.8357139	0.0071429									
550	29.60455	79.69002	1538.31 m	249	2:47pm	13	236.8071423	0.0071429									
600	29.60424	79.68982	1520.78 m	29.7	2:51pm	17	17.4785707	0.0071429									
650	29.60393	79.68951	1498.81 m	249	3:03pm	29	236.6928559	0.0071429									
700	29.60353	79.68929	1486.86 m	260	3:09pm	35	247.6499985	0.0071429									
750	29.60324	79.68892	1469.66 m	248	3:15pm	41	235.6071411	0.0071429									
800	29.60292	79.68871	1462.05 m	284	3:28pm	54	271.5142834	0.0071429									
			Elevation	mV	Time	Time Difference	Corrected mV	Factor	Remark	Revised 1 (mV)		Revised 2 (mV)		Revised 3(mV)		Revised 3(mV)	
B2(@800m)			1462.05 M	13.5	10:43AM					Time	mV	Time	mV				

Station No.	Latitude	Longitude	Elevation							11:49AM	6.02MV						
850	29.60246	79.68851	1442.46 M	-34.3	10.50AM	7	-35.0933331	0.1133333									
900	29.60206	79.68844	1421.76 M	-20	11:07AM	24	-22.7199992	0.1133333									
950	29.60165	79.6885	1420.30 M	-138	11:23AM	40	-142.533332	0.1133333									
1000	29.60118	79.68826	1413.80 M	-254	11:30AM	47	-259.3266651	0.1133333									

SP Line-5

			Elevation	mV	Time	Time Difference	Corrected mV	Factor	Remark	Revised 1 (mV)		Revised 2 (mV)		Revised 3(mV)		Revised 3(mV)	
B1(@400m)				36.8	1:17PM					Time	mV	Time	mV				
Station No.	Latitude	Longitude	Elevation							2:16pm	26.6mv	3:17pm	28.35mv	4:18pm	35.85mv		
0	29.60357	79.73107	1348.26 M	-9.79	2:53PM	37	-19.3014745	0.0286885									
50	29.6032	79.73094	1344.21 M	-42	2:28PM	12	-50.794262	0.0286885									
100	29.60288	79.73065	1331.32 M	-146	2:13PM	56	-155.6813528	0.1728813									
150	29.60266	79.73037	1321.83 M	-168	2:03PM	46	-175.9525398	0.1728813									
200	29.6024	79.73005	1309.97 M	-208	1:56PM	39	-214.7423707	0.1728813									
250	29.60208	79.72968	1300.05 M	-245	1:52PM	35	-251.0508455	0.1728813									
300	29.60182	79.72925	1284.25 M	-284	1:47PM	30	-289.186439	0.1728813									
350	29.60159	79.72881	1267.17 M	-540	1:25PM	8	-541.3830504	0.1728813									
400	29.60144	79.7284	1259.15 M	36.8	1:17PM	0	36.8	0.1728813									
450	29.60129	79.72793	1263.05 M	-850	3:36PM	19	-853.2860652	0.1229508									
500	29.60104	79.72751	1267.93 M	-136	3:40PM	23	-139.7778684	0.1229508									
550	29.60082	79.72708	1273.74 M	-93	3:45PM	28	-97.3926224	0.1229508									
600	29.60058	79.72664	1275.20 M	-87.7	3:48PM	31	-92.4614748	0.1229508									

			Elevation	mV	Time	Time Difference	Corrected mV	Factor	Remark	Revised 1 (mV)		Revised 2 (mV)		Revised 3(mV)		Revised 3(mV)	
B1(@400m)				36.8	1:17PM					Time	mV	Time	mV				
Station No.	Latitude	Longitude	Elevation							2:16pm	26.6mv	3:17pm	28.35mv	4:18pm	35.85mv		
650	29.60035	79.72617	1276.30 M	-130	3:51PM	34	-135.1303272	0.1229508									
700	29.60017	79.7257	1286.54 M	-118.6	3:54PM	37	-124.0991796	0.1229508									
750	29.60003	79.7252	1284.78 M	-118.1	3:57PM	40	-123.968032	0.1229508									
800	29.59992	79.72473	1279.39 M	-82.1	4:04PM	47	-88.8286876	0.1229508									

			Elevation	mV	Time	Time Difference	Corrected mV	Factor	Remark	Revised 1 (mV)		Revised 2 (mV)		Revised 3(mV)	
B2(@400m)				-0.32	4:45PM					Time	mV	Time	mV		
Station No.	Latitude	Longitude	Elevation							5:21pm	3.84mv				
850	29.59984	79.72422	1273.1M	-57.9	4:48PM	3	-58.1933331	0.0977777							
900	29.59961	79.7232	1272.13M	-131	5:01PM	16	-132.5644432	0.0977777							
950	29.59942	79.72323	1275.71M	-83.9	5:06PM	21	-85.9533317	0.0977777							
1000	29.59941	79.72282	1279.85M	-52.15	5:12PM	27	-54.7899979	0.0977777							

SP Line-06

			Elevation	mV	Time	Time Difference	Corrected mV	Factor	Remark	Revised 1 (mV)		Revised 2 (mV)		Revised 3(mV)		Revised 3(mV)	
B1(@350m)				**-20.95**	**11:37:00**					**Time**	**mV**	**Time**	**mV**				
Station No.	**Latitude**	**Longitude**	**Elevation (m)**							**12:30 PM**	**-23.2 mv**	**1:37 PM**	**-23.7 mv**	**2:30 PM**			
0	29.620197	79.715699	1476	-59.8	12:12 PM	35	-61.28584906	0.042452830 1886792									
50	29.620324	79.716184	2.67	-49.475	12:09 PM	32	-50.83349057	0.042452830 1886792									
100	29.620412	79.716657	1456	-73.1	12:04 PM	27	-74.24622642	0.042452830 1886792									
150	29.620525	79.717139	1437	-18.875	12:01 PM	24	-19.89386792	0.042452830 1886792									
200	29.620634	79.71763	1420	-5.34	11:55:00 AM	18	-6.104150943	0.042452830 1886792									
250	29.620735	79.718109	1406	-5.8975	11:51:00 AM	14	-6.491839623	0.042452830 1886792									
300	29.620849	79.718622	1392	-4.1075	11:45:00 AM	8	-4.447122642	0.042452830 1886792									
350	29.620969	79.719157	1367	-20.95	11:37:00 AM	0	-20.95	0.042452830 1886792	Base								
400	29.621089	79.719682	1354	1.22	12:56 PM	26	-1.724029851	0.007462686 56716	road								
450	29.621201	79.720185	1345	-27.025	1:03 PM	33	-30.02126866	0.007462686 56716	electric pole								
500	29.621303	79.720636	1337	-33.175	1:06 PM	36	-36.19365672	0.007462686 56716	road								
550	29.621398	79.721084	1323	-12.275	1:10 PM	40	-15.32350746	0.007462686 56716	road								
600	29.621504	79.721549	1311	-44.9	1:13 PM	43	-47.97089552	0.007462686 56716	road								
650	29.621614	79.72206	1316	-280	1:21 PM	51	-283.130597	0.007462686 56716	road								
700	29.621715	79.722522	1323	-386	1:25 PM	55	-389.1604478	0.007462686 56716	road								

			Elevation	mV	Time	Time Difference	Corrected mV	Factor	Remark	Revised 1 (mV)		Revised 2 (mV)	
B2(@1000m)			**1355**	**5.225**	**03:38:00**					**Time**	**mV**	**Time**	**mV**
Station No.	**Latitude**	**Longitude**	**Elevation**							**4:31 PM**	**4.31**		
750	29.621814	79.723012	1327	2.01	4:17 PM	39	1.336698113	0.017264150943396					
800	29.621936	79.723479	1327.23	2.26	4:14 PM	36	1.638490566	0.017264150943396					
850	29.622051	79.724019	1326	2.5	4:10 PM	32	1.94754717	0.017264150943396					

			Elevation	mV	Time	Time Difference	Corrected mV	Factor	Remark	Revised 1 (mV)		Revised 2 (mV)	
B2(@1000m)			1355	5.225	03:38:00					Time	mV	Time	mV
Station No.	Latitude	Longitude	Elevation							4:31 PM	4.31		
900	29.622163	79.724536	1332	4.498	4:05 PM	27	4.031867925	0.017264150943396					
950	29.622283	79.725043	1343	3.72	4:00 PM	22	3.340188679	0.017264150943396					
1000	29.622401	79.725555	1355	5.225	3:38 PM	0	5.225	0.017264150943396					
1050	29.622494	79.726035	1372	1.484	3:44 PM	6	1.380415094	0.017264150943396					
1100	29.622598	79.72651	1387	3.51	3:49 PM	11	3.32009434	0.017264150943396					

SP Line- 07

			Elevation	mV	Time	Time Difference	Corrected mV	Factor	Remark	Revised 1 (mV)		Revised 2 (mV)		Revised 3(mV)		Revised 3(mV)	
Day3B3(@350m)				-1.1	10:14:00					Time	mV	Time	mV				
Station No.	Latitude	Longitude	Elevation (m)							11:16:00 AM	-3.1						
0	29.618638	79.70947	1577.45	16.9	11:13:00 AM	59	14.99677446	0.03225806									
50	29.618607	79.70999	1577.97	29.68	11:09:00 AM	52	28.00258088	0.03225806									
100	29.618576	79.71051	1578.75	33.85	11:06:00 AM	50	32.237097	0.03225806									
150	29.618557	79.71102	1579.47	28.9	11:04:00 AM	50	27.287097	0.03225806									
200	29.61851	79.71155	1569.93	36.2	11:02:00 AM	48	34.65161312	0.03225806									
250	29.618497	79.71206	1562.88	26.8	11:00:00 AM	46	25.31612924	0.03225806									
300	29.618442	79.71261	1555.89	13	10:58:00 AM	44	11.58064536	0.03225806									
350	29.618422	79.7131	1553.33	-1.1	10:14:00 AM	0	-1.1	0.03225806									
400	29.618388	79.71365	1539.64	-11.2	10:17:00 AM	3	-11.29677418	0.03225806									
450	29.618345	79.71418	1517.74	-6.6	10:20:00 AM	6	-6.79354836	0.03225806									
500	29.61832	79.71471	1504.69	-35.3	10:22:00 AM	8	-35.55806448	0.03225806									
550	29.61828	79.71524	1491.7	-49	10:24:00 AM	10	-49.3225806	0.03225806									
600	29.618258	79.71576	1477.05	-57.3	10:27:00 AM	13	-57.71935478	0.03225806									
650	29.618216	79.7163	1465.38	-171	10:30:00 AM	16	-171.516129	0.03225806									
700	29.618185	79.71681	1460.55	-358	10:33:00 AM	19	-358.6129031	0.03225806									

			Elevation	mV	Time	Time Difference	Corrected mV	Factor	Remark	Revised 1 (mV)		Revised 2 (mV)		Revised 3(mV)		Revised 3(mV)	
Day1B1(@110m)				-3.213	12:29:00					Time	mV	Time	mV				
Station No.	Latitude	Longitude	Elevation (m)							1:25:00 AM	-4.998	2:20:00 AM	0.396				
750	29.618195	79.7168	1460.19	-384	1:00:00 AM	31	-384.988125	0.031875									
800	29.618215	79.71733	1457.24	-446	12:50:00 PM	21	-446.669375	0.031875									
850	29.618265	79.71785	1456.29	-192.25	12:47:00 PM	18	-192.82375	0.031875									
900	29.618281	79.71838	1450.11	-115.58	12:44:00 PM	15	-116.058125	0.031875									
950	29.618309	79.7189	1440.22	-54.025	12:40:00 PM	11	-54.375625	0.031875									
1000	29.618319	79.71943	1432.35	-1.59	12:36:00 PM	7	-1.813125	0.031875									
1050	29.618345	79.71997	1428.24	-1.988	12:33:00 PM	4	-2.1155	0.031875									
1100	29.618384	79.72049	1422.24	-3.213	12:29:00 PM	0	-3.213	0.031875									
1150	29.618421	79.72101	1411.81	-107.15	1:31:00 AM	6	-110.3342	0.0708									
1200	29.618452	79.72155	1397.34	-51.32	1:34:00 AM	9	-54.2918	0.0708									
1250	29.618507	79.72206	1379.02	44.875	1:38:00 AM	13	42.1864	0.0708									
1300	29.618554	79.72257	1359.6	70.648	1:44:00 AM	19	68.3842	0.0708									
1350	29.618576	79.72311	1341.22	124	1:48:00 AM	23	122.0194	0.0708									
1400	29.618648	79.72363	1320.67	-2.135	1:51:00 AM	26	-3.9032	0.0708									
1450	29.61869	79.72416	1305.43	287	1:57:00 AM	32	285.6566	0.0708									

			Elevation	mV	Time	Time Difference	Corrected mV	Factor	Remark	Revised 1 (mV)		Revised 2 (mV)		Revised 3(mV)		Revised 3(mV)	
Day2B2(@1600m)				-19.15	11.20					Time	mV	Time	mV				
Station No.	Latitude	Longitude	Elevation							12.17	-3.638	1.17	-3.642				
1500	29.61869	79.72416	1305.43	-4.035	11.58	38	6.3050014	0.2721053									
1550	29.618682	79.72467	1300.12	-69.57	11.54	34	-60.3184198	0.2721053									
1600	29.618713	79.7252	1307.43	-211.33	11.52	32	-202.6226304	0.2721053									
1650	29.618715	79.72572	1316.52	-454.67	11.38	13	-451.1326311	0.2721053									
1700	29.618699	79.72624	1321.66	-187.3	11.25	5	-185.9394735	0.2721053									
1750	29.618745	79.72677	1328.83	-19.15	11.2	0	-19.15	0.2721053									
1800	29.618738	79.72728	1340.49	54.74	12.25	8	39.23253333	0.0000666666									
1850	29.618719	79.7278	1353.53	40.975	12.29	12	25.4678	0.0000666666									
1900	29.618753	79.72833	1355.88	49.18	12.34	17	33.67313333	0.0000666666									
1950	29.618796	79.72886	1343.57	68.5	12.39	22	52.99346667	0.0000666666									

2000	29.618823	79.72938	1330.98	15.025	12.44	27	-0.481200002	0.0000666666										

SP Line-08

			Elevation	mV	Time	Time Difference	Corrected mV	Factor	Remark	Revised 1 (mV)		Revised 2 (mV)	
Day2_B3(@100m)				**5.91**	**13:18:00**					**Time**	**mV**	**Time**	**mV**
Station No.	**Latitude**	**Longitude**	**Elevation (m)**							**2:00 PM**	**3.94**		
0	29.613563	79.709719	1550.11	-2.63	1:53 PM	35	-4.2716645	0.0469047					
50	29.613578	79.710224	1545.65	-14.5	1:50 PM	32	-16.0009504	0.0469047					
100	29.613621	79.710745	1536.03	5.91	1:18 PM	0	5.91	0.0469047					
150	29.613662	79.711287	1521.95	-2.775	1:22 PM	4	-2.9626188	0.0469047					
200	29.613707	79.71179	1509.76	-6.94	1:26 PM	8	-7.3152376	0.0469047					
250	29.613725	79.712344	1491.91	-6.45	1:30 PM	12	-7.0128564	0.0469047					
300	29.613779	79.712871	1479.09	-1.875	1:37 PM	19	-2.7661893	0.0469047					
			Elevation	**mV**	**Time**	**Time Difference**	**Corrected mV**	**Factor**	**Remark**	**Revised 1 (mV)**		**Revised 2 (mV)**	
Day2_B2(@600m)				**-8.03**	**10:38:00**					**Time**	**mV**	**Time**	**mV**
Station No.	**Latitude**	**Longitude**	**Elevation**							**11:33**	**-18.40**	**12:37**	**-8.50**
300	29.613779	79.712871	1479.09	-6.74	12:21 PM	48	2.365	0.1546875					
350	29.613811	79.713392	1475.91	-251.75	12:16 PM	43	-241.8715625	0.1546875	-0.05891				
400	29.613856	79.713909	1480.92	-261	12:11 PM	38	-250.348125	0.1546875					
450	29.613874	79.714446	1487.06	-367.3	12:08 PM	35	-356.1840625	0.1546875					
500	29.613922	79.714968	1491.91	-176.75	11:57 AM	24	-163.9325	0.1546875					
550	29.613948	79.715466	1502.58	-55.4	11:49 AM	16	-41.345	0.1546875	Road				
600	29.614009	79.71596	1505.45	-8.03	10:38 AM	0	-8.03	0.1885454					
650	29.614029	79.716484	1491.67	-150.9	10:45 AM	7	-152.2198178	0.1885454					
700	29.614064	79.717003	1473.91	-154.5	10:52 AM	14	-157.1396356	0.1885454					
750	29.614086	79.717546	1456.76	-275.3	10:56 AM	18	-278.6938172	0.1885454	Road				
800	29.614109	79.718059	1442.48	-181.3	11:00 AM	22	-185.4479988	0.1885454					
850	29.61414	79.718592	1431.8	-127.5	11:03 AM	25	-132.213635	0.1885454					
900	29.614275	79.719118	1424.72	-115.13	11:07 AM	29	-120.5978166	0.1885454					
			Elevation	**mV**	Time	**Time Difference**	**Corrected mV**	**Factor**	**Remark**	**Revised 1 (mV)**		**Revised 2 (mV)**	
Day1_B1(@1250m)				**-1.335**	11:16 AM					**Time**	**mV**	**Time**	**mV**
Station No.	**Latitude**	**Longitude**	**Elevation**							**12:05**	**0.94**	**13:00**	**4.18**
900	29.614275	79.719118	1424.72	-144	12:39 PM	34	-136.4820909	0.0589090909					
950	29.614214	79.719632	1409.08	-34.07	12:34 PM	29	-26.84663636	0.0589090909					
1000	29.614253	79.720149	1393.66	41.3	12:29 PM	24	48.22881818	0.0589090909					
1050	29.614268	79.720679	1379.23	101.875	12:26 PM	21	108.6270909	0.0589090909					

1100	29.61434	79.721215	1361.69	117.53	12:21 PM	16	123.9875455	0.0589090909						
1150	29.614339	79.721744	1356.04	90.47	12:17 PM	12	96.69190909	0.0589090909						
1200	29.614388	79.722289	1350.84	12.03	12:13 PM	8	18.01627273	0.0589090909						
1250	29.614359	79.22761	1340.95	-1.335	11:16 AM	0	-1.335	0.00806122448979591						
1300	29.614435	79.723304	1331.18	-59.5	11:23 AM	7	-59.44357143	0.00806122448979591						
1350	29.6145	79.723804	1324.28	-109.8	11:26 AM	10	-109.7193878	0.00806122448979591						
1400	29.614524	79.724339	1316.31	-201.8	11:29 AM	13	-201.6952041	0.00806122448979591						
1450	29.614549	79.72486	1308.76	-207	11:31 AM	15	-206.8790816	0.00806122448979591						
1500	29.614601	79.725403	1301.37	-361.6	11:36 AM	20	-361.4387755	0.00806122448979591						
1550	29.614623	79.725872	1292.91	-2.725	11:40 AM	24	-2.531530612	0.00806122448979591						
1600	29.614674	79.72642	1291.55	-261.5	11:43 AM	27	-261.2823469	0.00806122448979591						

SP Line- 09

			Elevation	mV	Time	Time Difference	Corrected mV	Factor	Remark	Revised 1 (mV)		Revised 2 (mV)		Revised 3 (mV)		Revised 3(mV)	
Day2_B4(@250m)				**-8.32**	**11:45 AM**					**Time**	**mV**	**Time**	**mV**				
Station No.	**Latitude**	**Longitude**	**Elevation (m)**							**12:46 PM**	**-9.57**						
0	29.609927	79.710511	1592.38	-88.95	12:36 PM	51	-89.99508197	0.020491803									
50	29.60998	79.711111	1573.57	-56.425	12:33 PM	48	-57.40860656	0.020491803									
100	29.610031	79.711721	1545.7	170	12:29 PM	44	169.0983607	0.020491803									
150	29.610042	79.712253	1525.21	301	12:25 PM	40	300.1803279	0.020491803									
200	29.610086	79.712803	1510.32	89.25	12:21 PM	36	88.51229508	0.020491803									
250	29.61011	79.713361	1496.3	-8.32	11:45 AM	0	-8.32	0.020491803									
300	29.610158	79.713903	1478.35	157	11:48 AM	3	156.9385246	0.020491803									
350	29.610191	79.714554	1460.26	254	11:50 AM	5	253.897541	0.020491803									
400	29.610206	79.715092	1459.13	233	11:52 AM	7	232.8565574	0.020491803									
450	29.610215	79.715588	1454.95	166	11:54 AM	9	165.8155738	0.020491803									
500	29.610282	79.71616	1453.01	52.15	11:56 AM	11	51.92459016	0.020491803									
550	29.610295	79.716708	1442.05	39.4	11:58 AM	13	39.13360656	0.020491803									
600	29.610338	79.717255	1432.91	64.3	12:00 PM	15	63.99262295	0.020491803									
			Elevation	**mV**	**Time**	**Time Difference**	**Corrected mV**	**Factor**	**Remark**	**Revised 1 (mV)**		**Revised 2 (mV)**		**Revised 3(mV)**		**Revised 3(mV)**	
Day2_B3(@900m)			**1365.47**	**-1.2375**	**9:08 AM**					**Time**	**mV**	**Time**	**mV**				
Station No.	**Latitude**	**Longitude**	**Elevation**							**10:08 AM**	**-2.1075**						
600	29.610338	79.717255	1432.91	176	9:35 AM	27	175.6085	0.0145									
650	29.610368	79.717807	1425.29	160	9:31 AM	23	159.6665	0.0145									
700	29.610375	79.718394	1408.44	145	9:28 AM	20	144.71	0.0145									
750	29.610394	79.718928	1379.47	107.45	9:22 AM	14	107.247	0.0145									
800	29.610473	79.719516	1362.19	297	9:16 AM	8	296.884	0.0145									
850	29.610504	79.720174	1360.57	21.45	9:13 AM	5	21.3775	0.0145									
900	29.610535	79.720742	1365.47	-1.2375	9:08 AM	0	-1.2375	0.0145									
950	29.61058	79.72127	1365.85	83.6	10:02 AM	54	82.817	0.0145									
1000	29.610612	79.721819	1360.62	448	10:04 AM	56	447.188	0.0145									
			Elevation	**mV**	**Time**	**Time Difference**	**Corrected mV**	**Factor**	**Remark**	**Revised 1 (mV)**		**Revised 2 (mV)**		**Revised 3(mV)**		**Revised 3(mV)**	
Day1_B2(@1200m)			**1346.05**	**9.15**	**2:38 PM**					**Time**	**mV**	**Time**	**mV**				
Station No.	**Latitude**	**Longitude**	**Elevation**							**3:40 PM**	**-1.5525**						
1000	29.610612	79.721819	1360.62	-93.4	3:27 PM	49	-99.40447581	0.12254032258									
1050	29.610642	79.722379	1359.67	-72.425	3:23 PM	45	-77.93931452	0.12254032258									
1100	29.610671	79.722915	1352.23	-99.75	3:20 PM	42	-104.8966935	0.12254032258									

1150	29.610723	79.723473	1351.31	-52.35	3:17 PM	39	-57.12907258	0.12254032258									
1200	29.610719	79.724002	1346.05	9.15	2:38 PM	0	9.15	0.12254032258									
1250	29.610764	79.724527	1339.24	19.4	2:41 PM	3	19.03237903	0.12254032258									
1300	29.610789	79.725094	1330.58	-41.65	2:44 PM	6	-42.38524194	0.12254032258									
1350	29.610811	79.725649	1319.16	72.5	2:47 PM	9	71.3971371	0.12254032258									
1400	29.610845	79.726168	1309.32	35.5	2:50 PM	12	34.02951613	0.12254032258									
1450	29.610883	79.726695	1307.6	100.325	2:53 PM	15	98.48689516	0.12254032258									
1500	29.610932	79.727258	1314.11	105	2:57 PM	19	102.6717339	0.12254032258									
			Elevation	**mV**	**Time**	**Time Difference**	**Corrected mV**	**Factor**	**Remark**	**Revised 1 (mV)**		**Revised 2 (mV)**		**Revised 3(mV)**		**Revised 3(mV)**	
Day1_B1(@1800m)			**1273.4**	**27.6**	**11:28 AM**					**Time**	**mV**	**Time**	**mV**				
Station No.	**Latitude**	**Longitude**	**Elevation**							**12:16 PM**	**15.2**	**1:15 PM**	**-20.2**				
1500	29.610932	79.727258	1314.11	-61.85	1:01 PM	45	-17.86355932	0.0847457627									
1550	29.610959	79.727793	1318.21	-48.48	12:51 PM	35	-3.646101695	0.0847457627									
1600	29.610981	79.728332	1311.36	-74.375	12:47 PM	31	-29.20211864	0.0847457627									
1650	29.611015	79.728822	1293.58	-52.725	12:41 PM	25	-7.043644068	0.0847457627									
1700	29.611042	79.729359	1278.62	-16.73	12:33 PM	17	29.62932203	0.0847457627	River								
1750	29.611057	79.729896	1274.46	-14.35	12:27 PM	11	32.51779661	0.0847457627									
1800	29.611121	79.730461	1273.4	27.6	11:28 AM	0	27.6	0.258333333									
1850	29.611171	79.731	1278.82	6.273	11:34 AM	6	4.723000002	0.258333333									
1900	29.611142	79.731548	1278.89	5.45	11:36 AM	8	3.383333336	0.258333333									
1950	29.611164	79.732134	1276.95	0.81	11:40 AM	12	-2.289999996	0.258333333									
2000	29.611201	79.732681	1277.41	-9.765	11:43 AM	15	-13.64	0.258333333									
2050	29.611226	79.733214	1278.91	1.73	11:46 AM	18	-2.919999994	0.258333333									
2100	29.611254	79.733707	1282.02	-3.185	11:51 AM	23	-9.126666659	0.258333333									
2150	29.611271	79.734201	1289.81	-16	11:56 AM	28	-23.23333332	0.258333333	Road								

SP Line-10

			Elevation	mV	Time	Time Difference	Corrected mV	Factor	Remark	Revised 1 (mV)		Revised 2 (mV)	
Day1_B1(@350m)			1345.79	-8.12	9:34 AM					Time	mV	Time	mV
Station No.	Latitude	Longitude	Elevation (m)							10:36 AM	-8.7975	11:48 AM	-5.625
0	29.608588	79.728585	1287.28	104.9	10:16 AM	42	104.4410484	0.01092741935	River				
50	29.608215	79.728875	1269.42	151	10:12 AM	38	150.5847581	0.01092741935	River				
100	29.607819	79.729205	1274.34	105.675	10:05 AM	31	105.33625	0.01092741935					
150	29.607451	79.729498	1294.82	70	10:00 AM	26	69.7158871	0.01092741935					
200	29.607095	79.729769	1311.88	32.35	9:56 AM	22	32.10959677	0.01092741935					
250	29.606725	79.730064	1328.01	9.595	9:52 AM	18	9.398306452	0.01092741935	Road				
300	29.606302	79.730394	1336.5	17.575	9:39 AM	5	17.5203629	0.01092741935					
350	29.605904	79.730739	1345.79	-8.12	9:34 AM	0	-8.12	0.01092741935					
400	29.605528	79.731072	1355.52	-41.575	11:02 AM	26	-37.934375	0.0440625					
450	29.60511	79.731409	1368.09	-67.2	11:05 AM	29	-63.4271875	0.0440625					
500	29.604719	79.731728	1369.55	-85.3	11:07 AM	31	-81.4390625	0.0440625					
550	29.60431	79.732033	1352.57	-80.8	11:14 AM	38	-76.630625	0.0440625					
600	29.603957	79.732376	1337.56	-82.75	11:22 AM	46	-78.228125	0.0440625					
650	29.603591	79.73268	1322.64	-117.3	11:27 AM	51	-112.5578125	0.0440625	Road				
700	29.603177	79.733011	1303.07	-64.325	11:31 AM	55	-59.4065625	0.0440625					
			Elevation	mV	Time	Time Difference	Corrected mV	Factor	Remark	Revised 1 (mV)		Revised 2 (mV)	
Day1_B2(@900m)			1269.59	-13.325	12:40 PM					Time	mV	Time	mV
Station No.	Latitude	Longitude	Elevation							1:42 PM	-17.5		
700	29.603177	79.733011	1303.07	-155	1:04 PM	24	-156.616129	0.067338709677419					
750	29.60278	79.733353	1296.86	-690	1:00 PM	20	-691.3467742	0.067338709677419					
800	29.602339	79.733712	1286.99	-187	12:50 PM	10	-187.6733871	0.067338709677419					
850	29.601917	79.734062	1269.82	-6.945	12:46 PM	6	-7.349032258	0.067338709677419	River				
900	29.601495	79.734384	1269.59	-13.325	12:40 PM	0	-13.325	0.067338709677419					
950	29.601142	79.734677	1280.39	-116.9	1:19 PM	39	-119.5262097	0.067338709677419					
1000	29.600732	79.735062	1301.94	-57.15	1:25 PM	45	-60.18024194	0.067338709677419					
1050	29.600342	79.735357	1306.07	27.1	1:29 PM	49	23.80040323	0.067338709677419					
1100	29.599903	79.735734	1306.08	70.175	1:31 PM	51	66.74072581	0.067338709677419					

SP Line-11

			Elevation	mV	Time	Time Difference	Corrected mV	Factor	Remark	Revised 1 (mV)		Revised 2 (mV)	
Day2_B3(@350m)			**1688.48**	**-14.775**	**11:21 AM**					**Time**	**mV**	**Time**	**mV**
Station No.	**Latitude**	**Longitude**	**Elevation (m)**							**12:25 PM**	**-14.35**	**1:20 PM**	**-16**
0	29.647668	79.687358	1614.69	-65.4	11:50 AM	29	-65.20742188	0.006640625					
50	29.647527	79.687863	1631.09	-35.7	11:46 AM	25	-35.53398438	0.006640625					
100	29.647423	79.688386	1643.81	-13.95	11:43 AM	22	-13.80390625	0.006640625					
150	29.647304	79.688873	1655.23	-9.475	11:38 AM	17	-9.362109375	0.006640625					
200	29.647187	79.689387	1660.07	-5.24666	11:36 AM	15	-5.147050625	0.006640625					
250	29.647083	79.689904	1659.21	-51.4	11:32 AM	11	-51.32695313	0.006640625					
300	29.646961	79.690437	1672.28	-25.2	11:27 AM	6	-25.16015625	0.006640625					
350	29.646857	79.690952	1688.48	-14.775	11:21 AM	0	-14.775	0.006640625					
400	29.646719	79.691453	1705.74	12.5	12:31 PM	6	13.545	0.03					
450	29.646613	79.691959	1729.26	3.805	12:34 PM	9	4.76	0.03					
500	29.646505	79.692472	1753.83	33.9	12:39 PM	14	34.705	0.03					
550	29.646388	79.692981	1753.34	12.1	12:41 PM	16	12.845	0.03					
600	29.646275	79.693494	1740.11	20.25	12:44 PM	19	20.905	0.03					
650	29.646154	79.694013	1730.97	64.7	12:46 PM	21	65.295	0.03					
700	29.646042	79.694521	1717.8	58.6	12:49 PM	24	59.105	0.03					
			Elevation	**mV**	**Time**	**Time Difference**	**Corrected mV**	**Factor**	**Remark**	**Revised 1 (mV)**		**Revised 2 (mV)**	
Day2_B4(@900m)			**1664.31**	**-52.75**	**2:30 PM**					**Time**	**mV**	**Time**	**mV**
Station No.	**Latitude**	**Longitude**	**Elevation**							**3:04 PM**	**-49.2**		
700	29.646042	79.694521	1717.8	58.6	2:41 PM	11	59.74852941	0.104411765					
750	29.64592	79.695029	1708.36	54.2	2:38 PM	8	55.03529412	0.104411765					
800	29.645817	79.695541	1691.94	41.1	2:36 PM	6	41.72647059	0.104411765					
850	29.645696	79.696044	1681.43	33.6	2:33 PM	3	33.91323529	0.104411765					
900	29.645605	79.696562	1664.31	-52.75	2:30 PM	0	-52.75	0.104411765					
950	29.645466	79.697076	1646.19	-29	2:52 PM	22	-26.70294118	0.104411765					
1000	29.645353	79.697596	1627.45	-42	2:54 PM	24	-39.49411765	0.104411765					
1050	29.645241	79.698109	1601.9	-130	2:56 PM	26	-127.2852941	0.104411765					
			Elevation	**mV**	**Time**	**Time Difference**	**Corrected mV**	**Factor**	**Remark**	**Revised 1 (mV)**		**Revised 2 (mV)**	
Day1_B1 (@1350m)			**1502.02**	**-47.25**	**9:13 AM**					**Time**	**mV**	**Time**	**mV**
Station No.	**Latitude**	**Longitude**	**Elevation**							**10:12 AM**	**17.8**	**11:06 AM**	**12.4**
1050	29.645241	79.698109	1601.9	150	9:37 AM	24	161.979661	0.4991525423729					
1100	29.645122	79.698618	1585.87	261	9:33 AM	20	270.9830508	0.4991525423729					
1150	29.644995	79.699104	1575.53	247	9:30 AM	17	255.4855932	0.4991525423729					
1200	29.644899	79.69963	1563.29	239	9:26 AM	13	245.4889831	0.4991525423729					

1250	29.644779	79.700148	1546.17	225	9:22 AM	9	229.4923729	0.4991525423729	Road				
1300	29.644656	79.700693	1524.35	135	9:18 AM	5	137.4957627	0.4991525423729					
1350	29.644542	79.701211	1502.02	-47.25	9:13 AM	0	-47.25	0.4991525423729					
1400	29.644433	79.701723	1480.73	-81.7	10:16 AM	4	-21.65	0.1					
1450	29.644316	79.702234	1458.48	-71.7	10:19 AM	7	-11.35	0.1					
1500	29.644196	79.702717	1440.39	-11.54	10:22 AM	10	49.11	0.1					
1550	29.644093	79.703245	1424.84	166	10:25 AM	13	226.95	0.1					
1600	29.64398	79.703751	1419.35	240	10:29 AM	17	301.35	0.1	Nala				
1650	29.643862	79.704261	1417.73	184	10:33 AM	21	245.75	0.1					
1700	29.643749	79.704777	1410.53	267	10:37 AM	25	329.15	0.1					
			Elevation	**mV**	**Time**	**Time Difference**	**Corrected mV**	**Factor**	**Remark**	**Revised 1 (mV)**		**Revised 2 (mV)**	
Day1_B2(@1950m)			**1385.16**	**6.14**	**12:42 PM**					**Time**	**mV**	**Time**	**mV**
Station No.	**Latitude**	**Longitude**	**Elevation**							**1:34 PM**	**6.08**		
1700	29.643749	79.704777	1410.53	169	12:59 PM	17	168.9803846	0.00115384615384615					
1750	29.643629	79.705292	1406.21	183.5	12:54 PM	12	183.4861538	0.00115384615384615					
1800	29.64353	79.705818	1398.14	192	12:51 PM	9	191.9896154	0.00115384615384615					
1850	29.643393	79.70631	1391.31	18.5	12:49 PM	7	18.49192308	0.00115384615384615					
1900	29.643304	79.706823	1384.92	175	12:47 PM	5	174.9942308	0.00115384615384615					
1950	29.643183	79.707337	1385.16	6.14	12:42 PM	0	6.14	0.00115384615384615					
2000	29.643064	79.70784	1390.23	-52	1:13 PM	31	-52.03576923	0.00115384615384615					
2050	29.642945	79.708362	1397.72	13.4	1:15 PM	33	13.36192308	0.00115384615384615					
2100	29.642835	79.708864	1403.61	125	1:17 PM	35	124.9596154	0.00115384615384615					
2150	29.642722	79.709372	1400.16	137	1:19 PM	37	136.9573077	0.00115384615384615					
2200	29.642611	79.709861	1399.93	150	1:21 PM	39	149.955	0.00115384615384615					

SP Line-12

			Elevation	mV	Time	Time Difference	Corrected mV	Factor	Remark	Revised 1 (mV)		Revised 2 (mV)	
Day2_B2(@350m)			**1468.06**	**-16.9**	**11:19 AM**					**Time**	**mV**	**Time**	**mV**
Station No.	**Latitude**	**Longitude**	**Elevation (m)**							**12:28 PM**	**-6.42**	**12:55 PM**	**-6.66**
0	29.655996	79.702662	1578	123	12:45 PM	40	123.355552	0.0088888					
50	29.655902	79.703174	1570	98.6	12:42 PM	36	98.9199968	0.0088888	Mica Schist				
100	29.655802	79.703683	1568	-63.1	12:40 PM	32	-62.8155584	0.0088888					
150	29.655717	79.704196	1566	-110.5	12:38 PM	26	-110.2688912	0.0088888	Graphite Schist				
200	29.655628	79.704712	1560	-44.95	12:36 PM	20	-44.772224	0.0088888	Road				
250	29.655441	79.705231	1547	-20.8	12:33 PM	10	-20.711112	0.0088888					
300	29.655439	79.705742	1533	-46.95	12:29 PM	1	-46.9411112	0.0088888					
350	29.65534	79.706263	1519	-16.9	11:19 AM	0	-16.9	0.151884057971					
400	29.65524	79.706793	1501	5.69	11:22 AM	3	6.145652174	0.151884057971					
450	29.655167	79.707346	1482	27.75	11:25 AM	6	28.66130435	0.151884057971					
500	29.655074	79.707877	1463	39.55	11:28 AM	9	40.91695652	0.151884057971					
550	29.654982	79.708399	1448	89.6	11:32 AM	13	91.57449275	0.151884057971					
600	29.65486	79.708924	1447	24.75	11:34 AM	15	27.02826087	0.151884057971					
650	29.654784	79.709441	1454	95.65	11:43 AM	24	99.29521739	0.151884057971					
700	29.65469	79.709946	1463	89.65	11:56 AM	37	95.26971014	0.151884057971					
			Elevation	**mV**	**Time**	**Time Difference**	**Corrected mV**	**Factor**	**Remark**	**Revised 1 (mV)**		**Revised 2 (mV)**	
Day2_B1(@1050m)			**1503.93**	**2**	**12:00 PM**					**Time**	**mV**	**Time**	**mV**
Station No.	**Latitude**	**Longitude**	**Elevation**							**1:14 AM**	**0.97**		
700	29.65469	79.709946	1463	41.55	12:24 PM	24	41.21594595	0.013918919					
750	29.654584	79.710463	1476	42.6	12:20 PM	20	42.32162162	0.013918919					
800	29.654524	79.710994	1460.02	40.1	12:16 PM	16	39.8772973	0.013918919					
850	29.654444	79.711509	1464.6	12.8	12:13 PM	13	12.61905405	0.013918919					
900	29.654344	79.71204	1471.71	31.35	12:09 PM	9	31.22472973	0.013918919					
950	29.654256	79.712564	1474.76	46.6	12:07 PM	7	46.50256757	0.013918919					
1000	29.654166	79.713098	1486.23	30.3	12:03 PM	3	30.25824324	0.013918919					
1050	29.654072	79.713639	1503.93	2	12:00 PM	0	2	0.013918919					
1100	29.653978	79.714172	1518.87	-14.15	12:51 PM	51	-14.85986486	0.013918919					
1150	29.653871	79.71474	1529.34	-45.3	12:54 PM	54	-46.05162162	0.013918919					
1200	29.653785	79.715273	1544.33	-35.3	12:58 PM	58	-36.1072973	0.013918919					
1250	29.65369	79.71579	1571.44	-69.4	1:03 PM	63	-70.27689189	0.013918919					
1300	29.653606	79.716309	1584.52	-114.5	1:07 PM	67	-115.4325676	0.013918919					
			Elevation	**mV**	**Time**	**Time Difference**	**Corrected mV**	**Factor**	**Remark**	**Revised 1 (mV)**		**Revised 2 (mV)**	
Day1_B2(@1450m)			**1546.81**	**-4.91**	**12:52 PM**					**Time**	**mV**	**Time**	**mV**

Station No.	Latitude	Longitude	Elevation							2:08 PM	-8.03		
1300	29.653606	79.716309	1584.52	-28.1	2:04 PM	72	-31.05578947	0.041052632					
1350	29.653502	79.716836	1578.98	-13.6	2:02 PM	70	-16.47368421	0.041052632	Road				
1400	29.65343	79.71738	1561.12	-16.3	1:59 PM	67	-19.05052632	0.041052632					
1450	29.653318	79.717905	1552.82	-4.91	12:52 PM	0	-4.91	0.041052632					
1500	29.653229	79.718427	1535.62	16.4	12:56 PM	4	16.23578947	0.041052632					
1550	29.653137	79.718978	1514.14	15.4	12:58 PM	6	15.15368421	0.041052632					
1600	29.653043	79.719503	1499.46	1.43	1:01 PM	9	1.060526316	0.041052632					
1650	29.652917	79.720038	1495.25	-0.44	1:05 PM	13	-0.973684211	0.041052632	Nala				
1700	29.652824	79.720572	1418.73	-38.25	1:09 PM	17	-38.94789474	0.041052632					
1750	29.652734	79.721101	1462.48	-1.47	1:22 PM	30	-2.701578947	0.041052632					
1800	29.65264	79.721619	1443.29	-35.3	1:24 PM	32	-36.61368421	0.041052632					
			Elevation	mV	Time	Time Difference	Corrected mV	Factor	Remark	Revised 1 (mV)		Revised 2 (mV)	
Day1_B1(@2150m)			1546.81	-36.65	9:54 AM					Time	mV	Time	mV
Station No.	Latitude	Longitude	Elevation							10:54 AM	-0.35		
1800	29.65264	79.721619	1443.29	-15.9	10:47 AM	53	16.165	0.605					
1850	29.653551	79.722145	1425.6	-27.9	10:43 AM	49	1.745	0.605					
1900	29.652473	79.722677	1416.88	-19.375	10:39 AM	45	7.85	0.605					
1950	29.652393	79.723193	1417.61	-34.85	10:36 AM	42	-9.44	0.605					
2000	29.652293	79.723714	1417.83	-15.9	10:33 AM	39	7.695	0.605					
2050	29.652222	79.724251	1417.7	-7.345	10:31 AM	37	15.04	0.605					
2100	29.652134	79.724761	1417.06	-1.18	10:29 AM	35	19.995	0.605					
2150	29.652045	79.725276	1407.16	-36.65	9:54 AM	0	-36.65	0.605					
2200	29.651937	79.75813	1401.34	24.7	10:00 AM	6	28.33	0.605					
2250	29.651828	79.725813	1399.96	-8.91	10:04 AM	10	-2.86	0.605					
2300	29.651747	79.72691	1398.09	-52.75	10:07 AM	13	-44.885	0.605	Nala				
2350	29.651655	79.727427	1396.12	-61.05	10:09 AM	15	-51.975	0.605					
2400	29.651563	79.727975	1389.69	-57.3	10:12 AM	18	-46.41	0.605					

SP Line-13

			Elevation	mV	Time	Time Difference	Corrected mV	Factor	Remark	Revised 1 (mV)		Revised 2 (mV)	
Day1_B2(@300m)			**1468.06**	**14.9**	**12:56 PM**					**Time**	**mV**	**Time**	**mV**
Station No.	**Latitude**	**Longitude**	**Elevation (m)**							**1:57 PM**	**19.0**	**2:51 PM**	**14.1**
0	29.596831	79.688614	1350.64	18.4	2:37 PM	40	13.97037037	0.0907407407407					
50	29.597268	79.688834	1366.49	-18.9	2:33 PM	36	-22.96666667	0.0907407407407					
100	29.597695	79.689056	1382.44	-86.8	2:29 PM	32	-90.5037037	0.0907407407407					
150	29.598124	79.689274	1405.53	-95.05	2:23 PM	26	-98.20925926	0.0907407407407					
200	29.598564	79.689477	1432.05	-125	2:17 PM	20	-127.6148148	0.0907407407407	Road				
250	29.598978	79.68969	1449.74	-92.75	2:07 PM	10	-94.45740741	0.0907407407407					
300	29.599397	79.689895	1468.06	14.9	12:56 PM	0	14.9	0.0672131147540983					
350	29.599809	79.690094	1482.78	14.3	1:08 PM	12	15.10655738	0.0672131147540983					
400	29.600224	79.690303	1486.85	85.9	1:11 PM	15	86.90819672	0.0672131147540983					
450	29.600654	79.690508	1492.28	177	1:14 PM	18	178.2098361	0.0672131147540983					
500	29.601066	79.690716	1512.58	265	1:18 PM	22	266.4786885	0.0672131147540983					
550	29.601495	79.690936	1532.18	302	1:21 PM	25	303.6803279	0.0672131147540983					
600	29.601928	79.691145	1552.48	283	1:26 PM	30	285.0163934	0.0672131147540983					
			Elevation	**mV**	**Time**	**Time Difference**	**Corrected mV**	**Factor**	**Remark**	**Revised 1 (mV)**		**Revised 2 (mV)**	
Day1_B1(@950m)			**1664.31**	**0.785**	**10:33 AM**					**Time**	**mV**	**Time**	**mV**
Station No.	**Latitude**	**Longitude**	**Elevation**							**11:31 AM**	**-4.535**		
600	29.601928	79.691145	1552.48	-3.295	11:21 AM	48	-6.398448276	0.06465517241379					
650	29.602347	79.69135	1578.62	-9.18	11:17 AM	44	-12.02482759	0.06465517241379					
700	29.602766	79.691558	1599.93	-5.125	11:13 AM	40	-7.711206897	0.06465517241379					
750	29.603177	79.691773	1612.42	-0.66	11:09 AM	36	-2.987586207	0.06465517241379					
800	29.603597	79.691977	1604.79	24.8	11:04 AM	31	22.79568966	0.06465517241379					
850	29.604029	79.692182	1581.25	27.4	11:01 AM	28	25.58965517	0.06465517241379					
900	29.604436	79.692396	1562	33.3	10:56 AM	23	31.81293103	0.06465517241379					
950	29.604866	79.692599	1546.81	0.785	10:33 AM	0	0.785	0.06465517241379					
1000	29.605289	79.692817	1528.95	-28.25	10:39 AM	6	-28.63793103	0.06465517241379					
1050	29.605719	79.693019	1513.35	-83.8	10:45 AM	12	-84.57586207	0.06465517241379					

SP Line-14

			Elevation	mV	Time	Time Difference	Corrected mV	Factor	Remark	Revised 1 (mV)		Revised 2 (mV)	
Day2_B2(@350m)			**1688.48**	**-14.775**	**11:21 AM**					**Time**	**mV**	**Time**	**mV**
Station No.	**Latitude**	**Longitude**	**Elevation (m)**							**12:25 PM**	**-14.35**	**1:20 PM**	**-16**
0	29.654263	79.672205	1815.99	54.875	11:16 AM	21	55.01445313	0.006640625					
50	29.653977	79.672582	1799.71	19.975	11:13 AM	18	20.09453125	0.006640625					
100	29.653667	79.672992	1785.92	-14.25	11:10 AM	15	-14.15039063	0.006640625					
150	29.653384	79.673369	1776.15	-100.6	11:07 AM	14	-100.5070313	0.006640625					
200	29.653072	79.673772	1757.28	-39.9	11:03 AM	10	-39.83359375	0.006640625					
250	29.652805	79.67412	1737.53	-24.7	11:01 AM	8	-24.646875	0.006640625					
300	29.652528	79.674496	1717.75	-5.88	10:58 AM	5	-5.846796875	0.006640625					
350	29.652237	79.674876	1696.22	4.75	10:53 AM	0	4.75	0.006640625					
400	29.651954	79.675226	1679.32	-10.895	11:42 AM	17	-12.63	0.03					
450	29.651679	79.675608	1661.09	-96.15	11:44 AM	19	-97.945	0.03	Graphite soil				
500	29.651396	79.675973	1644.52	-175.5	11:46 AM	21	-177.355	0.03	Graphite soil				
550	29.651118	79.676339	1639.43	-252	11:49 AM	24	-253.945	0.03					
600	29.650806	79.676755	1629.2	-91.95	11:51 AM	26	-93.955	0.03					
650	29.650492	79.677157	1623.32	-193	11:53 AM	28	-195.065	0.03	Nala				
700	29.650196	79.677561	1624.24	-273	11:55 AM	30	-275.125	0.03					
750	29.649879	79.677972	1622.12	-45.4	11:57 AM	32	-47.585	0.03					
			Elevation	**mV**	**Time**	**Time Difference**	**Corrected mV**	**Factor**	**Remark**	**Revised 1 (mV)**		**Revised 2 (mV)**	
Day2_B4(@1000m)				**3.765**	**2:21 PM**					**Time**	**mV**	**Time**	**mV**
Station No.	**Latitude**	**Longitude**	**Elevation**							**2:50 PM**	**3.25**		
750	29.649879	79.677972	1622.12	-4.615	2:34 PM	13	-4.845862069	0.017758620689655					
800	29.649568	79.678374	1616.95	23.25	2:32 PM	11	23.05465517	0.017758620689655					
850	29.649277	79.67877	1602.33	44.15	2:30 PM	9	43.99017241	0.017758620689655					
900	29.648972	79.679167	1592.4	39.5	2:27 PM	6	39.39344828	0.017758620689655					
950	29.648678	79.679557	1586.98	45.5	2:24 PM	3	45.44672414	0.017758620689655	Nala				
1000	29.64838	79.679944	1588.1	3.765	2:21 PM	0	3.765	0.017758620689655					
1050	29.648064	79.680358	1597.01	4.95	2:45 PM	24	4.523793103	0.017758620689655					
1100	29.647779	79.680738	1601.65	-51.2	2:47 PM	26	-51.66172414	0.017758620689655					
			Elevation	**mV**	**Time**	**Time Difference**	**Corrected mV**	**Factor**	**Remark**	**Revised 1 (mV)**		**Revised 2 (mV)**	
Day2_B3 (@1250m)				**7.6**	**1:08 PM**					**Time**	**mV**	**Time**	**mV**
Station No.	**Latitude**	**Longitude**	**Elevation**							**2:00 PM**	**0.21**		
1100	29.647779	79.680738	1601.65	-33.05	1:15 PM	7	-34.04480769	0.142115384615384					
1150	29.647476	79.681145	1600.98	-46.5	1:13 PM	5	-47.21057692	0.142115384615384					
1200	29.647151	79.681554	1600.1	-24.9	1:11 PM	3	-25.32634615	0.142115384615384					
1250	29.646867	79.681946	1603.14	**7.6**	**1:08 PM**	0	7.6	0.142115384615384					
1300	29.646557	79.682336	1609.29	-17.3	1:25 PM	17	-19.71596154	0.142115384615384					

1350	29.646258	79.682735	1602.86	19.05	1:27 PM	19	16.34980769	0.142115384615384					
1400	29.645973	79.683128	1591.91	40.7	1:29 PM	21	37.71557692	0.142115384615384					
1450	29.645654	79.68353	1570.03	20.6	1:31 PM	23	17.33134615	0.142115384615384					
1500	29.645348	79.683928	1553.9	-95.8	1:34 PM	26	-99.495	0.142115384615384					
1550	29.645052	79.684323	1561.09	-180	1:37 PM	29	-184.1213462	0.142115384615384	Nala				
1600	29.644755	79.684714	1571.97	-75.6	1:40 PM	32	-80.14769231	0.142115384615384					
			Elevation	**mV**	**Time**	**Time Difference**	**Corrected mV**	**Factor**	**Remark**	**Revised 1 (mV)**		**Revised 2 (mV)**	
Day1_B1(@1950m)				**-9.015**	**11:02 AM**					**Time**	**mV**	**Time**	**mV**
Station No.	**Latitude**	**Longitude**	**Elevation**							**12:01 PM**	**-19.9**	**12:53 PM**	**-21.1**
1600	29.644755	79.684714	1571.97	-183	11:31 AM	29	-188.3502542	0.184491525423728					
1650	29.644467	79.685122	1589.89	-46.6	11:28 AM	26	-51.39677966	0.184491525423728					
1700	29.644148	79.685515	1609.22	-75.7	11:23 AM	21	-79.57432203	0.184491525423728					
1750	29.643864	79.685903	1624.91	-7.9725	11:20 AM	18	-11.29334746	0.184491525423728					
1800	29.643358	79.686296	1629.91	11.36	11:16 AM	14	8.777118644	0.184491525423728					
1850	29.643258	79.686696	1622.21	34.3	11:13 AM	11	32.27059322	0.184491525423728					
1900	29.642957	79.687079	1611.86	31.1	11:10 AM	8	29.6240678	0.184491525423728					
1950	29.642648	79.687468	1607.62	**-9.015**	**11:02 AM**	0	-9.015	0.184491525423728					
2000	29.642371	79.687864	1616.53	-26.3	12:08 PM	7	-38.54653846	0.0230769230769					
2050	29.642045	79.688256	1609.54	-12.55	12:11 PM	10	-24.86576923	0.0230769230769					
2100	29.641757	79.688658	1624.65	-20.8	12:17 PM	16	-33.25423077	0.0230769230769					
2150	29.641446	79.689059	1651.5	-114.2	12:22 PM	21	-126.7696154	0.0230769230769					
2200	29.641154	79.689447	1677.05	-454	12:25 PM	24	-466.6388462	0.0230769230769					
2250	29.640852	79.689836	1678.76	-211	12:28 PM	27	-223.7080769	0.0230769230769					
2300	29.640544	79.690249	1678.69	-171	12:32 PM	31	-183.8003846	0.0230769230769					

SP Line-15

			Elevation	mV	Time	Time Difference	Corrected mV	Factor	Remark	Revised 1 (mV)		Revised 2 (mV)	
Day1_B01(@350m)				**6.11**	**11:23 AM**					**Time**	**mV**	**Time**	**mV**
Station No.	**Latitude**	**Longitude**	**Elevation (m)**							**12:23 PM**	**-0.24**	**1:02 PM**	**-3.27**
0	29.632644	79.670014	1829.08	-63.4	11:53 AM	30	-66.335	0.097833333					
50	29.632999	79.67031	1814.46	-79.5	11:49 AM	26	-82.04366667	0.097833333					
100	29.633366	79.670617	1802.33	-61.3	11:45 AM	22	-63.45233333	0.097833333					
150	29.633738	79.670927	1783.23	-54.6	11:41 AM	18	-56.361	0.097833333					
200	29.634096	79.671221	1768.49	-33	11:37 AM	14	-34.36966667	0.097833333					
250	29.634459	79.671535	1757.78	3.3	11:33 AM	10	2.321666667	0.097833333					
300	29.634844	79.671833	1747.47	-24.3	11:30 AM	7	-24.98483333	0.097833333					
350	29.635205	79.672153	1738.99	6.11	11:23 AM	0	6.11	0.097833333					
400	29.635568	79.672453	1738.22	-11.4	12:28 PM	5	-21.16846154	0.077692307692					
450	29.635938	79.67276	1732.57	-10.85	12:32 PM	9	-20.92923077	0.077692307692					
500	29.636308	79.67307	1720.9	-25.7	12:35 PM	12	-36.01230769	0.077692307692					
550	29.636683	79.67338	1718.33	55.65	12:37 PM	14	45.18230769	0.077692307692					
600	29.637051	79.673686	1714.01	-7.9	12:39 PM	16	-18.52307692	0.077692307692					
650	29.637411	79.674001	1703.24	-18	12:41 PM	18	-28.77846154	0.077692307692					
700	29.637789	79.674311	1691.2	16.4	12:43 PM	20	5.466153846	0.077692307692					
750	29.638153	79.674619	1683.12	-23.45	12:46 PM	23	-34.61692308	0.077692307692					
			Elevation	**mV**	**Time**	**Time Difference**	**Corrected mV**	**Factor**	**Remark**	**Revised 1 (mV)**		**Revised 2 (mV)**	
Day2_B2(@1050m)				**-4.07**	**11:21 AM**					**Time**	**mV**	**Time**	**mV**
Station No.	**Latitude**	**Longitude**	**Elevation**							**12:22 PM**	**-4.63**		
750	29.638153	79.674619	1683.12	63.3	11:36 AM	15	63.16229508	0.0091803278688					
800	29.638532	79.679946	1680.78	39.55	11:34 AM	13	39.43065574	0.0091803278688					
850	29.63891	79.675248	1675.58	38.1	11:32 AM	11	37.99901639	0.0091803278688					
900	29.639268	79.675555	1660.36	7.64	11:29 AM	8	7.566557377	0.0091803278688					
950	29.639642	79.675864	1650.01	24.5	11:27 AM	6	24.44491803	0.0091803278688					
1000	29.640014	79.67617	1638.25	46.7	11:24 AM	3	46.67245902	0.0091803278688					
1050	29.640388	79.67649	1634.28	-4.07	11:21 AM	0	-4.07	0.0091803278688					
1100	29.640754	79.676789	1632.9	6.56	11:53 AM	32	6.266229508	0.0091803278688					
1150	29.641131	79.677099	1636.06	-3.1675	11:55 AM	34	-3.479631148	0.0091803278688					
1200	29.641493	79.6774	1646.54	-24.15	11:59 AM	38	-24.49885246	0.0091803278688					
1250	29.641872	79.677732	1651.64	-11.2	12:01 PM	40	-11.56721311	0.0091803278688					
1300	29.642237	79.678032	1648.07	-27.7	12:04 PM	43	-28.0947541	0.0091803278688					
1350	29.642603	79.678347	1637.61	-9.99	12:06 PM	45	-10.40311475	0.0091803278688					
			Elevation	**mV**	**Time**	**Time Difference**	**Corrected mV**	**Factor**	**Remark**	**Revised 1 (mV)**		**Revised 2 (mV)**	

Day2_B3 (@1500m)				-1.33	12:53 PM					Time	mV	Time	mV
Station No.	Latitude	Longitude	Elevation							1:32 PM	-4.63		
1350	29.642603	79.678347	1637.61	-69.2	1:18 PM	25	-71.31538462	0.08461538461538					
1400	29.642964	79.67865	1627.46	-42.25	1:13 PM	20	-43.94230769	0.08461538461538					
1450	29.643349	79.678965	1605.95	-9.3	1:11 PM	18	-10.82307692	0.08461538461538					
1500	29.643707	79.679276	1590.17	-1.33	12:53 PM	0	-1.33	0.08461538461538					
1550	29.644095	79.67959	1575.29	-0.9	12:56 PM	3	-1.153846154	0.08461538461538					
1600	29.644456	79.679892	1568.53	4.4	1:00 PM	7	3.807692308	0.08461538461538					

SP Line-16

			Elevation	mV	Time	Time Difference	Corrected mV	Factor	Remark	Revised 1 (mV)		Revised 2 (mV)	
Day1_B1(@300m)				**-38.5**	**10:46 AM**					**Time**	**mV**	**Time**	**mV**
Station No.	**Latitude**	**Longitude**	**Elevation (m)**							**11:46 AM**	**-50.6**	**12:42 PM**	**-44.5**
0	29.62295856	79.7154971	1395.41	-46.5	10:55:00 AM	9	-48.3149994	0.2016666					
50	29.62299388	79.71576734	1380.86	-18.15	11:10:00 AM	20	-22.183332	0.2016666					
100	29.62303655	79.7163224	1367.52	-6.23	11:20:00 AM	34	-13.0866644	0.2016666					
150	29.623083	79.71682	1367.96	-7.9	11:30:00 AM	44	-16.7733304	0.2016666					
200	29.62311001	79.71735666	1381.75	-46.4	11:39:00 AM	53	-57.0883298	0.2016666					
250	29.62317624	79.71787282	1399.16	-44.8	11:43:00 AM	57	-56.2949962	0.2016666					
300	29.62325697	79.71835816	1395.45	-38.5	10:46:00 AM	0	-38.5	0.2016666					
350	29.62325957	79.71883044	1381.12	-19	12:10:00 PM	24	-27.614284	0.1089285					
400	29.62321854	79.71943339	1366.45	0.0025	12:15:00 PM	29	-9.1564265	0.1089285					
450	29.62331223	79.71998727	1344.53	4.3	12:20:00 PM	34	-5.403569	0.1089285					
500	29.62337229	79.72045356	1324.58	10.11	12:27:00 PM	41	-0.3560685	0.1089285					
550	29.62336879	79.72102621	1313.35	18.5	12:30:00 PM	44	7.707146	0.1089285					
600	29.62338714	79.72153141	1313.56	-66.6	12:35:00 PM	49	-77.9374965	0.1089285					
650	29.62347079	79.72207985	1325.86	-279.5	12:40:00 PM	54	-291.382139	0.1089285					
			Elevation	**mV**	**Time**	**Time Difference**	**Corrected mV**	**Factor**	**Remark**	**Revised 1 (mV)**		**Revised 2 (mV)**	
Day1_B2(@800m)				**3.66**	**2:08:00 AM**					**Time**	**mV**	**Time**	**mV**
Station No.	**Latitude**	**Longitude**								**2:19:00 AM**	**3.75**	**2:59:00 AM**	**6.44**
650	29.62347079	79.72207985	1325.86	-178	1:57:00 AM	11	-177.9100002	0.0081818					
700	29.62350514	79.72256423	1335.04	-142	2:12:00 AM	4	-141.9672728	0.0081818					
750	29.62354671	79.72308312	1346.78	-4.71	2:15:00 AM	7	-4.6527274	0.0081818					
800	29.62359907	79.72358958	1352.03	3.75	2:08:00 AM	0	3.75	0.0081818					
850	29.62364556	79.72419196	1346.34	-1.108	2:23:00 AM	4	1.941	0.06725					
900	29.62368673	79.72468024	1340.93	114.4	2:27:00 AM	8	117.718	0.06725					
950	29.62371577	79.72514014	1351.52	84.5	2:30:00 AM	11	88.01975	0.06725					
1000	29.62377308	79.7257492	1359.71	-219	2:34:00 AM	15	-215.21125	0.06725					
1050	29.62381561	79.7262054	1370	-256	2:37:00 AM	18	-252.0095	0.06725					
1100	29.62380078	79.72671616	1327.72	-256	2:41:00 AM	22	-251.7405	0.06725					
1150	29.6238602	79.72727845	1397.53	-279	2:46:00 AM	27	-274.40425	0.06725					
			Elevation	**mV**	**Time**	**Time Difference**	**Corrected mV**	**Factor**	**Remark**	**Revised 1 (mV)**		**Revised 2 (mV)**	
Day2_B3(@1400m)				**0.735**	**11:37:00 AM**					**Time**	**mV**	**Time**	**mV**
Station No.	**Latitude**	**Longitude**								**12:35:00 PM**	**-1.97**	**1:18:00 PM**	**-6.51**
1150	29.6238602	79.72727845	1397.53	106.3	13:07	32	97.1463952	0.1055814					
1200	29.623864	79.727482	1398.03	-83.03	13:01	26	-91.5501164	0.1055814					
1250	29.623874	79.728001	1389.81	-52.45	12:56	21	-60.4422094	0.1055814					
1300	29.623888	79.728517	1369.72	-20.23	12:49	14	-27.4831396	0.1055814					

1350	29.623911	79.729029	1343.98	-12.73	12:41	7	-19.2440698	0.1055814					
1400	29.623904	79.729521	1320.96	0.735	11:37	0	0.735	0.0212931					
1450	29.623932	79.730047	1301.35	0.048	11:41	4	-0.0371724	0.0212931					
1500	29.62393	79.730586	1294.02	-30.23	11:45	8	-30.4003448	0.0212931					
1550	29.623944	79.731098	1301.45	-64.25	11:47	10	-64.462931	0.0212931					
1600	29.629967	79.731623	1317.03	-70.025	12:20	43	-70.9406033	0.0212931					
1650	29.623963	79.732146	1323.98	-54.58	12:17	40	-55.431724	0.0212931					
1700	29.623968	79.732692	1323.56	-57.9	12:03	26	-58.4536206	0.0212931					
1750	29.623989	79.733234	1322.58	-25.5	12:11	34	-26.2239654	0.0212931					

SP Line-17

			Elevation	mV	Time	Time Difference	Corrected mV	Factor	Remark	Revised 1 (mV)		Revised 2 (mV)	
Day1_B1(@350m)				**-8.105**	**10:20 AM**					**Time**	**mV**	**Time**	**mV**
Station No.	**Latitude**	**Longitude**	**Elevation (m)**							**11:40 AM**	**-1.02**	**1:16 PM**	**-60.5**
0	29.62580	79.71507	1326.12	50.9	10:42 AM		50.9	0.006641					
50	29.62592	79.71557	1330.35	26.7	10:46 AM		26.7	0.006641					
100	29.62597	79.71611	1327.08	22.25	10:53 AM		22.25	0.006641					
150	29.62606	79.71663	1324.55	34.43	11:08 AM		34.43333	0.006641					
200	29.62611	79.71711	1322.75	-3.4	11:20 AM		-3.4	0.006641					
250	29.62618	79.71764	1326.49	-42.6	11:24 AM		-42.6	0.006641					
300	29.62625	79.71814	1327.05	-21.45	11:28 AM		-21.45	0.006641					
350	29.62634	79.71866	1325.34	-1.02	11:40 AM		-1.02	0.006641					
400	29.62637	79.71921	1332.77	-32.675	11:44 AM		-31.45	0.03					
450	29.62645	79.71971	1349.07	-138	11:50 AM		-136.775	0.03					
500	29.62652	79.72027	1353.07	-211.25	11:55 AM		-210.025	0.03					
550	29.62658	79.72078	1378.34	-235.75	12:04 PM		-234.525	0.03					
600	29.62667	79.72133	1391.96	-248	12:25 PM		-246.775	0.03					
650	29.62674	79.72187	1390.79	-237.25	12:36 PM		-236.025	0.03					
			Elevation	**mV**	**Time**	**Time Difference**	**Corrected mV**	**Factor**	**Remark**	**Revised 1 (mV)**		**Revised 2 (mV)**	
Day1_B2(@900m)				**-17.29**	**2:09 PM**					**Time**	**mV**	**Time**	**mV**
Station No.	**Latitude**	**Longitude**	**Elevation**							**3:03 PM**	**7.445**		
650	29.62674	79.72187	1390.79	-213	14:35:00								
700	29.62674	79.72237	1377.08	-138	2:43:00 PM		-138	0.104412					
750	29.62684	79.72289	1378.75	-2.81	2:48:00 PM		-2.81	0.104412					
800	29.62694	79.72349	1394.82	-161	2:54:00 PM		-161	0.104412					
850	29.62685	79.72403	1398.99	-32.7	2:59:00 PM		-32.7	0.104412					
900	29.62707	79.72442	1403.18	7.46	3:03:00 PM		7.46	0.104412					
950	29.62713	79.72495	1411.98	32.38	3:11:00 PM		32.38	0.104412					
1000	29.62717	79.72545	1426.22	62.3	3:17:00 PM		62.3	0.104412					
1050	29.62725	79.72599	1435.14	-20.8	3:19:00 PM		-20.8	0.104412					
1100	29.62734	79.72652	1433.09	-17.03	3:23:00 PM		-17.03	0.104412					

SP Line- 18

			Elevation	mV	Time	Time Difference	Corrected mV	Factor	Remark	Revised 1 (mV)		Revised 2 (mV)	
Day1_B2(@350m)				**-19.6**	**1:52 PM**					**Time**	**mV**	**Time**	**mV**
Station No.	**Latitude**	**Longitude**	**Elevation (m)**							**2:52 PM**	**-18.7**		
0	29.62872	79.71472	1422.75	-124	2:41 PM	49	-123.265	0.015					
50	29.62874	79.71524	1423.55	-146	2:39 PM	47	-145.295	0.015					
100	29.6288	79.71524	1419.39	-193	2:37 PM	45	-192.325	0.015					
150	29.62885	79.71629	1428.05	-202.00	2:34 PM	42	-201.37	0.015					
200	29.6289	79.71682	1429.87	-96.15	2:32 PM	40	-95.55	0.015					
250	29.62892	79.71733	1427.08	29.9	2:30 PM	38	30.47	0.015					
300	29.62899	79.71787	1428.58	39.05	2:28 PM	36	39.59	0.015					
350	29.62903	79.71839	1436.34	-19.6	1:52 PM	0	-19.6	0.015					
400	29.62907	79.71889	1444.51	40.4	1:57 PM	5	41.55	0.015					
450	29.62912	79.71944	1461.74	85.8	1:59 PM	7	86.92	0.015					
500	29.62917	79.71993	1484.63	177	2:03 PM	11	178.06	0.015					
550	29.62923	79.72046	1500.58	193	2:08 PM	16	193.985	0.015					
			Elevation	**mV**	**Time**	**Time Difference**	**Corrected mV**	**Factor**	**Remark**	**Revised 1 (mV)**		**Revised 2 (mV)**	
Day1_B1(@900m)				**30.4**	**11:31 AM**					**Time**	**mV**	**Time**	**mV**
Station No.	**Latitude**	**Longitude**	**Elevation**							**12:23 PM**	**27.7**		
550	29.629232	79.720457	1500.58	-87.5	12:15 PM	44	-89.7846	0.05192308					
600	29.629272	79.720984	1492.3	-77.5	12:11 PM	40	-79.5769	0.05192308					
650	29.62933	79.7215	1495.18	-67.15	12:09 PM	38	-69.1231	0.05192308					
700	29.62938	79.72202	1503.62	-46.95	12:07 PM	36	-48.8192	0.05192308					
750	29.62943	79.72255	1510.23	-31.95	12:04 PM	33	-33.6635	0.05192308					
800	29.62948	79.72306	1512.81	-14.8	12:02 PM	31	-16.4096	0.05192308					
850	29.62951	79.72358	1502.48	31.8	11:59 AM	28	30.34615	0.05192308					
900	29.62956	79.7241	1486.63	30.4	11:31 AM	0	30.4	0.05192308					
950	29.62962	79.72462	1478.58	78.25	11:34 AM	3	78.09423	0.05192308					
1000	29.62966	79.72514	1469.91	81.65	11:36 AM	5	81.39038	0.05192308					
1050	29.62971	79.72568	1459.51	151	11:38 AM	7	150.6365	0.05192308					
1100	29.62976	79.7262	1448.48	131	11:40 AM	9	130.5327	0.05192308					
1150	29.62981	79.7282	1436.6	127	11:43 AM	12	126.3769	0.05192308					
1200	29.62986	79.72721	1429.65	146	11:45 AM	14	145.2731	0.05192308					

SP Line-19

			Elevation	mV	Time	Time Difference	Corrected mV	Factor	Remark	Revised 1 (mV)		Revised 2 (mV)	
Day1_B1(@350m)			**1473.22**	**-0.575**	**11:54 AM**					**Time**	**mV**	**Time**	**mV**
Station No.	**Latitude**	**Longitude**	**Elevation (m)**							**1:12 PM**	**-12.95**	**2:13 PM**	**-13.9**
0	29.620577	79.705193	1514.4	-4.57	1:00 PM	56	-13.45461538	0.1586538461538					
50	29.621013	79.705178	1503.58	8.29	12:56 PM	52	0.04	0.1586538461538					
100	29.621457	79.705181	1495.71	20.5	12:48 PM	44	13.51923077	0.1586538461538					
150	29.621947	79.705171	1494.07	16.875	12:43 PM	39	10.6875	0.1586538461538					
200	29.622403	79.705169	1494.71	25.1	12:32 PM	28	20.65769231	0.1586538461538					
250	29.622865	79.705148	1486.43	-18.4	12:19 PM	25	-22.36634615	0.1586538461538					
300	29.623337	79.705143	1476.32	-17.35	12:05 PM	11	-19.09519231	0.1586538461538					
350	29.623789	79.705136	1473.22	-0.575	11:54 AM	0	-0.575	0.1586538461538					
400	29.624266	79.705137	1472.36	-35.575	1:36 PM	24	-49.27377049	0.01557377					
450	29.624713	79.705112	1469.44	1.7725	1:40 PM	28	-11.98856557	0.01557377					
500	29.625186	79.705109	1467.26	-27.7	1:46 PM	34	-41.5545082	0.01557377					
550	29.625637	79.705108	1464.95	-18.35	1:54 PM	42	-32.32909836	0.01557377					
600	29.626092	79.705082	1459.21	-22.5	1:58 PM	46	-36.54139344	0.01557377					
650	29.626561	79.705075	1455.24	-37.55	2:01 PM	49	-51.63811475	0.01557377					
700	29.627017	79.705081	1447.26	-91.7	2:04 PM	52	-105.8348361	0.01557377					
			Elevation	**mV**	**Time**	**Time Difference**	**Corrected mV**	**Factor**	**Remark**	**Revised 1 (mV)**		**Revised 2 (mV)**	
Day1_B2(@850m)			**1407.58**	**-13.2**	**2:50 PM**					**Time**	**mV**	**Time**	**mV**
Station No.	**Latitude**	**Longitude**	**Elevation**							**3:47 PM**	**-4.9975**		
700	29.627017	79.705081	1447.26	-12.25	3:08 PM	18	-9.659736842	0.143903508771929					
750	29.627472	79.705063	1437.25	-58.5	3:00 PM	10	-57.06096491	0.143903508771929					
800	29.627931	79.705061	1429.84	-48.85	2:56 PM	6	-47.98657895	0.143903508771929					
850	29.628351	79.705054	1407.58	-13.2	2:50 PM	0	-13.2	0.143903508771929					
900	29.628727	79.705041	1383.02	-6.72	3:28 PM	38	-1.251666667	0.143903508771929					
950	29.629169	79.705034	1367.69	0.6825	3:33 PM	43	6.870350877	0.143903508771929					
1000	29.629594	79.705031	1360.71	-34.3	3:36 PM	46	-27.6804386	0.143903508771929	Nala				
1050	29.630058	79.705025	1355.56	21.8	3:38 PM	48	28.70736842	0.143903508771929					

1100	29.630532	79.705006	1353.17	3.1125	3:40 PM	50	10.30767544	0.143903508771929					

SP Line- 20

			Elevation	mV	Time	Time Difference	Corrected mV	Factor	Remark	Revised 1 (mV)		Revised 2 (mV)	
Day1_B2(@250m)				**0.7**	**12:30 PM**					**Time**	**mV**	**Time**	**mV**
Station No.	**Latitude**	**Longitude**	**Elevation (m)**							**1:33 PM**	**-0.26**	**2:31 PM**	**-2.465**
0	29.621457	79.708105	1464.93	-26.4	1:24 PM	54	-26.77714286	0.00698412698					
50	29.621958	79.708152	1452.44	-55.2	1:20 PM	50	-55.54920635	0.00698412698					
100	29.622395	79.708186	1440.37	-43.275	1:03 PM	33	-43.50547619	0.00698412698					
150	29.622823	79.708141	1421.24	1.335	12:56 PM	26	1.153412699	0.00698412698					
200	29.623233	79.708157	1401.28	-4.98	12:42 PM	12	-5.063809524	0.00698412698					
250	29.623713	79.708184	1387.73	0.7	12:30 PM	0	0.7	0.00698412698					
300	29.624194	79.708172	1383.75	14.1	1:56 PM	23	10.06060345	0.038017241379					
350	29.624625	79.708162	1393.68	-22.6	1:59 PM	26	-26.75344828	0.038017241379					
400	29.625094	79.708128	1405.36	-42.6	2:08 PM	35	-47.09560345	0.038017241379					
450	29.625537	79.708151	1413.32	-48.1	2:10 PM	37	-52.67163793	0.038017241379					
500	29.625993	79.708146	1404.5	-30.5	2:14 PM	41	-35.2237069	0.038017241379					
550	29.626448	79.708158	1392.34	-10.51	2:17 PM	44	-15.34775862	0.038017241379					
600	29.626936	79.708133	1395.28	-26.8	2:20 PM	47	-31.75181034	0.038017241379					
			Elevation	**mV**	**Time**	**Time Difference**	**Corrected mV**	**Factor**	**Remark**	**Revised 1 (mV)**		**Revised 2 (mV)**	
Day1_B1(@850m)				**2.34**	**11:15 AM**					**Time**	**mV**	**Time**	**mV**
Station No.	**Latitude**	**Longitude**	**Elevation**							**12:07 PM**	**-3.035**		
600	29.626936	79.708133	1395.28	-3.21	11:27 AM	12	-3.370384615	0.013365385					
650	29.627418	79.70814	1388.55	-3.375	11:25 AM	10	-3.508653846	0.013365385					
700	29.627873	79.708136	1379.15	-2.1	11:22 AM	7	-2.193557692	0.013365385					
750	29.628335	79.708103	1381.13	-2.4	11:20 AM	5	-2.466826923	0.013365385					
800	29.628807	79.708135	1379.75	-3.74	11:17 AM	2	-3.766730769	0.013365385					
850	29.629287	79.708115	1374.01	2.34	11:15 AM	0	2.34	0.013365385					
900	29.629689	79.708137	1353.96	31	11:43 AM	28	30.62576923	0.013365385					
950	29.630152	79.708127	1348.52	16.15	11:45 AM	30	15.74903846	0.013365385					
1000	29.630594	79.708126	1359.01	-5.4275	11:47 AM	32	-5.855192307	0.013365385	Nala				
1050	29.631085	79.708027	1369.4	-18	11:50 AM	35	-18.46778846	0.013365385					
1100	29.631495	79.708022	1386.97	-24.95	11:52 AM	37	-25.44451923	0.013365385					

SP Line-21

			Elevation	mV	Time	Time Difference	Corrected mV	Factor	Remark	Revised 1 (mV)		Revised 2 (mV)	
Day1_B2(@350m)				**-1.61**	**12:16 PM**					**Time**	**mV**	**Time**	**mV**
Station No.	**Latitude**	**Longitude**	**Elevation (m)**							**1:10 AM**	**-1.89**		
0	29.645386	79.729884	1380.2	29	12:32:00 PM	16	28.9170384	0.0051851					
50	29.645725	79.730209	1390.35	59.2	12:30:00 PM	14	59.1274086	0.0051851					
100	29.646069	79.730548	1401.78	-41.75	12:28:00 PM	12	-41.8122212	0.0051851					
150	29.646439	79.730892	1416.76	35.50	12:26:00 PM	10	35.448149	0.0051851					
200	29.646796	79.731232	1433.82	18.4	12:24:00 PM	8	18.3585192	0.0051851					
250	29.647146	79.731564	1441.8	21.3	12:21:00 PM	5	21.2740745	0.0051851					
300	29.647507	79.731905	1435.14	24.85	12:19:00 PM	3	24.8344447	0.0051851					
350	29.647859	79.732237	1428.59	-1.61	12:16:00 PM	0	-1.61	0.0051851					
400	29.648212	79.732597	1426.05	22.4	12:55:00 PM	39	22.1977811	0.0051851					
450	29.648574	79.732925	1418.59	6.305	12:57:00 PM	41	6.0924109	0.0051851					
500	29.648923	79.733262	1409.01	13	12:59:00 PM	43	12.7770407	0.0051851					
550	29.649285	79.73361	1400.74	-4.42	1:01:00 AM	45	-4.6533295	0.0051851					
600	29.649648	79.733945	1380.61	-24.4	1:04:00 AM	48	-24.6488848	0.0051851					
			Elevation	**mV**	**Time**	**Time Difference**	**Corrected mV**	**Factor**	**Remark**	**Revised 1 (mV)**		**Revised 2 (mV)**	
Day1_B1(@900m)				**0.295**	**11:50:00 AM**					**Time**	**mV**	**Time**	**mV**
Station No.	**Latitude**	**Longitude**	**Elevation**							**12:37:00 PM**	**-4.02**	**1:44:00 AM**	**-0.94**
600	29.649648	79.733945	1380.67	-7.51	1:15:00 AM	38	-9.9018638	0.0459701					
650	29.649997	79.734285	1365.1	-81.08	1:09:00 AM	32	-83.1960432	0.0459701					
700	29.650344	79.734621	1363.6	-85.42	12:57:00 PM	20	-86.984402	0.0459701					
750	29.650702	79.734971	1366.42	-41.4	12:52:00 PM	15	-42.7345515	0.0459701					
800	29.651053	79.735297	1373.01	-31.8	12:50:00 PM	13	-33.0426113	0.0459701					
850	29.65141	79.735643	1380.38	-5.83	12:45:00 PM	8	-6.8427608	0.0459701					
900	29.651764	79.735978	1386.05	-4.0225	11:50:00 AM	0	-4.0225	0.0792553					
950	29.651129	79.736313	1394.6	0.74	12:33:00 PM	43	-2.6679779	0.0792553					
1000	29.652496	79.73667	1406.87	-9.87	12:31:00 PM	41	-13.1194673	0.0792553					
1050	29.652859	79.737011	1413.55	-1.96	12:23:00 PM	33	-4.5754249	0.0792553					
1100	29.653206	79.737327	1409.15	30.15	12:19:00 PM	29	27.8515963	0.0792553					
1150	29.653559	79.737668	1398.57	36.23	12:15:00 PM	25	34.2486175	0.0792553					
1200	29.653920	79.737999	1383.24	49.48	12:08:00 PM	18	48.0534046	0.0792553					

SP Line-22

			Elevation	mV	Time	Time Difference	Corrected mV	Factor	Remark	Revised 1 (mV)	
Day1_B1(@350m)			**1694.65**	**4.89**	**10:28 AM**					**Time**	**mV**
Station No.	**Latitude**	**Longitude**	**Elevation (m)**							**11:29 AM**	**0.49**
0	29.65732	79.68712	1751.73	153	10:48 AM	20	151.557377	0.07213114754098			
50	29.65689	79.68728	1743.77	163	10:45 AM	17	161.7737705	0.07213114754098			
100	29.65647	79.6875	1737.74	156	10:42 AM	14	154.9901639	0.07213114754098			
150	29.65603	79.68767	1734.33	140	10:40 AM	12	139.1344262	0.07213114754098			
200	29.6556	79.68784	1725.29	136	10:37 AM	9	135.3508197	0.07213114754098			
250	29.65518	79.688	1709.04	129	10:34 AM	6	128.5672131	0.07213114754098			
300	29.65474	79.68817	1699.07	115.2	10:31 AM	3	114.9836066	0.07213114754098			
350	29.65432	79.68833	1694.65	4.89	10:28 AM	0	4.89	0.07213114754098			
400	29.65391	79.68851	1690.11	-100.55	11:08 AM	40	-103.4352459	0.07213114754098			
450	29.65347	79.68871	1684.34	-174	11:10 AM	42	-177.0295082	0.07213114754098			
500	29.65305	79.68888	1676.9	-193	11:13 AM	45	-196.2459016	0.07213114754098			
550	29.65264	79.6891	1669.2	-590	11:15 AM	47	-593.3901639	0.07213114754098			
600	29.65223	79.68924	1658.1	-373	11:18 AM	50	-376.6065574	0.07213114754098			
650	29.6518	79.68942	1654.71	-240	11:20 AM	52	-243.7508197	0.07213114754098			
700	29.65143	79.68961	1636.59	-209	11:22 AM	54	-212.895082	0.07213114754098			
750	29.65102	79.68976	1617.78	-164	11:25 AM	57	-168.1114754	0.07213114754098			
			Elevation	**mV**	**Time**	**Time Difference**	**Corrected mV**	**Factor**	**Remark**	**Revised 1 (mV)**	
Day1_B2(@900m)			1598.33	-11.16	12:40 PM					**Time**	**mV**
Station No.	**Latitude**	**Longitude**	**Elevation**							**1:38 AM**	**-11.92**
750	29.65102	79.68976	1617.78	-234	12:53 PM	13	-234.1703448	0.013103448275862			
800	29.65062	79.68996	1594.9	5.11	12:50 PM	10	4.978965517	0.013103448275862			
850	29.65023	79.69012	1586.07	4.095	12:47 PM	7	4.003275862	0.013103448275862			
900	29.64983	79.6903	1598.33	-11.16	12:40 PM	0	-11.16	0.013103448275862			
950	29.64933	79.69043	1623.4	-5.14	1:09 PM	29	-5.52	0.013103448275862			
1000	29.64893	79.69059	1644.23	4.74	1:14 PM	34	4.294482759	0.013103448275862			
1050	29.64851	79.6908	1665.01	-19.7	1:17 PM	37	-20.18482759	0.013103448275862			
1100	29.6481	79.691	1674.82	13.5	1:20 PM	40	12.97586207	0.013103448275862			
1150	29.64766	79.6912	1681.76	-27.7	1:23 PM	43	-28.26344828	0.013103448275862			
1200	29.64725	79.69138	1691.42	-43.2	1:25 PM	45	-43.78965517	0.013103448275862			

SP Line-23

			Elevation	mV	Time	Time Difference	Corrected mV	Factor	Remark	Revised 1 (mV)		Revised 2 (mV)	
Day1_B1(@350m)				**5.88**	**1:22 PM**					**Time**	**mV**	**Time**	**mV**
Station No.	**Latitude**	**Longitude**	**Elevation (m)**							**2:15 PM**	**1.76**	**2:53 PM**	**1.805**
0	29.65649	79.71726	1550.52	2.925	1:49 PM	29	0.67066038	0.077735849057					
50	29.65645	79.71676	1567.76	43.1	1:46 PM	26	41.0788679	0.077735849057					
100	29.65643	79.7173	1588.26	6.91	1:41 PM	21	5.27754717	0.077735849057					
150	29.65639	79.71781	1597.35	-7.04	1:38 PM	18	-8.43924528	0.077735849057					
200	29.65635	79.71835	1587.69	-33.55	1:31 PM	11	-34.4050943	0.077735849057					
250	29.65632	79.71887	1562.92	-175	1:29 PM	7	-175.544151	0.077735849057					
300	29.65627	79.71942	1550.57	-18.66	1:26 PM	4	-18.9709434	0.077735849057					
350	29.6562	79.71997	1546.14	5.88	1:22 PM	0	5.88	0.077735849057					
400	29.65621	79.72047	1536.94	23.1	2:22 PM	7	19.0167105	0.001184211					
450	29.65617	79.72	1509.66	16.8	2:25 PM	10	12.7131579	0.001184211					
500	29.65613	79.72153	1496.37	10.55	2:32 PM	17	6.45486842	0.001184211					
550	29.65611	79.72205	1495	2.765	2:40 PM	25	-1.33960526	0.001184211					
600	29.65606	79.72257	1479.24	11.88	2:45 PM	30	7.76947368	0.001184211					

SP Line-24

			Elevation	mV	Time	Time Difference	Corrected mV	Factor	Remark	Revised 1 (mV)		Revised 2 (mV)	
Day1_B1(@350m)			**1500.54**	**-11.075**	**10:50 AM**					**Time**	**mV**	**Time**	**mV**
Station No.	**Latitude**	**Longitude**	**Elevation (m)**							**11:51 AM**	**-32.25**	**12:37 PM**	**-4.785**
0	29.65574	79.71668	1578.38	193	12:26 PM	35	178.3927174	0.597065217					
50	29.65569	79.71719	1582.84	157	12:21 PM	30	145.3780435	0.597065217					
100	29.65568	79.71771	1572.67	165	12:17 PM	26	155.7663043	0.597065217					
150	29.65562	79.71824	1546.31	189	12:11 PM	20	183.3486957	0.597065217					
200	29.65561	79.71875	1527.03	186	12:07 PM	16	182.7369565	0.597065217					
250	29.65559	79.71979	1504.06	-36.35	11:58 AM	7	-34.23945652	0.597065217					
300	29.65555	79.71981	1498.95	-41.675	11:54 AM	3	-37.17619565	0.597065217					
350	29.65552	79.7203	1500.54	-11.075	10:50 AM	0	-11.075	0.347131147540983					
400	29.65547	79.72088	1473.44	49.3	10:57 AM	7	46.87008197	0.347131147540983					
450	29.65545	79.72143	1468.86	16.2	11:02 AM	12	12.03442623	0.347131147540983					
500	29.65538	79.72196	1477.52	-73.875	11:12 AM	22	-81.51188525	0.347131147540983					
550	29.65537	79.72249	1473.68	-64.375	11:19 AM	29	-74.44180328	0.347131147540983					
600	29.65533	79.72304	1552.61	-60.65	11:28 AM	38	-73.84098361	0.347131147540983					

SP Line- 25

			Elevation	mV	Time	Time Difference	Corrected mV	Factor	Remark	Revised 1 (mV)		Revised 2 (mV)	
Day1_B1(@250m)				**0.98**	**10:40 AM**					**Time**	**mV**	**Time**	**mV**
Station No.	**Latitude**	**Longitude**	**Elevation (m)**							**11:45 AM**	**-1.74**		
0	29.627	79.74162	1547.54	-22.78	11:00 AM	20	-23.01384615	0.0116923076923076					
50	29.62694	79.74214	1546.02	-9.2	10:56 AM	16	-9.387076923	0.0116923076923076					
100	29.6269	79.74266	1541.78	-12.4	10:52 AM	12	-12.54030769	0.0116923076923076					
150	29.62685	79.74319	1532.33	2.51	10:49 AM	9	2.404769231	0.0116923076923076					
200	29.6268	79.74368	1533.03	12.9	10:45 AM	5	12.84153846	0.0116923076923076					
250	29.62675	79.74416	1533.75	0.98	10:40 AM	0	0.98	0.0116923076923076					
300	29.6267	79.74471	1522.52	23.1	11:27 AM	47	22.55046154	0.0116923076923076					
350	29.62664	79.74525	1520.54	21.525	11:29 AM	49	20.95207692	0.0116923076923076					
400	29.62659	79.74577	1524.57	3.29	11:34 AM	54	2.658615385	0.0116923076923076					
450	29.62654	79.74628	1544.88	-130	11:37 AM	57	-130.6664615	0.0116923076923076					
500	29.62649	79.74681	1573.14	-421	11:39 AM	59	-421.6898462	0.0116923076923076					
550	29.62644	79.74734	1611.54	-486	11:41 AM	61	-486.7132308	0.0116923076923076					

SP Line- 26

			Elevation	mV	Time	Time Difference	Corrected mV	Factor	Remark	Revised 1 (mV)	
Day1_B1(@250m)			1570.59	-1.13	12:45 PM					Time	mV
Station No.	Latitude	Longitude	Elevation (m)							1:46 PM	-5.66
0	29.62515	79.74263	1569.34	10.46	1:43 PM	58	6.152786885	0.07426229508197			
50	29.62515	79.74316	1568.6	-22	1:40 PM	55	-26.08442623	0.07426229508197			
100	29.62513	79.74368	1574.47	-8.36	1:38 PM	53	-12.29590164	0.07426229508197			
150	29.62513	79.7442	1572.71	12.9	1:35 PM	50	9.186885246	0.07426229508197			
200	29.62512	79.74473	1570.59	-1.13	12:45 PM	0	-1.13	0.07426229508197			
250	29.62511	79.74525	1568.85	17.1	12:49 PM	4	16.80295082	0.07426229508197			
300	29.6251	79.74577	1573.53	47.65	12:52 PM	7	47.13016393	0.07426229508197			
350	29.6251	79.74629	1580.78	-45.1	12:55 PM	10	-45.84262295	0.07426229508197			
400	29.62508	79.74682	1601.2	-270.5	12:59 PM	14	-271.5396721	0.07426229508197			
450	29.62508	79.74735	1625.11	-306.5	1:03 PM	18	-307.8367213	0.07426229508197			
500	29.62507	79.74786	1656.93	-317	1:08 PM	23	-318.7080328	0.07426229508197			

Annexure XVIII_Self Potential (SP) Plots

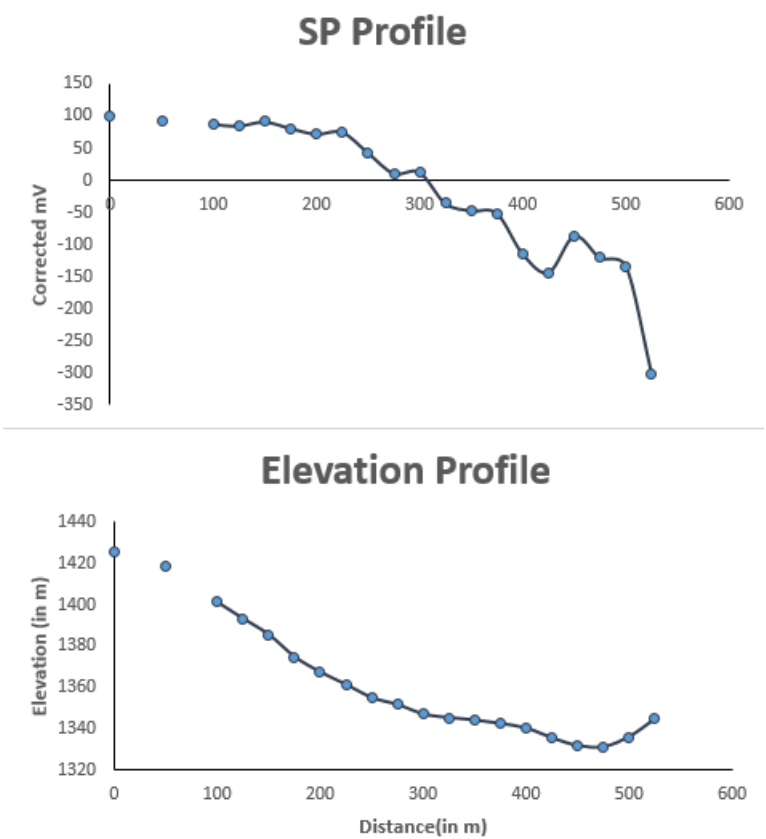

Fig 1: SP and Elevation Profile of Line 01

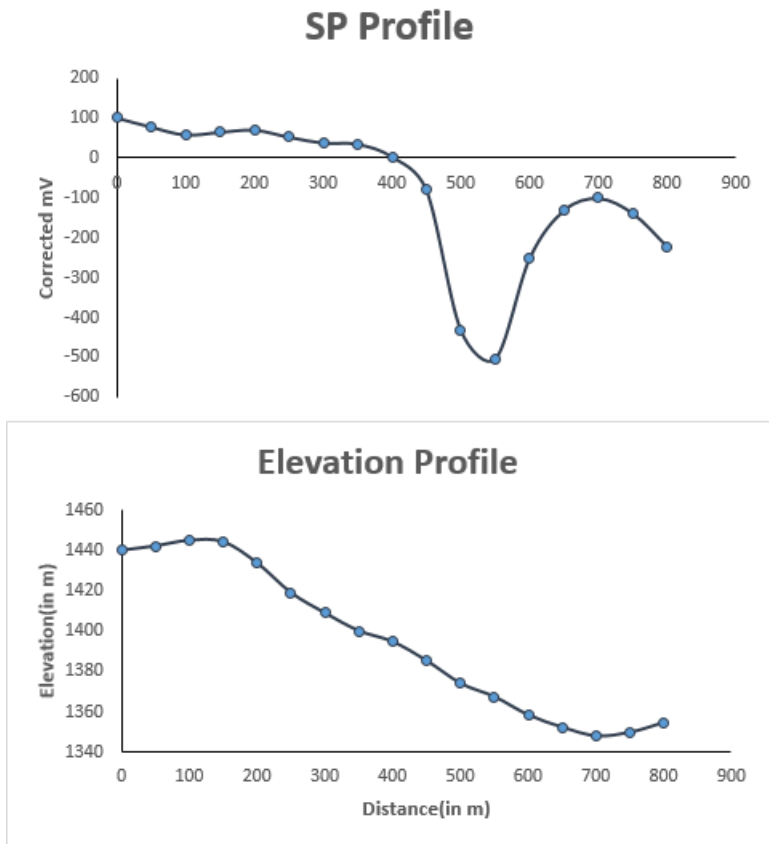

Fig 2: SP and Elevation Profile of Line 02

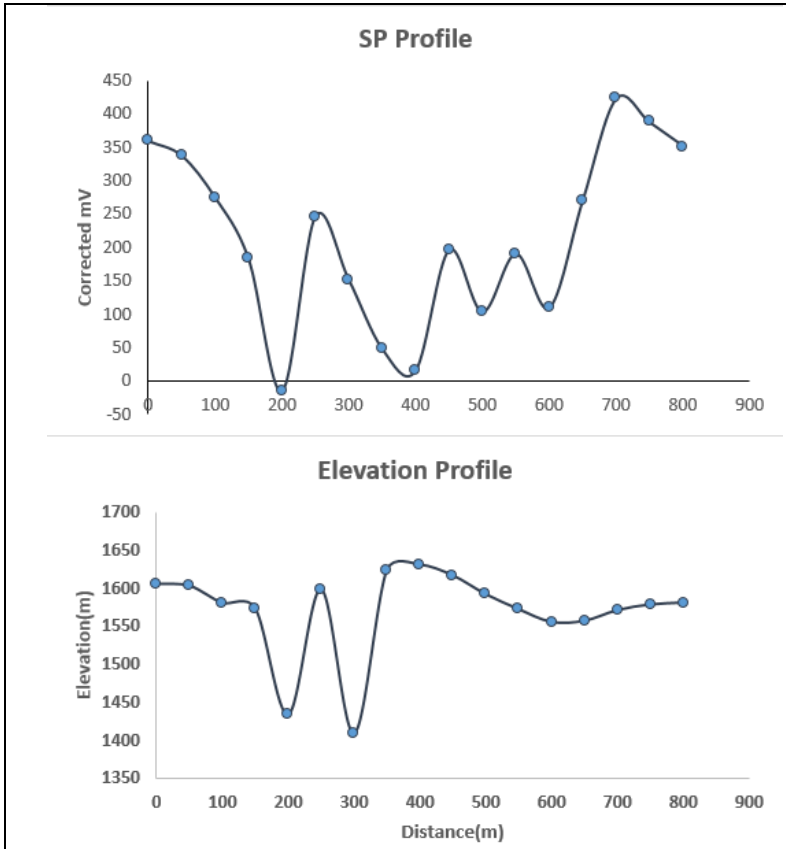

Fig 3: SP and Elevation Profile of Line 03

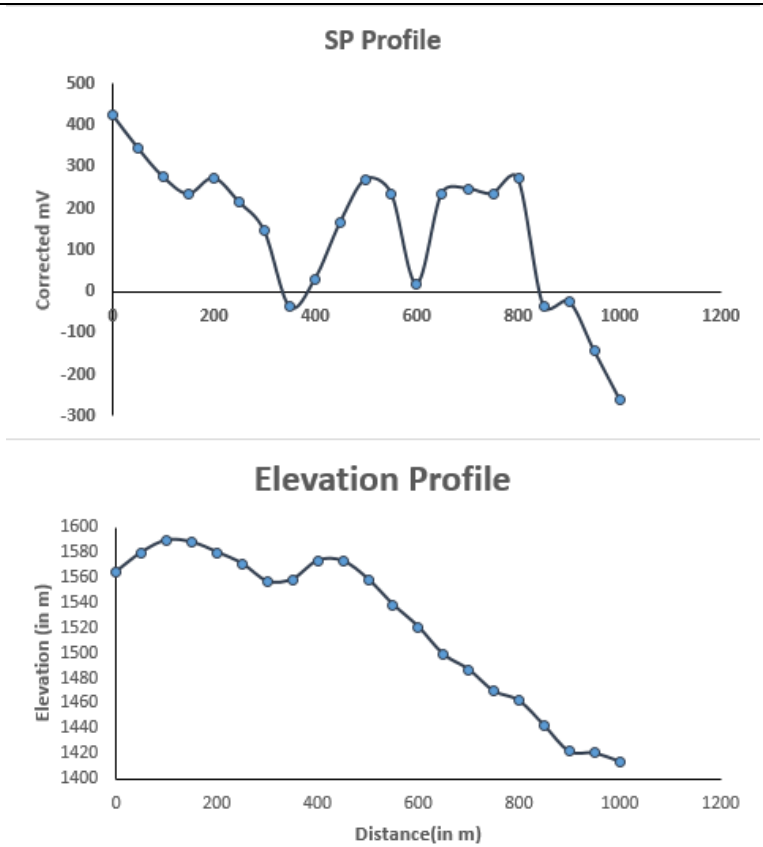

Fig 4: SP and Elevation Profile of Line 04

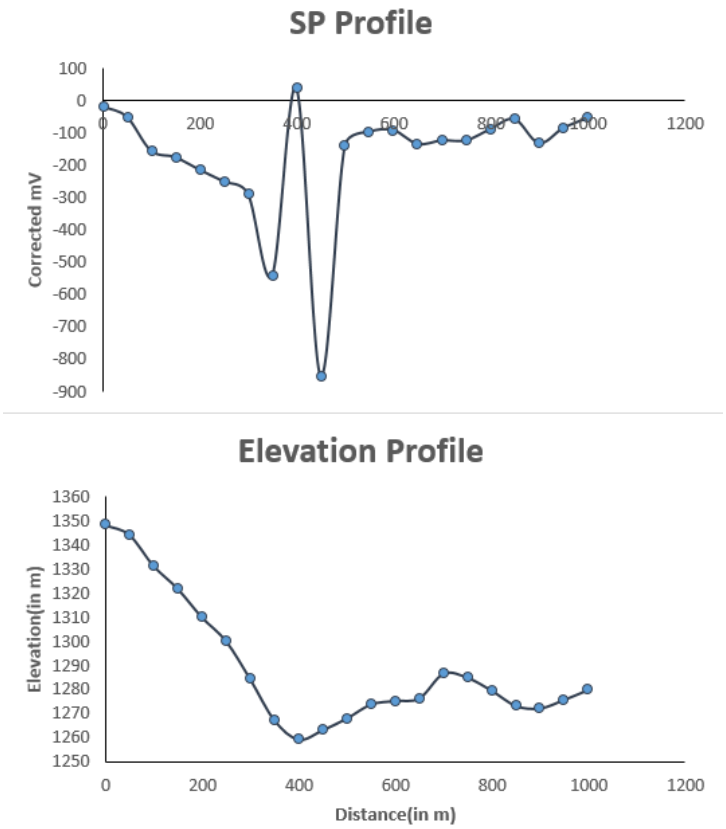

Fig 5: SP and Elevation Profile of Line 05

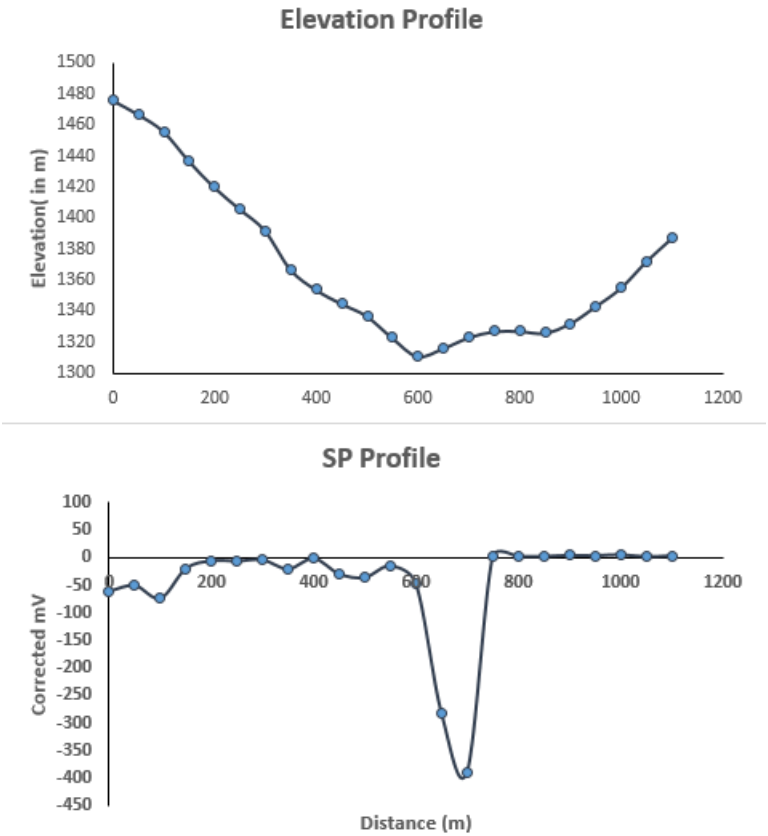

Fig 6: SP and Elevation Profile of Line 06

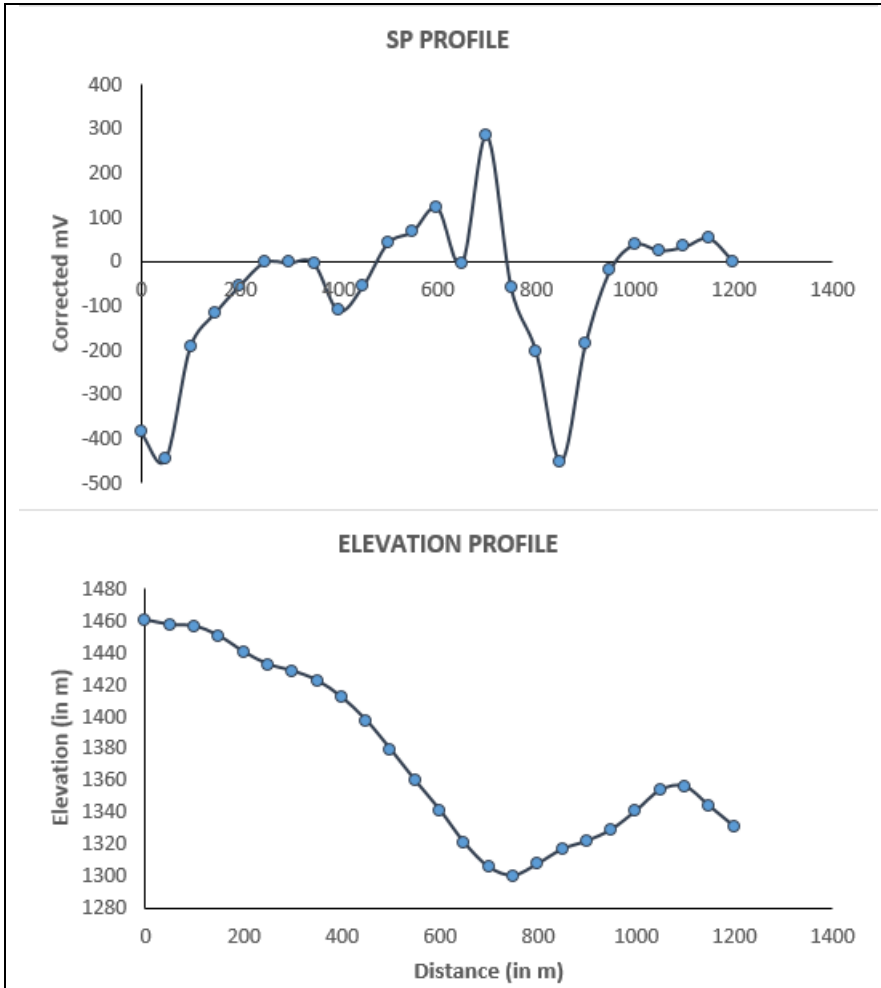

Fig 7: SP and Elevation Profile of Line 07

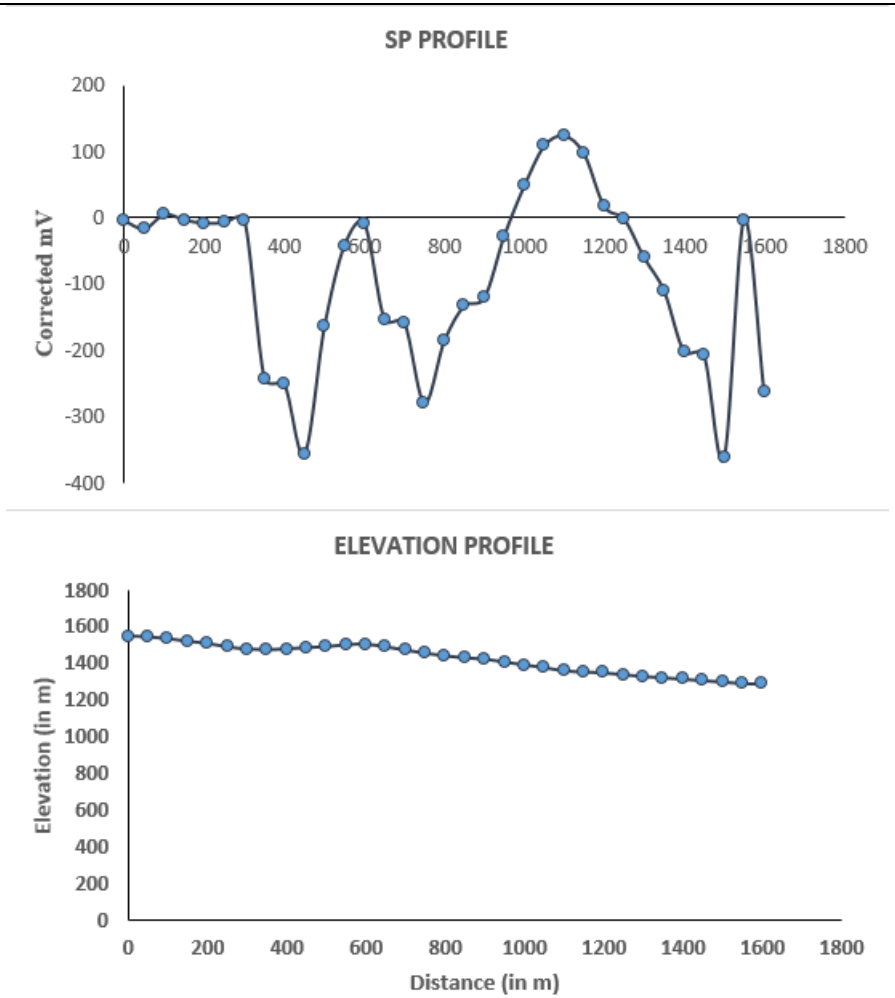

Fig 8: SP and Elevation Profile of Line 08

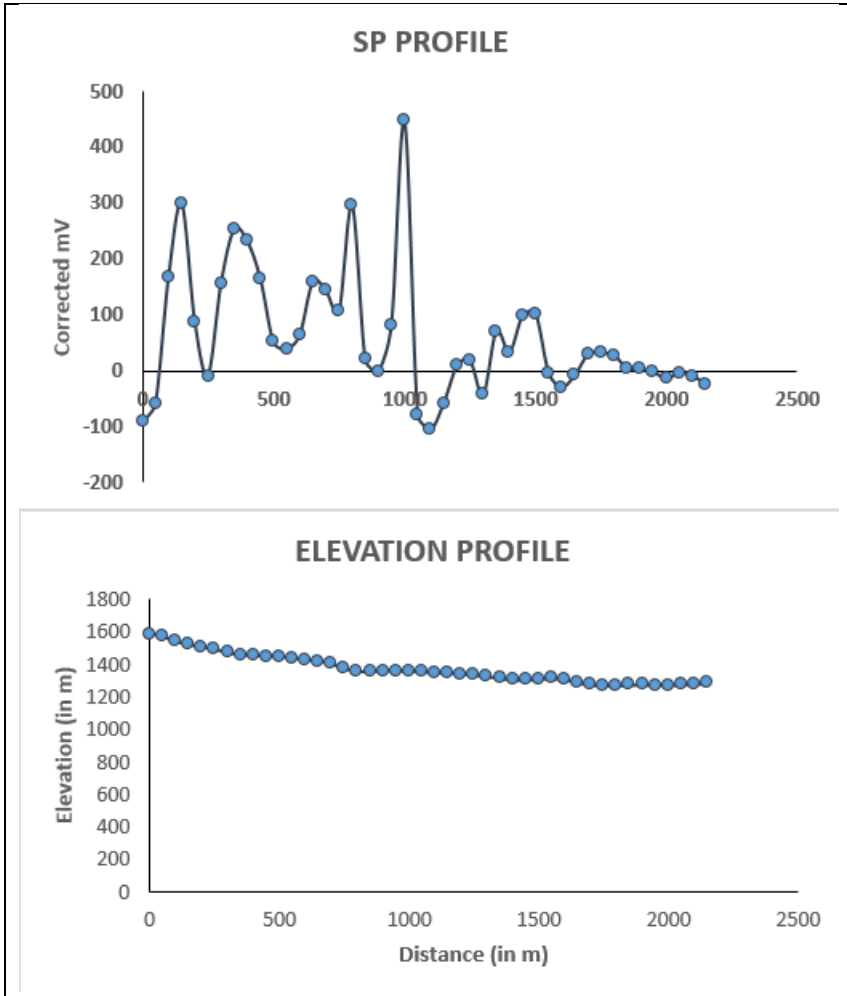

Fig 9: SP and Elevation Profile of Line 09

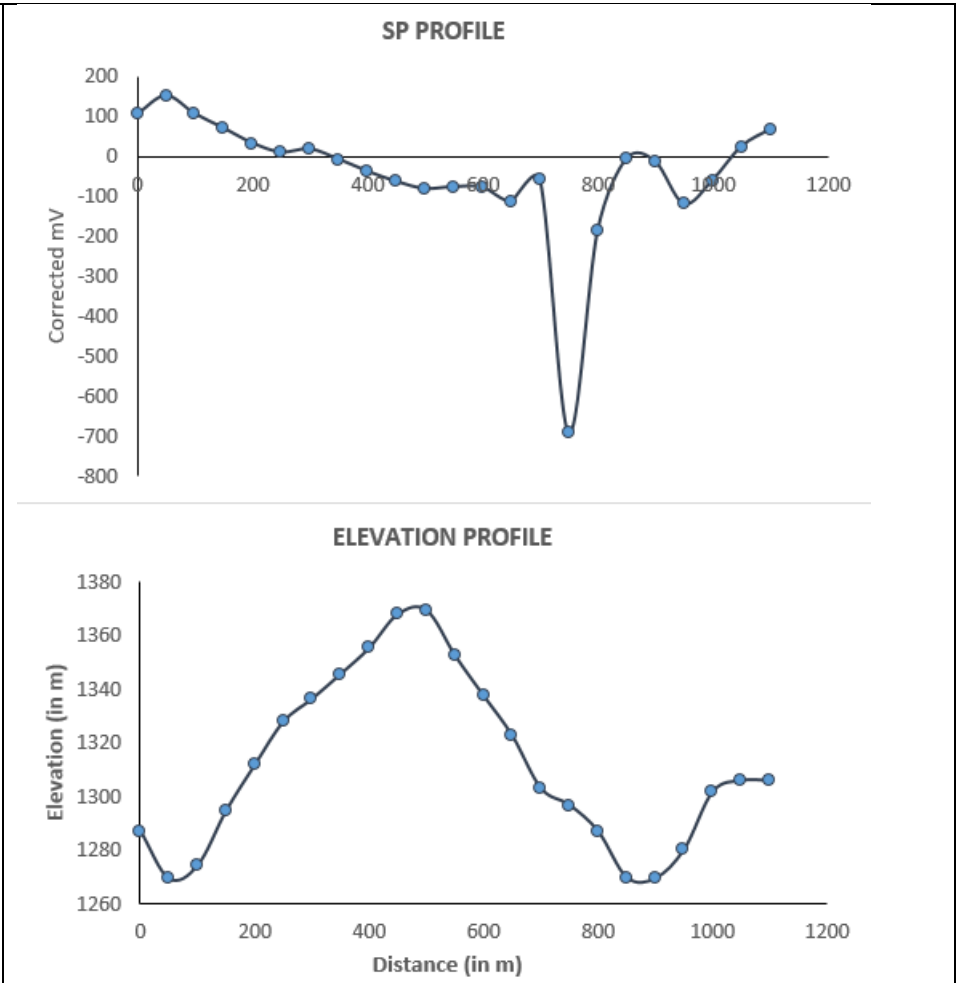

Fig 10: SP and Elevation Profile of Line 10

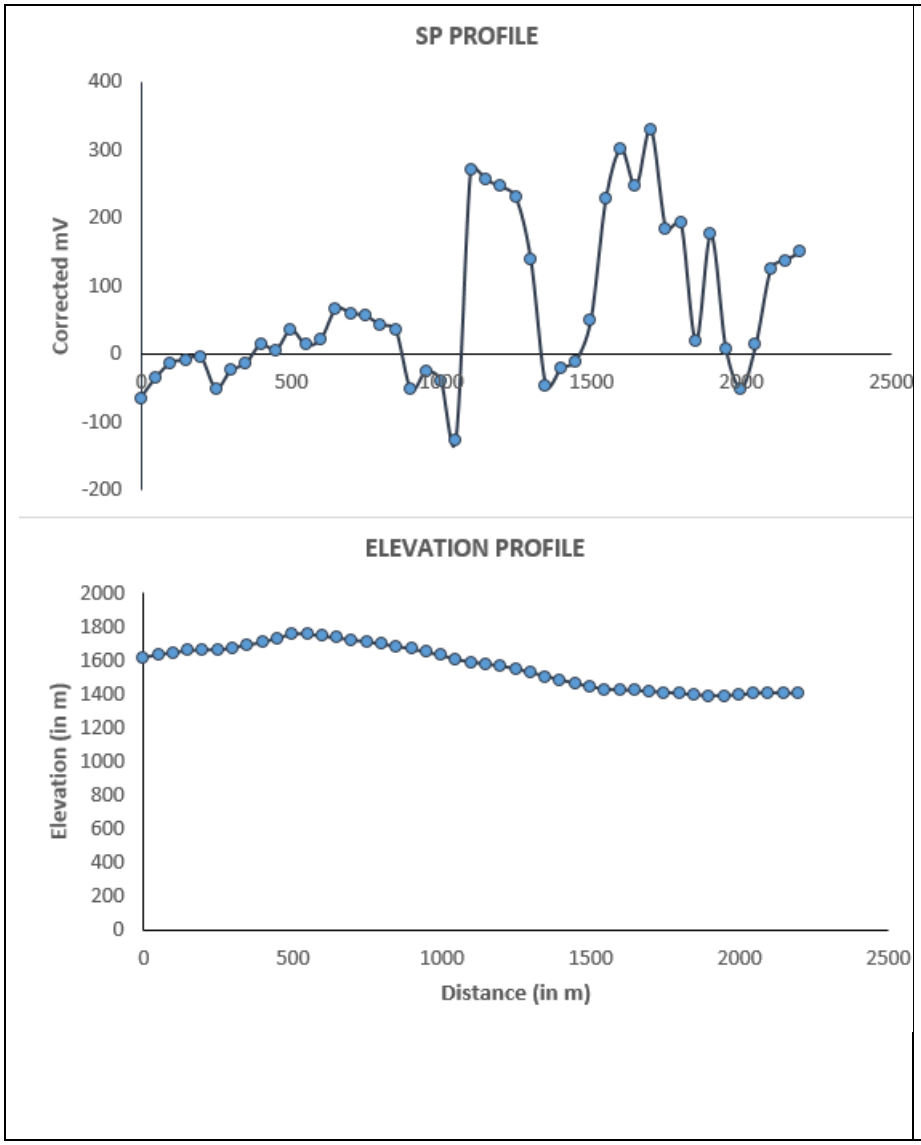
SP PROFILE
Corrected mV
400
300
200
100
0
-100
-200
0
500
1000
1500
2000
2500
ELEVATION PROFILE
Elevation (in m)
2000
1800
1600
1400
1200
1000
800
600
400
200
0
0
500
1000
1500
2000
2500
Distance (in m)

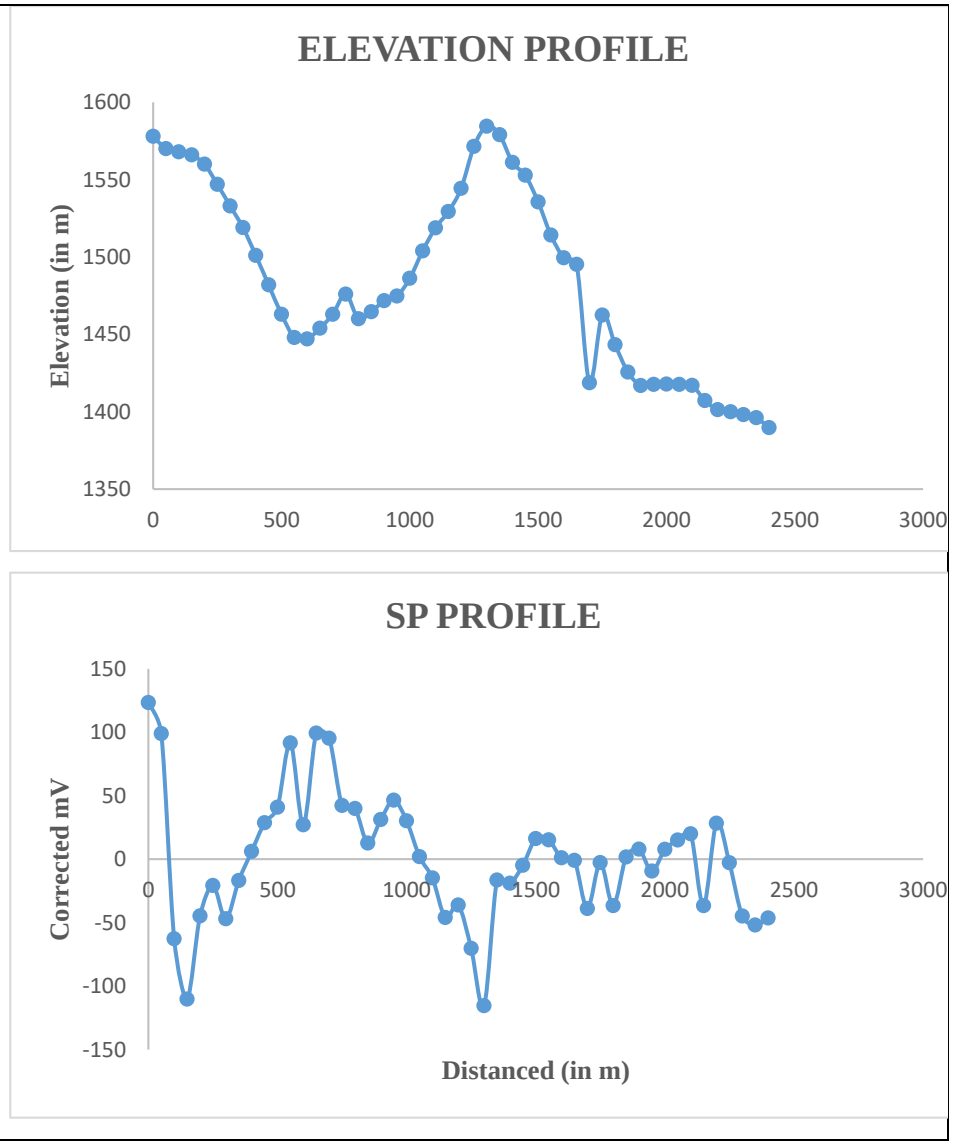
ELEVATION PROFILE
Elevation (in m)
1600
1550
1500
1450
1400
1350
0
500
1000
1500
2000
2500
3000
SP PROFILE
Corrected mV
150
100
50
0
-50
-100
-150
0
500
1000
1500
2000
2500
3000
Distanced (in m)

Fig 11: SP and Elevation Profile of Line 11

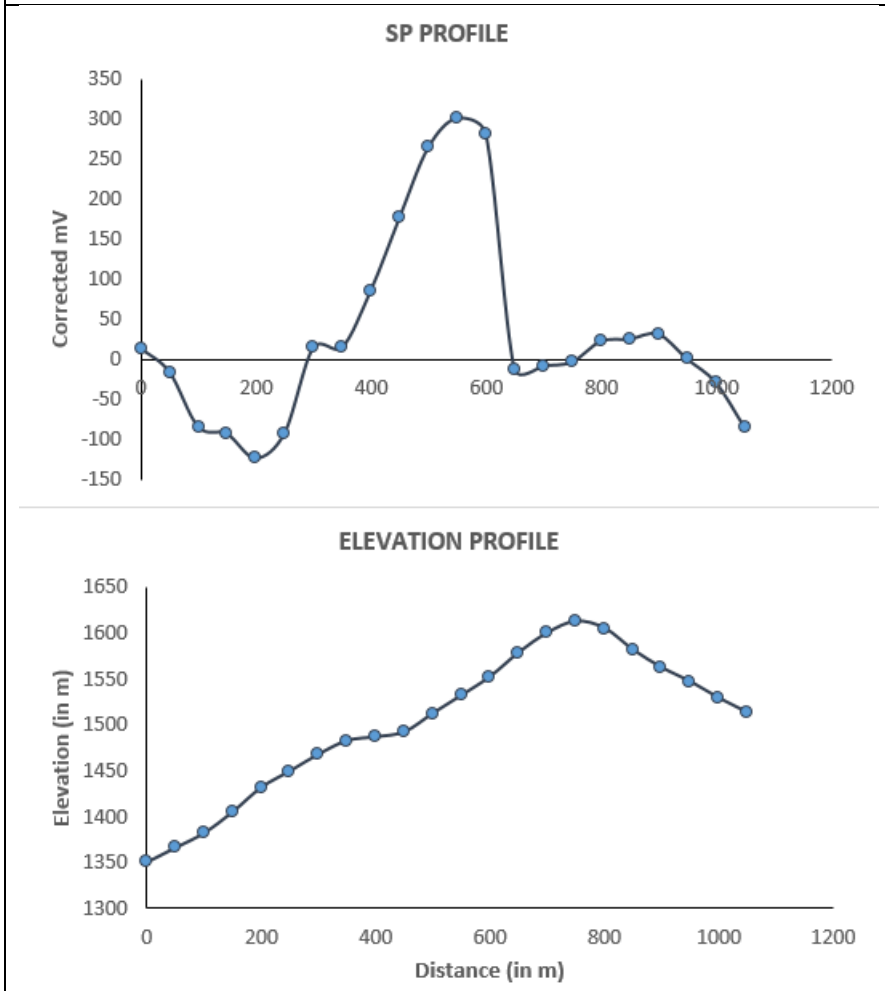

Fig 12: SP and Elevation Profile of Line 12

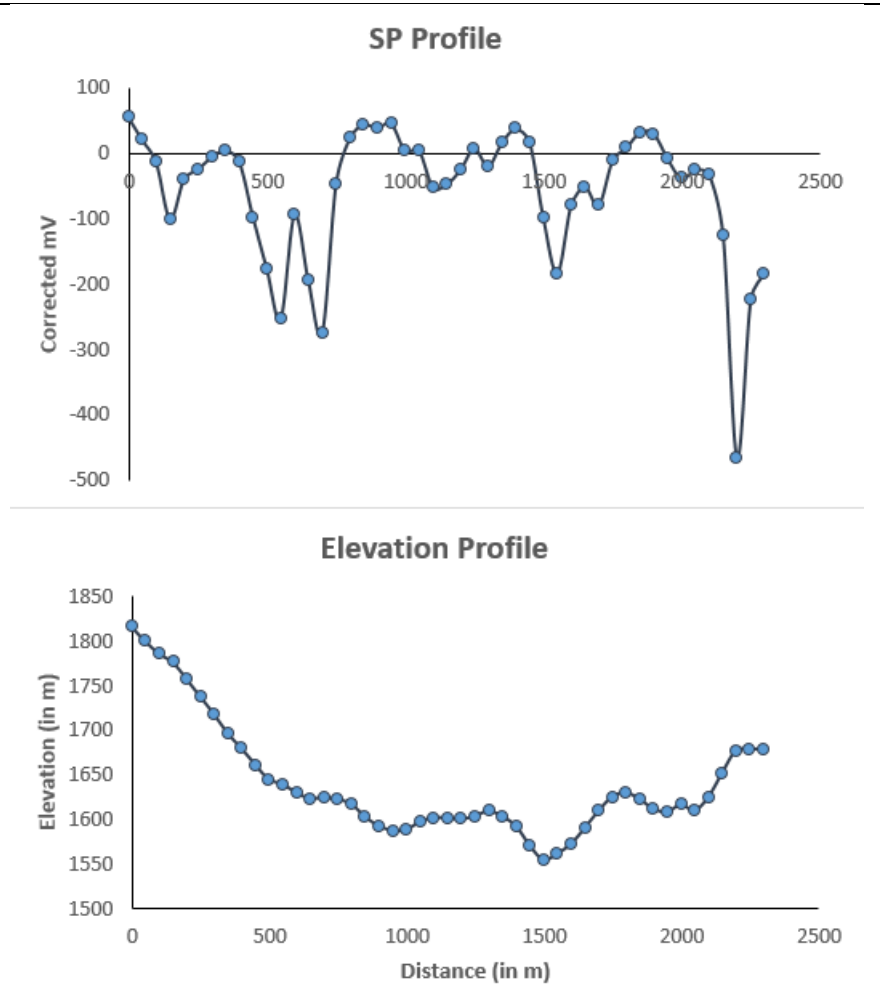

Fig 13: SP and Elevation Profile of Line 13

Fig 14: SP and Elevation Profile of Line 14

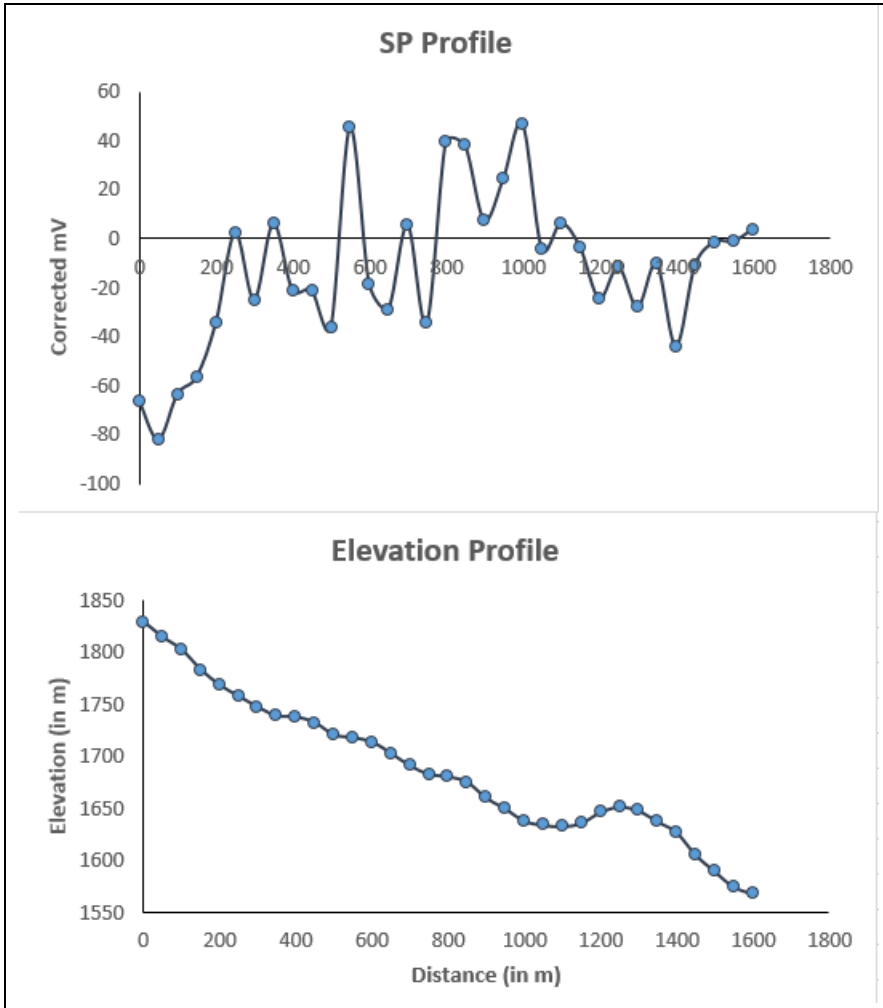

Fig 15: SP and Elevation Profile of Line 15

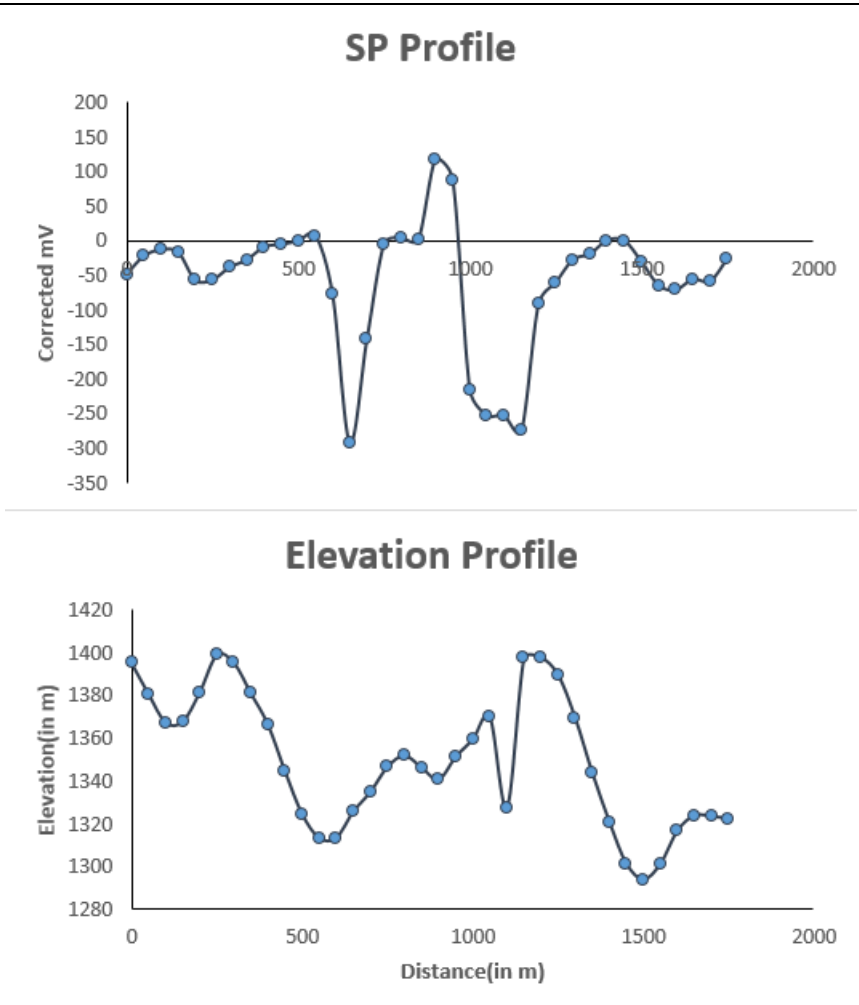

Fig 16: SP and Elevation Profile of Line 16

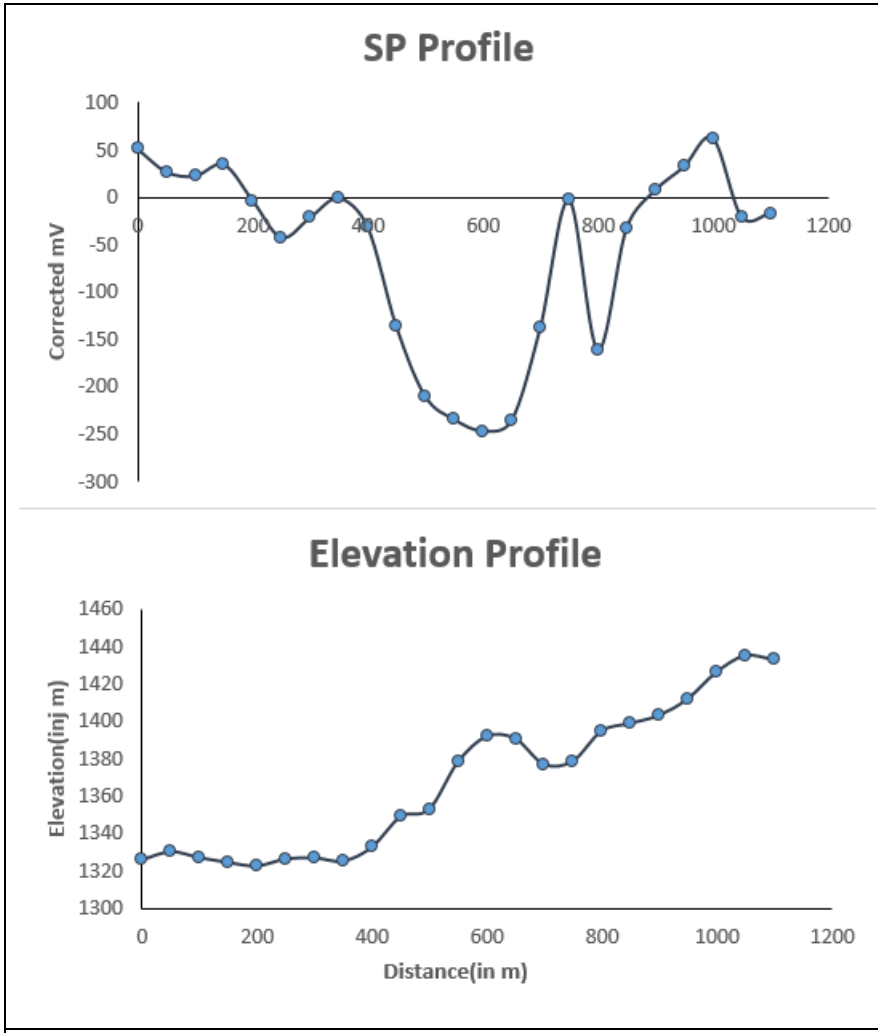

Fig 17: SP and Elevation Profile of Line 17

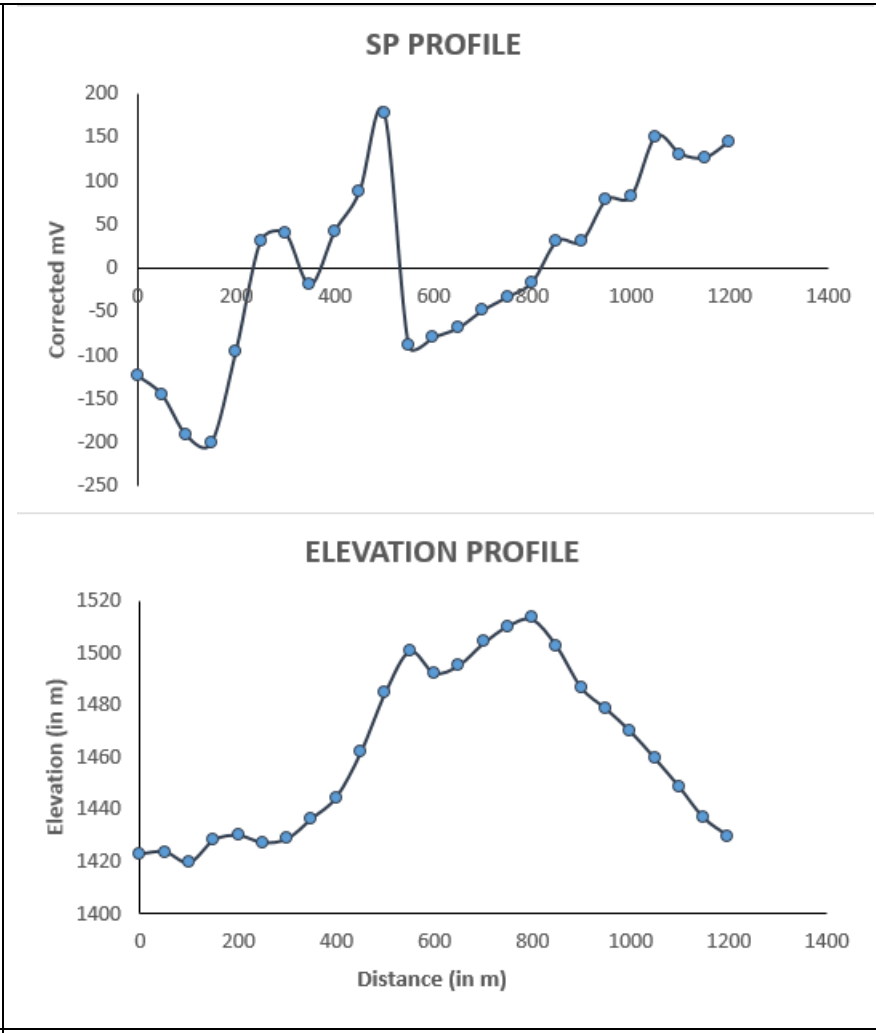

Fig 18: SP and Elevation Profile of Line 18

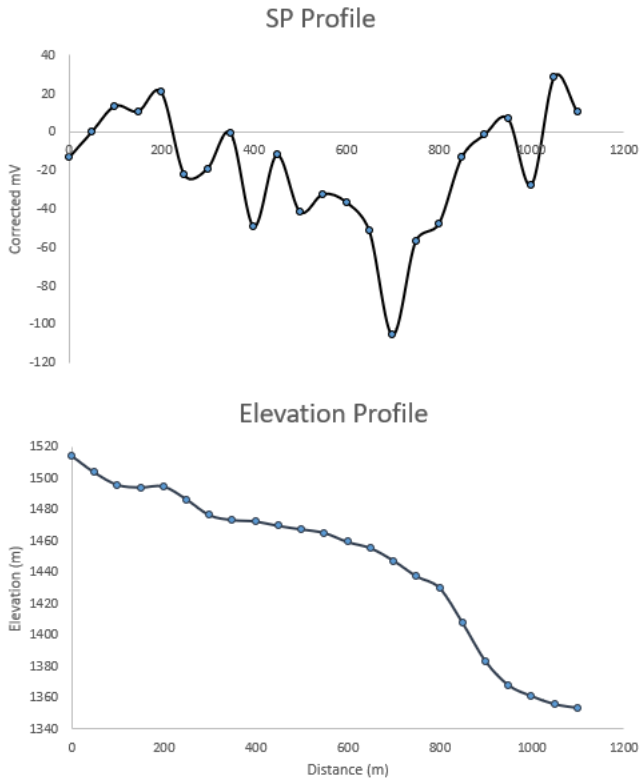

Fig 19: SP and Elevation Profile of Line 19

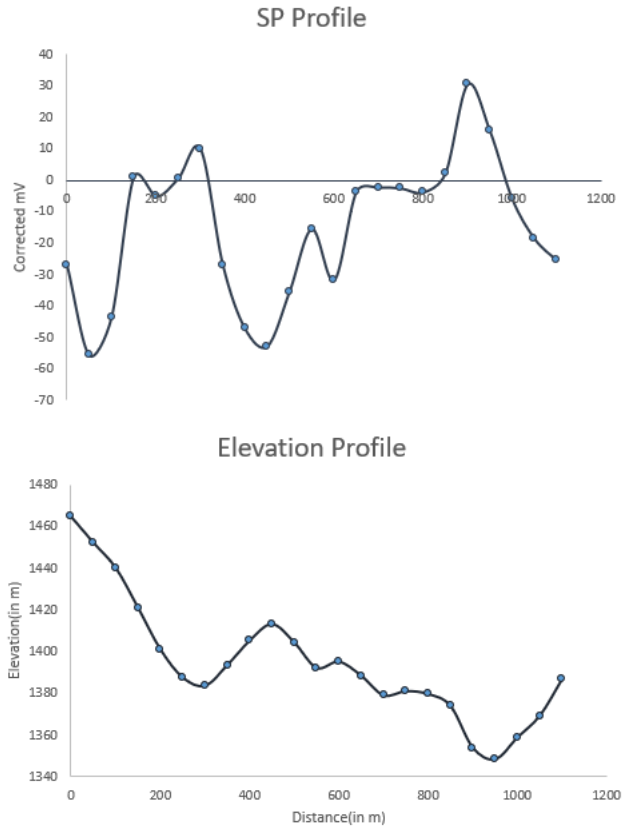

Fig 20: SP and Elevation Profile of Line 20

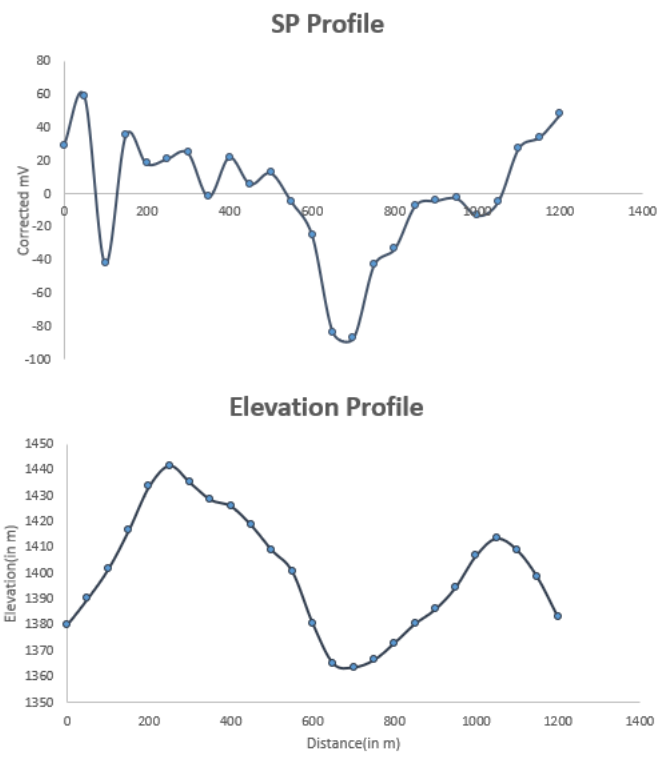

Fig 21: SP and Elevation Profile of Line 21

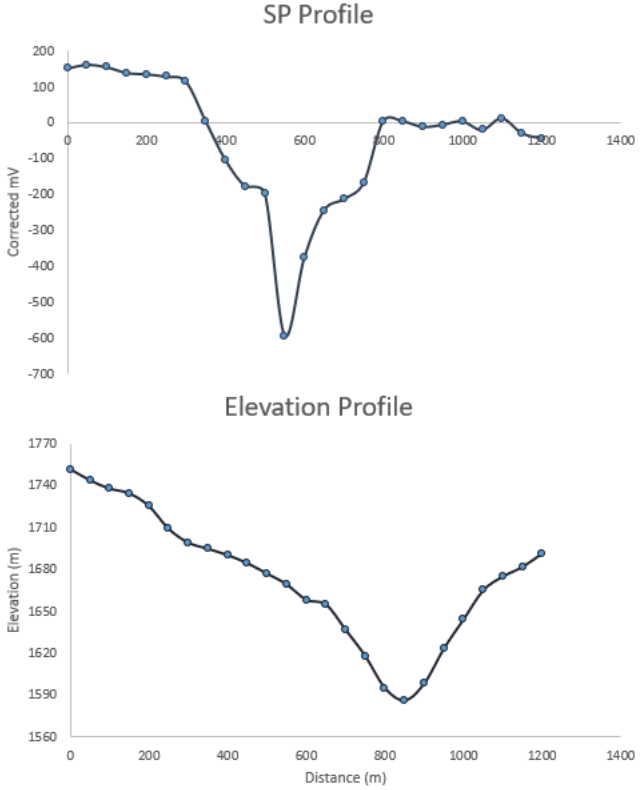

Fig 22: SP and Elevation Profile of Line 22

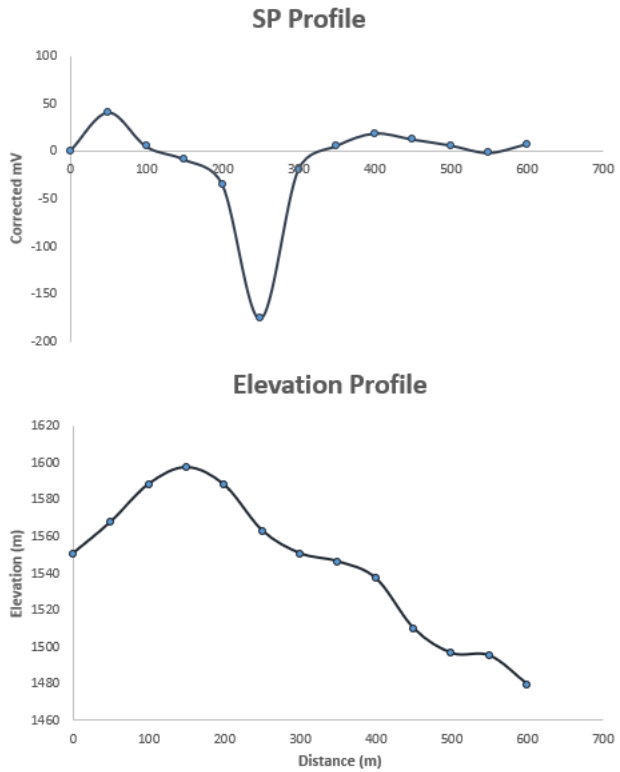

Fig 23: SP and Elevation Profile of Line 23

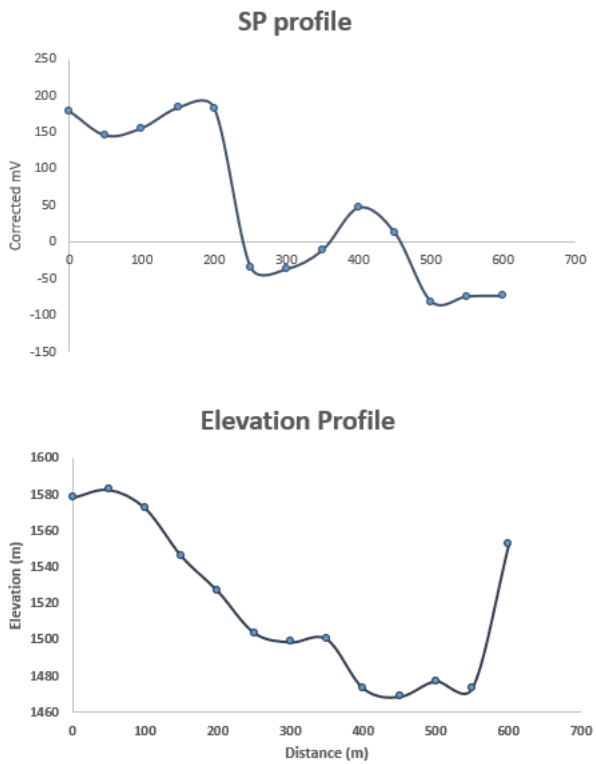

Fig 24: SP and Elevation Profile of Line 24

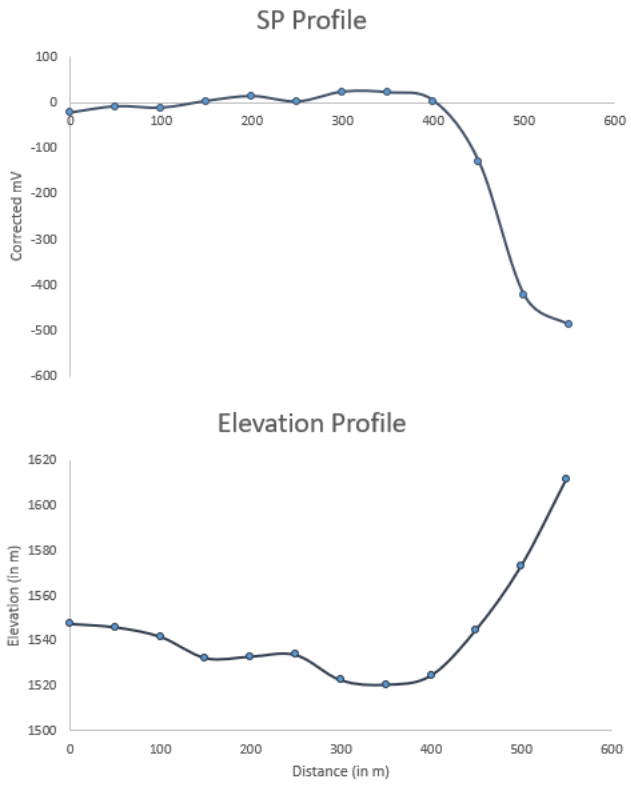

Fig 25: SP and Elevation Profile of Line 25

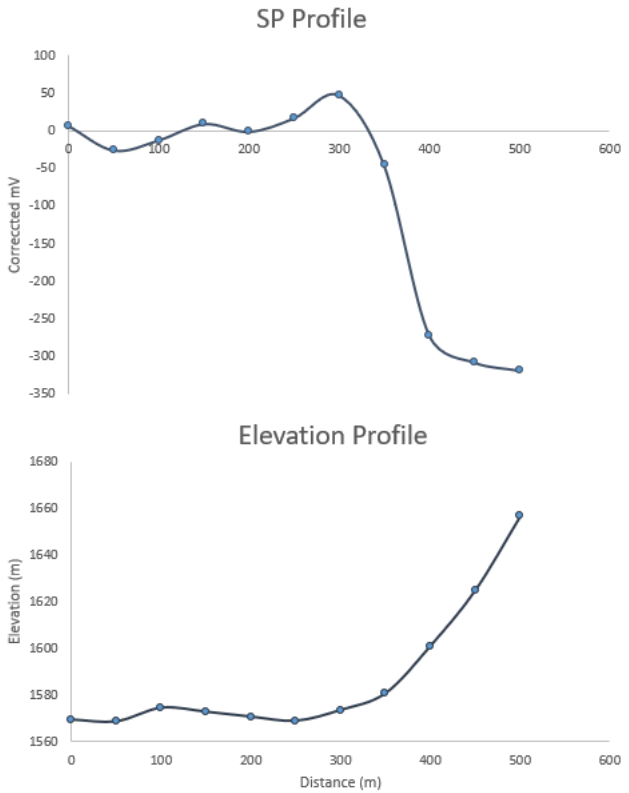

Fig 26: SP and Elevation Profile of Line 26

Annexure XIX_Resistivity (VES) Raw Data

AL_VES01

Date: 04/03/2025		VES-01							
Latitude	29.60553	Longitude	79.690505	Area	Phalshima	Elevation (m)	1567.0	Direction	80°E
S.N	Current Electrode Spacing (AB/2)	Potential Electrode Spacing (MN)	Resistance (Ohm)	K value	Aparent Resistivity (Rho_a)				
1	2.5	1	32.6	18.846	614.3796				
2	5	1	5.63	77.73975	437.6747925				
3	10	1	1.8	313.31475	563.96655				
4	15	1	0.884	705.93975	624.050739				
5	20	1	0.541	1255.61475	679.2875797500001				
6	25	1	0.372	1962.33975	729.990387				
7	30	1	0.236	2826.11475	666.963081				
8	35	1	0.144	3846.93975	553.9593239999999				
9	40	1	0.07735	5024.8147500000005	388.6694209125001				
10	45	1	0.0454	6359.73975	288.73218465				
11	50	1	0.0367	7851.71475	288.15793132500005				
12	60	1	0.0173	11306.81475	195.60789517499998				
13	70	1	0.00932	15390.11475	143.43586947				
14	80	1	0.00612	20101.61475	123.02188226999999				
15	90	1	0.0034	25441.31475	86.50047015				
16	100	1	0.0015	31409.21475	47.113822125				

AL_VES02

Date: 05/03/2025		VES-02							
Latitude	29.605801	Longitude	79.689172	Area	Phalshima	Elevation (m)	1583.0	Direction	80°E
S.N	Current Electrode Spacing (AB/2)	Potential Electrode Spacing (MN)	Resistance (Ohm)	K value	Aparent Resistivity (Rho_a)				
1	2.5	1	75.6	18.846	1424.7576				
2	5	1	17.7	77.73975	1375.993575				
3	10	1	1.21	313.31475	379.1108475				
4	15	1	0.344	705.93975	242.84327399999998				
5	20	1	0.125	1255.61475	156.95184375				
6	25	1	0.056	1962.33975	109.89102600000001				
7	30	1	0.024	2826.11475	67.82675400000001				
8	35	1	0.016	3846.93975	61.551036				
9	40	1	0.011	5024.8147500000005	55.27296225				

10	45	1	0.008	6359.73975	50.877918				
11	50	1	0.006	7851.71475	47.1102885				
12	60	1	0.00357	11306.81475	40.365328657499994				
13	70	1	0.002497	15390.11475	38.42911653075				
14	80	1	0.003245	20101.61475	65.22973986375				
15	90	1	0.06497	25441.31475	1652.9222193075002				
16	100	1	0.004246	31409.21475	133.3635258285				

AL_VES03

Date: 05/03/2025		VES-03							
Latitude	29.606188	Longitude	79.691518	Area	Phalshima	Elevation (m)	1551.0	Direction	80°E
S.N	Current Electrode Spacing (AB/2)	Potential Electrode Spacing (MN)	Resistance (Ohm)	K value	Aparent Resistivity (Rho_a)				
1	2.5	1	47.9	18.846	902.7234				
2	5	1	13.1	77.73975	1018.390725				
3	10	1	2.74	313.31475	858.4824150000001				
4	15	1	0.698	705.93975	492.74594549999995				
5	20	1	0.283	1255.61475	355.33897425				
6	25	1	0.13	1962.33975	255.10416750000002				
7	30	1	0.0715	2826.11475	202.067204625				
8	35	1	0.0375	3846.93975	144.260240625				
10	45	1	0.00882	6359.73975	56.09290459499999				
11	50	1	0.0075	7851.71475	58.887860625				
12	60	1	0.00611	11306.81475	69.0846381225				
13	70	1	0.005085	15390.11475	78.25873350375001				
14	80	1	0.00412	20101.61475	82.81865277000001				
15	90	1	0.00337	25441.31475	85.7372307075				
16	100	1	0.00553	31409.21475	173.6929575675				

AL_VES04

Date: 06/03/2025		VES-04							
Latitude	29.60692	Longitude	79.690166	Area	Phalshima	Elevation (m)	1575.0	Direction	90°E
S.N	Current Electrode Spacing (AB/2)	Potential Electrode Spacing (MN)	Resistance (Ohm)	K value	Aparent Resistivity (Rho_a)				
1	2.5	1	222	18.846	4183.812				
2	5	1	55.9	77.73975	4345.652025				
3	10	1	12.1	313.31475	3791.108475				
4	15	1	5.89	705.93975	4157.9851275				

5	20	1	3.74	1255.61475	4695.999165				
6	25	1	2.805	1962.33975	5504.362998750001				
7	30	1	2.13	2826.11475	6019.6244175				
8	35	1	1.35	3846.93975	5193.3686625				
9	40	1	0.854	5024.8147500000005	4291.1917965				
10	45	1	0.386	6359.73975	2454.8595434999997				
11	50	1	0.26	7851.71475	2041.445835				
12	70	1	0.0225	15390.11475	346.277581875				
13	80	1	0.00863	20101.61475	173.4769352925				
14	90	1	0.00775	25441.31475	197.1701893125				
15	100	1	0.00511	31409.21475	160.5010873725				
16	110	1	0.00171	38005.31475	64.98908822249999				
17	120	1	0.00214	45229.61475	96.791375565				
18	130	1	0.00587	53082.11475	311.5920135825				
19	140	1	0.00024	61562.81475	14.77507554				
20	150	1	0.0025	70671.71475	176.679286875				
21	160	1	0.00105	80408.81475	84.4292554875				
22	170	1	0.00193	90774.11475	175.1940414675				
23	180	1	0.00065	101767.61475	66.1489495875				
24	190	1	0.00114	113389.31475	129.263818815				
25	200	1	0.0015	125639.21475	188.458822125				

AL_VES05

Date: 06/03/2025		**VES-05**							
Latitude	**29.606943**	**Longitude**	**79.69269**	**Area**	**Phalshima**	**Elevation (m)**	**1575.0**	**Direction**	**90°E**
S.N	**Current Electrode Spacing (AB/2)**	**Potential Electrode Spacing (MN)**	**Resistance (Ohm)**	**K value**	**Aparent Resistivity (Rho_a)**				
1	2.5	1	76.65	18.846	1444.5459				
2	5	1	22.45	77.73975	1745.2573875				
3	10	1	4.86	313.31475	1522.709685				
4	15	1	1.69	705.93975	1193.0381775				
5	20	1	0.806	1255.61475	1012.0254885				
6	25	1	0.422	1962.33975	828.1073745				
7	30	1	0.305	2826.11475	861.9649987500001				
8	35	1	0.226	3846.93975	869.4083835				
9	40	1	0.174	5024.8147500000005	874.3177665000001				
10	45	1	0.137	6359.73975	871.28434575				
11	50	1	0.1047	7851.71475	822.0745343250001				
12	60	1	0.060525	11306.81475	684.34496274375				
13	70	1	0.03665	15390.11475	564.0477055875001				

AL_VES06

Date: 07/03/2025		VES-06							
Latitude	29.60729	Longitude	79.689196	Area	Phalshima	Elevation (m)	1585.0	Direction	90°E
S.N	Current Electrode Spacing (AB/2)	Potential Electrode Spacing (MN)	Resistance (Ohm)	K value	Aparent Resistivity (Rho_a)				
1	2.5	1	44.1	18.846	831.1086				
2	5	1	3.6	77.73975	279.86310000000003				
3	10	1	0.622	313.31475	194.8817745				
4	15	1	0.283	705.93975	199.78094925				
5	20	1	0.16	1255.61475	200.89836				
6	25	1	0.0846	1962.33975	166.01394285				
7	30	1	0.0507	2826.11475	143.284017825				
8	35	1	0.0401	3846.93975	154.26228397499997				
9	40	1	0.048	5024.8147500000005	241.191108				
10	45	1	0.0368	6359.73975	234.03842279999998				
11	50	1	0.0245	7851.71475	192.367011375				
12	60	1	0.01188	11306.81475	134.32495923				
13	70	1	0.00882	15390.11475	135.740812095				
14	80	1	0.00782	20101.61475	157.19462734500001				
15	90	1	0.00725	25441.31475	184.4495319375				
16	100	1	0.00531	31409.21475	166.7829303225				

AL_VES07

Date: 07/03/2025		VES-07							
Latitude	29.607317	Longitude	79.690957	Area	Phalshima	Elevation (m)	1579.0	Direction	90°E
S.N	Current Electrode Spacing (AB/2)	Potential Electrode Spacing (MN)	Resistance (Ohm)	K value	Aparent Resistivity (Rho_a)				
1	2.5	1	62.6	18.846	1179.7596				
2	5	1	15.8	77.73975	1228.28805				
3	10	1	2.33	313.31475	730.0233675000001				
4	15	1	0.684	705.93975	482.862789				
5	20	1	0.343	1255.61475	430.67585925000003				
6	25	1	0.182	1962.33975	357.14583450000003				
7	30	1	0.115	2826.11475	325.00319625000003				
8	35	1	0.079	3846.93975	303.90824025				
9	40	1	0.0582	5024.8147500000005	292.44421845000005				
10	45	1	0.0464	6359.73975	295.0919244				
11	50	1	0.0394	7851.71475	309.35756115				
12	60	1	0.0272	11306.81475	307.54536119999995				
13	70	1	0.0204	15390.11475	313.95834090000005				
14	80	1	0.016	20101.61475	321.625836				
15	90	1	0.0131	25441.31475	333.281223225				

16	100	1	0.01095	31409.21475	343.9309015125				

AL_VES08

Date: 07/03/2025		VES-08							
Latitude	29.607292	Longitude	79.692992	Area	Phalshima	Elevation (m)	1558.0	Direction	90°E
S.N	Current Electrode Spacing (AB/2)	Potential Electrode Spacing (MN)	Resistance (Ohm)	K value	Aparent Resistivity (Rho_a)				
1	2.5	1	89.8	18.846	1692.3708				
2	5	1	18.2	77.73975	1414.86345				
3	10	1	5.8	313.31475	1817.2255499999999				
4	15	1	3.11	705.93975	2195.4726225				
5	20	1	2.25	1255.61475	2825.1331875				
6	25	1	1.65	1962.33975	3237.8605875				
7	30	1	0.495	2826.11475	1398.9268012500002				
8	35	1	0.161	3846.93975	619.35729975				
9	40	1	0.102	5024.8147500000005	512.5311045				
10	45	1	0.0546	6359.73975	347.24179035000003				
11	50	1	0.0258	7851.71475	202.57424055				
12	60	1	0.019	11306.81475	214.82948025				
13	70	1	0.00462	15390.11475	71.102330145				
14	80	1	0.00437	20101.61475	87.8440564575				
15	90	1	0.0027	25441.31475	68.69154982500001				
16	100	1	0.0022	31409.21475	69.10027245				

AL_VES09

Date: 08/03/2025		VES-09							
Latitude	29.605476	Longitude	79.687265	Area	Phalshima	Elevation (m)	1607.0	Direction	80°E
S.N	Current Electrode Spacing (AB/2)	Potential Electrode Spacing (MN)	Resistance (Ohm)	K value	Aparent Resistivity (Rho_a)				
1	2.5	1	38.3	18.846	721.8018				
2	5	1	13.1	77.73975	1018.390725				
3	10	1	4.04	313.31475	1265.79159				
4	15	1	1.55	705.93975	1094.2066125000001				
5	20	1	0.51	1255.61475	640.3635225				
6	25	1	0.264	1962.33975	518.0576940000001				
7	30	1	0.17	2826.11475	480.43950750000005				
8	35	1	0.126	3846.93975	484.7144085				
9	40	1	0.0947	5024.8147500000005	475.84995682500005				

10	45	1	0.0741	6359.73975	471.25671547499996				
11	50	1	0.0587	7851.71475	460.895655825				
12	60	1	0.0372	11306.81475	420.61350869999995				
13	70	1	0.0224	15390.11475	344.7385704				
14	80	1	0.0139	20101.61475	279.412445025				
15	90	1	0.01163	25441.31475	295.8824905425				
16	100	1	0.00936	31409.21475	293.99025006				

AL_VES10

Date: 08/03/2025		VES-10							
Latitude	29.60669	Longitude	79.688145	Area	Phalshima	Elevation (m)	1628.0	Direction	90°E
S.N	Current Electrode Spacing (AB/2)	Potential Electrode Spacing (MN)	Resistance (Ohm)	K value	Aparent Resistivity (Rho_a)				
2	5	1	7.34	77.73975	570.609765				
3	10	1	1.89	313.31475	592.1648775				
4	15	1	1.034	705.93975	729.9417015				
5	20	1	0.588	1255.61475	738.301473				
6	25	1	0.431	1962.33975	845.76843225				
7	30	1	0.36	2826.11475	1017.4013100000001				
8	35	1	0.312	3846.93975	1200.245202				
9	40	1	0.26	5024.8147500000005	1306.451835				
10	45	1	0.221	6359.73975	1405.50248475				
11	50	1	0.193	7851.71475	1515.38094675				
12	60	1	0.147	11306.81475	1662.1017682499999				
13	70	1	0.116	15390.11475	1785.2533110000002				
14	80	1	0.0778	20101.61475	1563.90562755				
15	90	1	0.0386	25441.31475	982.0347493500001				
16	100	1	0.0266	31409.21475	835.4851123499999				

AL_VES11

Date: 08/03/2025		VES-11							
Latitude	29.607302	Longitude	79.686974	Area	Phalshima	Elevation (m)	1654.0	Direction	90°E
S.N	Current Electrode Spacing (AB/2)	Potential Electrode Spacing (MN)	Resistance (Ohm)	K value	Aparent Resistivity (Rho_a)				
1	2.5	1	107.1	18.846	2018.4065999999998				
2	5	1	25.6	77.73975	1990.1376				

3	10	1	4.45	313.31475	1394.2506375				
4	15	1	1.66	705.93975	1171.859985				
5	20	1	0.931	1255.61475	1168.97733225				
6	25	1	0.556	1962.33975	1091.060901				
7	30	1	0.432	2826.11475	1220.881572				
8	35	1	0.344	3846.93975	1323.347274				
9	40	1	0.272	5024.8147500000005	1366.7496120000003				
10	45	1	0.205	6359.73975	1303.7466487499998				
11	50	1	0.16	7851.71475	1256.2743600000001				
12	60	1	0.13	11306.81475	1469.8859175				
13	70	1	0.104	15390.11475	1600.571934				
14	80	1	0.0881	20101.61475	1770.9522594750001				
15	90	1	0.083	25441.31475	2111.62912425				
16	100	1	0.0783	31409.21475	2459.341514925				

AL_VES12

Date: 10/03/2025		VES-12							
Latitude	29.610115	Longitude	79.709442	Area	Sirar	Elevation (m)	1619.0	Direction	60°NE
S.N	Current Electrode Spacing (AB/2)	Potential Electrode Spacing (MN)	Resistance (Ohm)	K value	Aparent Resistivity (Rho_a)				
1	2.5	1	61.6	18.846	1160.9136				
2	5	1	7.93	77.73975	616.4762175				
3	10	1	1.58	313.31475	495.037305				
4	15	1	0.515	705.93975	363.55897125				
5	20	1	0.288	1255.61475	361.61704799999995				
7	30	1	0.111	2826.11475	313.69873725				
8	35	1	0.0693	3846.93975	266.592924675				
9	40	1	0.0546	5024.8147500000005	274.35488535				
10	45	1	0.0406	6359.73975	258.20543384999996				
11	50	1	0.0306	7851.71475	240.26247135				
12	60	1	0.0204	11306.81475	230.6590209				
13	70	1	0.0181	15390.11475	278.56107697500005				
14	80	1	0.0174	20101.61475	349.76809664999996				
15	90	1	0.0154	25441.31475	391.79624715000006				
16	100	1	0.0129	31409.21475	405.178870275				

AL_VES13

Date: 10/03/2025		VES-13							
Latitude	29.609303	Longitude	79.707942	Area	Sirar	Elevation (m)	1637.0	Direction	60°NE

S.N	Current Electrode Spacing (AB/2)	Potential Electrode Spacing (MN)	Resistance (Ohm)	K value	Aparent Resistivity (Rho_a)				
1	2.5	1	74.9	18.846	1411.5654000000002				
2	5	1	13.8	77.73975	1072.80855				
3	10	1	2.77	313.31475	867.8818575				
4	15	1	1.23	705.93975	868.3058925				
5	20	1	0.689	1255.61475	865.1185627499999				
6	25	1	0.406	1962.33975	796.7099385000001				
7	30	1	0.261	2826.11475	737.61594975				
8	35	1	0.178	3846.93975	684.7552754999999				
9	40	1	0.132	5024.8147500000005	663.2755470000001				
10	45	1	0.1015	6359.73975	645.513584625				
11	50	1	0.0762	7851.71475	598.3006639500001				
12	60	1	0.0479	11306.81475	541.596426525				
13	70	1	0.0355	15390.11475	546.349073625				
14	80	1	0.0247	20101.61475	496.50988432500003				
15	90	1	0.0186	25441.31475	473.20845435				
16	100	1	0.0131	31409.21475	411.460713225				

AL_VES14

Date: 11/03/2025		VES-14							
Latitude	29.609217	Longitude	79.708938	Area	Sirar	Elevation (m)	1624.0	Direction	60°NE
S.N	Current Electrode Spacing (AB/2)	Potential Electrode Spacing (MN)	Resistance (Ohm)	K value	Aparent Resistivity (Rho_a)				
1	2.5	1	274	18.846	5163.804				
2	5	1	91.6	77.73975	7120.9610999999995				
3	10	1	17.9	313.31475	5608.334024999999				
4	15	1	5.03	705.93975	3550.8769425				
5	20	1	2	1255.61475	2511.2295				
6	25	1	0.994	1962.33975	1950.5657115000001				
7	30	1	0.597	2826.11475	1687.19050575				
8	35	1	0.409	3846.93975	1573.3983577499998				
9	40	1	0.239	5024.8147500000005	1200.93072525				
10	45	1	0.176	6359.73975	1119.3141959999998				
11	50	1	0.123	7851.71475	965.76091425				
12	60	1	0.0736	11306.81475	832.1815656				
13	70	1	0.0524	15390.11475	806.4420129000001				
14	80	1	0.0346	20101.61475	695.51587035				
15	90	1	0.0269	25441.31475	684.3713667750001				
16	100	1	0.0294	31409.21475	923.43091365				

AL_VES15

Date: 11/03/2025		VES-15							
Latitude	29.608519	Longitude	79.707082	Area	Sirar	Elevation (m)	1604.0	Direction	60°NE
S.N	Current Electrode Spacing (AB/2)	Potential Electrode Spacing (MN)	Resistance (Ohm)	K value	Aparent Resistivity (Rho_a)				
2	5	1	11.7	77.73975	909.555075				
3	10	1	3.14	313.31475	983.8083150000001				
4	15	1	1.74	705.93975	1228.335165				
5	20	1	1.09	1255.61475	1368.6200775				
6	25	1	0.719	1962.33975	1410.92228025				
7	30	1	0.408	2826.11475	1153.054818				
8	35	1	0.311	3846.93975	1196.39826225				
9	40	1	0.215	5024.8147500000005	1080.33517125				
10	45	1	0.126	6359.73975	801.3272085				
11	50	1	0.0903	7851.71475	709.009841925				
12	60	1	0.0396	11306.81475	447.7498641				
13	70	1	0.0188	15390.11475	289.3341573				
14	80	1	0.00986	20101.61475	198.20192143500003				
15	90	1	0.00913	25441.31475	232.27920366749998				
16	100	1	0.00882	31409.21475	277.029274095				

AL_VES16

Date: 12/03/2025		VES-16							
Latitude	29.610748	Longitude	79.709067	Area	Sirar	Elevation (m)	1622.0	Direction	30°NE
S.N	Current Electrode Spacing (AB/2)	Potential Electrode Spacing (MN)	Resistance (Ohm)	K value	Aparent Resistivity (Rho_a)				
1	2.5	1	187	18.846	3524.202				
2	5	1	40	77.73975	3109.59				
3	10	1	9.3	313.31475	2913.8271750000004				
4	15	1	2.95	705.93975	2082.5222625				
5	20	1	1.5	1255.61475	1883.422125				
6	25	1	0.972	1962.33975	1907.394237				
7	30	1	0.62	2826.11475	1752.191145				
8	35	1	0.371	3846.93975	1427.21464725				
9	40	1	0.234	5024.8147500000005	1175.8066515000003				
10	45	1	0.135	6359.73975	858.56486625				
11	50	1	0.0905	7851.71475	710.580184875				
12	60	1	0.0382	11306.81475	431.92032344999996				
13	70	1	0.0211	15390.11475	324.731421225				

14	80	1	0.00244	20101.61475	49.047939989999996				
16	100	1	0.00167	31409.21475	52.4533886325				

AL_VES17

Date: 12/03/2025		VES-17							
Latitude	29.612206	Longitude	79.710265	Area	Sirar	Elevation (m)	1536.0	Direction	30°NE
S.N	Current Electrode Spacing (AB/2)	Potential Electrode Spacing (MN)	Resistance (Ohm)	K value	Aparent Resistivity (Rho_a)				
1	2.5	1	33.7	18.846	635.1102000000001				
2	5	1	8.35	77.73975	649.1269125				
3	10	1	3.01	313.31475	943.0773975				
4	15	1	0.666	705.93975	470.15587350000004				
5	20	1	0.235	1255.61475	295.06946624999995				
6	25	1	0.136	1962.33975	266.87820600000003				
7	30	1	0.0845	2826.11475	238.80669637500003				
8	35	1	0.0604	3846.93975	232.35516090000002				
9	40	1	0.0448	5024.8147500000005	225.11170080000002				
10	45	1	0.0326	6359.73975	207.32751584999997				
11	50	1	0.0261	7851.71475	204.929754975				
12	60	1	0.0215	11306.81475	243.09651712499996				
13	70	1	0.0185	15390.11475	284.717122875				
14	80	1	0.0164	20101.61475	329.66648190000006				
15	90	1	0.0166	25441.31475	422.32582485				
16	100	1	0.0152	31409.21475	477.4200642				

AL_VES18

Date: 13/03/2025		VES-18							
Latitude	29.609947	Longitude	79.708076	Area	Sirar	Elevation (m)	1631.0	Direction	30°NE
S.N	Current Electrode Spacing (AB/2)	Potential Electrode Spacing (MN)	Resistance (Ohm)	K value	Aparent Resistivity (Rho_a)				
1	2.5	1	94.4	18.846	1779.0624				
2	5	1	21.8	77.73975	1694.72655				
3	10	1	5.76	313.31475	1804.6929599999999				
4	15	1	2.28	705.93975	1609.54263				
5	20	1	1.3	1255.61475	1632.299175				
6	25	1	0.772	1962.33975	1514.926287				
7	30	1	0.533	2826.11475	1506.3191617500001				
8	35	1	0.357	3846.93975	1373.35749075				
9	40	1	0.314	5024.8147500000005	1577.7918315000002				

10	45	1	0.243	6359.73975	1545.4167592499998				
11	50	1	0.152	7851.71475	1193.460642				
12	60	1	0.0756	11306.81475	854.7951951				
13	70	1	0.0224	15390.11475	344.7385704				
14	80	1	0.0191	20101.61475	383.940841725				
15	90	1	0.0132	25441.31475	335.8253547				
16	100	1	0.1199	31409.21475	3765.964848525				

AL_VES19

Date: 13/03/2025		**VES-19**							
Latitude	**29.608661**	**Longitude**	**79.707496**	**Area**	**Sirar**	**Elevation (m)**	**1615.0**	**Direction**	**60°NE**
S.N	**Current Electrode Spacing (AB/2)**	**Potential Electrode Spacing (MN)**	**Resistance (Ohm)**	**K value**	**Aparent Resistivity (Rho_a)**				
1	2.5	1	63	18.846	1187.298				
2	5	1	15.2	77.73975	1181.6442				
3	10	1	3.35	313.31475	1049.6044125				
4	15	1	1.26	705.93975	889.484085				
5	20	1	0.609	1255.61475	764.66938275				
6	25	1	0.36	1962.33975	706.44231				
7	30	1	0.23	2826.11475	650.0063925000001				
8	35	1	0.152	3846.93975	584.734842				
9	40	1	0.1017	5024.8147500000005	511.02366007500007				
10	45	1	0.0687	6359.73975	436.91412082499994				
11	50	1	0.0463	7851.71475	363.534392925				
12	60	1	0.0267	11306.81475	301.89195382500003				
13	70	1	0.0196	15390.11475	301.6462491				
14	80	1	0.0137	20101.61475	275.39212207500003				
15	90	1	0.00602	25441.31475	153.156714795				
16	100	1	0.0433	31409.21475	1360.018998675				

AL_VES20

Date: 13/03/2025		**VES-20**							
Latitude	**29.608572**	**Longitude**	**79.70943**	**Area**	**Sirar**	**Elevation (m)**	**1606.0**	**Direction**	**0°N**
S.N	**Current Electrode Spacing (AB/2)**	**Potential Electrode Spacing (MN)**	**Resistance (Ohm)**	**K value**	**Aparent Resistivity (Rho_a)**				
1	2.5	1	185	18.846	3486.51				
2	5	1	46.6	77.73975	3622.6723500000003				
3	10	1	10.54	313.31475	3302.3374649999996				
4	15	1	5.1	705.93975	3600.292725				
5	20	1	3.2	1255.61475	4017.9672				

6	25	1	2.1	1962.33975	4120.913475				
7	30	1	1.41	2826.11475	3984.8217975000002				
8	35	1	0.901	3846.93975	3466.09271475				
9	40	1	0.53	5024.8147500000005	2663.1518175000006				
10	45	1	0.349	6359.73975	2219.54917275				
11	50	1	0.242	7851.71475	1900.1149695				
12	60	1	0.138	11306.81475	1560.3404355				
13	70	1	0.1065	15390.11475	1639.047220875				
14	80	1	0.0854	20101.61475	1716.6778996500002				
15	90	1	0.0749	25441.31475	1905.554474775				
16	100	1	0.0695	31409.21475	2182.9404251250003				

AL_VES21

Date: 26/03/2025		**VES-21**							
Latitude	**29.61199**	**Longitude**	**79.729737**	**Area**	**Bajyoli**	**Elevation (m)**	**1278.0**	**Direction**	**5°N**
S.N	**Current Electrode Spacing (AB/2)**	**Potential Electrode Spacing (MN)**	**Resistance (Ohm)**	**K value**	**Aparent Resistivity (Rho_a)**				
1	2.5	1	163	18.846	3071.898				
2	5	1	60.9	77.73975	4734.350775				
3	10	1	11.63	313.31475	3643.8505425000003				
4	15	1	4.08	705.93975	2880.23418				
5	20	1	1.93	1255.61475	2423.3364675				
6	25	1	1.161	1962.33975	2278.27644975				
7	30	1	0.792	2826.11475	2238.2828820000004				
8	35	1	0.585	3846.93975	2250.45975375				
9	40	1	0.46	5024.8147500000005	2311.4147850000004				
10	45	1	0.345	6359.73975	2194.1102137499997				
11	50	1	0.28	7851.71475	2198.4801300000004				
12	60	1	0.204	11306.81475	2306.590209				
15	90	1	0.0784	25441.31475	1994.5990764				
16	100	1	0.0616	31409.21475	1934.8076286				

AL_VES22

Date: 26/03/2025		**VES-22**							
Latitude	**29.610023**	**Longitude**	**79.730003**	**Area**	**Bajyoli**	**Elevation (m)**	**1276.0**	**Direction**	**5°N**
S.N	**Current Electrode Spacing (AB/2)**	**Potential Electrode Spacing (MN)**	**Resistance (Ohm)**	**K value**	**Aparent Resistivity (Rho_a)**				

1	2.5	1	197	18.846	3712.662				
2	5	1	27.9	77.73975	2168.939025				
3	10	1	7.52	313.31475	2356.1269199999997				
4	15	1	3.76	705.93975	2654.33346				
5	20	1	2.21	1255.61475	2774.9085975				
6	25	1	1.44	1962.33975	2825.76924				
7	30	1	1.015	2826.11475	2868.50647125				
8	35	1	0.738	3846.93975	2839.0415355				
9	40	1	0.544	5024.8147500000005	2733.4992240000006				
10	45	1	0.408	6359.73975	2594.7738179999997				
11	50	1	0.332	7851.71475	2606.7692970000003				
12	60	1	0.301	11306.81475	3403.35123975				
13	70	1	0.234	15390.11475	3601.2868515000005				
14	80	1	0.149	20101.61475	2995.14059775				
15	90	1	0.121	25441.31475	3078.39908475				
16	100	1	0.0842	31409.21475	2644.6558819499996				

AL_VES23

Date: 26/03/2025		**VES-23**							
Latitude	**29.613812**	**Longitude**	**79.729465**	**Area**	**Bajyoli**	**Elevation (m)**	**1318.0**	**Direction**	**5°N**
S.N	**Current Electrode Spacing (AB/2)**	**Potential Electrode Spacing (MN)**	**Resistance (Ohm)**	**K value**	**Aparent Resistivity (Rho_a)**				
1	2.5	1	28.3	18.846	533.3418				
2	5	1	7.61	77.73975	591.5994975				
3	10	1	1.9	313.31475	595.2980249999999				
4	15	1	0.861	705.93975	607.81412475				
5	20	1	0.463	1255.61475	581.34962925				
6	25	1	0.316	1962.33975	620.099361				
7	30	1	0.235	2826.11475	664.13696625				
8	35	1	0.186	3846.93975	715.5307935				
9	40	1	0.14	5024.8147500000005	703.4740650000001				
10	45	1	0.109	6359.73975	693.2116327499999				
11	50	1	0.0919	7851.71475	721.572585525				
12	60	1	0.0715	11306.81475	808.4372546249999				
13	70	1	0.0564	15390.11475	868.0024719				
14	80	1	0.0477	20101.61475	958.847023575				
15	90	1	0.0709	25441.31475	1803.7892157750002				
16	100	1	0.0356	31409.21475	1118.1680451				

AL_VES24

Date: 27/03/2025		VES-24							
Latitude	29.615762	Longitude	79.72915	Area	Bajyoli	Elevation (m)	1329.0	Direction	5°N
S.N	Current Electrode Spacing (AB/2)	Potential Electrode Spacing (MN)	Resistance (Ohm)	K value	Aparent Resistivity (Rho_a)				
1	2.5	1	14.3	18.846	269.49780000000004				
2	5	1	2.67	77.73975	207.5651325				
3	10	1	1.022	313.31475	320.2076745				
4	15	1	0.538	705.93975	379.7955855				
5	20	1	0.232	1255.61475	291.302622				
6	25	1	0.173	1962.33975	339.48477675				
7	30	1	0.131	2826.11475	370.22103225000006				
8	35	1	0.1037	3846.93975	398.927652075				
9	40	1	0.0848	5024.8147500000005	426.10429080000006				
10	45	1	0.0679	6359.73975	431.826329025				
11	50	1	0.0524	7851.71475	411.4298529				
12	60	1	0.0365	11306.81475	412.69873837499995				
13	70	1	0.0275	15390.11475	423.228155625				
14	80	1	0.0211	20101.61475	424.144071225				
15	90	1	0.016	25441.31475	407.06103600000006				
16	100	1	0.012	31409.21475	376.910577				

AL_VES25

Date: 27/03/2025		VES-25							
Latitude	29.624205	Longitude	79.712723	Area	Bajyoli	Elevation (m)	1362.0	Direction	0°N
S.N	Current Electrode Spacing (AB/2)	Potential Electrode Spacing (MN)	Resistance (Ohm)	K value	Aparent Resistivity (Rho_a)				
1	2.5	1	343	18.846	6464.178				
2	5	1	74	77.73975	5752.7415				
3	10	1	9.1	313.31475	2851.164225				
4	15	1	1.69	705.93975	1193.0381775				
5	20	1	0.739	1255.61475	927.89930025				
6	25	1	0.551	1962.33975	1081.24920225				
7	30	1	0.479	2826.11475	1353.7089652500001				
8	35	1	0.433	3846.93975	1665.72491175				
9	40	1	0.379	5024.8147500000005	1904.4047902500001				
10	45	1	0.312	6359.73975	1984.2388019999999				
11	50	1	0.255	7851.71475	2002.1872612500001				
12	60	1	0.186	11306.81475	2103.0675435				
13	70	1	0.131	15390.11475	2016.1050322500002				
14	80	1	0.1	20101.61475	2010.161475				
15	90	1	0.0793	25441.31475	2017.496259675				

16	100	1	0.0677	31409.21475	2126.403838575				

AL_VES26

Date: 27/03/2025		VES-26							
Latitude	29.61797	Longitude	79.72598	Area	Bajyoli	Elevation (m)	1310.0	Direction	5°N
S.N	Current Electrode Spacing (AB/2)	Potential Electrode Spacing (MN)	Resistance (Ohm)	K value	Aparent Resistivity (Rho_a)				
1	2.5	1	57.5	18.846	1083.645				
2	5	1	6.67	77.73975	518.5241325				
3	10	1	1.028	313.31475	322.087563				
4	15	1	0.441	705.93975	311.31942975				
5	20	1	0.211	1255.61475	264.93471224999996				
6	25	1	0.134	1962.33975	262.9535265				
7	30	1	0.101	2826.11475	285.43758975000003				
8	35	1	0.0846	3846.93975	325.45110285				
9	40	1	0.0719	5024.8147500000005	361.28418052500007				
10	45	1	0.0662	6359.73975	421.01477144999996				
11	50	1	0.0563	7851.71475	442.05154042500004				
12	60	1	0.0488	11306.81475	551.7725598000001				
13	70	1	0.0409	15390.11475	629.455693275				
14	80	1	0.0361	20101.61475	725.668292475				
15	90	1	0.0313	25441.31475	796.3131516750001				
16	100	1	0.0294	31409.21475	923.43091365				

AL_VES27

Date: 28/03/2025		VES-27							
Latitude	29.620125	Longitude	79.727978	Area	Bajyoli	Elevation (m)	1357.0	Direction	5°N
S.N	Current Electrode Spacing (AB/2)	Potential Electrode Spacing (MN)	Resistance (Ohm)	K value	Aparent Resistivity (Rho_a)				
1	2.5	1	60.7	18.846	1143.9522				
2	5	1	13.8	77.73975	1072.80855				
3	10	1	2.88	313.31475	902.3464799999999				
4	15	1	1.36	705.93975	960.07806				
5	20	1	0.744	1255.61475	934.177374				
6	25	1	0.477	1962.33975	936.03606075				
7	30	1	0.363	2826.11475	1025.87965425				
8	35	1	0.276	3846.93975	1061.7553710000002				
9	40	1	0.236	5024.8147500000005	1185.856281				
10	45	1	0.199	6359.73975	1265.58821025				

11	50	1	0.18	7851.71475	1413.308655				
12	60	1	0.15	11306.81475	1696.0222124999998				
13	70	1	0.122	15390.11475	1877.5939995				
14	80	1	0.0784	20101.61475	1575.9665964				
15	90	1	0.0475	25441.31475	1208.462450625				
16	100	1	0.0515	31409.21475	1617.574559625				

AL_VES28

Date: 28/03/2025		VES-28							
Latitude	29.622238	Longitude	79.727015	Area	Bajyoli	Elevation (m)	1391.0	Direction	5°N
S.N	Current Electrode Spacing (AB/2)	Potential Electrode Spacing (MN)	Resistance (Ohm)	K value	Aparent Resistivity (Rho_a)				
1	2.5	1	85	18.846	1601.91				
2	5	1	14.4	77.73975	1119.4524000000001				
3	10	1	2.28	313.31475	714.35763				
4	15	1	0.881	705.93975	621.93291975				
5	20	1	0.432	1255.61475	542.425572				
6	25	1	0.278	1962.33975	545.5304505				
7	30	1	0.199	2826.11475	562.3968352500001				
8	35	1	0.153	3846.93975	588.58178175				
9	40	1	0.127	5024.8147500000005	638.1514732500001				
10	45	1	0.114	6359.73975	725.0103315				
11	50	1	0.0941	7851.71475	738.846357975				
12	60	1	0.0756	11306.81475	854.7951951				
13	70	1	0.0673	15390.11475	1035.754722675				
14	80	1	0.0463	20101.61475	930.7047629250001				
15	90	1	0.0303	25441.31475	770.871836925				
16	100	1	0.0301	31409.21475	945.417363975				

AL_VES29

Date: 28/03/2025		VES-29							
Latitude	29.624091	Longitude	79.726833	Area	Bajyoli	Elevation (m)	1388.0	Direction	5°N
S.N	Current Electrode Spacing (AB/2)	Potential Electrode Spacing (MN)	Resistance (Ohm)	K value	Aparent Resistivity (Rho_a)				
1	2.5	1	15	18.846	282.69				
2	5	1	5.34	77.73975	415.130265				
3	10	1	1.062	313.31475	332.7402645				
4	15	1	0.44	705.93975	310.61349				
5	20	1	0.226	1255.61475	283.7689335				

6	25	1	0.158	1962.33975	310.0496805				
7	30	1	0.125	2826.11475	353.26434375				
8	35	1	0.108	3846.93975	415.469493				
9	40	1	0.0918	5024.8147500000005	461.2779940500001				
10	45	1	0.082	6359.73975	521.4986595				
11	50	1	0.0716	7851.71475	562.1827761				
12	60	1	0.0506	11306.81475	572.1248263499999				
13	70	1	0.0377	15390.11475	580.207326075				
14	75	1	0.0314	17667.33975	554.75446815				

AL_VES30

Date: 29/03/2025		VES-30							
Latitude	29.626693	Longitude	79.727052	Area	Bajyoli	Elevation (m)	1398.0	Direction	5°N
S.N	Current Electrode Spacing (AB/2)	Potential Electrode Spacing (MN)	Resistance (Ohm)	K value	Aparent Resistivity (Rho_a)				
1	2.5	1	70.7	18.846	1332.4122				
2	5	1	21.2	77.73975	1648.0827				
3	10	1	5.69	313.31475	1782.7609275000002				
4	15	1	2.68	705.93975	1891.9185300000001				
5	20	1	1.57	1255.61475	1971.3151575				
6	25	1	0.983	1962.33975	1928.9799742500002				
7	30	1	0.688	2826.11475	1944.3669479999999				
8	35	1	0.411	3846.93975	1581.09223725				
9	40	1	0.31	5024.8147500000005	1557.6925725				
10	45	1	0.216	6359.73975	1373.703786				
11	50	1	0.176	7851.71475	1381.9017959999999				
12	60	1	0.129	11306.81475	1458.57910275				
13	70	1	0.106	15390.11475	1631.3521635				
14	80	1	0.0928	20101.61475	1865.4298488				
15	90	1	0.0788	25441.31475	2004.7756023				
16	100	1	0.0612	31409.21475	1922.2439427				

AL_VES31

Date: 29/03/2025		VES-31							
Latitude	29.598697	Longitude	79.722645	Area	Pithauni	Elevation (m)	1270.0	Direction	90°E
S.N	Current Electrode Spacing (AB/2)	Potential Electrode Spacing (MN)	Resistance (Ohm)	K value	Aparent Resistivity (Rho_a)				
1	2.5	1	30.2	18.846	569.1492				
2	5	1	5.76	77.73975	447.78096				

3	10	1	1.29	313.31475	404.17602750000003				
4	15	1	0.383	705.93975	270.37492425				
5	20	1	0.159	1255.61475	199.64274525				
6	25	1	0.101	1962.33975	198.19631475000003				
7	30	1	0.073	2826.11475	206.30637675				
8	35	1	0.055	3846.93975	211.58168625				
9	40	1	0.0504	5024.8147500000005	253.25066340000004				
10	45	1	0.0392	6359.73975	249.30179819999998				
11	50	1	0.0358	7851.71475	281.09138805				
12	60	1	0.0299	11306.81475	338.07376102499995				
13	70	1	0.0218	15390.11475	335.50450155				
14	80	1	0.0147	20101.61475	295.493736825				
15	90	1	0.0157	25441.31475	399.428641575				
16	100	1	0.0993	31409.21475	3118.935024675				

AL_VES32

Date: 29/03/2025		VES-32							
Latitude	29.598333	Longitude	79.720349	Area	Pithauni	Elevation (m)	1270.0	Direction	90°E
S.N	Current Electrode Spacing (AB/2)	Potential Electrode Spacing (MN)	Resistance (Ohm)	K value	Aparent Resistivity (Rho_a)				
1	2.5	1	112.7	18.846	2123.9442				
2	5	1	19.5	77.73975	1515.925125				
3	10	1	3.1	313.31475	971.2757250000001				
4	15	1	0.858	705.93975	605.6963055				
5	20	1	0.345	1255.61475	433.18708874999993				
6	25	1	0.163	1962.33975	319.86137925				
7	30	1	0.083	2826.11475	234.56752425000002				
8	35	1	0.055	3846.93975	211.58168625				
9	40	1	0.0423	5024.8147500000005	212.549663925				
10	45	1	0.0318	6359.73975	202.23972405				
11	50	1	0.0235	7851.71475	184.515296625				
12	60	1	0.0154	11306.81475	174.12494715				
13	70	1	0.00664	15390.11475	102.19036194				
14	80	1	0.00501	20101.61475	100.7090898975				
15	90	1	0.00685	25441.31475	174.2730060375				
16	100	1	0.00879	31409.21475	276.0869976525				

AL_VES33

Date: 29/03/2025		VES-33							
Latitude	29.59837	Longitude	79.717603	Area	Biraura	Elevation (m)	1252.0	Direction	90°E

S.N	Current Electrode Spacing (AB/2)	Potential Electrode Spacing (MN)	Resistance (Ohm)	K value	Aparent Resistivity (Rho_a)				
1	2.5	1	98	18.846	1846.908				
2	5	1	34	77.73975	2643.1515				
3	10	1	8.39	313.31475	2628.7107525				
4	15	1	4.09	705.93975	2887.2935775				
5	20	1	2.02	1255.61475	2536.341795				
6	25	1	1.077	1962.33975	2113.43991075				
7	30	1	0.65	2826.11475	1836.9745875				
8	35	1	0.416	3846.93975	1600.326936				
9	40	1	0.259	5024.8147500000005	1301.4270202500002				
10	45	1	0.122	6359.73975	775.8882494999999				
11	50	1	0.131	7851.71475	1028.5746322500001				
12	60	1	0.076	11306.81475	859.317921				
13	70	1	0.0399	15390.11475	614.065578525				
14	80	1	0.024	20101.61475	482.438754				
15	90	1	0.016	25441.31475	407.06103600000006				
16	100	1	0.0186	31409.21475	584.21139435				

AL_VES34

Date: 07/04/2025		VES-34							
Latitude	29.597947	Longitude	79.71509	Area	Bhirora	Elevation (m)	1284.0	Direction	90°E
S.N	Current Electrode Spacing (AB/2)	Potential Electrode Spacing (MN)	Resistance (Ohm)	K value	Aparent Resistivity (Rho_a)				
1	2.5	1	79.6	18.846	1500.1416				
2	5	1	13.8	77.73975	1072.80855				
3	10	1	2.79	313.31475	874.1481525				
4	15	1	1.154	705.93975	814.6544715				
5	20	1	0.629	1255.61475	789.78167775				
6	25	1	0.395	1962.33975	775.12420125				
7	30	1	0.277	2826.11475	782.8337857500002				
8	35	1	0.22	3846.93975	846.326745				
9	40	1	0.169	5024.8147500000005	849.1936927500001				
10	45	1	0.148	6359.73975	941.2414829999999				
11	50	1	0.12	7851.71475	942.20577				
12	60	1	0.077	11306.81475	870.6247357499999				
13	70	1	0.0529	15390.11475	814.137070275				
14	80	1	0.0416	20101.61475	836.2271736				
16	100	1	0.0202	31409.21475	634.46613795				

AL_VES35

Date: 07/04/2025		VES-35							
Latitude	29.598025	Longitude	79.71269	Area	Bhirora	Elevation (m)	1288.0	Direction	90°E
S.N	Current Electrode Spacing (AB/2)	Potential Electrode Spacing (MN)	Resistance (Ohm)	K value	Aparent Resistivity (Rho_a)				
1	2.5	1	32.1	18.846	604.9566				
2	5	1	10.18	77.73975	791.390655				
3	10	1	3.37	313.31475	1055.8707075				
4	15	1	1.122	705.93975	792.0643995				
5	20	1	0.435	1255.61475	546.19241625				
6	25	1	0.301	1962.33975	590.66426475				
7	30	1	0.232	2826.11475	655.658622				
8	35	1	0.179	3846.93975	688.60221525				
9	40	1	0.124	5024.8147500000005	623.077029				
10	45	1	0.0984	6359.73975	625.7983914				
11	50	1	0.0778	7851.71475	610.8634075499999				
12	60	1	0.0496	11306.81475	560.8180116				
13	70	1	0.0321	15390.11475	494.02268347499995				
14	80	1	0.0257	20101.61475	516.611499075				
15	90	1	0.0201	25441.31475	511.37042647500004				
16	100	1	0.0152	31409.21475	477.4200642				

AL_VES36

Date: 07/04/2025		VES-36							
Latitude	29.598137	Longitude	79.709838	Area	Bhirora	Elevation (m)	1284.0	Direction	90°E
S.N	Current Electrode Spacing (AB/2)	Potential Electrode Spacing (MN)	Resistance (Ohm)	K value	Aparent Resistivity (Rho_a)				
1	2.5	1	103.8	18.846	1956.2148				
2	5	1	175	77.73975	13604.45625				
3	10	1	16.4	313.31475	5138.3619				
4	15	1	4.21	705.93975	2972.0063475				
5	20	1	1.9	1255.61475	2385.668025				
6	25	1	0.87	1962.33975	1707.2355825				
7	30	1	0.815	2826.11475	2303.28352125				
8	35	1	0.499	3846.93975	1919.62293525				
9	40	1	0.363	5024.8147500000005	1824.00775425				
10	45	1	0.293	6359.73975	1863.4037467499998				
11	50	1	0.263	7851.71475	2065.00097925				
12	60	1	0.133	11306.81475	1503.80636175				
13	70	1	0.097	15390.11475	1492.84113075				
14	80	1	0.228	20101.61475	4583.168163				

15	90	1	-0.0127	25441.31475	-323.104697325				
16	100	1	0.012	31409.21475	376.910577				

AL_VES37

Date: 08/04/2025		VES-37							
Latitude	29.601255	Longitude	79.724633	Area	Pithauni	Elevation (m)	1310.0	Direction	90°E
S.N	Current Electrode Spacing (AB/2)	Potential Electrode Spacing (MN)	Resistance (Ohm)	K value	Aparent Resistivity (Rho_a)				
1	2.5	1	8.67	18.846	163.39482				
2	5	1	2.16	77.73975	167.91786000000002				
3	10	1	0.769	313.31475	240.93904275				
4	15	1	0.446	705.93975	314.8491285				
5	20	1	0.3	1255.61475	376.684425				
6	25	1	0.223	1962.33975	437.60176425000003				
7	30	1	0.17	2826.11475	480.43950750000005				
8	35	1	0.136	3846.93975	523.183806				
9	40	1	0.112	5024.8147500000005	562.779252				
10	45	1	0.095	6359.73975	604.17527625				
11	50	1	0.083	7851.71475	651.6923242500001				
12	60	1	0.0631	11306.81475	713.460010725				
13	70	1	0.0449	15390.11475	691.0161522750001				
14	80	1	0.0343	20101.61475	689.485385925				
15	90	1	0.0284	25441.31475	722.5333389000001				
16	100	1	0.0245	31409.21475	769.525761375				

AL_VES38

Date: 08/04/2025		VES-38							
Latitude	29.601117	Longitude	79.721797	Area	Pithauni	Elevation (m)	1304.0	Direction	90°E
S.N	Current Electrode Spacing (AB/2)	Potential Electrode Spacing (MN)	Resistance (Ohm)	K value	Aparent Resistivity (Rho_a)				
1	2.5	1	28.4	18.846	535.2264				
2	5	1	4.6	77.73975	357.60285				
3	10	1	1.91	313.31475	598.4311725				
4	15	1	0.938	705.93975	662.1714855				
5	20	1	0.631	1255.61475	792.29290725				
6	25	1	0.411	1962.33975	806.52163725				
7	30	1	0.263	2826.11475	743.2681792500001				
8	35	1	0.191	3846.93975	734.76549225				

9	40	1	0.148	5024.8147500000005	743.672583				
10	45	1	0.115	6359.73975	731.37007125				
11	50	1	0.092	7851.71475	722.357757				
12	63	1	0.0438	12465.84375	546.00395625				
13	70	1	0.0401	15390.11475	617.143601475				
14	80	1	0.0213	20101.61475	428.164394175				
15	90	1	0.0198	25441.31475	503.7380320500001				
16	100	1	0.014	31409.21475	439.7290065				

AL_VES39

Date: 08/04/2025		VES-39							
Latitude	29.600973	Longitude	79.719142	Area	Pithauni	Elevation (m)	1337.0	Direction	90°E
S.N	Current Electrode Spacing (AB/2)	Potential Electrode Spacing (MN)	Resistance (Ohm)	K value	Aparent Resistivity (Rho_a)				
1	2.5	1	81	18.846	1526.526				
2	5	1	11.03	77.73975	857.4694425				
3	10	1	1.79	313.31475	560.8334025				
5	20	1	39.7	1255.61475	49847.905575000004				
6	25	1	0.405	1962.33975	794.7475987500001				
7	30	1	0.296	2826.11475	836.5299660000001				
8	35	1	0.253	3846.93975	973.27575675				
9	40	1	0.214	5024.8147500000005	1075.3103565000001				
10	45	1	0.208	6359.73975	1322.825868				
11	50	1	0.135	7851.71475	1059.98149125				
	55	1	0.109	9500.73975	1035.5806327500002				
12	60	1	0.13	11306.81475	1469.8859175				
13	70	1	0.127	15390.11475	1954.5445732500002				
14	80	1	0.089	20101.61475	1789.04371275				
15	90	1	0.0603	25441.31475	1534.111279425				
16	100	1	0.0486	31409.21475	1526.48783685				

AL_VES40

Date: 08/04/2025		VES-40							
Latitude	29.601362	Longitude	79.716703	Area	Pitauni	Elevation (m)	1330.0	Direction	90°E
S.N	Current Electrode Spacing (AB/2)	Potential Electrode Spacing (MN)	Resistance (Ohm)	K value	Aparent Resistivity (Rho_a)				
1	2.5	1	51.8	18.846	976.2228				
2	5	1	6.78	77.73975	527.075505				
3	10	1	1.25	313.31475	391.6434375				

4	15	1	0.603	705.93975	425.68166924999997				
5	20	1	0.396	1255.61475	497.223441				
6	25	1	0.239	1962.33975	468.99920025				
7	30	1	0.162	2826.11475	457.83058950000003				
8	35	1	0.125	3846.93975	480.86746875				
9	40	1	0.087	5024.8147500000005	437.15888325000003				
10	45	1	0.0651	6359.73975	414.01905772500004				
11	50	1	0.0524	7851.71475	411.4298529				
12	60	1	0.0397	11306.81475	448.880545575				
13	70	1	0.0301	15390.11475	463.242453975				
14	80	1	0.0264	20101.61475	530.6826294				
15	90	1	0.0231	25441.31475	587.694370725				
16	100	1	0.0127	31409.21475	398.89702732499995				

AL_VES41

Date: 09/04/2025		VES-41							
Latitude	29.601374	Longitude	79.713611	Area	Bhirora	Elevation (m)	1369.0	Direction	90°E
S.N	Current Electrode Spacing (AB/2)	Potential Electrode Spacing (MN)	Resistance (Ohm)	K value	Aparent Resistivity (Rho_a)				
1	2.5	1	31.8	18.846	599.3028				
2	5	1	5.16	77.73975	401.13711				
3	10	1	1.119	313.31475	350.59920525				
4	15	1	0.52	705.93975	367.08867000000004				
5	20	1	0.328	1255.61475	411.841638				
6	25	1	0.19	1962.33975	372.8445525				
7	30	1	0.126	2826.11475	356.0904585				
8	35	1	0.105	3846.93975	403.92867375				
9	40	1	0.089	5024.8147500000005	447.20851275				
10	45	1	0.0787	6359.73975	500.511518325				
11	50	1	0.07	7851.71475	549.6200325000001				
12	60	1	0.063	11306.81475	712.32932925				
13	70	1	0.0496	15390.11475	763.3496916				
15	90	1	0.0379	25441.31475	964.2258290250002				
16	100	1	0.0243	31409.21475	763.243918425				

AL_VES42

Date: 09/04/2025		VES-42							
Latitude	29.600835	Longitude	79.711577	Area	Bhirora	Elevation (m)	1373.0	Direction	90°E

S.N	Current Electrode Spacing (AB/2)	Potential Electrode Spacing (MN)	Resistance (Ohm)	K value	Aparent Resistivity (Rho_a)				
1	2.5	1	46.2	18.846	870.6852				
2	5	1	6.51	77.73975	506.08577249999996				
3	10	1	1.27	313.31475	397.9097325				
4	15	1	0.611	705.93975	431.32918725				
5	20	1	0.35	1255.61475	439.46516249999996				
6	25	1	0.23	1962.33975	451.33814250000006				
7	30	1	0.151	2826.11475	426.74332725				
8	35	1	0.108	3846.93975	415.469493				
9	40	1	0.091	5024.8147500000005	457.25814225000005				
10	45	1	0.0801	6359.73975	509.415153975				
11	50	1	0.0734	7851.71475	576.3158626500001				
12	60	1	0.0592	11306.81475	669.3634332				
13	70	1	0.0583	15390.11475	897.243689925				
14	80	1	0.0593	20101.61475	1192.025754675				
15	90	1	0.0544	25441.31475	1384.0075224				
16	100	1	0.0554	31409.21475	1740.07049715				

AL_VES43

Date: 09/04/2025		VES-43							
Latitude	29.601218	Longitude	79.709544	Area	Bhirora	Elevation (m)	1306.0	Direction	90°E
S.N	Current Electrode Spacing (AB/2)	Potential Electrode Spacing (MN)	Resistance (Ohm)	K value	Aparent Resistivity (Rho_a)				
1	2.5	1	18.5	18.846	348.651				
2	5	1	4.19	77.73975	325.7295525				
3	10	1	0.978	313.31475	306.4218255				
4	15	1	0.524	705.93975	369.91242900000003				
5	20	1	0.352	1255.61475	441.976392				
6	25	1	0.25	1962.33975	490.5849375				
7	30	1	0.197	2826.11475	556.74460575				
8	35	1	0.138	3846.93975	530.8776855000001				
9	40	1	0.136	5024.8147500000005	683.3748060000001				
10	45	1	0.1074	6359.73975	683.0360491499999				
11	50	1	0.0903	7851.71475	709.009841925				
12	60	1	0.0751	11306.81475	849.141787725				
13	70	1	0.0492	15390.11475	757.1936457				
14	80	1	0.0446	20101.61475	896.53201785				
15	90	1	0.036	25441.31475	915.887331				

16	100	1	0.0136	31409.21475	427.1653206				

AL_VES44

Date: 10/04/2025		VES-44							
Latitude	29.65521	Longitude	79.675633	Area	Matena	Elevation (m)	1767.0	Direction	50°NE
S.N	Current Electrode Spacing (AB/2)	Potential Electrode Spacing (MN)	Resistance (Ohm)	K value	Aparent Resistivity (Rho_a)				
1	2.5	1	651	18.846	12268.746				
2	5	1	74.1	77.73975	5760.515474999999				
3	10	1	14.3	313.31475	4480.400925				
4	15	1	4.03	705.93975	2844.9371925				
5	20	1	1.98	1255.61475	2486.117205				
6	25	1	1.153	1962.33975	2262.57773175				
7	30	1	0.765	2826.11475	2161.97778375				
8	35	1	0.437	3846.93975	1681.11267075				
9	40	1	0.242	5024.8147500000005	1216.0051695				
10	45	1	0.174	6359.73975	1106.5947164999998				
11	50	1	0.114	7851.71475	895.0954815				
12	60	1	0.062	11306.81475	701.0225144999999				
13	70	1	0.0204	15390.11475	313.95834090000005				
14	80	1	0.0156	20101.61475	313.5851901				
15	90	1	0.0146	25441.31475	371.44319535				
16	100	1	0.0734	31409.21475	2305.4363626500003				

AL_VES45

Date: 10/04/2025		VES-45							
Latitude	29.653851	Longitude	79.673988	Area	Matena	Elevation (m)	1773.0	Direction	50°NE
S.N	Current Electrode Spacing (AB/2)	Potential Electrode Spacing (MN)	Resistance (Ohm)	K value	Aparent Resistivity (Rho_a)				
1	2.5	1	210	18.846	3957.66				
2	5	1	45	77.73975	3498.28875				
3	10	1	7.89	313.31475	2472.0533775				
4	15	1	2.55	705.93975	1800.1463625				
5	20	1	0.9	1255.61475	1130.053275				
6	25	1	0.485	1962.33975	951.73477875				
7	30	1	0.329	2826.11475	929.7917527500001				
8	35	1	0.244	3846.93975	938.653299				
9	40	1	0.196	5024.8147500000005	984.8636910000001				
10	45	1	0.143	6359.73975	909.4427842499999				

11	50	1	0.119	7851.71475	934.35405525				
12	60	1	0.0775	11306.81475	876.2781431249999				
13	70	1	0.0616	15390.11475	948.0310686				
14	80	1	0.0462	20101.61475	928.6946014499999				
15	90	1	0.023	25441.31475	585.15023925				
16	100	1	0.0157	31409.21475	493.1246715749999				

AL_VES46

Date: 10/04/2025		VES-46							
Latitude	29.652688	Longitude	79.671698	Area	Matena	Elevation (m)	1809.0	Direction	50°NE
S.N	Current Electrode Spacing (AB/2)	Potential Electrode Spacing (MN)	Resistance (Ohm)	K value	Aparent Resistivity (Rho_a)				
1	2.5	1	110.6	18.846	2084.3676				
2	5	1	25.3	77.73975	1966.815675				
3	10	1	7.35	313.31475	2302.8634125				
4	15	1	4.08	705.93975	2880.23418				
5	20	1	2.63	1255.61475	3302.2667924999996				
6	25	1	1.006	1962.33975	1974.1137885				
7	30	1	0.599	2826.11475	1692.84273525				
8	35	1	0.405	3846.93975	1558.01059875				
9	40	1	0.316	5024.8147500000005	1587.8414610000002				
10	45	1	0.245	6359.73975	1558.1362387499998				
11	50	1	0.19	7851.71475	1491.8258025				
12	60	1	0.148	11306.81475	1673.408583				
13	70	1	0.1166	15390.11475	1794.48737985				
14	80	1	0.1108	20101.61475	2227.2589143				
15	90	1	0.0837	25441.31475	2129.438044575				
16	100	1	0.0592	31409.21475	1859.4255132				

AL_VES47

Date: 10/04/2025		VES-47							
Latitude	29.651613	Longitude	79.66915	Area	Matena	Elevation (m)	1819.0	Direction	50°NE
S.N	Current Electrode Spacing (AB/2)	Potential Electrode Spacing (MN)	Resistance (Ohm)	K value	Aparent Resistivity (Rho_a)				
1	2.5	1	123	18.846	2318.058				
2	5	1	25.2	77.73975	1959.0417				
3	10	1	4.83	313.31475	1513.3102425				
4	15	1	1.52	705.93975	1073.02842				
5	20	1	0.869	1255.61475	1091.12921775				
6	25	1	0.58	1962.33975	1138.157055				

7	30	1	0.434	2826.11475	1226.5338015				
8	35	1	0.343	3846.93975	1319.5003342500002				
9	40	1	0.279	5024.8147500000005	1401.9233152500003				
10	45	1	0.216	6359.73975	1373.703786				
11	50	1	0.156	7851.71475	1224.867501				
12	60	1	0.09	11306.81475	1017.6133275				
13	70	1	0.0746	15390.11475	1148.10256035				
14	80	1	0.0568	20101.61475	1141.7717178				
15	90	1	0.0372	25441.31475	946.4169087				
16	100	1	0.0362	31409.21475	1137.0135739500001				

AL_VES_48

Date: 11/04/2025		**VES-48**							
Latitude	**29.648505**	**Longitude**	**79.666772**	**Area**	**Mat**	**Elevation (m)**	**1772.0**	**Direction**	**50°NE**
S.N	**Current Electrode Spacing (AB/2)**	**Potential Electrode Spacing (MN)**	**Resistance (Ohm)**	**K value**	**Aparent Resistivity (Rho_a)**				
1	2.5	1	193	18.846	3637.278				
2	5	1	41.7	77.73975	3241.7475750000003				
3	10	1	9.24	313.31475	2895.02829				
4	15	1	3.53	705.93975	2491.9673175				
5	20	1	2.16	1255.61475	2712.12786				
6	25	1	1.34	1962.33975	2629.5352650000004				
7	30	1	0.827	2826.11475	2337.1968982500002				
8	35	1	0.477	3846.93975	1834.9902607499998				
9	40	1	0.307	5024.8147500000005	1542.6181282500002				
10	45	1	0.227	6359.73975	1443.66092325				
11	50	1	0.173	7851.71475	1358.3466517499999				
12	60	1	0.122	11306.81475	1379.4313995				
13	70	1	0.0769	15390.11475	1183.499824275				
14	80	1	0.0617	20101.61475	1240.269630075				
15	90	1	0.0453	25441.31475	1152.4915581750001				
16	100	1	0.037	31409.21475	1162.14094575				

AL_VES_49

Date: 11/04/2025		**VES-49**							
Latitude	**29.649747**	**Longitude**	**79.66829**	**Area**	**Mat**	**Elevation (m)**	**1727.0**	**Direction**	**50°NE**
S.N	**Current Electrode Spacing (AB/2)**	**Potential Electrode Spacing (MN)**	**Resistance (Ohm)**	**K value**	**Aparent Resistivity (Rho_a)**				

1	2.5	1	Resistivity over ranged						
2	5	1	227	77.73975	17646.92325				
3	10	1	34.5	313.31475	10809.358875				
4	15	1	5.26	705.93975	3713.243085				
5	20	1	0.656	1255.61475	823.683276				
6	25	1	0.309	1962.33975	606.36298275				
7	30	1	0.187	2826.11475	528.48345825				
8	35	1	0.1089	3846.93975	418.931738775				
9	40	1	0.095	5024.8147500000005	477.35740125000007				
10	45	1	0.1055	6359.73975	670.952543625				
11	50	1	0.0701	7851.71475	550.405203975				
12	60	1	0.0508	11306.81475	574.3861893				
13	70	1	0.084	15390.11475	1292.769639				
14	80	1	0.0663	20101.61475	1332.737057925				
15	90	1	0.0629	25441.31475	1600.258697775				
16	100	1	0.0392	31409.21475	1231.2412181999998				

AL_VES_50

Date: 11/04/2025		**VES-50**							
Latitude	**29.650477**	**Longitude**	**79.667683**	**Area**	**Mat**	**Elevation (m)**	**1782.0**	**Direction**	**50°NE**
S.N	**Current Electrode Spacing (AB/2)**	**Potential Electrode Spacing (MN)**	**Resistance (Ohm)**	**K value**	**Aparent Resistivity (Rho_a)**				
1	2.5	1	200	18.846	3769.2				
2	5	1	44.5	77.73975	3459.418875				
3	10	1	6.1	313.31475	1911.219975				
4	15	1	2.75	705.93975	1941.3343125000001				
5	20	1	1.36	1255.61475	1707.63606				
6	25	1	1.22	1962.33975	2394.054495				
7	30	1	0.652	2826.11475	1842.6268170000003				
8	35	1	0.688	3846.93975	2646.694548				
9	40	1	0.477	5024.8147500000005	2396.83663575				
10	45	1	0.278	6359.73975	1768.0076505000002				
11	50	1	0.303	7851.71475	2379.06956925				
12	60	1	0.283	11306.81475	3199.8285742499997				
13	70	1	0.0426	15390.11475	655.61888835				
14	80	1	0.0362	20101.61475	727.6784539500001				
15	90	1	0.0254	25441.31475	646.20939465				
16	100	1	0.0303	31409.21475	951.699206925				

AL_VES_51

Date: 11/04/2025		VES-51							
Latitude	29.64946	Longitude	79.66637	Area	Mat	Elevation (m)	1800.0	Direction	50°NE
S.N	Current Electrode Spacing (AB/2)	Potential Electrode Spacing (MN)	Resistance (Ohm)	K value	Aparent Resistivity (Rho_a)				
1	2.5	1	119.3	18.846	2248.3278				
2	5	1	31.8	77.73975	2472.12405				
3	10	1	7.09	313.31475	2221.4015775				
4	15	1	2.75	705.93975	1941.3343125000001				
5	20	1	1.22	1255.61475	1531.8499949999998				
6	25	1	0.716	1962.33975	1405.035261				
7	30	1	0.375	2826.11475	1059.79303125				
8	35	1	0.252	3846.93975	969.428817				
9	40	1	0.187	5024.8147500000005	939.6403582500001				
10	45	1	0.1033	6359.73975	656.961116175				
11	50	1	0.092	7851.71475	722.357757				
12	60	1	0.0568	11306.81475	642.2270778				
13	70	1	0.0387	15390.11475	595.597440825				
14	80	1	0.0343	20101.61475	689.485385925				
15	90	1	0.0323	25441.31475	821.7544664250001				
16	100	1	0.0462	31409.21475	1451.10572145				

AL_VES_52

Date: 12/04/2025		VES-52							
Latitude	29.6546	Longitude	79.67702	Area	Matena	Elevation (m)	1772.0	Direction	50°NE
S.N	Current Electrode Spacing (AB/2)	Potential Electrode Spacing (MN)	Resistance (Ohm)	K value	Aparent Resistivity (Rho_a)				
1	2.5	1	110.2	18.846	2076.8292				
2	5	1	19.3	77.73975	1500.377175				
3	10	1	3.51	313.31475	1099.7347725				
4	15	1	1.32	705.93975	931.8404700000001				
5	20	1	0.74	1255.61475	929.154915				
6	25	1	0.487	1962.33975	955.6594582500001				
7	30	1	0.33	2826.11475	932.6178675000001				
8	35	1	0.228	3846.93975	877.102263				
9	40	1	0.176	5024.8147500000005	884.367396				
10	45	1	0.132	6359.73975	839.485647				
11	50	1	0.107	7851.71475	840.1334782499999				
12	60	1	0.074	11306.81475	836.7042915				
13	70	1	0.052	15390.11475	800.285967				

14	80	1	0.0398	20101.61475	800.04426705				
15	90	1	0.034	25441.31475	865.0047015000001				
16	100	1	0.0293	31409.21475	920.289992175				

AL_VES_53

Date: 12/04/2025		VES-53							
Latitude	29.65395	Longitude	79.675245	Area	Matena	Elevation (m)	1723.0	Direction	50°NE
S.N	Current Electrode Spacing (AB/2)	Potential Electrode Spacing (MN)	Resistance (Ohm)	K value	Aparent Resistivity (Rho_a)				
1	2.5	1	340	18.846	6407.64				
2	5	1	70.5	77.73975	5480.652375				
3	10	1	10.17	313.31475	3186.4110075				
4	15	1	1.27	705.93975	896.5434825				
5	20	1	1.27	1255.61475	1594.6307325				
6	25	1	0.712	1962.33975	1397.185902				
7	30	1	0.487	2826.11475	1376.31788325				
8	35	1	0.385	3846.93975	1481.07180375				
9	40	1	0.302	5024.8147500000005	1517.4940545000002				
10	45	1	0.241	6359.73975	1532.6972797499998				
11	50	1	0.199	7851.71475	1562.49123525				
12	60	1	0.141	11306.81475	1594.2608797499997				
13	70	1	0.11	15390.11475	1692.9126225				
14	80	1	0.094	20101.61475	1889.5517865000002				
15	90	1	0.082	25441.31475	2086.1878095				
16	100	1	0.0677	31409.21475	2126.403838575				

AL_VES_54

Date: 13/04/2025		VES-54							
Latitude	29.652895	Longitude	79.673845	Area	Matena	Elevation (m)	1747.0	Direction	50°NE
S.N	Current Electrode Spacing (AB/2)	Potential Electrode Spacing (MN)	Resistance (Ohm)	K value	Aparent Resistivity (Rho_a)				
1	2.5	1	145	18.846	2732.67				
2	5	1	41.8	77.73975	3249.52155				
3	10	1	15	313.31475	4699.7212500000005				
4	15	1	6.06	705.93975	4277.994885				
5	20	1	2.72	1255.61475	3415.27212				
6	25	1	1.186	1962.33975	2327.3349435				
7	30	1	0.59	2826.11475	1667.4077025				
8	35	1	0.301	3846.93975	1157.92886475				

9	40	1	0.206	5024.8147500000005	1035.1118385				
10	45	1	0.159	6359.73975	1011.19862025				
11	50	1	0.131	7851.71475	1028.5746322500001				
12	60	1	0.0881	11306.81475	996.1303794749999				
13	70	1	0.0643	15390.11475	989.584378425				
14	80	1	0.0551	20101.61475	1107.598972725				
15	90	1	0.0437	25441.31475	1111.7854545750001				
16	100	1	0.0357	31409.21475	1121.308966575				

AL_VES_55

Date: 13/04/2025		VES-55							
Latitude	29.650715	Longitude	79.670435	Area	Matena	Elevation (m)	1762.0	Direction	50°NE
S.N	Current Electrode Spacing (AB/2)	Potential Electrode Spacing (MN)	Resistance (Ohm)	K value	Aparent Resistivity (Rho_a)				
1	2.5	1	193	18.846	3637.278				
2	5	1	56	77.73975	4353.426				
3	10	1	9.72	313.31475	3045.41937				
5	20	1	1.079	1255.61475	1354.8083152499999				
6	25	1	0.51	1962.33975	1000.7932725000001				
7	30	1	0.267	2826.11475	754.5726382500001				
8	35	1	0.16	3846.93975	615.51036				
9	40	1	0.117	5024.8147500000005	587.9033257500001				
10	45	1	0.087	6359.73975	553.2973582499999				
11	50	1	0.064	7851.71475	502.509744				
12	60	1	0.0438	11306.81475	495.23848604999995				
13	70	1	0.0316	15390.11475	486.3276261000001				
14	80	1	0.0214	20101.61475	430.17455565				
15	90	1	0.0202	25441.31475	513.91455795				
16	100	1	0.0181	31409.21475	568.5067869750001				

Sheet: AL_VES_56

Date: 13/04/2025		VES56							
Latitude	29.651807	Longitude	79.672083	Area	Matena	Elevation (m)	1787.0	Direction	50°NE
S.N	Current Electrode Spacing (AB/2)	Potential Electrode Spacing (MN)	Resistance (Ohm)	K value	Aparent Resistivity (Rho_a)				
1	2.5	1	73.9	18.846	1392.7194000000002				
2	5	1	22.5	77.73975	1749.144375				
3	10	1	4.91	313.31475	1538.3754225				

4	15	1	1.74	705.93975	1228.335165				
5	20	1	0.731	1255.61475	917.85438225				
6	25	1	0.391	1962.33975	767.2748422500001				
7	30	1	0.273	2826.11475	771.5293267500001				
8	35	1	0.212	3846.93975	815.5512269999999				
9	40	1	0.164	5024.8147500000005	824.0696190000001				
10	45	1	0.132	6359.73975	839.485647				
11	50	1	0.1082	7851.71475	849.55553595				
12	60	1	0.072	11306.81475	814.090662				
13	70	1	0.0488	15390.11475	751.0375998000001				
14	80	1	0.0373	20101.61475	749.790230175				
15	90	1	0.0314	25441.31475	798.85728315				
16	100	1	0.0281	31409.21475	882.598934475				

AL_VES57

Date:14/04/2025		VES57							
Latitude	29.654642	Longitude	79.695615	Area	Salla	Elevation (m)	1726.0	Direction	200°SW
S.N	Current Electrode Spacing (AB/2)	Potential Electrode Spacing (MN)	Resistance (Ohm)	K value	Aparent Resistivity (Rho_a)				
1	2.5	1	150	18.846	2826.9				
2	5	1	40.6	77.73975	3156.23385				
3	10	1	10.09	313.31475	3161.3458275				
4	15	1	3.29	705.93975	2322.5417775				
5	20	1	1.48	1255.61475	1858.30983				
6	25	1	0.783	1962.33975	1536.5120242500002				
7	30	1	0.488	2826.11475	1379.143998				
8	35	1	0.335	3846.93975	1288.72481625				
9	40	1	0.257	5024.8147500000005	1291.3773907500001				
10	45	1	0.2	6359.73975	1271.94795				
11	50	1	0.167	7851.71475	1311.23636325				
12	60	1	0.1136	11306.81475	1284.4541556				
13	70	1	0.0771	15390.11475	1186.5778472250001				
14	80	1	0.0567	20101.61475	1139.7615563250001				
15	90	1	0.0463	25441.31475	1177.932872925				
16	100	1	0.0408	31409.21475	1281.4959618				

AL_VES58

Date:14/04/2025		VES58							
Latitude	29.654642	Longitude	79.695615	Area	Salla	Elevation (m)	1730.0	Direction	200°SW

S.N	Current Electrode Spacing (AB/2)	Potential Electrode Spacing (MN)	Resistance (Ohm)	K value	Aparent Resistivity (Rho_a)				
1	2.5	1	82.6	18.846	1556.6796				
2	5	1	9.66	77.73975	750.965985				
3	10	1	2.66	313.31475	833.417235				
4	15	1	1.162	705.93975	820.3019895				
5	20	1	0.707	1255.61475	887.7196282499999				
6	25	1	0.464	1962.33975	910.525644				
7	30	1	0.29	2826.11475	819.5732775				
8	35	1	0.166	3846.93975	638.5919985				
9	40	1	0.121	5024.8147500000005	608.00258475				
10	45	1	0.089	6359.73975	566.0168377499999				
11	50	1	0.071	7851.71475	557.4717472499999				
12	60	1	0.0487	11306.81475	550.641878325				
13	70	1	0.0264	15390.11475	406.2990294				
14	80	1	0.0264	20101.61475	530.6826294				
15	90	1	0.0233	25441.31475	592.782633675				
16	100	1	0.0196	31409.21475	615.6206090999999				

AL_VES59

Date:14/04/2025		VES59							
Latitude	29.651119	Longitude	79.694777	Area	Salla	Elevation (m)	1709.0	Direction	200°SW
S.N	Current Electrode Spacing (AB/2)	Potential Electrode Spacing (MN)	Resistance (Ohm)	K value	Aparent Resistivity (Rho_a)				
1	2.5	1	33.5	18.846	631.341				
2	5	1	9.88	77.73975	768.0687300000001				
3	10	1	2.17	313.31475	679.8930075				
4	15	1	1.005	705.93975	709.46944875				
5	20	1	0.443	1255.61475	556.23733425				
6	25	1	0.253	1962.33975	496.47195675				
7	30	1	0.156	2826.11475	440.87390100000005				
8	35	1	0.103	3846.93975	396.23479425				
9	40	1	0.074	5024.8147500000005	371.8362915				
10	45	1	0.0592	6359.73975	376.4965932				
11	50	1	0.0509	7851.71475	399.652280775				
12	60	1	0.0367	11306.81475	414.96010132500004				
13	70	1	0.0255	15390.11475	392.447926125				
14	80	1	0.0162	20101.61475	325.64615895				

15	90	1	0.0115	25441.31475	292.575119625				
16	100	1	0.0093	31409.21475	292.105697175				

AL_VES60

Date:14/04/2025		VES60							
Latitude	29.649555	Longitude	79.694138	Area	Salla	Elevation (m)	1693.0	Direction	200°SW
S.N	Current Electrode Spacing (AB/2)	Potential Electrode Spacing (MN)	Resistance (Ohm)	K value	Aparent Resistivity (Rho_a)				
1	2.5	1	211	18.846	3976.506				
2	5	1	27.6	77.73975	2145.6171				
3	10	1	3.81	313.31475	1193.7291975				
4	15	1	1.074	705.93975	758.1792915000001				
5	20	1	0.555	1255.61475	696.86618625				
6	25	1	0.359	1962.33975	704.47997025				
7	30	1	0.24	2826.11475	678.26754				
8	35	1	0.156	3846.93975	600.122601				
9	40	1	0.0979	5024.8147500000005	491.92936402500004				
10	45	1	0.0705	6359.73975	448.36165237499995				
11	50	1	0.056	7851.71475	439.696026				
12	60	1	0.0374	11306.81475	422.87487165				
13	70	1	0.024	15390.11475	369.362754				
14	80	1	0.018	20101.61475	361.82906549999996				
15	90	1	0.0142	25441.31475	361.26666945000005				
16	100	1	0.0125	31409.21475	392.615184375				

AL_VES61

Date:17/04/2025		VES61							
Latitude	29.647782	Longitude	79.693775	Area	Salla	Elevation (m)	1733.0	Direction	200°SW
S.N	Current Electrode Spacing (AB/2)	Potential Electrode Spacing (MN)	Resistance (Ohm)	K value	Aparent Resistivity (Rho_a)				
1	2.5	1	248	18.846	4673.808				
2	5	1	65.7	77.73975	5107.501575				
3	10	1	10.34	313.31475	3239.674515				
4	15	1	2.34	705.93975	1651.899015				
5	20	1	0.747	1255.61475	937.94421825				
6	25	1	0.499	1962.33975	979.2075352500001				

7	30	1	0.327	2826.11475	924.1395232500001				
8	35	1	0.2525	3846.93975	971.352286875				
9	40	1	0.1865	5024.8147500000005	937.1279508750001				
10	45	1	0.134	6359.73975	852.2051265				
11	50	1	0.1033	7851.71475	811.082133675				
12	60	1	0.0657	11306.81475	742.857729075				
13	70	1	0.045425	15390.11475	699.0959625187501				
14	80	1	0.0305	20101.61475	613.099249875				
15	90	1	0.0192	25441.31475	488.47324319999996				
16	100	1	0.0154	31409.21475	483.70190715				

AL_VES62

Date:17/04/2025		**VES62**							
Latitude	**29.646096**	**Longitude**	**79.693243**	**Area**	**Salla**	**Elevation (m)**	**1743.0**	**Direction**	**200°SW**
S.N	**Current Electrode Spacing (AB/2)**	**Potential Electrode Spacing (MN)**	**Resistance (Ohm)**	**K value**	**Aparent Resistivity (Rho_a)**				
1	2.5	1	64.2	18.846	1209.9132				
2	5	1	13.2	77.73975	1026.1647				
3	10	1	1.7	313.31475	532.635075				
4	15	1	0.6535	705.93975	461.33162662499996				
5	20	1	0.263	1255.61475	330.22667925				
6	25	1	0.15	1962.33975	294.3509625				
7	30	1	0.0976	2826.11475	275.8287996				
8	35	1	0.0743	3846.93975	285.827623425				
9	40	1	0.0647	5024.8147500000005	325.105514325				
10	45	1	0.0576	6359.73975	366.32100959999997				
11	50	1	0.0551	7851.71475	432.629482725				
12	60	1	0.046	11306.81475	520.1134784999999				
13	70	1	0.0404	15390.11475	621.7606359				
14	80	1	0.04375	20101.61475	879.4456453125				
15	90	1	0.029175	25441.31475	742.2503578312501				
16	100	1	0.0258	31409.21475	810.35774055				

AL_VES63

Date:17/04/2025		**VES63**							
Latitude	**29.644368**	**Longitude**	**79.692682**	**Area**	**Salla**	**Elevation (m)**	**1773.0**	**Direction**	**200°SW**
S.N	**Current Electrode Spacing (AB/2)**	**Potential Electrode Spacing (MN)**	**Resistance (Ohm)**	**K value**	**Aparent Resistivity (Rho_a)**				

1	2.5	1	85.9	18.846	1618.8714000000002				
2	5	1	15.1	77.73975	1173.870225				
3	10	1	2.49	313.31475	780.1537275000001				
4	15	1	0.934	705.93975	659.3477265				
5	20	1	0.425	1255.61475	533.63626875				
6	25	1	0.245	1962.33975	480.77323875				
7	30	1	0.19	2826.11475	536.9618025000001				
8	35	1	0.149	3846.93975	573.1940227499999				
9	40	1	0.113	5024.8147500000005	567.8040667500001				
10	45	1	0.09	6359.73975	572.3765774999999				
11	50	1	0.074	7851.71475	581.0268915				
12	60	1	0.0453	11306.81475	512.198708175				
13	70	1	0.0326	15390.11475	501.71774085				
14	80	1	0.0258	20101.61475	518.62166055				
15	90	1	0.0191	25441.31475	485.929111725				
16	100	1	0.0174	31409.21475	546.52033665				

AL_VES64

Date:18/04/2025		VES64							
Latitude	29.642678	Longitude	79.692133	Area	Salla	Elevation (m)	1759.0	Direction	200°SW
S.N	Current Electrode Spacing (AB/2)	Potential Electrode Spacing (MN)	Resistance (Ohm)	K value	Aparent Resistivity (Rho_a)				
1	2.5	1	300	18.846	5653.8				
2	5	1	58.3	77.73975	4532.227425				
3	10	1	5.58	313.31475	1748.296305				
4	15	1	1.45	705.93975	1023.6126375				
5	20	1	0.486	1255.61475	610.2287685				
6	25	1	0.188	1962.33975	368.919873				
7	30	1	0.094	2826.11475	265.6547865				
8	35	1	0.077	3846.93975	296.21436074999997				
9	40	1	0.061	5024.8147500000005	306.51369975				
10	45	1	0.0519	6359.73975	330.070493025				
11	50	1	0.0455	7851.71475	357.253021125				
12	60	1	0.0379	11306.81475	428.528279025				
13	70	1	0.0313	15390.11475	481.71059167500005				
14	80	1	0.0238	20101.61475	478.41843105000004				
15	90	1	0.0225	25441.31475	572.429581875				
16	100	1	0.0157	31409.21475	493.1246715749999				

AL_VES65

Date:17/04/2025		VES65							

Latitude	29.640838	Longitude	79.691617	Area	Salla	Elevation (m)	1721.0	Direction	200°SW
S.N	Current Electrode Spacing (AB/2)	Potential Electrode Spacing (MN)	Resistance (Ohm)	K value	Aparent Resistivity (Rho_a)				
1	2.5	1	151	18.846	2845.746				
2	5	1	15.1	77.73975	1173.870225				
3	10	1	2.7	313.31475	845.949825				
4	15	1	0.979	705.93975	691.1150152499999				
5	20	1	0.508	1255.61475	637.852293				
6	25	1	0.344	1962.33975	675.0448739999999				
7	30	1	0.245	2826.11475	692.39811375				
8	35	1	0.188	3846.93975	723.224673				
9	40	1	0.155	5024.8147500000005	778.84628625				
10	45	1	0.129	6359.73975	820.40642775				
11	50	1	0.1057	7851.71475	829.926249075				
12	60	1	0.0822	11306.81475	929.4201724499999				
13	70	1	0.0558	15390.11475	858.7684030500001				
14	80	1	0.0441	20101.61475	886.481210475				
15	90	1	0.0232	25441.31475	590.2385022				
16	100	1	0.0233	31409.21475	731.834703675				

AL_VES66

Date:18/04/2025		VES66							
Latitude	29.639248	Longitude	79.691038	Area	Salla	Elevation (m)	1661.0	Direction	200°SW
S.N	Current Electrode Spacing (AB/2)	Potential Electrode Spacing (MN)	Resistance (Ohm)	K value	Aparent Resistivity (Rho_a)				
1	2.5	1	112.3	18.846	2116.4058				
2	5	1	22	77.73975	1710.2745				
3	10	1	3.85	313.31475	1206.2617875				
4	15	1	1.37	705.93975	967.1374575000001				
5	20	1	0.725	1255.61475	910.3206937499999				
6	25	1	0.389	1962.33975	763.3501627500001				
7	30	1	0.217	2826.11475	613.26690075				
8	35	1	0.155	3846.93975	596.27566125				
9	40	1	0.053	5024.8147500000005	266.31518175				
11	50	1	0.0142	7851.71475	111.49434945				
12	60	1	0.00525	11306.81475	59.360777437500005				
13	70	1	0.00418	15390.11475	64.330679655				
14	80	1	0.001	20101.61475	20.10161475				

AL_VES67

Date:18/04/2025		VES67							
Latitude	29.634167	Longitude	79.67694	Area	Balta	Elevation (m)	1691.0	Direction	150°SE
S.N	Current Electrode Spacing (AB/2)	Potential Electrode Spacing (MN)	Resistance (Ohm)	K value	Aparent Resistivity (Rho_a)				
1	2.5	1	103.7	18.846	1954.3302				
2	5	1	40	77.73975	3109.59				
3	10	1	13.2	313.31475	4135.7546999999995				
4	15	1	6.33	705.93975	4468.5986175				
5	20	1	3.43	1255.61475	4306.7585925				
6	25	1	2.01	1962.33975	3944.3028974999997				
7	30	1	1.3	2826.11475	3673.949175				
8	35	1	0.905	3846.93975	3481.4804737500003				
9	40	1	0.67	5024.8147500000005	3366.6258825000004				
10	45	1	0.53	6359.73975	3370.6620675				
11	50	1	0.429	7851.71475	3368.38562775				
12	60	1	0.284	11306.81475	3211.1353889999996				
13	70	1	0.167	15390.11475	2570.14916325				
14	80	1	0.126	20101.61475	2532.8034585				
15	90	1	0.0945	25441.31475	2404.204243875				
16	100	1	0.0644	31409.21475	2022.7534299				

AL_VES68

Date:18/04/2025		VES68							
Latitude	29.635725	Longitude	79.675778	Area	Balta	Elevation (m)	1648.0	Direction	150°SE
S.N	Current Electrode Spacing (AB/2)	Potential Electrode Spacing (MN)	Resistance (Ohm)	K value	Aparent Resistivity (Rho_a)				
1	2.5	1	147	18.846	2770.362				
2	5	1	42.2	77.73975	3280.61745				
3	10	1	11.43	313.31475	3581.1875925				
4	15	1	4.81	705.93975	3395.5701974999997				
5	20	1	2.46	1255.61475	3088.812285				
6	25	1	1.79	1962.33975	3512.5881525000004				
7	30	1	1.28	2826.11475	3617.4268800000004				
8	35	1	0.845	3846.93975	3250.66408875				
9	40	1	0.598	5024.8147500000005	3004.8392205				
10	45	1	0.425	6359.73975	2702.8893937499997				
11	50	1	0.315	7851.71475	2473.29014625				

12	60	1	0.177	11306.81475	2001.3062107499998				
13	70	1	0.129	15390.11475	1985.3248027500001				
14	80	1	0.0997	20101.61475	2004.130990575				
15	90	1	0.0752	25441.31475	1913.1868692000003				
16	100	1	0.0592	31409.21475	1859.4255132				

AL_VES69

Date:18/04/2025		VES69							
Latitude	29.637157	Longitude	79.67463	Area	Balta	Elevation (m)	1685.0	Direction	150°SE
S.N	Current Electrode Spacing (AB/2)	Potential Electrode Spacing (MN)	Resistance (Ohm)	K value	Aparent Resistivity (Rho_a)				
1	2.5	1	151	18.846	2845.746				
2	5	1	15.1	77.73975	1173.870225				
3	10	1	2.7	313.31475	845.949825				
4	15	1	0.979	705.93975	691.1150152499999				
5	20	1	0.508	1255.61475	637.852293				
6	25	1	0.344	1962.33975	675.0448739999999				
7	30	1	0.245	2826.11475	692.39811375				
8	35	1	0.188	3846.93975	723.224673				
9	40	1	0.155	5024.8147500000005	778.84628625				
10	45	1	0.129	6359.73975	820.40642775				
11	50	1	0.1057	7851.71475	829.926249075				
12	60	1	0.0822	11306.81475	929.4201724499999				
13	70	1	0.0558	15390.11475	858.7684030500001				
14	80	1	0.0441	20101.61475	886.481210475				
15	90	1	0.0232	25441.31475	590.2385022				
16	100	1	0.0233	31409.21475	731.834703675				

AL_VES70

Date:20/04/2025		VES70							
Latitude	29.638777	Longitude	79.673418	Area	Mat	Elevation (m)	1669.0	Direction	150°SE
S.N	Current Electrode Spacing (AB/2)	Potential Electrode Spacing (MN)	Resistance (Ohm)	K value	Aparent Resistivity (Rho_a)				
1	2.5	1	34.1	18.846	642.6486				
2	5	1	11.03	77.73975	857.4694425				
3	10	1	3.55	313.31475	1112.2673625				
4	15	1	1.66	705.93975	1171.859985				
5	20	1	0.84	1255.61475	1054.7163899999998				

6	25	1	0.531	1962.33975	1042.00240725				
7	30	1	0.379	2826.11475	1071.0974902500002				
8	35	1	0.267	3846.93975	1027.13291325				
9	40	1	0.195	5024.8147500000005	979.8388762500001				
10	45	1	0.143	6359.73975	909.4427842499999				
11	50	1	0.0959	7851.71475	752.979444525				
12	60	1	0.0749	11306.81475	846.8804247749999				
13	70	1	0.0527	15390.11475	811.0590473249999				
14	80	1	0.0396	20101.61475	796.0239441000001				
15	90	1	0.0306	25441.31475	778.50423135				
16	100	1	0.0286	31409.21475	898.30354185				

AL_VES71

Date:20/04/2025		**VES71**							
Latitude	**29.640817**	**Longitude**	**79.673412**	**Area**	**Mat**	**Elevation (m)**	**1704.0**	**Direction**	**150°SE**
S.N	**Current Electrode Spacing (AB/2)**	**Potential Electrode Spacing (MN)**	**Resistance (Ohm)**	**K value**	**Aparent Resistivity (Rho_a)**				
1	2.5	1	112	18.846	2110.752				
2	5	1	37.2	77.73975	2891.9187				
3	10	1	5.74	313.31475	1798.4266650000002				
4	15	1	1.48	705.93975	1044.79083				
5	20	1	0.594	1255.61475	745.8351614999999				
6	25	1	0.391	1962.33975	767.2748422500001				
7	30	1	0.259	2826.11475	731.96372025				
8	35	1	0.171	3846.93975	657.82669725				
9	40	1	0.164	5024.8147500000005	824.0696190000001				
10	45	1	0.088	6359.73975	559.6570979999999				
11	50	1	0.155	7851.71475	1217.01578625				
12	60	1	0.04	11306.81475	452.27259				
13	70	1	0.025	15390.11475	384.75286875000006				
14	80	1	0.0147	20101.61475	295.493736825				
15	90	1	0.025	25441.31475	636.03286875				
16	100	1	0.00979	31409.21475	307.4962124025				

AL_VES72

Date:20/04/2025		**VES72**							
Latitude	**29.641624**	**Longitude**	**79.671161**	**Area**	**Mat**	**Elevation (m)**	**1690.0**	**Direction**	**150°SE**
S.N	**Current Electrode**	**Potential Electrode**	**Resistance (Ohm)**	**K value**	**Aparent Resistivity (Rho_a)**				

	Spacing (AB/2)	Spacing (MN)							
1	2.5	1	62.8	18.846	1183.5288				
2	5	1	12.6	77.73975	979.52085				
3	10	1	2.77	313.31475	867.8818575				
4	15	1	1.095	705.93975	773.00402625				
5	20	1	0.636	1255.61475	798.570981				
6	25	1	0.483	1962.33975	947.81009925				
7	30	1	0.372	2826.11475	1051.314687				
8	35	1	0.289	3846.93975	1111.76558775				
9	40	1	0.196	5024.8147500000005	984.8636910000001				
10	45	1	0.127	6359.73975	807.68694825				
11	50	1	0.0932	7851.71475	731.7798147000001				
12	60	1	0.0635	11306.81475	717.982736625				
13	70	1	0.0467	15390.11475	718.718358825				
14	80	1	0.0367	20101.61475	737.729261325				
15	90	1	0.0261	25441.31475	664.0183149750001				
16	100	1	0.0237	31409.21475	744.3983895749999				

AL_VES73

Date:21/04/2025		VES73							
Latitude	29.643093	Longitude	79.670017	Area	Mat	Elevation (m)	1637.0	Direction	150°SE
S.N	Current Electrode Spacing (AB/2)	Potential Electrode Spacing (MN)	Resistance (Ohm)	K value	Aparent Resistivity (Rho_a)				
1	2.5	1	136	18.846	2563.056				
2	5	1	14.9	77.73975	1158.322275				
3	10	1	3.35	313.31475	1049.6044125				
4	15	1	1.55	705.93975	1094.2066125000001				
5	20	1	0.982	1255.61475	1233.0136845				
6	25	1	0.593	1962.33975	1163.66747175				
7	30	1	0.408	2826.11475	1153.054818				
8	35	1	0.298	3846.93975	1146.3880454999999				
9	40	1	0.209	5024.8147500000005	1050.1862827500001				
10	45	1	0.152	6359.73975	966.680442				
11	50	1	0.115	7851.71475	902.94719625				
12	60	1	0.05	11306.81475	565.3407375				
13	70	1	0.0279	15390.11475	429.38420152500004				
14	80	1	0.0174	20101.61475	349.76809664999996				
15	90	1	0.0134	25441.31475	340.91361765000005				
16	100	1	0.012	31409.21475	376.910577				

AL_VES74

Date:21/04/2025		VES74							
Latitude	29.642038	Longitude	79.669058	Area	Mat	Elevation (m)	1684.0	Direction	150°SE
S.N	Current Electrode Spacing (AB/2)	Potential Electrode Spacing (MN)	Resistance (Ohm)	K value	Aparent Resistivity (Rho_a)				
1	2.5	1	14.4	18.846	271.3824				
2	5	1	11.9	77.73975	925.103025				
3	10	1	2.1	313.31475	657.9609750000001				
4	15	1	0.824	705.93975	581.694354				
5	20	1	0.383	1255.61475	480.90044925				
6	25	1	0.202	1962.33975	396.39262950000006				
7	30	1	0.125	2826.11475	353.26434375				
8	35	1	0.088	3846.93975	338.530698				
9	40	1	0.0661	5024.8147500000005	332.14025497500006				
10	45	1	0.0524	6359.73975	333.2503629				
11	50	1	0.039	7851.71475	306.21687525				
12	60	1	0.0269	11306.81475	304.153316775				
13	70	1	0.0186	15390.11475	286.25613434999997				
14	80	1	0.01193	20101.61475	239.8122639675				
15	90	1	0.00857	25441.31475	218.0320674075				
16	100	1	0.00736	31409.21475	231.17182056000001				

AL_VES75

Date:29/04/2025		VES75							
Latitude	29.63755	Longitude	79.67251	Area	Mat	Elevation (m)	1732.0	Direction	150°SE
S.N	Current Electrode Spacing (AB/2)	Potential Electrode Spacing (MN)	Resistance (Ohm)	K value	Aparent Resistivity (Rho_a)				
1	2.5	1	195	18.846	3674.97				
2	5	1	42.8	77.73975	3327.2612999999997				
3	10	1	7.83	313.31475	2453.2544925				
4	15	1	2.67	705.93975	1884.8591325				
5	20	1	1.62	1255.61475	2034.0958950000002				
6	25	1	0.966	1962.33975	1895.6201985				
7	30	1	0.605	2826.11475	1709.79942375				
8	35	1	0.31	3846.93975	1192.5513225				
9	40	1	0.184	5024.8147500000005	924.565914				
10	45	1	0.106	6359.73975	674.1324135				
11	50	1	0.078	7851.71475	612.4337505				
12	60	1	0.0541	11306.81475	611.698677975				

13	70	1	0.0455	15390.11475	700.250221125					
14	80	1	0.0485	20101.61475	974.928315375					
15	90	1	0.0335	25441.31475	852.2840441250002					
16	100	1	0.0267	31409.21475	838.626033825					

AL_VES76

Date:21/04/2025		VES76							
Latitude		Longitude		Area		Elevation (m)		Direction	
S.N	**Current Electrode Spacing (AB/2)**	**Potential Electrode Spacing (MN)**	**Resistance (Ohm)**	**K value**	**Aparent Resistivity (Rho_a)**				
1	2.5	1	43.5	18.846	819.801				
2	5	1	15	77.73975	1166.096				
3	10	1	3.79	313.3148	1187.463				
4	15	1	1.76	705.9398	1242.454				
5	20	1	1.075	1255.615	1349.786				
6	25	1	0.779	1962.34	1528.663				
7	30	1	0.598	2826.115	1690.017				
8	35	1	0.483	3846.94	1858.072				
9	40	1	0.388	5024.815	1949.628				
10	45	1	0.324	6359.74	2060.556				
11	50	1	0.271	7851.715	2127.815				
12	60	1	0.182	11306.81	2057.840				
13	70	1	0.13	15390.11	2000.715				
14	80	1	0.099	20101.61	1990.060				
15	90	1	0.082	25441.31	2086.188				
16	100	1	0.0699	31409.21	2195.504				

AL_VES77

Date:21/04/2025		VES77							
Latitude		Longitude		Area		Elevation (m)		Direction	
S.N	**Current Electrode Spacing (AB/2)**	**Potential Electrode Spacing (MN)**	**Resistance (Ohm)**	**K value**	**Aparent Resistivity (Rho_a)**				
1	2.5	1	97.9	18.846	1845.023				
2	5	1	32.8	77.73975	2549.864				
3	10	1	9.23	313.3148	2891.895				
4	15	1	4	705.9398	2823.759				
5	20	1	2.19	1255.615	2749.796				
6	25	1	1.38	1962.34	2708.029				
7	30	1	0.868	2826.115	2453.068				
8	35	1	0.607	3846.94	2335.092				
9	40	1	0.433	5024.815	2175.745				

10	45	1	0.325	6359.74	2066.915				
11	50	1	0.247	7851.715	1939.374				
12	60	1	0.164	11306.81	1854.318				
13	70	1	0.118	15390.11	1816.034				
14	80	1	0.08865	20101.61	1782.008				
15	90	1	0.06505	25441.31	1654.958				
16	100	1	0.051225	31409.21	1608.937				

AL_VES78

Date:21/04/2025		VES78							
Latitude	29.636039	Longitude	79.673646	Area	Balta	Elevation (m)	1703.0	Direction	150°SE
S.N	Current Electrode Spacing (AB/2)	Potential Electrode Spacing (MN)	Resistance (Ohm)	K value	Aparent Resistivity (Rho_a)				
1	2.5	1	451	18.846	8499.546				
2	5	1	138	77.73975	10728.0855				
3	10	1	17	313.31475	5326.35075				
4	15	1	3.62	705.93975	2555.501895				
5	20	1	1.37	1255.61475	1720.1922075				
6	25	1	0.74	1962.33975	1452.131415				
7	30	1	0.515	2826.11475	1455.4490962500001				
8	35	1	0.42	3846.93975	1615.714695				
9	40	1	0.4205	5024.8147500000005	2112.934602375				
10	45	1	0.335	6359.73975	2130.51281625				
11	50	1	0.267	7851.71475	2096.40783825				
12	60	1	0.218	11306.81475	2464.8856155				
13	70	1	0.172	15390.11475	2647.099737				
14	80	1	0.08635	20101.61475	1735.7744336625				
15	90	1	0.07455	25441.31475	1896.6500146125002				
16	100	1	0.0437	31409.21475	1372.582684575				

AL_VES79

Date:29/04/2025		VES79							
Latitude	29.653363	Longitude	79.712169	Area	Balta	Elevation (m)	1704.0	Direction	150°SE
S.N	Current Electrode Spacing (AB/2)	Potential Electrode Spacing (MN)	Resistance (Ohm)	K value	Aparent Resistivity (Rho_a)				
1	2.5	1	72.1	18.846	1358.7966				
2	5	1	9.66	77.73975	750.965985				
3	10	1	1.37	313.31475	429.24120750000003				

4	15	1	0.669	705.93975	472.27369275				
5	20	1	0.333	1255.61475	418.11971175				
6	25	1	0.177	1962.33975	347.33413575				
7	30	1	0.11	2826.11475	310.87262250000003				
8	35	1	0.0728	3846.93975	280.0572138				
9	40	1	0.0495	5024.8147500000005	248.72833012500004				
10	45	1	0.0384	6359.73975	244.21400639999996				
11	50	1	0.0329	7851.71475	258.321415275				
12	60	1	0.0258	11306.81475	291.71582055				
13	70	1	0.0197	15390.11475	303.185260575				
14	80	1	0.0157	20101.61475	315.595351575				
15	90	1	0.0131	25441.31475	333.281223225				
16	100	1	0.01061	31409.21475	333.2517684975				

AL_VES80

Date:29/04/2025		VES80							
Latitude	29.632916	Longitude	79.676079	Area	Balta	Elevation (m)	1738.0	Direction	150°SE
S.N	Current Electrode Spacing (AB/2)	Potential Electrode Spacing (MN)	Resistance (Ohm)	K value	Aparent Resistivity (Rho_a)				
1	2.5	1	43.5	18.846	819.801				
2	5	1	15	77.73975	1166.096				
3	10	1	3.79	313.31475	1187.463				
4	15	1	1.76	705.93975	1242.454				
5	20	1	1.075	1255.61475	1349.786				
6	25	1	0.779	1962.33975	1528.663				
7	30	1	0.598	2826.11475	1690.017				
8	35	1	0.483	3846.93975	1858.072				
9	40	1	0.388	5024.8147500000005	1949.628				
10	45	1	0.324	6359.73975	2060.556				
11	50	1	0.271	7851.71475	2127.815				
12	60	1	0.182	11306.81475	2057.840				
13	70	1	0.13	15390.11475	2000.715				
14	80	1	0.099	20101.61475	1990.060				
15	90	1	0.082	25441.31475	2086.188				
16	100	1	0.0699	31409.21475	2195.504				

AL_VES81

Date:30/04/2025		VES81							
Latitude	29.655139	Longitude	79.712425	Area	Batgal	Elevation (m)	1497.0	Direction	05°N
S.N	Current Electrode	Potential Electrode Spacing (MN)	Resistance (Ohm)	K value	Aparent Resistivity (Rho_a)				

	Spacing (AB/2)								
1	2.5	1	59.5	18.846	1121.337				
2	5	1	10.28	77.73975	799.16463				
3	10	1	1.65	313.31475	516.9693374999999				
4	15	1	0.719	705.93975	507.57068025				
5	20	1	0.407	1255.61475	511.03520324999994				
6	25	1	0.2505	1962.33975	491.566107375				
7	30	1	0.178	2826.11475	503.0484255				
8	35	1	0.122	3846.93975	469.3266495				
9	40	1	0.0799	5024.8147500000005	401.48269852500005				
10	45	1	0.0542	6359.73975	344.69789445				
11	50	1	0.0384	7851.71475	301.5058464				
12	60	1	0.0263	11306.81475	297.369227925				
13	70	1	0.0182	15390.11475	280.10008845000004				
14	80	1	0.0142	20101.61475	285.44292945				
15	90	1	0.01132	25441.31475	287.99568297				
16	100	1	0.00606	31409.21475	190.339841385				

AL_VES82

Date:30/04/2025		VES82							
Latitude	29.653363	Longitude	79.712169	Area	Batgal	Elevation (m)	1495.0	Direction	05°N
S.N	Current Electrode Spacing (AB/2)	Potential Electrode Spacing (MN)	Resistance (Ohm)	K value	Aparent Resistivity (Rho_a)				
1	2.5	1	72.1	18.846	1358.7966				
2	5	1	9.66	77.73975	750.965985				
3	10	1	1.37	313.31475	429.24120750000003				
4	15	1	0.669	705.93975	472.27369275				
5	20	1	0.333	1255.61475	418.11971175				
6	25	1	0.177	1962.33975	347.33413575				
7	30	1	0.11	2826.11475	310.87262250000003				
8	35	1	0.0728	3846.93975	280.0572138				
9	40	1	0.0495	5024.8147500000005	248.72833012500004				
10	45	1	0.0384	6359.73975	244.21400639999996				
11	50	1	0.0329	7851.71475	258.321415275				
12	60	1	0.0258	11306.81475	291.71582055				
13	70	1	0.0197	15390.11475	303.185260575				
14	80	1	0.0157	20101.61475	315.595351575				
15	90	1	0.0131	25441.31475	333.281223225				
16	100	1	0.01061	31409.21475	333.2517684975				

AL_VES83

Date:21/04/2025		VES83							
Latitude	29.651396	Longitude	79.711859	Area	Batgal	Elevation (m)	1499.0	Direction	05°N
S.N	Current Electrode Spacing (AB/2)	Potential Electrode Spacing (MN)	Resistance (Ohm)	K value	Aparent Resistivity (Rho_a)				
1	2.5	1	338	18.846	6369.948				
2	5	1	62	77.73975	4819.8645				
3	10	1	8.04	313.31475	2519.05059				
4	15	1	2.26	705.93975	1595.4238349999998				
5	20	1	0.901	1255.61475	1131.30888975				
6	25	1	0.384	1962.33975	753.5384640000001				
7	30	1	0.26	2826.11475	734.789835				
8	35	1	0.211	3846.93975	811.70428725				
9	40	1	0.185	5024.8147500000005	929.59072875				
10	45	1	0.173	6359.73975	1100.2349767499998				
11	50	1	0.16	7851.71475	1256.2743600000001				
12	60	1	Rock	11306.81475					
13	70	1	0.122	15390.11475	1877.5939995				
14	80	1	0.107	20101.61475	2150.87277825				
15	90	1	0.0914	25441.31475	2325.33616815				
16	100	1	Rock	31409.21475					

AL_VES84

Date:30/04/2025		VES84							
Latitude	29.65509	Longitude	79.70983	Area	Batgal	Elevation (m)	1431.0	Direction	05°N
S.N	Current Electrode Spacing (AB/2)	Potential Electrode Spacing (MN)	Resistance (Ohm)	K value	Aparent Resistivity (Rho_a)				
1	2.5	1	162	18.846	3053.052				
2	5	1	26.9	77.73975	2091.199275				
3	10	1	5.84	313.31475	1829.75814				
4	15	1	1.54	705.93975	1087.147215				
5	20	1	0.431	1255.61475	541.1699572499999				
6	25	1	0.216	1962.33975	423.865386				
7	30	1	0.071	2826.11475	200.65414725				
8	35	1	0.0536	3846.93975	206.1959706				
9	40	1	0.0397	5024.8147500000005	199.48514557500002				
10	45	1	0.0416	6359.73975	264.5651736				
11	50	1	0.024	7851.71475	188.441154				
12	60	1	0.0296	11306.81475	334.6817166				

13	70	1	0.017	15390.11475	261.63195075000004				
14	80	1	0.0242	20101.61475	486.45907695				
15	90	1	0.0235	25441.31475	597.870896625				
16	100	1	0.0218	31409.21475	684.72088155				

AL_VES85

Date:30/04/2025		VES85							
Latitude	29.656935	Longitude	79.710375	Area	Batgal	Elevation (m)	1468.0	Direction	05°N
S.N	Current Electrode Spacing (AB/2)	Potential Electrode Spacing (MN)	Resistance (Ohm)	K value	Aparent Resistivity (Rho_a)				
1	2.5	1	595	18.846	11213.37				
2	5	1	122	77.73975	9484.2495				
3	10	1	15.8	313.31475	4950.37305				
4	15	1	3.29	705.93975	2322.5417775				
5	20	1	2.23	1255.61475	2800.0208924999997				
6	25	1	1.44	1962.33975	2825.76924				
7	30	1	1.017	2826.11475	2874.1587007499998				
8	35	1	0.64	3846.93975	2462.04144				
9	40	1	0.543	5024.8147500000005	2728.4744092500005				
10	45	1	0.418	6359.73975	2658.3712155				
11	50	1	0.34	7851.71475	2669.583015				
12	60	1	0.41	11306.81475	4635.7940475				
13	70	1	0.19	15390.11475	2924.1218025000003				
14	80	1	0.179	20101.61475	3598.18904025				
15	90	1	0.12	25441.31475	3052.95777				
16	100	1	0.256	31409.21475	8040.758976				

AL_VES86

Date:1/05/2025		VES86							
Latitude	29.652677	Longitude	79.709691	Area	Batgal	Elevation (m)	1514.0	Direction	05°N
S.N	Current Electrode Spacing (AB/2)	Potential Electrode Spacing (MN)	Resistance (Ohm)	K value	Aparent Resistivity (Rho_a)				
1	2.5	1	115.7	18.846	2180.4822				
2	5	1	19.9	77.73975	1547.021025				
3	10	1	3.4	313.31475	1065.27015				
4	15	1	1.4	705.93975	988.3156499999999				
5	20	1	0.636	1255.61475	798.570981				
6	25	1	0.589	1962.33975	1155.81811275				

7	30	1	0.502	2826.11475	1418.7096045				
8	35	1	0.404	3846.93975	1554.163659				
9	40	1	0.432	5024.8147500000005	2170.7199720000003				
10	45	1	0.278	6359.73975	1768.0076505000002				
11	50	1	0.199	7851.71475	1562.49123525				
12	60	1	0.104	11306.81475	1175.9087339999999				
13	70	1	0.063	15390.11475	969.5772292500001				
14	80	1	0.0392	20101.61475	787.9832982				
15	90	1	0.0568	25441.31475	1445.0666778000002				
16	100	1	0.0612	31409.21475	1922.2439427				

AL_VES87

Date:21/04/2025		VES87							
Latitude	29.651507	Longitude	79.709178	Area	Batgal	Elevation (m)	1481.0	Direction	05°N
S.N	Current Electrode Spacing (AB/2)	Potential Electrode Spacing (MN)	Resistance (Ohm)	K value	Aparent Resistivity (Rho_a)				
1	2.5	1	265	18.846	4994.19				
2	5	1	47.5	77.73975	3692.638125				
3	10	1	4.37	313.31475	1369.1854575				
4	15	1	1.96	705.93975	1383.64191				
5	20	1	1.02	1255.61475	1280.727045				
6	25	1	0.703	1962.33975	1379.52484425				
7	30	1	0.474	2826.11475	1339.5783915				
8	35	1	0.415	3846.93975	1596.4799962499999				
9	40	1	0.367	5024.8147500000005	1844.1070132500001				
10	45	1	0.585	6359.73975	3720.4477537499997				
11	50	1	0.273	7851.71475	2143.51812675				
12	60	1	0.354	11306.81475	4002.6124214999995				
13	70	1	0.459	15390.11475	7064.06267025				
14	80	1	0.157	20101.61475	3155.95351575				
15	90	1	0.136	25441.31475	3460.0188060000005				
16	100	1	0.151	31409.21475	4742.791427249999				

AL_VES88

Date:5/05/2025		VES88							
Latitude	29.628451	Longitude	79.706012	Area	PunakoteArea	Elevation (m)	1426.0	Direction	90°E
S.N	Current Electrode Spacing (AB/2)	Potential Electrode Spacing (MN)	Resistance (Ohm)	K value	Aparent Resistivity (Rho_a)				

1	2.5	1	366	18.846	6897.636				
2	5	1	50.9	77.73975	3956.953275				
3	10	1	1.44	313.31475	451.17323999999996				
4	15	1	1.95	705.93975	1376.5825125				
5	20	1	0.964	1255.61475	1210.412619				
6	25	1	0.679	1962.33975	1332.42869025				
7	30	1	0.67	2826.11475	1893.4968825000003				
8	35	1	0.552	3846.93975	2123.5107420000004				
9	40	1	0.395	5024.8147500000005	1984.8018262500002				
10	45	1	0.275	6359.73975	1748.9284312500001				
11	50	1	0.182	7851.71475	1429.0120845				
12	60	1	0.0897	11306.81475	1014.221283075				
13	70	1	0.0692	15390.11475	1064.9959407000001				
14	80	1	0.064	20101.61475	1286.503344				
15	90	1	0.0478	25441.31475	1216.0948450500002				
16	100	1	0.0401	31409.21475	1259.509511475				

AL_VES89

Date:05/05/2025		**VES89**							
Latitude	**29.628365**	**Longitude**	**79.708089**	**Area**	**Punakote Area**	**Elevation (m)**	**1383.0**	**Direction**	**90°E**
S.N	**Current Electrode Spacing (AB/2)**	**Potential Electrode Spacing (MN)**	**Resistance (Ohm)**	**K value**	**Aparent Resistivity (Rho_a)**				
1	2.5	1	65	18.846	1224.99				
2	5	1	13.8	77.73975	1072.80855				
3	10	1	3.18	313.31475	996.340905				
4	15	1	1.38	705.93975	974.1968549999999				
5	20	1	0.81	1255.61475	1017.0479475000001				
6	25	1	0.522	1962.33975	1024.3413495				
7	30	1	0.373	2826.11475	1054.14080175				
8	35	1	0.28	3846.93975	1077.1431300000002				
9	40	1	0.208	5024.8147500000005	1045.161468				
10	45	1	0.164	6359.73975	1042.997319				
11	50	1	0.141	7851.71475	1107.09177975				
12	60	1	0.0981	11306.81475	1109.198526975				
13	70	1	0.0682	15390.11475	1049.60582595				
14	80	1	0.0571	20101.61475	1147.802202225				
15	90	1	0.0379	25441.31475	964.2258290250002				
16	100	1	0.0339	31409.21475	1064.7723800249998				

AL_VES90

Date:05/05/2025		**VES90**							

Latitude	29.628355	Longitude	79.710216	Area	Punakote area	Elevation (m)	1338.0	Direction	90°E
S.N	Current Electrode Spacing (AB/2)	Potential Electrode Spacing (MN)	Resistance (Ohm)	K value	Aparent Resistivity (Rho_a)				
1	2.5	1	58.4	18.846	1100.6064				
2	5	1	11.3	77.73975	878.4591750000001				
3	10	1	4.2	313.31475	1315.9219500000002				
4	15	1	1.12	705.93975	790.6525200000001				
5	20	1	1.078	1255.61475	1353.5527005000001				
6	25	1	0.591	1962.33975	1159.74279225				
7	30	1	0.393	2826.11475	1110.66309675				
8	35	1	0.28	3846.93975	1077.1431300000002				
9	40	1	0.23	5024.8147500000005	1155.7073925000002				
10	45	1	0.183	6359.73975	1163.83237425				
11	50	1	0.151	7851.71475	1185.60892725				
12	60	1	0.1024	11306.81475	1157.8178304				
13	70	1	0.0669	15390.11475	1029.598676775				
14	80	1	0.0495	20101.61475	995.0299301250001				
15	90	1	0.0529	25441.31475	1345.845550275				
16	100	1	0.0376	31409.21475	1180.9864746				

AL_VES91

Date:05/05/2025		VES91							
Latitude	29.634612	Longitude	79.727032	Area	Digoli Area	Elevation (m)	1355.0	Direction	5°N
S.N	Current Electrode Spacing (AB/2)	Potential Electrode Spacing (MN)	Resistance (Ohm)	K value	Aparent Resistivity (Rho_a)				
1	2.5	1	191	18.846	3599.5860000000002				
2	5	1	24.15	77.73975	1877.4149625				
3	10	1	6.99	313.31475	2190.0701025000003				
4	15	1	1.94	705.93975	1369.523115				
5	20	1	1.3	1255.61475	1632.299175				
6	25	1	0.876	1962.33975	1719.0096210000002				
7	30	1	0.601	2826.11475	1698.49496475				
8	35	1	0.48	3846.93975	1846.53108				
9	40	1	0.446	5024.8147500000005	2241.0673785000004				
10	45	1	0.407	6359.73975	2588.41407825				
11	50	1	0.463	7851.71475	3635.34392925				
12	60	1	1.06	11306.81475	11985.223635				
13	70	1	0.195	15390.11475	3001.07237625				

AL_VES92

Date:05/05/2025		VES92							
Latitude	29.636268	Longitude	79.726792	Area	Digoli	Elevation (m)	1335.0	Direction	5°N
S.N	Current Electrode Spacing (AB/2)	Potential Electrode Spacing (MN)	Resistance (Ohm)	K value	Aparent Resistivity (Rho_a)				
1	2.5	1	65.3	18.846	1230.6438				
2	5	1	16.1	77.73975	1251.609975				
3	10	1	4.02	313.31475	1259.525295				
4	15	1	1.8	705.93975	1270.69155				
5	20	1	0.648	1255.61475	813.638358				
6	25	1	0.32	1962.33975	627.9487200000001				
7	30	1	0.201	2826.11475	568.0490647500001				
8	35	1	0.153	3846.93975	588.58178175				
9	40	1	0.125	5024.8147500000005	628.1018437500001				
10	45	1	0.1225	6359.73975	779.0681193749999				
11	50	1	0.0768	7851.71475	603.0116928				
12	60	1	0.0745	11306.81475	842.357698875				
13	70	1	0.0445	15390.11475	684.860106375				
14	80	1	0.0304	20101.61475	611.0890884				
15	90	1	0.0201	25441.31475	511.37042647500004				
16	100	1	0.0132	31409.21475	414.6016347				

AL_VES93

Date:05/05/2025		VES93							
Latitude	29.6381	Longitude	79.726537	Area	Digoli	Elevation (m)	1383.0	Direction	5°N
S.N	Current Electrode Spacing (AB/2)	Potential Electrode Spacing (MN)	Resistance (Ohm)	K value	Aparent Resistivity (Rho_a)				
1	2.5	1	102.2	18.846	1926.0612				
2	5	1	13.1	77.73975	1018.390725				
3	10	1	2.36	313.31475	739.4228099999999				
4	15	1	1.177	705.93975	830.89108575				
5	20	1	0.713	1255.61475	895.25331675				
6	25	1	0.519	1962.33975	1018.4543302500001				
7	30	1	0.4	2826.11475	1130.4459000000002				
8	35	1	0.428	3846.93975	1646.490213				
9	40	1	0.258	5024.8147500000005	1296.4022055000003				
10	45	1	0.205	6359.73975	1303.7466487499998				
11	50	1	0.195	7851.71475	1531.08437625				

12	60	1	0.177	11306.81475	2001.3062107499998				
13	70	1	0.136	15390.11475	2093.0556060000004				
14	80	1	0.203	20101.61475	4080.6277942500005				
15	90	1	0.0816	25441.31475	2076.0112836000003				
16	100	1	0.077	31409.21475	2418.50953575				

AL_VES94

Date:05/05/2025		VES94							
Latitude	29.614889	Longitude	79.721577	Area	Bataldeon	Elevation (m)	1334.0	Direction	170°SE
S.N	Current Electrode Spacing (AB/2)	Potential Electrode Spacing (MN)	Resistance (Ohm)	K value	Aparent Resistivity (Rho_a)				
1	2.5	1	384	18.846	7236.864				
2	5	1	68.6	77.73975	5332.946849999999				
3	10	1	10.67	313.31475	3343.0683825				
4	15	1	3.27	705.93975	2308.4229825				
5	20	1	1.91	1255.61475	2398.2241725				
6	25	1	1.46	1962.33975	2865.016035				
7	30	1	1.091	2826.11475	3083.29119225				
8	35	1	1.018	3846.93975	3916.1846655				
9	40	1	0.553	5024.8147500000005	2778.7225567500004				
10	45	1	0.345	6359.73975	2194.1102137499997				
11	50	1	0.268	7851.71475	2104.2595530000003				
12	60	1	0.291	11306.81475	3290.2830922499998				
13	70	1	0.209	15390.11475	3216.53398275				
14	80	1	0.0923	20101.61475	1855.379041425				
15	90	1	0.1125	25441.31475	2862.1479093750004				
16	100	1	0.0986	31409.21475	3096.9485743499995				

AL_VES95

Date:05/05/2025		VES95							
Latitude	29.61317	Longitude	79.722189	Area	Bataldeon	Elevation (m)	1396.0	Direction	170°SE
S.N	Current Electrode Spacing (AB/2)	Potential Electrode Spacing (MN)	Resistance (Ohm)	K value	Aparent Resistivity (Rho_a)				
1	2.5	1	299	18.846	5634.954				
2	5	1	102.7	77.73975	7983.872325				
3	10	1	32	313.31475	10026.072				
4	15	1	15	705.93975	10589.09625				
5	20	1	9.04	1255.61475	11350.757339999998				

6	25	1	5.78	1962.33975	11342.323755000001				
7	30	1	3.44	2826.11475	9721.83474				
8	35	1	2.08	3846.93975	8001.63468				
9	40	1	1.26	5024.8147500000005	6331.266585				
10	45	1	0.965	6359.73975	6137.14885875				
11	50	1	0.764	7851.71475	5998.710069				
12	60	1		11306.81475	0				
13	70	1		15390.11475	0				
14	80	1		20101.61475	0				
15	90	1		25441.31475	0				
16	100	1		31409.21475	0				

AL_VES96

Date:05/05/2025		VES96							
Latitude	**29.628757**	**Longitude**	**79.721063**	**Area**	**Bataldeon**	**Elevation (m)**	**1476.0**	**Direction**	**0°N**
S.N	**Current Electrode Spacing (AB/2)**	**Potential Electrode Spacing (MN)**	**Resistance (Ohm)**	**K value**	**Aparent Resistivity (Rho_a)**				
1	2.5	1	130	18.846	2449.98				
2	5	1	19.9	77.73975	1547.021025				
3	10	1	5.54	313.31475	1735.763715				
4	15	1	2.29	705.93975	1616.6020275				
5	20	1	1.24	1255.61475	1556.96229				
6	25	1	0.803	1962.33975	1575.7588192500002				
7	30	1	0.514	2826.11475	1452.6229815000002				
8	35	1	0.317	3846.93975	1219.47990075				
9	40	1	0.231	5024.8147500000005	1160.73220725				
10	45	1	0.173	6359.73975	1100.2349767499998				
11	50	1	0.149	7851.71475	1169.90549775				
12	60	1	0.107	11306.81475	1209.82917825				
13	70	1	0.0939	15390.11475	1445.131775025				
14	80	1	0.0837	20101.61475	1682.505154575				
15	90	1	0.0393	25441.31475	999.8436696750001				
16	100	1	0.0683	31409.21475	2145.249367425				

AL_VES97

Date:07/05/2025		**VES97**							
Latitude	**29.609274**	**Longitude**	**79.711866**	**Area**	**Sirar**	**Elevation (m)**	**1458.0**	**Direction**	**10°N**
S.N	**Current Electrode**	**Potential Electrode**	**Resistance (Ohm)**	**K value**	**Aparent Resistivity (Rho_a)**				

	Spacing (AB/2)	Spacing (MN)							
1	2.5	1	248	18.846	4673.808				
2	5	1	100.1	77.73975	7781.7489749999995				
3	10	1	52.5	313.31475	16449.024375				
4	15	1	25.3	705.93975	17860.275675				
5	20	1	29.7	1255.61475	37291.758075				
6	25	1	7	1962.33975	13736.378250000002				
7	30	1	0.21	2826.11475	593.4840975				
8	35	1	4.56	3846.93975	17542.04526				
9	40	1	0.248	5024.8147500000005	1246.154058				
10	45	1	0.501	6359.73975	3186.2296147499997				
11	50	1	0.703	7851.71475	5519.75546925				
12	60	1	0.789	11306.81475	8921.07683775				
13	70	1	0.226	15390.11475	3478.1659335000004				
14	80	1	0.114	20101.61475	2291.5840815				
15	90	1	0.269	25441.31475	6843.713667750001				
16	100	1	0.0521	31409.21475	1636.420088475				

AL_VES98

Date:07/05/2025		VES98							
Latitude	29.611447	Longitude	79.712296	Area	Sirar	Elevation (m)	1457.0	Direction	10°N
S.N	Current Electrode Spacing (AB/2)	Potential Electrode Spacing (MN)	Resistance (Ohm)	K value	Aparent Resistivity (Rho_a)				
1	2.5	1	42.1	18.846	793.4166				
2	5	1	13.5	77.73975	1049.486625				
3	10	1	3.75	313.31475	1174.9303125000001				
4	15	1	1.5	705.93975	1058.909625				
5	20	1	0.712	1255.61475	893.9977019999999				
6	25	1	0.362	1962.33975	710.3669895				
7	30	1	0.208	2826.11475	587.831868				
8	35	1	0.136	3846.93975	523.183806				
9	40	1	0.103	5024.8147500000005	517.55591925				
10	45	1	0.082	6359.73975	521.4986595				
11	50	1	0.0698	7851.71475	548.04968955				
12	60	1	0.05	11306.81475	565.3407375				
13	70	1	0.0394	15390.11475	606.37052115				
14	80	1	0.0389	20101.61475	781.952813775				
15	90	1	0.0369	25441.31475	938.7845142750001				
16	100	1	0.0158	31409.21475	496.26559305000006				

AL_VES99

Date:07/05/2025		VES99							
Latitude	29.607795	Longitude	79.711306	Area	Sirar	Elevation (m)	1602.0	Direction	10°N
S.N	Current Electrode Spacing (AB/2)	Potential Electrode Spacing (MN)	Resistance (Ohm)	K value	Aparent Resistivity (Rho_a)				
1	2.5	1	85.3	18.846	1607.5638				
2	5	1	18.5	77.73975	1438.185375				
3	10	1	2.51	313.31475	786.4200225				
4	15	1	1.095	705.93975	773.00402625				
5	20	1	0.737	1255.61475	925.38807075				
6	25	1	0.546	1962.33975	1071.4375035				
7	30	1	0.402	2826.11475	1136.0981295000001				
8	35	1	0.277	3846.93975	1065.60231075				
9	40	1	0.158	5024.8147500000005	793.9207305000001				
10	45	1	0.121	6359.73975	769.5285097499999				
11	50	1	0.0829	7851.71475	650.907152775				
12	60	1	0.0516	11306.81475	583.4316411				
13	70	1	0.0495	15390.11475	761.8106801250001				
14	80	1	0.0324	20101.61475	651.2923179				
15	90	1	0.034	25441.31475	865.0047015000001				
16	100	1	0.0177	31409.21475	555.943101075				

AL_VES100

Date:08/05/2025		VES100							
Latitude	29.600162	Longitude	79.729779	Area	Pithauni	Elevation (m)	1274.0	Direction	90°E
S.N	Current Electrode Spacing (AB/2)	Potential Electrode Spacing (MN)	Resistance (Ohm)	K value	Aparent Resistivity (Rho_a)				
1	2.5	1	270	18.846	5088.42				
2	5	1	59.7	77.73975	4641.063075				
3	10	1	7.95	313.31475	2490.8522625				
4	15	1	2.49	705.93975	1757.7899775				
5	20	1	0.831	1255.61475	1043.4158572499998				
6	25	1	0.5	1962.33975	981.169875				
7	30	1	0.231	2826.11475	652.83250725				
8	35	1	0.196	3846.93975	754.0001910000001				
9	40	1	0.143	5024.8147500000005	718.54850925				
10	45	1	0.151	6359.73975	960.32070225				

11	50	1	0.0982	7851.71475	771.03838845				
12	60	1	0.0675	11306.81475	763.209995625				
13	70	1	0.0897	15390.11475	1380.493293075				
14	80	1	0.0324	20101.61475	651.2923179				
15	90	1	0.0666	25441.31475	1694.3915623500002				
16	100	1	0.0427	31409.21475	1341.173469825				

AL_VES101

Date:08/05/2025		VES101							
Latitude	29.600105	Longitude	79.732096	Area	Pithauni	Elevation (m)	1266.0	Direction	90°E
S.N	Current Electrode Spacing (AB/2)	Potential Electrode Spacing (MN)	Resistance (Ohm)	K value	Aparent Resistivity (Rho_a)				
1	2.5	1	78.6	18.846	1481.2956				
2	5	1	17.7	77.73975	1375.993575				
3	10	1	3.22	313.31475	1008.873495				
4	15	1	1.49	705.93975	1051.8502275				
5	20	1	0.868	1255.61475	1089.873603				
6	25	1	0.524	1962.33975	1028.2660290000001				
7	30	1	0.359	2826.11475	1014.57519525				
8	35	1	0.237	3846.93975	911.72472075				
9	40	1	0.161	5024.8147500000005	808.99517475				
10	45	1	0.1152	6359.73975	732.6420191999999				
11	50	1	0.1008	7851.71475	791.4528468				
12	60	1	0.0837	11306.81475	946.380394575				
13	70	1	0.0521	15390.11475	801.8249784750001				
14	80	1	0.0384	20101.61475	771.9020064				
15	90	1	0.0248	25441.31475	630.9446058				
16	100	1	0.0171	31409.21475	537.097572225				

AL_VES102

Date:08/05/2025		VES102							
Latitude	29.600221	Longitude	79.727471	Area	Pithauni	Elevation (m)	1258.0	Direction	90°E
S.N	Current Electrode Spacing (AB/2)	Potential Electrode Spacing (MN)	Resistance (Ohm)	K value	Aparent Resistivity (Rho_a)				
1	2.5	1	7.33	18.846	138.14118				
2	5	1	0.432	77.73975	33.583572				
3	10	1	0.0384	313.31475	12.031286399999999				
4	15	1	0.0154	705.93975	10.87147215				

5	20	1	0.00853	1255.61475	10.710393817499998				
6	25	1	0.00512	1962.33975	10.047179520000002				
7	30	1	0.00426	2826.11475	12.039248835				
8	35	1	0.00256	3846.93975	9.84816576				
9	40	1	0.0017	5024.8147500000005	8.542185075				
10	45	1	0.0017	6359.73975	10.811557574999998				
11	50	1	0.00085	7851.71475	6.6739575375				
12	60	1	0.0018	11306.81475	20.35226655				
13	70	1	0.0017	15390.11475	26.163195075				
14	80	1	0.00505	20101.61475	101.5131544875				
15	90	1	0.00151	25441.31475	38.4163852725				
16	100	1	0.00202	31409.21475	63.446613795000005				

AL_VES103

Date:09/05/2025		VES103							
Latitude	29.655557	Longitude	79.7180102	Area	Batgal	Elevation (m)	1553.0	Direction	0°N
S.N	Current Electrode Spacing (AB/2)	Potential Electrode Spacing (MN)	Resistance (Ohm)	K value	Aparent Resistivity (Rho_a)				
1	2.5	1	27.6	18.846	520.1496000000001				
2	5	1	4.38	77.73975	340.500105				
3	10	1	0.927	313.31475	290.44277325				
4	15	1	0.369	705.93975	260.49176775				
5	20	1	0.2	1255.61475	251.12295				
6	25	1	0.127	1962.33975	249.21714825				
7	30	1	0.839	2826.11475	2371.11027525				
8	35	1	0.561	3846.93975	2158.13319975				
9	40	1	0.445	5024.8147500000005	2236.04256375				
10	45	1	0.389	6359.73975	2473.93876275				
11	50	1	0.313	7851.71475	2457.58671675				
12	60	1	0.268	11306.81475	3030.226353				
13	70	1	0.157	15390.11475	2416.24801575				
14	80	1	0.131	20101.61475	2633.3115322500003				
15	90	1	0.126	25441.31475	3205.6056585				
16	100	1	0.1112	31409.21475	3492.7046801999995				

AL_VES104

Date:09/05/2025		VES104							
Latitude	29.653382	Longitude	79.718303	Area	Batgal	Elevation (m)	1540.0	Direction	0°N
S.N	Current Electrode	Potential Electrode	Resistance (Ohm)	K value	Aparent Resistivity (Rho_a)				

	Spacing (AB/2)	Spacing (MN)							
1	2.5	1	192	18.846	3618.432				
2	5	1	34.8	77.73975	2705.3433				
3	10	1	4.65	313.31475	1456.9135875000002				
4	15	1	1.62	705.93975	1143.622395				
5	20	1	0.889	1255.61475	1116.24151275				
6	25	1	0.591	1962.33975	1159.74279225				
7	30	1	0.477	2826.11475	1348.0567357500001				
8	35	1	0.365	3846.93975	1404.13300875				
9	40	1	0.317	5024.8147500000005	1592.86627575				
10	45	1	0.265	6359.73975	1685.33103375				
11	50	1	0.255	7851.71475	2002.1872612500001				
12	60	1	0.153	11306.81475	1729.94265675				
13	70	1	0.0981	15390.11475	1509.7702569750002				
14	80	1	0.0526	20101.61475	1057.34493585				
15	90	1	0.0627	25441.31475	1595.1704348250003				
16	100	1	0.0688	31409.21475	2160.9539747999997				

AL_VES105

Date:09/05/2025		VES105							
Latitude	29.657678	Longitude	79.718173	Area	Batgal	Elevation (m)	1621.0	Direction	0°N
S.N	Current Electrode Spacing (AB/2)	Potential Electrode Spacing (MN)	Resistance (Ohm)	K value	Aparent Resistivity (Rho_a)				
1	2.5	1	150	18.846	2826.9				
2	5	1	34.8	77.73975	2705.3433				
3	10	1	3.4	313.31475	1065.27015				
4	15	1	0.765	705.93975	540.04390875				
5	20	1	0.364	1255.61475	457.043769				
6	25	1	0.0186	1962.33975	36.49951935				
7	30	1	0.106	2826.11475	299.5681635				
8	35	1	0.0743	3846.93975	285.827623425				
9	40	1	0.0541	5024.8147500000005	271.842477975				
10	45	1	0.0404	6359.73975	256.9334859				
11	50	1	0.0298	7851.71475	233.98109955				
12	60	1	0.0142	11306.81475	160.55676945				
13	70	1	0.0096	15390.11475	147.7451016				
14	80	1	0.00707	20101.61475	142.1184162825				
15	90	1	0.00404	25441.31475	102.78291159000001				
16	100	1	0.00353	31409.21475	110.87452806750001				

AL_VES106

Date:10/05/2025		VES106							
Latitude	29.626067	Longitude	79.743637	Area	Udalgaon	Elevation (m)	1547.0	Direction	0°N
S.N	Current Electrode Spacing (AB/2)	Potential Electrode Spacing (MN)	Resistance (Ohm)	K value	Aparent Resistivity (Rho_a)				
1	2.5	1	34.3	18.846	646.4177999999999				
2	5	1	8.95	77.73975	695.7707624999999				
3	10	1	2.78	313.31475	871.015005				
4	15	1	1.38	705.93975	974.1968549999999				
5	20	1	0.878	1255.61475	1102.4297505				
6	25	1	0.647	1962.33975	1269.63381825				
7	30	1	0.505	2826.11475	1427.18794875				
8	35	1	0.374	3846.93975	1438.7554665				
9	40	1	0.298	5024.8147500000005	1497.3947955				
10	45	1	0.208	6359.73975	1322.825868				
11	50	1	0.1059	7851.71475	831.4965920249999				
12	60	1	0.0657	11306.81475	742.857729075				
13	70	1	0.0521	15390.11475	801.8249784750001				
14	80	1	0.0401	20101.61475	806.074751475				
15	90	1	0.0273	25441.31475	694.5478926750001				
16	100	1	0.0222	31409.21475	697.28456745				

AL_VES107

Date:10/05/2025		VES107							
Latitude	29.627355	Longitude	79.744115	Area	Udalgaon	Elevation (m)	1515.0	Direction	0°N
S.N	Current Electrode Spacing (AB/2)	Potential Electrode Spacing (MN)	Resistance (Ohm)	K value	Aparent Resistivity (Rho_a)				
1	2.5	1	50.3	18.846	947.9538				
2	5	1	16	77.73975	1243.836				
3	10	1	4.51	313.31475	1413.0495225				
4	15	1	1.78	705.93975	1256.572755				
5	20	1	0.915	1255.61475	1148.88749625				
6	25	1	0.554	1962.33975	1087.1362215000001				
7	30	1	0.341	2826.11475	963.7051297500001				
8	35	1	0.208	3846.93975	800.163468				
9	40	1	0.145	5024.8147500000005	728.59813875				
10	45	1	0.082	6359.73975	521.4986595				
11	50	1	0.0615	7851.71475	482.880457125				
12	60	1	0.0657	11306.81475	742.857729075				

13	70	1	0.0316	15390.11475	486.3276261000001				
14	80	1		20101.61475	0				
15	90	1		25441.31475	0				
16	100	1		31409.21475	0				

AL_VES108

Date:10/05/2025		VES108							
Latitude	29.624357	Longitude	79.743788	Area	Udalgaon	Elevation (m)	1605.0	Direction	0°N
S.N	Current Electrode Spacing (AB/2)	Potential Electrode Spacing (MN)	Resistance (Ohm)	K value	Aparent Resistivity (Rho_a)				
1	2.5	1	155	18.846	2921.13				
2	5	1	39.2	77.73975	3047.3982				
3	10	1	10.09	313.31475	3161.3458275				
4	15	1	3.46	705.93975	2442.551535				
5	20	1	1.21	1255.61475	1519.2938474999999				
6	25	1	0.443	1962.33975	869.3165092500001				
7	30	1	0.194	2826.11475	548.2662615				
8	35	1	0.394	3846.93975	1515.6942615				
9	40	1	0.0824	5024.8147500000005	414.04473540000004				
10	45	1	0.0495	6359.73975	314.807117625				
11	50	1	0.01098	7851.71475	86.211827955				
12	60	1	-0.1152	11306.81475	-1302.5450592				
13	70	1	-0.169	15390.11475	-2600.9293927500003				

AL_VES109

Date:11/05/2025		VES109							
Latitude	29.638306	Longitude	79.702035	Area	Barakot	Elevation (m)	1517.0	Direction	0°N
S.N	Current Electrode Spacing (AB/2)	Potential Electrode Spacing (MN)	Resistance (Ohm)	K value	Aparent Resistivity (Rho_a)				
1	2.5	1	64	18.846	1206.144				
2	5	1	16.7	77.73975	1298.253825				
3	10	1	2.41	313.31475	755.0885475				
4	15	1	0.438	705.93975	309.2016105				
5	20	1	0.214	1255.61475	268.7015565				
6	25	1	0.131	1962.33975	257.06650725000003				
7	30	1	0.0819	2826.11475	231.45879802500002				
8	35	1	0.0612	3846.93975	235.4327127				
9	40	1	0.0475	5024.8147500000005	238.67870062500003				

10	45	1	0.0404	6359.73975	256.9334859				
11	50	1	0.0339	7851.71475	266.173130025				
12	60	1	0.0233	11306.81475	263.448783675				
13	70	1	0.00909	15390.11475	139.89614307750003				
14	80	1	0.01011	20101.61475	203.2273251225				
15	90	1	0.00404	25441.31475	102.78291159000001				
16	100	1	0.0129	31409.21475	405.178870275				

AL_VES110

Date:11/05/2025		VES110							
Latitude	29.639959	Longitude	79.702231	Area	Barakot	Elevation (m)	1499.0	Direction	0°N
S.N	Current Electrode Spacing (AB/2)	Potential Electrode Spacing (MN)	Resistance (Ohm)	K value	Aparent Resistivity (Rho_a)				
1	2.5	1	84.5	18.846	1592.487				
2	5	1	17.3	77.73975	1344.8976750000002				
3	10	1	2.73	313.31475	855.3492675				
4	15	1	1.017	705.93975	717.94072575				
5	20	1	0.374	1255.61475	469.5999165				
6	25	1	0.186	1962.33975	364.9951935				
7	30	1	0.121	2826.11475	341.95988475				
8	35	1	0.0779	3846.93975	299.676606525				
9	40	1	0.0576	5024.8147500000005	289.4293296				
10	45	1	0.0197	6359.73975	125.28687307499999				
11	50	1	-0.00939	7851.71475	-73.72760150250001				
12	60	1	-0.0632	11306.81475	-714.5906922				
13	70	1	-0.0401	15390.11475	-617.143601475				
14	80	1	-0.0546	20101.61475	-1097.54816535				
15	90	1	0.0307	25441.31475	781.048362825				
16	100	1	0.0307	31409.21475	964.262892825				

AL_VES111

Date:11/05/2025		VES111							
Latitude	29.636416	Longitude	79.702035	Area	Barakot	Elevation (m)	1535.0	Direction	0°N
S.N	Current Electrode Spacing (AB/2)	Potential Electrode Spacing (MN)	Resistance (Ohm)	K value	Aparent Resistivity (Rho_a)				
1	2.5	1	92.4	18.846	1741.3704				
2	5	1	15.1	77.73975	1173.870225				
3	10	1	2.25	313.31475	704.9581875				

4	15	1	1.153	705.93975	813.94853175				
5	20	1	0.657	1255.61475	824.93889075				
6	25	1	0.447	1962.33975	877.16586825				
7	30	1	0.3095	2826.11475	874.682515125				
8	35	1	0.2475	3846.93975	952.117588125				
9	40	1	0.201	5024.8147500000005	1009.9877647500001				
10	45	1	0.1705	6359.73975	1084.335627375				
11	50	1	0.142	7851.71475	1114.9434944999998				
12	60	1	0.1036	11306.81475	1171.3860081				
13	70	1	0.0817	15390.11475	1257.372375075				
14	80	1	0.0666	20101.61475	1338.7675423500002				
15	90	1	0.0551	25441.31475	1401.8164427250001				
16	100	1	0.0463	31409.21475	1454.246642925				

AL_VES112

Date:12/05/2025		VES112							
Latitude	29.643035	Longitude	79.721267	Area	Deora	Elevation (m)	1453.0	Direction	90°E
S.N	Current Electrode Spacing (AB/2)	Potential Electrode Spacing (MN)	Resistance (Ohm)	K value	Aparent Resistivity (Rho_a)				
1	2.5	1	76.4	18.846	1439.8344000000002				
2	5	1	15.7	77.73975	1220.514075				
3	10	1	2.78	313.31475	871.015005				
4	15	1	0.748	705.93975	528.042933				
5	20	1	0.402	1255.61475	504.7571295				
6	25	1	0.259	1962.33975	508.24599525				
7	30	1	0.199	2826.11475	562.3968352500001				
8	35	1	0.144	3846.93975	553.9593239999999				
9	40	1	0.118	5024.8147500000005	592.9281405				
10	45	1	0.1057	6359.73975	672.224491575				
11	50	1	0.0925	7851.71475	726.283614375				
12	60	1	0.0837	11306.81475	946.380394575				
13	70	1	0.0435	15390.11475	669.469991625				
14	80	1	0.0316	20101.61475	635.2110261				
15	90	1	0.0171	25441.31475	435.04648222500003				
16	100	1	0.00597	31409.21475	187.5130120575				

AL_VES113

Date:12/05/2025		VES113							
Latitude	29.642916	Longitude	79.723764	Area	Deora	Elevation (m)	1406.0	Direction	90°E

S.N	Current Electrode Spacing (AB/2)	Potential Electrode Spacing (MN)	Resistance (Ohm)	K value	Aparent Resistivity (Rho_a)				
1	2.5	1	129	18.846	2431.134				
2	5	1	24	77.73975	1865.754				
3	10	1	5.54	313.31475	1735.763715				
4	15	1	1.57	705.93975	1108.3254075				
5	20	1	0.789	1255.61475	990.68003775				
6	25	1	0.555	1962.33975	1089.09856125				
7	30	1	0.39	2826.11475	1102.1847525				
8	35	1	0.27	3846.93975	1038.6737325000001				
9	40	1	0.216	5024.8147500000005	1085.3599860000002				
10	45	1	0.169	6359.73975	1074.79601775				
11	50	1	0.138	7851.71475	1083.5366355				
12	60	1	0.119	11306.81475	1345.5109552499998				
13	70	1	0.0667	15390.11475	1026.520653825				
14	80	1	0.0667	20101.61475	1340.777703825				
15	90	1	0.0475	25441.31475	1208.462450625				
16	100	1	0.0303	31409.21475	951.699206925				

AL_VES114

Date:13/05/2025		VES114							
Latitude	29.641722	Longitude	79.665775	Area	Mat	Elevation (m)	1783.0	Direction	0°N
S.N	Current Electrode Spacing (AB/2)	Potential Electrode Spacing (MN)	Resistance (Ohm)	K value	Aparent Resistivity (Rho_a)				
1	2.5	1	230	18.846	4334.58				
2	5	1	38.4	77.73975	2985.2064				
3	10	1	2.5	313.31475	783.286875				
4	15	1	0.493	705.93975	348.02829675				
5	20	1	0.221	1255.61475	277.49085974999997				
6	25	1	0.145	1962.33975	284.53926375				
7	30	1	0.0956	2826.11475	270.17657010000005				
8	35	1	0.0726	3846.93975	279.28782585				
9	40	1	0.0692	5024.8147500000005	347.71718070000003				
10	45	1	0.0512	6359.73975	325.6186752				
11	50	1	0.0572	7851.71475	449.1180837				
12	60	1	0.0246	11306.81475	278.14764285				
13	70	1	0.0273	15390.11475	420.15013267500007				
14	80	1	0.0512	20101.61475	1029.2026752000002				
15	90	1	0.0412	25441.31475	1048.1821677				
16	100	1	0.0538	31409.21475	1689.81575355				

AL_VES115

Date:13/05/2025		VES115							
Latitude	29.640207	Longitude	79.665642	Area	Mat	Elevation (m)	1795.0	Direction	0°N
S.N	Current Electrode Spacing (AB/2)	Potential Electrode Spacing (MN)	Resistance (Ohm)	K value	Aparent Resistivity (Rho_a)				
1	2.5	1	66.6	18.846	1255.1435999999999				
2	5	1	9.02	77.73975	701.212545				
3	10	1	1.104	313.31475	345.89948400000003				
4	15	1	0.371	705.93975	261.90364725				
5	20	1	0.157	1255.61475	197.13151575				
6	25	1	0.0488	1962.33975	95.76217980000001				
7	30	1	0.0455	2826.11475	128.58822112500002				
8	35	1	0.0274	3846.93975	105.40614915				
9	40	1	0.0294	5024.8147500000005	147.72955365				
10	45	1	0.0143	6359.73975	90.944278425				
11	50	1	0.01056	7851.71475	82.91410776000001				
12	60	1	0.01156	11306.81475	130.70677851				
13	70	1	0.00729	15390.11475	112.1939365275				
14	80	1	0.0121	20101.61475	243.229538475				

AL_VES116

Date:13/05/2025		VES116							
Latitude	29.643973	Longitude	79.665699	Area	Mat	Elevation (m)	1771.0	Direction	0°N
S.N	Current Electrode Spacing (AB/2)	Potential Electrode Spacing (MN)	Resistance (Ohm)	K value	Aparent Resistivity (Rho_a)				
1	2.5	1	115.3	18.846	2172.9438				
2	5	1	27.9	77.73975	2168.939025				
3	10	1	5.72	313.31475	1792.1603699999998				
4	15	1	2.46	705.93975	1736.611785				
5	20	1	1.21	1255.61475	1519.2938474999999				
6	25	1	0.458	1962.33975	898.7516055000001				
7	30	1	0.265	2826.11475	748.9204087500001				
8	35	1	0.216	3846.93975	830.938986				
9	40	1	0.163	5024.8147500000005	819.0448042500001				
10	45	1	0.124	6359.73975	788.607729				
11	50	1	0.166	7851.71475	1303.3846485000001				
12	60	1	0.161	11306.81475	1820.39717475				

13	70	1	0.141	15390.11475	2170.00617975				
14	80	1	0.186	20101.61475	3738.9003435				
15	90	1	0.196	25441.31475	4986.4976910000005				
16	100	1	0.128	31409.21475	4020.379488				

AL_VES117

Date:14/05/2025		VES117							
Latitude	29.603313	Longitude	79.689033	Area	Phalshima	Elevation (m)	1481.0	Direction	140°SE
S.N	Current Electrode Spacing (AB/2)	Potential Electrode Spacing (MN)	Resistance (Ohm)	K value	Aparent Resistivity (Rho_a)				
1	2.5	1	21.8	18.846	410.8428				
2	5	1	1.54	77.73975	119.719215				
3	10	1	0.189	313.31475	59.21648775				
4	15	1	0.0727	705.93975	51.321819825				
5	20	1	0.0367	1255.61475	46.081061325				
6	25	1	0.0154	1962.33975	30.22003215				
7	30	1	0.0137	2826.11475	38.717772075000006				
8	35	1	0.01024	3846.93975	39.39266304				
9	40	1	0.00728	5024.8147500000005	36.580651380000006				
10	45	1	0.0111	6359.73975	70.593111225				
11	50	1	0.00597	7851.71475	46.8747370575				
12	60	1	0.01024	11306.81475	115.78178304000001				
13	70	1	0.00939	15390.11475	144.5131775025				
14	80	1	0.0128	20101.61475	257.30066880000004				
15	90	1	0.0171	25441.31475	435.04648222500003				
16	100	1	0.00426	31409.21475	133.803254835				

AL_VES118

Date:14/05/2025		VES118							
Latitude	29.602123	Longitude	79.690509	Area	Phalshima	Elevation (m)	1555.0	Direction	140°SE
S.N	Current Electrode Spacing (AB/2)	Potential Electrode Spacing (MN)	Resistance (Ohm)	K value	Aparent Resistivity (Rho_a)				
1	2.5	1	34	18.846	640.764				
2	5	1	6.47	77.73975	502.9761825				
3	10	1	1.64	313.31475	513.83619				
4	15	1	0.788	705.93975	556.280523				
5	20	1	0.433	1255.61475	543.6811867499999				
6	25	1	0.219	1962.33975	429.75240525000004				

7	30	1	0.157	2826.11475	443.70001575000003				
8	35	1	0.0999	3846.93975	384.309281025				
9	40	1	0.0803	5024.8147500000005	403.49262442500003				
10	45	1	0.0709	6359.73975	450.905548275				
11	50	1	0.0666	7851.71475	522.9242023500001				
12	60	1	0.0564	11306.81475	637.7043519				
13	70	1	0.0472	15390.11475	726.4134162				
14	80	1	0.0973	20101.61475	1955.887115175				
15	90	1	0.0675	25441.31475	1717.2887456250003				
16	100	1	0.0649	31409.21475	2038.458037275				

AL_VES119

Date:14/05/2025		VES119							
Latitude	29.604893	Longitude	687617	Area	Phalshima	Elevation (m)	1570.0	Direction	140°SE
S.N	Current Electrode Spacing (AB/2)	Potential Electrode Spacing (MN)	Resistance (Ohm)	K value	Aparent Resistivity (Rho_a)				
1	2.5	1	169	18.846	3184.974				
2	5	1	16.7	77.73975	1298.253825				
3	10	1	1.8	313.31475	563.96655				
4	15	1	0.803	705.93975	566.86961925				
5	20	1	0.407	1255.61475	511.03520324999994				
6	25	1	0.258	1962.33975	506.28365550000007				
7	30	1	0.251	2826.11475	709.35480225				
8	35	1	0.175	3846.93975	673.21445625				
9	40	1	0.138	5024.8147500000005	693.4244355000001				
10	45	1	0.00342	6359.73975	21.750309944999998				
11	50	1	-0.00462	7851.71475	-36.274922145				
12	60	1	0.0453	11306.81475	512.198708175				
13	70	1	0.0512	15390.11475	787.9738752000001				
14	80	1	0.0526	20101.61475	1057.34493585				
15	90	1	0.0897	25441.31475	2282.085933075				
16	100	1	0.0957	31409.21475	3005.8618515749995				

AL_VES120

Date:15/05/2025		VES120							
Latitude	29.612882	Longitude	79.727792	Area	Bataldeon	Elevation (m)	1287.0	Direction	160°SE
S.N	Current Electrode Spacing (AB/2)	Potential Electrode Spacing (MN)	Resistance (Ohm)	K value	Aparent Resistivity (Rho_a)				

1	2.5	1	20.2	18.846	380.68919999999997				
2	5	1	3.59	77.73975	279.08570249999997				
3	10	1	0.883	313.31475	276.65692425000003				
4	15	1	0.548	705.93975	386.854983				
5	20	1	0.358	1255.61475	449.51008049999996				
6	25	1	0.262	1962.33975	514.1330145000001				
7	30	1	0.193	2826.11475	545.44014675				
8	35	1	0.142	3846.93975	546.2654445				
9	40	1	0.1187	5024.8147500000005	596.445510825				
10	45	1	0.0965	6359.73975	613.7148858749999				
11	50	1	0.0811	7851.71475	636.7740662250001				
12	60	1	0.0521	11306.81475	589.085048475				
13	70	1	0.0361	15390.11475	555.583142475				
14	80	1	0.0134	20101.61475	269.36163765000003				
15	90	1	0.01195	25441.31475	304.02371126250006				
16	100	1		31409.21475	0				

AL_VES121

Date:15/05/2025		VES121							
Latitude	29.614697	Longitude	79.726623	Area	Bajyoli	Elevation (m)	1294.0	Direction	160°SE
S.N	Current Electrode Spacing (AB/2)	Potential Electrode Spacing (MN)	Resistance (Ohm)	K value	Aparent Resistivity (Rho_a)				
1	2.5	1	50.6	18.846	953.6076				
2	5	1	19.9	77.73975	1547.021025				
3	10	1	4.02	313.31475	1259.525295				
4	15	1	0.759	705.93975	535.80827025				
5	20	1	0.123	1255.61475	154.44061424999998				
6	25	1	0.0601	1962.33975	117.936618975				
7	30	1	0.00298	2826.11475	8.421821955				
8	35	1	0.00192	3846.93975	7.38612432				
9	40	1	0.00131	5024.8147500000005	6.582507322500001				
10	45	1	0.00606	6359.73975	38.540022885				
11	50	1	0.00404	7851.71475	31.720927590000002				
12	60	1	0.00404	11306.81475	45.67953159				
13	70	1	0.00252	15390.11475	38.783089170000004				

AL_VES122

Date:16/05/2025		VES122							
Latitude	29.617878	Longitude	79.727395	Area	Bajyoli	Elevation (m)	1355.0	Direction	160°SE

S.N	Current Electrode Spacing (AB/2)	Potential Electrode Spacing (MN)	Resistance (Ohm)	K value	Aparent Resistivity (Rho_a)				
1	2.5	1	80.4	18.846	1515.2184000000002				
2	5	1	15.8	77.73975	1228.28805				
3	10	1	2.66	313.31475	833.417235				
4	15	1	0.792	705.93975	559.104282				
5	20	1	0.388	1255.61475	487.178523				
6	25	1	0.208	1962.33975	408.166668				
7	30	1	0.147	2826.11475	415.43886825				
8	35	1	0.108	3846.93975	415.469493				
9	40	1	0.0784	5024.8147500000005	393.9454764				
10	45	1	0.0627	6359.73975	398.755682325				
11	50	1	0.0531	7851.71475	416.92605322500003				
12	60	1	0.0427	11306.81475	482.800989825				
13	70	1	0.035	15390.11475	538.65401625				
14	80	1	0.031	20101.61475	623.15005725				
15	90	1	0.0275	25441.31475	699.636155625				
16	100	1	0.0282	31409.21475	885.73985595				

AL_VES123

Date:16/05/2025		VES123							
Latitude	29.619768	Longitude	79.727395	Area	Bajyoli	Elevation (m)	1350.0	Direction	160°SE
S.N	Current Electrode Spacing (AB/2)	Potential Electrode Spacing (MN)	Resistance (Ohm)	K value	Aparent Resistivity (Rho_a)				
1	2.5	1	67.8	18.846	1277.7588				
2	5	1	10.67	77.73975	829.4831325				
3	10	1	2.05	313.31475	642.2952375				
4	15	1	0.954	705.93975	673.4665215				
5	20	1	0.658	1255.61475	826.1945055				
6	25	1	0.469	1962.33975	920.33734275				
7	30	1	0.379	2826.11475	1071.0974902500002				
8	35	1	0.276	3846.93975	1061.7553710000002				
9	40	1	0.23	5024.8147500000005	1155.7073925000002				
11	50	1	0.164	7851.71475	1287.681219				
12	60	1	0.132	11306.81475	1492.4995470000001				
13	70	1	0.105	15390.11475	1615.96204875				
14	80	1	0.082	20101.61475	1648.3324095				
15	90	1	0.0504	25441.31475	1282.2422634000002				
16	100	1	0.041	31409.21475	1287.77780475				

AL_VES124

Date:16/05/2025		VES124							
Latitude	29.616246	Longitude	79.729065	Area	Bajyoli	Elevation (m)	1328.0	Direction	160°SE
S.N	Current Electrode Spacing (AB/2)	Potential Electrode Spacing (MN)	Resistance (Ohm)	K value	Aparent Resistivity (Rho_a)				
1	2.5	1	60.8	18.846	1145.8368				
2	5	1	9.29	77.73975	722.2022774999999				
3	10	1	1.62	313.31475	507.56989500000003				
4	15	1	0.711	705.93975	501.92316224999996				
5	20	1	0.478	1255.61475	600.1838505				
6	25	1	0.326	1962.33975	639.7227585				
7	30	1	0.224	2826.11475	633.049704				
8	35	1	0.161	3846.93975	619.35729975				
9	40	1	0.125	5024.8147500000005	628.1018437500001				
10	45	1	0.0981	6359.73975	623.890469475				
11	50	1	0.0789	7851.71475	619.500293775				
12	60	1	0.0546	11306.81475	617.35208535				
13	70	1	0.0394	15390.11475	606.37052115				

AL_VES125

Date:17/05/2025		VES125							
Latitude	29.639482	Longitude	79.721326	Area	Digoli	Elevation (m)	1381.0	Direction	280°NW
S.N	Current Electrode Spacing (AB/2)	Potential Electrode Spacing (MN)	Resistance (Ohm)	K value	Aparent Resistivity (Rho_a)				
1	2.5	1	148	18.846	2789.208				
2	5	1	18.7	77.73975	1453.733325				
3	10	1	3.99	313.31475	1250.1258525				
4	15	1	1.88	705.93975	1327.16673				
5	20	1	1.42	1255.61475	1782.9729449999998				
6	25	1	1.35	1962.33975	2649.1586625000004				
7	30	1	0.951	2826.11475	2687.63512725				
8	35	1	1.84	3846.93975	7078.369140000001				
9	40	1	1.085	5024.8147500000005	5451.92400375				
10	45	1	0.879	6359.73975	5590.21124025				
11	50	1	0.734	7851.71475	5763.1586265				
12	60	1	0.556	11306.81475	6286.589001				
13	70	1	0.513	15390.11475	7895.12886675				
14	80	1	0.699	20101.61475	14051.028710249999				

15	90	1	0.874	25441.31475	22235.7090915				
16	100	1	0.148	31409.21475	4648.563783				

AL_VES126

Date:17/05/2025		VES126							
Latitude	29.638806	Longitude	79.721018	Area	Digoli	Elevation (m)	1358.0	Direction	280°NW
S.N	Current Electrode Spacing (AB/2)	Potential Electrode Spacing (MN)	Resistance (Ohm)	K value	Aparent Resistivity (Rho_a)				
1	2.5	1	167	18.846	3147.282				
2	5	1	18.6	77.73975	1445.95935				
3	10	1	3.35	313.31475	1049.6044125				
4	15	1	1.62	705.93975	1143.622395				
5	20	1	0.961	1255.61475	1206.6457747499999				
6	25	1	0.778	1962.33975	1526.7003255000002				
7	30	1	0.662	2826.11475	1870.8879645000002				
8	35	1	0.237	3846.93975	911.72472075				
9	40	1	0.266	5024.8147500000005	1336.6007235000002				
10	45	1	0.183	6359.73975	1163.83237425				
11	50	1	0.272	7851.71475	2135.666412				
12	60	1	0.268	11306.81475	3030.226353				
13	70	1	0.333	15390.11475	5124.90821175				
14	80	1	0.132	20101.61475	2653.413147				
15	90	1	0.119	25441.31475	3027.51645525				
16	100	1	0.0888	31409.21475	2789.1382698				

AL_VES127

Date:17/05/2025		VES127							
Latitude	29.639989	Longitude	79.719518	Area	Digoli	Elevation (m)	1377.0	Direction	280°NW
S.N	Current Electrode Spacing (AB/2)	Potential Electrode Spacing (MN)	Resistance (Ohm)	K value	Aparent Resistivity (Rho_a)				
1	2.5	1	180	18.846	3392.28				
2	5	1	26.7	77.73975	2075.651325				
3	10	1	2.47	313.31475	773.8874325				
4	15	1	1.073	705.93975	757.47335175				
5	20	1	0.638	1255.61475	801.0822105				
6	25	1	0.439	1962.33975	861.46715025				
7	30	1	0.365	2826.11475	1031.5318837500001				
8	35	1	0.275	3846.93975	1057.9084312500001				

9	40	1	0.242	5024.8147500000005	1216.0051695				
10	45	1	0.188	6359.73975	1195.631073				
11	50	1	0.176	7851.71475	1381.9017959999999				
12	60	1	0.0997	11306.81475	1127.2894305749999				
13	70	1	0.0931	15390.11475	1534.394440575				
14	80	1		20101.61475	1871.460333225				
15	90	1		25441.31475	0				
16	100	1		31409.21475	0				

AL_VES128

Date:19/05/2025		VES128							
Latitude	29.615051	Longitude	79.714551	Area	Sirar	Elevation (m)	1526.0	Direction	0°N
S.N	Current Electrode Spacing (AB/2)	Potential Electrode Spacing (MN)	Resistance (Ohm)	K value	Aparent Resistivity (Rho_a)				
1	2.5	1	89.1	18.846	1679.1786				
2	5	1	20.3	77.73975	1578.116925				
3	10	1	5.51	313.31475	1726.3642725				
4	15	1	2.46	705.93975	1736.611785				
5	20	1	1.32	1255.61475	1657.41147				
6	25	1	0.836	1962.33975	1640.516031				
7	30	1	0.575	2826.11475	1625.0159812499999				
8	35	1	0.428	3846.93975	1646.490213				
9	40	1	0.357	5024.8147500000005	1793.8588657500002				
10	45	1	0.265	6359.73975	1685.33103375				
11	50	1	0.215	7851.71475	1688.11867125				
12	60	1	0.125	11306.81475	1413.35184375				
13	70	1	0.088	15390.11475	1354.330098				
14	80	1	0.089	20101.61475	1789.04371275				
15	90	1	0.0627	25441.31475	1595.1704348250003				
16	100	1	0.156	31409.21475	4899.837501				

AL_VES129

Date:19/05/2025		VES129							
Latitude	29.61692	Longitude	79.714567	Area	Sirar	Elevation (m)	1533.0	Direction	0°N
S.N	Current Electrode Spacing (AB/2)	Potential Electrode Spacing (MN)	Resistance (Ohm)	K value	Aparent Resistivity (Rho_a)				
1	2.5	1	26.7	18.846	503.1882				
2	5	1	5.16	77.73975	401.13711				

3	10	1	0.63	313.31475	197.3882925				
4	15	1	0.219	705.93975	154.60080525				
5	20	1	0.143	1255.61475	179.55290924999997				
6	25	1	0.0976	1962.33975	191.52435960000003				
7	30	1	0.0753	2826.11475	212.80644067500003				
8	35	1	0.0602	3846.93975	231.58577294999998				
9	40	1	0.0465	5024.8147500000005	233.65388587500001				
10	45	1	0.0344	6359.73975	218.77504739999998				
11	50	1	0.0253	7851.71475	198.648383175				
12	60	1	0.0136	11306.81475	153.77268059999997				
13	70	1	0.01112	15390.11475	171.13807602				
14	80	1	0.00909	20101.61475	182.7236780775				
15	90	1	0.00859	25441.31475	218.54089370250003				
16	100	1	0.00707	31409.21475	222.06314828249998				

AL_VES130

Date:19/05/2025		VES130							
Latitude	29.618933	Longitude	79.714647	Area		Elevation (m)	1498.0	Direction	0°N
S.N	Current Electrode Spacing (AB/2)	Potential Electrode Spacing (MN)	Resistance (Ohm)	K value	Aparent Resistivity (Rho_a)				
1	2.5	1	75.3	18.846	1419.1037999999999				
2	5	1	17.1	77.73975	1329.349725				
3	10	1	2.55	313.31475	798.9526125				
4	15	1	0.926	705.93975	653.7002085				
5	20	1	0.506	1255.61475	635.3410635				
6	25	1	0.348	1962.33975	682.894233				
7	30	1	0.292	2826.11475	825.225507				
8	35	1	0.243	3846.93975	934.80635925				
9	40	1	0.205	5024.8147500000005	1030.08702375				
10	45	1	0.149	6359.73975	947.6012227499999				
11	50	1	0.1027	7851.71475	806.371104825				
12	60	1	0.0875	11306.81475	989.3462906249999				
13	70	1	0.0797	15390.11475	1226.592145575				
14	80	1	0.0555	20101.61475	1115.6396186250001				
15	90	1	0.0393	25441.31475	999.8436696750001				
16	100	1	0.0237	31409.21475	744.3983895749999				

AL_VES131

Date:12/05/2025		VES131							
Latitude	29.620917	Longitude	79.714201	Area		Elevation (m)	1484.0	Direction	0°N

S.N	Current Electrode Spacing (AB/2)	Potential Electrode Spacing (MN)	Resistance (Ohm)	K value	Aparent Resistivity (Rho_a)				
1	2.5	1	139	18.846	2619.594				
2	5	1	32.8	77.73975	2549.8637999999996				
3	10	1	8.62	313.31475	2700.7731449999997				
4	15	1	2.73	705.93975	1927.2155175				
5	20	1	1.38	1255.61475	1732.7483549999997				
6	25	1	0.642	1962.33975	1259.8221195				
7	30	1	0.358	2826.11475	1011.7490805				
8	35	1	0.234	3846.93975	900.1839015				
9	40	1	0.155	5024.8147500000005	778.84628625				
10	45	1	0.1203	6359.73975	765.076691925				
11	50	1	0.105	7851.71475	824.43004875				
12	60	1	0.0657	11306.81475	742.857729075				
13	70	1	0.0555	15390.11475	854.151368625				
14	80	1	0.0498	20101.61475	1001.06041455				
15	90	1		25441.31475	0				
16	100	1		31409.21475	0				

AL_VES132

Date:12/05/2025		VES132							
Latitude	29.622825	Longitude	79.717715	Area		Elevation (m)	1408.0	Direction	180°S
S.N	Current Electrode Spacing (AB/2)	Potential Electrode Spacing (MN)	Resistance (Ohm)	K value	Aparent Resistivity (Rho_a)				
1	2.5	1	99.8	18.846	1880.8308				
2	5	1	25.4	77.73975	1974.58965				
3	10	1	6.01	313.31475	1883.0216475				
4	15	1	1.96	705.93975	1383.64191				
5	20	1	0.839	1255.61475	1053.4607752499999				
6	25	1	0.699	1962.33975	1371.67548525				
7	30	1	0.506	2826.11475	1430.0140635				
8	35	1	0.348	3846.93975	1338.735033				
9	40	1	0.3	5024.8147500000005	1507.4444250000001				
10	45	1	0.253	6359.73975	1609.01415675				
11	50	1	0.215	7851.71475	1688.11867125				
12	60	1	0.168	11306.81475	1899.5448780000002				
13	70	1	0.133	15390.11475	2046.8852617500002				
14	80	1	0.1033	20101.61475	2076.496803675				
15	90	1	0.0862	25441.31475	2193.04133145				
16	100	1	0.0632	31409.21475	1985.0623722000003				

AL_VES133

Date:20/05/2025		VES133							
Latitude	29.62103	Longitude	79.717755	Area	Bataldeon	Elevation (m)	1418.0	Direction	180°S
S.N	Current Electrode Spacing (AB/2)	Potential Electrode Spacing (MN)	Resistance (Ohm)	K value	Aparent Resistivity (Rho_a)				
1	2.5	1	237	18.846	4466.502				
2	5	1	62.2	77.73975	4835.412450000001				
3	10	1	13.5	313.31475	4229.749125				
4	15	1	4.94	705.93975	3487.3423650000004				
5	20	1	2.72	1255.61475	3415.27212				
6	25	1	1.48	1962.33975	2904.26283				
7	30	1	0.838	2826.11475	2368.2841605				
8	35	1	0.664	3846.93975	2554.367994				
9	40	1	0.594	5024.8147500000005	2984.7399615				
10	45	1	0.431	6359.73975	2741.04783225				
11	50	1	0.517	7851.71475	4059.33652575				
12	60	1	0.239	11306.81475	2702.32872525				
13	70	1	0.193	15390.11475	2970.29214675				
14	80	1	0.267	20101.61475	5367.131138250001				
15	90	1	0.236	25441.31475	6004.150281				
16	100	1	0.138	31409.21475	4334.4716355				

AL_VES134

Date:20/05/2025		VES134							
Latitude	29.619167	Longitude	79.717777	Area	Bataldeon	Elevation (m)	1415.0	Direction	180°S
S.N	Current Electrode Spacing (AB/2)	Potential Electrode Spacing (MN)	Resistance (Ohm)	K value	Aparent Resistivity (Rho_a)				
1	2.5	1	76.1	18.846	1434.1806				
2	5	1	13	77.73975	1010.61675				
3	10	1	1.81	313.31475	567.0996975				
4	15	1	0.67	705.93975	472.97963250000004				
5	20	1	0.404	1255.61475	507.26835900000003				
6	25	1	0.281	1962.33975	551.4174697500001				
7	30	1	0.214	2826.11475	604.7885565				
8	35	1	0.146	3846.93975	561.6532035				
9	40	1	0.129	5024.8147500000005	648.2011027500001				
10	45	1	0.108	6359.73975	686.851893				

11	50	1	0.0914	7851.71475	717.64672815				
12	60	1	0.064	11306.81475	723.636144				
13	70	1	0.0538	15390.11475	827.98817355				
14	80	1		20101.61475	0				
15	90	1		25441.31475	0				
16	100	1		31409.21475	0				

AL_VES135

Date:21/05/2025		VES135							
Latitude	29.636037	Longitude	79.702761	Area	Barakot	Elevation (m)	1525.0	Direction	120°SE
S.N	Current Electrode Spacing (AB/2)	Potential Electrode Spacing (MN)	Resistance (Ohm)	K value	Aparent Resistivity (Rho_a)				
1	2.5	1	192	18.846	3618.432				
2	5	1	42.6	77.73975	3311.71335				
3	10	1	8.03	313.31475	2515.9174424999997				
4	15	1	3.11	705.93975	2195.4726225				
5	20	1	1.46	1255.61475	1833.1975349999998				
6	25	1	0.892	1962.33975	1750.4070570000001				
7	30	1	0.648	2826.11475	1831.3223580000001				
8	35	1	0.471	3846.93975	1811.90862225				
9	40	1	0.312	5024.8147500000005	1567.7422020000001				
10	45	1	0.29	6359.73975	1844.3245274999997				
11	50	1	0.214	7851.71475	1680.2669564999999				
12	60	1	0.127	11306.81475	1435.96547325				
13	70	1	0.0982	15390.11475	1511.30926845				
14	80	1	0.0675	20101.61475	1356.858995625				
15	90	1	0.0521	25441.31475	1325.492498475				
16	100	1	0.0435	31409.21475	1366.300841625				

AL_VES136

Date:21/05/2025		VES136							
Latitude	29.635529	Longitude	79.704859	Area	Barakot	Elevation (m)	1489.0	Direction	120°SE
S.N	Current Electrode Spacing (AB/2)	Potential Electrode Spacing (MN)	Resistance (Ohm)	K value	Aparent Resistivity (Rho_a)				
1	2.5	1	123	18.846	2318.058				
2	5	1	31.7	77.73975	2464.350075				
3	10	1	5.74	313.31475	1798.4266650000002				
4	15	1	1.73	705.93975	1221.2757675				

5	20	1	0.782	1255.61475	981.8907345				
6	25	1	0.431	1962.33975	845.76843225				
7	30	1	0.332	2826.11475	938.2700970000001				
8	35	1	0.203	3846.93975	780.9287692500001				
9	40	1	0.167	5024.8147500000005	839.1440632500002				
10	45	1	0.154	6359.73975	979.3999214999999				
11	50	1	0.162	7851.71475	1271.9777895				
12	60	1	0.1087	11306.81475	1229.050763325				
13	70	1	0.0829	15390.11475	1275.840512775				
14	80	1	0.0733	20101.61475	1473.4483611750002				
15	90	1	0.049	25441.31475	1246.6244227500001				
16	100	1	0.0871	31409.21475	2735.7426047249996				

AL_VES137

Date:21/05/2025		VES137							
Latitude	29.634989	Longitude	79.706912	Area	Barakot	Elevation (m)	1480.0	Direction	120°SE
S.N	Current Electrode Spacing (AB/2)	Potential Electrode Spacing (MN)	Resistance (Ohm)	K value	Aparent Resistivity (Rho_a)				
1	2.5	1	93.5	18.846	1762.101				
2	5	1	28.6	77.73975	2223.35685				
3	10	1	6.24	313.31475	1955.0840400000002				
4	15	1	2.08	705.93975	1468.3546800000001				
5	20	1	1.016	1255.61475	1275.704586				
6	25	1	0.598	1962.33975	1173.4791705				
7	30	1	0.412	2826.11475	1164.359277				
8	35	1	0.28	3846.93975	1077.1431300000002				
9	40	1	0.312	5024.8147500000005	1567.7422020000001				
10	45	1	0.901	6359.73975	5730.12551475				
11	50	1	4.41	7851.71475	34626.0620475				
12	60	1	2.13	11306.81475	24083.5154175				
13	70	1	3.51	15390.11475	54019.3027725				
14	80	1	2.99	20101.61475	60103.8281025				
15	90	1		25441.31475	0				
16	100	1		31409.21475	0				

AL_VES138

Date:22/05/2025		VES138							
Latitude	29.634463	Longitude	79.709095	Area	Barakot	Elevation (m)	1457.0	Direction	120°SE
S.N	Current Electrode	Potential Electrode	Resistance (Ohm)	K value	Aparent Resistivity (Rho_a)				

	Spacing (AB/2)	Spacing (MN)							
1	2.5	1	185	18.846	3486.51				
2	5	1	46.1	77.73975	3583.802475				
3	10	1	13.8	313.31475	4323.74355				
4	15	1	5.75	705.93975	4059.1535625				
5	20	1	2.21	1255.61475	2774.9085975				
6	25	1	1.54	1962.33975	3022.003215				
7	30	1	1.28	2826.11475	3617.4268800000004				
8	35	1	0.954	3846.93975	3669.9805214999997				
9	40	1	1.55	5024.8147500000005	7788.4628625000005				
10	45	1	1.64	6359.73975	10429.973189999999				
11	50	1	2.19	7851.71475	17195.2553025				
12	60	1	1.32	11306.81475	14924.99547				
13	70	1	1.88	15390.11475	28933.41573				
14	80	1	1.116	20101.61475	22433.402061000004				
15	90	1	0.649	25441.31475	16511.41327275				
16	100	1	0.196	31409.21475	6156.206091				

AL_VES139

Date:22/05/2025		VES139							
Latitude	29.63399	Longitude	79.711049	Area	Barakot	Elevation (m)	1442.0	Direction	120°SE
S.N	Current Electrode Spacing (AB/2)	Potential Electrode Spacing (MN)	Resistance (Ohm)	K value	Aparent Resistivity (Rho_a)				
1	2.5	1	85.7	18.846	1615.1022				
2	5	1	24.7	77.73975	1920.171825				
3	10	1	7.39	313.31475	2315.3960025				
4	15	1	3.54	705.93975	2499.026715				
5	20	1	1.35	1255.61475	1695.0799125				
6	25	1	3.08	1962.33975	6044.00643				
7	30	1	2.02	2826.11475	5708.751795				
8	35	1	3.42	3846.93975	13156.533945				
9	40	1	2.14	5024.8147500000005	10753.103565000001				
10	45	1	1.73	6359.73975	11002.3497675				
11	50	1	1.88	7851.71475	14761.22373				
12	60	1	1.34	11306.81475	15151.131765				
13	70	1	1.38	15390.11475	21238.358355				
14	80	1	1.61	20101.61475	32363.599747500004				
15	90	1	0.998	25441.31475	25390.4321205				
16	100	1	0.348	31409.21475	10930.406733				

AL_VES140

Date:23/05/2025		VES140							
Latitude	29.597968	Longitude	79.687957	Area	Jhasertana	Elevation (m)	1416.0	Direction	90°E
S.N	Current Electrode Spacing (AB/2)	Potential Electrode Spacing (MN)	Resistance (Ohm)	K value	Aparent Resistivity (Rho_a)				
1	2.5	1	112.6	18.846	2122.0596				
2	5	1	34.1	77.73975	2650.925475				
3	10	1	5.85	313.31475	1832.8912874999999				
4	15	1	2.34	705.93975	1651.899015				
5	20	1	1.191	1255.61475	1495.4371672500001				
6	25	1	0.653	1962.33975	1281.40785675				
7	30	1	0.392	2826.11475	1107.836982				
8	35	1	0.268	3846.93975	1030.979853				
9	40	1	0.198	5024.8147500000005	994.9133205000002				
10	45	1	0.174	6359.73975	1106.5947164999998				
11	50	1	0.139	7851.71475	1091.38835025				
12	60	1	0.1196	11306.81475	1352.2950440999998				
13	70	1	0.1018	15390.11475	1566.71368155				
14	80	1	0.0623	20101.61475	1252.330598925				

AL_VES141

Date:23/05/2025		VES141							
Latitude	29.597795	Longitude	79.690558	Area	Jhasertana	Elevation (m)	1396.0	Direction	90°E
S.N	Current Electrode Spacing (AB/2)	Potential Electrode Spacing (MN)	Resistance (Ohm)	K value	Aparent Resistivity (Rho_a)				
1	2.5	1	48.6	18.846	915.9156				
2	5	1	19.3	77.73975	1500.377175				
3	10	1	5.26	313.31475	1648.0355849999999				
4	15	1	1.66	705.93975	1171.859985				
5	20	1	0.988	1255.61475	1240.5473729999999				
6	25	1	0.618	1962.33975	1212.7259655				
7	30	1	0.441	2826.11475	1246.3166047500001				
8	35	1	0.333	3846.93975	1281.0309367500001				
9	40	1	0.243	5024.8147500000005	1221.02998425				
10	45	1	0.203	6359.73975	1291.02716925				
11	50	1	0.142	7851.71475	1114.9434944999998				
12	60	1	0.0572	11306.81475	646.7498037				
13	70	1	0.0487	15390.11475	749.498588325				

AL_VES142

Date:23/05/2025		VES142							
Latitude	29.597764	Longitude	79.693049	Area	Tatik	Elevation (m)	1402.0	Direction	90°E
S.N	Current Electrode Spacing (AB/2)	Potential Electrode Spacing (MN)	Resistance (Ohm)	K value	Aparent Resistivity (Rho_a)				
1	2.5	1	161	18.846	3034.206				
2	5	1	25.2	77.73975	1959.0417				
3	10	1	3.05	313.31475	955.6099875				
4	15	1	1.011	705.93975	713.7050872499999				
5	20	1	0.39	1255.61475	489.6897525				
6	25	1	0.196	1962.33975	384.61859100000004				
7	30	1	0.136	2826.11475	384.35160600000006				
8	35	1	0.1137	3846.93975	437.397049575				
9	40	1	0.0782	5024.8147500000005	392.9405134500001				
10	45	1	0.0626	6359.73975	398.11970835				
11	50	1	0.0805	7851.71475	632.063037375				
12	60	1	0.0654	11306.81475	739.46568465				
13	70	1	0.0516	15390.11475	794.1299211				
14	80	1	0.0854	20101.61475	1716.6778996500002				
15	90	1	0.0832	25441.31475	2116.7173872				
16	100	1	0.0647	31409.21475	2032.1761943249996				

AL_VES143

Date:23/05/2025		VES143							
Latitude	29.597841	Longitude	79.695422	Area	Tatik	Elevation (m)	1390.0	Direction	90°E
S.N	Current Electrode Spacing (AB/2)	Potential Electrode Spacing (MN)	Resistance (Ohm)	K value	Aparent Resistivity (Rho_a)				
1	2.5	1	87.7	18.846	1652.7942				
2	5	1	17.4	77.73975	1352.67165				
3	10	1	3.19	313.31475	999.4740525				
4	15	1	1.59	705.93975	1122.4442025				
5	20	1	1.041	1255.61475	1307.09495475				
6	25	1	0.665	1962.33975	1304.9559337500002				
7	30	1	0.485	2826.11475	1370.66565375				
8	35	1	0.394	3846.93975	1515.6942615				
9	40	1	0.287	5024.8147500000005	1442.12183325				
10	45	1	0.225	6359.73975	1430.94144375				
11	50	1	0.198	7851.71475	1554.6395205000001				

12	60	1	0.161	11306.81475	1820.39717475				
13	70	1	0.1092	15390.11475	1680.6005307000003				
14	80	1	0.088	20101.61475	1768.942098				
15	90	1	0.0617	25441.31475	1569.729120075				
16	100	1	0.0445	31409.21475	1397.7100563749998				

AL_VES144

Date:24/05/2025		VES144							
Latitude	29.649461	Longitude	79.711742	Area	Deora	Elevation (m)	1492.0	Direction	05°N
S.N	Current Electrode Spacing (AB/2)	Potential Electrode Spacing (MN)	Resistance (Ohm)	K value	Aparent Resistivity (Rho_a)				
1	2.5	1	132	18.846	2487.672				
2	5	1	10.96	77.73975	852.0276600000001				
3	10	1	3.17	313.31475	993.2077575				
4	15	1	1.36	705.93975	960.07806				
5	20	1	0.666	1255.61475	836.2394235				
6	25	1	0.351	1962.33975	688.78125225				
7	30	1	0.251	2826.11475	709.35480225				
8	35	1	0.218	3846.93975	838.6328655				
9	40	1	0.156	5024.8147500000005	783.8711010000001				
10	45	1	0.161	6359.73975	1023.91809975				
11	50	1	0.148	7851.71475	1162.053783				
12	60	1	0.574	11306.81475	6490.111666499999				
13	70	1	0.208	15390.11475	3201.143868				
14	80	1	0.109	20101.61475	2191.07600775				
15	90	1	0.135	25441.31475	3434.5774912500005				
16	100	1	0.125	31409.21475	3926.15184375				

AL_VES145

Date:24/05/2025		VES145							
Latitude	29.647518	Longitude	79.711185	Area	Deora	Elevation (m)	1406.0	Direction	05°N
S.N	Current Electrode Spacing (AB/2)	Potential Electrode Spacing (MN)	Resistance (Ohm)	K value	Aparent Resistivity (Rho_a)				
1	2.5	1	20.3	18.846	382.5738				
2	5	1	5.04	77.73975	391.80834				
3	10	1	1.81	313.31475	567.0996975				
4	15	1	0.991	705.93975	699.58629225				
5	20	1	0.689	1255.61475	865.1185627499999				

6	25	1	0.514	1962.33975	1008.6426315000001				
7	30	1	0.432	2826.11475	1220.881572				
8	35	1	0.336	3846.93975	1292.571756				
9	40	1	0.315	5024.8147500000005	1582.81664625				
10	45	1	0.233	6359.73975	1481.81936175				
11	50	1	0.199	7851.71475	1562.49123525				
12	60	1	0.141	11306.81475	1594.2608797499997				
13	70	1	0.142	15390.11475	2185.3962945				
14	80	1	0.1041	20101.61475	2092.578095475				
15	90	1	0.136	25441.31475	3460.0188060000005				
16	100	1	0.168	31409.21475	5276.7480780000005				

AL_VES146

Date:24/05/2025		**VES146**							
Latitude	**29.645566**	**Longitude**	**79.710983**	**Area**	**Deora**	**Elevation (m)**	**1380.0**	**Direction**	**05°N**
S.N	**Current Electrode Spacing (AB/2)**	**Potential Electrode Spacing (MN)**	**Resistance (Ohm)**	**K value**	**Aparent Resistivity (Rho_a)**				
1	2.5	1	20.1	18.846	378.80460000000005				
2	5	1	3.66	77.73975	284.527485				
3	10	1	0.899	313.31475	281.66996025000003				
4	15	1	0.543	705.93975	383.32528425000004				
5	20	1	0.377	1255.61475	473.36676074999997				
6	25	1	0.296	1962.33975	580.852566				
7	30	1	0.238	2826.11475	672.6153105				
8	35	1	0.173	3846.93975	665.5205767499999				
9	40	1	0.145	5024.8147500000005	728.59813875				
10	45	1	0.117	6359.73975	744.0895507500001				
11	50	1	0.105	7851.71475	824.43004875				
12	60	1	0.0873	11306.81475	987.084927675				
13	70	1	0.0531	15390.11475	817.215093225				
14	80	1	0.042	20101.61475	844.2678195000001				
15	90	1	0.0375	25441.31475	954.049303125				
16	100	1	0.0327	31409.21475	1027.081322325				

AL_VES147

Date:26/05/2025		**VES147**							
Latitude	**29.643593**	**Longitude**	**79.709104**	**Area**	**Naini**	**Elevation (m)**	**1411.0**	**Direction**	**05°N**
S.N	**Current Electrode**	**Potential Electrode**	**Resistance (Ohm)**	**K value**	**Aparent Resistivity (Rho_a)**				

	Spacing (AB/2)	Spacing (MN)							
1	2.5	1	19.8	18.846	373.1508				
2	5	1	4.58	77.73975	356.04805500000003				
3	10	1	0.995	313.31475	311.74817625000003				
4	15	1	0.531	705.93975	374.85400725				
5	20	1	0.319	1255.61475	400.54110525				
6	25	1	0.223	1962.33975	437.60176425000003				
7	30	1	0.172	2826.11475	486.09173699999997				
8	35	1	0.141	3846.93975	542.4185047499999				
9	40	1	0.113	5024.8147500000005	567.8040667500001				
10	45	1	0.0943	6359.73975	599.723458425				
11	50	1	0.0787	7851.71475	617.9299508250001				
12	60	1	0.0546	11306.81475	617.35208535				
13	70	1	0.0392	15390.11475	603.2924982				
14	80	1	0.0257	20101.61475	516.611499075				
15	90	1	0.0269	25441.31475	684.3713667750001				
16	100	1	0.0224	31409.21475	703.5664104				

AL_VES148

Date:26/05/2025		VES148							
Latitude	29.645584	Longitude	79.709552	Area	Naini	Elevation (m)	1406.0	Direction	05°N
S.N	Current Electrode Spacing (AB/2)	Potential Electrode Spacing (MN)	Resistance (Ohm)	K value	Aparent Resistivity (Rho_a)				
1	2.5	1	8.45	18.846	159.24869999999999				
2	5	1	2.53	77.73975	196.6815675				
3	10	1	0.731	313.31475	229.03308225				
4	15	1	0.322	705.93975	227.3125995				
5	20	1	0.2105	1255.61475	264.306904875				
6	25	1	0.151	1962.33975	296.31330225				
7	30	1	0.124	2826.11475	350.43822900000004				
8	35	1	0.0958	3846.93975	368.53682805				
9	40	1	0.0792	5024.8147500000005	397.96532820000004				
10	45	1	0.0669	6359.73975	425.466589275				
11	50	1	0.0548	7851.71475	430.27396830000004				
12	60	1	0.0405	11306.81475	457.925997375				
13	70	1	0.0317	15390.11475	487.866637575				
14	80	1	0.0262	20101.61475	526.6623064500001				
15	90	1	0.0216	25441.31475	549.5323986000001				
16	100	1	0.0181	31409.21475	568.5067869750001				

AL_VES149

Date:26/05/2025		VES149							
Latitude	29.647432	Longitude	79.709457	Area	Naini	Elevation (m)	1398.0	Direction	05°N
S.N	Current Electrode Spacing (AB/2)	Potential Electrode Spacing (MN)	Resistance (Ohm)	K value	Aparent Resistivity (Rho_a)				
1	2.5	1	96.1	18.846	1811.1006				
2	5	1	22.4	77.73975	1741.3704				
3	10	1	5.03	313.31475	1575.9731925				
4	15	1	2.05	705.93975	1447.1764875				
5	20	1	1.21	1255.61475	1519.2938474999999				
6	25	1	0.881	1962.33975	1728.8213197500002				
7	30	1	0.427	2826.11475	1206.75099825				
8	35	1	0.292	3846.93975	1123.306407				
9	40	1	0.309	5024.8147500000005	1552.6677577500002				
10	45	1	0.188	6359.73975	1195.631073				
11	50	1	0.167	7851.71475	1311.23636325				
12	60	1	0.151	11306.81475	1707.3290272499999				
13	70	1	0.159	15390.11475	2447.02824525				
14	80	1	0.393	20101.61475	7899.93459675				
15	90	1	0.0698	25441.31475	1775.8037695500002				
16	100	1	0.159	31409.21475	4994.06514525				

AL_VES150

Date:26/05/2025		VES150							
Latitude	29.649622	Longitude	79.709606	Area	Naini	Elevation (m)	1410.0	Direction	05°N
S.N	Current Electrode Spacing (AB/2)	Potential Electrode Spacing (MN)	Resistance (Ohm)	K value	Aparent Resistivity (Rho_a)				
1	2.5	1	40	18.846	753.84				
2	5	1	12.6	77.73975	979.52085				
3	10	1	3.36	313.31475	1052.73756				
4	15	1	1.72	705.93975	1214.21637				
5	20	1	1.015	1255.61475	1274.4489712499999				
6	25	1	0.6405	1962.33975	1256.878609875				
7	30	1	0.388	2826.11475	1096.532523				
8	35	1	0.256	3846.93975	984.816576				
9	40	1	0.161	5024.8147500000005	808.99517475				
10	45	1	0.116	6359.73975	737.729811				
11	50	1	0.0854	7851.71475	670.53643965				
12	60	1	0.0576	11306.81475	651.2725296				

13	70	1	0.0384	15390.11475	590.9804064				
14	80	1		20101.61475	0				
15	90	1		25441.31475	0				
16	100	1		31409.21475	0				

AL_VES151

Date:27/05/2025		VES151							
Latitude	29.651094	Longitude	79.683597	Area	Matena	Elevation (m)	1646.0	Direction	80°E
S.N	Current Electrode Spacing (AB/2)	Potential Electrode Spacing (MN)	Resistance (Ohm)	K value	Aparent Resistivity (Rho_a)				
1	2.5	1	229	18.846	4315.734				
2	5	1	46.1	77.73975	3583.802475				
3	10	1	5.66	313.31475	1773.3614850000001				
4	15	1	2.33	705.93975	1644.8396175				
5	20	1	1.41	1255.61475	1770.4167974999998				
6	25	1	0.876	1962.33975	1719.0096210000002				
7	30	1	0.613	2826.11475	1732.40834175				
8	35	1	0.447	3846.93975	1719.58206825				
9	40	1	0.383	5024.8147500000005	1924.5040492500002				
10	45	1	0.381	6359.73975	2423.06084475				
11	50	1	0.305	7851.71475	2394.77299875				
12	60	1	0.187	11306.81475	2114.37435825				
13	70	1	0.129	15390.11475	1985.3248027500001				
14	80	1		20101.61475	0				
15	90	1		25441.31475	0				
16	100	1		31409.21475	0				

AL_VES152

Date:27/05/2025		VES152							
Latitude	29.651048	Longitude	79.685899	Area	Matena	Elevation (m)	1672.0	Direction	80°E
S.N	Current Electrode Spacing (AB/2)	Potential Electrode Spacing (MN)	Resistance (Ohm)	K value	Aparent Resistivity (Rho_a)				
1	2.5	1	115.4	18.846	2174.8284000000003				
2	5	1	26.6	77.73975	2067.87735				
3	10	1	4.56	313.31475	1428.71526				
4	15	1	1.24	705.93975	875.36529				
5	20	1	0.558	1255.61475	700.6330305				
6	25	1	0.333	1962.33975	653.4591367500001				

7	30	1	0.272	2826.11475	768.7032120000001				
8	35	1	0.194	3846.93975	746.3063115				
9	40	1	0.151	5024.8147500000005	758.7470272500001				
10	45	1	0.126	6359.73975	801.3272085				
11	50	1	0.1011	7851.71475	793.808361225				
12	60	1	0.0743	11306.81475	840.0963359250001				
13	70	1	0.0667	15390.11475	1026.520653825				
14	80	1	0.0511	20101.61475	1027.192513725				
15	90	1	0.044	25441.31475	1119.417849				
16	100	1	0.0369	31409.21475	1159.000024275				

AL_VES153

Date:27/05/2025		VES153							
Latitude	29.651232	Longitude	79.688018	Area	Matena	Elevation (m)	1598.0	Direction	80°E
S.N	Current Electrode Spacing (AB/2)	Potential Electrode Spacing (MN)	Resistance (Ohm)	K value	Aparent Resistivity (Rho_a)				
1	2.5	1	249	18.846	4692.654				
2	5	1	67.2	77.73975	5224.1112				
3	10	1	13.9	313.31475	4355.075025				
4	15	1	4.805	705.93975	3392.0404987499996				
5	20	1	1.89	1255.61475	2373.1118775				
6	25	1	1.005	1962.33975	1972.1514487499999				
7	30	1	0.609	2826.11475	1721.1038827500001				
8	35	1	0.668	3846.93975	2569.7557530000004				
9	40	1	0.362	5024.8147500000005	1818.9829395000002				
10	45	1	0.268	6359.73975	1704.410253				
11	50	1	0.216	7851.71475	1695.970386				
12	60	1	0.169	11306.81475	1910.85169275				
13	70	1	0.153	15390.11475	2354.68755675				
14	80	1	0.1046	20101.61475	2102.62890285				
15	90	1	0.156	25441.31475	3968.8451010000003				
16	100	1		31409.21475	0				

AL_VES154

Date:27/05/2025		VES154							
Latitude		Longitude	79.690246	Area	Matena	Elevation (m)	1625.0	Direction	80°E
S.N	Current Electrode	Potential Electrode	Resistance (Ohm)	K value	Aparent Resistivity (Rho_a)				

	Spacing (AB/2)	Spacing (MN)							
1	2.5	1	100.9	18.846	1901.5614				
2	5	1	27.1	77.73975	2106.747225				
3	10	1	5.29	313.31475	1657.4350275				
4	15	1	2.12	705.93975	1496.59227				
5	20	1	1.114	1255.61475	1398.7548315000001				
6	25	1	0.659	1962.33975	1293.18189525				
7	30	1	0.437	2826.11475	1235.0121457500002				
8	35	1	0.316	3846.93975	1215.632961				
9	40	1	0.23	5024.8147500000005	1155.7073925000002				
10	45	1	0.164	6359.73975	1042.997319				
11	50	1	0.119	7851.71475	934.35405525				
12	60	1	0.0622	11306.81475	703.28387745				
13	70	1	0.0485	15390.11475	746.420565375				
14	80	1	0.0227	20101.61475	456.30665482500007				
15	90	1	0.0268	25441.31475	681.8272353000001				
16	100	1	0.0172	31409.21475	540.2384936999999				

Annexure XX_Resistivity (2D) Models

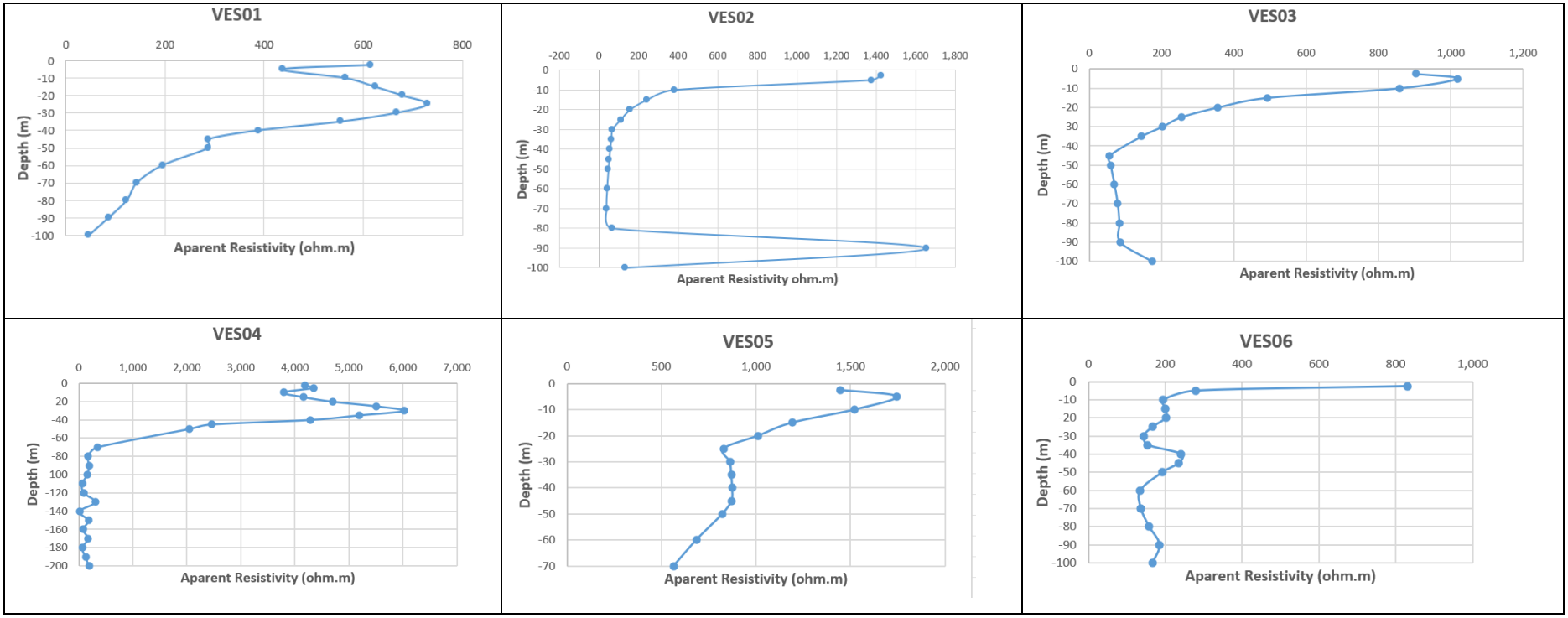

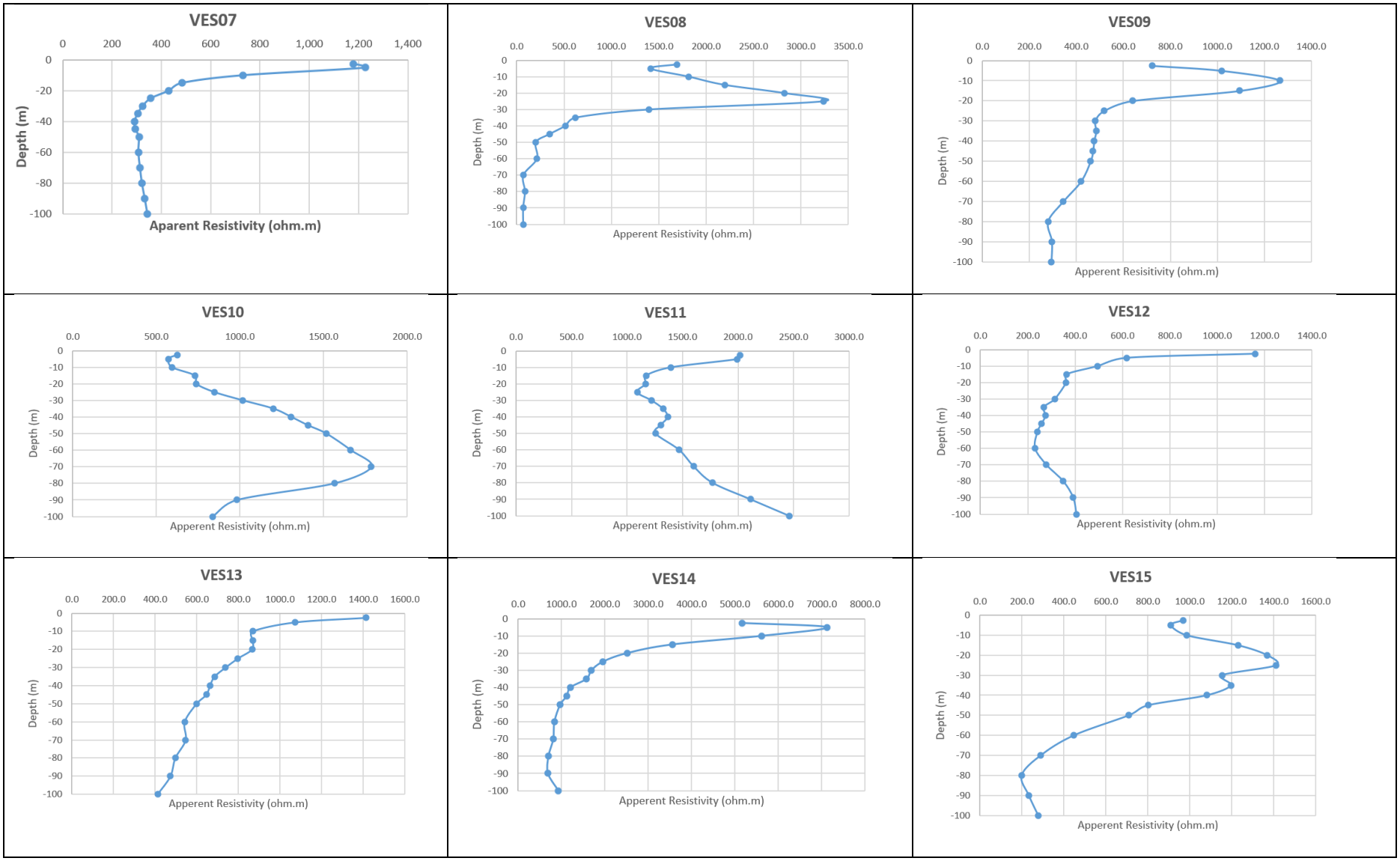
VES07
Depth (m)
Aparent Resistivity (ohm.m)
VES08
Depth (m)
Apperent Resistivity (ohm.m)
VES09
Depth (m)
Apperent Resisitivity (ohm.m)
VES10
Depth (m)
Apperent Resistivity (ohm.m)
VES11
Depth (m)
Apperent Resistivity (ohm.m)
VES12
Depth (m)
Apperent Resistivity (ohm.m)
VES13
Depth (m)
Apperent Resistivity (ohm.m)
VES14
Depth (m)
Apperent Resistivity (ohm.m)
VES15
Depth (m)
Apperent Resistivity (ohm.m)

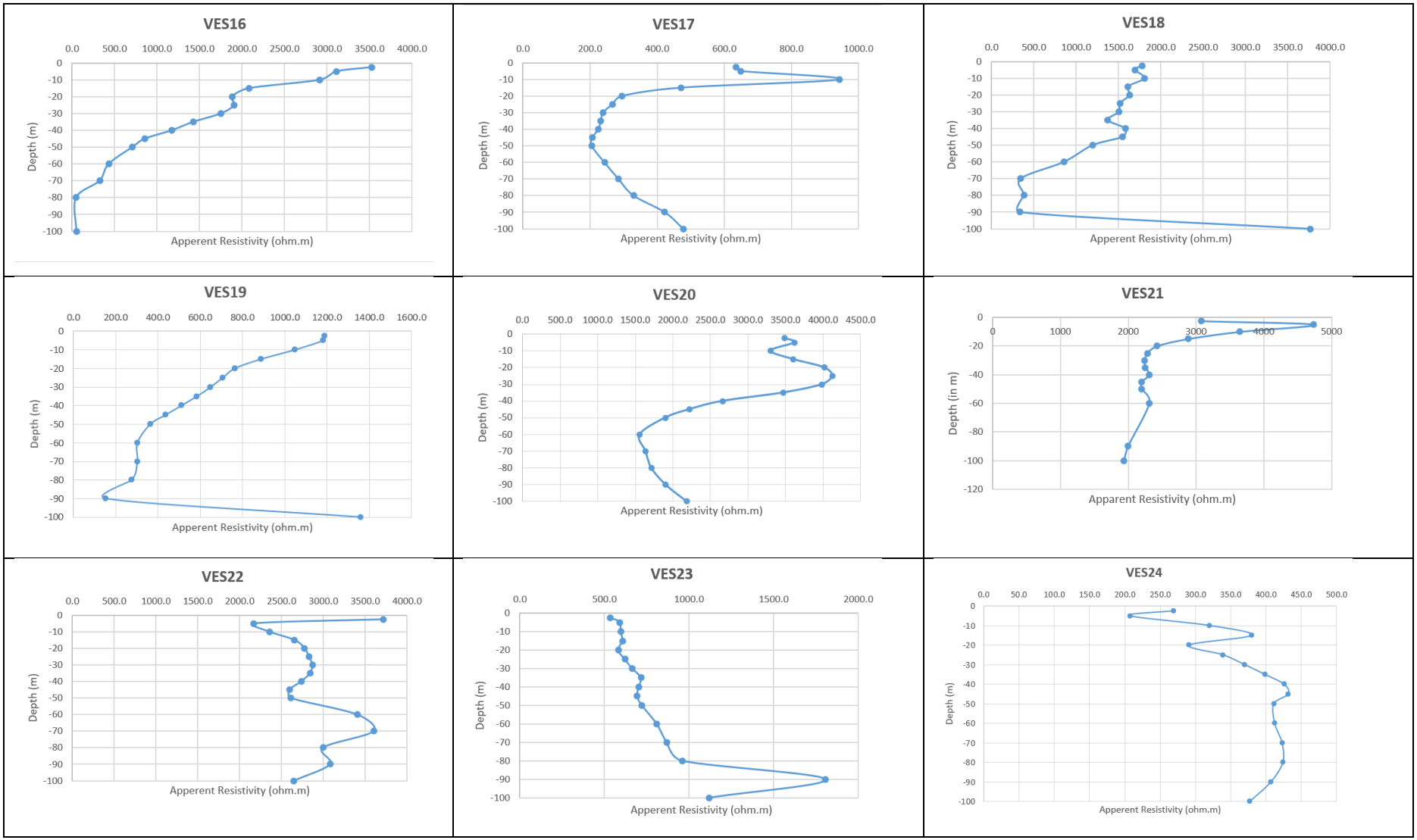
VES16
Depth (m)
Apperent Resistivity (ohm.m)
VES17
Depth (m)
Apperent Resistivity (ohm.m)
VES18
Depth (m)
Apperent Resistivity (ohm.m)
VES19
Depth (m)
Apperent Resistivity (ohm.m)
VES20
Depth (m)
Apperent Resistivity (ohm.m)
VES21
Depth (in m)
Apparent Resistivity (ohm.m)
VES22
Depth (m)
Apperent Resistivity (ohm.m)
VES23
Depth (m)
Apperent Resistivity (ohm.m)
VES24
Depth (m)
Apperent Resistivity (ohm.m)

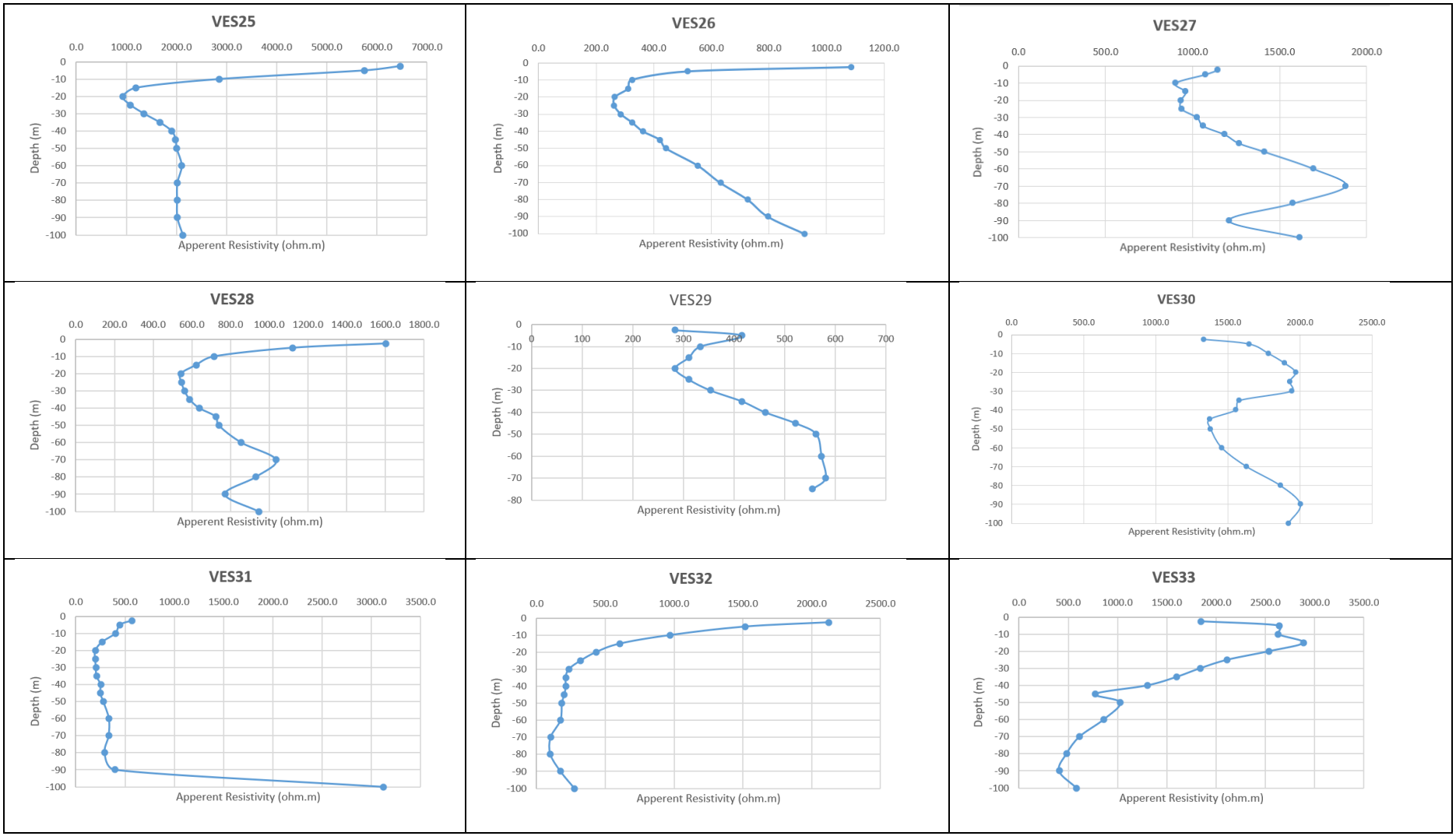
VES25
0.0 1000.0 2000.0 3000.0 4000.0 5000.0 6000.0 7000.0
0 -10 -20 -30 -40 -50 -60 -70 -80 -90 -100
Depth (m)
Apperent Resistivity (ohm.m)
VES26
0.0 200.0 400.0 600.0 800.0 1000.0 1200.0
0 -10 -20 -30 -40 -50 -60 -70 -80 -90 -100
Depth (m)
Apperent Resistivity (ohm.m)
VES27
0.0 500.0 1000.0 1500.0 2000.0
0 -10 -20 -30 -40 -50 -60 -70 -80 -90 -100
Depth (m)
Apperent Resistivity (ohm.m)
VES28
0.0 200.0 400.0 600.0 800.0 1000.0 1200.0 1400.0 1600.0 1800.0
0 -10 -20 -30 -40 -50 -60 -70 -80 -90 -100
Depth (m)
Apperent Resistivity (ohm.m)
VES29
0 100 200 300 400 500 600 700
0 -10 -20 -30 -40 -50 -60 -70 -80
Depth (m)
Apperent Resistivity (ohm.m)
VES30
0.0 500.0 1000.0 1500.0 2000.0 2500.0
0 -10 -20 -30 -40 -50 -60 -70 -80 -90 -100
Depth (m)
Apperent Resistivity (ohm.m)
VES31
0.0 500.0 1000.0 1500.0 2000.0 2500.0 3000.0 3500.0
0 -10 -20 -30 -40 -50 -60 -70 -80 -90 -100
Depth (m)
Apperent Resistivity (ohm.m)
VES32
0.0 500.0 1000.0 1500.0 2000.0 2500.0
0 -10 -20 -30 -40 -50 -60 -70 -80 -90 -100
Depth (m)
Apperent Resistivity (ohm.m)
VES33
0.0 500.0 1000.0 1500.0 2000.0 2500.0 3000.0 3500.0
0 -10 -20 -30 -40 -50 -60 -70 -80 -90 -100
Depth (m)
Apperent Resistivity (ohm.m)

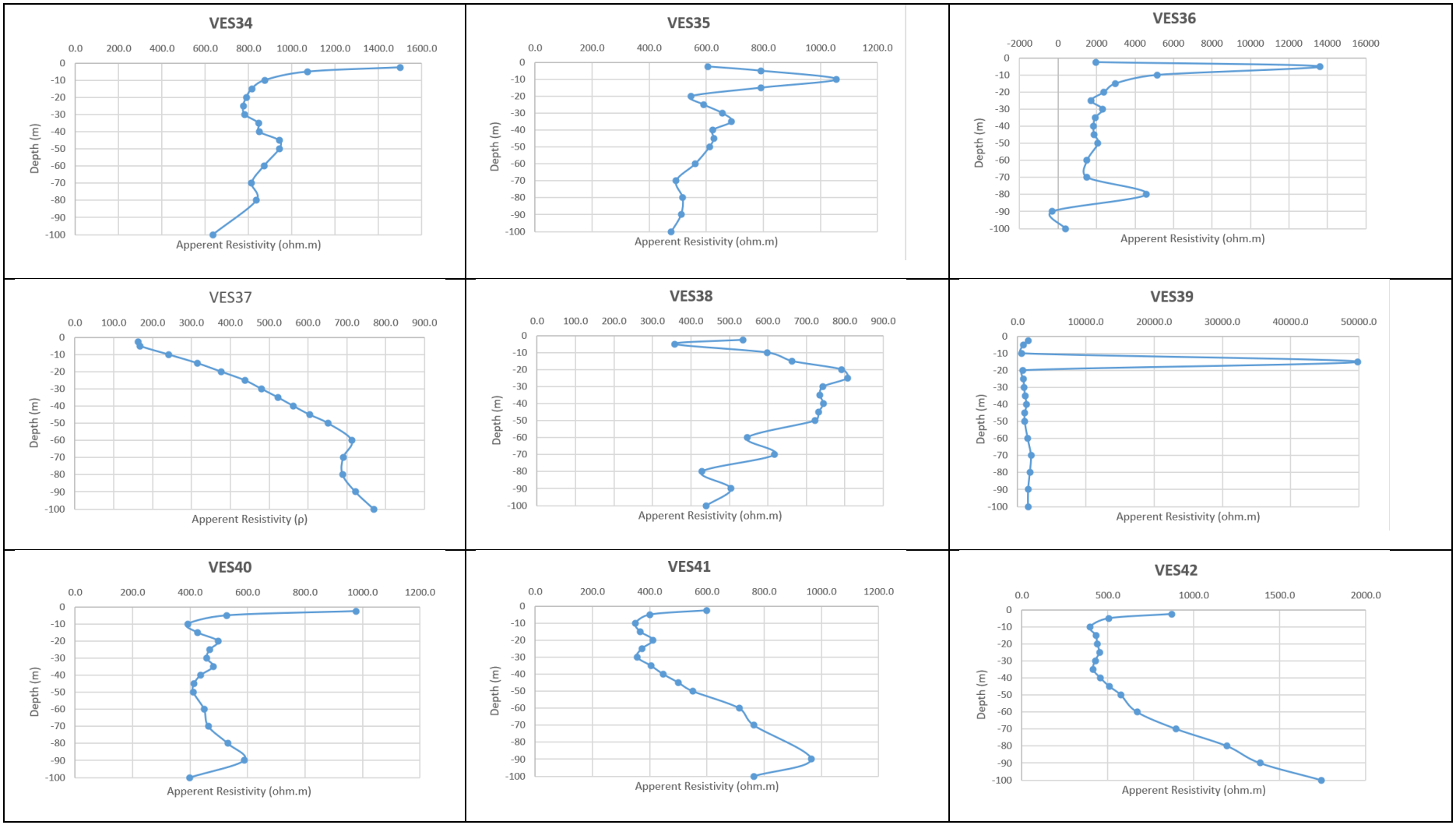
VES34
0.0 200.0 400.0 600.0 800.0 1000.0 1200.0 1400.0 1600.0
0 -10 -20 -30 -40 -50 -60 -70 -80 -90 -100
Depth (m)
Apperent Resistivity (ohm.m)
VES35
0.0 200.0 400.0 600.0 800.0 1000.0 1200.0
0 -10 -20 -30 -40 -50 -60 -70 -80 -90 -100
Depth (m)
Apperent Resistivity (ohm.m)
VES36
-2000 0 2000 4000 6000 8000 10000 12000 14000 16000
0 -10 -20 -30 -40 -50 -60 -70 -80 -90 -100
Depth (m)
Apperent Resistivity (ohm.m)
VES37
0.0 100.0 200.0 300.0 400.0 500.0 600.0 700.0 800.0 900.0
0 -10 -20 -30 -40 -50 -60 -70 -80 -90 -100
Depth (m)
Apperent Resistivity (ρ)
VES38
0.0 100.0 200.0 300.0 400.0 500.0 600.0 700.0 800.0 900.0
0 -10 -20 -30 -40 -50 -60 -70 -80 -90 -100
Depth (m)
Apperent Resistivity (ohm.m)
VES39
0.0 10000.0 20000.0 30000.0 40000.0 50000.0
0 -10 -20 -30 -40 -50 -60 -70 -80 -90 -100
Depth (m)
Apperent Resistivity (ohm.m)
VES40
0.0 200.0 400.0 600.0 800.0 1000.0 1200.0
0 -10 -20 -30 -40 -50 -60 -70 -80 -90 -100
Depth (m)
Apperent Resistivity (ohm.m)
VES41
0.0 200.0 400.0 600.0 800.0 1000.0 1200.0
0 -10 -20 -30 -40 -50 -60 -70 -80 -90 -100
Depth (m)
Apperent Resistivity (ohm.m)
VES42
0.0 500.0 1000.0 1500.0 2000.0
0 -10 -20 -30 -40 -50 -60 -70 -80 -90 -100
Depth (m)
Apperent Resistivity (ohm.m)

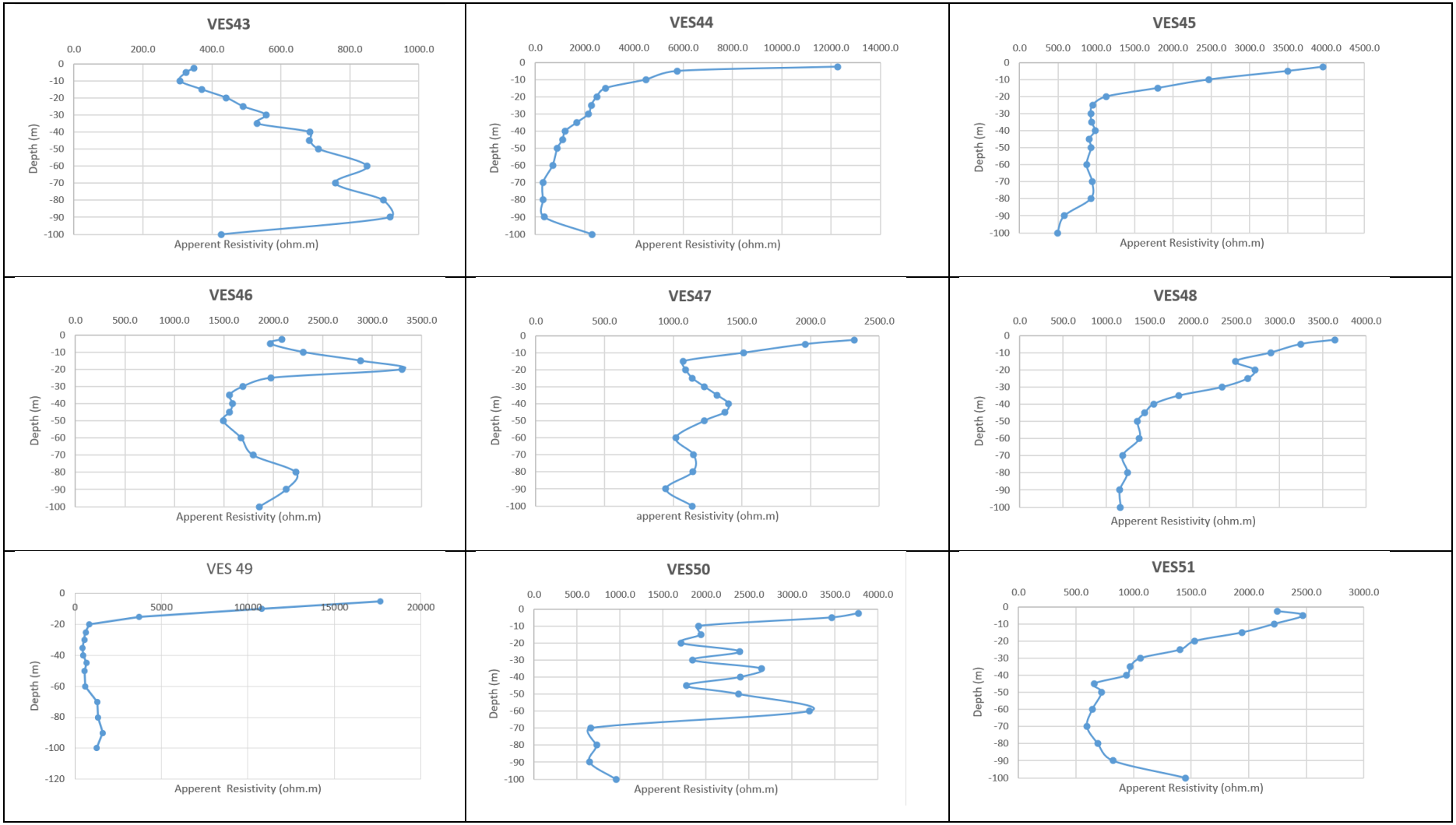
VES43
0.0 200.0 400.0 600.0 800.0 1000.0
0 -10 -20 -30 -40 -50 -60 -70 -80 -90 -100
Depth (m)
Apperent Resistivity (ohm.m)
VES44
0.0 2000.0 4000.0 6000.0 8000.0 10000.0 12000.0 14000.0
0 -10 -20 -30 -40 -50 -60 -70 -80 -90 -100
Depth (m)
Apperent Resistivity (ohm.m)
VES45
0.0 500.0 1000.0 1500.0 2000.0 2500.0 3000.0 3500.0 4000.0 4500.0
0 -10 -20 -30 -40 -50 -60 -70 -80 -90 -100
Depth (m)
Apperent Resistivity (ohm.m)
VES46
0.0 500.0 1000.0 1500.0 2000.0 2500.0 3000.0 3500.0
0 -10 -20 -30 -40 -50 -60 -70 -80 -90 -100
Depth (m)
Apperent Resistivity (ohm.m)
VES47
0.0 500.0 1000.0 1500.0 2000.0 2500.0
0 -10 -20 -30 -40 -50 -60 -70 -80 -90 -100
Depth (m)
apperent Resistivity (ohm.m)
VES48
0.0 500.0 1000.0 1500.0 2000.0 2500.0 3000.0 3500.0 4000.0
0 -10 -20 -30 -40 -50 -60 -70 -80 -90 -100
Depth (m)
Apperent Resistivity (ohm.m)
VES 49
0 5000 10000 15000 20000
0 -20 -40 -60 -80 -100 -120
Depth (m)
Apperent Resistivity (ohm.m)
VES50
0.0 500.0 1000.0 1500.0 2000.0 2500.0 3000.0 3500.0 4000.0
0 -10 -20 -30 -40 -50 -60 -70 -80 -90 -100
Depth (m)
Apperent Resistivity (ohm.m)
VES51
0.0 500.0 1000.0 1500.0 2000.0 2500.0 3000.0
0 -10 -20 -30 -40 -50 -60 -70 -80 -90 -100
Depth (m)
Apperent Resistivity (ohm.m)

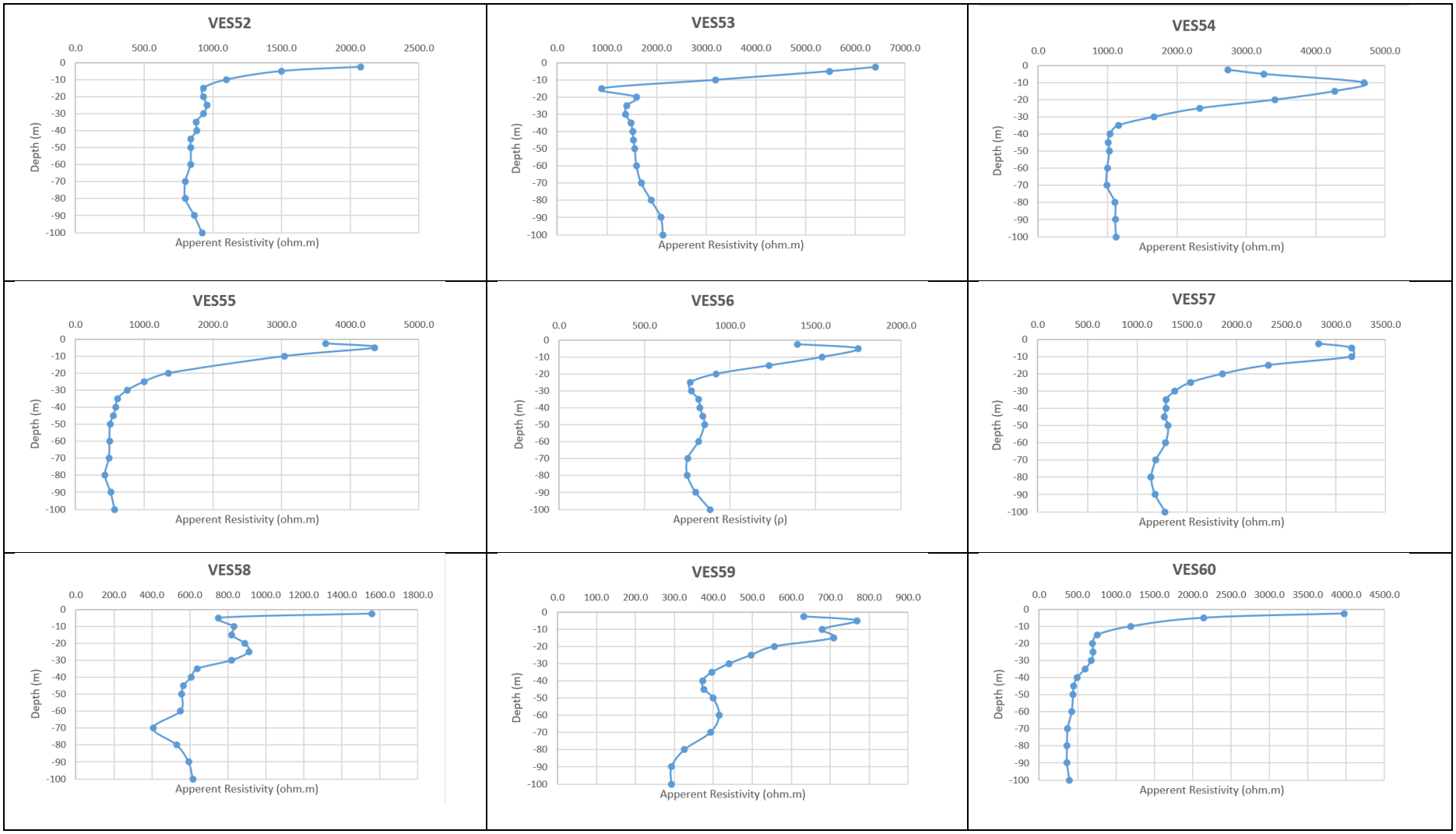
VES52
0.0 500.0 1000.0 1500.0 2000.0 2500.0
0 -10 -20 -30 -40 -50 -60 -70 -80 -90 -100
Depth (m)
Apperent Resistivity (ohm.m)
VES53
0.0 1000.0 2000.0 3000.0 4000.0 5000.0 6000.0 7000.0
0 -10 -20 -30 -40 -50 -60 -70 -80 -90 -100
Depth (m)
Apperent Resistivity (ohm.m)
VES54
0.0 1000.0 2000.0 3000.0 4000.0 5000.0
0 -10 -20 -30 -40 -50 -60 -70 -80 -90 -100
Depth (m)
Apperent Resistivity (ohm.m)
VES55
0.0 1000.0 2000.0 3000.0 4000.0 5000.0
0 -10 -20 -30 -40 -50 -60 -70 -80 -90 -100
Depth (m)
Apperent Resistivity (ohm.m)
VES56
0.0 500.0 1000.0 1500.0 2000.0
0 -10 -20 -30 -40 -50 -60 -70 -80 -90 -100
Depth (m)
Apperent Resistivity (ρ)
VES57
0.0 500.0 1000.0 1500.0 2000.0 2500.0 3000.0 3500.0
0 -10 -20 -30 -40 -50 -60 -70 -80 -90 -100
Depth (m)
Apperent Resistivity (ohm.m)
VES58
0.0 200.0 400.0 600.0 800.0 1000.0 1200.0 1400.0 1600.0 1800.0
0 -10 -20 -30 -40 -50 -60 -70 -80 -90 -100
Depth (m)
Apperent Resistivity (ohm.m)
VES59
0.0 100.0 200.0 300.0 400.0 500.0 600.0 700.0 800.0 900.0
0 -10 -20 -30 -40 -50 -60 -70 -80 -90 -100
Depth (m)
Apperent Resistivity (ohm.m)
VES60
0.0 500.0 1000.0 1500.0 2000.0 2500.0 3000.0 3500.0 4000.0 4500.0
0 -10 -20 -30 -40 -50 -60 -70 -80 -90 -100
Depth (m)
Apperent Resistivity (ohm.m)

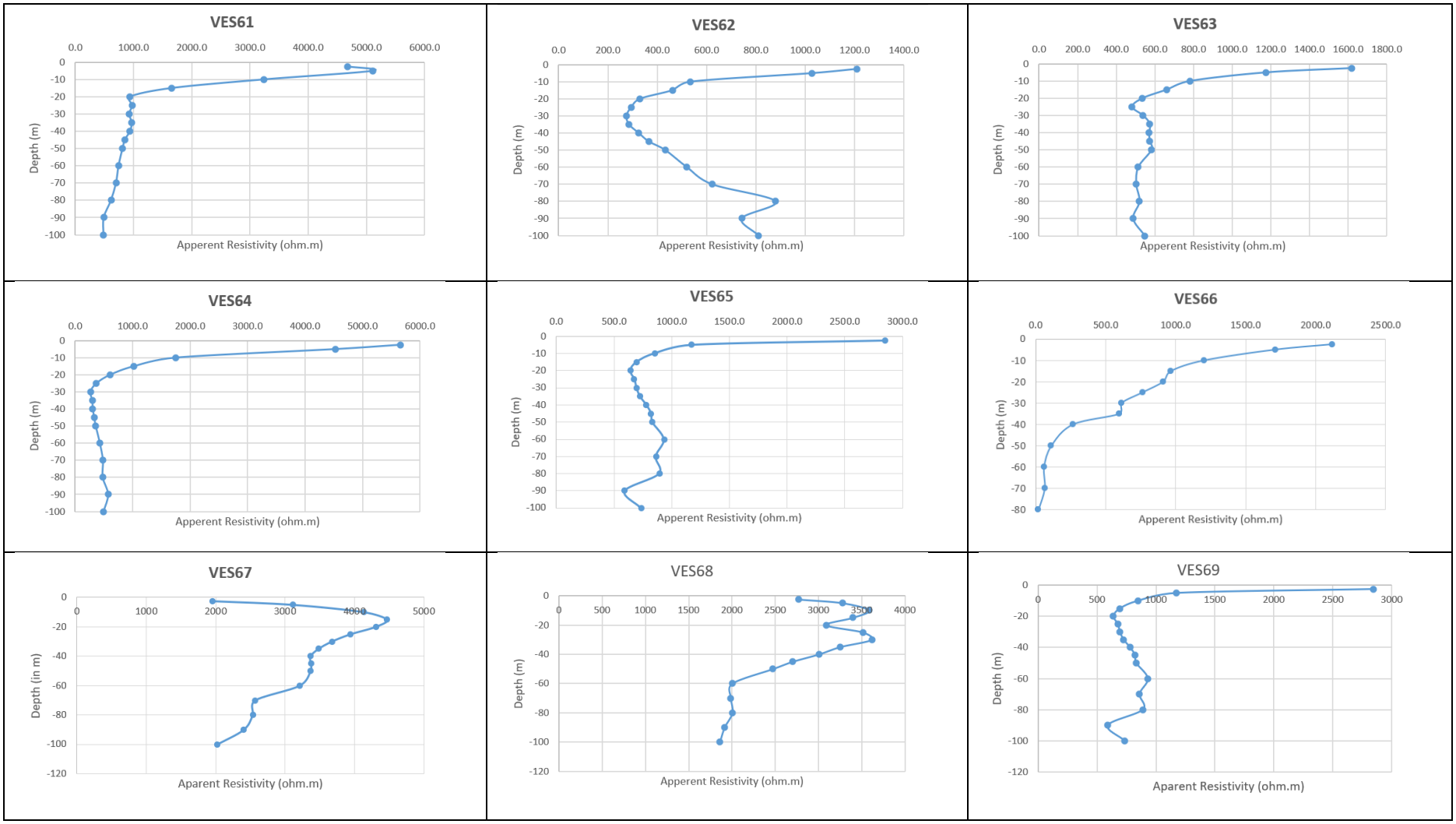
VES61
Depth (m)
Apperent Resistivity (ohm.m)
VES62
Depth (m)
Apperent Resistivity (ohm.m)
VES63
Depth (m)
Apperent Resistivity (ohm.m)
VES64
Depth (m)
Apperent Resistivity (ohm.m)
VES65
Depth (m)
Apperent Resistivity (ohm.m)
VES66
Depth (m)
Apperent Resistivity (ohm.m)
VES67
Depth (in m)
Aparent Resistivity (ohm.m)
VES68
Depth (m)
Apperent Resistivity (ohm.m)
VES69
Depth (m)
Aparent Resistivity (ohm.m)

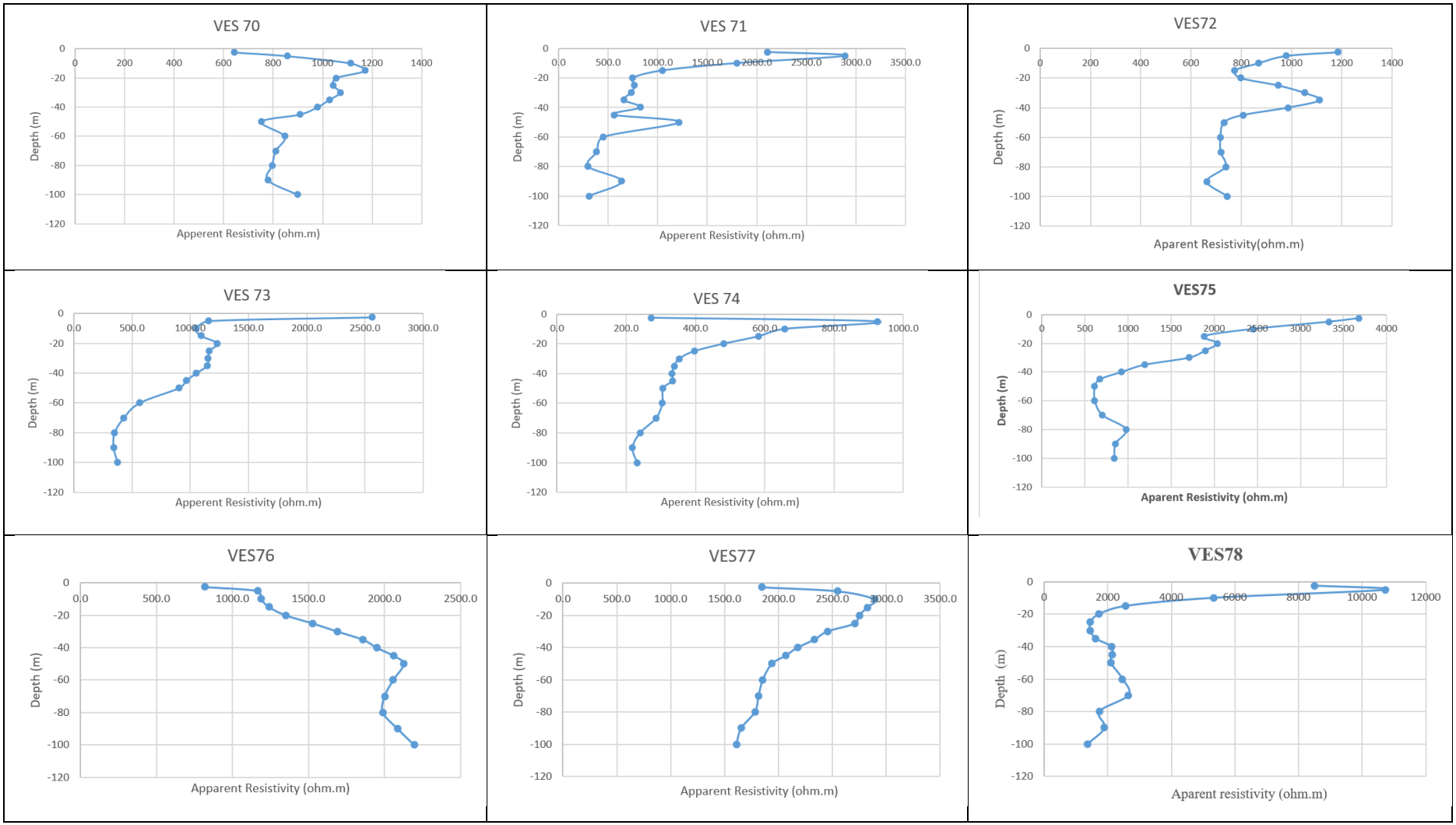
VES 70
Depth (m)
Apperent Resistivity (ohm.m)
VES 71
Depth (m)
Apperent Resistivity (ohm.m)
VES72
Depth (m)
Aparent Resistivity(ohm.m)
VES 73
Depth (m)
Apperent Resistivity (ohm.m)
VES 74
Depth (m)
Aperent Resistivity (ohm.m)
VES75
Depth (m)
Aparent Resistivity (ohm.m)
VES76
Depth (m)
Apparent Resistivity (ohm.m)
VES77
Depth (m)
Apparent Resistivity (ohm.m)
VES78
Depth (m)
Aparent resistivity (ohm.m)

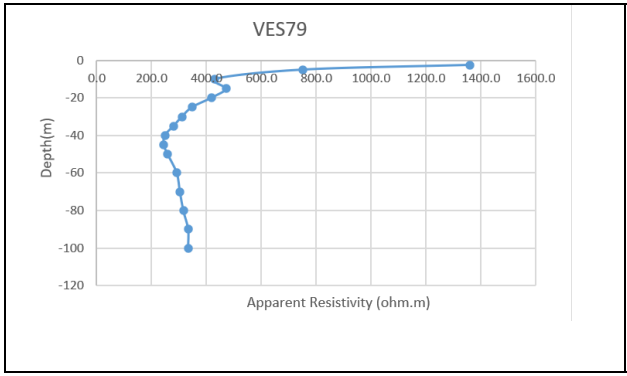
VES79
Depth(m)
Apparent Resistivity (ohm.m)

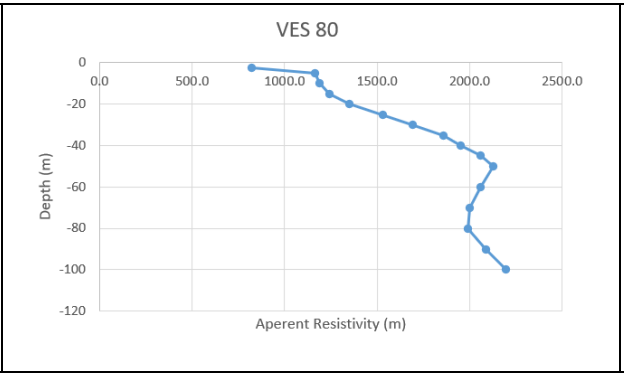
VES 80
Depth (m)
Aperent Resistivity (m)

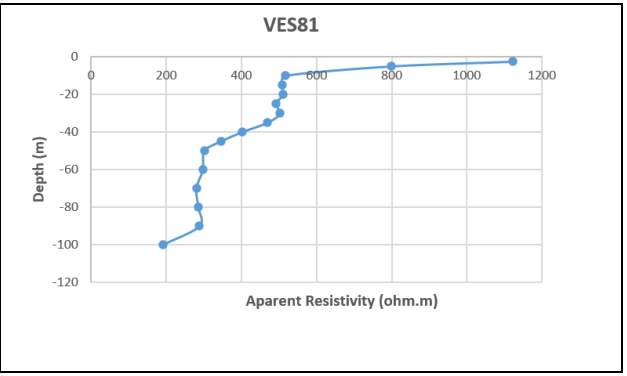
VES81
Depth (m)
Aparent Resistivity (ohm.m)

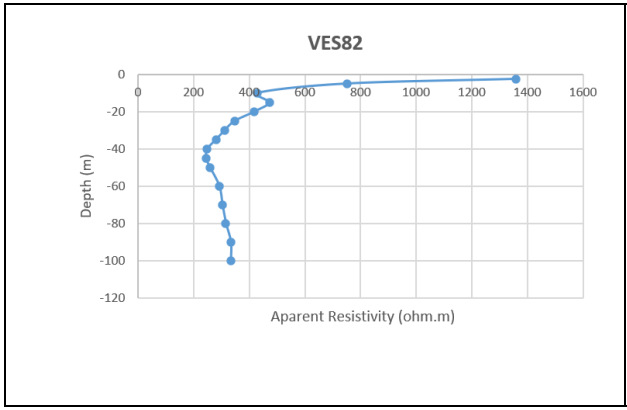
VES82
Depth (m)
Aparent Resistivity (ohm.m)

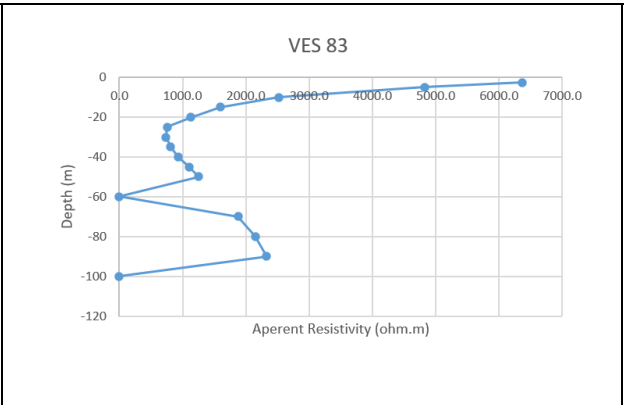
VES 83
Depth (m)
Aperent Resistivity (ohm.m)

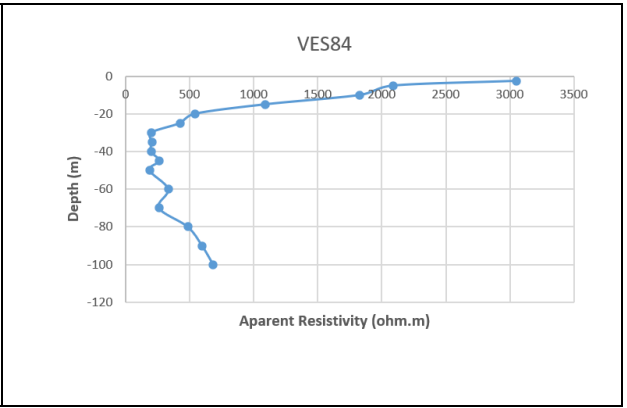
VES84
Depth (m)
Aparent Resistivity (ohm.m)

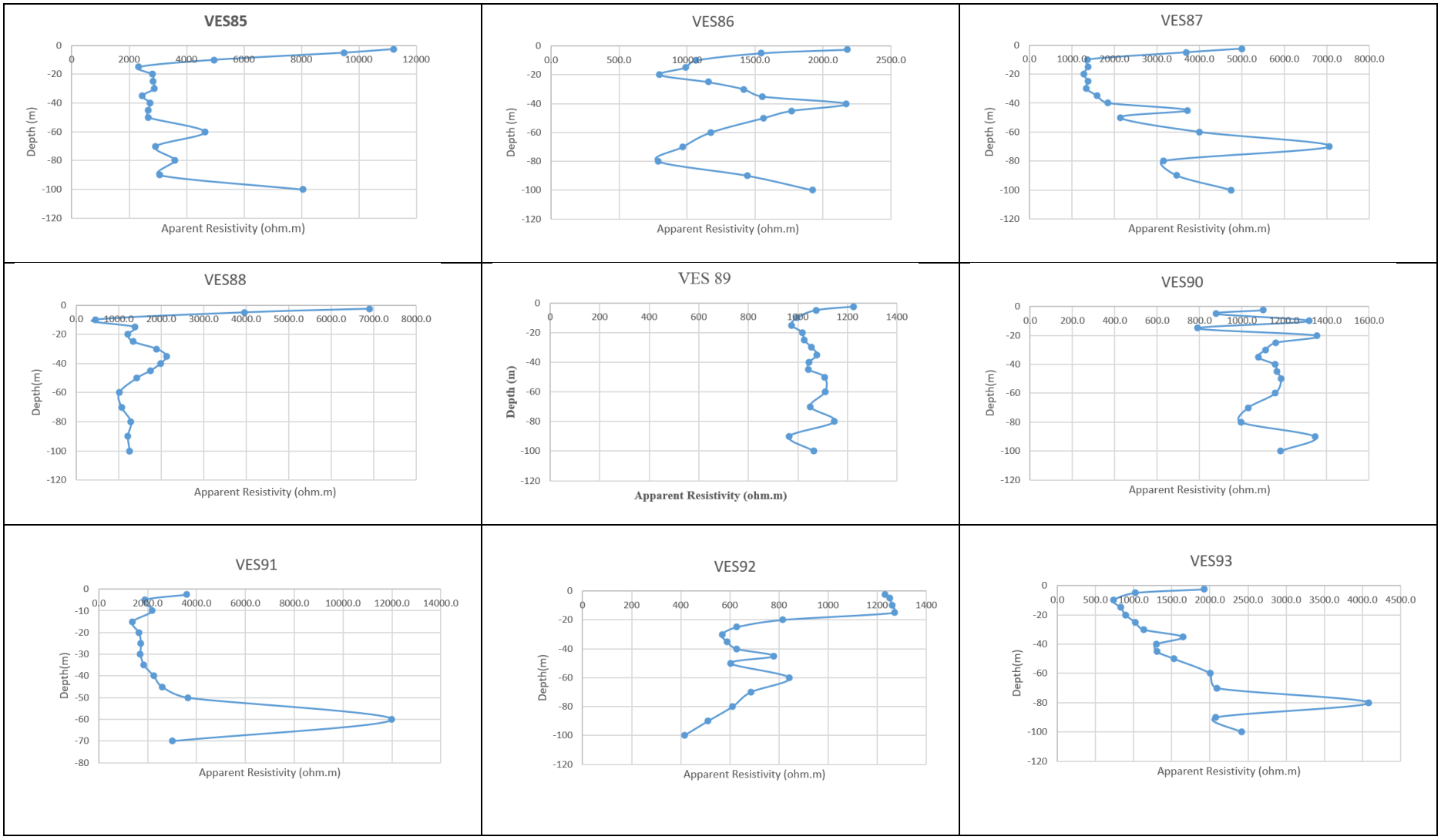
VES85
Depth (m)
Aparent Resistivity (ohm.m)
VES86
Depth (m)
Apparent Resistivity (ohm.m)
VES87
Depth (m)
Apparent Resistivity (ohm.m)
VES88
Depth(m)
Apparent Resistivity (ohm.m)
VES 89
Depth (m)
Apparent Resistivity (ohm.m)
VES90
Depth(m)
Apparent Resistivity (ohm.m)
VES91
Depth(m)
Apparent Resistivity (ohm.m)
VES92
Depth(m)
Apparent Resistivity (ohm.m)
VES93
Depth(m)
Apparent Resistivity (ohm.m)

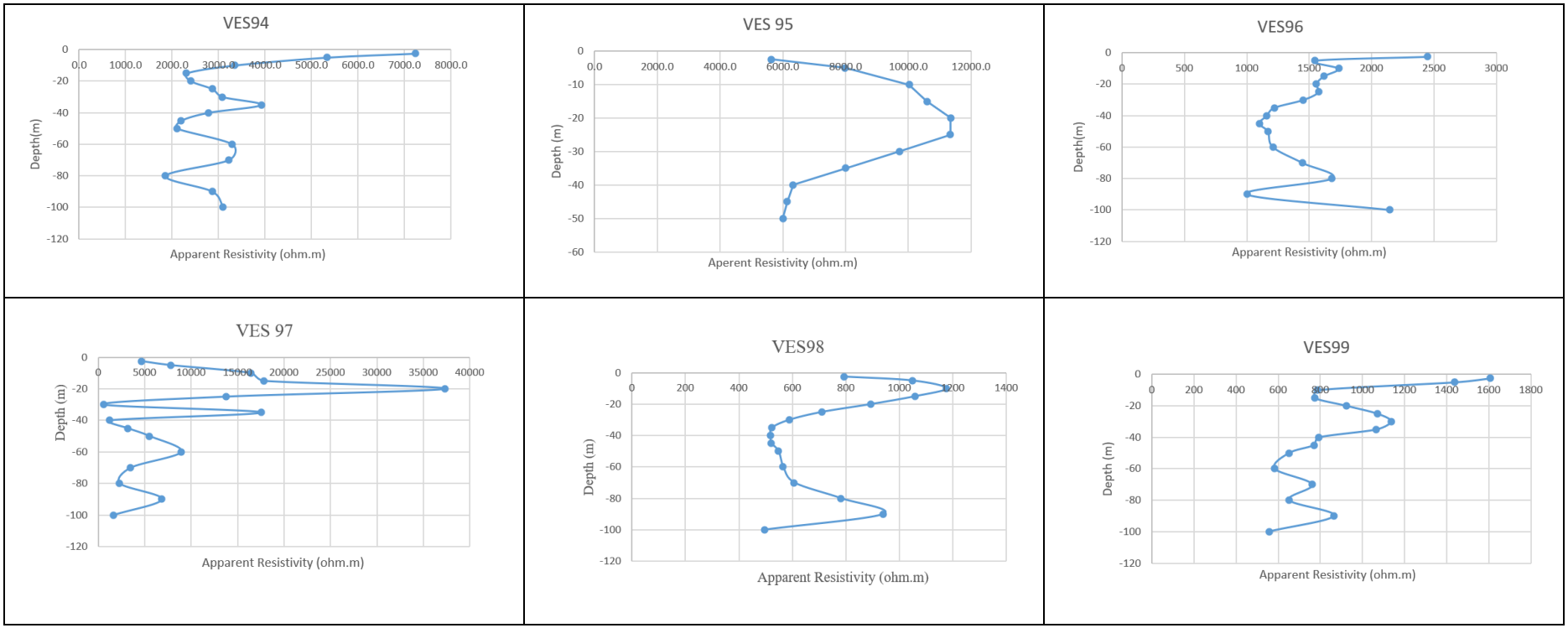
VES94
Depth(m)
Apparent Resistivity (ohm.m)
VES 95
Depth (m)
Aperent Resistivity (ohm.m)
VES96
Depth(m)
Apparent Resistivity (ohm.m)
VES 97
Depth (m)
Apparent Resistivity (ohm.m)
VES98
Depth (m)
Apparent Resistivity (ohm.m)
VES99
Depth (m)
Apparent Resistivity (ohm.m)

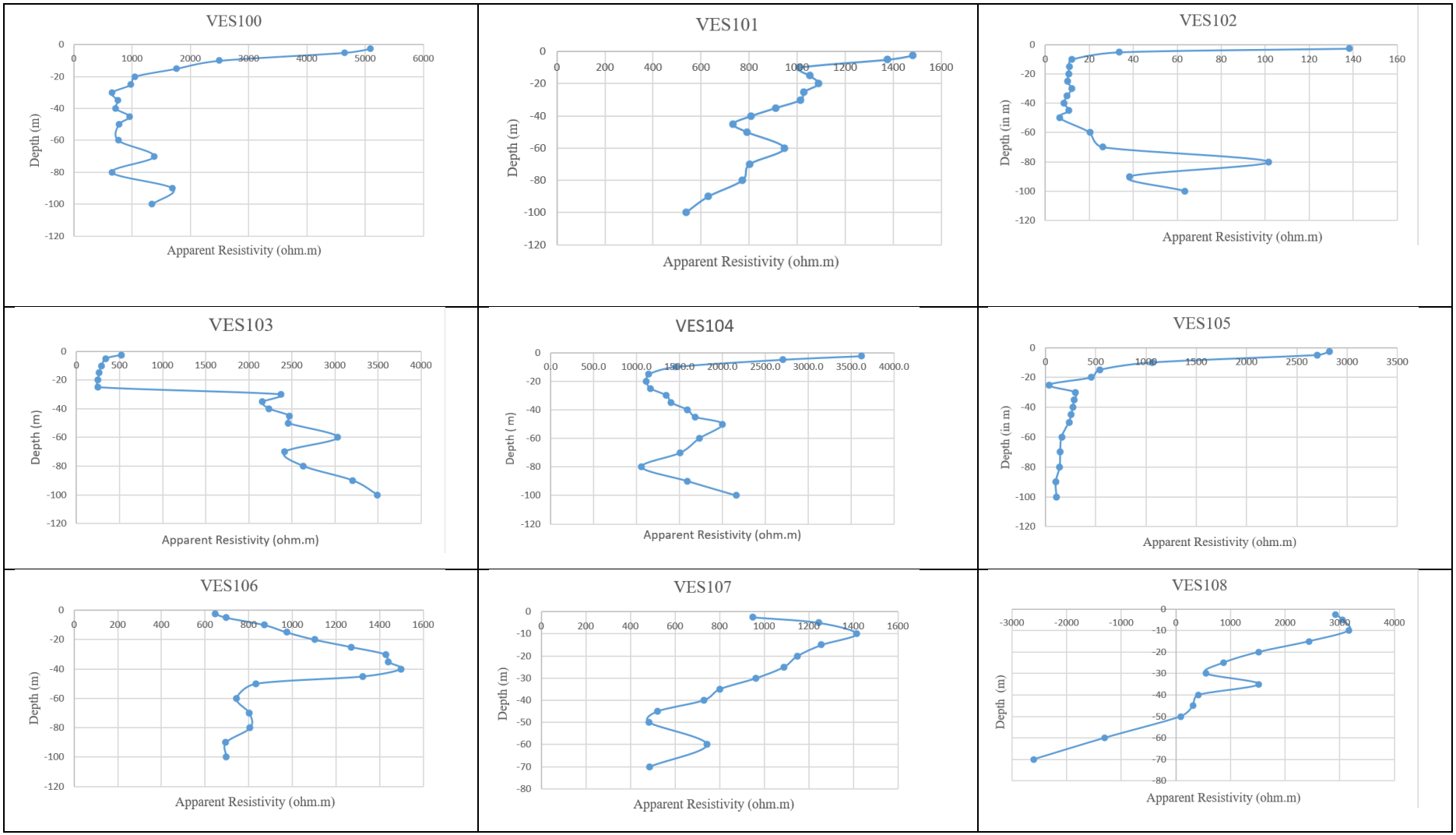
VES100
Depth (m)
Apparent Resistivity (ohm.m)
VES101
Depth (m)
Apparent Resistivity (ohm.m)
VES102
Depth (in m)
Apparent Resistivity (ohm.m)
VES103
Depth (m)
Apparent Resistivity (ohm.m)
VES104
Depth (m)
Apparent Resistivity (ohm.m)
VES105
Depth (in m)
Apparent Resistivity (ohm.m)
VES106
Depth (m)
Apparent Resistivity (ohm.m)
VES107
Depth (m)
Apparent Resistivity (ohm.m)
VES108
Depth (m)
Apparent Resistivity (ohm.m)

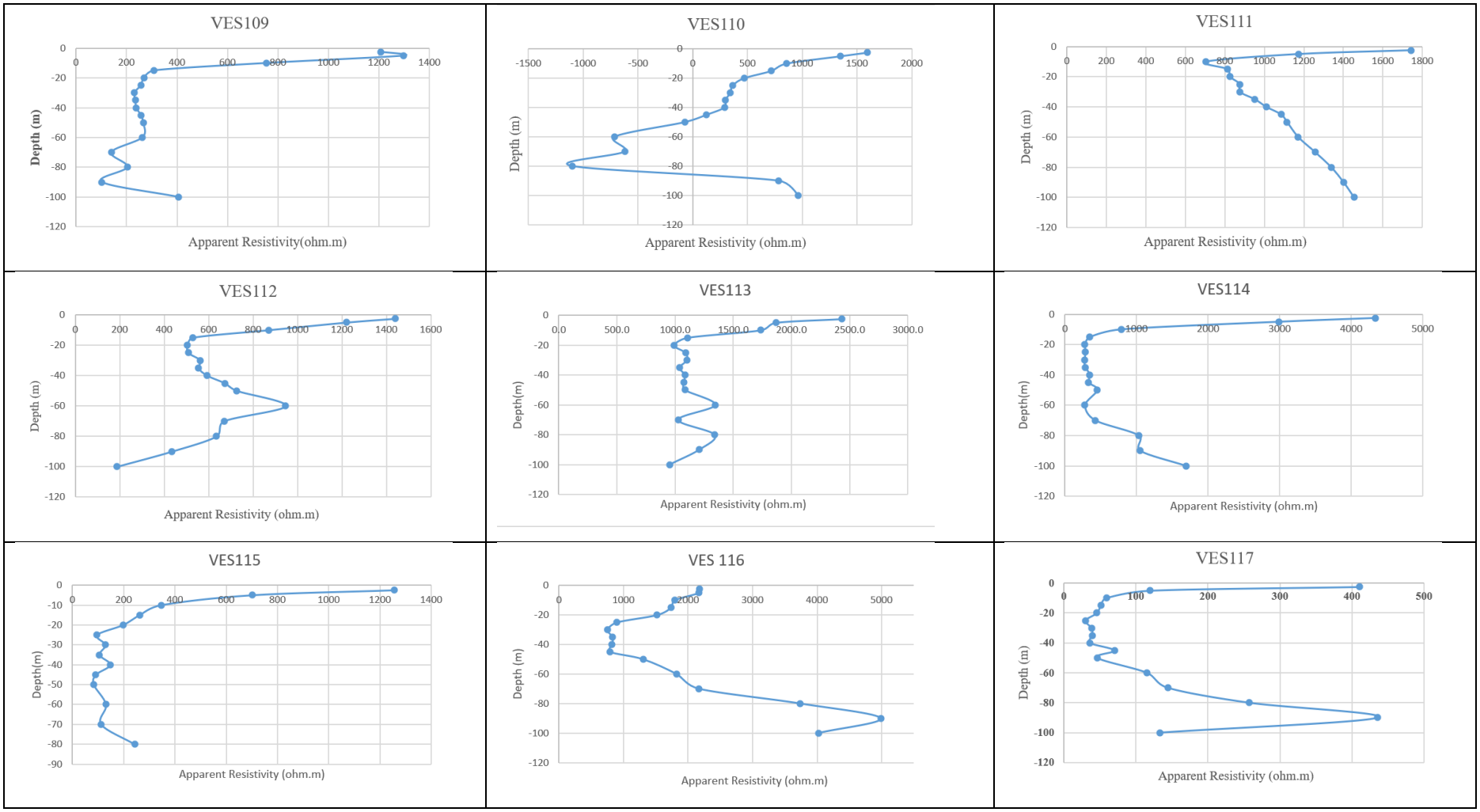
VES109
Depth (m)
Apparent Resistivity(ohm.m)
VES110
Depth (m)
Apparent Resistivity (ohm.m)
VES111
Depth (m)
Apparent Resistivity (ohm.m)
VES112
Depth (m)
Apparent Resistivity (ohm.m)
VES113
Depth(m)
Apparent Resistivity (ohm.m)
VES114
Depth(m)
Apparent Resistivity (ohm.m)
VES115
Depth(m)
Apparent Resistivity (ohm.m)
VES 116
Depth (m)
Apparent Resistivity (ohm.m)
VES117
Depth (m)
Apparent Resistivity (ohm.m)

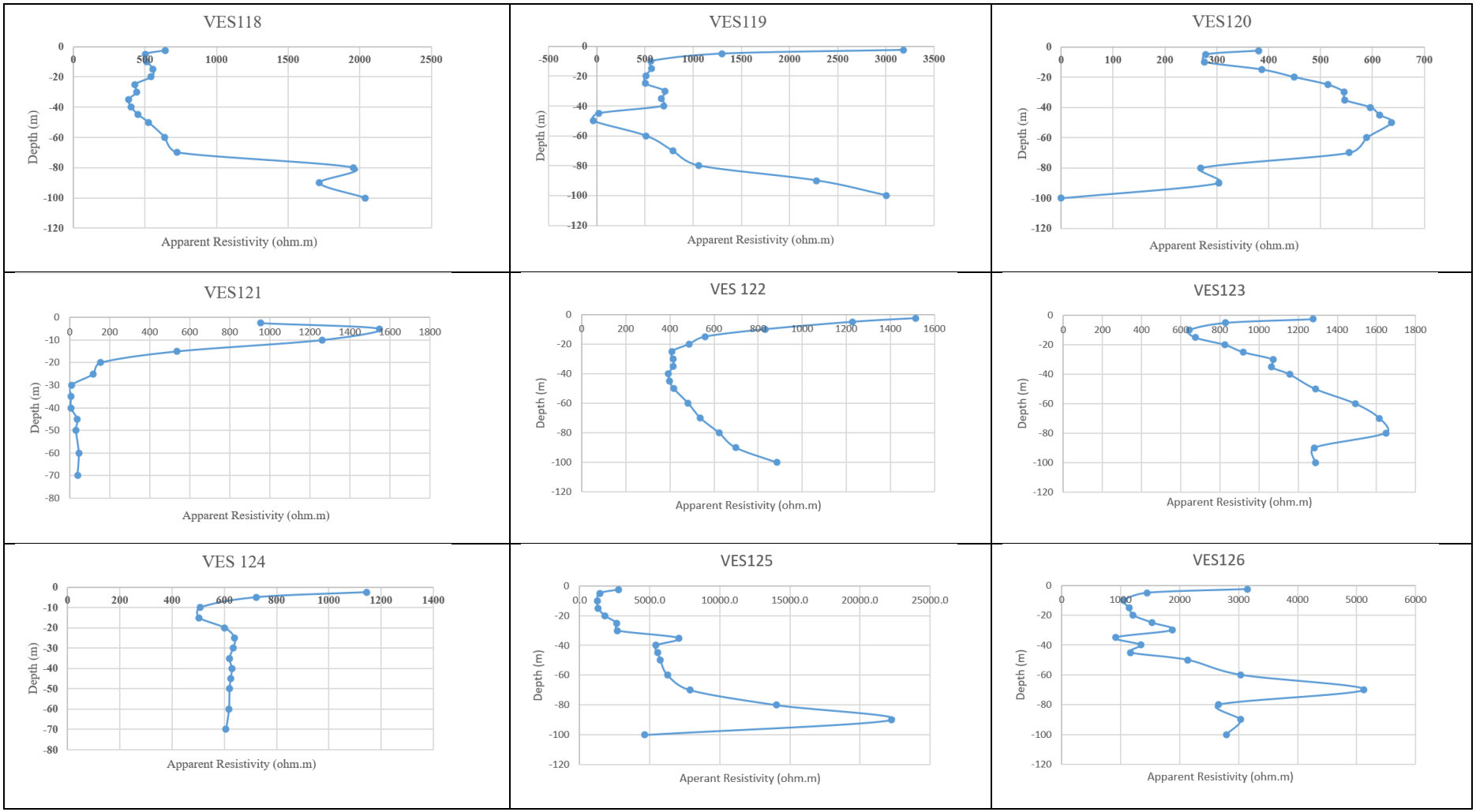
VES118
Depth (m)
Apparent Resistivity (ohm.m)
VES119
Depth (m)
Apparent Resistivity (ohm.m)
VES120
Depth (m)
Apparent Resistivity (ohm.m)
VES121
Depth (m)
Apparent Resistivity (ohm.m)
VES 122
Depth (m)
Apparent Resistivity (ohm.m)
VES123
Depth (m)
Apparent Resistivity (ohm.m)
VES 124
Depth (m)
Apparent Resistivity (ohm.m)
VES125
Depth (m)
Aperant Resistivity (ohm.m)
VES126
Depth (m)
Apparent Resistivity (ohm.m)

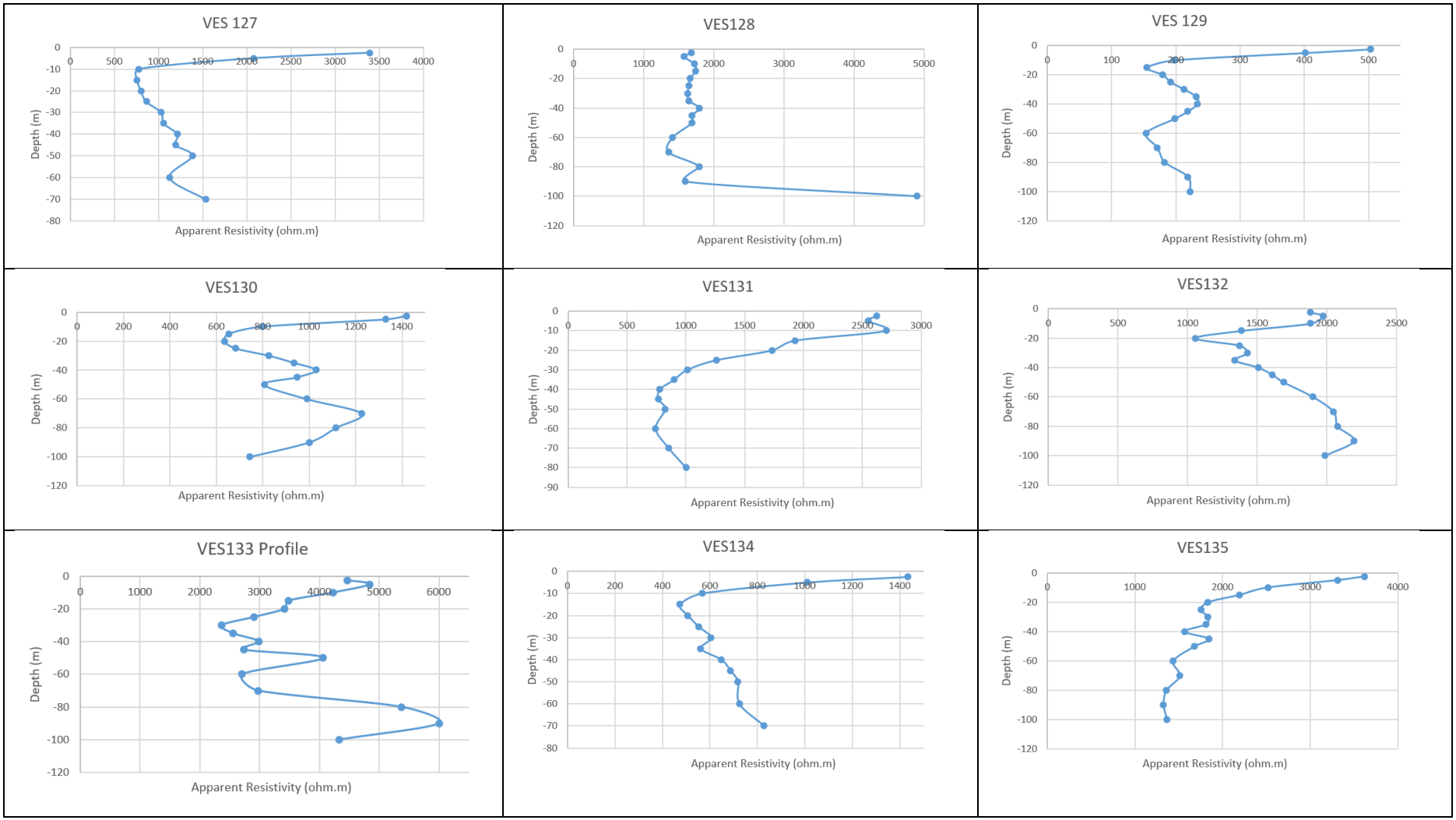
VES 127
Depth (m)
Apparent Resistivity (ohm.m)
VES128
Depth (m)
Apparent Resistivity (ohm.m)
VES 129
Depth (m)
Apparent Resistivity (ohm.m)
VES130
Depth (m)
Apparent Resistivity (ohm.m)
VES131
Depth (m)
Apparent Resistivity (ohm.m)
VES132
Depth (m)
Apparent Resistivity (ohm.m)
VES133 Profile
Depth (m)
Apparent Resistivity (ohm.m)
VES134
Depth (m)
Apparent Resistivity (ohm.m)
VES135
Depth (m)
Apparent Resistivity (ohm.m)

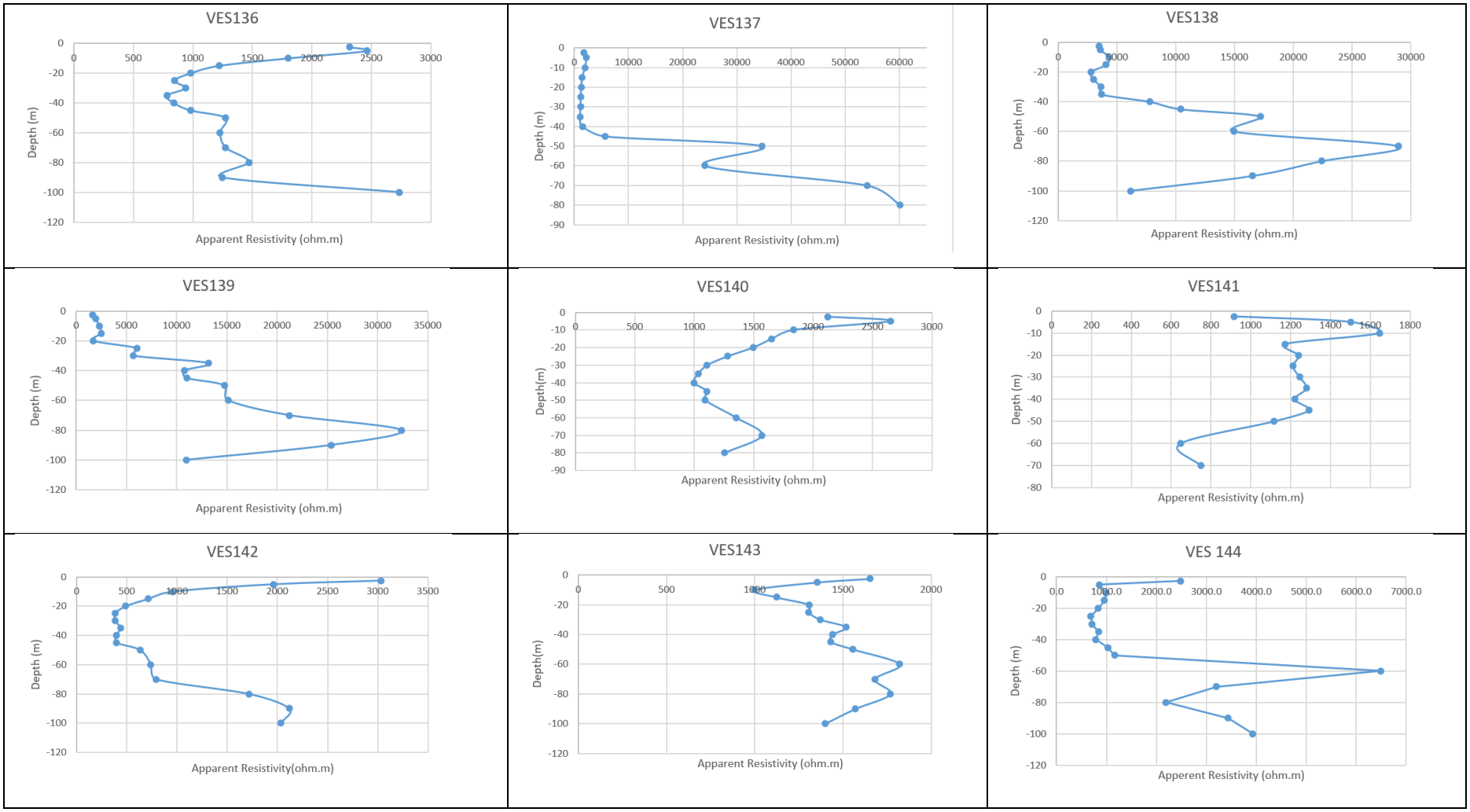
VES136
Depth (m)
Apparent Resistivity (ohm.m)
VES137
Depth (m)
Apparent Resistivity (ohm.m)
VES138
Depth (m)
Apparent Resistivity (ohm.m)
VES139
Depth (m)
Apparent Resistivity (ohm.m)
VES140
Depth(m)
Apparent Resistivity (ohm.m)
VES141
Depth (m)
Apperent Resistivity (ohm.m)
VES142
Depth (m)
Apparent Resistivity(ohm.m)
VES143
Depth(m)
Apparent Resistivity (ohm.m)
VES 144
Depth (m)
Apperent Resistivity (ohm.m)

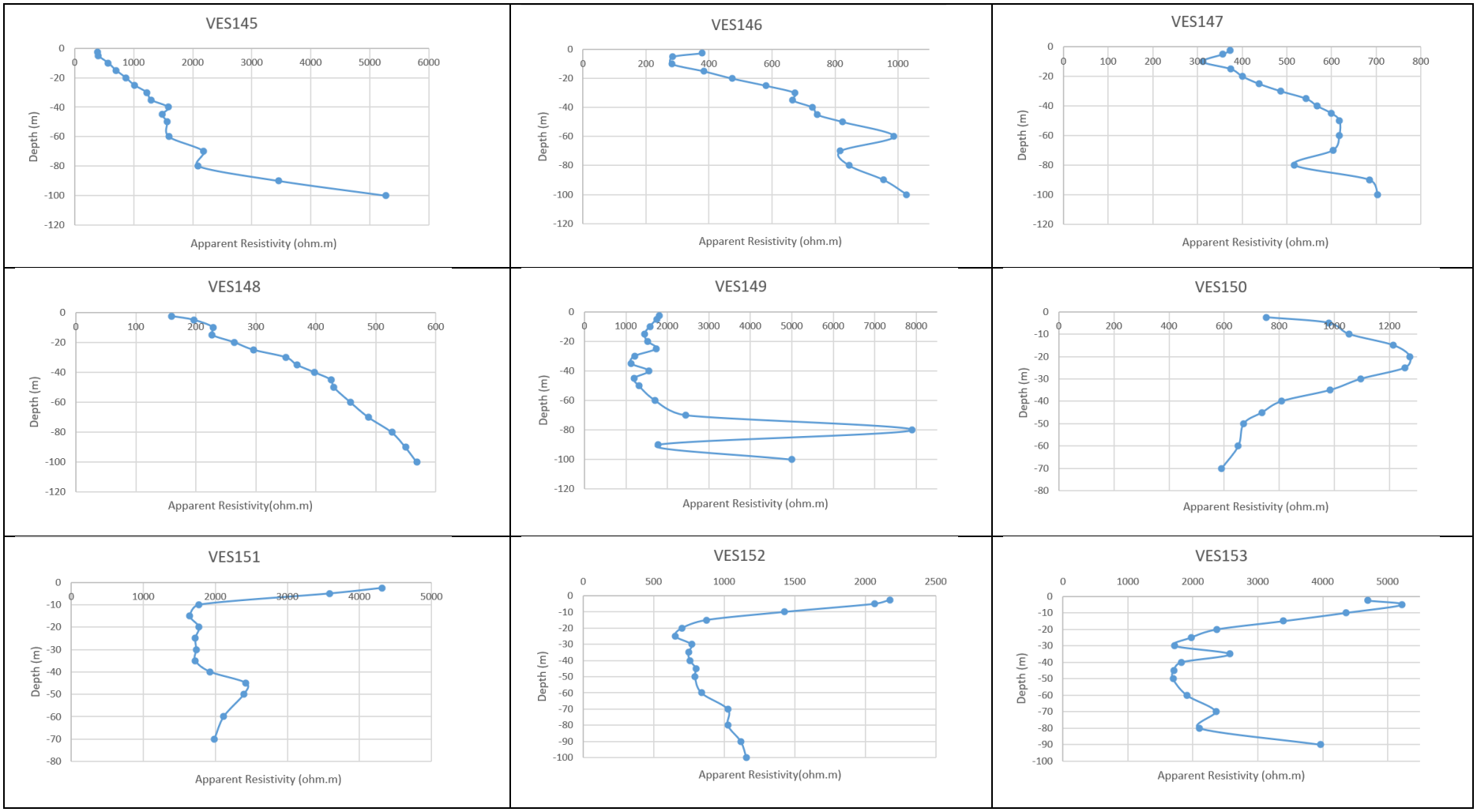
VES145
Depth (m)
Apparent Resistivity (ohm.m)
VES146
Depth (m)
Apparent Resistivity (ohm.m)
VES147
Depth (m)
Apparent Resistivity (ohm.m)
VES148
Depth (m)
Apparent Resistivity(ohm.m)
VES149
Depth (m)
Apparent Resistivity (ohm.m)
VES150
Depth (m)
Apparent Resistivity (ohm.m)
VES151
Depth (m)
Apparent Resistivity (ohm.m)
VES152
Depth (m)
Apparent Resistivity(ohm.m)
VES153
Depth (m)
Apparent Resistivity (ohm.m)

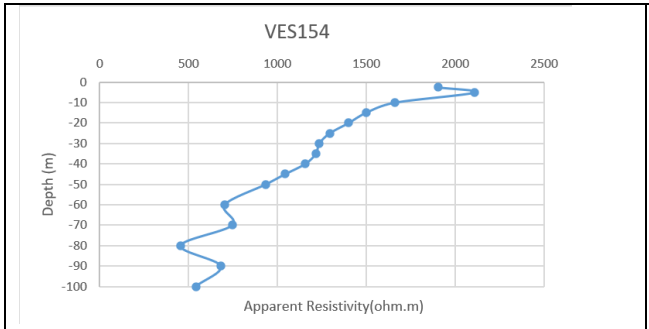 VES154 0 500 1000 1500 2000 2500 0 -10 -20 -30 -40 -50 -60 -70 -80 -90 -100 Depth (m) Apparent Resistivity(ohm.m)		

Annexure XXI_Details of Petrographical Description of Borehole Samples

Sl. No	Sample ID	BH_ID	Depth (m)	Study Result
1	110071	GSPL/AL/BH-01	36.75	Quartz-sericite-graphite schist with quartz- carbonate veins. Coarse grained flakey graphite notes which are not parallel to the foliation (post deformation graphite formation). Smaller graphite flakes are syn deformational. Pyrite present.
2	110076	GSPL/AL/BH-01	81.4	quartz-sericite-graphite schist. Dessiminated pyrite of various size. Amorphos graphite scattered in the slide.
3	114201	GSPL/AL/BH-01	25.2	Alternate bands of quartz with secondary carbonates and bands rich in muscovite, chlorite, graphite and pyrite. Graphite occurs as concordant bands within the schist, with very fine graphite flakes/sringers are aligned parallel to the schistosity. Three distinct graphite-bearing bands have been identified, of which the middle band contains the highest concentration of graphite, comprising approximately 15–20% of the band. Apatite and epidote are noted within the graphite-rich bands. Pyrite is abundantly present and is closely associated with the graphite-rich horizons.
4	114202	GSPL/AL/BH-01	40.5	quartz–muscovite/sericite–graphite schist with a few quartz veins. The veins comprise polycrystalline quartz with secondary carbonates. Fine specks of graphite with irregular grain boundaries are disseminated throughout the thin section. Pyrite is profusely developed and minor chalcopyrite is also observed
5	114203	GSPL/AL/BH-01	58.3	graphite bearing quartz-mica schist. Dessiminated pyrite of various size. Medium sized grains of graphite with irregular grain boundary scattered in the rock.
6	113501	GSPL/AL/BH-03	53.36	Under the petrographic microscope, graphite appears completely opaque in plane- polarized light (PPL), showing black colour with sharp grain boundaries. It commonly occurs in flaky and often aligned parallel to the foliation in schists. In crossed polars (XPL), graphite remains black due to its opacity and does not show interference colour. The chalcopyrite occurs in disseminated form.
7	114204	GSPL/AL/BH-03	39.2	In thin section, the rock shows a well-developed schistose texture with strong foliation defined by the parallel alignment of platy minerals of chlorite and muscovite. Chlorite appears pale to green in plane-polarized light with weak pleochroism and shows low first-order interference colour under crossed polars. Muscovite is colourless in PPL, exhibits perfect cleavage and displays bright second-order interference colours in XPL. Quartz is commonly present as colourless, anhedral grains with low first-order gray interference colours. The rock is chlorite muscovite schist.
8	114205	GSPL/AL/BH-03	43.5	Pyrite appears pale brass-yellow in reflected light with high reflectance and cubic crystal form although in section part of it shows. In transmitted light it is opaque, appearing black in both PPL and XPL with no interference colours.
9	114206	GSPL/AL/BH-03	66.7	Graphite flakes occurring within recrystallized quartz appear as opaque, black, platy to flaky grains in thin section. In plane-polarized light (PPL) and crossed polars (XPL), graphite remains completely black due to its opacity, while the surrounding quartz is colourless in PPL and shows low first-order gray interference colours in XPL. The quartz typically exhibits a granoblastic texture with interlocking, equigranular crystals formed by recrystallization during metamorphism. Graphite flakes may occur as inclusions within quartz grains or along grain boundaries, sometimes showing alignment parallel to foliation.
10	114207	GSPL/AL/BH-02	27.8	In thin section, pyrite and chalcopyrite occurring in schist appear as opaque sulphide minerals. In transmitted light (PPL and XPL), both remain black due to their opacity. In reflected light, pyrite shows a pale brass-yellow colour with high reflectance and commonly cubic form, whereas chalcopyrite appears deeper brassy yellow with slightly lower reflectance and may show anisotropy. These sulphides commonly occur as disseminated grains or along foliation planes within the schist.
11	114208	GSPL/AL/BH-05	47.8	Intense chlorite–muscovite schist in thin section shows a strongly foliated, lepidoblastic texture with well-aligned platy minerals. Chlorite appears pale to green in plane-polarized light (PPL) with weak pleochroism and low first-order interference colour in crossed polars (XPL). Muscovite is colourless in PPL, displays perfect basal cleavage and shows bright second-order interference colour in XPL. Quartz is present as interlocking, anhedral grains with low first-order gray interference colour. The strong alignment of chlorite and muscovite reflects high foliation development during low- to medium-grade regional metamorphism.
12	113523	GSPL/AL/BH-07	44.57	Graphite occurs as opaque, black, platy to flaky grains enclosed within recrystallized quartz in thin section. Under plane-polarized light (PPL) as well as crossed nicols (XPL), graphite remains completely opaque and appears black, whereas quartz is colourless in PPL and displays low first-order grey interference colours in XPL. The quartz grains commonly show a granoblastic texture characterized by interlocking, equigranular crystals formed due to metamorphic recrystallization. Graphite flakes are present both as inclusions within quartz grains and along grain boundaries, locally exhibiting preferred orientation parallel to the foliation, indicating deformation and metamorphic alignment.
13	113514	GSPL/AL/BH-05	40.35	Graphite is present as opaque, black, flaky to platy grains associated with recrystallized quartz in thin section. The graphite remains completely black under both plane-polarized light (PPL) and crossed polarized light (XPL) owing to its opaque nature. The surrounding quartz appears

Sl. No	Sample ID	BH_ID	Depth (m)	Study Result
				colourless in PPL and exhibits low first-order grey interference colours in XPL. Quartz grains commonly display a granoblastic texture consisting of interlocking, equigranular crystals formed during metamorphic recrystallization. Graphite flakes occur either as inclusions within quartz grains or concentrated along grain boundaries and locally show a preferred alignment parallel to the foliation, reflecting metamorphic deformation and mineral segregation.
14	114209	BH-06	20.5	Graphite occurs as opaque, black, flaky to platy grains within recrystallized quartz. The graphite remains completely opaque under both plane-polarized light (PPL) and crossed polars (XPL). Quartz is colourless in PPL and shows low first-order grey interference colours in XPL, displaying a granoblastic texture formed by metamorphic recrystallization. Graphite flakes occur as inclusions within quartz and along grain boundaries, locally aligned parallel to foliation, indicating metamorphic deformation and mineral segregation
15	114210	BH-06	50.4	Graphite occurs as opaque, black, platy to flaky grains enclosed within recrystallized quartz. Under both PPL and XPL, graphite remains completely opaque, whereas quartz appears colourless in PPL and displays low first-order grey interference colours in XPL. The quartz shows a granoblastic texture with interlocking, equigranular recrystallized grains. Graphite flakes occur as inclusions within quartz and along grain boundaries, locally aligned parallel to foliation, indicating metamorphic recrystallization and deformation.
16	113541	BH-06	75.3	Graphite occurs as opaque, black, flaky grains within recrystallized quartz. Quartz appears colourless in PPL and shows low first-order grey interference colours in XPL, displaying a granoblastic recrystallized texture. Graphite flakes occur as inclusions and along grain boundaries, locally aligned parallel to foliation, indicating metamorphic deformation.
17	110085	BH-02	42.15	Under the petrographic microscope, graphite appears completely opaque and black in plane-polarized light (PPL) with well-defined grain boundaries. It commonly occurs as flaky grains, locally aligned parallel to foliation in schistose rocks. In crossed polars (XPL), graphite remains black and shows no interference colours due to its opaque nature. Chalcopyrite occurs in disseminated form within the rock matrix.
18	114211	BH-07	27.3	Under the petrographic microscope, graphite is observed as opaque, black grains in plane-polarized light (PPL) with distinct grain boundaries. It typically occurs as flaky aggregates showing preferred orientation parallel to foliation in schistose rocks. In crossed polars (XPL), graphite remains completely black and lacks interference colours because of its opacity. Chalcopyrite is present as disseminated mineralization within the rock matrix.
19	114212	BH-08	38	Graphite occurs as opaque, black, flaky to platy grains within recrystallized quartz. The graphite remains completely opaque under both plane-polarized light (PPL) and crossed polars (XPL). Quartz is colourless in PPL and shows low first-order grey interference colours in XPL, displaying a granoblastic texture formed by metamorphic recrystallization. Graphite flakes occur as inclusions within quartz and along grain boundaries, locally aligned parallel to foliation, indicating metamorphic deformation and mineral segregation
20	114213	BH-10	13.5	Graphite occurs as opaque, black, flaky to platy grains within recrystallized quartz and remains completely black under both PPL and XPL. Quartz appears colourless in PPL and shows low first-order grey interference colours in XPL with granoblastic, equigranular texture. Graphite flakes occur as inclusions and along grain boundaries, locally aligned parallel to foliation.
21	114214	BH-11	31.6	Graphite occurs as opaque, black, platy to flaky grains enclosed within recrystallized quartz in thin section. It remains completely black under both plane-polarized light (PPL) and crossed polars (XPL) due to its opaque nature. The surrounding quartz appears colourless in PPL and displays low first-order grey interference colours in XPL, exhibiting a granoblastic texture of interlocking, equigranular recrystallized grains. Graphite flakes are present as inclusions within quartz as well as along grain boundaries, locally aligned parallel to foliation, indicating metamorphic recrystallization and deformation.
22	114215	BH-11	62.8	Graphite is present as opaque, black, platy to flaky grains associated with recrystallized quartz and remains black in both PPL and XPL. Quartz appears colourless in PPL and exhibits low first-order grey interference colours in XPL with a granoblastic recrystallized texture. Graphite commonly occurs along grain boundaries or as inclusions within quartz, locally showing foliation-parallel alignment.
23	114216	BH-11	73.8	graphite bearing quartz-mica schist. Desseminated pyrite of various size. Medium sized grains of graphite with irregular grain boundary scattered in the rock.
24	114217	BH-04	8.5	Graphite occurs as opaque, black, platy to flaky grains within recrystallized quartz and remains completely black under both PPL and XPL. Quartz is colourless in PPL and shows low first-order grey interference colours in XPL, displaying a granoblastic recrystallized texture. Graphite flakes are present along grain boundaries and as inclusions within quartz, locally aligned parallel to foliation.
25	114218	BH-04	27.9	Graphite occurs as opaque, black, flaky to platy grains within recrystallized quartz and remains completely black under both PPL and XPL. Quartz appears colourless in PPL and shows low first-order grey interference colours in XPL with granoblastic, equigranular texture. Graphite flakes occur as inclusions and along grain boundaries, locally aligned parallel to foliation.

Annexure XXII_XRF Data of Borehole Samples with Additional 2 Elements Sn, W (All data in %)

SL No	Sample ID	Borehole No	From (m)	To (m)	Length	Al_2O_3	BaO	CaO	Cr_2O_3	Fe_2O_3	K_2O	MgO	MnO	Na_2O	P_2O_5	SiO_2	SO_3	SnO_2	TiO_2	V_2O_5	WO_3	LOI@ 950°C
1	110071	BH-01	36.5	37	0.5	9.553	0.253	8.124	0.068	4.137	2.864	5.801	0.089	0.333	0.273	49.186	0.103	<0.05	0.48	0.251	0.094	17.40
2	110076	BH-01	81	82	1	12.82	0.23	3.26	<0.05	3.05	2.05	1.70	0.05	2.64	0.10	64.40	2.48	<0.05	0.36	0.07	<0.05	6.33
3	110081	BH-02	19	20	1	13.95	0.21	3.08	0.06	3.81	2.45	3.27	<0.05	1.17	0.10	59.91	1.05	<0.05	0.44	0.14	0.06	10.00
4	110082	BH-02	22	23	1	10.83	0.76	3.56	<0.05	4.38	2.68	3.42	<0.05	0.37	0.08	61.49	4.16	<0.05	0.41	<0.05	<0.05	7.71
5	110083	BH-02	27	28	1	9.451	0.137	4.27	0.059	3.717	1.95	1.26	0.059	0.991	0.149	66.885	2.169	<0.05	0.312	0.063	0.05	8.07
6	110085	BH-02	42	43	1	10.92	<0.05	2.26	<0.05	5.47	2.04	1.77	0.10	3.11	0.16	71.33	0.16	<0.05	0.69	<0.05	<0.05	1.67
7	113617	BH-03	12	13	1	9.77	1.30	<0.05	0.08	4.71	2.68	1.28	<0.05	<0.05	0.06	75.83	<0.05	<0.05	0.50	<0.05	<0.05	3.64
8	110097	BH-03	27	28	1	9.40	0.08	0.21	0.08	3.51	3.05	1.57	<0.05	0.17	0.08	65.76	4.97	<0.05	0.44	0.28	<0.05	10.29
9	113612	BH-03	31	32	1	10.71	0.09	0.34	0.08	4.20	3.31	2.30	<0.05	0.42	0.17	56.21	10.96	<0.05	0.51	0.29	<0.05	10.15
10	110098	BH-03	46	47	1	8.21	0.07	2.37	0.08	3.54	2.73	2.34	<0.05	<0.05	0.08	65.56	5.17	<0.05	0.41	0.20	<0.05	9.07
11	110100	BH-03	59	60	1	6.64	0.07	2.74	0.05	3.08	2.02	0.85	<0.05	0.50	0.10	72.72	5.23	<0.05	0.30	0.31	<0.05	5.26
12.1	113502	BH-03	65	66	1	3.94	0.15	0.44	0.06	1.46	1.38	0.56	<0.05	<0.05	0.06	82.81	1.93	<0.05	0.15	0.37	<0.05	6.54
12.2	113502	BH-03	65	66	1	3.85	0.15	0.44	0.06	1.41	1.36	0.55	<0.05	<0.05	0.06	83.02	1.94	<0.05	0.15	0.36	<0.05	6.49
13	113503	BH-04	10	11	1	10.97	0.32	0.45	<0.05	2.75	2.44	1.16	<0.05	1.89	0.10	70.86	1.39	<0.05	0.43	0.17	<0.05	6.90
14	113504	BH-04	15	16	1	4.90	0.24	0.10	0.08	2.34	1.54	0.65	<0.05	0.19	0.10	80.56	0.88	<0.05	0.23	0.24	<0.05	7.84
15	113505	BH-04	18	19	1	6.61	0.21	6.80	0.06	2.51	2.02	2.94	<0.05	0.79	0.18	61.58	3.82	<0.05	0.31	0.17	<0.05	11.85
16	113508	BH-04	31	32	1	12.87	0.09	1.36	<0.05	5.32	3.23	2.07	<0.05	1.88	0.22	54.96	4.24	<0.05	0.61	0.09	<0.05	12.88
17	113509	BH-04	54.5	55.5	1	13.26	0.19	1.21	<0.05	5.38	3.19	2.02	0.09	1.80	0.17	58.23	0.39	<0.05	0.62	<0.05	<0.05	13.32
18	113510	BH-05	6	7	1	16.89	0.54	1.64	<0.05	7.76	4.33	3.35	0.07	2.10	0.14	57.44	0.44	<0.05	0.80	<0.05	<0.05	4.34
19	113511	BH-05	15	16	1	10.46	1.25	0.14	0.06	5.06	2.92	1.60	<0.05	0.32	0.17	65.85	1.29	<0.05	0.47	0.22	<0.05	10.06
20	113512	BH-05	28	29	1	12.38	<0.05	0.75	0.06	4.05	1.64	2.04	<0.05	3.81	0.11	62.79	6.26	<0.05	0.41	<0.05	<0.05	5.51
21	113513	BH-05	32	33	1	9.80	0.07	0.47	<0.05	2.81	2.34	1.02	<0.05	1.47	0.14	70.93	4.14	<0.05	0.38	0.32	<0.05	5.94
22	113514	BH-05	40	41	1	11.30	0.10	3.07	0.07	5.10	2.98	1.55	<0.05	0.58	0.25	57.56	6.62	<0.05	0.51	0.42	<0.05	9.59
23	113515	BH-05	44	45	1	12.42	<0.05	2.00	0.09	5.14	4.00	2.02	<0.05	0.38	0.22	55.84	6.58	<0.05	0.60	0.53	<0.05	9.99
24	113605	BH-05	48	49	1	11.70	0.05	2.96	0.09	4.81	3.74	2.20	<0.05	0.37	0.33	50.23	10.71	<0.05	0.56	0.61	<0.05	11.14
25	113516	BH-05	61	62	1	8.00	0.06	4.15	<0.05	3.57	2.29	1.06	<0.05	1.09	0.11	67.21	5.11	<0.05	0.32	0.08	<0.05	6.76
26	113517	BH-05	72	73	1	13.02	0.08	3.20	<0.05	9.63	3.23	2.10	<0.05	1.56	0.17	39.32	14.40	<0.05	0.61	0.28	<0.05	11.92
27	113541	BH-06	75	76	1	16.87	0.22	1.20	<0.05	7.20	4.49	2.77	0.07	1.68	0.15	58.90	1.89	<0.05	0.72	<0.05	<0.05	3.68
28	113543	BH-06	87	88	1	13.69	0.08	2.26	<0.05	7.86	3.72	2.29	0.06	1.11	0.15	56.51	5.47	<0.05	0.53	0.06	<0.05	6.07
29	113547	BH-06	105	106	1	14.78	0.12	1.70	<0.05	7.15	2.79	2.38	<0.05	2.51	0.14	59.01	4.01	<0.05	0.53	<0.05	<0.05	4.60

SL No	Sample ID	Borehole No	From (m)	To (m)	Length	Al_2O_3	BaO	CaO	Cr_2O_3	Fe_2O_3	K_2O	MgO	MnO	Na_2O	P_2O_5	SiO_2	SO_3	SnO_2	TiO_2	V_2O_5	WO_3	LOI@ 950°C
30	113518	BH-07	9	10	1	10.99	0.13	0.81	<0.05	5.50	3.67	1.98	0.05	1.94	0.15	69.32	0.76	<0.05	0.76	<0.05	<0.05	3.70
31	113519	BH-07	14	15	1	12.77	0.20	1.12	<0.05	4.75	2.40	1.56	0.08	2.20	0.16	72.11	<0.05	<0.05	0.63	<0.05	<0.05	1.86
32	113520	BH-07	29	30	1	17.09	0.43	1.82	<0.05	8.16	4.20	3.39	0.08	2.36	0.16	58.61	0.16	<0.05	0.72	<0.05	<0.05	2.64
33	113521	BH-07	30	31	1	15.76	0.38	1.82	<0.05	5.38	3.04	2.19	<0.05	2.10	0.12	64.71	0.17	<0.05	0.57	<0.05	<0.05	3.60
34	113522	BH-07	35	36	1	10.66	0.52	0.48	<0.05	4.91	2.23	1.67	<0.05	0.90	0.20	72.48	0.75	<0.05	0.43	0.05	<0.05	4.55
35	113524	BH-08	18	19	1	12.19	0.40	1.18	<0.05	4.48	2.15	1.61	0.07	2.21	0.16	73.01	<0.05	<0.05	0.65	<0.05	<0.05	1.65
36	113525	BH-08	21.5	22.5	1	12.76	0.42	1.13	<0.05	4.73	2.36	1.65	0.06	2.41	0.16	71.75	<0.05	<0.05	0.63	<0.05	<0.05	1.69
37	113526	BH-08	28.5	29.5	1	14.59	0.29	1.32	<0.05	5.92	3.34	2.25	0.08	2.32	0.15	66.56	0.23	<0.05	0.64	<0.05	<0.05	2.14
38	113528	BH-08	37.5	38.5	1	12.54	<0.05	1.38	<0.05	13.03	3.03	2.12	<0.05	1.32	0.10	42.33	14.19	<0.05	0.53	0.05	<0.05	9.17
39.1	113529	BH-08	43	44	1	13.52	0.16	1.41	<0.05	7.82	3.14	2.20	0.08	1.74	0.17	62.18	3.76	<0.05	0.59	<0.05	<0.05	3.06
39.2	113529	BH-08	43	44	1	13.60	0.16	1.43	<0.05	7.87	3.18	2.16	0.08	1.78	0.17	61.95	3.80	<0.05	0.59	<0.05	<0.05	3.07
40	113571	BH-09	3	4	1	7.84	1.53	0.05	0.08	2.38	1.94	0.94	<0.05	0.08	0.09	79.32	<0.05	<0.05	0.35	0.27	<0.05	5.41
41.1	113576	BH-09	44	45	1	12.69	0.08	1.27	<0.05	5.44	2.59	1.79	0.10	1.90	0.14	71.82	<0.05	<0.05	0.61	<0.05	<0.05	1.58
41.2	113576	BH-09	44	45	1	12.82	0.08	1.28	<0.05	5.52	2.61	1.81	0.10	1.88	0.14	71.63	<0.05	<0.05	0.61	<0.05	<0.05	1.58
42	113567	BH-10	5	6	1	2.34	<0.05	0.23	<0.05	0.78	0.69	0.22	<0.05	<0.05	<0.05	92.68	0.24	<0.05	0.09	<0.05	<0.05	2.48
43	113568	BH-10	21	22	1	8.10	0.22	0.49	0.07	3.28	2.19	1.01	<0.05	0.22	0.12	75.59	1.11	<0.05	0.36	0.14	<0.05	6.95
44	113557	BH-11	11.5	12.5	1	16.97	0.37	1.12	<0.05	6.80	4.25	3.15	0.06	2.11	0.15	63.06	0.23	<0.05	0.72	<0.05	<0.05	0.84
45	113559	BH-11	31	32	1	13.98	0.07	1.81	<0.05	5.79	3.27	2.65	0.05	2.54	0.14	65.52	2.57	<0.05	0.59	<0.05	<0.05	0.82
46.1	113562	BH-11	53.1	54.1	1	12.56	0.17	1.26	<0.05	4.92	2.35	1.99	0.06	2.87	0.16	72.00	<0.05	<0.05	0.62	<0.05	<0.05	0.94
46.2	113562	BH-11	53.1	54.1	1	12.51	0.17	1.32	<0.05	5.01	2.36	1.97	0.07	2.88	0.17	71.88	<0.05	<0.05	0.63	<0.05	<0.05	0.94
47	113566	BH-11	80.6	81.6	1	13.41	<0.05	1.49	<0.05	5.74	2.33	2.18	0.09	2.83	0.16	69.95	0.11	<0.05	0.71	<0.05	<0.05	0.82
48	113583	BH-11	91	92	1	15.72	0.06	3.02	0.06	3.88	4.74	1.38	0.07	3.17	0.17	66.17	0.11	<0.05	0.46	<0.05	<0.05	0.91
49	113622	BH-12	26.5	27.8	1.3	7.79	0.16	1.16	<0.05	3.20	2.23	0.77	<0.05	0.40	0.10	82.85	0.78	<0.05	0.34	0.07	<0.05	8.27
50	113624	BH-12	31	33	2	9.87	0.06	1.19	0.08	6.56	2.64	1.47	0.16	0.79	0.08	66.57	9.97	<0.05	0.40	<0.05	<0.05	4.74
51	113629	BH-12	54.5	56	1.5	9.48	0.14	3.66	0.06	3.41	2.48	2.44	<0.05	1.45	0.14	70.96	5.07	<0.05	0.34	0.23	<0.05	12.61

Annexure XXIII_XRF Data of Borehole Check Samples (All data in %)

Sl. No	Sample ID	BH-ID	From (m)	To (m)	Lab	Al_2O_3	BaO	CaO	Cr_2O_3	Fe_2O_3	K_2O	MgO	MnO	Na_2O	P_2O_5	SiO_2	SO_3	SnO_2	TiO_2	V_2O_5	WO_3	LOI@ 950°C
1	110076	GSPL/AL/BH-01	81	82	BV	12.82	0.23	3.26	<0.05	3.05	2.05	1.70	0.05	2.64	0.10	64.40	2.48	<0.05	0.36	0.07	<0.05	6.33
	113636				Shiva	**10.72**	**0.30**	**4.33**	**0.04**	**3.69**	**2.32**	**1.77**	**0.05**	**2.35**	**0.09**	**61.72**	**4.45**	-	**0.38**	**0.04**	-	**7.64**
2	110071	GSPL/AL/BH-01	36.5	37	BV	9.55	0.25	8.12	0.07	4.14	2.86	5.80	0.09	0.33	0.27	49.19	0.10	<0.05	0.48	0.25	0.09	17.40
	113637				Shiva	**10.85**	**0.25**	**2.21**	**0.08**	**5.67**	**3.71**	**3.48**	**0.02**	**0.27**	**0.10**	**50.22**	**9.59**	-	**0.60**	**0.28**	-	**12.45**
3	110097	GSPL/AL/BH-03	27	28	BV	9.40	0.08	0.21	0.08	3.51	3.05	1.57	<0.05	0.17	0.08	65.76	4.97	<0.05	0.44	0.28	<0.05	10.29
	113645				Shiva	**9.17**	**0.21**	**0.20**	**0.07**	**4.02**	**2.98**	**1.63**	**0.00**	**0.13**	**0.08**	**65.64**	**5.23**	-	**0.45**	**0.27**	-	**9.74**
4	113583	GSPL/AL/BH-11	91	92	BV	15.72	0.06	3.02	0.06	3.88	4.74	1.38	0.07	3.17	0.17	66.17	0.11	<0.05	0.46	<0.05	<0.05	0.91
	113648				Shiva	**15.02**	**0.07**	**2.79**	**0.02**	**3.67**	**3.58**	**1.12**	**0.07**	**2.81**	**0.09**	**69.36**	**0.05**	-	**0.38**	**0.01**	-	**0.91**
5	113517	GSPL/AL/BH-05	72	73	BV	13.02	0.08	3.20	<0.05	9.63	3.23	2.10	<0.05	1.56	0.17	39.32	14.40	<0.05	0.61	0.28	<0.05	11.92
	113649				Shiva	**11.44**	**0.10**	**2.87**	**0.05**	**8.49**	**3.08**	**2.12**	**0.05**	**1.36**	**0.16**	**44.66**	**11.61**	-	**0.59**	**0.28**	-	**12.90**

Annexure XXIV_XRF Data of Borehole Check Samples with 2 Additional Elements (Sn, W)

Sl. No	Sample ID	BH-ID	From (m)	To (m)	Lab	SnO_2 (%)	WO_3 (%)	Sn (in ppm)	W (in ppm)
1	110076	GSPL/AL/BH-01	81	82	BV	<0.05	<0.05	< 394	< 396.5
	113636				Shiva	-	-	7.12	0.61
2	110071	GSPL/AL/BH-01	36.5	37	BV	<0.05	0.094	< 394	745.4
	113637				Shiva	-	-	8.97	2.48
3	110097	GSPL/AL/BH-03	27	28	BV	<0.05	<0.05	< 394	< 396.5
	113645				Shiva	-	-	3.38	6.94
4	113583	GSPL/AL/BH-11	91	92	BV	<0.05	<0.05	< 394	< 396.5
	113648				Shiva	-	-	7.73	0.87
5	113517	GSPL/AL/BH-05	72	73	BV	<0.05	<0.05	< 394	< 396.5
	113649				Shiva	-	-	7.42	2.58

Annexure XXV_ICPMS Data of Borehole Samples (All data in ppm)

SL	Sample ID	Borehole No	From (m)	To (m)	Li	Be	Sc	V	Mn	Cr	Co	Ni	Cu	Zn	Ga	Ge	Se	Rb	Sr	Y
1	110065	GSPL/AL/BH-01	14	15	38.93	2.96	17.28	105.65	160.13	954.42	23.05	62.43	42.22	116.86	26.37	0.02	11.17	158.98	92.65	33.53
2	110066	GSPL/AL/BH-01	19	20.32	23.51	2.56	14.53	205.46	232.60	46.13	11.15	54.31	191.35	46.50	18.74	0.04	20.54	132.07	93.90	20.15
3	110067	GSPL/AL/BH-01	20.32	21.32	11.41	1.40	10.45	106.83	182.54	75.55	8.09	109.90	267.75	50.73	9.01	0.05	12.14	46.47	59.86	26.23
4	110068	GSPL/AL/BH-01	35	35.5	35.94	2.76	13.80	1383.45	367.65	128.57	11.66	322.05	325.72	876.36	20.76	0.04	37.84	133.09	80.65	104.48
5	110069	GSPL/AL/BH-01	35.5	36	34.36	2.47	11.76	1405.81	336.72	155.08	10.68	323.17	453.81	949.95	18.42	0.03	32.07	134.79	80.12	88.51
6	110070	GSPL/AL/BH-01	36	36.5	35.94	2.61	10.54	1594.60	347.03	107.26	11.24	326.60	334.37	945.68	16.04	0.04	28.49	127.11	53.24	84.93
7	110071	GSPL/AL/BH-01	36.5	37	43.75	1.91	9.33	1028.75	230.93	395.44	8.17	250.73	524.27	688.55	16.32	0.02	27.14	155.93	173.72	72.99
8.1	**110072**	GSPL/AL/BH-01	49	50	17.55	1.98	7.40	261.74	108.57	493.76	8.69	32.90	39.40	175.61	11.95	0.01	14.29	79.47	242.91	31.36
8.2	**110072**	GSPL/AL/BH-01	49	50	16.13	2.16	6.98	259.12	105.72	488.13	8.26	29.86	40.11	173.27	12.99	0.00	16.38	81.00	239.09	29.64
9	110073	GSPL/AL/BH-01	53	54	20.61	2.33	8.29	641.61	180.92	345.55	10.28	54.78	101.16	573.62	17.58	0.02	22.94	88.06	190.21	45.36
10	110074	GSPL/AL/BH-01	57	58	23.38	2.36	9.66	391.68	112.76	309.80	10.85	51.33	96.75	329.74	16.83	0.00	19.42	90.18	172.52	30.26
11	110077	GSPL/AL/BH-01	58.25	59.25	19.24	2.39	11.23	333.45	192.49	317.67	11.39	53.62	142.95	388.91	18.71	0.20	9.29	100.53	178.58	36.18
12	110088	GSPL/AL/BH-01	62	63	22.48	2.21	8.83	748.75	179.17	328.86	10.37	73.16	156.18	659.69	17.25	0.17	8.26	97.09	140.61	53.11
13	110075	GSPL/AL/BH-01	72	72.5	22.52	2.22	10.66	794.54	257.34	197.10	9.68	111.86	172.60	379.74	16.80	0.00	24.19	96.93	187.04	46.33
14	110078	GSPL/AL/BH-01	73	74	18.20	2.06	7.92	218.22	130.22	406.36	8.60	18.90	39.75	107.99	15.98	0.13	5.40	83.71	212.36	29.12
15	110089	GSPL/AL/BH-01	78	79	15.66	1.44	6.54	784.38	221.95	505.14	12.89	227.99	311.02	492.09	12.16	0.21	12.33	63.44	150.80	48.49
16	110090	GSPL/AL/BH-01	79	80	17.34	1.73	7.14	759.86	271.08	195.34	7.30	112.52	259.34	390.35	12.67	0.18	9.49	71.78	120.09	40.57
17	110076	GSPL/AL/BH-01	81	82	17.05	1.84	7.47	381.28	186.89	364.20	8.25	57.88	102.31	322.29	15.45	0.01	16.06	90.19	194.83	32.10
18	110079	GSPL/AL/BH-01	84	85	25.85	2.85	13.35	187.05	186.39	495.92	15.96	44.65	49.92	130.26	23.45	0.20	5.90	136.52	201.17	29.12
19	110091	GSPL/AL/BH-01	89	90	18.84	1.75	8.22	250.74	120.99	344.12	12.22	69.71	112.81	207.44	17.38	0.14	5.52	79.78	131.81	28.04

SL	Sample ID	Borehole No	From (m)	To (m)	Zr	Nb	Mo	Ag	Cd	In	Sn	Sb	Te	Cs	Ba	La	Ce	Pr	Nd	Sm
1	110065	GSPL/AL/BH-01	14	15	2.28	9.73	0.15	-0.19	0.10	0.11	3.71	<0.000	0.00	9.51	603.94	40.95	82.73	9.47	36.69	7.39
2	110066	GSPL/AL/BH-01	19	20.32	0.83	7.52	12.39	0.52	0.33	0.06	3.03	4.48	0.00	2.69	698.56	34.29	69.87	8.33	33.35	6.83
3	110067	GSPL/AL/BH-01	20.32	21.32	0.56	3.16	6.81	0.01	0.33	0.10	1.17	2.62	0.00	1.37	1581.69	20.29	51.83	7.44	33.66	7.17
4	110068	GSPL/AL/BH-01	35	35.5	1.10	12.95	160.14	2.08	13.54	0.10	2.26	16.39	0.00	9.23	720.75	35.93	67.70	10.89	50.51	11.86
5	110069	GSPL/AL/BH-01	35.5	36	1.07	12.14	155.14	5.14	14.72	0.09	2.43	31.80	0.00	9.94	1062.88	36.29	63.55	9.82	42.39	9.84
6	110070	GSPL/AL/BH-01	36	36.5	1.38	13.77	163.44	1.94	14.43	0.11	2.37	16.75	1.16	7.35	2715.15	16.46	29.75	5.28	26.83	7.79
7	110071	GSPL/AL/BH-01	36.5	37	1.01	7.67	121.06	12.37	10.13	0.06	1.54	156.96	0.60	16.57	1771.49	29.01	49.89	7.78	34.35	8.41
8.1	**110072**	GSPL/AL/BH-01	49	50	0.33	6.81	5.62	0.75	3.17	0.04	1.52	7.85	0.00	4.31	819.53	25.42	46.61	5.81	22.74	4.93
8.2	**110072**	GSPL/AL/BH-01	49	50	0.45	7.19	4.72	0.66	3.21	0.03	1.51	8.45	0.00	4.29	1230.08	23.77	44.08	5.42	23.03	4.82
9	110073	GSPL/AL/BH-01	53	54	0.75	8.14	15.86	0.89	11.06	0.09	2.11	8.61	0.00	4.55	1393.88	32.63	56.07	7.85	32.20	7.02
10	110074	GSPL/AL/BH-01	57	58	0.47	7.90	9.94	1.14	2.96	0.06	1.84	7.71	0.00	4.56	1185.67	26.72	48.66	6.05	25.46	4.98
11	110077	GSPL/AL/BH-01	58.25	59.25	1.55	8.47	19.90	2.14	3.33	0.04	2.03	2.48	<0.05	4.53	2828.94	34.84	59.58	7.87	32.03	6.84
12	110088	GSPL/AL/BH-01	62	63	1.43	6.61	22.67	5.93	7.27	0.05	1.82	6.03	0.67	5.99	2029.17	37.67	60.61	8.67	34.35	7.84
13	110075	GSPL/AL/BH-01	72	72.5	1.10	9.22	46.85	0.85	6.73	0.06	1.88	8.96	0.00	8.51	2274.81	33.71	59.08	8.29	35.19	7.66
14	110078	GSPL/AL/BH-01	73	74	0.68	6.36	6.28	1.07	1.88	0.01	1.35	2.43	<0.05	4.38	2477.57	27.86	48.27	6.07	23.29	4.72
15	110089	GSPL/AL/BH-01	78	79	1.02	6.85	70.61	10.29	10.27	0.04	1.46	6.32	<0.05	5.04	1487.57	35.26	54.09	9.09	38.26	8.27
16	110090	GSPL/AL/BH-01	79	80	1.27	7.25	58.65	15.69	9.09	0.03	1.44	6.49	<0.05	5.14	2391.21	33.87	53.56	8.16	35.22	7.08
17	110076	GSPL/AL/BH-01	81	82	0.64	6.94	16.81	0.10	2.81	0.05	1.57	4.37	0.00	4.09	2534.03	26.96	46.95	6.15	25.31	4.92
18	110079	GSPL/AL/BH-01	84	85	0.76	8.45	7.80	0.79	1.11	0.05	2.59	2.45	<0.05	8.58	7067.30	40.26	75.31	8.35	32.07	6.53
19	110091	GSPL/AL/BH-01	89	90	1.43	7.90	20.43	3.10	3.41	0.03	1.85	5.08	<0.05	4.66	2357.40	33.44	59.36	7.45	29.86	5.39

SL	Sample ID	Borehole No	From (m)	To (m)	Eu	Gd	Tb	Dy	Ho	Er	Tm	Yb	Lu	Hf	Ta	W	Tl	Pb	Bi	Th	U
1	110065	GSPL/AL/BH-01	14	15	1.46	7.60	1.03	6.57	1.25	3.82	0.51	3.42	0.44	0.06	0.65	2.57	1.19	27.56	0.65	16.19	3.08
2	110066	GSPL/AL/BH-01	19	20.32	1.27	5.52	0.68	3.90	0.72	2.14	0.30	2.03	0.28	0.05	0.66	3.46	1.30	50.00	0.70	19.74	12.04
3	110067	GSPL/AL/BH-01	20.32	21.32	1.58	6.45	0.81	4.98	0.96	3.08	0.40	2.83	0.41	0.03	0.24	1.68	0.74	13.84	0.35	7.42	16.04
4	110068	GSPL/AL/BH-01	35	35.5	2.76	15.06	2.22	15.74	3.28	10.42	1.38	8.94	1.09	0.06	1.01	4.25	2.40	57.82	0.41	13.03	41.79
5	110069	GSPL/AL/BH-01	35.5	36	2.25	12.28	1.79	13.02	2.68	8.62	1.16	7.56	1.04	0.06	0.94	4.01	2.50	23.31	0.52	12.64	42.37
6	110070	GSPL/AL/BH-01	36	36.5	2.32	10.75	1.75	12.74	2.71	8.80	1.16	7.32	0.99	0.23	1.67	3.74	2.45	48.06	0.66	8.50	43.45
7	110071	GSPL/AL/BH-01	36.5	37	1.73	10.27	1.49	10.46	2.19	7.19	1.01	6.81	0.94	0.02	0.55	2.57	3.03	48.75	0.64	9.60	36.56
8.1	**110072**	GSPL/AL/BH-01	49	50	1.50	5.05	0.73	5.00	1.00	3.00	0.42	2.82	0.38	0.04	0.48	1.19	1.32	37.51	0.17	7.59	4.45
8.2	**110072**	GSPL/AL/BH-01	49	50	1.32	4.96	0.67	4.58	0.93	2.90	0.40	2.57	0.36	0.03	0.55	1.28	1.31	39.21	0.17	7.23	4.13
9	110073	GSPL/AL/BH-01	53	54	1.66	7.62	1.09	7.39	1.48	4.73	0.61	4.11	0.51	0.06	0.68	2.01	1.25	34.31	0.18	8.85	10.22
10	110074	GSPL/AL/BH-01	57	58	1.36	5.65	0.74	5.05	1.01	3.20	0.45	3.16	0.48	0.04	0.59	1.29	1.22	67.14	0.26	8.50	5.71
11	110077	GSPL/AL/BH-01	58.25	59.25	1.58	6.57	0.93	6.40	1.22	3.74	0.53	3.63	0.50	0.06	0.46	33.18	1.18	50.45	0.22	10.21	6.41
12	110088	GSPL/AL/BH-01	62	63	1.69	8.15	1.16	7.83	1.64	5.16	0.73	4.70	0.64	<0.05	0.18	28.82	1.31	30.36	0.24	9.02	12.84
13	110075	GSPL/AL/BH-01	72	72.5	1.94	8.01	1.08	7.46	1.46	4.50	0.64	4.21	0.63	0.07	0.75	2.21	1.56	80.07	0.32	9.79	17.47
14	110078	GSPL/AL/BH-01	73	74	1.25	4.96	0.67	4.55	0.92	2.83	0.40	2.66	0.35	<0.05	0.26	36.18	1.20	80.95	0.18	7.57	4.83
15	110089	GSPL/AL/BH-01	78	79	1.84	9.09	1.19	7.59	1.51	4.72	0.65	4.37	0.59	0.06	0.41	64.64	1.14	60.26	0.36	7.24	24.47
16	110090	GSPL/AL/BH-01	79	80	1.72	7.65	1.04	6.65	1.32	4.07	0.53	3.59	0.51	<0.05	0.43	88.37	1.21	66.22	0.28	7.67	22.69
17	110076	GSPL/AL/BH-01	81	82	1.48	5.28	0.76	5.10	1.00	3.27	0.44	3.02	0.41	0.02	0.51	1.48	1.32	58.45	0.19	7.65	9.76
18	110079	GSPL/AL/BH-01	84	85	1.67	5.92	0.79	5.35	1.02	3.01	0.39	2.60	0.34	0.06	0.27	8.80	1.33	56.28	0.21	13.21	6.77
19	110091	GSPL/AL/BH-01	89	90	1.30	5.63	0.73	4.77	0.92	2.78	0.38	2.47	0.34	0.05	0.51	30.64	0.88	26.17	0.21	9.33	10.82

SL	Sample ID	Borehole No	From (m)	To (m)	Li	Be	Sc	V	Mn	Cr	Co	Ni	Cu	Zn	Ga	Ge	Se	Rb	Sr	Y
20	110080	GSPL/AL/BH-02	13	14	29.14	2.29	12.48	1022.09	418.56	123.22	10.27	205.82	323.89	555.82	18.43	0.28	10.70	119.66	108.04	50.84
21	110092	GSPL/AL/BH-02	15	16	22.88	1.50	8.47	819.13	368.04	172.12	13.26	225.27	398.72	530.58	16.39	0.34	12.59	79.45	83.71	83.94
22	110093	GSPL/AL/BH-02	17	18	24.41	1.63	7.84	789.05	325.80	190.32	13.88	217.19	380.21	511.48	14.16	0.27	12.15	74.40	99.54	70.02
23	110094	GSPL/AL/BH-02	19	20	23.44	1.69	8.42	710.56	406.80	165.91	17.37	194.10	409.50	459.53	16.40	0.34	14.42	80.54	78.88	91.34
24	110081	GSPL/AL/BH-02	19	20	28.68	2.71	11.68	882.95	329.98	176.00	9.78	149.67	246.35	382.90	18.12	0.26	12.33	110.91	144.39	81.24
25	110082	GSPL/AL/BH-02	22	23	36.47	2.41	19.35	98.47	176.87	211.16	12.04	29.66	27.51	124.90	17.94	0.16	5.70	121.13	122.17	24.42
26	110083	GSPL/AL/BH-02	27	28	18.55	1.90	8.00	424.79	329.31	423.80	9.62	75.39	120.84	260.19	13.19	0.12	5.96	81.61	130.01	27.88
27	110086	GSPL/AL/BH-02	29.3	30.3	56.22	2.82	10.79	81.33	151.46	527.87	15.98	33.71	31.78	82.12	18.30	0.14	4.76	156.75	80.43	15.92
28	110084	GSPL/AL/BH-02	34	35	7.66	0.71	8.51	29.64	159.90	136.31	2.80	7.53	16.86	31.38	4.63	0.10	2.83	27.88	75.12	14.39
29.1	**110085**	GSPL/AL/BH-02	42	43	20.58	2.20	11.25	68.55	161.35	725.07	11.65	21.28	25.61	55.57	18.69	0.24	4.21	88.45	85.52	29.80
29.2	**110085**	GSPL/AL/BH-02	42	43	21.43	2.12	11.74	69.16	163.30	722.69	11.92	22.08	25.40	59.08	19.93	0.22	4.58	88.92	87.88	30.70
30	110087	GSPL/AL/BH-02	48	49	21.32	2.42	10.82	81.65	209.86	566.10	14.23	40.31	32.03	65.31	18.03	0.11	2.56	106.94	87.61	20.54

SL	Sample ID	Borehole No	From (m)	To (m)	Zr	Nb	Mo	Ag	Cd	In	Sn	Sb	Te	Cs	Ba	La	Ce	Pr	Nd	Sm
20	110080	GSPL/AL/BH-02	13	14	1.34	9.92	87.76	1.65	8.89	0.06	2.31	4.51	0.68	9.24	1551.22	39.19	67.15	10.08	43.71	10.25
21	110092	GSPL/AL/BH-02	15	16	1.63	8.75	77.97	2.00	9.21	0.08	1.91	4.62	0.05	6.61	1899.11	44.02	71.29	11.36	49.35	11.63
22	110093	GSPL/AL/BH-02	17	18	0.99	8.80	75.08	1.56	9.69	0.06	1.74	3.75	0.05	6.62	1804.03	41.51	67.98	10.67	46.19	10.71
23	110094	GSPL/AL/BH-02	19	20	1.08	9.92	59.14	1.64	8.18	0.05	1.84	5.11	1.31	7.53	1447.65	45.96	78.11	12.11	51.75	12.64
24	110081	GSPL/AL/BH-02	19	20	1.18	11.19	51.46	1.52	6.84	0.04	2.05	5.29	0.05	9.77	2272.14	39.37	67.91	10.35	45.34	11.00
25	110082	GSPL/AL/BH-02	22	23	0.77	9.46	3.14	0.67	0.81	0.05	2.57	10.68	0.05	9.33	615.50	26.00	52.23	6.34	24.92	5.40
26	110083	GSPL/AL/BH-02	27	28	0.89	5.19	38.33	0.85	5.67	0.02	1.44	0.10	0.05	4.51	1722.81	25.69	43.81	5.79	24.19	4.78
27	110086	GSPL/AL/BH-02	29.3	30.3	1.46	8.72	1.52	0.65	0.12	0.06	2.78	0.88	0.66	30.45	774.70	30.21	61.08	6.85	26.89	5.44
28	110084	GSPL/AL/BH-02	34	35	0.53	1.83	1.16	0.20	0.06	0.01	0.34	0.63	0.05	3.65	1851.52	9.73	19.10	2.69	11.67	2.60
29.1	**110085**	GSPL/AL/BH-02	42	43	4.13	10.33	0.23	0.09	0.05	0.05	2.19	2.33	0.05	3.74	616.70	42.42	83.36	9.12	36.12	7.26

29.2	**110085**	GSPL/AL/BH-02	42	43	4.64	10.55	0.30	0.08	0.05	0.05	2.21	2.12	0.05	4.07	617.67	43.40	84.59	9.50	36.46	6.85
30	110087	GSPL/AL/BH-02	48	49	1.77	6.78	2.52	0.20	0.10	0.09	2.67	1.65	0.05	5.38	1491.85	31.54	60.59	6.82	26.04	5.10

SL	Sample ID	Borehole No	From (m)	To (m)	Eu	Gd	Tb	Dy	Ho	Er	Tm	Yb	Lu	Hf	Ta	W	Tl	Pb	Bi	Th	U
20	110080	GSPL/AL/BH-02	13	14	2.11	10.22	1.29	8.27	1.61	5.03	0.70	4.74	0.69	0.06	0.48	29.56	1.86	89.03	0.72	11.62	29.12
21	110092	GSPL/AL/BH-02	15	16	2.40	13.42	1.86	12.54	2.63	8.22	1.11	7.28	0.94	0.05	0.46	37.61	1.35	48.17	0.62	11.12	30.01
22	110093	GSPL/AL/BH-02	17	18	2.27	11.56	1.56	10.57	2.19	6.83	0.89	6.08	0.87	0.05	0.41	32.91	1.32	63.21	0.63	10.36	28.85
23	110094	GSPL/AL/BH-02	19	20	2.54	15.24	2.13	14.42	2.93	9.18	1.18	8.04	1.04	0.06	0.69	68.93	1.33	67.06	0.67	11.84	28.56
24	110081	GSPL/AL/BH-02	19	20	2.37	13.01	1.87	13.31	2.69	8.10	1.15	7.61	1.05	0.07	0.75	59.34	1.87	64.92	0.81	12.08	21.82
25	110082	GSPL/AL/BH-02	22	23	1.21	5.25	0.74	5.05	0.93	3.06	0.41	2.88	0.42	0.06	0.76	25.98	1.78	135.53	0.49	12.03	2.72
26	110083	GSPL/AL/BH-02	27	28	1.15	5.00	0.65	4.17	0.87	2.73	0.38	2.69	0.41	0.05	0.25	51.28	1.06	38.76	0.55	6.78	19.83
27	110086	GSPL/AL/BH-02	29.3	30.3	0.90	4.39	0.56	3.49	0.60	1.81	0.24	1.72	0.23	0.06	0.56	6.28	1.23	145.67	0.44	11.03	2.12
28	110084	GSPL/AL/BH-02	34	35	0.64	2.77	0.38	2.18	0.47	1.34	0.19	1.40	0.19	0.05	0.11	9.08	0.44	24.41	0.29	3.38	1.91
29.1	**110085**	GSPL/AL/BH-02	42	43	1.29	6.66	0.92	5.86	1.10	3.21	0.44	2.77	0.37	0.05	0.73	6.83	0.65	57.43	0.19	15.29	2.53
29.2	**110085**	GSPL/AL/BH-02	42	43	1.32	6.86	0.93	5.91	1.11	3.35	0.45	2.91	0.37	0.05	0.74	6.92	0.68	55.90	0.20	15.71	2.58
30	110087	GSPL/AL/BH-02	48	49	1.04	4.70	0.64	4.05	0.77	2.32	0.34	2.09	0.26	0.09	0.49	13.95	0.79	34.16	0.29	10.54	2.57

SL	Sample ID	Borehole No	From (m)	To (m)	Li	Be	Sc	V	Mn	Cr	Co	Ni	Cu	Zn	Ga	Ge	Se	Rb	Sr	Y
31	113618	GSPL/AL/BH-03	7	8	29.52	0.91	11.87	51.64	324.41	132.93	25.81	104.55	200.94	276.63	14.01	0.27	10.16	90.72	124.64	54.62
32	113617	GSPL/AL/BH-03	12	13	23.32	2.96	14.03	120.89	55.35	463.24	2.34	20.57	71.55	69.96	15.65	<0.1	2.77	83.06	98.16	14.02
33	113616	GSPL/AL/BH-03	15	16	13.02	1.22	7.52	876.61	35.32	543.17	1.71	45.59	89.91	127.62	10.10	<0.1	4.21	62.28	84.42	21.11
34	110095	GSPL/AL/BH-03	22	23	18.57	1.79	8.05	712.31	64.18	480.47	6.20	84.54	164.54	205.71	12.87	0.21	9.99	76.99	113.02	58.51
35	113615	GSPL/AL/BH-03	23	24	26.60	2.43	8.83	1296.36	61.75	625.70	9.13	137.31	403.99	291.44	15.29	<0.1	11.56	84.44	94.87	54.17
36	113614	GSPL/AL/BH-03	24	25	24.97	2.38	7.41	1553.55	61.74	582.71	10.60	161.61	519.23	318.82	14.92	0.13	10.94	81.66	93.56	56.73
37	110097	GSPL/AL/BH-03	27	28	27.80	2.39	12.11	1715.51	42.68	757.07	12.11	243.37	365.83	782.25	18.14	0.30	11.62	113.61	51.21	65.16
38	113613	GSPL/AL/BH-03	29	30	30.19	2.13	10.97	1846.60	52.53	488.96	15.74	383.11	547.13	1524.04	14.92	0.24	13.46	107.27	76.32	59.93
39	113612	GSPL/AL/BH-03	31	32	35.40	2.51	12.72	1601.64	52.00	452.29	15.92	364.97	424.41	1366.61	15.11	0.16	14.35	127.10	92.14	58.87
40	110096	GSPL/AL/BH-03	38	39	24.20	1.67	9.35	944.97	145.99	568.21	17.13	470.22	295.31	1144.66	14.49	0.27	15.94	85.72	97.15	76.18
41	110099	GSPL/AL/BH-03	41	42	21.69	2.64	5.85	259.88	135.68	391.18	6.95	55.04	396.13	165.55	13.27	0.12	5.77	59.79	224.99	32.24
42	110098	GSPL/AL/BH-03	46	47	28.58	1.57	10.45	1265.75	127.31	813.46	7.30	286.70	332.73	1076.33	17.97	0.26	18.96	113.83	54.67	96.59
43	113501	GSPL/AL/BH-03	53	54	25.92	2.68	8.91	2758.56	95.29	611.85	15.18	155.49	81.72	664.63	20.47	0.54	21.54	113.60	93.66	54.40
44	110100	GSPL/AL/BH-03	59	60	16.69	1.62	5.09	1838.42	132.92	490.94	9.06	82.58	128.49	664.87	13.16	0.17	10.36	76.85	117.80	46.93
45.1	113502	GSPL/AL/BH-03	65	66	12.31	1.18	5.94	2326.94	40.13	598.38	6.29	216.48	608.12	535.70	10.14	0.25	8.28	52.11	29.33	52.60
45.2	113502	GSPL/AL/BH-03	65	66	11.10	1.29	5.93	2313.69	35.85	590.81	6.09	212.41	596.47	540.56	10.65	0.21	9.63	53.39	28.49	51.03
46.1	113611	GSPL/AL/BH-03	73	75	11.93	1.21	5.85	1501.15	254.57	527.41	12.78	151.06	380.08	694.95	10.78	0.15	9.87	61.74	95.52	44.18
46.2	113611	GSPL/AL/BH-03	73	75	12.12	1.57	5.96	1516.40	252.47	546.07	13.02	151.09	397.12	710.76	10.03	0.19	10.02	63.38	98.02	43.89

SL	Sample ID	Borehole No	From (m)	To (m)	Zr	Nb	Mo	Ag	Cd	In	Sn	Sb	Te	Cs	Ba	La	Ce	Pr	Nd	Sm
31	113618	GSPL/AL/BH-03	7	8	3.79	4.97	2.30	0.60	0.62	0.03	1.27	1.10	<0.05	10.32	4415.43	42.36	109.27	12.27	52.37	12.98
32	113617	GSPL/AL/BH-03	12	13	27.24	10.00	50.15	<0.05	0.17	0.06	3.12	1.28	0.67	4.06	10832.53	12.32	27.50	2.69	9.79	1.95
33	113616	GSPL/AL/BH-03	15	16	3.59	5.96	42.82	<0.05	0.38	0.21	2.20	1.56	<0.05	2.57	3688.54	23.66	31.32	4.10	15.39	2.92
34	110095	GSPL/AL/BH-03	22	23	3.53	8.25	45.64	<0.05	0.96	0.07	1.47	4.51	<0.05	6.28	2499.12	35.07	63.48	8.64	33.18	6.93
35	113615	GSPL/AL/BH-03	23	24	6.25	11.35	190.02	0.54	1.03	0.08	2.87	3.10	<0.05	7.20	3060.38	20.98	37.76	5.50	24.13	5.83
36	113614	GSPL/AL/BH-03	24	25	6.86	12.03	170.40	0.47	2.28	0.08	5.05	3.69	<0.05	6.18	3211.24	19.85	35.63	5.49	23.52	5.79
37	110097	GSPL/AL/BH-03	27	28	4.39	10.39	158.85	<0.05	20.92	0.08	2.96	3.73	0.79	6.11	724.34	27.24	53.57	8.20	34.91	8.00
38	113613	GSPL/AL/BH-03	29	30	4.98	11.55	206.37	1.12	36.33	0.09	3.12	5.37	0.71	7.67	1354.67	32.63	50.69	8.66	37.32	8.66
39	113612	GSPL/AL/BH-03	31	32	3.79	13.18	150.60	0.27	36.48	0.06	3.09	2.81	<0.05	8.36	1154.75	32.90	61.13	8.71	35.85	8.19
40	110096	GSPL/AL/BH-03	38	39	3.03	6.16	191.93	<0.05	17.05	0.08	2.12	4.89	<0.05	4.42	617.84	26.65	49.35	7.10	29.74	7.22
41	110099	GSPL/AL/BH-03	41	42	5.49	7.58	12.59	<0.05	2.74	0.01	1.68	2.87	<0.05	4.25	1161.19	25.69	47.77	5.64	22.28	4.93
42	110098	GSPL/AL/BH-03	46	47	3.31	9.85	126.04	0.13	20.32	0.07	2.07	3.69	<0.05	6.27	672.72	34.53	60.83	9.59	40.63	10.17
43	113501	GSPL/AL/BH-03	53	54	3.69	11.69	133.51	0.99	21.34	0.04	2.50	6.81	<0.05	4.31	424.40	48.58	81.42	12.76	50.42	10.79
44	110100	GSPL/AL/BH-03	59	60	12.75	6.45	110.47	<0.05	21.15	0.05	1.87	4.16	<0.05	2.48	587.45	23.37	39.78	5.91	25.24	5.53
45.1	113502	GSPL/AL/BH-03	65	66	5.84	6.16	211.25	1.98	14.05	0.01	1.83	5.03	0.80	1.93	1328.67	30.65	34.93	8.12	35.59	8.50
45.2	113502	GSPL/AL/BH-03	65	66	5.93	5.88	210.42	1.89	14.06	0.01	2.02	5.57	0.75	1.90	1320.04	29.65	34.53	7.95	35.23	8.18
46.1	113611	GSPL/AL/BH-03	73	75	4.06	5.95	197.07	6.21	15.97	0.04	2.02	4.29	<0.05	3.83	1407.73	34.42	50.32	8.19	34.43	7.60
46.2	113611	GSPL/AL/BH-03	73	75	4.40	6.25	200.02	5.98	16.45	0.05	1.92	4.36	<0.05	4.18	1390.95	34.37	50.41	8.00	35.28	7.65

SL	Sample ID	Borehole No	From (m)	To (m)	Eu	Gd	Tb	Dy	Ho	Er	Tm	Yb	Lu	Hf	Ta	W	Tl	Pb	Bi	Th	U
31	113618	GSPL/AL/BH-03	7	8	3.11	12.96	1.79	11.02	2.83	7.26	0.79	7.51	0.71	<0.05	0.29	37.91	2.01	7.02	0.12	13.17	7.79
32	113617	GSPL/AL/BH-03	12	13	1.50	1.88	0.29	2.13	0.39	1.34	<0.1	1.59	<0.01	<0.05	0.74	12.54	0.92	<0.1	0.76	7.83	3.43
33	113616	GSPL/AL/BH-03	15	16	0.91	3.33	0.39	2.56	0.56	1.83	<0.1	1.79	0.08	<0.05	0.26	5.78	0.86	<0.1	<0.1	6.90	10.37
34	110095	GSPL/AL/BH-03	22	23	1.76	7.93	1.12	7.48	1.89	5.02	0.61	5.02	0.48	<0.05	0.22	14.39	0.84	5.72	0.17	9.75	21.17
35	113615	GSPL/AL/BH-03	23	24	1.50	6.84	1.03	7.36	2.08	5.48	0.55	5.33	0.40	<0.05	0.77	14.30	1.45	4.97	0.22	6.29	44.40
36	113614	GSPL/AL/BH-03	24	25	1.50	7.64	1.12	7.81	2.24	5.78	0.63	5.76	0.43	<0.05	0.83	14.62	1.42	19.70	0.29	5.74	46.06
37	110097	GSPL/AL/BH-03	27	28	1.79	9.52	1.32	8.75	2.13	5.77	0.67	5.70	0.53	<0.05	0.63	7.32	1.20	18.63	0.57	11.27	46.54
38	113613	GSPL/AL/BH-03	29	30	2.02	9.07	1.19	8.00	2.16	5.55	0.57	5.23	0.44	<0.05	0.75	9.81	1.56	13.87	0.37	9.65	53.02
39	113612	GSPL/AL/BH-03	31	32	1.90	8.80	1.14	7.41	2.09	5.50	0.57	5.09	0.39	<0.05	0.89	7.58	1.61	2.32	0.22	12.21	43.55
40	110096	GSPL/AL/BH-03	38	39	1.59	9.41	1.42	9.44	2.32	6.17	0.76	6.75	0.76	<0.05	0.15	14.58	0.88	30.11	0.40	8.26	53.03
41	110099	GSPL/AL/BH-03	41	42	1.19	5.35	0.72	4.73	0.95	2.67	0.23	2.44	0.16	<0.05	0.37	1.73	0.81	<0.1	<0.1	7.33	8.25
42	110098	GSPL/AL/BH-03	46	47	1.93	12.23	1.70	11.92	3.00	8.16	0.98	8.14	0.81	<0.05	0.63	9.08	1.47	106.50	0.87	10.77	53.83
43	113501	GSPL/AL/BH-03	53	54	2.20	10.62	1.29	7.67	1.75	4.36	0.44	3.97	0.32	<0.05	0.92	4.66	1.73	24.82	0.44	12.34	84.36
44	110100	GSPL/AL/BH-03	59	60	1.01	6.67	0.96	6.19	1.45	3.89	0.39	4.00	0.28	0.11	0.34	3.32	1.15	8.13	0.23	6.54	17.25
45.1	113502	GSPL/AL/BH-03	65	66	1.72	9.96	1.28	8.24	1.90	4.84	0.51	4.46	0.33	<0.05	<0.1	6.84	0.78	10.11	0.33	4.74	54.29
45.2	113502	GSPL/AL/BH-03	65	66	1.55	9.22	1.25	8.28	1.84	4.73	0.50	4.25	0.31	<0.05	<0.1	6.86	0.74	10.40	0.30	4.44	53.37
46.1	113611	GSPL/AL/BH-03	73	75	1.56	7.81	0.98	6.22	1.58	4.46	0.34	3.69	0.20	0.23	0.38	298.04	0.84	16.54	0.37	7.11	39.24
46.2	113611	GSPL/AL/BH-03	73	75	1.70	7.92	0.98	6.29	1.62	4.16	0.41	3.67	0.24	0.22	0.40	307.30	0.89	15.59	0.45	7.47	42.94

SL	Sample ID	Borehole No	From (m)	To (m)	Li	Be	Sc	V	Mn	Cr	Co	Ni	Cu	Zn	Ga	Ge	Se	Rb	Sr	Y
47	113503	GSPL/AL/BH-04	10	11	19.81	2.81	7.77	1052.37	41.88	424.13	3.48	13.95	27.41	48.32	14.89	<0.1	6.17	95.03	180.40	12.47
48	113504	GSPL/AL/BH-04	15	16	15.03	1.59	6.63	1459.65	45.60	754.95	4.71	51.32	128.64	130.73	11.39	0.12	12.44	53.27	36.10	46.35
49	113505	GSPL/AL/BH-04	18	19	23.45	1.65	6.75	1041.12	209.52	549.28	8.92	172.85	335.31	536.53	12.15	0.29	10.24	96.97	165.63	69.37
50	113506	GSPL/AL/BH-04	19	20	22.31	2.03	6.99	784.22	291.94	506.32	10.06	130.42	285.00	1016.13	13.88	0.38	12.99	86.52	152.46	70.49
51	113507	GSPL/AL/BH-04	23	24	27.10	2.30	8.39	135.32	387.75	295.94	12.40	48.03	28.19	126.93	16.76	0.11	3.57	121.97	175.06	19.64
52	113508	GSPL/AL/BH-04	31	32	26.92	2.62	11.46	546.07	346.34	264.43	16.40	89.47	68.86	186.35	21.84	0.23	9.21	141.91	154.58	37.36
53	113509	GSPL/AL/BH-04	54.5	55.5	35.29	2.26	11.29	95.01	706.72	195.84	14.93	39.58	22.57	93.85	21.11	0.24	5.19	143.33	116.01	31.91

SL	Sample ID	Borehole No	From (m)	To (m)	Zr	Nb	Mo	Ag	Cd	In	Sn	Sb	Te	Cs	Ba	La	Ce	Pr	Nd	Sm
47	113503	GSPL/AL/BH-04	10	11	2.04	7.47	27.67	<0.05	0.17	0.03	2.25	5.12	<0.05	2.57	2850.34	17.76	25.39	2.83	8.83	1.66
48	113504	GSPL/AL/BH-04	15	16	9.57	8.84	107.50	0.61	0.87	0.03	2.30	7.50	<0.05	2.04	2156.31	27.75	40.17	7.07	30.05	6.41
49	113505	GSPL/AL/BH-04	18	19	2.57	9.64	82.15	1.36	15.69	0.02	2.15	29.12	<0.05	8.67	1934.56	23.74	39.59	6.49	28.04	7.83
50	113506	GSPL/AL/BH-04	19	20	3.04	6.55	50.57	1.13	11.71	0.02	1.79	9.07	0.78	6.48	739.00	36.62	63.49	9.48	40.80	10.21
51	113507	GSPL/AL/BH-04	23	24	2.89	8.98	9.00	<0.05	0.42	0.05	2.25	2.90	<0.05	7.87	5425.38	30.83	57.70	6.44	22.83	4.84
52	113508	GSPL/AL/BH-04	31	32	2.74	12.42	26.55	<0.05	1.96	0.05	2.94	2.56	<0.05	4.85	759.09	46.25	90.50	10.03	38.08	7.47
53	113509	GSPL/AL/BH-04	54.5	55.5	2.03	12.68	1.23	<0.05	0.14	0.06	3.42	1.98	<0.05	6.98	1707.42	47.12	92.10	9.80	35.21	6.86

SL	Sample ID	Borehole No	From (m)	To (m)	Eu	Gd	Tb	Dy	Ho	Er	Tm	Yb	Lu	Hf	Ta	W	Tl	Pb	Bi	Th	U
47	113503	GSPL/AL/BH-04	10	11	0.73	2.02	0.26	1.58	0.24	0.86	<0.1	0.74	<0.000	<0.05	0.20	1.51	1.00	20.44	0.19	8.91	8.21
48	113504	GSPL/AL/BH-04	15	16	1.49	7.73	0.99	6.60	1.53	4.16	0.47	4.39	0.32	0.11	0.65	2.61	0.67	19.88	0.30	6.64	26.94
49	113505	GSPL/AL/BH-04	18	19	1.91	10.24	1.49	10.14	2.49	6.22	0.78	6.34	0.61	<0.05	0.78	1.92	1.58	26.24	0.40	7.36	25.94
50	113506	GSPL/AL/BH-04	19	20	2.31	11.84	1.57	10.54	2.53	6.48	0.74	6.49	0.59	<0.05	0.16	24.82	1.01	13.66	0.23	8.31	21.87
51	113507	GSPL/AL/BH-04	23	24	1.60	4.32	0.59	3.37	0.60	1.63	<0.1	1.54	<0.01	<0.05	0.50	1.77	0.77	10.14	0.13	9.11	4.99
52	113508	GSPL/AL/BH-04	31	32	1.46	7.05	0.94	6.09	1.23	3.43	0.27	3.27	0.20	<0.05	0.84	2.70	1.82	<0.1	0.15	15.10	15.48
53	113509	GSPL/AL/BH-04	54.5	55.5	1.51	6.58	0.89	5.63	1.13	3.04	0.26	2.94	0.18	<0.05	0.65	2.09	0.77	16.69	<0.1	16.40	3.34

SL	Sample ID	Borehole No	From (m)	To (m)	Li	Be	Sc	V	Mn	Cr	Co	Ni	Cu	Zn	Ga	Ge	Se	Rb	Sr	Y
54	113510	GSPL/AL/BH-05	6	7	39.33	3.17	17.20	170.07	564.71	235.07	17.21	34.31	58.62	119.81	28.78	0.16	7.56	211.83	160.42	31.08
55	113610	GSPL/AL/BH-05	10	11	14.87	1.79	7.60	67.10	183.50	186.25	11.57	38.95	16.87	83.04	14.37	<0.1	2.79	71.31	149.12	18.64
56	113511	GSPL/AL/BH-05	15	16	21.19	2.44	7.76	1170.96	76.56	526.31	2.36	20.30	137.49	86.54	18.79	<0.1	8.75	115.57	76.40	17.50
57	113609	GSPL/AL/BH-05	23	24	26.30	2.28	10.01	824.17	122.77	368.03	13.03	80.85	663.13	210.16	16.08	0.35	23.12	123.62	182.82	60.67
58	113608	GSPL/AL/BH-05	25	26	16.17	2.30	9.19	945.21	80.80	211.70	13.44	68.34	244.41	310.09	15.41	0.22	16.32	94.08	93.28	77.41
59	113512	GSPL/AL/BH-05	28	29	18.03	2.15	7.37	106.21	89.01	552.54	12.27	70.42	60.46	106.22	17.26	0.20	9.59	81.87	241.54	31.14
60	113513	GSPL/AL/BH-05	32	33	17.29	1.96	6.65	2089.62	57.26	469.36	27.29	237.15	171.94	1724.06	17.11	0.48	16.37	91.34	111.93	76.12
61	113607	GSPL/AL/BH-05	35	36	22.94	2.51	10.81	1073.39	509.06	369.29	22.97	100.97	221.89	1722.51	20.32	0.29	16.20	122.18	81.41	102.26
62	113606	GSPL/AL/BH-05	38	39	28.37	3.23	13.04	3683.43	295.48	558.53	15.11	154.06	276.20	2730.96	20.88	0.33	21.22	149.15	106.40	72.97
63	113514	GSPL/AL/BH-05	40	41	24.61	3.38	10.25	2443.45	288.60	562.09	12.77	129.53	216.71	1478.97	18.37	<0.1	23.96	129.83	114.34	83.64
64	113515	GSPL/AL/BH-05	44	45	32.78	4.39	14.19	3486.02	245.64	893.89	15.53	186.56	339.55	2368.78	23.68	0.40	24.28	160.94	132.53	94.85
65	113605	GSPL/AL/BH-05	48	49	28.47	3.08	11.54	3739.38	343.93	559.60	13.89	175.43	271.17	2848.15	19.43	0.30	22.23	154.28	136.13	101.03
66	113604	GSPL/AL/BH-05	50	51	23.21	2.80	10.55	2872.27	403.71	406.06	14.93	154.86	226.60	1930.31	18.54	0.23	20.03	127.53	154.42	93.50
67	113603	GSPL/AL/BH-05	55	56	25.92	3.26	12.31	2926.03	253.97	354.03	27.71	172.11	217.04	1981.71	19.83	0.24	18.98	132.58	142.40	91.37
68	113516	GSPL/AL/BH-05	61	62	22.06	1.72	5.22	500.03	244.60	322.64	10.55	70.44	238.24	596.47	12.80	<0.1	10.90	72.51	366.50	31.88
69	113555	GSPL/AL/BH-05	65	66	17.60	2.89	6.78	909.47	184.83	327.37	10.43	72.64	195.89	682.70	14.51	<0.1	13.55	80.74	243.03	40.59
70	113554	GSPL/AL/BH-05	69	70	21.93	1.44	6.07	322.47	307.71	263.67	8.31	33.65	34.25	178.33	12.04	<0.1	9.75	105.55	458.17	27.51
71	113517	GSPL/AL/BH-05	72	73	32.93	3.72	12.05	1502.49	297.12	356.97	34.90	180.98	295.55	814.30	21.73	<0.1	28.16	141.73	217.65	53.63
72	113556	GSPL/AL/BH-05	74	75	33.15	3.90	14.52	405.24	628.76	240.19	21.01	91.22	170.72	280.37	25.57	<0.1	16.97	170.33	343.39	38.25

SL	Sample ID	Borehole No	From (m)	To (m)	Zr	Nb	Mo	Ag	Cd	In	Sn	Sb	Te	Cs	Ba	La	Ce	Pr	Nd	Sm
54	113510	GSPL/AL/BH-05	6	7	<0.1	16.17	3.19	0.23	<0.05	0.10	4.69	0.32	0.54	8.90	4856.64	54.65	112.37	11.66	41.97	8.50
55	113610	GSPL/AL/BH-05	10	11	2.56	5.47	10.30	<0.05	<0.05	0.03	1.59	0.58	<0.05	4.09	751.83	24.81	46.61	4.75	18.79	3.03
56	113511	GSPL/AL/BH-05	15	16	<0.1	10.18	42.48	1.58	0.45	0.02	3.53	13.97	<0.05	3.64	10823.93	38.29	68.19	10.07	37.10	5.74
57	113609	GSPL/AL/BH-05	23	24	3.11	8.28	52.12	3.74	0.54	0.06	2.25	2.79	<0.05	6.79	426.87	30.15	58.25	8.50	38.14	9.58
58	113608	GSPL/AL/BH-05	25	26	2.83	7.79	66.26	0.71	44.14	0.08	2.51	2.55	<0.05	2.63	805.77	31.25	53.92	9.06	40.83	9.39
59	113512	GSPL/AL/BH-05	28	29	3.80	7.94	1.25	<0.05	7.68	0.01	1.36	3.00	0.74	4.33	431.67	25.04	54.49	6.95	29.07	6.50
60	113513	GSPL/AL/BH-05	32	33	2.34	7.67	32.71	0.48	24.03	0.09	2.21	3.33	<0.05	2.68	628.33	30.49	58.29	10.24	48.37	11.38
61	113607	GSPL/AL/BH-05	35	36	2.77	9.06	108.57	1.56	11.25	0.07	3.09	2.25	<0.05	4.71	650.71	38.51	67.42	10.95	50.38	11.72
62	113606	GSPL/AL/BH-05	38	39	2.51	11.75	113.94	4.81	52.23	0.15	3.54	2.74	<0.05	3.70	694.92	44.43	71.61	11.37	48.51	9.92
63	113514	GSPL/AL/BH-05	40	41	<0.1	10.08	63.75	4.20	28.62	0.08	3.15	24.28	1.30	3.25	852.62	41.76	64.74	11.13	47.65	10.95
64	113515	GSPL/AL/BH-05	44	45	3.15	12.24	119.67	2.68	46.15	0.10	3.57	4.09	<0.05	4.94	436.19	43.06	71.58	13.25	54.95	11.17
65	113605	GSPL/AL/BH-05	48	49	2.57	10.96	111.58	3.18	55.12	0.14	3.43	3.28	<0.05	5.37	498.50	38.87	65.37	11.51	49.53	11.55
66	113604	GSPL/AL/BH-05	50	51	4.99	10.28	119.29	2.89	35.76	0.11	3.13	3.56	0.72	4.07	473.85	33.66	57.92	9.82	42.84	9.79
67	113603	GSPL/AL/BH-05	55	56	2.66	11.07	108.57	3.28	36.85	0.09	2.96	4.17	0.70	4.75	316.09	36.70	71.71	10.88	45.96	10.35
68	113516	GSPL/AL/BH-05	61	62	1.85	5.84	26.86	17.17	11.85	0.06	1.79	33.84	<0.05	3.08	512.22	18.29	34.43	4.97	20.78	4.45
69	113555	GSPL/AL/BH-05	65	66	<0.1	6.56	27.73	6.78	15.44	0.05	2.36	32.63	<0.05	2.86	1022.93	30.75	48.52	7.56	30.06	6.20
70	113554	GSPL/AL/BH-05	69	70	<0.1	6.60	11.43	2.60	3.56	0.02	1.28	32.95	<0.05	7.15	1296.36	24.82	43.28	5.22	20.87	4.15
71	113517	GSPL/AL/BH-05	72	73	<0.1	13.17	65.83	4.60	16.06	0.05	3.46	25.58	<0.05	9.11	678.65	44.31	83.87	10.33	41.52	8.27
72	113556	GSPL/AL/BH-05	74	75	<0.1	15.00	21.04	3.99	4.07	0.07	3.53	26.72	<0.05	9.86	2564.10	52.58	100.71	10.71	40.69	7.84

SL	Sample ID	Borehole No	From (m)	To (m)	Eu	Gd	Tb	Dy	Ho	Er	Tm	Yb	Lu	Hf	Ta	W	Tl	Pb	Bi	Th	U
54	113510	GSPL/AL/BH-05	6	7	2.06	7.38	1.01	5.76	1.17	3.34	0.49	3.15	0.39	0.11	1.36	3.18	1.18	16.81	0.28	21.13	5.16
55	113610	GSPL/AL/BH-05	10	11	0.72	3.40	0.49	2.94	0.64	1.96	<0.1	1.60	<0.01	<0.05	0.31	<0.1	0.22	6.17	<0.1	8.48	1.52
56	113511	GSPL/AL/BH-05	15	16	2.25	4.02	0.52	2.77	0.61	1.76	0.28	1.83	0.31	0.11	0.89	2.98	1.78	12.05	0.34	7.53	11.93
57	113609	GSPL/AL/BH-05	23	24	2.17	10.86	1.47	9.59	2.51	6.18	0.63	6.27	0.43	<0.05	0.55	1.35	1.96	4.88	0.23	9.85	26.44
58	113608	GSPL/AL/BH-05	25	26	1.77	11.61	1.57	11.07	3.07	7.68	0.78	6.80	0.62	<0.05	0.37	5.57	1.00	<0.1	0.10	8.13	33.00
59	113512	GSPL/AL/BH-05	28	29	1.50	6.57	0.86	5.14	1.07	2.80	0.23	2.63	0.14	<0.05	0.50	0.41	1.71	0.41	0.11	7.24	13.76
60	113513	GSPL/AL/BH-05	32	33	3.27	12.73	1.68	10.81	2.58	6.70	0.75	6.50	0.63	<0.05	0.39	1.50	1.12	6.44	0.28	7.03	12.88
61	113607	GSPL/AL/BH-05	35	36	2.53	13.92	1.91	12.92	3.78	9.42	0.99	8.18	0.81	<0.05	0.58	17.28	1.30	<0.1	0.24	11.38	25.34
62	113606	GSPL/AL/BH-05	38	39	1.97	10.58	1.38	9.02	2.47	6.44	0.61	5.51	0.45	<0.05	0.72	3.77	1.65	<0.1	0.19	12.22	64.69
63	113514	GSPL/AL/BH-05	40	41	2.20	12.57	1.73	11.84	2.44	7.40	1.00	6.30	0.86	0.09	0.88	2.78	1.63	<0.1	0.21	11.03	37.70
64	113515	GSPL/AL/BH-05	44	45	2.33	13.81	1.94	12.75	3.12	7.84	0.91	7.15	0.65	<0.05	0.85	3.63	1.92	10.92	0.23	12.22	59.87
65	113605	GSPL/AL/BH-05	48	49	2.55	13.82	1.90	12.54	3.68	8.89	0.86	7.51	0.64	<0.05	0.80	2.94	1.95	<0.1	0.21	11.52	61.16
66	113604	GSPL/AL/BH-05	50	51	2.15	12.26	1.69	11.38	3.21	8.21	0.84	7.60	0.67	<0.05	0.81	4.83	1.43	2.46	0.29	10.71	54.03
67	113603	GSPL/AL/BH-05	55	56	2.48	11.20	1.58	10.97	3.11	7.85	0.80	7.13	0.61	<0.05	0.81	3.49	1.41	10.82	0.31	11.91	57.19
68	113516	GSPL/AL/BH-05	61	62	1.17	5.02	0.66	4.03	0.92	2.39	0.19	2.35	0.09	<0.05	0.17	1.20	0.99	79.03	0.89	5.48	30.09
69	113555	GSPL/AL/BH-05	65	66	1.49	6.18	0.89	5.79	1.20	3.75	0.48	3.55	0.46	0.10	0.47	2.13	1.18	16.19	0.65	7.13	17.33
70	113554	GSPL/AL/BH-05	69	70	1.25	3.70	0.59	3.43	0.77	2.34	0.36	2.23	0.31	0.09	0.53	0.95	1.87	<0.1	0.20	6.97	8.62
71	113517	GSPL/AL/BH-05	72	73	1.63	8.28	1.15	6.82	1.50	4.50	0.63	4.07	0.55	0.10	1.25	3.41	1.88	3.55	0.72	13.31	40.52
72	113556	GSPL/AL/BH-05	74	75	1.78	7.20	0.99	5.86	1.21	3.53	0.49	3.39	0.45	0.14	1.33	2.94	2.27	6.10	0.58	18.18	14.46

SL	Sample ID	Borehole No	From (m)	To (m)	Li	Be	Sc	V	Mn	Cr	Co	Ni	Cu	Zn	Ga	Ge	Se	Rb	Sr	Y
73	113530	GSPL/AL/BH-06	14	15	32.61	3.20	11.46	82.03	443.15	178.21	15.50	28.45	19.90	79.99	23.14	<0.1	5.91	178.65	227.85	33.16
74	113531	GSPL/AL/BH-06	17	18	23.44	1.71	9.18	67.29	334.23	221.67	9.88	17.35	14.35	76.96	17.75	<0.1	7.71	109.49	164.68	34.11
75	113532	GSPL/AL/BH-06	23	24	19.16	2.50	9.36	72.05	521.10	186.24	11.24	21.59	14.21	71.05	17.93	<0.1	6.79	134.16	176.73	32.15
76	113533	GSPL/AL/BH-06	27	28	13.79	2.21	4.67	37.15	467.46	271.91	7.48	18.42	10.75	49.34	10.26	<0.1	3.45	77.69	158.70	13.79
77	113534	GSPL/AL/BH-06	33	34	14.02	2.10	4.73	36.28	534.04	273.45	7.46	27.69	19.97	50.65	10.16	<0.1	4.14	75.34	158.87	13.82
78	113535	GSPL/AL/BH-06	41	42	30.59	3.66	10.91	156.36	451.32	247.46	16.53	57.50	48.74	154.61	20.37	0.12	6.67	158.75	185.80	30.78
79	113536	GSPL/AL/BH-06	48.5	49.5	28.64	2.68	11.16	172.94	519.93	204.22	15.14	66.68	42.24	146.86	22.31	0.22	5.58	132.72	135.97	26.34
80	113537	GSPL/AL/BH-06	55.5	56.5	21.11	2.81	8.64	64.12	543.51	143.15	10.44	21.88	14.13	85.12	17.40	<0.1	5.62	123.01	181.43	28.20
81	113538	GSPL/AL/BH-06	61	62	23.26	3.43	9.77	81.20	680.43	183.24	12.41	26.63	24.58	157.53	18.29	<0.1	8.54	129.99	195.20	27.82
82	113539	GSPL/AL/BH-06	66	67	25.72	3.01	10.62	77.50	527.45	172.60	13.40	27.43	13.50	68.93	20.56	<0.1	6.45	147.17	230.97	30.02
83.1	**113540**	GSPL/AL/BH-06	70	71	30.89	3.28	10.20	89.22	415.02	145.18	16.84	33.03	58.41	69.93	19.29	<0.1	5.34	155.76	164.68	31.59
83.2	**113540**	GSPL/AL/BH-06	70	71	30.11	3.13	10.45	87.15	415.02	146.19	18.47	33.03	58.41	67.16	20.55	<0.1	5.13	155.38	162.63	31.59
84	113541	GSPL/AL/BH-06	75	76	40.71	3.17	16.69	187.46	529.56	219.40	21.39	70.85	54.81	214.25	29.59	0.29	5.86	200.28	152.48	37.44
85	113542	GSPL/AL/BH-06	81	82	27.93	2.55	10.14	152.74	414.88	187.78	15.70	45.79	29.90	92.47	19.83	<0.1	5.36	140.91	154.83	33.40
86	113543	GSPL/AL/BH-06	87	88	33.23	2.90	13.75	355.14	483.44	175.80	22.36	124.28	68.06	234.26	23.75	0.33	6.56	157.58	130.67	43.24
87	113544	GSPL/AL/BH-06	93	94	27.16	3.32	10.80	82.08	363.84	175.68	15.81	34.85	31.37	101.80	19.55	<0.1	5.52	158.80	162.09	28.79
88	113545	GSPL/AL/BH-06	97	98	31.64	2.45	10.46	352.14	386.52	240.53	17.70	74.39	49.26	254.05	20.35	<0.1	7.91	160.90	136.95	37.71
89	113546	GSPL/AL/BH-06	102	103	35.23	1.39	11.26	582.70	492.47	211.69	17.39	99.57	57.62	248.90	23.18	<0.1	7.85	185.69	77.87	43.80
90	113547	GSPL/AL/BH-06	105	106	31.35	3.45	11.32	257.52	343.82	216.30	21.85	86.57	67.36	133.35	19.88	<0.1	6.47	139.88	209.76	37.37

SL	Sample ID	Borehole No	From (m)	To (m)	Zr	Nb	Mo	Ag	Cd	In	Sn	Sb	Te	Cs	Ba	La	Ce	Pr	Nd	Sm
73	113530	GSPL/AL/BH-06	14	15	<0.1	14.02	1.20	0.21	0.07	0.07	3.26	15.15	<0.05	10.11	2230.11	51.67	101.05	10.24	38.91	7.11
74	113531	GSPL/AL/BH-06	17	18	<0.1	12.43	0.84	0.21	0.19	0.05	2.58	7.50	<0.05	3.48	862.53	54.96	105.96	11.05	41.20	7.82
75	113532	GSPL/AL/BH-06	23	24	<0.1	6.41	2.17	0.15	0.12	0.04	2.91	18.24	<0.05	6.22	1994.39	51.99	101.23	10.28	38.96	7.35
76	113533	GSPL/AL/BH-06	27	28	<0.1	1.75	0.68	0.12	<0.05	0.03	0.90	13.77	<0.05	3.43	2239.11	20.95	40.76	4.13	15.47	2.74
77	113534	GSPL/AL/BH-06	33	34	<0.1	1.56	0.43	0.08	<0.05	<0.01	0.79	5.65	<0.05	3.43	2062.21	19.85	38.43	4.05	14.91	2.81
78	113535	GSPL/AL/BH-06	41	42	<0.1	6.71	20.30	0.41	1.17	0.07	3.12	18.56	<0.05	5.54	1407.13	45.19	87.79	9.09	34.73	6.39
79	113536	GSPL/AL/BH-06	48.5	49.5	2.79	5.15	19.71	<0.05	0.97	0.07	2.68	2.63	<0.05	4.03	691.26	44.19	86.75	9.27	32.91	6.20
80	113537	GSPL/AL/BH-06	55.5	56.5	<0.1	7.29	1.18	0.14	0.30	0.04	2.14	18.04	<0.05	6.55	1093.15	42.80	83.28	8.56	31.10	6.12
81	113538	GSPL/AL/BH-06	61	62	<0.1	6.61	1.09	0.21	0.72	0.06	2.33	20.02	<0.05	5.00	1130.03	41.26	80.01	8.20	32.04	5.89
82	113539	GSPL/AL/BH-06	66	67	<0.1	12.48	1.04	0.04	0.14	0.06	2.59	13.11	<0.05	7.62	1055.83	46.03	90.27	9.36	33.71	6.76
83.1	**113540**	GSPL/AL/BH-06	70	71	<0.1	8.60	1.63	0.21	0.16	0.10	2.87	9.55	<0.05	8.40	1252.49	50.69	90.13	9.59	37.24	6.73
83.2	**113540**	GSPL/AL/BH-06	70	71	<0.1	8.63	1.84	0.19	0.19	0.09	3.08	9.84	<0.05	8.99	1251.39	50.57	108.15	9.62	37.19	7.03
84	113541	GSPL/AL/BH-06	75	76	2.72	14.95	9.52	<0.05	0.46	0.12	4.94	2.52	0.82	12.09	2080.31	54.44	104.88	11.50	41.37	8.33
85	113542	GSPL/AL/BH-06	81	82	<0.1	4.54	14.56	0.26	1.57	0.08	3.09	13.35	<0.05	5.76	1345.83	47.17	91.10	9.58	35.99	7.59
86	113543	GSPL/AL/BH-06	87	88	3.09	7.40	48.57	<0.05	4.04	0.10	5.02	3.86	<0.05	5.33	740.89	47.93	94.31	10.38	39.28	7.87
87	113544	GSPL/AL/BH-06	93	94	<0.1	5.59	2.03	0.29	0.42	0.07	3.17	22.88	<0.05	5.58	1301.60	39.98	79.31	8.51	31.38	6.99
88	113545	GSPL/AL/BH-06	97	98	<0.1	8.09	38.61	0.47	4.06	0.09	3.65	22.33	<0.05	6.59	1407.12	45.81	88.65	9.51	36.83	7.18
89	113546	GSPL/AL/BH-06	102	103	<0.1	5.45	31.10	0.30	6.02	0.10	3.96	12.76	<0.05	6.99	1734.32	46.51	89.11	9.78	37.09	7.38
90	113547	GSPL/AL/BH-06	105	106	<0.1	8.79	37.52	0.41	1.97	0.11	3.35	20.52	<0.05	7.33	1050.00	53.54	102.34	10.74	39.98	8.22

SL	Sample ID	Borehole No	From (m)	To (m)	Eu	Gd	Tb	Dy	Ho	Er	Tm	Yb	Lu	Hf	Ta	W	Tl	Pb	Bi	Th	U
73	113530	GSPL/AL/BH-06	14	15	1.71	6.85	0.95	5.86	1.12	3.34	0.46	3.02	0.40	0.09	0.98	1.29	1.32	<0.1	0.18	18.09	2.95
74	113531	GSPL/AL/BH-06	17	18	1.83	7.22	0.95	5.89	1.12	3.39	0.45	2.98	0.37	0.17	0.89	1.01	0.51	<0.1	0.18	22.48	3.36
75	113532	GSPL/AL/BH-06	23	24	1.57	6.45	0.92	5.30	1.10	3.19	0.43	2.76	0.33	0.11	0.50	1.88	1.11	7.59	0.16	23.80	3.89
76	113533	GSPL/AL/BH-06	27	28	0.64	2.31	0.37	1.95	0.47	1.29	0.20	1.41	0.17	0.07	0.12	1.06	0.75	18.27	<0.1	7.18	1.27
77	113534	GSPL/AL/BH-06	33	34	0.57	2.32	0.35	2.03	0.45	1.35	0.21	1.62	0.24	<0.05	0.11	0.53	1.16	<0.1	<0.1	6.40	1.25
78	113535	GSPL/AL/BH-06	41	42	1.36	6.23	0.87	4.89	1.06	3.01	0.41	2.60	0.33	0.07	0.77	2.25	1.42	2.74	0.41	15.22	6.39
79	113536	GSPL/AL/BH-06	48.5	49.5	1.26	6.33	0.78	4.81	0.90	2.34	0.17	2.20	0.08	<0.05	0.27	1.80	0.95	6.05	0.38	16.79	5.76
80	113537	GSPL/AL/BH-06	55.5	56.5	1.33	5.53	0.78	4.62	0.93	2.67	0.38	2.59	0.31	0.08	0.50	1.12	1.65	50.08	0.14	15.84	2.58
81	113538	GSPL/AL/BH-06	61	62	1.27	5.83	0.79	4.55	0.94	2.63	0.34	2.31	0.26	0.09	0.63	1.41	1.57	<0.1	0.26	14.54	2.72
82	113539	GSPL/AL/BH-06	66	67	1.36	6.16	0.86	4.93	1.05	2.77	0.41	2.60	0.34	0.06	0.91	0.80	1.28	<0.1	0.18	17.04	3.00
83.1	**113540**	GSPL/AL/BH-06	70	71	1.39	6.31	0.86	5.34	1.04	3.00	0.43	2.70	0.34	0.08	0.53	1.13	1.14	11.99	0.17	16.58	3.67
83.2	**113540**	GSPL/AL/BH-06	70	71	1.59	6.82	0.93	6.28	1.23	3.65	0.49	2.82	0.37	0.08	0.58	1.15	1.16	12.97	0.21	16.77	4.02
84	113541	GSPL/AL/BH-06	75	76	1.67	7.65	1.05	6.27	1.37	3.72	0.31	3.23	0.21	<0.05	1.16	2.13	1.09	11.48	0.36	18.73	7.84
85	113542	GSPL/AL/BH-06	81	82	1.53	6.60	0.90	5.48	1.11	3.50	0.44	3.28	0.39	0.11	0.39	1.66	0.90	<0.1	0.46	16.49	9.02
86	113543	GSPL/AL/BH-06	87	88	1.57	7.86	1.05	6.43	1.42	3.78	0.38	3.68	0.25	<0.05	0.49	2.16	0.81	9.18	0.66	16.45	26.54
87	113544	GSPL/AL/BH-06	93	94	1.34	5.86	0.84	5.29	1.04	2.98	0.42	2.76	0.35	0.11	0.61	2.14	0.97	4.45	0.33	13.78	3.05
88	113545	GSPL/AL/BH-06	97	98	1.57	6.83	0.94	5.88	1.20	3.80	0.48	3.33	0.42	0.12	0.80	2.57	0.96	41.59	0.71	15.46	16.57
89	113546	GSPL/AL/BH-06	102	103	1.62	7.14	1.02	6.17	1.37	4.11	0.58	3.74	0.52	0.09	0.43	2.38	1.07	<0.1	0.86	15.76	16.85
90	113547	GSPL/AL/BH-06	105	106	1.52	7.53	0.97	5.86	1.19	3.57	0.50	3.48	0.42	0.10	0.77	2.13	0.95	<0.1	0.70	15.60	17.45

SL	Sample ID	Borehole No	From (m)	To (m)	Li	Be	Sc	V	Mn	Cr	Co	Ni	Cu	Zn	Ga	Ge	Se	Rb	Sr	Y
91	113518	GSPL/AL/BH-07	9	10	32.60	3.15	9.94	160.02	413.90	196.36	7.81	23.26	38.64	90.83	19.08	<0.1	3.23	132.43	103.11	11.88
92	113519	GSPL/AL/BH-07	14	15	26.21	1.94	8.40	59.65	587.40	187.13	10.50	33.08	16.56	66.03	16.82	<0.1	8.03	117.07	128.63	33.92
93.1	**113550**	GSPL/AL/BH-07	22	23	27.06	2.04	8.11	67.37	618.78	239.67	18.91	49.71	11.47	81.50	17.13	<0.1	6.83	114.92	132.44	36.34
93.2	**113550**	GSPL/AL/BH-07	22	23	27.62	2.65	8.47	67.42	618.78	243.60	18.93	49.71	11.46	83.16	18.02	<0.1	7.03	115.25	132.74	36.11
94	113520	GSPL/AL/BH-07	29	30	49.29	4.24	15.64	134.10	642.02	243.06	24.74	56.80	46.37	139.24	27.20	<0.1	8.56	213.64	162.44	31.93
95	113521	GSPL/AL/BH-07	30	31	34.43	3.18	11.98	98.29	366.41	196.13	12.16	38.72	28.85	96.33	19.83	<0.1	4.97	145.06	192.07	27.91
96	113522	GSPL/AL/BH-07	35	36	27.82	2.52	12.42	309.18	367.97	272.32	18.28	61.69	77.11	135.52	16.29	<0.1	7.12	111.11	94.34	26.26
97	113549	GSPL/AL/BH-07	41	42	18.41	1.71	7.26	51.87	490.67	180.38	7.82	22.81	13.35	43.28	12.26	<0.1	3.17	81.03	116.03	24.05
98	113523	GSPL/AL/BH-07	44	45	23.38	1.97	9.15	67.79	487.94	165.16	9.43	22.83	14.91	56.25	18.28	<0.1	5.81	114.58	148.24	32.46
99	113548	GSPL/AL/BH-07	48.5	49.5	23.24	2.15	9.72	70.01	558.51	181.96	9.47	23.38	12.79	50.83	16.85	<0.1	8.40	109.69	121.27	35.86

SL	Sample ID	Borehole No	From (m)	To (m)	Zr	Nb	Mo	Ag	Cd	In	Sn	Sb	Te	Cs	Ba	La	Ce	Pr	Nd	Sm
91	113518	GSPL/AL/BH-07	9	10	<0.1	19.23	13.22	0.42	0.08	0.07	4.17	38.43	<0.05	2.12	1209.40	24.83	51.06	5.00	17.55	3.54
92	113519	GSPL/AL/BH-07	14	15	<0.1	12.45	0.59	0.04	<0.05	0.03	2.32	16.26	<0.05	4.02	1787.96	46.10	91.32	9.50	35.06	7.01
93.1	**113550**	GSPL/AL/BH-07	22	23	<0.1	15.56	0.89	0.10	0.59	0.05	2.32	20.98	<0.05	3.09	1471.50	50.91	100.42	10.38	37.72	7.61
93.2	**113550**	GSPL/AL/BH-07	22	23	<0.1	15.70	0.89	0.11	0.57	0.05	2.58	18.36	<0.05	3.12	1470.50	51.81	100.55	10.78	38.92	7.72
94	113520	GSPL/AL/BH-07	29	30	<0.1	13.91	0.74	0.23	0.11	0.09	3.95	13.16	<0.05	12.90	3836.86	56.85	112.11	11.32	42.19	8.44
95	113521	GSPL/AL/BH-07	30	31	<0.1	10.84	0.97	0.21	0.09	0.06	2.69	13.79	<0.05	7.98	3427.59	40.99	80.39	8.47	31.13	6.20
96	113522	GSPL/AL/BH-07	35	36	<0.1	6.97	23.23	1.24	1.10	0.06	3.26	14.00	<0.05	10.17	4685.26	29.89	51.96	5.93	22.37	5.02
97	113549	GSPL/AL/BH-07	41	42	<0.1	10.71	0.74	0.10	<0.05	0.05	2.16	26.33	<0.05	7.22	357.16	33.07	64.63	6.77	25.86	4.98
98	113523	GSPL/AL/BH-07	44	45	<0.1	9.70	1.51	0.12	<0.05	0.07	3.34	14.46	<0.05	11.66	537.22	45.04	89.99	9.35	35.26	6.87
99	113548	GSPL/AL/BH-07	48.5	49.5	<0.1	13.18	0.45	0.07	<0.05	0.04	2.90	22.68	<0.05	6.11	546.01	54.94	109.03	10.98	40.31	7.95

SL	Sample ID	Borehole No	From (m)	To (m)	Eu	Gd	Tb	Dy	Ho	Er	Tm	Yb	Lu	Hf	Ta	W	Tl	Pb	Bi	Th	U
91	113518	GSPL/AL/BH-07	9	10	0.72	2.72	0.37	2.28	0.44	1.26	0.20	1.42	0.16	0.11	2.80	3.58	1.19	1.11	0.55	12.11	7.08
92	113519	GSPL/AL/BH-07	14	15	1.45	6.65	0.95	5.71	1.17	3.59	0.47	3.21	0.41	0.08	1.09	1.17	0.53	0.67	0.11	19.34	2.67
93.1	**113550**	GSPL/AL/BH-07	22	23	1.36	7.17	0.98	5.84	1.20	3.47	0.49	3.30	0.41	0.09	1.91	1.80	0.68	<0.1	0.20	20.86	3.14
93.2	**113550**	GSPL/AL/BH-07	22	23	1.58	7.30	1.02	5.93	1.26	3.61	0.51	3.39	0.42	0.08	1.87	1.74	0.63	<0.1	0.17	22.24	3.09
94	113520	GSPL/AL/BH-07	29	30	2.03	7.54	0.96	5.63	1.15	3.40	0.45	2.86	0.37	0.08	0.96	1.81	1.10	12.38	0.35	19.51	3.74
95	113521	GSPL/AL/BH-07	30	31	1.68	5.64	0.76	4.63	0.97	2.67	0.37	2.57	0.33	0.13	0.75	1.96	0.70	10.10	0.35	13.93	3.11
96	113522	GSPL/AL/BH-07	35	36	1.56	4.20	0.59	3.74	0.82	2.59	0.38	2.61	0.39	0.09	0.42	3.96	0.99	<0.1	0.35	10.79	11.60
97	113549	GSPL/AL/BH-07	41	42	0.87	4.44	0.69	4.02	0.82	2.36	0.32	2.02	0.29	0.15	1.33	2.19	0.64	<0.1	0.21	11.26	1.80
98	113523	GSPL/AL/BH-07	44	45	1.22	6.50	0.91	5.67	1.10	3.34	0.43	2.99	0.40	0.09	0.73	1.97	0.59	3.07	0.23	15.96	3.36
99	113548	GSPL/AL/BH-07	48.5	49.5	1.34	7.12	1.01	5.82	1.17	3.49	0.47	3.21	0.44	0.06	1.07	1.78	0.78	<0.1	0.19	19.94	2.75

SL	Sample ID	Borehole No	From (m)	To (m)	Li	Be	Sc	V	Mn	Cr	Co	Ni	Cu	Zn	Ga	Ge	Se	Rb	Sr	Y
100	113524	GSPL/AL/BH-08	18	19	26.22	2.07	12.16	85.16	505.81	235.14	12.41	26.14	14.01	93.01	20.62	<0.1	6.15	103.95	166.60	33.13
101	113525	GSPL/AL/BH-08	21.5	22.5	33.30	0.84	14.48	124.17	458.64	39.25	14.35	33.67	11.40	166.10	15.28	<0.1	3.57	73.72	472.69	15.82
102	113551	GSPL/AL/BH-08	25.5	26.5	24.74	1.74	8.16	68.13	442.90	266.36	9.80	34.08	12.23	66.00	17.67	0.25	5.27	112.49	143.88	30.31
103	113526	GSPL/AL/BH-08	28.5	29.5	35.08	2.84	14.02	91.46	624.08	253.72	17.79	48.79	31.47	99.69	23.62	0.22	4.64	170.33	140.36	31.04
104	113527	GSPL/AL/BH-08	33	34	28.98	2.19	8.80	68.56	481.89	188.65	11.02	30.03	11.79	63.24	18.79	0.23	3.94	117.87	122.29	28.53
105	113528	GSPL/AL/BH-08	37.5	38.5	20.72	3.51	11.29	313.66	383.23	263.87	22.86	100.87	90.82	184.81	17.50	0.15	9.92	146.53	127.05	16.60
106	113552	GSPL/AL/BH-08	40.55	41.55	29.60	2.45	8.78	70.32	808.57	205.88	14.60	50.71	20.53	88.79	18.88	0.24	5.42	104.09	145.73	37.19
107.1	113529	GSPL/AL/BH-08	43	44	31.22	2.96	11.55	111.06	643.93	259.00	23.36	89.63	40.33	136.86	21.97	0.30	5.26	151.20	113.76	37.03
107.2	113529	GSPL/AL/BH-08	43	44	30.42	2.85	12.03	109.75	645.27	255.11	23.00	88.98	41.59	138.38	21.74	0.36	6.52	153.29	116.51	37.38
108	113553	GSPL/AL/BH-08	48	49	28.63	2.70	11.77	365.66	412.74	222.76	18.16	81.91	44.18	178.86	19.52	0.22	5.12	152.19	112.59	35.21

SL	Sample ID	Borehole No	From (m)	To (m)	Zr	Nb	Mo	Ag	Cd	In	Sn	Sb	Te	Cs	Ba	La	Ce	Pr	Nd	Sm
100	113524	GSPL/AL/BH-08	18	19	3.67	12.70	0.69	0.30	0.63	0.06	4.86	9.63	<0.05	3.34	3610.19	52.94	102.83	10.63	39.79	7.48
101	113525	GSPL/AL/BH-08	21.5	22.5	1.01	3.90	4.24	9.37	0.36	0.04	1.17	33.80	<0.05	4.28	3778.39	15.37	32.31	3.74	16.80	3.74
102	113551	GSPL/AL/BH-08	25.5	26.5	2.68	12.99	<0.1	<0.05	0.28	0.07	2.43	2.37	0.80	2.90	2324.13	48.82	96.79	9.87	35.72	6.65
103	113526	GSPL/AL/BH-08	28.5	29.5	2.54	13.56	1.01	<0.05	0.17	0.06	3.39	2.30	1.63	5.78	2687.77	45.02	88.38	9.26	33.74	6.66
104	113527	GSPL/AL/BH-08	33	34	2.24	12.18	<0.1	<0.05	<0.05	0.06	2.83	2.26	0.76	2.45	2332.20	46.72	91.77	9.87	34.45	6.32
105	113528	GSPL/AL/BH-08	37.5	38.5	4.97	11.13	69.75	<0.05	2.87	0.04	2.57	9.26	<0.05	2.65	187.77	21.18	44.49	5.02	18.68	3.61
106	113552	GSPL/AL/BH-08	40.55	41.55	3.37	11.22	<0.1	<0.05	0.54	0.07	2.57	2.47	<0.05	4.71	1031.36	43.17	85.69	9.00	33.09	7.17
107.1	113529	GSPL/AL/BH-08	43	44	2.94	11.72	12.81	<0.05	0.50	0.07	3.10	2.94	0.69	6.89	1467.09	46.47	92.39	9.84	37.37	7.40
107.2	113529	GSPL/AL/BH-08	43	44	2.43	10.98	12.45	<0.05	0.50	0.09	2.98	2.81	0.70	7.16	1459.22	48.07	94.64	10.05	37.14	7.08
108	113553	GSPL/AL/BH-08	48	49	3.16	12.66	26.82	<0.05	2.23	0.10	2.94	3.81	0.81	5.62	1478.27	41.84	81.80	8.96	32.68	6.81

SL	Sample ID	Borehole No	From (m)	To (m)	Eu	Gd	Tb	Dy	Ho	Er	Tm	Yb	Lu	Hf	Ta	W	Tl	Pb	Bi	Th	U
100	113524	GSPL/AL/BH-08	18	19	1.86	7.48	0.90	5.55	1.06	3.11	0.43	2.71	0.37	0.13	0.86	0.88	1.00	23.16	0.13	20.38	2.95
101	113525	GSPL/AL/BH-08	21.5	22.5	0.90	3.12	0.45	2.44	0.54	1.59	0.21	1.50	0.21	2.69	0.39	3.65	0.58	19.49	0.65	3.05	0.77
102	113551	GSPL/AL/BH-08	25.5	26.5	1.51	7.12	0.88	5.30	1.09	2.90	0.25	2.60	0.14	<0.05	1.08	0.75	0.56	9.49	0.15	19.97	3.01
103	113526	GSPL/AL/BH-08	28.5	29.5	1.58	6.47	0.88	5.21	1.08	2.90	0.24	2.83	0.13	<0.05	0.99	1.28	1.05	13.13	0.25	16.64	3.33
104	113527	GSPL/AL/BH-08	33	34	1.42	6.43	0.84	5.03	0.97	2.68	0.18	2.49	0.12	<0.05	0.93	1.05	0.60	5.84	0.13	18.53	2.68
105	113528	GSPL/AL/BH-08	37.5	38.5	0.75	3.36	0.48	2.85	0.45	1.54	<0.1	1.48	0.01	<0.05	0.87	1.45	2.95	21.84	0.36	11.11	15.12
106	113552	GSPL/AL/BH-08	40.55	41.55	1.46	7.07	1.00	6.11	1.30	3.37	0.31	3.02	0.22	<0.05	0.78	0.70	0.51	12.52	0.31	16.05	2.90
107.1	113529	GSPL/AL/BH-08	43	44	1.46	7.67	0.98	5.98	1.27	3.47	0.29	3.13	0.22	<0.05	0.78	1.33	1.04	10.15	0.28	17.31	4.56
107.2	113529	GSPL/AL/BH-08	43	44	1.56	7.56	1.00	6.07	1.33	3.26	0.34	3.42	0.22	<0.05	0.77	1.31	0.99	9.95	0.24	17.55	4.72
108	113553	GSPL/AL/BH-08	48	49	1.41	6.62	0.92	5.54	1.21	3.13	0.27	3.17	0.20	<0.05	0.65	1.39	0.94	10.16	0.26	15.03	13.28

SL	Sample ID	Borehole No	From (m)	To (m)	Li	Be	Sc	V	Mn	Cr	Co	Ni	Cu	Zn	Ga	Ge	Se	Rb	Sr	Y
109	113571	GSPL/AL/BH-09	3	4	16.07	2.09	10.71	1502.34	51.96	441.12	3.15	18.91	165.86	66.66	12.16	<0.1	6.48	69.84	120.39	29.01
110	113572	GSPL/AL/BH-09	8	9	6.84	0.42	4.07	35.76	142.32	205.64	3.36	11.77	13.88	37.07	1.88	<0.1	0.90	30.70	24.92	8.64
111	113573	GSPL/AL/BH-09	16	17	13.47	1.42	8.56	494.30	508.13	306.97	8.82	30.84	153.97	118.07	8.30	<0.1	4.77	68.74	94.43	20.61
112	113574	GSPL/AL/BH-09	26	27	35.01	2.39	12.93	186.48	372.05	263.05	17.27	51.67	57.87	134.69	20.83	0.11	4.08	152.24	110.66	20.92
113	113575	GSPL/AL/BH-09	39	40	38.67	2.41	10.17	175.17	480.32	216.11	20.41	56.74	63.62	152.44	22.70	<0.1	2.58	154.28	71.97	14.75
114.1	113576	GSPL/AL/BH-09	44	45	27.34	2.24	11.15	90.87	712.94	171.44	15.86	40.41	27.30	104.00	15.91	0.12	4.57	119.12	112.78	27.51
114.2	113576	GSPL/AL/BH-09	44	45	27.23	2.28	10.74	91.45	708.47	170.98	15.84	40.39	27.66	102.18	16.00	0.14	4.37	117.20	112.86	27.97

SL	Sample ID	Borehole No	From (m)	To (m)	Zr	Nb	Mo	Ag	Cd	In	Sn	Sb	Te	Cs	Ba	La	Ce	Pr	Nd	Sm
109	113571	GSPL/AL/BH-09	3	4	2.97	6.54	44.11	<0.05	0.86	0.04	2.16	1.94	0.67	3.09	12956.86	27.16	39.03	5.62	22.47	4.31
110	113572	GSPL/AL/BH-09	8	9	2.96	2.22	0.66	<0.05	0.33	0.03	1.01	0.29	<0.05	1.68	1193.26	6.06	12.16	1.24	5.74	1.23
111	113573	GSPL/AL/BH-09	16	17	2.20	5.20	12.40	<0.05	1.64	0.04	1.96	1.01	<0.05	2.73	9119.24	19.76	36.78	4.05	15.56	2.71
112	113574	GSPL/AL/BH-09	26	27	2.08	12.88	5.33	<0.05	1.06	0.12	3.90	0.28	<0.05	7.51	2599.46	29.31	59.48	6.20	25.17	5.21
113	113575	GSPL/AL/BH-09	39	40	2.19	15.55	3.53	<0.05	0.77	0.11	4.69	0.93	<0.05	4.88	1840.44	19.46	50.42	4.13	16.29	3.20
114.1	113576	GSPL/AL/BH-09	44	45	9.93	10.23	0.95	<0.05	0.62	0.07	2.85	0.58	<0.05	5.55	713.70	33.66	68.32	6.88	26.64	5.31
114.2	113576	GSPL/AL/BH-09	44	45	9.70	10.49	0.97	<0.05	0.54	0.08	3.23	0.56	<0.05	5.13	712.50	35.24	71.77	7.29	28.29	5.36

SL	Sample ID	Borehole No	From (m)	To (m)	Eu	Gd	Tb	Dy	Ho	Er	Tm	Yb	Lu	Hf	Ta	W	Tl	Pb	Bi	Th	U
109	113571	GSPL/AL/BH-09	3	4	2.61	4.62	0.60	3.85	0.93	2.82	0.20	2.68	0.12	<0.05	0.22	7.89	0.91	<0.1	0.17	8.43	9.13
110	113572	GSPL/AL/BH-09	8	9	0.21	1.35	0.20	1.08	<0.1	0.58	<0.1	0.58	<0.01	<0.05	<0.1	2.69	<0.05	<0.1	<0.1	2.53	1.60
111	113573	GSPL/AL/BH-09	16	17	1.66	3.06	0.48	2.73	0.69	2.32	0.15	2.54	0.10	<0.05	0.24	196.66	0.45	<0.1	0.12	6.41	7.00
112	113574	GSPL/AL/BH-09	26	27	1.15	4.91	0.68	3.36	0.73	1.88	<0.1	1.62	<0.01	<0.05	0.86	47.01	0.79	1.63	0.17	11.28	3.86
113	113575	GSPL/AL/BH-09	39	40	0.81	3.51	0.45	2.63	0.51	1.52	<0.1	1.24	<0.01	<0.05	1.08	33.72	0.85	0.84	0.14	9.40	4.05
114.1	113576	GSPL/AL/BH-09	44	45	1.06	5.51	0.74	4.56	1.04	2.94	0.21	2.66	0.10	<0.05	0.80	17.21	0.48	0.95	0.21	13.37	2.96
114.2	113576	GSPL/AL/BH-09	44	45	1.16	5.85	0.76	4.71	1.10	2.78	0.22	2.66	0.12	<0.05	0.75	15.62	0.43	1.01	0.18	13.84	3.05

SL	Sample ID	Borehole No	From (m)	To (m)	Li	Be	Sc	V	Mn	Cr	Co	Ni	Cu	Zn	Ga	Ge	Se	Rb	Sr	Y
115	113567	GSPL/AL/BH-10	5	6	4.17	0.33	4.89	193.65	85.32	296.11	1.70	15.91	16.46	54.16	1.53	<0.1	0.52	30.25	21.90	6.70
116	113579	GSPL/AL/BH-10	9	10	7.26	0.64	8.67	677.55	28.28	394.66	1.57	11.33	75.97	6.01	5.29	<0.1	1.65	56.32	25.98	11.96
117	113580	GSPL/AL/BH-10	11	12	6.95	0.56	8.29	583.82	88.56	387.49	0.41	5.46	21.59	5.49	5.56	<0.1	1.42	45.48	33.87	11.71
118	113581	GSPL/AL/BH-10	15	16	7.93	0.64	10.55	366.44	24.22	409.13	0.98	21.63	88.14	87.59	5.36	<0.1	2.71	46.71	75.13	16.23
119	113582	GSPL/AL/BH-10	16	17	10.58	0.67	7.77	1216.12	44.73	574.08	0.83	10.39	41.00	17.94	8.21	<0.1	1.79	66.67	61.37	6.52
120	113568	GSPL/AL/BH-10	21	22	24.16	1.75	8.81	840.63	42.19	446.32	3.84	100.31	358.85	356.60	14.21	0.16	7.59	91.59	91.07	29.37
121	113569	GSPL/AL/BH-10	22	23	22.47	1.92	7.82	772.73	41.55	299.94	4.29	102.98	385.64	420.00	12.44	0.16	7.87	80.77	86.46	31.77
122	113570	GSPL/AL/BH-10	27	28	4.94	0.51	5.75	123.15	50.97	308.64	1.67	12.73	88.40	25.40	2.34	<0.1	1.30	34.38	20.52	6.62

SL	Sample ID	Borehole No	From (m)	To (m)	Zr	Nb	Mo	Ag	Cd	In	Sn	Sb	Te	Cs	Ba	La	Ce	Pr	Nd	Sm
115	113567	GSPL/AL/BH-10	5	6	2.74	1.54	34.77	<0.05	0.35	0.03	0.91	0.60	<0.05	0.46	423.01	3.29	5.44	0.60	2.78	0.40
116	113579	GSPL/AL/BH-10	9	10	3.16	3.06	29.31	<0.05	0.05	0.03	1.31	0.95	<0.05	1.34	340.27	9.25	16.89	2.13	9.67	1.93
117	113580	GSPL/AL/BH-10	11	12	2.59	2.80	9.53	<0.05	<0.05	0.01	1.10	1.23	<0.05	0.99	332.19	7.82	12.93	1.22	5.33	0.75
118	113581	GSPL/AL/BH-10	15	16	3.61	2.59	58.36	0.11	0.27	0.03	1.08	1.34	0.67	1.10	367.22	9.47	18.04	2.31	9.20	1.83
119	113582	GSPL/AL/BH-10	16	17	3.47	5.75	43.80	<0.05	0.25	0.04	2.04	1.69	<0.05	2.20	618.21	6.86	10.63	1.14	5.19	0.79
120	113568	GSPL/AL/BH-10	21	22	3.69	8.29	46.54	3.70	0.94	0.06	2.41	10.36	<0.05	5.74	1941.03	32.80	58.79	8.62	36.22	7.11
121	113569	GSPL/AL/BH-10	22	23	4.06	7.54	43.16	4.69	1.75	0.07	2.42	9.27	<0.05	5.70	1700.71	30.53	53.51	7.64	33.54	7.35
122	113570	GSPL/AL/BH-10	27	28	2.44	1.11	54.06	0.22	<0.05	0.03	1.06	0.85	<0.05	1.25	475.68	5.99	12.31	1.40	5.95	0.88

SL	Sample ID	Borehole No	From (m)	To (m)	Eu	Gd	Tb	Dy	Ho	Er	Tm	Yb	Lu	Hf	Ta	W	Tl	Pb	Bi	Th	U
115	113567	GSPL/AL/BH-10	5	6	<0.1	0.55	0.11	0.56	<0.1	0.35	<0.1	0.46	<0.01	<0.05	<0.1	0.88	0.15	<0.1	0.10	1.28	1.37
116	113579	GSPL/AL/BH-10	9	10	0.28	1.44	0.22	1.35	0.18	0.85	<0.1	0.97	<0.01	<0.05	0.11	2.79	0.32	<0.1	0.23	5.38	4.78
117	113580	GSPL/AL/BH-10	11	12	<0.1	0.86	0.16	0.91	0.16	0.76	<0.1	1.10	<0.01	<0.05	<0.1	2.30	0.29	<0.1	0.11	2.72	2.62
118	113581	GSPL/AL/BH-10	15	16	0.29	1.72	0.26	1.77	0.33	1.28	<0.1	1.34	<0.01	<0.05	<0.1	1.76	0.29	<0.1	<0.1	3.14	11.66
119	113582	GSPL/AL/BH-10	16	17	<0.1	1.02	0.13	0.71	<0.1	0.40	<0.1	0.47	<0.01	<0.05	0.33	24.11	0.51	<0.1	0.15	3.00	12.42
120	113568	GSPL/AL/BH-10	21	22	1.50	6.37	0.72	4.02	0.96	2.59	0.17	2.41	0.13	<0.05	0.52	44.02	1.10	<0.1	0.33	8.28	18.80

121	113569	GSPL/AL/BH-10	22	23	1.47	6.22	0.74	4.28	1.04	2.81	0.19	2.79	0.14	<0.05	0.47	70.87	0.91	<0.1	0.37	7.94	18.70
122	113570	GSPL/AL/BH-10	27	28	0.14	0.97	0.15	0.76	<0.1	0.39	<0.1	0.49	<0.01	<0.05	<0.1	1.61	0.14	<0.1	<0.1	2.47	1.51

SL	Sample ID	Borehole No	From (m)	To (m)	Li	Be	Sc	V	Mn	Cr	Co	Ni	Cu	Zn	Ga	Ge	Se	Rb	Sr	Y
123	113577	GSPL/AL/BH-11	2	3	21.61	2.42	11.56	573.01	187.59	266.00	10.39	98.77	202.28	283.41	16.52	0.12	6.23	97.96	92.58	23.92
124	113578	GSPL/AL/BH-11	4	5	19.03	2.49	10.70	213.77	237.88	191.40	15.25	65.37	67.74	385.75	15.78	0.11	3.78	126.93	116.36	20.61
125	113557	GSPL/AL/BH-11	11.5	12.5	40.21	3.75	17.94	150.32	517.13	212.73	26.16	46.89	53.62	164.42	28.59	0.36	6.74	193.70	179.17	29.25
126	113584	GSPL/AL/BH-11	15	16	38.72	3.44	15.78	124.87	725.27	187.54	22.72	46.63	61.37	179.68	25.94	0.19	5.10	182.75	168.83	27.63
127	113558	GSPL/AL/BH-11	24	25	19.60	2.12	8.47	313.68	78.36	265.76	33.70	201.53	101.36	1461.05	15.50	0.19	10.15	94.76	168.67	38.55
128	113585	GSPL/AL/BH-11	29	30	18.79	1.95	8.20	389.43	424.91	308.61	12.82	64.91	90.97	426.71	12.70	0.12	8.64	97.81	165.76	39.22
129	113559	GSPL/AL/BH-11	31	32	29.72	2.51	13.62	233.82	410.98	243.60	17.39	46.32	47.35	186.61	21.52	0.21	4.57	159.03	198.69	25.63
130.1	113601	GSPL/AL/BH-11	33	34	19.65	2.17	10.44	309.01	370.28	225.91	7.84	28.10	29.27	78.19	16.57	<0.1	3.40	109.36	126.47	28.39
130.2	113601	GSPL/AL/BH-11	33	34	19.92	2.35	10.06	304.68	367.05	222.36	7.55	26.97	29.50	76.08	14.63	<0.1	3.45	102.02	125.25	28.96
131	113560	GSPL/AL/BH-11	39.1	40.1	26.11	0.87	7.81	62.63	251.42	187.12	9.50	29.27	2.56	26.69	16.13	0.14	3.07	94.49	115.27	10.22
132	113561	GSPL/AL/BH-11	46.1	47.1	28.04	2.16	10.51	79.27	627.09	156.16	14.54	31.43	25.67	67.95	20.38	0.32	3.60	134.37	115.35	25.96
133.1	113562	GSPL/AL/BH-11	53.1	54.1	22.17	2.18	8.91	73.62	500.41	150.95	13.13	28.80	16.26	46.49	19.17	0.28	3.39	93.14	106.04	24.60
133.2	113562	GSPL/AL/BH-11	53.1	54.1	22.37	2.35	9.16	73.95	505.04	148.79	13.27	29.58	16.31	47.13	20.11	0.27	3.49	94.58	105.57	25.16
134	113563	GSPL/AL/BH-11	62.1	63.1	21.53	2.46	11.82	216.87	381.97	131.66	16.66	80.81	45.44	107.58	20.77	0.18	6.03	132.92	102.00	26.73
135	113564	GSPL/AL/BH-11	69.1	70.1	21.35	2.36	11.71	84.93	549.13	161.52	16.91	37.96	26.18	65.95	21.29	0.32	5.16	128.36	123.68	29.00
136	113565	GSPL/AL/BH-11	75.1	76.1	21.83	1.37	11.27	360.85	176.94	321.16	11.60	72.16	64.95	32.62	14.48	0.30	5.69	58.98	83.73	37.97
137	113566	GSPL/AL/BH-11	80.6	81.6	22.07	2.45	12.59	93.96	667.80	131.71	15.42	36.02	18.22	58.60	20.07	0.36	6.24	105.75	116.41	30.33
138	113602	GSPL/AL/BH-11	87	88	28.29	2.58	14.79	96.17	981.23	182.05	15.69	39.56	16.81	73.50	19.24	0.17	3.74	133.42	108.83	36.29
139	113583	GSPL/AL/BH-11	91	92	26.63	3.62	8.68	53.74	503.71	99.16	6.81	8.95	0.92	47.98	17.80	<0.1	3.34	163.11	166.82	26.84

SL	Sample ID	Borehole No	From (m)	To (m)	Zr	Nb	Mo	Ag	Cd	In	Sn	Sb	Te	Cs	Ba	La	Ce	Pr	Nd	Sm
123	113577	GSPL/AL/BH-11	2	3	2.87	8.56	22.54	<0.05	2.20	0.09	2.81	3.12	<0.05	3.94	2322.06	34.21	60.72	7.14	27.74	5.55
124	113578	GSPL/AL/BH-11	4	5	2.21	8.07	17.19	<0.05	3.72	0.06	2.81	2.28	<0.05	7.23	2586.26	27.17	51.24	5.27	19.30	3.71
125	113557	GSPL/AL/BH-11	11.5	12.5	3.09	14.36	0.79	<0.05	0.98	0.12	4.00	2.89	<0.05	12.07	3375.39	44.31	87.82	9.22	34.67	5.83
126	113584	GSPL/AL/BH-11	15	16	2.31	12.81	14.77	<0.05	0.49	0.08	3.50	1.21	<0.05	15.03	2296.80	45.96	90.47	9.02	33.68	6.85
127	113558	GSPL/AL/BH-11	24	25	2.66	6.88	13.25	0.62	4.92	0.03	1.66	2.64	<0.05	4.60	608.38	28.58	53.37	6.63	25.96	5.34
128	113585	GSPL/AL/BH-11	29	30	2.38	8.79	29.72	0.42	4.39	0.05	2.00	1.12	<0.05	3.52	1734.56	34.04	58.67	7.19	28.03	6.08
129	113559	GSPL/AL/BH-11	31	32	1.99	8.57	4.94	<0.05	1.06	0.07	2.61	2.30	<0.05	10.97	753.97	35.56	73.19	7.83	28.66	5.73
130.1	113601	GSPL/AL/BH-11	33	34	32.91	8.96	16.83	<0.05	0.83	0.07	4.35	1.00	<0.05	4.81	4884.72	27.89	53.34	5.91	23.46	4.77
130.2	113601	GSPL/AL/BH-11	33	34	31.78	8.19	17.57	<0.05	0.78	0.08	4.91	0.96	<0.05	4.95	4881.78	26.69	51.36	5.82	22.74	4.67
131	113560	GSPL/AL/BH-11	39.1	40.1	2.97	5.05	0.55	0.69	0.09	0.05	0.77	2.36	<0.05	8.98	792.58	31.21	59.41	6.42	23.83	4.52
132	113561	GSPL/AL/BH-11	46.1	47.1	2.74	12.27	<0.1	<0.05	<0.05	0.08	3.24	2.03	<0.05	4.11	1593.69	40.57	79.54	8.44	30.61	5.94
133.1	113562	GSPL/AL/BH-11	53.1	54.1	2.91	11.96	0.15	<0.05	<0.05	0.04	2.69	2.08	<0.05	2.96	1507.63	41.06	80.91	8.70	30.89	6.09
133.2	113562	GSPL/AL/BH-11	53.1	54.1	3.08	12.52	0.11	<0.05	<0.05	0.04	2.68	2.28	<0.05	3.13	1497.97	40.52	80.61	8.76	30.98	6.34
134	113563	GSPL/AL/BH-11	62.1	63.1	2.32	5.75	18.67	<0.05	1.27	0.08	3.59	2.09	<0.05	12.26	1490.32	40.78	78.74	8.68	31.12	6.05
135	113564	GSPL/AL/BH-11	69.1	70.1	2.32	7.75	1.04	<0.05	0.09	0.08	2.79	2.15	<0.05	5.53	874.73	43.45	84.22	9.06	31.91	6.89
136	113565	GSPL/AL/BH-11	75.1	76.1	2.42	4.76	23.97	<0.05	0.07	0.04	1.44	2.15	<0.05	3.99	1134.11	30.09	56.06	7.13	28.23	6.16
137	113566	GSPL/AL/BH-11	80.6	81.6	2.27	11.19	0.31	<0.05	<0.05	0.10	2.91	2.19	<0.05	4.60	377.97	40.61	81.65	8.91	32.80	6.73
138	113602	GSPL/AL/BH-11	87	88	2.95	7.95	1.05	<0.05	<0.05	0.07	3.42	0.24	<0.05	6.64	505.00	37.06	73.88	7.80	29.98	5.87
139	113583	GSPL/AL/BH-11	91	92	3.19	11.47	22.71	<0.05	<0.05	0.06	3.54	0.34	<0.05	8.97	552.78	31.75	63.08	6.76	24.33	5.27

SL	Sample ID	Borehole No	From (m)	To (m)	Eu	Gd	Tb	Dy	Ho	Er	Tm	Yb	Lu	Hf	Ta	W	Tl	Pb	Bi	Th	U
123	113577	GSPL/AL/BH-11	2	3	1.40	5.24	0.64	3.67	0.84	2.18	0.13	2.02	0.05	<0.05	0.52	15.26	0.78	3.80	0.32	10.89	6.84
124	113578	GSPL/AL/BH-11	4	5	1.03	3.84	0.54	3.30	0.70	2.12	0.12	1.85	0.07	<0.05	0.35	9.34	0.83	1.54	0.13	9.43	6.27
125	113557	GSPL/AL/BH-11	11.5	12.5	1.78	6.76	0.85	5.14	1.08	2.72	0.26	2.61	0.12	<0.05	1.10	1.99	0.98	9.40	0.23	17.30	6.92
126	113584	GSPL/AL/BH-11	15	16	1.45	6.10	0.81	4.72	1.07	2.80	0.22	2.55	0.12	<0.05	0.87	5.39	1.08	10.40	0.27	15.22	4.53
127	113558	GSPL/AL/BH-11	24	25	1.43	6.36	0.89	5.72	1.27	3.47	0.32	3.41	0.26	<0.05	0.24	0.72	0.73	<0.1	<0.1	7.68	9.30
128	113585	GSPL/AL/BH-11	29	30	1.64	6.18	0.88	5.63	1.39	3.80	0.26	3.34	0.20	<0.05	0.60	9.29	0.74	<0.1	0.14	9.80	11.47
129	113559	GSPL/AL/BH-11	31	32	1.10	5.49	0.69	4.12	0.85	2.37	0.16	2.00	0.06	<0.05	0.41	1.64	0.81	<0.1	0.19	12.20	4.32
130.1	113601	GSPL/AL/BH-11	33	34	1.52	5.30	0.67	4.00	0.96	2.68	0.19	2.54	0.12	0.50	0.38	3.72	0.65	<0.1	0.16	9.42	3.67
130.2	113601	GSPL/AL/BH-11	33	34	1.59	4.96	0.65	4.10	0.95	2.67	0.19	2.68	0.11	0.47	0.40	3.30	0.60	<0.1	0.14	9.26	3.41
131	113560	GSPL/AL/BH-11	39.1	40.1	0.79	4.29	0.50	2.46	0.29	0.74	<0.1	0.53	<0.01	<0.05	0.33	0.44	0.98	21.61	0.19	9.07	1.12
132	113561	GSPL/AL/BH-11	46.1	47.1	1.33	5.68	0.76	4.58	0.90	2.46	0.19	2.40	0.11	<0.05	0.94	1.72	0.34	<0.1	0.16	13.94	2.57
133.1	113562	GSPL/AL/BH-11	53.1	54.1	1.33	6.13	0.78	4.47	0.88	2.29	0.16	2.34	0.08	<0.05	0.97	1.07	0.14	<0.1	0.13	14.85	2.37
133.2	113562	GSPL/AL/BH-11	53.1	54.1	1.30	6.04	0.79	4.44	0.86	2.30	0.19	2.37	0.09	<0.05	1.06	1.15	0.17	<0.1	0.16	14.82	2.33
134	113563	GSPL/AL/BH-11	62.1	63.1	1.30	6.20	0.78	4.75	0.94	2.51	0.19	2.28	0.07	<0.05	0.37	2.37	0.62	5.20	0.57	14.23	6.32
135	113564	GSPL/AL/BH-11	69.1	70.1	1.29	6.22	0.83	4.97	1.01	2.61	0.26	2.73	0.15	<0.05	0.46	1.09	0.34	2.47	0.23	14.31	3.05
136	113565	GSPL/AL/BH-11	75.1	76.1	1.27	6.60	0.91	5.89	1.31	3.40	0.36	3.38	0.21	<0.05	0.15	1.37	<0.05	<0.1	0.59	9.08	9.68
137	113566	GSPL/AL/BH-11	80.6	81.6	1.30	6.76	0.92	5.47	1.11	2.86	0.23	2.68	0.18	<0.05	0.88	1.27	0.29	<0.1	0.22	14.55	2.76
138	113602	GSPL/AL/BH-11	87	88	1.20	5.87	0.85	5.60	1.44	3.99	0.31	3.70	0.21	<0.05	0.42	1.54	0.51	<0.1	<0.1	13.78	2.55
139	113583	GSPL/AL/BH-11	91	92	0.88	5.15	0.71	4.27	0.94	2.69	0.19	2.67	0.09	<0.05	1.27	1.46	0.50	12.19	0.22	14.03	4.63

SL	Sample ID	Borehole No	From (m)	To (m)	Li	Be	Sc	V	Mn	Cr	Co	Ni	Cu	Zn	Ga	Ge	Se	Rb	Sr	Y
140	113619	GSPL/AL/BH-12	16	17.5	22.75	1.97	10.44	104.53	123.37	227.62	2.43	14.64	17.58	23.15	13.79	0.17	0.87	114.76	86.84	4.09
141	113620	GSPL/AL/BH-12	20	21	69.94	1.50	9.80	309.55	280.98	395.33	25.65	86.75	146.06	353.01	12.22	0.17	5.82	71.18	122.93	21.97
142	113621	GSPL/AL/BH-12	23.5	24.5	57.84	1.74	12.77	188.68	155.69	323.49	3.28	20.91	56.83	726.37	18.46	0.15	4.89	123.94	97.47	33.02
143	113622	GSPL/AL/BH-12	26.5	27.8	43.94	1.58	12.43	396.39	60.55	248.72	10.44	135.32	361.25	543.73	13.52	0.15	12.60	85.93	118.21	25.78
144.1	113623	GSPL/AL/BH-12	29.5	31	24.32	1.85	12.19	249.70	51.56	234.63	13.39	93.39	1060.97	298.03	20.65	0.17	11.91	108.33	143.61	25.43
144.2	113623	GSPL/AL/BH-12	29.5	31	23.96	1.37	11.65	251.91	55.03	233.79	13.20	88.99	1055.69	302.05	18.30	0.16	10.64	107.02	144.15	24.75
145	113624	GSPL/AL/BH-12	31	33	33.35	1.57	13.47	143.09	47.25	207.19	11.18	62.53	417.92	383.64	14.50	0.16	7.99	90.17	114.14	16.31
146	113625	GSPL/AL/BH-12	34.5	36	24.25	1.92	13.92	131.29	65.92	270.71	9.38	102.69	165.19	519.01	10.70	0.16	4.84	63.25	130.57	13.66
147	113626	GSPL/AL/BH-12	40.5	42	31.87	2.60	22.29	87.54	134.64	201.53	7.42	81.15	36.07	1581.81	15.04	0.14	4.13	77.66	180.54	18.00
148	113627	GSPL/AL/BH-12	45	46	29.58	1.68	7.54	662.02	142.61	355.16	8.87	210.12	225.75	892.82	9.58	0.15	3.87	71.45	141.70	23.88
149	113628	GSPL/AL/BH-12	51.5	53	25.19	2.18	4.89	17.23	611.28	27.37	13.79	19.40	11834.88	8235.63	24.19	0.15	10.86	88.06	244.47	10.10
150	113629	GSPL/AL/BH-12	54.5	56	29.59	2.83	11.73	1380.52	141.33	393.41	9.57	227.37	325.16	716.80	14.66	0.16	6.38	92.81	238.73	12.58

SL	Sample ID	Borehole No	From (m)	To (m)	Zr	Nb	Mo	Ag	Cd	In	Sn	Sb	Te	Cs	Ba	La	Ce	Pr	Nd	Sm
140	113619	GSPL/AL/BH-12	16	17.5	1.62	7.81	0.80	<0.05	<0.05	<0.1	2.58	1.18	<0.1	3.22	604.81	16.99	37.77	4.54	14.92	1.78
141	113620	GSPL/AL/BH-12	20	21	1.91	3.72	15.00	0.64	0.45	<0.1	1.75	6.60	<0.1	13.35	758.70	26.86	68.32	11.05	46.26	7.85

142	113621	GSPL/AL/BH-12	23.5	24.5	4.71	7.64	6.70	0.16	0.35	<0.1	3.69	2.01	<0.1	17.20	1214.25	30.18	74.24	7.90	32.10	5.64
143	113622	GSPL/AL/BH-12	26.5	27.8	3.63	5.54	22.56	1.31	3.44	<0.1	2.55	4.10	<0.1	13.17	1395.95	27.33	57.98	7.46	33.02	7.03
144.1	113623	GSPL/AL/BH-12	29.5	31	1.99	8.81	21.44	1.51	0.10	<0.1	3.86	4.15	<0.1	4.70	1117.64	35.06	72.56	8.67	34.54	7.14
144.2	113623	GSPL/AL/BH-12	29.5	31	1.55	9.04	21.60	1.49	0.11	<0.1	4.01	4.02	<0.1	4.71	1113.02	34.39	70.87	8.41	34.17	6.95
145	113624	GSPL/AL/BH-12	31	33	2.00	6.76	5.48	0.15	<0.05	<0.1	2.61	7.92	<0.1	10.76	719.93	17.15	44.19	5.88	25.41	5.90
146	113625	GSPL/AL/BH-12	34.5	36	18.87	4.22	6.66	0.19	11.45	<0.1	2.36	7.20	<0.1	5.34	1470.11	13.32	29.40	3.94	15.71	3.57
147	113626	GSPL/AL/BH-12	40.5	42	5.51	7.15	2.34	<0.05	3.09	<0.1	3.08	3.20	1.29	4.94	2436.20	20.00	50.31	5.52	22.78	4.92
148	113627	GSPL/AL/BH-12	45	46	1.75	4.81	53.13	0.78	8.84	<0.1	1.96	3.97	<0.1	7.46	4158.41	22.32	36.73	5.94	23.59	5.09
149	113628	GSPL/AL/BH-12	51.5	53	151.10	11.58	50.72	66.76	30.91	3.44	10.64	363.17	22.68	4.67	1799.33	30.05	61.76	6.71	25.79	4.89
150	113629	GSPL/AL/BH-12	54.5	56	3.72	7.07	79.35	3.80	9.48	<0.1	2.63	19.95	<0.1	4.17	1532.13	25.56	49.08	7.69	32.69	5.98

SL	Sample ID	Borehole No	From (m)	To (m)	Eu	Gd	Tb	Dy	Ho	Er	Tm	Yb	Lu	Hf	Ta	W	Tl	Pb	Bi	Th	U
140	113619	GSPL/AL/BH-12	16	17.5	0.17	1.20	0.16	0.89	0.15	0.45	<0.1	0.35	0.06	0.11	0.64	2.70	0.66	<0.1	<0.1	7.90	2.47
141	113620	GSPL/AL/BH-12	20	21	1.19	6.23	0.76	4.78	0.85	2.54	0.35	2.73	0.37	<0.1	0.27	3.47	0.35	35.73	<0.1	6.58	6.16
142	113621	GSPL/AL/BH-12	23.5	24.5	0.95	4.84	0.59	3.67	0.68	2.03	0.38	2.16	0.32	0.15	0.62	19.57	0.78	115.49	0.13	13.28	2.55
143	113622	GSPL/AL/BH-12	26.5	27.8	1.74	6.28	0.77	4.89	0.93	2.95	0.41	2.96	0.45	0.11	0.50	6.73	0.49	49.14	0.20	10.03	13.10
144.1	113623	GSPL/AL/BH-12	29.5	31	1.48	6.79	0.88	5.35	0.98	2.84	0.38	2.62	0.33	0.10	0.73	4.00	0.88	47.59	0.15	11.30	9.99
144.2	113623	GSPL/AL/BH-12	29.5	31	1.37	6.73	0.92	5.31	1.03	2.85	0.42	2.82	0.39	0.12	0.75	4.14	0.89	49.73	0.15	11.41	10.08
145	113624	GSPL/AL/BH-12	31	33	1.08	4.88	0.66	3.90	0.73	2.13	0.31	1.98	0.30	0.12	0.54	3.58	0.96	32.40	0.23	10.06	8.40
146	113625	GSPL/AL/BH-12	34.5	36	0.84	3.44	0.56	2.97	0.56	1.60	0.22	1.61	0.26	<0.1	0.33	10.68	0.49	43.98	0.12	9.12	23.81
147	113626	GSPL/AL/BH-12	40.5	42	1.22	4.59	0.64	4.64	0.79	3.79	0.34	2.49	0.34	0.12	0.60	2.40	0.86	131.12	0.16	12.65	13.39
148	113627	GSPL/AL/BH-12	45	46	1.37	4.76	0.56	7.51	0.71	2.27	0.32	2.42	0.40	<0.1	0.39	2.92	1.17	49.26	<0.1	6.77	26.54
149	113628	GSPL/AL/BH-12	51.5	53	1.06	4.52	0.53	2.56	0.34	0.71	<0.1	0.51	0.07	4.13	0.93	7.88	3.85	12085.77	64.02	10.64	3.77
150	113629	GSPL/AL/BH-12	54.5	56	1.28	4.24	0.46	2.50	0.47	1.29	0.20	1.48	0.26	0.12	0.46	4.18	1.36	65.82	0.46	11.01	29.80

Annexure XXVI_ICPMS Data of Borehole Check Samples (All data in ppm)

SL No	Sample ID	Borehole ID	From (m)	To (m)	Lab Name	Li	Be	B	Sc	V	Mn	Cr	Co	Ni	Cu	Zn	Ga	Ge	Se	Rb	Sr	Y
1.1	110071	GSPL/AL/BH-01	36.5	37	BV	43.75	1.91		9.33	1028.75	230.93	395.44	8.17	250.73	524.27	688.55	16.32	0.02	27.14	155.93	173.72	72.99
1.2	113637				Shiva	33.46	1.83	< 5	12.38	-	-	-	11.47	-	-	-	15.15	<0.5	16.43	145.07		99.50
2.1	110076	GSPL/AL/BH-01	81	82	BV	17.05	1.84		7.47	381.28	186.89	364.20	8.25	57.88	102.31	322.29	15.45	0.01	16.06	90.19	194.83	32.10
2.2	113636				Shiva	17.22	1.95	< 5	7.46	-	-	-	8.53	-	-	-	12.71	<0.5	7.15	89.36		24.37
3.1	110097	GSPL/AL/BH-03	27	28	BV	27.80	2.39		12.11	1715.51	42.68	757.07	12.11	243.37	365.83	782.25	18.14	0.30	11.62	113.61	51.21	65.16
3.2	113645				Shiva	26.69	2.13	< 5	12.35	-	-	-	11.75	-	-	-	15.30	<0.5	12.82	109.93		58.50
4.1	110100	GSPL/AL/BH-03	59	60	BV	16.69	1.62		5.09	1838.42	132.92	490.94	9.06	82.58	128.49	664.87	13.16	0.17	10.36	76.85	117.80	46.93
4.2	113641				Shiva	19.04	2.24	< 5	8.13	-	-	-	11.64	-	-	-	14.21	<0.5	22.93	93.63		48.85
5.1	113508	GSPL/AL/BH-04	31	32	BV	26.92	2.62		11.46	546.07	346.34	264.43	16.40	89.47	68.86	186.35	21.84	0.23	9.21	141.91	154.58	37.36
5.2	113640				Shiva	24.08	2.13	< 5	10.85	-	-	-	12.40	-	-	-	16.35	<0.5	6.62	125.26		29.54
6.1	113512	GSPL/AL/BH-05	28	29	BV	18.03	2.15		7.37	106.21	89.01	552.54	12.27	70.42	60.46	106.22	17.26	0.20	9.59	81.87	241.54	31.14
6.2	113647				Shiva	17.47	1.98	< 5	8.71	-	-	-	11.52	-	-	-	14.57	<0.5	7.91	84.03		31.24
7.1	113514	GSPL/AL/BH-05	40	41	BV	24.61	3.38		10.25	2443.45	288.60	562.09	12.77	129.53	216.71	1478.97	18.37	<0.1	23.96	129.83	114.34	83.64
7.2	113650				Shiva	27.50	3.03	< 5	12.64	-	-	-	16.30	-	-	-	19.22	<0.5	29.43	128.15		68.01
8.1	113517	GSPL/AL/BH-05	72	73	BV	32.93	3.72		12.05	1502.49	297.12	356.97	34.90	180.98	295.55	814.30	21.73	<0.1	28.16	141.73	217.65	53.63
8.2	113649				Shiva	30.55	2.31	< 5	12.35	-	-	-	35.87	-	-	-	17.64	<0.5	29.96	119.10		68.65
9.1	113535	GSPL/AL/BH-06	41	42	BV	30.59	3.66		10.91	156.36	451.32	247.46	16.53	57.50	48.74	154.61	20.37	0.12	6.67	158.75	185.80	30.78
9.2	113638				Shiva	31.26	2.74	< 5	12.18	-	-	-	17.11	-	-	-	18.37	<0.5	5.97	138.46		27.31
10.1	113541	GSPL/AL/BH-06	75	76	BV	40.71	3.17		16.69	187.46	529.56	219.40	21.39	70.85	54.81	214.25	29.59	0.29	5.86	200.28	152.48	37.44
10.2	113646				Shiva	29.98	3.12	< 5	12.88	-	-	-	14.78	-	-	-	17.94	<0.5	2.78	145.20		31.84
11.1	113520	GSPL/AL/BH-07	29	30	BV	49.29	4.24		15.64	134.10	642.02	243.06	24.74	56.80	46.37	139.24	27.20	<0.1	8.56	213.64	162.44	31.93

SL No	Sample ID	Borehole ID	From (m)	To (m)	Lab Name	Li	Be	B	Sc	V	Mn	Cr	Co	Ni	Cu	Zn	Ga	Ge	Se	Rb	Sr	Y
11.2	113644				Shiva	56.04	3.48	< 5	20.14	-	-	-	27.91	-	-	-	26.47	<0.5	2.51	221.81		28.70
12.1	113528	GSPL/AL/BH-08	37.5	38.5	BV	20.72	3.51		11.29	313.66	383.23	263.87	22.86	100.87	90.82	184.81	17.50	0.15	9.92	146.53	127.05	16.60
12.2	113642				Shiva	21.99	3.27	< 5	12.47	-	-	-	21.40	-	-	-	16.97	<0.5	16.25	152.45		21.44
13.1	113580	GSPL/AL/BH-10	11	12	BV	6.95	0.56		8.29	583.82	88.56	387.49	0.41	5.46	21.59	5.49	5.56	<0.1	1.42	45.48	33.87	11.71
13.2	113643				Shiva	9.12	0.63	< 5	8.34	-	-	-	1.77	-	-	-	5.78	<0.5	2.13	41.80		10.08
14.1	113559	GSPL/AL/BH-11	31	32	BV	29.72	2.51		13.62	233.82	410.98	243.60	17.39	46.32	47.35	186.61	21.52	0.21	4.57	159.03	198.69	25.63
14.2	113639				Shiva	26.93	2.33	< 5	13.26	-	-	-	15.64	-	-	-	18.00	<0.5	5.30	137.14		28.73
15.1	113583	GSPL/AL/BH-11	91	92	BV	26.63	3.62		8.68	53.74	503.71	99.16	6.81	8.95	0.92	47.98	17.80	<0.1	3.34	163.11	166.82	26.84
15.2	113648				Shiva	28.23	3.44	< 5	9.31	-	-	-	6.60	-	-	-	18.00	<0.5	2.39	165.77		32.92

SL No	Sample ID	Borehole ID	From (m)	To (m)	Lab Name	Zr	Nb	Mo	Ag	Cd	In	Sn	Sb	Te	Cs	Ba	La	Ce	Pr	Nd	Sm
1.1	110071	GSPL/AL/BH-01	36.5	37	BV	1.01	7.67	121.06	12.37	10.13	0.06	1.54	156.96	0.60	16.57	1771.49	29.01	49.89	7.78	34.35	8.41
1.2	113637				Shiva		9.18	116.15		9.36	<0.5	8.97	23.95	<0.5	10.08	-	35.20	64.08	9.52	41.91	10.73
2.1	110076	GSPL/AL/BH-01	81	82	BV	0.64	6.94	16.81	0.10	2.81	0.05	1.57	4.37	0.00	4.09	2534.03	26.96	46.95	6.15	25.31	4.92
2.2	113636				Shiva		3.73	7.05		0.84	<0.5	7.12	1.17	<0.5	4.18	-	25.89	47.69	5.63	22.03	4.54
3.1	110097	GSPL/AL/BH-03	27	28	BV	4.39	10.39	158.85	<0.05	20.92	0.08	2.96	3.73	0.79	6.11	724.34	27.24	53.57	8.20	34.91	8.00
3.2	113645				Shiva		7.89	129.18		11.68	<0.5	3.38	<0.5	<0.5	5.72	-	28.76	57.20	8.36	37.19	8.89
4.1	110100	GSPL/AL/BH-03	59	60	BV	12.75	6.45	110.47	<0.05	21.15	0.05	1.87	4.16	<0.05	2.48	587.45	23.37	39.78	5.91	25.24	5.53
4.2	113641				Shiva		5.95	93.84		14.07	<0.5	5.67	4.47	<0.5	3.55	-	30.79	49.89	7.78	32.20	7.03
5.1	113508	GSPL/AL/BH-04	31	32	BV	2.74	12.42	26.55	<0.05	1.96	0.05	2.94	2.56	<0.05	4.85	759.09	46.25	90.50	10.03	38.08	7.47
5.2	113640				Shiva		8.92	8.54		1.52	<0.5	5.24	<0.5	<0.5	4.15	-	36.28	74.02	8.14	31.03	5.96
6.1	113512	GSPL/AL/BH-05	28	29	BV	3.80	7.94	1.25	<0.05	7.68	0.01	1.36	3.00	0.74	4.33	431.67	25.04	54.49	6.95	29.07	6.50
6.2	113647				Shiva		6.67	3.22		5.52	<0.5	5.36	0.61	<0.5	4.45	-	29.02	57.90	6.85	28.07	6.13
7.1	113514	GSPL/AL/BH-05	40	41	BV	<0.1	10.08	63.75	4.20	28.62	0.08	3.15	24.28	1.30	3.25	852.62	41.76	64.74	11.13	47.65	10.95
7.2	113650				Shiva		7.67	43.33		15.58	<0.5	7.42	0.92	<0.5	3.42	-	39.29	58.63	9.98	40.30	8.70
8.1	113517	GSPL/AL/BH-05	72	73	BV	<0.1	13.17	65.83	4.60	16.06	0.05	3.46	25.58	<0.05	9.11	678.65	44.31	83.87	10.33	41.52	8.27
8.2	113649				Shiva		9.29	48.26		11.99	<0.5	6.28	6.13	<0.5	7.29	-	34.58	69.89	9.25	39.80	8.74
9.1	113535	GSPL/AL/BH-06	41	42	BV	<0.1	6.71	20.30	0.41	1.17	0.07	3.12	18.56	<0.05	5.54	1407.13	45.19	87.79	9.09	34.73	6.39
9.2	113638				Shiva		1.85	12.36		<0.5	<0.5	8.82	<0.5	<0.5	5.42	-	37.16	76.53	8.28	31.49	6.11
10.1	113541	GSPL/AL/BH-06	75	76	BV	2.72	14.95	9.52	<0.05	0.46	0.12	4.94	2.52	0.82	12.09	2080.31	54.44	104.88	11.50	41.37	8.33
10.2	113646				Shiva		8.47	9.71		<0.5	<0.5	5.03	<0.5	<0.5	8.47	-	42.23	86.17	9.47	35.03	6.83
11.1	113520	GSPL/AL/BH-07	29	30	BV	<0.1	13.91	0.74	0.23	0.11	0.09	3.95	13.16	<0.05	12.90	3836.86	56.85	112.11	11.32	42.19	8.44
11.2	113644				Shiva		14.43	3.38		<0.5	<0.5	5.54	<0.5	<0.5	12.34	-	51.85	107.75	10.97	40.83	7.77
12.1	113528	GSPL/AL/BH-08	37.5	38.5	BV	4.97	11.13	69.75	<0.05	2.87	0.04	2.57	9.26	<0.05	2.65	187.77	21.18	44.49	5.02	18.68	3.61
12.2	113642				Shiva		9.92	52.31		<0.5	<0.5	6.39	7.40	<0.5	2.76	-	26.91	57.80	6.45	25.06	5.24
13.1	113580	GSPL/AL/BH-10	11	12	BV	2.59	2.80	9.53	<0.05	<0.05	0.01	1.10	1.23	<0.05	0.99	332.19	7.82	12.93	1.22	5.33	0.75
13.2	113643				Shiva		0.98	8.36		<0.5	<0.5	5.23	<0.5	<0.5	1.15	-	8.00	13.82	1.63	5.84	1.08
14.1	113559	GSPL/AL/BH-11	31	32	BV	1.99	8.57	4.94	<0.05	1.06	0.07	2.61	2.30	<0.05	10.97	753.97	35.56	73.19	7.83	28.66	5.73
14.2	113639				Shiva		7.38	8.24		0.78	<0.5	2.47	<0.5	<0.5	8.71	-	32.33	65.94	7.17	26.79	5.45
15.1	113583	GSPL/AL/BH-11	91	92	BV	3.19	11.47	22.71	<0.05	<0.05	0.06	3.54	0.34	<0.05	8.97	552.78	31.75	63.08	6.76	24.33	5.27
15.2	113648				Shiva		11.54	1.23		<0.5	<0.5	7.73	<0.5	<0.5	9.08	-	31.40	67.22	7.50	27.89	6.07

SL No	Sample ID	Borehole ID	From (m)	To (m)	Lab Name	Eu	Gd	Tb	Dy	Ho	Er	Tm	Yb	Lu	Hf	Ta	W	Tl	Pb	Bi	Th	U
1.1	110071	GSPL/AL/BH-01	36.5	37	BV	1.73	10.27	1.49	10.46	2.19	7.19	1.01	6.81	0.94	0.02	0.55	2.57	3.03	48.75	0.64	9.60	36.56
1.2	113637				Shiva	4.11	13.07	2.05	13.26	2.82	8.76	1.23	7.32	1.06	<0.5	1.08	2.48	1.90	-	<0.5	12.62	37.43
2.1	110076	GSPL/AL/BH-01	81	82	BV	1.48	5.28	0.76	5.10	1.00	3.27	0.44	3.02	0.41	0.02	0.51	1.48	1.32	58.45	0.19	7.65	9.76
2.2	113636				Shiva	3.23	5.44	0.64	3.85	0.82	2.31	<0.5	2.17	<0.5	<0.5	<0.5	0.61	0.94	-	1.19	7.25	4.46
3.1	110097	GSPL/AL/BH-03	27	28	BV	1.79	9.52	1.32	8.75	2.13	5.77	0.67	5.70	0.53	<0.05	0.63	7.32	1.20	18.63	0.57	11.27	46.54
3.2	113645				Shiva	3.19	9.37	1.28	9.49	1.72	5.26	0.78	4.99	0.81	<0.5	0.77	6.94	1.26	-	0.59	12.70	36.68
4.1	110100	GSPL/AL/BH-03	59	60	BV	1.01	6.67	0.96	6.19	1.45	3.89	0.39	4.00	0.28	0.11	0.34	3.32	1.15	8.13	0.23	6.54	17.25
4.2	113641				Shiva	3.33	8.33	1.10	7.14	1.45	4.47	0.60	3.82	0.63	<0.5	0.67	3.54	1.36	-	<0.5	9.34	25.59
5.1	113508	GSPL/AL/BH-04	31	32	BV	1.46	7.05	0.94	6.09	1.23	3.43	0.27	3.27	0.20	<0.05	0.84	2.70	1.82	<0.1	0.15	15.10	15.48
5.2	113640				Shiva	4.09	7.61	0.77	4.58	0.96	2.98	<0.5	2.61	<0.5	<0.5	1.20	2.68	1.74	-	<0.5	16.30	6.31
6.1	113512	GSPL/AL/BH-05	28	29	BV	1.50	6.57	0.86	5.14	1.07	2.80	0.23	2.63	0.14	<0.05	0.50	0.41	1.71	0.41	0.11	7.24	13.76
6.2	113647				Shiva	3.90	7.24	0.84	5.20	0.98	3.04	<0.5	2.64	<0.5	0.50	0.69	<0.5	1.07	-	<0.5	9.43	11.62
7.1	113514	GSPL/AL/BH-05	40	41	BV	2.20	12.57	1.73	11.84	2.44	7.40	1.00	6.30	0.86	0.09	0.88	2.78	1.63	<0.1	0.21	11.03	37.70
7.2	113650				Shiva	8.48	10.37	1.45	9.37	1.92	5.89	0.83	4.82	0.74	<0.5	0.85	1.36	1.37	-	<0.5	11.58	23.45
8.1	113517	GSPL/AL/BH-05	72	73	BV	1.63	8.28	1.15	6.82	1.50	4.50	0.63	4.07	0.55	0.10	1.25	3.41	1.88	3.55	0.72	13.31	40.52
8.2	113649				Shiva	3.14	10.38	1.29	8.32	1.73	5.41	0.76	4.82	0.68	<0.5	1.13	2.58	1.44	-	<0.5	13.42	37.09
9.1	113535	GSPL/AL/BH-06	41	42	BV	1.36	6.23	0.87	4.89	1.06	3.01	0.41	2.60	0.33	0.07	0.77	2.25	1.42	2.74	0.41	15.22	6.39
9.2	113638				Shiva	2.10	8.03	0.80	4.81	0.87	2.79	<0.5	2.39	<0.5	<0.5	<0.5	3.50	1.14	-	<0.5	15.61	4.26
10.1	113541	GSPL/AL/BH-06	75	76	BV	1.67	7.65	1.05	6.27	1.37	3.72	0.31	3.23	0.21	<0.05	1.16	2.13	1.09	11.48	0.36	18.73	7.84
10.2	113646				Shiva	2.36	8.87	0.93	5.60	1.08	3.28	<0.5	2.96	<0.5	<0.5	0.75	0.80	0.77	-	<0.5	18.17	5.64
11.1	113520	GSPL/AL/BH-07	29	30	BV	2.03	7.54	0.96	5.63	1.15	3.40	0.45	2.86	0.37	0.08	0.96	1.81	1.10	12.38	0.35	19.51	3.74
11.2	113644				Shiva	5.07	10.14	0.95	5.32	1.06	3.15	<0.5	2.86	<0.5	<0.5	1.69	3.08	0.98	-	<0.5	22.82	3.43
12.1	113528	GSPL/AL/BH-08	37.5	38.5	BV	0.75	3.36	0.48	2.85	0.45	1.54	<0.1	1.48	0.01	<0.05	0.87	1.45	2.95	21.84	0.36	11.11	15.12
12.2	113642				Shiva	2.12	6.45	0.65	3.81	0.73	2.34	<0.5	1.97	<0.5	<0.5	1.09	0.99	3.40	-	<0.5	14.78	13.13
13.1	113580	GSPL/AL/BH-10	11	12	BV	<0.1	0.86	0.16	0.91	0.16	0.76	<0.1	1.10	<0.01	<0.05	<0.1	2.30	0.29	<0.1	0.11	2.72	2.62
13.2	113643				Shiva	<0.5	1.53	<0.5	1.17	<0.5	0.85	<0.5	0.84	<0.5	2.01	<0.5	1.22	<0.5	-	<0.5	2.72	2.39
14.1	113559	GSPL/AL/BH-11	31	32	BV	1.10	5.49	0.69	4.12	0.85	2.37	0.16	2.00	0.06	<0.05	0.41	1.64	0.81	<0.1	0.19	12.20	4.32
14.2	113639				Shiva	5.76	7.40	0.71	4.02	0.82	2.43	<0.5	1.92	<0.5	<0.5	0.90	1.35	1.22	-	<0.5	13.53	5.52
15.1	113583	GSPL/AL/BH-11	91	92	BV	0.88	5.15	0.71	4.27	0.94	2.69	0.19	2.67	0.09	<0.05	1.27	1.46	0.50	12.19	0.22	14.03	4.63
15.2	113648				Shiva	1.16	7.67	0.87	5.40	1.08	3.35	<0.5	3.07	<0.5	<0.5	2.16	0.87	0.64	-	<0.5	17.91	5.37

Annexure XXVII_Proximate Analysis of Graphite for Borehole Samples (All data in %)

SL No	Sample ID	BH-ID	From (m)	To (m)	Length	IM %	VM %	ASH %	FC %
1	110068	GSPL/AL/BH-01	35	35.5	0.5	0.88	3.85	88.83	6.44
2	110069	GSPL/AL/BH-01	35.5	36	0.5	0.58	4.14	90	5.28
3	110070	GSPL/AL/BH-01	36	36.5	0.5	0.57	4.13	89.5	5.8
4	110071	GSPL/AL/BH-01	36.5	37	0.5	0.69	8.5	83.25	7.56
5	110072	GSPL/AL/BH-01	49	50	1	0.7	5.34	92.85	1.11
6	110073	GSPL/AL/BH-01	53	54	1	0.9	3.96	93.8	1.34
7	110074	GSPL/AL/BH-01	57	58	1	0.55	3.97	94.57	0.91
8	110077	GSPL/AL/BH-01	58.25	59.25	1	0.18	3.83	95.5	0.49
9	110088	GSPL/AL/BH-01	62	63	1	0.54	3.43	93.85	2.18
10	110075	GSPL/AL/BH-01	72	72.5	0.5	0.72	4.51	92.27	2.5
11	110078	GSPL/AL/BH-01	73	74	1	0.67	4.27	93	2.06
12	110089	GSPL/AL/BH-01	78	79	1	0.53	4.54	90.61	4.32
13	110090	GSPL/AL/BH-01	79	80	1	0.57	2.89	93.67	2.87
14	110076	GSPL/AL/BH-01	81	82	1	0.46	4.27	94.19	1.08
15	110079	GSPL/AL/BH-01	84	85	1	0.68	2.65	94.58	2.09
16	110091	GSPL/AL/BH-01	89	90	1	0.49	2.76	95.79	0.96
17	110080	GSPL/AL/BH-02	13	14	1	0.7	3.54	90.91	4.85
18	110093	GSPL/AL/BH-02	17	18	1	0.33	5.73	91.02	2.92
19	110081	GSPL/AL/BH-02	19	20	1	0.69	3.58	90.09	5.64
20	110082	GSPL/AL/BH-02	22	23	1	0.6	5.01	93.42	0.97
21	110083	GSPL/AL/BH-02	27	28	1	0.63	4.33	92.91	2.13
22	110086	GSPL/AL/BH-02	29.3	30.3	1	0.71	4.75	93.73	0.81
23	110084	GSPL/AL/BH-02	34	35	1	0.56	3.29	95.26	0.89
24	113616	GSPL/AL/BH-03	15	16	1	0.54	1.86	93.75	3.85
25	110095	GSPL/AL/BH-03	22	23	1	0.88	1.94	93.33	3.85
26	113615	GSPL/AL/BH-03	23	24	1	0.37	2.57	90.7	6.36
27	113614	GSPL/AL/BH-03	24	25	1	0.45	2.5	90.7	6.35
28	110097	GSPL/AL/BH-03	27	28	1	0.4	2.49	90.24	6.87
29	113613	GSPL/AL/BH-03	29	30	1	0.28	2.72	88.68	8.32
30	113612	GSPL/AL/BH-03	31	32	1	0.25	2.78	89.66	7.31
31	110096	GSPL/AL/BH-03	38	39	1	0.6	3.77	87.23	**8.4**
32	110098	GSPL/AL/BH-03	46	47	1	0.44	3.81	89.46	6.29
33	113501	GSPL/AL/BH-03	53	54	1	0.59	3.13	92.27	4.01
34	110100	GSPL/AL/BH-03	59	60	1	0.58	1.04	97.07	1.31
35	113504	GSPL/AL/BH-04	15	16	1	0.78	1.29	91.64	6.29
36	113505	GSPL/AL/BH-04	18	19	1	0.52	6.19	89.89	3.4
37	113508	GSPL/AL/BH-04	31	32	1	0.42	2.42	96.11	1.05
38	113512	GSPL/AL/BH-05	28	29	1	0.55	2.88	94.73	1.84
39	113513	GSPL/AL/BH-05	32	33	1	0.53	2.17	94.21	3.09
40	113515	GSPL/AL/BH-05	44	45	1	0.49	4.76	91.4	3.35
41	113605	GSPL/AL/BH-05	48	49	1	0.47	4.02	89.77	5.74

SL No	Sample ID	BH-ID	From (m)	To (m)	Length	IM %	VM %	ASH %	FC %
42	113516	GSPL/AL/BH-05	61	62	1	0.62	4.65	93.22	1.51
43	113541	GSPL/AL/BH-06	75	76	1	0.49	2.44	96.07	1
44	113543	GSPL/AL/BH-06	87	88	1	0.38	3.36	95.06	1.2
45	113528	GSPL/AL/BH-08	37.5	38.5	1	0.57	5.38	91.03	3.02
46	113571	GSPL/AL/BH-09	3	4	1	0.79	1.91	94.31	2.99
47	113580	GSPL/AL/BH-10	11	12	1	0.57	0.48	96.51	2.44
48	113582	GSPL/AL/BH-10	16	17	1	0.61	0.9	95.39	3.1
49	113568	GSPL/AL/BH-10	21	22	1	0.86	3.19	93.8	2.15
50	113559	GSPL/AL/BH-11	31	32	1	0.47	2.46	96.06	1.01
51	113622	GSPL/AL/BH-12	26.5	27.8	1	0.78	3.18	91.98	4.06
52	113623	GSPL/AL/BH-12	29.5	31	1	0.58	3.24	93.83	2.34
53	113624	GSPL/AL/BH-12	31	33	2	0.61	4.17	93.39	1.83
54	113629	GSPL/AL/BH-12	54.5	56	1.5	0.51	4.53	88.04	6.92

Annexure XXVIII_Details of Borehole Litholog

GSPL/Almora/BH-01
29.636734°N, 79.726113°E
Vertical Borehole (RL- 1363 m)

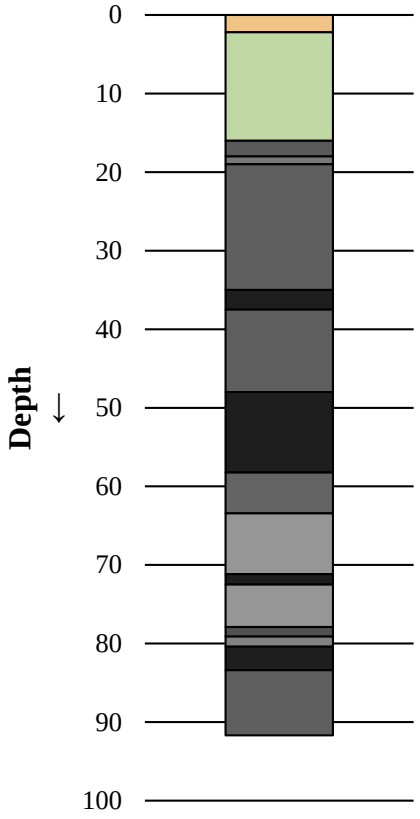

From (m)	To (m)	Thickness (m)	V (ppm)	FC%
14	15	1	105.65	
15	16	1		
16	17	1		
17	18	1		
18	19	1		
19	20.32	1.32	205.46	
20.32	21.32	1	106.83	
21.32	23	1.68		
23	24	1		
24	25	1		
25	26	1		
26	27	1		
27	28	1		
28	29	1		
29	30	1		
30	31	1		
31	32	1		
32	33	1		
33	34	1		
34	35	1		
35	35.5	0.5	1383.45	6.44
35.5	36	0.5	1405.81	5.28
36	36.5	0.5	1594.60	5.8
36.5	37	0.5	1028.75	7.56
37	38	1		
38	39	1		

From (m)	To (m)	Thickness (m)	V (ppm)	FC%
39	40	1		
40	41	1		
41	42	1		
42	43	1		
43	44	1		
44	45	1		
45	46	1		
46	47	1		
47	48	1		
48	49	1		
49	50	1	261.74	1.11
50	51	1		
51	52	1		
52	53	1		
53	54	1	641.61	1.34
54	55	1		
55	56	1		
56	57	1		
57	58	1	391.68	0.91
58	58.25	0.25		
58.25	59.25	1	333.45	0.49
59.25	60	0.75		
60	61	1		
61	62	1		
62	63	1	748.75	2.18

From (m)	To (m)	Thickness (m)	V (ppm)	FC%
63	64	1		
64	65	1		
65	66	1		
66	67	1		
67	68	1		
68	69	1		
69	70	1		
70	71	1		
71	72	1		
72	72.5	0.5	794.54	2.5
72.5	73	0.5		
73	74	1	218.22	2.06
74	75	1		
75	76	1		
76	77	1		
77	78	1		
78	79	1	784.38	4.32
79	80	1	759.86	2.87
80	81	1		
81	82	1	381.28	1.08
82	83	1		
83	84	1		
84	85	1	187.05	2.09
85	86	1		
86	87	1		
87	88	1		
88	89	1		
89	90	1	250.74	0.96

Colour Code	From (m)	To (m)	Lithology
	0	2.2	Weathered mica schist with topsoil
	2.2	16	Sericite–Mica Schist
	16	18	Weathered graphitic schist
	18	19	Graphite schist with quartz vein
	19	35	Medium Grade Graphite schist
	35	37.5	High Grade Graphite schist
	37.5	48	Medium Grade Graphite schist
	48	58.25	High Grade Graphite schist
	58.25	63.43	Medium Grade Graphite schist (partly weathered)
	63.43	71.18	Low Grade Graphite schist
	71.18	72.5	High Grade Graphite schist
	72.5	77.9	Low Grade Graphite schist
	77.9	79.13	Weathered high-grade graphite
	79.13	80.4	Low to Medium Grade Graphite schist
	80.4	83.4	High Grade Graphite schist
	83.4	91.7	Medium Grade Graphite schist

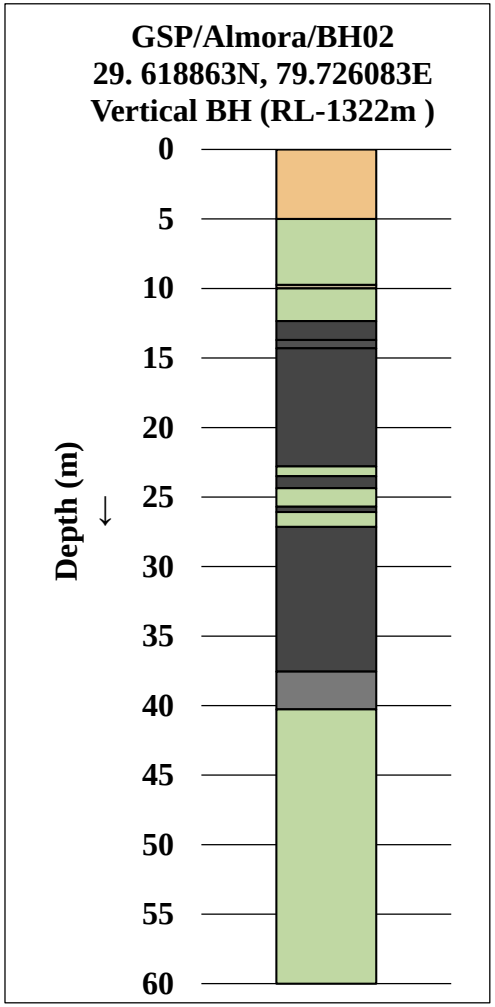

From (m)	To (m)	Thickness (m)	V (ppm)	FC%
13	14	1	1022.09	4.85
14	15	1		
15	16	1	819.13	
16	17	1		
17	18	1	789.05	2.92
18	19	1		
19	20	1	710.56	5.64
20	21	1		
21	22	1		
22	23	1	98.47	0.97
23	24	1		
24	25	1		
25	26	1		
26	27	1		
27	28	1	424.79	2.13
28	29	1		
29.3	30.3	1	81.33	0.81
30	31	1		
31	32	1		
32	33	1		
33	34	1		
34	35	1	29.64	0.89
35	36	1		
36	37	1		
37	38	1		
38	39	1		
39	40	1		
40	41	1		
41	42	1		
42	43	1	68.55	
43	44	1		
44	45	1		
45	46	1		
46	47	1		
47	48	1		
48	49	1	81.65	

Colour Code	From (m)	To (m)	Lithology
	0	5	Weathered mica schist with topsoil
	5	9.74	Sericite Mica Schist
	9.74	10	Quartz Graphite Schist
	10	12.35	Sericite Mica Schist
	12.35	13.7	High Grade Graphite Schist (sulphide-rich)
	13.7	14.3	Medium to High Grade Graphite Schist
	14.3	22.8	High Grade Graphite Schist (sulphide-rich)
	22.8	23.5	Sericite Mica Schist
	23.5	24.36	High Grade Graphite Schist (sulphide-rich)
	24.36	25.7	Sericite Mica Schist
	25.7	26.08	High Grade Graphite Schist (sulphide-rich)
	26.08	27.15	Sericite Mica Schist
	27.15	37.56	High Grade Graphite Schist (sulphide-rich)
	37.56	40.27	Medium Grade Graphite Schist
	40.27	60	Sericite Mica Schist

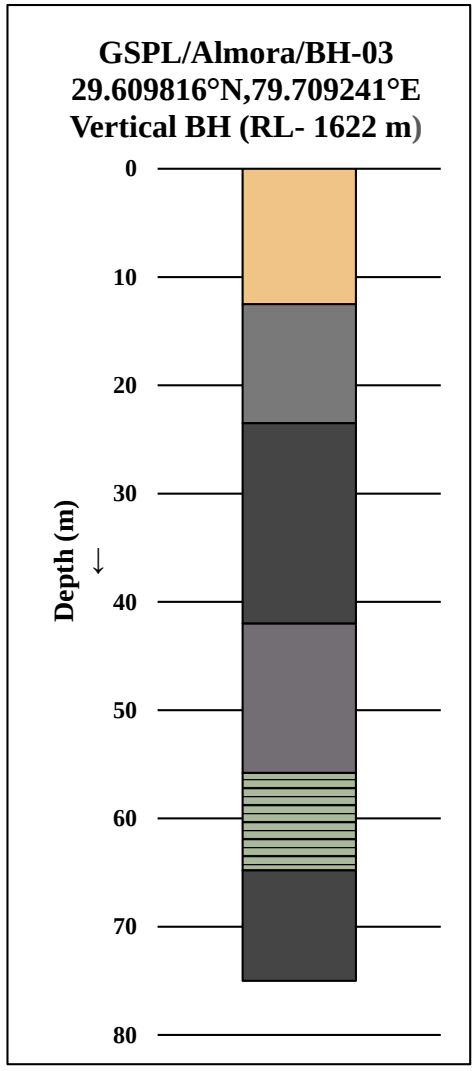

From (m)	To (m)	Thickness (m)	V (ppm)	FC%
7	8	1	51.64	
8	9	1		
9	10	1		
10	11	1		
11	12	1		
12	13	1	120.89	
13	14	1		
14	15	1		
15	16	1	876.61	3.85
16	17	1		
17	18	1		
18	19	1		
19	20	1		
20	21	1		
21	22	1		
22	23	1	712.31	3.85
23	24	1	1296.36	6.36
24	25	1	1553.55	6.35
25	26	1		
26	27	1		
27	28	1	1715.51	6.87
28	29	1		
29	30	1	1846.60	8.32
30	31	1		
31	32	1	1601.64	7.31
32	33	1		
33	34	1		
34	35	1		
35	36	1		
36	37	1		
37	38	1		
38	39	1	944.97	8.4
39	40	1		
40	41	1		
41	42	1	259.88	
42	43	1		
43	44	1		
44	45	1		
45	46	1		
46	47	1	1265.75	6.29
47	48	1		
48	49	1		
49	50	1		
50	51	1		
51	52	1		
52	53	1		

From (m)	To (m)	Thickness (m)	V (ppm)	FC%
53	54	1	2758.56	4.01
54	55	1		
55	56	1		
56	57	1		
57	58	1		
58	59	1		
59	60	1	1838.42	1.31
60	61	1		
61	62	1		
62	63	1		
63	64	1		
64	65	1		
65	66	1	2326.94	
66	67	1		
67	68	1		
68	69	1		
69	70	1		
70	71	1		
71	72	1		
72	73	1		
73	75	2	1501.15	
73	75	2	1516.40	

Colour Code	From (m)	To (m)	Lithology
	0	12.5	Weathered mica schist with topsoil
	12.5	23.5	Medium Grade Graphite Schist
	23.5	42	High Grade Graphite Schist
	42	55.8	Graphitic Sericite Schist
	55.8	64.8	Graphitic Quartzite
	64.8	75	High Grade Graphite Schist

GSPL/Almora/BH-04
29.638587°N, 79.701410°E
Vertical BH (RL- 1531 m)

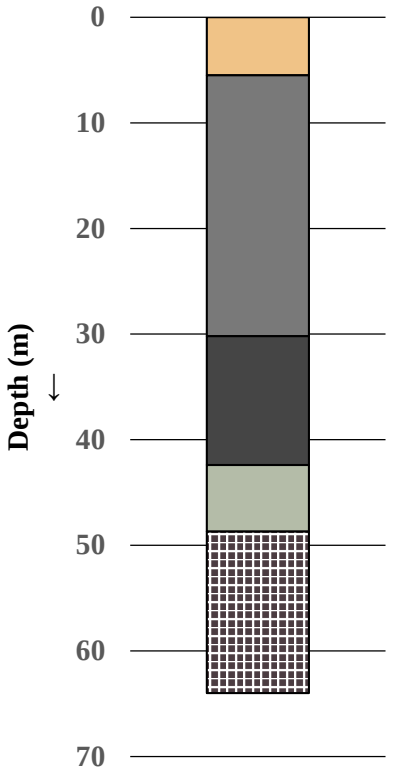

From (m)	To (m)	Thickness (m)	V (ppm)	FC%
10	11	1	1052.37	
11	12	1		
12	13	1		
13	14	1		
14	15	1		
15	16	1	1459.65	6.29
16	16	1		
17	17	1		
18	19	1	1041.12	3.4
19	20	1	784.22	
20	21	1		
21	22	1		
22	23	1		
23	24	1	135.32	
24	25	1		
25	26	1		
26	27	1		
27	28	1		
28	29	1		
29	30	1		
30	31	1		
31	32	1	546.07	1.05
32	33	1		
33	34	1		
34	35	1		
35	36	1		
36	37	1		
37	38	1		
38	39	1		
39	40	1		
40	41	1		
41	42	1		
42	43	1		
43	44	1		
44	45	1		
45	46	1		
46	47	1		
47	48	1		
48	49	1		
49	50	1		
50	51	1		
51	52	1		
52	53	1		
53	54.5	1.5		
54.5	55.5	1	95.01	

Colour Code	From (m)	To (m)	Lithology
	0	5.5	Weathered mica schist with topsoil
	5.5	30.2	Medium Grade Graphite Schist
	30.2	42.4	High Grade Graphite Schist
	42.4	48.7	Graphite Quartzite intercalated with Sericite Schist
	48.7	64	Biotite Mica Schist intercalated with thin Graphite Band

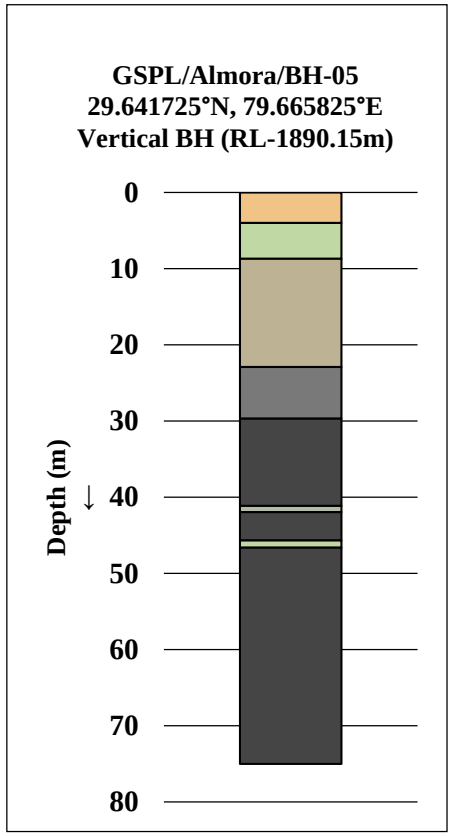

From (m)	To (m)	Thickness (m)	V (ppm)	FC%
6	7	1	170.07	
7	8	1		
8	9	1		
9	10	1		
10	11	1	67.10	
11	12	1		
12	13	1		
13	14	1		
14	15	1		
15	16	1	1170.96	
16	17	1		
17	18	1		
18	19	1		
19	20	1		
20	21	1		
21	22	1		
22	23	1		
23	24	1	824.17	
24	25	1		
25	26	1	945.21	
26	27	1		
27	28	1		
28	29	1	106.21	1.84
29	30	1		
30	31	1		
31	32	1		
32	33	1	2089.62	3.09
33	34			
34	35	1		
35	36	1	1073.39	
36	37	1		
37	38	1		
38	39	1	3683.43	
39	40	1		
40	41	1	2443.45	
41	42	1		
42	43	1		
43	44	1		
44	45	1	3486.02	3.35
45	46	1		
46	47	1		
47	48	1		
48	49	1	3739.38	5.74
49	50	1		
50	51	1	2872.27	

From (m)	To (m)	Thickness (m)	V (ppm)	FC%
51	52	1		
52	53	1		
53	54	1		
54	55	1		
55	56	1	2926.03	
56	57	1		
57	58	1		
58	59	1		
59	60	1		
60	61	1		
61	62	1	500.03	1.51
62	63	1		
63	64	1		
64	65	1		
65	66	1	909.47	
66	67	1		
67	68	1		
68	69	1		
69	70	1	322.47	
70	71	1		
71	72	1		
72	73	1	1502.49	
73	74	1		
74	75	1	405.24	

Colour Code	From (m)	To (m)	Lithology
	0	4	Weathered mica schist with topsoil
	4	8.7	Sericite Mica Schist
	8.7	22.9	Quartz Graphitic Schist
	22.9	29.7	Medium Grade Graphite Schist
	29.7	41.15	High Grade Graphite Schist
	41.15	41.95	Sericitic Graphite Schist
	41.95	45.67	High Grade Graphite Schist
	45.67	46.62	Sericite Mica Schist
	46.62	75	High Grade Graphite Schist

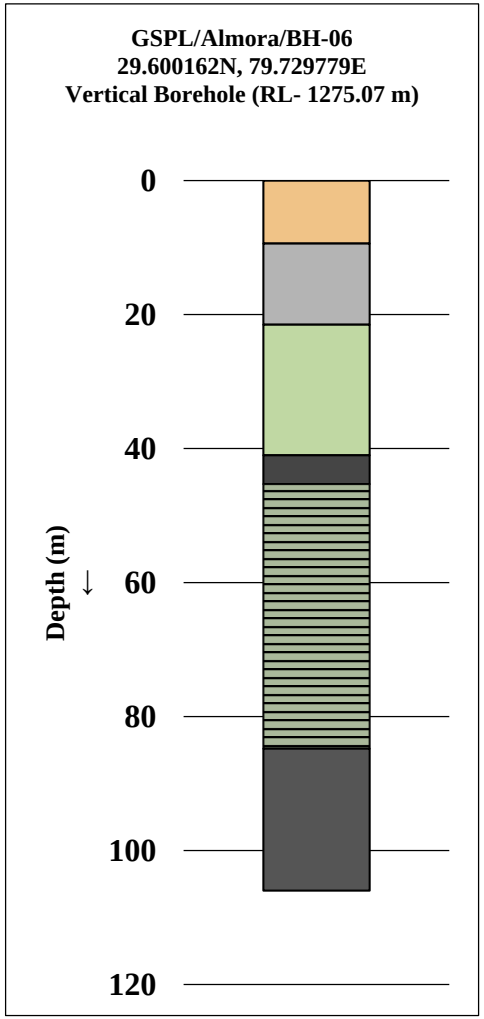

From (m)	To (m)	Thickness (m)	V (ppm)	FC%
14	15	1	82.03	
15	16	1		
16	17	1		
17	18	1	67.29	
18	19	1		
19	20	1		
20	21	1		
21	22	1		
22	23	1		
23	24	1	72.05	
24	25	1		
25	26	1		
26	27	1		
27	28	1	37.15	
28	29	1		
29	30	1		
30	31	1		
31	32	1		
32	33	1		
33	34	1	36.28	
34	35	1		
35	36	1		
36	37	1		
37	38	1		
38	39	1		
39	40	1		
40	41	1		
41	42	1	156.36	
42	43	1		
43	44	1		
44	45	1		
45	46	1		
46	47	1		
47	48.5	1.5		
48.5	49.5	1	172.94	
49.5	50.5	1		
50.5	51.5	1		
51.5	52.5	1		
52.5	53.5	1		
53.5	54.5	1		
54.5	55.5	1		
55.5	56.5	1	64.12	
56.5	57	1		
57	58	1		

From (m)	To (m)	Thickness (m)	V (ppm)	FC%
58	59	1		
59	60	1		
60	61	1		
61	62	1	81.20	
62	63	1		
63	64	1		
64	65	1		
65	66	1		
66	67	1	77.50	
67	68	1		
68	69	1		
69	70	1		
70	71	1	89.22	
71	72	1		
72	73	1		
73	74	1		
74	75	1		
75	76	1	187.46	1
76	77	1		
77	78	1		
78	79	1		
79	80	1		
80	81	1		
81	82	1	152.74	
82	83	1		
83	84	1		
84	85	1		
85	86	1		
86	87	1		

From (m)	To (m)	Thickness (m)	V (ppm)	FC%
87	88	1	355.14	1.2
88	89	1		
89	90	1		
90	91	1		
91	92	1		
92	93	1		
93	94	1	82.08	
94	95	1		
95	96	1		
96	97	1		
97	98	1	352.14	
98	99	1		
99	100	1		
100	101	1		
101	102	1		
102	103	1	582.70	
103	104	1		
104	105	1		
105	106	1	257.52	

Colour Code	From (m)	To (m)	Lithology
	0	9.4	Weathered mica schist with topsoil
	9.4	21.5	Graphite–Sericite Schist
	21.5	41	Sericite Mica Schist
	41	45.3	High Grade Graphite Schist
	45.3	84.8	Graphitic Quartzite
	84.8	106	High-Grade Graphite Schist to Graphitic Quartzite

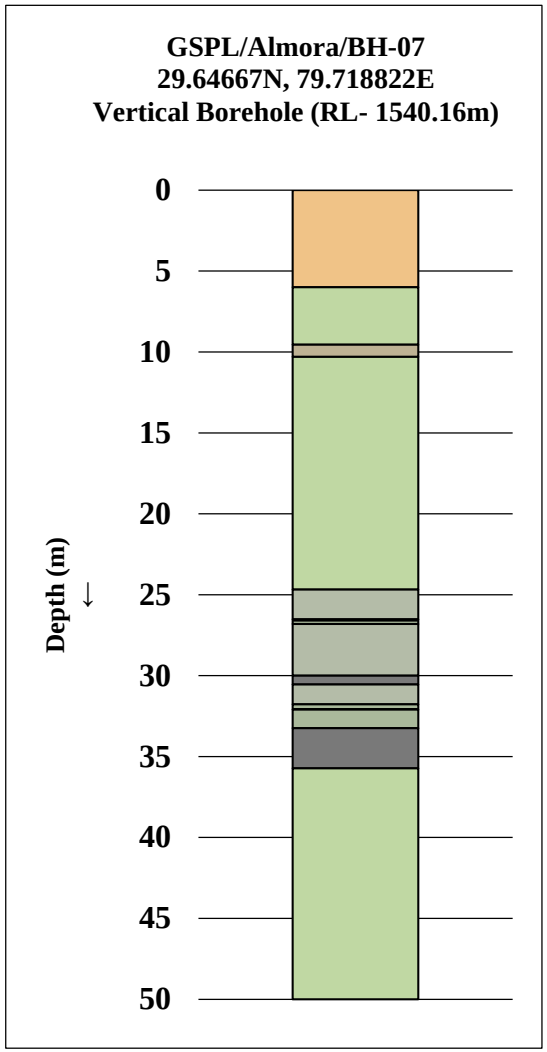

From (m)	To (m)	Thickness (m)	V (ppm)	FC%
9	10	1	160.02	
10	11	1		
11	12	1		
12	13	1		
13	14	1		
14	15	1	59.65	
15	16	1		
16	17	1		
17	18	1		
18	19	1		
19	20	1		
20	21	1		
21	22	1		
22	23	1	67.37	
23	24	1		
24	25	1		
25	26	1		
26	27	1		
27	28	1		
28	29	1		
29	30	1	134.10	
30	31	1	98.29	
31	32	1		
32	33	1		
33	34	1		
34	35	1		
35	36	1	309.18	
36	37	1		
37	38	1		
38	39	1		
39	40	1		
40	41	1		
41	42	1	51.87	
42	43	1		
43	44	1		
44	45	1	67.79	
45	46	1		
46	47	1		
47	48.5	1.5		
48.5	49.5	1	70.01	

Colour Code	From (m)	To (m)	Lithology
	0	6	Weathered mica schist with topsoil
	6	9.55	Sericite Mica Schist
	9.55	10.3	Quartz Graphitic Schist
	10.3	24.7	Sericite Mica Schist
	24.68	26.5	Graphitic Sericite Schist
	26.52	26.8	Graphitic Quartzite
	26.81	30	Graphitic Sericite Schist
	30	30.6	Graphite Schist Moderate Grade
	30.55	31.8	Graphitic Sericite Schist
	31.77	32.1	Sericite Mica Schist
	32.1	33.3	Graphitic Quartzite
	33.25	35.7	Graphite Schist Moderate Grade
	35.73	50	Sericite Mica Schist

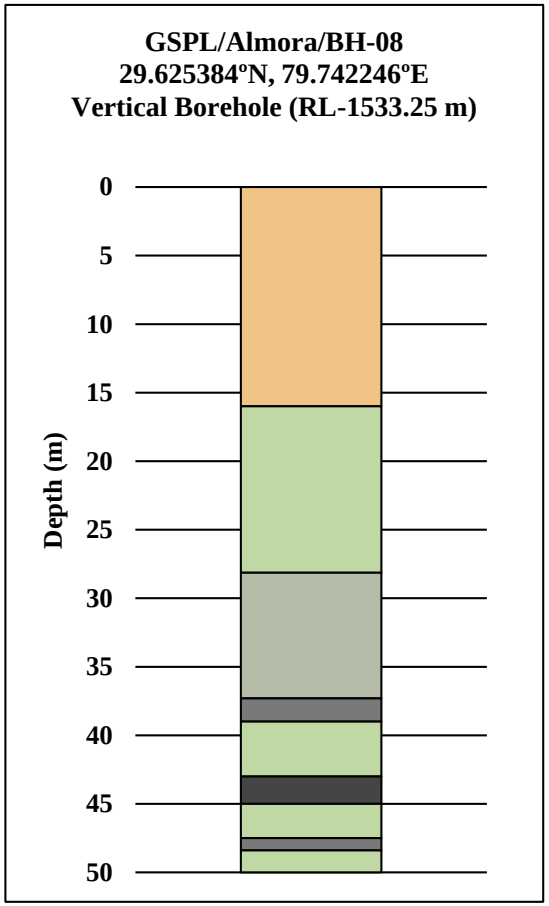

From (m)	To (m)	Thickness (m)	V (ppm)	FC%
18	19	1	85.16	
19	20	1		
20	21.5	1.5		
21.5	22.5	1	124.17	
22.5	23.5	1		
23.5	24.5	1		
24.5	25.5	1		
25.5	26.5	1	68.13	
26.5	27.5	1		
27.5	28.5	1		
28.5	29.5	1	91.46	
29.5	31	1.5		
31	32	1		
32	33	1		
33	34	1	68.56	
34	35	1		
35	36	1		
36	37.5	1.5		
37.5	38.5	1	313.66	3.02
38.5	39.5	1		
39.5	40.5	1		
40.5	41.5	1	70.32	
41.5	43	1.5		
43	44	1	111.06	
44	45	1		
45	46	1		
46	47	1		
47	48	1		
48	49	1	365.66	

Colour Code	From (m)	To (m)	Lithology
	0	16	Weathered mica schist with topsoil
	16	28.14	Sericite Mica Schist
	28.14	37.3	Graphitic Sericite Schist
	37.3	39	Medium Grade Graphite Schist
	39	43	Sericite Mica Schist
	43	45	High Grade Graphite Schist
	45	47.5	Graphitic Sericite Schist
	47.5	48.4	Medium Grade Graphite Schist
	48.4	50	Sericite Mica Schist

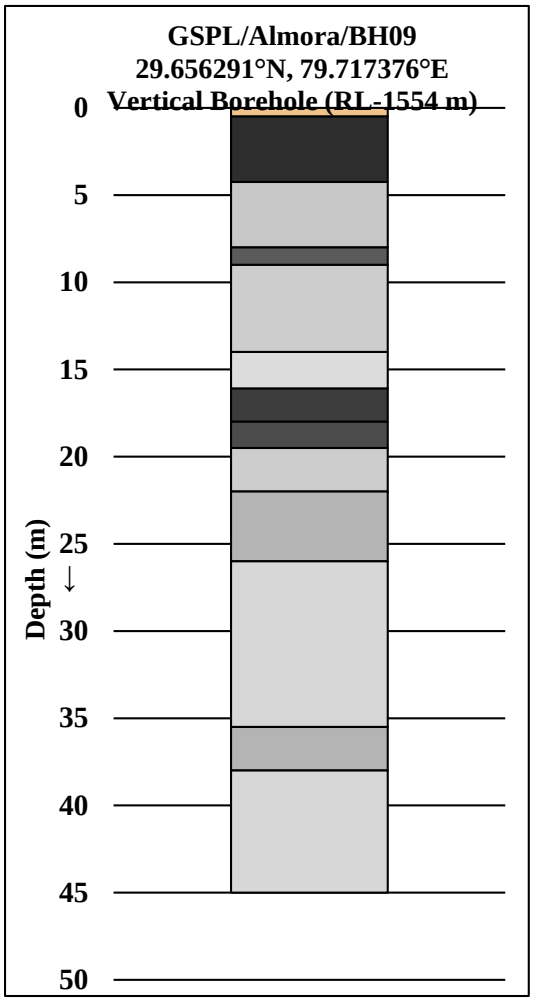

From (m)	To (m)	Thickness (m)	V (ppm)	FC (%)
3	4	1	1502.34	2.99
4	5	1		
5	6	1		
6	7	1		
7	8	1		
8	9	1	35.76	
9	10	1		
10	11	1		
11	12	1		
12	13	1		
13	14	1		
14	15	1		
15	16	1		
16	17	1	494.30	
17	18	1		
18	19	1		
19	20	1		
20	21	1		
21	22	1		
22	23	1		
23	24	1		
24	25	1		
25	26	1		
26	27	1	186.48	
27	28	1		
28	29	1		
29	30	1		
30	31	1		
31	32	1		
32	33	1		
33	34	1		
34	35	1		
35	36	1		
36	37	1		
37	38	1		
38	39	1		
39	40	1	175.17	
40	41	1		
41	42	1		
42	43	1		
43	44	1		
44	45	1	90.87	

Colour Code	From (m)	To (m)	Lithology
	0	0.5	Weathered mica schist with topsoil
	0.5	4.25	Highly weathered graphitic schist, sludgy
	4.25	8	Highly weathered mica schist, sludgy
	8	9	Intercalated mica schist and graphitic schist
	9	14	Highly weathered mica schist, sludgy
	14	16.1	Loose / highly weathered mica schist
	16.1	18	Loose / highly weathered graphitic schist
	18	19.5	Loose mixed mica schist with dominant graphitic schist
	19.5	22	Highly weathered mica schist, sludgy
	22	26	Mica schist
	26	35.5	Loose/ weathered mica schist
	35.5	38	Mica schist
	38	45	Loose/ weathered mica schist

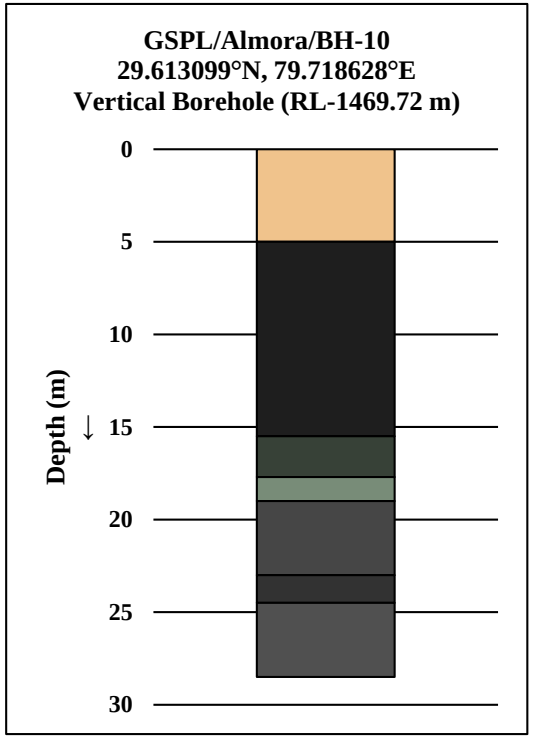

From (m)	To (m)	Thickness (m)	V (ppm)	FC (%)
5	6	1	193.65	
6	7	1		
7	8	1		
8	9	1		
9	10	1	677.55	
10	11	1		
11	12	1	583.82	2.44
12	13	1		
13	14	1		
14	15	1		
15	16	1	366.44	
16	17	1	1216.12	3.1
17	18	1		
18	19	1		
19	20	1		
20	21	1		
21	22	1	840.63	2.15
22	23	1	772.73	
23	24	1		
24	25	1		
25	26	1		
26	27	1		
27	28	1	123.15	

Colour Code	From (m)	To (m)	Lithology
	0	5	Top Soil mixed with Sericite.
	5	15.5	High-grade graphitic schist (enriched in redox-sensitive elements)
	15.5	17.7	Graphitic schist (low redox-sensitive elements), locally greenish
	17.7	19	Highly weathered greenish schist (sludgy)
	19	23	Highly weathered graphitic schist (sludgy)
	23	24.5	Loose / friable high-grade graphitic schist
	24.5	28.5	Weathered high-grade graphitic schist

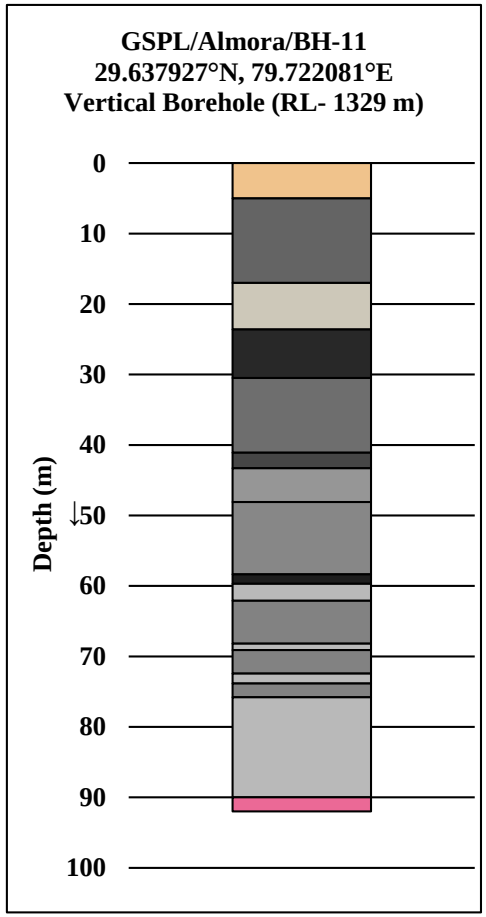

From (m)	To (m)	Thickness (m)	V (ppm)	FC (%)
2	3	1	573.01	
3	4	1		
4	5	1	213.77	
5	6	1		
6	7	1		
7	8	1		
8	9	1		
9	10	1		
10	11.5	1.5		
11.5	12.5	1	150.32	
12.5	13.5	1		
13.5	15	1.5		
15	16	1	124.87	
16	17	1		
17	18	1		
18	19	1		
19	20	1		
20	21	1		
21	22	1		
22	23	1		
23	24	1		
24	25	1	313.68	
25	26	1		
26	27	1		
27	28	1		
28	29	1		
29	30	1	389.43	
30	31	1		
31	32	1	233.82	1.01
32	33	1		
33	34	1	309.01	
33	34	1	304.68	
34	35	1		
35	36	1		
36	37	1		
37	38	1		
38	39.1	1.1		
39.1	40.1	1	62.63	
40.1	41.1	1		
41.1	42.1	1		
42.1	43.1	1		
43.1	44.1	1		
44.1	45.1	1		

From (m)	To (m)	Thickness (m)	V (ppm)	FC (%)
45.1	46.1	1		
46.1	47.1	1	79.27	
47.1	48.1	1		
48.1	49.1	1		
49.1	50.1	1		
50.1	51.1	1		
51.1	52.1	1		
52.1	53.1	1		
53.1	54.1	1	73.62	
54.1	55.1	1		
55.1	56.1	1		
56.1	57.1	1		
57.1	58.1	1		
58.1	59.1	1		
59.1	60.1	1		
60.1	61.1	1		
61.1	62.1	1		
62.1	63.1	1	216.87	
63.1	64.1	1		
64.1	65.1	1		

From (m)	To (m)	Thickness (m)	V (ppm)	FC (%)
65.1	66.1	1		
66.1	67.1	1		
67.1	68.1	1		
68.1	69.1	1		
69.1	70.1	1	84.93	
70.1	71.1	1		
71.1	72.1	1		
72.1	73.1	1		
73.1	74.1	1		
74.1	75.1	1		
75.1	76.1	1		
76.1	77.1	1	360.85	
77.1	78.1	1		
78.1	79.1	1		
79.1	80.6	1.5		
80.6	81.6	1		
81.6	83	1.4	93.96	
83	84	1		
84	85	1		
85	86	1		
86	87	1		
87	88	1		
88	89	1	96.17	
89	90	1		
90	91	1		
23	24	1		
91	92	1	53.74	

Colour Code	From (m)	To (m)	Lithology
	0	5	Weathered mica schist with topsoil
	5	17	Graphite–sericite (sludgy/weathered)
	17	23.6	Sericite (minor graphite)
	23.6	30.5	High-grade graphite schist
	30.5	41.1	Intercalated graphite & mica schist
	41.1	43.3	Moderate-grade graphite schist
	43.3	48.1	Mica schist with disseminated graphite (altered, quartz veins)
	48.1	58.4	Mica schist with graphite bands (with quartz)
	58.4	59.7	High-grade graphite band (sulphidic)
	59.7	62.1	Mica schist
	62.1	68.2	Mica schist with thin graphite bands (repetitive)
	68.2	69.1	Mica schist
	69.1	72.5	Mica schist with thin graphite bands
	72.5	73.9	Mica schist
	73.9	75.8	Mica schist with thin graphite bands
	75.8	90	Mica schist
	90	92	Foliated granite

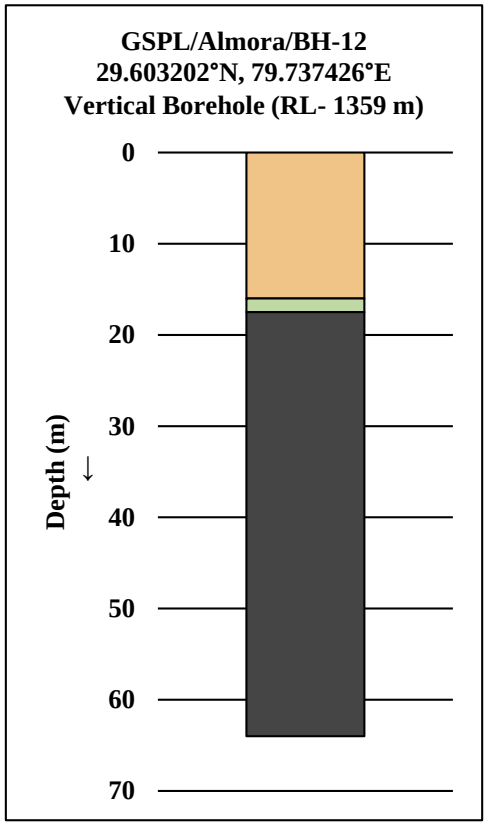

From (m)	To (m)	Thickness (m)	V (ppm)	FC (%)
16	17.5	1.5	104.53	
17.5	18.5	1		
18.5	20	1.5		
20	21	1	309.55	
21	22	1		
22	23.5	1.5		
23.5	24.5	1	188.68	
24.5	25.5	1		
25.5	26.5	1		
26.5	27.8	1.3	396.39	4.06
27.8	29.5	1.7		
29.5	31	1.5	249.70	
29.5	31	1.5	251.91	2.34
31	33	2	143.09	1.83
33	34.5	1.5		
34.5	36	1.5	131.29	
36	37	1		
37	38	1		

From (m)	To (m)	Thickness (m)	V (ppm)	FC (%)
38	39	1		
39	40.5	1.5		
40.5	42	1.5	87.54	
42	43	1		
43	44	1		
44	45	1		
45	46	1	662.02	
46	47	1		
47	48	1		
48	49	1		
49	50	1		
50	51.5	1.5		
51.5	53	1.5	17.23	
53	54.5	1.5		
54.5	56	1.5	1380.52	6.92

Colour code	From (m)	To (m)	Lithology
	0	16	Weathered mica schist with topsoil
	16	17.5	Sericite Mica Schist
	17.5	64	Graphite Schist

Annexure XXIX_Details of Drill Core Preservation

Borehole No	From Depth	To Depth	Meterage	Lithology	Core Box No	Total meterage	Total No of Boxes
BH-01	12	16	4	Sericite–Mica Schist	4	20	5
BH-01	20	24	4	Medium Grade Graphite schist	6		
BH-01	24	28	4	Medium Grade Graphite schist	7		
BH-01	32	36	4	Medium Grade Graphite schist	9		
BH-01	72	76	4	Low Grade Graphite schist	19		
BH-02	4	8	4	Sericite Mica Schist	2	24	6
BH-02	12	16	4	Graphite Schist	4		
BH-02	32	36	4	High Grade Graphite Schist (sulphide-rich)	9		
BH-02	40	44	4	Sericite Mica Schist	11		
BH-02	44	48	4	Sericite Mica Schist	12		
BH-02	48	52	4	Sericite Mica Schist	13		
BH-03	12	16	4	Medium Grade Graphite Schist	4	20	5
BH-03	16	20	4	Medium Grade Graphite Schist	5		
BH-03	20	24	4	Medium Grade Graphite Schist			
BH-03	52	56	4	Graphitic Sericite Schist	14		
BH-03	56	60	4	Graphitic Quartzite	15		
BH-04	4	8	4	Weathered mica schist with topsoil	2	32	8
BH-04	8	12	4	Medium Grade Graphite Schist	3		
BH-04	12	16	4	Medium Grade Graphite Schist	4		
BH-04	36	40	4	High Grade Graphite Schist	10		
BH-04	40	44	4	Graphite Quartzite intercalated with Sericite Schist	11		
BH-04	44	48	4	Graphite Quartzite intercalated with Sericite Schist	12		
BH-04	52	56.5	4.5	Biotite Mica Schist intercalated with thin Graphite Band	14		
BH-04	56.5	60	3.5	Biotite Mica Schist intercalated with thin Graphite Band	15		
BH-05	4	8	4	Sericite Mica Schist	2	28	7
BH-05	8	12	4	Quartz Graphite schist	3		
BH-05	12	16	4	Quartz Graphite schist	4		

Borehole No	From Depth	To Depth	Meterage	Lithology	Core Box No	Total meterage	Total No of Boxes
BH-05	20	24	4	Quartz Graphite schist	6		
BH-05	24	28	4	Medium Grade Graphite Schist	7		
BH-05	32	36	4	High Grade Graphite Schist	9		
BH-05	68	72	4	High Grade Graphite Schist	18		
BH-06	8	12	4	Weathered mica schist with topsoil	3	42	10
BH-06	12	16	4	Graphite–Sericite Schist	4		
BH-06	16	20	4	Graphite–Sericite Schist	5		
BH-06	20	25	5	Sericite Mica Schist	6		
BH-06	25	29	4	Sericite Mica Schist	7		
BH-06	33	37	4	Sericite Mica Schist	9		
BH-06	42	46.5	4.5	High Grade Graphite Schist	11		
BH-06	46.5	50.5	4	Graphitic Quartzite	12		
BH-06	54.5	58.5	4	Graphitic Quartzite	14		
BH-06	58.5	63	4.5	Graphitic Quartzite	15		
BH-07	0	4	4	Weathered mica schist with topsoil	1	50	13
BH-07	4	8	4	Sericite Mica Schist	2		
BH-07	8	12	4	Quartz Graphite schist	3		
BH-07	12	16	4	Sericite Mica Schist	4		
BH-07	16	20	4	Sericite Mica Schist	5		
BH-07	20	24	4	Sericite Mica Schist	6		
BH-07	24	28	4	Graphitic Sericite Schist	7		
BH-07	28	32	4	Graphitic Sericite Schist	8		
BH-07	32	36	4	Sericite Mica Schist	9		
BH-07	36	40	4	Sericite Mica Schist	10		
BH-07	40	44	4	Sericite Mica Schist	11		
BH-07	44	48.5	4.5	Sericite Mica Schist	12		
BH-07	48.5	50	1.5	Sericite Mica Schist	13		
BH-08	20	24.5	4.5	Sericite Mica Schist	6	30	7
BH-08	24.5	28.5	4	Sericite Mica Schist	7		
BH-08	28.5	33	4.5	Graphitic Sericite Schist	8		
BH-08	33	37.8	4.8	Graphitic Sericite Schist	9		
BH-08	37.8	41.5	3.7	Sericite Mica Schist	10		
BH-08	41.5	46.5	5	High Grade Graphite Schist	11		

Borehole No	From Depth	To Depth	Meterage	Lithology	Core Box No	Total meterage	Total No of Boxes
BH-08	46.5	50	3.5	Sericite Mica Schist	12		
BH-09	20	24	4	Mica Schist	6	8	2
BH-09	24	28	4	Mica Schist	7		
BH-10	4	8	4	High-grade graphite schist (enriched in redox-sensitive elements)	2	13	3
BH-10	8	12	4	High-grade graphite schist (enriched in redox-sensitive elements)	3		
BH-10	17	22	5	Highly weathered greenish schist (sludgy)	5		
BH-11	12.5	16.5	4	Graphite–sericite (sludgy/weathered)	4	24.7	6
BH-11	29	33	4	High-grade graphite schist	8		
BH-11	33	37	4	Intercalated graphite and mica schist	9		
BH-11	37	41.1	4.1	Intercalated graphite and mica schist	10		
BH-11	77.1	81.6	4.5	Mica schist	20		
BH-11	81.6	85.7	4.1	Mica schist	21		
BH-12	43.3	48.4	5.1	Graphite Schist	10	9.9	2
BH-12	48.4	53.2	4.8	Graphite Schist	11		
						Total – 301.6 m	**Total- 74**

Annexure XXX_Construction of Concrete Pillar (12"x12"x30")

Figure 14.37: Concrete pillaring at Borehole-01

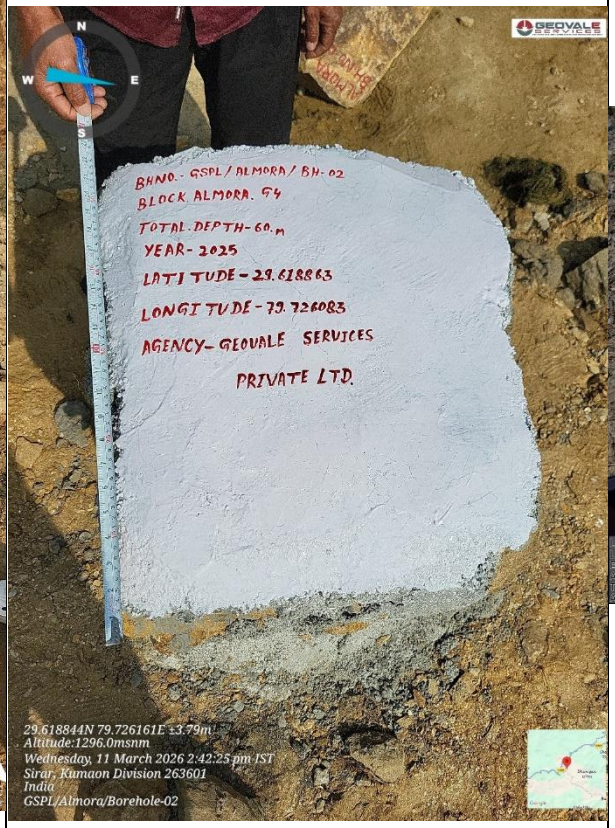

Figure 14.38: Concrete pillaring at Borehole-02

Figure 14.39: Concrete pillaring of Borehole-03

Figure 14.40: Concrete pillaring at Borehole-04

Figure 14.41: Concrete pillaring at Borehole-05

Figure 14.42: Concrete pillaring at Borehole-06

Figure 14.43: Concrete pillaring of Borehole-07

Figure 14.44: Concrete pillaring at Borehole-08

Figure 14.45: Concrete pillaring of Borehole-09

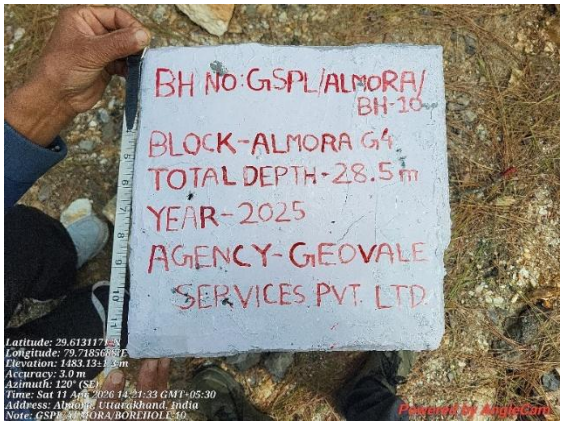

Figure 14.46: Concrete pillaring of Borehole-10

Figure 14.47: Concrete pillaring at Borehole-11

Figure 14.48: Concrete pillaring at Borehole-12